VOLUME 28 / NUMBER 8
APRIL 23, 1990
ACC. NOS. N90-15882 TO N90-16706

STAR

AN ABSTRACT JOURNAL

Scientific and Technical Aerospace Reports

PRODUCED BY THE
SCIENTIFIC AND TECHNICAL
INFORMATION
DIVISION

NASA

NATIONAL AERONAUTICS AND SPACE ADMINISTRATION

WHAT YOU CAN DO FOR *STAR*

All users of this abstract service are urged to forward reports to be considered for announcement in *STAR*. This will aid NASA in its efforts to provide the fullest possible coverage of all scientific and technical publications that might support aeronautics and space research and development. If you have prepared relevant reports (other than those that you will transmit to NASA, DOD, or DOE through the usual contract- or grant-reporting channels), please send them for consideration to the NASA Scientific and Technical Information Facility, P.O. Box 8757, BWI Airport, MD 21240.

Reprints of journal articles, book chapters, and conference papers are also welcome. These will be considered for announcement in *STAR*'s companion journal, *International Aerospace Abstracts*.

You may specify a particular source to be included in a report announcement if you wish; otherwise the report will be placed on public sale at the National Technical Information Service. Copyrighted publications will be announced but not distributed or sold.

PURCHASE OF *STAR*

The semimonthly issues are available to registered users on annual subscription from the NASA Scientific and Technical Information Facility, ATTN: Registration Services, P.O. Box 8757, BWI Airport, MD 21240. *STAR* is publicly available on annual subscription from the Superintendent of Documents, U.S. Government Printing Office, Washington, DC 20402.

PUBLISHED BY:

UNITED STATES GOVERNMENT
NATIONAL AERONAUTICS AND SPACE ADMINISTRATION
SCIENTIFIC AND TECHNICAL INFORMATION DIVISION
Scientific and Technical Aerospace Reports, Volume 28, is prepared by the NASA Scientific and Technical Information Facility operated for the National Aeronautics and Space Administration by RMS Associates.

The Administrator of the National Aeronautics and Space Administration has determined that the publication of this periodical is necessary in the transaction of the public business required by law of this agency. Use of funds for printing this periodical has been approved by the Director of the Office of Management and Budget through March 22, 1991.

US ISSN 0036-8741

Scientific and Technical Aerospace Reports (STAR) is issued twice a month and contains abstracts and indexes of meeting papers, conference proceedings, and unlimited distribution reports that have been added to the NASA Scientific and Technical Information Database during the preceding period. These citations may also be accessed online via NASA/RECON or via AIAA's Aerospace Database (File 108) through Dialog Information Services, Inc.

STAR subject coverage includes all aerospace-related areas that will help NASA achieve its mission. Material is gathered from all over the world and includes significant input from many countries under exchange and access agreements.

Consult the indexes at the back of this volume to help zero in on what you are looking for. These include:

Subject Index
Personal Author Index
Corporate Source Index
Contract Number Index
Report/Accession Number Index

STAR's companion abstract journal *International Aerospace Abstracts* should be used if you are looking for references to periodicals, books, and published meeting papers or conference proceedings.

Questions and comments should be addressed to:

NASA Scientific and Technical Information Facility
User Services
P.O. Box 8757
BWI Airport, MD 21240
301-621-0150

VOLUME 28 NUMBER 8 / APRIL 23, 1990

TABLE OF CONTENTS

AERONAUTICS

Includes aeronautics (general); aerodynamics; air transportation and safety; aircraft communications and navigation; aircraft design, testing and performance; aircraft instrumentation; aircraft propulsion and power; aircraft stability and control; and research and support facilities (air).

For related information see also *Astronautics.*

01 AERONAUTICS (GENERAL) **N.A.**

02 AERODYNAMICS **1017**

Includes aerodynamics of bodies, combinations, wings, rotors, and control surfaces; and internal flow in ducts and turbomachinery.

For related information see also *34 Fluid Mechanics and Heat Transfer.*

03 AIR TRANSPORTATION AND SAFETY **1019**

Includes passenger and cargo air transport operations; and aircraft accidents.

For related information see also *16 Space Transportation* and *85 Urban Technology and Transportation.*

04 AIRCRAFT COMMUNICATIONS AND NAVIGATION **1020**

Includes digital and voice communication with aircraft; air navigation systems (satellite and ground based); and air traffic control.

For related information see also *17 Space Communications, Spacecraft Communications, Command and Tracking* and *32 Communications and Radar.*

05 AIRCRAFT DESIGN, TESTING AND PERFORMANCE **1021**

Includes aircraft simulation technology.

For related information see also *18 Spacecraft Design, Testing and Performance* and *39 Structural Mechanics.* For land transportation vehicles see *85 Urban Technology and Transportation.*

06 AIRCRAFT INSTRUMENTATION **N.A.**

Includes cockpit and cabin display devices; and flight instruments.

For related information see also *19 Spacecraft Instrumentation* and *35 Instrumentation and Photography.*

07 AIRCRAFT PROPULSION AND POWER **1024**

Includes prime propulsion systems and systems components, e.g., gas turbine engines and compressors; and onboard auxiliary power plants for aircraft.

For related information see also *20 Spacecraft Propulsion and Power, 28 Propellants and Fuels,* and *44 Energy Production and Conversion.*

08 AIRCRAFT STABILITY AND CONTROL **1025**

Includes aircraft handling qualities; piloting; flight controls; and autopilots.

For related information see also *05 Aircraft Design, Testing and Performance.*

09 RESEARCH AND SUPPORT FACILITIES (AIR) **1028**

Includes airports, hangars and runways; aircraft repair and overhaul facilities; wind tunnels; shock tubes; and aircraft engine test stands.

For related information see also *14 Ground Support Systems and Facilities (Space).*

ASTRONAUTICS

Includes astronautics (general); astrodynamics; ground support systems and facilities (space); launch vehicles and space vehicles; space transportation; space communications, spacecraft communications, command and tracking; spacecraft design, testing and performance; spacecraft instrumentation; and spacecraft propulsion and power.

For related information see also *Aeronautics.*

12 ASTRONAUTICS (GENERAL) **1033**

For extraterrestrial exploration see *91 Lunar and Planetary Exploration.*

13 ASTRODYNAMICS **1033**

Includes powered and free-flight trajectories; and orbital and launching dynamics.

14 GROUND SUPPORT SYSTEMS AND FACILITIES (SPACE) **1033**

Includes launch complexes, research and production facilities; ground support equipment, e.g., mobile transporters; and simulators.

For related information see also *09 Research and Support Facilities (Air).*

15 LAUNCH VEHICLES AND SPACE VEHICLES **N.A.**

Includes boosters; operating problems of launch/space vehicle systems; and reusable vehicles.

For related information see also *20 Spacecraft Propulsion and Power.*

16 SPACE TRANSPORTATION **1034**

Includes passenger and cargo space transportation, e.g., shuttle operations; and space rescue techniques.

For related information see also *03 Air Transportation and Safety* and *18 Spacecraft Design, Testing and Performance.* For space suits see *54 Man/System Technology and Life Support.*

17 SPACE COMMUNICATIONS, SPACECRAFT COMMUNICATIONS, COMMAND AND TRACKING **1035**

Includes telemetry; space communications networks; astronavigation and guidance; and radio blackout.

For related information see also *04 Aircraft Communications and Navigation* and *32 Communications and Radar.*

18 SPACECRAFT DESIGN, TESTING AND PERFORMANCE 1036

Includes satellites; space platforms; space stations; spacecraft systems and components such as thermal and environmental controls; and attitude controls.

For life support systems see *54 Man/System Technology and Life Support.* For related information see also *05 Aircraft Design, Testing and Performance, 39 Structural Mechanics,* and *16 Space Transportation.*

19 SPACECRAFT INSTRUMENTATION N.A.

For related information see also *06 Aircraft Instrumentation* and *35 Instrumentation and Photography.*

20 SPACECRAFT PROPULSION AND POWER 1037

Includes main propulsion systems and components, e.g. rocket engines; and spacecraft auxiliary power sources.

For related information see also *07 Aircraft Propulsion and Power, 28 Propellants and Fuels, 44 Energy Production and Conversion,* and *15 Launch Vehicles and Space Vehicles.*

CHEMISTRY AND MATERIALS

Includes chemistry and materials (general); composite materials; inorganic and physical chemistry; metallic materials; nonmetallic materials; propellants and fuels; and materials processing.

23 CHEMISTRY AND MATERIALS (GENERAL) N.A.

24 COMPOSITE MATERIALS 1039

Includes physical, chemical, and mechanical properties of laminates and other composite materials.

For ceramic materials see *27 Nonmetallic Materials.*

25 INORGANIC AND PHYSICAL CHEMISTRY 1040

Includes chemical analysis, e.g., chromatography; combustion theory; electrochemistry; and photochemistry.

For related information see also *77 Thermodynamics and Statistical Physics.*

26 METALLIC MATERIALS 1043

Includes physical, chemical, and mechanical properties of metals, e.g., corrosion; and metallurgy.

27 NONMETALLIC MATERIALS 1047

Includes physical, chemical, and mechanical properties of plastics, elastomers, lubricants, polymers, textiles, adhesives, and ceramic materials.

For composite materials see *24 Composite Materials.*

28 PROPELLANTS AND FUELS 1052

Includes rocket propellants, igniters and oxidizers; their storage and handling procedures; and aircraft fuels.

For related information see also *07 Aircraft Propulsion and Power, 20 Spacecraft Propulsion and Power,* and *44 Energy Production and Conversion.*

29 MATERIALS PROCESSING 1053

Includes space-based development of products and processes for commercial application.

For biological materials see *55 Space Biology.*

ENGINEERING

Includes engineering (general); communications and radar; electronics and electrical engineering; fluid mechanics and heat transfer; instrumentation and photography; lasers and masers; mechanical engineering; quality assurance and reliability; and structural mechanics.

For related information see also *Physics.*

31 ENGINEERING (GENERAL) 1054

Includes vacuum technology; control engineering; display engineering; cryogenics; and fire prevention.

32 COMMUNICATIONS AND RADAR 1055

Includes radar; land and global communications; communications theory; and optical communications.

For related information see also *04 Aircraft Communications and Navigation* and *17 Space Communications, Spacecraft Communications, Command and Tracking.* For search and rescue see *03 Air Transportation and Safety,* and *16 Space Transportation.*

33 ELECTRONICS AND ELECTRICAL ENGINEERING 1059

Includes test equipment and maintainability; components, e.g., tunnel diodes and transistors; microminiaturization; and integrated circuitry.

For related information see also *60 Computer Operations and Hardware* and *76 Solid-State Physics.*

34 FLUID MECHANICS AND HEAT TRANSFER 1062

Includes boundary layers; hydrodynamics; fluidics; mass transfer and ablation cooling.

For related information see also *02 Aerodynamics* and *77 Thermodynamics and Statistical Physics.*

35 INSTRUMENTATION AND PHOTOGRAPHY 1072

Includes remote sensors; measuring instruments and gauges; detectors; cameras and photographic supplies; and holography.

For aerial photography see *43 Earth Resources and Remote Sensing.* For related information see also *06 Aircraft Instrumentation* and *19 Spacecraft Instrumentation.*

36 LASERS AND MASERS 1082

Includes parametric amplifiers.

For related information see also *76 Solid-State Physics.*

37 MECHANICAL ENGINEERING 1083

Includes auxiliary systems (nonpower); machine elements and processes; and mechanical equipment.

38 QUALITY ASSURANCE AND RELIABILITY 1086

Includes product sampling procedures and techniques; and quality control.

39 STRUCTURAL MECHANICS 1087

Includes structural element design and weight analysis; fatigue; and thermal stress.

For applications see *05 Aircraft Design, Testing and Performance* and *18 Spacecraft Design, Testing and Performance.*

GEOSCIENCES

Includes geosciences (general); earth resources and remote sensing; energy production and conversion; environment pollution; geophysics; meteorology and climatology; and oceanography.

For related information see also *Space Sciences.*

42 GEOSCIENCES (GENERAL) 1090

43 EARTH RESOURCES AND REMOTE SENSING 1090

Includes remote sensing of earth resources by aircraft and spacecraft; photogrammetry; and aerial photography.

For instrumentation see *35 Instrumentation and Photography.*

44 ENERGY PRODUCTION AND CONVERSION 1095

Includes specific energy conversion systems, e.g., fuel cells; global sources of energy; geophysical conversion; and windpower.

For related information see also *07 Aircraft Propulsion and Power, 20 Spacecraft Propulsion and Power,* and *28 Propellants and Fuels.*

45 ENVIRONMENT POLLUTION 1098

Includes atmospheric, noise, thermal, and water pollution.

46 GEOPHYSICS 1099

Includes aeronomy; upper and lower atmosphere studies; ionospheric and magnetospheric physics; and geomagnetism.

For space radiation see *93 Space Radiation.*

47 METEOROLOGY AND CLIMATOLOGY 1102

Includes weather forecasting and modification.

48 OCEANOGRAPHY N.A.

Includes biological, dynamic, and physical oceanography; and marine resources.

For related information see also *43 Earth Resources and Remote Sensing.*

LIFE SCIENCES

Includes life sciences (general); aerospace medicine; behavioral sciences; man/system technology and life support; and space biology.

51 LIFE SCIENCES (GENERAL) 1104

52 AEROSPACE MEDICINE 1104

Includes physiological factors; biological effects of radiation; and effects of weightlessness on man and animals.

53 BEHAVIORAL SCIENCES N.A.

Includes psychological factors; individual and group behavior; crew training and evaluation; and psychiatric research.

54 MAN/SYSTEM TECHNOLOGY AND LIFE SUPPORT 1105

Includes human engineering; biotechnology; and space suits and protective clothing.

For related information see also *16 Space Transportation.*

55 SPACE BIOLOGY 1106

Includes exobiology; planetary biology; and extraterrestrial life.

MATHEMATICAL AND COMPUTER SCIENCES

Includes mathematical and computer sciences (general); computer operations and hardware; computer programming and software; computer systems; cybernetics; numerical analysis; statistics and probability; systems analysis; and theoretical mathematics.

59 MATHEMATICAL AND COMPUTER SCIENCES (GENERAL) 1106

60 COMPUTER OPERATIONS AND HARDWARE 1106

Includes hardware for computer graphics, firmware, and data processing.

For components see *33 Electronics and Electrical Engineering.*

61 COMPUTER PROGRAMMING AND SOFTWARE 1107

Includes computer programs, routines, algorithms, and specific applications, e.g., CAD/CAM.

62 COMPUTER SYSTEMS 1113

Includes computer networks and special application computer systems.

63 CYBERNETICS N.A.

Includes feedback and control theory, artificial intelligence, robotics and expert systems.

For related information see also *54 Man/System Technology and Life Support.*

64 NUMERICAL ANALYSIS 1115

Includes iteration, difference equations, and numerical approximation.

65 STATISTICS AND PROBABILITY N.A.

Includes data sampling and smoothing; Monte Carlo method; and stochastic processes.

66 SYSTEMS ANALYSIS N.A.

Includes mathematical modeling; network analysis; and operations research.

67 THEORETICAL MATHEMATICS 1117

Includes topology and number theory.

PHYSICS

Includes physics (general); acoustics; atomic and molecular physics; nuclear and high-energy physics; optics; plasma physics; solid-state physics; and thermodynamics and statistical physics.

For related information see also *Engineering.*

70 PHYSICS (GENERAL) 1118

For precision time and time interval (PTTI) see *35 Instrumentation and Photography;* for geophysics, astrophysics or solar physics see *46 Geophysics, 90 Astrophysics,* or *92 Solar Physics.*

71 ACOUSTICS 1119
Includes sound generation, transmission, and attenuation.
For noise pollution see *45 Environment Pollution.*

72 ATOMIC AND MOLECULAR PHYSICS 1119
Includes atomic structure, electron properties, and molecular spectra.

73 NUCLEAR AND HIGH-ENERGY PHYSICS 1122
Includes elementary and nuclear particles; and reactor theory.
For space radiation see *93 Space Radiation.*

74 OPTICS 1122
Includes light phenomena and optical devices.
For lasers see *36 Lasers and Masers.*

75 PLASMA PHYSICS 1123
Includes magnetohydrodynamics and plasma fusion.
For ionospheric plasmas see *46 Geophysics.* For space plasmas see *90 Astrophysics.*

76 SOLID-STATE PHYSICS 1127
Includes superconductivity.
For related information see also *33 Electronics and Electrical Engineering* and *36 Lasers and Masers.*

77 THERMODYNAMICS AND STATISTICAL PHYSICS 1134
Includes quantum mechanics; theoretical physics; and Bose and Fermi statistics.
For related information see also *25 Inorganic and Physical Chemistry* and *34 Fluid Mechanics and Heat Transfer.*

SOCIAL SCIENCES

Includes social sciences (general); administration and management; documentation and information science; economics and cost analysis; law, political science, and space policy; and urban technology and transportation.

80 SOCIAL SCIENCES (GENERAL) N.A.
Includes educational matters.

81 ADMINISTRATION AND MANAGEMENT 1136
Includes management planning and research.

82 DOCUMENTATION AND INFORMATION SCIENCE 1136
Includes information management; information storage and retrieval technology; technical writing; graphic arts; and micrography.
For computer documentation see *61 Computer Programming and Software.*

83 ECONOMICS AND COST ANALYSIS N.A.
Includes cost effectiveness studies.

84 LAW, POLITICAL SCIENCE AND SPACE POLICY N.A.
Includes NASA appropriation hearings; aviation law; space law and policy; international law; international cooperation; and patent policy.

85 URBAN TECHNOLOGY AND TRANSPORTATION 1138
Includes applications of space technology to urban problems; technology transfer; technology assessment; and surface and mass transportation.
For related information see *03 Air Transportation and Safety, 16 Space Transportation,* and *44 Energy Production and Conversion.*

SPACE SCIENCES

Includes space sciences (general); astronomy; astrophysics; lunar and planetary exploration; solar physics; and space radiation.
For related information see also *Geosciences.*

88 SPACE SCIENCES (GENERAL) 1138

89 ASTRONOMY 1138
Includes radio, gamma-ray, and infrared astronomy; and astrometry.

90 ASTROPHYSICS 1140
Includes cosmology; celestial mechanics; space plasmas; and interstellar and interplanetary gases and dust.
For related information see also *75 Plasma Physics.*

91 LUNAR AND PLANETARY EXPLORATION 1152
Includes planetology; and manned and unmanned flights.
For spacecraft design or space stations see *18 Spacecraft Design, Testing and Performance.*

92 SOLAR PHYSICS 1153
Includes solar activity, solar flares, solar radiation and sunspots.
For related information see *93 Space Radiation.*

93 SPACE RADIATION 1153
Includes cosmic radiation; and inner and outer earth's radiation belts.
For biological effects of radiation see *52 Aerospace Medicine.* For theory see *73 Nuclear and High-Energy Physics.*

GENERAL

Includes aeronautical, astronautical, and space science related histories, biographies, and pertinent reports too broad for categorization; histories or broad overviews of NASA programs.

99 GENERAL 1154

Note: N.A. means that no abstracts were assigned to this category for this issue.

SUBJECT INDEX I-1
PERSONAL AUTHOR INDEX I-51
CORPORATE SOURCE INDEX I-59
CONTRACT NUMBER INDEX I-71
REPORT/ACCESSION NUMBER INDEX .. I-73
APPENDIX—ABOUT STAR A-1

TYPICAL CITATION AND ABSTRACT

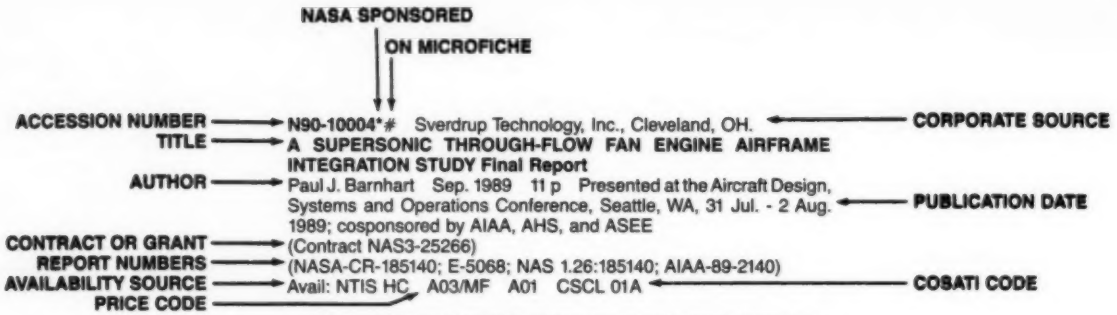
NASA SPONSORED
ON MICROFICHE
ACCESSION NUMBER
N90-10004*# Sverdrup Technology, Inc., Cleveland, OH.
CORPORATE SOURCE
TITLE
A SUPERSONIC THROUGH-FLOW FAN ENGINE AIRFRAME INTEGRATION STUDY Final Report
AUTHOR
Paul J. Barnhart Sep. 1989 11 p Presented at the Aircraft Design, Systems and Operations Conference, Seattle, WA, 31 Jul. - 2 Aug. 1989; cosponsored by AIAA, AHS, and ASEE
PUBLICATION DATE
CONTRACT OR GRANT
(Contract NAS3-25266)
REPORT NUMBERS
(NASA-CR-185140; E-5068; NAS 1.26:185140; AIAA-89-2140)
AVAILABILITY SOURCE
Avail: NTIS HC A03/MF A01 CSCL 01A
COSATI CODE
PRICE CODE

Engine airframe integration effects are investigated for superonsic through-flow fan engines installed on a Mach 3.20 supersonic cruise vehicle. Six different supersonic through-flow fan engine installations covering the effects of engine size, nacelle contour, nacelle placement, and approximate bypass plume effects are presented. The different supersonic through-flow fan installations are compared with a conventional turbine bypass engine configuration on the same basic airframe. The supersonic through-flow fan engine integrations are shown to be comparable to the turbine bypass engine configuration on the basis of installed nacelle wave drag. The supersonic through-flow fan engine airframe integrated vehicles have superior aerodynamic performance on the basis of maximum lift-to-drag ratio than the turbine bypass engine installation over the entire operating Mach number range from 1.10 to 3.20. When approximate bypass plume modeling is included, the supersonic through-flow fan engine configuration shows even larger improvements over the turbine bypass engine configuration. Author

VOLUME 28 NUMBER 8 / APRIL 23, 1990

Scientific and Technical Aerospace Reports

A Semimonthly Publication of the National Aeronautics and Space Administration

01 AERONAUTICS (GENERAL)

No abstracts in this category.

02 AERODYNAMICS

Includes aerodynamics of bodies, combinations, wings, rotors, and control surfaces; and internal flow in ducts and turbomachinery.

For related information see also *34 Fluid Mechanics and Heat Transfer.*

N90-15882*# National Aeronautics and Space Administration. Langley Research Center, Hampton, VA.
ROTOR INDUCED-INFLOW-RATIO MEASUREMENTS AND CAMRAD CALCULATIONS
Danny R. Hoad Washington Jan. 1990 28 p Original contains color illustrations
(DA Proj. 1L1-62211-A-47-AA)
(NASA-TP-2946; L-16594; NAS 1.60:2946; AVSCOM-TM-89-B-010) Avail: NTIS HC A03/MF A01 CSCL 01A

Comparison of the inflow calculations between an analytical rotor wake method and rotor inflow measurements using a laser velocimeter was presented. The inflow measurements were made near a 4-bladed rotor system using rectangular planform blades operating in forward flight at a thrust coefficient of 0.0064, and at 3 rotor advance ratios: 0.15, 0.23, and 0.30. The inflow measurements were made at azimuthal increments of 30 degrees at 3.0 inches (approximately 1 chord) above the plane formed by the tips of the blades, and radial locations from 20 to 110 percent of blade span. The experimental measurements showed that as the advance ratio (m) increased, the induced upflow region moved progressively from the forward 20 percent of the rotor disc at m = 0.15 to covering most of the forward half of the rotor disc at m = 0.30. The induced inflow characteristics at all advance ratios were found to be unsymmetrical about the longitudinal centerline. The maximum downwash was found to be in the rear portion of the disc and skewed toward the advancing blade side. The comparisons with the analytical method Comprehensive Analytical Model of Rotorcraft Aerodynamics and Dynamics (CAMRAD) show that the region of induced upflow over the rotor disc was effectively modeled only at the advance ratio of 0.15. The method consistently indicated the largest values of induced inflow ratio to be on the retreating-blade side of the rotor disc (opposite from that measured). The importance of the choice of rotor trim option is examined and results of two trim selections are detailed. Author

N90-15883 Princeton Univ., NJ.
THE STRUCTURE OF SUPERSONIC TURBULENT BOUNDARY LAYERS SUBJECTED TO CONCAVE SURFACE CURVATURE Ph.D. Thesis
John Francis Donovan 1989 352 p
Avail: Univ. Microfilms Order No. DA8910891

The behavior of a supersonic turbulent boundary layer subjected to the perturbations associated with short regions of two-dimensional concave surface curvature, was studied. Two flows were studied. One was a relatively weak case and one was a relatively strong case. Both flows severely distorted the boundary layer, as evidenced by an alteration of the mean velocity profiles, and caused an increase in wall stress of 50 percent in the first case and 100 percent in the second. Hotwire anemometry and high-speed data acquisition were the primary tools used in this investigation. Instantaneously, large gradients in the streamwise mass flux (termed mass flux fronts) inclined at an average angle of 50 degrees to the wall were found to extend across the boundary layer. These mass flux fronts are associated with large contributions to the Reynolds averaged shear stress. The strong perturbation caused the angle of inclination of these fronts to increase by 10 degrees, whereas there was no change in the weak perturbation. Significant differences in the average flowfield associated with the mass flux fronts were also caused by the perturbation. In addition to the experimental work, calculations of the flows were made. A calculation method developed by Bradshaw, Ferris, and Atwell was modified to allow reasonable agreement of the calculated wall stress with the experimentally determined values. Using this method, the relative importance of the curvature and bulk compression effects were determined. Dissert. Abstr.

N90-15884*# National Aeronautics and Space Administration. Langley Research Center, Hampton, VA.
AN EXPERIMENTAL INVESTIGATION OF THRUST VECTORING TWO-DIMENSIONAL CONVERGENT-DIVERGENT NOZZLES INSTALLED IN A TWIN-ENGINE FIGHTER MODEL AT HIGH ANGLES OF ATTACK
Francis J. Capone, Mary L. Mason, and Laurence D. Leavitt Washington Feb. 1990 123 p
(NASA-TM-4155; L-16563; NAS 1.15:4155) Avail: NTIS HC A06/MF A01 CSCL 01A

An investigation was conducted in the Langley 16-Foot Transonic Tunnel to determine thrust vectoring capability of subscale 2-D convergent-divergent exhaust nozzles installed on a twin engine general research fighter model. Pitch thrust vectoring was accomplished by downward rotation of nozzle upper and lower flaps. The effects of nozzle sidewall cutback were studied for both unvectored and pitch vectored nozzles. A single cutback sidewall was employed for yaw thrust vectoring. This investigation was conducted at Mach numbers ranging from 0 to 1.20 and at angles of attack from -2 to 35 deg. High pressure air was used to simulate jet exhaust and provide values of nozzle pressure ratio up to 9. Author

N90-15885*# George Washington Univ., Washington, DC. Joint Inst. for Advancement of Flight Sciences.
FLOW SEPARATION IN SHOCK WAVE BOUNDARY LAYER INTERACTIONS AT HYPERSONIC SPEEDS Final Report
A. Hamed (Cincinnati Univ., OH.) Washington NASA Feb. 1990 46 p
(Contract NAS1-18458)
(NASA-CR-4274; NAS 1.26:4274) Avail: NTIS HC A03/MF A01 CSCL 01A

An assessment is presented for the experimental data on separated flow in shock wave turbulent boundary layer interactions at hypersonic and supersonic speeds. The data base consists mainly of two dimensional and axisymmetric interactions in

compression corners or cylinder-flares, and externally generated oblique shock interactions with boundary layers over flat plates or cylindrical surfaces. The conditions leading to flow separation and the subsequent changes in the flow empirical correlations for incipient separation are reviewed. The effects of the Mach number, Reynolds number, surface cooling and the methods of detecting separation are discussed. The pertinent experimental data for the separated flow characteristics in separated turbulent boundary layer shock interaction are also presented and discussed. Author

N90-15886*# National Aeronautics and Space Administration. Langley Research Center, Hampton, VA.
ASSESSMENT OF COMPUTATIONAL PREDICTION OF TAIL BUFFETING
John W. Edwards Jan. 1990 42 p
(NASA-TM-101613; NAS 1.15:101613) Avail: NTIS HC A03/MF A01 CSCL 01A

Assessments of the viability of computational methods and the computer resource requirements for the prediction of tail buffeting are made. Issues involved in the use of Euler and Navier-Stokes equations in modeling vortex-dominated and buffet flows are discussed and the requirement for sufficient grid density to allow accurate, converged calculations is stressed. Areas in need of basic fluid dynamics research are highlighted: vorticity convection, vortex breakdown, dynamic turbulence modeling for free shear layers, unsteady flow separation for moderately swept, rounded leading-edge wings, vortex flows about wings at high subsonic speeds. An estimate of the computer run time for a buffeting response calculation for a full span F-15 aircraft indicates that an improvement in computer and/or algorithm efficiency of three orders of magnitude is needed to enable routine use of such methods. Attention is also drawn to significant uncertainties in the estimates, in particular with regard to nonlinearities contained within the modeling and the question of the repeatability or randomness of buffeting response. Author

N90-15887# Centre d'Etudes et de Recherches, Toulouse (France). Dept. d'Etudes et de Recherches en Aerothermodynamique.
EXPERIMENTAL INVESTIGATION OF A THREE-DIMENSIONAL WAKE. PART 2: SPECTRAL AND TURBULENT ENERGY ANALYSIS
G. Pailhas and V. Jayaraman (National Aeronautical Lab., Bangalore, India) May 1989 48 p
(Contract STPA-85-95-004-35)
(ONERA-RT-32/5025-AYD-Pt-2; DERAT-32/5025-20-Pt-2; ETN-90-96083) Avail: NTIS HC A03/MF A01

The study is devoted to the understanding of the behavior of the energy containing eddies in a three dimensional pressure gradient wake. The spectral analysis and turbulent kinetic energy balance are considered. The results obtained reveal the following remarks: the spectra for the near wake X-stations are different in nature as compared to the far stations ones; for larger values of X, near the wake centerline, the slope of the spectra in the sub-inertial range follows a classical power law of the form K to the power of minus 5/3; the transfer of the energy towards the low frequencies related to the formation of large scale eddies appears to be evident. The dissipative length scales are obtained. The calculation of higher order moments permitted access to the turbulent transort velocity. The results obtained in the present study reinforce the previous observations that the behavior of such a dissymmetric pressure gradient wake is different from that of a classical two and three dimensional wake. ESA

N90-15888# Royal Aerospace Establishment, Farnborough (England).
WEAPON AERODYNAMICS OVERVIEW
D. N. Foster Jan. 1989 59 p Presented at RAE's One-Day Conference on Weapon Aerodynamics, Farnborough, England, 1 Dec. 1988
(RAE-TM-Aero-2150; BR110498; ETN-90-96137) Copyright Avail: NTIS HC A04/MF A01

The problems currently facing the weapon aerodynamicist are discussed. The origins of these problems and the methods available to predict and to solve them are analyzed. The results lead to the following conclusions: the extensive database on loads and moments for a wide variety of conventional missile configurations enable the applicability of semi-empirical methods to be extended, and contribute to the validation of computational fluid dynamics methods; the measurement of flowfield and surface pressure characteristics provides the understanding of the flow around a missile, and also severe test cases for computational fluid dynamics methods; the increase of maximum Mach number puts more emphasis on the measurement and prediction of kinetic heating effects; solutions to eliminate the random variation of out-of-plane forces, generated at very high angles of incidence, are needed; the effect of intakes on overall aerodynamic characteristics is large, but may be beneficial; and significant aerodynamic problems, requiring extensive aerodynamic research, may be encountered for unconventional shapes. ESA

N90-15889# European Space Agency, Paris (France).
WIND TUNNEL TESTS OF THE INFLUENCE OF AEROFOIL THICKNESS ON THE NORMAL FORCE AND PITCHING MOMENT OF TWO SLENDER WINGS AT TRANSONIC AND SUPERSONIC MACH NUMBERS
Helmut Esch (Deutsche Forschungs- und Versuchsanstalt fuer Luft- und Raumfahrt, Cologne, Germany, F.R.) Aug. 1989 190 p Transl. into ENGLISH of Windkanalmessungen zum Einfluss der Profildicke von zwei Geometrisch Einfachen, Schlanken Fluegeln im Trans- und Ueberschallgeschwindigkeitsbereich Original language document was announced as N88-27171
(ESA-TT-1129; DFVLR-FB-88-17; ETN-90-96189) Avail: NTIS HC A09/MF A02; original German report available from DFVLR, VB-PL-DO, Postfach 90 60 58, 5000 Cologne, Federal Republic of Germany, 67.50 deutsche marks

Forces at subsonic, transonic, and supersonic Mach numbers are measured. The investigation is performed in order to determine the influence of aerofoil thickness and shape on the normal force and pitching moment of slender wings. Both wings, a rectangular and a clipped delta wing, had hexagonal wing sections. The wing thickness, the edge angle and edge radius are varied. The tests are carried out in a trisonic wind tunnel at Mach numbers between 0.5 and 4. In supersonic flow, the incidence varied between -10 deg and 90 deg. ESA

N90-15890*# National Aeronautics and Space Administration. Langley Research Center, Hampton, VA.
IMPROVED TANGENT-CONE METHOD FOR THE AERODYNAMIC PRELIMINARY ANALYSIS SYSTEM (APAS) VERSION OF THE HYPERSONIC ARBITRARY-BODY PROGRAM
Christopher I. Cruz and Gregory J. Sova (Rockwell International Corp., El Segundo, CA.) Feb. 1990 10 p
(NASA-TM-4165; L-16404; NAS 1.15:4165) Avail: NTIS HC A02/MF A01 CSCL 01A

The Aerodynamic Preliminary Analysis System (APAS) utilizes a modified version of the Hypersonic Arbitrary-Body Program (HABP) Mark 3 code in its analysis rationale. Four methods are considered for incorporation into the code as the tangent-cone method. The combination of second-order slender body theory and the approximate solution of Hammitt and Murthy shows the best agreement with the exact numerical solutions and is thus included in the APAS production version of the HABP code. Author

N90-15891*# Old Dominion Univ., Norfolk, VA. Dept. of Mechanical Engineering and Mechanics.
APPLICATION OF LAGRANGIAN BLENDING FUNCTIONS FOR GRID GENERATION AROUND AIRPLANE GEOMETRIES Final Report, period ended 30 Sep. 1989
Jamshid S. Abolhassani, Ideen Sadrehaghighi, and Surendra N. Tiwari Feb. 1990 29 p
(Contract NAS1-18584)
(NASA-CR-186318; NAS 1.26:186318) Avail: NTIS HC A03/MF A01 CSCL 01A

A simple procedure was developed and applied for the grid generation around an airplane geometry. This approach is based on a transfinite interpolation with Lagrangian interpolation for the blending functions. A monotonic rational quadratic spline interpolation was employed for the grid distributions. Author

N90-15892*# National Aeronautics and Space Administration. Langley Research Center, Hampton, VA.
PERSONAL COMPUTER STUDY OF FINITE-DIFFERENCE METHODS FOR THE TRANSONIC SMALL DISTURBANCE EQUATION
Samuel R. Bland Dec. 1989 19 p Presented at the 3rd International Congress of Fluid Mechanics, Cairo, Egypt, 2-4 Jan. 1990
(NASA-TM-102582; NAS 1.15:102582) Avail: NTIS HC A03/MF A01 CSCL 01A

Calculation of unsteady flow phenomena requires careful attention to the numerical treatment of the governing partial differential equations. The personal computer provides a convenient and useful tool for the development of meshes, algorithms, and boundary conditions needed to provide time accurate solution of these equations. The one-dimensional equation considered provides a suitable model for the study of wave propagation in the equations of transonic small disturbance potential flow. Numerical results for effects of mesh size, extent, and stretching, time step size, and choice of far-field boundary conditions are presented. Analysis of the discretized model problem supports these numerical results. Guidelines for suitable mesh and time step choices are given. Author

N90-15893*# Institute for Computer Applications in Science and Engineering, Hampton, VA.
EULER AND NAVIER-STOKES COMPUTATIONS FOR TWO-DIMENSIONAL GEOMETRIES USING UNSTRUCTURED MESHES Final Report
D. J. Mavriplis Jan. 1990 31 p Submitted for publication
(Contracts NAS1-18107; NAS1-18605)
(NASA-CR-181977; NAS 1.26:181977; ICASE-90-3) Avail: NTIS HC A03/MF A01 CSCL 01A

A general purpose unstructured mesh solver for steady-state two-dimensional inviscid and viscous flows is described. The efficiency and accuracy of the method are enhanced by the simultaneous use of adaptive meshing and an unstructured multigrid technique. A method for generating highly stretched triangulations in regions of viscous flow is outlined, and a procedure for implementing an algebraic turbulence model on unstructured meshes is described. Results are shown for external and internal inviscid flows and for turbulent viscous flow over a multi-element airfoil configuration. Author

N90-15894*# National Aeronautics and Space Administration. Langley Research Center, Hampton, VA.
STRUCTURAL DYNAMICS DIVISION RESEARCH AND TECHNOLOGY ACCOMPLISHMENTS FOR FY 1989 AND PLANS FOR FY 1990
Jacqueline G. Smith and James E. Gardner Jan. 1990 190 p
(NASA-TM-101683; NAS 1.15:101683) Avail: NTIS HC A09/MF A01 CSCL 01A

The purpose is to present the Structural Dynamics Division's research accomplishments for FY 1989 and research plans for FY 1990. The work under each Branch (technical area) is described in terms of highlights of accomplishments during the past year and highlights of plans for the current year as they relate to five year plans for each technical area. This information will be useful in program coordination with other government organizations and industry in areas of mutual interest. Author

N90-16252# Deutsche Forschungs- und Versuchsanstalt fuer Luft- und Raumfahrt, Brunswick (Germany, F.R.). Hauptabteilung Windkanaele.
USE OF THE FILM-OF-OIL TECHNIQUE FOR PROFILE MEASUREMENTS IN THE TRANSONIC WIND TUNNEL BRUNSWICK (TWB) [EINSATZ DER OELANSTRICHTECHNIK BEI PROFILMESSUNGEN IM TRANSSONISCHEN WINDKANAL BRAUNSCHWEIG (TWB)]
W. Puffert-Meissner *In* DGLR, Two-Dimensional Measuring Techniques 1988 p 189-199 In GERMAN (For primary document see N90-16236 08-35)
Avail: NTIS HC A12/MF A02

03 AIR TRANSPORTATION AND SAFETY

Includes passenger and cargo air transport operations; and aircraft accidents.

For related information see also *16 Space Transportation* and *85 Urban Technology and Transportation.*

N90-15895# National Transportation Safety Board, Washington, DC.
AIRCRAFT ACCIDENT REPORT: DELTA AIR LINES, INC., BOEING 727-232, N473DA, DALLAS-FORT WORTH INTERNATIONAL AIRPORT, TEXAS, AUGUST 31, 1988
26 Sep. 1989 137 p
(PB89-910406; NTSB/AAR-89/04) Avail: NTIS HC A07/MF A01 CSCL 01C

The crash of Delta flight 1141 while taking off at the Dallas-Forth Worth, Texas on August 31, 1988 is examined. The safety issues discussed include flightcrew procedures; wake vortices; engine performance; airplane flaps and slats; takeoff warning system; cockpit discipline; airplane rescue and firefighting; emergency evacuation; and survival factors. Recommendations addressing these issues were made to the Federal Aviation Administration, the American Association of Airport Executives, the Airport Operations Council International, and the National Fire Protection Association. Author

N90-15896# Royal Signals and Radar Establishment, Malvern (England).
THE AUTOMATIC DETECTION OF ANTI-COLLISION LIGHTS
Brian A. Wyndham Feb. 1989 19 p Sponsored by Civil Aviation Authority, London, England
(RSRE-Memo-4272; BR110168; ETN-90-96116) Copyright
Avail: NTIS HC A03/MF A01

The techniques for the automatic detection of anti-collision lights, are presented. It is a warning system to be applied in light aircraft and helicopters. Instances of mid-air collisions and near-misses between aircraft at low level emphasize the need for some form of aid to provide earlier visual warning of potentially dangerous situations. The nature of the problem to be overcome, and proposals for the use of a cockpit image sensor and advanced image processing techniques, are described. ESA

N90-15897 Civil Aviation Authority, London (England).
UK AIRMISSES INVOLVING COMMERCIAL AIR TRANSPORT, SEPTEMBER TO DECEMBER 1988
1989 50 p
(ISSN-0951-6301; ETN-90-96148) Copyright Avail: Civil Aviation Authority, Greville House, 37 Gratton Road, Cheltenham, England, 5 sterling pounds

Airmisses in the United Kingdom involving commercial air transport aircrafts, from Sep. - Dec. 1988, are reported. An airmiss is said to occur when a pilot considers that his aircraft may be endangered by the proximity of another aircraft. The following topics are emphasized: the purpose and the investigation of the airmiss reports, the categorization of the airmisses, the involvement of commercial air transport aircrafts, and the relation of airmisses to flying hours. ESA

N90-15898*# National Aeronautics and Space Administration. Ames Research Center, Moffett Field, CA.
PILOTED SIMULATION OF A GROUND-BASED TIME-CONTROL CONCEPT FOR AIR TRAFFIC CONTROL
Thomas J. Davis and Steven M. Green Jun. 1989 11 p Presented at the AIAA American Control Conference, Pittsburgh, PA, Jun. 1989
(NASA-TM-101085; A-89085; NAS 1.15:101085) Avail: NTIS HC A03/MF A01 CSCL 01C

A concept for aiding air traffic controllers in efficiently spacing traffic and meeting scheduled arrival times at a metering fix was developed and tested in a real time simulation. The automation aid, referred to as the ground based 4-D descent advisor (DA), is based on accurate models of aircraft performance and weather conditions. The DA generates suggested clearances, including both top-of-descent-point and speed-profile data, for one or more aircraft in order to achieve specific time or distance separation objectives. The DA algorithm is used by the air traffic controller to resolve conflicts and issue advisories to arrival aircraft. A joint simulation was conducted using a piloted simulator and an advanced concept air traffic control simulation to study the acceptability and accuracy of the DA automation aid from both the pilot's and the air traffic controller's perspectives. The results of the piloted simulation are examined. In the piloted simulation, airline crews executed controller issued descent advisories along standard curved path arrival routes, and were able to achieve an arrival time precision of + or - 20 sec at the metering fix. An analysis of errors generated in turns resulted in further enhancements of the algorithm to improve the predictive accuracy. Evaluations by pilots indicate general support for the concept and provide specific recommendations for improvement. Author

N90-15977*# National Aeronautics and Space Administration. Lyndon B. Johnson Space Center, Houston, TX.
ASSURED CREW RETURN CAPABILITY ARCHITECTURE
J. W. Craig *In* ESA, Crew Safety and Rescue in Space: An International Approach Aug. 1989 p 21-26 (For primary document see N90-15974 08-16)
Copyright Avail: NTIS HC A04/MF A01; ESA Publications Div., ESTEC, Noordwijk, Netherlands, 30 Dutch guilders CSCL 22A

N90-15978# Glavkosmos, Moscow (USSR).
ON THE SELECTION OF CREWMEMBER RESCUE MEANS FOR MANNED SPACE LAUNCH SYSTEMS
G. I. Severin *In* ESA, Crew Safety and Rescue in Space: An International Approach Aug. 1989 p 27-30 (For primary document see N90-15974 08-16)
Copyright Avail: NTIS HC A04/MF A01; ESA Publications Div., ESTEC, Noordwijk, Netherlands, 30 Dutch guilders

04 AIRCRAFT COMMUNICATIONS AND NAVIGATION

Includes digital and voice communication with aircraft; air navigation systems (satellite and ground based); and air traffic control.

For related information see also *17 Space Communications, Spacecraft Communications, Command and Tracking* and *Communications and Radar.*

N90-15899# Advisory Group for Aerospace Research and Development, Neuilly-Sur-Seine (France). Guidance and Control Panel.
ADVANCES IN TECHNIQUES AND TECHNOLOGIES FOR AIR VEHICLE NAVIGATION AND GUIDANCE
Walter M. Hollister (Massachusetts Inst. of Tech., Cambridge.) 1990 13 p Presented at the 48th Guidance and Control Panel Symposium, Lisbon, Portugal, 9-12 May 1989
(AGARD-AR-276; ISBN-92-835-0528-X) Copyright Avail: NTIS HC A03/MF A01; Non-NATO Nationals requests available only from AGARD/Scientific Publications Executive

Papers were presented covering the following topics: terrain reference navigation methods; positioning by image processing or Global Positioning System (GPS); mission and sensor management; new techniques and algorithms; sensor technology; and systems applications. Author

N90-15900# Royal Signals and Radar Establishment, Malvern (England). Software Engineering Section.
THE APPLICATION OF Z TO THE SPECIFICATION OF AIR TRAFFIC CONTROL SYSTEMS. 1: AN INITIAL SPECIFICATION OF THE RADAR PROCESSING ACTIVITY
L. N. Simcox Apr. 1989 60 p Sponsored by Civil Aviation Authority, London, England
(RSRE-Memo-4280; BR111060; ETN-90-96119) Copyright Avail: NTIS HC A04/MF A01

This initial investigation into the formal specification language Z and its applicability to air traffic control systems is described. The software corresponding to the initial radar plot processing in the multi-radar automatic tracking system at the London Air Traffic Control Centre (LATCC) is used. An informal pseudo code description of the radar plot processing function is taken as the requirements and converted into a formal specification in the Z language. The specification is partly validated, using a Royal Signals and Radar Establishment Z syntax and type checking tool. The experiences gained and potential benefits for the Civil Aviation Authority are discussed. ESA

N90-15901# Stuttgart Univ. (Germany, F.R.). Inst. of Geodesy.
GPS NETWORK ANALYSIS: THE INFLUENCE OF STOCHASTIC PRIOR INFORMATION OF ORBITAL ELEMENTS ON GROUND STATION POSITION MEASURES
Wojciech Pachelski, Dariusz Lapucha, and Klaus Budde 1988 113 p Sponsored by Sonderforschungsbereich 228 and IAESTE
(TR-4-1988; ISSN-0933-2839; ETN-90-95862) Avail: NTIS HC A06/MF A01

Factors which might be causes of possible biases and accuracy characteristics of Global Positioning System (GPS) results are investigated. Stochastic prior orbital information on groundstation coordinates and on interstation vector components, distances and distant ratios are investigated. Results of a number of test calculations show influence of stochastic a priori GPS-orbital information on all three types of interstation measures, while station coordinates are weakly estimable following weak data origin definition. The measurements tend to converge at a certain value, and their mean errors became larger. ESA

N90-15927# Messerschmitt-Boelkow-Blohm G.m.b.H., Munich (Germany, F.R.).
NAVIGATION OF AUTONOMOUS AIR VEHICLES BY PASSIVE IMAGING SENSORS
H. Zinner, R. Schmidt, and D. Wolf *In* AGARD, Guidance and Control of Unmanned Air Vehicles Aug. 1989 14 p Sponsored in part by German Ministry of Defence (For primary document see N90-15924 08-08)
Copyright Avail: NTIS HC A09/MF A02; Non-NATO Nationals requests available only from AGARD/Scientific Publications Executive

N90-15928# Aerospatiale, Paris (France). Div. Engins Tactiques.
NAVIGATION UP-DATE USING RADAR MAPPING: ASSESSMENT AND OPTIMISATION SIMULATION TOOL
J. P. Guyvarch *In* AGARD, Guidance and Control of Unmanned Air Vehicles Aug. 1989 11 p In FRENCH (For primary document see N90-15924 08-08)
Copyright Avail: NTIS HC A09/MF A02; Non-NATO Nationals requests available only from AGARD/Scientific Publications Executive

N90-15935# Lockheed Missiles and Space Co., Austin, TX.
NAVIGATION AND GUIDANCE TESTING OF THE LOCKHEED/US ARMY AQUILA REMOTELY PILOTED VEHICLE

Steven L. Ferguson *In* AGARD, Guidance and Control of Unmanned Air Vehicles Aug. 1989 13 p (For primary document see N90-15924 08-08)
Copyright Avail: NTIS HC A09/MF A02; Non-NATO Nationals requests available only from AGARD/Scientific Publications Executive

05 AIRCRAFT DESIGN, TESTING AND PERFORMANCE

Includes aircraft simulation technology.

For related information see also *18 Spacecraft Design, Testing and Performance* and *39 Structural Mechanics*.For land transportation vehicles see *85 Urban Technology and Transportation*.

N90-15902*# National Aeronautics and Space Administration. Langley Research Center, Hampton, VA.
EVALUATION OF TWO TRANSPORT AIRCRAFT AND SEVERAL GROUND TEST VEHICLE FRICTION MEASUREMENTS OBTAINED FOR VARIOUS RUNWAY SURFACE TYPES AND CONDITIONS. A SUMMARY OF TEST RESULTS FROM JOINT FAA/NASA RUNWAY FRICTION PROGRAM
Thomas J. Yager, William A. Vogler (PRC Kentron, Inc., Hampton, VA.), and Paul Baldasare Washington Feb. 1990 301 p (NASA-TP-2917; L-16536; NAS 1.60:2917) Avail: NTIS HC A14/MF A02 CSCL 01C

Tests with specially instrumented NASA Boeing 737 and 727 aircraft together with several different ground friction measuring devices were conducted for a variety of runway surface types and conditions. These tests are part of joint FAA/NASA Aircraft/Ground Vehicle Runway Friction Program aimed at obtaining a better understanding of aircraft ground handling performance under adverse weather conditions and defining relationships between aircraft and ground vehicle tire friction measurements. Aircraft braking performance on dry, wet, snow and ice-covered runway conditions is discussed as well as ground vehicle friction data obtained under similar runway conditions. For a given contaminated runway surface condition, the correlation between ground vehicles and aircraft friction data is identified. The influence of major test parameters on friction measurements such as speed, test tire characteristics, type and amount of surface contaminant, and ambient temperature are discussed. The effect of surface type on wet friction levels is also evaluated from comparative data collected on grooved and ungrooved concrete and asphalt surfaces.
Author

N90-15903 Purdue Univ., West Lafayette, IN.
ANALYTICAL TECHNIQUES FOR TRACKING FILTER IMPLEMENTATION Ph.D. Thesis
Daniel Gleason 1988 203 p
Avail: Univ. Microfilms Order No. DA8911908

Two fundamental shortcomings to currently employed tracking filters are addressed. First, a nonlinear analysis is presented in which a tracking filter that incorporates aircraft orientation in both the system model and measurements is compared to a tracker that uses only standard radar measurements. The addition of the orientation information enhances the tracking filter performance because, in general, aircraft orientation is strongly correlated with the acceleration of the aircraft. Improved position estimation and prediction is demonstrated with the tracking filter that incorporates orientation information. The second fundamental cause of tracking filter errors (i.e., unknown system inputs) is investigated using linear analysis techniques. First, an analysis technique is developed using frequency and time domain methodologies for determining tracking filter gains for a system with unknown exogenous inputs. An analysis technique is also developed to determine the difference in tracking filter error covariance histories using variable structure models. This leads to a means for calculating process noise levels to achieve error covariance equivalent models. In addition, a three state, constant gain discrete tracking filter is investigated to determine filter gain behavior as a function of process and measurement noise levels, and measurement sampling times. A limiting analysis is presented to determine the asymptotic behavior of the filter gains.
Dissert. Abstr.

N90-15904# Advisory Group for Aerospace Research and Development, Neuilly-Sur-Seine (France). Structures and Materials Panel.
FUEL TANK TECHNOLOGY
Nov. 1989 171 p In ENGLISH and FRENCH Meeting held in Ottawa, Ontario, 23-28 Apr. 1989
(AGARD-R-771; ISBN-92-835-0534-4) Copyright Avail: NTIS HC A08/MF A01; Non-NATO Nationals requests available only from AGARD/Scientific Publications Executive

Experiences and information concerning aircraft fuel tank technology, and information concerning current design practices were exchanged and detection and repair of fuel leaks and modification practices to improve fuel tank integrity were discussed. For individual titles, see N90-15905 through N90-15916.

N90-15905# British Aerospace Public Ltd. Co., Kingston-upon-Thames (England).
INTEGRAL FUEL TANK SEALING PRACTICE AT BRITISH AEROSPACE (KINGSTON)
G. N. Sheridan *In* AGARD, Fuel Tank Technology Nov. 1989 7 p (For primary document see N90-15904 08-05)
Copyright Avail: NTIS HC A08/MF A01; Non-NATO Nationals requests available only from AGARD/Scientific Publications Executive

The current integral fuel tank sealing and repair procedures at British Aerospace (Kingston) were reviewed. It describes the materials and processes used in the design and initial manufacture of integral fuel tanks. The methods used for the repair of leaks in integral fuel tanks are described. The need to review the current procedures for use on future aircraft using composite materials is highlighted.
Author

N90-15906# Avions Marcel Dassault, Saint-Cloud (France).
INTEGRAL FUEL TANKS - DESIGN, PRODUCTION, AGING, REPAIR [LES RESERVOIRS DE CARBURANT STRUCTURAUX CONCEPTION, REALISATION, VIEILLISSEMENT, REPARATION]
C. A. Picard *In* AGARD, Fuel Tank Technology Nov. 1989 12 p In FRENCH (For primary document see N90-15904 08-05)
Copyright Avail: NTIS HC A08/MF A01; Non-NATO Nationals requests available only from AGARD/Scientific Publications Executive

The advantages of using integral tanks for aircraft fuel containment are discussed and compared to those of flexible fuel tanks. The design elements of integral tanks that ensure leak-proof characteristics are described including joints, fasteners, and ports. Various types of leakage problems are outlined and repair methods are discussed. Finally, the problem of microbial corrosion is addressed.
Transl. by M.G.

N90-15907# Aeritalia S.p.A., Turin (Italy). Defence Aircraft Group.
AIRCRAFT FUEL TANK CONSTRUCTION AND TESTING EXPERIENCE
Ernesto Liossi and Corrado Bianco *In* AGARD, Fuel Tank Technology Nov. 1989 18 p (For primary document see N90-15904 08-05)
Copyright Avail: NTIS HC A08/MF A01; Non-NATO Nationals requests available only from AGARD/Scientific Publications Executive

The evolution of aircraft structures manufacturing technology has moved the choice of solutions for fuel tanks, from welded sheet metal components to flexible rubber fuel cells up to now when airplanes manufacturers are going to address their choices, toward more extensive adoption of integral fuel tanks. The Aeritalia experience in fuel tanks construction is presented with a short view on flexible fuel tank applications (advantages and

disadvantages) and the technological solutions adopted for integral fuel tanks constuction and performances quality assurance. The integral fuel tanks are designed as primary structures to sustain high loads, therefore the critical target is to obtain a leak proof structure and to guarantee no leakage for the aircraft service-life.
Author

N90-15908# Royal Air Force, Dereham (England).
THE REPAIR OF AIRCRAFT INTEGRAL FUEL TANKS IN THE RAF: A USER'S VIEW OF FUEL TANK TECHNOLOGY
G. Dawson *In* AGARD, Fuel Tank Technology Nov. 1989 8 p (For primary document see N90-15904 08-05)
Copyright Avail: NTIS HC A08/MF A01; Non-NATO Nationals requests available only from AGARD/Scientific Publications Executive

The sealing and repair of aircraft fuel tanks was a thorn in the side of aircraft maintenance personnel for a considerable number of years. In the Royal Air Force in particular, repairing and resealing integral fuel tanks was always difficult and has frequently required several attempts to achieve an acceptable seal. In justifying this repair expenditure, it would be easy to conclude that all problems resulted from poor design, ineffective sealants, poor information or even bad weather. However, although all of these factors play a part in repair procedures, some problems were generated for ourselves, and these require considerable commitment on the part of the managers to resolve. Some progress was already made in resolving the more critical of the problems, and the success rate in effective, long-term repairs has begun to improve. However, it is expected that the process of gradual improvement will continue for the foreseeable future. In order to achieve this improvement, a number of areas of concern were summarized, beginning with background to fuel tank repair in the RAF, and including Health and Safety problems, leak testing, tank venting, surface preparation and resealing. In each area both equipment and procedures are being continually improved in order to reduce aircraft downtime and improve repair effectiveness at all depths of maintenance. Finally, the problems generated by aircraft design, and in particular access provided to integral fuel tanks are examined. As in the other areas, we have identified problems and suggested improvements for future aircraft as well as highlighting the reliability and maintainability implications of poor design. The problems faced by Royal Air Force maintenance engineers in repairing aircraft integral fuel tanks are documented.
Author

N90-15909# Royal Aircraft Establishment, Farnborough (England). Materials and Structures Dept.
THE EFFECT OF PRIMER AGE ON ADHESION OF POLYSULPHIDE SEALANT **c27**
S. P. Wilford and J. Day *In* AGARD, Fuel Tank Technology Nov. 1989 7 p (For primary document see N90-15904 08-05)
Copyright Avail: NTIS HC A08/MF A01; Non-NATO Nationals requests available only from AGARD/Scientific Publications Executive

Sealants used in aircraft integral fuel tanks must adhere well to primed substrate surfaces. The adhesion of polysulphide sealant (PR1422) to primed aluminum alloy surfaces of different primer age was studied with respect to the effect on lap-shear strength of ageing in fuel at 100 C. Freshly primed surfaces, 1 day old, were compared with a range of older primed surfaces. With a standard epoxy chromate primer, primer age has a very marked effect on lap-shear strength, the value after 10 days in fuel (Avtur) at 100 C being a factor of 2 less for 2 to 20 week old primed specimens as compared to a freshly primed one. In contrast, similar studies using three tolerant epoxy chromate primers indicate that primer age has much less effect on the adhesion of PR1422 sealant to these primers, lap shear strengths after ageing in fuel at 100 C showing much less dependence on primer age. These results would appear to be very relevant to both repair and manufacture of integral fuel tanks.
Author

N90-15910# Products Research and Chemical Corp., Glendale, CA. Aerospace Div.
IMPROVED PERFORMANCE POLYSULFIDE BASED SEALANT **c27**
Ahmed Sharaby *In* AGARD, Fuel Tank Technology Nov. 1989 9 p (For primary document see N90-15904 08-05)
Copyright Avail: NTIS HC A08/MF A01; Non-NATO Nationals requests available only from AGARD/Scientific Publications Executive

It was recently discovered that low viscosity mercaptan terminated polymers which exhibit application and performance properties superior to their precursor materials can be obtained by chemical modification of Thiokol LP polymers. For example, these chemically modified Thioko! LP polymers, known as Permapol P-5 polymers, can be formulated and cured using similar methods as LP polymers to give elastomeric materials which, compared to the same LP polymer based materials, exhibit: superior ozone and UV radiation resistance; higher physical properties; better fuel resistance; higher temperature resistance; greater compatibility with traditional plasticizers; better adhesion to many substrates after exposure to liquids such as aromatic hydrocarbon containing fuels; and better resistance to permeability of inert gases and fuel vapors. The properties and uses, of this new class of polymers, in some sealant formulations are described as compared to their precursor materials, the Thiokol LP polymer.
Author

N90-15911# Products Research and Chemical Corp., Glendale, CA.
FUEL RESISTANT COATINGS FOR METAL AND COMPOSITE FUEL TANKS **c27**
Santo Randazzo *In* AGARD, Fuel Tank Technology Nov. 1989 20 p (For primary document see N90-15904 08-05)
Copyright Avail: NTIS HC A08/MF A01; Non-NATO Nationals requests available only from AGARD/Scientific Publications Executive

Coating systems based on fuel resistant polythioether polyurethane polymers were developed. These systems are formulated to provide a secondary seal and thereby protect the interior of composite fuel tanks. In addition to fuel resistance the systems have excellent physical properties, low specific gravity and prevent fuel leakage even after severe impact damage to the composite tank. Reduction of mechanical damage, prevention of water penetration into the composite, and prevention of leakage through composite imperfections are other desirable properties of these coatings. Data are presented showing the fuel resistance and hydrolytic stability of these new materials. The retention of physical properties is tabulated after prolonged environmental exposure to fuel and water. Impact damage data on coated composites and metal is presented using different energy levels of impact and various thicknesses of coating. The effectiveness of these coatings in sealing composite tanks, both before and after impact damage, is demonstrated. Fuel and water permeability data are presented. Rapid cure characteristics are also illustrated making these coatings of particular value for production lines. Coating procedures for sealing disposable or integral fuel tanks without use of faying surface sealants are discussed. Results on adhesion to metals, composites and conventional aerospace sealants are presented. Ease of repair, surface preparation and product application are also discussed when sealing simple or complex fuel tanks. The chemistry of polythioether polyurethane polymers is also discussed and compared to conventional polyurethane materials, illustrating how these new coatings provide a new dimension in aircraft sealing technology.
Author

N90-15912# Air Force Wright Aeronautical Labs., Wright-Patterson AFB, OH.
SPRAY SEALING: A BREAKTHROUGH IN INTEGRAL FUEL TANK SEALING TECHNOLOGY **c31**
Martin D. Richardson and J. H. Zadarnowski (McDonnell Aircraft Co., Saint Louis, MO.) *In* AGARD, Fuel Tank Technology Nov. 1989 12 p (For primary document see N90-15904 08-05)
Copyright Avail: NTIS HC A08/MF A01; Non-NATO Nationals

requests available only from AGARD/Scientific Publications Executive

In a continuing effort to increase readiness, a new approach to sealing integral fuel tanks is being developed. The technique seals potential leak sources by spraying elastomeric materials inside the tank cavity. Laboratory evaluations project an increase in aircraft supportability and reliability, an improved maintainability, decreasing acquisition and life cycle costs. Increased usable fuel volume and lower weight than conventional bladders improve performance. Concept feasibility was demonstrated on sub-scale aircraft fuel tanks. Materials were selected by testing sprayable elastomers in a fuel tank environment. Chemical stability, mechanical properties, and dynamic durability of the elastomer are being evaluated at the laboratory level and in sub-scale and full scale aircraft component fatigue tests. The self sealing capability of sprayable materials is also under development. Ballistic tests show an improved aircraft survivability, due in part to the elastomer's mechanical properties and its ability to damp vibrations. New application equipment, system removal, and repair methods are being investigated. Author

N90-15913# Messerschmitt-Boelkow-Blohm G.m.b.H., Munich (Germany, F.R.). Military Aircraft Div.

DESIGN PHILOSOPHY AND CONSTRUCTION TECHNIQUES FOR INTEGRAL FUSELAGE FUEL TANKS

G. Kagerbauer, M. Voglsinger, and L. Lemmer *In* AGARD, Fuel Tank Technology Nov. 1989 20 p (For primary document see N90-15904 08-05)

Copyright Avail: NTIS HC A08/MF A01; Non-NATO Nationals requests available only from AGARD/Scientific Publications Executive

The fuel tanks of modern military aircraft are designed as integral fuel tanks. The design features and sealing systems which were adopted for integral fuselage fuel tanks, to satisfy the requirement for tightness during the entire service life, are presented. The design aim was to minimize penetrations into the fuel compartments and to reduce the probability of fuel leaks by the application of redundant sealing barriers. The adopted sealing systems for the sealing of internal metallic substructure, and to an outer CFRP skin are described. Selected sealing systems were tested in a representative sideskin test box in fatigue and the experience gained was introduced into the design of a fuselage sealing box to aircraft standard which was also tested in fatigue. The representative fuel tank structure of the sealing box was used to demonstrate accessability for repair and to proof that repair actions to the sealing system are possible with suitable equipment. Author

N90-15914# Lockheed Aeronautical Systems Co., Marietta, GA.

FUEL TANK EXPLOSION PROTECTION

M. E. Borders, G. E. Knowles, D. E. Meadows, C. C. Randall, T. F. Christian, Jr., and T. M. Jennings (Warner Robins Air Logistics Center, Robins AFB, GA.) *In* AGARD, Fuel Tank Technology Nov. 1989 17 p (For primary document see N90-15904 08-05)

Copyright Avail: NTIS HC A08/MF A01; Non-NATO Nationals requests available only from AGARD/Scientific Publications Executive

The modernization of military aircraft has included the addition of fuel tank fire/explosion protection. A military transport, like any other aircraft, is susceptible to fuel tank explosions from a number of sources, including combat gunfire. Studies have shown that the fuel tanks are the largest single contributor to the vulnerability from high explosive incendiary (HEI) rounds for transport aircraft. Since no aircraft has the inherent capability to suppress flames within the fuel tank ullage, it is important to provide a tank explosion protection system that prevents fires and explosions inside the fuel tanks during all modes of aircraft operation. The Lockheed Aeronautical Systems Company and the United States Air Force have acquired considerable knowledge about explosive suppressant foam through its use in the Lockheed-built C-130 aircraft. This foam material prevents or limits flame and pressure wave propagation and acts as an anti-slosh baffle. In-service experience with the foam is discussed. Associated maintenance problems and impacts on man-hours, weight, and cost is also reviewed. The status of the new foam materials being developed to eliminate electrostatic problems with the present explosion suppressant foam will be stated and assessed. Alternative techniques and methods to achieve fuel tank explosion protection were proposed for the C-130 and will be compared to the performance of the foam installation. Finally, explosion suppression is put into perspective with other C-130 wing modernization features. Author

N90-15915# McDonnell Aircraft Co., Saint Louis, MO. Structural Dynamics Dept.

A DYNAMICIST'S VIEW OF FUEL TANK SKIN DURABILITY

M. A. Ferman, M. D. Healey, W. H. Unger, and Martin D. Richardson (Air Force Wright Aeronautical Labs., Wright-Patterson AFB, OH.) *In* AGARD, Fuel Tank Technology Nov. 1989 17 p (For primary document see N90-15904 08-05)

Copyright Avail: NTIS HC A08/MF A01; Non-NATO Nationals requests available only from AGARD/Scientific Publications Executive

Widespread leakage of fuel tanks in military aircraft is believed to be aggravated by small cracks induced by premature fatigue of skins from fluid structure interaction loading and dynamics. A developing method is shown that will help improve designs to avoid this recently recognized problem. The technique treats flat panels, curved panels, and stiffened panels. Parallel panels configured as sides or top and bottom pairs are included. Panels of a representative fuel tank section of typical aircraft construction were analyzed, tested, and are included. This method was under steady and careful development for a number of years so that high confidence would be established at each step. A well balanced analytical and experimental approach was taken. It is now mature and ready for full scale application. Author

N90-15916# Air Force Wright Research and Development Center, Wright-Patterson AFB, OH.

INTEGRAL FUEL TANK CERTIFICATION AND TEST METHODS

Martin D. Richardson *In* AGARD, Fuel Tank Technology Nov. 1989 13 p (For primary document see N90-15904 08-05)

Copyright Avail: NTIS HC A08/MF A01; Non-NATO Nationals requests available only from AGARD/Scientific Publications Executive

Fuel tanks make up a significant structural volume of present aircraft designs. Life cycle costs and the repair of fuel tank leaks are significant. The efforts accomplished, and now in progress, to develop methods to certify the fuel containment integrity of future USAF aircraft are described. The methods use the idea of combining the aircraft structural durability testing requirements with a fuel tank certification requirement. The application of this concept during the development phase of a new aircraft design will enable deficiencies in fuel tank sealing designs to be discovered early, before production begins. The work accomplished to date using C-130 wing fuel tank components, has shown that this approach is possible and does provide valid results. The requirement to employ environmental exposures, including the use of actual jet fuels, and not water or simulants, is emphasized. Author

N90-15917# Royal Aerospace Establishment, Farnborough (England).

THE DEVELOPMENT OF A LOW COST DATA LOGGING SYSTEM FOR FLIGHT TRIALS BASED ON AN IBM COMPATIBLE PC

A. P. Manning Jan. 1989 24 p

(RAE-TM-FM-16; BR110742; ETN-90-96130) Copyright Avail: NTIS HC A03/MF A01

The development of a data logging system based on an IBM compatible Personal Computer (PC), is described. It is extended to both the airborne and ground based data recording capabilities. The new system supplements the existing Modular Data Acquisition System (MODAS) fitted to the research aircraft. The compatibility with existing recovery and plotting systems, is maintained. It

provides a portable record/replay capability and allows operations remote from base with immediate access to data, currently between sorties and potentially between runs in a sortie. ESA

N90-15930# Lockheed Missiles and Space Co., Austin, TX.
UNMANNED AIR VEHICLES PAYLOADS AND SENSORS
Grover S. Amick *In* AGARD, Guidance and Control of Unmanned Air Vehicles Aug. 1989 18 p (For primary document see N90-15924 08-08)
Copyright Avail: NTIS HC A09/MF A02; Non-NATO Nationals requests available only from AGARD/Scientific Publications Executive

N90-15931# Lockheed Missiles and Space Co., Austin, TX.
AUTOMATED SEARCH TECHNIQUES APPLIED TO OPTICAL PAYLOADS IN UNMANNED AIR VEHICLES
Robert L. Moody and James L. Thompson *In* AGARD, Guidance and Control of Unmanned Air Vehicles Aug. 1989 7 p (For primary document see N90-15924 08-08)
Copyright Avail: NTIS HC A09/MF A02; Non-NATO Nationals requests available only from AGARD/Scientific Publications Executive

N90-15932# Merit Technology, Inc., Plano, TX.
AN INTELLIGENCE-DRIVEN RPV MISSION PLANNER
Klaus Dannenberg, Mel Barney, and Chuck Kirklen *In* AGARD, Guidance and Control of Unmanned Air Vehicles Aug. 1989 8 p (For primary document see N90-15924 08-08)
Copyright Avail: NTIS HC A09/MF A02; Non-NATO Nationals requests available only from AGARD/Scientific Publications Executive

N90-15933# Lockheed Missiles and Space Co., Austin, TX.
DISTRIBUTION OF HARDWARE AND SOFTWARE ELEMENTS IN UNMANNED AIR VEHICLE SYSTEMS
Larry D. Sauvain *In* AGARD, Guidance and Control of Unmanned Air Vehicles Aug. 1989 10 p (For primary document see N90-15924 08-08)
Copyright Avail: NTIS HC A09/MF A02; Non-NATO Nationals requests available only from AGARD/Scientific Publications Executive

N90-15934# British Aerospace Public Ltd. Co., Lancashire (England). Military Aircraft Div.
TECHNOLOGY AND EVALUATION OF UNMANNED AIR VEHICLES
George R. Seyfang *In* AGARD, Guidance and Control of Unmanned Air Vehicles Aug. 1989 5 p (For primary document see N90-15924 08-08)
Copyright Avail: NTIS HC A09/MF A02; Non-NATO Nationals requests available only from AGARD/Scientific Publications Executive

06 AIRCRAFT INSTRUMENTATION

Includes cockpit and cabin display devices; and flight instruments.

For related information see also *19 Spacecraft Instrumentation* and *35 Instrumentation and Photography.*

No abstracts in this category.

07 AIRCRAFT PROPULSION AND POWER

Includes prime propulsion systems and systems components, e.g., gas turbine engines and compressors; and onboard auxilliary power plants for aircraft.

For related information see also *20 Spacecraft Propulsion and Power, 28 Propellants and Fuels,* and *44 Energy Production and Conversion.*

N90-15918# Department of the Air Force, Washington, DC.
EXTERNALLY VAPORIZING SYSTEM FOR TURBINE COMBUSTOR Patent
Clifford C. Gleason, inventor (to AF) and Edward E. Ekstedt, inventor (to AF) 13 Jun. 1989 5 p Filed 10 Sep. 1986 Supersedes US-Patent-Appl-SN-905439
(AD-D014284; US-Patent-4,838,029; US-Patent-Appl-SN-905439) Avail: US Patent and Trademark Office CSCL 21/5

The present invention relates to turbine engines, and, in particular, relates to a combustor therein. The present invention is directed toward providing a combustor in which the undesirable characteristics of prior liquid fuel systems are overcome in light of the advantages of a purely gaseous system. The externally vaporizing system of the present invention incorporates an auxiliary burner which is supplied with compressor discharge air at a rate which is regulated to the main fuel flow rate. The auxiliary burner is operated at approximately stoichiometric fuel-air-ratio, in order to provide very-hot, nearly-inert gases for vaporizing the main fuel supply. The main fuel is sprayed in the auxiliary burner exit gas stream where rapid mixing and evaporation occur. The resulting vaporized fuel/inert gas mixture (at about 800 F, preferably) is then ducted and distributed to the individual main combustor fuel injectors where it is injected into the premixing ducts. GRA

N90-15919# Royal Aerospace Establishment, Farnborough (England).
PERFORMANCE OF A HIGHLY-LOADED HP COMPRESSOR
W. J. Calvert, R. B. Ginder, I. R. I. McKenzie, and D. J. Way Feb. 1989 11 p Presented at the 34th International Gas Turbine and Aeroengine Congress and Exposition, Toronto, Ontario, 5-8 Jun. 1989
(RAE-TM-P-1149; BR110401; ETN-90-96126) Copyright Avail: NTIS HC A03/MF A01

A 4 stage axial research compressor, representative of the rearmost stages of a highly loaded military or civil compression system, is designed and tested. It is a large scale compressor, with extended inter-row gaps, to facilitate the acquisition of detailed aerodynamic data. Its design pressure ratio is exceeded by a factor of 4.0, and a peak polytropic efficiency at design speed of 89 percent is obtained. The flow profiles obtained from area traversing at stator exits are presented and discussed. The performance is measured and an inviscid-viscous blade-to-blade method, is incorporated. ESA

N90-15920# Royal Aerospace Establishment, Farnborough (England). Propulsion Dept.
AERODYNAMIC AND HEAT TRANSFER MEASUREMENTS ON BLADING FOR A HIGH RIM-SPEED TRANSONIC TURBINE
R. C. Kingcombe, S. P. Harasgama, N. P. Leversuch, and E. T. Wedlake Mar. 1989 11 p Presented at the 34th ASME International Gas Turbine and Aeroengine Congress, Toronto, Ontario, 5-8 Jun. 1989
(RAE-TM-P-1151; BR110400; ETN-90-96127) Copyright Avail: NTIS HC A03/MF A01

A high rim speed turbine incorporating 3-D features is designed and tested. The cold flow turbine testing, with performance measurements, rotor exit traversing and surface static pressure measurements on the vane and rotor, is performed. The vane is tested in annular cascade on the isentropic light piston cascade. Surface heat transfer measurements on the vanes and endwalls and aerodynamic information are given. The data is compared with design predictions and the reasons for the differences observed are explored. ESA

N90-15921 Royal Aerospace Establishment, Farnborough (England).
CYCLE ANALYSIS FOR HELICOPTER GAS TURBINE ENGINES
A. D. Bewley Apr. 1989 12 p Presented at the 34th ASME International Gas Turbine and Aeroengine Congress and Exposition, Toronto, Ontario, 5-8 Jun. 1989
(RAE-TM-P-1154; BR110402; ETN-90-96128) Copyright Avail: NTIS HC A03/MF A01

The performance potential of a 1000 kW gas turbine engine is determined in terms of specific fuel consumption and specific power. Compressor and turbine efficiencies are assumed size dependent. The cycle temperature is determined from the material capability and cooling technology available. Heat exchanger cycle engines for helicopters are considered. As cycle temperatures increase, a low pressure ratio engine with a single stage gas generator turbine provides the most cost effective solution. The heat exchanger cycle is attractive only for those helicopter missions where endurance or fuel conservaton is the dominating requirement. ESA

N90-15922# Royal Aerospace Establishment, Farnborough (England).
A UK PERSPECTIVE ON THE UNIFORM ENGINE TEST PROGRAMME
M. Holmes, A. R. Osborn, and J. C. Ascough Jun. 1989 26 p Presented at the 1989 European Propulsion Forum on Modern Techniques and Developments in Engine and Component Testing, Bath, England, 19-21 Apr. 1989; sponsored by the Royal Aeronautical Society, AAAF, and DGLR
(RAE-TM-P-1172; BR110949; ETN-90-96129) Copyright Avail: NTIS HC A03/MF A01

The uniform engine test program and the test results are given. The program provides the opportunity for aeroengine test facilities in Europe and North America for the evaluation of the test procedures and methods of analysis. It is achieved by testing the same engines over an agreed range of operating conditions. Nozzle coefficients are used as a basis for comparing gross thrust and airflow measurements. The differences in some of the other performance parameters are compared with the predicted precision and bias errors. ESA

N90-15923*# National Aeronautics and Space Administration. Lewis Research Center, Cleveland, OH.
ASSESSMENT OF WORM GEARING FOR HELICOPTER TRANSMISSIONS
Lev Chaiko Jan. 1990 16 p Prepared in cooperation with Army Aviation Systems Command, Cleveland, OH
(DA Proj. 1L1-61102-AH-45)
(NASA-TM-102441; E-5212; NAS 1.15:102441; AVSCOM-TM-89-C-010) Avail: NTIS HC A03/MF A01 CSCL 13I

A high-efficiency hydrostatic worm gear drive for helicopter transmissions is assessed. The example given is for a large cargo helicopter with three 4000-kW engines and transmission reduction ratio of 110. Also contained are: an efficiency calculation, a description of the test stand for evaluating the feasibility of worm gear hydrostatic mesh, a weight calculation, and a comparison with conventional helicopter transmissions of the same power and transmission reduction ratio. Author

08 AIRCRAFT STABILITY AND CONTROL

Includes aircraft handling qualities; piloting; flight controls; and autopilots.

For related information see also *05 Aircraft Design, Testing and Performance.*

N90-15924# Advisory Group for Aerospace Research and Development, Neuilly-Sur-Seine (France). Guidance and Control Panel.
GUIDANCE AND CONTROL OF UNMANNED AIR VEHICLES
Aug. 1989 191 p In ENGLISH and FRENCH Symposium held in San Francisco, CA, 4-7 Oct. 1988
(AGARD-CP-436; ISBN-92-835-0523-9) Copyright Avail: NTIS HC A09/MF A02; Non-NATO Nationals requests available only from AGARD/Scientific Publications Executive

The following topics were discussed: operational concepts, requirements and systems, vehicle guidance and control, optical systems, systems external to the vehicle, and evaluation and test. For individual titles, see N90-15925 through N90-15935.

N90-15925# Ecole Nationale de l'Aeronautique et de l'Espace, Toulouse (France).
SYNTHESIS OF CONTROL LAW, ON A RPV, IN ORDER TO MINIMIZE THE NUMBER OF SENSORS
Jean-Luc Boiffier *In* AGARD, Guidance and Control of Unmanned Air Vehicles Aug. 1989 17 p Sponsored by ENSAE and Centre d'Etudes et de Recherche, Toulouse, France (For primary document see N90-15924 08-08)
Copyright Avail: NTIS HC A09/MF A02; Non-NATO Nationals requests available only from AGARD/Scientific Publications Executive

Two 25 kg Remotely Piloted Vehicles (RPVs) were built and the capabilities in flight were demonstrated. This RPV is equipped with a digital computer which enables the plane to be under automatic control for a sea skimmer flight. A 50 kg RPV project, with a 20 kg payload under 300 W, for a flight of 2500 m high and 6 hour flying time is now being developed. The first flight is planned for 1990. These specifications need to pay special attention to the weights. One kilo represents 15 percent of the performance. The airplane configuration was optimized to minimize the weights of the airframe and fuel. Optimal wing area, aspect ratio, area ratio between front and rear lifting surfaces, were found. The avionic systems were treated with the same effort. In particular, control laws were studied in order to reduce the number of sensors needed to control and guide the plane. A method is described for avoiding the installation of a vertical gyroscope, which is a heavy sensor, for this kind of RPV. The lighter the plane is, the more this proposition is interesting. The plane and turbulence are described, and the automatic lateral control is presented. The following topics are approached: adjustment of the natural mode of the plane in order to reduce the sensitivity of the plane under the effect of turbulence, basic control law by LQ method, installation of wash-out filters on the measurement to avoid drift sensors effect, optimization of the wash-out frequency, and general performances with and without bank and heading angle measurement. Author

N90-15926# METEOR Costruzioni Aeronautiche ed Elettroniche S.p.A., Ronchi dei Legionari (Italy).
MIRACH 100 FLIGHT CONTROL SYSTEM
Anes Sbuelz *In* AGARD, Guidance and Control of Unmanned Air Vehicles Aug. 1989 17 p (For primary document see N90-15924 08-08)
Copyright Avail: NTIS HC A09/MF A02; Non-NATO Nationals requests available only from AGARD/Scientific Publications Executive

The Mirach 100 air-vehicle is a multipurpose RPV-UMA, suited to intelligence missions of target recognition, acquisition, and identification up to 150 km. It is a high-subsonic speed, jet-powered drone having a ceiling altitude of 9000 m and 1 hour endurance. Different arrangements of the base air-vehicle allow higher altitudes

or wider endurances according to the mission operational requirements. The flight control system of the Mirach 100 is mainly a compound of already tested in flight components. Autopilot function includes a full control system of stabilization on two axes, simply designed to improve reliability and safety of guidance. Mechanization is based on a simple analogic control circuit of the actuators that drive the control surfaces of the aircraft, stabilized through the vertical gyroscope feed-back; the gyroscope is installed in the air-vehicle fore structure. Guidance function includes a complete control system based on altitude, heading and velocity integrated in the flight controller which runs the whole aircraft, pay load included. Navigation function is based on a OMEGA/VLF receiver and navigator, suited to memorize a flight plan formed with up to 99 geographical points sequentially navigated, starting from any of it. From the computation a wind parameter is estimated which includes the on-board sensor errors, giving improved navigation performances even when the omega-receiver operates in marginal conditions. The drone is guided to follow the programmed flight plan. Complete avionics and aircraft itself were modeled on a computer for dynamic and static stability analysis and performance computations; the results obtained were compared with those recorded during the Mirach 100 test flights performed at the experimental range Salto di Quirra in Sardinia. Test flights gave excellent results about steering, guidance and navigation. The altitude and speed control were obtained with an accuracy that went far beyond the expectations, reaching the accuracy level of the sensor used in the testing program. Author

N90-15927# Messerschmitt-Boelkow-Blohm G.m.b.H., Munich (Germany, F.R.).

NAVIGATION OF AUTONOMOUS AIR VEHICLES BY PASSIVE IMAGING SENSORS **c04**

H. Zinner, R. Schmidt, and D. Wolf *In* AGARD, Guidance and Control of Unmanned Air Vehicles Aug. 1989 14 p Sponsored in part by German Ministry of Defence (For primary document see N90-15924 08-08)

Copyright Avail: NTIS HC A09/MF A02; Non-NATO Nationals requests available only from AGARD/Scientific Publications Executive

Navigation systems of autonomous vehicles must provide information that enables the control of flight and information about the environment that allows for the perception of the 3-D scene. Passive imaging sensors with the appropriate algorithms can supply both types of information. A concept is presented that evaluates the optical flow field across the image plane in order to derive the quantities necessary for the guidance and control of the vehicle. The quality of information processing is improved by incorporating knowledge of the environment and the dynamics of the vehicle. In various computer simulations, the performance of an observer is compared with an Extended Kalman Filter. The concept is applied to two kinds of unmanned vehicles: to an autonomous unpropelled submunition, which has to detect, to classify, and to track ground vehicles, and to the fiber-optic guided missile that serves as a testbed towards systems of higher autonomy. Author

N90-15928# Aerospatiale, Paris (France). Div. Engins Tactiques.

NAVIGATION UP-DATE USING RADAR MAPPING: ASSESSMENT AND OPTIMISATION SIMULATION TOOL **c04**

J. P. Guyvarch *In* AGARD, Guidance and Control of Unmanned Air Vehicles Aug. 1989 11 p In FRENCH (For primary document see N90-15924 08-08)

Copyright Avail: NTIS HC A09/MF A02; Non-NATO Nationals requests available only from AGARD/Scientific Publications Executive

The idea of an air-to-ground missile, fired from a safe distance and having all-weather capabilities, is a suitable strategy for the aerial attack of terrestrial targets. The guidance precision required exceeds the capabilities of an inertial system alone. The missile would also be equipped with a millimeter-wave radar sensor that permits localization through cartography. This principle implies that trajectory selection be made at the time of mission preparation and provisional maps be incorporated into the memory of the missile before firing. In order to estimate the probability of mission success and aid in the making of provisional maps, a method for the numerical simulation of the entire system was developed. The simulation is validated and progressively enhanced with actual data obtained in the course of sensor experimentation.

Transl. by M.G.

N90-15929# Ferranti Defence Systems Ltd., Edinburgh (Scotland). Dept. of Electro-Optics.

ELECTRO-OPTIC SENSORS FOR SURVEILLANCE AND TARGET ACQUISITION **c74**

J. W. Jack and A. Houston *In* AGARD, Guidance and Control of Unmanned Air Vehicles Aug. 1989 20 p (For primary document see N90-15924 08-08)

Copyright Avail: NTIS HC A09/MF A02; Non-NATO Nationals requests available only from AGARD/Scientific Publications Executive

The synthesis of a compact electro-optical payload suitable for tactical reconnaissance, target spotting and fire control is described. The selection criteria for the electro-optical sensors comprizing an imaging sensor, lens, and laser are discussed and the performance of an actual system is predicted. The predicted performance is compared with the results of flight trials in which an equipment was used to acquire, range and designate ground targets. Finally the experience of using the equipment against ground targets in collaboration with fixed wing aircraft is discussed. Author

N90-15930# Lockheed Missiles and Space Co., Austin, TX.

UNMANNED AIR VEHICLES PAYLOADS AND SENSORS **c05**

Grover S. Amick *In* AGARD, Guidance and Control of Unmanned Air Vehicles Aug. 1989 18 p (For primary document see N90-15924 08-08)

Copyright Avail: NTIS HC A09/MF A02; Non-NATO Nationals requests available only from AGARD/Scientific Publications Executive

The Lockheed Corporation developed a family of payload sensors for use in unmanned air vehicle applications. The program was initially conceived as an extension of the U.S. Army Aquila Remotely Piloted Vehicle (RPV) Program and is applicable to a much wider variety of uses and applications. The design concept utilized a universal gimbal platform with interchangeable sensor spheres. The concept and implementation process was directed to develop a low-cost sensor system which could easily accommodate new sensors as they become available. The system has been developed and demonstrated using the Lockheed Altair UAV system and is available for use. A family of seven sensor types were successfully demonstrated, and others are in development. The system is known as the Lockheed Adaptive Modular Payload System (LAMPS). Author

N90-15931# Lockheed Missiles and Space Co., Austin, TX.

AUTOMATED SEARCH TECHNIQUES APPLIED TO OPTICAL PAYLOADS IN UNMANNED AIR VEHICLES **c05**

Robert L. Moody and James L. Thompson *In* AGARD, Guidance and Control of Unmanned Air Vehicles Aug. 1989 7 p (For primary document see N90-15924 08-08)

Copyright Avail: NTIS HC A09/MF A02; Non-NATO Nationals requests available only from AGARD/Scientific Publications Executive

The missions of the U.S. Army Aquila Remotely Piloted Vehicle (RPV) system include reconnaissance and target acquisition. To aid the operator in the accomplishment of these missions, Lockheed has developed automated target search software which ensures a thorough, systematic search of a designated area and reduces the operator workload while the search is being conducted. Various factors, internal and external to the unmanned air vehicle (UAV) system, are discussed which affect the probability of detecting a target of military interest. Search parameters were implemented within the software to optimize the capabilities of the Aquila System to detect targets under varying environmental conditions. The automated search algorithm (autosearch) was

successfully demonstrated in flights conducted by the Army in a Force Development Test and Experimentation (FDT and E).
Author

N90-15932# Merit Technology, Inc., Plano, TX.
AN INTELLIGENCE-DRIVEN RPV MISSION PLANNER **c05**
Klaus Dannenberg, Mel Barney, and Chuck Kirklen *In* AGARD, Guidance and Control of Unmanned Air Vehicles Aug. 1989 8 p (For primary document see N90-15924 08-08)
Copyright Avail: NTIS HC A09/MF A02; Non-NATO Nationals requests available only from AGARD/Scientific Publications Executive

The time required to plan Remotely Piloted Vehicles (RPV) missions can be greatly reduced by the application of technology currently available. Additionally, the effectiveness of these missions can be increased significantly. The application of expert system based processing of near real time intelligence, route planning techniques, and high resolution graphics to the RPV mission planning process can result in an integrated planning aid that accomplishes both a savings in planning time and an increase in mission effectiveness. Expertise in RPV mission planning is acquired by the repetitive performance of planning and observing actual RPV missions. The requirements for these systems are driven by mission requirements, and are often heavily derived from the tools available. The new tools suggested will have a significant impact on the planning process. The development of the system suggested will require participation by these experts. The most time consuming part of an RPV mission planning exercise is the collection and assimilation of relevant intelligence data. These data include enemy threat tactical, communication, and situation data, as well as friendly tactical, communication, and situation data. A system that collects and filters these data was demonstrated. The heart of this system, the Intelligence-Driven Mission Planning Station (IMPS), successfully provided relevant intelligence data for the Wild Weasel defense suppression mission. The combination of onboard sensors and stored terrain data bases have made possible the development of algorithms that select optimum routings for air-to-ground penetration missions. Optimal route generation can first be exercised in the ground based mission planner, and the resulting data can be used to provide onboard mission replanning. The graphics required to plan an effective RPV mission quickly include plan view, God's-eye view, perspective view, and analytical statistical graphs. All these capabilities were successfully developed, demonstrated, and delivered in the form Battle Area Simulation (BATS) software package. Author

N90-15933# Lockheed Missiles and Space Co., Austin, TX.
DISTRIBUTION OF HARDWARE AND SOFTWARE ELEMENTS IN UNMANNED AIR VEHICLE SYSTEMS **c05**
Larry D. Sauvain *In* AGARD, Guidance and Control of Unmanned Air Vehicles Aug. 1989 10 p (For primary document see N90-15924 08-08)
Copyright Avail: NTIS HC A09/MF A02; Non-NATO Nationals requests available only from AGARD/Scientific Publications Executive

Future unmanned air vehicle systems will be highly automated in order to accomplish their intended mission. These increased levels of automation are best achieved when the computer and man-machine interface elements are incorporated into the initial system design. Adequate capacity, growth capabilities and the maximum use of previously developed system elements are essential considerations in the computer hardware selection. The software structure must be modular, maintainable and have adequate configuration management tools to assure that the correct software is in use at all times. Since additional unplanned mission requirements may evolve, it is important that the man-machine interface elements be easily reconfigured. The basis for these assertions and how they were achieved within the ground control station portion of the Lockheed Demonstration and Research Test System will be addressed. Author

N90-15934# British Aerospace Public Ltd. Co., Lancashire (England). Military Aircraft Div.
TECHNOLOGY AND EVALUATION OF UNMANNED AIR VEHICLES **c05**
George R. Seyfang *In* AGARD, Guidance and Control of Unmanned Air Vehicles Aug. 1989 5 p (For primary document see N90-15924 08-08)
Copyright Avail: NTIS HC A09/MF A02; Non-NATO Nationals requests available only from AGARD/Scientific Publications Executive

The 15 years of UMA studies and experimental work done at BAe indicate that all of the technologies required to allow UMA to fulfull the air-to-ground roles in increasingly dangerous scenarios now exist. There appears to be the potential for significant savings in peacetime operating costs with UMA, although there would have to be changes to the services' infrastructure to gain all of these potential savings. Author

N90-15935# Lockheed Missiles and Space Co., Austin, TX.
NAVIGATION AND GUIDANCE TESTING OF THE LOCKHEED/US ARMY AQUILA REMOTELY PILOTED VEHICLE **c04**
Steven L. Ferguson *In* AGARD, Guidance and Control of Unmanned Air Vehicles Aug. 1989 13 p (For primary document see N90-15924 08-08)
Copyright Avail: NTIS HC A09/MF A02; Non-NATO Nationals requests available only from AGARD/Scientific Publications Executive

The Lockheed/U.S. Army Aquila Remotely Piloted Vehicle test program is described. The Aquila system is described, the data collection system discussed, and then particular tests required for testing the various navigation and guidance functions of the Aquila are described. Author

N90-15936*# Georgia Inst. of Tech., Atlanta. School of Aerospace Engineering.
SINGULAR PERTURBATION ANALYSIS OF AOTV-RELATED TRAJECTORY OPTIMIZATION PROBLEMS Final Report
Anthony J. Calise and Gyoung H. Bae Jan. 1990 53 p (Grant NAG1-660)
(NASA-CR-186202; NAS 1.26:186202) Avail: NTIS HC A04/MF A01 CSCL 01C

The problem of real time guidance and optimal control of Aeroassisted Orbit Transfer Vehicles (AOTV's) was addressed using singular perturbation theory as an underlying method of analysis. Trajectories were optimized with the objective of minimum energy expenditure in the atmospheric phase of the maneuver. Two major problem areas were addressed: optimal reentry, and synergetic plane change with aeroglide. For the reentry problem, several reduced order models were analyzed with the objective of optimal changes in heading with minimum energy loss. It was demonstrated that a further model order reduction to a single state model is possible through the application of singular perturbation theory. The optimal solution for the reduced problem defines an optimal altitude profile dependent on the current energy level of the vehicle. A separate boundary layer analysis is used to account for altitude and flight path angle dynamics, and to obtain lift and bank angle control solutions. By considering alternative approximations to solve the boundary layer problem, three guidance laws were derived, each having an analytic feedback form. The guidance laws were evaluated using a Maneuvering Reentry Research Vehicle model and all three laws were found to be near optimal. For the problem of synergetic plane change with aeroglide, a difficult terminal boundary layer control problem arises which to date is found to be analytically intractable. Thus a predictive/corrective solution was developed to satisfy the terminal constraints on altitude and flight path angle. A composite guidance solution was obtained by combining the optimal reentry solution with the predictive/corrective guidance method. Numerical comparisons with the corresponding optimal trajectory solutions show that the resulting performance is very close to optimal. An attempt was made to obtain numerically optimized trajectories for the case where heating rate is constrained. A first order state

variable inequality constraint was imposed on the full order AOTV point mass equations of motion, using a simple aerodynamic heating rate model. Author

N90-15937*# Boeing Aerospace Co., Kent, WA.
CREW EMERGENCY RETURN VEHICLE AUTOLAND FEASIBILITY STUDY
J. A. Bossi, M. A. Langehough, and K. L. Lee Dec. 1989 168 p
(Contract NAS1-18762)
(NASA-CR-181940; NAS 1.26:181940) Avail: NTIS HC A08/MF A01 CSCL 22B

The crew emergency return vehicle (CERV) autoland feasibility study focused on determining the controllability of the NASA Langley high lift over drag CERV for performing an automatic landing at a prescribed runway. An autoland system was developed using integral linear quadratic Gaussian (LQG) design techniques. The design was verified using a nonlinear 6 DOF simulation. Simulation results demonstrate that the CERV configuration is a very flyable configuration for performing an autoland mission. Adequate stability and control was demonstrated for wind turbulence and wind shear. Control surface actuator requirements were developed. Author

N90-15938*# National Aeronautics and Space Administration. Ames Research Center, Moffett Field, CA.
A SURVEY OF NONUNIFORM INFLOW MODELS FOR ROTORCRAFT FLIGHT DYNAMICS AND CONTROL APPLICATIONS
Robert T. N. Chen Nov. 1989 65 p Presented at the 15th European Rotorcraft Forum, Amsterdam, Netherlands, 12-15 Sep. 1989
(NASA-TM-102219; A-89220; NAS 1.15:102219) Avail: NTIS HC A04/MF A01 CSCL 01C

The results of a brief survey of nonuniform inflow models was summarized for the calculation of induced velocities at and near a lifting rotor in and out of ground effect. The survey, conducted from the perspective of flight dynamics and control applications, covers a spectrum of flight conditions including hover, vertical flight, and low-speed and high-speed forward flight, and reviews both static and dynamic aspects of the inflow. A primary emphasis is on the evaluation of various simple first harmonic inflow models developed over the years, in comparison with more sophisticated methods developed for use in performance and airload computations. The results of correlation with several sets of test data obtained at the rotor out of ground effect indicate that the Pitt/Peters first harmonic inflow model works well overall. For inflow near the rotor or in ground effect, it is suggested that charts similar to those of Heyson/Katzoff and Castles/De Leeuw of NACA be produced using modern free-wake methods for use in flight dynamic analyses and simulations. Author

09 RESEARCH AND SUPPORT FACILITIES (AIR)

Includes airports, hangars and runways; aircraft repair and overhaul facilities; wind tunnels; shock tubes; and aircraft engine test stands.

For related information see also *14 Ground Support Systems and Facilities (Space)*.

N90-15939# Advisory Group for Aerospace Research and Development, Neuilly-Sur-Seine (France). Fluid Dynamics Panel.
SPECIAL COURSE ON ADVANCES IN CRYOGENIC WIND TUNNEL TECHNOLOGY
Nov. 1989 373 p Course held in Rhode-Saint-Genese, Belgium, 5-9 Jun. 1989
(AGARD-R-774; ISBN-92-835-0532-8) Copyright Avail: NTIS HC A16/MF A03; Non-NATO Nationals requests available only from AGARD/Scientific Publications Executive

Current concerns with trying to build and use cryogenic wind tunnels are addressed as specifically as possible. This course covered both the theory and practice of cryogenic wind tunnel design, operation, and use. A brief review is provided for the development and early use of cryogenic tunnels and then covered all aspects of the design and operation of cryogenic tunnels and then covered all aspects of the design and operation of cryogenic tunnels. Among the areas covered were: cryogenic engineering and safety, properties of materials at cryogenic temperatures, tunnel design requirements, model design and construction, automatic tunnel control, data acquisition, data accuracy, flow visualization, productivity, and costs of models and operation. The status of cryogenic wind tunnel projects in AGARD countries and in the rest of the world was also presented. For individual titles, see N90-15940 through N90-15962.

N90-15940# Southampton Univ. (England). Dept. of Aeronautics and Astronautics.
INTRODUCTION TO CRYOGENIC WIND TUNNELS
M. J. Goodyer *In* AGARD, Special Course on Advances in Cryogenic Wind Tunnel Technology Nov. 1989 11 p (For primary document see N90-15939 08-09)
Copyright Avail: NTIS HC A16/MF A03; Non-NATO Nationals requests available only from AGARD/Scientific Publications Executive

The cryogenic wind tunnel was conceived as a way of increasing Reynolds number in a wind tunnel while avoiding an increase in its size. This it does very effectively and with some other surprisingly beneficial effects. Important among these is a reduction of tunnel drive power and the ability for the first time in a wind tunnel test to identify the separate effects of Reynolds number, Mach number and dynamic pressure. A brief introduction at the fundamental level highlighting some of the characteristics of cryogenic wind tunnels and their flows is presented. Author

N90-15941*# National Aeronautics and Space Administration. Langley Research Center, Hampton, VA.
THE NASA LANGLEY 0.3-METER TRANSONIC CRYOGENIC TUNNEL
Edward J. Ray *In* AGARD, Special Course on Advances in Cryogenic Wind Tunnel Technology Nov. 1989 21 p (For primary document see N90-15939 08-09)
Copyright Avail: NTIS HC A16/MF A03; Non-NATO Nationals requests available only from AGARD/Scientific Publications Executive CSCL 14B

The Langley 0.3-Meter Transonic Cryogenic Tunnel (0.3-m TCT) was placed in operation at NASA's Langley Research Center in 1973. This facility was the world's first cryogenic pressure tunnel. The 0.3-m TCT can operate from ambient to cryogenic temperatures at absolute pressures ranging from about 1 to 6 atmospheres. Three major test section concepts were developed and refined in this unique facility. The 0.3-m TCT was a leader in the evolution of cryogenic pressure wind tunnel test techniques, instrumentation, control strategy and model technology. An overview is presented of the evolution and 15 years of experience with the 0.3-m TCT. The historical background concentrates on the technical challenges and proof-of-concept validations during the establishment of the first cryogenic pressure wind tunnel. The various test section concepts are described. Highlights of operational experience and test results determined from these first time exploratory tests are presented. Operating costs and effective test techniques for the 0.3-m TCT are discussed. Finally, current and future plans for the facility are presented. Author

N90-15942*# National Aeronautics and Space Administration. Langley Research Center, Hampton, VA.
THE US NATIONAL TRANSONIC FACILITY, NTF
Walter E. Bruce, Jr. and Blair B. Gloss *In* AGARD, Special Course on Advances in Cryogenic Wind Tunnel Technology Nov. 1989 27 p (For primary document see N90-15939 08-09)
Copyright Avail: NTIS HC A16/MF A03; Non-NATO Nationals requests available only from AGARD/Scientific Publications Executive CSCL 14B

The construction of the National Transonic Facility was completed in September 1982 and the start-up and checkout of

tunnel systems were performed over the next two years. In August 1984, the Operational Readiness Review (ORR) was conducted and the facility was declared operational for final checkout of cryogenic instrumentation and control systems, and for the aerodynamic calibration and testing to commence. Also, the model access system for the cryogenic mode of operation would be placed into operation along with tunnel testing. Since the ORR, a host of operating problems resulting from the cryogenic environment were identified and solved. These range from making mechanical and electrical systems functional to eliminating temperature induced model vibration to coping with the outgassing of moisture from the thermal insulation. Additionally, a series of aerodynamic tests have demonstrated data quality and provided research data on several configurations. Some of the more significant efforts are reviewed since the ORR and the NTF status concerning hardware, instrumentation and process controls systems, operating constraints imposed by the cryogenic environment, and data quality are summarized. Author

N90-15943# Deutsche Forschungsanstalt fuer Luft- und Raumfahrt, Cologne (Germany, F.R.).
THE KRYO-KANAL KOELN (KKK): DESCRIPTION OF THE TUNNEL CONVERSION. THERMAL INSULATION, INSTRUMENTATION, OPERATIONAL EXPERIENCE, TEST RESULTS AND OPERATING COSTS
F. Viehweger *In* AGARD, Special Course on Advances in Cryogenic Wind Tunnel Technology Nov. 1989 17 p (For primary document see N90-15939 08-09)
Copyright Avail: NTIS HC A16/MF A03; Non-NATO Nationals requests available only from AGARD/Scientific Publications Executive

The construction of the Kryo-Kanal Koeln was completed in May 1985. After check out of all systems the aerodynamic and cryogenic calibration was started one year later and completed in the third quarter of 1988. During this time operating problems in the circuit and in the subsystems resulting from the cryogenic mode of operation were identified and solved. Some basic tests were performed to understand the physics of the desorption of moisture from the internal insulation. The aerodynamic tests demonstrated the flow quality in the test section. The experimental experience and the test results gathered during the calibration phase are reviewed. Author

N90-15944# Deutsche Forschungsanstalt fuer Luft- und Raumfahrt, Cologne (Germany, F.R.).
AUTOMATIC CONTROL OF KKK: REQUIREMENTS, SENSORS, ACTUATORS, AND CONTROL PERFORMANCE RESULTS
R. Kronen *In* AGARD, Special Course on Advances in Cryogenic Wind Tunnel Technology Nov. 1989 11 p (For primary document see N90-15939 08-09)
Copyright Avail: NTIS HC A16/MF A03; Non-NATO Nationals requests available only from AGARD/Scientific Publications Executive

After the modification of the low speed wind tunnel at the DLR Research Center at Cologne to a cryogenic wind tunnel a new control system was necessary. For lay out of the control system and for studying the tunnel behavior some mathematical models were developed. The models and the controller were tested by computerized simulations. Furthermore the control system was tested with the real tunnel for the run-up, testing, run-down phases. Author

N90-15945# ETW G.m.b.H., Cologne (Germany, F.R.).
THE EUROPEAN TRANSONIC WINDTUNNEL (ETW)
Xavier Bouis *In* AGARD, Special Course on Advances in Cryogenic Wind Tunnel Technology Nov. 1989 16 p (For primary document see N90-15939 08-09)
Copyright Avail: NTIS HC A16/MF A03; Non-NATO Nationals requests available only from AGARD/Scientific Publications Executive

The construction phase of the European Transonic Wind Tunnel started recently at Cologne, West Germany. Ambitious goals in aerodynamic quality and cost-effectiveness are reflected in the design philosophy. The main features of the future facility are presented. Author

N90-15946# Centre d'Etudes et de Recherches, Toulouse (France). Dept. d'Aerothermodynamique.
THE CRYOGENIC INDUCTION TUNNEL T2 AT TOULOUSE
Jean-Pierre Archambaud *In* AGARD, Special Course on Advances in Cryogenic Wind Tunnel Technology Nov. 1989 12 p (For primary document see N90-15939 08-09)
Copyright Avail: NTIS HC A16/MF A03; Non-NATO Nationals requests available only from AGARD/Scientific Publications Executive

The activity of the ONERA-CERT in the aerodynamic cryogenic experimental branch is presented. Firstly, the T2 induction wind tunnel is described, acting in cryogenic conditions since 1981, and the flow characteristics are indicated. Then the hollow model conception and its cooling during the run are developed and the importance of the wall temperature measurements underlined. The presence of ice particles in the flow, tripping the transition on the model, is discussed; an efficient solution is given, providing fairly good results on a laminar profile at high Reynolds number. Finally cryogenic test results on a three-dimensional model are shown. Author

N90-15947# Deutsche Forschungsanstalt fuer Luft- und Raumfahrt, Goettingen (Germany, F.R.). Inst. fuer Experimentelle Stroemungsmechanik.
THE CRYOGENIC LUDWIEG TUBE TUNNEL AT GOETTINGEN
G. Hefer *In* AGARD, Special Course on Advances in Cryogenic Wind Tunnel Technology Nov. 1989 7 p (For primary document see N90-15939 08-09)
Copyright Avail: NTIS HC A16/MF A03; Non-NATO Nationals requests available only from AGARD/Scientific Publications Executive

At the Research Center Goettingen of the DLR a cryogenic Ludwieg tube wind tunnel for transonic operation was constructed. The tunnel, having an effective run time of 1 second, a test section of 0.4 x 0.35 m squared, and a maximum stagnation pressure of 10 bars, is to be operated with nitrogen at temperatures between ambient and 120 K, achieving a Reynolds number of 70 x 10(exp 6) based on a model chord of 0.15 m. This lecture gives a brief review of the Ludwieg tube concept, the main design features of the tunnel, and the status of the project and presents the first results of the calibration. Author

N90-15948*# National Aeronautics and Space Administration. Langley Research Center, Hampton, VA.
OTHER CRYOGENIC WIND TUNNEL PROJECTS
Robert A. Kilgore *In* AGARD, Special Course on Advances in Cryogenic Wind Tunnel Technology Nov. 1989 12 p (For primary document see N90-15939 08-09)
Copyright Avail: NTIS HC A16/MF A03; Non-NATO Nationals requests available only from AGARD/Scientific Publications Executive CSCL 14B

The first cryogenic tunnel was built in 1972. Since then, many cryogenic wind-tunnel projects were started at aeronautical research centers around the world. Some of the more significant of these projects are described which are not covered by other lecturers at this Special Course. Described are cryogenic wind-tunnel projects in five countries: China (Chinese Aeronautical Research and Development Center); England (College of Aeronautics at Cranfield, and Royal Aerospace Establishment-Bedford); Japan (National Aerospace Laboratory, University of Tsukuba, and National Defense Academy); United States (Douglas Aircraft Co., University of Illinois at Urbana-Champaign and NASA Langley); and U.S.S.R. (Central Aero-Hydronamics Institute (TsAGI), Institute of Theoretical and Applied Mechanics (ITAM), and Physical-Mechanical Institute at Kharkov (PMI-K). Author

N90-15949# Cryogenic, Marine and Materials Consultants, Southampton (England).
CRYOGENIC ENGINEERING AND MATERIALS
D. A. Wigley *In* AGARD, Special Course on Advances in Cryogenic Wind Tunnel Technology Nov. 1989 18 p (For primary document see N90-15939 08-09)
Copyright Avail: NTIS HC A16/MF A03; Non-NATO Nationals requests available only from AGARD/Scientific Publications Executive

The effects of cryogenic temperatures on the mechanical and physical properties of materials are summarized. Heat capacity and thermal conductivity are considered in the context of conservation of liquid nitrogen, thermal stability of the gas stream and the response time for changes in operating temperature. Particular attention is given to the effects of differential expansion and failure due to thermal fatigue. Factors affecting safety are discussed, including hazards created due to the inadvertent production of liquid oxygen and the physiological effects of exposure to liquid and gaseous nitrogen, such as cold burns and asphyxiation. The preference for using fcc metals at low temperatures is explained in terms of their superior toughness and the limitations on the use of ferritic steels is also considered. Nonmetallic materials are discussed, mainly in the context of their LOX compatibility and their use in the form of foams and fibers as insulants, seals, and fiber-reinforced composites. Author

N90-15950# Office National d'Etudes et de Recherches Aeronautiques, Paris (France).
INSTRUMENTATION FOR CRYOGENIC WIND TUNNELS
Maurice Bazin *In* AGARD, Special Course on Advances in Cryogenic Wind Tunnel Technology Nov. 1989 31 p (For primary document see N90-15939 08-09)
Copyright Avail: NTIS HC A16/MF A03; Non-NATO Nationals requests available only from AGARD/Scientific Publications Executive

The possibilities of adapting existing instrumentation for use in the ETW cryogenic wind tunnel were investigated. These efforts must be continued, especially for balances, but recent work was devoted to systems with a direct impact on the design of the wind tunnel test section. This is the case in particular for all the optical methods whose use in ETW for flow visualization (external flow-field and transition detection), accurate model attitude measurements and deformation measurements will contribute to the quality of the tests. Author

N90-15951# Centre d'Etudes et de Recherches, Toulouse (France). Dept. d'Aerothermodynamique.
FUNDAMENTAL CONSIDERATIONS IN TESTING IN CRYOGENIC WIND TUNNELS
Andre Mignosi *In* AGARD, Special Course on Advances in Cryogenic Wind Tunnel Technology Nov. 1989 12 p (For primary document see N90-15939 08-09)
Copyright Avail: NTIS HC A16/MF A03; Non-NATO Nationals requests available only from AGARD/Scientific Publications Executive

The cryogenic technology for wind tunnel testing is strongly connected with the aerodynamic requirements. A number of aerodynamic problems mainly related to cryogenic testing are examined. The various factors are described which are involved in achieving the best similarity possible between an aircraft in flight and the model in the wind tunnel. The second part covers the analysis of these factors: effect of a non-adiabatic wall, boundary layer transition, two-dimensional and three-dimensional tests, effects of the Reynolds number. It is attempted to alternate theoretical considerations with practical examples in order to illustrate the importance of experimental/theoretical correlations. Author

N90-15952*# National Aeronautics and Space Administration. Langley Research Center, Hampton, VA.
TEST TECHNIQUES FOR CRYOGENIC WIND TUNNELS
Pierce L. Lawing *In* AGARD, Special Course on Advances in Cryogenic Wind Tunnel Technology Nov. 1989 12 p (For primary document see N90-15939 08-09)
Copyright Avail: NTIS HC A16/MF A03; Non-NATO Nationals requests available only from AGARD/Scientific Publications Executive CSCL 14B

Some of the testing techniques developed for transonic cryogenic tunnels are presented. Techniques are emphasized which required special development or were unique because of the opportunities offered by cryogenic operation. Measuring the static aerodynamic coefficients normally used to determine component efficiency is discussed. The first topic is testing of two dimensional airfoils at transonic Mach numbers and flight values of Reynolds number. Three dimensional tests of complete configurations and sidewall mounted wings are also described. Since flight Reynolds numbers are of interest, free transition must be allowed. A discussion is given of wind tunnel and model construction effects on transition location. Time dependent phenomena, fluid mechanics, and measurement techniques are examined. The time dependent, or unsteady, aerodynamic test techniques described include testing for flutter, buffet, and oscillating airfoil characteristics. In describing non-intrusive laser techniques, discussions are given regarding optical access, seeding, forward scatter lasers, two-spot lasers, and laser holography. Methods of detecting transition and separation are reported and a new type of skin friction balance is described. Author

N90-15953# Southampton Univ. (England). Dept. of Aeronautics and Astronautics.
FLOW VISUALIZATION IN THE CRYOGENIC WIND TUNNEL
M. J. Goodyer *In* AGARD, Special Course on Advances in Cryogenic Wind Tunnel Technology Nov. 1989 11 p (For primary document see N90-15939 08-09)
Copyright Avail: NTIS HC A16/MF A03; Non-NATO Nationals requests available only from AGARD/Scientific Publications Executive

A range of flow visualization methods for possible application to model testing in the large cryogenic wind tunnel is described. Desirable features are outlined, including the flow details which should be revealed by the various methods. The risks of model and tunnel contamination are discussed, also the coverage of the model surface to be expected, the advance planning and complexity of model design and tunnel equipment required by the visualization method, and the prospects of generating multiple flow images during one tunnel run. The methods to be outlined are at an early stage of development but in all cases there is some cryogenic experience to support their consideration for use in the cryogenic environment. None is well established for use at the highest Reynolds number conditions attainable in the cryogenic pressure tunnel. Author

N90-15954# Cryogenic, Marine and Materials Consultants, Southampton (England).
MATERIALS AND TECHNIQUES FOR MODEL CONSTRUCTION
D. A. Wigley *In* AGARD, Special Course on Advances in Cryogenic Wind Tunnel Technology Nov. 1989 19 p (For primary document see N90-15939 08-09)
Copyright Avail: NTIS HC A16/MF A03; Non-NATO Nationals requests available only from AGARD/Scientific Publications Executive

The problems confronting the designer of models for cryogenic wind tunnel models are discussed with particular reference to the difficulties in obtaining appropriate data on the mechanical and physical properties of candidate materials and their fabrication technologies. The relationship between strength and toughness of alloys is discussed in the context of maximizing both and avoiding the problem of dimensional and microstructural instability. All major classes of materials used in model construction are considered in some detail and in the Appendix selected numerical data is given for the most relevant materials. The stepped-specimen program to investigate stress-induced dimensional changes in alloys is discussed in detail together with interpretation of the initial results. The methods used to bond model components are considered with particular reference to the selection of filler alloys and

temperature cycles to avoid microstructural degradation and loss of mechanical properties. Author

N90-15955# Cryogenic, Marine and Materials Consultants, Southampton (England).
SOME RECENT DEVELOPMENTS IN MATERIALS AND TECHNIQUES FOR MODEL FABRICATION
D. A. Wigley *In* AGARD, Special Course on Advances in Cryogenic Wind Tunnel Technology Nov. 1989 10 p (For primary document see N90-15939 08-09)
Copyright Avail: NTIS HC A16/MF A03; Non-NATO Nationals requests available only from AGARD/Scientific Publications Executive

Three topics are considered: the laminated thin sheet technology used in fabrication of a model of the X29A canard that enabled a uniquely high number of pressure orifices to be placed in a thin airfoil; the different configurations of sample used for studies on materials and fabrication techniques for model construction; and the long term objective of creating a handbook, database or expert system to bring together the information already available and indicate those areas where further work is needed. Author

N90-15956*# National Aeronautics and Space Administration. Langley Research Center, Hampton, VA.
MODELS FOR CRYOGENIC WIND TUNNELS
Pierce L. Lawing *In* AGARD, Special Course on Advances in Cryogenic Wind Tunnel Technology Nov. 1989 14 p (For primary document see N90-15939 08-09)
Copyright Avail: NTIS HC A16/MF A03; Non-NATO Nationals requests available only from AGARD/Scientific Publications Executive CSCL 14B

Model requirements, types of model construction methods, and research in new ways to build models are discussed. The 0.3-m Transonic Cryogenic Tunnel was in operation for 16 years and many 2-D airfoil pressure models were tested. In addition there were airfoil models dedicated to transition detection techniques and other specialized research. There were also a number of small 3-D models tested. A chronological development in model building technique is described which led to the construction of many successful models. The difficulties of construction are illustrated by discussing several unsuccessful model fabrication attempts. The National Transonic Facility, a newer and much larger tunnel, was used to test a variety of models including a submarine, transport and fighter configurations, and the Shuttle Orbiter. A new method of building pressure models was developed and is described. The method is centered on the concept of bonding together plates with pressure channels etched into the bond planes, which provides high density pressure instrumentation with minimum demand on parent model material. With care in the choice of materials and technique, vacuum brazing can be used to produce strong bonds without blocking pressure channels and with no bonding voids between channels. Using multiple plates, a 5 percent wing with 96 orifices was constructed and tested in a transonic cryogenic wind tunnel. Samples of test data are presented and future applications of the technology are suggested. Author

N90-15957*# National Aeronautics and Space Administration. Langley Research Center, Hampton, VA.
AUTOMATIC CONTROL OF CRYOGENIC WIND TUNNELS
S. Balakrishna *In* AGARD, Special Course on Advances in Cryogenic Wind Tunnel Technology Nov. 1989 15 p (For primary document see N90-15939 08-09)
Copyright Avail: NTIS HC A16/MF A03; Non-NATO Nationals requests available only from AGARD/Scientific Publications Executive CSCL 14B

Inadequate Reynolds number similarity in testing of scaled models affects the quality of aerodynamic data from wind tunnels. This is due to scale effects of boundary-layer shock wave interaction which is likely to be severe at transonic speeds. The idea of operation of wind tunnels using test gas cooled to cryogenic temperatures has yielded a quantrum jump in the ability to realize full scale Reynolds number flow similarity in small transonic tunnels. In such tunnels, the basic flow control problem consists of obtaining and maintaining the desired test section flow parameters. Mach number, Reynolds number, and dynamic pressure are the three flow parameters that are usually required to be kept constant during the period of model aerodynamic data acquisition. The series of activity involved in modeling, control law development, mechanization of the control laws on a microcomputer, and the performance of a globally stable automatic control system for the 0.3-m Transonic Cryogenic Tunnel (TCT) are discussed. A lumped multi-variable nonlinear dynamic model of the cryogenic tunnel, generation of a set of linear control laws for small perturbation, and nonlinear control strategy for large set point changes including tunnel trajectory control are described. The details of mechanization of the control laws on a 16 bit microcomputer system, the software features, operator interface, the display and safety are discussed. The controller is shown to provide globally stable and reliable temperature control to + or - 0.2 K, pressure to + or - 0.07 psi and Mach number to + or - 0.002 of the set point value. This performance is obtained both during large set point commands as for a tunnel cooldown, and during aerodynamic data acquisition with intrusive activity like geometrical changes in the test section such as angle of attack changes, drag rake movements, wall adaptation and sidewall boundary-layer removal. Feasibility of the use of an automatic Reynolds number control mode with fixed Mach number control is demonstrated. Author

N90-15958*# National Aeronautics and Space Administration. Langley Research Center, Hampton, VA.
EXPERIENCE WITH STRAIN-GAGE BALANCES FOR CRYOGENIC WIND TUNNELS
M. Susan Williams *In* AGARD, Special Course on Advances in Cryogenic Wind Tunnel Technology Nov. 1989 14 p (For primary document see N90-15939 08-09)
Copyright Avail: NTIS HC A16/MF A03; Non-NATO Nationals requests available only from AGARD/Scientific Publications Executive CSCL 14B

The U.S. National Transonic Facility (NTF) is a cryogenic wind tunnel build to meet the United States' needs for high Reynolds number testing. The facility was declared operational in August 1984, and since that time numerous models were tested in the NTF using unheated strain-gage balances to measure aerodynamic forces. The difficulty in accurately measuring forces and moments of models in conventional wind tunnels becomes more challenging at cryogenic conditions. The Force and Strain Instrumentation Section of the Instrument Research Division at NASA Langley Research Center designed and fabricated the balances to measure forces at cryogenic temperatures without thermally controlling the balance temperature. Presented are balance results from a recent cryogenic test program in the NTF. The data indicated the accuracy with which aerodynamic forces are determined using current instrumentation and test methods as well as identified areas for future research. Author

N90-15959*# National Aeronautics and Space Administration. Langley Research Center, Hampton, VA.
CRYOGENIC BALANCES FOR THE US NTF Status Report
Alice T. Ferris *In* AGARD, Special Course on Advances in Cryogenic Wind Tunnel Technology Nov. 1989 10 p (For primary document see N90-15939 08-09)
Copyright Avail: NTIS HC A16/MF A03; Non-NATO Nationals requests available only from AGARD/Scientific Publications Executive CSCL 14B

Force balances were used to obtain aerodynamic data in the National Transonic Facility (NTF) wind tunnel since it became operational in 1983. These balances were designed, fabricated, gaged, and calibrated to Langley Research Center's specifications to operate over the temperature range of -320 F to +140 F without thermal control. Some of the materials and procedures developed to obtain a balance that would perform in this environment are reviewed. The degree of success in using these balances thus far is reported. Some of the problem areas that

need additional work are specified and some of the progress addressing these problems is described. Author

N90-15960*# National Aeronautics and Space Administration. Langley Research Center, Hampton, VA.
SAFETY AND CRYOGENIC WIND TUNNELS
Edward J. Ray *In* AGARD, Special Course on Advances in Cryogenic Wind Tunnel Technology Nov. 1989 18 p (For primary document see N90-15939 08-09)
Copyright Avail: NTIS HC A16/MF A03; Non-NATO Nationals requests available only from AGARD/Scientific Publications Executive CSCL 14B

The Langley 0.3-Meter Transonic Cryogenic Tunnel (0.3-m TCT) was placed in operation at NASA's Langley Research Center in 1973 as the world's first cryogenic pressure tunnel. The 0.3-m TCT can operate from ambient to cryogenic temperatures over an absolute pressure range from about 1 to 6 atmospheres. Three major test section concepts were developed and refined in this unique facility. The 0.3-m TCT is a leader in the development of various cryogenic pressure wind tunnel experimental techniques, instrumentation, control, model technology and safety standards. The safety experience gained is examined. During this period of advanced research, new operating techniques, training policies, and procedures had to be established. The paper deals with the Do's and Don'ts of cryogenic wind tunnel testing. Hazards and safety requirements which are unique to cryogenic testing are discussed. Highlights of experience and lessons learned with the 0.3-m TCT are reviewed. Author

N90-15961# Office National d'Etudes et de Recherches Aeronautiques, Paris (France).
PRODUCTIVITY AND CRYOGENIC WIND TUNNELS
J. Christophe *In* AGARD, Special Course on Advances in Cryogenic Wind Tunnel Technology Nov. 1989 14 p (For primary document see N90-15939 08-09)
Copyright Avail: NTIS HC A16/MF A03; Non-NATO Nationals requests available only from AGARD/Scientific Publications Executive

After a brief review of the situation of existing cryogenic wind tunnels, the thermal balance of five wind tunnels is discussed. This discussion of the thermal balance is then generalized to suggest guidelines for the designers of future cryogenic wind tunnels. Finally, with the same concern, unconventional schemes are examined. Author

N90-15962*# National Aeronautics and Space Administration. Langley Research Center, Hampton, VA.
ENERGY MANAGEMENT AND RECOVERY
Pierce L. Lawing *In* AGARD, Special Course on Advances in Cryogenic Wind Tunnel Technology Nov. 1989 9 p (For primary document see N90-15939 08-09)
Copyright Avail: NTIS HC A16/MF A03; Non-NATO Nationals requests available only from AGARD/Scientific Publications Executive CSCL 14B

Energy management is treated by first exploring the energy requirements for a cryogenic tunnel. The requirement is defined as a function of Mach number, Reynolds number, temperature, and tunnel size. A simple program and correlation is described which allow calculation of the energy required. Usage of energy is also addressed in terms of tunnel control and research operation. The potential of a new wet expander is outlined in terms of cost saved by reliquefying a portion of the exhaust. The expander is described as a potentially more efficient way of recovering a fraction of the cold nitrogen gas normally exhausted to the atmosphere from a cryogenic tunnel. The role of tunnel insulation systems is explored in terms of requirements, safety, cost, maintenance, and efficiency. A detailed description of two external insulation systems is given. One is a rigid foam with a fiber glass and epoxy shell. The other is composed of glass fiber mats with a flexible outer vapor barrier; this system is nitrogen purged. The two systems are compared with the purged system being judged superior.
Author

N90-15963# European Space Agency, Paris (France).
PRESSURE MEASUREMENT TECHNIQUE IN THE WIND TUNNEL DIVISION OF DFVLR Status Report, 1988
Ruediger Siebert Oct. 1989 52 p Original language document was announced as N89-25243
(ESA-TT-1145; DFVLR-Mitt-88-11; ETN-90-96190) Avail: NTIS HC A04/MF A01; original German version available from DFVLR, VB-PL-DO, Postfach 90 60 58, 5000 Cologne, Fed. Republic of Germany, 19.50 DM

Information for users of the DFVLR wind tunnels in Brunswick, Goetingen and Cologne (Germany, F.R.) is presented. The general concept, technical details and status of the pressure measuring technique are described. The data on all the available pressure sensors and pressure measuring systems are provided. A modern and powerful pressure measurement technique available for wind tunnel users is described. Compatible measuring systems permit use on various wind tunnels. An adequate measure of flexibility is retained and it is possible to react quickly even to varying requirements. ESA

N90-15964*# National Aeronautics and Space Administration. Lewis Research Center, Cleveland, OH.
AN ELECTRONIC PRESSURE PROFILE DISPLAY SYSTEM FOR AERONAUTIC TEST FACILITIES
Mark R. Woike 1990 13 p Proposed for presentation at the International Instrumentation Symposium, Denver, CO, 6-10 May 1990; sponsored by Instrument Society of America
(NASA-TM-102478; E-5265; NAS 1.15:102478) Avail: NTIS HC A03/MF A01 CSCL 14B

The NASA Lewis Research Center has installed an Electronic Pressure Profile Display system. This system provides for the real-time display of pressure readings on high resolution graphics monitors. The Electronic Pressure Profile Display system will replace manometer banks currently used in aeronautic test facilities. The Electronic Pressure Profile Display system consists of an industrial type Digital Pressure Transmitter (DPT) unit which interfaces with a host computer. The host computer collects the pressure data from the DPT unit, converts it into engineering units, and displays the readings on a high resolution graphics monitor in bar graph format. Software was developed to accomplish the above tasks and also draw facility diagrams as background information on the displays. Data transfer between host computer and DPT unit is done with serial communications. Up to 64 channels are displayed with one second update time. This paper describes the system configuration, its features, and its advantages over existing systems. Author

N90-15965*# National Aeronautics and Space Administration. Lewis Research Center, Cleveland, OH.
A NUMERICAL SIMULATION OF THE FLOW IN THE DIFFUSER OF THE NASA LEWIS ICING RESEARCH TUNNEL
Harold E. Addy, Jr. and Theo G. Keith, Jr. (Toledo Univ., OH.) 1990 11 p Presented at the 28th Aerospace Sciences Meeting, Reno, NV, 8-11 Jan. 1990; sponsored by AIAA
(NASA-TM-102480; E-5270; NAS 1.15:102480; AIAA-90-0488)
Avail: NTIS HC A03/MF A01 CSCL 14B

The flow in the diffuser section of the Icing Research Tunnel at the NASA Lewis Research Center is numerically investigated. To accomplish this, an existing computer code is utilized. The code, known as PARC3D, is based on the Beam-Warming algorithm applied to the strong conservation law form of the complete Navier-Stokes equations. The first portion of the paper consists of a brief description of the diffuser and its current flow characteristics. A brief discussion of the code work follows. Predicted velocity patterns are then compared with the measured values. Author

12 ASTRONAUTICS (GENERAL)

For extraterrestrial exploration see *91 Lunar and Planetary Exploration.*

N90-15966# Congress of the United States, Washington, DC.
ROUND TRIP TO ORBIT. HUMAN SPACEFLIGHT ALTERNATIVES: SPECIAL REPORT
1989 127 p
(OTA-ISC-419; LC-89-600744) Avail: NTIS HC A07/MF A01

Technologies and systems are examined for transporting astronauts and scientists to and from low-earth orbit, and some of the policy choices that Congress faces in this critical aspect of the U.S. Government's space program are explained. A variety of ways are analyzed to make the Space Shuttle system safer and more reliable. It also explores several proposed systems to replace the Shuttle early in the next century, and examines proposals for a Space Station crew escape system. Finally, the National Aerospace Plane is discussed, and it is compared with other potential future launch systems. Cargo-only launch vehicles are not examined except insofar as their use may affect the need for crew-carrying launchers. Author

N90-15967# Helsinki Univ. of Technology, Espoo (Finland). Space Technology Lab.
LABORATORY OF SPACE TECHNOLOGY Annual Report, 1988
Martti Hallikainen, ed. May 1989 28 p
(PB90-110651; ISBN-951-754-928-8; ISSN-0786-8154; Rept-1)
Avail: NTIS HC A03/MF A01 CSCL 22A

Activities of the Laboratory of Space Technology in 1988 are described. The Laboratory was officially established in November 1988, although it has been an independent organizational unit within the University since September 1987. The Laboratory is responsible for teaching space technology at the University. The main area in research is airborne and spaceborne microwave remote sensing, including instrumentation, measurements and interpretation of experimental results. The laboratory was co-organizer of a 5-day course, Seminar on Space Techniques, for 60 attendees in March. Preparations for hosting the EARSel General Assembly and Symposium in 1989 and IGARSS '91 in 1991 were started. Author

N90-15968# European Space Agency, Paris (France).
MISSION TO MARS. REPORT OF THE MARS EXPLORATION STUDY TEAM
A. F. Chicarro, G. E. N. Scoon (European Space Agency. European Space Research and Technology Center, ESTEC, Noordwijk, Netherlands), M. Coradini, and Bruce Battrick, ed. Jul. 1989 213 p Original contains color illustrations
(ESA-SP-1117; ISBN-92-9092-040-8; ISSN-0379-6566; ETN-90-96200) Copyright Avail: NTIS HC A10/MF A02; ESA Publications Div., ESTEC, Noordwijk, Netherlands, 60 Dutch guilders

The objectives and the activities carried out by the Mars Exploration Study Team (MEST) are reported. Taking into account the key scientific issues, for a better understanding of the formation and evolution of Mars, and the results achieved by post missions to Mars, three areas of action are identified by MEST: two involve science from the surface (geophysics, minerology and meteorology), and the third involves the supporting technology for mission scenarios. The options evaluated during the course of the ESA internal study, which concentrated on orbiter instrumentation, a network of small Mars surface stations, and elements of a Mars rover, are summarized. ESA

N90-15969# Technische Univ., Berlin (Germany, F.R.). Inst. fuer Luft- und Raumfahrt.
A FOUNDATION FOR THE DESIGN OF AN ASTRONAUTICS SPECIFICATION SYSTEM BASED ON DYNAMIC MOTIVATION ANALYSIS [ENTWURF EINES RAUMFAHRTSPEZIFISCHEN ZIELSYSTEMS AUF DER BASIS EINER DYNAMISCHEN MOTIVATIONSANALYSE]
Goekhan Kayal 1 Mar. 1989 69 p In GERMAN; ENGLISH summary
(ILR-Mitt-220; ETN-90-95356) Avail: NTIS HC A04/MF A01

Arguments for or against astronautics are categorized. A dynamic evaluation of these arguments for the U.S. and Western Europe is presented. A general view of the changes of meaning and frequency of motivations since the fifties is presented. The trends show that arguments from all areas of human life provide significant motivation for the further development of astronautics. The system of objectives on which this analysis is based, is judged in relation to relative priorities from two points of view for four points in time. The approximation formula provides evaluations for the period 1955 to 1995. ESA

N90-15970# Technische Univ., Berlin (Germany, F.R.). Inst. fuer Luft- und Raumfahrt.
THE FIRST 1000 DAYS OF A FUTURE LUNAR BASE
H. Hermann Koelle, Thorsten Alt, Christian Becker, Danieel Dallmann, Roland Glasmachers, Bernhard Hufenbach, Hakan Kayal, Rene Kleessen, Eckhard Krabel, and Andreas Kuechler et al 1 May 1989 61 p
(ILR-Mitt-224; ETN-90-95821) Avail: NTIS HC A04/MF A01

A theoretical study of the planning and organization to establish a lunar base is presented. The lunar base is assumed to be on the lunar equator. An initial assembly crew of twelve would be required for initial operations. The average monthly working hours are assumed to be 200 hours per person. The lunar modules for the initial base are limited to a mass of 20 metric tons, a diameter of 4.20 m and a length of 9.60 cm. The study aims at a lunar crew size of 48 by the end of the first 1000 day build up period. ESA

13 ASTRODYNAMICS

Includes powered and free-flight trajectories; and orbital and launching dynamics.

N90-15971# Royal Aerospace Establishment, Farnborough (England).
ON MEAN ELEMENTS FOR SATELLITE ORBITS PERTURBED BY THE ZONAL HARMONICS OF THE GEOPOTENTIAL
R. H. Gooding Jul. 1989 10 p Presented at the 27th COSPAR Meeting on Advances in Space Research, Espoo, Finland, 21 Jul. 1988 Submitted for publication
(RAE-TM-Space-371; BR110918; ETN-90-96134) Copyright
Avail: NTIS HC A02/MF A01

The mean elements to the perturbations of a satellite caused by the Earth's zonal harmonic J(sub 2) are studied. It is shown how elements can be defined so that perturbations in spherical coordinates take an especially simple form. The first order effects of J(sub 2) are concentrated on, with formulae given to connect the preferred elements to the elements of Kozai. The extension to second order in J(sub 2) and the first order in the general zonal harmonic are considered. ESA

14 GROUND SUPPORT SYSTEMS AND FACILITIES (SPACE)

Includes launch complexes, research and production facilities; ground support equipment, e.g., mobile transporters; and simulators.

For related information see also *09 Research and Support Facilities (Air).*

N90-15972# Royal Signals and Radar Establishment, Malvern (England).
TACTICAL UK MILITARY SATELLITE GROUND TERMINALS: A RESEARCH AND DEVELOPMENT REVIEW
P. J. Skilton 1 Jan. 1989 63 p
(RSRE-Memo-4262; BR110081; ETN-90-96114) Copyright
Avail: NTIS HC A04/MF A01

A review of tactical satellite ground terminals in service with United Kingdom and NATO forces is given. A background to the military space segment available to the United Kingdom, U.S. and NATO provides a relevant perspective to the tactical terminal program. Satellite communication to a moving vehicle, prototype vehicles, and radio equipment, are described. Future trends in space and ground segment hardware are included. ESA

N90-15973# Sandia National Labs., Albuquerque, NM. Thermomechanical and Physical Div.
THE USE OF HYPERVELOCITY LAUNCHERS TO EXPLORE PREVIOUSLY INACCESSIBLE STATES OF MATTER
J. R. Asay, T. G. Trucano, and R. S. Hawke (Lawrence Livermore National Lab., CA.) 1989 16 p Presented at the Hypervelocity Impact Symposium, San Antonio, TX, 12-14 Dec. 1989 Sponsored in part by DNA
(Contract DE-AC04-76DP-00789)
(DE90-004088; SAND-89-0596C; CONF-891214-13) Avail: NTIS HC A03/MF A01

The dynamic response of materials at very high pressure and temperature is important in a wide variety of scientific and programmatic applications. Thermodynamic regions of interest include the high-pressure response of condensed phases and the highly expanded states of materials. Since these regimes are normally studied with flat-plate impact techniques, it is necessary that projectile velocities achievable with high-velocity launchers be sufficient to access the desired thermodynamic regions. In this paper, we discuss the equation-of-state regions that would be accessible with a plate impact capability of 15 km/s and summarize the status of a hypervelocity launcher under development which will provide the required velocity capability. DOE

15 LAUNCH VEHICLES AND SPACE VEHICLES

Includes boosters; operating problems of launch/space vehicle systems; and reusable vehicles.

For related information see also *20 Spacecraft Propulsion and Power.*

No abstracts in this category.

16 SPACE TRANSPORTATION

Includes passenger and cargo space transportation, e.g., shuttle operations; and space rescue techniques.

For related information see also *03 Air Transportation and Safety* and *18 Spacecraft Design, Testing and Performance.* For space suits see *54 Man/System Technology and Life Support.*

N90-15974# European Space Agency, Paris (France).
CREW SAFETY AND RESCUE IN SPACE: AN INTERNATIONAL APPROACH
Valerie David, ed. and T. D. Guyenne, ed. Aug. 1989 70 p Workshop held in Le Bourget, France, 7 Jun. 1989; sponsored by NASA, Agenzia Spaziale Italiana, Canadian Space Agency, CNES, DFVLR, Glavkosmos, and the National Space Development Agency
(ESA-SP-300; ISBN-92-9029-042-4; ISSN-0379-6566; ETN-90-96196) Copyright Avail: NTIS HC A04/MF A01; ESA Publications Div., ESTEC, Noordwijk, Netherlands, 30 Dutch guilders

The 1989 workshop on crew safety and rescue operations in space are presented. The safety and rescue during space transportation and orbit activities and the interoperability between manned space systems are the main topics. The workshop provided the opportunity of exchanging space technology knowledge. A consensus on the need of implementing international safety and rescue operations emerged. The goals and limitations of space rescue, concerning launch, reentry and orbital phases are underlined. It is pointed out that the same infrastructure needed to support in-space international rendezvous and docking must also be put into place to enhance terrestrial capabilities for rescue of astronauts and cosmonauts returning from space under emergency conditions. For individual titles, see N90-15975 through N90-15982.

N90-15975*# National Aeronautics and Space Administration. Lyndon B. Johnson Space Center, Houston, TX.
SAFETY AND RESCUE DURING STS OPERATIONS
Bryan OConnor *In* ESA, Crew Safety and Rescue in Space: An International Approach Aug. 1989 p 9-12 (For primary document see N90-15974 08-16)
Copyright Avail: NTIS HC A04/MF A01; ESA Publications Div., ESTEC, Noordwijk, Netherlands, 30 Dutch guilders CSCL 22B

The space shuttle means, provided to the crew, of abort/escape for noncatastrophic mishap scenaries, during Space Transportation Systems (STS) operations, are discussed. From vehicle ingress until launch, the crew can escape the launch pad by use of slidewire baskets. For various emergencies during ascent, the crew can fly an intact abort. Such aborts include return to launch site, transoceanic abort landing, abort once around, and abort to orbit. The crew can fly the orbiter to an emergency airfield, or to an over ocean bailout for more serious ascent or on-orbit emergencies. For failures during landing, the crew can quickly egress the orbiter from the overhead hatch, or by use of an inflatable slide mounted at the side hatch. ESA

N90-15976# Glavkosmos, Moscow (USSR).
EVA SPACE SUIT. GENERAL CONCEPTS OF DESIGN AND ARRANGEMENT **c54**
G. I. Severin, V. I. Svertshek, and I. P. Abramov *In* ESA, Crew Safety and Rescue in Space: An International Approach Aug. 1989 p 13-17 (For primary document see N90-15974 08-16)
Copyright Avail: NTIS HC A04/MF A01; ESA Publications Div., ESTEC, Noordwijk, Netherlands, 30 Dutch guilders

The Extra Vehicular Activities (EVA) space suit, used by the Soviets, is presented. It is a semi-rigid type of suit. High reliability of a space suit and its subsystems and an adequate cosmonaut mobility are considered in the space suit development process. Space suit system design concepts and associated study results are reviewed. Methods to provide space suit reliability are presented. ESA

N90-15977*# National Aeronautics and Space Administration. Lyndon B. Johnson Space Center, Houston, TX.
ASSURED CREW RETURN CAPABILITY ARCHITECTURE **c03**
J. W. Craig *In* ESA, Crew Safety and Rescue in Space: An International Approach Aug. 1989 p 21-26 (For primary document see N90-15974 08-16)
Copyright Avail: NTIS HC A04/MF A01; ESA Publications Div., ESTEC, Noordwijk, Netherlands, 30 Dutch guilders CSCL 22A

The fundamental elements of the spacecraft Assured Crew Return Capability (ACRC) are discussed. These elements are access, response time, crew transfer, and the availability of landing sites. The use of an embedded operations concept identified as an essential element of the ACRC architecture. Several rescue assets are identified and evaluated as primary elements of an overall ACRC architecture. The investigation results lead to the following conclusions: optimum on-orbit rescue capability is provided by a rescue system integral to the operational vehicle; ground based rescue provides the most practical coverage for stranded transportation vehicles; and due to infrequent and unexpected use of ACRC, crew operations must be kept simple. ESA

N90-15978# Glavkosmos, Moscow (USSR).
ON THE SELECTION OF CREWMEMBER RESCUE MEANS FOR MANNED SPACE LAUNCH SYSTEMS **c03**
G. I. Severin *In* ESA, Crew Safety and Rescue in Space: An International Approach Aug. 1989 p 27-30 (For primary document see N90-15974 08-16)
Copyright Avail: NTIS HC A04/MF A01; ESA Publications Div., ESTEC, Noordwijk, Netherlands, 30 Dutch guilders

The role of crew member rescue systems in the provision of manned space launch system flight safety is considered. The rescue system requirements are identified. Jettisonable cabins and ejection seat comparative analysis is given. Main parameters of an ejection seat developed in the USSR are presented. Flight certification of the seat is performed using high speed and high altitude aircraft (airborne laboratories) which allowed test ejections under conditions close to the actual. ESA

N90-15979*# National Aeronautics and Space Administration. Lyndon B. Johnson Space Center, Houston, TX.
SYSTEMS INTEROPERABILITY APPROACH APOLLO/SOYUZ TEST PROJECT
Donald C. Wade *In* ESA, Crew Safety and Rescue in Space: An International Approach Aug. 1989 p 33-36 (For primary document see N90-15974 08-16)
Copyright Avail: NTIS HC A04/MF A01; ESA Publications Div., ESTEC, Noordwijk, Netherlands, 30 Dutch guilders CSCL 22B

The aproach used to design and develop the hardware and to insure the compatibility of existing systems used for the Apollo/Soyuz test project mission, are described. This mission used slightly modified Apollo and Soyuz spacecraft, a new jointly designed docking system, a new docking module (used as an airlock), and many existing flight and ground systems. The working groups major responsibilities and the documentation to control the technical agreements and information exchange are summarized. ESA

N90-15980# Glavkosmos, Moscow (USSR).
CREW SAFETY AND RESCUE AIDS
Yuri P. Semyenov *In* ESA, Crew Safety and Rescue in Space: An International Approach Aug. 1989 p 37-42 (For primary document see N90-15974 08-16)
Copyright Avail: NTIS HC A04/MF A01; ESA Publications Div., ESTEC, Noordwijk, Netherlands, 30 Dutch guilders

The Soviet program concerning crew safety and rescue aids is summarized. Complex procedures to ensure safety in all phases of the mission are envisaged. The program includes the steps of orbit insertion with the help of booster, orbital flight and recovery. The possibility to expand feasibilities for crew rescue by using spacecraft of different countries in orbital flight phases are considered. The problem of manned spacecraft/stations systems compatibility is analyzed. It involves radiocommunication systems, orbital rendezvous control systems, docking units, internal atmospheres. In this case, spacecraft additional equipping and technical decisions changes are needed. ESA

N90-15981# National Space Development Agency, Tokyo (Japan).
NASDA'S APPROACH TO THE INTEROPERABILITY OF SAFETY AND RESCUE IN SPACE
Masanori Homma *In* ESA, Crew Safety and Rescue in Space: An International Approach Aug. 1989 p 43-45 (For primary document see N90-15974 08-16)
Copyright Avail: NTIS HC A04/MF A01; ESA Publications Div., ESTEC, Noordwijk, Netherlands, 30 Dutch guilders

The present status of the National Space Development Agency of Japan (NASDA) activity, is described. The future plans concerning the issue of First National Processing (FMPT) and Japanese Experiment Module (JEM) which are manned space activities in development phase in Japan, are discussed. In the design of JEM, the safety and rescue has the high priority. The future programs research consists of rendezvous docking, data relay satellite network and reentry vehicle. It is shown that the requirement of interoperability can not be neglected. ESA

N90-15982# European Space Agency, Paris (France).
RVD SCENARI AND INTERFACES BETWEEN HERMES AND SPACE STATION
J.-J. Capart *In its* Crew Safety and Rescue in Space: An International Approach Aug. 1989 p 47-52 (For primary document see N90-15974 08-16)
Copyright Avail: NTIS HC A04/MF A01; ESA Publications Div., ESTEC, Noordwijk, Netherlands, 30 Dutch guilders

The European manned transportation system, Hermes, operational at the end of the century, is examined. The range of missions, for which Hermes is designed are presented. The adaptability of Hermes to visit diferent stations, and to various in-orbit interventions both external and internal (with the support of a manipulator arm and extravehicular suit) are illustrated. The possible scenarios for crew transport and rescue missions are discussed. An approach for improving the interoperability of manned systems, by international cooperation and standardization, is provided. ESA

N90-16199# European Space Agency. Centre Spatial de Toulouse (France). Hermes Project Dept.
THE HERMES DEVELOPMENT PROGRAM
J. Herholz *In* DGLR, Flows with Separation 1988 p 377-396 (For primary document see N90-16169 08-34)
Avail: NTIS HC A17/MF A03

17 SPACE COMM., SPACECRAFT COMM., COMMAND & TRACKING

Includes telemetry; space communications networks; astronavigation and guidance; and radio blackout.

For related information see also *04 Aircraft Communications and Navigation* and *32 Communications and Radar.*

N90-15983*# National Aeronautics and Space Administration. Lewis Research Center, Cleveland, OH.
A BURST COMPRESSION AND EXPANSION TECHNIQUE FOR VARIABLE-RATE USERS IN SATELLITE-SWITCHED TDMA NETWORKS
James M. Budinger Mar. 1990 19 p Prepared for presentation at the 13th International Communication Satellite Systems Conference, Los Angeles, CA, 11-15 Mar. 1990; sponsored in part by AIAA
(NASA-TM-102414; E-5177; NAS 1.15:102414; AIAA-90-0850)
Avail: NTIS HC A03/MF A01 CSCL 17B

A burst compression and expansion technique is described for asynchronously interconnecting variable-data-rate users with cost-efficient ground terminals in a satellite-switched, time-division-multiple-access (SS/TDMA) network. Compression and expansion buffers in each ground terminal convert between lower rate, asynchronous, continuous-user data streams and higher-rate TDMA bursts synchronized with the satellite-switched timing. The technique described uses a first-in, first-out (FIFO) memory approach which enables the use of inexpensive clock sources by both the users and the ground terminals and obviates the need for elaborate user clock synchronization processes. A continous range of data rates from kilobits per second to that approaching the modulator burst rate (hundreds of megabits per second) can be accommodated. The technique was developed for use in the NASA Lewis Research Center System Integration, Test, and Evaluation (SITE) facility. Some key features of the technique have also been implemented in the gound terminals developed at NASA Lewis for use in on-orbit evaluation of the Advanced Communications Technology Satellite (ACTS) high burst rate (HBR) system. Author

18 SPACECRAFT DESIGN, TESTING AND PERFORMANCE

Includes satellites; space platforms; space stations; spacecraft systems and components such as thermal and environmental controls; and attitude controls.

For life support systems see *54 Man/System Technology and Life Support.* For related information see also *05 Aircraft Design, Testing and Performance, 39 Structural Mechanics,* and *16 Space Transportation.*

N90-15984# Department of the Air Force, Washington, DC.
DEFENSE TO LASER LIGHT IRRADIATION Patent
James D. Barry, inventor (to AF) and Chandler J. Kennedy, inventor (to AF) 1 Aug. 1989 7 p Filed 6 Jan. 1982 Supersedes US-Patent-Appl-SN-338198
(AD-D014286; US-Patent-4,852,452; US-Patent-Appl-SN-338198; US-Patent-Class-89-1.11) Avail: US Patent and Trademark Office CSCL 17/4

A satellite defends itself by having a plurality of corner cube retroreflectors with shutters, each having a laser light sensor. It is assumed that the attacker first must obtain positional and range information with a pulsed laser. When one of the sensors detects these low power laser pulses, it causes the shutter of the corner cube array to open and return the pulses with sufficient strength to saturate or damage the attack sensors. GRA

N90-15985*# Rockwell International Corp., Canoga Park, CA. Energy Technology Engineering Center.
THE GEVALTIG: AN INERTIAL FUSION POWERED MANNED SPACECRAFT DESIGN FOR OUTER SOLAR SYSTEM MISSIONS Final Report
K. A. Murray Oct. 1989 53 p
(NASA Order C-32002-J)
(NASA-CR-185163; NAS 1.26:185163; ETEC-89-7) Avail: NTIS HC A04/MF A01 CSCL 22B

The Gevaltig is an inertial fusion powered rocket engine capable of manned missions to other planets with round trip mission times as low as 100 days. The Gevaltig design was previously described for a mission to Mars. This effort defines the spacecraft components in terms of mass and presents a mission analysis for a manned trip to Titan, a moon of Saturn. The Gevaltig component masses are provided as a function of fuel pellet ignition frequency. These variable mass components include the fuel tank, radiators, structure and EM pumps. Fixed mass components include the drivers, coil, coil shield, power processing system, payload, crew shield and laser mirrors. A 6 MW nuclear reactor is included in the design for startup purposes. Various combinations of thrust, mission duration and specific impulse were evaluated to determine a reasonable mission scenario for the Titan mission. The mission analysis yielded several viable mission scenarios, with round trip durations of 370 to 500 days and initial (launch) masses from lunar orbit of 2500 to 20,000 metric tons. Author

N90-15986# Consiglio Nazionale delle Ricerche, Frascati (Italy). Ist. di Fisica dello Spazio Interplanetario.
HOLLOW-CATHODE EXPERIMENTS TO SUPPORT ELECTRODYNAMIC TETHER APPLICATIONS
G. Vannaroni, U. Guidoni, C. B. Cosmovici, and F. DeVenuto Mar. 1989 21 p Sponsored by Piano Spaziale Nazionale, Rome, Italy
(IFSI-89-5; ETN-90-96167) Avail: NTIS HC A03/MF A01

Interaction experiments between two hollow cathode plasma sources are carried out in a plasma chamber. The experiment is performed in order to simulate the electrodynamic phenomena of the tethered satellite system orbiting at ionospheric altitudes. The interaction region is investigated by means of Langmuir and emissive probes. Plasma parameter maps are carried out applying different voltage polarizations to the hollow cathode plasma contactor with respect to the ambient plasma. The results show the presence of two regions, the first where a double layer is formed, and the second presenting an electron heating effect. ESA

N90-15987# Consiglio Nazionale delle Ricerche, Frascati (Italy). Ist. di Fisica dello Spazio Interplanetario.
ELECTRICAL CHARACTERISTICS MEASUREMENTS FOR THE TSS-1 SATELLITE PAINTING
G. Vannaroni and U. Guidoni Apr. 1989 22 p
(IFSI-89-7; ETN-90-96169) Avail: NTIS HC A03/MF A01

The measurements performed in order to determine the electrical characteristics of some space paints are presented. These paints are going to be used as thermal coating of the external surface of the Tethered Satellite System number one (TSS-1) satellite. Painted samples used as Langmuir probes are tested in a plasma chamber, under plasma conditions close to ionospheric ones. The classical current-voltage technique is used to measure the volume resistivity of the paints. The results pointed out that all the painted samples behave as poor conductors compared with naked aluminum. For the NS43C paint, a quasi linear decrease of resistivity is found when the voltage applied across the layer is increased above 100V. ESA

N90-15988# Consiglio Nazionale delle Ricerche, Frascati (Italy). Ist. di Fisica dello Spazio Interplanetario.
RETE EXPERIMENT ACTIVITY AT THE TSS-1 POCC
U. Guidoni May 1989 36 p
(IFSI-89-12; ETN-90-96174) Avail: NTIS HC A03/MF A01

The Tethered Satellite System (TSS) project, with the Payload Operation Control Center (POCC) support requirements for Research Electrical Tethered Effect (RETE) real time activity during the TSS-1 mission is reported. Data access, reduction and display requirements are covered for the RETE Electrical Ground Support Equipment (EGSE), and information on the ground support of the experiment is addressed. The RETE activity requires full accessibility of its own data. This implies the request to have RETE telemetry streeped from the incoming telemetry stream and routed to the experiment's EGSE. A set of monitors, where the main aspects of the mission are summarized in real time, are needed, for the scientific return of the mission. ESA

N90-15989# European Space Agency, Paris (France).
COLUMBUS: A USER'S INTRODUCTION
Jocelyne Landeau, ed. and Norman Longdon, ed. Sep. 1989 33 p Original contains color illustrations
(ESA-BR-62; ISBN-92-9092-027-0; ISSN-0250-1589; ETN-90-96206) Copyright Avail: NTIS HC A03/MF A01; ESA Publications Div., ESTEC, Noordwijk, Netherlands, 30 Dutch guilders

Basic information about Columbus elements and their operations are given. Columbus is the program by which ESA participates in the international space station Freedom, which is based on a manned core station. The station is planned to be launched and assembled from 1995 onwards. The main objectives of the Columbus program are to: provide an in-orbit and a ground infrastructure which are compatible with the needs of European and international users from the mid-1990s onwards; develop further European capabilities in manned spaceflight: co-operate with the U.S. and other partners in an international space station in which Columbus is Europe's contribution; ensure the development of a European capability; ensure that the technological research and key technological development required for manned space flight and for the in-orbit operations, both manned and automatic, are carried out. The possibilities that Columbus offers to the users, and the user support access to Columbus, are considered. ESA

N90-15990# Technische Univ., Berlin (Germany, F.R.). Inst. fuer Luft- und Raumfahrt.
A MODULAR HABITATION UNIT ADAPTED FOR SERVICE IN LOW EARTH AND GEOSTATIONARY EARTH ORBITS [SYSTEMENTWURF EINER MODULAREN WOHNANLAGE MIT VARIABLER SCHWERKRAFT FUER ERDUMLAUFBAHNEN UNTER BESONDERER BERUECKSICHTIGUNG BETRIEBLICHER ERFORDERNISSE]
Jens Lassmann 20 Sep. 1988 93 p In GERMAN; ENGLISH

summary
(ILR-Mitt-217; ETN-90-95355) Avail: NTIS HC A05/MF A01

A possible concept for an extraterrestrial habitation unit is presented. It would provide an Earthlike environment and is designed to operate in orbit heights varying from 400 km (low earth orbit) to 36,000 km (geostationary earth orbit). Operational design aspects are described. Cost evaluations are presented.
ESA

19 SPACECRAFT INSTRUMENTATION

For related information see also *06 Aircraft Instrumentation* and *35 Instrumentation and Photography.*

No abstracts in this category.

20 SPACECRAFT PROPULSION AND POWER

Includes main propulsion systems and components, e.g., rocket engines; and spacecraft auxilliary power sources.

For related information see also *07 Aircraft Propulsion and Power, 28 Propellants and Fuels, 44 Energy Production and Conversion,* and *15 Launch Vehicles and Space Vehicles.*

N90-15991*# Morton Thiokol, Brigham City, UT. Space Operations.
SPACE SHUTTLE PRODUCTION VERIFICATION MOTOR 1 (PV-1) STATIC FIRE Final Test Report
Aug. 1989 142 p
(Contract NAS8-30490)
(NASA-CR-183784; NAS 1.26:183784; TWR-17592-Rev-B) Avail: NTIS HC A07/MF A01 CSCL 21H

All inspection and instrumentation data indicate that the PV-1 static test firing conducted 18 Aug. 1988 was successful. With the exception of the intentionally flawed joints and static test modifications, PV-1 was flight configuration. Fail-safe flaws guaranteeing pressure to test the sealing capability of primary O-rings were included in the aft field joint, case-to-nozzle joint, and nozzle internal Joint 5. The test was conducted at ambient conditions, with the exception of the field joints and case/nozzle joints which were maintained at a minimum of 75 F. Ballistics performance values were within specification requirements. The PV-1 motor exhibited chamber pressure oscillations similar to previously tested Space Shuttle redesigned solid rocket motors, particularly QM-7. The first longitudinal mode oscillations experienced by PV-1 were the strongest ever measured in a Space Shuttle motor. Investigation into this observation is being conducted. Joint insulation performed as designed with no evidence of gas flow within unflawed forward field joints. The intentionally flawed center and aft case field joint insulation performance was excellent. There was no evidence of hot gas past the center field joint capture feature O-ring, the case-to-nozzle joint primary O-ring, or the aft field joint primary O-ring. O-ring seals and barriers with assured pressure at the flaws showed erosion and heat effect, but all sealed against passage of hot gases with the exception of the aft field joint capture feature O-ring. There was no evidence of erosion, heat effect, or blowby on any O-ring seals or barriers at the unflawed joints. Nozzle performance was nominal with typical erosion. Post-test examination revealed that the forward nose ring was of the old high performance motor design configuration with the 150-deg ply angle. All nozzle components remained intact for post-test evaluation. The thrust vector control system operated correctly. The water deluge system, CO2 quench, and other test equipment performed as planned during all required test operations.
Author

N90-15992*# National Aeronautics and Space Administration. Lewis Research Center, Cleveland, OH.
DESIGN OF A THRUST STAND FOR HIGH POWER ELECTRIC PROPULSION DEVICES
Thomas W. Haag 1989 15 p Presented at the 25th Joint Propulsion Conference, Monterey, CA, 10-14 Jul. 1989; sponsored by AIAA, ASEE, ASME and SAE Previously announced in IAA as A89-47110
(NASA-TM-102372; E-5104; NAS 1.15:102372; AIAA-89-2829)
Avail: NTIS HC A03/MF A01 CSCL 21C

A thrust stand for use with high power electric propulsion devices was designed and tested. The thrust stand was specifically tailored to the needs of a 100 to 250 kW magnetoplasmadynamic (MPD) thruster program currently in progress at the NASA Lewis Research Center. The thrust stand structure was built as an inverted pendulum arrangement, supported at the base by water-cooled electrical power flexures. Thrust stand tares due to thruster discharge current were demonstrated to be negligible. Tares due to an applied field magnet current, after considerable effort, were reduced to less than 3.0 percent of measured thrust. These tares, however, could be determined independently and subtracted from the indicated thrust measurement. A detailed description is given for the thrust stand design and operation with a 100 kW class MPD device. Other thrust stand tares due to vibration and thermal effects are discussed, along with issues of accuracy and repeatability.
Author

N90-15993# Rocket Research Corp., Redmond, WA.
PULSED PLASMA MISSION ENDURANCE TEST Final Technical Report, Sep. 1984 - Jul. 1989
Joseph R. Cassidy Aug. 1989 151 p
(Contract F04611-84-C-0060)
(AD-A213462; AFAL-TR-88-105) Avail: NTIS HC A08/MF A01 CSCL 21/3

The objectives of this program were to evaluate the performance and to conduct a life investigation of one millipound Teflon Pulsed Plasma Thruster (PPT). The goal of the life demonstration was a total impulse of 70,000 lbf-s (312,000 N-S) or 14 million pulses. The PPT thruster was designed for satellite stationkeeping and drag make-up propulsion applications. It is extremely simple in concept, utilizing a solid propellant (Teflon), a simple electrode geometry (rails), and a common form of energy storage (capacitors). In application at the millipound level, this simplicity demonstrated itself ably in test flights aboard the LES-6 spacecraft, the SMS spacecraft, and on the Navy TIP and NOVA satellites. The PPT thrusters performed flawlessly in their role of drag make-up and precision spacecraft positional control. Scaling the PPT thruster to the millipound level for North-South stationkeeping application proved to be somewhat more difficult. The configuration changes required to achieve the higher thrust level complicated the design and made the component requirements more stringent. The background, program description, and test results from the PPT Mission Endurance Test program are provided. It also provides a lessons learned overview of the program to benefit future programs. Where appropriate, specific problem areas are addressed with a detailed description of the problems encountered and RRC recommended fixes for these problems.
GRA

N90-15994# Department of the Air Force, Washington, DC.
ADVANCED COMPOSITE POLAR BOSS Patent
Hugh M. Reynolds, inventor (to AF) and Curt M. Kawabata, inventor (to AF) 1 Aug. 1989 10 p Filed 16 Oct. 1987 Supersedes US-Patent-Appl-SN-109810
(AD-D014287; US-Patent-4,852,347; US-Patent-Appl-SN-109810)
Avail: US Patent and Trademark Office CSCL 21/8

Composite polar bosses applied in rocket motor cases have desirable characteristics. The lead time for a boss can be reduced from 6 to 12 months to 4 to 6 months. Weight savings for the boss/nozzle assembly are about 20 to 40 percent. A composite polar boss which attaches nozzle assemblies to solid fueled rocket motor cases is disclosed. This polar boss is a carbonized fabrication which sits within a circumferential indentation within the motor

case, and has a threaded inner circumference which permits the nozzle assembly to be attached thereto. The materials of the boss are selected to permit a service temperature of up to 3,200 F. GRA

N90-15995# Argonne National Lab., IL.
DYNAMICS ANALYSES OF SPACE POWER SYSTEMS USING THE SALT CODE
Howard K. Geyer, Samit K. Bhattacharyya, Nelson A. Hanan, and Julie M. Livingston (Westinghouse Electric Corp., Pittsburgh, PA.) 1989 10 p Presented at the 7th Symposium on Space Nuclear Power Systems, Albuquerque, NM, 7-11 Jan. 1990
(Contract W-31-109-eng-38)
(DE90-002274; CONF-900109-12) Avail: NTIS HC A02/MF A01

The dynamic behavior of large space power systems has been identified as a significant technical issue. To date several analyses of reactor kinetics have been reported in the literature, but there have been few (if any) studies of the dynamic response of the entire space power system. The problem is complex and required analytical methods are not generally available. Furthermore, given the conceptual state of current MMW space power systems designs, dynamic models of components are not generally available. The SALT code was used to perform preliminary analyses of the startup and shutdown transients of several proposed MMW system designs. A description is provided of the code methodology along with the results of the analyses performed for the NERVA derivative reactor (NDR) system. DOE

N90-15996*# Little (Arthur D.), Inc., Cambridge, MA.
CONCEPTUAL DESIGN OF A MOVING BELT RADIATOR SHUTTLE-ATTACHED EXPERIMENTS: TECHNICAL REQUIREMENT DOCUMENT
Jerry L. Aguilar Nov. 1989 63 p
(Contract NAS3-25356)
(NASA-CR-185168; NAS 1.26:185168) Avail: NTIS HC A04/MF A01 CSCL 10B

The technical requirements for a shuttle-attached Moving Belt Radiator (MBR) experiment are defined. The MBR is an advanced radiator concept in which a rotating belt radiates thermal energy to space. The requirements for integrating the MBR experiment in the shuttle bay are discussed. Requirements for the belt material and working fluid are outlined along with some possible options. The proposed size and relationship to a full scale Moving Belt Radiator are defined. The experiment is defined with the primary goal of dynamic testing and a secondary goal of demonstrating the sealing and heat transfer characteristics. A perturbation system which will simulate a docking maneuver or other type of short term acceleration is proposed for inclusion in the experimental apparatus. A deployment and retraction capability which will aid in evaluating the dynamics of a belt during such a maneuver is also described. The proposed test sequence for the experiment is presented. Details of the conceptual design are not presented herein, but rather in a separate Final Report. Author

N90-15997# Royal Armament Research and Development Establishment, Fort Halstead (England).
BURST PRESSURE PREDICTION OF METALLIC/FIBRE REINFORCED ROCKET MOTOR CASES USING AN ELASTO-PLASTIC INSTABILITY ANALYSIS
A. Groves and J. Margetson Jun. 1989 28 p
(RARDE-1/89; BR110718; ETN-90-96141) Copyright Avail: NTIS HC A03/MF A01

A numerical elasto-plastic instability analysis is developed. The prediction of the axial burst pressure of metallic rocket motor cases, circumferentially reinforced with a pre-tensioned fiber overwind, is carried out. Numerical derived burst pressure values are compared with experimental results. An analytical burst pressure analysis is also derived, based on numerical and experimental observations. The numerical analysis is applied for predicting the burst pressure of an unwound motor and overwound motors exhibiting hoop bursts through fiber failure. These burst pressure values are in good agreement with experimentally derived burst pressure results. ESA

N90-15998# European Space Agency, Paris (France).
FLIGHT EXPERIMENT HARDWARE FOR SOUNDING ROCKET INVESTIGATIONS. MATERIALS SCIENCE AND FLUID SCIENCES
J. Hunt, ed. Aug. 1989 35 p Original contains color illustrations
(ESA-SP-1116; ISBN-92-9092-036-X; ISSN-0379-6566; ETN-90-96199) Copyright Avail: NTIS HC A03/MF A01; ESA Publications Div., ESTEC, Noordwijk, Netherlands, 20 Dutch guilders

The hardware development for ESA sounding rocket activities are reported. The TEXUS (Technologische Experimente Unter Schwerelosigkeit) and MASER (Materials Science Experiment Rocket) programs, are examined. The common features of TEXUS and MASER are analyzed. The following topics of each program are considered: sequence of flight events, concept of the experiment modules, data transmission and telescience and description of the experiment modules. A questionnaire for submission proposals is provided. ESA

N90-15999# European Space Agency, Paris (France).
FROM SMALL BEGINNINGS... THE STORY OF ESRO'S SOUNDING ROCKET PROGRAMME IN CELEBRATION OF THE TWENTY-FIFTH ANNIVERSARY OF THE FIRST ESRO SOUNDING ROCKET LAUNCH
Derek Eaton, A. Pedersen, and Norman Longdon, ed. Sep. 1989 30 p Original contains color illustrations
(ESA-BR-60; ISBN-92-9092-015-7; ISSN-0250-1589; ETN-90-96205) Copyright Avail: NTIS HC A03/MF A01; ESA Publications Div., ESTEC, Noordwijk, Netherlands, 30 Dutch guilders

The story of the ESRO'S sounding rocket program from 1964 to 1972 is summarized. Questions involving the meaning, the purposes, the achievements, the launch sites, and the payloads of sounding rockets, are discussed. It is shown that the evolution of technological developments of hardware led to an increasing reliability of hardware and operations so that a success rate of 50 percent in 1965 improved to 93 percent in 1972. The space science evolution by means of sounding rockets, is analyzed. ESA

N90-16000# Technische Univ., Delft (Netherlands). Faculty of Aerospace Engineering.
SOLID FUEL COMBUSTION CHAMBER, PHASE 10 Progress Report No. 11, Jan. - Jun. 1987
H. Wittenberg, P. A. O. G. Korting, T. Wijchers, P. J. M. Elands, F. Dijkstra, R. P. vandenBeg, and J. vandenBrand Nov. 1987 32 p Sponsored by the Netherlands Technology Foundation and the Organization for Applied Scientific Research Prepared in cooperation with Prins Maurits Lab. TNO
(LR-536; PML-1987-C141; ETN-90-95998) Avail: NTIS HC A03/MF A01

The tenth phase of the solid fuel combustion chamber project is described. The aim of the project is a better understanding of the flow and the combustion processes, occurring in solid fuel grains. In the scope of the work, the following topics are presented: the project management, the list of persons involved, the theoretical developments, the experiments performed, and the optical equipment applied. The financial support, the planned near and long term activities, the users committee, the publications and contacts are also included. ESA

N90-16001# Technische Univ., Delft (Netherlands). Faculty of Aerospace Engineerings.
SOLID FUEL COMBUSTION CHAMBER Progress Report No. 12, Jul. - Dec. 1987
H. Wittenberg, P. A. O. G. Korting, B. T. C. Zandbergen, T. Wijchers, P. J. M. Elands, J. P. deWilde, and F. Dijkstra Apr. 1988 46 p Sponsored in cooperation by the Organization for Applied Scientific Research Prepared in cooperation with Prins Maurits Lab. TNO

(Contracts STW-DLR-15-0120; TUDLR-A2L3-81-04)
(LR-555; PML-1988-C32; SFCC-Publ-52; ETN-90-96000) Avail: NTIS HC A03/MF A01

The development phase of the solid fuel combustion chamber project, between July and December 1987 is reported. The research activities carried out in this period are reviewed. the mass flow modeling, as a function of the heat flux, the experiments with hydroxy terminated poly butadene fuels, and the evaluation of the laser Doppler anemometry technique for focal flow velocity measurements, are discussed. The project support and personnel, the program status and the near term activities, are also included. ESA

23 CHEMISTRY AND MATERIALS (GENERAL)

No abstracts in this category.

24 COMPOSITE MATERIALS

Includes physical, chemical, and mechanical properties of laminates and other composite materials.

For ceramic materials see *27 Nonmetallic Materials*.

N90-16002# National Inst. of Standards and Technology, Gaithersburg, MD. National Engineering Lab.
ASSESSING THE FLAMMABILITY OF COMPOSITE MATERIALS
Thomas J. Ohlemiller Jan. 1989 27 p Sponsored by David W. Taylor Naval Ship Research and Development Center, Annapolis, MD
(PB90-112996; NISTIR-89/4032) Avail: NTIS HC A03/MF A01 CSCL 11D

A comprehensive approach to properly characterizing the flammability of composite materials is outlined. Laboratory-scale tests are described which provide measures of material ignitability, flame spread rate and heat release rate. Rather than expressing the measures as arbitrary indices, they are interpreted in terms of models of the controlling phenomena designed to provide information that can be generalized to full scale contexts, particularly compartment fires. GRA

N90-16003# Sandia National Labs., Albuquerque, NM. Joining and Physical Metallurgy Div.
EVALUATION OF POTENTIAL COLD X RAY SHIELD MATERIALS TESTED ON PROTO II
James P. Lucas Dec. 1989 46 p
(Contract DE-AC04-76DR-00789)
(DE90-004348; SAND-89-8224) Avail: NTIS HC A03/MF A01

Several composite materials were irradiated with cold x rays of photon energies of 1 and 3 keV line radiation generated by imploding Ne and Ar gas using the Proto II accelerator. The materials were exposed to fluences of up to 60 cal/sq cm. Continuous reinforced carbon phenolic and carbon-carbon composites and an inorganic rigid SiO2 fiber-Al2 O3 fiber composite were tested. Examination of the irradiated surfaces of all materials revealed varying degrees and types of damage with fluences levels. The surface of irradiated reinforced carbon phenolic (RCP) composite was characterized by blowoff debris and melting of the matrix resin. The melt depth of RCP materials increased as the fluence increased. Surface fibers of irradiated inorganic fibrous composite (IFC) exhibited severe melting, but the extent of surface blowoff debris was considerably less than that of RCP materials. Both melting and blowoff were minimal on the surface of irradiated reinforced carbon-carbon (RCC) composite, even at high fluence levels. Interior spall and delamination were seen in exposed RCP material above an apparent threshold fluence of approximately 15 cal/sq cm. Of the composite materials tested, RCC appeared to be the most attractive material for cold x ray shielding. DOE

N90-16004*# National Aeronautics and Space Administration. Hugh L. Dryden Flight Research Facility, Edwards, CA.
OPEN-MODE DELAMINATION STRESS CONCENTRATIONS IN HORSESHOE AND ELLIPTIC COMPOSITE CURVED BARS SUBJECTED TO END FORCES
William L. Ko and Raymond H. Jackson Washington Jan. 1990 25 p
(NASA-TM-4164; H-1567; NAS 1.15:4164) Avail: NTIS HC A03/MF A01 CSCL 11D

The multilayer theory of anisotropic elasticity and a finite element method were used to analyze the open-mode delamination stress concentrations in horseshoe and elliptic laminated composite curved bars. Two types of laminations, solid laminations and sandwich laminations, were analyzed. It was found that the open-mode delamination stress concentration could be greatly increased in these two types of curved bars by decreasing their aspect ratios. The open-mode delamination stress concentration generated in the solid laminations was found to be far more severe than that generated in the sandwich laminations. The horseshoe curved bar may be used to determine both the open-mode delamination strength of solidly laminated composites and the open-mode debonding strength of sandwiched laminated composites. However, the elliptic curved bar is only good for determining the open-mode delamination strength of solidly laminated composites. Author

N90-16005# Oak Ridge National Lab., TN.
THE STRUCTURE OF SILICA-POLYSILOXANE COMPOSITES AND ITS EFFECTS ON THEIR ELASTOMERIC PROPERTIES
Dale W. Schaefer, L. Jian, C. C. Sun, D. McCarthy, C. Y. Jiang, Y. P. Ning, J. E. Mark (Cincinnati Univ., OH.), and Steve Spooner 1989 3 p Presented at the Ultrastructure Processing of Ceramics, Glasses and Composites, Miami, FL, 20-23 Feb. 1990
(Contracts DE-AC05-84OR-21400; DE-AC04-76DP-00789; DAAL03-86-K-0032; AF-AFOSR-0020-83; NSF DMR-84-15082)
(DE89-014768; CONF-900213-1) Avail: NTIS HC A01/MF A01

Two factors have limited the understanding of the microstructure of complex phase-separated materials: the absence of unambiguous methods for characterizing structure, and the lack of reasonable models to predict structure based on chemical and physical parameters. Substantial progress, however, has been made in both these areas because of advances in instrumentation, advances in the interpretation of scattering from disordered systems, and advances in the development of simple models for complex disorderly growth processes. We attempt to build on these advances to enhance our understanding of composites. DOE

N90-16006# Oak Ridge Y-12 Plant, TN.
ZrO2 SINTERED COMPACT AND METHOD FOR ITS PRODUCTION
Ryoji Inoue and Hisao Hara 1989 7 p Transl. into ENGLISH of Japanese Patent Application No. 62-226859 (5 Oct. 1987)
(Contract DE-AC05-84OS-21400)
(DE90-004125; Y/TR-89-8) Avail: NTIS HC A02/MF A01

Conventionally, a ZrO2 sintered compact that has been made by adding a small amount of Y2O3 to ZrO2 is generally sub-stable tetragonal and is tough at low temperatures because of stress-induced transformation from the tetragonal to the monoclinic phase. Thus such compacts have been used primarily for tools that are used at low temperatures, such as cutlery. The addition of HfO2 is effective for raising the temperature at which the tetragonal crystal of a ZrO2 sintered compact is stabilized and thus for improving its toughness at higher temperatures: i.e., for keeping the tetragonal crystal in a sub-stable state even at high temperatures. However, when HfO2 was substituted for ZrO2 in a ZrO2 sintered compact containing Y2O3, it was not possible to obtain an adequate toughness at high temperatures. With reference to the above discussion, the purpose of this invention is to provide

a ZrO2 sintered compact and a method for its production whereby the ZrO2 sintered compact is made superior in toughness at high temperatures by selecting the most appropriate stabilizer. DOE

N90-16007*# National Aeronautics and Space Administration. Marshall Space Flight Center, Huntsville, AL.
INSTRUMENTED IMPACT AND RESIDUAL TENSILE STRENGTH TESTING OF EIGHT-PLY CARBON EOPOXY SPECIMENS
A. T. Nettles Jan. 1990 43 p
(NASA-TP-2981; NAS 1.60:2981) Avail: NTIS HC A03/MF A01 CSCL 11D

Instrumented drop weight impact testing was utilized to examine a puncture-type impact on thin carbon-epoxy coupons. Four different material systems with various eight-ply lay-up configurations were tested. Specimens were placed over a 10.3-mm diameter hole and impacted with a smaller tup (4.2-mm diameter) than those used in previous studies. Force-time plots as well as data on absorbed energy and residual tensile strength were gathered and examined. It was found that a critical impact energy level existed for each material tested, at which point tensile strength began to rapidly decrease with increasing impact energy. Author

N90-16008*# National Aeronautics and Space Administration. Lewis Research Center, Cleveland, OH.
PROBABILISTIC SIMULATION OF UNCERTAINTIES IN COMPOSITE UNIAXIAL STRENGTHS
C. C. Chamis and T. A. Stock (Cleveland State Univ., OH.) 1990 16 p Presented at the 45th Annual Conference of the Society of Plastics Industry Reinforced Plastics, Washington, DC, 12-16 Feb. 1990
(NASA-TM-102483; E-5269; NAS 1.15:102483) Avail: NTIS HC A03/MF A01 CSCL 11D

Probabilistic composite micromechanics methods are developed that simulate uncertainties in unidirectional fiber composite strengths. These methods are in the form of computational procedures using composite mechanics with Monte Carlo simulation. The variables for which uncertainties are accounted include constituent strengths and their respective scatter. A graphite/epoxy unidirectional composite (ply) is studied to illustrate the procedure and its effectiveness to formally estimate the probable scatter in the composite uniaxial strengths. The results show that ply longitudinal tensile and compressive, transverse compressive and intralaminar shear strengths are not sensitive to single fiber anomalies (breaks, intergacial disbonds, matrix microcracks); however, the ply transverse tensile strength is.
Author

25 INORGANIC AND PHYSICAL CHEMISTRY

Includes chemical analysis, e.g., chromatography; combustion theory; electrochemistry; and photochemistry.

For related information see also *77 Thermodynamics and Statistical Physics.*.

N90-16009 Michigan Univ., Ann Arbor.
SWIRL-STABILIZED FLAMES: FLUID DYNAMICS, MIXING, AND FLAME STABILITY LIMITS Ph.D. Thesis
Ruey-Hung Chen 1988 112 p
Avail: Univ. Microfilms Order No. DA8907011

Several unique features of swirl-stabilized flames were quantified and explained in this study. Results can be categorized into the following four areas: (1) Recirculation strength was measured and various trends were determined; (2) The fuel-air mixing process was visualized in swirl flames, which was not done in the past; and (3) Flame length, which is a measure of overall fuel-air mixing, was measured and various trends were determined. A simple scaling analysis was developed which explained several of the measured trends in the flame length data and why swirl flame lengths do not scale in the same manner as jet flames; (4) Three distinct flame blowout limits were measured; they are due to excessive swirl, very weak swirl, and excessive fuel jet momentum, respectively. Laser Doppler Velocimetry (LDV) was used to obtain relevant velocity data. It was found that: (1) the density change due to combustion promotes recirculation; (2) increasing swirl and Reynolds numbers affect the inlet boundary conditions in a favorable manner to cause recirculation; and (3) increasing fuel jet momentum weakens recirculation strength and destabilizes the flame. Comparisons were drawn with bluff-body flows and vortex breakdown phenomena observed in water flows. It was found that Reynolds number effects that had been reported for water flow studies are similar to effects observed in the present flame. Dissert. Abstr.

N90-16010# Wisconsin Univ., Madison.
THE EIGHTEENTH CONFERENCE ON STOCHASTIC PROCESSES AND THEIR APPLICATIONS Final Report
D. Griffeath, J. Kuelbs, and T. Kurtz 1 Jul. 1989 103 p Conference held in Madison, WI, 25 Jun. - 1 Jul. 1989; sponsored by NSF, AFOSR, ARO, NSA and ONR
(Contract DAAL03-89-G-0029)
(AD-A212301; ARO-26196.1-MA-CF) Avail: NTIS HC A06/MF A01 CSCL 12/2

Topics addressed include: stochastic processes; hypoelliptic processes; Witten-Sander models; differential geometry; two-dimensional percolation; cellular automata; diffeomorphisms; and Boltzmann equations of motion. B.G.

N90-16011# Stanford Univ., CA. Dept. of Materials Science and Engineering.
SOLID-STATE ELECTROLYTE CATALYSIS FOR METHANE AND OXYGEN SYNTHESIS Annual Report No. 1, 1 Aug. 1987 - 31 Jul. 1988
Turgut M. Guer, Henry Wise, and Robert A. Huggins Sep. 1988 15 p
(Contract GRI-5087-260-1534)
(PB90-100231; GRI-89/0038) Avail: NTIS HC A03/MF A01 CSCL 07D

The performance of an oxygen-ion conducting electrochemical cell for enhancing the conversion of CO2 to CH4 and O2 was investigated. An oxide-ion conducting solid electrolyte in an electrochemical reactor configuration was used to carry out surface catalysis for the breakage of carbon-oxygen bonds as well as formation of carbon-hydrogen bonds, and removal of oxygen by ionic migration through the solic electrolyte. Experiments with CO2-H2 reaction mixtures on Ni and Pt catalyst electrodes in contact with a zirconia solid electrolyte show that CO2 is converted to CH4 at an increased rate under DC biased conditions. The solid state electrochemical approach resulted in enhancements of up to two orders of magnitude in the methanation rate of CO2, despite the use of a configuration that was not optimized. The mechanistic sequence of the reation involves the formation of CO, which is reduced to C(sub s), which is then hydrogenated to CH4. GRA

N90-16012# SRI International Corp., Menlo Park, CA.
MECHANISMS OF THE ELECTROCHEMISTRY OF SMALL ORGANIC MOLECULES Annual Report, Mar. 1988 - Feb. 1989
K. W. Frese, Jr. and M. Cinnibulk Jun. 1989 65 p
(Contract GRI-5083-260-0922; SRI Proj. PYU-7142)
(PB90-100785; GRI-89/0127) Avail: NTIS HC A04/MF A01 CSCL 07D

The mechanisms of electrochemical reactions of small molecules, including CH4, CO2, CO, and C2H4, were investigated. The reactions included oxidations, reductions, and coupling of radicals to achieve higher carbon content molecules. Modeling work included development of the role of the thermodynamics of the rate limiting step in a consecutive step electrochemical reaction. GRA

N90-16013*# Lockheed Engineering and Sciences Co., Houston, TX.
DEMONSTRATION OF THE FEASIBILITY OF LASER INDUCED FLUORESCENCE FOR ARC JET FLOW DIAGNOSTICS

Sivaram Arepalli Oct. 1989 29 p
(Contract NAS9-17900)
(NASA-CR-185595; NAS 1.26:185595; LESC-27642; Rept-83-102)
Avail: NTIS HC A03/MF A01 CSCL 07D

Laser Induced Fluorescence (LIF) studies are carried out on nitric oxide and oxygen molecules in the arc jet flows at the NASA Johnson Space Center Reentry Testing Facility. Measurements are taken in the free stream and from a blunt body shock layer. Tests are performed under different flow conditions to determine the feasibility and sensitivity of the LIF technique for various species. This is developed as a part of high enthalpy flow diagnostics and will be useful to elucidate the rotational and vibrational temperatures. Adequate sensitivity for the detection of O(2) and NO is demonstrated. Proposed improvements of the existing system are presented. Author

N90-16014# George Mason Univ., Fairfax, VA.
ANALYSIS AND EVALUATION OF TECHNICAL DATA ON THE PHOTOCHROMIC AND NON-LINEAR OPTICAL PROPERTIES OF MATERIALS Quarterly Report No. 3
Robert F. Cozzens 1 Sep. 1989 4 p
(Contract DAAB07-89-C-F404; ARPA Order 6631)
(AD-A214050) Avail: NTIS HC A01/MF A01 CSCL 07/4

The overall goal of this effort is to provide technical assistance to Dr. Frank Patten (DARPA) in evaluating data on materials, especially polymers, that may be useful in the development of optical limiters for the protection of eyes and electro-optic sensors from exposure to damaging levels of laser radiation. A principle task is to assist in the development of a predictive capability in assessing the viability of various protective approaches and to determine the theoretical limitations which may exist in the use of organic materials as optical switches and limiters. Two generic molecular structures which offer the greatest near term promise for high chi-3 systems are the phthalocyanine structures and ladder polymers, especially those containing heteronuclear atoms (S or N) in the aromatic ring. In addition, both of these molecular systems tend to be thermally stable, enabling them to survive relatively large doses of absorbed laser radiation. Phthalocynanine chromphores are generally deeply colored and thus strong light absorbers. They may be limited to use as resonant chi-3 materials. Analysis and discussion of an ablative mirror/optical fuse system located at the focus of an optical device used for eye/sensor hardening has been undertaken as a tangential effort under this project. GRA

N90-16015# York Univ., Downsview (Ontario). Dept. of Chemistry.
ELECTROCHEMICAL PARAMETERIZATION OF METAL COMPLEX REDOX POTENTIALS, USING THE RUTHENIUM(III)/RUTHENIUM(II) COUPLE TO GENERATE A LIGAND ELECTROCHEMICAL SERIES Technical Report, Aug. 1989 - Aug. 1990
A. B. P. Lever 20 Oct. 1989 55 p Sponsored in part by Natural Sciences and Engineering Research Council, Ottawa, Ontario
(Contract N00014-84-G-0201)
(AD-A214439; TR-27) Avail: NTIS HC A04/MF A01 CSCL 07/4

A ligand electrochemical parameter, El (L), is described to generate a series which may be used to predict M(n)/M(n-1) redox potentials by assuming that all ligand contributions are additive. In this fashion it performs a similar purpose to the Dq parameter in electronic spectroscopy. The parameter is defined as 1/6 that of the Ru(III)/Ru(II) potential for species RuL6 in acetontrile. The El(L) values for over 200 ligands are presented and the model is tested over a wide range of coordination complexes and organometallic species. The redox potential of a M(n)/M(n-1) couple is defined to be equal to:-E(calc) = f Sigma EL (L) + c. The values of f and C, which are tabulated, depend upon the metal and redox couple, and upon spin state and stereochemistry, but, in organic solvents, are generally insensitive to the net charge of the species. Consideration is given to synergism, the potentials of isomeric species, and the situations where the ligand additivity model is expected to fail. In this initial study, the redox couples are restricted almost exclusively to those involving the loss or addition of an electron to the tzg (in Oh) sublevel. GRA

N90-16016# Sao Paulo Univ. (Brazil). Inst. de Quimica.
CARBON-13 NUCLEAR MAGNETIC RESONANCE OF HETEROCYCLIC SALTS AND ITS PRECURSORS Ph.D. Thesis
Haydee Rodrigues Freire 1989 92 p In PORTUGUESE; ENGLISH summary
(DE89-635768; INIS-BR-1583) Avail: NTIS (US Sales Only) HC A05/MF A01

The synthesis of 1,2,3,6-tetrahydro 1,1-dimethyl 3-oxo 5-phenylpyridinium bromides containing the following 4' substituents: H, Me, Cl, Br, OMe, and NO2, is described. The phenacyl bromides were characterized by their melting points and by their infrared and proton NMR spectra. Some studies on the C-13 NMR spectra of the phenacyl bromides, the quartenary ammonium salts, and the cyclic salts are given. The effect of substituents on the electronic structure of these compounds and on the chemical shifts of the different carbon atoms in terms of electronic and steric effects are discussed. DOE

N90-16017# Princeton Univ., NJ. Dept. of Mechanical and Aerospace Engineering.
COMPREHENSIVE MECHANISMS FOR COMBUSTION CHEMISTRY: AN EXPERIMENTAL AND NUMERICAL STUDY WITH EMPHASIS ON APPLIED SENSITIVITY ANALYSIS Technical Progress Report, 15 Mar. 1987 - 1 Nov. 1989
Frederick L. Dryer Nov. 1989 117 p
(Contract DE-FG02-86ER-13503)
(DE90-003904; DOE/ER-13503/3) Avail: NTIS HC A06/MF A01

This research program is an integrated effort for determining the reaction mechanisms responsible for the oxidation of hydrocarbon structures under conditions representative of combustion environments. The experimental aspects of the program are presently conducted in a flow reactor facility which permits chemical kinetic observations at atmospheric pressure, in the temperature range of about 850 K to 1200 K, and for reaction times the order of 10 to 1000 msec. Specifically addressed is the oxidation and pyrolysis of ethanol, methanol, and formaldehyde. DOE

N90-16018# California Univ., Berkeley. Lawrence Berkeley Lab. Applied Sciences Div.
THE CONTINUOUS CRYSTALLIZATION OF SULFUR FORMED BY THE LIQUID-PHASE REACTION OF HYDROGEN SULFIDE AND SULFUR DIOXIDE Ph.D. Thesis
Craig A. Stevens and Scott Lynn Sep. 1989 199 p
(Contract DE-AC03-76SF-00098)
(DE90-003991; LBL-27956) Avail: NTIS HC A09/MF A01

The crystallization of elemental sulfur is a unit operation in a process being developed to remove hydrogen sulfide from industrial gas streams. The sulfur is formed by the irreversible, liquid-phase reaction of hydrogen sulfide (H2S) and sulfur dioxide (SO2). Low-temperature sulfur solubility data in triethylene glycol dimethyl ether (Triglyme) and diethylene glycol methyl ether (DGM) were collected. The effects of temperature and water concentration in the solvents on sulfur solubility were correlated. The thermal crystallization of sulfur from Triglyme was studied in a laboratory-scale experimental crystallizer. The dependence of crystal-size distribution on residence time, slurry density, impeller power input, and water concentration in the solvent was determined. A crystallization model, applicable to the experimental crystallizer, was derived from population balance theory and verified using the experimental data. The crystallization kinetics of the sulfur/Triglyme system were obtained from the crystallization model. The reactive crystallization of sulfur formed by the reaction between H2S and SO2 was also studied. A reactor/crystallizer model was developed from the reaction kinetics and from the thermal crystallization kinetics. Reactive crystallization experiments verified the model. An industrial-sized reactor/crystallizer was designed from the model. DOE

N90-16019# Oak Ridge National Lab., TN. Chemical Technology Div.

USING INORGANIC MEMBRANES TO SEPARATE GASES: R AND D STATUS REVIEW

B. Zane Egan Nov. 1989 70 p

(Contract DE-AC05-84OR-21400)

(DE90-004386; ORNL/TM-11345) Avail: NTIS HC A04/MF A01

This report describes the preparation, properties, and utilization of inorganic membranes, primarily emphasizing the research and development aspects related to the separation of gases. Included are definitions, a brief historical background, a comparison of inorganic and polymeric membranes, a discussion of separation mechanisms, descriptions of various preparation or fabrication methods, studies and applications of inorganic membranes related to gas separations, and compilation of information on commercially available porous materials. The information is evaluated in terms of limitations, needs, and prospects for future development. The major types of gas transport through porous membranes are discussed in terms of viscous flow, free-molecule (Knudsen) flow, surface diffusion, capillary condensation, surface adsorption, ion exchange, and molecular sieving. Membrane preparation and fabrication techniques include: extrusion, powder suspension, molten salt inclusion, phase separation and leaching, nuclear track etching, dynamic deposition, anodic oxidation, pyrolysis, particle dispersion/slipcasting, and thin film deposition. Metallic, porous glass, ceramic, and metallic oxide membranes for separating various gases are tabulated. The needs for improved membrane materials, metal-to-nonmetal seals which will withstand high temperatures and pressures, and better membrane characterization techniques are discussed. DOE

N90-16020# Argonne National Lab., IL. Materials Science Div.

NEW ELECTRICALLY CONDUCTING SOLIDS BASED ON NICKEL(II) - BIS(1,3-DITHIOLE-2-THIONE-4,5-DISELENOLATE)

Aravinda M. Kini, Mark A. Beno, S. Budz, H. H. Wang, and Jack M. Williams 1989 12 p Presented at the Materials Research Society Fall Meeting, Boston, MA, 27 Nov. - 1 Dec. 1989

(Contract W-31-109-eng-38)

(DE90-003788; CONF-891119-30) Avail: NTIS HC A03/MF A01

Electrochemical oxidation of the metal-organic complex, nickel(II)-bis(1,3-dithiole 2-thione 4,5-diselenolate) or Ni(dsit)2(sup -2), yields highly conducting salts, in which the stoichiometry and packing arrangement depends critically on the site of the counter-cations incorporated. Smaller counter-cations, e.g., tetramethylammonium and tetramethylphosphonium ions, yield salts with a 1:2 cation N:(dsit)2 stoichiometry, while the larger tetraethylammonium ion yields a salt with 2:2 stoichiometry. In both these salts, the Ni(dsit)2 units occur as tightly bound dimers, in which coordination geometry of nickel is a unique, but not unprecedented square-pyramidal type. Moreover, the packing arrangement of (Ni(dsit)2)2 dimer units in both (Me4N)(Ni(dsit)2)2 and (Me4P)(Ni(dsit)2)2 is (kappa)-type, similar to that found in the organic superconductor with the highest-known T(sub c) (10.4 K), (kappa)-(BEDT-TTF)2Cu(NCS)2. Both these salts possess good room temperature conductivities, (sigma(sub rt) = 36 and 19 S./cm respectively), but the temperature dependence of their conductivities is characteristic of semiconductors with small bandgaps (E(sub g) = 0.11 and 0.13 eV respectively). The 2:2 salt (Et4N)2(Ni(dsit)2)2, on the other hand, has a substantially lower room temperature conductivity, about six orders of magnitude smaller than that of the 1:2 salts. DOE

N90-16021# Institut Franco-Allemand de Recherches, Saint-Louis (France).

MULTIDIMENSIONAL NUMERICAL SIMULATION OF LARGE CALIBER IGNITION PROCESSES

D. Hensel and R. Heiser (EMI Ltd., Hayes, England) 5 Oct. 1988 25 p Presented at the 5th Anglo-German Meeting on Internal Ballistics, Meppen and Unterluess, Fed. Republic of Germany, 1-10 Jun. 1988

(ISL-CO-233/88; ETN-90-96092) Avail: NTIS HC A03/MF A01

Multidimensional two phase models for predicting phenomena associated with the ignition of granular charge are presented. In order to avoid ignition problems, the ignitor and the propellant must be adapted to each other. A computational model which yields detailed informaton about the processes occurring during the ignition period and which can be used for adapting the ignitor to the propellant, is developed. The model describes the interaction of both components as an axisymmetric two phase flow. By this tool, the investigation of the ignition and combustion of a charge is possible. This model allows the study of gas pressure, intergranular stress and temperature and the analysis of the dependency on the ignitor's position, its thermodynamic properties and its venting characteristics. This capability is underlined by computational results. ESA

N90-16022# Institut National des Sciences Appliquees de Lyon, Villeurbanne (France). Lab. de Genie Electrique et de Ferroelectricite.

STUDY OF PHASE TRANSFORMATIONS LIQUID-SOLID-SOLID OF ULTRAFINE PARTICLES Ph.D. Thesis [ETUDE DES TRANSFORMATIONS LIQUIDE-SOLIDE-SOLIDE DE MATERIAUX FINEMENT DIVISES]

Martinie Bernard 1989 178 p In FRENCH

(ISAL-89-0019; ETN-90-96036) Avail: NTIS HC A09/MF A02

Research into phase transformations of ultrafine particles dependent on their size, is described. AgNO3, AgI, CsCl, CsNO3 and RbCl are passed through pores ranging between 3.5 nm and 100 nm. The nucleation behavior within the pores is studied. The results are analyzed to determine the phenomena causing the lowering of transition temperatures in solid to solid transitions. ESA

N90-16023# Laboratoire d'Automatique et d'Analyse des Systemes, Toulouse (France). Div. Composants Electroniques.

STUDY OF SILICON NITRIDE pH RESPONSE TO THE FABRICATION OF MICROELECTRONIC SENSORS Ph.D. Thesis - Toulouse Univ.

Christophe Lefevre 1989 162 p In FRENCH; ENGLISH summary

(LAAS-89229; ETN-90-96040) Avail: NTIS HC A08/MF A01

The sensitivity and time behavior of the pH response of an Si3N4 membrane elaborated by LPCVD (low pressure chemical vapor deposition) is studied. Experimental data obtained from the study of the capacitance of the electrolyte/Si3N4/SiO2/Si system is presented. The influence of such parameters as fabrication processes of Si3N4, electrode encapsulation techniques and soaking modes of electrodes between two measurements is analyzed in relation to the pH characteristics of these structures. A new mode of encapsulation is proposed. Such encapsulation ensures complete isolation of the components, in order to measure the real characteristics of one silicon nitride material. Faradic currents occur with diffusion of hydrogenous species across the membrane. They show the limits of the silicon nitride passivation. A point of zero charge occurs at 6.5 pH according to the site-binding theory. This theory explains the mechanism governing the Si3N4 pH behavior and provides a theoretical analysis of such structures. ESA

N90-16024# Kernforschungsanlage, Juelich (Germany, F.R.). Inst. fuer Nukleare Sicherheitsforschung.

KINETICS OF THE GRAPHITE/OXYGEN REACTION IN THE IN-PORE DIFFUSION CONTROLLED REGIME. PART 3: INFLUENCE OF BOUNDARY LAYER DIFFUSION IN KINETIC EXPERIMENTS AT TEMPERATURES 970K TO 1170K

Hans-Klemens Hinssen and Rainer Moormann Jun. 1989 31 p In GERMAN; ENGLISH summary

(JUEL-2284-Pt-3; ISSN-0366-0885; ETN-90-96073) Avail: NTIS HC A03/MF A01

A reevalution of experimental data for the kinetics of the reaction between oxygen and nuclear graphites at temperatures 970 to 1170K is presented. This reevalution mainly covers an improved handling of the influence of boundary layer diffusion (mass transfer) on the measured rates. It is demonstrated, that a remarkable

influence of boundary layer diffusion exists down to rather low temperatures. Rates for the in-pore diffusion controlled regime, presented earlier are corrected to higher values which increase with increasing temperature. The maximum correction factor is 1.6. ESA

N90-16025# Oak Ridge National Lab., TN. Analytical Chemistry Div.
PERFORMANCE OF AN INDUCTIVELY COUPLED PLASMA-MASS SPECTROMETER ANALYZER SYSTEM Foreign Travel Report, 13-17 Nov. 1989
J. H. Stewart and W. H. Christie 17 Nov. 1989 29 p
(Contract DE-AC05-84OR-21400)
(DE90-004002; ORNL/FTR-3488) Avail: NTIS HC A03/MF A01

The Analytical Chemistry Division was notified on Monday, October 25, 1989, that the new ICP-MS analyzer fabrication was completed and the system would be ready for the detailed performance testing required for shipping approval on November 13, 1989. The travelers promptly prepared travel authorization forms and obtained certified NIST (NBS) and EPA reference materials to be utilized for the equipment certification. The tests began on November 13 as scheduled and concluded on Thursday, November 16. The analyzer system was well made, the VG staff was knowledgeable, and completely cooperative. A new quality assurance feature of acceptance was introduced into this purchase, and we met with the VG Quality Assurance Manager, Mr. Steven Ward. He impressed us with his concern for producing the highest quality product and agreed to fill out the ORNL QA certification document. DOE

N90-16026# Tennessee Univ., Knoxville. Measurement and Control Engineering Center.
ON-LINE CHEMICAL COMPOSITION ANALYZER DEVELOPMENT Final Report
Arlene A. Garrison, Emil C. Muly, Michael J. Roberts, and Charles F. Moore Jul. 1989 116 p
(Contract DE-FC07-88ID-12691)
(DE90-004079; DOE/ID-12691/1) Avail: NTIS HC A06/MF A01

The energy consumed in distillation processes in the United States represents nearly 3 percent of the total national energy consumption. If effective control of distillation columns can be accomplished, it was estimated that it would result in a reduction in the national energy consumption of 0.3 percent (1). Real time control based on mixture composition could achieve these savings. However, the major distillation processes represent diverse applications and at present there does not exist a proven on-line chemical composition sensor technology which can be used to control these diverse processes in real time. DOE

26 METALLIC MATERIALS

Includes physical, chemical, and mechanical properties of metals, e.g., corrosion; and metallurgy.

N90-16027# State Univ. of New York, Albany.
SURFACE STUDIES AT THE NSLS Progress Summary Report
Nov. 1989 4 p
(Contract DE-FG02-86ER-45239)
(DE90-003173; DOE/ER-45239/T1) Avail: NTIS HC A01/MF A01

The most significant results obtained in the past six months are the growth and the identification of a new, body-centered-tetragonal, phase of copper. The new phase was grown epitaxially on a surface of palladium, and seems to confirm a prediction recently made by theorists at the University of Pennsylvania. A LEED intensity analysis was completed of the c(2 x 2) phase formed by Mn on Pd at low coverages, and have established that this phase is probably a Pd3Mn alloy with a Cu3Au structure. A study of the c(2 x 2) phase obtained by deposition of Mn on a Cu surface has so far produced no solution, despite intense calculational efforts and photoemission experiments. The evaluation of the photoemission experiments on Ag surfaces was completed successfully. DOE

N90-16028# Department of the Air Force, Washington, DC.
HIGH TEMPERATURE ALUMINUM-BASE ALLOY Patent
Yashwant R. Mahajan, inventor (to AF), Young-Won Kim, inventor (to AF), and Francis H. Froes, inventor (to AF) 25 Jul. 1989 2 p Filed 13 Feb. 1989 Supersedes US-Patent-Appl-SN-310448 (AD-D014270; US-Patent-4,851,193; US-Patent-Appl-SN-310448)
Avail: US Patent and Trademark Office CSCL 11/6

In accordance with the present invention, there is provided an improved alloy consisting essentially of about 6 to 10 weight percent Fe and about 3 to 10 weight percent Gd, balance aluminum. In a presently preferred embodiment, the weight ratio of iron to gadolinium is in the range of about 1:1 to 2.2:1. In addition to aluminum, iron and gadolinium, the alloy can contain refractory metals of at least about 0.1 wt. percent and up to about 1.0 wt. percent tungsten, 1.0 wt. percent tantalum, 1.5 wt. percent molybdenum, and/or 1.5 wt. percent niobium. Preferably, the total amount of these strengtheners should not exceed about 5 wt. percent and preferably should not exceed the iron and gadolinium content. The alloys are produced by any of the known rapid solidification processes for producing particulate materials. Suitable processes include gas atomization, drum splat, twin roll atomization, chill block melt spinning, planar flow casting, and the like. GRA

N90-16029# Department of the Air Force, Washington, DC.
METHOD TO PRODUCE TITANIUM ALLOY ARTICLES WITH HIGH FATIGUE AND FRACTURE RESISTANCE Patent
Francis H. Froes, inventor (to AF) and Daniel Eylon, inventor (to AF) 9 May 1989 6 p Filed 6 May 1988 Supersedes US-Patent-Appl-SN-198804
(AD-D014278; US-Patent-4,828,793; US-Patent-Appl-SN-198804)
Avail: US Patent and Trademark Office CSCL 11/6

A method for producing an integral titanium alloy article having at least two regions, each region having a distinct microstructure, which comprises the steps of: (1) providing a suitable mold for the article; (2) introducing a first titanium alloy into a first portion of the mold; (3) introducing a second titanium alloy in powder form into a second portion of the mold; and (4) hot compacting the first and second alloys in the mold to produce a substantially fully dense article. The second alloy may be the hydrided version of the first alloy, or may have a different overall composition from the first alloy, or may be hydrided and have a different overall composition from the first alloy. GRA

N90-16030# Department of the Air Force, Washington, DC.
METHOD FOR REFINING MICROSTRUCTURES ON PREALLOYED TITANIUM POWDER COMPACTS Patent
Daniel Eylon, inventor (to AF) and Francis H. Froes, inventor (to AF) 23 May 1989 6 p Filed 4 Dec. 1987 Supersedes US-Patent-Appl-SN-128842
(AD-D014280; US-Patent-4,832,760; US-Patent-Appl-SN-128842)
Avail: US Patent and Trademark Office CSCL 11/6

This abstract discloses a method for improving the microstructure of prealloyed titanium alloy compacted articles which comprises the steps of hydrogenating the article at temperature of about 780 to 1020 C to a hydrogen level of 0.50 to 1.50 weight percent, cooling the thus-hydrogenated article to room temperature at a controlled rate, heating the thus-cooled, hydrogenated article to a temperature of about 650 to 750 C and applying a vacuum to dehydrogenate the article. GRA

N90-16031# Department of the Air Force, Washington, DC.
METHOD OF MARKING TITANIUM ALLOY ARTICLES HAVING DISTINCT MICROSTRUCTURAL REGIONS CORRESPONDING TO HIGH CREEP AND FATIGUE RESISTANCE Patent
Daniel Eylon, inventor (to AF) and Francis H. Froes, inventor (to AF) 25 Jul. 1989 7 p Filed 8 Nov. 1988 Supersedes US-Patent-Appl-SN-270146

(AD-D014283; US-Patent-4,851,055; US-Patent-Appl-SN-270146) Avail: US Patent and Trademark Office CSCL 11/6

A method for producing an integral titanium alloy article having at least two regions, each region having a distinct microstructure is provided. The method comprises heat treating one or more selected region(s) of the article at a temperature greater than the beta-transus temperature of the region(s), while simultaneously heat treating the remaining region(s) of the article at a temperature below the beta-transus temperature of the remaining region(s). GRA

N90-16032# Naval Ship Research and Development Center, Bethesda, MD. Ship Materials Engineering Dept.

EFFECTS OF HIGH RATE SHEAR ON THE MICROSTRUCTURE AND DEFORMATION AND FRACTURE BEHAVIOR OF TWO HIGH STRENGTH STEELS

E. M. Hackett Apr. 1989 171 p

(AD-A214107; DTRC/SME-89/27) Avail: NTIS HC A08/MF A01 CSCL 11/6

The shear localization behavior of two high strength steels was evaluated at loading rates ranging from quasi-static to impact. The steels evaluated were similar in yield strength, but had different levels of toughness. The steel with superior toughness was direct quenched (DQ). The second steel was quenched and tempered (Q and T). Fatigue precracked Dual Notched Shear (DNS) specimens, loaded in mode II (in-plane shear), were employed. The objectives were to measure energy density variations with loading rate, estimate the temperatures achieved in the shear zones of the specimens and examine micromechanisms of localized shear deformation as related to the microstructures of the steels. Temperatures in the shear zones were estimated from energy absorption characteristics and compared with temperatures measured adjacent to the fatigue crack tips, to assess compliance with adiabatic conditions. GRA

N90-16033# State Univ. of New York, Albany.

STAINLESS STEEL PASSIVITY Report, 1 Oct. 1988 - 30 Sep. 1989

C. R. Clayton 30 Sep. 1989 6 p

(AD-A214108) Avail: NTIS HC A02/MF A01 CSCL 11/6

Additions of nitrogen to molybdenum bearing and (essentially) Mo free stainless steels result in much higher improvements in general corrosion resistance and pitting resistance. The most dramatic improvements are observed in the Mo bearing steels. This enquiry is attempting to model the roles of N and Mo in passivity. X Ray Photoelectron Spectroscopy (XPS) was utilized along with electrochemical analysis and a new surface doping treatment devised in order to facilitate this study. GRA

N90-16034# State Univ. of New York, Stony Brook. Dept. of Materials Science and Engineering.

AN XPS AND ELECTROCHEMICAL STUDY OF THE INFLUENCE OF MOLYBDENUM AND NITROGEN ON THE PASSIVITY OF AUSTENITIC STAINLESS STEEL

R. D. Willenbruch, C. R. Clayton, M. Oversluizen, D. Kim, and Y. Lu 24 Oct. 1989 13 p

(Contract N00014-89-J-1068)

(AD-A214267) Avail: NTIS HC A03/MF A01 CSCL 11/6

In previous surface studies of N bearing stainless steels exposed to acidic environments it was determined that N is anodically segregated as a surface nitride phase. Herein, the nature of the surface nitride and its role in the passivity of each of the constituent elements comprising a Mo bearing stainless steel is examined. To facilitate this study, surface nitrides were generated electrochemically at room temperature on the surface of high purity samples of Cr, Mo, Fe and Ni and on the surface of types 304, 317LX, 904L and A16X stainless steels. The effect of the surface nitriding treatment on the anodic kinetics of the stainless steels was in close agreement with the effect of N alloying. The surface nitriding of Cr resulted in the complete elimination of the active nose in deaerated 0.1 MHC1. GRA

N90-16035# Carnegie-Mellon Univ., Pittsburgh, PA. Dept. of Metallurgical Engineering and Materials Science.

FUNDAMENTAL STUDIES OF BETA PHASE DECOMPOSITION MODES IN TITANIUM ALLOYS Interim Technical Report, 1 Oct. 1988 - 30 Sep. 1989

Hubert I. Aaronson, T. Furuhara, and Y. Mou 31 Oct. 1989 78 p

(Grant AF-AFOSR-0303-84; AF Proj. 2306)

(AD-A214424; AFOSR-89-1356TR) Avail: NTIS HC A05/MF A01 CSCL 11/6

An experimental investigation of the interfacial structure of the broad faces of windmanstatten alpha plates and of grain boundary alpha allotriomorphs formed in a Ti-7.15 W/O (6.62 A/O) Cr alloy was completed. A supporting modeling study was also made of the structure of these BCC: HCP interfaces, using both a computer modeling technique and the bollmann O-lattice method. No misfit dislocations were found at any of the interfaces examined on either morphology. Instead, c- or (c+a)-type misfit-compensating ledges of variable height eliminated the need for one set of misfit dislocations; structural ledges removed the requirement for the other set. The former ledges were readily imaged with conventional tem; they are straight and uniformly spaced. Direct observation of structural ledges required the use of atomic resolution tem. Hot-stage tem confirmed the mobility of growth ledges and the immobility of c-type ledges. GRA

N90-16036# Argonne National Lab., IL. Materials and Components Technology Div.

THE ONSET OF BOILING OF THE LIQUID ALKALI METALS

Robert E. Holtz and Paul A. Lottes 1989 7 p Presented at the 7th Symposium on Space Nuclear Power Systems, Albuquerque, NM, 7-11 Jan. 1990

(Contract W-31-109-eng-38)

(DE90-002276; CONF-900109-13) Avail: NTIS HC A02/MF A01

Studies pertinent to the liquid superheat required to initiate boiling and the subsequent behavior of the two phase fluid have been conducted for many years. Knowledge of the incipient boiling superheats is important because of the proposed use of liquid metals as reactor coolants, Rankine cycle working fluids, and heat rejection fluids in space energy conversion systems. Some of the parameters that have been postulated to influence the incipient boiling superheats and the subsequent two phase flow behavior of the alkali metals include the system pressure, the pressure-temperature-time history, heat flux, liquid purity, dissolved gas content, surface condition, nuclear radiation, heating method, length of time of operation (for example, aging), liquid velocity, and the approach to boiling. The prediction of incipient boiling superheats is complex, and the influence of some of these parameters needs additional clarification. DOE

N90-16037# Los Alamos National Lab., NM.

ELASTIC MODULI OF COPPER: ELECTRONIC STRUCTURE CONTRIBUTIONS FROM PSEUDOPOTENTIALS AND FULL-POTENTIAL LINEAR MUFFIN-TIN ORBITAL BAND STRUCTURE CALCULATIONS

Galen K. Straub and John M. Wills Nov. 1989 46 p

(Contract W-7405-eng-36)

(DE90-004423; LA-11522-MS) Avail: NTIS HC A03/MF A01

The elastic moduli of copper were determined from the electronic structure by using an empty core pseudopotential model and first-principles full-potential linear muffin-tin orbital (FPLMTO) band calculations. General second order stress-strain coefficients are determined from strain derivatives of the total energy. The pseudo-potential model includes d-state interactions and results in an effective pair-wise interaction between ions. In terms of the pair-wise interaction and its derivatives, formulas for the second order elastic constants are given. FPLMTO calculations are presented for the total energy and its derivatives of Cu based on a self consistent local density functional Hamiltonian with no shape approximation to the potential. Pseudopotential and FPLMTO results for the elastic moduli and their pressure derivatives are compared at pressures of zero and one Mbar. DOE

N90-16038# Gandhi (Indira) Centre for Atomic Research, Kalpakkam (India).
INTERPLANAR SPACING FOR VARIOUS PHASES IN AUSTENITIC STAINLESS STEELS
R. V. Nandedkar 1988 15 p
(DE90-602350; IGC-104) Avail: NTIS (US Sales Only) HC A03/MF A01

Austenitic stainless steels are candidate materials for fast breeder and future fusion reactors. The selection of these materials, especially the type of austenitic stainless steel depends upon both the starting microstructure or the changes in it produced by either environment (corrosive or radiation) or applied stresses. These stresses could be compressive, cyclic or tensile. The starting microstructure is governed by the thermo-mechanical treatment. Any austenitic stainless steel, being a multicomponent system is prone to have many second phase particles as well as intermetallic compounds depending upon the thermomechanical treatment and/or irradiation conditions. The identification of these phases is usually performed using a transmission electron microscope. Electron diffraction patterns are analyzed to identify a phase, coupled with elemental analysis if the microscope is equipped with analytical facilities. This report gives a compilation of different interplanar spacings for various phases one normally encounters in austenitic stainless steels. The lattice parameters (a,b,c) and interplaner spacings (dspg) are expressed in nanometres. The crystal structure is also indicated. Alpha, beta, gamma are the cell angles in degrees. In many steels, if zirconium is present as an impurity, some zirconium based intermetallics are formed. Interplaner spacings for these are also included. DOE

N90-16039# Technical Research Centre of Finland, Helsinki. Metals Lab.
LONG TERM CREEP STRENGTH OF SILVER ALLOYED COPPER
Pertti Auerkari and Stefan Sandlin Dec. 1988 26 p Sponsored in part by Industrial Power Co. Ltd., Helsinki, Finland
(DE90-602367; YJT-88-14) Avail: NTIS (US Sales Only) HC A03/MF A01

The long term creep strength of silver alloyed copper has been estimated using literature creep data for materials with less than 0.1 percent Ag. The available data was very limited, and it was necessary to test the differences between various data sets and extrapolation methods. Assuming constant stress level and constant or changing temperature, the creep behavior has been assessed using mainly Larson-Miller and theta-projection approaches. The calculations indicate that the different extrapolation methods and data sources can yield strongly different life estimates. With the available incomplete data the theta projection method may give the conservative life predictions, whereas the Larson-Miller approach grossly overestimates creep life. It is recommended that supplementary data is acquired to better assess the long term creep properties of canisters in repository conditions. DOE

N90-16040# Delaware Univ., Newark.
SELECTIVITY OF THE REACTIONS OF OXYGENATES ON TRANSITION METAL SURFACES Progress Report, 15 Dec. 1988 - 14 Dec. 1989
Mark A. Barteau 1989 6 p
(Contract DE-FG02-84ER-13290)
(DE90-003911; DOE/ER-13290/5) Avail: NTIS HC A02/MF A01

The goal of this research was to understand, by means of surface science studies, the elementary processes involved in the synthesis of higher oxygenates on transition metals, and the dependence of these processes upon the nature of the surface. A considerable body of work was completed; (Ph.D. Thesis of J. Lynn Davis, 1988) on the reactions of alcohols, aldehydes, and carboxylic acids on clean and oxygen-containing Pd(111) surfaces. Work during the past year focused on the surface chemistry of rhodium. Both interesting similarities and differences were found between rhodium and palladium. Comparison of the two sheds light on common reaction networks among the transition metals, and on the differences between them which permit control of selectivities in catalytic reactions. DOE

N90-16041# Pacific Northwest Lab., Richland, WA. Dept. of Materials Science.
MICROSTRUCTURAL EXPLANATION FOR IRRADIATION EMBRITTLEMENT OF V-15Cr-5Ti
D. S. Gelles, S. Ohnuki, B. A. Loomis, H. Takahashi (Hokkaido Univ., Sapporo, Japan), and F. A. Garner Nov. 1989 21 p Presented at the 4th International Conference on Fusion Reactor Materials, Kyoto, Japan, 4-8 Dec. 1989
(Contract DE-AC06-76RL-01830)
(DE90-004112; PNL-SA-17021; CONF-891204-8) Avail: NTIS HC A03/MF A01

Vanadium alloys are candidate materials for first wall fusion reactor applications based on low induced activity and heat resistant response. However, recent results have indicated that modest levels of neutron irradiation damage in V-15Cr-5Ti lead to severe degradation of mechanical properties. In order to explain the observed behavior, specimens of V-15Cr-5Ti have been examined by transmission electron microscopy following irradiation at 600 C to 14 dpa in the Fast Flux Test Facility (FFTF). The conditions examined included two heats of V-15Cr-5Ti with very different oxygen contents and, in one case, a section of a charpy specimen demonstrated to have very poor impact resistance. Specimens irradiated at 420 and 520 C were also examined to confirm density change measurements that indicated swelling levels as high as 2.5 percent. Following irradiation at 600 C, a complex microstructure was found that included a perfect dislocation network of line segments and loops, faulted loops, a high density of black spot damage and a high density of rod-shaped precipitates. Heat-to-heat variations did not appear to significantly alter these microstructural features; instead the density of large blocky precipitates, believed to be TiO2, was found to have increased with increasing oxygen content. Only two of the specimens irradiated at 600 C contained voids, whereas none of the specimens irradiated at 420 or 520 C contained voids. DOE

N90-16042# Pacific Northwest Lab., Richland, WA.
PHASE EVOLUTION DURING NEUTRON IRRADIATION OF COMMERCIAL Fe-Cr-Mn ALLOYS
J. M. McCarthy and F. A. Garner Dec. 1989 9 p Presented at the 4th International Conference on Fusion Reactor Materials, Kyoto, Japan, 4-8 Dec. 1989
(Contract DE-AC06-76RL-01830)
(DE90-004113; PNL-SA-16980; CONF-891204-9) Avail: NTIS HC A02/MF A01

Earlier irradiation studies on simple Fe-Mn and Fe-Cr-Mn alloys in the annealed condition showed that these alloys exhibited a higher level of phase instability than do comparable Fe-Cr-Ni alloys. Contributing to this instability was the tendency of iron to segregate at microstructural sinks due to the operation of the inverse Kirkendall effect. This segregation, combined with the addition of various solutes and the application of typical thermomechanical treatments to produce the commercial alloys, added complexity to the phase evolution of Fe-Cr-Mn alloys. This complexity included the intergranular and intragranular precipitation of M23, C6 carbide, alpha ferrite, and sigma. These phases can have detrimental effects on mechanical and corrosion properties. Provided that the phase transformations to sigma and carbides can be controlled, the commercial austenitic Fe-Cr-Mn alloys appear to be suitable starting compositions for the development of low activation alloys for service in fusion reactors. DOE

N90-16043# Royal Aerospace Establishment, Farnborough (England).
FATIGUE AND IMPACT STRENGTH OF DIFFUSION BONDED TITANIUM ALLOY JOINTS
T. S. Baker and P. G. Partridge Feb. 1989 24 p Presented at Diffusion Bonding International Conference, Bedford, England, 7-8 Jul. 1987

(RAE-TM-MAT/STR-1123; BR110503; ETN-90-96135) Copyright Avail: NTIS HC A03/MF A01

The fatigue and impact strengths for diffusion bonded butt joints in IMI 318 and IMI 550 titanium alloys are reported. Different diffusion bonding parameters are used to produce bonds with parent metal tensile strengths but different void contents. The results are related to metallographic and fractographic data. The results show that the absence of pores in a bond does not itself guarantee parent metal impact strength since this is also affected by microstructural and textural inhomogeneities in the joint region. Fatigue strength is shown to be reduced when clusters of pores are present. The relative impact strengths of joints which had parent metal tensile and fatigue strengths are 49 percent (IMI 318) and 25 percent (IMI 550). ESA

N90-16044# Kernforschungsanlage, Juelich (Germany, F.R.). Inst. fuer Reaktorwerkstoffe.

THE INFLUENCE OF CARBIDE PRECIPITATION ON THE CREEP RUPTURE BEHAVIOR OF HIGH TEMPERATURE ALLOYS Thesis - Technische Hocshule Aachen

R. vonderGracht, P. J. Ennis, A. Czyrska-Filemonowicz, W. J. Quadakkers, H. Schuster, and H. Nickel Jul. 1988 139 p In GERMAN; ENGLISH summary

(JUEL-2211; ISSN-0366-0885; ETN-90-95326) Avail: NTIS HC A07/MF A01

The effect of carbon content on the creep behavior of Ni Cr22 Co12 Mo (INCONEL 617) and X10 NiCrAlTi 3220H (INCOLOY 800H), investigated at 850 C and 950 C, is described. Tests on the commercial alloys in a decarburizing atmosphere are carried out. Pre-carburized specimens exhibit a significantly higher creep rupture strength than solution treated specimens and specimens tested in a carburizing atmosphere. The tests on alloys of different initial carbon contents show that the secondary creep rate decreases with increasing carbon content. Specimens tested in a decarburizing atmosphere exhibit a very high creep rate after only a few hours of testing. The rupture times for specimens tested in the decarburizing atmosphere are an order of magnitude shorter than those of specimens tested in air or in carburizing atmospheres at the same temperature and stress. The very low creep rupture strength of the decarburized material is attributed to the absence of grain boundary carbides, with the result that grain boundary sliding was enhanced. Consequently the rapid formation of grain boundary pores and cracks occurred. ESA

N90-16045# Etablissement Technique Central de l'Armement, Arcueil (France). Dept. Physique des Surfaces.

STRUCTURAL ANALYSIS OF ZIRCONIUM-ALUMINUM PLASMA DEPOSITS [ANALYSE STRUCTURALE DE DEPOTS PLASMA DE ZIRCONE-ALUMINE]

M. C. Foujanet, J. P. Lumet, and J. L. Derep 10 May 1989 21 p In FRENCH Presented at the 1st Plasma-Technique Symposium, Lucerne, Switzerland, May 1988

(ETCA-89-R-073; ETN-90-95927) Avail: NTIS HC A03/MF A01

Structural composites of partially stabilized zirconium and aluminum are created by atmospheric plasma projection and studied. The microstructure of the power from the projected deposit and from the reheated powder are analyzed. Different phases present in the powder are identified by x ray diffraction. ESA

N90-16046# Pacific Northwest Lab., Richland, WA.

FRACTURE TOUGHNESS OF FERRITIC ALLOYS AT VERY HIGH NEUTRON EXPOSURES

M. L. Hamilton and F. H. Huang (Westinghouse Hanford Co., Richland, WA.) 1989 15 p Presented at the 4th International Conference on Fusion Reactor Materials, Kyoto (Japan), 4-8 Dec. 1989

(Contract DE-AC06-76RL-01830)

(DE90-004519; PNL-SA-16982; CONF-891204-10) Avail: NTIS HC A03/MF A01

Fracture toughness tests were performed on a number of heats of both HT9 and modified 9Cr to 1Mo irradiated in the Fast Flux Test Facility (FFTF) to doses ranging from 35 to over 100 dpa at temperatures of 400 to 600 C. Virtually no additional degradation was observed in either toughness or tearing modulus beyond that observed in the Experimental Breeder Reactor 2 (EBR-2) at 15 dpa. The FFTF data base for these alloys is compared to that of similar specimens irradiated in the High Flux Isotope Reactor (HFIR) and EBR-2. DOE

N90-16047# Pacific Northwest Lab., Richland, WA.

IRRADIATION CREEP AND SWELLING OF ANNEALED TYPE 304L STAINLESS STEEL AT APPROXIMATELY 390 C AND HIGH NEUTRON FLUENCE

D. L. Porter, F. A. Garner, and G. D. Hudman (Argonne National Lab., IL.) 18 Nov. 1989 7 p Presented at the 4th International Conference on Fusion Reactor Materials, Kyoto, Japan, 4-8 Dec. 1989

(Contracts DE-AC06-76RL-01830; W-31-109-eng-38)

(DE90-004521; PNL-SA-16986; CONF-891204-11) Avail: NTIS HC A02/MF A01

The objective of this effort is to determine the mechanisms involved in radiation-induced deformation of structural materials and apply these insights toward extrapolation of available fast reactor data to fusion-relevant conditions. The irradiation-induced creep and swelling of annealed AISI 304L in EBR-II at approximately 390 C have been investigated to exposures on the order of 80 dpa and compared with the behavior of AISI 316 stainless steel. It is shown that swelling and creep of various austenitic steels are strongly interactive phenomena. While swelling depends on stress, displacement rate, composition and cold-work level, the creep rate directly depends only on the stress level and the instantaneous swelling rate. The creep-swelling coupling coefficient does not appear to be very sensitive to composition, cold work level or temperature. DOE

N90-16048# Oak Ridge National Lab., TN.

SELECTION OF CORROSION-RESISTANT MATERIALS FOR USE IN MOLTEN NITRATE SALTS

P. F. Tortorelli, P. S. Bishop, and J. R. DiStefano Oct. 1989 50 p

(Contract DE-AC05-84OR-21400)

(DE90-004351; ORNL/TM-11162) Avail: NTIS HC A04/MF A01

Investigations of the corrosion of various metals, alloys, and ceramics in high temperature nitrate salt melts revealed that relatively few materials have acceptable compatibility in a 650 C, NaNO3(-KNO3)-Na2O2 environment that was chemically characteristic of the MOLTOX (trademark) chemical air separation process. Corrosion in these systems was controlled by the stabilities of the salt and solid-state surface oxides (whether they were ore-existing or formed upon exposure), the salt's oxide ion activity (strongly influenced by Na2O2 additions), and the physical condition of the solid surfaces. In general, refractory/reactive metals and alloys (with the exception of zirconium and hafnium), cobalt, nickel, NiMo, TiAl, austenitic steel, and Ni-Cr-Fe alloys were found to corrode quite readily because of rapid oxidation and/or dissolution in the salt. DOE

N90-16049# Pacific Northwest Lab., Richland, WA.

SYNTHESIS OF AIR-SINTERABLE LANTHANUM CHROMITE POWDERS

L. A. Chick, J. L. Bates, L. R. Pederson, and H. E. Kissinger Oct. 1989 10 p Presented at the Electrochemical Society Fall Meeting, Hollywood, FL, 15-20 Oct. 1989

(Contract DE-AC06-76RL-01830)

(DE90-004681; PNL-SA-17010; CONF-8910107-7) Avail: NTIS HC A02/MF A01

Lanthanum chromites, used as current interconnections in solid oxide fuel cells (SOFCs), have high electrical conductivity and are chemically stable. However, they are difficult to fabricate under conditions compatible with other SOFC components. A novel powder synthesis technique, the glycine/nitrate process, has been developed that produces chromite powders that can be sintered to near-full density in air at 1823 K. This paper describes the glycine/nitrate process for the synthesis and fabrication of

lanthanum chromites. The sintering behavior and properties of a series of glycine/nitrate-produced lanthanum chromites are discussed. Some of the materials produced by this method match the thermal expansion of the electrolyte and maintain high electrical conductivity. DOE

N90-16050# State Univ. of New York, Stony Brook.
THEORETICAL STUDIES OF CHEMISORPTION AND SURFACE REACTIONS ON NICKEL AND SILICON Progress Report, 15 Jun. 1987 - 1 Dec. 1989
Jerry L. Whitten 1 Dec. 1989 16 p Prepared in cooperation with North Carolina State Univ., Raleigh
(Contract DE-FG02-84ER-45100)
(DE90-004849; DOE/ER-45100/13) Avail: NTIS HC A03/MF A01

The research is part of a theoretical program on the structure of molecules adsorbed on solid surfaces and dissociative chemisorption with emphasis on transition metal substrates and electronic materials. An embedding theory for treating chemisorption on metals is further developed and applied to the reaction of hydrocarbon fragments and hydrogen coadsorbed on nickel, the dissociation of water on nickel, and the systems H/Ni, NH3/Ni, and C6H6/Ni. The main emphasis is on the energetics of adsorption as a function of surface site, the potential energy for adsorbate motion between surface sites and the energetics of surface reactions. Equilibrium geometries, vibrational frequencies and ionization potentials are also calculated. Preliminary work on the description of Si(100) surfaces was completed in preparation of H/Si and N/Si adsorption studies. Studies of pi bonding on Si(111) were also completed and work was begun on the Auger ionization of F/Si. The original form of the embedding theory was extended to make use of an effective potential representation of the bulk electrons interacting with the embedded surface region. Effective core potentials for Fe were developed. DOE

N90-16051# Oak Ridge National Lab., TN. Metals and Ceramic Div.
MODELING DISLOCATION EVOLUTION IN IRRADIATED ALLOYS
R. E. Stoller 1988 31 p Presented at the TMS Fall Meeting, Chicago, IL, 25-30 Sep. 1988
(Contract DE-AC05-84OR-21400)
(DE90-004921; CONF-8809322-2) Avail: NTIS HC A03/MF A01

Neutron irradiation of structural materials leads to such observable changes as creep and void swelling. These effects are due to differential partitioning of point defects. Although most radiation-produced point defects recombine with an antidefect, a very small fraction of the defects survive. The surviving defect fraction is directly related to the density and type of extended defects that act as point defect sinks. Defect partitioning requires the presence of more than one type of sink and that at least one of the sinks has a capture efficiency for either vacancies or interstitials that is different from that of the other sink(s). For example, dislocations provide the interstitial bias that drives swelling and the ration of the dislocation to cavity sink strength determines the swelling rate. These sink strengths change during irradiation and an explicit model of their evolution is required to simulate swelling or creep. Such a model was developed; the influence of various model assumptions and parameters is discussed. The model simulates the evolution of Frank faulted interstitial loops, providing a dislocation source and the glide/climb of the dislocation network leading to annihilation of dislocation segments. Good agreement is found between model predictions and experimental data. Swelling simulations are shown to be quite sensitive to the dislocation model. DOE

N90-16052# Battelle Columbus Labs., OH.
DESIGN OF COUPLED OR UNCOUPLED MULTIFILAMENTARY SSC-TYPE STRANDS WITH ALMOST ZERO RETAINED MAGNETIZATION AT FIELDS NEAR 0.3 T
E. W. Collings, K. R. Marken, Jr., and M. D. Sumption 1989 8 p Presented at the International Cryogenic Materials Conference, Los Angeles, CA, 24-28 Jul. 1989
(Contract DE-AC02-86ER-40296)
(DE90-005391; CONF-890701-26) Avail: NTIS HC A02/MF A01

Multifilamentary Cu-matrix strands with interfilamentary spacing as small as 0.2 microns can be almost fully decoupled by the addition of 0.5 wt percent Mn to the interfilamentary Cu. Decoupling in this way seems to be beneficial from a field-stability standpoint. On the other hand, the elimination of coupling does little to reduce residual strand-magnetization at the injection field of about 0.3 T when that field is approached, as usual, along the shielding branch of M(H). This residual diamagnetic magnetization (say M sub R) of the winding material is responsible for unwanted distortion (multipole formation) of the dipolar field. It is demonstrated that M sub R can be locally cancelled to zero by associating the strand with a small volume-fraction (less than 2 percent, depending on filament diameter) of pure Ni or any other low-field-saturable ferromagnetic material. The presence of the Ni has little effect on the shape of the M(H) hysteresis loop of the strand, other than to shift its wings uniformly in the +M (when H is positive) and minus M directions, respectively. In practice, the Ni could be administered as: (1) additional filaments, (2) interfilamentary barriers, or (3) an electroplated layer on the outside of the strand. DOE

N90-16053*# National Aeronautics and Space Administration. Lewis Research Center, Cleveland, OH.
PRODUCTION AND PROCESSING OF Cu-Cr-Nb ALLOYS
David L. Ellis, Gary M. Michal (Case Western Reserve Univ., Cleveland, OH.), and Norman W. Orth Jan. 1990 14 p
(NASA-TM-102495; E-5286; NAS 1.15:102495) Avail: NTIS HC A03/MF A01 CSCL 11F

A new Cu-based alloy possessing high strength, high conductivity, and good stability at elevated temperatures was recently produced. This paper details the melting of the master alloys, production of rapidly solidified ribbon, and processing of the ribbon to sheet by hot pressing and hot rolling. Author

N90-16688*# Randolph-Macon Coll., Ashland, VA. Dept. of Chemistry.
STUDY OF METAL CORROSION USING ac IMPEDANCE TECHNIQUES IN THE STS LAUNCH ENVIRONMENT
Luz M. Calle *In* University of Central Florida, NASA/ASEE Summer Faculty Fellowship Program Oct. 1989 p 24-57 (For primary document see N90-16686 08-99)
Avail: NTIS HC A18/MF A03 CSCL 11F

N90-16698*# Murray State Univ., KY. Dept. of Engineering Technology.
THE EFFECTS OF HYDROGEN EMBRITTLEMENT OF TITANIUM
Delbert J. Taylor *In* University of Central Florida, NASA/ASEE Summer Faculty Fellowship Program Oct. 1989 p 292-302 (For primary document see N90-16686 08-99)
Avail: NTIS HC A18/MF A03 CSCL 11F

27 NONMETALLIC MATERIALS

Includes physical, chemical, and mechanical properties of plastics, elastomers, lubricants, polymers, textiles, adhesives, and ceramic materials.

For composite materials see *24 Composite Materials.*

N90-16054# NATO Advanced Study Inst., Brussels (Belgium).
STRUCTURE-PROPERTY RELATIONSHIPS IN ION-BEAM SURFACE-MODIFIED CERAMICS: THEORY AND APPLICATIONS
9 Sep. 1988 49 p
(AD-A212785; R/D-5956-MS-02) Avail: NTIS HC A03/MF A01 CSCL 11/2

Topics addressed include: ceramic defects; ion beam alloying; hardness and wear resistance; ion energy dissipation and sputtering; ion beam mixing; ion implanation; microstructural

characterization; ion beam and laser treatment; tribology; thin films; mechanical properties; radiation damage; irradiation; and optical waveguides. B.G.

N90-16055# Argonne National Lab., IL.
DEVELOPMENT OF A DIAMOND INSULATOR FOR THERMIONIC APPLICATIONS
Ankur Purohit, Samit K. Bhattacharyya, J. Vandersande, C. Wood, and E. Kennel (Air Force Wright Aeronautical Labs., Wright-Patterson AFB, OH.) 1989 36 p Presented at the 1989 Thermionic Conversion Specialists Conference, Eindhoven, Netherlands, 9-12 Oct. 1989
(Contract W-31-109-eng-38)
(DE90-002849; CONF-8910301-1) Avail: NTIS HC A03/MF A01

Diamond (D) and Diamond Like Carbon (DLC) films and thick sections are being considered for several applications, one of which is as electrical insulators for the converter of the in-core thermionic generator. The purpose of this work is to: (1) optimize several methods of D and DLC depositions, (2) characterize the thermomechanical, optical and electrical properties at room and elevated temperatures, and (3) determine the effects of fast neutron and gamma irradiation on the structure and properties of these films. D and DLC films using a variety of H2/CH4 gas mixtures, were deposited on silicon and niobium substrates, using four different deposition techniques. The resultant films were examined using optical and scanning electron microscopy and Raman spectroscopy. DOE

N90-16056# Los Alamos National Lab., NM.
EFFECT OF CARBON ON ION BEAM MIXING OF Fe-Ti BILAYERS
Juha Pekka Hirvonen, Michael Nastasi, Reijo Lappalainen, Kurt Sickafus, and Peter Borgeson, ed. 1989 7 p Presented at the Materials Research Society Fall Meeting, Boston, MA, 27 Nov. - 2 Dec. 1989
(Contract W-7405-eng-36)
(DE90-003650; LA-UR-89-4009; CONF-891119-13) Avail: NTIS HC A02/MF A01

The influence of implanted carbon on ion beam mixing of a Fe-Ti system was investigated. Carbon was introduced into bilayer samples by implanting C-13 isotopes. The implantation energies were selected to set the mean range of carbon ions in either the iron or titanium layer. The effect of implanted carbon on 400 keV Ar ion mixing in the temperature range from 0 to 300 C was studied using Rutherford backscattering spectroscopy at the energy of 5 MeV. Changes in carbon concentration profiles were probed utilizing the resonance of the nuclear reaction C-13(p, gamma)N-14 at the proton energy of 1.748 MeV. The measurements revealed that mixing was not affected by carbon implanted into the titanium layer. However, carbon in the iron layer remarkably retarded mixing at all temperatures investigated. Significant changes in carbon depth distributions were observed only when the sample with implanted carbon in the iron layer was mixed at 300 C. These results are explained in terms of the enhanced mobility of carbon in an evaporated iron film which allows segregation to the interface. At low temperatures, however, vacancy-carbon interaction in iron may have a contribution to the retarded ion beam mixing. DOE

N90-16057# Los Alamos National Lab., NM. Materials Science and Technology Div.
SILICON-BASED COATINGS ON NIOBIUM METAL
Paul D. Stupik, Thomas R. Jervis, Michael Nastasi, Michell M. Donovan, and Andy R. Barron (Harvard Univ., Cambridge, MA.) 1989 7 p Presented at the Materials Research Society Fall Meeting, Boston, MA, 27 Nov. - 2 Dec. 1989
(Contract W-7405-eng-36)
(DE90-003651; LA-UR-89-4008; CONF-891119-12) Avail: NTIS HC A02/MF A01

Silicon coatings on niobium substrates were subjected to thermal, ion beam and laser mixing, and the effectiveness of the different methods for the synthesis of graded interfaces was compared. The resulting metal/silicon interfaces were characterized by x ray photoelectron spectroscopy (XPS), Auger electron spectroscopy (AES) and the Rutherford backscattering (RBS). DOE

N90-16058# Los Alamos National Lab., NM.
THE PHYSICAL PROPERTIES OF MICROCELLULAR COMPOSITE FOAMS
Alice M. Nyitray, Joel M. Williams, David Onn, and Adam Witek (Delaware Univ., Newark.) 1989 7 p Presented at the Materials Research Society Fall Meeting, Boston, MA, 27 Nov. - 2 Dec. 1989
(Contract W-7405-eng-36)
(DE90-003658; LA-UR-89-3940; CONF-891119-12) Avail: NTIS HC A02/MF A01

Recently a method of preparing microcellular composite foams was reported. In this procedure an open-celled polystyrene foam is prepared by the polymerization of a high-internal-phase water-in-oil emulsion containing styrene, divinylbenzene, surfactant, free-radial initiator and water. After drying, the cells of the polystyrene foam are then filled with other materials such as aerogel or resoles. The physical properties of these materials, e.g., surface area, density, thermal conductivity, and compressive strength will be presented. DOE

N90-16059# Department of the Air Force, Washington, DC.
MOLYBDENUM DISULFIDE-MOLYBDENUM OXIDE LUBRICANTS Patent
Phillip W. Centers, inventor (to Air Force) 9 May 1989 4 p Filed 13 Apr. 1988 Supersedes US-Patent-Appl-SN-181355
(AD-D014253; US-Patent-4,828,729; US-Patent-Appl-SN-181135; US-Patent-Class-252-25) Avail: U.S. Patent and Trademark Office CSCL 11/8

This abstract discloses a solid lubricating material consisting essentially of an intimate mixture of about 15 to 50 mole percent molybdenum trioxide, balance molybdenum disulfide. The material is particularly useful under extreme environmental conditions such as very high temperature or vacuum. The material may be used in powder form, compacted into a pellet or other desired shape, incorporated into a grease composition or incorporated into a resin-bonded solid film lubricant. GRA

N90-16060# Department of the Air Force, Washington, DC.
METHOD OF MAKING CARBON DIOXIDE AND CHLORINE FREE FLUORIDE-BASED GLASS Patent
Joseph J. Hutta, inventor (to Air Force) 27 Jun. 1989 4 p Filed 20 Jun. 1988 Supersedes US-Patent-Appl-SN-213007
(AD-D014260; US-Patent-4,842,631; US-Patent-Appl-SN-213007; US-Patent-Class-65-32.5) Avail: U.S. Patent and Trademark Office CSCL 11/2

The present invention relates to an improved method of making fluoride-base glass free of certain contaminants, and in particular, free of carbon dioxide and chlorine. Considerable effort has expended to develop heavy metal fluoride glasses (HMFG) as a viable family of infrared-transparent optical-materials for application as fiber waveguides and as bulk optical components. The present process is directed to typical heavy metal fluoride glasses of the compositions: (XF4+BaF2+LaF3+AlF3+YF) where X is either zirconium or hafnium and Y can represent sodium, lithium, lead, indium, or no addition. For example, the melt mixture may contain multi-component fluorides, or, alternatively, the mixed oxides or oxyfluorides plus ammonium bifluoride (NH4HF2) in a crucible, preferably made of a nonreactive inert precious metal such as platinum, platinum alloys or gold but also including vitreous or pyrolytic carbon. This crucible is placed within a furnace contained within a vacuum chamber. The chamber is evacuated to around 110 torr and then backfilled with sulphur hexafluoride (SF6) to a slight positive pressure. The mixture is then rapidly heated to about 800 + or - 10 C, held there at temperature for a brief period then rapidly cooled. The present invention is a process of providing, high optical quality heavy metal fluoride glasses that lack devitrification, straie, seed, internal bubbles, crystalline inclusions, dissolved CO2 and chlorine contamination or other defects. GRA

N90-16061# Department of the Air Force, Washington, DC.
POROUS CERAMIC BODIES Patent
Clarence A. Andersson, inventor (to AF), Deborah P. Partlow, inventor (to AF), and Bulent E. Yoldas, inventor (to AF) 9 May 1989 4 p Filed 5 Feb. 1987
(AD-D014277; US-Patent-4,828,774; US-Patent-Appl-SN-011085; US-Patent-Class-264-60) Avail: US Patent and Trademark Office CSCL 11/2

This invention relates to porous ceramic bodies. Renewed interest in lightweight porous ceramics was stimulated by the need for materials having low thermal expansion, low dielectric constant, and/or low density for certain high-tech applications. It is the objective to provide an improved method for fabricating porous ceramic bodies. In accordance with the present invention there is provided an improved method for making a lightweight porous ceramic body which comprises the steps of: providing a ceramic polymer solution; blending high-strength fibers with the polymer solution to provide a mixture; felting the mixture; drying the resulting felt; and firing the dried felt. Alternatively, the fibers may be felted, then impregnated with the ceramic polymer solution, then dried and fired. The polymer solution is an inorganic oxide network containing glass-forming elements such as Si, Al, Ti, Zr and the like and optionally, modifying elements such as Mg, B and the like. The oxide network is formed by controlled hydrolysis of an organo-metallic compound such as a metal alkoxide. GRA

N90-16062# University of Southern Mississippi, Hattiesburg. Dept. of Polymer Science.
COPOLYMERS FOR DRAG REDUCTION IN MARINE PROPULSION: NEW MOLECULAR STRUCTURES WITH ENHANCED EFFECTIVENESS Quarterly Report, 1 Jun. - 31 Aug. 1989
C. L. McCormick and R. D. Hester Aug. 1989 4 p
(Contract N00014-89-J-1893)
(AD-A214444) Avail: NTIS HC A01/MF A01 CSCL 07/6

The following is reported: (1) Synthesis: The first phase of synthetic research began with initial emphasis placed on preparation of copolymers of acrylamide with diacetone acrylamide with diacetone acrylamide (AM-DAMM) and ampholytic terpolymers of acrylamide and sodium 2-acrylamido-2-methylpropane dimethylammonium chloride with sodium-2-acrylamido-2-methylpropane sulfonate (ADASAM series) or with sodium-3-acrylamido 3-methyl-butanoate (ADABAM series); (2) Molecular Characterization: Construction of the proposed preparation scale size exclusion chromatography system is well underway. The system will be able to separate high molecular weight water soluble polymers for subsequent drag reduction studies; and (3) Friction Reduction Measurements: Construction of the proposed tube flow apparatus for measurement of drag reduction is completed. Testing of polyethylene oxide and polyacrylamide standards is in progress. GRA

N90-16063# Sao Paulo Univ. (Brazil). Inst. de Fisica.
PAIRS OF CHALCOGEN IMPURITIES IN SILICON M.S. Thesis
Helio FerreiradePaula, Jr. 1988 109 p In PORTUGUESE; ENGLISH summary
(DE89-635767; INIS-BR-1567) Avail: NTIS (US Sales Only) HC A06/MF A01

The electronic structure of complex defects in silicon involving oxygen and sulfur (O-O, S-O and S-S), occupying different positions in the host crystal is studied. It is shown that the many-electron effects (via configuration interaction) are important to describe the correct ground state. The orbital base set is obtained through the LCAO-MO-INDO/S method. DOE

N90-16064# Lawrence Livermore National Lab., CA.
SILICON MEMBRANE FORMATION Final Report
Charles E. Hunt (California Univ., Davis.) May 1989 6 p
(Contract W-7405-eng-48)
(DE90-003022; UCRL-21193) Avail: NTIS HC A02/MF A01

Experiments in the formation of silicon membranes by the use of electrochemical and nonelectro-activated chemical etching were performed. The starting material in the experiments is MOS-grade Si wafers. Application of the rotating disc (electrode) to the etch process is included. The results show that isotropic chemical thinning can benefit from the rotating disc system and that some electrochemical etching techniques can benefit over normal turbulent agitation methods. The experiments and results are described. DOE

N90-16065# Texas Univ., Austin. Dept. of Chemical Engineering.
SYNTHESIS AND ANALYSIS OF NOVEL POLYMERS WITH POTENTIAL FOR PROVIDING BOTH HIGH PERMSELECTIVITY AND PERMEABILITY IN GAS SEPARATION APPLICATIONS Progress Report, Dec. 1988 - Nov. 1989
W. J. Koros and D. R. Paul 28 Nov. 1989 7 p
(Contract DE-FG05-86ER-13507)
(DE90-003907; DOE/ER-13507/5) Avail: NTIS HC A02/MF A01

During the first eight months of project support under the renewal proposal, the following important experimental, analytical and publication objectives consistent with the project goal to develop advanced materials for gas separation membrane applications were achieved. Synthesized and characterized additional polycarbonate materials beyond those specified in the original proposal to test ideas developed in the course of the work with the originally proposed polycarbonate materials. Completed synthesis and characterization of the originally-proposed polysulfones in the renewal proposal. Also synthesized and begun characterization of additional polysulfone materials beyond those proposed in the renewal proposal to test ideas developed in the course of the work with the originally proposed materials. Began work to synthesize the systematic family of polyesters described in the renewal proposal. DOE

N90-16066# Sandia National Labs., Albuquerque, NM.
SHOCK-INDUCED REACTION SYNTHESIS OF ALUMINIDES AND SILICIDES
N. N. Thadhani, M. J. Costello, I. Song (New Mexico Inst. of Mining and Technology, Socorro.), S. Work, and R. A. Graham 1989 13 p Presented at the Metallurgical Society Fall Meeting: Materials Week, Indianapolis, IN, 1-5 Oct. 1989
(Contract DE-AC04-76DP-00789)
(DE90-003948; SAND-89-2703C; CONF-891024-7) Avail: NTIS HC A03/MF A01

Shock-induced reaction synthesis (SRS) is used for solid state processing of Ni-Al, Ni-Si, and Nb-Si type compounds, starting with elemental powder mixtures. The constituent elemental powders are blended in different stoichiometries and packed at 65 percent density in stainless steel capsules. A steel flyer plate, accelerated by the detonation of an explosive, impacts the powder containing capsules embedded in a steel recovery fixture backed by a momentum trap. The shock wave generated upon impact triggers a self-sustaining, exothermic reaction between the elemental powder constituents, thereby synthesizing the compound and at the same time consolidating the porous mass into 12mm diameter by 5mm thick compacts. The characteristics of the SRS technique and the structural features of the shock synthesized products will be discussed. DOE

N90-16067# Brookhaven National Lab., Upton, NY. Dept. of Applied Science.
MASS LOSS DURING X RAY MICROANALYSIS
Klas Themmer, Per Spanne (Linkoeping Univ., Sweden), and Keith W. Jones Oct. 1989 9 p Presented at the 5th International Conference on PIXE and Its Analytical Applications, Amsterdam, Netherlands, 20-26 Aug. 1989 Submitted for publication
Sponsored in part by Swedish Medical Research Council; Swedish Society of Medicine; and National Inst. of Health Biotechnology Research Resource
(Contract DE-AC02-76CH-00016)
(DE90-003954; BNL-43452; CONF-8908165-3) Avail: NTIS HC A02/MF A01

Mass loss during photon and proton irradiation of polymer films, tissue samples and gelatin standards is studied. No difference in

relative hydrogen loss is seen when varying the sample thickness. A dependence of the loss rate on the temperature in the irradiated volume is demonstrated by varying the proton irradiation parameters. The effects of the mass loss on the accuracy of the x ray microanalysis are discussed and the absorbed doses from protons and photons to produce equivalent loss are compared. DOE

N90-16068# Pacific Northwest Lab., Richland, WA.
DESIGN, CHARACTERIZATION, AND OPTICAL PROPERTIES OF PHOSPHAZENE-BASED POLYMERS
Gregory J. Exarhos and William D. Samuels Nov. 1989 6 p Presented at the 34th Conference on Magnetism and Magnetic Materials, Boston, MA, 27 Nov. - 1 Dec. 1989 Submitted for publication
(Contract DE-AC06-76RL-01830)
(DE90-004111; PNL-SA-17227; CONF-891117-12) Avail: NTIS HC A02/MF A01

Physical properties intrinsic to linear inorganic polymer systems can be modified through replacement of chemical groups external to the chain backbone. This substitution also perturbs chemical bonding along the chain which can further influence polymer properties. Several phosphazene polymers deposited as thin dielectric films exhibit extended ultraviolet transmission. Second harmonic generation (SHG) was observed in these polymers as well as in cyclic polymer precursors. The relative magnitude of SHG is found to correlate both with the nature of the substitutional group and molecular conformation. Influence of these parameters on substrate-film adhesion and measured optical properties is discussed in terms of substitutional group electronegativity, and electronic charge localization in the polymer chain which is probed using molecular spectroscopic techniques. DOE

N90-16069# Sandia National Labs., Albuquerque, NM.
CHARACTERIZATION OF B AND N IMPLANTED FUSED SILICA
G. W. Arnold, R. K. Brow, M. J. Carr, and J. C. Barbour 1989 11 p Presented at the Materials Research Society Fall Meeting, Boston, MA, 27 Nov. - 2 Dec. 1989
(Contract DE-AC04-76DP-00789)
(DE90-004198; SAND-89-1822C; CONF-891119-40) Avail: NTIS HC A03/MF A01

The implantation of B and N into fused silica can result in chemical incorporation into the glass with a consequent larger increase in refractive index than is possible due to volume compaction alone. B implantation produces anomalously large concentrations of oxygen-vacancy defects which aid in the accommodation of B into a borosilicate layer. N implants can result in unreacted N accumulations in addition to N incorporated into an Si-oxynitride layer. The unreacted N can also be incorporated by implantation damage (e.g., Si, Ar, Kr) -- before or after N implantation -- which provides additional occupancy sites. These results are important with respect to the use of implantation-produced waveguides for optoelectronic devices. DOE

N90-16070# Oak Ridge National Lab., TN. Metals and Ceramics Div.
METALS AND CERAMICS DIVISION MATERIALS SCIENCES PROGRAM Annual Progress Report, period ending 30 Apr. 1989
J. O. Stiegler, comp. Sep. 1989 298 p
(Contract DE-AC05-84OR-21400)
(DE90-004371; ORNL/TM-11281) Avail: NTIS HC A13/MF A02

This report summarizes the activities of the Materials Sciences Program in the Oak Ridge National Laboratory (ORNL) Metals and Ceramics Division for the period July 1, 1987 to April 30, 1989. The program is directed at uncovering principles for the scientific design of materials. The efforts emphasize three classes of materials: high-temperature metallic alloys based on intermetallic compounds, structural ceramics, and radiation-resistant alloys. The principal elements of Materials Science and Engineering, synthesis/processing, characterization, properties, and performance, are incorporated in all of these programs to achieve a full understanding of the relationships among the elements. A first-principles theory provides understanding of the structure of alloy systems. Surfaces and interfaces of ceramic systems are investigated through ion beam and molecular beam epitaxy activities. Major emphasis is placed on structural characterization capabilities to furnish the link between processing and performance. DOE

N90-16071# Oak Ridge National Lab., TN. Metals and Ceramics Div.
AN INVESTIGATION OF ELASTIC GUIDED WAVES FOR CERAMIC JOINT EVALUATION
W. A. Simpson, Jr. and R. W. McClung Oct. 1989 44 p
(Contract DE-AC05-84OR-21400)
(DE90-004400; ORNL/TM-10931) Avail: NTIS HC A03/MF A01

The rapid development of ceramic technology has led to the widespread use of ceramics in applications traditionally reserved for metals. Many of these applications, however, require the use of ceramics bonded to other ceramics or to metals in order to achieve the requisite strength. The presence of unbonding in such ceramic joints can now be reliably detected by previously developed ultrasonic techniques, but what is needed is a nondestructive approach which is capable of assessing bond strength directly. A possible tool to achieve this goal is the use of guided elastic waves propagating in the braze layer of a typical ceramic joint. We describe the theory of guided waves in the center layer of a general three-layer solid. The secular determinant is found, and roots of the secular equation are determined numerically for cases of interest in ceramic joining. Both guided and leaky modes are described, and it is shown that dispersive Stoneley waves can occur for these materials. In addition, the evanescent nature of the guided waves in the bounding solids raises the possibility of determining the elastic properties of the oxygen depletion layer adjacent to the braze in oxide ceramics. Possible models for incomplete bonding and the effect of this condition in the ultrasonic parameters are also discussed. DOE

N90-16072*# Sverdrup Technology, Inc., Cleveland, OH.
THERMODYNAMIC ANALYSIS OF CHEMICAL STABILITY OF CERAMIC MATERIALS IN HYDROGEN-CONTAINING ATMOSPHERES AT HIGH TEMPERATURES Final Report
Ajay K. Misra Jan. 1990 26 p
(Contracts NAS3-25266; NRA-88-ARC-1(BJY))
(NASA-CR-4271; E-4954; NAS 1.26:4271) Avail: NTIS HC A03/MF A01 CSCL 11C

The chemical stability of several ceramic materials in hydrogen-containing environments was analyzed with thermodynamic considerations in mind. Equilibrium calculations were made as a function of temperature, moisture content, and total system pressure. The following ceramic materials were considered in this study: SiC, Si3N4, SiO2, Al2O3, mullite, ZrO2, Y2O3, CaO, MgO, BeO, TiB2, TiC, HfC, and ZrC. On the basis of purely thermodynamic arguments, upper temperature limits are suggested for each material for long-term use in H2-containing atmospheres. Author

N90-16073# Institut National des Sciences Appliquees de Lyon, Villeurbanne (France). Lab. des Materiaux Macromoleculaires.
DEVELOPMENT OF AN ELASTOMERIC ADDITIVE TO IMPROVE THE IMPACT RESISTANCE OF UNSATURATED POLYESTER NETWORKS Ph.D. Thesis [MISE AU POINT D'UN ELASTOMERE DESTINE A L'AMELIORATION DE LA TENUE A L'IMPACT DE RESEAUX POLYESTER INSATURES]
Laurent Suspene 1989 249 p In FRENCH Sponsored by Societe Norsclor
(ISAL-89-0006; ETN-90-95514) Avail: NTIS HC A11/MF A02

Impact resistance of unsaturated polyester is improved by adding an elastomer while the prepolymer is still dissolved in styrene. The interfacial tension of the mixtures is measured using different techniques and is shown to vary with varying interaction

parameters. By changing the end links of the elastomer chain, or by making copolymer blocks, one can decrease the interfacial tension in order to obtain a stable emulsion with no sedimentation. Correlation studies linking interfacial tension and elastomer particle size to impact resistance of the material are described. ESA

N90-16074# Institut National des Sciences Appliquees de Lyon, Villeurbanne (France). Lab. Genie Electrique et Ferroelectricite.
PIEZOELECTRIC CERAMIC MODELING AND CHARACTERIZATION AT HIGH LEVELS OF MECHANICAL ACTIVITY Ph.D. Thesis [MODELISATION ET CARACTERISATION SOUS HAUT NIVEAU DE SOLLICITATION MECANIQUE DES CERAMIQUES PIEZOELECTRIQUES]
Pascal Champ 1989 272 p In FRENCH Sponsored by the DCAN; Direction des Recherches, Etudes et Techniques, Paris, France, and Societe Thomson Sintra ASM
(ISAL-89-0030; ETN-90-95707) Avail: NTIS HC A12/MF A02

A theoretical modeling technique developed for choosing the piezoelectric ceramic best suited for power emission under certain conditions is described. The technique is used to compare the performance of a wide variety of components. Results obtained by the technique are substantiated by vibration amplitude measurements at the emitting surface of a resonator. Laser interferometry is used to measure the vibration amplitude. A study of the thermal responses of the samples of piezoelectric ceramics agrees with a classification scheme based solely on electric response. The advantage of measuring the resonance of the ceramic samples longitudinally rather than in three dimensions is described. ESA

N90-16075# Brookhaven National Lab., Upton, NY.
SOFT MODES, FREEZING, AND NONLINEAR RESPONSE OF A DIPOLAR GLASS
K. B. Lyons, P. A. Fleury, H. Chou, J. Kjems, S. Shapiro, and D. Rytz (Hughes Research Labs., Malibu, CA.) 1989 11 p Presented at the 1st USA/USSR Workshop on Ferroelectricity, Boulder, CO, 9-14 Jul. 1989 Prepared in cooperation with Risoe National Lab., Roskilde, Denmark
(Contract DE-AC02-76CH-00016)
(DE90-003647; BNL-43410; CONF-8907111-1) Avail: NTIS HC A03/MF A01

A careful study of the polarization dynamics near the dipolar glass transition, utilizing both neutron and light scattering reveals a dichotomy in the behavior, on the one hand suggesting ordered domains of macroscopic extent and on the other clearly indicating dynamic cluster behavior in the same temperature region. An examination of this evidence leads us to suggest a percolated cluster model for the dipolar glass phase in KTa(1-x)Nb(x)O3 (KTN). DOE

N90-16076# Oak Ridge National Lab., TN.
ISOTOPE DRIVEN CRITICAL SCATTERING AND PHASE SEPARATION FROM MIXTURES OF DEUTERATED AND PROTONATED POLYMERS Foreign Travel Report, 7-15 Nov. 1989
G. D. Wignall Dec. 1989 13 p Presented at the Taniguchi Conference on Neutron Scattering from Polymers, Kyoto, Japan, 7-10, 11 Nov. 1989; also presented at Tokai, Japan, 15 Nov. 1989
(Contract DE-AC05-84OR-21400)
(DE90-003976; ORNL/FTR-3496) Avail: NTIS HC A03/MF A01

The traveler attended the Taniguchi Conference on Polymer Research by Neutron Scattering and presented an invited lecture entitled, Isotope Driven Critical Scattering and Phase Separation from Mixtures of Deuterated and Protonated Polymers. The traveler visited Kyoto University and performed experiments comparing the performance of the Kyoto University and ORNL SAXS instruments. Finally, the traveler visited JAERI and gave a seminar entitled, Small-Angle Scattering: Why so much time and money to study the origin of Q-space. DOE

N90-16077# Babcock and Wilcox Co., Lynchburg, VA.
ASSESSMENT OF STRENGTH LIMITING FLAWS IN CERAMIC HEAT EXCHANGER COMPONENTS FinaL Report, 4 Dec. 1986 - 31 Jan. 1989
J. R. Bower, J. P. Sandifer, M. O. Robertson, K. R. Waeber, and M. P. Macdonald Jan. 1989 135 p
(Contract DE-AC07-84ID-12566)
(DE90-004086; DOE/ID-12566/3) Avail: NTIS HC A07/MF A01

The ability to predict energy efficient lifetimes for ceramic heat exchanger components is necessary for their design, manufacture, and sale. The ability to inspect components for critical defects and adherence to specifications is also vital. In this second phase of a three phase program new instrumentation was added to the existing NDE capabilities, mechanical testing was carried out to determine material properties, and a fracture mechanics model was developed. The new instrumentation is a TOFAM system and a CT scanner. The TOFAM was developed at Idaho National Engineering Laboratory. It is an ultrasonic scanning system, with the capability of producing a magnified image of the part being scanned, and a color coded image showing the depth of any defects located. The CT scanner is based on a microfocus x ray system, and reconstructions use code supplied by Sandia National Laboratory. Both of these systems are capable of working with full size heat exchanger tubes. The mechanical testing program was carried out on C-rings at both room temperature and at 1230 C, and on pressurized tube segments at room temperature. Acoustic Emission monitoring was used to detect slow crack growth in all test conditions. DOE

N90-16078# Central Research Inst. of Electric Power Industry, Tokyo (Japan).
ANALYTICAL STUDY ON THE DECREASING METHOD OF THERMAL STRESS FOR CERAMIC GAS TURBINES
T. Mimaki, T. Abe, T. Hismatsu, H. Miyata, and T. Machida Nov. 1988 43 p In JAPANESE; ENGLISH summary
(DE90-734934; CRIE-W-88014) Avail: NTIS (US Sales Only) HC A03/MF A01

The authors subjected the following three points to numerical analysis in search of a method for decreasing thermal stresses produced in ceramic stator vanes of gas turbines. The first point is to adopt a structural design which makes it possible to release large thermal strains generated in a limited part of the vane even in stationary motion. The analysis confirmed that a suitable slit made in that part of the vane reduced the maximum thermal stress by about 30 percent. The second point is to use a kind of high conductivity ceramics to decrease thermal shock stress produced in the vane at the emergency stop of gas turbine. It was found that the use of hot pressed silicon carbide reduced the transient stress by about one half as compared with the use of ordinary silicon carbide. The third point is to improve the stoppage equipment to be operated at the emergency shut down of the gas turbine. Simulation analysis proved the system which makes use of fluid resistance to be more efficient than that heretofore in use. DOE

N90-16079# Sandia National Labs., Albuquerque, NM.
DIBLOCK COPOLYMERS AT SURFACES
Peter F. Green, Thomas M. Christensen, Thomas P. Russell, and Spiros H. Anastasiadis (International Business Machines Corp., San Jose, CA.) 1989 19 p Presented at the Materials Research Society Fall Meeting, Boston, MA, 27 Nov. - 2 Dec. 1989
(Contract DE-AC04-76DP-00789)
(DE90-005406; SAND-89-2788C; CONF-891119-59) Avail: NTIS HC A03/MF A01

The surface properties of symmetric microphase separated diblock copolymers of polystyrene (PS) and polymethylmethacrylate (PMMA) were investigated using x ray photoelectron spectroscopy (XPS), the specular reflectivity of neutrons and secondary ion mass spectrometry (SIMS). PS, the lower surface energy component, exhibited a preferential affinity for the free surface. For copolymers that are far from the bulk microphase separation transition (MST), the surface consists of a layer of pure PS. When the system is

close to the MST the surface is a mixture of PS and PMMA. The PS surface excess can be described by a N-(1/2) dependence, where N is the number of segments that comprise the copolymer chain. It is shown that the surface undergoes an ordering transition at a temperature T sub s that is above that of the bulk MST. The ordering of the bulk lamellar morphology is induced by an ordering at the surface. This is analogous to the ferromagnetic order observed in systems such as Gd at temperatures above the bulk Curie temperature. The results here are discussed in light of previous work on copolymer surfaces and in light of mean field theory. DOE

N90-15909# Royal Aircraft Establishment, Farnborough (England). Materials and Structures Dept.
THE EFFECT OF PRIMER AGE ON ADHESION OF POLYSULPHIDE SEALANT
S. P. Wilford and J. Day *In* AGARD, Fuel Tank Technology Nov. 1989 7 p (For primary document see N90-15904 08-05) Copyright Avail: NTIS HC A08/MF A01; Non-NATO Nationals requests available only from AGARD/Scientific Publications Executive

N90-15910# Products Research and Chemical Corp., Glendale, CA. Aerospace Div.
IMPROVED PERFORMANCE POLYSULFIDE BASED SEALANT
Ahmed Sharaby *In* AGARD, Fuel Tank Technology Nov. 1989 9 p (For primary document see N90-15904 08-05) Copyright Avail: NTIS HC A08/MF A01; Non-NATO Nationals requests available only from AGARD/Scientific Publications Executive

N90-15911# Products Research and Chemical Corp., Glendale, CA.
FUEL RESISTANT COATINGS FOR METAL AND COMPOSITE FUEL TANKS
Santo Randazzo *In* AGARD, Fuel Tank Technology Nov. 1989 20 p (For primary document see N90-15904 08-05) Copyright Avail: NTIS HC A08/MF A01; Non-NATO Nationals requests available only from AGARD/Scientific Publications Executive

28 PROPELLANTS AND FUELS

Includes rocket propellants, igniters, and oxidizers; their storage and handling procedures; and aircraft fuels.

For related information see also *07 Aircraft Propulsion and Power, 20 Spacecraft Propulsion and Power,* and *44 Energy Production and Conversion.*

N90-16080# Defence Science and Technology Organization, Salisbury (Australia).
TRACKING FLARES
I. L. Thompson 1989 17 p
(ISBN-0-642-13583-5) Copyright Avail: NTIS HC A03/MF A01

A major requirement of experimental missile firings is that the position and attitude of the missile be known during flight. At Woomera extensive use was made of optical tracking systems which were more accurate than contemporary radar sets, provided the missile remained in view. The design and manufacture of a series of tracking flares developed to extend the range of visibility are described. Author

N90-16081# Defence Science and Technology Organization, Salisbury (Australia).
METAL VAPORISERS: BICENTENNIAL SERIES OF FIVE HISTORICAL MONOGRAPHS
I. R. Johnston 1988 17 p
(ISBN-0-642-13584-3) Avail: NTIS HC A03/MF A01

Metal vaporizer units, developed at the Weapons Research Establishment and deployed from Woomera launched rockets, were used to produce gigantic glow clouds at altitudes in excess of 80 km. These clouds were tracked and various upper atmospheric parameters such as neutral wind, the interrelationship of the wind with the earth's magnetic field and the effect of both on the ionized atmosphere, were measured. The design and development of various vaporizers are chronicles from humble beginnings to the production of reliable units for use. Author

N90-16082# Sandia National Labs., Albuquerque, NM. Initiating and Pyrotechnic Components Div.
VERY LOW ENERGY IGNITION OF PYROTECHNICS USING A SEMICONDUCTOR BRIDGE (SCB)
C. B. McCampbell (SCB Technologies, Inc., Albuquerque, NM.), R. W. Bickes, Jr., and S. L. Schlobohm Nov. 1989 17 p Presented at the Annual American Defense Preparedness Association Meeting, New Orleans, LA, 3-4 Oct. 1989
(Contract DE-AC04-76DP-00789)
(DE90-002645; SAND-89-2259; CONF-8910224-1) Avail: NTIS HC A03/MF A01

Electroexplosive devices conventionally use small metal bridgewires (hot wires) to ignite pyrotechnic and other energetic powders. Typically, hot-wire pyrotechnic ignition takes place a few milliseconds after a current pulse of at least 20 mJ is applied to the bridgewire. In contrast, we report here a new means for ignition that produces a usable explosive output in less than 125 microsec after application of a current pulse of less than 2 mJ energy to the device. Our igniter is a semiconductor bridge (SCB) which is a heavily doped polysilicon region defined on a silicon substrate. Despite the low energies needed for powder ignition, SCBs have excellent no-fire characteristics, better than the hot wires, because of the intimate contact of the SCB bridge with the underlying substrate. In addition, experiments show very good electrostatic discharge characteristics; application of the current pulse obtained from a 500-pF capacitor charged to 25 kV to our SCB test devices in series with a 5000-Omega resistor produced no bridge damage. The energy required for explosive ignition with SCBs is discussed as a function of bridge size and ESD tests. Also briefly discussed are SCB processing and die mounting procedures that lend themselves to automated component assembly. DOE

N90-16083# Department of the Air Force, Washington, DC.
SYNTHESIS OF TETRAFLUOROHYDRAZINE Patent
Miles R. Palmer, inventor (to AF) 23 May 1989 4 p Filed 7 Sep. 1988 Supersedes US-Patent-Appl-SN-241179 (AD-D014281; US-Patent-4,832,931; US-Patent-Appl-SN-241179; US-Patent-Class-423-406) Avail: US Patent and Trademark Office CSCL 21/9

High purity tetrafluorohydrazine is synthesized by reacting nitrogen trifluoride with silicon at an elevated temperature. The reaction occurs only periodically and at a low concentration of NF3. Immediate cooling of the reaction material produces tetrafluorohydrazine and silicon tetrafluoride. Alkaline hydrolysis removes substantially all impurities. Tetrafluorohydrazine is further recovered by cryogenic trapping from the remaining impurities. Tetrafluorohydrazine is useful as a high energy oxidizer as a rocket propellant. For example, when it reacts with hydrazine a specific impulse of about 300 is possible. This value may be compared with those for reaction of oxygen and hydrazine, for which the calculated specific impulse is 273 sec. and the flame temperature is 3000 K. It will be seen that tetrafluorohydrazine provides almost as high a specific impulse, but it differs from oxygen in being storable in liquid condition at normal temperatures, while liquid oxygen requires low temperatures which bring many problems. Tetrafluorohydrazine can also be reacted with ammonia to provide a source of high energy and high impulse. Thus, tetrafluorohydrazine may be stored in missiles which are ready for immediate launching. The present invention is directed at a single step process that produces tetrafluorohydrazine without these undesirable characteristics. GRA

N90-16084# California Univ., Berkeley. Lawrence Berkeley Lab. Applied Sciences Div.
DEVELOPMENT AND EVALUATION OF A PROCESS TO PRODUCE HYDROGEN FROM COAL Ph.D. Thesis

Thomas E. Colson and Scott Lynn Aug. 1989 47 p
(Contract DE-AC03-76SF-00098)
(DE90-003937; LBL-27955) Avail: NTIS HC A03/MF A01

This thesis is a study of a proposed process to produce hydrogen from coal via coal gasification and the water-gas shift (WGS) reaction. A novel aspect of the process is the use of the U.C. Berkeley Sulfur Recovery Process (UCBSRP) for removal of CO2 and H2S from the gasified coal (Neumann 1986 and Sciamanna 1986). The CO(sub 2) is recovered as a purified product and the H(sub 2)S is recovered as elemental sulfur. DOE

N90-16085# Oak Ridge National Lab., TN.
ALCOHOL AND BLENDS AS MOTOR FUELS Foreign Trip Report, 11-18 Nov. 1989
R. N. McGill 4 Dec. 1989 15 p
(Contract DE-AC05-84OR-21400)
(DE90-003517; ORNL/FTR-3490) Avail: NTIS HC A02/MF A01

Participation is reported in the 11th meeting of the Executive Committee on Alcohols and Alcohol Blends as Motor Fuels (International Energy Agency). Participating countries in addition to the U.S. are Canada, Italy, Finland, Japan, Sweden, New Zealand (absent). A representative of West Germany was in attendance as an observer and also to make a technical presentation. The status of three existing annexes was reviewed and two new annexes were approved in principle with details to be discussed in the next meeting. An invitation was extended for the committee to hold its next meeting in June 1990 in Los Angeles, California. In other informal discussions during the travel period, it was learned that the organizing committee of the International Symposium on Alcohol Fuels wishes for the U.S. to host the symposium in 1993. DOE

N90-16086# Heidelberg Univ. (Germany, F.R.).
APPLICATION OF THE SINGULARITY-SEPARATING METHOD TO COMPUTING PROBLEMS OF SOLID-PROPELLANT COMBUSTION IN A CLOSED VESSEL
Xionghua Wu and Youlan Zhu (Academia Sinica, Beijing, China) Nov. 1988 14 p Sponsored in part by the AvH Foundation; Chinese National Natural Science Foundation; and the Tongji University Science Foundation
(Preprint-489; ETN-90-95876) Avail: NTIS HC A03/MF A01

The Singularity-Separating Method (SSM) is used to calculate the flow field resulting from a solid-propellant combustion in a closed tube. Comparisons between the results obtained and results obtained by the Random Choice Method (RCM) are presented. The singularity separating method considers all discontinuity lines in the flow field as internal boundary lines. The difference scheme is used only in subregions with continuous solution. Using the SSM, accurate numerical results are obtained even near the discontinuity lines or boundaries. ESA

29 MATERIALS PROCESSING

Includes space-based development of products and processes for commercial applications.

For biological materials see *55 Space Biology*.

N90-16087*# National Aeronautics and Space Administration. Lewis Research Center, Cleveland, OH.
CONCEPTUAL DESIGN FOR THE SPACE STATION FREEDOM MODULAR COMBUSTION FACILITY
17 May 1989 63 p Presented at the MCF Assessment Workshop, Cleveland, OH, 17-18 May 1989; sponsored by NASA, Washington
(NASA-TM-102037; E-4786; NAS 1.15:102037) Avail: NTIS HC A04/MF A01 CSCL 22A

A definition study and conceptual design for a combustion science facility that will be located in the Space Station Freedom's baseline U.S. Laboratory module is being performed. This modular, user-friendly facility, called the Modular Combustion Facility, will be available for use by industry, academic, and government research communities in the mid-1990's. The Facility will support research experiments dealing with the study of combustion and its byproducts. Because of the lack of gravity-induced convection, research into the mechanisms of combustion in the absence of gravity will help to provide a better understanding of the fundamentals of the combustion process. The background, current status, and future activities of the effort are covered. Author

N90-16088# European Space Agency, Paris (France).
EXPERIMENT FACILITIES FOR MATERIALS AND FLUID SCIENCES EMBARKED ON EURECA-1
Valerie David, ed. Aug. 1989 23 p Original contains color illustrations
(ESA-SP-1118; ISBN-92-9092-044-0; ISSN-0379-6566; ETN-90-96201) Copyright Avail: NTIS HC A03/MF A01; ESA Publications Div., ESTEC, Noordwijk, Netherlands, 20 Dutch guilders

The mission profiles and the performance characteristics of the European Retrievable Carrier (Eureca) are described. Eureca is designed to conduct a long duration microgravity investigation requiring low levels of residual acceleration. The Eureca-1 mission is scheduled for 1991 (launch with shuttle flight number 46 in May 1991 and retrieval with flight number 51 in January 1992). A concise overview of the facilities to be flown on Eureca-1 for materials and fluid sciences experiments is given. Since the Eureca satellite is unmanned; experiments have to be automated or teleoperated from the ground. Lists of the planned experiments for each facility are included. ESA

N90-16089# European Space Agency, Paris (France).
EXPERIMENT FACILITIES FOR MATERIALS AND FLUID SCIENCES EMBARKED ON SPACELAB
Norman Longdon, ed. Aug. 1989 57 p Original contains color illustrations
(ESA-SP-1120; ISBN-92-9092-052-1; ISSN-0379-6566; ETN-90-96202) Copyright Avail: NTIS HC A04/MF A01; ESA Publications Div., ESTEC, Noordwijk, Netherlands, 30 Dutch guilders

Information on the facilities and experiment modules for Spacelab missions are provided. The experiments conducted with fluid systems under microgravity conditions, where gravity-driven convection, sedimentation, and hydrostatic pressure are almost eliminated, are considered. Physical and physico-chemical processes such as capillarity, flow and transport processes, near critical point phenomena, and crystal growth from the melt, the vapor phase and from solutions, are included. This report is useful in identifying and defining new hardware developments, in avoiding duplications and also in arriving at a coherent picture of flight experiment hardware in Europe. ESA

N90-16090# Universitaet der Bundeswehr, Neubiberg (Germany, F.R.). Inst. fuer Raumfahrttechnik.
RESPONSE OF A ROTATING FINITE ANNULAR LIQUID LAYER TO AXIAL EXCITATION
Helmut F. Bauer 1988 44 p
(LRT-WE-9-FB-15(1988); ETN-90-96063) Avail: NTIS HC A03/MF A01

Experiments carried out on a solidly rotating finite annular liquid layer are described. The liquid layer, consisting of a non-viscous liquid, is subjected to axial harmonic excitation in a zero gravity environment. The response of the free liquid surface elevation and the velocity in radial and axial directions is determined. Data is obtained over a wide forcing frequency range and in the hyperbolic range for different diameter ratios. ESA

31 ENGINEERING (GENERAL)

Includes vacuum technology; control engineering; display engineering; cryogenics; and fire prevention.

N90-16091# Oak Ridge National Lab., TN. Engineering Physics and Mathematics Div.

ELECTROPLATING SIMULATION

L. J. Gray, G. E. Giles, J. S. Bullock, and P. W. McKenzie (Oak Ridge Y-12 Plant, TN.) 1989 14 p Presented at the European Conference on Mathematics in Industry, Glasgow, Scotland, 28-31 Aug. 1989 Prepared in cooperation with IBM Norway, Bergen
(Contract DE-AC05-84OR-21400)
(DE90-003683; CONF-8908186-1) Avail: NTIS HC A03/MF A01

A simulation of a three-dimensional electroplating process which includes a model of the heat flow generated during the plating is presented. The steady state temperature distribution in the cell is coupled to the electric field through the nonlinear polarization (overvoltage) boundary conditions and the temperature dependence of the electrolyte conductivity. As the conductivity directly influences the deposition rate, variations due to temperature can have an impact on the shape of the plated part. The thermal and electrostatic problems are simultaneously solved using the boundary element method, and a simple iterative scheme is employed to satisfy the boundary conditions. A newly developed boundary element procedure for crack geometries is used to cope with the thin shielding present in the cell. Utilizing this technique, a computationally expensive and cumbersome multidomain decomposition of the region is avoided. DOE

N90-16092# General Atomic Co., San Diego, CA.

D3-D CRYOGENIC CONTROL SYSTEM UPGRADE

G. L. Campbell and J. J. Gilgallon Nov. 1989 4 p Presented at the 13th International Symposium on Fusion Engineering, Knoxville, TN, 2-6 Oct. 1989 Submitted for publication
(Contract DE-AC03-89ER-51114; GA Proj. 3466)
(DE90-003290; GA-A-19747; CONF-891007-92) Avail: NTIS HC A01/MF A01

The helium liquefier and distribution system at the DIII-D tokamak facility was upgraded with the addition of a programmable logic controller, color graphic operator interfaces and analog data acquisition system. This new system provides extended monitoring, control capability as well as centralized datalogging, trending and alarm reporting. Other objectives included offsite (remote) monitoring and control via phone modem and a hardware basis for automation of liquefier operation and maintenance. It is now also possible to accomplish connection and coordination with other DIII-D control systems. It was required that most of the installation and checkout of the new control system be done during operating periods. For this reason, and reliability concerns, the upgrade hardware was designed and installed as an additional independent system rather than a replacement control system. DOE

N90-16093# Technical Research Centre of Finland, Espoo. Lab. of Electrical and Automation Engineering.

FEASIBILITY OF COOL STORAGE SYSTEMS IN REFRIGERATION

Yehia ElMahgary, Veikko Kekkonen, Ari Laitinen, and Hannu Pihala May 1989 81 p
(DE90-728179; VTT-TUTK-620; ISBN-951-38-3253-8; ISSN-0358-5077) Avail: NTIS (US Sales Only) HC A05/MF A01

In the present report, the economic viability and technical feasibility of selected cool storage systems are considered. Cool storage has clear potential for several applications: in connection with air-conditioning systems, domestic refrigerating and freezing systems; commercially e.g., in the dairy and vegetable industries; and in deep freezing, as in the meat industry. Air-conditioning has limited significance in Finland. For this reason it was not investigated in this study. In domestic refrigeration and freezing two systems were investigated; a controlled cooling/heating system and a simple built-in system in individual refrigerators and freezers. The central cooling/heating system in houses was found to be economically unattractive. It also has several technical drawbacks. The simple built-in system appeared to be promising. The amount of savings is rationally a function of the difference between day and night tariffs and the costs of installing an automatic switch and storage media. In the vegetable and dairy industries cool storage also has considerable potential. Several systems were investigated in this respect and compared to the conventional system. The cool storage system using Cristopia balls, one of the most common commercial systems available in Europe, was not economical at a tariff difference of 10 p/k Wh or more. Cool storage for freezing in meat plants was also investigated. DOE

N90-16094# Sandia National Labs., Albuquerque, NM.

DIGITAL SYSTEM FOR MONITORING AND CONTROLLING REMOTE PROCESSES

Dennis P. Roach 1989 19 p Presented at the Winter Annual Meeting of the ASME , San Francisco, CA, 10-15 Dec. 1989
(Contract DE-AC04-76DP-00789)
(DE90-003935; SAND-89-1608C; CONF-891208-26) Avail: NTIS HC A03/MF A01

The need to operate increasingly complex and potentially hazardous facilities at higher degrees of efficiency can be met through the development of automated process control systems. The availability of microcomputers capable of interfacing to data acquisition and control equipment results in the possibility of developing such systems at low investment costs. An automated control system is described which maintains a constant or time varying pressure in a pressure vessel. Process control data acquisition and analysis is carried out using a commercially available microcomputer and data scanner interface device. In this system, a computer interface is developed to allow precision positioning of custom designed proportional valves. Continuous real time process control is achieved through a direct digital control algorithm. The advantages to be gained by adapting this system to other process control applications is discussed. The modular design and ability of this system to operate many types of hardware control mechanisms makes it adaptable to a wide variety of industrial applications. DOE

N90-16095# Lawrence Livermore National Lab., CA.

ELECTRODE/WORKPIECE COMBINATIONS

J. J. Benedict 19 Oct. 1989 7 p Presented at the Machine Tool Subgroup and Machineability Technical Exchange Meeting, Las Vegas, NV, 23-26 Oct. 1989
(Contract W-7405-eng-48)
(DE90-003919; UCRL-102200; CONF-8910318-1) Avail: NTIS HC A02/MF A01

Of the many machine tool operations available in the shop today, plunge cut Electrical Discharge Machining (EDM) has become an increasingly useful method of materials fabrication. It is a necessary tool for the research and development type of work performed at the Lawrence Livermore National Laboratory (LLNL). With advancing technology, plunge cut EDMs are more efficient, faster, have greater accuracy and are able to produce better surface finishes. They have been in the past and will continue to be an important part of the production of quality parts in both the Precision and NC Shop. It should be kept in mind that as a non-traditional machining process, EDMing is a time consuming process that can be a very expensive method of producing parts. For this reason, it must be used in the most efficient manner in order to make it a cost-effective means of fabrication, although technology has advanced to the point of state-of-the-art equipment, there is currently a void in available technical information needed for use with this process. The type of information sought after concerns the area of electrode/workpiece combinations. This is in reference to the task of choosing the correct electrode material for the specific workpiece material encountered. A brief description of the EDM process will help in understanding the electrode/workpiece relationship. DOE

N90-15912# Air Force Wright Aeronautical Labs., Wright-Patterson AFB, OH.
SPRAY SEALING: A BREAKTHROUGH IN INTEGRAL FUEL TANK SEALING TECHNOLOGY
Martin D. Richardson and J. H. Zadarnowski (McDonnell Aircraft Co., Saint Louis, MO.) *In* AGARD, Fuel Tank Technology Nov. 1989 12 p (For primary document see N90-15904 08-05)
Copyright Avail: NTIS HC A08/MF A01; Non-NATO Nationals requests available only from AGARD/Scientific Publications Executive

N90-16692*# Savannah State Coll., GA. Dept. of Engineering Technology.
ANALYSIS OF THE 60-Hz POWER SYSTEM AT KSC: THE ORSINO SUBSTATION
Alex O. Kalu *In* University of Central Florida, NASA/ASEE Summer Faculty Fellowship Program Oct. 1989 p 125-158 (For primary document see N90-16686 08-99)
Avail: NTIS HC A18/MF A03 CSCL 10B

32 COMMUNICATIONS AND RADAR

Includes radar; land and global communications; communications theory; and optical communications.

For related information see also *04 Aircraft Communications and Navigation* and *17 Space Communications, Spacecraft Communications, Command and Tracking.* For search and rescue see *03 Air Transportation and Safety,* and *16 Space Transportation.*

N90-16096 British Broadcasting Corp., Kingswood (England). Engineering Div.
USE OF AN HF ACTIVE MONITORING ARRAY IN THE PRESENCE OF HIGH LEVEL INTERFERENCE
K. L. Beeke 1989 9 p
(BBC-RD-1989/7) Avail: Issuing Activity

An electronically-steerable, active receiving array for HF was developed at BBC Research Department a few years ago. An investigation is being carried out to find the limiting operating conditions for the array, i.e., under what maximum levels of interference it can be operated satisfactorily. Typically, it was found that if interference levels are greater than about 100 dB/microV/m, then some form of screening will be required, especially if the wanted signal level is very low and on a frequency close to an intermodulation product of the interfering signals. Author

N90-16097 British Broadcasting Corp., Kingswood (England). Engineering Div.
THE FIRST YEAR'S WORK OF RACE PROJECT 1036 WTDM BROADBAND CUSTOMER PREMISES NETWORK
A. Oliphant 1989 15 p
(BBC-RD-1989/6) Avail: Issuing Activity

The first year's work on the Research and development Advanced Communications technology in Europe (RACE) is described. The aim is to develop a Broadband Customer Premises Network (BCPN) suitable for broadband service providers and for a wide range of applications in industry, commerce, education, and public services. The BCPN uses a combination of wavelength-division multiplexing and electrical time-division multiplexing to give a total capacity on a single bearer of over 38 Gbit/s. During the first year a detailed technical specification was agreed by the partners. Technical progress is reported in electrical multiplexing up to 2.5 Gbit/s, control and packaging of high speed laser transmitters, optical star couplers, optical demultiplexers, optical receivers, and system control. Author

N90-16098 British Broadcasting Corp., Kingswood (England). Engineering Div.
SATELLITE BROADCASTING: REQUIREMENTS FOR THE RECEIVING ANTENNA
J. H. Stott 1989 23 p
(BBC-RD-1989/5) Avail: Issuing Activity

The receiving antenna plays a significant part in the reception of television signals broadcast from a satellite in so-called Direct Broadcasting by Satellite (DBS). The performance of the antenna must be sufficiently good to ensure that signals are received without suffering adverse effects of noise or interference. A hypothetical receiver specification was used during the planning of satellite broadcasting at the World Administrative Radio Conference in 1977 (WARC-77), but while this is in general sufficient it may not always be necessary. Furthermore, the different trade-offs involved in the antenna designs (including flat-plate types) may mean that the same result can most effectively be obtained with a very different specification. The various requirements are explained, and examples are given for incomplete or lower-power use of the WARC-77 allocations. It provides a useful background to related research reports which describe work on flat-plate antennas. Author

N90-16099# Defence Science and Technology Organization, Salisbury (Australia).
THE DEVELOPMENT OF OVER-THE-HORIZON RADAR IN AUSTRALIA
D. H. Sinnott 1989 42 p
(ISBN-0-642-13561-4) Avail: NTIS HC A03/MF A01

The development of over-the-horizon radar (OTHR) in Australia is so closely tied to the word JINDALEE in the minds of most peple that one might imagine that the history of Defence Science and Technology Organization (DSTO's) Project JINDALEE, spanning the years 1975 to 1985, is the total history of OTHR in Australiia. It is not the case. While JINDALEE saw the development of OTHR technology and the commissioning and testing of two experimental OTHR systems, the history extends in both direction outside the decade in which project Jindalee was running. In this Monograph, the story of the OTHR in Australia is sought from its origins in ionospheric soundings in the 1950s to the present. Necessarily much of the story is that of JINDALEE but, fascinating though this is, the earlier work which laid the basis for DSTO's enormously successful project is equally interesting. For it is a record of work which advanced with little official support or recognition and which required the force of several major personalities to keep up its momentum. OTHR was and continues to be an important and high-profile area of DSTO research. It is very apt that, in the Bicentennial year, a record of Australian OTHR research should be published. It is the hope of this monography that the record might prove to be not just a history of events which made up the story of the development of OTHR but also convey something of the flavor of defense research in this country. Author

N90-16100# Essex Corp., Westlake Village, CA.
MANPRINT (MANPOWER AND PERSONNEL INTEGRATION) EVALUATION: AN/TRC-170 DIGITAL TROPOSCATTER RADIO SYSTEM Final Report, Oct. 1986 - Jan. 1988
Gregory S. Krohn and Samuel E. Bowser Jun. 1989 78 p
(Contract MDA903-86-C-0341; DA Proj. 793)
(AD-A211799; ARI-RR-1524) Avail: NTIS HC A05/MF A01
CSCL 23/2

This document describes the Manpower and Personnel Integration (MANPRINT) Evaluation of the AN/TRC-170 Digital Troposcatter Radio System. The MANPRINT evaluation was conducted in support of the AN/TRC-170 Follow-On Operational Test and Evaluation (FOT and E) by the U.S. Army Research Institute for the Behavioral and Social Sciences (ARI). The FOT and E was conducted by the U.S. Army Operational Test and Evaluation Agency (OTEA) at Fort Huachuca, AZ, from September 1986 through January 1987. The purpose of the MANPRINT Evaluation was to identify human factors engineering, system safety, health hazards, training, and manpower factors leading to refinements in the AN/TRC-170 system. The MANPRINT evaluation methodology included structured interviews, on-site observations of operations and maintenance, and measures of task performance times. There were 24 MANPRINT findings involving equipment assembly and disassembly, materials handling procedures, and safety during road marches. GRA

N90-16101# National Inst. of Standards and Technology, Boulder, CO. Electromagnetic Fields Div.
X-BAND ATMOSPHERIC ATTENUATION FOR AN EARTH TERMINAL MEASUREMENT SYSTEM
Michael H. Francis Jul. 1989 46 p Sponsored by Camp Parks Communications Annex
(PB90-100736; NISTIR-89/3918) Avail: NTIS HC A03/MF A01 CSCL 20N

The National Institute of Standards and Technology has developed an Earth Terminal Measurement System to be used by the Camp Parks Communications Annex in determining satellite effective isotropic radiated power and antenna gain. In determining these quantities the effect of atmospheric attenuation must be taken into account. An overview is provided of the methods used for determining atmospheric attenuation with emphasis on a tipping-curve method. An error analysis is also provided. GRA

N90-16102# Helsinki Univ. of Technology, Espoo (Finland). Radio Lab.
HELSINKI UNIVERSITY OF TECHNOLOGY RADIO LABORATORY Annual Report, 1988
Antti Raeisaenen, ed. Apr. 1989 26 p
(PB90-110677; ISBN-951-754-888-5; ISSN-0355-5712; S-179)
Avail: NTIS HC A03/MF A01 CSCL 17B

Activities of the Radio Laboratory are described for the year 1988. Research is discussed in three areas: (1) Millimeter Wave Techniques -- (22 GHz receiver for Radioastron satellite, coaxial MESFT-and HEMT-amplifiers for 22.2 GHz, 40 to 50 GHz Schottky-mixer receiver, 100 GHz SIS mixer, millimeter-wave frequency multipliers, quasi-optics studies, and anechoic chamber measurements); (2) Industrial Microwave Applications -- (microwave hygrometer, measurement of the water mass per unit area of paper, and high-resolution portable impulse radar); and (3) Microwave and Millimeter Wave Propagation -- (atmospheric attenuation studies, and development of a measurement system for propagation studies at mm-waves. GRA

N90-16103*# Ohio State Univ., Columbus. ElectroScience Lab.
HIGH-FREQUENCY ASYMPTOTIC METHODS FOR ANALYZING THE EM SCATTERING BY OPEN-ENDED WAVEGUIDE CAVITIES
R. J. Burkholder and P. H. Pathak Sep. 1989 271 p
(Grant NAG3-476)
(NASA-CR-186244; NAS 1.26:186244; ESL-TR-719630-3) Avail: NTIS HC A12/MF A02 CSCL 20N

Four high-frequency methods are described for analyzing the electromagnetic (EM) scattering by electrically large open-ended cavities. They are: (1) a hybrid combination of waveguide modal analysis and high-frequency asymptotics, (2) geometrical optics (GO) ray shooting, (3) Gaussian beam (GB) shooting, and (4) the generalized ray expansion (GRE) method. The hybrid modal method gives very accurate results but is limited to cavities which are made up of sections of uniform waveguides for which the modal fields are known. The GO ray shooting method can be applied to much more arbitrary cavity geometries and can handle absorber treated interior walls, but it generally only predicts the major trends of the RCS pattern and not the details. Also, a very large number of rays need to be tracked for each new incidence angle. Like the GO ray shooting method, the GB shooting method can handle more arbitrary cavities, but it is much more efficient and generally more accurate than the GO method because it includes the fields diffracted by the rim at the open end which enter the cavity. However, due to beam divergence effects the GB method is limited to cavities which are not very long compared to their width. The GRE method overcomes the length-to-width limitation of the GB method by replacing the GB's with GO ray tubes which are launched in the same manner as the GB's to include the interior rim diffracted field. This method gives good accuracy and is generally more efficient than the GO method, but a large number of ray tubes needs to be tracked. Author

N90-16104*# National Aeronautics and Space Administration. Pasadena Office, CA.
STRIPLINE FEED FOR A MICROSTRIP ARRAY OF PATCH ELEMENTS WITH TEARDROP SHAPED PROBES Patent Application
John Huang, inventor (to NASA) 7 Sep. 1989 24 p
(Contract NAS7-918)
(NASA-Case-NPO-17548-1-CU; NAS 1.71:NPO-17548-1-CU; US-Patent-Appl-SN-404293) Avail: NTIS HC A03/MF A01 CSCL 20N

A circularly polarized microstrip array antenna utilizing a honeycomb substrate made of dielectric material to support on one side the microstrip patch elements in an array, and on the other side a stripline circuit for feeding the patch elements in subarray groups of four with angular orientation and phase for producing circularly polarized radiation, preferably at a 0, 90, 180, and 270 degree relationship is described. The probe used for coupling each feed point in the stripline circuit to a microstrip patch element is teardrop shaped in order to introduce capacitance between the coupling probe and the metal sheet of the stripline circuit that serves as an antenna ground plane. The capacitance thus introduced tunes out inductance of the probe. The shape of the teardrop probe is not critical. The probe capacitance required is controlled by the maximum diameter for the teardrop shaped probe, which can be empirically determined for the operating frequency. An aluminum baffle around each subarray blocks out surface wave between subarrays. NASA

N90-16105# Department of the Air Force, Washington, DC.
METHOD FOR ELIMINATING SELF-SCREENING NOISE JAMMING IN RADAR SYSTEMS Patent
Charles B. Clarkson, inventor (to AF) 25 Jul. 1989 4 p Filed 22 Jan. 1970 Supersedes US-Patent-Appl-SN-012517
(AD-D014271; US-Patent-4,851,847; US-Patent-Appl-SN-012517)
Avail: US Patent and Trademark Office CSCL 17/4

A method for eliminating self-screening noise jamming from the main beam of a radar in order to reveal the skin echoes of aircraft at the same angle, including the aircraft carrying the jammer by using a main antenna and an auxiliary antenna located a short distance apart, delaying the signal from the auxiliary antenna decorrelating the signals and cancelling the jamming signals. GRA

N90-16106# Department of the Air Force, Washington, DC.
SEQUENTIAL RAPID COMMUNICATION VISUAL DISPLAYS Patent
Ethel Matin, inventor (to AF) and Kenneth R. Boff, inventor (to AF) 4 Jul. 1989 12 p Filed 28 Aug. 1987 Supersedes US-Patent-Appl-SN-090500
(AD-D014282; US-Patent-4,845,645; US-Patent-Appl-SN-090500)
Avail: US Patent and Trademark Office CSCL 14/2

The rapid communication (RAP-COM) microprocessor controlled memory display system and method operates by presenting real-time data in rapid temporal succession at one spatial location. It can be embodied as a stand-alone instrument or as a small display window within a larger integrated display. It can be incorporated, for example, within larger display configurations in military crew stations, nuclear power plants, air-traffic control centers, space stations, or industrial process control plants. RAP-COM has two advantages over conventional display formats. First, it reduces the amount of required display space by presenting information in sequentially in one location rather than simultaneously in several locations. Second it speeds the rate of system-to-operator information transfer by eliminating the time needed for the scanning saccadic eye movements that access information from conventional spatially separated displays. GRA

N90-16107# Naval Ship Research and Development Center, Bethesda, MD. Ship Materials Engineering Dept.
PLASMON EXCITATION IN THE SCATTERING OF ELECTROMAGNETIC WAVES FROM GOOD CONDUCTORS Final Report, 1 Oct. 1988 - 1 Sep. 1989

Clifford R. Schumacher Jul. 1989 19 p
(AD-A214026; DTRC/SME-89/025) Avail: NTIS HC A03/MF A01 CSCL 20/14

Excellent Drude model fits were reported to the Kramers-Kroning analysis of measurements of the optical constants of 15 metals: Ti, Fe, Co, Ni, Pt, V, Pd, W, Pb, Cu, Mo, Ta, Ag, Au, and Al. The resulting values of plasma and damping frequencies not only provide excellent fits to the measured values of the conductivity but also were shown to predict the frequency dependence of the dielectric constant. All static values of the dielectric constant of these 15 metals were negative and very large, but increased monotonically with increasing frequency, passing through zero in the optical range between wavelengths of 1,000 and 6,000A. This behavior was interpreted as plasmon excitation, and very sharply peaked loss factors were calculated. Furthermore, the novel behavior of the dielectric constant caused a large impedance discontinuity that kept the reflection coefficient very nearly equal to 1 unit until it dropped very rapidly at the plasma resonance frequency to values approaching zero as photon energies reached the electron volt range. GRA

N90-16108# Naval Ocean Systems Center, San Diego, CA.
LOW-ALTITUDE MILLIMETER-WAVE PROPAGATION IN THE EVAPORATION DUCT Final Report, Oct. 1984 - Jul. 1989
K. D. Anderson Jul. 1989 32 p Sponsored by ONR, Arlington, VA
(AD-A214432; NOSC/TR-1300) Avail: NTIS HC A03/MF A01 CSCL 20/14

One-way, low altitude radio propagation measurements at 94 GHz and simultaneous surface meteorological measurements were made on a 40.6-km over-the-horizon, over-water path along the southern California coast to assess the effects of the evaporation duct on signal propagation. More than 2000 hours of received signal power were recorded in eight measurement periods from July 1986 through July 1987. The average received power was 63 dB greater than expected for propagation in a nonducting, or standard, atmosphere; 90 percent of the measurements were at least 55 dB greater than the standard atmosphere. Predictions of transmission loss based on the observed surface meteorology compared favorably to the measured transmission loss; on the average, the predictions underestimated the transmission loss by 10 dB. The reliability and reasonable accuracy of the model provided a strong justification for utilizing the technique to assess millimeter-wave communication and radar systems operating in many, if not all, ocean regions. GRA

N90-16109# International Centre for Theoretical Physics, Trieste (Italy).
ON AVERAGED FORCE ACTING ON A PARTICLE IN HF ELECTROMAGNETIC FIELD
J. F. Ogunniyi and D. D. Tskhakaya (Academy of Sciences of the Georgian SSR, Tbilisi.) Jun. 1989 8 p Submitted for publication
(DE90-600984; IC-89/146) Avail: NTIS (US Sales Only) HC A02/MF A01

A general expression is obtained for the time averaged force acting on a particle immersed in a magnetic field in the presence of HF quasiplanar, quasimonochromatic electromagnetic wave. Here, averaging is done over the period of the HF wave. It is shown that this averaged force is proportional to the time derivative of the squared HF wave amplitude. The force also includes a term proportional to the gradient of the time constant magnetic field and is connected with the induced magnetic moment in the HF field. DOE

N90-16110*# Jet Propulsion Lab., California Inst. of Tech., Pasadena.
MT'S ALGORITHM: A NEW ALGORITHM TO SEARCH FOR THE OPTIMUM SET OF MODULATION INDICES FOR SIMULTANEOUS RANGE, COMMAND, AND TELEMETRY
Tien Manh Nguyen 1 Aug. 1989 90 p
(Contract NAS7-918)
(NASA-CR-186259; NAS 1.26:186259; JPL-89-20) Avail: NTIS HC A05/MF A01 CSCL 17B

MT's algorithm was developed as an aid in the design of space telecommunications systems when utilized with simultaneous range/command/telemetry operations. This algorithm provides selection of modulation indices for: (1) suppression of undesired signals to achieve desired link performance margins and/or to allow for a specified performance degradation in the data channel (command/telemetry) due to the presence of undesired signals (interferers); and (2) optimum power division between the carrier, the range, and the data channel. A software program using this algorithm was developed for use with MathCAD software. This software program, called the MT program, provides the computation of optimum modulation indices for all possible cases that are recommended by the Consultative Committee on Space Data System (CCSDS) (with emphasis on the squarewave, NASA/JPL ranging system). Author

N90-16111# European Space Agency, Paris (France).
REFLECTION FROM LAYERED MEDIA WITH SPECIAL ATTENTION TO THE MICROWAVE REGION
Juergen Preissner (Deutsche Forschungs- und Versuchsanstalt fuer Luft- und Raumfahrt, Oberpfaffenhofen, Germany, F.R.) Oct. 1989 56 p Original language document was announced as N89-26287
(ESA-TT-1155; DFVLR-Mitt-89-03; ETN-90-96191) Avail: NTIS HC A04/MF A01; original German version from DFVLR, VB-PL-DO, Postfach 90 60 58, 5000 Cologne, Fed. Republic of Germany, 19 DM

Reflection at the plane of multi-layered media is described. The mathematical formulation and a developed computer program are given. Selected calculations show the dependence of the reflection on the layer configuration, layer thickness, angle of incidence and frequency. Examples of possible application, such as the measurement of the thickness of a layer of oil and reduction of reflection are discussed. Results and measurements are compared. ESA

N90-16112# European Space Agency, Paris (France).
NECESSITY AND BENEFIT OF THE X-SAR SPACE SHUTTLE EXPERIMENT
Wolfgang Keydel and Herwig Oettl (Deutsche Forschungs- und Versuchsanstalt fuer Luft- und Raumfahrt, Oberpfaffenhofen, Germany, F.R.) Oct. 1989 38 p Transl. into ENGLISH of Notwendigkeit und Nutzen des X-SAR-Space-Shuttle-Experiments Original language document was announced as N89-24688
(ESA-TT-1164; DFVLR-Mitt-88-29; ETN-90-96192) Avail: NTIS HC A03/MF A01; original German version available from DFVLR, VB-PL-DO, Postfach 90 60 58, 5000 Cologne, Federal Republic of Germany, 26.50 deutsche marks

The X-band (9.6 GHz) Synthetic Aperture Radar (X-SAR) is studied. It is the first space qualified SAR in X-band. The X-SAR is to be flown on several Shuttle missions as part of the U.S. Radarlab program for Earth observation. The examples shown clearly indicate that the X-band is an extremely valuable and important frequency range for areas of remote sensing. X-band measurements supply valuable additions to measurements in the L- and C-bands. It can be applied to the classification of cultivated land surfaces and of ice and snow and for finding pollution in rivers, lakes and on the seas. ESA

N90-16113# European Space Agency, Paris (France).
SATELLITE SYSTEMS INTEGRATED WITH THE TERRESTRIAL CELLULAR NETWORK FOR MOBILE COMMUNICATIONS
E. DelRe (Florence Univ., Italy) and W. R. Burke, ed. Aug. 1989 69 p
(ESA-STR-228; ISBN-92-9092-001-7; ISSN-0379-4067; ETN-90-96203) Copyright Avail: NTIS HC A04/MF A01

An integrated satellite/cellular system with reference to the Pan-European standardized digital cellular network is investigated. The integrated system uses the same protocols except for the radio frequency part of the physical layer and the synchronization

strategy in the access phase. Cellular systems based on terrestrial infrastructures are proposed, to satisfy the needs of future users of land mobile communications. For a faster wide-area coverage, the integration of a satellite system with the terrestrial cellular network is a possible approach, provided that the same protocols are used in the two environments. From the preliminary investigations a satellite link at 270.833 kbit/s seems to be feasible from a technical point of view. ESA

N90-16114 Forschungsinstitut fuer Hochfrequenzphysik, Werthhoven (Germany, F.R.).
THE PHYSICAL FOUNDATIONS OF RADIOMETRY AND THEIR APPLICATIONS IN THE mm-WAVEBAND [PHYSIKALISCHE GRUNDLAGEN DER RADIOMETRIE UND IHRE ANWENDUNGEN IN MM-WELLENBEREICH]
H. H. Fuchs Dec. 1988 44 p In GERMAN; ENGLISH summary
(Rept-12-88; Lfd-281; ETN-90-95346) Copyright Avail: Forschungsinstitut fuer Hochfrequenzphysik, Wachtberg-Werthhoven, Federal Republic of Germany

The fundamental principles of radiometry are reviewed. The performance and operational characteristics of radiometers are presented. Applications in the mm-waveband are discussed and examples given. The importance of temperature contrast and the attenuating influence of the atmosphere in determining the range performance of a radiometer are discussed. Possible applications of scanning radiometric sensors on airborne platforms are described. Future development concepts in radiometry including improvement in receivers and their sensing possibilities are discussed. ESA

N90-16115# Southampton Univ. (England). Inst. of Sound and Vibration Research.
AN ANALYSIS OF THE TIME VARIATION OF THE FREQUENCY RESPONSE OF THE LMS ADAPTIVE LINE ENHANCER
R. Y. John Jun. 1989 35 p Sponsored by the ARE, Teddington, England
(ISVR-TR-175; ETN-90-95530) Avail: NTIS HC A03/MF A01

The analysis which quantifies (in a statistical sense) the variation of the LMS ALE's frequency response with time is presented. An upper bound is generated for the rate of change of the frequency response, and it is explained why the spurious broadband streaks are an inevitable feature of the LMS ALE. The physical form of the detector output is given. It is shown that when the input signal to noise ratio is low, the frequency response displays broadband coherence over time which results in the appearance of false lines. ESA

N90-16116 Max-Planck-Inst. fuer Physik und Astrophysik, Garching (Germany, F.R.). Inst. fuer Extraterrestrische Physik.
NATURAL AND MAN-MADE EMISSIONS AT 1.0 TO 5.6 MHz MEASURED BETWEEN 10 AND 18 R SUB E
J. LaBelle, R. A. Treumann, M. H. Boehm, and K. Gewecke Jul. 1989 24 p Submitted for publication Original contains color illustrations
(Grant NSF ATM-88-13654)
(MPE-Preprint-146; ISSN-0178-0719; ETN-90-95854) Copyright Avail: Fachinformationszentrum Karlsruhe, 7514 Eggenstein-Leopoldshafen 2, Federal Republic of Germany

A survey undertaken of the 1.0 to 5.6 MHz electric field spectrum measured at distances of 15 to 18 R(sub E) (100,000 to 120,000 km) from the Earth is described. Auroral Kilometric Radiation (AKR) emissions were taken into consideration in order to resolve interference sources. For the times of weak or absent AKR, the results of this survey may be summarized as follows: for local times of roughly 0800 to 1600 (dayside), a nearly constant level was recorded which at 1 to 3.2 MHz was equal to the galactic background level, and at 3.2 to 5.6 MHz was above the galactic background level and probably was due to spacecraft-generated noise. At other local times, the same nearly constant level was sometimes recorded, but frequently bursts of noise at 3 to 5.6 MHz were observed. These bursts seem more likely to represent ionospheric breakthrough of manmade radiation rather than natural emissions. A comparison with previous satellite observations implies that the terrestrial background level in this frequency range may have increased considerably between 1970 to 1985. ESA

N90-16117# Bonn Univ. (Germany, F.R.). Inst. fuer Physik.
THE LIDAR EXPERIMENT AT ANDOYA, NORWAY, DURING THE SUMMER OF 1988 Thesis [DAS NATRIUM-LIDARGERAET IN ANDOYA, NORWEGEN. IM SOMMER 1988 UND FILMISCHE DARSTELLUNG DYNAMISCHER PROZESSE IN DER MESOPAUSENREGION]
Matthias Alpers Apr. 1989 105 p In GERMAN; ENGLISH summary
(Bonn-IR-89-16; ISSN-0172-8741; ETN-90-95910) Avail: NTIS HC A06/MF A01

The instruments used in the lidar experiment are described. Integration of a wavelength meter into the instruments increased spectral resolving power over a greater bandwidth. A second Fabry-Perot-Etalon for daylight measurements, integrated into the detecting part of the experiment, is described. Experiments in adjusting this filter are outlined. A technique for the transposition of sodium density profiles into a movie is presented. Application of this technique to the measurements of October 21 and 22 in 1987 is described. ESA

N90-16118# Central Research Inst. of Electric Power Industry, Tokyo (Japan). Energy and Environment Lab.
MICROWAVE SCREENING ON DIGITAL RADIO COMMUNICATION LINKS DUE TO MULTICIRCUIT POWER TRANSMISSION LINES
Y. Serizawa and K. Takeshita May 1989 23 p In JAPANESE; ENGLISH summary
(DE90-734950; CRIE-T-88079) Avail: NTIS (US Sales Only) HC A03/MF A01

A method of estimating multicircuit power transmission line interference on digital radio links was developed and applied to several kinds of digital radio systems. In this method, any conductors in the first Fresnel zone on a radio path could be accounted for in the calculation of the interference (equivalent C/N degradation or screening loss). General characteristics of the interference (distance dependency between power transmission line and radio site, power transmission line length dependency in the first Fresnel zone, angle dependency between power transmission line and radio polarization) were calculated. As a result, in some cases, the interference increased even if the power transmission line departed from the center of the radio propagation path, and the use of vertical polarization was effective to reduce the interference. The power transmission line (187kV, four circuits) interference on the radio link (19.7km, 2GHz, 4PSK, 1.5Mb/s) was estimated to be 0.1dB or less in equivalent C/N degradation. DOE

N90-16119# Oak Ridge Gaseous Diffusion Plant, TN. Data Systems Engineering Organization.
ISSUES AND APPROACHES FOR ELECTRONIC DOCUMENT APPROVAL AND TRANSMITTAL USING DIGITAL SIGNATURES AND TEXT AUTHENTICATION: PROTOTYPE DOCUMENTATION
M. E. Boling 30 Sep. 1989 63 p
(Contract DE-AC05-84OT-21400)
(DE90-003382; K/DSRD-205) Avail: NTIS HC A04/MF A01

Prototypes were assembled pursuant to recommendations made in report K/DSRD-96, Issues and Approaches for Electronic Document Approval and Transmittal Using Digital Signatures and Text Authentication, and to examine and discover the possibilities for integrating available hardware and software to provide cost effective systems for digital signatures and text authentication. These prototypes show that on a LAN, a multitasking, windowed, mouse/keyboard menu-driven interface can be assembled to provide easy and quick access to bit-mapped images of documents, electronic forms and electronic mail messages with a means to sign, encrypt, deliver, receive or retrieve and authenticate text and signatures. In addition they show that some of this same

software may be used in a classified environment using host to terminal transactions to accomplish these same operations. Finally, a prototype was developed demonstrating that binary files may be signed electronically and sent by point to point communication and over ARPANET to remote locations where the authenticity of the code and signature may be verified. Related studies on the subject of electronic signatures and text authentication using public key encryption were done within the Department of Energy. These studies include timing studies of public key encryption software and hardware and testing of experimental user-generated host resident software for public key encryption. This software used commercially available command-line source code. These studies are responsive to an initiative within the Office of the Secretary of Defense (OSD) for the protection of unclassified but sensitive data. It is notable that these related studies are all built around the same commercially available public key encryption products from the private sector and that the software selection was made independently by each study group. DOE

33 ELECTRONICS AND ELECTRICAL ENGINEERING

Includes test equipment and maintainability; components, e.g., tunnel diodes and transistors; microminiaturization; and integrated circuitry.

For related information see also *60 Computer Operations and Hardware* and *76 Solid-State Physics*.

N90-16120# Synergic Communication Services, Inc., Columbus, OH.

NINTH BATTERY AND ELECTROCHEMICAL CONTRACTORS' CONFERENCE: EXTENDED ABSTRACTS

Nov. 1989 332 p Conference held in Alexandria, VA, 13-17 Nov. 1989 Sponsored in part by Electric Power Research Inst., Palo Alto, CA Prepared in cooperation with Battelle Pacific Northwest Labs., Richland, WA

(Contract DE-AC06-76RL-01830)

(DE89-016837; CONF-891132-Summ) Avail: NTIS HC A15/MF A02

This document contains the extended abstracts for presentations scheduled for the Ninth Battery and Electrochemical Contractors' Conference, highlighting research supporting by the U.S. Department of Energy and the Electric Power Research Institute. It is intended to be a technical overview for engineers and scientists in government, industry, and academia who are interested in learning more about electrochemical energy storage. The abstracts are grouped according to the following technical sessions: Introductory Session; Sodium/Sulfur Battery Development; Planning, Analysis, and Technology Transfer; Fuel Cells; Zinc/Bromine Battery Development; Aqueous Battery Development; Non-Aqueous Batteries; Battery Testing and Evaluation; and Metal/Air Batteries. DOE

N90-16121# Stanford Linear Accelerator Center, CA.

RECENT PROGRESS IN RELATIVISTIC KLYSTRON RESEARCH

M. A. Allen, R. S. Callin, H. Deruyter, K. R. Eppley, K. S. Fant, W. R. Fowkes, H. A. Hoag, R. F. Koontz, T. L. Lavine, and G. A. Loew et al Aug. 1989 6 p Presented at the International Conference on High Energy Accelerators, Tsukuba, Japan, 20-26 Aug. 1989 Prepared in cooperation with Lawrence Livermore National Lab., California Univ., Berkeley, Lawrence Berkeley Lab., and Haimson Research Corp.

(Contracts DE-AC03-76SF-00515; W-7405-eng-48; DE-AC03-76SF-00098)

(DE90-000942; SU-SLAC-PUB-5070; CONF-890803-22; LBL-27760; UCRL-101688) Avail: NTIS HC A02/MF A01

Experimental work is now under way by collaborators at LLNL, SLAC, and LBL to investigate relativistic klystrons as a possible RF power source for future high-gradient accelerators. How to overcome the previously reported problem of high-power RF pulse shortening was solved and peak RF power levels of 290 MW were achieved. The RF from a relativistic klystron was used to power a short, 11.4-GHz high-gradient accelerator. The measured momentum spectrum of the accelerated electron beam corresponds to an accelerating gradient of 84 MV/m. DOE

N90-16122# Edgerton, Germeshausen and Grier, Inc., Idaho Falls, ID.

ASSESSMENT OF BATTERY TECHNOLOGIES FOR ELECTRIC VEHICLES, VOLUME 1

E. Z. Ratner, ed., P. C. Symons, ed., W. Walsh, ed., C. J. Warde, ed. (Warde Associates, Inc., Greensboro, NC.), and G. L. Henriksen, ed. Aug. 1989 63 p

(Contract DE-AC07-76ID-01570)

(DE90-002049; DOE/ID-10243) Avail: NTIS HC A04/MF A01

To help guide future EV battery R and D programs, the U.S. Department of Energy (DOE) commissioned a comprehensive assessment of viable secondary battery technologies. A total of 55 battery developers from the United States, Canada, Europe, Asia, and Africa, were solicited to submit battery design concepts for an Improved Dual-Shaft Electric Propulsion (IDSEP) van. A team of seven representatives from DOE laboratories and ten independent EV and Battery consultants evaluated 42 design concepts. Using six criteria, five technical/economic criteria and a maturity/technical barriers criterion, the Assessment Team identified 12 most-promising batteries. DOE

N90-16123# California Univ., Berkeley. Lawrence Berkeley Lab.

BROAD-BEAM MULTI-AMPERE METAL ION SOURCE

Ian G. Brown, James E. Galvin, Robert A. MacGill, and Frank J. Paoloni (Wollongong Univ., Australia) Jun. 1989 9 p Presented at the International Conference on Ion Sources, Berkeley, CA, 10-14 Jul. 1989

(Contract DE-AC03-76SF-00098)

(DE90-003106; LBL-26842; CONF-890703-25) Avail: NTIS HC A03/MF A01

An embodiment of the MEVVA (metal vapor vacuum arc) high current metal ion source was developed in which the beam is formed from a 10 cm diameter set of extractor grids and which produces a peak beam current of up to several Amperes. The source, MEVVA V, operates in a pulsed mode with a pulse width at present 0.25 ms and a repetition rate of up to several tens of pulses per second (power supply limited). The multicathode feature that was developed for the prior source version, MEVVA IV, was incorporated here also; one can switch between any of 18 separate cathodes and thus metallic beam species. Maximum beam extraction voltage is over 90 kV, and since the ion charge state typically from Q = 1 to 5, depending on the metal employed, the ion energy in the extracted beam can thus be up to several hundred keV. This source is a new addition to the MEVVA family of metal ion sources, and the operational regimes and the limits to the source performance are being investigated. The source is described and some preliminary results are presented. DOE

N90-16124*# National Aeronautics and Space Administration. Pasadena Office, CA.

ORGANIC CATHODE FOR A SECONDARY BATTERY Patent Application

Ratnakumar V. Bugga, inventor (to NASA), Salvador DiStefano, inventor (to NASA), Roger M. Williams, inventor (to NASA), and Clyde P. Bankston, inventor (to NASA) 7 Sep. 1989 20 p

(Contract NAS7-918)

(NASA-Case-NPO-17604-1-CU; NAS 1.71:NPO-17604-1-CU; US-Patent-Appl-SN-404288) Avail: NTIS HC A03/MF A01 CSCL 09A

A liquid catholyte for a battery based on liquid metal such as sodium anode and a solid, ceramic separator such as beta alumina (BASE) comprises a mixture of a Group I-III metal salt such as sodium tetrachloroaluminate and a minor amount of an organic carbonitrile depolarizer having at least one adjacent ethylenic band such as 1 to 40 percent by weight of tetracyanoethylene. The tetracyanoethylene forms an adduct with the molten metal salt. NASA

N90-16125# Department of the Army, Washington, DC.
SAW (SURFACE ACOUSTIC WAVE) TRANSDUCER WITH IMPROVED BUS-BAR DESIGN Patent Application
Elio A. Mariani, inventor (to Army) and Clinton S. Hartmann, inventor (to Army) 25 Sep. 1989 15 p
(AD-D014250; US-Patent-Appl-SN-412054) Avail: NTIS HC A03/MF A01 CSCL 09/4

A surface acoustic wave (SAW) transducer comprises a piezoelectric substrate, a paid of metal bus bars positioned on the substrate parallel to and separated from each other a preselected distance and a plurality of interdigital electrode fingers extending from each of the metal bus bars. A plurality of slots are positioned along each metal bus bar so that the bus bar metallization is reduced and the acoustic wave velocity is increased in the metal bus bar region. GRA

N90-16126# Department of the Air Force, Washington, DC.
COMMAND OPERATED LIQUID METAL OPENING SWITCH Patent
James M. Gruden, inventor (to Air Force) 27 Jun. 1989 11 p Filed 13 Oct. 1987 Supersedes US-Patent-Appl-SN-107185
(AD-D014262; US-Patent-4,841,834; US-Patent-Appl-SN-107185) Avail: U.S. Patent and Trademark Office CSCL 10/2

A very low inductance, very low resistance, command operated repetitive high current opening switch is described which uses a Lorentz force to move a conductive liquid between a conducting region and an insulated region between two electrodes. In a specific embodiment, a cylindrical outer electrode coaxially surrounds in a spaced relationship a generally cylindrical inner electrode. The annular space between the inner and outer electrodes is divided into first and second sections along the length of the electrodes. Intermeshing continuous spiral fins are defined on the facing surfaces of the inner and outer electrodes surrounding the second section. An electrically conductive liquid is sealed inside the first and second annular sections in an amount sufficient to substantially fill only one of the annular sections, so that electric current can flow between the outer electrode and the inner electrode through the liquid whenever any of the liquid is inside the first annular section, but the insulation prevents the flow of electric current flow between the outer electrode and the inner electrode when all of the liquid is inside the second annular section. GRA

N90-16127# Department of the Air Force, Washington, DC.
LARGE ANGLE OFF-AXIS BEAM STEERING OF A PHASED TELESCOPE ARRAY Patent
Patricia J. Wallentine, inventor (to AF), Mark G. Baciak, inventor (to AF), Richard A. Carreras, inventor (to AF), Elinor L. Coates, inventor (to AF), and David G. Haralson, inventor (to AF) 16 May 1989 6 p Filed 14 Apr. 1988 Supersedes US-Patent-Appl-SN-181480
(AD-D014269; US-Patent-4,831,246; US-Patent-Appl-SN-181480) Avail: US Patent and Trademark Office CSCL 20/6

A system and method for large angle off-axis steering of the composite beam from a phased array telescope system. GRA

N90-16128 Department of the Navy, Washington, DC.
OPFET (OPTICAL FIELD-EFFECT TRANSISTOR) DEMODULATOR-DOWNCONVERTER FOR DETECTING MICROWAVE MODULATED OPTICAL SIGNALS Patent
Christen Rauscher, inventor (to Navy) 8 Aug. 1989 8 p Filed 28 May 1987 Supersedes US-Patent-Appl-SN-054976
(AD-D014294; US-Patent-4,856,095; US-Patent-Appl-SN-054976; US-Patent-Class-455-619) Avail: U.S. Patent and Trademark Office CSCL 09/1

A field-effect transistor performs four functions, namely signal demodulation, generation of a local oscillator signal, generation of harmonics of this local oscillator signal through frequency multiplication, and mixing of the demodulated signal with either the local oscillator signal or one of its harmonics to produce a signal at a lower intermediate frequency; the field-effect transistor being the key element in a demodulator-downconversion circuit. GRA

N90-16129# Sandia National Labs., Albuquerque, NM.
SIZING AND SELECTION OF BATTERIES FOR STAND-ALONE PHOTOVOLTAIC SYSTEMS
Richard N. Chapman and Jay L. Chamberlin 1990 14 p Presented at the 5th Annual Battery Conference on Applications and Advances, Long Beach, CA, 16-18 Jan. 1990
(Contract DE-AC04-76DP-00789)
(DE90-002990; SAND-89-2134C; CONF-900138-3) Avail: NTIS HC A03/MF A01

The process used to design battery subsystems for stand-alone photovoltaic systems is presented in two steps; sizing and selection. The sizing step gives the raw usable capacity required for the application. A nomographic technique and a computer simulation technique for sizing are reviewed. The second step, which is presented in a worksheet format, gives the final battery capacity and its configuration based on the characteristics of the selected cell and the working environment. A design example is given to illustrate the sizing and selection processes. DOE

N90-16130# Lawrence Livermore National Lab., CA.
ELECTRICAL SAFETY IN THE HIGH VOLTAGE LABORATORY
L. B. Gordon (Auburn Univ., AL.), D. L. Counts, W. W. Hofer, C. W. Jordan, A. E. Kirkewoog, and B. R. Schleicher Jun. 1989 5 p Presented at the 7th Institute of Electrical and Electronics Engineers Pulsed Power Conference, Monterey, CA, 12-14 Jun. 1989
(Contract W-7405-eng-48)
(DE90-003026; UCRL-100652; CONF-890665-52) Avail: NTIS HC A01/MF A01

In the process of reevaluating the thoroughness and long term retention of existing electrical safety training programs at Lawrence Livermore National Lab, a new, intensive training program was developed. Although it encompasses the electrical safety of utility power it is primarily designed to include the specialized safety issues present in the high energy or pulsed power laboratory. The unique approach is to expose the technical person likely to work in such a hazardous location to a dynamic, thorough, and motivating presentation designed to leave a long lasting appreciation for the issue of laboratory safety. It is believed that this approach is critical to establish and maintain the sense of long term safety awareness in an individual that is necessary to assure a continually safe work environment. The newly developed electrical safety awareness course uses a variety of multi-media techniques to accomplish the above goals. The design and content is presented of the course as well as the results from the initial presentations. DOE

N90-16131# Sandia National Labs., Albuquerque, NM. Plasma Theory Div.
THEORETICAL AND EXPERIMENTAL INVESTIGATION OF AXIAL POWER EXTRACTION FROM A MAGNETICALLY INSULATED TRANSMISSION LINE OSCILLATOR
Raymond W. Lemke, Gary E. DeMuth, and Albert W. Biggs (Alabama Univ., Huntsville.) 1989 10 p Presented at the SPIE Optics, Electro-Optics and Laser Applications in Science and Engineering Conference and Exhibition, Los Angeles, CA, 20-25 Jan. 1990
(Contract DE-AC04-76DP-00789)
(DE90-003486; SAND-89-2733C; CONF-900140-1) Avail: NTIS HC A02/MF A01

The utility of the magnetically insulated transmission line oscillator (MILO) as a high power microwave source depends on how efficiently power can be extracted from it. A slow-wave stepped transformer was designed for the purpose of axially extracting microwave power from a 3.6 GHz coaxial MILO. The slow-wave transformer design was optimized using particle-in-cell simulation, and tested in experiments performed on the HPM Simulation Division's GEMINI and GYPSY water Blumlein pulse power sources. The slow-wave stepped transformer design was summarized, and MILO axial power extraction experiments which yielded up to 300 MW of radiated power were described. DOE

N90-16132# Oak Ridge National Lab., TN. Instrument and Controls Div.

BILATERAL FORCE REFLECTION FOR TELEOPERATORS WITH MASTERS AND SLAVES WITH DISSIMILAR AND POSSIBLY REDUNDANT KINEMATICS

J. F. Jansen and S. M. Babcock Nov. 1989 49 p

(Contract DE-AC05-84OR-21400)

(DE90-004392; ORNL/TM-11326) Avail: NTIS HC A03/MF A01

Several bilateral control techniques and methods for exploiting redundant slaves are investigated as a part of research to develop and analyze bilateral, force-reflecting control methodologies for teleoperator systems with kinematic dissimilar masters and slaves. The study indicates that, with force/torque sensing at the wrist, and an impedance type of controller with the appropriate joint compensation, a significant improvement in performance and controllability of a teleoperator system can be achieved. DOE

N90-16133# Alabama Univ., Huntsville.

EVALUATION OF A NEW CHARGE ALGORITHM FOR A LEAD-ACID BATTERY WITH GELLED ELECTROLYTE USING A 96V GEL CELL 4 AS A TEST BATTERY Final Report, FY 1988

Dieter K. Nowak Oct. 1989 46 p

(Contract DE-FG08-87NV-10672)

(DE90-003420; DOE/NV-10672/1) Avail: NTIS HC A04/MF A01

A summary is reported of test results obtained utilizing the new UAH charge algorithm for Lead-Acid batteries with gelled electrolyte. The battery performance data for a 96V Phase 4 Gel/Cell battery pack was tested in a Jet Industries Electrica vehicle. It was shown that the new charge concept is sound although there can be problems with batteries that are highly imbalanced and where excessive electronic noise is experienced on the electronic signal feed-back line that carries the voltage sensor signals from the battery. Additional work is needed to add intelligence to the charge algorithm in terms of a better ability to extract the beginning of gas development from the voltage spread function. This can probably be accomplished by scanning the voltages more often and including that data into the function analysis by adding software filters. The Phase 4 Gel/Cell battery performance was found to be about 20 percent lower than that of the Phase 3 Gel/Cell battery. Problems with cell valve leakage were encountered in the Phase 4 Gel/Cell that pose a threat to battery life although so far no battery module has been lost. DOE

N90-16134# Grenoble-1 Univ. (France). Techniques de l'Informatique, des Mathematiques; Microelectronique; Microscopie Quantitative.

BUILT IN TEST OF FOLDED PLAs

A. O. Fernandes and B. Courtois Oct. 1988 25 p

(IMAG-RR-758-I; ETN-90-95693) Avail: NTIS HC A03/MF A01

A built-in self test of topologically optimized Programmable Logic Arrays (PLAs) is examined. A review of PLA optimization techniques is presented. From these techniques, the built-in self test scheme is selected. This scheme is shown to be an improvement over other existing schemes. Its convenience in handling topologically optimized PLAS is shown. The application of the scheme to different optimization techniques is discussed in detail. The compatibility of other built-in self tests for PLA methods with topological optimization is discussed. ESA

N90-16135# Grenoble-1 Univ. (France). Lab. de Genie Informatique.

VLSI INTEGRATED CIRCUIT TESTS [TEST DES CIRCUITS INTEGRES VLSI]

A. Verdillon Nov. 1988 52 p In FRENCH

(IMAG-RR-763-I; ETN-90-95697) Avail: NTIS HC A04/MF A01

Different techniques for testing Very Large Scale Integration integrated circuits are discussed. The overlong testing times required by some of these techniques are pointed out. A fault modeling procedure is presented. Boolean function testing for multiple fault combinations is discussed. The technique calls for overlong testing times. It is concluded that synthesis and analysis algorithms are needed in order to interpret test results. The need for circuit testing must be taken into account at the time of creating the integrated circuit. Specialized parallel processing computers must be developed to lower test result analysis and synthesis times. ESA

N90-16136# Laboratoire d'Automatique et d'Analyse des Systemes, Toulouse (France).

A PHYSICAL AND NUMERICAL STUDY OF THE TURN-OFF BEHAVIOR OF BIPOLAR POWER TRANSISTORS Ph.D. Thesis - Toulouse Univ.

Mohammed Ramdani 1989 146 p In FRENCH; ENGLISH summary

(LAAS-89185; ETN-90-95706) Avail: NTIS HC A07/MF A01

The turn-off switching process of bipolar power transistors using inductive load circuits is discussed. A one-dimensional simulation model which emphasizes the charge dynamics in the slightly-doped collector region is described. Good agreement is obtained between computed and measured switching times t sub s and t sub f. The impact of the main physical device parameters on t sub s and t sub f is discussed as well as the effect of the base drive and the influence of the snubber capacitor. A qualitative explanation of the dv/dt phenomenon in inverter bridges is proposed. ESA

N90-16137# Central Research Inst. of Electric Power Industry, Tokyo (Japan). Energy and Environment Lab.

APPLICATION OF ac IMPEDANCE METHOD FOR DIAGNOSIS OF LITHIUM SECONDARY BATTERY DEGRADATION. PRELIMINARY STUDY WITH AA SIZE Li/MoS2 CELLS

Karoru Ishihara and Kazuma Kumai Dec. 1989 37 p In JAPANESE; ENGLISH summary

(DE90-702474; CRIE-T-88010) Avail: NTIS (US Sales Only) HC A03/MF A01

This report describes the possible application of ac impedance analysis for diagnosis of cell capacity degradation of AA size Li/MoS2 secondary cells. Electronic internal resistivity R(sub s), the interfacial resistivity between the lithium negative electrode and the electrolyte R(sub n), and the constant parameter of Werburg impedance S(sub p) which can be accurately and easily lead from the impedance spectrum on a complex plane were selected as useful parameters to detect the cell degradation. The R(sub s) and the S(sub p) increased with decrease of cell capacity which may originate in positive electrode materials through the charge-discharge cycles. The R(sub n) is sensitive to the dendrite formation and the propagation on the surface lithium electrode, indicating the possibility of dendrite detection. The diagnosis of lithium secondary cells by the ac impedance method was found to be a useful method to estimate degraded parts or causes of degradation. Especially, S(sub p) obtained from the low frequency region is useful to detect the degradation of a positive electrode material which has large influences on the cell capacity degradation. DOE

N90-16138# Oak Ridge National Lab., TN.

ON THE HEMP (HIGH-ALTITUDE ELECTROMAGNETIC PULSE) RESPONSE OF PROTECTIVE RELAYS

D. E. Thomas, Carl M. Wiggins (BDM Corp., Albuquerque, NM.), and Paul R. Barnes 1990 8 p Presented at the IEEE Power Engineering Society Winter Meeting, Atlanta, GA, 4-9 Feb. 1990

(Contract DE-AC05-84OR-21400)

(DE90-003718; CONF-900202-3) Avail: NTIS HC A02

An assessment of the susceptibility of protective relays to the transients produced by high altitude electromagnetic pulse (HEMP) events is presented. Several mechanisms responsible for coupling of HEMP to relay terminals are examined. The predicted relay responses to HEMP events are compared to measured data on a solid state based relay's impulse. DOE

N90-16139# California Univ., Berkeley. Lawrence Berkeley Lab. Applied Science Div.
CYCLE-LIFE IMPROVEMENT OF Zn/NiOOH CELLS BY THE ADDITION OF Ca(OH)2 TO THE ZINC ELECTRODE Ph.D. Thesis
Rajiv Jain, Frank R. McLarnon, and Elton J. Cairns Aug. 1989 151 p
(Contract DE-AC03-76SF-00098)
(DE90-004040; LBL-25332) Avail: NTIS HC A08/MF A01

The addition of Ca(OH)2 to the zinc electrode of Zn/NiOOH cells was investigated in order to determine its effect on reducing the rate of Zinc redistribution. Cells containing 0, 10, 25, and 40 mol percent Ca(OH)2 in the zinc electrode were constructed and tested. Ca(OH)2 was found to form a calcium zincate complex with the zincate supersaturated KOH solution created during the discharge half-cycle. As Ca(OH)2 is insoluble in the electrolyte, the formation of this complex (containing two Zn atoms to one Ca) significantly reduces the Zinc redistribution rate. Electrodes with only 10 percent Ca(OH)2 were found to contain insufficient Ca(OH)2 to complex with enough Zinc to make a dramatic improvement on cycle life. The 25 percent-Ca(OH)2 electrodes, however, were found to retain their capacity beyond 150 deep discharge cycles, with indication that further Zinc redistribution would occur very slowly. The Zinc utilization of the Ca-containing electrodes showed dramatic improvement over the Ca-free zinc electrodes. DOE

N90-16140# Oak Ridge National Lab., TN.
STEEP FRONT IMPULSE TESTS ON A SOLID-STATE RELAY
Tom M. Salas, Carl M. Wiggins (BDM Corp., Albuquerque, NM.), and Paul R. Barnes 1990 7 p Presented at the IEEE Power Engineering Society Winter Meeting, Atlanta, GA, 4-9 Feb. 1990
(Contract DE-AC05-84OR-21400)
(DE90-004243; CONF-900202-4) Avail: NTIS HC A02/MF A01

A protective relay, subjected to a high voltage steep front impulse, was shown to fail in the laboratory. Laboratory experiments were performed to characterize the response of a protective relay to steep front impulses. These impulses may be the result of a nuclear induced high altitude electromagnetic pulse. Tests were also conducted to quantify the protection offered by a surge protection package on the dc circuits of a relay system. Results from these tests were used to assess the vulnerability of a protective relay. DOE

34 FLUID MECHANICS AND HEAT TRANSFER

Includes boundary layers; hydrodynamics; fluidics; mass transfer; and ablation cooling.

For related information see also *02 Aerodynamics* and *77 Thermodynamics and Statistical Physics.*

N90-16141 Illinois Univ., Urbana-Champaign.
A NUMERICAL AND EXPERIMENTAL INVESTIGATION OF MULTIPLE SHOCK WAVE/TURBULENT BOUNDARY LAYER INTERACTIONS IN A RECTANULAR DUCT Ph.D. Thesis
Bruce Frederick Carroll 1988 270 p
Avail: Univ. Microfilms Order No. DA8908640

A combined numerical and experimental investigation of multiple shock wave/turbulent boundary layer interactions in nearly constant area supersonic duct flows was performed. The flow characteristics of two shock train interactions, one with an initial Mach number of 2.45, the other at Mach 1.6, were investigated using spark Schlieren photography, surface oil flow visualization, and mean wall pressure measurements. The experiments were performed in 76.2 mm wide rectangular ducts with nominal heights of 38.1 and 35.6 mm for the Mach 2.45 and 1.6 interactions, respectively. The Mach 2.45 interaction was oblique and asymmetric in nature with large scale boundary layer separation present. The experimental investigation was coordinated with a numerical study of the shock train phenomenon. The computations use the explicit, time-dependent, second-order accurate MacCormack scheme to solve the mass averaged Navier-Stokes equations. Turbulence is modeled via the Baldwin-Lomax algebraic model and the Wilcox-Rubesin two-equation model. The Wilcox-Rubesin calculation shows very good agreement with the experimental results with the only major difference being that the computation predicted boundary layer separation under the shock. The Baldwin-Lomax calculation shows only a limited ability to capture the features of this shock train flow. Dissert. Abstr.

N90-16142# ETS, Inc., Roanoke, VA.
AMBIENT TEST RIG (ATR) FLOW STUDIES: A LAMINAR FLOW, REDUCED ENTRAINMENT ELECTROSTATIC PRECIPITATOR Technical Progress Report
Oct. 1988 34 p
(Contract DE-AC22-88PC-88865)
(DE90-000144; DOE/PC-88865/T1) Avail: NTIS HC A03/MF A01

Results of flow testing on a Reduced Entrainment Precipitator Ambient Test Rig are presented. The Reduced Entrainment Precipitator concept involves drawing a portion of the main precipitator flow through hollow, porous collecting plates. The purposes of flow through porous collecting plates (side flow) are to provide a dust layer clamping force, and to reduce turbulence with the precipitator. Achievement of these goals should reduce re-entrainment, and result in increased precipitator efficiency. The increased efficiency should be especially evident at higher precipitator main flow velocities. Flow tests conducted included pilot tube velocity traverses, smoke (turbulence) visualization, and measurements of turbulence and velocity with a (fast-response) hot-wire anemometer. DOE

N90-16143# Los Alamos National Lab., NM.
A BRIEF DESCRIPTION OF LATTICE GAS MODELS FOR MULTIPHASE FLOWS AND MAGNETOHYDRODYNAMICS
H. Chen, S. Chen, G. D. Doolen, and W. H. Matthaeus (Delaware Univ., Newark.) 1989 16 p Presented at the Santa Fe Institute Summer School on Complex Systems, Santa Fe, NM, 5-30 Jun. 1989
(Contract W-7405-eng-36)
(DE90-003653; LA-UR-89-3984; CONF-8906239-2) Avail: NTIS HC A03/MF A01

Lattice gas models for multiphase fluids and for magnetohydrodynamic fluids are briefly described. DOE

N90-16144# State Univ. of New York, Stony Brook. Dept. of Applied Mathematics and Statistics.
ANOMALOUS WAVES IN SHOCK WAVE - FLUID INTERFACE COLLISIONS
John W. Grove 1989 14 p Repr. from Contemporary Mathematics, 1989 Submitted for publication
(Contracts DAAL03-89-K-0017; DAAG29-85-K-0188)
(AD-A213584; ARO-26616.6-MA) Avail: NTIS HC A02/MF A01 CSCL 20/4

The acceleration of a fluid interface by a shock wave consists of three basic regimes. The first of these is the actual collision phase during which the interface is impulsively accelerated. The second two phases are characterized by the growth of surface instabilities in the interface, either in the initial small amplitude linear regime, or the long term non-linear growth of unstable modes. These three phases occur on sharply different time scales. The small amplitude collision between a shock wave and a fluid material interface produces locally self-similar diffracted waves that correspond to solutions of Riemann problems for a steady flow. As the amplitude between the interacting waves grows, these pseudo-stationary waves bifurcate into a variety of different patterns. If the shock is incident in the material with higher acoustic impedance reflected Prandtl-Meyer rarefaction waves are produced, and the bifurcation is analogous to a transition from a regular to a Mach reflection when the reflected wave is a rarefaction instead of a shock. An enhanced description of these interactions is obtained by incorporating an analysis of the bifurcations into a

front tracking code. Two numerical examples, a planar shock passing over a bubble, and an expanding shock impacting a planar contact are discussed. GRA

N90-16145# Wisconsin Univ., Madison. Center for the Mathematical Sciences.
INTERDISCIPLINARY RESEARCH IN VISCOELASTICITY AND RHEOLOGY Final Technical Report, May 1987 - May 1989
David S. Malkus, John A. Nohel, Deborah Brandon, Robert C. Rogers, and Athanassios E. Tzavaras 25 Aug. 1989 13 p
(Grant AF-AFOSR-0191-87; AF Proj. 2304)
(AD-A213630; AFOSR-89-1274TR) Avail: NTIS HC A03/MF A01 CSCL 20/4

A deep understanding of viscoelasticity and rheology is crucial to advanced materials engineering and process design. Examples of such advanced materials are high-strength polymers and additives for lubricants; process design problems include spinning of synthetic fibers and injection molding. The materials involved in these technologies are often highly elastic and very viscous. As a consequence, they often display behavior intermediate between that of a solid and that of a fluid, and their dynamic response involves multiple time-scales. The goal is to understand the predictions of equations of motion coupled with various constitutive assumptions for advanced, complex materials and to put this knowledge to use in modelling, the design of algorithms, and the computational solution of practical problems. To achieve the goals, an interdisciplinary program has adapted and extended tools in nonlinear analysis of partial differential equations, analytical and computational techniques for hyperbolic conservation laws, and computational techniques from nonlinear structural dynamics. GRA

N90-16146# Woods Hole Oceanographic Inst., MA.
LABORATORY STUDIES OF ISOLATED EDDIES IN A ROTATING FLUID
J. A. Whitehead 1989 13 p Repr. from Mesoscale/Synoptic Coherent Structures in Geophysical Turbulence (Amsterdam, Netherlands, Eisevier Science), 1989
(Contracts N00014-87-K-0007; NR-83-004; NSF OCE-84-16100; NSF OCE-87-14842)
(AD-A213903) Avail: NTIS HC A02/MF A01 CSCL 20/4

Numerous laboratory techniques have been used to generate isolated eddies in a rotating fluid, but they can all be divided into two categories; those in which the eddies are directly produced by inserting or withdrawing fluid, and those in which eddies are produced by an instability or separation process. Two examples are reviewed for the latter category. Dipole eddies in a homogeneous rotating fluid have been produced by Flierl, Stern, and Whitehead. In most cases, modification was observed due to a third vortex. This is usually accompanied by a curved track of the vortex pairs. Recent studies have focused on isolated eddies which form from rather general and nondescript initial conditions. Baroclinic eddies in a rotating fluid with a sloping bottom were produced by squirting dense salt water up the sloping bottom and along the eastern wall. The jet stagnated in shallow water and was ejected normal to the wall. For certain parameters (volume flux of jet, etc.), a coherent lens of dense bottom water formed and propagated west with an overlying cyclonic vortex. The circulation in the bottom lens, on the other hand, was relatively weak. No such eddy forms when the depth of fresh water is relatively deep, and a regime diagram is given for the formation of the coherent eddies. The pressure field determined from analysis of the density distribution and using streak photographs is discussed in terms of an integral theorem for coherent eddies. The westward propagation is also related to previous theories. GRA

N90-16147# Department of the Air Force, Washington, DC.
EXPANDABLE RADIATOR Patent
Donald L. Reinmuller, inventor (to Air Force) 27 Jun. 1989 5 p Filed 11 Oct. 1988 Supersedes US-Patent-Appl-SN-255803
(AD-D014258; US-Patent-4,842,045; US-Patent-Appl-SN-255803) Avail: U.S. Patent and Trademark Office CSCL 22/5

An expandable heat rejection system for radiating heat from a source of heat on a spacecraft or like vehicle is described and comprises a fluid heat exchange medium in operative circulating heat exchange relationship with the source for absorbing heat by evaporation of a liquid phase or the medium, an elongate inflatable sleeve defining an expandable and collapsible volume closed at a first end and including an inlet and outlet at a second end and further defining a condensation surface on the inner surface of the sleeve and a heat radiating surface on the outer surface of the sleeve, a reel attachable to the vehicle and operatively attached to the first end of the sleeve for selectively winding and unwinding the sleeve in response to pressure generated within the system. GRA

N90-16148# Laboratorio de Computacao Cientifica, Rio de Janeiro (Brazil).
FEED BACK PETROV-GALERKIN METHODS FOR CONVECTION DOMINATED PROBLEMS
Eduardo G. D. doCarmo (Universidade Federal do Rio de Janeiro, Brazil) and Augusto Cesar Galeao Sep. 1988 30 p Submitted for publication
(DE89-636436; LNCC-034/88; ISSN-0101-6113) Avail: NTIS (US Sales Only) HC A03/MF A01

The Petrov-Galerkin method is adaptively applied to convection dominated problems. To this end, a feedback function is created which increases the control of derivatives in the direction of the gradient of the approximate solution. This leads to a method with good stability properties close to boundary layers and high accuracy in those regions where regular solutions do occur. Author

N90-16149# ETS, Inc., Roanoke, VA.
AMBIENT FLOW STUDIES AND PARTICULATE COLLECTION MEASUREMENTS: A LAMINAR FLOW, REDUCED ENTRAINMENT ELECTROSTATIC PRECIPITATOR
Gary P. Greiner, Dale A. Furlong, and Mark A. Bahner May 1989 142 p
(Contract DE-AC22-88PC-88865)
(DE90-001457; DOE/PC-88865/T2) Avail: NTIS HC A07/MF A01

This report describes ambient temperature testing of an electrostatic precipitator having a portion of the main precipitator flow drawn through porous (fabric) plates. The effects of flow through the plates (side flow) on precipitator turbulence and particulate removal efficiency are investigated. Ambient temperature particulate removal efficiency measurements are conducted on both indoor air dust, and on injected coal fly ash. DOE

N90-16150# General Atomic Co., San Diego, CA.
NONLINEAR WAVE COUPLING AND CLUMPS IN DRIFT WAVE TURBULENCE THEORY
R. R. Dominguez Jul. 1989 9 p Presented at the Workshop on Coherent Structure in Plasma, Nagoya, Japan, Mar. 1989 Submitted for publication
(Contract DE-AC03-89ER-53277; GA Proj. 3468)
(DE90-004103; GA-A-19794; CONF-8903180-1) Avail: NTIS HC A02/MF A01

Anomalous transport mediated by drift wave turbulence has been studied by many authors using weak and renormalized turbulence theory. Additional nonlinear effects coming from three-wave coupling have been studied in simple models by Waltz and for drift waves by Waltz and Dominguez. At the same time, the clump theory of Dupree has been extended and applied to drift wave turbulence. In the present work, how the discreteness effects associated with clumps may be combined with the nonlinear wave coupling formalism is discussed. It is shown that both the nonlinear wave coupling and clump correlation act as sources for the spectral density in k, and w, with a comparison between the two effects being presented. DOE

N90-16151# Purdue Univ., West Lafayette, IN. Boiling and Two-Phase Flow Lab.
THICKNESS, VELOCITY, AND TEMPERATURE MEASUREMENTS IN FALLING LIQUID FILMS Final Report
Issam A. Mudawar, William G. Tiederman, Tae-Hwan Lyu, Ronald

A. Houpt, and John E. Koskie Nov. 1989 153 p
(Contract DE-FG02-85ER-13398)
(DE90-004290; DOE/ER-13398/11) Avail: NTIS HC A08/MF A01

Liquid films are encountered in many industrial applications such as heat exchangers and chemical process equipment. Therefore, there is significant interest in the prediction of heat and mass transport associated with film flow. As in any convective form of heat or mass transport, the fluid mechanics of the system strongly influence the resulting transport. This paper includes the results of experiments performed to define better the hydrodynamic characteristics of developing liquid films on vertical surfaces. In particular, this study provides data on water films at high Reynolds numbers (greater than) 10,000), and films of more viscous mixtures of water and propylene glycol. Statistical characteristics of film thickness that account for development length between 0.293 m and 1.913 m are presented over new ranges of Reynolds numbers and viscosities. Photographic analysis of film motion was also performed to investigate the three-dimensional structure of the waves. DOE

N90-16152 Utah Univ., Salt Lake City.
VORTICITY AMPLIFICATION IN NONORTHOGONAL STAGNATION FLOW Ph.D. Thesis
Kirk Dee Hagen 1989 145 p
Avail: Univ. Microfilms Order No. DA8923092

The objective is to advance a possible generation mechanism for experimentally observed streamwise vortices in the near region of an internal free shear layer. By modeling the nonorthogonal stagnation point of a flow restrictor as a symmetrical wedge in cross flow, it is shown by analysis that cross and streamwise vorticity having scales larger than a neutral value can amplify in the stagnation region. Hot-wire probe surveys of the stagnation streamline ahead of a wedge in cross flow reveal a general amplification of natural and grid-generated turbulence of low frequenices. Sublimation tests using wedges of paradichlorobenzene fail to reveal streamwise vortex structures near the stagnation point in a natural turbulence environment. Streamwise vortices are observed, however, for conditions that fall under a unique threshold of incipient vortex formation curve. Vortex wavelength at the stagnation point scales with grid mesh size, and is an increasing function of grid separation distance. The study is successful in corroborating the essential features of vorticity amplification and extending the theory to include a nonplanar geometry, but additional research of the problem in the original flow restrictor configuration is recommended.
Dissert. Abstr.

N90-16153# Institut Franco-Allemand de Recherches, Saint-Louis (France).
PLUME SHAPE OPTIMIZATION OF SMALL ATTITUDE CONTROL THRUSTERS WITH RESPECT TO IMPINGEMENT AND THRUST
K. W. Naumann 9 Aug. 1988 28 p Presented at the 16th International Symposium of Rarefied Gas Dynamics, Pasadena, CA, 10-15 Jul. 1988
(ISL-CO-220/88; ETN-90-96087) Avail: NTIS HC A03/MF A01

A comparative description of plumes emanating from different nozzles, similar to those of typical small hydrazine thrusters, is presented. The objective is to point out the effect of nozzle design on free jet expansion. The investigation shows an optimum nozzle wall angle exists which causes the minimal spreading plume. With increasing nozzle size and stagnation pressure the plume spreads wider. In this case the optimum nozzle wall angle is clearly marked concerning the thrust efficiency and minimization of impingement effects, the use of smaller thrusters with large wall angles is favorable. ESA

N90-16154# Institut Franco-Allemand de Recherches, Saint-Louis (France).
DIRECT MONTE CARLO CALCULATIONS ON EXPANSION WAVE STRUCTURE NEAR A WALL
F. Seiler and B. Schmidt (Karlsruhe Univ., Germany, F.R.) 21 Nov. 1988 18 p Presented at the 16th International Symposium on Rarefied Gas Dynamics, Pasadena, CA, 10-16 Jul. 1988
(ISL-CO-249/88; ETN-90-96096) Avail: NTIS HC A03/MF A01

The influence of the boundary layer on the structure of a centered rarefaction wave moving along a wall is investigated. The gas kinetic direct simulation Monte Carlo method is used and compared with a one dimensional isentropic continuum solution given by the method of characteristics. In the simulation study the real gas flow is modeled statistically at atomic level for a monatomic, perfect gas with three degrees of freedom. The centered two dimensional rarefaction wave is generated by a piston, which is suddenly set in motion and then moves with constant velocity. If the gas temperature is initially set equal to the wall temperature only small density and temperature gradients appear towards the wall. In the case of a cooler wall, the weak expansion wave structure far away from the wall changes next to the wall into a steep wave behavior. When the piston speed exceeds the maximum possible flow velocity, towards the wall, no density gradients are observed, whereas for the temperature and velocity distribution the boundary layer effect is clearly visible. ESA

N90-16155# Aeronautical Research Inst. of Sweden, Stockholm. Aerodynamics Dept.
ADAPTIVE LOCAL GRID REFINEMENT FOR THE COMPRESSIBLE 3-D EULER EQUATIONS
Thilo Schoenfeld 1989 33 p
(Contract FMV-FlygFL-82260-88-061-73-001)
(FFA-TN-1989-40; ETN-90-96149) Avail: NTIS HC A03/MF A01

A method is presented based on a three-dimensional Euler code, using the explicit finite volume technique and a Runge-Kutta scheme, and applied in an adaptive version for the transonic flow around wings. The method allows embedded subgrids at two levels of refinement. Computations are performed with both various fixed refined grids and in an adaptive version applying a pressure or density gradient sensor. When comparing the results of embedded grid computations with calculations on only a total coarse or fine mesh, it can be stated that the local grid refinement technique is an effective framework to obtain well-resolved solutions with, at the same time, a minimum of grid points. ESA

N90-16156# Centre d'Etudes et de Recherches, Toulouse (France). Dept. d'Etudes et de Recherches en Mecanique et Energetique des Systemes.
STUDY OF FLOW AROUND A SPHERE IN A HYDRAULIC TEST TUNNEL Final Report [ETUDE EN TUNNEL HYDRAULIQUE DE L'ECOULEMENT AUTOUR D'UNE SPHERE]
Christine Lempereur, Christian Berger, Gerard Lavergne, Daniel Gallot, Pascal Gaudin, Francois Stephan, and Beatrice Tico Feb. 1989 53 p In FRENCH
(Contract DRET-87-002-019)
(CERT-1/2313/MES; Rept-1/231/00/DERMES; ETN-90-95026)
Avail: NTIS HC A04/MF A01

A three dimensional study of trajectory around a sphere is described. A special software program is developed to take into consideration the time and space parameters involved. A second study is carried out to establish a method of calculating, with flow corrections, the average flow around a sphere in the presence of side walls. Qualitative visualizations of the flow are provided. The instabilities within the wake are characterized. The need for improvements in three dimensional laser lighting is stressed. Light sources adapted to such purposes need to be developed. ESA

N90-16157# Institut Franco-Allemand de Recherches, Saint-Louis (France).
A NUMERIC ANALYSIS OF INCOMPRESSIBLE, VISCOUS FLOW AROUND A SYMMETRICAL BODY OF REVOLUTION [NUMERISCHE UNTERSUCHUNGEN DER INKOMPRESSIBLEN REIBUNGSBEHAFTETEN STROEMUNG UM DREHKOERPER]
W. Czichowsky 16 Jun. 1987 31 p In GERMAN Presented at the 2nd GARTEUR AG-09 Meeting, Ottobrunn, Federal Rep. of Germany, 10-11 Jun. 1987

(ISL-CO-215/87; ETN-90-95029) Avail: NTIS HC A03/MF A01

The influence of base surface geometry on the flow around a symmetrical body of revolution is investigated. Its influence on the drag coefficient is also analyzed. A finite difference method is used in calculating the incompressible flow. This method is based on turbulent eddy equations and on the Poisson equation. By using a curved coordinate system, the flow field is converted into a rectangular domain. The differential equations are written out in finite form and are solved by means of an implicit method. ESA

N90-16158# Heidelberg Univ. (Germany, F.R.).
USING THE SINGULARITY-SEPARATING METHOD TO STUDY HOW TO DECREASE THE PRESSURE AT THE END OF A TUBE
Xionghua Wu and Youlan Zhu (Academia Sinica, Beijing, China) Nov. 1988 20 p Sponsored in part by the AvH Foundation; Chinese National Natural Science Foundation; and the Tongji University Science Foundation
(Preprint-490; ETN-90-95877) Avail: NTIS HC A03/MF A01

The Singularity-Separating Method (SSM) is used to calculate the flow field in tubes with rapidly changing cross-section areas. How to decrease the pressure at the end of a tube is studied. The central principle behind SSM is that all discontinuity lines in the flow fields are considered as internal boundary lines. The difference scheme is only used in the subregions with continuous solution. One-sided difference scheme and boundary conditions are adopted on the boundaries and are linear or nonlinear equations. The solutions on the boundaries can be obtained by solving these equations. A software program for unsteady aerodynamic problems in one dimension is developed in order to deal with complicated SSM codes. ESA

N90-16159# Heidelberg Univ. (Germany, F.R.). Inst. fuer Angewandte Mathematik.
NUMERICAL ANALYSIS OF NONSTATIONARY FLUID FLOW (A SURVEY)
R. Rannacher Nov. 1988 22 p Sponsored by DFG, Bonn, Fed. Republic of Germany
(Preprint-492; ETN-90-95878) Avail: NTIS HC A03/MF A01

Aspects of numerical approximation of the nonstationary Navier-Stokes equations are discussed. Criteria used in choosing appropriate timestepping schemes is given particular attention. The importance of the smoothing property and of the global regularity property in computing flow is outlined. Their importance in the range of moderate Reynolds numbers is supported by rigorous theoretical analysis. For numerical simulation of convection dominated flows it is shown that additional numerical damping is necessary. ESA

N90-16160# Heidelberg Univ. (Germany, F.R.). Inst. fuer Angewandte Mathematik.
EXTRAPOLATION TECHNIQUES FOR FINITE ELEMENT APPROXIMATIONS OF STOKES AND NAVIER-STOKES FLOW OVER A BACKWARD FACING STEP
H. Blum, J. Harig, and S. Mueller Jan. 1989 17 p Sponsored by DFG, Bonn, Fed. Republic of Germany
(Preprint-499; ETN-90-95879) Avail: NTIS HC A03/MF A01

The effect of reentry corners for standard finite element discretizations of the Stokes equations is studied. In viscous flow over a backwards facing step the pollution effect is relatively localized. Richardson extrapolation is used to recover full accuracy on the basis of asymptotic error expansion. The method can be used for velocity as well as pressure. Tests of the Stokes and Navier-Stokes equations are presented. ESA

N90-16161 Gesellschaft fuer Mathematik und Datenverarbeitung, Saint Augustin (Germany, F.R.). Inst. fuer Methodische Grundlagen.
THE SUPRENUM ARCHITECTURE AND ITS APPLICATION TO COMPUTATIONAL FLUID DYNAMICS
Karl Solchenbach and Clemens-August Thole May 1989 20 p
(Contracts BMFT-ITR-8601-9; MWMT-323-860-5200)
(GMD-389; ISSN-0723-0508; ETN-90-95881) Copyright Avail: Gesellschaft fuer Mathematik und Datenverarbeitung mbH, Schloss Birlinghoven, Postfach 12 40, D-5205, Saint Augustin 1, Fed. Rep. of Germany

A short overview of the Suprenum supercomputer project is presented. The architecture and hardware components are outlined. The development of Suprenum is characterized by the simultaneous construction of hardware and application software packages. The software packages available are listed. The fundamental parallelization technique based on grid algorithms and grid partitioning is described. Some estimation of performance results are provided. ESA

N90-16162# Ruhr Univ., Bochum (Germany, F.R.). Inst. fuer Thermo- und Fluiddynamik.
MEASUREMENT OF THE p, v, T BEHAVIOR UNDER MICROGRAM CONDITIONS Final Report
Norbert Kurzeja, Bruno Pieperbeck, and Wolfgang Wagner Aug. 1988 29 p In GERMAN; ENGLISH summary
(Contract BMFT-01-QV-094A)
(ETN-90-95906) Avail: NTIS HC A03/MF A01

An apparatus based on the p, v, T multicell method designed to give extremely accurate measurements of pressure, density and temperature behavior in the critical region of pure fluids is described. The reconstruction of the block of measuring cells and the improved design of the thermostat is described. Equipment for purification of the fluid sulfur hexafluoride used as the measuring fluid is described. Computer generated estimations of the influence of impurities and gravity on the accuracy of the measurements are outlined. ESA

N90-16163# Bonn Univ. (Germany, F.R.). Sonderforschungsbereich 256.
DECAY ESTIMATES FOR THE COMPRESSIBLE NAVIER-STOKES EQUATIONS IN THE HALF-SPACE
Klaus Deckelnick Sep. 1988 32 p Sponsored by DFG, Bonn, Fed. Republic of Germany
(Preprint-46; ETN-90-95911) Avail: NTIS HC A03/MF A01

Equations which describe the motion of a viscous compressible fluid in the half space are discussed. Explicit estimates for the rate with which the instationary solution converges to the corresponding stationary state are established by means of a differential inequality. ESA

N90-16164# Bonn Univ. (Germany, F.R.). Sonderforschungsbereich 256.
VISUALIZATION OF 2 AND 3 DIMENSIONAL FLOWS
Harald Duvenbeck and Alfred Schmidt Mar. 1989 20 p In GERMAN; ENGLISH summary
(Rept-1; ETN-90-95912) Avail: NTIS HC A03/MF A01

Aspects and problems of the visualization of numerically computed flows on two dimensional manifolds and in three dimensional domains is discussed. An outline of the numerical algorithms used to solve the partial differential equations of fluid dynamics (Navier-Stokes equations) is presented. Various forms of flow visualization are compared. ESA

N90-16165# Office National d'Etudes et de Recherches Aerospatiales, Toulouse (France). Dept. d'Etudes et de Recherches en Aerothermodynamique.
CALCULATION OF TURBULENT CHOPPY FLOW MIXING Final Report [CALCULS D'ECOULEMENTS CISAILLES TURUBLENTS ET DE LEUR MELANGE]
Pascal Gendre 1988 196 p In FRENCH
(Contract DRET-86-34-810-00-470-75-01)
(ETN-90-95929) Avail: NTIS HC A09/MF A02

A mathematical model for calculating turbulent detached flow involving resolution of Navier-Stokes equations is presented. Turbulent detached flow over a wing and over a turbine blade are investigated. The algorithm used in the forward marching method is described. A more robust calculation method needed to handle the high detached flow values is developed. Using this method a

mathematical model is developed and its performance is described. ESA

N90-16166# Universitaet der Bundeswehr, Neubiberg (Germany, F.R.). Inst. fuer Raumfahrttechnik.
VIBRATIONAL BEHAVIOR OF A VISCOUS COLUMN WITH A FREE LIQUID SURFACE
Helmut F. Bauer 1989 36 p
(LRT-WE-9-FB-1(1989); ETN-90-96064) Avail: NTIS HC A03/MF A01

The vibrational behavior of a viscous liquid column is investigated. For an axial length larger than the length of the circumference, the liquid column is unstable in its axisymmetric motion. For axial wavelengths below this magnitude, the viscous liquid exhibits not only oscillatory motion behavior, but behaves as a frictionless liquid. There are ranges of pure decaying motion just below specific axial waves lengths and for very small wavelengths. In the range of wavelengths between these two, the liquid motion is of damped oscillatory character. All this indicates that g-jitter in experiments carried out on space missions may not be detrimental. ESA

N90-16167# Universitaet der Bundeswehr, Neubiberg (Germany, F.R.). Inst. fuer Raumfahrttechnik.
SMALL AMPLITUDE LIQUID OSCILLATIONS IN A RECTANGULAR CONTAINER UNDER ZERO-GRAVITY
Helmut F. Bauer and Werner Eidel 1989 50 p
(LRT-WE-9-FB-2(1989); ETN-90-96065) Avail: NTIS HC A03/MF A01

Free and forced sloshing in rectangular tanks under zero gravity are investigated. It is shown that the natural sloshing frequencies of the liquid increase with an increase in contact angle to a maximum value slightly above a contact angle of pi over two. The frequencies decrease from that point on. A completely nonwetting liquid has larger natural frequencies than a completely wetting liquid. Under zero gravity conditions, a nonwetting liquid exhibits reduced sloshing mass, indicating that the influence of liquids with small contact angles on the dynamics of a vehicle with liquid containers, may be pronounced. ESA

N90-16168# Universitaet der Bundeswehr, Neubiberg (Germany, F.R.). Inst. fuer Raumfahrttechnik.
LINEAR LIQUID OSCILLATIONS IN CYLINDRICAL CONTAINERS UNDER ZERO-GRAVITY
Helmut F. Bauer and Werner Eidel 1989 38 p
(LRT-WE-9-FB-5(1989); ETN-90-96066) Avail: NTIS HC A03/MF A01

Free and forced sloshing in a container under zero gravity conditions is investigated. The liquid surface exhibits surface tension effects which depend on the magnitude of the contact angle to the wall. The natural frequencies of the liquid are found to increase with an increase in the contact angle to a maximum value of pi over two after which it decreases. The sloshing mass of a wetting liquid was found to be considerably larger under zero-gravity than under normal gravity. Non-wetting liquid exhibits reduced sloshing masses. By coating the container wall on the inside with a hydrophobic material, the sloshing mass is reduced. ESA

N90-16169# Deutsche Gesellschaft fuer Luft- und Raumfahrt, Bonn (Germany, F.R.). Arbeitsgemeinschaft Stroemungen mit Ablosung.
FLOWS WITH SEPARATION
1988 394 p Partly in ENGLISH and GERMAN The 6th DGLR-Fach-Symposium was held in Brunswick, Fed. Republic of Germany, 8-10 Nov. 1988 Sponsored by BMFT, Bonn, Fed. Republic of Germany
(DGLR-Papers-88-05; ISBN-3-922010-42-3; ETN-90-95008)
Avail: NTIS HC A17/MF A03

Eleven contributions treat the laminar flow behavior of aircraft, a subject of utmost importance for future passenger aircrafts, with emphasis on phenomenology and the prediction of laminar-turbulent transition. Seven contributions treat flow separation on slim delta wings in subsonic flow and at large angles of attack. Ten contributions present numerical calculation methods: further development of boundary layer methods, improved turbulence models, consideration of curvature, solving Navier-Stokes equations. The Hermes development program is presented. For individual titles, see N90-16170 through N90-16199.

N90-16170# Deutsche Gesellschaft fuer Luft- und Raumfahrt, Bonn (Germany, F.R.). Inst. fuer Experimentelle Stroemungsmechanik.
EXPERIMENTS ON THE LAMINAR-TURBULENT TRANSITION ON SWEPT WINGS [EXPERIMENTE ZUM UMSCHLAG LAMINAR-TURBULENT AM SCHIEBENDEN FLUEGEL]
H. Bippes and B. Mueller *In its* Flows with Separation 1988 p 3-16 In GERMAN (For primary document see N90-16169 08-34)
Avail: NTIS HC A17/MF A03

Some basic experiments were conducted for the investigation of the laminar-turbulent transition on swept wings, in connection with theoretical work. The geometry of the models was selected in such a way that each time a single instability mechanism is dominant. The neighborhood of the leading edge is found to be the most complicated region. Preliminary tests on a wing with a concavely curved profile part show that such surfaces are very unstable, even in three dimensional boundary layers. With respect to cross flow instability the nonlinear domain of the continuous excitation of the boundary layer was analyzed; this instability is dominant in three dimensional boundary layers, in contrast with predictions of linear stability theory. Wind tunnel experiments at different degrees of turbulence show complicated correlations between initial perturbations and transition in three dimensional boundary layers. ESA

N90-16171# Deutsche Forschungs- und Versuchsanstalt fuer Luft- und Raumfahrt, Goettingen (Germany, F.R.). Inst. fuer Theoretische Stroemungsmechanik.
METHOD FOR THE PRIMARY STABILITY ANALYSIS OF THE THREE DIMENSIONAL, COMPRESSIBLE BOUNDARY LAYER FLOWS [VERFAHREN ZUR PRIMAEREN STABILITAETSANALYSE DREIDIMENSIONALER, KOMPRESSIBLER GRENZSCHICHTSTROEMUNGEN]
U. Ehrenstein *In* DGLR, Flows with Separation 1988 p 17-26 In GERMAN (For primary document see N90-16169 08-34)
Avail: NTIS HC A17/MF A03

A method for the solution of the compressible, linear disturbance differential equations is described, with a view to the establishment of possible multi-purpose stability characteristics of three-dimensional, compressible, boundary layer flows. The method treats the basic equation system for the stability problem as a boundary value problem within the boundary layer. The boundary conditions are only fulfilled if after iteration an eigenvalue is obtained such that the eigenvalue problem can be formulated following a temporal as well as a spatial theory. This allows the strategies used in the framework of the laminar flow control technology for the determination of so-called N-factors to be taken into account. The program package COSTA (compressible flow stability analyzer) is under development. ESA

N90-16172# Messerschmitt-Boelkow-Blohm G.m.b.H., Bremen (Germany, F.R.). Transport- und Verkehrsflugzeuge.
AN EFFICIENT SOLVER OF THE EIGENVALUE PROBLEM OF THE LINEAR STABILITY EQUATIONS FOR THREE DIMENSIONAL, COMPRESSIBLE BOUNDARY-LAYER FLOWS
Geza Schrauf *In* DGLR, Flows with Separation 1988 p 27-38 (For primary document see N90-16169 08-34)
Avail: NTIS HC A17/MF A03

A compressible stability code was developed as a tool for the design of natural-laminar-flow airfoils. The code is based on a general set of stability equations which allows one to examine the influence of non-parallelity or non-zero pressure gradients. It also allows streamline and surface curvature to be included. ESA

N90-16173# Deutsche Forschungs- und Versuchsanstalt fuer Luft- und Raumfahrt, Goettingen (Germany, F.R.). Inst. fuer Theoretische Stroemungsmechanik.

NUMERICAL SIMULATION OF THE NONLINEAR EVOLUTION OF A PERTURBATION IN A THREE DIMENSIONAL BOUNDARY LAYER [NUMERISCHE SIMULATION DER NICHTLINEAREN STOERUNGSENTWICKLUNG IN EINER DREIDIMENSIONALEN GRENZSCHICHT]

F. Meyer and L. Kleiser *In* DGLR, Flows with Separation 1988 p 39-40 In GERMAN (For primary document see N90-16169 08-34)

Avail: NTIS HC A17/MF A03

The laminar-turbulent transition in three dimensional boundary layers due to the cross flow instability was numerically simulated by the integration of the Navier-Stokes equations, using a spectral method. The temporal evolution of perturbations are periodic in the directions parallel to the wall. The basic flow was the Falker-Stan-Cooke profile. A primary stability analysis predicts wavelengths and frequencies in agreement with experiments. The fully three dimensional, nonlinear interaction between cross flow vortices and current perturbations is illustrated. The cross flow vortex amplitudes and the excited fluctuations tend to saturate, in agreement with previous results and experiments. ESA

N90-16174# Technische Hochschule, Darmstadt (Germany, F.R.). Fachgebiet Aerodynamik und Messtechnik.

SEMI-EMPIRICAL TRANSITION CRITERIA FOR THE DESIGN OF LAMINAR PROFILES [SEMI-EMPIRISCHE TRANSITIONSKRITERIEN FUER DEN ENTWURF VON LAMINARPROFILEN]

S. Stroh and P. Thiede (Messerschmitt-Boelkow-Blohm G.m.b.H., Bremen, Germany, F.R.) *In* DGLR, Flows with Separation 1988 p 41-53 In GERMAN (For primary document see N90-16169 08-34)

Avail: NTIS HC A17/MF A03

Laminar-turbulent transition predictions were made, with a view to the reliable design of laminar flow airfoils. The primary instability and the length of the excitation region were universally calculated for the solutions of the compressible boundary equations. This data base was used for the establishment of a simplified transition criterium for compressible profile boundary layers. Test calculations for incompressible and compressible profile flows show good agreement with measurements and linear stability calculations. The transition prediction is better, the more precisely the condition of constant pressure gradient in the excitation region is fulfilled. The criterium is especially suited for the design of laminar profiles. ESA

N90-16175# Technische Univ., Berlin (Germany, F.R.). Inst. fuer Luft- und Raumfahrt.

DETECTION OF FLOW INSTABILITIES AT AIRFOIL PROFILES USING PIEZOELECTRIC ARRAYS [DETEKTION VON STROEMUNGSINSTABILITAETEN AN TRAGFLUEGELPROFILEN MIT HILFE VON PIEZO-ARRAYS]

W. Nitsche, P. Mirow, and T. Doerfler *In* DGLR, Flows with Separation 1988 p 55-65 In GERMAN (For primary document see N90-16169 08-34)

Avail: NTIS HC A17/MF A03

The possibilities of piezoelectric sensor arrays for the investigation and analysis of laminar-turbulent flow at airfoil profiles, with a view to the characterization of the flow conditions as well as to the detection of flow instabilities in the transition region are discussed. Both wind tunnel tests and free flight tests demonstrated that piezoelectric foil arrays are a valuable and practicable aid in current laminar airfoil research. ESA

N90-16176# Physikalisch-Technische Bundesanstalt, Brunswick (Germany, F.R.).

OPTICAL FLOW MEASURING METHOD USING DIODE LASERS, PHASE COUPLED ARRAYS, AND HIGH FREQUENCY PULSED DIODE LASERS [OPTISCHE STROEMUNGSMESSVERFAHREN MIT DIODENLASERN, PHASENGEKOPPELTEN ARRAYS UND HOCHFREQUENT GEPULSTEN DIODENLASERN]

D. Dopheide, M. Faber, G. Reim, and G. Taux *In* DGLR, Flows with Separation 1988 p 67-75 In GERMAN (For primary document see N90-16169 08-34)

Avail: NTIS HC A17/MF A03

The use of miniature Laser Doppler Anemometers (LDAs), based on semiconductor diode lasers and avalanche photodiodes, is outlined. It is shown that GaAlAs diode lasers with index and gain guided construction can be used in the LDA technique; index guided diodes have slight advantages compared to gain guided diodes. Silicon avalanche diode with quantum efficiencies of 90 percent combined with GaAlAs diode lasers are the ideal combination for LDA applications. A 70 mW semiconductor LDA has the same signal to noise ratios as the usual gas laser LDA with 200 mW output power (Ar-ion system). ESA

N90-16177# Deutsche Forschungs- und Versuchsanstalt fuer Luft- und Raumfahrt, Brunswick (Germany, F.R.). Inst. fuer Entwurfsaerodynamik.

DETERMINATION OF THE N-FACTOR IN THE BRUNSWICK (FEDERAL REP. OF GERMANY) TRANSONIC WIND TUNNEL USING MEASUREMENTS OF PRESSURE DISTRIBUTIONS AND TRANSITION POINTS, AND THE SALLY METHOD [BESTIMMUNG DES N-FAKTORS IM TRANSSONISCHEN WINDKANAL BRAUNSCHWEIG (TWB) ANHAND VON DRUCKVERTEILUNGS- UND UMSCHLAGPUNKTMESSUNGEN UND DEM SALLY-VERFAHREN]

H. Koester and R. Mueller *In* DGLR, Flows with Separation 1988 p 77-92 In GERMAN (For primary document see N90-16169 08-34)

Avail: NTIS HC A17/MF A03

The N-factors (amplitude amplification exponent) of the Brunswick transonic wind tunnel were determined. The most diverse (mainly laminar) profiles in the Mach number range 0.3 to 0.95 were tested. The transition points were determined using the IR technique, and the pressure distributions were measured, allowing deduction of the N-factors at which the laminar-turbulent boundary layer transition occurs. ESA

N90-16178# Deutsche Forschungs- und Versuchsanstalt fuer Luft- und Raumfahrt, Brunswick (Germany, F.R.). Inst. fuer Entwurfsaerodynamik.

DIRECT MEASUREMENT OF LAMINAR INSTABILITY AMPLIFICATION FACTORS IN FLIGHT

S. J. Miley, K.-H. Horstmann, B. Ketthaus, C.-P. Krueckeberg, and H. Wandert *In* DGLR, Flows with Separation 1988 p 93-102 (For primary document see N90-16169 08-34)

Avail: NTIS HC A17/MF A03

An instrumentation system and methodology were developed to measure the physical parameters of Tollmein-Schlichting (TS) waves on a wing of the LFU 205 research aircraft in flight. Highly position accurate boundary layer traversing mechanisms were used. Probe positioning and data recording were performed under computer software control. Special attention in the software development was given to the research environment of the aircraft cabin. The external disturbance environment was also measured and made available with the TS data. ESA

N90-16179# Messerschmitt-Boelkow-Blohm G.m.b.H., Bremen (Germany, F.R.). Transport- und Verkehrsflugzeuge.

DEVELOPMENT OF TRANSITION CRITERIA ON THE BASIS OF E TO THE N POWER FOR THREE DIMENSIONAL WING BOUNDARY LAYERS [ENTWICKLUNG VON TRANSITIONSKRITERIEN AUF E SUP N BASIS FUER DREIDIMENSIONALE FLUEGELGRENZSCHICHTEN]

H. Bieler and G. Redeker (Deutsche Forschungs- und

Versuchsanstalt fuer Luft- und Raumfahrt, Brunswick, Germany, F.R.) *In* DGLR, Flows with Separation 1988 p 103-116 In GERMAN (For primary document see N90-16169 08-34)
Avail: NTIS HC A17/MF A03

Criteria for the laminar-turbulent transition on laminar flow airfoils were established for wing design purposes. Flight tests with the ATTAS research aircraft provided a data base for the experimental determination of N-factors where N = amplitude amplification exponent. Cross flow instability, Tollmein-Schlichting instability, and attachment line contamination were observed. The IR method provided a global picture of the transition line, without affecting the flow itself. Boundary layer stability analyses using the Orr-Sommerfeld solver SALLY for several flight conditions give N-factor threshold values for the Tollmein-Schlichting and for the cross flow instability. Curvature effects, compressibility effects, and interactions between the disturbances could not be taken into account. ESA

N90-16180# Messerschmitt-Boelkow-Blohm G.m.b.H., Bremen (Germany, F.R.).
THE PRECISE CALCULATION OF THE INVISCID LEADING EDGE FLOW ON A LAMINAR AIRFOIL USING SIMPLE METHODS AND VERIFICATION BY MEASUREMENTS ON THE TLF PILOT MODEL [DIE GENAUE BERECHNUNG DER REIBUNGSFREIEN NASENUMSTROEMUNG AM LAMINARFLUEGEL MIT EINFACHEN METHODEN UND VERIFIKATION DURCH MESSUNGEN AM TLF-PILOTMODELL]
K. D. Klevenhusen, H. Jakob, K. Becker, and R. Henke *In* DGLR, Flows with Separation 1988 p 129-140 In GERMAN (For primary document see N90-16169 08-34)
Avail: NTIS HC A17/MF A03

The inviscid flow on the leading edge of a laminar flow airfoil was calculated using the program package LISWA (locally infinite swept wind analysis), and compared with measurements on a pilot model. It is shown that the flow can be very accurately calculated with LISWA, and can be usefully combined with a more complicated method, such as the three dimensional Euler code. The LISWA results agree very well with experimental results for a supersonic case on the small pilot model without fuselage TLF (transonic laminar flow). The LISWA method allows interpretation of missing points in a limited series of measurements, avoiding the very expensive use of large models and wind tunnels with a view to stability calculations. ESA

N90-16181# Technische Univ., Brunswick (Germany, F.R.). Inst. fuer Stroemungsmechanik.
WIND TUNNEL INVESTIGATIONS ON THE CONFIGURATION OF THE INTERNATIONAL VORTEX FLOW EXPERIMENT [WINDKANALUNTERSUCHUNGEN AN DER KONFIGURATION DES INTERNATIONALEN VORTEX FLOW EXPERIMENT]
H.-Chr. Oelker *In* DGLR, Flows with Separation 1988 p 141-157 In GERMAN (For primary document see N90-16169 08-34)
Avail: NTIS HC A17/MF A03

Wind tunnel experiments were performed with a view to the systematic investigation of vortex interferences and the short range coupled canard type configuration international vortex flow experiment on Euler-code validation. The force and pressure distributions resulting from the wind tunnel experiments demonstrate the basic mechanism of the interference between both wings, leading to an increase of the maximum lift coefficient in comparison with wings without canard type configuration. The flow field measurements show that the vortex system coming off the tail unit continues up to behind the wing and can be univocally identified. ESA

N90-16182# Deutsche Forschungs- und Versuchsanstalt fuer Luft- und Raumfahrt, Goettingen (Germany, F.R.). Inst. fuer Experimentelle Stroemungsmechanik.
FLOW FIELD VISUALIZATION STUDY ON A 65 DEG DELTA WING AT M = 0.85
Karl-Aloys Buetefisch and K. Hartmann *In* DGLR, Flows with Separation 1988 p 159-168 Presented at the 16th ICAS Congress, Jerusalem, Israel, 28 Aug. - 2 Sep. 1988 Submitted for publication (For primary document see N90-16169 08-34)
Avail: NTIS HC A17/MF A03

Flow field visualization experiments were performed in a transonic wind tunnel on a delta wing with rounded leading edge as a contribution to the international vortex flow experiment. The aim was to provide a better understanding of the physical behavior of the flow field that is strongly dominated by the formation, development, and decay of vortices. In addition to force, pressure, and velocity measurements the flow was visualized using the laser light sheet and the oil flow technique. The development of the primary and secondary vortex system was observed. Sudden changes of the flow field structure were found. The digital image processing system provided quantitative data on the positions of the vortices. ESA

N90-16183# Universitaet der Bundeswehr, Neubiberg (Germany, F.R.). Inst. fuer Luftfahrttechnik und Leichtbau.
A NONLINEAR VORTEX-LATTICE METHOD FOR THE CALCULATION OF INTERFERENCE EFFECTS BETWEEN FREE VORTEX SHEETS AND WINGS [EIN NICHTLINEARES WIRBELGITTERVERFAHREN ZUR BERECHNUNG VON INTERFERENZEFFEKTEN ZWISCHEN FREIEN WIRBELSCHICHTEN UND TRAGFLAECHEN]
R. Behr and S. Wagner *In* DGLR, Flows with Separation 1988 p 169-180 In GERMAN (For primary document see N90-16169 08-34)
(Contract DFG-Wa-424/3)
Avail: NTIS HC A17/MF A03

A vortex-lattice method for flow calculations on single and coupled airfoils with and without leading edge flow separation is presented. Using a time-dependent procedure, the formation and position of the separated shear sheets in the flow field are determined. The problems due to the induced velocities in the immediate neighborhood of the discretized vortex sheets were solved, allowing examination of strongly rolled up shear sheets that occur especially in leading edge vortices. Wing loading and flow fields are predicted with acceptable accuracy with a relatively small calculation effort, as demonstrated by comparisons with experiments. ESA

N90-16184# Deutsche Forschungs- und Versuchsanstalt fuer Luft- und Raumfahrt, Brunswick (Germany, F.R.). Inst. for Design Aerodynamics.
RESEARCH ON THREE DIFFERENT EULER'S SCHEMES APPLIED TO A DELTA WING WITH VORTICAL FLOWS
J. M. A. Longo *In* DGLR, Flows with Separation 1988 p 181-193 Prepared in cooperation with MBB GmbH, Bremen, Federal Rep. of Germany (For primary document see N90-16169 08-34)
Avail: NTIS HC A17/MF A03

The capability of the numerical solution of the Euler equations to predict vortex flow fields around a sharp leading edge cropped delta wing at moderate to high angles of attack was investigated for subsonic and transonic flow regimes. The solution of the Euler equations discretized on a given grid is independent of the numerical scheme used to solve the Euler equations, and also of the grid topology and the convergence level. Only the numerical dissipation is responsible for the deviation in the solutions. The dominant effect is related to the truncation error, which is drastically reduced by a proper mesh design in places where high flow grandients are expected. The comparison of computed results with experimental data proves that Euler solvers are a valuable engineering tool for total forces prediction including vortex bursting phenomena and vortex-shock wave interaction. ESA

N90-16185# Technische Hochschule, Aachen (Germany, F.R.). Inst. fuer Luft- und Raumfahrt.
FORCE AND MOMENT MEASUREMENTS ON DELTA WINGS IN UNSTEADY FLOW [KRAFT- UND MOMENTENMESSUNGEN AN DELTAFLUEGELN BEI INSTATIONAERER ANSTROEMUNG]
Bernd Steckemetz *In* DGLR, Flows with Separation 1988

p 195-207 In GERMAN (For primary document see N90-16169 08-34)
Avail: NTIS HC A17/MF A03

Based on flow observations on delta wings in a water tunnel, force and moment measurements were performed for unsteady flow in a subsonic wind tunnel. The influence of an angle of attack disturbance with a fixed delta wing in a gust field and for a wing maneuver was analyzed. Substantial phase shifts in the force and moment balance were found in unsteady flows. A comparison with water tumel results shows the correlation with the time-dependent bursting of the leading edge vortex. The effects of the flight mechanics derivatives for a delta wing configuration were calculated with a semiempirical approach. Strong effects of the phase shifts occurring in the force and moment balance on the angle of attack oscillation were found. ESA

N90-16186# Deutsche Forschungs- und Versuchsanstalt fuer Luft- und Raumfahrt, Goettingen (Germany, F.R.). Inst. fuer Theoretische Stroemungsmechanik.

NUMERICAL SIMULATION OF THE LAMINAR AND TURBULENT THREE DIMENSIONAL FLOW ON A DELTA WING WITH SHARP LEADING EDGE [NUMERISCHE SIMULATION DER LAMINAREN UND TURBULENTEN DREIDIMENSIONALEN STROEMUNG UM EINEN DELTAFLUEGEL MIT SCHARFER VORDERKANTE]

A. Hilgenstock *In* DGLR, Flows with Separation 1988 p 209-220 In GERMAN (For primary document see N90-16169 08-34)
Avail: NTIS HC A17/MF A03

The flows about a 65 deg swept delta wing were simulated using a block structured three dimensional Navier-Stokes computer program. The computational grid generation was performed with an algebraic method. Grid refinements reveal the strong sensitivity of the solution to refinement in the direction perpendicular to the surface. The numerical results agree well with experimental data. ESA

N90-16187# Technische Hochschule, Aachen (Germany, F.R.). Aerodynamisches Inst.

NUMERICAL SIMULATION OF A BUBBLE SHAPED BURSTING VORTEX [NUMERISCHE SIMULATION EINES BLASENFOERMIG AUFPLATZENDEN WIRBELS]

M. Breuer and D. Haenel *In* DGLR, Flows with Separation 1988 p 221-231 In GERMAN (For primary document see N90-16169 08-34)
Avail: NTIS HC A17/MF A03

The breakdown of an isolated vortex, embedded in an inviscid nonrotational flow, was simulated by solving the Navier-Stokes equations for an unsteady, three dimensional, incompressible and laminar flow. The integration method for the incompressible conservation equations is described. It is based on the principle of artificial compressibility, but was extended for unsteady flow. The calculated vortex flows show the time evolution of the bubble shaped breakdown phenomenon and the internal structure of the breakdown bubble. ESA

N90-16188# Stuttgart Univ. (Germany, F.R.). Mathematisches Inst.

FINITE ELEMENT CALCULATIONS FOR TRANSONIC FLOWS TAKING INTO ACCOUNT SEVERAL FAR FIELD BOUNDARY CONDITIONS [FINITE ELEMENT BERECHNUNGEN FUER TRANSONISCHE STROEMUNGEN UNTER BERUECKSICHTIGUNG VERSCHIEDENER FERNFELDRANDBEDINGUNGEN]

H. Berger, G. Warnecke, and W. Wendland *In* DGLR, Flows with Separation 1988 p 233-243 In GERMAN Sponsored by the Stiftung Volkswagen (For primary document see N90-16169 08-34)
Avail: NTIS HC A17/MF A03

Some preliminary approaches were mathematically investigated in the framework of a systematic treatment of the far field boundary conditions on the finite boundary of the computation domain. The emphasis was on the global boundary conditions in the form of integral conditions. A finite element method for the nonlinear complete potential equation was coupled with a boundary element method for the Prandtl-Glauert linearization in the outer field. Preliminary results are presented. ESA

N90-16189# Universitaet der Bundeswehr, Neubiberg (Germany, F.R.). Inst. fuer Luftfahrttechnik und Leichtbau.

CALCULATION OF THE FLOW FIELD OF A MULTIBLADE HELICOPTER ROTOR USING A EULER METHOD INCLUDING THE WAKE [BERECHNUNG DES STROEMUNSFELDES EINES MEHRBLAETTRIGEN HUBSCHRAUBERROTORS MIT HILFE EINES EULER-VERFAHRENS UNTER EINBEZIEHUNG DES NACHLAUFES]

S. Wagner, E. Kraemer, and J. Hertel *In* DGLR, Flows with Separation 1988 p 243-254 In GERMAN (For primary document see N90-16169 08-34)
(Contract BMFT-514-8891-LFF-8440)
Avail: NTIS HC A17/MF A03

A method for the calculation of the subsonic and transonic flow about a multiblade helicopter rotor in hover flight based on the solution of the Euler equations is presented. Blade-vortex interference was taken into account. It is shown that the Euler equations are very well suited for the description of vortex transport, and hence for the treatment of the main problem of a steady rotor flow, i.e., the blade-vortex interference, without the need of an external vortex model. The results agree with measurements on a model rotor, and represent the effects of lattice topology and the distance of the far field boundary on the vortex propagation. ESA

N90-16190# Messerschmitt-Boelkow-Blohm G.m.b.H., Bremen (Germany, F.R.).

AN INTERACTIVE METHOD FOR THE FLOW CALCULATION OF AIRFOILS WITH LOCAL SEPARATION REGIONS [EIN INTERAKTIVES VERFAHREN ZUR STROEMUNGSBERECHNUNG VON TRAGFLUEGELPROFILEN MIT LOKALEN ABLOESEGEBIETEN]

F. Arnold, B. Schalau, and F. Thiele (Technische Univ., Berlin, Germany, F.R.) *In* DGLR, Flows with Separation 1988 p 255-266 In GERMAN (For primary document see N90-16169 08-34)
Avail: NTIS HC A17/MF A03

The turbulent flow of the airfoil profile NACA4412 for different angles of attack was calculated using an interactive method. The inverse formulation of the applied difference method for the boundary layer flow allows the calculation of local separation regions that occur at the profile trailing edge for large angles of attack and that can propagate up to the wake. The comparison of the results with measurements shows that, depending on the applied turbulence modeling, the interactive method is suitable for the calculation of airfoil flow with local separation region, even in the off-design domain. The calculation effort is substantially less than for Navier-Stokes solvers. ESA

N90-16191# Messerschmitt-Boelkow-Blohm G.m.b.H., Bremen (Germany, F.R.). Transport- und Verkehrsflugzeuge.

CALCULATION OF THE FLAP PROFILE FLOWS WITH SEPARATION BASED ON COUPLED POTENTIAL AND BOUNDARY LAYER SOLUTIONS [BERECHNUNG VON KLAPPENPROFILSTROEMUNGEN MIT ABLOESUNG AUF DER BASIS GEKOPPELTER POTENTIAL- UND GRENZSCHICHTLOESUNGEN]

G. Dargel and H. Jakob *In* DGLR, Flows with Separation 1988 p 267-278 In GERMAN (For primary document see N90-16169 08-34)
Avail: NTIS HC A17/MF A03

A method for the calculation of flap system flows, based on iteratively coupled potential and boundary layer solutions was developed with a view to the design of high lift systems for passenger and transport aircrafts. The inclusion of the wake in the calculation method allows the determination of the interaction between wake and flap flow which is very important for the calculation of the flap pressure distribution. Trailing edge

separations were calculated. The calculation of the aerodynamic coefficients was substantially improved and could be extended to stalling. Test calculations show that the modeling of separated turbulent boundary layer flow and wakes and their interaction must be improved. ESA

N90-16192# Messerschmitt-Boelkow-Blohm G.m.b.H., Bremen (Germany, F.R.). Transport- und Verkehrsflugzeuge.
INVERSE SOLUTIONS FOR BOUNDARY LAYERS WITH SEPARATION OR CLOSE TO SEPARATION UNDER LOCALLY INFINITE SWEPT WING CONDITIONS [INVERSE LOESUNGEN FUER ABLOESENAHE/ABGELOESTE GRENZSCHICHTEN UNTER LOCALLY INFINITE SWEPT WING BEDINGUNGEN]
E. Elsholz *In* DGLR, Flows with Separation 1988 p 279-288 In GERMAN (For primary document see N90-16169 08-34)
Avail: NTIS HC A17/MF A03

An inverse Locally Infinite Swept Wing (LISW) difference method for quasi three dimensional wall and wake boundary layer flows with partial separated flow regions is described. The LISW method solves the Prandtl boundary layer equations for turbulent, compressible fluids, assuming a locally infinitely extended swept wing in a surface coordinate system. The function and efficiency of the method are illustrated by two test cases. Compared with integral methods the LISW method requires larger calculation times, but allows a simple exchange of turbulence models and a simpler adaptation to changed boundary conditions. ESA

N90-16193# Deutsche Forschungs- und Versuchsanstalt fuer Luft- und Raumfahrt, Goettingen (Germany, F.R.). Inst. fuer Experimentelle Stroemungsmechanik.
NUMERICAL BOUNDARY LAYER CALCULATIONS ON THE DFVLR ELLIPSOID OF REVOLUTION [NUMERISCHE GRENZSCHICHTRECHNUNGEN AM DFVLR-ROTATIONSELLIPSOID]
F. Menter *In* DGLR, Flows with Separation 1988 p 289-300 In GERMAN (For primary document see N90-16169 08-34)
Avail: NTIS HC A17/MF A03

Two methods for the calculation of three dimensional viscous flow problems are presented. The numerical calculations were performed on the DFVLR ellipsoid of revolution for an angle of attack of 10 deg and a Reynolds number of 7.7 times 10 to the 6th power. The first method solves the three dimensional boundary layer equations of first order in curvilinear orthogonal coordinates for a given pressure distribution. The second method integrates the parabelized Navier-Stokes equations spatially, allowing the successive integration of single velocity profiles, completely analogous with a boundary layer method. For a given potential theory pressure distribution the solution of the boundary layer equations shows a discontinuity in the region of strong interaction with the external flow. This problem could be avoided by the second method, allowing the calculation of a numerical solution over almost the whole body. ESA

N90-16194*# National Aeronautics and Space Administration. Langley Research Center, Hampton, VA. Inst. fuer Entwurfsaerodynamik.
CONVERGENCE SPEEDING UP IN THE CALCULATION OF THE VISCOUS FLOW ABOUT AN AIRFOIL [KONVERGENZBESCHLEUNIGUNG BEI DER BERECHNUNG DER REIBUNGSBEHAFTETEN UMSTROEMUNG EINES TRAGFLUEGELS]
R. Radespiel and C. Rossow (Deutsche Forschungs- und Versuchsanstalt fuer Luft- und Raumfahrt, Brunswick, Germany, F.R.) *In* DGLR, Flows with Separation 1988 p 301-312 In GERMAN (For primary document see N90-16169 08-34)
Avail: NTIS HC A17/MF A03 CSCL 20D

A finite volume method to solve the three dimensional Navier-Stokes equations was developed. It is based on a cell-vertex scheme with central differences and explicit Runge-Kutta time steps. A good convergence for a stationary solution was obtained by the use of local time steps, implicit smoothing of the residues, a multigrid algorithm, and a carefully controlled artificial dissipative term. The method is illustrated by results for transonic profiles and airfoils. The method allows a routine solution of the Navier-Stokes equations. ESA

N90-16195# Imperial Coll. of Science and Technology, London (England). Inst. of Mechanical Engineering.
A FINITE VOLUME CALCULATION METHOD FOR THREE DIMENSIONAL, COMPLEX FLOWS [EIN FINITES-VOLUMEN-BERECHNUNGSVERFAHREN FUER DREIDIMENSIONALE, KOMPLEXE STROEMUNGEN]
A. D. Gosman and M. Peric (Erlangen-Nuremberg Univ., Germany, F.R.) *In* DGLR, Flows with Separation 1988 p 313-326 In GERMAN (For primary document see N90-16169 08-34)
Avail: NTIS HC A17/MF A03

A compact version of a finite volume method for fully elliptic three dimensional flows is presented. The conservation equations and their fully implicit discretization are outlined. The coupling between pressure and velocities and the solution algorithm are explained. The method can be applied for the prediction of laminar or turbulent, steady and unsteady, incompressible (also incompressible up to a Mach number of about 0.6) three dimensional flows. The numerical grid is adapted to the boundary of the solution domain and does not have to be orthogonal or smooth. Examples demonstrate that the method is suited for the investigation of complex flows. ESA

N90-16196# Dornier System G.m.b.H., Friedrichshafen (Germany, F.R.). Numerische Stroemungsmechanik.
PERIODICALLY UNSTEADY EFFECTS ON PROFILES, INDUCED BY SEPARATION [DURCH ABLOESUNG INDUZIERTE, PERIODISCH-INSTATIONAERE EFFEKTE AN PROFILEN]
Edgar A. Gerteisen *In* DGLR, Flows with Separation 1988 p 327-341 In GERMAN (For primary document see N90-16169 08-34)
Avail: NTIS HC A17/MF A03

The possibilities of allowing larger time steps in time accurate methods were investigated, with a view to the application of Euler and Navier-Stokes methods for the analysis of nonlinear phenomena. Almost no gain was obtained for the time accurate multigrid formulation; the time step could be enhanced by maximum one order of magnitude. The fully implicit approximation of the Euler flux terms is a suitable means (through the stabilization of the algorithm) for an efficient time accurate flow calculation. ESA

N90-16197# Deutsche Forschungs- und Versuchsanstalt fuer Luft- und Raumfahrt, Brunswick (Germany, F.R.). Inst. fuer Entwurfsaerodynamik.
CALCULATION OF TWO AND THREE DIMENSIONAL SUPER AND HYPERSONIC FLOWS BY SOLVING THE EULER EQUATIONS [BERECHNUNG VON ZWEI- UND DREIDIMENSIONALEN UEBER- UND HYPERSCHALLSTROEMUNGEN DURCH LOESUNG DER EULER-GLEICHUNGEN]
N. Kroll, H. Li, J. Schoene, and Th. Sonar *In* DGLR, Flows with Separation 1988 p 343-364 In GERMAN (For primary document see N90-16169 08-34)
Avail: NTIS HC A17/MF A03

An explicit finite volume method with cell-vortex discretization for the calculation of supersonic and hypersonic flow fields is presented. The method is based on the solution of the Euler equations. Air in chemical equilibrium can be taken into account. The spatial discretization was simplified for the calculation of conical flow fields. Numerical results for a cone, an analytically defined front body, and two different conical delta wings are presented and compared with experimental data. The method was extended to a total variation diminishing scheme; the first results show a better determination of shocks and an enhanced robustness of the method. ESA

N90-16198# Deutsche Forschungs- und Versuchsanstalt fuer Luft- und Raumfahrt, Goettingen (Germany, F.R.). Inst. fuer Theoretische Stroemungsmechanik.
NUMERICAL SIMULATION OF LAMINAR HYPERSONIC FLOWS ABOUT AN ELLIPSOID [NUMERISCHE SIMULATION LAMINARER HYPERSCHALL-STROEMUNGEN UM ELLIPSOIDE]
S. Riedelbauch and B. Mueller *In* DGLR, Flows with Separation 1988 p 365-376 In GERMAN (For primary document see N90-16169 08-34)
Avail: NTIS HC A17/MF A03

The laminar hypersonic flow about a double ellipsoid, which idealizes the nose and cockpit of a spacecraft, were numerically simulated. The calculation method solves the three dimensional thin layer Navier-Stokes equations in a conservative formulation on a surface oriented calculation grid using an implicit/explicit finite difference technique. The conservative formulation allows the correct calculation of embedded compression shocks, while the head wave was treated with a shock-fitting procedure. The calculated flow fields about the ellipsoid show shock-shock and shock-boundary layer interactions in connection with separated flow. Wall flow lines and heat transfer agree qualitatively very well with film-of-oil and thermographic pictures. ESA

N90-16199# European Space Agency. Centre Spatial de Toulouse (France). Hermes Project Dept.
THE HERMES DEVELOPMENT PROGRAM **c16**
J. Herholz *In* DGLR, Flows with Separation 1988 p 377-396 (For primary document see N90-16169 08-34)
Avail: NTIS HC A17/MF A03

The Hermes program is presented. The role of the Hermes system, the development program, the technical challenges, and the system verification program are outlined. The program includes a considerable number of novelties for the European space community in a variety of areas ranging from management techniques to be applied to large programs, over new technologies and techniques, to the verification and qualification of complex interfaces with other space and ground based systems. This requires the involvement and cooperation of available resources all over Europe. ESA

N90-16200# Illinois Inst. of Tech., Chicago.
GRID-INDEPENDENT WALL LAYER TURBULENCE MODEL FOR COMPLEX FLOW CALCULATIONS
Mark J. Jennings and Thomas Morel (Ricardo-ITI, Westmont, IL.) 1989 7 p Presented at the 7th Symposium on Turbulent Shear Flows, Stanford, CA, 21-23 Aug. 1989
(Contract DE-AC04-86AL-33183)
(DE90-003500; CONF-8908163-1) Avail: NTIS HC A02/MF A01

A new modeling approach was developed for the near wall region in turbulent flows, to be used as an alternative to wall functions in multi-dimensional flow simulation codes. The model involves the solution of a set of boundary layer equations on a finely resolved 1-D grid spanning the wall layer (below y(+)--50). The wall layer grid is dynamically scaled to provide sufficient resolution of the near wall flow regardless of the resolution of the bulk flow grid. The wall layer solution does not rely on the assumption of turbulence equilibrium (production-dissipation), making it applicable to complex flows involving separation and reattachment. Comparison to skin friction and heat transfer data in sudden expansion flows shows that the new model performs significantly better than the wall functions. DOE

N90-16201# Department of Energy, Idaho Falls, ID.
INDUSTRIAL HEAT PUMP ASSESSMENT STUDY
R. N. Chappell, S. J. Priebe, and G. L. Wilfert (Battelle Northwest Labs., Richland, WA.) Mar. 1989 50 p Prepared for Bonneville Power Administration, Portlane, OR Prepared in cooperation with Idaho National Engineering Lab., Idaho Falls, ID
(Contract DE-AI79-87BP-36246)
(DE90-004541; DOE/BP-36246/1) Avail: NTIS HC A04/MF A01

This report summarizes preliminary studies that assess the potential of industrial heat pumps for reduction of process heating requirements in industries receiving power from the Bonneville Power Administration (BPA). This project was initiated at the request of BPA to determine the potential of industrial heat pumps in BPA's service area. Working from known heat pump principles and from a list of BPA's industrial customers, the authors estimated the fuel savings potential for six industries. Findings indicate that the pulp and paper industry would yield the greatest fuel savings and increased electrical consumption. Assessments presented in this report represent a cooperative effort between The Idaho National Engineering Laboratory (INEL), and Battelle-Northwest Laboratories. DOE

N90-16240# Technische Hochschule, Aachen (Germany, F.R.). Stosswellenlabor.
CODED TRAJECTORIES FOR THE INVESTIGATION OF STRONGLY UNSTEADY FLOW FIELDS [KODIERTE BAHNSPUREN ZUR UNTERSUCHUNG STARK INSTATIONAERER STROEMUNGSFELDER]
W. Kerres and H. Groenig *In* DGLR, Two-Dimensional Measuring Techniques 1988 p 43-57 In GERMAN (For primary document see N90-16236 08-35)
Avail: NTIS HC A12/MF A02

N90-16241# Deutsche Forschungs- und Versuchsanstalt fuer Luft- und Raumfahrt, Berlin (Germany, F.R.). Abteilung Turbulenzforschung.
VISUALIZATION OF INSTABILITY FORMS OF A ROUND FREE JET USING A LIGHT SHEET METHOD [SICHTBARMACHUNG VON INSTABILITAETSFORMEN EINES RUNDEN FREISTRAHLS DURCH EINE LICHTSCHNITTMETHODE]
B. Lehmann and B. Barsikow *In* DGLR, Two-Dimensional Measuring Techniques 1988 p 59-66 In GERMAN (For primary document see N90-16236 08-35)
Avail: NTIS HC A12/MF A02

N90-16244# Karlsruhe Univ. (Germany, F.R.). Inst. fuer Stroemungslehre und Stroemungsmaschinen.
DIGITAL IMAGE INTERPRETATION FOR OPTICAL FLOW MEASUREMENT METHODS: SYSTEM DESCRIPTION AND PRELIMINARY APPLICATION EXAMPLES [DIGITALE BILDAUSWERTUNG FUER OPTISCHE STROEMUNGSMESSVERFAHREN: SYSTEMBESCHREIBUNG UND ERSTE ANWENDUNGSBEISPIELE]
G. Schnerr *In* DGLR, Two-Dimensional Measuring Techniques 1988 p 93-104 In GERMAN (For primary document see N90-16236 08-35)
(Contract DFG-Zi/18-31-1)
Avail: NTIS HC A12/MF A02

N90-16245# Duits-Nederlandse Windtunnel, North East Polder (Netherlands).
THE DETERMINATION OF VORTEX SEPARATION FREQUENCIES BY MEANS OF LASER LIGHT SHEET IMAGES
K. Pengel *In* DGLR, Two-Dimensional Measuring Techniques 1988 p 105-110 (For primary document see N90-16236 08-35)
(DNW-WTI-88.038) Avail: NTIS HC A12/MF A02

N90-16253# Erlangen-Nuremberg Univ. (Germany, F.R.). Lehrstuhl fuer Stroemungsmechanik.
FLOW VISUALIZATION OF WATER FLOWS USING THE CRYSTAL VIOLET METHOD [STROEMUNGSSICHTBARMACHUNG VON WASSERSTROEMUNGEN MIT HILFE DES KRISTALLVIOLETTVERFAHRENS]
G. Dimaczek, C. Eh, and C. Tropea *In* DGLR, Two-Dimensional Measuring Techniques 1988 p 201-210 In GERMAN (For primary document see N90-16236 08-35)
Avail: NTIS HC A12/MF A02

N90-16255# Duits-Nederlandse Windtunnel, North East Polder (Netherlands).
SURFACE FLOW VISUALIZATION WITH SHEAR STRESS SENSITIVIVE LIQUID CRYSTALS
K. Pengel *In* DGLR, Two-Dimensional Measuring Techniques 1988 p 223-232 Original contains color illustrations (For primary document see N90-16236 08-35)
(DNW-WTI-88.039) Avail: NTIS HC A12/MF A02

35 INSTRUMENTATION AND PHOTOGRAPHY

Includes remote sensors; measuring instruments and gages; detectors; cameras and photographic supplies; and holography.

For aerial photography see *43 Earth Resources and Remote Sensing*. For related information see also *06 Aircraft Instrumentation*, and *19 Spacecraft Instrumentation*.

N90-16202*# Southwest Research Inst., San Antonio, TX.
STAND ALONE PRESSURE MEASUREMENT DEVICE (SAPMD) FOR THE SPACE SHUTTLE ORBITER, PART 1 Final Report
Bill Tomlinson Jan. 1989 89 p
(Contract NAS9-17601; SwRI Proj. 15-1062)
(NASA-CR-172119-Pt-1; NAS 1.26:172119-Pt-1) Avail: NTIS HC A05/MF A01 CSCL 14B

The specifications for the Stand Alone Pressure Measurement Device (SAPMD) are as follows: the SAPMD shall measure ambient pressure at the surface of the Orbiter TPS in the range of 0 to 15 pounds per square inch absolute (PSIA). Measurement will begin at solid rocket booster (SRB) ignition as sensed by appropriate vibration sensing elements in the SAPMD. Pressure and corresponding real-time data are to be recorded every one tenth second for 140 seconds and at the end of the recording period, the operation will be discontinued with the data preserved for interrogation subsequent to Orbiter re-entry and landing. The type and size of the battery shall be such as to allow the vibration sensing elements and a real-time clock to be initialized a minimum of 30 day prior to launch and still provide power as necessary to perform the 140 second data recording period after SRB ignition. Battery installation shall be in such a manner as to allow battery replacement without removing the SAPMD from its position or removing more than one TPS tile. The SAPMD must be mounted in specific locations under tile of the TPS. To accommodate such mounting, the absolute maximum physical dimensions much not exceed 6.0 inches in length, 1.5 inches in width, and 0.4 inches in height, and the device shall be of such configuration that it can be bonded to the Orbiter skin at the joint line of two TPS tiles with the pressure sensing port at the surface of the tile. The SAPMD must remain operational in the temperature range of -40 to +85 C and survive storage temperature of -55 to +125 C. The pressure port must withstand 934 C without causing damage to the TPS during entry and must remain functional at 262 C during ascent. The accuracy of the pressure measurement must be plus or minus one-half PSIA over a temperature range of 0 to +36 C. All the specifications were met and verified by prototype testing and documented in the enclosed test data. Four flight-qualified models were fabricated and of these, two were delivered and successfully flown in the cargo bay of STS-26.
Author

N90-16203*# Southwest Research Inst., San Antonio, TX.
STAND ALONE PRESSURE MEASUREMENT DEVICE (SAPMD) FOR THE SPACE SHUTTLE ORBITER, PART 2
Bill Tomlinson Jan. 1989 78 p
(Contract NAS9-17601; SwRI Proj. 15-1062)
(NASA-CR-172119-Pt-2; NAS 1.26:172119-Pt-2) Avail: NTIS HC A05/MF A01 CSCL 14B

The Stand Alone Pressure Measurement Device (SAPMD) specifications are examined. The HP.SAPMD GSE software is listed; the HP/SGA readme program is presented; and the SPMD acceptance test procedure is described. B.G.

N90-16204*# National Aeronautics and Space Administration. Langley Research Center, Hampton, VA.
VISUAL INFORMATION PROCESSING FOR TELEVISION AND TELEROBOTICS
Friedrich O. Huck, ed. and Stephen K. Park, ed. (College of William and Mary, Williamsburg, VA.) Washington Nov. 1989 263 p Workshop held in Williamsburg, VA, 10-12 May 1989
(NASA-CP-3053; L-16665; NAS 1.55:3053) Avail: NTIS HC A12/MF A02 CSCL 14B

This publication is a compilation of the papers presented at the NASA conference on Visual Information Processing for Television and Telerobotics. The conference was held at the Williamsburg Hilton, Williamsburg, Virginia on May 10 to 12, 1989. The conference was sponsored jointly by NASA Offices of Aeronautics and Space Technology (OAST) and Space Science and Applications (OSSA) and the NASA Langley Research Center. The presentations were grouped into three sessions: Image Gathering, Coding, and Advanced Concepts; Systems; and Technologies. The program was organized to provide a forum in which researchers from industry, universities, and government could be brought together to discuss the state of knowledge in image gathering, coding, and processing methods. For individual titles, see N90-16205 through N90-16224.

N90-16205*# College of William and Mary, Williamsburg, VA. Dept. of Computer Science.
LINEAR DIGITAL IMAGING SYSTEM FIDELITY ANALYSIS
Stephen K. Park *In* NASA, Langley Research Center, Visual Information Processing for Television and Telerobotics Nov. 1989 p 3-10 (For primary document see N90-16204 08-35)
Avail: NTIS HC A12/MF A02 CSCL 14B

The combined effects of imaging gathering, sampling and reconstruction are analyzed in terms of image fidelity. The analysis is based upon a standard end-to-end linear system model which is sufficiently general so that the results apply to most line-scan and sensor-array imaging systems. Shift-variant sampling effects are accounted for with an expected value analysis based upon the use of a fixed deterministic input scene which is randomly shifted (mathematically) relative to the sampling grid. This random sample-scene phase approach has been used successfully by the author and associates in several previous related papers. Author

N90-16206*# College of William and Mary, Williamsburg, VA.
MODEL-BASED QUANTIFICATION OF IMAGE QUALITY
Rajeeb Hazra, Keith W. Miller, and Stephen K. Park *In* NASA, Langley Research Center, Visual Information Processing for Television and Telerobotics Nov. 1989 p 11-22 (For primary document see N90-16204 08-35)
Avail: NTIS HC A12/MF A02 CSCL 14B

In 1982, Park and Schowengerdt published an end-to-end analysis of a digital imaging system quantifying three principal degradation components: (1) image blur - blurring caused by the acquisition system, (2) aliasing - caused by insufficient sampling, and (3) reconstruction blur - blurring caused by the imperfect interpolative reconstruction. This analysis, which measures degradation as the square of the radiometric error, includes the sample-scene phase as an explicit random parameter and characterizes the image degradation caused by imperfect acquisition and reconstruction together with the effects of undersampling and random sample-scene phases. In a recent paper Mitchell and Netravelli displayed the visual effects of the above mentioned degradations and presented subjective analysis about their relative importance in determining image quality. The primary aim of the research is to use the analysis of Park and Schowengerdt to correlate their mathematical criteria for measuring image degradations with subjective visual criteria. Insight gained from this research can be exploited in the end-to-end design of optical systems, so that system parameters (transfer functions of the acquisition and display systems) can be designed relative to each other, to obtain the best possible results using quantitative measurements. Author

N90-16207*# College of William and Mary, Williamsburg, VA. Dept. of Computer Science.

OPTIMAL FOCAL-PLANE RESTORATION

Stephen E. Reichenbach and Stephen K. Park *In* NASA, Langley Research Center, Visual Information Processing for Television and Telerobotics Nov. 1989 p 23-32 (For primary document see N90-16204 08-35)

Avail: NTIS HC A12/MF A02 CSCL 14B

Image restoration can be implemented efficiently by calculating the convolution of the digital image and a small kernel during image acquisition. Processing the image in the focal-plane in this way requires less computation than traditional Fourier-transform-based techniques such as the Wiener filter and constrained least-squares filter. Here, the values of the convolution kernel that yield the restoration with minimum expected mean-square error are determined using a frequency analysis of the end-to-end imaging system. This development accounts for constraints on the size and shape of the spatial kernel and all the components of the imaging system. Simulation results indicate the technique is effective and efficient. Author

N90-16208*# Rochester Univ., NY. Inst. of Optics.

CODED-APERTURE IMAGING IN NUCLEAR MEDICINE

Warren E. Smith, Harrison H. Barrett, and John N. Aarsvold (Arizona Univ., Tucson.) *In* NASA, Langley Research Center, Visual Information Processing for Television and Telerobotics Nov. 1989 p 33-45 Sponsored by National Cancer Inst. (For primary document see N90-16204 08-35)

Avail: NTIS HC A12/MF A02 CSCL 14B

Coded-aperture imaging is a technique for imaging sources that emit high-energy radiation. This type of imaging involves shadow casting and not reflection or refraction. High-energy sources exist in x ray and gamma-ray astronomy, nuclear reactor fuel-rod imaging, and nuclear medicine. Of these three areas nuclear medicine is perhaps the most challenging because of the limited amount of radiation available and because a three-dimensional source distribution is to be determined. In nuclear medicine a radioactive pharmaceutical is administered to a patient. The pharmaceutical is designed to be taken up by a particular organ of interest, and its distribution provides clinical information about the function of the organ, or the presence of lesions within the organ. This distribution is determined from spatial measurements of the radiation emitted by the radiopharmaceutical. The principles of imaging radiopharmaceutical distributions with coded apertures are reviewed. Included is a discussion of linear shift-variant projection operators and the associated inverse problem. A system developed at the University of Arizona in Tucson consisting of small modular gamma-ray cameras fitted with coded apertures is described. Author

N90-16209*# Westinghouse Electric Corp., Baltimore, MD. Advanced Technology Div.

CONTEXT DEPENDENT ANTI-ALIASING IMAGE RECONSTRUCTION

Paul R. Beaudet, A. Hunt, and N. Arlia (Westinghouse Research and Development Center, Pittsburgh, PA.) *In* NASA, Langley Research Center, Visual Information Processing for Television and Telerobotics Nov. 1989 p 47-56 (For primary document see N90-16204 08-35)

Avail: NTIS HC A12/MF A02 CSCL 14B

Image Reconstruction has been mostly confined to context free linear processes; the traditional continuum interpretation of digital array data uses a linear interpolator with or without an enhancement filter. Here, anti-aliasing context dependent interpretation techniques are investigated for image reconstruction. Pattern classification is applied to each neighborhood to assign it a context class; a different interpolation/filter is applied to neighborhoods of differing context. It is shown how the context dependent interpolation is computed through ensemble average statistics using high resolution training imagery from which the lower resolution image array data is obtained (simulation). A quadratic least squares (LS) context-free image quality model is described from which the context dependent interpolation coefficients are derived. It is shown how ensembles of high-resolution images can be used to capture the a priori special character of different context classes. As a consequence, a priori information such as the translational invariance of edges along the edge direction, edge discontinuity, and the character of corners is captured and can be used to interpret image array data with greater spatial resolution than would be expected by the Nyquist limit. A Gibb-like artifact associated with this super-resolution is discussed. More realistic context dependent image quality models are needed and a suggestion is made for using a quality model which now is finding application in data compression. Author

N90-16210*# Westinghouse Electric Corp., Baltimore, MD. Advanced Technology Div.

CONTEXT DEPENDENT PREDICTION AND CATEGORY ENCODING FOR DPCM IMAGE COMPRESSION

Paul R. Beaudet *In* NASA, Langley Research Center, Visual Information Processing for Television and Telerobotics Nov. 1989 p 57-69 (For primary document see N90-16204 08-35)

Avail: NTIS HC A12/MF A02 CSCL 14B

Efficient compression of image data requires the understanding of the noise characteristics of sensors as well as the redundancy expected in imagery. Herein, the techniques of Differential Pulse Code Modulation (DPCM) are reviewed and modified for information-preserving data compression. The modifications include: mapping from intensity to an equal variance space; context dependent one and two dimensional predictors; rationale for nonlinear DPCM encoding based upon an image quality model; context dependent variable length encoding of 2x2 data blocks; and feedback control for constant output rate systems. Examples are presented at compression rates between 1.3 and 2.8 bits per pixel. The need for larger block sizes, 2D context dependent predictors, and the hope for sub-bits-per-pixel compression which maintains spacial resolution (information preserving) are discussed. Author

N90-16211*# National Aeronautics and Space Administration. Langley Research Center, Hampton, VA.

IMAGE GATHERING AND CODING FOR DIGITAL RESTORATION: INFORMATION EFFICIENCY AND VISUAL QUALITY

Friedrich O. Huck, Sarah John, Judith A. McCormick, and Ramkumar Narayanswamy (Science and Technology Corp., Hampton, VA.) *In its* Visual Information Processing for Television and Telerobotics Nov. 1989 p 71-91 (For primary document see N90-16204 08-35)

Avail: NTIS HC A12/MF A02 CSCL 14B

Image gathering and coding are commonly treated as tasks separate from each other and from the digital processing used to restore and enhance the images. The goal is to develop a method that allows us to assess quantitatively the combined performance of image gathering and coding for the digital restoration of images with high visual quality. Digital restoration is often interactive because visual quality depends on perceptual rather than mathematical considerations, and these considerations vary with the target, the application, and the observer. The approach is based on the theoretical treatment of image gathering as a communication channel (J. Opt. Soc. Am. A2, 1644(1985); 5,285(1988). Initial results suggest that the practical upper limit of the information contained in the acquired image data range typically from approximately 2 to 4 binary information units (bifs) per sample, depending on the design of the image-gathering system. The associated information efficiency of the transmitted data (i.e., the ratio of information over data) ranges typically from approximately 0.3 to 0.5 bif per bit without coding to approximately 0.5 to 0.9 bif per bit with lossless predictive compression and Huffman coding. The visual quality that can be attained with interactive image restoration improves perceptibly as the available information increases to approximately 3 bifs per sample. However, the perceptual improvements that can be attained with further increases in information are very subtle and depend on the target and the desired enhancement. Author

N90-16212*# National Aeronautics and Space Administration. Lewis Research Center, Cleveland, OH.
DATA COMPRESSION FOR THE MICROGRAVITY EXPERIMENTS
Khalid Sayood, Wayne A. Whyte, Jr., Karen S. Anderson, Mary Jo Shalkhauser, and Anne M. Summers (Nebraska Univ., Lincoln.) *In* NASA, Langley Research Center, Visual Information Processing for Television and Telerobotics Nov. 1989 p 93-107 Sponsored in part by NASA, Goddard Space Flight Center (For primary document see N90-16204 08-35)
(Grants NAG3-806; NAG5-916)
Avail: NTIS HC A12/MF A02 CSCL 14B

Researchers present the environment and conditions under which data compression is to be performed for the microgravity experiment. Also presented are some coding techniques that would be useful for coding in this environment. It should be emphasized that researchers are currently at the beginning of this program and the toolkit mentioned is far from complete. Author

N90-16213*# National Aeronautics and Space Administration. Goddard Space Flight Center, Greenbelt, MD.
DETECTION OF EDGES USING LOCAL GEOMETRY
J. A. Gualtieri and M. Manohar *In* NASA, Langley Research Center, Visual Information Processing for Television and Telerobotics Nov. 1989 p 109-119 (For primary document see N90-16204 08-35)
Avail: NTIS HC A12/MF A02 CSCL 14B

Researchers described a new representation, the local geometry, for early visual processing which is motivated by results from biological vision. This representation is richer than is often used in image processing. It extracts more of the local structure available at each pixel in the image by using receptive fields that can be continuously rotated and that go to third order spatial variation. Early visual processing algorithms such as edge detectors and ridge detectors can be written in terms of various local geometries and are computationally tractable. For example, Canny's edge detector has been implemented in terms of a local geometry of order two, and a ridge detector in terms of a local geometry of order three. The edge detector in local geometry was applied to synthetic and real images and it was shown using simple interpolation schemes that sufficient information is available to locate edges with sub-pixel accuracy (to a resolution increase of at least a factor of five). This is reasonable even for noisy images because the local geometry fits a smooth surface - the Taylor series - to the discrete image data. Only local processing was used in the implementation so it can readily be implemented on parallel mesh machines such as the MPP. Researchers expect that other early visual algorithms, such as region growing, inflection point detection, and segmentation can also be implemented in terms of the local geometry and will provide sufficiently rich and robust representations for subsequent visual processing. Author

N90-16214*# Ecole Polytechnique Federale de Lausanne (Switzerland). Signal Processing Lab.
HIGH COMPRESSION IMAGE AND IMAGE SEQUENCE CODING
Murat Kunt *In* NASA, Langley Research Center, Visual Information Processing for Television and Telerobotics Nov. 1989 p 121-131 (For primary document see N90-16204 08-35)
Avail: NTIS HC A12/MF A02 CSCL 14B

The digital representation of an image requires a very large number of bits. This number is even larger for an image sequence. The goal of image coding is to reduce this number, as much as possible, and reconstruct a faithful duplicate of the original picture or image sequence. Early efforts in image coding, solely guided by information theory, led to a plethora of methods. The compression ratio reached a plateau around 10:1 a couple of years ago. Recent progress in the study of the brain mechanism of vision and scene analysis has opened new vistas in picture coding. Directional sensitivity of the neurones in the visual pathway combined with the separate processing of contours and textures has led to a new class of coding methods capable of achieving compression ratios as high as 100:1 for images and around 300:1 for image sequences. Recent progress on some of the main avenues of object-based methods is presented. These second generation techniques make use of contour-texture modeling, new results in neurophysiology and psychophysics and scene analysis. Author

N90-16215*# California Univ., Irvine.
IMAGE PROCESSING BY INTENSITY-DEPENDENT SPREAD (IDS)
Tom N. Cornsweet *In* NASA, Langley Research Center, Visual Information Processing for Television and Telerobotics Nov. 1989 p 133-144 (For primary document see N90-16204 08-35)
(Contract NAS1-18468)
Avail: NTIS HC A12/MF A02 CSCL 14B

As retinal illuminance is lowered, the human visual system integrates the effects of photon absorptions over larger areas and longer times. A theory of the process that might underlie these changes is called Intensity-Dependent Spread (IDS). Each input point gives rise to a pattern of excitation that spreads to a region of the total excitation it sees. The unique aspect of the theory is the assumption that, although the amplitude of the excitation pattern at its center increases with input illuminance, its width decreases in such a way that its volume remains constant. Application of this theory to image processing reveals that it displays a number of unexpected and potentially useful properties. Among them are edge enhancement and independence from scene illumination. Author

N90-16216*# Old Dominion Univ., Norfolk, VA.
FROM PRIMAL SKETCHES TO THE RECOVERY OF INTENSITY AND REFLECTANCE REPRESENTATIONS
Rachel Alter-Gartenberg, Ramkumar Narayanswamy, and Karen S. Nolker (Computer Sciences Corp., Hampton, VA.) *In* NASA, Langley Research Center, Visual Information Processing for Television and Telerobotics Nov. 1989 p 145-163 (For primary document see N90-16204 08-35)
Avail: NTIS HC A12/MF A02 CSCL 14B

A local change in intensity (edge) is a characteristic that is preserved when an image is filtered through a bandpass filter. Primal sketch representations of images, using the bandpass-filtered data, have become a common process since Marr proposed his model for early human vision. Here, researchers move beyond the primal sketch extraction to the recovery of intensity and reflectance representations using only the bandpass-filtered data. Assessing the response of an ideal step edge to the Laplacian of Gaussian (NAb/A squared G) filter, they found that the resulting filtered data preserves the original change of intensity that created the edge in addition to the edge location. Using the filtered data, they can construct the primal sketches and recover the original (relative) intensity levels between the boundaries. It was found that the result of filtering an ideal step edge with the Intensity-Dependent Spatial Summation (IDS) filter preserves the actual intensity on both sides of the edge, in addition to the edge location. The IDS filter also preserves the reflectance ratio at the edge location. Therefore, one can recover the intensity levels between the edge boundaries as well as the (relative) reflectance representation. The recovery of the reflectance representation is of special interest as it erases shadowing degradations and other dependencies on temporal illumination. This method offers a new approach to low-level vision processing as well as to high data-compression coding. High compression can be gained by transmitting only the information associated with the edge location (edge primitives) that is necessary for the recovery Author

N90-16217*# National Aeronautics and Space Administration. Langley Research Center, Hampton, VA.
ISOLATING CONTOUR INFORMATION FROM ARBITRARY IMAGES
Daniel J. Jobson *In its* Visual Information Processing for Television and Telerobotics Nov. 1989 p 177-190 (For primary document

see N90-16204 08-35)
Avail: NTIS HC A12/MF A02 CSCL 14B

Aspects of natural vision (physiological and perceptua.) serve as a basis for attempting the development of a general processing scheme for contour extraction. Contour information is assumed to be central to visual recognition skills. While the scheme must be regarded as highly preliminary, initial results do compare favorably with the visual perception of structure. The scheme pays special attention to the construction of a smallest scale circular difference-of-Gaussian (DOG) convolution, calibration of multiscale edge detection thresholds with the visual perception of grayscale boundaries, and contour/texture discrimination methods derived from fundamental assumptions of connectivity and the characteristics of printed text. Contour information is required to fall between a minimum connectivity limit and maximum regional spatial density limit at each scale. Results support the idea that contour information, in images possessing good image quality, is (centered at about 10 cyc/deg and 30 cyc/deg). Further, lower spatial frequency channels appear to play a major role only in contour extraction from images with serious global image defects. Author

N90-16218*# Microtronics Associates, Pittsburgh, PA.
PARALLEL ASYNCHRONOUS SYSTEMS AND IMAGE PROCESSING ALGORITHMS
D. D. Coon and A. G. U. Perera (Pittsburgh Univ., PA.) *In* NASA, Langley Research Center, Visual Information Processing for Television and Telerobotics Nov. 1989 p 191-201 (For primary document see N90-16204 08-35)
Avail: NTIS HC A12/MF A02 CSCL 14B

A new hardware approach to implementation of image processing algorithms is described. The approach is based on silicon devices which would permit an independent analog processing channel to be dedicated to evey pixel. A laminar architecture consisting of a stack of planar arrays of the device would form a two-dimensional array processor with a 2-D array of inputs located directly behind a focal plane detector array. A 2-D image data stream would propagate in neuronlike asynchronous pulse coded form through the laminar processor. Such systems would integrate image acquisition and image processing. Acquisition and processing would be performed concurrently as in natural vision systems. The research is aimed at implementation of algorithms, such as the intensity dependent summation algorithm and pyramid processing structures, which are motivated by the operation of natural vision systems. Implementation of natural vision algorithms would benefit from the use of neuronlike information coding and the laminar, 2-D parallel, vision system type architecture. Besides providing a neural network framework for implementation of natural vision algorithms, a 2-D parallel approach could eliminate the serial bottleneck of conventional processing systems. Conversion to serial format would occur only after raw intensity data has been substantially processed. An interesting challenge arises from the fact that the mathematical formulation of natural vision algorithms does not specify the means of implementation, so that hardware implementation poses intriguing questions involving vision science. Author

N90-16219*# Naval Research Lab., Washington, DC.
NEURAL NETWORKS FOR DATA COMPRESSION AND INVARIANT IMAGE RECOGNITION
Sheldon Gardner *In* NASA, Langley Research Center, Visual Information Processing for Television and Telerobotics Nov. 1989 p 203-213 (For primary document see N90-16204 08-35)
Avail: NTIS HC A12/MF A02 CSCL 14B

An approach to invariant image recognition (I2R), based upon a model of biological vision in the mammalian visual system (MVS), is described. The complete I2R model incorporates several biologically inspired features: exponential mapping of retinal images, Gabor spatial filtering, and a neural network associative memory. In the I2R model, exponentially mapped retinal images are filtered by a hierarchical set of Gabor spatial filters (GSF) which provide compression of the information contained within a pixel-based image. A neural network associative memory (AM) is used to process the GSF coded images. We describe a 1-D shape function method for coding of scale and rotationally invariant shape information. This method reduces image shape information to a periodic waveform suitable for coding as an input vector to a neural network AM. The shape function method is suitable for near term applications on conventional computing architectures equipped with VLSI FFT chips to provide a rapid image search capability. Author

N90-16220*# Odetics, Inc., Anaheim, CA.
KNOWLEDGE-BASED IMAGING-SENSOR FUSION SYSTEM
George Westrom *In* NASA, Langley Research Center, Visual Information Processing for Television and Telerobotics Nov. 1989 p 215-229 (For primary document see N90-16204 08-35)
(Contracts NAS1-18816; NAS1-18664)
Avail: NTIS HC A12/MF A02 CSCL 14B

An imaging system which applies knowledge-based technology to supervise and control both sensor hardware and computation in the imaging system is described. It includes the development of an imaging system breadboard which brings together into one system work that we and others have pursued for LaRC for several years. The goal is to combine Digital Signal Processing (DSP) with Knowledge-Based Processing and also include Neural Net processing. The system is considered a smart camera. Imagine that there is a microgravity experiment on-board Space Station Freedom with a high frame rate, high resolution camera. All the data cannot possibly be acquired from a laboratory on Earth. In fact, only a small fraction of the data will be received. Again, imagine being responsible for some experiments on Mars with the Mars Rover: the data rate is a few kilobits per second for data from several sensors and instruments. Would it not be preferable to have a smart system which would have some human knowledge and yet follow some instructions and attempt to make the best use of the limited bandwidth for transmission. The system concept, current status of the breadboard system and some recent experiments at the Mars-like Amboy Lava Fields in California are discussed. Author

N90-16221*# Alabama Univ., Huntsville. Dept. of Computer Science.
A KNOWLEDGE-BASED MACHINE VISION SYSTEM FOR SPACE STATION AUTOMATION
Laure J. Chipman and H. S. Ranganath *In* NASA, Langley Research Center, Visual Information Processing for Television and Telerobotics Nov. 1989 p 231-241 (For primary document see N90-16204 08-35)
(Contract NCC8-16)
Avail: NTIS HC A12/MF A02 CSCL 14B

A simple knowledge-based approach to the recognition of objects in man-made scenes is being developed. Specifically, the system under development is a proposed enhancement to a robot arm for use in the space station laboratory module. The system will take a request from a user to find a specific object, and locate that object by using its camera input and information from a knowledge base describing the scene layout and attributes of the object types included in the scene. In order to use realistic test images in developing the system, researchers are using photographs of actual NASA simulator panels, which provide similar types of scenes to those expected in the space station environment. Figure 1 shows one of these photographs. In traditional approaches to image analysis, the image is transformed step by step into a symbolic representation of the scene. Often the first steps of the transformation are done without any reference to knowledge of the scene or objects. Segmentation of an image into regions generally produces a counterintuitive result in which regions do not correspond to objects in the image. After segmentation, a merging procedure attempts to group regions into meaningful units that will more nearly correspond to objects. Here, researchers avoid segmenting the image as a whole, and instead use a knowledge-directed approach to locate objects in the scene. The

knowledge-based approach to scene analysis is described and the categories of knowledge used in the system are discussed. Author

N90-16222*# Optivision, Inc., Davis, CA.
A PROGRAMMABLE IMAGE COMPRESSION SYSTEM
Paul M. Farrelle *In* NASA, Langley Research Center, Visual Information Processing for Television and Telerobotics Nov. 1989 p 241-250 (For primary document see N90-16204 08-35)
Avail: NTIS HC A12/MF A02 CSCL 14B

A programmable image compression system which has the necessary flexibility to address diverse imaging needs is described. It can compress and expand single frame video images (monochrome or color) as well as documents and graphics (black and white or color) for archival or transmission applications. Through software control, the compression mode can be set for lossless or controlled quality coding; the image size and bit depth can be varied; and the image source and destination devices can be readily changed. Despite the large combination of image data types, image sources, and algorithms, the system provides a simple consistent interface to the programmer. This system (OPTIPAC) is based on the TITMS320C25 digital signal processing (DSP) chip and has been implemented as a co-processor board for an IBM PC-AT compatible computer. The underlying philosophy can readily be applied to different hardware platforms. By using multiple DSP chips or incorporating algorithm specific chips, the compression and expansion times can be significantly reduced to meet performance requirements. Author

N90-16223*# Fairchild Weston Systems, Inc., Syosset, NY.
HYBRID LZW COMPRESSION
H. Garton Lewis, Jr. and William B. Forsyth *In* NASA, Langley Research Center, Visual Information Processing for Television and Telerobotics Nov. 1989 p 251-259 (For primary document see N90-16204 08-35)
Avail: NTIS HC A12/MF A02 CSCL 14B

The Science Data Management and Science Payload Operations subpanel reports from the NASA Conference on Scientific Data Compression (Snowbird, Utah in 1988) indicate the need for both lossless and lossy image data compression systems. The ranges developed by the subpanel suggest ratios of 2:1 to 4:1 for lossless coding and 2:1 to 6:1 for lossy predictive coding. For the NASA Freedom Science Video Processing Facility it would be highly desirable to implement one baseline compression system which would meet both of these criteria. Presented here is such a system, utilizing an LZW hybrid coding scheme which is adaptable to either type of compression. Simulation results are presented with the hybrid LZW algorithm operating in each of its modes. Author

N90-16224*# Martin Marietta Corp., Denver, CO. Astronautics Group.
CONNECTIONIST MODEL-BASED STEREO VISION FOR TELEROBOTICS
William Hoff and Donald Mathis *In* NASA, Langley Research Center, Visual Information Processing for Television and Telerobotics Nov. 1989 p 261-270 (For primary document see N90-16204 08-35)
Avail: NTIS HC A12/MF A02 CSCL 14B

Autonomous stereo vision for range measurement could greatly enhance the performance of telerobotic systems. Stereo vision could be a key component for autonomous object recognition and localization, thus enabling the system to perform low-level tasks, and allowing a human operator to perform a supervisory role. The central difficulty in stereo vision is the ambiguity in matching corresponding points in the left and right images. However, if one has a priori knowledge of the characteristics of the objects in the scene, as is often the case in telerobotics, a model-based approach can be taken. Researchers describe how matching ambiguities can be resolved by ensuring that the resulting three-dimensional points are consistent with surface models of the expected objects. A four-layer neural network hierarchy is used in which surface models of increasing complexity are represented in successive layers. These models are represented using a connectionist scheme called parameter networks, in which a parametrized object (for example, a planar patch p=f(h,m sub x, m sub y) is represented by a collection of processing units, each of which corresponds to a distinct combination of parameter values. The activity level of each unit in the parameter network can be thought of as representing the confidence with which the hypothesis represented by that unit is believed. Weights in the network are set so as to implement gradient descent in an energy function. Author

N90-16225# Eltron Research, Inc., Aurora, IL.
ADVANCED BIOSENSORS FOR AMINO ACID DETECTION Report, 1-31 Oct. 1989
R. L. Cook, J. Patel, and A. F. Sammells 31 Oct. 1989 11 p (Contract N00014-89-C-0250)
(AD-A214029) Avail: NTIS HC A03/MF A01 CSCL 06/1

Reported is work directed towards characterizing an advanced biosensor technology compatible for the real time indirect optical detection of amino acids as typified by e-phen-ylalanine, e-doA, E-Tryptophan and related compounds. The technical strategy involves the indirect optical detection of amines and amino acids by monitoring changes induced in the visible spectra of immobilized chromagenic acyclic polyether host molecules to which the amine or amino acid becomes associated. Syntheses are currently proceeding for preparation of chromagenic acyclic polyether host molecules into which selected amino acids will become incorporated, resulting in induced color changes, detectable when these molecular species are immobilized onto a fiber optic. Design and fabrication of synchronous sample-and-hold circuitry for detection of small optical changes from the fiber optic has largely been completed. GRA

N90-16226 Department of the Navy, Washington, DC.
COLINEAR FLUCTUATING WALL SHEAR STRESS AND FLUCTUATING PRESSURE TRANSDUCER Patent
William L. Keith, inventor (to Navy) 8 Aug. 1989 6 p Filed 25 Apr. 1988 Supersedes US-Patent-Appl-SN-185728 (AD-D014296; US-Patent-4,854,174; US-Patent-Appl-SN-185728; US-Patent-Class-73-714) Avail: U.S. Patent and Trademark Office CSCL 13/7

This patent discloses a unique combination of two transducers. A hot film shear stress gauge and a piezoelectric pressure transducer are coaxially located along the longitudinal centerline of a cylindrical metal shell. The hot film shear stress gauge is exposed to the fluid while the pressure transducer is positioned directly below. Conductors are attached to each and the remaining volume filled with plastic to form a colinear unit. The conductors attached to the hot film element provide power while the conductors attached to the piezoelectric transducer transmit pressure produced electrical signals therefrom. The resulting configuration allows the measurement of fluctuating shear stress and fluctuating pressure to be made simultaneously at a single spatial location at a solid wall bounding a turbulent fluid flow layer. GRA

N90-16227 Department of the Navy, Washington, DC.
LIQUID LEVEL MEASUREMENT SYSTEM FOR ANALOG AND DIGITAL READOUT Patent
Ernest A. Dahl, inventor (to Navy) 15 Aug. 1989 6 p Filed 27 Jun. 1988 Supersedes US-Patent-Appl-SN-213032 (AD-D014297; US-Patent-4,857,894; US-Patent-Appl-SN-213032; US-Patent-Class-340-619) Avail: U.S. Patent and Trademark Office CSCL 14/2

An elongated level sensor system has an optical prism formation moulded or cut in a side, and includes a plurality of LED light sources and corresponding photo cells positioned along its length. Light from the LED sources are reflected off the prism surfaces to respective photocells when there is no liquid present in the area, thereby indicating no liquid media present. When liquid surrounds a particular section, light from the LED is not reflected from the prism surfaces, but is refracted out; the change in photocell voltage then indicates the presence of liquid storage areas, and read out simultaneously at a remote sensor/alarm panel. GRA

N90-16228# City Univ., London (England). Dept. of Electrical, Electronic and Information Engineering.
A SIMPLE FIBER OPTIC AUTOCORRELATION TACHOMETER
K. T. V. Grattan (Sira Inst. Ltd., Chislehurst, England), J. Jiwei, A. W. Palmer, and B. T. Meggitt 1987 8 p Submitted for publication
(ETN-90-96146) Avail: NTIS HC A02/MF A01

The principle of a simple and inexpensive optical fiber based correlation technique is demonstrated. It is to be applied for the monitoring of the slow rotation of a shaft of an electric motor. The use and possible extension of the techniques employed are discussed. To be an effective online measurement system, a high operational speed, achieved with more sophisticated and rapid analog/digital conversion and analysis, is required. Finer features of the shaft to be studied can be interrogated to give the autocorrelation pattern. ESA

N90-16229# Consiglio Nazionale delle Ricerche, Frascati (Italy). Ist. di Fisica dello Spazio Interplanetario.
TWO POSSIBLE CONFIGURATIONS FOR THE TOP-HAT ELECTROSTATIC ANALYZER: A NUMERICAL STUDY
M. B. Bavassano-Cattaneo, R. Bruno, and V. Formisano Nov. 1989 24 p
(IFSI-88-18; ETN-90-96157) Avail: NTIS HC A03/MF A01

Two possible configurations for an electrostatic analyzer are studied numerically. The aim is to compare, through the results of a three dimensional numerical simulation, the performances of the top hat electrostatic analyzer with a similar flat hat configuration. The configuration studied here differs, in the top hat version, from the standard top hat analyzer (classical top hat) for the presence of a grounded collimator. Both analyzers have a sharper energy resolution than the classical top hat in spite of a smaller geometric factor. The deflection ratio is comparable for the top hat and the flat hat. The sequence of histograms shown suggests that focussing is expected to occur at negative angles for the flat hat. ESA

N90-16230# Consiglio Nazionale delle Ricerche, Frascati (Italy). Ist. di Fisica dello Spazio Interplanetario.
CIS-2 ANALYZER DERIVATION OF HARDWARE PARAMETERS
V. Formisano, E. Amata, P. Baldetti, M. B. Bavassano, G. Bellucci, R. Bruno, M. Candidi, P. Cerulli-Irelli, G. Chionchio, and A. DiLellis et al Jun. 1989 25 p
(IFSI-89-13; ETN-90-96175) Avail: NTIS HC A03/MF A01

The intrinsic parameters defining the geometric factor of an electrostatic analyzer, named Cluster CIS-2, are discussed. The proposed values of the angular and energy resolutions are respectively 5.6 degrees and 0.08. The following observations are reviewed: solar wind and backstreaming ions, magnetosheath, plasma mantle, lobe, and plasma sheet boundary layer. The characteristic parameters of flown electrostatic analyzers are also reviewed. Concerning the proposed equipment, simulation studies on spherical and flat top geometries are suggested. ESA

N90-16231# Consiglio Nazionale delle Ricerche, Frascati (Italy). Ist. di Fisica dello Spazio Interplanetario.
THE VISIBLE CHANNEL OF OMEGA-VIMS
V. Formisano, G. Bellucci, G. Chionchio, A. Carusi, F. Capaccioni, A. Coradini, A. Adriani, M. Viterbini, R. Bathia, and F. Angrilli Aug. 1989 43 p Prepared in cooperation with Padua Univ., Italy
(IFSI-89-14; ETN-90-96176) Avail: NTIS HC A03/MF A01

OMEGA-VIMS (Observatoire pour la Mineralogie, l'Eau, les Glaces et l'Activite - Visual and Infrared Mapping Spectrometer) is an infrared spectrometer selected for the Soviet mission Mars 94. The instrumentation is designed to support remote sensing of planetary surfaces by an infrared multispectral imager. It provides recognition of planetary bodies in the spectral range 0.30 to 1.05 microns. The main purpose of a visible channel for OMEGA-VIMS is to extend the mapping capability towards short wavelengths and to help the identification on the surface of features mapped in the infrared range. One of the purposes of this work is to explore the possibility of including the present design of the visible channel on missions, in terms of scientific return and technical feasibility. The optical, mechanical, electronical designs, together with considerations on interfacing problems, are presented. ESA

N90-16232# Institut Franco-Allemand de Recherches, Saint-Louis (France).
MINIATURE LASER DOPPLER ANEMOMETER WITH A DIODE LASER [MINIATUR-LASER-DOPPLER-ANEMOMETER MIT HALBLEITERLASER]
S. Damp 19 Aug. 1988 11 p In GERMAN Presented at the 2nd Kongressmesse fuer Industrielle Messtechnik, Wiesbaden, Federal Rep. of Germany, 27-29 Sep. 1988
(ISL-CO-224/88; ETN-90-95032) Avail: NTIS HC A03/MF A01

A miniature laser Doppler anemometer, 11 cm by 4 cm by 4 cm in size, is described. It contains complete electronic circuitry needed to ensure correct functioning of the diode laser as well as preamplification of the signal from the receptor. Thanks to the beam trajectories, the set-up can be assembled from standard, low cost, optical components. The results of preliminary tests show that the setup works well. A sturdier version, and a system for measuring two components at once, are under study. ESA

N90-16233# Grenoble-1 Univ. (France). Lab. de Techniques de l'Informatique; Mathematiques; Microelectronique; Microscopie Quantitative.
REMOTE USE OF AN ELECTRON BEAM TESTER (EBT)
G. Baille, F. Conquet, B. Devautour, and T. Gouyon Oct. 1988 106 p In FRENCH; ENGLISH summary
(IMAG-RR-760-I; ETN-90-95694) Avail: NTIS HC A06/MF A01

The first remote use of the TIM3 experimental electron beam tester is described. Thanks to modern lines, it is possible to manage the TESSIE exerciser from any remote terminal. The test pattern memory can be loaded, dumped or modified. The output pattern memory (analysis) can be loaded with circuit truth tables or with the answers given by a golden chip, dumped in a file for future use. Other remote management possibilities are described. Future developments such as transmission of images, simulation and test tool techniques are outlined. ESA

N90-16234 Max-Planck-Inst. fuer Physik und Astrophysik, Garching (Germany, F.R.).
THE MPI/AIT X RAY IMAGER (MAXI): HIGH SPEED PN-CCD'S FOR X RAY DETECTION
L. Strueder, H. Braeuninger, M. Meier, P. Predehl, C. Reppin, M. Sterzik, J. Truemper, P. Cattaneo, D. Hauff, and G. Lutz (Max-Planck-Inst. fuer Physik und Astrophysik, Munich, Germany, F.R.) et al Jun. 1989 18 p Presented at the 5th European Symposium on Semiconductor Detectors, Munich, Federal Rep. of Germany,21-23 Feb. 1989 Submitted for publication Prepared in cooperation with Tuebingen Univ., Politecnico di Milano, Brookhave National Lab., Pavia Univ., Fraunhafer Inst. for Microelectronics, and Messerschmitt-Boelkow-Blohm GmbH
(MPE-Preprint-154; ISSN-0178-0719; ETN-90-95856) Copyright Avail: Fachinformationszentrum Karlsruhe, 7514 Eggenstein-Leopoldshafen 2, Federal Republic of Germany

The MPI/AIT X ray Imager (MAXI), part of a proposal submitted to ESA as focal plane instrumentation of the X ray Multi Mirror Mission (XMM) is presented. A fully depleted (sensitive) pn Charge Coupled Device (CCD) of 280 micrometers thickness with a homogenous sensitivity area of 36 square centimeters and a pixel size of 150 by 150 square micrometers, is proposed. This CCD is well matched with the telescope's angular resolution of 30 arc sec. X ray sensitivity and other performance characteristics of the telescope are outlined. Tests carried out on prototype components of the camera system are described. ESA

N90-16235# Institut National des Sciences Appliquees de Lyon, Villeurbanne (France). Lab. de Genie Electrique et Ferroelectricite.

MECHANOELECTRIC CONVERSION BY UNIAXIAL CONSTRAINT IN PIEZOELECTRIC GENERATORS: OPTIMIZATION OF ELECTRICAL, MECHANICAL, AND PHYSICO-CHEMICAL PARAMETERS OF MATERIALS Ph.D. Thesis [CONVERSION MECANOELECTRIQUE PAR CONTRAINTE UNIAXIALE DANS LES GENERATEURS PIEZOELECTRIQUES: OPTIMISATION DES PARAMETRES ELECTRIQUES, MECANIQUES ET PHYSICO-CHIMIQUES DES MATERIAUX]

Hagop Ohanessian 1989 382 p In FRENCH

(ISAL-89-0020; ETN-90-96038) Avail: NTIS HC A17/MF A03

Shock compression phenomena are analyzed in order to establish optimization criteria. Electrical and mechanical criteria are established for the experimental apparatus. The dielectric and piezoelectric properties of the materials used are studied. The characteristics of short term uniaxial compression are defined. Optimal utilization criteria for generators under capacitative, linear, and spark producing loads are established. Materials used are characterized and their piezoelectric properties are optimized. An optimal material for electrical generation under uniaxial compression is defined. ESA

N90-16236# Deutsche Gesellschaft fuer Luft- und Raumfahrt, Bonn (Germany, F.R.). Arbeitsgemeinschaft Stroemungen mit Ablosung.

TWO-DIMENSIONAL MEASURING TECHNIQUES [2D-MESSTECHNIK]

1988 271 p Partly in ENGLISH and GERMAN Workshop held in Markdorf, Fed. Republic of Germany, 18-19 Oct. 1988 Sponsored by BMFT, Bonn, Fed. Republic of Germany Original contains color illustrations

(DGLR-Papers-88-04; ISBN-3-922010-41-5; ETN-90-95007)

Avail: NTIS HC A12/MF A02

In the field of density and velocity field measurements, quantitative interferometry, phase-coupled diode arrays, non-enclosed liquid crystal tracers, laser Doppler scanning, and particle-image-velocimetry are discussed. In the field of flow visualization, the use of coded trajectories, (laser) light sheet methods, the smoke wire technique, digital image interpretation, sublimation methods, the film-of-oil technique, the crystal violet method, thermochromatic liquid crystals, shear stress sensitive liquid crystals, preheated liquid crystals, and infrared thermography are presented. In the field of wall sensor arrays, the determination of dynamic surface forces using piezoelectric arrays, and the determination of the unsteady pressure distribution at the surface of a gas turbine blade using piezofoil sensors are outlined. For individual titles, see N90-16237 through N90-16258.

N90-16237# Deutsche Gesellschaft fuer Luft- und Raumfahrt, Bonn (Germany, F.R.).

QUANTATIVE INTERFEROMETRY [QUANTITATIVE INTERFOMETRIE]

H.-H. Bartels, B. Bretthauer, G. E. A. Meier (Max-Planck-Inst. fuer Stroemungsforschung, Goettingen, Germany, F.R.), and R. Wenskus *In its* Two-Dimensional Measuring Techniques 1988 p 5-2 In GERMAN (For primary document see N90-16236 08-35)

Avail: NTIS HC A12/MF A02

Interferograms of classical and holographic interferometers were digitized using a TV camera with a view to computer evaluation. After an image preprocessing depending on the quality of the images, the shape of the interference stripes were extracted from the interferogram as closed traverses free of redundant points using a controlled threshold procedure. After the elimination of possible line interruptions of the closed traverses due to a lack of contrast or resolution, this representation was stored as a basis for the further processing of the interferograms. The amount of data can in this way be reduced to about 1/10 as compared to the original image. After an extensive automatic numbering of the interference stripes (closed traverses) the object functions can be represented quasi-three-dimensionally using polynomial approximations on a triangular raster through the closed traverse points. ESA

N90-16238# Physikalisch-Technische Bundesanstalt, Brunswick (Germany, F.R.).

HIGH FREQUENCY PULSED DIODE LASERS AND PHASE-COUPLED DIODE ARRAYS FOR AERODYNAMICS [HOCHFREQUENT GEPULSTE DIODENLASER UND PHASENGEKOPPELTE DIODENARRAYS FUER DIE AERODYNAMIK] **c36**

D. Dopheide, M. Faber, G. Reim, and H. Pfeifer (Institut Franco-Allemand de Recherches, Saint-Louis, France) *In* DGLR, Two-Dimensional Measuring Techniques 1988 p 25-30 In GERMAN (For primary document see N90-16236 08-35)

Avail: NTIS HC A12/MF A02

Novel Laser Doppler Anemometer (LDA) techniques suitable for wind tunnel research are presented. The advantages and disadvantages of miniature LDAs with diode lasers and avalanche diodes are reviewed. High power diode lasers with output powers up to 1000 mW are described. High frequency pulsed diode lasers with signal integrator and/or digital pulse analysis are introduced. Phase-coupled diode laser arrays for high speed measurements are presented. The possibilities of the techniques for laser Doppler applications are discussed. ESA

N90-16239# Max-Planck-Inst. fuer Stroemungsforschung, Goettingen (Germany, F.R.).

SIMULTANEOUS DETERMINATION OF TEMPERATURE AND VELOCITY FIELDS IN A THERMAL CONVECTION FLOW WITH NON-ENCLOSED LIQUID CRYSTAL TRACERS [SIMULTANE ERFASSUNG VON TEMPERATUR- UND GESCHWINDIGKEITSFELDERN IN EINER THERMISCHEN KONVEKTIONSSTROEMUNG MIT UNGEKAPSELTEN FLUESSIGKRISTALLTRACERN]

W. J. Hiller, St. Koch, and T. A. Kowalewski *In* DGLR, Two-Dimensional Measuring Techniques 1988 p 31-39 In GERMAN Original contains color illustrations (For primary document see N90-16236 08-35)

Avail: NTIS HC A12/MF A02

A measuring procedure is developed for the simultaneous visualization of velocity and temperature fields with a view to the investigation of a thermally driven convection flow in a cubical cell. The method is based on the fact that nonenclosed liquid crystal tracers, suspended in the flow medium, reflect white light wavelength selectively depending on their temperature. The measurement of the wavelength of the reflected light gives the temperature of the tracer, providing the temperature of the immediately surrounding medium. The measurement accuracy is 0.1 C. The application is limited to a very small number of fluids, due to the chemical instability of the tracer substances. The velocity is determined from the change of the spatial position of the tracer. ESA

N90-16240# Technische Hochschule, Aachen (Germany, F.R.). Stosswellenlabor.

CODED TRAJECTORIES FOR THE INVESTIGATION OF STRONGLY UNSTEADY FLOW FIELDS [KODIERTE BAHNSPUREN ZUR UNTERSUCHUNG STARK INSTATIONAERER STROEMUNGSFELDER] **c34**

W. Kerres and H. Groenig *In* DGLR, Two-Dimensional Measuring Techniques 1988 p 43-57 In GERMAN (For primary document see N90-16236 08-35)

Avail: NTIS HC A12/MF A02

Two-dimensional flow fields were quantitatively measured using coded trajectories of particles. The use of a special exposure pattern allows the determination of direction, velocity, and accelerations. Three-dimensional flow domains can be recognized from the incomplete pattern. This technique has a high time (1 ms) and spatial (3 to 5 mm) resolution. It is illustrated by the flow on a NACA 0012 profile with a 30 deg angle of attack. The flow velocity profiles demonstrate the possibility of the quantitative evaluation using the method of coded trajectories. ESA

N90-16241# Deutsche Forschungs- und Versuchsanstalt fuer Luft- und Raumfahrt, Berlin (Germany, F.R.). Abteilung Turbulenzforschung.

VISUALIZATION OF INSTABILITY FORMS OF A ROUND FREE JET USING A LIGHT SHEET METHOD [SICHTBARMACHUNG VON INSTABILITAETSFORMEN EINES RUNDEN FREISTRAHLS DURCH EINE LICHTSCHNITTMETHODE] **c34**

B. Lehmann and B. Barsikow *In* DGLR, Two-Dimensional Measuring Techniques 1988 p 59-66 In GERMAN (For primary document see N90-16236 08-35)

Avail: NTIS HC A12/MF A02

The instability behavior of a round thermal free jet was investigated using a laser light sheet method with a view to combustion engineering applications. A 4 W Ar laser was used for the light sheet, and SiC or tobacco smoke were used as optically scattering tracers. The laser beam is transformed into a light plane using a cylindrical lens. As in the case of cold free jets axisymmetric flow structures were found; they are however essentially stabilized with respect to the cold case due to the effect of the density gradients resulting from the temperature differences. Instability forms with azimuthally distributed structures were also observed; their development is coupled with the occurrence of the axisymmetric structures; they interfere locally with ring vortices which probably leads to jetlike eruptions as supported by model calculations. ESA

N90-16242# Siegen Univ., (Germany, F.R.). Inst. fuer Fluid- und Thermodynamik.

VISUALIZATION OF GAS FLOWS USING THE SMOKE WIRE TECHNIQUE [VISUALISIERUNG VON GASSTROEMUNGEN MIT DER RAUCHDRAHT-TECHNIK]

A. Leder and D. Geropp *In* DGLR, Two-Dimensional Measuring Techniques 1988 p 67-78 In GERMAN Original contains color illustrations (For primary document see N90-16236 08-35)

Avail: NTIS HC A12/MF A02

The optimization of flow visualization using the smoke wire technique is investigated. This technique is especially suitable for visualization flow structures in the low velocity range. The principles of the smoke wire technique are described, and the manifold possibilities for the visualization of complex flow fields are elucidated. In particular, this technique allows color differentiation between flow regions and the easy adaptation of the smoke injection of the model geometry. Curved flow surfaces can be visualized. ESA

N90-16243# Deutsche Forschungs- und Versuchsanstalt fuer Luft- und Raumfahrt, Goettingen (Germany, F.R.). Inst. fuer Experimentelle Stroemungsmechanik.

FLOW FIELD VISUALIZATION USING LASER LIGHT SHEET METHODS. QUANTITATIVE ANALYSIS USING IMAGE PROCESSING [STROEMUNGSFELDSICHTBARMACHUNG MITTELS LASER-LICHTSCHNITTVERFAHREN. QUANTITATIVE ANALYSE DURCH EINSATZ DER BILDVERARBEITUNG] **c36**

Sabine Foerster and Juergen Kompenhans *In* DGLR, Two-Dimensional Measuring Techniques 1988 p 79-91 In GERMAN (For primary document see N90-16236 08-35)

Avail: NTIS HC A12/MF A02

Application and evaluation possibilities of the laser light sheet method and the applied image processing system are discussed. The laser beam is transferred into a light plane using a cylindrical lens. Laser light sheet technique and image analysis allows relatively simple, statements concerning flow structures and their spatial changes in the form of vortex trajectories. Such results are suitable for verification of theoretical considerations and to be taken into account in calculation methods. ESA

N90-16244# Karlsruhe Univ. (Germany, F.R.). Inst. fuer Stroemungslehre und Stroemungsmaschinen.

DIGITAL IMAGE INTERPRETATION FOR OPTICAL FLOW MEASUREMENT METHODS: SYSTEM DESCRIPTION AND PRELIMINARY APPLICATION EXAMPLES [DIGITALE BILDAUSWERTUNG FUER OPTISCHE STROEMUNGSMESSVERFAHREN: SYSTEMBESCHREIBUNG UND ERSTE ANWENDUNGSBEISPIELE] **c34**

G. Schnerr *In* DGLR, Two-Dimensional Measuring Techniques 1988 p 93-104 In GERMAN (For primary document see N90-16236 08-35)

(Contract DFG-Zi/18-31-1)

Avail: NTIS HC A12/MF A02

A system for the digital acquisition and processing of flow images, obtained by Schlieren and interference methods, is presented. All the hardware components are selected, taking into account the special requirements. The complete pictures can be stored with a maximum video frequency of 25 Hz. Short illumination times of pictures were realized via hardware and software control. The evaluation of Mach-Zehnder interferograms is described. A method for the quantitative determination of condensation fronts in Schlieren pictures of transonic flows is presented. This method is suitable for the localization of compression and expansion fronts in compressible flows. The advantages of this technique are fast qualitative and quantitative experimental information and substantially improved resolution and reproducibility. Substantial investments are shown to be required. ESA

N90-16245# Duits-Nederlandse Windtunnel, North East Polder (Netherlands).

THE DETERMINATION OF VORTEX SEPARATION FREQUENCIES BY MEANS OF LASER LIGHT SHEET IMAGES **c34**

K. Pengel *In* DGLR, Two-Dimensional Measuring Techniques 1988 p 105-110 (For primary document see N90-16236 08-35)

(DNW-WTI-88.038) Avail: NTIS HC A12/MF A02

The laser light sheet method is used for the investigation of the flow around wind tunnel models. Rotating mirrors are used to generate the light sheet from the laser beam. Extremely short exposure times of the smoke particles can be realized. A 30 Hz beam sweeping frequency leads to an illumination time of 1 micron for each particle which is at a distance of 3 m from the mirror. Instantaneous images of a periodically changing flow are obtained, and recorded with a video system. Strouhal numbers are determined from the video signals. The example of the wake vortices of an outdoor mirror is presented. The frequency of the noise generated by this mirror was derived from flow visualization pictures. ESA

N90-16246# Volkswagen A.G., Wolfsburg (Germany, F.R.). Forschung Messtechnik.

FLOW VISUALIZATION USING THE LASER LIGHT SHEET METHOD IN VEHICLE AERODYNAMICS AND COMBUSTION CHAMBER ENGINEERING [STROEMUNGSSICHTBARMACHUNG MIT DEM LASER-LICHTSCHNITT-VERFAHREN IN DER FAHRZEUGAERODYNAMIK UND DER BRENNRAUMMESSTECHNIK] **c36**

Werner Hentschel *In* DGLR, Two-Dimensional Measuring Techniques 1988 p 111-119 In GERMAN (For primary document see N90-16236 08-35)

Avail: NTIS HC A12/MF A02

Laser light sheet flow visualization is applied in the automobile industry with a view to the reduction of air resistance. Using high power lasers a plane is cut out of the 3-D flow field and the course of flow in the plane is analyzed. In vehicle aerodynamics the flow phenomena are mainly visualized with smoke in the tail region of automobiles and in the wake, in planes parallel as well as perpendicular to the flow direction. For the investigation of flow phenomena in the combustion chamber of Otto and Diesel engines, the laser light sheet method is used on a series motor

with optical access, the so-called flow motor. Typical results and requirements for future automated evaluation methods are discussed. ESA

N90-16247# Technische Hochschule, Darmstadt (Germany, F.R.). Fachgebiet Aerodynamik und Messtechnik.
ANALYSIS OF THE MEASURING RANGE AND THE ACCURACY OF AN EXISTING PARTICLE IMAGE VELOCIMETRY SYSTEM [ANALYSE DES MESSBEREICHS UND DER GENAUIGKEIT EINES BESTEHENDEN PARTICLE-IMAGE-VELOCIMETRY-SYSTEMS]
A. Bloch and P. Heller *In* DGLR, Two-Dimensional Measuring Techniques 1988 p 121-133 In GERMAN (For primary document see N90-16236 08-35)
Avail: NTIS HC A12/MF A02

The measuring range and the systematic and random measuring errors of a Particle Image Velocimetry (PIV) method with digital image processing system, allowing a fully automatic data acquisition, are studied. The analyzed PIV system is briefly described. The PIV method allows a quantitative flow visualization in a 2-D flow plane. It combines the advantages of an instantaneous flow field observation and a flow velocity determination, and allows the analysis of complex flow fields. The possible sources of errors are listed and their order of magnitude is estimated. The magnitude of the maximum possible global error is empirically determined. ESA

N90-16248# Deutsche Forschungs- und Versuchsanstalt fuer Luft- und Raumfahrt, Goettingen (Germany, F.R.). Inst. fuer Experimentelle Stroemungsmechanik.
FURTHER DEVELOPMENT OF THE PIV METHOD FOR USE IN THE LARGE WIND TUNNEL [WEITERENTWICKLUNG DER PIV-METHODE IM HINBLICK AUF DEN EINSATZ IM GROSSEN WINDKANAL]
Rainer Hoecker and Juergen Kompenhans *In* DGLR, Two-Dimensional Measuring Techniques 1988 p 135-144 In GERMAN (For primary document see N90-16236 08-35)
Avail: NTIS HC A12/MF A02

The PIV (particle image velocimetry) method for the instantaneous determination of magnitude and direction of the flow velocimetry in a 2-D field is further developed for application in a wind tunnel. The separation of measurement and evaluation shortens the measuring times in the wind tunnel. At the side of the recording techniques, a fast distance focusing, a control of the particle density, and a runoff control for the laser flash lamps are realized. Besides data evaluation, a brightness control, a direct observation, and a direct evaluation are realized. Some experimental examples are presented. ESA

N90-16249# Technische Univ., Berlin (Germany, F.R.). Inst. fuer Luft- und Raumfahrt.
DETERMINATION OF DYNAMIC SURFACE FORCES USING PIEZOELECTRIC ARRAYS [ERFASSUNG DYNAMISCHER OBERFLAECHENKRAEFTE MIT PIEZO-ARRAYS]
W. Nitsche and P. Mirow *In* DGLR, Two-Dimensional Measuring Techniques 1988 p 145-156 In GERMAN (For primary document see N90-16236 08-35)
Avail: NTIS HC A12/MF A02

The experimental determination of static and dynamic surface forces on flow bodies using piezoelectric arrays is outlined. The fundamentals of the piezo-array sensor technique (sensor construction, signal separation, and signal transmission) are presented. Practical applications of piezo-arrays in the fields of airfoil aerodynamics and general flow investigations are explained. The obtained measuring results are purely qualitative. ESA

N90-16250# Karlsruhe Univ. (Germany, F.R.). Lehrstuhl fuer Thermische Stroemungsmaschinen.
THE USE OF PIEZOFOIL SENSORS FOR THE DETERMINATION OF THE UNSTEADY PRESSURE DISTRIBUTION AT THE SURFACE OF A GAS TURBINE BLADE [EINSATZ VON PIEZOFOLIEN-SENSOREN ZUR BESTIMMUNG DER INSTATIONAEREN DRUCKVERTEILUNG AN DER OBERFLAECHE EINER GASTURBINENSCHAUFEL]
K. Dullenkopf and J. Lauber *In* DGLR, Two-Dimensional Measuring Techniques 1988 p 157-168 In GERMAN (For primary document see N90-16236 08-35)
Avail: NTIS HC A12/MF A02

The use of piezoelectric sensors made of Polyvinylidenefluoride (PVDF) in flow measurement techniques is outlined. The main advantage of the foil is the possibility of adherence to any body without a change of structure and offers in many cases new and interesting aspects. Qualitative statements can be obtained in a relatively simple way. A quantitative analysis of the sensor signals requires some effort as well as careful testing. The further processing of the sensor signals using digital signal analysis provides many possibilities of qualitative and quantitative evaluation. ESA

N90-16251# Messerschmitt-Boelkow-Blohm G.m.b.H., Bremen (Germany, F.R.). Transport- und Verkehrsflugzeuge.
THE USE OF SUBLIMATION METHODS FOR THE RECOGNITION OF TRANSITION AT LOW SPEED [UEBER DEN EINSATZ VON SUBLIMATIONSVERFAHREN ZUR TRANSITIONS- ERKENNUNG IM LOW SPEED]
R. Henke *In* DGLR, Two-Dimensional Measuring Techniques 1988 p 169-187 In GERMAN (For primary document see N90-16236 08-35)
Avail: NTIS HC A12/MF A02

Sublimation methods are used for the recognition of laminar turbulent transition on VFW-614 profile as well as in a free jet in the MBB low speed wind tunnel, with view to the elucidation of the effect of several perturbing bodies on the transition. The sublimation method chosen is the naphthalene method, and the infrared method is used to explain the resulting additional roughness. The experiments show that the naphthalene film strongly affects the transition position. Both methods revealed effects, such as the presence of water droplets, which can lead to wrong interpretations. ESA

N90-16252# Deutsche Forschungs- und Versuchsanstalt fuer Luft- und Raumfahrt, Brunswick (Germany, F.R.). Hauptabteilung Windkanaele.
USE OF THE FILM-OF-OIL TECHNIQUE FOR PROFILE MEASUREMENTS IN THE TRANSONIC WIND TUNNEL BRUNSWICK (TWB) [EINSATZ DER OELANSTRICHTECHNIK BEI PROFILMESSUNGEN IM TRANSSONISCHEN WINDKANAL BRAUNSCHWEIG (TWB)] **c02**
W. Puffert-Meissner *In* DGLR, Two-Dimensional Measuring Techniques 1988 p 189-199 In GERMAN (For primary document see N90-16236 08-35)
Avail: NTIS HC A12/MF A02

The film-of-oil technique is applied in the TWB to support and interpret pressure distribution measurements on profiles in difficult flow conditions as well as for the investigation of sidewall effects on the profile flow. The film consists of silicone oil and colored powder; the mixture depends on the conditions. A video camera records the evolution of the film during the tests. The picture clearly shows the type and strength of the sidewall effect with increasing Mach number and angle of attack. The use of the film-of-oil technique as an interpretation aid for measured pressure distributions is demonstrated on a helicopter rotor blade. Infrared pictures show that the technique has its limitations in the determination of the laminar turbulent boundary layer transition since the film affects the boundary layer condition. ESA

N90-16253# Erlangen-Nuremberg Univ. (Germany, F.R.). Lehrstuhl fuer Stroemungsmechanik.
FLOW VISUALIZATION OF WATER FLOWS USING THE CRYSTAL VIOLET METHOD [STROEMUNGSSICHTBARMACHUNG VON WASSERSTROEMUNGEN MIT HILFE DES KRISTALLVIOLETTVERFAHRENS] **c34**
G. Dimaczek, C. Eh, and C. Tropea *In* DGLR, Two-Dimensional Measuring Techniques 1988 p 201-210 In GERMAN (For primary document see N90-16236 08-35)
Avail: NTIS HC A12/MF A02

A method for the visualization of water flows using the indicator colorant crystal violet is developed. The colorant is coated on thin carrier material. The indicator sheet is glued onto the surface to be investigated. The colorant diffuses from the carrier material and is transported in the flow direction by convective transport. A picture of the flow structures in the neighborhood of the wall is taken. The method allows a quick, qualitative 2-D representation of these water flow structures, even at optically inaccessible locations. ESA

N90-16254# Karlsruhe Univ. (Germany, F.R.). Lehrstuhl fuer Thermische Stroemungsmaschinen.
UNSTEADY HEAT TRANSFER MEASUREMENT USING THERMOCHROMATIC LIQUID CRYSTALS AS TEMPERATURE INDICATORS [INSTATIONAERE WAERMEUEBERGANGSMESSUNG UNTER NUTZUNG VON THERMOCHROMEN FLUESSIGKRISTALLEN ALS TEMPERATURINDIKATOREN]
C. Hirsch, K.-H. Platzer, D. E. Metzger (Arizona State Univ., Tempe.), and S. Wittig *In* DGLR, Two-Dimensional Measuring Techniques 1988 p 211-221 In GERMAN Sponsored in part by the Alexander von Humboldt Foundation (For primary document see N90-16236 08-35)
Avail: NTIS HC A12/MF A02

A measuring system for the two-dimensional, unsteady measurement of heat transfer in gas turbines, based on the so called thick wall technique, is developed. The temperature sensors are thermochromatic liquid crystals, which are optically indicated using computer assisted image processing in real time. The automatic color recognition allows the measurement of spatial distributions of heat transfer coefficients on complex geometries with simple apparatus. Preliminary results of measurements on a covered, rotating disk, agree well with data in the literature. ESA

N90-16255# Duits-Nederlandse Windtunnel, North East Polder (Netherlands).
SURFACE FLOW VISUALIZATION WITH SHEAR STRESS SENSITIVIVE LIQUID CRYSTALS **c34**
K. Pengel *In* DGLR, Two-Dimensional Measuring Techniques 1988 p 223-232 Original contains color illustrations (For primary document see N90-16236 08-35)
(DNW-WTI-88.039) Avail: NTIS HC A12/MF A02

The use of non-capsulated liquid crystals, which react directly to wall shear forces, for surface flow visualization, is presented. The temperature sensitivity is avoided by producing a mixture with an event temperature (first red indication temperature) above the expected investigation temperature range. Below the event temperature the liquid crystals are only sensitive to shear stress, resulting in a wavelength variation of the reflected light. The analysis of video pictures from a low speed wind tunnel lead to information about the wall shear stress distribution on an Airbus wing, and in particular about the detection of the laminar to turbulent boundary layer transition. ESA

N90-16256# Deutsche Forschungs- und Versuchsanstalt fuer Luft- und Raumfahrt, Goettingen (Germany, F.R.). Inst. fuer Experimentelle Stroemungsmechanik.
QUANTITATIVE HEAT TRANSFER MEASUREMENTS USING HEATED LIQUID CRYSTALS [QUANTITATIVE WAERMEUEBERGANGSMESSUNGEN MIT GEHEIZTEN FLUESSIGKRISTALLEN]
Karl-Aloys Buetefisch and Horst Ahlbrecht *In* DGLR, Two-Dimensional Measuring Techniques 1988 p 233-244 In GERMAN (For primary document see N90-16236 08-35)
Avail: NTIS HC A12/MF A02

Quantitative heat transfer measurements are performed on models in wind tunnels using preheated liquid crystals. In order to avoid the disadvantage of liquid crystals the choice of which imposes a temperature range, they are electrically preheated to a temperature above that expected during the tests, and then cooled by the flow along the model. This method allows the stationary determination of the temperature distribution at the surface of models. Measurements at a flat plate for the cases of a laminar and a turbulent boundary layer give heat transfer coefficients that agree well with theoretical expectations. ESA

N90-16257# Karlsruhe Univ. (Germany, F.R.). Lehrstuhl fuer Thermische Stroemungsmaschinen.
DETERMINATION OF THE HEAT TRANSFER COEFFICIENTS IN SEPARATED FLOWS USING AN INFRARED CAMERA [BESTIMMUNG DER WAERMEUEBERGANGSZAHLEN IN ABGELOESTEN STROEMUNGEN MIT HILFE EINER INFRAROTKAMERA]
V. Scherer, A. Pfeiffer, and S. Wittig *In* DGLR, Two-Dimensional Measuring Techniques 1988 p 245-253 In GERMAN (For primary document see N90-16236 08-35)
Avail: NTIS HC A12/MF A02

A method for a fast and contactless measurement of wall temperatures using an IR thermocamera is presented, with a view to the determination of local heat transfer coefficients on bodies in a flow. The method is based on the boundary condition of constant heat flow. The data evaluation is simple, since for constant heat flow the surface temperature is a direct measure for the heat transfer coefficients. A further advantage is that the time and cost intensive instrumentation and calibration of thermoelements can be avoided. The method provides a detailed, two-dimensional picture of the heat transfer. ESA

N90-16258# Deutsche Forschungs- und Versuchsanstalt fuer Luft- und Raumfahrt, Porz (Germany, F.R.). Hauptabteilung Windkanaele.
INVESTIGATION OF ABLATION PHENOMENA USING IR THERMOGRAPHY IN A HYPERSONIC WIND TUNNEL [UNTERSUCHUNG VON ABLATIONSVORGAENGEN MITTELS DER IR-THERMOGRAPHIE IN EINEM HYPERSCHALL WINDKANAL]
A. Henckels and F. Mauer *In* DGLR, Two-Dimensional Measuring Techniques 1988 p 255-264 In GERMAN (For primary document see N90-16236 08-35)
Avail: NTIS HC A12/MF A02

In a series of tests in a hypersonic wind tunnel the heat resistance of an insulating material is investigated using an IR camera and modern image processing techniques. Samples are mounted in the surface of a flat plate model in a tangential flow. The evolution of the temperature distribution is observed by the IR camera, enabling monitoring of the formation of regions of enhanced heat transfer due to forced turbulence and cellular ablation structures. The image processing allows the calculation of the heat flow at arbitrary locations of the surface. ESA

N90-16259# Oak Ridge National Lab., TN. Instrumentation and Controls Div.
MODELING A SELF-CALIBRATING THERMOCOUPLE FOR USE IN A SMART TEMPERATURE MEASUREMENT SYSTEM
F. R. Ruppel 1989 7 p Presented at the IEEE Instrumentation and Measurement Technology, San Jose, CA, 13-15 Feb. 1990
(Contract DE-AC05-84OR-21400)
(DE90-003697; CONF-900228-1) Avail: NTIS HC A02/MF A01

A smart temperature measurement system was developed that consists of a commercially available self-calibrating thermocouple connected to a data-acquisition system with a specially designed algorithm capable of automatically detecting the calibration temperature of the self-calibrating thermocouple. The self-calibrating thermocouple has a high-purity, low melting point metal encapsulated near its thermojunction. The

time-temperature record of the thermocouple forms a plateau at the phase transition temperature of the encapsulated metal, providing a single-point calibration. Since the plateau is usually not horizontal, a major effort of the work reported here was to determine which point of the phase transition plateau is the actual phase transition temperature. A finite difference computer simulation program was written to explain the thermodynamic behavior of the system. Based on a literature review and simulation analysis, a method was developed to recognize which point on the melting or freezing plateau curve is the actual phase transition temperature of the encapsulated metal. The known phase transition temperature is compared to the reported melting or freezing point of the encapsulated metal to determine the magnitude of error in the thermocouple output. DOE

N90-16260# Los Alamos National Lab., NM.
END-ON SOFT X RAY IMAGING OF FIELD-REVERSED CONFIGURATIONS (FRCS) ON THE FIELD-REVERSAL-C (FRX-C)/LARGE SCALE MODIFICATION (LSM) EXPERIMENT
D. P. Taggart, R. J. Gribble, A. D. Bailey, III, and S. Sugimoto (Osaka Univ., Japan) 1989 7 p Presented at the 11th US/Japan Workshop on Field-Reversed Configurations and Compact Toroids, Los Alamos, NM, 7-9 Nov. 1989
(Contract W-7405-eng-36)
(DE90-004863; LA-UR-89-4237; CONF-8911130-9) Avail: NTIS HC A02/MF A01

Recently, a prototype soft x ray pinhole camera was fielded on FRX-C/LSM at Los Alamos and TRX at Spectra Technology. The soft x ray FRC images obtained using this camera stand out in high contrast to their surroundings. It was particularly useful for studying the FRC during and shortly after formation when, at certain operating conditions, flute-like structures at the edge and internal structures of the FRC were observed which other diagnostics could not resolve. Building on this early experience, a new soft x ray pinhole camera was installed on FRX-C/LSM, which permits more rapid data acquisition and briefer exposures. It will be used to continue studying FRC formation and to look for internal structure later in time which could be a signature of instability. The initial operation of this camera is summarized. DOE

N90-16700*# Pennsylvania State Univ., Erie. Dept. of Mechanical Engineering.
LOW FLOW VORTEX SHEDDING FLOWMETER
Charles J. Waugaman *In* University of Central Florida, NASA/ASEE Summer Faculty Fellowship Program Oct. 1989 p 324-357 (For primary document see N90-16686 08-99)
Avail: NTIS HC A18/MF A03 CSCL 14B

36 LASERS AND MASERS

Includes parametric amplifiers.
For related information see also *76 Solid-State Physics.*

N90-16261# National Oceanic and Atmospheric Administration, Boulder, CO. Wave Propagation Lab.
STATISTICS OF A REFLECTED LASER BEAM IN THE TURBULENT ATMOSPHERE (PATH CORRELATION)
James H. Churnside and Richard J. Lataitis Sep. 1989 93 p
(PB90-113994; NOAA-TM-ERL-WPL-172) Avail: NTIS HC A05/MF A01 CSCL 20E

The statistics of the angle of arrival and of the irradiance of a reflected laser beam in the turbulent atmosphere are calculated. The angle-of-arrival fluctuations of a reflected beam depend strongly on the reflector characteristics; convex surfaces produce smaller fluctuations than concave surfaces do. The irradiance fluctuations on a path folded by a large reflector are generally larger than those that would be observed on a single path of the same total length. GRA

N90-16262# Brookhaven National Lab., Upton, NY.
PROPOSAL FOR A STUDY OF LASER ACCELERATION OF ELECTRONS USING MICROGRATING STRUCTURES AT ATF
W. Chen, J. Claus, R. C. Fernow, J. Fischer, J. C. Gallardo, H. G. Kirk, H. Kramer, Z. Li, R. B. Palmer, and J. Rogers et al 29 Oct. 1989 24 p Prepared in cooperation with Los Alamos National Lab., NM, Princeton Univ., NJ, and California Univ., Los Angeles
(Contract DE-AC02-76CH-00016)
(DE90-003699; BNL-43465) Avail: NTIS HC A03/MF A01

A new method of particle acceleration was investigated by using a short-pulse CO2 laser as the power source and grating-like structures as accelerator cavities. Phase 1 of this program is intended to demonstrate the principle of the method. The laser light is focused to a 3 mm line on the surface of the microstructure. The structure is used to transform the electric field pattern of the incoming transversely polarized laser beam to a mode which has a component along the electron beam direction in the vicinity of the surface. With 6 mJ of laser energy and a 6 ps pulse length, the electric field in the spot will be around 1 GV/m. The electron beam from the Brookhaven Accelerator Test Facility (ATF) will be focused transversely within the few micron transverse dimension of the microstructure. The maximum expected acceleration for a 1 GV/m field and a 3 mm acceleration length is 3 MeV. DOE

N90-16263# Department of the Air Force, Washington, DC.
DIFFRACTION LIMITED DICHROIC COMBINER DIODE LASER Patent
William L. Casey, inventor (to AF) 18 Apr. 1989 10 p Filed 10 Nov. 1986 Supersedes US-Patent-Appl-SN-928356
(AD-D014291; US-Patent-4,823,357; US-Patent-Appl-SN-928356)
Avail: US Patent and Trademark Office CSCL 09/3

A laser transmitter is disclosed in which the laser combines the outputs of numerous laser diodes using dichroic combination to produce a high power, diffraction limited beam which may be transmitted at minimum beam divergence using the full aperture of the transmitter telescope. The individual diode beams are combined and superimposed in the laser, and are transmitted superimposed in the near and far field of the transmitter telescope. The dichroic combining process is as follows. A collimate beam of a first wavelength is directed at a narrowband or long wave pass filter which is tilted slightly (about 10 degrees). This beam passes through the filter. A beam of a second wavelength is directed toward the exist side of the filter (which acts as a mirror) at such an angle that the second beam is reflected colinear with the first beam and superimposed on it. This process of superimposing the laser beams continues as each laser beam from the laser diodes is added to form a combined laser beam. GRA

N90-16264# Sira Inst. Ltd., Chislehurst (England).
DISTANCE MEASUREMENT USING LASER DIODES
B. T. Meggitt and A. W. Palmer (City Univ., London, England) 1989 8 p Presented at Poster Session FOS, Olympia, Greece, 26 Apr. 1989
(ETN-90-96144) Avail: NTIS HC A02/MF A01

The techniques for accurate distance measurement using laser diodes are discussed. The time of flight measurement, the laser diode intensity modulation and the interferometric ranging are described. The multisource heterodyne and the heterodyne frequency modulated continuous wave interferometries are included. The scheme presented shows high resolution and simplified optical configuration. The development of external cavity laser diodes with frequency sweeps in excess of 60 GHz offers a possibility of resolutions down to submicrons. ESA

N90-16265# Max-Planck-Inst. fuer Meteorologie, Hamburg (Germany, F.R.).
BACKSCATTERING EFFECTS IN DIAL DUE TO WATER VAPOR Thesis - Hamburg Univ. [BODENGEBUNDENE DIAL-WASSERDAMPFMESSUNG: BERUECKSICHTIGUNG DER DOPPLERVERBREITERUNG DER LASERLINIE DURCH RAYLEIGHRUECKSTREUUNG]
Albert Ansmann 1989 89 p In GERMAN; ENGLISH summary
Original contains color illustrations
(Contracts BMFT-KF-10056; BMFT-KF-10110)

(Ser-Wiss-Abhandl-89; ETN-90-95350) Avail: NTIS HC A05/MF A01; G.M.L. Wittenborne Soehne, 2000 Hamburg 13, Federal Republic of Germany, 28 deutsche marks

Doppler broadening of a backscattered laser line and the consideration of this effect in the evaluation of a ground based H2O measurement using the Differential Absorption Lidar (DIAL) technique are described. Results are obtained by error analysis. Correction of the Doppler broadening effect is not necessary, when Rayleigh backscattering is negligible. In cases where Rayleigh backscattering is not negligible, but particle backscattering is relatively homogeneous, uncertainties in the input parameters used in the retrieval must be expected. Care has to be taken in the analysis of H2O DIAL measurements when layers with steep gradients of particle backscatter are present. ESA

N90-16266# Hamburg Univ. (Germany, F.R.). Inst. fuer Angewandte Physik.

EUROLASER DEFINITION PHASE, SOLID STATE LASERS WORKING GROUP: ACTIVE MEDIUM, LASER ACTIVE CRYSTALS Final Report, 31 Dec. 1987

Guenter Huber and Klaus Peterman 17 Jul. 1987 15 p In GERMAN; ENGLISH summary

(Contract BMFT-13-EU-00214)

(ETN-90-95899) Avail: NTIS HC A03/MF A01

A comparison of the most important aspects and parameters of materials to be used in the EURECA solid state laser project is presented. Garnets, alexandrite, sapphire fluorides and glasses are evaluated for their potential usefulness. The materials Nd:YAG, Nd:GSGG, Nd:Glass, and alexandrite are selected for the initial phase of EURECA. Materials to be used in the second phase are presented. ESA

N90-16267# Max-Planck-Inst. fuer Stroemungsforschung, Goettingen (Germany, F.R.).

SHOCK THICKNESS MEASUREMENTS WITH LASER BEAMS Thesis

M. Herrmann Apr. 1989 60 p In GERMAN; ENGLISH summary

(MPIS-7/1989; ISSN-0436-1199; ETN-90-96055) Avail: NTIS HC A04/MF A01

Measurements of shock thicknesses in argon, nitrogen and PP1 (Perfluoro n-hexan, C6F14) are presented. The reflective coefficient of a laser beam on the shock front is measured. To determine the shock thickness, a one-parameter model for the shock front structure is assumed. The parameter, shock thickness, is then calculated from the measured reflectivity. In PP1 the measurements reveal a dependence of shock thickness on density which is not accounted for by normalization with the mean free path ahead of the shock, and an unexpected dependence on Mach number. Ways of qualitatively describing these results are presented. ESA

N90-16268# Battelle Inst., Frankfurt am Main (Germany, F.R.).

EUROLASER DEFINITION PHASE: A COMPARISON OF HIGH POWER LASERS AVAILABLE [DEFINITIONSPHASE: FESTKOERPERLASER, ARBEITSPAKET GESAMTSYSTEM: ANALYSE DER TECHNIK. BAND 2: DATENBLAETTER FUER KOMMERZIELLE FESTKOERPER-HOCHLEISTUNGSLASER]

1 Mar. 1989 24 p Partly in ENGLISH and GERMAN

(Contract BMFT-FKZ-13-EU-00018/2)

(ETN-90-96061) Avail: NTIS HC A03/MF A01

The technical and performance data for commercially available high power Nd:YAG lasers is presented. Twenty one different lasers are presented. For each laser, the pulse width, pulse energy, beam quality, beam mode and all other pertinent technical data are presented in tabular form. The price of each laser and the length of the warranty are listed. Thirteen of the lasers are pulsed, the remaining eight are continuous wave lasers. ESA

N90-16238# Physikalisch-Technische Bundesanstalt, Brunswick (Germany, F.R.).

HIGH FREQUENCY PULSED DIODE LASERS AND PHASE-COUPLED DIODE ARRAYS FOR AERODYNAMICS [HOCHFREQUENT GEPULSTE DIODENLASER UND PHASENGEKOPPELTE DIODENARRAYS FUER DIE AERODYNAMIK]

D. Dopheide, M. Faber, G. Reim, and H. Pfeifer (Institut Franco-Allemand de Recherches, Saint-Louis, France) *In* DGLR, Two-Dimensional Measuring Techniques 1988 p 25-30 In GERMAN (For primary document see N90-16236 08-35)

Avail: NTIS HC A12/MF A02

N90-16243# Deutsche Forschungs- und Versuchsanstalt fuer Luft- und Raumfahrt, Goettingen (Germany, F.R.). Inst. fuer Experimentelle Stroemungsmechanik.

FLOW FIELD VISUALIZATION USING LASER LIGHT SHEET METHODS. QUANTITATIVE ANALYSIS USING IMAGE PROCESSING [STROEMUNGSFELDSICHTBARMACHUNG MITTELS LASER-LICHTSCHNITTVERFAHREN. QUANTITATIVE ANALYSE DURCH EINSATZ DER BILDVERARBEITUNG]

Sabine Foerster and Juergen Kompenhans *In* DGLR, Two-Dimensional Measuring Techniques 1988 p 79-91 In GERMAN (For primary document see N90-16236 08-35)

Avail: NTIS HC A12/MF A02

N90-16246# Volkswagen A.G., Wolfsburg (Germany, F.R.). Forschung Messtechnik.

FLOW VISUALIZATION USING THE LASER LIGHT SHEET METHOD IN VEHICLE AERODYNAMICS AND COMBUSTION CHAMBER ENGINEERING [STROEMUNGSSICHTBARMACHUNG MIT DEM LASER-LICHTSCHNITT-VERFAHREN IN DER FAHRZEUGAERODYNAMIK UND DER BRENNRAUMMESSTECHNIK]

Werner Hentschel *In* DGLR, Two-Dimensional Measuring Techniques 1988 p 111-119 In GERMAN (For primary document see N90-16236 08-35)

Avail: NTIS HC A12/MF A02

37 MECHANICAL ENGINEERING

Includes auxiliary systems (nonpower); machine elements and processes; and mechanical equipment.

N90-16269# Edgerton, Germeshausen and Grier, Inc., Idaho Falls, ID.

NATIONAL PROGRAM PLAN FOR ELECTRIC VEHICLE BATTERY RESEARCH AND DEVELOPMENT: TECHNICAL PLAN

G. L. Henriksen, David L. Douglas, and C. J. Warde (Warde Associates, Inc., Greensboro, NC.) Aug. 1989 70 p

(Contract DE-AC07-76ID-01570)

(DE90-002023; DOE/ID-10219) Avail: NTIS HC A04/MF A01

Electric vehicles (EVs) offer the prospect of reducing U.S. petroleum fuel usage and air pollution in major metropolitan areas. In 1987, DOE-EHP commissioned a two-phase study at INEL to produce a national plan for R and D on battery technology -- the limiting component in EVs. The battery assessment phase identified the most-promising technologies from a comprehensive list of viable EV batteries. This multi-year R and D program plan identifies development schedules, milestones, and tasks directed at resolving the critical technical and economic issues for the most-promising developmental batteries: bipolar lead/acid, flow-through lead/acid, iron/air, lithium/iron sulfide, nickel/iron, sodium/metal chloride, sodium/sulfur, zinc/air, and zinc/bromine. DOE

N90-16270# Edgerton, Germeshausen and Grier, Inc., Idaho Falls, ID.

AN APPROACH FOR TESTING FUEL-CELL/BATTERY HYBRID POWER SOURCES FOR BUS APPLICATIONS

25 May 1989 48 p Prepared in cooperation with U.S. Fuel

Cells, Inc.
(Contract DE-AC07-76ID-01570)
(DE90-002090; EGG-EP-8581) Avail: NTIS HC A03/MF A01

The principal objectives of this report are to describe an approach and outline general procedures for safe operation and testing of fuel cell/battery hybrid power sources, to discuss likely criteria for evaluating the system performance and relative merits of such power sources in a transportation application, and to describe the expected configuration and operation of the specific power systems now under development for the Department of Energy (DOE) sponsored transit bus program. DOE

N90-16271# Edgerton, Germeshausen and Grier, Inc., Idaho Falls, ID.
ELECTRIC AND HYBRID VEHICLES: TECHNICAL BACKGROUND REPORT FOR THE DOE FLEXIBLE AND ALTERNATIVE FUELS STUDY
William Hamilton (Hamilton, William, Santa Barbara, CA) 21 Jul. 1989 103 p
(Contract DE-AC07-76ID-01570)
(DE90-002218; DOE/ID-10252) Avail: NTIS HC A06/MF A01

This report was prepared to provide background information on electric and hybrid vehicles (EHVs) for a Department of Energy assessment of the costs and benefits of flexible and alternative fuel use in the U.S. transportation sector. As required by the assessment, this report focuses on the potential characteristics and impacts of large-scale EHV production and use, rather than on the policies, decisions, activities and events which might be required to assure the introduction of EHVs into U.S. transportation on such a scale. This report is primarily a composite of existing papers and reports on EHVs. It offers new calculations only where necessary to assemble a consistent and reasonably complete picture. Its emphasis is on results and conclusions rather than analytic methods or available data. It is intentionally brief. In comparison, the EHV test reports and technical papers from which it draws would fill a bookshelf. DOE

N90-16272*# National Aeronautics and Space Administration. Langley Research Center, Hampton, VA.
MECHANICAL STRAIN ISOLATOR MOUNT Patent Application
Gordon E. James, inventor (to NASA) (TRW Space Technology Labs., Redondo Beach, CA.) 27 Nov. 1989 7 p Sponsored by NASA
(NASA-Case-LAR-13580-1; NAS 1.71:LAR-13580-1; US-Patent-Appl-SN-441673) Avail: NTIS HC A02/MF A01 CSCL 13I

Certain devices such as optical instruments must preserve their alignmental integrity while being subjected to mechanical strain. A mechanical strain isolator mount is provided to preserve the alignmental integrity of an alignment sensitive instrument. An alignment sensitive instrument is mounted on a rectangular base. Flexural legs are connected at their proximal ends to the rectangular base. Flexural legs are also spaced parallel to the sides. Mounting pads are connected to the legs at the distal end and the mechanical strain isolator mount is attached to the substrate by means of threaded bolts. When a mounting pad and its respective leg is subjected to lateral strain in either the X or Y direction via the substrate, the respective leg relieves the strain by bending in the direction of the strain. An axial strain on a mounting pad in the Z direction is relieved by a rotational motion of the legs in the direction of the strain. When the substrate is stress free, the flexural legs return to their original condition and thus preserve the original alignment integrity of the alignment sensitive instrument. NASA

N90-16273# Department of the Air Force, Washington, DC.
AUTOMATIC PRESTART OR POST SHUTOFF ENGINE LUBRICATOR Patent
James R. Andres, inventor (to Air Force) 2 May 1989 9 p Filed 28 Apr. 1988 Supersedes US-Patent-Appl-SN-187143 (AD-D014259; US-Patent-4,825,826; US-Patent-Appl-SN-187143)
Avail: U.S. Patent and Trademark Office CSCL 11/8

A system for automatically injecting lubricating oil into the lubricating system of an engine prior to startup of the engine or following shutdown of the engine is described which comprises a solenoid controlled spring loaded piston and cylinder arrangement which is filled with oil under pressure during normal engine operation and a control circuit responsive to the ignition switch of the engine for controlled or metered release of oil from the cylinder either just prior to engine startup or after engine shutdown. GRA

N90-16274# Department of the Air Force, Washington, DC.
QUICK DISCONNECT DUCT COUPLER Patent
Douglas D. Dierksmeier, inventor (to Air Force) 13 Jun. 1989 4 p Filed 24 Sep. 1987 Supersedes US-Patent-Appl-SN-100385 (AD-D014265; US-Patent-4,838,584; US-Patent-Appl-SN-100385)
Avail: U.S. Patent and Trademark Office CSCL 13/11

A coupling device is disclosed which utilizes the first and second contiguous L-shaped coupling members affixed to terminal duct portions, and a slidable clamp having a T-shaped trough for gripping the L-shaped coupling members when slid thereover, locking them together to the close the duct. The clamp is slid away from coupling members to rapidly open the duct. GRA

N90-16275# Department of the Air Force, Washington, DC.
CONTINUOUSLY VARIABLE GEAR DRIVE TRANSMISSION Patent
Vann Y. Won, inventor (to Air Force) 8 Aug. 1989 14 p Filed 20 May 1987 Supersedes US-Patent-Appl-SN-052641 (AD-D014268; US-Patent-4,854,190; US-Patent-Appl-SN-052641)
Avail: U.S. Patent and Trademark Office CSCL 13/6

The invention comprises an all gear transmission mechanism capable of producing a wide range of speed outputs, including very high torque at low speed and very high speed at low torque. This result is provided by a combination of epicyclic gearing and differential gearing. The invention also includes an all gear feedback mechanism for sustaining desired operating speeds and torques as well as for performing rapid changes in gear ratio that produce rapid acceleration and deceleration of output shaft rotation. The invention comprises an all gear mechanism for a continuously variable transmission that provides a wide range of output speeds and torques. The Basic element of the transmission is a floating gear assembly can either comprise a floating gearbox or a floating gear arrangement incorporated into a differential assembly with idler gears. Various controlling mechanisms are shown and described which include first and second mechanical feedback loops. With these speed control systems, the output gear ratio can be made to change either linearly to geometrically to produce a desired output speed and torque. GRA

N90-16276# Sandia National Labs., Albuquerque, NM.
DIESEL STARTING SYSTEM MONITOR: PROTOTYPE DEVELOPMENT
T. M. DeBey Jul. 1989 24 p
(Contract DE-AC04-76DP-00789)
(DE90-004425; SAND-88-7058) Avail: NTIS HC A04/MF A01

The U.S. Department of Energy (DOE) effort to extend the operational lives of commercial nuclear power plants is examining methods for predicting the performance of specific equipment. The focus is on predictive monitoring as a means for reducing equipment surveillance, maintenance, and outages. Realizing these goals will result in nuclear plants that are more reliable, have lower maintenance costs, and have longer lives. A prognostic monitoring system is described which was developed to predict starting performance in emergency diesels. A prototype system was built and tested on an engine at Sandia National Laboratories. DOE

N90-16277# Oak Ridge National Lab., TN. Engineering Technology Div.
RESULTS FROM THE THIRD YEAR OF OPERATION OF THE FEDERAL METHANOL FLEET AT LAWRENCE BERKELEY LABORATORY
R. N. McGill, B. H. West, S. L. Hillis, and J. W. Hodgson (Tennessee Univ., Knoxville.) Dec. 1989 29 p
(Contract DE-AC05-84OR-21400)

(DE90-003306; ORNL/TM-11401) Avail: NTIS HC A03/MF A01

Lawrence Berkeley Laboratory has completed three years of operation of ten vehicles for the Federal Methanol Fleet Project; five of the vehicles are fueled with methanol. Nearly 74,000 miles were accumulated on the ten vehicles during the third year, bringing the total for three years to over 280,000 miles. The five gasoline cars in the project at Berkeley have been retired from service by the General Services Administration, but the five methanol cars will continue to be monitored. Recent emissions tests of the methanol cars revealed higher emissions than when the cars were originally tested in 1985, and evidence suggests that there has been some deterioration of emissions control by the catalytic converters. Rates of accumulation of wear metals in the lubricating oil of the methanol engines improved during the third year; only iron remains appreciably elevated in the oil when compared to that of the gasoline engines. Drivers continued to express a high degree of satisfaction with the performance of the methanol cars as compared to that of the gasoline cars. DOE

N90-16278# Sandia National Labs., Albuquerque, NM. Thermomechanical/Physical and Process Research Div.

STABILITY AND FRAGMENTATION OF EJECTA IN HYPERVELOCITY IMPACT

D. E. Grady and S. L. Passman 1989 16 p Presented at the Hypervelocity Impact Symposium, San Antonio, TX, 12-14 Dec. 1989

(Contract DE-AC04-76DP-00789)

(DE90-004087; SAND-89-0507C; CONF-891214-14) Avail: NTIS HC A03/MF A01

The present study offers an explanation for the behavior of debris ejected from the back surface of a target impacted by a high velocity projectile. Such debris is observed to expand as a ductile bubble and then fragment through surface instabilities when a critical expansion is achieved. An approximate model of hypervelocity impact developed by Swift et al. (1983), which assumes as expanding spherical shell of matter for the debris cloud, is introduced to motivate the analysis. We then solve for the spherically symmetric motion of, and pressures within, a spherical shell of ideal incompressible fluid subjected to inner and outer pressure boundary conditions. The solution is specialized to the freely expanding spherical shell (no pressure on the inner and outer boundaries). We then specialize further to the thin freely expanding spherical shell. Material response is extended to ideal incompressible plasticity and solutions for the radial and circumferential stress distributions are determined. Experimental results from high velocity impact tests of lead and uranium projectiles on lead and uranium targets using multiple flash radiography diagnostics (Grady et al., 1985) are compared with the theory. Although data are limited and the material and kinematic parameters somewhat uncertain, the comparison supports the physics and analysis put forth in this study. DOE

N90-16279# Sandia National Labs., Albuquerque, NM. Interconnections Div.

CONNECTOR SELECTION PROGRAM IMPLEMENTATION NOTES, VERSION 1.0

Nicole E. Sevier Nov. 1989 116 p

(Contract DE-AC04-76DP-00789)

(DE90-004983; SAND-89-1619) Avail: NTIS HC A06/MF A01

The connector selection program is a database application that allows engineers to locate information about connectors that meet their requirements. This document describes the design and implementation of the database, the data input application, and the user interface. Nijssen's Information Analysis Methodology (NIAM) was used to characterize the connector data requirements which yielded the database design. This design was transformed into database record structures that were implemented in the relational database management software ORACLE. After the database was in place, data input screens were created to capture the connector data, analyze it, and place it in the proper database record structures. Finally, a user interface was designed and developed that displays or prints the information contained in the database, associated drawings, and documentation related to the program and its data. DOE

N90-16280 Pennsylvania State Univ., University Park.

ON-LINE ESTIMATION OF MECHANICAL NONLINEARITIES IN COMPLIANT TWO-LINK ROBOT MANIPULATORS Ph.D. Thesis

Intak Bae 1989 136 p

Avail: Univ. Microfilms Order No. DA8922015

Estimation schemes for mechanical nonlinearities such as Coulomb friction and gear backlash in compliant two-link robot manipulators have been developed and evaluated. During the estimation, sinusoidal control inputs were applied to each joint individually, and a recursive least squares parameter identifier was used to estimate the nonlinearities based on the measurements of the output joint angles. A compliant planar two-link manipulator with work envelope and payload capacity comparable to a PUMA 760 was modeled. Dynamics of the compliant robot manipulator consist of two components-rigid body dynamics and first mode vibrational dynamics. Lagrangian methods were employed to establish the dynamic equations with nonlinear friction effects. The performance of the parameter estimation scheme was evaluated through the use of computer simulation. The simulations were executed using both PID feedback controllers and computed torque open-loop controllers, and the performance of both cases was examined. Dissert. Abstr.

N90-16281# Institut National des Sciences Appliquees de Lyon, Villeurbanne (France). Lab. de Mecanique des Contacts.

INVESTIGATION OF ROUGH ELASTOHYDRODYNAMIC CONTACT Ph.D. Thesis [FONCTIONNEMENT DU CONTACT ELASTOHYDRODYNAMIQUE RUGUEUX]

Louis Flamand 1989 269 p In FRENCH Sponsored by the Direction des Recherches, Etudes et Techniques, Paris, France; French Marine Nationale; Electricite de France; Turbomeca S.A.; SNR; SNECMA; Aerospatiale; SEP, Vernon, France; and Graffenstaden

(ISAL-89-0029; ETN-90-96035) Avail: NTIS HC A12/MF A02

The elastohydrodynamic contact points which exist between most mechanical components, gears, bearings, cams, and their separation by lubricants submitted to high pressures, are investigated. The rugosity of these contact points can lead to surface failure. The theoretical and practical aspects of such friction points are analyzed. A failure estimation criterion is proposed and correlated with experimental results. A method for evaluating the health of mechanical parts through analysis of wear deposits in the lubricant is presented. ESA

N90-16282# Sandia National Labs., Albuquerque, NM. Thermomechanical and Physical Div.

STUDIES OF DENSITY DISTRIBUTIONS IN ONE-DIMENSIONAL SHOCK-INDUCED DEBRIS CLOUDS

J. R. Asay and T. G. Trucano 1989 17 p Presented at the Hypervelocity Impact Symposium, San Antonio, TX, 12-14 Dec. 1989 Sponsored in part by DNA

(Contract DE-AC04-76DP-00789)

(DE90-004089; SAND-89-0595C; CONF-891214-12) Avail: NTIS HC A03/MF A01

The vaporization of target and projectile materials in hypervelocity impact events is known to substantially influence target interaction effects. In this paper, two experimental techniques are presented for studying shock-induced vaporization for one-dimensional motion. One uses velocity interferometry to measure the motion history produced when a one-dimensional vapor cloud stagnates against a laser window. The other employs fast radiography to measure the density distributions in one-dimensional vapor clouds. Data obtained for shock-induced vaporization in lead and cadmium with these techniques have been compared to computer simulations, which indicate: (1) good agreement for small amounts of vapor and for small propagation distances, and (2) increasing disagreement as the degree of vaporization increases. These results suggest that either diffusing

flow between the vapor and liquid phases occurs under these conditions, or that vaporization kinetics are important. DOE

N90-16283# Los Alamos National Lab., NM.
DESIGN OF A SPHEROMAK COMPRESSOR DRIVEN BY HIGH EXPLOSIVES
Ivars Henins, Juan C. Fernandez, Thomas R. Jarboe (Seattle Univ., WA.), Stanley P. Marsh, George J. Marklin, Robert M. Mayo, and Fred J. Wysocki 1989 5 p Presented at the 11th US/Japan Workshop on Field-Reversed Configurations and Compact Toroids, Los Alamos, NM, 6-9 Nov. 1989
(Contract W-7405-eng-36)
(DE90-003652; LA-UR-89-4006; CONF-8911130-8) Avail: NTIS HC A01/MF A01

High energy density spheromaks can be used to accelerate a thin section of the flux conserver wall to high velocities. The energy density of a spheromak, formed by conventional helicity injection into a flux conserver, can be increased by reducing the flux conserver volume after the spheromak is formed. A method of accomplishing this is by imploding one wall of the flux conserver with high explosives. The velocity of a wall driven by high explosives is about 3 to 5 km/sec, which is not exceptionally fast. Magnetic equilibrium calculations show that for some imploding flux conserver geometries, the energy density of the spheromak can be suddenly increased on an Alfven time scale by the tendency of the spheromak to maintain a state of minimum energy per unit helicity, which is equivalent to minimizing lambda = mu (sub 0)j/B. In this process, as the initial flux conserver dimensions are reduced under the explosive drive, the characteristic lambda of the configuration increases. Then, if there is an attached flux conserver region whose dimensions are such that its lambda becomes lower than for the imploding region, the spheromak will quickly transfer to this region, even if its volume is smaller, thus increasing the energy per unit volume. This is called the natural switching feature of spheromaks. The simplest such geometry is a cylindrical flux conserver with one end being driven by high explosives. An attached, smaller diameter on-axis cylinder has a thin end wall which is accelerated when the spheromak switches into the smaller cylinder. DOE

N90-16284# Westinghouse Savannah River Co., Aiken, SC. Robotics Group.
EXAMPLES OF ROBOTS AND TELEOPERATORS AT THE SAVANNAH RIVER SITE
Clyde R. Ward, Frank M. Heckendorn, and Richard C. Vandewlle 1989 7 p Presented at the IEEE Nuclear Science Symposium and Exhibits, San Francisco, CA, 27-29 Oct. 1989 Submitted for publication
(Contract DE-AC09-89SR-18035)
(DE90-004659; WSRC-RP-89-799; CONF-891087-12) Avail: NTIS HC A02/MF A01

The Savannah River Site manufactures nuclear materials for the U.S. Department of Energy. In recent years robots and mobile teleoperators have been used to reduce the radiation exposure of personnel at this site. Two examples of robots that have significantly reduced radiation exposure are the Shielded Cells Waste Handling Robot and the Shielded Cells Sample Handling Robot. The Shielded Cells Waste Handling Robot has been in operation for over four years. It removes cans of radioactive waste from the Shielded Cells, seals the can in a plastic bag, and places the cans in a waste drum. The Shielded Cells Sample Handling Robot has been in operation for only a few months. It opens a door to one of the Shielded Cells, removes a radioactive sample from a shielded container, laces it in the cell, and closes the door. Two examples of tasks where mobile teleoperators have significantly reduced radiation exposure are removal of a contaminated junction box, and lead removal from radioactive vessels. DOE

N90-16285# Du Pont de Nemours (E. I.) and Co., Aiken, SC. Robotics Technology.
EXPERT SYSTEM CONTROL OF A SIX-LEGGED WALKING TELEROBOT
Kevin R. DeVries 1989 6 p Presented at the 3rd ANS Topical Meeting on Robotics and Remote Systems, Charleston, SC, 13-16 Mar. 1989
(Contract DE-AC09-76SR-00001)
(DE90-004661; DP-MS-88-94; CONF-890304-38) Avail: NTIS HC A02/MF A01

The Robotics Technology Group of the Savannah River Laboratory has implemented a three-stage expert system for a six-legged walking telerobot. Remote operation of this machine requires the knowledge of a highly skilled operator. Stability, size, and mode of operation considerations must take place continuously, in general, much more so than with a typical wheeled vehicle. The technology employed provides for quasi-real-time computer control, manual control, and an expert advisor -- all in the same package, which runs on the IBM PC/AT. DOE

N90-16286*# National Aeronautics and Space Administration. Lewis Research Center, Cleveland, OH.
DYNAMIC ANALYSIS OF GEARED ROTORS BY FINITE ELEMENTS
Ahmet Kahraman, H. Nevzat Ozguven, Donald R. Houser (Ohio State Univ., Columbus.), and James J. Zakrajsek Jan. 1990 22 p Prepared in cooperation with Army Aviation Systems Command, Cleveland, OH
(Grant NAG3-773; DA Proj. 1L1-62209-A4-7A)
(NASA-TM-102349; E-5058; NAS 1.15:102349; AVSCOM-TM-89-C-006) Avail: NTIS HC A03/MF A01 CSCL 13I

A finite-element model of a geared rotor system on flexible bearings was developed. The model includes the rotary inertia of shaft elements, the axial loading on shafts, flexibility and damping of bearings, material damping of shafts and the stiffness and the damping of gear mesh. The coupling between the torsional and transverse vibrations of gears were considered in the model. A constant mesh stiffness was assumed. The analysis procedure can be used for forced vibration analysis of geared rotors by calculating the critical speeds and determining the response of any point on the shaft to mass unbalances, geometric eccentricities of gears and displacement transmission error excitation at the mesh point. The dynamic mesh forces due to these excitations can also be calculated. The model has been applied to several systems for the demonstration of its accuracy and for studying the effect of bearing compliances on system dynamics. Author

N90-16696*# Florida Inst. of Tech., Melbourne. Dept. of Mechanical and Aerospace Engineering.
ON THE SELECTION OF MATERIALS FOR CRYOGENIC SEALS AND THE TESTING OF THEIR PERFORMANCE
John M. Russell *In* University of Central Florida, NASA/ASEE Summer Faculty Fellowship Program Oct. 1989 p 226-269 (For primary document see N90-16686 08-99)
Avail: NTIS HC A18/MF A03 CSCL 11A

N90-16701*# California Polytechnic State Univ., San Luis Obispo. Dept. of Engineering Technology.
MATHEMATICAL MODEL FOR ADAPTIVE CONTROL SYSTEM OF ASEA ROBOT AT KENNEDY SPACE CENTER
Omar Zia *In* University of Central Florida, NASA/ASEE Summer Faculty Fellowship Program Oct. 1989 p 358-381 (For primary document see N90-16686 08-99)
Avail: NTIS HC A18/MF A03 CSCL 13I

38 QUALITY ASSURANCE AND RELIABILITY

Includes product sampling procedures and techniques; and quality control.

N90-16287# Sandia National Labs., Albuquerque, NM. Exploratory Batteries Div.
FAULT TREE ANALYSIS: A TOOL FOR BATTERY SAFETY AND RELIABILITY STUDIES
Samuel C. Levy 1989 7 p Presented at the 5th Annual Battery Conference on Applications and Advances, Long Beach,

CA, 16-18 Jan. 1990
(Contract DE-AC04-76DP-00789)
(DE90-002582; SAND-89-2312C; CONF-900138-2) Avail: NTIS HC A02/MF A01

Fault tree analysis was used by engineers as a means of defining system failure. It provides a method of system examination which increases the level of understanding of the system and is helpful in logically determining the underlying causes of potential failures. A fault tree is composed of a number of symbols, describing different types of events, which are operated on by logic gates. Construction of a battery fault tree is discussed in terms of two types of event and two logic gates. An example is given of how fault tree analysis was used to determine the cause of a safety incident. A string of lithium cells on test for several years suddenly vented violently. Fault tree analysis quickly pointed out the underlying faults leading to this event, and a means of prevention was suggested. DOE

N90-16288# Brookhaven National Lab., Upton, NY. Dept. of Physics.
SLOW POSITRON DEFECT PROFILING OF SILICON EPILAYERS
Erik Tandberg, Peter J. Schultz, T. E. Jackman, M. W. Denhoff, G. C. Aers (National Research Council of Canada, Ottawa, Ontario), K. G. Lynn, and B. Nielsen 1988 4 p Repr. from Positron Annihilation (Singapore, World Scientific Publishers), 1988 Presented at the 8th International Conference on Positron Annihilation, Gent, Belgium, 29 Aug. - 3 Sep. 1988
(Contract DE-AC02-76CH-00016)
(DE90-003958; BNL-43482; CONF-8808122-18) Avail: NTIS HC A01/MF A01

Over the last decade, positrons have been used as a probe to nondestructively study and depth profile defects in dilute concentrations (parts per million) in solids. Only recently have positrons been used to profile buried defects in ultra-thin epitaxial layers of semiconductors. Recent results are discussed which involve the modeling of defects and electric fields in homoepitaxial layers of silicon grown by molecular beam epitaxy (MBE) on a Si(100) substrate. Also discussed are some of the limitations of the modelling technique and future prospects. DOE

N90-16289# Aeritalia S.p.A., Turin (Italy). Gruppo Velivola da Combattimento.
STRUCTURAL CHARACTERIZATION OF SPACELAB [CARATTERISTICHE DELLA STRUTTURA DELLO SPACELAB]
Mario Balocco, Franco Cipri, and Arnaldo Tonso 1989 10 p In ITALIAN
(ETN-90-95214) Avail: NTIS HC A02/MF A01

The quality level of Spacelab weldings is investigated in order to examine the feasibility of the proposed control procedures. The parameters adopted for x ray inspection are also studied. Improvements in x ray control are adopted including a reduction in the source to object distance, a double film imaging technique and a two sources two films procedure. The improved procedures show that expected life of Spacelab welding is longer than the specified requirements. ESA

N90-16290# Central Research Inst. of Electric Power Industry, Tokyo (Japan). Energy and Environment Lab.
THEORETICAL STUDY ON CREEP DAMAGE DETECTION BY ULTRA-SONIC WAVE MEASUREMENT
Masaaki Matsubara and Akihito Nitta Dec. 1988 33 p In JAPANESE; ENGLISH summary
(DE90-702472; CRIE-T-88014) Avail: NTIS (US Sales Only) HC A03/MF A01

A theoretical study on the application of an ultrasonic wave measurement to detect the creep damage of a steam turbine rotor material, is described. From a reference survey, it was found that there are many studies on the application of an ultrasonic method to detect creep damage in consideration of the effectiveness of the method. The author developed a theoretical evaluation method of change in ultrasonic wave attenuation and velocity with progress in creep damage by using the creep cavity growth model. This method enables one to grasp the approximate changes of ultrasonic variables accompanied by the progress of creep damage. Furthermore, it was found theoretically that the change in attenuation is a more appropriate parameter than the change in velocity to detect the creep damage for the rotor material. DOE

39 STRUCTURAL MECHANICS

Includes structural element design and weight analysis; fatigue; and thermal stress.

For applications see *05 Aircraft Design, Testing and Performance* and *18 Spacecraft Design, Testing and Performance.*

N90-16291 Stanford Univ., CA.
ELEMENT-BY-ELEMENT PRECONDITIONING TECHNIQUES FOR LARGE-SCALE, VECTORIZED FINITE ELEMENT ANALYSIS IN NONLINEAR SOLID AND STRUCTURAL MECHANICS Ph.D. Thesis
Robert Mark Ferencz 1989 296 p
Avail: Univ. Microfilms Order No. DA8919424

Solving coupled linear systems of equations is the dominant cost of linear and nonlinear implicit finite element simulations in three dimensions. Direct methods, i.e., algorithms based upon Gaussian elimination, are traditionally used for two-dimensional simulations. However, direct methods display unfavorable asymptotic cost growth for three-dimensional applications, leading the computational mechanics community to reexamine the utility of iterative linear equation solving. Element-by-element (EBE) preconditioned iterative algorithms have shown considerable promise in small-scale, academic investigations. However, iterative methods, being motivated by a desire for computational economy, will not be accepted by the engineering community until they are evaluated for large-scale applications. Vectorized EBE pre-conditioners, and the conjugate gradient (CG) and Lanczos iterative drivers are being implemented, in a general-purpose, large-scale simulation code for nonlinear solid and structural mechanics. This implementation has included developing software which in turn writes vectorized FORTRAN modules for each of the major EBE operations, for a element with a user-specified number of degrees of freedom. Performance of the EBE preconditioned conjugate gradient (EBE/PCG) methods is reported and compared with direct solution for a number of large-scale engineering analyses. A simple measure of mesh connectivity is introduced, and its usefulness in predicting the relative efficiency of direct and iterative solutions is illustrated. The utility of a Lanczos algorithm incorporating partial reorthogonalization is also investigated. Dissert. Abstr.

N90-16292*# National Aeronautics and Space Administration. Langley Research Center, Hampton, VA.
ANALYSIS AND TESTING OF AXIAL COMPRESSION IN IMPERFECT SLENDER TRUSS STRUTS
Mark S. Lake and Nicholas Georgiadis Washington Feb. 1990 30 p
(NASA-TM-4174; L-16712; NAS 1.15:4174) Avail: NTIS HC A03/MF A01 CSCL 20K

The axial compression of imperfect slender struts for large space structures is addressed. The load-shortening behavior of struts with initially imperfect shapes and eccentric compressive end loading is analyzed using linear beam-column theory and results are compared with geometrically nonlinear solutions to determine the applicability of linear analysis. A set of developmental aluminum clad graphite/epoxy struts sized for application to the Space Station Freedom truss are measured to determine their initial imperfection magnitude, load eccentricity, and cross sectional area and moment of inertia. Load-shortening curves are determined from axial compression tests of these specimens and are correlated with theoretical curves generated using linear analysis. Author

N90-16293*# National Aeronautics and Space Administration. Langley Research Center, Hampton, VA.
LOAD-SHORTENING BEHAVIOR OF AN INITIALLY CURVED ECCENTRICALLY LOADED COLUMN
W. B. Fichter and Mark W. Pinson Dec. 1989 22 p
(NASA-TM-101643; NAS 1.15:101643) Avail: NTIS HC A03/MF A01 CSCL 20K

To explore the feasibility of using buckled columns to provide a soft support system for simulating a free-free boundary condition in dynamic testing, the nonlinear load-shortening behavior of initially imperfect, eccentrically loaded slender columns is analyzed. Load-shortening curves are obtained for various combinations of load eccentricity and uniform initial curvature and are compared, for reference purposes, with the limiting case of the classical elastica. Results for numerous combinations of initial curvature and load eccentricity show that, over a wide range of shortening, an axially loaded slender column exhibits load-deflection compliance which is of the same order as that of a straight but otherwise identical cantilever beam under lateral tip loading. Author

N90-16294*# Virginia Polytechnic Inst. and State Univ., Blacksburg. Dept. of Engineering Science and Mechanics.
FATIGUE LIFE ESTIMATES FOR HELICOPTER LOADING SPECTRA
A. K. Khosrovaneh, N. E. Dowling, A. P. Berens, and J. P. Gallagher (Dayton Univ., OH.) Dec. 1989 108 p
(Grant NAG1-822)
(NASA-CR-181941; NAS 1.26:181941) Avail: NTIS HC A06/MF A01 CSCL 20K

Helicopter loading histories applied to notch metal samples are used as examples, and their fatigue lives are calculated by using a simplified version of the local strain approach. This simplified method has the advantage that it requires knowing the loading history in only the reduced form of ranges and means and number of cycles from the rain-flow cycle counting method. The calculated lives compare favorably with test data. Author

N90-16295# Air Force Inst. of Tech., Wright-Patterson AFB, OH. School of Engineering.
IMPROVED SOLUTION TECHNIQUES FOR THE EIGENSTRUCTURE OF FRACTIONAL ORDER SYSTEMS M.S. Thesis
Michele L. Deveraux Dec. 1988 97 p
(AD-A213844; AFIT/GAE/AA/88D-08) Avail: NTIS HC A05/MF A01 CSCL 20/11

The structural problem of a viscoelastically damped rod is considered. A four parameter fractional derivative viscoelastic model rather than the traditional viscous model is used to describe the stress-strain relationship. The introduction of fractional order derivatives leads to high order matrix equations, which are cumbersome and time consuming to solve. Thus, there exists a motivation to seek alternate solution techniques. An existing technique, modified matrix iteration, is presented, and a new one, employing spectrum shift concepts, is proposed. The spectrum shift technique is shown to be significantly more efficient. GRA

N90-16296# Department of the Air Force, Washington, DC.
VIBRATION DAMPING COMPOSITION SUITABLE FOR OUTER SPACE TEMPERATURE VARIATIONS Patent
Creed E. Blevins, inventor (to AF) 18 Apr. 1989 4 p Filed 19 Apr. 1988 Supersedes US-Patent-Appl-SN-183200
(AD-D014288; US-Patent-4,822,834; US-Patent-Appl-SN-183200) Avail: US Patent and Trademark Office CSCL 11/10

It is thus a principal object of the invention to provide an improved constrained layer composite damping material having a high loss factor throughout an extended temperature range of about -100 to +160 F. The composition of the present invention includes a composition of two different elastomers, a thermoplastic polymer, a plasticizer and a reinforcing filler. The first elastomer has a glass transitional point temperature of -50 F, the second elastomer has a glass transitional point temperature of +60 F and the thermoplastic material has a glass transitional point temperature of +130 F. GRA

N90-16297# Los Alamos National Lab., NM. Dynamic Testing Section.
ANALYSIS OF NONLINEAR SYSTEMS USING ARMA (AUTOREGRESSIVE MOVING AVERAGE) MODELS
Norman F. Hunter, Jr. 1990 8 p Presented at the 8th International Modal Analysis Conference, Kissimmee, FL, 29 Jan. - 1 Feb. 1990
(Contract W-7405-eng-36)
(DE90-002395; LA-UR-89-3375; CONF-900139-2) Avail: NTIS HC A02/MF A01

While many vibration systems exhibit primarily linear behavior, a significant percentage of the systems encountered in vibration and model testing are mildly to severely nonlinear. Analysis methods for such nonlinear systems are not yet well developed and the response of such systems is not accurately predicted by linear models. Nonlinear ARMA (autoregressive moving average) models are one method for the analysis and response prediction of nonlinear vibratory systems. The background is reviewed of linear and nonlinear ARMA models, and the application of these models to nonlinear vibration systems are illustrated. The advantages and disadvantages of ARMA models and emphasizing prospects for future development are summarized. DOE

N90-16298# Sandia National Labs., Albuquerque, NM. Experimental Mechanics Dept.
AN INTRODUCTION TO SHAKER SHOCK SIMULATIONS
Jonathan D. Rogers 1989 8 p Presented at the 8th International Modal Analysis Conference, Orlando, FL, 29 Jan. - 1 Feb. 1990
(Contract DE-AC04-76DP-00789)
(DE90-003057; SAND-89-1729C; CONF-900145-1) Avail: NTIS HC A02/MF A01

The use of shakers in shock testing is addressed. A brief review of the shock response spectrum is given with its applications to test specification. The capabilities and limitations of shaker shock simulations are discussed with regard to both classical pulses and transient vibration inputs. Methods for performing shaker shock simulations are presented. DOE

N90-16299# Technical Research Centre of Finland, Espoo. Lab. of Heating and Ventilating.
MEASUREMENT OF REFLECTION AND IMPEDANCE IN A BEAM BY THE STRUCTURAL INTENSITY TECHNIQUE
Tapio Lahti and Jukka Linjama Jun. 1989 66 p
(DE90-728212; VTT-TUTK-625; ISBN-951-38-3498-0; ISSN-0358-5077) Avail: NTIS (US Sales Only) HC A04/MF A01

In the one-dimensional propagation of vibration energy, the structural intensity methods can be extended to the determination of the mechanical impedance and reflection coefficient. A short survey of respective measurement of acoustic impedance is presented, and the principles of structural intensity measurements in beams are reviewed. Then, analogously to acoustics, frequency domain expressions are derived for estimating the impedance and reflection coefficient in a beam. The developed techniques are also extended to a special application, the division of the partly reflective general field into perfectly propagating and standing parts. Separation based on the reflection coefficient is suggested and compared to a known impedance-based approach. In laboratory experiments with bending waves in a simple beam, the various methods for estimating the impedance and reflection coefficient were tested and compared. The known method of measuring reflection of sound waves in ducts was shown to be applicable in beams. The simplest suggested method for estimating the impedance, which was based on the known wave impedance and the estimated reflection coefficient, gave the most reliable results. Also the character of the field separation methods was demonstrated in the experiments. The method based on the reflection coefficient appeared preferable, but the disadvantage is that it cannot be applied in fields with more than one dimension. DOE

N90-16300# Royal Aerospace Establishment, Farnborough (England).
FRAG REQUIREMENTS FOR CONTROL OF FATIGUE TESTING
R. Cook May 1989 28 p
(RAE-TM-MAT/STR-1130; BR110773; ETN-90-96136) Copyright Avail: NTIS HC A03/MF A01

Parts of the Fatigue Research Advisory Group (FRAG) investigations are reported. The accuracy requirements of load application, calibration requirements and test data that must be recorded, are defined. Various methods of control are described. They may be used to achieve the testing accuracy requirements. The requirements are applicable to both fatigue testing machines and single actuator test rigs. ESA

N90-16301# Royal Aerospace Establishment, Farnborough (England).
CALIBRATION OF A PULSED POTENTIAL CRACK MONITOR FOR USE IN FATIGUE CRACK GROWTH STUDIES
J. Newman, A. Jefferson, P. J. Gregson (Southampton Univ., England), and P. D. Pitcher Apr. 1989 21 p Sponsored in cooperation with British Aerospace Public Ltd.
(Contract MOD-2040/411/XR-MAT)
(RAE-TM-M/S-1126; BR110495; ETN-90-96138) Copyright Avail: NTIS HC A03/MF A01

A pulsed direct current is used to generate a potential drop as a function of crack length. Experimental values of potential drop and crack length are obtained for three test piece geometries: a center crack specimen, a holed specimen, and a compact tension specimen. Computed values are generated using a FORTRAN program and are compared with the experimental results. The accuracy of the technique and its consequences on potential probe positioning for both short and long cracks are discussed. ESA

N90-16302 Fraunhofer-Inst. fuer Betriebsfestigkeit, Darmstadt (Germany, F.R.).
REVIEW OF INVESTIGATIONS ON AERONAUTICAL FATIGUE IN THE FEDERAL REPUBLIC OF GERMANY Review Period, Jun. 1987 - May 1989
O. Buxbaum and H. Huth 1989 58 p Presented at the 21st International Committee on Aeronautical Fatigue Conference, Jerusalem, Israel, 1989
(LBF-S-182; ISSN-0721-5320; ETN-90-95873) Copyright Avail: Fachinformationszentrum Karlsruhe, 7514
Eggenstein-Leopoldshafen 2, Federal Republic of Germany

Results of investigations carried out by West German industrial and research organizations in the field of fatigue are presented. The results of fatigue tests on specimens and components under constant amplitude, program, and random loading are presented. Investigations in the areas of cyclic stress-strain behavior, crack propagation, fracture strength, and residual strength are described. investigations of composite materials, especially of graphite/ epoxies and their properties under environmental influence are outlined. ESA

N90-16303# Fraunhofer Inst. fuer Werkstoffmechanik, Freiburg (Germany, F.R.).
NUMERICAL SIMULATION OF CREEP CRACK GROWTH EXPERIMENTS Final Report
Thomas Hollstein and Reinhold Kienzler Dec. 1988 53 p
(Contract BMFT-03-K-0503-3)
(IWM-W-4/88; ETN-90-95908) Avail: NTIS HC A04/MF A01

Creep crack growth at 550 C under laboratory air conditions in the 21 CrMoNiV 5 7 steel is described by a power law using the C integral. Within the scatterband, some indications of dependencies on specimen size (triaxiality), crack length and crack growth seem to exist. The initial crack growth rate is described independent of geometry by the initial values of the stress intensity factor K. No difference between creep crack growth rates under vacuum and laboratory air conditions is observed. Calculations on the basis of a Norton power law are in good agreement with experimental results for stationary creep conditions. The use of an exponential fit yields an even better description of the experimental results. The consideration of primary creep leads to a realistic simulation of the transient region. ESA

N90-16304# Institut National des Sciences Appliquees de Lyon, Villeurbanne (France). Lab. de Mecanique des Contacts.
A QUANTITATIVE ANALYSIS OF SLIP PHENOMENA ALONG A DRY CONTACT SURFACE BETWEEN TWO BODIES IN COMPARISON TO INTERFACIAL CRACK PROPAGATION Ph.D. Thesis [ETUDE QUANTITATIVE DES PHENOMENES DE GLISSEMENTS DANS UN CONTACT SEC A DEUX CORPS PAR COMPARAISON AVEC LA PROPAGATION D'UNE FISSURE INTERFACIALE]
Moufid Mouwakeh 1989 209 p In FRENCH Sponsored by Direction des Recherches, Etudes et Techniques, Paris, France
(ISAL-89-0032; ETN-90-96044) Avail: NTIS HC A10/MF A02

A technique of analyzing local perturbations caused by slip phenomena is described. It involves an interpretation of the phenomena as if they were manifestations of frictional interfacial crack propagation. This technique developed by Pogri works better than the Coulomb friction laws in analyzing this type of situation. The technique is tested using an actual crack propagation test. It is shown that the energy released during a slip is almost directly comparable to a frictional crack propagating itself along the slip interface. ESA

N90-16305# Oak Ridge National Lab., TN. Engineering Physics and Mathematics Div.
MATERIAL RESPONSES TO INCIDENT X RAYS
M. S. Smith 1989 6 p Presented at the HEART Conference, Monterey, CA, 12-16 Feb. 1990 Sponsored in part by AF
(Contract DE-AC05-84OR-21400)
(DE89-015366; CONF-900216-1) Avail: NTIS HC A02/MF A01

This paper discusses results of hydrodynamic calculations to assess the thermo-mechanical response of various materials to energy loadings from incident x rays. A beryllium mirror surface impurity study was performed to determine what effect surface impurities contribute to the material response. A second study, the LAMPSHADE survivability analysis, was conducted to ascertain whether the satellite debris shield would survive various x ray energy loadings. The PUFF-TFT code was used to assess the material response from incident x rays. The PUFF code calculates stress wave formation and propagation by numerical integration of the conservation equations in a one-dimensional Lagrangian coordinate system. The TFT package accounts for the effects of dose enhancement due to the transport of secondary particles with ranges comparable to the thickness of the thin material layers and thermal conduction between thin material layers. These two modifications (among others) more accurately portray the degree of energy sharing between thin layers, thereby modifying the expected energy depositions based on normal x ray interactions and possibly altering the anticipated thermo-mechanical response of the medium. DOE

N90-16306# Oak Ridge National Lab., TN.
EXPERIENCES WITH THREE-POINT BENDING TEST SPECIMENS FOR DETERMINING THE CRACK-ARREST FRACTURE TOUGHNESS K(SUB Ia) IN LOW-ALLOY STEEL
Guenther Schneeweiss and Thomas Varga (Technische Hochschule, Vienna, Austria) 1989 33 p
(Contract DE-AC05-84OR-21400)
(DE90-004120; ORNL/tr-89/52) Avail: NTIS HC A03/MF A01

The use of a smaller and simpler specimen than the standard crack arrest specimens (Robertson, CCA) appears to be more advantageous. Through instrument testing on three point bending test specimens, the advantages and disadvantages of this type of specimen were to be determined. The selected bending test specimen is suited for determining K(sub Ia): the crack arrest fracture toughness determined with the latter and by means of the CCA-specimen lies within the same dispersion range (material ASTM A 533 B). DOE

N90-16307# McElroy (Ralph) Co., Austin, TX.
BAM: GERMAN FEDERAL INSTITUTE FOR MATERIALS RESEARCH AND TESTING, BERLIN
1989 77 p Transl. into ENGLISH of unidentified German document Prepared for ORNL, TN
(Contract DE-AC05-84OR-21400)
(DE90-004293; ORNL/tr-89/48) Avail: NTIS HC A05/MF A01

The present report continues the documentation of findings of elastic-plastic FE analyses of an experimentally investigated pressure vessel with axial semielliptical exterior surface cracks, applicability of approximation methods of calculation of J will be discussed, results of calculations and experiments will be compared and in particular the dependence of the local J (Delta a) curves on the multiaxial nature of the stress state at the crack front will be investigated. DOE

N90-16308# Swedish Inst. for Materials Testing, Boras.
CYCLIC FATIGUE OF HOT-ISOSTATIC-PRESSED SILICON NITRIDE
Lennart Carlsson 1989 27 p
(PB90-122649; SP-RAPP-1989:43; ISBN-91-7848-193-7; ISSN-0284-5172) Avail: NTIS HC A03/MF A01 CSCL 20K

Cyclic fatigue was studied for hot isostatic pressed silicon nitride at room temperature. The number of cycles to failture was 10 to the 6th power at a maximum stress of 70 percent of the 4 point bending strength and 10 to the 4th power cycles at 95 percent of the bending strength. The behavior was found not to be time-dependent but cycle-dependent, at least at the lowest stresses. Scanning electron fractographs revealed numerous small cracks in the fatigued area. The findings are consistent with a qualitative model, in which cracks are developed in the glassy phase in the grain boundaries. The cracks grow under the cyclic stress until the sample fails according to the Griffith law. Author

42 GEOSCIENCES (GENERAL)

N90-16309# Department of Energy, Washington, DC. Engineering and Geosciences Div.
SUMMARIES OF PHYSICAL RESEARCH IN THE GEOSCIENCES
Dec. 1989 148 p
(DE90-004993; DOE/ER-0430) Avail: NTIS HC A08/MF A01

The Department of Energy supports research in the geosciences in order to provide a sound foundation of fundamental knowledge in those areas of the geosciences which are germane to the Department of Energy's many missions. The Division of Engineering and Geosciences, part of the Office of Basic Energy Sciences of the Office of Energy Research, supports the Geosciences Research Program. The participants in this program include Department of Energy laboratories, industry, universities, and other governmental agencies. These activities are formalized by a contact or grant between the Department of Energy and the organization performing the work providing funds for salaries, equipment, research materials, and overhead. The summaries in this document, prepared by the investigators, describe the scope of the individual programs. The Geoscience Research Program includes in geology, petrology, geophysics, geochemistry, solar physics, solar-terrestrial relationships, aeronomy, seismology, and natural resource modeling and analysis, including their various subdivisions and interdisciplinary areas. All such research is related either or indirectly to the Department of Energy's long-range technological needs. DOE

43 EARTH RESOURCES AND REMOTE SENSING

Includes remote sensing of earth resources by aircraft and spacecraft; photogrammetry; and aerial photography.

For instrumentation see *35 Instrumentation and Photography.*

N90-16310 Arizona Univ., Tucson.
CLOUD PHASE DISCRIMINATION BY NEAR-INFRARED REMOTE SENSING Ph.D. Thesis
Peter Andrew Pilewskie 1989 119 p
Avail: Univ. Microfilms Order No. DA8915982

A ground based near infrared spectroradiometer was built and used to measure relative spectral reflectance from cumulus congestus and cumulonimbus clouds during the 1985 and 1986 Arizona summer monsoon seasons. Thermodynamic phase was inferred from spectral features in the regions between 1.55 to 1.75 and 2.1 to 2.3 microns where there are distant differences between absorption in liquid water and ice and absorption by water vapor is very weak. Although liquid water and ice are nearly transparent in the visible, they absorb weakly in the near infrared and that absorption is amplified by multiple scattering in clouds. Reflectance measurements are simple to make, requiring neither high spectral resolution nor absolute detector response. Three distinct aspects of differences between absorption in liquid water and ice were used to infer phase: (1) Ratio of the signal at 1.65 microns to that at 2.2 microns; (2) Wavelength of peak signal in the 1.65 microns water vapor transmission window; and (3) Half-bandwidth of the 2.1 to 2.3 microns feature. Representative spectra are presented and analyzed on the basis of the predicted behavior of liquid water and ice cloud absorption. The results are consistent with young cumuli rapidly glaciating as they reach cooler levels, well before evidence of anvil formation of fibrous structure, contrary to the notion that phase can be inferred from visible cloud features. Dissert. Abstr.

N90-16311# Washington Univ., Seattle. Dept. of Statistics.
ICE FLOE IDENTIFICATION IN SATELLITE IMAGES USING MATHEMATICAL MORPHOLOGY AND CLUSTERING ABOUT PRINCIPAL CURVES Technical Report, 1 Sep. 1988 - 31 Aug. 1989
Jeffrey D. Banfield and Adrian E. Raftery Aug. 1989 35 p
(Contracts N00014-88-K-0265; N00014-89-J-1114)
(AD-A213854; TR-172) Avail: NTIS HC A03/MF A01 CSCL 08/2

Identification of ice floes and their outlines in satellite images is important for understanding physical processes in the polar regions, for transportation in ice covered seas and for the design of offshore structures intended to survive in the presence of ice. At present this is done manually, a long and tedious process which precluded full use of the great volume of relevant images now available. An automatic and accurate method is described for identifying ice floes and their outlines. Floe outlines are modeled as closed principal curves (Hastie and Stuetzle, 1989), a flexible class of smooth non-parametric curves. A robust method of estimating closed principal curves which reduces both bias and variance is proposed. Initial estimates of floe outlines come from the erosion-propagation (EP) algorithm, which combines erosion from mathematical morphology with local propagation of information about floe edges. The edge pixel from the EP algorithm are grouped into floe outlines using a new clustering algorithm. This extends existing clustering methods by allowing groups to be centered about principal curves rather than points or lines. This may open the way to efficient feature extraction using cluster analysis in images more generally. The method is implemented in an object-oriented programming environment for which it is well suited, and is quite computationally efficient. GRA

N90-16312*# Jet Propulsion Lab., California Inst. of Tech., Pasadena.
SCIENCE PLAN FOR THE ALASKA SAR FACILITY PROGRAM. PHASE 1: DATA FROM THE FIRST EUROPEAN SENSING SATELLITE, ERS-1
Frank D. Carsey 1 Sep. 1989 101 p Presented at the Chena Hot Springs, Alaska Meeting, Jul. 1987 and Aug. 1988
(Contract NAS7-918)
(NASA-CR-185028; JPL-Publ-89-14; NAS 1.26:185028) Avail: NTIS HC A06/MF A01 CSCL 08B

Science objectives, opportunities and requirements are discussed for the utilization of data from the Synthetic Aperture Radar (SAR) on the European First Remote Sensing Satellite, to be flown by the European Space Agency in the early 1990s. The principal applications of the imaging data are in studies of geophysical processes taking place within the direct-reception area of the Alaska SAR Facility in Fairbanks, Alaska, essentially the area within 2000 km of the receiver. The primary research that will be supported by these data include studies of the oceanography and sea ice phenomena of Alaskan and adjacent polar waters and the geology, glaciology, hydrology, and ecology of the region. These studies focus on the area within the reception mask of ASF, and numerous connections are made to global processes and thus to the observation and understanding of global change. Processes within the station reception area both affect and are affected by global phenomena, in some cases quite critically. Requirements for data processing and archiving systems, prelaunch research, and image processing for geophysical product generation are discussed. Author

N90-16313*# National Aeronautics and Space Administration. Ames Research Center, Moffett Field, CA.
COMPUTER-AIDED BOUNDARY DELINEATION OF AGRICULTURAL LANDS
Thomas D. Cheng, Gary L. Angelici, Robert E. Slye, and Matt Ma (TGS Technology, Inc., Moffett Field, CA.) Nov. 1989 24 p Original contains color illustrations
(NASA-TM-102243; A-89264; NAS 1.15:102243) Avail: NTIS HC A03/MF A01 CSCL 08B

The National Agricultural Statistics Service of the United States Department of Agriculture (USDA) presently uses labor-intensive aerial photographic interpretation techniques to divide large geographical areas into manageable-sized units for estimating domestic crop and livestock production. Prototype software, the computer-aided stratification (CAS) system, was developed to automate the procedure, and currently runs on a Sun-based image processing system. With a background display of LANDSAT Thematic Mapper and United States Geological Survey Digital Line Graph data, the operator uses a cursor to delineate agricultural areas, called sampling units, which are assigned to strata of land-use and land-cover types. The resultant stratified sampling units are used as input into subsequent USDA sampling procedures. As a test, three counties in Missouri were chosen for application of the CAS procedures. Subsequent analysis indicates that CAS was five times faster in creating sampling units than the manual techniques were. Author

N90-16314 Forschungsinstitut fuer Informationsverarbeitung, Ettlingen (Germany, F.R.).
QUANTITATIVE EVALUATION OF OBJECT-CHANGES IN MULTITEMPORAL AGRISAR IMAGERY
K. Behrens, M. Doebele, A. Ebert, A. Hohrath, G. Koehler, and E. Mauer Mar. 1988 59 p In GERMAN; ENGLISH summary
(Contract BMFT-523-4001-01QS87069)
(FIM-195; ETN-90-95348) Copyright Avail: Forschungsinstitut fuer Informationsverarbeitung und Mustererkennung, Eisenstockstrasse 12, D-7505 Ettlingen 6, Fed. Republic of Germany

The analysis of qualitative changes in multitemporal digital synthetic aperture radar (SAR) images is discussed. Numerical evaluations of image quality for each scene are extracted. The need for effective automatic SAR image analysis to handle the large existing and planned amount of SAR data is stressed. An automatic digital image evaluation technique is described. Significant object intensity changes in multitemporal data are analyzed. Image preprocessing methods and advanced image analysis operations are used. Data change detection methods are tailored to the different abstraction levels of the data required. Examples of each kind of change analysis are presented and the results compared. ESA

N90-16315# Technische Univ., Hanover (Germany, F.R.). Fachbereich Bauingenieur- und Vermessungswesen.
REGIONAL HEIGHT DETERMINATION USING GRAVIMETRIC AND TOPOGRAPHICAL DATA Ph.D. Thesis
Heiner Denker 1988 136 p In GERMAN; ENGLISH summary
(UH-156; ISSN-0174-1454; ETN-90-95352) Avail: NTIS HC A07/MF A01

Point and mean gravity data, a global geopotential model and geological and topographic information, are used in providing the corresponding height reference surface with compatible accuracy to that of the Global Positioning System (GPS). The data sets are combined by least square collocation using a remove-restore technique in which the topography is taken into account by a Residual Terrain Model (RTM) reduction. The applicability of these algorithms is demonstrated in two test areas: White Sands, New Mexico and Northern Germany. ESA

N90-16316 Deutsche Geodaetische Kommission, Munich (Germany, F.R.).
DYNAMIC ANALYSIS OF THE GEODETIC NETWORKS ORIGINATING FROM THE NAVSTAR/GLOBAL POSITIONING SYSTEM (GPS) SATELLITES Ph.D. Thesis - Stuttgart Univ. [DYNAMISCHE ANALYSE GEODAETISCHER NETZE AUF DER BASIS VON GPS-PHASENBEOBACHTUNGEN]
Wolfgang Lindlohr 1988 155 p In GERMAN; ENGLISH summary
(Ser-C-346; ISBN-3-7696-9394-9; ISSN-0065-5325;
ETN-90-95883) Copyright Avail: Fachinformationszentrum Karlsruhe, 7514 Eggenstein-Leopoldshafen 2, Fed. Republic of Germany

The originally undifferentiated carrier beat phases emitted from Navstar/Global Positioning System (GPS) satellites are used to determine coordinates, coordinate differences and baseline lengths by a dynamic analysis of geodetic networks. Analysis of the displacement field and its related deformation elements at the surface of the Earth is discussed. The investigations are based on a division of the displacement fields into global, regional, and local parts. The global and regional effects have to be reduced before the local parts can be investigated. ESA

N90-16317 Deutsche Geodaetische Kommission, Munich (Germany, F.R.).
INTEGRATED GEODETIC NETWORK ANALYSIS WITH STOCHASTIC PRIOR INFORMATION ABOUT THE GRAVITY FIELD AND REFERENCE ELLIPSOID Ph.D. Thesis - Stuttgart Univ.
Francis W. Odhiambo Aduol 1989 113 p In GERMAN; ENGLISH summary Sponsored by Akademischer Austauchdienstes
(Ser-C-351; ISBN-3-7696-9399-X; ISSN-0065-5325;
ETN-90-95886) Copyright Avail: Fachinformationszentrum Karlsruhe, 7514 Eggensteinn-Leopoldshafen 2, Fed. Republic of Germany

Within the framework of integrated 3-D network adjustment procedures, the comprehensive estimation of local geodetic data parameters in both physical and geometric space are considered. The model parameters for parameter estimation are defined through a model potential and a reference ellipsoid. The respective model parameters are treated in the estimation process as stochastic prior information. Models for incorporating the prior information into the estimation process as stochastic and dynamic on the one hand and as stochastic but static on the other hand are considered. In order to numerically test the considered procedures, two real geodetic networks of differing extents and observational material are analyzed. The consequence of incorrectly treating

the gravity field and reference ellipsoid parameters as exact restrictions when they in fact ought to be viewed as stochastic prior information is investigated. The results are analyzed against the background of previous adjustments of the test networks, in which the model parameters had been treated as exact restrictions. Besides confirming the rigor of establishing local geodetic data: through the integrated analysis of both physical and geometric geodetic observations, the results underline the significance of incorporating model parameters into the estimation process as stochastic prior information. ESA

N90-16318# Deutsche Forschungs- und Versuchsanstalt fuer Luft- und Raumfahrt, Oberpfaffenhofen (Germany, F.R.). Abteilung Fernerkundungsanwendungen.

PROCEEDINGS OF THE 5TH USER SEMINAR OF THE GERMAN REMOTE SENSING DATA CENTER OF THE DFVLR

Feb. 1989 130 p Partly in ENGLISH and GERMAN Seminar held in Oberpfaffenhofen, Fed. Republic ofGermany, 6-7 Jun. 1988 Original contains color illustrations

(DFVLR-Mitt-89-04; ETN-90-95296) Avail: NTIS HC A07/MF A01; DFVLR, VB-PL-DO, Postfach 90 60 58, 5000 Cologne, Fed. Republic of Germany, 52 Deutsche marks

The application potential of satellite data of the NOAA, LANDSAT, and SPOT satellites is presented in 21 contributions. The main emphasis is on the evaluation of NOAA-data for meteorological and oceanographic applications on the one hand, and on investigations by Federal Governmental Agencies of planning, inventory, monitoring, statistics and geoscientific development aid on the other hand. For individual titles, see N90-16319 through N90-16339.

N90-16319# Deutsche Forschungs- und Versuchsanstalt fuer Luft- und Raumfahrt, Oberpfaffenhofen (Germany, F.R.). Hauptabteilung Angewandte Datentechnik.

INTRODUCTION TO THE FRAMEWORK AND TASKS OF THE DFD [EINFUEHRUNG IN DAS UMFELD UND DIE AUFGABEN DES DFD]

Winfried Markwitz *In its* Proceedings of the 5th User Seminar of the German Remote Sensing Data Center of the DFVLR Feb. 1989 p 11-14 In GERMAN Original contains color illustrations (For primary document see N90-16318 08-43)

Avail: NTIS HC A07/MF A01; DFVLR, VB-PL-DO, Postfach 90 60 58, 5000 Cologne, Fed. Republic of Germany, 52 DM

The use of the space information potential is discussed. The enormous, steadily growing information potential opens many possible tasks in the fields of environment survey, inventories, and planning, especially for public services. However, the operational use of this potential data obtained in space requires the introduction and financing of new and efficient procedures, as well as the continuity of the supply of data, national data archives, and the formation of experts. Concrete and important tasks of the DFD (Deutsches Fernerkundungsdatenzentrum, German Remote Sensing Data Center) are the participation in large international and national projects, as well as the development of methods and systems for data evaluation ESA

N90-16320# Deutsche Forschungs- und Versuchsanstalt fuer Luft- und Raumfahrt, Oberpfaffenhofen (Germany, F.R.). Angewandte Datentechnik.

THE INTERACTIVE SYSTEM METEOROLOGY AND ITS USE IN METEOROLOGY AND OCEANOGRAPHY [DAS ISM UND SEINE ANWENDUNG IN METEOROLOGIE UND OZEANOGRAPHIE]

Thomas Koenig *In its* Proceedings of the 5th User Seminar of the German Remote Sensing Data Center of the DFVLR Feb. 1989 p 15-19 In GERMAN Original contains color illustrations (For primary document see N90-16318 08-43)

Avail: NTIS HC A07/MF A01; DFVLR, VB-PL-DO, Postfach 90 60 58, 5000 Cologne, Fed. Republic of Germany, 52 DM

In the framework of the replacement of hardware components, the Interactive System Meteorology (ISM) was developed, based on the Interactive Meteorological Image Processing System. The ISM was developed on Perkin-Elmer computers. It is conceived as a multi-operator system with an extended systems infrastructure. Access to ISM from almost any location is possible via the DATEX-P network of the Federal Postal Administration. Commands for data preprocessing and for physical handling of the data are available to the user. The contributions to different measuring campaigns are listed. ESA

N90-16321# Deutsche Forschungs- und Versuchsanstalt fuer Luft- und Raumfahrt, Oberpfaffenhofen (Germany, F.R.). Inst. fuer Physik der Atmosphaere.

DETERMINATION OF OPTICAL PORPERTIES OF CLOUDS FROM NOAA-AVHRR DATA USING APOLLO [BESTIMMUNG OPTISCHER EIGENSCHAFTEN VON WOLKEN AUS NOAA-AVHRR-DATEN MIT APOLLO]

K. T. Kriebel *In its* Proceedings of the 5th User Seminar of the German Remote Sensing Data Center of the DFVLR Feb. 1989 p 21-25 In GERMAN Original contains color illustrations (For primary document see N90-16318 08-43)

Avail: NTIS HC A07/MF A01; DFVLR, VB-PL-DO, Postfach 90 60 58, 5000 Cologne, Fed. Republic of Germany, 52 DM

The multispectral information from the advanced very high resolution radiometer (AVHRR) was used in the Apollo (AVHRR processing scheme over clouds, land and ocean) scheme to classify each pixel with respect to its cloud coverage degree. Preliminary comparison with flight measurements shows that optical thickness and liquid water content of water clouds can be determined with an accuracy better than about 50 percent. For ice clouds (cirrus), plausible values of optical thickness and ice water content were obtained. This allows the operational determination of optical properties of clouds which can be used for the description of initial values in numerical weather forecasting models. ESA

N90-16322# Deutsche Forschungs- und Versuchsanstalt fuer Luft- und Raumfahrt, Oberpfaffenhofen (Germany, F.R.). Hauptabteilung Angewandte Datentechnik.

RECOGNITION AND DISTINCTION OF CLOUDS, SNOW, AND ICE USING AVHRR DATA [ERKENNUNG UND UNTERSCHEIDUNG VON WOLKEN, SCHNEE UND EIS MIT HILFE VON AVHRR-DATEN]

Gerhard Gesell *In its* Proceedings of the 5th User Seminar of the German Remote Sensing Data Center of the DFVLR Feb. 1989 p 27-31 In GERMAN Original contains color illustrations (For primary document see N90-16318 08-43)

Avail: NTIS HC A07/MF A01; DFVLR, VB-PL-DO, Postfach 90 60 58, 5000 Cologne, Fed. Republic of Germany, 52 DM

Cloud recognition algorithms were used for the classification and interpretation of multispectral AVHRR advanced very high resolution radiometer (AVHRR) information. Starting from the properties of several cloud types, the algorithms subject the measured reflectivities or black body temperatures to a threshold test, or analyze the statistical distributions of these quantities over a smaller part of the image, resulting in a snow and ice classification. ESA

N90-16323# Freie Univ., Berlin (Germany, F.R.). Zentraleinrichtung fuer Audiovisuelle Methoden.

SATELLITE IMAGE SEQUENCES FOR MOTION ANALYSIS AND CHANGE DETECTION [SATELLITENBILDSEQUENZEN FUER BEWEGUNGSANALYSE UND CHANGE DETECTION]

Christian Zick *In* DFVLR, Proceedings of the 5th User Seminar of the German Remote Sensing Data Center of the DFVLR Feb. 1989 p 33-35 In GERMAN Original contains color illustrations (For primary document see N90-16318 08-43)

Avail: NTIS HC A07/MF A01; DFVLR, VB-PL-DO, Postfach 90 60 58, 5000 Cologne, Fed. Republic of Germany, 52 DM

Techniques and representation forms were developed for change detection of remote sensing data, with a view to analysis of sequences of image data from geostationary satellites (Meteosat). Several Meteosat film scenes demonstrate the application possibilities for quantitative and qualitative cloud motion analysis. ESA

N90-16324# Freie Univ., Berlin (Germany, F.R.). Inst. fuer Geophysikalische Wissenschaften.

PRELIMINARY EXPERIENCES WITH A NOVEL METHOD FOR THE DETERMINATION OF DISPLACEMENT VECTOR FIELDS AND SATELLITE IMAGE SEQUENCES [ERSTE ERFAHRUNGEN MIT EINER NEUEN METHODE ZUR BESTIMMUNG VON VERSCHIEBUNGSVEKTORFELDERN AUS SATELLITENBILDFOLGEN]

Anke Eriksson *In* DFVLR, Proceedings of the 5th User Seminar of the German Remote Sensing Data Center of the DFVLR Feb. 1989 p 37-38 In GERMAN (For primary document see N90-16318 08-43)

Avail: NTIS HC A07/MF A01; DFVLR, VB-PL-DO, Postfach 90 60 58, 5000 Cologne, Fed. Republic of Germany, 52 DM

Displacement vectors are calculated from digital image sequences in image regions with homogeneous or linear gray value variations using a directed smoothness requirement. Real discontinuities are not covered by this method. The calculation of the displacement vector field is formulated as a minimization problem, for which the solution is a system of nonlinear partial differential equations. Tests with Meteosat-WV-image sequences gave the basic structure of the wind fields via the displacement vector fields. Several problems emerged which require more extensive testing. ESA

N90-16325# European Space Agency. ESRIN, Frascati (Italy). Earthnet.

ESA/EARTHNET Status Report [ESA/EARTHNET: EIN STATUS REPORT]

Juerg Lichtenegger *In* DFVLR, Proceedings of the 5th User Seminar of the German Remote Sensing Data Center of the DFVLR Feb. 1989 p 39-41 In GERMAN (For primary document see N90-16318 08-43)

Avail: NTIS HC A07/MF A01; DFVLR, VB-PL-DO, Postfach 90 60 58, 5000 Cologne, Fed. Republic of Germany, 52 DM

The status of the ESA/Earthnet program is outlined. The data of several long range reconnaissance satellites is operationally received. LANDSAT data is prepared by Earthnet and commercialized by Eurimage. The status of the long range reconnaissance missions, LANDSAT 5 MSS and TM, SPOT, and MOS-1, is given. ESA

N90-16326# SPOT Image Corp., Toulouse (France).

SPOT AFTER TWO YEARS IN OPERATION: AN APPRAISAL OF RESULTS AND A REVIEW OF SELECTED APPLICATIONS

J. C. Rivereau and M. Pousse *In* DFVLR, Proceedings of the 5th User Seminar of the German Remote Sensing Data Center of the DFVLR Feb. 1989 p 43-46 (For primary document see N90-16318 08-43)

Avail: NTIS HC A07/MF A01; DFVLR, VB-PL-DO, Postfach 90 60 58, 5000 Cologne, Fed. Republic of Germany, 52 DM

The results of the first two years of SPOT in orbit are reviewed. During this period 662,000 images of the earth were acquired. In addition to the 8 directly receiving stations currently in operation, 5 new stations were expected to begin receiving SPOT in 1988. Out of the total archived scenes, about 25 percent are usable and represent a cloud cover of under 10 percent, while 50 percent are not usable at all (cloud cover more than 7/8). The market share taken by SPOT products rose steadily during these first two years and the SPOT specific capabilities attracted new customers. The usefulness of SPOT data in all fields of remote sensing was demonstrated. The most striking results were obtained in the field of cartography. The main manufacturers in stereoplotting equipment have now specific software adapted to the SPOT data. ESA

N90-16327# Freiburg Univ. (Germany, F.R.). Inst. fuer Physische Geographie.

EVALUATION OF THE PASTURE POTENTIAL IN THE DRY AREAS OF KENYA USING COMBINED EARTH RECONNAISSANCE [DIE BEWERTUNG DES WEIDEPOTENTIALS IN DEN TROCKENGEBIETEN KENIAS MIT HILFE DER KOMBINIERTEN ERDERKUNDUNG]

Ruediger Maeckel *In* DFVLR, Proceedings of the 5th User Seminar of the German Remote Sensing Data Center of the DFVLR Feb. 1989 p 47-51 In GERMAN Original contains color illustrations (For primary document see N90-16318 08-43)

Avail: NTIS HC A07/MF A01; DFVLR, VB-PL-DO, Postfach 90 60 58, 5000 Cologne, Fed. Republic of Germany, 52 DM

The fundamentals of land use and long term planning in the dry areas of Kenya were studied using LANDSAT-MSS data. The land qualification types were classified according to vegetation, soil, limitations to the use, phytomass and capacity, and requirements for use. ESA

N90-16328# Wuerzburg Univ. (Germany, F.R.). Inst. fuer Geographie.

FOREST MAPPING NUERENBERG GERMAN NATIONAL FOREST WITH SPECIAL EMPHASIS ON THE SPECTRAL REFLECTION BEHAVIOR OF PINE TREES [WALDKARTIERUNG IM NUERNBERG REICHSWALD UNTER BESONDERER BERUECKSICHTIGUNG DES SPEKTRALEN REFLEXIONSVERHALTENS BEI DER KIEFER]

Juergen Janoth *In* DFVLR, Proceedings of the 5th User Seminar of the German Remote Sensing Data Center of the DFVLR Feb. 1989 p 53-55 In GERMAN Original contains color illustrations (For primary document see N90-16318 08-43)

Avail: NTIS HC A07/MF A01; DFVLR, VB-PL-DO, Postfach 90 60 58, 5000 Cologne, Fed. Republic of Germany, 52 DM

Multitemporal LANDSAT-TM data is used to detect location-determined differences in forest vegetation. The images form the basis for a careful signature analysis and for several maximum likelihood classifications. The results show that there exist three natural age types of pine-trees, and that differences in the reflection behavior are correlated with location. ESA

N90-16329# Technische Univ., Munich (Germany, F.R.). Geologisches Inst.

ATTEMPT TO DRAW CONCLUSIONS CONCERNING THE GEOLOGICAL SUBSOIL FROM THE VEGETATION USING DIGITAL IMAGE PROCESSING OF TM DATA [VERSUCH EINES RUECKSCHLUSSES AUS DER VEGETATION AUF DEN GEOLOGISCHEN UNTERGRUND MIT HILFE DIGITALER BILDVERARBEITUNG NACH TM-DATEN]

Tobias Wever *In* DFVLR, Proceedings of the 5th User Seminar of the German Remote Sensing Data Center of the DFVLR Feb. 1989 p 57-62 In GERMAN Original contains color illustrations (For primary document see N90-16318 08-43)

Avail: NTIS HC A07/MF A01; DFVLR, VB-PL-DO, Postfach 90 60 58, 5000 Cologne, Fed. Republic of Germany, 52 DM

The extent to which conclusions can be drawn concerning the geological subsoil in humid areas where this subsoil is masked by soil or vegetation is investigated. There exists a clear correlation between soil type (grain size) and crop yield, the determining factor being the ground water, providing a point where remote sensing can hook in. A second point is the surprisingly high degree of correlation between cultivation of the soil and geological subsoil. The results show clay-like soils (pseudogley) can be discriminated from sandy soils by the spectral signature as well as by the cultivation of the soil. However, the method only allows large differences to be determinated. ESA

N90-16330# Freiburg Univ. (Germany, F.R.). Inst. fuer Physische Geographie.

THE DETERMINATION OF SUBSCALE STRUCTURES IN THERMAL IMAGES [DIE ERFASSUNG SUBSKALIGER STRUKTUREN IN THERMALBILDERN]

D. Scherer *In* DFVLR, Proceedings of the 5th User Seminar of the German Remote Sensing Data Center of the DFVLR Feb. 1989 p 63-67 In GERMAN Original contains color illustrations (For primary document see N90-16318 08-43)

Avail: NTIS HC A07/MF A01; DFVLR, VB-PL-DO, Postfach 90 60 58, 5000 Cologne, Fed. Republic of Germany, 52 DM

A method is presented to improve the spatial resolution of thermal images via the calculation of synthetic temperature distributions. From the heat budget equation, regression models were deduced, containing long wavelength emission, radiation,

height, and percentage of thermally relevant classes. From the thermal image the radiation temperature and hence the long wavelength emission of each pixel were calculated. From the height model a topographic model was obtained, allowing the calculation of radiation. The contribution of the classes to each pixel of the thermal image can be obtained from the land use classification. Regressions then provide the regression quantities as well as the variance reconnaissance. The synthetic distribution of the long wavelength emission and the corresponding, highly resolved radiation temperatures are then calculated. ESA

N90-16331# Deutsche Forschungs- und Versuchsanstalt fuer Luft- und Raumfahrt, Oberpfaffenhofen (Germany, F.R.). Hauptabteilung Angewandte Datentechnik.

INVESTIGATION OF THE BACKSCATTER BEHAVIOR OF SELECTED TEST AREAS IN TWO GEOCODED SEASAT-SAR SCENES IN GREATER BONN (FED. REPUBLIC OF GERMANY) [UNTERSUCHUNG UEBER DAS RUECKSTREUVERHALTEN AUSGEWAEHLTER TESTGEBIETE IN ZWEI GEOKODIERTEN SEASAT-SAR-SZENEN IM GROSSRAUM BONN]

Eva Boensch *In its* Proceedings of the 5th User Seminar of the German Remote Sensing Data Center of the DFVLR Feb. 1989 p 69-72 In GERMAN Original contains color illustrations (For primary document see N90-16318 08-43)

Avail: NTIS HC A07/MF A01; DFVLR, VB-PL-DO, Postfach 90 60 58, 5000 Cologne, Fed. Republic of Germany, 52 DM

Two geocoded SEASAT-SAR scenes were analyzed to provide information for geoscientific research. It is shown that geocoded data make it possible to have pixel accuracy, and to superimpose information from topographic maps and models, and from aerial pictures, directly onto satellite pictures, providing a guarantee for an exact definition of the test areas. The radar data allows the recognition of geological and geomorphological phenomena, as well as the demarcation of natural and cultural spatial units (agriculture, forest, settlement). ESA

N90-16332# Deutsche Forschungs- und Versuchsanstalt fuer Luft- und Raumfahrt, Oberpfaffenhofen (Germany, F.R.). Hauptabteilung Angewandte Datentechnik.

INVESTIGATION OF THE TOPOGRAPHIC COMPONENTS OF THE IMAGE CONTENT OF RADAR PICTURES [UNTERSUCHUNG DER TOPOGRAPHISCHEN KOMPONENTE DES BILDINHALTES VON RADARBILDERN]

Thomas Bayer *In its* Proceedings of the 5th User Seminar of the German Remote Sensing Data Center of the DFVLR Feb. 1989 p 73-76 In GERMAN Original contains color illustrations (For primary document see N90-16318 08-43)

Avail: NTIS HC A07/MF A01; DFVLR, VB-PL-DO, Postfach 90 60 58, 5000 Cologne, Fed. Republic of Germany, 52 DM

A simple empirical method was developed for the extraction of the topographic components in pictures of orbit supported SAR (synthetic aperture radar) systems. The coded SAR pictures were analyzed using a digital height model. The tests show a good general agreement with the theoretically expected results of the measurements of the backscatter coefficient as a function of the local incidence angle. A synthetic picture, representing the average effect of the local incidence angle in the original picture is produced. This picture is a first approximation of the representation of the topographic components of the backscatter valve in the original. The final results are in the form of synthetic, color-coded pictures. Settlements, cultivated areas, and water surface can be very clearly discriminated. ESA

N90-16333# Institut fuer Angewandte Geodaesie, Frankfurt am Main (Germany, F.R.).

FOCAL RESEARCH EFFORT POINTS OF THE INSTITUTE OF APPLIED GEODESY IN THE FIELD OF DIGITAL IMAGE PROCESSING [ARBEITSSCHWERPUNKTE DES INSTITUTS FUER ANGEWANDTE GEODAESIE IN DER DIGITALEN BILDVERARBEITUNG]

H. Schmidt-Falkenberg and B.-S. Schulz *In* DFVLR, Proceedings of the 5th User Seminar of the German Remote Sensing Data Center of the DFVLR Feb. 1989 p 77-81 In GERMAN (For primary document see N90-16318 08-43)

Avail: NTIS HC A07/MF A01; DFVLR, VB-PL-DO, Postfach 90 60 58, 5000 Cologne, Fed. Republic of Germany, 52 DM

Research efforts in the fields of photogrammetry and remote sensing were performed. Photogrammetric measurements were conducted with a view to earth reconnaissance, earth survey, and topography survey, using digital images of electromagnetic radiation in several spectral ranges. The results are stored in topographic and thematic data bases, which can be used for landscape models. ESA

N90-16334# Bundesanstalt fuer Geowissenschaften und Rohstoffe, Hannover (Germany, F.R.).

UTILIZATION OF REMOTE SENSING IN GEOSCIENTIFIC DEVELOPMENT AND PROJECTS [ANWENDUNG DER FERNERKUNDUNG IN GEOWISSENSCHAFTLICHEN ENTWICKLUNGSHILFEPROJEKTEN]

D. Bannert and W. Kruck *In* DFVLR, Proceedings of the 5th User Seminar of the German Remote Sensing Data Center of the DFVLR Feb. 1989 p 83-86 In GERMAN Original contains color illustrations (For primary document see N90-16318 08-43)

Avail: NTIS HC A07/MF A01; DFVLR, VB-PL-DO, Postfach 90 60 58, 5000 Cologne, Fed. Republic of Germany, 52 DM

The current and planned development aid projects in the fields of hydrology and soil science, based on remote sensing, and in particular, satellite remote sensing, are listed. The satellite data are processed in the image processing system GLOBUS. ESA

N90-16335# Bundesforschungsanstalt fuer Landeskunde und Raumordnung, Bonn (Germany, F.R.).

USE OF REMOTE SENSING DATA FOR LAND AND BUILDING STATISTICS [NUTZUNG VON FERNERKUNDUNGSDATEN FUER ZWECKE DER GRUNDSTUECKS- UND GEBAEUDESTATISTIK]

Volkmar Kroesch *In* DFVLR, Proceedings of the 5th User Seminar of the German Remote Sensing Data Center of the DFVLR Feb. 1989 p 87-88 In GERMAN Original contains color illustrations (For primary document see N90-16318 08-43)

Avail: NTIS HC A07/MF A01; DFVLR, VB-PL-DO, Postfach 90 60 58, 5000 Cologne, Fed. Republic of Germany, 52 DM

Aerial pictures and other remote sensing data were used for land and building statistics. Large scale aerial pictures allow detailed mapping. Smaller scale pictures allow the discrimination of settlement types according to type and density. Satellite pictures seem to provide higher geometric resolution. ESA

N90-16336# Technische Univ., Berlin (Germany, F.R.). Inst. fuer Landschafts- und Freiraumplanung.

USE OF REMOTE SENSING IN OPERATIONAL INVENTORY AND MONITORING AGRICULTURAL AND FORESTRY TASKS [EINZBEZIEHUNG DER FERNERKUNDUNG IN OPERATIONELLE INVENTUR- UND UEBERWACHUNGSAUFGABEN DER LAND- UND FORSTWIRTSCHAFT]

H. Kenneweg *In* DFVLR, Proceedings of the 5th User Seminar of the German Remote Sensing Data Center of the DFVLR Feb. 1989 p 89-95 In GERMAN Original contains color illustrations (For primary document see N90-16318 08-43)

Avail: NTIS HC A07/MF A01; DFVLR, VB-PL-DO, Postfach 90 60 58, 5000 Cologne, Fed. Republic of Germany, 52 DM

The operational use of remote sensing data, with a view to inventories and monitoring in the fields of agriculture and forestry, is explained. Examples are given to illustrate the use. ESA

N90-16337# Bundesanstalt fuer Gewaesserkunde, Koblenz (Germany, F.R.).

SUPPORT OF HYDROLOGICAL MODELS CALCULATIONS BY SATELLITE DATA [UNTERSTUETZUNG HYDROLOGISCHER MODELLRECHNUNGEN DURCH SATELLITENDATEN]

Herrman G. Mendel *In* DFVLR, Proceedings of the 5th User Seminar of the German Remote Sensing Data Center of the DFVLR Feb. 1989 p 97-100 In GERMAN Original contains

color illustrations (For primary document see N90-16318 08-43) Avail: NTIS HC A07/MF A01; DFVLR, VB-PL-DO, Postfach 90 60 58, 5000 Cologne, Fed. Republic of Germany, 52 DM

Experiences with the combined use of ground and satellite data in hydrology models are presented. The high correlation between upper cloud boundary temperature and the intensity of the precipitation, as well as between draining off and land use type are noted. ESA

N90-16338# Statistisches Bundesamt, Wiesbaden (Germany, F.R.).

STATISTICAL INFORMATION SYSTEM FOR CULTIVATION OF THE SOIL. USE OF REMOTE SENSING IN OFFICIAL STATISTICS [STATISCHES INFORMATIONSSYSTEM ZUR BODENNUTZUNG. EINSATZ VON FERNERKUNDUNG IN DER AMTLICHEN STATISTIK]

Walter Radermacher *In* DFVLR, Proceedings of the 5th User Seminar of the German Remote Sensing Data Center of the DFVLR Feb. 1989 p 101-107 In GERMAN Original contains color illustrations (For primary document see N90-16318 08-43) Avail: NTIS HC A07/MF A01; DFVLR, VB-PL-DO, Postfach 90 60 58, 5000 Cologne, Fed. Republic of Germany, 52 DM

The concept of a statistical information system for cultivation of the soil is under study. The system aims at the following characteristics: capability to process aerial pictures; satellite pictures and digital topographic maps; interpretation of aerial pictures on scale 1:32,000; as an interpretation basis the topographic maps TK25; systematic determination of cultivation types in agreement with the data users; and units of cultivation. ESA

N90-16339# Freie Univ., Berlin (Germany, F.R.). Inst. fuer Weltraumtechnik.

TM LAND USE CLASSIFICATION OF A REGION. UTILIZATION FOR PLANNING AND STATISTICS [TM LANDNUTZUNGSKLASSIFIKATION EINER REGION. NUTZEN FUER PLANUNG UND STATISTIK]

Christiane Schmullius *In* DFVLR, Proceedings of the 5th User Seminar of the German Remote Sensing Data Center of the DFVLR Feb. 1989 p 109-113 In GERMAN Original contains color illustrations (For primary document see N90-16318 08-43) Avail: NTIS HC A07/MF A01; DFVLR, VB-PL-DO, Postfach 90 60 58, 5000 Cologne, Fed. Republic of Germany, 52 DM

Satellite picture data is used for land use mapping. A land use map of the region of the Upper Rhine with 16 land use classes is digitally established based on LANDSAT-5 TM data. The analysis of the phenological situation shows that the development of vegetation is dominated by local effects. The classification accuracy of land use types is 93.8 percent. The agreement between satellite data and official land statistics is best for water surfaces and global surfaces. ESA

44 ENERGY PRODUCTION AND CONVERSION

Includes specific energy conversion systems, e.g., fuel cells; global sources of energy; geophysical conversion; and windpower.

For related information see also *07 Aircraft Propulsion and Power, 20 Spacecraft Propulsion and Power,* and *28 Propellants and Fuels.*

N90-16340# Spectracom, Canoga Park, CA.

SPECTRAL SENSITIVITY OF DEVICE POWER OUTPUT FOR TANDEM A-Si ALLOY SOLAR CELLS Final Report, 21 May 1986 - 31 May 1988

K. Eskenas May 1989 26 p Prepared for Midwest Research Inst., Golden, CO

(Contract DE-AC02-83CH-10093)

(DE89-009421; SERI/STR-211-3510) Avail: NTIS HC A03/MF A01

The purpose of this project was to investigate the feasibility of single and multifunction a:Si alloy solar cells when considered under solar spectra corresponding to a typical day or year. In order to determine the spectral sensitivity of single and tandem solar cell devices, a computer model was developed. Modeled spectral irradiance data for clear sky conditions was computed using the SERI SPCTRL2 computer code. It was found that the normalized integrated power output over the course of a typical day or year was very similar for the modeled single junction and 2- and 4-terminal tandem devices. The implication of this result is that spectral changes from varying atmospheric conditions (air mass) affect total integrated power output in a manner that is relatively independent of device configuration. DOE

N90-16341# Ceramatec, Inc., Salt Lake City, UT.

DEVELOPMENT OF PLANAR GEOMETRY SOLID OXIDE FUEL CELLS Annual Technical Progress Report, 1 Dec. 1987 - 31 Dec. 1988

Ashok C. Khandkar and A. V. Virkar (Utah Univ., Salt Lake City.) Jan. 1989 55 p

(Contract GRI-5086-294-1292)

(PB90-100769; PROG-88608804; GRI-89/0154) Avail: NTIS HC A04/MF A01 CSCL 10A

The progress made towards the development of planar geometry SOFCs is summarized. Graded composite electrolytes, suitable for use in a fuel cell, were developed using two phase Bi2O3 solid solutions heterogeneously doped with ZrO2. Efforts are underway to minimize microstructural voids at heterogeneous interfaces via alternative processing techniques. Electrode/electrolyte interface characterization studies are in progress. Electrode performance was improved at planar SOFC electrolyte interfaces. GRA

N90-16342# Los Alamos National Lab., NM.

LOW RISK LOW POWER HEAT PIPE/THERMOELECTRIC SPACE POWER SUPPLY

W. A. Ranken, P. J. Drivas, and V. Raag (Thermo Electron Corp., Waltham, MA.) 1989 9 p Presented at the 7th Symposium on Space Nuclear Power Systems, Albuquerque, NM, 7-11 Jan. 1990

(Contract W-7405-eng-36)

(DE89-014817; LA-UR-89-1952; CONF-900109-2) Avail: NTIS HC A02/MF A01

This paper discusses guidelines directed towards achieving low mass reactor power systems and describes a system that combines features -- a number borrowed from earlier concepts -- that reduce mass at the same time as they reduce development risk and increase reliability. DOE

N90-16343# California Univ., Berkeley. Lawrence Berkeley Lab. Earth Sciences Div.

SOME CONSIDERATIONS ON RESOURCE EVALUATION OF THE GEYSERS

Gudmundur S. Bodvarsson, Scott Gaulke, and Mark Ripperda Aug. 1989 11 p Presented at the Annual Meeting of the Geothermal Resources Council, Santa Rosa, CA, 1-4 Oct. 1989

(Contract DE-AC03-76SF-00098)

(DE90-002119; LBL-27598; CONF-891031-9) Avail: NTIS HC A03/MF A01

Although large amounts of data have been collected at The Geysers, some reservoir parameters, such as initial liquid saturation, matrix permeability and the fracture network characteristics, are still poorly known. These parameters greatly affect results of resource evaluation and predictions of reservoir behavior. Several 2-D fractured porous medium models were developed for The Geysers; these models differ in assumptions regarding the initial liquid saturation and matrix permeabilities. These models indicate that the permeability-thickness product (kH) of the fracture network ranges from 10 to 75 Dm (30,000 to 225,000 md/ft) and matrix permeability ranges from 1 to 3 micro-Darcies. All three models yielded surprisingly similar predictions regarding the future generating capacities of different areas. DOE

N90-16344# Sandia National Labs., Albuquerque, NM. Wind Energy Research Div.
RAINFLOW COUNTING ALGORITHM FOR THE LIFE2 FATIGUE ANALYSIS CODE
L. L. Schluter and H. J. Sutherland 1989 3 p Presented at the 9th ASME Wind Energy Symposium, New Orleans, LA, 14-17 Jan. 1990
(Contract DE-AC04-76DP-00789)
(DE90-002834; SAND-89-1795C; CONF-900136-3) Avail: NTIS HC A01/MF A01

The LIFE2 computer code is a fatigue/fracture analysis code that is specialized to the analysis of wind turbine components. The numerical formulation of the code uses a series of cycle count matrices to describe the cyclic stress states imposed upon the turbine. In this formulation, each stress cycle is counted or binsed according to the magnitude of its mean stress and alternating stress components and by the operating condition of the turbine. A set of numerical algorithms are described that were incorporated into the LIFE2 code. These algorithms determine the cycle count matrices for a turbine component using stress-time histories of the imposed stress states. Example problems are used to illustrate the use of these algorithms. DOE

N90-16345# Sandia National Labs., Albuquerque, NM. Wind Energy Research Div.
PERFORMANCE PREDICTIONS FOR AN INTERMEDIATE-SIZED VAWT BASED ON PERFORMANCE OF THE 34-m VAWT TEST BED
Henry M. Dodd 1989 17 p Presented at the 9th ASME Wind Energy Symposium, New Orleans, LA, 14-17 Jan. 1990
(Contract DE-AC04-76DP-00789)
(DE90-002835; SAND-89-1536C; CONF-900136-4) Avail: NTIS HC A03/MF A01

The DOE/Sandia 34-m Vertical Axis Wind Turbine (VAWT) Test Bed is a research turbine that has been in operation for over a year. With the advanced technology components incorporated in the turbine (including airfoils, structures and variable speed operation), its performance can be used to predict next generation commercial VAWT potential. This paper begins with the predicted and measured performance results obtained from the Test Bed and applies these results to a hypothetical commercial machine of the same size. The effects of a number of parameters are included in the performance analyses. First, the importance of siting considerations are presented, including wind frequency distributions (both real and Rayleigh) and mean wind speed and wind shear effects. Next, the paper shows the relative contribution of variable speed operation to improved performance and discusses other aspects of variable speed. The predicted performance of a 34-m VAWT is compared to existing machines, with annual energy capture per unit of swept area being the primary comparative metric. Finally, some cost of energy considerations associated with these technological advances are covered. DOE

N90-16346# Oak Ridge National Lab., TN.
ABSORPTION FLUIDS DATA SURVEY: 1989 UPDATE Topical Report No. 1
R. A. Macriss and T. S. Zawacki 1989 40 p Prepared in cooperation with Institute of Gas Technology, Chicago, IL
(Contract DE-AC05-84OR-21400)
(DE90-003985; ORNL/Sub-84-47989/4) Avail: NTIS HC A03/MF A01

This is an update of a series of prior reports on absorption fluids and data, ORNL/Sub/84-47989/1, 2, and 3. It covers additional data developed and published mainly during 1985 to 1988, and cites 44 additional references. Seventy-four different worldwide publications containing data relating to properties of binary, ternary, and multicomponent absorption fluids were identified. Of these, 30 manuscripts include applications of absorption fluid properties data toward evaluation, assessment, or design of chillers or heat pumps but do not include actual fluid properties data. The remaining 44 publications date as far back as 1929, but over 50 percent of these documents were published between 1985 and 1988. The texts of the 44 manuscripts are in English, German, Japanese, Russian, or French. The absorption fluids discussed in the 44 documents are combinations of 9 different refrigerant compounds and 30 single, 7 binary, and 1 ternary absorbent compounds. DOE

N90-16347# Giner, Inc., Waltham, MA.
IMPROVED ANODE CATALYSTS FOR COAL GAS-FUELED PHOSPHORIC ACID FUEL CELLS Progress Report, 3 Jun. - 2 Sep. 1989
Nancy Kackley and John A. Kosek Sep. 1989 10 p
(Contract DE-AC21-88MC-25170)
(DE90-004016; DOE/MC-25170/2779) Avail: NTIS HC A02/MF A01

The development, optimization and demonstration of contaminant-tolerant anode catalyst formulations for phosphoric acid fuel cells is the overall objective of this project. The goal is to develop supported catalyst systems that will not only be able to operate on feed gases containing high levels of CO, H2S, and COS, but will, in fact, encourage the shift reaction to convert the CO to additional H2 or anodically convert CO to CO2, boosting the power content of the fuel gas. Of CO conversion is not feasible, a secondary goal is to demonstrate CO- and H2S-tolerant catalysts so that gas cleanup requirements can be minimized. Upper limits for individual contaminant concentrations and mixtures of contaminant gases that can be tolerated by the advanced anode catalysts will be determined. This quarter, the two catalysts selected for testing were Pt-Ti-Ru and Pt-Ti-ZA, hydrogen/hydrogen cell testing continued. DOE

N90-16348# Oak Ridge National Lab., TN. Energy Div.
FEDERAL ROLES TO REALIZE NATIONAL ENERGY-EFFICIENCY OPPORTUNITIES IN THE 1990S
Eric Hirst Oct. 1989 47 p
(Contract DE-AC05-84OR-21400)
(DE90-004410; ORNL/CON-290) Avail: NTIS HC A03/MF A01

Improving energy efficiency throughout the U.S. economy is a vital component of our nation's energy future, with many benefits. Improving efficiency can: save money consumers, increase economic productivity and international competitiveness, reduce oil and gas prices by reducing the demand for foreign oil, enhance national security by lowering oil imports, reduce the adverse environmental consequences of fuel cycles, especially acid rain and global warming, add diversity and flexibility to the nation's portfolio of energy resources, respond to public interest in, and support of, energy efficiency. The primary purpose of this report is to suggest expanded roles for the U.S. Department of Energy (DOE) in improving energy efficiency during the 1990s. In an ideal world, the normal workings of the market place would yield optimal energy-efficiency purchase and operating decisions. Unfortunately, distortions in fuel prices, limited access to capital, misplaced incentives, lack of information, and difficulty in processing information complicate energy-related decision making. Thus, consumers in all sectors of the economy underinvest in energy-efficient systems. These market barriers, coupled with growing concern about environmental quality, justify a larger Federal role. DOE

N90-16349# Japan Atomic Energy Research Inst., Takasaki.
RADIATION RESISTANCE OF SOLAR CELLS FOR SPACE APPLICATION. 1: STUDY ON THE IRRADIATION PROCEDURE OF ELECTRON BEAMS
Hiroshi Mitsui, Ryuichi Tanaka, Hiromi Sunaga, Takao Kanazawa, Susumu Tanaka, Yasuyuki Haruyama, Takashi Agematsu, Sumio Matsuda, Takashi Noguchi, and Takashi Tamura (National Space Development Agency, Tokyo, Japan) et al Jul. 1989 172 p In JAPANESE; ENGLISH summary
(DE90-719546; JAERI-M-89-085) Avail: NTIS (US Sales Only) HC A08/MF A01

A 50 micron thick ultrathin silicon solar cell and a 280 micron thick high performance AlGaAs/GaAs solar cell with high radiation resistance were recently developed by National Space Development Agency of Japan (NASDA). In order to study the

radiation resistance of these cells, a joint research was performed between Japan Atomic Energy Research Institute (JAERI) and NASDA from 1984 through 1987. In this research, the irradiation method of electron beams, the effects of the irradiation conditions on the deterioration of solar cells by electron beams, and the annealing effects of the radiation damage in solar cells were investigated. The space radiation environment which artificial satellites will encounter, the solar cells used, and the experimental methods are described. In addition to these, the results of the study on the irradiation procedure of electron beams are reported. In the study of the irradiation method of electron beams, three methods, that is, the fixed irradiation method, the moving irradiation method, and the spot irradiation method were examined. In the fixed irradiation method and moving one, stationary solar cells and solar cells moving by conveyer were irradiated by scanning electron beams, respectively. On the other hand, in the spot irradiation method, stationary solar cells were irradiated by non-scanning steady electron beams. It was concluded that the fixed irradiation method was the most proper method. In addition to this some pieces of information were obtained with respect to the changes in the electrical characteristics of solar cells caused by the irradiation of electron beams. DOE

N90-16350# Argonne National Lab., IL. Energy Systems Div.
CONCEPTUAL DESIGN ANALYSIS FOR HYBRID-CYCLE OTEC PLANTS FOR CO-PRODUCTION OF ELECTRIC POWER AND DESALINATED WATER
T. Rabas, C. B. Panchal, and L. Genens 1989 11 p Presented at the International Conference on Ocean Energy Recovery, Honolulu, HI, 28-30 Nov. 1989 Submitted for publication
(Contract W-31-109-eng-38)
(DE90-003551; CONF-8911151-1) Avail: NTIS HC A03/MF A01

Hybrid-cycle Ocean Thermal Energy Conversion (OTEC) power plants are shown to be potentially the most flexible and cost effective in obtaining any specific mix of electrical power and desalinated water. This paper describes two particular hybrid configurations. One achieves maximum power production and the other achieves maximum water production for a given cold sea-water flow rate and pipe size. When power is the desired commodity and desalinated water is the by-product, the most effective configuration is the conventional hybrid cycle. When only water production is required, the desired configuration combines a multistage flash evaporator and a closed-cycle power OTEC plant, the latter generates the power to run the support equipment with no net or minimal power generation. DOE

N90-16351 Technische Univ., Delft (Netherlands). Inst. for Windenergy.
DEFINITION, TRANSFORMATION-FORMULAE AND MEASUREMENTS OF TIPVANE ANGLES
A. Bruining Oct. 1987 56 p Sponsored by the Netherlands Ministry of Economic Affairs
(IW-R510; ISBN-90-6275-424-4; ETN-90-96002) Copyright Avail: Delft Univ. Press, Stevinweg 1, 2628 CN Delft, Netherlands

The theoretical background of different angle systems used to define tipvane attitude in 3-D space is outlined. Different Euler equations are used for the various, wind tunnel, towing tank, and full scale tipvane models. The influence of rotor blade flapping angle on tipvane angles is described. The tipvane attitude measuring method is outlined in relationship to the Euler angle system. Side effects on the angle of attack of the tipvane due to rotation, translation, and curving of the tipvane are described. ESA

N90-16352# Midwest Research Inst., Golden, CO. Solar Energy Research Inst.
SERI (SOLAR ENERGY RESEARCH INSTITUTE) SOLAR RADIATION RESOURCE ASSESSMENT PROJECT Annual Progress Report, 1988
R. L. Hulstrom, E. Maxwell, C. Riordan, M. Rymes, and T. Stoffel Oct. 1989 77 p
(Contract DE-AC02-83CH-10093)
(DE89-009456; SERI/PR-215-3500) Avail: NTIS HC A05/MF A01

The earth receives vast amounts of energy from the sun in the form of incident solar radiation. Solar radiation drives the earth's weather and sustains life. As a result of the increasing costs, uncertain availability, and potentially severe environmental impacts of other sources of energy, insolation is being considered as a clean renewable energy source for our needs for heating, cooling, electricity, and fuels. Widespread interest and activities were initiated immediately after the oil embargo of the mid-1970s. For many applications, the insolation must be converted to a different form, such as heat, electricity, or a fuel (liquid, gas, or solid). A technology that can do this is known as a solar energy conversion device or technology. A wide range of candidate technologies is being developed. Some of these technologies include photovoltaics (converting insolation to electricity), solar thermal (converting insolation to heat), solar thermal-electric (converting insolation to heat, then to electricity), and biomass (converting insolation to biomass and then to fuels). DOE

N90-16353# Argonne National Lab., IL. Energy Systems Div.
EXPERIMENTAL INVESTIGATION OF CONDENSATION OF STEAM IN THE PRESENCE OF NONCONDENSABLE GASES FOR OPEN-CYCLE SURFACE CONDENSERS
C. B. Panchal and John C. Telotte (Florida State Univ., Tallahassee.) 1989 11 p Presented at the International Conference on Ocean Energy Recovery, Honolulu, HI, 28-30 Nov. 1989 Submitted for publication
(Contract W-31-109-eng-38)
(DE90-003552; CONF-8911151-2) Avail: NTIS HC A03/MF A01

Two experimental investigations are being carried out for determination of the effects of noncondensable gases on the rate of condensation in the open-cycle surface condenser. A single-channel test apparatus is being installed in Florida for a fundamental study of low-pressure condensation in the laminar-flow regime. The prototypical condenser configurations are tested in the Heat and Mass Transfer Scoping Test Apparatus (HMTSTA) facility in Hawaii. A series of tests have been conducted using existing condenser units in the HMTSTA. The data are analyzed and compared with theoretical predictions. DOE

N90-16354# New Energy Development Organization, Tokyo (Japan).
INVESTIGATION AND STUDY ON COMPRESSED AIR STORAGE POWER GENERATION SYSTEM, PART 2
Mar. 1989 159 p In JAPANESE and ENGLISH Prepared in cooperation with Electric Power Development Co. Ltd., Tokyo, Japan
(DE90-702648; NEDOJ-P-8825-Pt-2) Avail: NTIS (US Sales Only) HC A08/MF A01

Compressed air storage power generation system (CAES) was studied. As a system for response to peak loads, both output and efficiency were better than those of the previous year due to the study on the temperature of the turbine's inlet. As a system for response to peak and middle loads, steam power generation, which makes use of exhaust heat from the aftercooler and the low pressure turbine's outlet, was integrated into the system, and its heat efficiency was better than that of the usual thermal power generation. However, it is inferior to the latest LNG combined cycle power generation and it does not appeal much as a middle load power source. Deformation strength characteristics of the underground cavity rocks were clarified, and a multi-structure lining method was suggested. Its location area is restricted by the layer distribution. Construction cost per kW is 220,000 yen, and the power generation prime cost is a little higher than that of pumped storage power generation. As a pumped storage power station has difficulty in finding suitable location and is higher in costs, CAES can be put into existence as a system for response to peak loads in view of economy in the future. DOE

45 ENVIRONMENT POLLUTION

Includes atmospheric, noise, thermal, and water pollution.

N90-16355# National Oceanic and Atmospheric Administration, Silver Spring, MD. Air Resources Lab.
ECC (ELECTROCHEMICAL CONCENTRATION CELL) OZONESONDE OBSERVATIONS AT SOUTH POLE, ANTARCTICA, DURING 1988
W. D. Komhyr, J. A. Lathrop, R. W. Poston, and T. O. Mullen (National Oceanic and Atmospheric Administration, Boulder, CO.) Jun. 1989 284 p
(PB90-110172; NOAA-DR-ERL-ARL-18) Avail: NTIS HC A13/MF A02 CSCL 13B

Atmospheric ozone vertical distributions, air temperatures, and wind speed and wind direction data are presented for 67 balloon electrochemical concentration cell ozonesonde soundings made at South Pole, Antarctica, in 1988. GRA

N90-16356# Environmental Protection Agency, Washington, DC. Office of Research and Development.
SCIENTIFIC LINKAGES IN GLOBAL CHANGE
Peter R. Jutro, Robert C. Worrest, and Anthony C. Janetos 16 Jun. 1989 18 p Sponsored by Air and Waste Management Association, Pittsburgh, PA
(PB90-112608; EPA/600/D-89/126) Avail: NTIS HC A03/MF A01 CSCL 13B

In the atmosphere, certain trace gases both promote global warming and deplete the ozone layer. The primary radiatively active trace gases which affect global warming are carbon dioxide, nitrous oxide, chlorofluorocarbons, methane, and tropospheric ozone. In the troposphere, the atmosphere up to 10 miles above the earth's surface, these compounds function as greenhouse gases. Many of these gases also influence the concentration of ozone in the stratosphere, the atmospheric layer located between 10 to 30 miles above the earth's surface. The diffuse layer of ozone in the stratosphere protects life on earth from harmful solar radiation. A reduction of the layer could have very important impacts on the earth's systems. Interactions exist in various ecological processes as well. Physical, chemical, and biological activities of plants and animals are affected directly by global climate change and by increased ultraviolet radiation resulting from depletion of stratospheric ozone. GRA

N90-16357# National Oceanic and Atmospheric Administration, Silver Spring, MD. Air Resources Lab.
ECC (ELECTROCHEMICAL CONCENTRATION CELL) OZONESONDE OBSERVATIONS AT MIRNY, ANTARCTICA, DURING 1988
W. D. Komhyr, J. A. Lathrop (National Oceanic and Atmospheric Administration, Boulder, CO.), V. N. Arbuzova, V. U. Khattatov, P. G. Nureyev, V. V. Rudakov, and I. V. Zamyshlayev Sep. 1989 132 p Sponsored by NASA, Washington Prepared in cooperation with Central Aerological Observatory, Dolgoprudnyi (USSR)
(PB90-113960; NOAA-DR-ERL-ARL-19) Avail: NTIS HC A07/MF A01 CSCL 13B

Atmospheric ozone vertical distributions, air temperatures, and wind speed and direction data are presented for 40 balloon electrochemical concentration cell ozone soundings made at Mirny, Antarctica, in 1988. GRA

N90-16358# National Center for Atmospheric Research, Boulder, CO. Climate and Global Dynamics Div.
INTERCONNECTEDNESS IN NATURE AND IN SCIENCE: THE CASE OF CLIMATE AND CLIMATE MODELING Ph.D. Thesis - Colorado Univ.
Laurence P. Goldberg 1989 211 p
(Grant NSF ATM-87-09659)
(PB90-113986; NCAR/CT-121) Avail: NTIS HC A10/MF A02 CSCL 13B

Key aspects are reviewed of the history of conventional, hierarchically oriented, philosophical perspectives on science developed and within positivistic, historical, and systems traditions, and reviews, extends, and unifies recent alternatives to these traditions in recognition of the emerging research program within the philosophy of science. In keeping with the spirit of the program, the authors systematically apply its perspectives and methods to a single area of science, namely climate modeling. Climate modeling is an especially appropriate test case for the new philosophy of science because the complexities of the climate system and explanation and interdisciplinary cooperation in climate modeling all defy conventional forms of hierarchical analysis. Alternative perspectives are applied to explore: the complex interactions among and within the climate subsystems; the need to consider processes that are spatially and temporally unresolved by climate models in model confirmation; and the close forms of interdisciplinary cooperation required for adequate climate model development. Author

N90-16359# National Environmental Satellite Service, Washington, DC. Office of Research and Applications.
OPERATIONAL OZONE MONITORING WITH THE GLOBAL OZONE MONITORING RADIOMETER (GOMR)
Walter G. Planet, ed. Aug. 1989 33 p
(PB90-114034; NOAA-TM-NESDIS-28) Avail: NTIS HC A03/MF A01 CSCL 13B

The Global Ozone Monitoring Radiometer (GOMR) is planned for the next series of operational polar-orbiting meteorological satellites. The GOMR is conceived of being composed of two components: a nadir sounder for determining total ozone amounts and a limb sounder for determining vertical stratospheric distributions of temperature, ozone and other trace gases of importance to ozone photochemistry. GRA

N90-16360# Environmental Protection Agency, Washington, DC. Office of Research and Development.
POTENTIAL IMPACT OF STRATOSPHERIC OZONE DEPLETION ON MARINE ECOSYSTEMS
Robert C. Worrest, Hermann Gucinski, and John T. Hardy (Oregon State Univ., Corvallis.) 7 Dec. 1988 11 p Sponsored by Climate Inst., Washington, DC
(PB90-112616; EPA/600/D-89/125) Avail: NTIS HC A03/MF A01 CSCL 13B

As a result of stratospheric ozone depletion, ultraviolet-B radiation (290 to 320 nm; UV-B) reaching marine environments is likely to increase over the next few decades. Available information suggests that UV-B radiation can have variety of deleterious effects on marine ecosystem. It is pointed out that the current uncertainties in existing information and speculates on the range of possible effects. It is hoped that controversial aspects will stimulate discussion and additional needed research. Author

N90-16361# Argonne National Lab., IL.
ASSESSMENT OF THE IMPORTANCE OF ACIDIC FOGWATER AND CLOUDWATER IN AFFECTING TERRESTRIAL VEGETATION: SOME IMPORTANT CASE STUDIES
P. M. Irving and C. Eagar (Forest Service, Broomall, PA.) 1989 30 p Presented at the 82nd Annual APCA Meeting, Anaheim, CA, 25-30 Jun. 1989
(Contract W-31-109-eng-38)
(DE90-002216; CONF-890692-23) Avail: NTIS HC A03/MF A01

The purpose of this paper is to present some examples of terrestrial effects of concern as case studies to demonstrate the methodology to be used for answering questions of the NAPAP Integrated Assessment. The two examples presented, one each for forestry and crops, represent what is probably the worst case for possible acidic rain effects on crops and forests. Both examples revolve around hypotheses centering on stress from acidic fogwater or cloudwater. Because it is likely that additional information will become available prior to the publication of the Integrated Assessment, it should be understood that the analyses and interpretations presented on the following pages are subject to change when NAPAP publishes its final Assessment in 1990. DOE

N90-16362# Argonne National Lab., IL. Energy Systems Div.
ENVIRONMENTAL, HEALTH, AND SAFETY CONCERNS ASSOCIATED WITH NONPETROLEUM FUEL USE IN US TRANSPORTATION Progress Report No. 1
J. B. Rajan, C. L. Saricks, M. K. Singh, and W. J. Walsh Jun. 1989 57 p
(Contract W-31-109-eng-38)
(DE90-004367; ANL/ES-163) Avail: NTIS HC A04/MF A01

This report qualitatively examines the environmental, health, and safety concerns associated with the use of three alternative fuels in the US transportation system: methanol, compressed natural gas, and electricity. For each of these fuels, the results are presented for a literature review, discussions with specialists, and recent data from in-use fleet tests and summarizes the state of knowledge of their potential air pollution contribution from end use and process emissions relative to gasoline and diesel fuels. Carbon monoxide, particulate matter, ozone precursors (oxides of nitrogen and volatile organics), and carbon dioxide (from processing activities) are emphasized. Methanol-fueled vehicles are expected to have emissions comparable to their gasoline counterparts at least during the initial years, albeit with higher emissions of formaldehyde. Methanol production from coal may result in higher emissions of carbon dioxide. Compressed natural gas vehicles have the potential to reduce emissions of carbon dioxide and nonmethane hydrocarbons relative to conventional fuels. Electric vehicles using recharge power from nuclear or renewable energy sources hold the greatest promise for reduced air emissions. The manufacture and disposal of materials from lead-acid and nickel-iron batteries present safety concerns related to the potential emission of toxic materials. DOE

N90-16363# Oak Ridge National Lab., TN. Environmental Sciences Div.
ENVIRONMENTAL, HEALTH, AND CFC SUBSTITUTION ASPECTS OF THE OZONE DEPLETION ISSUE
R. I. VanHook, P. D. Fairchild, W. Fulkerson, A. M. Perry, J. D. Regan, and G. E. Taylor Nov. 1989 47 p
(Contract DE-AC05-84OR-21400)
(DE90-004404; ORNL-6552; ORNL-ESD-3308) Avail: NTIS HC A03/MF A01

In 1974 chlorofluorocarbons (CFCs) were identified as playing a major role in depleting the stratospheric ozone layer, a process which could potentially result in increasing levels of UV(B) radiation. Substantial progress has been made in the ensuing years, especially after the surprising discovery of the ozone hole in Antarctica in 1984. Investigation of this hole's development has led to improved understanding of heterogeneous gas-solid phase reaction kinetics occurring in the stratosphere, but there are still uncertainties in the developing theory of ozone depletion. The connection between global CFC production and stratospheric ozone depletion is plainly evident. It is also evident that the long atmospheric lifetimes of these synthetic organic chemicals lead to decadal time frames between the response on CFC emissions and the reaction of chlorine with stratospheric ozone molecules. It is generally accepted that complete CFC phaseout is required to alleviate this situation; however, even if emissions could be reduced to zero immediately, ozone depletion would continue for many decades although at a declining rate. A critical question to be addressed is that of the actual timing of the CFC phaseout. It appears to us that the decision to phase out CFCs completely (i.e., a 90 percent or 100 percent phaseout vs 50 percent phaseout as called for in the Montreal Protocol) is much more important than whether the phaseout occurs within the next 5 years or the next 10 years. DOE

N90-16364# Sandia National Labs., Albuquerque, NM. Strategic Technologies Div.
A QUALITATIVE ARCHITECTURE FOR UNDERSTANDING POLICY RESPONSES TO GLOBAL CHANGE
Dennis Engi 1989 8 p Presented at the 9th Miami International Congress on Energy and Environment, Miami Beach, FL, 11-13 Dec. 1989
(Contract DE-AC04-76DP-00789)
(DE90-003936; SAND-89-1338C; CONF-891210-2) Avail: NTIS HC A02/MF A01

An architecture is presented which will provide qualitative clarification of the principal cause-and-effect relationships among various policy options and the resulting impacts on anthropogenic greenhouse gas emissions. A fundamental product of analyzing the Global Change issue in the context of this architecture is the conceptual identification and internalization of conventionally external costs. The robust policy portfolios which evolve from this analysis will, by design, recognize the international dimension and be driven by adaptive incrementalism in order to avoid ill-conditioned and/or major, short-term, infrastructural changes to the energy systems. DOE

N90-16365# GKSS-Forschungszentrum Geesthacht (Germany, F.R.).
SIMULATION OF POLLUTANT TRANSPORT USING A MESOSCALE GRID CIRCULATION MODEL [BERECHNUNG DER ANFANGSBEDINGUNGEN FUER DEN STOFFTRANSPORT IN MESOSKALIGEN ZIRKULATIONSMODELLEN]
K. Bigalke and M. Schatzmann (Hamburg Univ., Germany, F.R.) 1989 217 p In GERMAN; ENGLISH summary
(GKSS-89/E/24; ISSN-0344-9629; ETN-90-96071) Copyright Avail: NTIS HC A10/MF A02

A numerical model developed for predicting the dispersion of pollutants emitted from a stack into the atmosphere is presented. The model is made up of an integral model used to simulate the jetlike nearfield of the dispersing plume, and of a diffusion model for the subsequent phase dominated by atmospheric turbulence. The two submodels are linked to each other. A detailed computer readout of the model accompanies test results. ESA

N90-16366# Los Alamos National Lab., NM.
PROCEEDINGS OF THE CONFERENCE ON TECHNOLOGY-BASED CONFIDENCE BUILDING: ENERGY AND ENVIRONMENT
John C. Allred, ed., Roger C. Eckhardt, ed., and Arthur S. Nichols, ed. Nov. 1989 27 p Conference held in Santa Fe, NM, 9-14 Jul. 1989; sponsored by California Univ.
(Contract W-7405-eng-36)
(DE90-003363; LA-UR-89-3440-Exc; CONF-8907103-Exc) Avail: NTIS HC A03/MF A01

This document contains excerpts from the proceedings of the conference on, Technology-Based Confidence Building: Energy and the Environment. It contains the agenda for the conference and a document on, Global Warming and Energy Use; a presentation on, From Militarism to Environmentalism: a New Focus of U.S.-Soviet Relations; a workshop on environmental challenges; a summary address on, Science, Technology, and World Affairs; an address entitled, Energy: the Coin of International Understanding; and concluding remarks. DOE

46 GEOPHYSICS

Includes aeronomy; upper and lower atmosphere studies; ionospheric and magnetospheric physics; and geomagnetism.

For space radiation see *93 Space Radiation.*

N90-16367 Washington Univ., Seattle.
THE EFFECT OF OROGRAPHIC FORCING ON THE MEAN FLOW OF THE STRATOSPHERE Ph.D. Thesis
Mark Douglas Iredell 1988 167 p
Avail: Univ. Microfilms Order No. DA8906909

Previous simple modeling studies have suggested a positive feedback mechanism in the interaction between the mean westerly flow of the stratosphere and the planetary waves propagating up from the troposphere. It is hypothesized that there exists a critical orographic forcing below which the stratosphere remains relatively quiet but above which the stratosphere is prone to sudden warmings of the polar regions. In order to test this hypothesis, a hybrid

version of the NCAR Community Climate Model is developed and used to determine the sensitivity of the mean flow of the stratosphere orographically forced planetary waves in the troposphere. The time-averaged stratospheric jet becomes weaker nearly linearly with increased orography in the model. The fraction of wave activity transmitting through the lower stratosphere is rather independent of orography. A quiet regime in the winter stratosphere is identified by a strong zonal jet located near 60 N that is maintained by a regular amount of planetary wave activity propagating up from the high-latitude troposphere into the stratospheric jet axis. The quiet regime is sometimes interrupted by sudden warming events when bursts of wave activity from the troposphere rapidly decelerate the stratospheric jet. While wave events occur in every model case, their frequency and strength increase substantially when the orography is increased to its normal level in the Northern Hemisphere. Major warmings occur only after the stratosphere is preconditioned by minor warmings that shift the stratospheric jet axis poleward. Dissert. Abstr.

N90-16368# Defence Science and Technology Organization, Salisbury (Australia).
UPPER ATMOSPHERE RESEARCH
K. H. Lloyd 1989 32 p
(ISBN-0-642-13582-7) Avail: NTIS HC A03/MF A01

From 1960 until 1977 the Weapons Research Establishment (WRE) undertook research into determining the properties of the upper atmosphere by the use of sounding rockets fired from the Woomera rocket range. This Monograph describes the experiments which were conducted. The experiments were aimed at measuring the temperature, density, constituents, ionization, and motions of the upper atmosphere between 60 and 200 km, about which at that time little was known. Many of the experiments were conducted in collaboration with Australian and overseas universities and research institutes, this work is also described. Author

N90-16369 Colorado State Univ., Fort Collins.
THE RESPONSE OF THE ATMOSPHERIC CONVECTIVE BOUNDARY LAYER TO SURFACE INHOMOGENEITIES Ph.D. Thesis
Mark Gregory Hadfield 1988 418 p
Avail: Univ. Microfilms Order No. DA8911794

Large-eddy simulations (LES) of the atmospheric convective boundary layer were conducted with a surface sensible heat flux that either is constant or varies on a spatial scale comparable to the boundary layer depth. The horizontally homogeneous simulations were compared with previous LES, laboratory and atmospheric studies. The dynamics of the simulated turbulence and the model's sensitivity to the subgrid diffusivity were investigated. In general the present model gives results similar to previous large-eddy simulations. All the LES models simulate a field of convective eddies having approximately the correct velocity and spatial scales, and with the crucial property that kinetic energy is transported vigorously upwards through the middle levels. Several failings of the models were identified, including a tendency to underpredict temperature variance and to overpredict vertical velocity skewness in the upper boundary layer. The surface heat-flux variations are one-dimensional and sinusoidal with a wave-length between one and four times the boundary layer depth. Simulations were carried out with zero wind or with a light mean wind perpendicular to the perturbations. Several effects were identified, though some are evident only after a gread deal of averaging. They include mean circulations in phase with the surface perturbations, modulation of the turbulence throughout the boundary layer and modifications (usually slight) to the profiles of horizontally averaged statistics. The mean boundary layer depth remains horizontally uniform. Most of the effects increase as the wavelength of the surface perturbation is increased and decrease with an imposed mean wind. Dissert. Abstr.

N90-16370 Colorado State Univ., Fort Collins.
MESOSCALE ANALYSIS BY NUMERICAL MODELLING COUPLED WITH SATELLITE-BASED SOUNDING Ph.D. Thesis
Alan Edmund Lipton 1988 205 p
Avail: Univ. Microfilms Order No. DA8911813

The development of a system for time-continuous mesoscale analysis and its use in studying the distribution of summertime convective cloud development in the Northeastern Colorado region are discussed. There are two basic components of the system--a numerical model and an algorithm for retrieving temperatures and water vapor concentrations from satellite data. The primary distinguishing feature of the new method is that there is an intimate coupling of the retrieval and modeling processes. Water vapor concentrations and ground surface temperatures were the foci of the analyses. The coupled analysis method was compared with other related methods by means of two-dimensional simulations and a three-dimensional case study. Analyses in which surface temperatures were derived from satellite-retrievals were compared with the alternative of relying on energy balance computations. The energy balance computations were so sensitive to soil characteristics, which were simulated as unknown, that the satellite retrieval method gave better results even with cloud contamination. In the case study, the horizontal and time variations of satellite-retrieved surface temperatures correspond closely to the conventional shelter temperature observations, but had much greater detail. In contrast, the energy balance-based temperatures tended to increase too quickly during the morning and lacked some of the observed gradients. For water vapor analysis the coupled method generally was the most valuable of the several methods considered because it exploited the major strengths of the numerical model and the satellite data while making it relatively easy to recognize any impacts of their weaknesses.
Dissert. Abstr.

N90-16371 Saint Louis Univ., MO.
DIAGNOSTIC AND KINEMATIC FIELDS ASSOCIATED WITH CURVED AND STRAIGHT JET STREAKS USING A TWO-LAYER PRIMITIVE EQUATION MODEL Ph.D. Thesis
Richard Charles Molinaro 1988 224 p
Avail: Univ. Microfilms Order No. DA8912779

The changes in the diagnostic and kinematic fields due to magnitude and curvature of jet streaks were studied using a two-layer primitive equation model. Thirteen (3 straight-line, 3 cyclonic, 3 anticyclonic, 1 low-level easterly, 2 baroclinic and 1 beta) jet streak case studies were performed along with three operational jet streak case studies. Results indicate a consistent weakening of the wind maximum for straight-line, cyclonic, anticyclonic and beta jet streak cases where the upper and lower-level waves were in phase during the model run. For the low-level easterly and baroclinic simulations the weakening of the jet maximum was much less; during one baroclinic case the magnitude of the wind even grew. Kinematic vertical motion fields displayed a consistent pattern of change during the jet streak motion along the top of a ridge or base of a trough, thus permitting the development of conceptual models for the evolution of the jet streak. Kinematic, along- and cross-contour omegas were computed from operational data. The resultant fields were not as well-defined as the primitive model cases but displayed similar features. Also a statistical analysis was performed by perturbing the original data and comparing the original resultant fields. The correlation coefficient was high for the kinematic omegas but low for the along- and cross-contour omegas. However, the perturbed fields still retained the major features of the original resultant fields. Dissert. Abstr.

N90-16372 California Univ., Los Angeles.
MULTIPLE FLOW REGIMES IN THE NORTHERN HEMISPHERE WINTER Ph.D. Thesis
Masahide Kimoto 1989 220 p
Avail: Univ. Microfilms Order No. DA8914064

Recurrent patterns in atmospheric circulation during a Northern Hemisphere winter were studied. The phase-space structure of observed 700mb geopotential height anomalies was examined using statistical techniques. Large-scale flow patterns that appear repeatedly and persist beyond synoptic time scales are objectively identified by a systematic search for the local maxima of multivariate

probability density functions (PDFs). This search is carried out in the phase space coordinatized by a few dominant spatial modes represented by empirical orthogonal functions (EOFs) of the sample covariance matrix of the height anomalies. The inherent difficulty in investigating multivariate PDFs with a limited number of samples is overcome by focusing on physically interesting parts of the phase space. First, visually hemispheric circulations are examined with the aid of bivariate PDFs to find indications of multiple regions in phase space which physically represent zonal and blocked flow regimes in the eastern halves of the two major oceans. An algorithm for classification is then based on multivariate PDFs, tailored to take the small-sample problem into account by discarding the information on the phase-space distance from the climatological mean. Based on the observed partial decoupling between the Pacific and the Atlantic-Eurasian sector, a classification algorithm is then applied to the regional data in these sectors. A total of 13 regional flow regimes are found. The temporal evolution of large-scale circulations is analyzed by a Markov-chain description based on the classification results. The existence of preferred routes of transition between various flow regimes is confirmed. Furthermore, cycles of regimes appear as candidates for intrinsic oscillations of both regional and hemispheric circulations. A synoptic characterization of the onsets and breaks of flow regimes is given by using a composition technique. It is shown how conditions external to the extratropics may favor the probability of appearance of some of the Northern Hemisphere flow regimes by studying statistical relations with the Southern Oscillation Index of the equatorial Central Pacific. Dissert. Abstr.

N90-16373 Alaska Univ., Fairbanks.
EFFECTS OF GRAVITY WAVES ON THE POLAR O2 AND OH AIRGLOW Ph.D. Thesis
Rodney Allen Viereck 1988 118 p
Avail: Univ. Microfilms Order No. DA8918593

The effect of gravity waves on the OH (87 km) and O2 (95 km) airglow emissions was examined using spectroscopic airglow data. The data was obtained from Longyearbyen, Svalbard, and Fairbanks, Alaska using Ebert-Fastie spectrometers and a system of Meridian Scanning Photometers. The spectrometers scanned in wavelength from 8200A to 8750A which included the airflow emissions from the OH(6 to 2) Meinel band and the O2(0 to 1) atmospheric band. The analysis was done by fitting a synthetic spectrum to the data and thereby the rotational temperature was calculated as well as the band intensity of each of the emissions. The rotational temperatures were assumed to represent the temperature of the emission region. Gravity waves were assumed to modify the density and temperature of the atmosphere in the region of the airflow emissions. These modifications were measured as fluctuations in the band intensity and rotational temperatures of the two emissions. In order to compare the data with theoretical models, it was necessary to calculate two parameters. The vertical and horizontal wavelengths, the phase speeds, and the propagation directions of several specific gravity wave examples were examined. During a 60 hour period of data, three well defined gravity waves were observed. The propagation directions implied a moving source south of the observing station. Dissert. Abstr.

N90-16374# Naval Ocean Systems Center, San Diego, CA.
LIDAR TECHNIQUE FOR ADJUSTING AEROSOL MODEL NUMBER DENSITIES TO EXISTING CONDITIONS Final Report, 30 Sep. 1988 - 30 Sep. 1989
H. G. Hughes and M. R. Paulson Sep. 1989 26 p
(AD-A213846; NOSC/TD-1637) Avail: NTIS HC A03/MF A01 CSCL 04/1

A technique is introduced by which the total number density of the LOWTRAN 7 Navy Maritime Aerosol Model is adjusted to represent existing atmospheric conditions. Measurements of the vertical profile of relative humidity and surface wind speeds are used with the model to determine the aerosol extinction and backscatter coefficients variations with altitude. Using the single scatter lidar (light detection and ranging) equation, these parameters are then used to calculate a range compensated power, S(h), from an airborne system. An iterative method is used by which the calculated S(h) values are adjusted to agree with corresponding measured values. Examples are presented of extinction and backscatter coefficients variations with range from the lidar calculated using adjusted size distribution. Also presented are the computer program and operating instructions for adjusting the size distributions at each altitude. GRA

N90-16375# Naval Ocean Systems Center, San Diego, CA.
ATMOSPHERIC TRANSMITTANCE DETERMINATION FROM A TWO-ANGLE MEASUREMENT OF RADIANCE CHANGE Final Report, Jun. 1987 - Nov. 1988
J. Smith and H. G. Hughes Sep. 1989 14 p
(AD-A213847; NOSC/TD-1636) Avail: NTIS HC A03/MF A01 CSCL 04/1

An experimental technique is described for estimating atmospheric transmittance to space from the ground. Using an idealized model for atmospheric absorption, it is shown that the measurement of the ratio of radiance gradients at two different zenith angles can be used to estimate the clear-sky transmittance. Transmittance obtained with this technique were compared with LOWTRAN 6 calculations using measured profiles of meteorological parameters. Results show the modeled transmittances to be in agreement with 10 percent for zenith angles above the horizon. GRA

N90-16376# International Centre for Theoretical Physics, Trieste (Italy).
ARE GRAVITONS WINDOWS TO HIGHER DIMENSIONS
Leszek M. Sokolowski (Jagellonian Univ., Cracow, Poland) May 1989 11 p Sponsored in part by Polish Research Programme
(DE90-600756; IC-89/99) Avail: NTIS (US Sales Only) HC A03/MF A01

A plane-fronted gravitational wave with parallel rays (pp wave) interacting with the radius of the internal space (the dilaton field) is studied for any number of dimensions. In 4-D the wave reduces to a Kerr-Schild wave coupled to the dilaton. It is distinguished from an ordinary system gravitational-wave-scalar-field by a special relation between one of its invariants and the source. DOE

N90-16377# Consiglio Nazionale delle Ricerche, Frascati (Italy). Ist. di Fisica dello Spazio Interplanetario.
POLAR CUSPS LATITUDINAL SHIFT AND ITS RELATION TO THE IMF-By COMPONENT
M. Candidi, G. Mastrantonio, S. Orsini, and C.-I. Meng (Johns Hopkins Univ., Laurel, MD.) Sep. 1988 35 p Submitted for publication Sponsored by Piano Spazio Nazionale, Rome, Italy
(Grants AF-AFOSR-0101-88; NSF ATM-87-13212)
(IFSI-88-14; ETN-90-96153) Avail: NTIS HC A03/MF A01

A study of the low altitude polar cusp regions, using the Defense Meteorological Satellite Program (DMSP) F2 and F4 satellites, is presented. The electron data acquisition is carried out during 54 quasi-simultaneous traversals of the same polar cusp region. Electron precipitation data is used to determine the cusps morphology and behavior for varying orientations of the Interplanetary Magnetic Field (IMF) at different magnetic local times. Indication of a systematic shift of the equatorward boundary is found. It can be observed in the morning cusp region toward the pole (the equator) in the Southern Hemisphere for positive (negative) By with respect to its position at noon (as detected simultaneously by the other satellite). ESA

N90-16378# Consiglio Nazionale delle Ricerche, Frascati (Italy). Ist. di Fisica dello Spazio Interplanetario.
ON THE STRUCTURE OF THE TAIL MAGNETIC FIELD
M. Candidi, S. Orsini, M. Stokholm, H. Balsiger, and R. C. Elphic (California Univ., Los Angeles.) Nov. 1988 34 p Sponsored by the Piano Spaziale Nazionale, Rome, Italy Original contains color illustrations
(IFSI-88-19; ETN-90-96158) Avail: NTIS HC A03/MF A01

The configuration of the magnetic field in the Earth's geometric tail is studied. The results in the lobe region and in the plasma sheet boundary layer region are compared. A systematic enhancement of the By component of the field is detected in the

plasma sheet boundary layer with respect to the lobe; this enhancement leads to a lower rate of flaring of the magnetic field lines in the lobe with respect to the plasma sheet boundary layer. This observation is a signature of field aligned currents at the boundary. The direction of such field aligned currents agrees with the nightside region two current system. ESA

N90-16379 Institut d'Aeronomie Spatiale de Belgique, Brussels.
A DOUBLE FOCUSSING MASS-SPECTROMETER FOR SIMULTANEOUS ION MEASUREMENTS IN THE STRATOSPHERE
R. Moor, E. Kopp, U. Jenzer, H. Ramseyer, U. Walchli, E. Arijs, D. Nevejans, J. Ingels, D. Fussen, and A. Barassin et al 1989 27 p Presented at the 9th ESA Symposium on European Rocket and Balloon Programs and Related Research, Lahnstein, Fed. Republic of Germany, 3-7 Apr. 1989 Submitted for publication Sponsored by the Swiss National Science Foundation; the Belgian National Science Foundation; CNES and CNRS
(Aeronomica-Acta-A-350-1989; ISSN-0065-3713; ETN-90-96034) Avail: Institut d'Aeronomie Spatiale de Belgique, 3 Avenue Circulaire, B-1180 Brussels, Belgium

A modified Mattauch-Herzog analyzer developed for positive ion measurements in the mass range of 12 to 500 microns is described. The design parameters and first laboratory tests results obtained with it are described. The ions are mass-separated in combined toroidal electrostatic and constant magnetic fields. The simultaneous measurement of a spectrum part is achieved with the use of two detectors. They consist of a 1 in. microchannel plate, an attached phosphor screen, a fiberoptic seal and a linear position sensitive light detector. Ambient atmospheric ions are sampled through a small orifice. The atmospheric air density is reduced in the inlet region of the instrument with a liquid helium cryopump. An octopole HF-field is integrated into the ion optics in order to reduce the ion loss. The analyzer will be upgraded for negative ions. ESA

N90-16380# Centre National d'Etudes Spatiales, Toulouse (France).
TERRESTRIAL MAGNETOSPHERE MAGNETIC FIELD MODELS [LES MODELES DE CHAMP MAGNETIQUE DE LA MAGNETOSPHERE TERRESTRE]
Jean-Claude Kosik 10 May 1989 90 p In FRENCH
(Rept-89/CT/DTI/MS/AS/154; ETN-90-96043) Avail: NTIS HC A05/MF A01

Different magnetosphere models developed between 1960 to 1989 are described. These models are divided into three main groups: models with calculated magnetopause; models with imposed magnetopause; and models based on physical data. Almost all recent models are imposed magnetopause based. Only a few recent models take actual experimental measurements into account. Filiation between old and new models is shown in diagrammatic form. Practical applications of theoretical models are discussed. ESA

47 METEOROLOGY AND CLIMATOLOGY

Includes weather forecasting and modification.

N90-16381 Colorado State Univ., Fort Collins.
THE CHEMISTRY AND DYNAMICS OF MARINE STRATOCUMULUS Ph.D. Thesis
Stephan Randolph Kawa 1988 126 p
Avail: Univ. Microfilms Order No. DA8911804

Ozone chemistry and meteorological processes occurring in the eastern North Pacific stratocumulus regime were studied. This climatological regime is characterized by widespread, persistent low clouds and an air history that does not include contact with continents for many days. The approach was the analysis of observational data from the Dynamics and Chemistry of Marine Stratocumulus (DYCOMS) experiment. Components of the regional ozone budget were investigated. Measurements of sea-surface deposition rate were smaller than most previous estimates. Net Photochemical production/destruction rate in the marine boundary layer was estimated using the ozone conservation relation. This rate, averaged over the flights, results in a small sink for ozone. This is an important verification of photochemical model predictions. Finally, the common presence of sharply defined concentration layers in the free troposphere was documented. These layers are shown to affect boundary layer concentration through entrainment and their possible origins are discussed. Dynamical and thermodynamical processes controlling stratocumulus cloud layer were investigated. The entrainment rate of free tropospheric air into the cloud layer was calculated using a new method. This rate is compared to thermodynamic fluxes and previous estimates toward parameterization of entrainment for mixed-layer models. Budgets and mean distributions were also examined for several cases which are not typical of the generally cloudy conditions.
Dissert. Abstr.

N90-16382# Forest Service, Portland, OR. Pacific Northwest Research Station.
CLIMATIC SUMMARIES AND DOCUMENTATION FOR THE PRIMARY METEOROLOGICAL STATION, H. J. ANDREWS EXPERIMENTAL FOREST, 1972 TO 1984
Frederick A. Bierlmaier and Arthur McKee (Oregon State Univ., Corvallis.) Jun. 1989 61 p Original contains color illustrations
(PB90-104373; FSGTR-PNW-242) Avail: NTIS HC A04/MF A01 CSCL 04B

The primary meteorology station at H. J. Andrews Experimental Forest in the Willamette National Forest is described as is the automatic digital data logger, sensors, and data processing procedures used in measuring air temperature, dewpoint temperature, windspeed, precipitation, and solar radiation. The quasi-Mediterranean climate has mild, moist winters and warm dry summers. GRA

N90-16383# ASTeR, Inc., Fort Collins, CO.
A DYNAMIC MODEL FOR FORECASTING NEW CLOUD DEVELOPMENT Final Report, 1 Nov. 1987 - 19 Dec. 1988
William R. Cotton, Ray McAnelly, Craig Tremback, and Robert Walko 19 Dec. 1988 87 p
(Contract F19628-87-C-0182; AF Proj. 6670)
(AD-A213939; AFGL-TR-89-0011) Avail: NTIS HC A05/MF A01 CSCL 04/2

The primary goal of this research is to develop a mesoscale model capable of predicting regions of convective outbreak. The model is to be initialized by a simple soundings(s) and during the data assimilation period single Doppler radar data are to be assimilated into the model fields. The model should be capable of producing forecasts of convective development on a mini-computer system. The model should cover a 100 km by 100 km domain with a minimum resolution of 5 km. The benchmark mini-computer system used for model development is the DEC Micro-Vax II. The basic model used for this study is the Colorado State University Regional Atmospheric Modeling System (RAMS). The overall features of RAMS are described in Appendix A. In the following sections, the various versions are described of RAMS that were developed for this project, the methods of 4-D assimilation of single Doppler radar data, preliminary testing and evaluation procedures and results. The real data cases used to test the model is then described along with the methods of single Doppler wind retrieval, and the results of testing the model. GRA

N90-16384# Japan Atomic Energy Research Inst., Ibaraki. Dept. of Environmental Safety Research.
VERIFICATION STUDY OF A THREE-DIMENSIONAL LOCAL SCALE ATMOSPHERIC MODEL PHYSIC AT SEACOAST REGION
Hiromi Yamazawa Jun. 1989 48 p
(DE90-719560; JAERI-M-89-082) Avail: NTIS (US Sales Only) HC A03/MF A01

The performance of a three-dimensional numerical atmospheric model (PHYSIC) was examined over a seacoast region with the data observed during the field tracer experiment at the Tokai site. The main frame of PHYSIC is made up of the momentum equations

with the hydrostatic and Boussinesq approximation, the second-order turbulence closure model level 2.5 by Yamada and other basic equations of physical processes in the atmosphere. A terrain following Z sub asterisk coordinate system is used. The present model successfully predicts the temporal change of wind field within twenty hours from the evening to the next noon. The occurrence and structure of sea breeze are simulated satisfactorily. The model performance concerning the eddy diffusivities is thought to be reasonable, although the direct comparison between the calculation and observation is restricted to the wind and temperature profiles by the limited observation data. This was supported by an additional calculation with a diagnostic model of turbulence quantities. DOE

N90-16385# World Meteorological Organization, Geneva (Switzerland).
GUIDE ON THE GLOBAL OBSERVING SYSTEM
1989 224 p Revised
(WMO-488-Rev; ISBN-92-63-10488-3; ETN-90-95755) Copyright Avail: NTIS MF A01; American Meteorological Society, World Publ. Centre, 45 Beacon Street, Boston, MA 02108; 42 Swiss francs; World Meterological Organization, Secy. General, P.O. Box No. 2300, CH-1211 Geneva 2, Switzerland, 42

This guide deals with the organization and implementation of the Global Observing System, one of the three essential elements of the World Weather Watch. Technical regulations, practices, procedures and specifications which participants in the program must comply with, are outlined. The surface-based subsystem is described. The space-based subsystem is described. Quality control of data is discussed. Monitoring of the global observing system and improved operational observing systems are discussed. ESA

N90-16386# World Meteorological Organization, Geneva (Switzerland).
WORLD WEATHER WATCH. GLOBAL OBSERVING SYSTEM-SATELLITE SUB-SYSTEM. INFORMATION ON METEOROLOGICAL AND OTHER ENVIRONMENTAL SATELLITES, SECOND EDITION
1989 161 p Revised
(WMO-411-Ed-2; ISBN-92-63-12411-6; ETN-90-95759) Copyright Avail: NTIS MF A01; American Meteorological Society, WMO Publications Centre, 45 Beacon St., Boston, MA 02108, 37 Swiss francs; World Meteorological Organization, Secretary General, P.O. Box 2300, CH-1211 Geneva 2, Switzerland, 37

The global network of meteorological and environmental satellites is described. A general background survey of the subject is presented. The physical basis for remote sensing is explained. Sensor characteristics are described. Future developments in remote sensing are discussed. The main fields of data collection: cloud wind vector, sea surface temperature, atmospheric temperature, and atmospheric moisture are defined. The data and product archives are described. The data collecting system is outlined. ESA

N90-16387# Central Research Inst. of Electric Power Industry, Tokyo (Japan). Energy and Environment Lab.
LIGHTNING OBSERVATIONS ON JAPAN SEA COAST IN WINTER
Jan. 1989 131 p In JAPANESE; ENGLISH summary
(DE90-702485; CRIE-T-10) Avail: NTIS (US Sales Only) HC A07/MF A01

Accidents along transmission lines caused by lightning in winter have a singularity which cannot be explained by the anti-lightning technology of summer lightning studied so far. A long-term investigation of this singularity since 1978 along the Japan Sea coast, is reported. During the investigation, electro-technology was introduced and observation equipment such as lightning stroke wave measurement equipment and lightning stroke photographing equipment were developed for collecting data. Comparing summer and winter lightning, there is hardly any difference between the two in the physical quantity of lightning discharge's elementary processes such as leaders and turnstrokes. Special features of lightning in winter are that there are many lightning strokes of straight polarity and that there is much upward lightning. It was found that these features are caused by the fact that the bottom of the lightning cloud is low, and that various discharge forms are caused, accordingly, by the correlated positions of the lightning clouds and high buildings. Other observations include the striking feature of lightning to high towers and transmission lines, overvoltages on a distribution line induced by a lightning stroke, electric fields, and electromagnetic waves from lightning. Basic data for lightning insulation is also proposed. DOE

N90-16388# Central Research Inst. of Electric Power Industry, Tokyo (Japan). Energy and Environment Lab.
CHARACTERISTICS OF ELECTROMAGNETIC WAVE FORMS WITH LIGHTNING IN WINTER SEASON (2): CHARACTERISTICS IN FREQUENCY DOMAIN
May 1989 19 p In JAPANESE; ENGLISH summary
(DE90-734989; CRIE-T-88092) Avail: NTIS (US Sales Only) HC A03/MF A01

This report summarized results of frequency analysis on electromagnetic wave forms generated with lightning activities in order to clarify the winter lightning characteristics from the viewpoint of electromagnetic wave and improve the detecting rate of winter lightning from the obtained characteristics by using the lightning location system which uses the electromagnetic wave containing the lightning position and tracking system. Frequency characteristics of triangular shape appear only below 300kHz and the frequency distribution near peaks is sharp like a pencil. Peak frequency is 13kHz or less. Frequency characteristics of bi-polar oscillation reach 500kHz or more and the frequency distribution is dull like a hill. Further, peak frequncies distribute in wider range from 13kHz to 76kHz. From the above mentioned, a lightning detection method equipped with the multiple band pass filters was proposed, indicating problems when the system will be put into the practical use. DOE

N90-16389*# National Aeronautics and Space Administration. Marshall Space Flight Center, Huntsville, AL.
NEW ATMOSPHERIC TURBULENCE MODEL FOR SHUTTLE APPLICATIONS
C. G. Justus, C. W. Campbell, M. K. Doubleday (BDM Corp., Huntsville, AL.), and D. L. Johnson Washington Jan. 1990 52 p
(NASA-TM-4168; NAS 1.15:4168) Avail: NTIS HC A04/MF A01 CSCL 04B

An updated NASA atmospheric turbulence model, from 0 to 200 km altitude, which was developed to be more realistic and less conservative when applied to space shuttle reentry engineering simulation studies involving control system fuel expenditures is presented. The prior model used extreme turbulence (3 sigma) for all altitudes, whereas in reality severe turbulence is patchy within quiescent atmospheric zones. The updated turublence model presented is designed to be more realistic. The prior turbulence statistics (sigma and L) were updated and were modeled accordingly. Author

N90-16690*# Auburn Univ., AL. Dept. of Aerospace Engineering.
ROCKET-TRIGGERED LIGHTNING STRIKES AND FOREST FIRE IGNITION
James H. Fenner *In* University of Central Florida, NASA/ASEE Summer Faculty Fellowship Program Oct. 1989 p 85-101 (For primary document see N90-16686 08-99)
Avail: NTIS HC A18/MF A03 CSCL 04B

48 OCEANOGRAPHY

Includes biological, dynamic, and physical oceanography; and marine resources.

For related information see also *43 Earth Resources and Remote Sensing.*

No abstracts in this category.

51 LIFE SCIENCES (GENERAL)

N90-16390# Catholic Univ. of America, Washington, DC. Vitreous State Lab.
MECHANISMS OF MICROWAVE INDUCED DAMAGE IN BIOLOGIC MATERIALS Annual Report, 22 Sep. 1986 - 21 Sep. 1987
M. Mullins, M. Penafiel, R. Mohr, C. Montrose, T. Litovitz, and C. Grosse Jan. 1988 69 p
(Contract DAMD17-86-C-6260; DA Proj. 3E1-6277-A-878)
(AD-A213480) Avail: NTIS HC A04/MF A01 CSCL 06/2

An interdisciplinary team of biologists, physicists, and electrical engineers was related to tackle the problem of microwave damage to biological systems. Work is described in five purposely overlapping areas: design and construction of microwave exposure chambers; investigation of the effects of microwave irradiation on the metabolic activity of several cell lines and an interferon system; investigation of the mechanisms of microwave absorption in DNA solutions; theoretical studies of the inhomogeneous deposition of microwave energy in the region of DNA and cells in suspension; and molecular dynamic (MD) computer simulation of electric field effects on long chain (DNA-like) molecules. GRA

N90-16689*# Massachusetts Univ., Amherst. Dept. of Plant and Soil Sciences.
DYNAMICS OF CARBON DIOXIDE EXCHANGE OF A WHEAT COMMUNITY GROWN IN A SEMI-CLOSED ENVIRONMENT
Kenneth A. Corey *In* University of Central Florida, NASA/ASEE Summer Faculty Fellowship Program Oct. 1989 p 58-84 (For primary document see N90-16686 08-99)
Avail: NTIS HC A18/MF A03 CSCL 06B

N90-16695*# Purdue Univ., West Lafayette, IN. Dept. of Agricultural Engineering.
PLANT FEATURES MEASUREMENTS FOR ROBOTICS
Gaines E. Miles *In* University of Central Florida, NASA/ASEE Summer Faculty Fellowship Program Oct. 1989 p 203-225 (For primary document see N90-16686 08-99)
Avail: NTIS HC A18/MF A03 CSCL 06C

52 AEROSPACE MEDICINE

Includes physiological factors; biological effects of radiation; and effects of weightlessness on man and animals.

N90-16391*# National Aeronautics and Space Administration. Pasadena Office, CA.
APPARATUS FOR IMAGING DEEP ARTERIAL AND CORONARY LESIONS Patent Application
James A. Rooney, inventor (to NASA), Richard C. Heyser, inventor (to NASA), and Dennis H. LeCroissette, inventor (to NASA) 1 Dec. 1989 24 p
(Contract NAS7-918)
(NASA-Case-NPO-17439-1-CU; NAS 1.71:NPO-17439-1-CU; US-Patent-Appl-SN-444248) Avail: NTIS HC A03/MF A01 CSCL 06B

A reflection-mode ultrasonic system uses time-delay spectrometry (TDS) for imaging of variations in a property of deep arterial and coronary tissue within a volume at a range from a transmitting transducer. A receiving transducer mounted concentric with the transmitting transducer provides a return signal that is demodulated by the sweep of the TDS using a balanced mixer to present a complex signal representative of a property within a volume of tissue. The complex signal is amplified and filtered before mixing with a frequency signal from a local generator to establish a zero range reference for A-scan display of the return signal, but before display the offset return signal is transformed by a fast Fourier transform processor from the frequency domain to a time domain to present the return signal for display as a time-based range signal. A B-scan display may be provided by additionally scanning the transducers in a linear path across the tissue. NASA

N90-16392# Army Aeromedical Research Lab., Fort Rucker, AL. Biodynamics Research Div.
SIMULATOR SICKNESS IN THE UH-60 (BLACK HAWK) FLIGHT SIMULATOR Final Report
Daniel W. Gower, Jr. and Jennifer Fowlkes (Essex Corp., Orlando, FL.) Sep. 1989 75 p
(AD-A214434; USAARL-89-25) Avail: NTIS HC A04/MF A01 CSCL 06/10

The U.S. Army Aeromedical Research Laboratory conducted field studies of operational flight simulators to assess the incidence and severity of simulator sickness. Simulator sickness here refers to the constellation of motion sickness related symptoms that occur in simulators due to visual representation, motion base representation, or combination of the two representations of flight. The incidence rates and relative frequency of specific symptoms are presented. Correlational factors such as recent simulator experience, current state of health, overall flight expereience, mission scenario, and flight dynamics are presented. The Army's flight simulators are ranked in comparision to the 10 Navy simulators studied by the Naval training systems Center, Orlando, Florida. The study further reinforces the need for studies to understand perceptual rearrangement, adaptation/readaptation, and pilot susceptibility to the effects of simulation. Design criteria for simulators, as well as those training guidelines necessary to cope with this phenomenon also must be addressed. GRA

N90-16393# Oak Ridge National Lab., TN. Health and Safety Research Div.
SHORT-TERM BIOASSAYS MAY BE USEFUL IN EVALUATING FIBER/WHISKER HAZARDS
Clay E. Easterly Nov. 1989 27 p Presented at the ANSI Subcommittee Meeting, Orlando, FL, 28-29 Nov. 1989
(Contract DE-AC05-84OR-21400)
(DE90-003707; CONF-8911148-1-Vugraphs) Avail: NTIS HC A03/MF A01

The utility of short-term bioassays for predicting hazards has been the focus of many individual efforts in the past. The World Health Organization concludes that a combination of tests may be useful in detecting excess formation of fibrous tissue in the lung as a result of reparative or reactive processes. Further, some consistency has been observed between specific in vitro assays and the induction of mesotheliomas induced in in vivo assays. For the most part such studies of correlation were very qualitative and were performed using mechanistic concepts to match the in vitro studies with whole animal studies. An alternative method to viewing the in vitro to in vivo correlation will be presented in this talk. Much of the focus will be on work performed by L. R. Glass during his dissertation research. Based on the alternative method, a plan for testing this concept on fibers will be presented. The abstract is this paper's only text; the remainder consists of viewgraphs. DOE

N90-16693*# North Carolina Univ., Greensboro. Dept. of Mathematics.
FACTOR ANALYTIC REDUCTION OF THE CAROTID-CARDIAC BAROREFLEX PARAMETERS
David A. Ludwig *In* University of Central Florida, NASA/ASEE

Summer Faculty Fellowship Program Oct. 1989 p 159-170
(For primary document see N90-16686 08-99)
Avail: NTIS HC A18/MF A03 CSCL 06P

53 BEHAVIORAL SCIENCES

Includes psychological factors; individual and group behavior; crew training and evaluation; and psychiatric research.

No abstracts in this category.

54 MAN/SYSTEM TECHNOLOGY AND LIFE SUPPORT

Includes human engineering; biotechnology; and space suits and protective clothing.

For related information see also *16 Space Transportation.*

N90-16394# Department of the Navy, Washington, DC.
HELMET-MOUNTED HEAD RESTRAINT Patent Application
Michael H. Patterson, inventor (to Navy) 3 Nov. 1988 12 p
(AD-D014233; US-Patent-Appl-SN-266955) Avail: NTIS HC A03/MF A01 CSCL 06/11

A head restraint for the occupant of a vehicle seat is disclosed, which restrains the forward and downward movement of the occupant's head when subjected to large deceleration forces. The restraint includes a strap assembly which encircles the back of the occupant's head and releasably connects to his helmet adjacent to each of his ears at two locations. A retaining strap is slidably connected by a loop to the strap assembly and extends behind the head to a retracting means fixed in the seat. The retracting means pulls the head back against the seat when the deceleration forces exceed a predetermined level, as during flight maneuvers. During normal flight conditions, the occupant is able to move his head freely from side to side as the strap assembly slides through the loop. GRA

N90-16395# Decision Science Consortium, Inc., Reston, VA.
USER INTERACTION WITH SELF-LEARNING SYSTEMS Final Report, Dec. 1988 - Jul. 1989
Martin A. Tolcott, Paul E. Lehner, and Theresa M. Mullin Aug. 1989 81 p
(Contract F33615-88-C-0540)
(AD-A214280; AAMRL-TR-89-029) Avail: NTIS HC A05/MF A01 CSCL 12/9

This research investigated how users interact with an expert system in which underlying values change as a function of the situation or of the planning time horizon. The problem context was the prioritization of tactical air strike targets, and Air Force targeteers were the experimental subjects. Their task was to explain why the system made the recommendations it did. The expert system was simulated in storyboard form. It was found that users who were given a good conceptual model of the expert system, in the form of a brief summary of its step-by-step processes, performed better than those whose model of the system was relatively poor. Users whose displays were relatively user-oriented (geographic, top-down, and simplified) did not consistently differ in performance from users whose displays were relatively aid-oriented (data-intensive matrices). However, the aid-oriented displays seem to encourage users to make more frequent reference to three tables (available to all subjects) containing important information about the expert assessments on which the aid's algorithms operated. Users would typically generate their own solutions, using criteria and heuristics that often differed from those used by the aid, and question the expert system solution. GRA

N90-16396# Royal Aerospace Establishment, Farnborough (England).
KEEPING THE PILOT IN THE LOOP
R. G. White Feb. 1989 20 p Presented at Flight Deck Display and Pilot Performance, Bedford, England, 4 Apr. 1989
(RAE-TM-FM-18; BR109681; ETN-90-96131) Copyright Avail: NTIS HC A03/MF A01

Evaluation of pilot performance is investigated. Questions concerning ways of informing the pilot when a problem arises and ways to show him that he must develop a solution are discussed. The manifestation of this dilemma at different stages in the history of flight, and cockpit systems needed to tackle it, are analyzed. The need for a totally integrated avionic system incorporating automatic monitoring and a suite of integrated displays is demonstrated. ESA

N90-16397 Ludwig-Maximilians-Universitaet, Munich (Germany, F.R.). Inst. fuer Medizinische Psychologie.
ASSESSMENT OF VISUAL FUNCTION IN AEROSPACE MEDICINE Final Report
Ingo Rentschler, Hans Strasburger, Bernhard Treutwein, and Walter Encke Feb. 1989 143 p In GERMAN; ENGLISH summary
(Contracts BMVg-InSan-I-0784-V-6385; BMVg-InSan-I-0784-V-6386)
(BMVg-FBWM-89-5; ETN-90-95872) Copyright Avail: Dokumentations- und Fachinformationszentrum der Bundeswehr, Friedrich-Ebert-Allee 34, 5300 Bonn, Federal Republic of Germany

Three aspects of visual function in aerospace environments are investigated. The recognition of digital displays in the cockpit, the analysis of temporal visual processing in aerospace medicine, and the implementation of a user friendly system for the psychophysical analysis of visual function in aerospace medicine, are discussed. It is concluded that digital displays should not be used for monitoring signals in the cockpit. Two techniques for analyzing deficiencies in the visual capacity to process temporal information are presented. A direct dialog between user and computer is measured using a statistically optimal procedure of maximum likelihood parameter estimation. ESA

N90-16398# Dornier System G.m.b.H., Friedrichshafen (Germany, F.R.). Dept. of Environmental Control and Life Support Systems.
DNSS: GERMAN/NORWEGIAN WORK TEAM SPACE SUBSEA. ENVIRONMENTAL CONTROL AND LIFE SUPPORT SUBSYSTEMS (TECHNICAL MATTERS), PHASE 2 Final Report
Ingo Borchers, Ingo Dathe, Josef Hackstein, Andreas Kreis, Helmut Preiss, Marion Stieb-Stabel, and Rainer Stoepler Oct. 1987 12 p In GERMAN; ENGLISH summary
(Contract BMFT-FE-01-TQ-8602-AK/PA1)
(ETN-90-95905) Avail: NTIS HC A03/MF A01

Monitoring and control methods used to avoid microbiological contamination in the Hermes and Columbus programs are discussed. A critical analysis of the components of the environmental control and life support subsystem is presented. Components of the environmental control and life support system were the main noise sources in the Spacelab project. Analytical investigations concerning noise production for a variable speed fan are presented. Primary and secondary noise sources are taken into account in optimizing noise reduction. A universal test bench used to verify the analytical data is presented. ESA

N90-16399*# National Aeronautics and Space Administration. Ames Research Center, Moffett Field, CA.
A SPACE-TIME DISCRETIZATION PROCEDURE FOR WAVE PROPAGATION PROBLEMS
Sanford Davis Nov. 1989 42 p
(NASA-TM-102215; A-89212; NAS 1.15:102215) Avail: NTIS HC A03/MF A01 CSCL 20N

Higher order compact algorithms are developed for the numerical simulation of wave propagation by using the concept of a discrete dispersion relation. The dispersion relation is the imprint of any linear operator in space-time. The discrete dispersion relation is derived from the continuous dispersion relation by examining

the process by which locally plane waves propagate through a chosen grid. The exponential structure of the discrete dispersion relation suggests an efficient splitting of convective and diffusive terms for dissipative waves. Fourth- and eighth-order convection schemes are examined that involve only three or five spatial grid points. These algorithms are subject to the same restrictions that govern the use of dispersion relations in the constructions of asymptotic expansions to nonlinear evolution equations. A new eighth-order scheme is developed that is exact for Courant numbers of 1, 2, 3, and 4. Examples are given of a pulse and step wave with a small amount of physical diffusion. Author

N90-15976# Glavkosmos, Moscow (USSR).
EVA SPACE SUIT. GENERAL CONCEPTS OF DESIGN AND ARRANGEMENT
G. I. Severin, V. I. Svertshek, and I. P. Abramov *In* ESA, Crew Safety and Rescue in Space: An International Approach Aug. 1989 p 13-17 (For primary document see N90-15974 08-16) Copyright Avail: NTIS HC A04/MF A01; ESA Publications Div., ESTEC, Noordwijk, Netherlands, 30 Dutch guilders

55 SPACE BIOLOGY

Includes exobiology; planetary biology; and extraterrestrial life.

N90-16400*# National Aeronautics and Space Administration. Ames Research Center, Moffett Field, CA.
COMPUTATION OF THE UNSTEADY FACILITATED TRANSPORT OF OXYGEN IN HEMOGLOBIN
Sanford Davis Jan. 1990 33 p
(NASA-TM-102251; A-90011; NAS 1.15:102251) Avail: NTIS HC A03/MF A01 CSCL 06C

The transport of a reacting permeant diffusing through a thin membrane is extended to more realistic dissociation models. A new nonlinear analysis of the reaction-diffusion equations, using implicit finite-difference methods and direct block solvers, is used to study the limits of linearized and equilibrium theories. Computed curves of molecular oxygen permeating through hemoglobin solution are used to illustrate higher-order reaction models, the effect of concentration boundary layers at the membrane interfaces, and the transient buildup of oxygen flux. Author

59 MATHEMATICAL AND COMPUTER SCIENCES (GENERAL)

N90-16401*# Institute for Computer Applications in Science and Engineering, Hampton, VA.
TRIANGLE BASED TVD SCHEMES FOR HYPERBOLIC CONSERVATION LAWS Final Report
Louis J. Durlofsky, Stanley Osher, and Bjorn Engquist (California Univ., Los Angeles.) Jan. 1990 31 p Submitted for publication Sponsored in part by DARPA and Chevron Oil Field Research Co.
(Contracts NAS1-18605; NCA-2372; NAG1-270; N00014-86-K-0691; NSF DMS-88-11863)
(NASA-CR-181984; NAS 1.26:181984; ICASE-90-10) Avail: NTIS HC A03/MF A01 CSCL 12A

A triangle based total variation diminishing (TVD) scheme for the numerical approximation of hyperbolic conservation laws in two space dimensions is constructed. The novelty of the scheme lies in the nature of the preprocessing of the cell averaged data, which is accomplished via a nearest neighbor linear interpolation followed by a slope limiting procedures. Two such limiting procedures are suggested. The resulting method is considerably more simple than other triangle based non-oscillatory approximations which, like this scheme, approximate the flux up to second order accuracy. Numerical results for linear advection and Burgers' equation are presented. Author

60 COMPUTER OPERATIONS AND HARDWARE

Includes hardware for computer graphics, firmware, and data processing.

For components see *33 Electronics and Electrical Engineering.*

N90-16402# Air Force Inst. of Tech., Wright-Patterson AFB, OH. School of Engineering.
DYNAMIC ARCHITECTURE COMPUTER M.S. Thesis
Patrick E. Price Dec. 1988 241 p
(AD-A214262; AFIT/GE/ENG/89D-40) Avail: NTIS HC A11/MF A02 CSCL 12/6

A computer was designed that could process a large variety of calculations with a minimum of hardware. This requires a computer that can change its structure to match the demands of the problem currently being calculated. Computer image generation was selected as an example problem. The processing requirements of real time computer image generation require calculation of very large real numbers as well as very small logical variables. The results demonstrate that, in a best case analysis, a dynamic architecture computer can demonstrate an improvement in processing speed over conventional single instruction single data computers. GRA

N90-16403# Oak Ridge National Lab., TN.
PVM (PARALLEL VIRTUAL MACHINE): A FRAMEWORK FOR PARALLEL DISTRIBUTED COMPUTING
V. S. Sunderam (Emory Univ., Atlanta, GA.) 1989 28 p
(Contract DE-AC05-84OR-21400)
(DE90-004390; ORNL/TM-11375) Avail: NTIS HC A03/MF A01

The PVM system is a programming environment for the development and execution of large concurrent or parallel applications that consist of many interacting, but relatively independent, components. It is intended to operate on a collection of heterogeneous computing elements interconnected by one or more networks. The participating processors may be scalar machines, multiprocessors, or special-purpose computers, enabling application components to execute on the architecture most appropriate to the algorithm. PVM provides a straightforward and general interface that permits the description of various types of algorithms (and their interactions), while the underlying infrastructure permits the execution of applications on a virtual computing environment that supports multiple parallel computation models. PVM contains facilities for concurrent, sequential, or conditional execution of application components, is portable to a variety of architectures, and supports failure detection (and certain forms of recovery) at the process and processor levels. DOE

N90-16404# Royal Signals and Radar Establishment, Malvern (England).
THE SMITE APPROACH TO SECURITY
P. F. Terry Aug. 1989 63 p
(Contract RSRE-A94c/2711)
(RSRE-89014; BR111536; ETN-90-96125) Copyright Avail: NTIS HC A04/MF A01

SMITE is a novel computer architecture implementing a new security policy model. It is the name of the third phase of the secure communications processor research program and is proposed as the best available technology. It may be used to develop information systems for operational use where high assurance of complex confidentialty and integrity based security policies is required. The results of work carried out are reported. A review of the architecture proposals, the essential architectural elements and the security oriented top level model, are considered. A baseline definition of SMITE to aid the future way forward for the project, is provided. ESA

N90-16405# Centre National d'Etudes Spatiales, Toulouse (France).
UNIX INTERNALS. PART 1: INTERTASK COMMUNICATION IN UNIX. PART 2: UNIX FILE SYSTEM [LES INTERNES D'UNIX. 1: COMMUNICATIONS ENTRE TACHES SOUS UNIX. 2: LE SYSTEME DE FICHIERS UNIX]
Monique Cima Sep. 1989 228 p In FRENCH; ENGLISH summary
(CNES-NT-122-Pt-1/2; ETN-90-96042) Copyright Avail: NTIS HC A11/MF A02

Two studies, performed in the computing facilities and services division of CNES (Centre National d'Etudes Spatiales) are described. The internal mechanisms in the UNIX operating system, the interprocessor communications and the file system, are outlined. A complete view of the different ways of communicating, and the available application fields of each one is presented. The file system operation and special implementation aspects are explained. Performance test results are presented. Differences between the Berkely 4.2 and the System 5 systems are discussed. ESA

N90-16406# Grenoble-1 Univ. (France). Lab. Structures Discretes et Didactique.
SPANNING TREES OF HYPERCUBES WITH A MAXIMUM OF SIXTEEN PEAKS [LE PLONGEMENT DANS L'HYPERCUBE DES ARBRES D'AU PLUS 16 SOMMETS]
Jean-Marie Laborde Jun. 1989 41 p In FRENCH; ENGLISH summary
(IMAG-RR-755-I; ETN-90-96045) Avail: NTIS HC A03/MF A01

A verification of Havel's conjecture about spanning trees of hypercubes is presented. The conjecture is slightly reformulated and checked for cubes with a dimension of at most four. Possible applications in designing algorithms for computers with hypercube architecture are investigated. ESA

N90-16687*# California State Univ., Fresno. Dept. of Computer Science.
FORMALISMS FOR USER INTERFACE SPECIFICATION AND DESIGN
Brent J. Auernheimer *In* University of Central Florida, NASA/ASEE Summer Faculty Fellowship Program Oct. 1989 p 1-23 (For primary document see N90-16686 08-99)
Avail: NTIS HC A18/MF A03 CSCL 09B

61 COMPUTER PROGRAMMING AND SOFTWARE

Includes computer programs, routines, alogorithms, and specific applications, e.g., CAD/CAM.

N90-16407*# Alabama Univ., Tuscaloosa. Dept. of Mathematics.
STOCHASTIC MODEL OF THE NASA/MSFC GROUND FACILITY FOR LARGE SPACE STRUCTURES WITH UNCERTAIN PARAMETERS: THE MAXIMUM ENTROPY APPROACH, PART 2 Final Report, 23 May 1988 - 22 Nov. 1989
Wei Shen Hsia Nov. 1989 64 p
(Grant NAG8-081)
(NASA-CR-186009; NAS 1.26:186009) Avail: NTIS HC A04/MF A01 CSCL 09B

A validated technology data base is being developed in the areas of control/structures interaction, deployment dynamics, and system performance for Large Space Structures (LSS). A Ground Facility (GF), in which the dynamics and control systems being considered for LSS applications can be verified, was designed and built. One of the important aspects of the GF is to verify the analytical model for the control system design. The procedure is to describe the control system mathematically as well as possible, then to perform tests on the control system, and finally to factor those results into the mathematical model. The reduction of the order of a higher order control plant was addressed. The computer program was improved for the maximum entropy principle adopted in Hyland's MEOP method. The program was tested against the testing problem. It resulted in a very close match. Two methods of model reduction were examined: Wilson's model reduction method and Hyland's optimal projection (OP) method. Design of a computer program for Hyland's OP method was attempted. Due to the difficulty encountered at the stage where a special matrix factorization technique is needed in order to obtain the required projection matrix, the program was successful up to the finding of the Linear Quadratic Gaussian solution but not beyond. Numerical results along with computer programs which employed ORACLS are presented. Author

N90-16408*# North Carolina Agricultural and Technical State Univ., Greensboro. Dept. of Electrical Engineering.
THE DEVELOPMENT OF TWO-DIMENSIONAL OBJECT IDENTIFICATION TECHNIQUES Final Report
Gary Lebby and Earnest E. Sherrod 18 Dec. 1989 42 p
(Grant NAG1-870)
(NASA-CR-186203; NAS 1.26:186203) Avail: NTIS HC A03/MF A01 CSCL 09B

This report marks the end of the first year of an anticipated three year effort to study methods for numerically identifying objects according to shape in two dimensions. The method is based upon comparing the unit gradient of an observed object and the unit gradient of a standard object over a specified range of points. The manner in which the gradients are compared forms the basis of a shape recognition scheme, which is then applied to simple closed plane figures. The gradient based method is calibrated by using various distorted objects in comparison with a set of standard reference objects. The use of pattern recognition techniques for computer identification of two-dimensional figures will be investigated during the second and third years of this project. Author

N90-16409# National Taiwan Univ., Taipei.
DIGITAL IMAGE CODING AND COMPRESSION Report, Aug. 1986 - Jul. 1987
Su-Chang Pei 1987 120 p
(Contract NSC-76-0404-E002-17)
(PB90-110958) Avail: NTIS HC A06/MF A01 CSCL 09B

Digital image coding and compression have many practical applications such as image data storage, medical image compression, tele-conference, view data, and digital television. Also, in the future Integrated Service Digital Network, voice and image data are combined together for transmission, so the techniques of coding and compression are very important. The report includes spatial, transform and hybrid coding, vector quantization and progressive image transmission coding. GRA

N90-16410*# National Aeronautics and Space Administration. Lyndon B. Johnson Space Center, Houston, TX.
DISCRETE EVENT SIMULATION TOOL FOR ANALYSIS OF QUALITATIVE MODELS OF CONTINUOUS PROCESSING SYSTEMS Patent Application
Jane T. Malin, inventor (to NASA), Bryan D. Basham, inventor (to NASA), and Richard A. Harris, inventor (to NASA) (Mitre Corp., McLean, VA.) 14 Jul. 1988 70 p Sponsored by NASA
(NASA-Case-MSC-21465-1; NAS 1.71:MSC-21465-1; US-Patent-Appl-SN-219295) Avail: NTIS HC A04/MF A01 CSCL 09B

An artificial intelligence design and qualitative modeling tool is disclosed for creating computer models and simulating continuous activities, functions, and/or behavior using developed discrete event techniques. Conveniently, the tool is organized in four modules: library design module, model construction module, simulation module, and experimentation and analysis. The library design module supports the building of library knowledge including component classes and elements pertinent to a particular domain of continuous activities, functions, and behavior being modeled. The continuous behavior is defined discretely with respect to invocation statements, effect statements, and time delays. The

functionality of the components is defined in terms of variable cluster instances, independent processes, and modes, further defined in terms of mode transition processes and mode dependent processes. Model construction utilizes the hierarchy of libraries and connects them with appropriate relations. The simulation executes a specialized initialization routine and executes events in a manner that includes selective inherency of characteristics through a time and event schema until the event queue in the simulator is emptied. The experimentation and analysis module supports analysis through the generation of appropriate log files and graphics developments and includes the ability of log file comparisons. NASA

N90-16411*# National Aeronautics and Space Administration. Lyndon B. Johnson Space Center, Houston, TX.
BUS PROGRAMMABLE SLAVE MODULE Patent Application
William A. Hall, inventor (to NASA) (Krug International, Houston, TX.) 15 Mar. 1989 27 p
(NASA-Case-MSC-21387-1; NAS 1.71:MSC-21387-1; US-Patent-Appl-SN-323748) Avail: NTIS HC A03/MF A01 CSCL 09B

A bus programmable slave module card for use in a computer control system is disclosed which comprises a master computer and one or more slave computer modules interfacing by means of a bus. Each slave module includes its own microprocessor, memory, and control program for acting as a single loop controller. The slave card includes a plurality of memory means (S1, S2...) corresponding to a like plurality of memory devices (C1, C2...) in the master computer, for each slave memory means its own communication lines connectable through the bus with memory communication lines of an associated memory device in the master computer, and a one-way electronic door which is switchable to either a closed condition or a one-way open condition. With the door closed, communication lines between master computer memory (C1, C2...) and slave memory (S1, S2...) are blocked. In the one-way open condition invention, the memory communication lines or each slave memory means (S1, S2...) connect with the memory communication lines of its associated memory device (C1, C2...) in the master computer, and the memory devices (C1, C2...) of the master computer and slave card are electrically parallel such that information seen by the master's memory is also seen by the slave's memory. The slave card is also connectable to a switch for electronically removing the slave microprocessor from the system. With the master computer and the slave card in programming mode relationship, and the slave microprocessor electronically removed from the system, loading a program in the memory devices (C1, C2...) of the master accomplishes a parallel loading into the memory devices (S1, S2...) of the slave. NASA

N90-16412# Los Alamos National Lab., NM.
FRAC-IN-THE-BOX UTILIZATION
Dave G. Collins and James T. West Jun. 1989 28 p
(Contract W-7405-eng-36)
(DE90-003648; LA-11606-MS) Avail: NTIS HC A03/MF A01

FRAC-IN-THE-BOX is a computer code developed to calculate the fractions of rectangular parallelepiped mesh cell volumes that are intersected by combinatorial geometry type zones. The geometry description used in the code is a subset of the combinatorial geometry used in SABRINA. The input file may be read into SABRINA and three dimensional plots made of the input geometry. The volume fractions for those portions of the geometry that are too complicated to describe with the geometry routines provided in FRAC-IN-THE-BOX may be calculated in SABRINA and merged with the volume fractions computed for the remainder of the geometry. DOE

N90-16413# Oak Ridge National Lab., TN.
CASE TOOL EVALUATION SYSTEM
P. L. Green, P. V. Andreae, W. J. Pennewell, L. A. Clinard, B. Thomas, Jr., and P. M. Tarrant 1989 166 p Sponsored in part by Navy, Dept. of Justice, and Defense Security Assistance Agency
(Contract DE-AC05-84OR-21400)
(DE90-003698; K/DSRD-112-Vol-1) Avail: NTIS HC A08/MF A01

An automated system that uses an analytical approach to evaluate Computer-Aided Software Engineering (CASE) tools is currently being developed. This system is referred to as the CASE Tool Evaluation System. The following general criteria will be used: overall tool functionality; tool stability; cost; interfaces with other software; customization; ease of use; output produced; hardware and operating system needs; documentation; training and vendor support; repository interface; methodologies; and vendor stability. in Phase 1 CASE tools will be eliminated that do not meet certain must-have characteristics specified by the user. Phase 2 will further reduce the size of the tool list by retaining those tools that possess desirable, but not absolutely necessary characteristics, also specified by the user. Phase 3 will employ the Analytic Hierarchy Process, developed by Dr. Thomas L. Saaty, to rank the tools. Users will be able to supply tools of their own choosing, in addition to tools that are generated via normal use of the system. All three phases will interact with a database that stores objective information about CASE tools. The use of the Analytic Hierarchy process (AHP) distinguishes this method of CASE tool evaluation from others. As used in this system, the AHP is a method of breaking down the complex, unstructured problem of selecting a CASE tool into its component evaluation criteria and candidate tools. These criteria and tools are arranged into a hierarchical order. Each criterion and tool is assigned a subjective numerical value (by experts or users or both). These values are then synthesized to determine which have the highest priority. The result will be a ranked list of CASE tools tailored to the needs and desires of the user. DOE

N90-16414*# Naval Postgraduate School, Monterey, CA. Dept. of Computer Science.
AN EMPIRICAL COMPARISON OF SOFTWARE FAULT TOLERANCE AND FAULT ELIMINATION Progress Report, Mar. 1986 - Jul. 1989
Timothy J. Shimeall and Nancy G. Leveson (California Univ., Irvine.) Jul. 1989 56 p Sponsored in part by State of California and TRW, Inc.
(Grants NAG1-668; NSF DCR-85-21398)
(NASA-CR-186313; NAS 1.26:186313; AD-A214184; NPS52-89-047) Avail: NTIS HC A04/MF A01 CSCL 09/2

Reliability is an important concern in the development of software for modern systems. Some researchers have hypothesized that particular fault-handling approaches or techniques are so effective that other approaches or techniques are superfluous. The authors have performed a study that compares two major approaches to the improvement of software, software fault elimination and software fault tolerance, by examination of the fault detection obtained by five techniques: run-time assertions, multi-version voting, functional testing augmented by structural testing, code reading by stepwise abstraction, and static data-flow analysis. This study has focused on characterizing the sets of faults detected by the techniques and on characterizing the relationships between these sets of faults. The results of the study show that none of the techniques studied is necessarily redundant to any combination of the others. Further results reveal strengths and weakness in the fault detection by the techniques studied and suggest directions for future research. GRA

N90-16415# Naval Oceanographic Office, Bay Saint Louis, MS.
ZBTAB: ZENITH-248 VERSION OF BLUGTAB Technical Note, Feb. - Apr. 1989
James J. Kohsmann Jun. 1989 13 p
(AD-A214279; NOO-TN-03-89) Avail: NTIS HC A03/MF A01 CSCL 17/1

A version of BLUGTAB able to run interactively on a Zenith-2 48 PC is now operative. The program is called ZBTAB to indicate its relation to BLUGTAB and its ability to run on the Zenith computer. The main difference between ZBTAB and the UNIVAC counterpart is that the Z-248 version does not include the option to access databases. The results of tests made on an Indian

Ocean parameter set for three frequencies and a sample interactive session are included in this report. Comparison of numerical output from ZBTAB and the UNIVAC version of BLUGTAB shows less than 0.02 percent difference between bottom-loss values. The BLUGTAB program generates bottom-loss values versus grazing angle for up to six frequencies at a time. It allows both interactive input and input from various databases resident on the UNIVAC system. The PC version of the program does not have access to these databases and can only operate in an interactive input mode. GRA

N90-16416# SRI International Corp., Menlo Park, CA. Computer Science Lab.
ALGORITHMS FOR FAULT TOLERANT DISTRIBUTED SYSTEMS Final Technical Report, Feb. 1985 - Feb. 1988
Leslie Lamport, P. Michael Melliar-Smith, Louise Moser, Ira Greenberg, and John Rushby Oct. 1989 214 p
(Contract F30602-85-C-0024)
(AD-A214447; RADC-TR-89-162) Avail: NTIS HC A10/MF A02 CSCL 12/7

The research described is presented in six parts: (1) On Interprocess Communication studies interprocess communication without assuming any lower level communication primitives. A formalism is developed for reasoning about concurrent systems that does not assume an atomic grain of action; (2) The Intersecting Broadcast Machine is a novel array processor architecture, capable of processing efficiently programs whose arbitrary or complex structure would make them difficult to map onto conventional array processors. The architecture also supports fault tolerant operation; (3) Broadcast Protocols for Distributed Systems considers how the broadcast character of communications media such as Ethernet and packet radio can be exploited to yield reliable communication with very little overhead; (4) Extending Interval Logic to Real Time Systems presents a technique for the formal expression of the real time constraints that are critical to the specification of fault tolerant distributed systems; (5) Consistency of Replicated Information in Multichannel Fault Tolerant Systems considers the possibility of using similar, but not identical, processing in the replicas of a fault tolerant system. Conventional fault tolerant systems using replicate processing require the replicas to be identical, so that they can be compared by exact match algorithms. This exact replication increases the risk that a common fault will affect all replicas and cause system failure; and (6) Experimental Implementation and Evaluation of the TRANS Broadcast Protocol describes an implementation and evaluation of the broadcast protocols outlined in part 3. GRA

N90-16417# Laboratorio de Computacao Cientifica, Rio de Janeiro (Brazil).
AN ALGORITHM TO COMPUTE THE SQUARE ROOT OF 3X3 POSITIVE DEFINITE MATRIX
Leopoldo P. Franca Jun. 1988 26 p
(DE89-635711; LNCC-022/88; ISSN-0101-6113) Avail: NTIS (US Sales Only) HC A03/MF A01

An efficient closed form to compute the square root of a 3 x 3 positive definite matrix is presented. The derivation employs the Cayley-Hamilton theorem avoiding calculation of eigenvectors. It is shown that evaluation of one eigenvalue of the square root matrix is needed and can not be circumvented. The algorithm is robust and efficient. DOE

N90-16418# Sandia National Labs., Albuquerque, NM.
CAE (COMPUTER-AIDED ENGINEERING) TOOLS' LIMITATIONS CASE STUDY: AN SSI (SMALL SCALE INTEGRATED) DESIGN TO AN ASIC (APPLICATION SPECIFIC INTEGRATED CIRCUIT)
Jeff Everts 1989 5 p Presented at the 1990 DAZIX Users' Group Meeting, San Francisco, CA, 23-25 Jan. 1990
(Contract DE-AC04-76DP-00789)
(DE90-002902; SAND-89-2712; CONF-900146-1) Avail: NTIS HC A01/MF A01

Every computer-aided engineering (CAE) tool has its limitations and shortcomings. Knowing where the pitfalls lie and how to get around them is extremely valuable. The problems and limitations encountered using the Daisy Systems suite of digital design tools (on a Logician 386 and a PKK386 MegaLogician, running DNIX 5.02A) to redesign a 169 small scale integrated (SSI) component design into an application specific integrated circuit (ASIC) gate array are examined. Deficiencies were found in the libraries, ACE, MDLS, DTA, MCFS, and the Hotline support. Some solutions and workarounds to these deficiencies are presented. DOE

N90-16419# Los Alamos National Lab., NM.
CREATING THE NEXT GENERATION CONTROL SYSTEM SOFTWARE
David E. Schultz 1989 12 p Presented at the International Conference on Accelerator and Large Experimental Physics Control Systems, Vancouver, British Columbia, 30 Oct. - 3 Nov. 1989
(Contract W-7405-eng-36)
(DE90-003391; LA-UR-89-3685; CONF-891094-10) Avail: NTIS HC A03/MF A01

A new 1980's style support package for future accelerator control systems is proposed. It provides a way to create accelerator applications software without traditional programming. Visual Interactive Applications (VIA) is designed to meet the needs of expanded accelerator complexes in a more cost effective way than past experience with procedural languages by using technology from the personal computer and artificial intelligence communities. DOE

N90-16420# Los Alamos National Lab., NM.
A 3-D MEASUREMENT SYSTEM USING OBJECT-ORIENTED FORTH
Kenneth B. Butterfield 1989 8 p Presented at the 1989 FORML Conference, Pacific Grove, CA, 24-26 Nov. 1989
(Contract W-7405-eng-36)
(DE90-003393; LA-UR-89-3679; CONF-8911140-1) Avail: NTIS HC A02/MF A01

Discussed is a system for storing 3-D measurements of points that relates the coordinate system of the measurement device to the global coordinate system. The program described here used object oriented FORTH to store the measured points as sons of the measuring device location. Conversion of local coordinates to absolute coordinates is performed by passing messages to the point objects. Modifications to the object oriented FORTH system are also described. DOE

N90-16421# Fermi National Accelerator Lab., Batavia, IL. Theoretical Physics Div.
THE THEORY OF HYBRID STOCHASTIC ALGORITHMS
A. D. Kennedy (Florida State Univ., Tallahassee.) 21 Nov. 1989 26 p Presented at the Workshop on Probabilistic Methods in Quantum Field Theory and Quantum Gravity, Cargese, France, 21-27 Aug. 1989
(Contracts DE-AC02-76CH-03000; DE-FC05-85ER-25000)
(DE90-003941; FNAL/C-89/237-T; CONF-8908189-1; FSU-SCRI-89-147) Avail: NTIS HC A03/MF A01

These lectures introduce the family of Hybrid Stochastic Algorithms for performing Monte Carlo calculations in Quantum Field Theory. After explaining the basic concepts of Monte Carlo integration, the properties are discussed of Markov processes and one particularly useful example of them: the Metropolis algorithm. Building upon this framework, the Hybrid and Langevin algorithms are considered from the viewpoint that they are approximate versions of the Hybrid Monte Carlo method; and thus Molecular Dynamics are considered using the Leapfrog algorithm. The lectures conclude by reviewing recent progress in these areas, explaining higher order integration schemes, the asymptotic large volume behavior of the various algorithms, and some simple exact results obtained by applying them to free field theory. It is attempted throughout to give simple yet correct proofs of the various results encountered. DOE

N90-16422# Oak Ridge National Lab., TN. Computing and Telecomunications Div.
EZVIDEO, FORTRAN GRAPHICS ROUTINES FOR THE IBM AT

M. R. Patterson, J. T. Holdeman, R. C. Ward, and W. L. Jackson Oct. 1989 29 p
(Contract DE-AC05-84OR-21400)
(DE90-004409; ORNL/CSD/TM-265) Avail: NTIS HC A03/MF A01

A set of IBM PC-based FORTRAN plotting routines called EZVIDEO is described in this report. These routines are written in FORTRAN and can be called from FORTRAN programs. EZVIDEO simulates a subset of the well-known DISSPLA graphics calls and makes plots directly on the IBM AT display screen. Screen dumps can also be made to an attached LaserJet or Epson printer to make hard copy without using terminal emulators. More than forty DISSPLA calls are simulated by the EZVIDEO routines. Typical screen plots require about 10 seconds (s), and good hard copy of the screen image on a laser printer requires less than 2 minutes (min). This higher-resolution hard copy is adequate for most purposes because of the enhanced resolution of the screen in the EGA and VGA modes. These EZVIDEO routines give the IB, AT user a stand-alone capability to make useful scientific or engineering plots directly on the AT, using data generated in FORTRAN programs. The routines will also work on the IBM PC or XT in CGA mode, but they require more time and yield less resolution. DOE

N90-16423*# National Aeronautics and Space Administration. Ames Research Center, Moffett Field, CA.
BASIC MATHEMATICAL FUNCTION LIBRARIES FOR SCIENTIFIC COMPUTATION
David C. Galant Dec. 1989 28 p
(NASA-TM-102256; A-90015; NAS 1.15:102256) Avail: NTIS HC A03/MF A01 CSCL 09B

Ada packages implementing selected mathematical functions for the support of scientific and engineering applications were written. The packages provide the Ada programmer with the mathematical function support found in the languages Pascal and FORTRAN as well as an extended precision arithmetic and a complete complex arithmetic. The algorithms used are fully described and analyzed. Implementation assumes that the Ada type FLOAT objects fully conform to the IEEE 754-1985 standard for single binary floating-point arithmetic, and that INTEGER objects are 32-bit entities. Codes for the Ada packages are included as appendixes. Author

N90-16424*# PRC Kentron, Inc., Hampton, VA. Aerospace Technologies Div.
CPU TIMING ROUTINES FOR A CONVEX C220 COMPUTER SYSTEM
Mary Ann Bynum Dec. 1989 22 p
(Contract NAS1-18000)
(NASA-CR-181950; NAS 1.26:181950) Avail: NTIS HC A03/MF A01 CSCL 09B

The timing routines available on the CONVEX C220 computer system in the Structural Mechanics Division (SMD) at NASA Langley Research Center are examined. The function of the timing routines, the use of the timing routines in sequential, parallel, and vector code, and the interpretation of the results from the timing routines with respect to the CONVEX model of computing are described. The timing routines available on the SMD CONVEX fall into two groups. The first group includes standard timing routines generally available with UNIX 4.3 BSD operating systems, while the second group includes routines unique to the SMD CONVEX. The standard timing routines described in this report are /bin/csh time,/bin/time, etime, and ctime. The routines unique to the SMD CONVEX are getinfo, second, cputime, toc, and a parallel profiling package made up of palprof, palinit, and palsum. Author

N90-16425# Royal Signals and Radar Establishment, Malvern (England).
THE NEW PROGRAMMING
C. S. E. Phillips and B. D. Bramson, ed. May 1989 29 p
(RSRE-Memo-4249; BR111061; ETN-90-96112) Copyright Avail: NTIS HC A03/MF A01

An approach to the design of computer programs, targeted at the so called software crisis, is presented. The sequential mode of thinking that underpins conventional programming is shown to be unnecessary, complicated and impractical for all but the most trivial of problems. In new programming, the flow of data is the only factor of importance. A new computer is defined as a nonsequential machine whose elemental processors are not required to execute their proecesses in an ordered sequence. Such a machine is easier to design and easier to prove correct than its sequential counterpart. ESA

N90-16426# Royal Signals and Radar Establishment, Malvern (England).
THE INSIDE-OUTSIDE ALGORITHM: FURTHER EXPERIMENTS ON THREE AND FOUR LETTER WORD SPELLING AND IMPLEMENTATION ON AN ARRAY PROCESSOR
Lorraine Dodd 1 Mar. 1989 24 p
(RSRE-Memo-4256; BR110021; ETN-90-96113) Copyright Avail: NTIS HC A03/MF A01

An application of the inside-outside algorithm to learning rules for the spelling of English words is described. The experiments examine the effect of using prior knowledge and further experiments compare stochastic regular grammars with stochastic context-free grammars. The problems of using the inside-outside algorithm are discussed and an implementation on an array processor is described. The question of not designating special pre-terminal symbols and allowing the non-terminals to be unrestricted in their roles as pre or non-terminals, is investigated. ESA

N90-16427# Royal Signals and Radar Establishment, Malvern (England).
A PERSISTENT HEAP FOR ALGOL 68
S. J. Rees, G. Cliff, P. D. Hammond, and N. E. Peeling Feb. 1989 13 p
(RSRE-Memo-4268; BR109992; ETN-90-96115) Copyright Avail: NTIS HC A03/MF A01

A method of extending the KeepSake procedures, to facilitate the production of a persistent heap, is described. KeepSake is a multiuser data base kernel, which extends a programming language to enable simple data structures to be written to disc. KeepSake cannot be called by the user directly on compound data structures. In the suggested method, all the data structures in the programming language can be written to disc. The software is produced in the form of two procedures, Persist and Unpersist. It is developed using ALGOL 68 on a VAX/VMS system and can be easily applied to other languages and machines. ESA

N90-16428# Royal Signals and Radar Establishment, Malvern (England).
ALVEY MMI007. OBJECT IDENTIFICATION FROM 2D IMAGES: THE RSRE CONTRIBUTION
P. Fretwell and R. Series May 1989 23 p Original contains color illustrations
(RSRE-Memo-4277; BR110853; ETN-90-96117) Copyright Avail: NTIS HC A03/MF A01

The Alvey program is a government scheme to improve the United Kingdoms competitiveness in the field of information technology. A consortia was formed in 1984 to tackle the subjects in a complicated environment from 2-D images. The RSRE (Royal Signals and Radar Establishment) contribution to the MMI007 project is reported. The main achievements of the project are: the development of a rich edge finder, suitable for parallel machines, the use of fractal dimension for line classification, the use of statistical measures for cueing, the use of Prolog to improve performance of image features, and the appraisal of fuzzy logic for reasoning. ESA

N90-16429# Royal Signals and Radar Establishment, Malvern (England).
BEAMFORMING PRE-PROCESSORS FOR HIGH DISCRIMINATION ALGORITHMS
J. L. Mather Aug. 1989 32 p
(RSRE-Memo-4304; BR111532; ETN-90-96121) Copyright Avail: NTIS HC A03/MF A01

The method for processing time reduction in high resolution algorithms is examined. This is achieved by means of a beamforming preprocessor. High discrimination algorithms based on numerical techniques such as eigen analysis are considered for use in future antenna array systems. In addition to being computationally expensive, such algorithms are only able to achieve significantly enhanced within-beam resolution at high signal to noise ratios. The Monte Carlo results demonstrated that such preprocessing can significantly improve the ability of a number of high discrimination algorithms to extract signal parameters from noise data. Beamforming pre-processing has a beneficial effect on data taken from an array whose calibration is randomly perturbed. Using a non-linear array, such processing is demonstrated to be equally applicable to alternative array geometries. ESA

N90-16430# Royal Signals and Radar Establishment, Malvern (England).
PATTERN MATCHING IN ML: A CASE STUDY IN REFINEMENT
R. Macdonald, G. P. Randell, and C. T. Sennett May 1989 59 p
(RSRE-89004; BR110583; ETN-90-96122) Copyright Avail: NTIS HC A04/MF A01

A case study in data refinement is reported. It is the process of taking a formal specification written in terms of abstract values and converting it into a concrete form suitable for implementation. The case study takes a non-trivial problem, namely pattern matching in the language ML. The refinement process and proof obligations incurred, concluding with an implementation in Algol68, is presented. The strengths and weaknesses of the formal developmet process, are discussed. The results show that the formal development process is useful and a cost effective technique for developing software formal proof adds to the assurance, but complete formality obscures. Proof needs to be undertaken within a context using both formal and informal elements. The structure of the proof and the way it is delivered to an evaluator ought to follow intuitive, informal, proof methods. ESA

N90-16431# Royal Signals and Radar Establishment, Malvern (England).
THE NODEN HARDWARE DESCRIPTION LANGUAGE
C. H. Pygott Aug. 1989 38 p
(RSRE-89011; BR111665; ETN-90-96123) Copyright Avail: NTIS HC A03/MF A01

The syntax and semantics of the NODEN Hardware Description Language (NODEN HDL), are described. NODEN is a suite of programs designed to perform hardware analysis on moderately complex blocks of logic, to prove the correspondence between the specification and implementation of a circuit. It is intended that circuits to be analyzed should be described in the NODEN-HDL. The language description file, the integer constant declarations, the type declarations, the functional unit definitions and the changes from previous versions, are discussed. ESA

N90-16432# Royal Signals and Radar Establishment, Malvern (England).
THE ALGEBRA OF THE NODEN ANALYSER
C. H. Pygott Aug. 1989 36 p
(RSRE-89012; BR111545; ETN-90-96124) Copyright Avail: NTIS HC A03/MF A01

NODEN is a suite of programs designed to perform hardware analysis on moderately complex blocks of logic, to prove the correspondence between the specification and implementation of a circuit. It is intended that circuits to be analyzed are described in the NODEN Hardware Description Language, NODEN-HDL. The basic features of NODEN, the circuits it can reason about and the operations performed by the analyzer in terms of set operations, are described. The possible representations that can be used for sets, and the operations on them, are discussed. A comparison of the performance of a number of different analyzers, based on different internal representations, when used on an actual application, is performed. ESA

N90-16433# Royal Signals and Radar Establishment, Malvern (England).
TOOL SUPPORT FOR THE PRODUCTION OF HIGH INTEGRITY SOFTWARE
C. T. Sennett Apr. 1989 28 p
(RSRE-89005; BR110738; ETN-90-96210) Copyright Avail: NTIS HC A03/MF A01

The software tools required for the production of trusted software are discussed. The guidelines given by the U.K. systems security confidence levels are followed. The following topics are analyzed: specification of security requirements, architectural definition, implementation, evaluation, document preparation, and configuration control. Recommendations for the development of new tools and techniques are given. ESA

N90-16434# Grenoble-1 Univ. (France). Lab. d'Informatique Fondamentale et d'Intelligence Artificielle.
APPEARANCE ANALYSIS FROM CAD MODELS
Ge Chen Oct. 1988 42 p
(IMAG-RR-756-I-IMAG-88-LIFIA; ETN-90-95704) Avail: NTIS HC A03/MF A01

An analytical Computer Aided Design (CAD) method for computing all the characteristic views of a 3-D polyhedral object, and the regions on the viewing sphere from which each characteristic view can be seen, is presented. A characteristic view is defined as a class of topologically equivalent views. This kind of analysis is useful for geometric reasoning and object recognition. The method proceeds in two major steps: an auxiliary object defined by the convex hull is computed and second, the viewing hemisphere is analytically cut into sections of equivalent appearance, by a computation essentially based on surface normals. The case of convex objects and the case of concave objects, by the introduction of auxiliary surfaces, are currently handled. ESA

N90-16435# Centre de Recherches Scientifiques et Techniques de l'Industrie des Fabrications Metalliques, Brussels (Belgium). Section Construction Mecanique.
LOW-COST VOLUMETRIC MODELING [LA MODELISATION VOLUMIQUE A PRIX MODERE]
Richard Aerens, Jan DeFraine, and Marc Deniel Sep. 1989 78 p In FRENCH Sponsored by the Institut pour l'Encouragement de la Recherche Scientifique dans l'Industrie et l'Agriculture
(CRIF-MC-85; ETN-90-96029) Avail: NTIS HC A05/MF A01

Volumetric modeling research using personal computers is described. It is shown that a personal computer cannot handle modeling problems in which the pieces measured have cylindrical or conic parts. These dramatically increase computational complexity and call for a more powerful computer. Software used in analyzing solids with curved surfaces are reviewed. The advantages and disadvantages of facet analysis are discussed. Limitations in available software are pointed out and future software developments are predicted. ESA

N90-16436# Laboratoire d'Automatique et d'Analyse des Systemes, Toulouse (France). Groupe Robotique et Intelligence Artificielle.
OPTIMIZATION OF MONOTONIC INFERENCE ALGORITHMS IN PROPOSITIONAL AND FIRST ORDER LOGIC Ph.D. Thesis - Toulouse Univ.
Gonzalo Escalada-Imaz 1989 200 p In FRENCH; ENGLISH summary
(LAAS-89204; ETN-90-96039) Avail: NTIS HC A09/MF A02

Monotonic inference algorithms are used to improve the deduction capabilities of propositional and first order logic. The considered knowledge representation formalism is decomposed into several subformalisms, going from the simple case dealing with horn propositional expressions to the most general case treating normal forms in first order logic. Some inference engines for a class of rule-based systems in propositional logic are presented. A computer theorem prover, a first order unification algorithm and an inference control scheme for first order calculus

are presented. All these methods are shown to be significant improvements over pre-existent methods. ESA

N90-16437# Laboratoire d'Automatique et d'Analyse des Systemes, Toulouse (France).
SOFTWARE DEPENDABILITY GROWTH CHARACTERIZATION, MODELING AND EVALUATION Ph.D. Thesis - Inst. National Polytechnique de Toulouse
Karama Kanoun 1989 178 p In FRENCH; ENGLISH summary
(LAAS-89320; ETN-90-96041) Avail: NTIS HC A09/MF A02

Software dependability modeling and evaluations both theoretical and practical, are considered. Software behavior is modeled in different situations including immediate correction of faults, delayed corrections, and specification changes. A knowledge model is established for each situation and these are approached by action models which are less detailed and thus less complex. A software dependability evaluation method is proposed and applied to two different systems. The method is based on the collection and processing of failure data. The data set is pre-processed so as to be sure that it is homogeneous and to identify periods of time during which reliability increases or decreases. Reliability growth models are applied separately to these periods, and predictions are significantly improved. The relevance of the proposed method is shown through its application to the software of two switching systems. ESA

N90-16438# Oak Ridge National Lab., TN. Engineering Physics and Mathematics Div.
DESIGN AND IMPLEMENTATION OF A MULTI-SENSOR FUSION ALGORITHM ON A HYPERCUBE COMPUTER ARCHITECTURE
Charles W. Glover 1989 16 p Presented at the SPIE Symposium on Advances in Intelligent Robotic Systems, Philadelphia, PA, 5-11 Nov. 1989
(Contract DE-AC05-84OR-21400)
(DE90-003682; CONF-8911125-2) Avail: NTIS HC A03/MF A01

A multi-sensor integration (MSI) algorithm written for sequential single processor computer architecture was transformed into a concurrent algorithm and implemented in parallel on a multi-processor hypercube computer architecture. This paper presents the philosophy and methodologies used in the decomposition of the sequential MSI algorithm, and its transformation into a parallel MSI algorithm. The parallel MSI algorithm was implemented on a NCUBE (trademark) hypercube computer. The performance of the parallel MSI algorithm was measured and compared against its sequential counterpart by running test case scenarios through a simulation program. The simulation program allows the user to define the trajectories of all players in the scenarios, and to pick the sensor suites of the players and their operating characteristics. DOE

N90-16439# Sandia National Labs., Albuquerque, NM. Primary Standards Lab.
RESULTS OF ERROR CORRECTION TECHNIQUES APPLIED ON TWO HIGH ACCURACY COORDINATE MEASURING MACHINES
C. Pace, T. Doiron, D. Stieren, B. Borchardt, and R. Veale (National Inst. of Standards and Technology, Gaithersburg, MD.) 1990 11 p Presented at the Measurement Science Conference, Anaheim, CA, 8-9 Feb. 1990
(Contract DE-AC04-76DP-00789)
(DE90-003341; SAND-89-2820C; CONF-900250-1) Avail: NTIS HC A03

The Primary Standards Laboratory at Sandia National Laboratories (SNL) and the Precision Engineering Division at the National Institute of Standards and Technology (NIST) are in the process of implementing software error correction on two nearly identical high accuracy coordinate measuring machines (CMMs). Both machines are Moore Special Tool Company M-48 CMMs which are fitted with laser positioning transducers. Although both machines were manufactured to high tolerance levels, the overall volumetric accuracy was insufficient for calibrating standards to the levels both laboratories require. The error mapping procedure was developed at NIST in the mid 1970's on an earlier but similar model. The error mapping procedure was originally very complicated and did not make any assumptions about the rigidness of the machine as it moved, each of the possible error motions was measured at each point of the error map independently. A simpler mapping procedure was developed during the early 1980's which assumed rigid body motion of the machine. This method was used to calibrate lower accuracy machines with a high degree of success and similar software correction schemes have been implemented by many CMM manufacturers. The rigid body model has not yet been used on highly repeatable CMMs such as the M48. Early mapping data is presented for the two M48 CMMs. The SNL CMM was manufactured in 1985 and has been in service for approximately four years, whereas the NIST CMM was delivered in early 1989. DOE

N90-16440# Lawrence Livermore National Lab., CA. Tool Design Group.
COMPUTER AIDED DESIGN BASED OPTICAL SYSTEM MODELING
Paul Geraghty 12 Sep. 1989 42 p Presented at the 6th DOE Workshop on Computer-Aided Engineering, Santa Fe, NM, 23-24 Oct. 1989 Submitted for publication
(Contract W-7405-eng-48)
(DE90-003453; UCRL-101940; CONF-8910220-2) Avail: NTIS HC A03/MF A01

The feasibility of an optical system is usually first determined through experiment. If the system performance during the experiment deviates from what is anticipated, the source of the deviation is isolated and corrected, then the system is tested again. Any new anomaly detected during the second test must be corrected and the system must be tested once more. This design cycle is repeated as many times as necessary to produce the desired system performance. Typically, the experiment is in the form of a bench test. With the advent of CAD systems with sophisticated programming and 3-D capabilities, optical systems can now be tested on a computer before components are bought and test fixtures are fabricated. Modeling the optical system on a computer provides an opportunity for cost savings and reduced design time by finding major design flaws before hardware is made. As an example, consider an optical system that uses a laser, beamsplitter, and two detectors to measure the translation and rotation of a piece of mechanical hardware. The beamsplitter and detectors would be defined as surfaces using the CAD software and their properties would be stored as entity attributes. The laser beam path would be defined as a series of lines starting from an origin and ending at the detectors. The optical modeling program, written in the CAD system programming language, would determine the laser path using the optical properties and surface geometry stored in the CAD data base. The modeling program could also simulate movement of the mechanical hardware, pass the coordinate readings of the detectors to the system data acquisition program, and compare the known movements with the derived movements, making it possible to test the validity of the data acquisition program as well as the optical system. DOE

N90-16441# Massachusetts Univ., Amherst. Automation and Robotics Lab.
INTERPRETATION OF CAD (COMPUTER AIDED DESIGN) MODELS THROUGH IGES (INITIAL GRAPHICS EXCHANGE SPECIFICATION) INTERFACE
Bartholomew O. Nnaji and Tzong-Shyan Kang 1989 58 p Sponsored in part by Digital Equipment Corp.
(Grant NSF DMC-86-10417)
(PB90-121294; NSF/ENG-89049) Avail: NTIS HC A04/MF A01 CSCL 09B

A scheme is described for recognizing and representing features for CAD data extracted using Initial Graphics Exchange Specification interface. The concepts developed are based on graph-based feature representation, where features are represented by a set of faces as well as their topological adjacency.

Strategies for classifying features and methods of decomposing a complicated feature into several simpler features for recognition purposes are discussed. Author

N90-16699*# Lehigh Univ., Bethlehem, PA. Dept. of Industrial Engineering.
OFF-LINE ROBOT PROGRAMMING AND GRAPHICAL VERIFICATION OF PATH PLANNING
Gregory L. Tonkay *In* University of Central Florida, NASA/ASEE Summer Faculty Fellowship Program Oct. 1989 p 303-323 (For primary document see N90-16686 08-99)
Avail: NTIS HC A18/MF A03 CSCL 09B

N90-16702*# Missouri Univ., Rolla. Dept. of Computer Science.
INVESTIGATION OF IGES FOR CAD/CAE DATA TRANSFER
George W. Zobrist *In* University of Central Florida, NASA/ASEE Summer Faculty Fellowship Program Oct. 1989 p 382-413 (For primary document see N90-16686 08-99)
Avail: NTIS HC A18/MF A03 CSCL 09B

62 COMPUTER SYSTEMS

Includes computer networks and special application computer systems.

N90-16442*# National Aeronautics and Space Administration. Goddard Space Flight Center, Greenbelt, MD.
THE 2ND SYMPOSIUM ON THE FRONTIERS OF MASSIVELY PARALLEL COMPUTATIONS
Ronnie Mills, ed. (ST Systems Corp., Lanham, MD.) Washington IEEE Computer Society Press 1988 721 p Symposium held in Fairfax, VA, 10-12 Oct. 1988; sponsored by NASA, Goddard Space Flight Center, IEEE, and George Mason Univ. Sponsored by Active Memory Technology, Digital Equipment Corp., LORAL Defence Systems, Martin Marietta Aerospace, Science Applications Research, ST Systems Corp., and Thinking Machines Corp.
(NASA-TM-101918; NAS 1.15:101918; IEEE-Order-892; LC-88-82088; IEEE-Catalog-88CH2649-2; ISBN-0-8186-0892-7; SAN-264-620X) Avail: NTIS HC A99/MF A04 CSCL 09B

Programming languages, computer graphics, neural networks, massively parallel computers, SIMD architecture, algorithms, digital terrain models, sort computation, simulation of charged particle transport on the massively parallel processor and image processing are among the topics discussed. For individual titles, see N90-16443 through N90-16454.

N90-16443*# National Aeronautics and Space Administration. Goddard Space Flight Center, Greenbelt, MD.
HOW TO CLUSTER IN PARALLEL WITH NEURAL NETWORKS
Behzad Kamgar-Parsi, J. A. Gualtieri, Judy E. Devaney, and Behrooz Kamgar-Parsi (George Mason Univ., Fairfax, VA.) *In its* The 2nd Symposium on the Frontiers of Massively Parallel Computations 1988 p 31-38 (For primary document see N90-16442 08-62)
Avail: NTIS HC A99/MF A04 CSCL 09B

Partitioning a set of N patterns in a d-dimensional metric space into K clusters - in a way that those in a given cluster are more similar to each other than the rest - is a problem of interest in astrophysics, image analysis and other fields. As there are approximately K(N)/K (factorial) possible ways of partitioning the patterns among K clusters, finding the best solution is beyond exhaustive search when N is large. Researchers show that this problem can be formulated as an optimization problem for which very good, but not necessarily optimal solutions can be found by using a neural network. To do this the network must start from many randomly selected initial states. The network is simulated on the MPP (a 128 x 128 SIMD array machine), where researchers use the massive parallelism not only in solving the differential equations that govern the evolution of the network, but also by starting the network from many initial states at once, thus obtaining many solutions in one run. Researchers obtain speedups of two to three orders of magnitude over serial implementations and the promise through Analog VLSI implementations of speedups comensurate with human perceptual abilities. Author

N90-16444*# Institute for Computer Applications in Science and Engineering, Hampton, VA.
OVERVIEW AND EXTENSIONS OF A SYSTEM FOR ROUTING DIRECTED GRAPHS ON SIMD ARCHITECTURES
Sherryl Tomboulian *In* NASA, Goddard Space Flight Center, The 2nd Symposium on the Frontiers of Massively Parallel Computations 1988 p 63-67 (For primary document see N90-16442 08-62)
(Contract NAS1-18107)
Avail: NTIS HC A99/MF A04 CSCL 09B

Many problems can be described in terms of directed graphs that contain a large number of vertices where simple computations occur using data from adjacent vertices. A method is given for parallelizing such problems on an SIMD machine model that uses only nearest neighbor connections for communication, and has no facility for local indirect addressing. Each vertex of the graph will be assigned to a processor in the machine. Rules for a labeling are introduced that support the use of a simple algorithm for movement of data along the edges of the graph. Additional algorithms are defined for addition and deletion of edges. Modifying or adding a new edge takes the same time as parallel traversal. This combination of architecture and algorithms defines a system that is relatively simple to build and can do fast graph processing. All edges can be traversed in parallel in time O(T), where T is empirically proportional to the average path length in the embedding times the average degree of the graph. Additionally, researchers present an extension to the above method which allows for enhanced performance by allowing some broadcasting capabilities. Author

N90-16445*# North Carolina State Univ., Raleigh. Dept. of Computer Science.
PARALLEL ALGORITHMS FOR INTERACTIVE MANIPULATION OF DIGITAL TERRAIN MODELS
E. W. Davis, D. F. McAllister, and V. Nagaraj *In* NASA, Goddard Space Flight Center, The 2nd Symposium on the Frontiers of Massively Parallel Computations 1988 p 133-136 (For primary document see N90-16442 08-62)
Avail: NTIS HC A99/MF A04 CSCL 09B

Interactive three-dimensional graphics applications, such as terrain data representation and manipulation, require extensive arithmetic processing. Massively parallel machines are attractive for this application since they offer high computational rates, and grid connected architectures provide a natural mapping for grid based terrain models. Presented here are algorithms for data movement on the massive parallel processor (MPP) in support of pan and zoom functions over large data grids. It is an extension of earlier work that demonstrated real-time performance of graphics functions on grids that were equal in size to the physical dimensions of the MPP. When the dimensions of a data grid exceed the processing array size, data is packed in the array memory. Windows of the total data grid are interactively selected for processing. Movement of packed data is needed to distribute items across the array for efficient parallel processing. Execution time for data movement was found to exceed that for arithmetic aspects of graphics functions. Performance figures are given for routines written in MPP Pascal. Author

N90-16446*# National Aeronautics and Space Administration. Goddard Space Flight Center, Greenbelt, MD.
SORT COMPUTATION
John E. Dorband *In its* The 2nd Symposium on the Frontiers of Massively Parallel Computations 1988 p 137-141 (For primary document see N90-16442 08-62)
Avail: NTIS HC A99/MF A04 CSCL 09B

Sorting has long been used to organize data in preparation for further computation, but sort computation allows some types of computation to be performed during the sort. Sort aggregation and sort distribution are the two basic forms of sort computation.

Sort aggregation generates an accumulative or aggregate result for each group of records and places this result in one of the records. An aggregate operation can be any operation that is both associative and commutative, i.e., any operation whose result does not depend on the order of the operands or the order in which the operations are performed. Sort distribution copies the value from a field of a specific record in a group into that field in every record of that group. Author

N90-16447*# Institute for Computer Applications in Science and Engineering, Hampton, VA.
DYNAMICALLY ALLOCATING SETS OF FINE-GRAINED PROCESSORS TO RUNNING COMPUTATIONS
David Middleton *In* NASA, Goddard Space Flight Center, The 2nd Symposium on the Frontiers of Massively Parallel Computations 1988 p 191-194 (For primary document see N90-16442 08-62)
Avail: NTIS HC A99/MF A04 CSCL 09B

Researchers explore an approach to using general purpose parallel computers which involves mapping hardware resources onto computations instead of mapping computations onto hardware. Problems such as processor allocation, task scheduling and load balancing, which have traditionally proven to be challenging, change significantly under this approach and may become amenable to new attacks. Researchers describe the implementation of this approach used by the FFP Machine whose computation and communication resources are repeatedly partitioned into disjoint groups that match the needs of available tasks from moment to moment. Several consequences of this system are examined. Author

N90-16448*# Maryland Univ., College Park. Dept. of Physics and Astronomy.
STOCHASTIC SIMULATION OF CHARGED PARTICLE TRANSPORT ON THE MASSIVELY PARALLEL PROCESSOR
James A. Earl *In* NASA, Goddard Space Flight Center, The 2nd Symposium on the Frontiers of Massively Parallel Computations 1988 p 237-240 (For primary document see N90-16442 08-62)
(Grant NGR-21-002-066)
Avail: NTIS HC A99/MF A04 CSCL 09B

Computations of cosmic-ray transport based upon finite-difference methods are afflicted by instabilities, inaccuracies, and artifacts. To avoid these problems, researchers developed a Monte Carlo formulation which is closely related not only to the finite-difference formulation, but also to the underlying physics of transport phenomena. Implementations of this approach are currently running on the Massively Parallel Processor at Goddard Space Flight Center, whose enormous computing power overcomes the poor statistical accuracy that usually limits the use of stochastic methods. These simulations have progressed to a stage where they provide a useful and realistic picture of solar energetic particle propagation in interplanetary space. Author

N90-16449*# National Aeronautics and Space Administration. Goddard Space Flight Center, Greenbelt, MD.
ESTIMATING WATER FLOW THROUGH A HILLSLOPE USING THE MASSIVELY PARALLEL PROCESSOR
Judy E. Devaney (Science Applications Research, Lanham, MD.), P. J. Camillo, and R. J. Gurney *In its* The 2nd Symposium on the Frontiers of Massively Parallel Computations 1988 p 249-256 (For primary document see N90-16442 08-62)
(Contract NAS5-28200)
Avail: NTIS HC A99/MF A04 CSCL 09B

A new two-dimensional model of water flow in a hillslope has been implemented on the Massively Parallel Processor at the Goddard Space Flight Center. Flow in the soil both in the saturated and unsaturated zones, evaporation and overland flow are all modelled, and the rainfall rates are allowed to vary spatially. Previous models of this type had always been very limited computationally. This model takes less than a minute to model all the components of the hillslope water flow for a day. The model can now be used in sensitivity studies to specify which measurements should be taken and how accurate they should be to describe such flows for environmental studies. Author

N90-16450*# National Aeronautics and Space Administration. Goddard Space Flight Center, Greenbelt, MD.
SCAN LINE GRAPHICS GENERATION ON THE MASSIVELY PARALLEL PROCESSOR
John E. Dorband *In its* The 2nd Symposium on the Frontiers of Massively Parallel Computations 1988 p 327-329 (For primary document see N90-16442 08-62)
Avail: NTIS HC A99/MF A04 CSCL 09B

Described here is how researchers implemented a scan line graphics generation algorithm on the Massively Parallel Processor (MPP). Pixels are computed in parallel and their results are applied to the Z buffer in large groups. To perform pixel value calculations, facilitate load balancing across the processors and apply the results to the Z buffer efficiently in parallel requires special virtual routing (sort computation) techniques developed by the author especially for use on single-instruction multiple-data (SIMD) architectures. Author

N90-16451*# National Aeronautics and Space Administration. Goddard Space Flight Center, Greenbelt, MD.
PARALLEL ALGORITHM FOR DETERMINING MOTION VECTORS IN ICE FLOE IMAGES BY MATCHING EDGE FEATURES
M. Manohar, H. K. Ramapriyan, and J. P. Strong *In its* The 2nd Symposium on the Frontiers of Massively Parallel Computations 1988 p 343-347 (For primary document see N90-16442 08-62)
Avail: NTIS HC A99/MF A04 CSCL 09B

A parallel algorithm is described to determine motion vectors of ice floes using time sequences of images of the Arctic ocean obtained from the Synthetic Aperture Radar (SAR) instrument flown on-board the SEASAT spacecraft. Researchers describe a parallel algorithm which is implemented on the MPP for locating corresponding objects based on their translationally and rotationally invariant features. The algorithm first approximates the edges in the images by polygons or sets of connected straight-line segments. Each such edge structure is then reduced to a seed point. Associated with each seed point are the descriptions (lengths, orientations and sequence numbers) of the lines constituting the corresponding edge structure. A parallel matching algorithm is used to match packed arrays of such descriptions to identify corresponding seed points in the two images. The matching algorithm is designed such that fragmentation and merging of ice floes are taken into account by accepting partial matches. The technique has been demonstrated to work on synthetic test patterns and real image pairs from SEASAT in times ranging from .5 to 0.7 seconds for 128 x 128 images. Author

N90-16452*# National Aeronautics and Space Administration. Goddard Space Flight Center, Greenbelt, MD.
IMAGE SEGMENTATION BY ITERATIVE PARALLEL REGION GROWING WITH APPLICATION TO DATA COMPRESSION AND IMAGE ANALYSIS
James C. Tilton *In its* The 2nd Symposium on the Frontiers of Massively Parallel Computations 1988 p 357-360 (For primary document see N90-16442 08-62)
Avail: NTIS HC A99/MF A04 CSCL 09B

Image segmentation can be a key step in data compression and image analysis. However, the segmentation results produced by most previous approaches to region growing are suspect because they depend on the order in which portions of the image are processed. An iterative parallel segmentation algorithm avoids this problem by performing globally best merges first. Such a segmentation approach, and two implementations of the approach on NASA's Massively Parallel Processor (MPP) are described. Application of the segmentation approach to data compression and image analysis is then described, and results of such application are given for a LANDSAT Thematic Mapper image. Author

N90-16453*# Microelectronics Center of North Carolina, Research Triangle Park.
BLITZEN: A HIGHLY INTEGRATED MASSIVELY PARALLEL MACHINE
D. W. Blevins, E. W. Davis, R. A. Heaton, and J. H. Reif (Duke Univ., Durham, NC.) *In* NASA, Goddard Space Flight Center, The 2nd Symposium on the Frontiers of Massively Parallel Computations 1988 p 399-406 Previously announced in IAA as A89-32316 (For primary document see N90-16442 08-62)
(Contracts NAG5-966; N00014-80-C-0647; N00014-87-K-0310; N00014-88-K-0458; DAAL03-88-K-0195; NSF CCR-86-96134; AF-AFOSR-0386-87)
Avail: NTIS HC A99/MF A04 CSCL 09B

The architecture and VLSI design of a new massively parallel processing array chip are described. The BLITZEN processing element array chip, which contains 1.1 million transistors, serves as the basis for a highly integrated, miniaturized, high-performance, massively parallel machine that is currently under development. Each processing element has 1K bits of static RAM and performs bit-serial processing with functional elements for arithmetic, logic, and shifting. Author

N90-16454*# National Aeronautics and Space Administration. Goddard Space Flight Center, Greenbelt, MD.
A GENERIC FINE-GRAINED PARALLEL C
L. Hamet and John E. Dorband *In its* The 2nd Symposium on the Frontiers of Massively Parallel Computations 1988 p 625-628 (For primary document see N90-16442 08-62)
Avail: NTIS HC A99/MF A04 CSCL 09B

With the present availability of parallel processors of vastly different architectures, there is a need for a common language interface to multiple types of machines. The parallel C compiler, currently under development, is intended to be such a language. This language is based on the belief that an algorithm designed around fine-grained parallelism can be mapped relatively easily to different parallel architectures, since a large percentage of the parallelism has been identified. The compiler generates a FORTH-like machine-independent intermediate code. A machine-dependent translator will reside on each machine to generate the appropriate executable code, taking advantage of the particular architectures. The goal of this project is to allow a user to run the same program on such machines as the Massively Parallel Processor, the CRAY, the Connection Machine, and the CYBER 205 as well as serial machines such as VAXes, Macintoshes and Sun workstations. Author

N90-16455# Massachusetts Inst. of Tech., Cambridge. Lab. for Computer Science.
ON THE EFFICIENT EXPLOITATION OF SPECULATION UNDER DATA FLOW PARADIGMS OF CONTROL
Richard M. Soley Nov. 1989 165 p
(Contract N00014-84-K-0099)
(AD-A214112; MIT/LCS/TR-443) Avail: NTIS HC A08/MF A01 CSCL 12/6

Data flow architectures to exploit the parallelism in large scientific codes are now taking form. However, no approach to exploiting speculative, searching parallelism has been explored, even though (or perhaps because) the potential parallelism of such applications is tremendous. A view of speculation as a process which may proceed in parallel in a controlled fashion is explored, using examples from actual symbolic processing situations. The central issue of exploiting this parallelism is the dynamic containment of the resources necessary to execute large speculative codes. Efficient structures (graph schemata and architectural support) are shown for executing highly speculative programs (such as expert systems) under a data flow executing paradigm. Controls over cross-procedure parallelism in an extensible manner are presented, with applications to the various current problems of data flow computation. Approaches to scheduling, prioritization and search tree pruning are considered, evaluated and compared. GRA

63 CYBERNETICS

Includes feedback and control theory, artificial intelligence, robotics and expert systems.

For related information see also *54 Man/System Technology and Life Support.*

N90-16691*# Oklahoma State Univ., Stillwater. Dept. of Psychology.
THE DAB MODEL OF DRAWING PROCESSES
Larry W. Hochhaus *In* University of Central Florida, NASA/ASEE Summer Faculty Fellowship Program Oct. 1989 p 102-124 (For primary document see N90-16686 08-99)
Avail: NTIS HC A18/MF A03 CSCL 09B

N90-16697*# Mississippi State Univ., State College. Dept. of Mechanical Engineering.
ARTIFICIAL INTELLIGENCE IN PROCESS CONTROL: KNOWLEDGE BASE FOR THE SHUTTLE ECS MODEL
A. Kent Stiffler *In* University of Central Florida, NASA/ASEE Summer Faculty Fellowship Program Oct. 1989 p 270-291 (For primary document see N90-16686 08-99)
Avail: NTIS HC A18/MF A03 CSCL 09B

64 NUMERICAL ANALYSIS

Includes iteration, difference equations, and numerical approximation.

N90-16456# International Centre for Theoretical Physics, Trieste (Italy).
THEORY OF SINGULAR LAGRANGIANS
Jose F. Carinena (Zaragoza Univ., Spain) Apr. 1989 47 p Submitted for publication
(DE90-600735; IC-89/61) Avail: NTIS (US Sales Only) HC A03/MF A01

The Lagrangian description of a system in Dirac's approach is analyzed from a geometric viewpoint. The geometric tools used in such a description are those of (pre-) symplectic geometry. The theory of Hamiltonian dynamical systems is presented, showing how both the Hamiltonian and Lagrangian approaches arise as particular cases when the Lagrangian is regular and the case of pre-symplectic systems corresponding to the case of Lagrangian being singular is carefully analyzed. DOE

N90-16457# International Centre for Theoretical Physics, Trieste (Italy).
SIMPLE PROOF OF RENORMALIZATION GROUP EQUATION IN THE MINIMAL SUBTRACTION SCHEME
K. G. Chetyrkin (Academy of Sciences, USSR, Moscow) Apr. 1989 18 p Submitted for publication
(DE90-600758; IC-88/418) Avail: NTIS (US Sales Only) HC A03/MF A01

A simple combinatorial proof is given of the renormalization group equation in the minimal subtraction scheme. Being mathematically rigorous, the proof avoids both the notorious complexity of techniques using parametric representations of Feynman diagrams and heuristic arguments of usual proofs calling up bare fields living in the space-time of complex dimension. It also copes easily with the general case of Green functions of arbitrary number of composite fields. DOE

N90-16458# Johns Hopkins Univ., Baltimore, MD. Dept. of Electrical and Computer Engineering.
ON THE RECIPROCITY OF STATE VECTORS IN BOUNDARY VALUE MODELS
Howard L. Weinert 22 Sep. 1989 8 p
(Contract N00014-89-J-1642)
(AD-A214104; JHU/ECE-89-14) Avail: NTIS HC A02/MF A01 CSCL 12/2

It is proven that the state vector of a two-point boundary value model is a reciprocal processes. GRA

N90-16459# Los Alamos National Lab., NM.
COMPLEX AVAILABILITY PROBLEMS SOLVED WITH SIMULATION
Gene J. Schroeder and Marvin M. Johnson (South Dakota School of Mines and Technology, Rapid City.) 1990 20 p Presented at the Reliability and Maintainability Symposium, Los Angeles, CA, Jan. 1990
(Contract W-7405-eng-36)
(DE89-012610; LA-UR-89-1383; CONF-900108-1) Avail: NTIS HC A03/MF A01

System owners and operators are increasingly emphasizing the actual amount of time equipment is capable of performing its intended function. For military systems, added complexity, longer service life requirements, reduced periodic maintenance, and less frequent checkouts are increasing system availability requirements. However, these factors compound the difficulty in estimating the system's true availability. With dormant or semi-dormant systems, the amount of time a system appears available may differ form the real availability. The difference in real and apparent availability is often the result of a transition from an operational but dormant state to an inoperational but dormant state. The major contributions from this research are: the development of the concept of complex availability that applies to systems which combine two or more elements of instantaneous, mission system, or steady-state availability; and the development of a modeling technique to estimate the real availability for a system which involves complex availability. DOE

N90-16460# Laboratorio de Computacao Cientifica, Rio de Janeiro (Brazil). Dept. of Research and Development.
UNIFORM STABILITY FOR TIME-VARYING INFINITE-DIMENSIONAL DISCRETE LINEAR SYSTEMS
C. S. Kubrusly (Catholic Univ., Rio de Janeiro, Brazil) Sep. 1988 31 p Revised Submitted for publication
(DE89-635712; LNCC-033/88; ISSN-0101-6113) Avail: NTIS (US Sales Only) HC A03/MF A01

Stability for time-varying discrete linear systems in a Banach space is investigated. A fairly complete collection of necessary and sufficient conditions for uniform asymptotic equistability for input-free systems is established. This includes uniform and strong power equistability, and uniform and strong l(sub p)-equistability, among other technical conditions which also play an essential role in stability theory. It is also shown that uniform asymptotic equistability for input-free systems is equivalent to each of the following concepts of uniform stability for forced systems: l(sub p)-input l(sub p)-state, c(sub o)-input c(sub o)-state, bounded-input bounded-state, l(sub p greater than 1)-input bounded-state, c(sub o)-input bounded-state, and convergent-input bounded-state; which are also equivalent to their nonuniform counterparts. For time-varying convergent systems, the above is also equivalent to convergent-input convergent-state stability. The proofs presented here are all elementary in the sense that they are based essentially only on the Banach-Steinhaus theorem. DOE

N90-16461# Laboratorio de Computacao Cientifica, Rio de Janeiro (Brazil).
AND STILL, A NEW BEGINNING: THE GALERKIN LEAST-SQUARES GRADIENT METHOD
Leopoldo P. Franca and Eduardo G. DutradoCarmo (Universidade Federal do Rio de Janeiro, Brazil) Aug. 1988 34 p
(DE89-636435; LNCC-030/88; ISSN-0101-6113) Avail: NTIS (US Sales Only) HC A03/MF A01

A finite element method is proposed to solve a scalar singular diffusion problem. The method is constructed by adding to the standard Galerkin a mesh-dependent term obtained by taking the gradient of the Euler-Lagrange equation and multiplying it by its least-squares. For the one-dimensional homogeneous problem the method is designed to develop a nodal exact solution. An error estimate shows that the method converges optimally for any value of the singular parameter. Numerical results demonstrate the good stability and accuracy properties of the method. DOE

N90-16462# Laboratorio de Computacao Cientifica, Rio de Janeiro (Brazil).
A NEW FINITE ELEMENT FORMULATION FOR CFD:8. THE GALERKIN/LEAST-SQUARES METHOD FOR ADVECTIVE-DIFFUSIVE EQUATIONS
Thomas J. R. Hughes, Gregory M. Hulbert (Stanford Univ., CA.), and Leopoldo P. Franca Oct. 1988 35 p Submitted for publication
(DE89-636437; LNCC-037/88; ISSN-0101-6113) Avail: NTIS (US Sales Only) HC A03/MF A01

Galerkin least squares finite element methods are presented for advective-diffusive equations. Galerkin least squares represents a conceptual simplification of SUPG, and is in fact applicable to a wide variety of other problem types. A convergence analysis and error estimates are presented. Author

N90-16463# Los Alamos National Lab., NM. Analysis and Testing Group.
RESTORING FORCE METHOD AND RESPONSE ESTIMATION
Elton G. Endebrock 1989 7 p Presented at the 8th International Modal Analysis Conference, Kissimmee, FL, 29 Jan. - 1 Feb. 1990
(Contract W-7405-eng-36)
(DE90-002394; LA-UR-89-3376; CONF-900139-1) Avail: NTIS HC A02/MF A01

The restoring force method is briefly outlined. Signal modifications that are necessary to successfully determine restoring force functions are discussed and illustrated. Restoring force functions for a base and a force excited system were determined and their effectiveness demonstrated by comparing measured and predicted signals. Additional developments that would make the restoring force method more general are suggested. DOE

N90-16464# International Centre for Theoretical Physics, Trieste (Italy).
MULTIPLET CLASSIFICATION OF HIGHEST WEIGHT MODULES OVER QUANTUM UNIVERSAL ENVELOPING ALGEBRAS: THE U(SUB q)(sl(3,C)) EXAMPLE
V. K. Dobrev May 1989 15 p
(DE90-600720; IC-89/142) Avail: NTIS (US Sales Only) HC A03/MF A01

The multiplet classification approach is extended to the quantum universal enveloping algebras U sub q (G), where G is any simple Lie algebra. In the case when the deformation parameter q is a root of unity we classify into multiplets and explicitly parametrize all highest weight modules (HWM) over U sub q (sl(2,C)) and U sub q (sl(3,C)). As a consequence we classify all irreducible HWM over U sub q (sl(3,C)) and give the dimensions of some of them. The same is done for U sub q (sl(2,C)) reproducing the results obtained earlier by other methods. DOE

N90-16465# Laboratorio de Computacao Cientifica, Rio de Janeiro (Brazil).
HIDDEN REGULARITY FOR A STRONGLY NONLINEAR WAVE EQUATION
Jaime E. M. Rivera Aug. 1988 22 p
(DE90-600742; LNCC-028/88; ISSN-0101-6113) Avail: NTIS (US Sales Only) HC A03/MF A01

The nonlinear wave equation u double prime - delta(u) + f(u) = v in Q = omega times O,T; u(0) = u(sub 0), u'(0) = u(sub 1) in omega; u(x,t) = 0 on sigma = gamma times O,T where f is a continuous function satisfying lim(sub s) sup yields + infinity times f(s)/s is greater than - infinity, and omega is a bounded domain of R(sup n) with smooth boundary gamma, is analyzed. It is shown that there exists a solution for the presented nonlinear wave equation that satisfies the regularity condition: partial derivative u/eta epsilon L squared (sigma). Moreover, it is shown that there exists a constant C is greater than 0, such that, the partial derivative of u/eta is less than C (E(0) + the absolute value of v squared (sub Q)). DOE

N90-16466# Rome Univ. (Italy). Dipt. di Fisica.
STOCHASTIC ACTION OF DYNAMICAL SYSTEMS ON CURVED MANIFOLDS. THE ISOKINETIC DEVELOPING MAP ON TRAJECTORIES
Ettore Aldrovandi, Daniela Dohrn (Salerno Univ., Italy), and Francesco Guerra 28 Apr. 1989 10 p Sponsored in part by the Italian Ministry of Public Education
(Preprint-666; ETN-90-95270) Avail: NTIS HC A02/MF A01

For a dynamical system on a curved configurational manifold, the definition of the classical action functional is extended to the case of diffusions. A Cartan nonintegrable isokinetic developing map, transforms trajectories on the curved manifold into trajectories on the flat initial tangent space. The main result is the absence of the Pauli-De Witt curvature term in the expression of the stochastic action functional. Considering the importance of the Pauli-De Witt term in the quantum mechanical behavior of dynamical systems on curved manifolds, it is interesting that the problem can be considered from a purely geometric point of view. The reason for this is discussed. ESA

N90-16467# Technische Univ., Eindhoven (Netherlands). Dept. of Mathematics and Computing Science.
THE ALGEBRAIC RICCATI EQUATION AND SINGULAR OPTIMAL CONTROL
A. H. W. Geerts Apr. 1989 19 p
(Memo-COSOR-89-11; ETN-90-95272) Avail: NTIS HC A03/MF A01

A class of nonnegative definite linear quadratic optimal control problems are linked to a subset of the set of real symmetric matrices that satisfy the dissipation inequality. This important subset is characterized by means of a certain algebraic Riccati equation and a linear condition. Every positive semidefinite element of the subset is attached in a one-to-one way to a certain subspace of a properly defined factor space. If the input weighting matrix in the cost functional is positive semidefinite, then the known results on bijective relations between positive semidefinite solutions of the algebraic Riccati equation and certain subspaces of the state space are recovered. ESA

N90-16468 Gesellschaft fuer Mathematik und Datenverarbeitung, Saint Augustin (Germany, F.R.). Inst. fuer Methodische Grundlagen.
MULTIGRID METHODS FOR TWO- AND THREE-DIMENSIONAL POISSON-TYPE EQUATIONS ON THE SPHERE
Saulo R. M. Barros Jun. 1989 44 p
(GMD-391; ISSN-0723-0508; ETN-90-95882) Copyright Avail: Gesellschaft fuer Mathematik und Datenverarbeitung mbH, Schloss Birlinghoven, Postfach 12 40, D-5205 Saint Augustin 1, Fed. Rep. of Germany

The efficient solution of two and three dimensional Poisson- and Helmholtz-type equations on the sphere with multigrid methods is outlined. The strong anisotropic behavior of the Laplacian in spherical coordinates poses severe requirements on the relaxation procedures, in order to attain a full multigrid effectiveness. The introduction of a combined relaxation technique results in high efficiency, even in cases with varying anisotropy direction, where alternating line- or plane-relaxations would normally be required. The combination of this relaxation technique with semi-coarsening strategies is studied. The multigrid solvers developed are shown to be competitive with two dimensional, direct fast solvers, in cases where the latter can be applied. The optimal computational complexity of the multigrid methods, their broad applicability (in contrast to fast direct solvers) and their high efficiency in three spatial dimensions are demonstrated. ESA

N90-16469# Universitaet der Bundeswehr, Neubiberg (Germany, F.R.). Forschungsschwerpunkt Simulation, Optimierung Deterministischer, Stochastischer Dynamischer Systeme.
OPTIMAL STEP SIZES IN SEMI-STOCHASTIC APPROXIMATION PROCEDURES
Kurt Marti and Ernst Ploechinger Dec. 1988 117 p
(ETN-90-95888) Avail: NTIS HC A06/MF A01

Several semistochastic approximation methods for improvement of stochastic approximation algorithms are presented. Many problems in stochastic optimization can be modeled by a mean value minimization problem. Time consuming computation of derivatives of the function can be omitted if the mean value minimization problem is solved by means of a stochastic approximation algorithm. Methods of improving on these algorithms are presented. ESA

N90-16470# Massachusetts Inst. of Tech., Cambridge.
AN IMPLICIT TIME-INTEGRATION PROCEDURE FOR A SET OF INTERNAL VARIABLE CONSTITUTIVE EQUATIONS FOR ISOTROPIC ELASTO-VISCOPLASTICITY
A. M. Lush, G. Weber, and L. Anand 1989 50 p
(Grant NSF MEA-83-15117)
(PB90-121302; NSF/ENG-89047) Avail: NTIS HC A03/MF A01 CSCL 12A

Researchers have formulated a fully-implicit, Euler backward time integration procedure for a set of internal variable constitutive equations for isothermal, isotropic elasto-viscoplasticity with isotropic hardening. The time-integration procedure is a generalization of the well-known radial-return algorithm of classical rate-independent plasticity and should, therefore, be well suited for implementation in large-scale finite element codes. As an example, the procedure has been implemented in the finite element code ABAQUS, and using he isothermal version of a recently proposed set of specific constitutive equations, the results of two sample problems are shown. Author

65 STATISTICS AND PROBABILITY

Includes data sampling and smoothing; Monte Carlo method; and stochastic processes.

No abstracts in this category.

66 SYSTEMS ANALYSIS

Includes mathematical modeling; network analysis; and operations research.

No abstracts in this category.

67 THEORETICAL MATHEMATICS

Includes topology and number theory.

N90-16471# Sandia National Labs., Albuquerque, NM.
ASYMPTOTICALLY FAST TRIANGULARIZATION OF MATRICES OVER RINGS
James L. Hafner (International Business Machines Corp., San Jose, CA.) and Kevin S. McCurley 1989 8 p Presented at the ACM/SIAM Symposium on Discrete Algorithms, San Francisco, CA, 20-24 Jan. 1990
(Contract DE-AC04-76DP-00789)
(DE90-003161; SAND-89-2581C; CONF-900148-1) Avail: NTIS HC A02/MF A01

Problems were considered which relate to the computation of Hermite and Smith normal forms of integer matrices, and more generally matrices over a principal ideal ring. First, we show that if the matrix A is m x n, with rank m and integer entries bounded in absolute value by T, then the Hermite normal form can be computed in O(m squared nB(m log(mT))) bit operations, where B(t) denotes a function that bounds the time required to perform the extended Euclidean algorithm on two t bit integers. Furthermore it is shown that the Smith normal form can be computed in O(m

cubed nB(m log(mT))log(mT)) bit operations. In the second part of the paper we apply fast matrix multiplication techniques to the problem of triangularizing a matrix over a ring using elementary column operations. It was also proved that matrix inversion and multiplication are equivalent in complexity over an arbitrary Principal Ideal Domain, generalizing a result of Bunch and Hopcroft. The general results were then applied to obtain an algorithm for triangularizing integer matrices that has a faster running timer than the known Hermite normal form algorithms. The triangular matrix that is computed has small entries like the Hermite normal form, and will suffice for many applications. A probabilistic method was discussed for calculating Smith normal forms. DOE

70 PHYSICS (GENERAL)

For precision time and time interval (PTTI) see *35 Instrumentation and Photography;* for geophysics, astrophysics or solar physics see *46 Geophysics, 90 Astrophysics,* or *92 Solar Physics.*

N90-16472# National Science Foundation, Washington, DC. Div. of Science Resource Studies.
PROJECT SUMMARIES Report, FY 1988
Sep. 1988 86 p
(PB90-103987; NSF-88-336) Avail: NTIS HC A05/MF A01 CSCL 20C

Summaries are included of over 68 projects that were in work during FY 1988 in the National Science Foundation's Division of Science Resources Studies. The projects concern the collection, interpretation, and analysis of data on characteristics, education, and employment of human resources (scientists, engineers, and technicians); on government, industry, and university funding of science and technology; on outputs and impacts of science and technology. Summaries of overviews of science and technology resources data and of data-system evaluations also are included. GRA

N90-16473# International Centre for Theoretical Physics, Trieste (Italy).
INTEGRABLE CLASSICAL SYSTEMS IN HIGHER DIMENSIONS
S. C. Mishra and D. Parashar (Delhi Univ., India) May 1989 11 p Submitted for publication Sponsored in part by UGC, India
(DE90-600737; IC-89/88) Avail: NTIS (US Sales Only) HC A03/MF A01

A general method for the construction of the second constant of motion (up to second order) for higher dimensional classical systems is carried out. Correspondingly, the first and the second order potential equations are obtained whose solutions can directly provide the integrable systems. DOE

N90-16474# Academy of Sciences (USSR), Novosibirsk. Inst. Yadernoj Fiziki.
LANGMUIR WAVE INTERACTION WITH ION-SOUND ONE. PART 1: STOCHASTIC EFFECTS
N. S. Buchelnikova and E. P. Matochkin 1988 60 p In RUSSIAN; ENGLISH summary
(DE90-603368; IYaF-88-139-Pt-1) Avail: NTIS (US Sales Only) HC A04/MF A01

The numerical experiments (PJC-method) were made to study the stochastic phenomena by the interaction of Langmuir wave and ion-sound wave. The conversion of the Langmuir wave on the ion-sound wave leads to the excitation of Langmuir wave modes N=N(sub e) + or - (beta) N(sub i), (beta) = 1,2,3. The damping of the electric field is determined by trapping of electron by the main (beta = 1,2) conversion modes and by the stochastic instability of the electron motion (the stochastic layers formation). Evolution of the stochastic layers leads to acceleration of a part of the electrons and to formation of short tails of the velocity distribution function. The Langmuir wave in the homogeneous plasma is described. The role of the ion nonlinearities (the formation of the density and velocity fronts and of the double electric layers) in the evolution of the stochasticity is shown. DOE

N90-16475# Department of the Air Force, Washington, DC.
ROTATING DOPPLER FREQUENCY SHIFTER Patent
Uve H. Lammers, inventor (to AF) and Richard A. Marr, inventor (to AF) 16 May 1989 6 p Filed 24 May 1988
(AD-D014279; US-Patent-4,830,479; US-Patent-Appl-SN-197935) Avail: US Patent and Trademark Office CSCL 20/6

A rotating Doppler Frequency shifter comprises spiral members which surrounded a first mirror affixed to a rotating shaft, and a second mirror affixed to an arm which extends from the shaft and rotates therewith. Each spiral member has a reflective inner surface which is shaped such as to reflect a signal impinging thereon back along its entry path. This arrangement provides for a continuous Doppler frequency shifting of the input signal. GRA

N90-16476# Technische Univ., Vienna (Austria). Inst. of Applied and Technical Physics.
ANISOTROPY AND MICROSTRUCTURE OF HIGH COERCIVITY RARE EARTH IRON PERMANENT MAGNETS, LIST OF PAPERS PUBLISHED
1989 211 p
(Contract DAJA45-88-C-0010)
(AD-A214160; R/D-5295-MS-01) Avail: NTIS HC A10/MF A02 CSCL 20/3

Some of the papers published at the Inst. of Applied and Technical Physics are presented. Some representative titles are: Temperature Dependence of Anisotropy Fields and Initial Susceptibility in R2Fe14B Compounds; Magnetic and Anisotropy Studies of Nd-Fe-B Based Permanent Magnets; The Hard Magnetic Properties of Sintered Nd-Fe-B Permanent Magnets; Magnetic Phase Transitions and Magnetic Anisotropy in Nd2Fe(14-x)Co(x)B Compounds; Investigation of the Hysteresis Loop and the Magnetic Anisotropy of Nd-Fe-B Based Permanent Magnets; Does a Co Substitution Really Improve the Temperature Dependence of Nd-Fe-B Based Permanent Magnets; Magnetic Anisotropy in the System La2Fe(14-x)Co(x)B and its Relation to the System Nd2Fe(14-x)Co(x)B; The Effect of Substitution of Al on the Magnetic Properties of Nd15Fe78B7 Permanent Magnets; Electron Microscope Study of Precipitation in a Niobium Containing (Nd,Dy)-Fe-B Sintered Magnet; Microstructural Evidence for the Magnetic Surface Hardening of Dy203-Doped N15Fe77B8 Magnets; Magnetic Anisotropy in Pr2 (Fe(1-x)COx)14B Compounds; Anisotropy and Hysteresis Studies of Highly Substituted Nd-Fe-B Based Permanent Magnets; Electron Microscopy of Nd-Fe-B Based Magnets; and The Influence of Dopants on Microstructure and Coercivity of Nd-Fe-B Sintered Magnets. GRA

N90-16477# Tokyo Univ., Tanashi (Japan). Inst. for Nuclear Study.
DISSIPATION MECHANISM OF THE LARGE-AMPLITUDE COLLECTIVE MOTION. DYNAMICAL EVOLUTION OF A COLLECTIVE BUNDLE OF TRAJECTORIES IN THE TDHF PHASE SPACE FOR A SIMPLE SOLUBLE MODEL
Masayuki Matsuo, Fumihiko Sakata, and Toshio Marumori (Tsukuba Univ., Ibaraki, Japan) Jun. 1989 43 p Sponsored in part by Ministry of Education, Science, and Culture
(DE90-719557; INS-751) Avail: NTIS (US Sales Only) HC A03/MF A01

A new microscopic origin responsible for the dissipation process of the large-amplitude collective motion is discussed in terms of the dynamics of distribution function in the time-dependent Hartree Fock (TDHF) phase space. With the use of a simple soluble model, the origin is illustrated by numerically solving the master equation in the microscopic theory of nuclear collective dynamics which was proposed aiming at studying the order-to-chaos transitions of the large-amplitude nuclear collective motion. In this framework, collectivity of the system is expressed by a bundle of trajectories in the TDHF phase space and the dissipation process is related to the diffusive property of the bundle of trajectories. It is clarified that the microscopic dynamics responsible for the dissipation

process originates from the dynamical fluctuation part of the coupling between the collective (relevant) and intrinsic (irrelevant) degrees of freedom. DOE

71 ACOUSTICS

Includes sound generation, transmission and attenuation. For noise pollution see *45 Environmental Pollution.*

N90-16478 North Carolina State Univ., Raleigh.
A COMPUTATIONAL AND EXPERIMENTAL STUDY OF STEADY AND TRANSIENT ACOUSTIC ENERGY FLOW FROM A COMPLEX MECHANICAL STRUCTURE Ph.D. Thesis
Du Hwan Chun 1989 280 p
Avail: Univ. Microfilms Order No. DA8909245

The steady state and transient acoustic energy flow from a complex mechanical structure with special applications to a hand operated punch press was investigated by both numerical and experimental methods. A numerical technique based on the boundary element method is presented for determining the transient acoustic field of an arbitrarily shaped 3-D body. The numerical implementation is improved by combining explicit and implicit time integration methods in order to achieve better numerical stability and computational efficiency. The acoustic energy maps obtained from the surface velocity, pressure, and acoustic energy flux density on the punch press surface and in the far field have identified the transient noise source and the transient wave mechanism. Some important effects due to the nature of the transient signal in digital signal processing techniques are illustrated. The experimental analysis is focused on the application of the surface acoustic intensity probe to transient measurement. As a conclusion, whereas methods based on conventional steady state modal analysis, which neglects non-resonant frequency components, have so far failed to reduce the overall transient impact noise level, it would appear that successful noise reduction from transient impact machines must focus on the complete suppression of the non-resonant modes which contribute to the broadband energy content of the radiated sound as well as the resonant peaks of the noise spectrum. Dissert. Abstr.

N90-16479# Department of the Air Force, Washington, DC.
ULTRASONIC ASSISTED PAINT REMOVAL METHOD Patent
Theodore J. Reinhart, inventor (to Air Force) 6 Jun. 1989 9 p Filed 7 Jul. 1987 Supersedes US-Patent-Appl-SN-070499 (AD-D014264; US-Patent-4,836,858; US-Patent-Appl-SN-070499; US-Patent-Class-134-1) Avail: U.S. Patent and Trademark Office CSCL 01/3

This abstract discloses paint or other protective coating removal method involving the use of reciprocal motion ultrasonic frequency mechanical energy applied to the coating by a variety of tool and abrasive substrate members in the company of surface preparation agents, such as coolant, heating, softening, and/or abrasive agents. The invention is particularly applicable and disclosed in terms of, protective coating removal from aircraft such as is often necessary for replacement or in the reutilization of aircraft with different identification markings. The coating removal method is environmentally and human operator safe in comparison with presently used coating removal methods such as abrasive blasting and chemical solvent removal. GRA

N90-16480# Brookhaven National Lab., Upton, NY. Dept. of Applied Mathematics.
SOLVING TIME HARMONIC WAVE PROBLEMS ON VECTOR PROCESSORS
C. I. Goldstein 1989 15 p Presented at the 2nd IMACS Symposium on Computational Acoustics, Princeton, NJ, 15-17 Mar. 1989
(Contract DE-AC02-76CH-00016; NSF DMS-85-12188)
(DE90-003956; BNL-43477; CONF-8903179-1) Avail: NTIS HC A03/MF A01

The numerical solution of multi-dimensional Helmholtz and related boundary value problems is important in various acoustic models. A great deal of research has previously been done in connection with the development of radiation boundary conditions, as well as finite difference and finite element discretizations of the boundary value problem and the solution of the resulting sparse, indefinite, non-selfadjoint system of linear equations. This includes the development, analysis and implementation of a preconditioned conjugate gradient iterative method applied to the normal equations (PCGN). Due to the large number of waves that must be resolved, the use of vector and parallel supercomputers is essential for the practical solution of large problems. Various issues are discussed dealing with the effective solution of 2 and 3-D Helmholtz problems on vector computers. In particular, a Helmholtz solver previously developed by the author was vectorized and implemented on an IBM 3090-180 with vector facility at Brookhaven National Laboratory. The code can treat Helmholtz type problems with variable index of refraction and different radiation conditions in Cartesian and cylindrical waveguides as well as in the exterior of a bounded obstacle. It was also applied to 3-D parabolic type wave models. Most of the computation involves the solution of the resulting large, sparse system of linear equations. Both the PCGN algorithm and multigrid preconditioner were completely vectorized. Various aspects are discussed of the numerical algorithm and the issues involved in the vectorization of the code. Timing results on the IBM 3090 are also given and demonstrate that the code vectorizes very well. DOE

N90-16694*# Indiana Univ.-Purdue Univ., Fort Wayne. Dept. of Engineering.
MODELING THE NEAR ACOUSTIC FIELD OF A ROCKET DURING LAUNCH
David W. Mauritzen *In* University of Central Florida, NASA/ASEE Summer Faculty Fellowship Program Oct. 1989 p 171-202 (For primary document see N90-16686 08-99)
Avail: NTIS HC A18/MF A03 CSCL 20A

72 ATOMIC AND MOLECULAR PHYSICS

Includes atomic structure, electron properties, and molecular spectra.

N90-16481# Lund Univ. (Sweden). Dept. of Physics.
ON THE OBSERVATION OF A TRANSITION FROM FUSION TO MULTIFRAGMENTATION IN HIGH MULTIPLICITY O16 INDUCED REACTIONS
B. Jakobsson, G. Jonsson, L. Karlsson, V. Kopljar, B. Noren, K. Soderstrom, F. Schussler, E. Monnand, H. Nifenecker, and G. Fai (Kent State Univ., OH.) et al Apr. 1989 26 p Prepared in cooperation with Niels Bohr Inst., Co penhagen, Denmark
(LUIP-8812; LUNFD6/(NFFK-7095)1-24(1988); ISSN-0348-9329)
Avail: NTIS HC A03/MF A01

High multiplicity O-16 + Br and O-16 + Ag collisions were studied from 10 to 220 A MeV on an event-by-event basis. The collisions with the highest multiplicity are fusion-like for energies below 35 A MeV where at highest energies the onset of multifragmentation (two or more medium mass fragments) is observed with a charge distribution which gets less and less wide with increasing energy. Correlations between high moments of the charge distribution and the maximum charge or the total multiplicity were studied. These correlations are generally well described by statistical models. The predicted clear signal of critical behavior is however not observed. Author

N90-16482*# Minnesota Univ., Minneapolis. Dept. of Chemistry and Supercomputer Inst.
GENERAL CONTRACTION OF GAUSSIAN BASIS SETS. PART 2: ATOMIC NATURAL ORBITALS AND THE CALCULATION OF ATOMIC AND MOLECULAR PROPERTIES
Jan Almloef and Peter R. Taylor (Eloret Corp., Sunnyvale, CA.) 1989 38 p
(Contract NCC2-371; NSF CHE-86-10809)
(NASA-CR-186201; NAS 1.26:186201) Avail: NTIS HC A03/MF A01 CSCL 20H

A recently proposed scheme for using natural orbitals from atomic configuration interaction (CI) wave functions as a basis set for linear combination of atomic orbitals (LCAO) calculations is extended for the calculation of molecular properties. For one-electron properties like multipole moments, which are determined largely by the outermost regions of the molecular wave function, it is necessary to increase the flexibility of the basis in these regions. This is most easily done by uncontracting the outmost Gaussian primitives, and/or by adding diffuse primitives. A similar approach can be employed for the calculation of polarizabilities. Properties which are not dominated by the long-range part of the wave function, such as spectroscopic constants or electric field gradients at the nucleus, can generally be treated satisfactorily with the original atomic natural orbital (ANO) sets. Author

N90-16483*# National Aeronautics and Space Administration. Ames Research Center, Moffett Field, CA.
THEORETICAL INVESTIGATIONS OF THE STRUCTURES AND BINDING ENERGIES OF Be(SUB n) AND Mg(SUB n) (n = 3-5) CLUSTERS
Timothy J. Lee, Alistair P. Rendell, and Peter R. Taylor (Eloret Corp., Sunnyvale, CA.) 1989 23 p
(Contract NCC2-371)
(NASA-TM-101931; NAS 1.15:101931) Avail: NTIS HC A03/MF A01 CSCL 20H

Researchers determined the equilibrium geometries and binding energies of Be and Mg trimers, tetramers and pentamers using single and double excitation coupled cluster (CCSD) and complete active space self-consistent-field (CASSCF) multireference configuration interaction (MRCI) wave functions in conjunction with extended atomic basis sets. Best estimates of the cluster binding energies are 24, 83 and 110 kcal/mole for Be3, Be4 and Be5; and 9, 31 and 41 kcal/mole for Mg3, Mg4 and Mg5, respectively. A comparison of the MRCI and CCSD results shows that even the best single-reference approach (limited to single and double excitations) is not capable of quantitative accuracy in determining the binding energies of Be and Mg clusters. Author

N90-16484# California Univ., Berkeley. Lawrence Berkeley Lab. Materials and Chemical Sciences Div.
A SEARCH FOR THE ELECTRIC DIPOLE OF THE ELECTRON Ph.D. Thesis
Kamal Fuad Abdullah (California Univ., Berkeley.) Aug. 1989 111 p
(Contract DE-AC03-76SF-00098)
(DE90-001572; LBL-27723) Avail: NTIS HC A06/MF A01

A new upper limit is reported on the electric dipole moment (EDM) of the electron of d(sub e) = 0.1 (plus minus) 3.2 x 10(exp -26) e/cm. This precision is one hundred times better than any previously published limit and a factor of two better than that of unofficial reports. Recently there has been a great deal of theoretical interest in the possibility of a non-zero electron EDM. Models such as the left-right-symmetric Standard Model and an off-standard model with new heavy neutrinos are constrained by the new limit on d(sub e). A non-zero electron EDM would violate the time reversal and parity space-time symmetries. T-violation was observed in neutral kaon decay and is still not fully explained by the Standard Model. Our experimental technique involves searching for an energy shift, linear in applied electric field, between the m(sub F) = 1 and m(sub F) = -1 magnetic sublevels of the F=1 hyperfine level of the 6(exp 2)P(exp 1/2) ground state of atomic thallium. If the electron has a non-zero EDM, this thallium state will exhibit an atomic electric dipole moment that is roughly 600 times larger. The energy shift is detected with the technique of magnetic resonance spectroscopy, employing separated oscillating fields, applied to an atomic beam of thallium. In the approach, any relative phase-shift between the m(sub F) = (plus minus)1 components of the F=1 wavefunction acquired by the atom as it travels through an electric field is detected through interference with two separate oscillating magnetic fields located on either side of the electric field. The new level of precision is achieved through several improvements on previous experiments including employment of a vertical apparatus, two opposing atomic beams, and optical pumping for atomic state selection and analysis. DOE

N90-16485# Physical Sciences, Inc., Andover, MA.
ROTATIONAL ENERGY TRANSFER IN METASTABLE STATES OF HETERONUCLEAR MOLECULES Final Report, 1 Jun. 1986 - 31 Aug. 1989
Steven J. Davis, Karl Holtzclaw, and L. G. Piper 26 Oct. 1989 101 p
(Contract F49620-86-C-0061; AF Proj. 2303)
(AD-A214425; PSI-1006/TR-976; AFOSR-89-1340TR) Avail: NTIS HC A06/MF A01 CSCL 20/5

The objective of this program was to measure and interpret state-to-state R-T transfer rate coefficients for selected interhalogen molecules. Spectrally resolved CW laser induced fluorescence was the experimental method used. A CW dye laser excites pure quantum states. The resolved fluorescence of the laser excited level and the collisionally populated J' levels are analyzed. Nearly 1000 state-to-state rate coefficients were determined for R-T transfer in IF(B). Collision partners include He, Ne, Ar, Kr, Xe, N2, and CF4. Rate coefficients were also determined for several initially excited J': 13, 27, 35 and 72. R-T transfer were also investigated during vibrationally inelastic collisions for both I2 and IF. In addition, R-T rate coefficients in ICl(B), were measured. GRA

N90-16486# Sao Paulo Univ. (Brazil). Inst. de Fisica.
STUDIES OF ELASTIC SCATTERING AND CROSS SECTIONS OF THE C-12 + Si-28 SYSTEM M.S. Thesis
Jose MartinsdeOliveiru, Jr. 1988 110 p In PORTUGUESE; ENGLISH summary
(DE89-635990; INIS-BR-1569) Avail: NTIS (US Sales Only) HC A06/MF A01

Angular distributions of the elastic scattering of the system C(12)+Si(28) were measured at the energies E(sub CM) = 14.70; 16.08; 18.90; 20.97; 21.87 MeV, in the angular range 15(exp 0) less than theta (CM) less than or + 170(sup 0), with angular steps of 1(sup 0). Other seven angular distributions measured by Villari, Ost and Cheng at energies E(sub CM) = 17.50; 19.60; 20.30; 22.40; 23.80; 24.50 and 25.20 MeV, were also used in the analysis. The angular distributions Were reproduced by optical model calculations and new optical potentials for the system C(12)+Si(28) were obtained. Calculations of the total reaction cross section from the elastic scattering data using a model independent method were done. The results were compared with fusion cross section data and with total reaction cross sections obtained via optical model calculations. Finally experimental angular distributions were analyzed by phase shift analysis and the problem of unicity and ambiguities of the scattering matrix S(l) was discussed. DOE

N90-16487# International Centre for Theoretical Physics, Trieste (Italy).
ON CONDENSATION DRIVEN BY ELECTROSTATIC INTERACTIONS IN MACROIONIC SOLUTIONS
Z. Badirkhan and M. P. Tosi (Trieste Univ., Italy) Apr. 1989 10 p Submitted for publication Sponsored in part by Ministero della Pubblica Istruzione, Italy and Consiglio Nazionale delle Ricerche, Italy
(DE89-636072; IC-89/60) Avail: NTIS (US Sales Only) HC A02/MF A01

Liquid-vapor phase separation, as it normally follows from attractive interactions, is demonstrated under pure Coulomb interactions for the primitive model of macroionic solutions in the mean spherical approximation and related to observations on dilute solutions of highly charged latex particles. It is stressed that the corresponding effective pair potential between macro-ions is of the DLVO repulsive type. DOE

N90-16488# Oak Ridge National Lab., TN.
HEAVY ION INELASTIC SCATTERING WITH A 4(pi) GAMMA DETECTOR

E. E. Gross 1989 10 p Presented at the 13th Symposium on Nuclear Physics, Oaxtepec, Mexico, 3-6 Jan. 1990
(Contract DE-AC05-84OR-21400)
(DE90-002709; CONF-900147-1) Avail: NTIS HC A02/MF A01

Heavy ion inelastic scattering with a new technique that uses a 4(pi) gamma-ray detector in coincidence with charged particle detectors is applied to (24)Mg(200 MeV) + (208)Pb scattering. In addition to differential cross sections, a complete particle-gamma angular correlation is obtained for decay of the 2(sub 1)(sup +) (1.37 MeV) state of (24)Mg. The data are analyzed in coupled-channels. The correlation data proves to be especially sensitive to the static quadrupole moment. DOE

N90-16489*# Lawrence Livermore National Lab., CA.
DEVELOPMENT OF LOW DENSITY SILICA AEROGEL AS A CAPTURE MEDIUM FOR HYPER-VELOCITY PARTICLES
Lawrence W. Hrubesh 1 Oct. 1989 23 p
(Contract W-7405-eng-48)
(NASA-CR-185930; NAS 1.26:185930; DE90-003990; UCRL-21234) Avail: NTIS HC A03/MF A01 CSCL 19H

The objective is to develop micro-porous silica aerogel glass with optimal properties for its potential use as a capture medium of hyper-velocity particles. The important properties for this application are identified as ultra-low bulk density (i.e., is less than 0.1 gm/cc), high transparency to visible light, and purity (absence of organic and inorganic contaminants). The approach is to expand on existing knowledge and experience concerning sol-gel chemistry and the extraction technology which is now used to routinely produce clear silica aerogel monoliths at densities higher than 0.1 gm/cc. The existing technology is being pushed toward ultra-low density aerogels and any limitations impeding the development of this material with optimal properties for the particle capture application are being identified. DOE

N90-16490# Tokyo Univ., Tanashi (Japan). Inst. for Nuclear Study.
POSSIBLE MEASUREMENT OF THE GRAVITATIONAL ACCELERATION OF MOLECULES, ATOMS, NUCLEI, ELEMENTARY PARTICLES, AND ANTIPARTICLES
Hidezumi Terazawa Jun. 1989 11 p
(DE90-719559; INS-752) Avail: NTIS (US Sales Only) HC A03/MF A01

A possible laboratory measurement of the gravitational acceleration of ionized molecules, ionized atoms, nuclei, charged elementary particles and charged antiparticles is proposed. It is simple by detecting their falling distance to an accuracy of the order of 1(mu)m after one turn of circular orbit with a radius of the order of 1m in the variable static homogeneous weak magnetic field of the orders of 10(exp -3)/gauss, which is available in the air-core spectrometer. The technical points are also presented and discussed in detail. DOE

N90-16491# Los Alamos National Lab., NM.
NEUTRINO OSCILLATIONS: AN ESSAY IN HONOR OF FELIX BOEHM
S. P. Rosen 1989 16 p Presented at the Symposium in Honor of Felix Boehm, Pasadena, CA, 7-9 Sep. 1989
(Contract W-7405-eng-36)
(DE90-003223; LA-UR-89-4026; CONF-8909273-1) Avail: NTIS HC A03/MF A01

Briefly reviewed is the theory of neutrino oscillations and the MSW effect and report on new calculations by Rosen and Gelb for solar neutrino-electron scattering. The aim of these calculations is to try to use the scattering process as a means of choosing between the three types of MSW solutions for the (sup 37)Cl experiment. Both the efficiency and the resolution of the Kamiokande II detector are taken into account and the ratio R of the MSW prediction to the standard solar model prediction is calculated for different cuts on the minimum electron energy. It was found that the adiabatic solution requires R to be less than 1/3, the large angle one requires it to be less than 2/3, and the nonadiabatic one restricts it to a value close to 1/2. The central value of the published KII data is close to 1/2, but the errors are too large to exclude the other solutions. DOE

N90-16492# Virginia Univ., Charlottesville. Inst. of Nuclear and Particle Physics.
Q-2 AND A DEPENDENCE OF DELTA (1232) ELECTROEXCITATION IN NUCLEI
R. M. Sealock 1989 14 p Presented at the Excited Baryons Conference, Troy, NY, 4-6 Aug. 1988 Submitted for publication
(Contract DE-FG05-89ER-40501)
(DE90-003470; CONF-8808198-5) Avail: NTIS HC A03/MF A01

Inclusive electron scattering measurements from SLAC of delta electroexcitation in nuclei are presented. Electrons with energies of 0.96, 1.1, 1.3 and 1.5 GeV were scattered from H, He-4, C, Fe and W at 37.5 degrees and detected with the End Station A 1.6 GeV/c spectrometer. The Q(sup 2) at the delta peak ranged from 0.2 to 0.5 (GeV/c)sup 2. For all nuclear targets the delta peak position shifts for higher invariant mass as Q(sup 2) increases and in all but one case is above that of the free nucleon. Cross sections were fitted by the form (sigma) = cA(sup b). For the delta region b varies from 0.99 to 1.02 with uncertainties of plus or minus 0.01. For the dip region, A dependence is observed that is consistent with the effects of Fermi broadening of the quasielastic and delta peaks. Transverse form factors have been calculated and fitted by the function 1/(1 + Q(sup 2)/(Lambda)(sup 2)). The A and invariant mass dependences of Lambda are discussed. DOE

N90-16493# Rensselaer Polytechnic Inst., Troy, NY. Dept. of Physics.
THEORETICAL ASPECTS OF ELECTROWEAK AND OTHER INTERACTIONS IN MEDIUM ENERGY NUCLEAR PHYSICS
Interim Project Report
Nimai C. Mukhopadhyay 8 Dec. 1989 28 p
(Contract DE-FG02-88ER-40448)
(DE90-004015; DOE/ER-40448/2) Avail: NTIS HC A03/MF A01

In the project year 1989/1990, progress was made towards the theoretical modeling of the photoproduction of eta-mesons off nucleons and in complex nuclei. Exploration of hadron models produced interesting perspectives on the violation of gauge invariance due to truncation of the quark model space. New projects in perturbative quantum chromodynamics and spectrum generating algebras for hadrons were started. DOE

N90-16494# Max-Planck-Inst. fuer Stroemungsforschung, Goettingen (Germany, F.R.).
LECTURE NOTES ON SUPERSONIC MOLECULAR BEAM SOURCES
E. L. Knuth (California Univ., Los Angeles.) Nov. 1988 36 p Presented at a Max-Planck Institut fuer Stroemungsforschung Conference, 30 Apr. 1987 - 21 May 1987
(MPIS-20/1988; ISSN-0436-1199; ETN-90-95332) Avail: NTIS HC A03/MF A01

Notes on supersonic molecular beams are presented. Beam density distributions, Mach number focusing and beam flux are discussed. Relaxation processes in flow systems are reviewed. The sudden freeze approximation is described. Free jets with successive freezing points are discussed. Diagrams and equations are presented to illustrate these lecture notes. ESA

N90-16495# Rome Univ. (Italy). Dipt. di Fisica.
NEUTRINO INTERACTIONS
M. Diemoz, F. Ferroni, Luciano Maiani, G. Martinelli, and E. Longo 2 May 1989 231 p
(Nota-Interna-934; ETN-90-95816) Avail: NTIS HC A11/MF A02

The experimental results of neutrino research, past and present, are reviewed. It is concluded that all of the neutrino experiments agree with each other within reasonable error, and are consistent with electroproduction experiments. All the results can be interpreted in the framework of the Quantum Chromodynamics

(QCD) improved parton model. However the small discrepancies between charged and neutral leptoproduction are not understood. It is not known if these discrepancies and difficulties in the high statistics QCD analysis must be attributed to systematic effects or are an indication of possible failure of the parton model at low Q to the second power values. ESA

73 NUCLEAR AND HIGH-ENERGY PHYSICS

Includes elementary and nuclear particles; and reactor theory.

For space radiation see *93 Space Radiation.*

N90-16496*# National Aeronautics and Space Administration. Lewis Research Center, Cleveland, OH.

SCALING STUDY FOR SP-100 REACTOR TECHNOLOGY

A. C. Marshall (Sandia National Labs., Albuquerque, NM.) and B. McKissock 1989 8 p Presented at the 7th Symposium on Space Nuclear Power Systems, Albuquerque, NM, 7-11 Jan. 1990 (Contract DE-AC04-76DP-00789)

(NASA-TM-897140; NAS 1.15:897140; DE89-014967; SAND-89-1635C; CONF-900109-4) Avail: NTIS HC A02/MF A01 CSCL 18I

Several ways were explored of extending SP-100 reactor technology to higher power levels. One approach was to use the reference SP-100 pin design and increase the fuel pin length and the number of fuel pins as needed to provide higher capability. The impact on scaling of a modified and advanced SP-100 reactor technology was also explored. Finally, the effect of using alternative power conversion subsystems, with SP-100 reactor technology was investigated. One of the principal concerns for any space based system is mass; consequently, this study focused on estimating reactor, shield, and total system mass. The RSMASS code (Marshall 1986) was used to estimate reactor and shield mass. Simple algorithms developed at NASA-Lewis were used to estimate the balance of system mass. Power ranges from 100 kWe to 10 MWe were explored assuming both one year and seven years of operation. Thermoelectric, Stirling, Rankine, and Brayton power conversion systems were investigated. The impact on safety, reliability, and other system attributes, caused by extending the technology to higher power levels, was also investigated. DOE

74 OPTICS

Includes light phenomena; and optical devices.

For lasers see *36 Lasers and Masers.*

N90-16497# Helsinki Univ. of Technology, Espoo (Finland). Electromagnetics Lab.

GEOMETRICAL OPTICS IN INHOMOGENEOUS CHIRAL MEDIA WITH APPLICATION TO POLARIZATION CORRECTION IN INHOMOGENEOUS LENS ANTENNAS

Ismo V. Lindell, Ari H. Sihvola, Ari J. Viitanen, and Sergei A. Tretyakov Jun. 1989 26 p Sponsored in part by Academy of Finland and Ministry of Education of Finland

(PB90-110669; ISBN-951-754-929-6; ISSN-0784-848X; Rept-48) Avail: NTIS HC A03/MF A01 CSCL 20F

A novel geometric optics method for inhomogeneous chiral media is introduced applying normalized wave fields, which are certain complex combinations of the electric and magnetic fields. It is seen that for sufficiently small values of the chirality parameter, the geometrical optics rays can be calculated as for achiral media and the main effect of the chirality is rotation of polarization along the ray. Thus, adding chirality to inhomogeneous lens antennas, their polarization properties can be improved. As an example, the Maxwell fish eye lens is analyzed and two possible expressions for a chirality distribution capable of eliminating the inherent cross polarization are derived. GRA

N90-16498# Helsinki Univ. of Technology, Espoo (Finland). Dept. of Technical Physics.

DETERMINATION OF HYPERFINE STRUCTURES AND RYDBERG CONVERGENCE LIMITS OF SELECTED OPTICAL TRANSITIONS IN Nb-93 USING RESONANCE IONIZATION SPECTROSCOPY

H. M. Lauranto, I. H. Auterinen, T. T. Kajava, K. M. Nyholm, and R. R. E. Salomaa 29 May 1989 21 p

(PB90-110719; TKK-F-A654; ISBN-951-754-914-8; ISSN-0355-7790) Avail: NTIS HC A03/MF A01 CSCL 20F

Several two and three step schemes for resonance ionization of Nb-93 with field ionization of Rydberg levels were investigated in the context of feasibility studies of using Nb-93/Nb-93 isomer ratio determination for fast neutron dosimetry. Hyperfine structures of various states of Nb-93 were measured. The Rydberg spectra of the excitation schemes were measured and corresponding ionization limits estimated. GRA

N90-16499# Department of the Navy, Washington, DC.

REFLECTOMETERS Patent

Keith A. Snail, inventor (to Navy) 28 Mar. 1989 12 p Filed 9 Oct. 1987 Supersedes US-Patent-Appl-SN-106469

(AD-D014249; US-Patent-4,815,858; US-Patent-Appl-SN-106469) Avail: U.S. Patent and Trademark Office CSCL 20/6

Systems for measuring the diffuse reflectances of various samples are constructed to include a primary mirror (e.g., an ellipsoidal mirror) and a secondary mirror (e.g., a compound parabolic concentrator) cooperating with a radiation source, and a radiation detector. GRA

N90-16500# Rochester Univ., NY.

HIGH SPEED SIGNAL EXTRACTION USING ELECTRO-OPTIC TECHNIQUES Final Technical Report, Jan. 1986 - Sep. 1987

John Nees and Gerard Mourou Oct. 1989 27 p

(Contract F30602-81-C-0206; AF Proj. 2338)

(AD-A214446; RADC-TR-89-181) Avail: NTIS HC A03/MF A01 CSCL 20/6

Preliminary experiments were done on several test methods to determine which one could best provide a low loading test environment. The range of techniques considered for signal extraction included direct and external modulation of semiconductor laser light. For the laser based modulation both gain and loss control were considered. Under gain controlled laser modulation using available semiconductor lasers, the max. efficiency of the laser would cause unwanted current loading of the device under test (DUT). Using loss modulation in laser diodes, efficient modulation can be obtained with only small loading effects; however, these diodes are very temperature sensitive and will not give the necessary performance under a variety of temperature. External modulation by electroabsorption was also inadequate due to temperature sensitivity. There are polymers which exhibit electro-optic co-efficients orders of magnitude greater than conventional crystals, but for some reason these effects fade with time. Finally, U of R considered confined wave modulators. The integrated Mach-Zender modulation can be directly connected to optical fibers without polarizers. This technique was the one determined to be the most viable in producing a low loading signal extraction method. GRA

N90-16501# Brookhaven National Lab., Upton, NY. Instrumentation Div.

SURFACE TOPOGRAPHY MEASUREMENTS OVER THE 1 METER TO 10 MICROMETER SPATIAL PERIOD BANDWIDTH

Peter Z. Takacs, Karen Furenlid, Robert A. DeBiasse, and Eugene L. Church (Army Armament Research and Development Command, Dover, NJ.) Sep. 1989 9 p Presented at the 33rd SPIE Annual International Technical Symposium on Optical and Optoelectronic Applied Science and Engineering, San Diego, CA, 6-11 Aug. 1989

(Contract DE-AC02-76CH-00016)

(DE90-003642; BNL-42519; CONF-890836-20) Avail: NTIS HC A03/MF A01

A recently-developed long-trace surface profiling instrument

(LTP) is now in operation in our laboratory measuring surface profiles on grazing incidence aspheres and also conventional optical surfaces. The LTP characterizes surface height profiles in a non-contact manner over spatial periods ranging from 1 meter (the maximum scan length) to 2 mm (the Nyquist period for 1 mm sampling period) and complements the range of our WYKO NCP-1000 2.5X surface roughness profiler (5 mm to 9.8 micron). Using these two instruments, we can fully characterize both figure and finish of an optical surface in the same way that we normally characterize surface finish, e.g., by means of the power spectral density function in the spatial frequency domain. A great deal of information about the distribution of figure errors over various spatial frequency ranges is available from this data, which is useful for process control and predicting performance at the desired wavelength and incidence angle. In addition, the LTP is able to measure the absolute radius of curvature on long-radius optics with high precision and accuracy. Angular errors in the optical head are measured in real time by an electronic autocollimator as the head traverses the linear air bearing slide. Measurements of kilometer radius optics can be made very quickly and the data analyzed in a format that is very easy to understand. DOE

N90-16502# Royal Signals and Radar Establishment, Malvern (England).
ENHANCED PERFORMANCE IR FOCAL PLANE ARRAYS USING ADAPTIVE SUBTRACTION
R. A. Ballingall and I. D. Blenkinsop 28 Apr. 1989 11 p
(RSRE-Memo-4286; BR111059; ETN-90-96120) Copyright Avail: NTIS HC A03/MF A01

A compact, adaptive circuit, realiable at the pixel level of infrared focal plane detector arrays, is described. The technique removes unwanted currents from the array, allowing more signal current to be integrated at the pixel. This can be used to improve performance, improve uniformity of signals from the array and simplify associated electronics. The choice of this scheme depends on the system in which it is employed. ESA

N90-16503# Sira Inst. Ltd., Chislehurst (England).
PROPOSED CONCEPT FOR THE VISIBLE/INFRARED IMAGING RADIOMETER FOR SECOND GENERATION METEOSAT
B. Kunkel, F. Blechinger, J. L. Bezy, G. Ratier, D. R. Lobb, M. A. Cutter, E. Hettlage, E. OMongain, A. F. J. Morgownik, and B. C. Taylor (British Aerospace Dynamics Group, Bristol, England) 1989 10 p Presented at the SIRA Optics in Space and Defence Conference, Sep. 1989 Submitted for publication
(ETN-90-96145) Avail: NTIS HC A02/MF A01

The Meteosat Second Generation (MSG) is planned to replace the current system. The emphasis is given on a three axis stabilized platform for MSG, but the current spin stabilized concept may be maintained for cost reasons. The instrument described represents the core payload element in either satellite version; the total payload is expected to consist of: a Visible/Infrared Imaging Radiometer (VIRI) and an IR Vertical Sounder (IRS). The technical concept for the VIRI, is presented. A revised set of requirements for an imager designated EVIRI (Enhanced VIRI) is summarized. ESA

N90-16504# Consiglio Nazionale delle Ricerche, Frascati (Italy). Inst. di Fisica dello Spazio Interplanetario.
MULTISQUEEZING OF MECHANICAL STATES AND BACK-ACTION EVASION MEASUREMENTS
Franco Bordoni and R. Onofrio (Rome Univ., Italy) Apr. 1989 24 p
(IFSI-89-6; ETN-90-96168) Avail: NTIS HC A03/MF A01

A technique to improve the squeezing of the mechanical noise in a back action evasion measurement is proposed. The scheme is based on the use of a parametric multipump system, and approaches a stroboscopic measurement. A simple model of the back action evasion effect is developed. Experimental evidence of a significant increase in the squeezing with respect to the two pump scheme, in accordance with the model, is reported. A close analogy between the concepts developed and similar concepts in quantum optics is observed. The work may be considered as the mechanical counterpart of nonlinear quantum optics developments. ESA

N90-16505# Institut National des Sciences Appliquees de Lyon, Villeurbanne (France). Lab. d'Automatique et de Micro-Informatique Industrielle.
ORDER FILTERS, MEDIAN RECURSIVE FILTER: ANALYSIS AND EVALUATION OF PERFORMANCE IN IMAGE PROCESSING Ph.D. Thesis [FILTRES D'ORDRE, FILTRE MEDIAN RECURSIF: ANALYSE ET EVALUATION DES PERFORMANCES EN TRAITEMENT D'IMAGE]
Mohamed Mouhoub 1989 151 p In FRENCH
(ISAL-89-0017; ETN-90-96037) Avail: NTIS HC A08/MF A01

The analysis and implementation of local image processing operators is described. These operators, using order filtration, allow for a smoothing of image perturbations (noise) while maintaining the transition intensities determined by the contour of the objects. Statistical properties of the median recursive filter are investigated. Techniques of contour detection are outlined. An operator using both median recursive filtration and differentiation is described. Its performance is analyzed and compared with that of the Canny-Deriche operator. ESA

N90-16506# California Univ., Berkeley. Lawrence Berkeley Lab. Applied Science Div.
CHROMATIC DISPERSION COMPENSATION IN A FRESNEL LENS BY MEANS OF A DIFFRACTION GRATING
Kenneth C. Johnson Aug. 1989 13 p Presented at the 33rd SPIE Annual International Technical Symposium on Optical and Optoelectronic Applied Science and Engineering, San Diego, CA, 6-11 Aug. 1989
(Contract DE-AC03-76SF-00098)
(DE90-004030; LBL-27950; CONF-890836-22) Avail: NTIS HC A03/MF A01

A Fresnel lens's imaging performance can be seriously impaired by chromatic dispersion which typically doubles the diameter of the focused sun image in a solar concentrator. This problem can be alleviated by means of a molded diffraction grating whose diffraction induced dispersion offsets and substantially cancels the lens's intrinsic refractive index dispersion. The grating lines would comprise a second tier of small scale, Fresnel-type facets superimposed on the lens facets, with a typical grating facet height of about 40 microinches and a facet width ranging from about 1 milliinch at the edge of the lens to around 5 or 10 milliinches near the center. In its primary intended application the grating would function in a core daylighting system to improve the optical performance of a collector which focuses direct sunlight into fiber optic couplers. For this application chromatic dispersion would be reduced by an order of magnitude with only a 2 percent loss in optical efficiency. DOE

N90-15929# Ferranti Defence Systems Ltd., Edinburgh (Scotland). Dept. of Electro-Optics.
ELECTRO-OPTIC SENSORS FOR SURVEILLANCE AND TARGET ACQUISITION
J. W. Jack and A. Houston *In* AGARD, Guidance and Control of Unmanned Air Vehicles Aug. 1989 20 p (For primary document see N90-15924 08-08)
Copyright Avail: NTIS HC A09/MF A02; Non-NATO Nationals requests available only from AGARD/Scientific Publications Executive

75 PLASMA PHYSICS

Includes magnetohydrodynamics and plasma fusion.

For ionospheric plasmas see *46 Geophysics*. For space plasmas see *90 Astrophysics*.

N90-16507# Los Alamos National Lab., NM.
TOROIDAL MAGNETIC FIELDS IN TERMS OF FIELD-LINE INVARIANTS

H. Ralph Lewis 1989 5 p Presented at the International Conference on Plasma Physics, New Delhi, India, 22-28 Nov. 1989
(Contract W-7405-eng-36)
(DE89-016610; LA-UR-89-2913; CONF-891182-1) Avail: NTIS HC A01/MF A01

Toroidal magnetic fields are discussed in terms of field-line invariants in magnetic fusion research. DOE

N90-16508# Solmecs Ltd., Jerusalem (Israel).
DEVELOPMENT OF A WET VAPOR HOMOGENEOUS LIQUID METAL MHD POWER SYSTEM Semiannual Report, Oct. 1988 - Mar. 1989
Apr. 1989 49 p
(Contract DE-AC22-88PC-88653)
(DE90-001468; DOE/PC-88653/T1) Avail: NTIS HC A03/MF A01

During the period covered by this report (October 1988 to March 1989), the following work was done: the mixing stream condensation process was analyzed, and a theoretical model for simulating this process was modified. A parametric study is being conducted at the present time; the separation processes were analyzed; and the experimental system was specified and its design is at present in an advanced stage. The mixing stream condensation process was analyzed. For the parameters defined in the SOW of this project the process was found to be a mist flow direct contact condensation, where the hot gas mixture consisting of inert gas and vapor is the continuous phase, and the subcooled liquid on which the vapor is condensed if the droplets dispersed phase. Two possibilities of creating the mist flow were considered. The first, injecting the cold Liquid Metal (LM) into the Mixing Streams Condenser (MSC) entrance as a jet and breaking it into LM fragments and the fragments into droplets by momentum transfer breakup mechanism. The second, atomizing the cooled LM stream into little droplets (approximately 100 micrometers in diameter) and accelerating them by the gas. The second possibility was preferred due to its much higher heat and mass transfer surface and coefficients relative to the first one. DOE

N90-16509# General Atomic Co., San Diego, CA.
INITIAL DEUTERIUM CONFINEMENT STUDIES IN DIII-D TOKAMAK: DIII-D MILESTONE REPORT NUMBER 58
J. C. DeBoo, D. P. Schissel, K. Burrell, and H. StJohn Aug. 1989 12 p
(Contract DE-AC03-89ER-51114)
(DE90-003942; GA-A-19803) Avail: NTIS HC A03/MF A01

The operational space of DIII-D was extended to include high current, high power deuterium neutral beam heating of deuterium discharges in both the single null and double null configurations. Recent completion of the neutron shielding of the DIII-D facility has allowed operation in these new parameter regimes while maintaining a low neutron dose at the site boundary. The plasma current and neutral beam power ranges with D(0) yields D(+) operation were extended to P(sub T) is less than or equal to 12 MW and I(sub p) is less than or equal to 2.5 MA. Comparison of H-mode discharges in pure H with those in pure D indicates a continuing superior confinement in deuterium for values of q is greater than or equal to 3; however at lower values of q the confinement becomes similar. Analysis of the energy confinement in this regime has shown no major differences in current or power scaling compared to H(0) yields D(+) operation. Energy confinement during the ELMing phase of D(0) yields D(+) H-mode discharges scales linearly with the plasma current and deteriorates with neutral beam power. Recent, ongoing time dependent analysis of discharges with long ELM-free periods following the L to H transition indicate that the energy confinement time may be independent of power so that power degradation may be a manifestation of ELMs. DOE

N90-16510# Oak Ridge National Lab., TN. Fusion Energy Div.
ATF-2 STUDIES
J. F. Lyon, B. A. Carreras, N. Dominguez, L. Dresner, C. L. Hedrick, S. P. Hirshman, M. S. Lubell, J. W. Lue, R. N. Morris (Martin Marietta Energy Systems, Inc., Oak Ridge, TN.), and S. L. Painter et al Oct. 1989 34 p
(Contract DE-AC05-84OR-21400)
(DE90-004380; ORNL/TM-11254) Avail: NTIS HC A03/MF A01

Design studies for a low-aspect-ratio, large next-generation stellarator, ATF-2, with high-current-density, high-field, stable NbTi/Cu helical windings are described. The design parameters are an average plasma radius of 0.52 m, a major radius of 2 m, and a field on axis of 4 to 5 T, with 10 to 15 MW of heating power. Such a device would be comparable in scope to other next-generation stellarators but would have roughly the same aspect ratio as the tokamaks without, however, the need for current drive to sustain steady-state operation. A number of low-aspect-ratio physics issues need to be addressed in the design of ATF-2, primarily compromises between high-beta capability and good confinement properties. A six-field-period Compact Torsatron is chosen as a reference design for ATF-2, and its main features and performance predictions are discussed. An integrated (beta capability and confinement) optimization approach and optimization of superconducting windings are also discussed. DOE

N90-16511# Oak Ridge National Lab., TN.
NEAR-TERM DIRECTIONS IN THE WORLD STELLARATOR PROGRAM
J. F. Lyon Oct. 1989 26 p
(Contract DE-AC05-84OR-21400)
(DE90-004381; ORNL/TM-11255) Avail: NTIS HC A03/MF A01

Interest in stellarators has increased because of the progress being made in the development of this concept and the inherent advantages of stellarators as candidates for an attractive, steady-state fusion reactor. Three new stellarator experiments started operation in 1988, and three more are scheduled to start in the next few years. In addition, design studies have started on large next-generation stellarator experiments for the mid-1990s. These devices are designed to test four basic approaches to stellarator configuration optimization. This report describes how these devices complement each other in exploring the potential of the stellarator concept and what main issues they will address during the next decade. DOE

N90-16512# Oak Ridge National Lab., TN. Applied Technology Div.
STRESS ANALYSIS OF THE PRINCETON PLASMA PHYSICS LABORATORY 1/2- X 1/2-INCH SHEAR/COMPRESSION TEST FIXTURE
H. W. Blake Oct. 1989 115 p
(Contract DE-AC05-84OR-21400)
(DE90-004401; ORNL/ATD-23) Avail: NTIS HC A06/MF A01

A finite element stress analysis was performed on a test fixture developed at the Princeton Plasma Physics Laboratory, which is utilized to test specimens of sheet insulating materials for the Compact Ignition Tokamak. The fixture is a newer version of one that had been previously analyzed. The new fixture was developed to test smaller-sized specimens that have had prior radiation exposure. The original fixture was utilized to test larger, unexposed specimens. The smaller specimens are of an appropriate size (0.5 (times) 0.5 in.) to fit into the test cell of a reactor. The internal stresses in the fixture and specimen were determined for two different conditions of loading. The uniformity of stress within the specimen as it related to the design of the fixture was examined. Two different geometrical shapes for the new fixture were analyzed. An assessment of the potential for specimen slippage is provided for a particular value of the coefficient of friction between the specimen and fixture. Results for a no-slip condition are also given. DOE

N90-16513# International Centre for Theoretical Physics, Trieste (Italy).
THEORETICAL STUDY OF COLD NUCLEAR FUSION USING BARRIER PENETRATION APPROACH
S. K. Gupta and Raj K. Gupta (Panjab Univ., Chandigarh, India)

Jun. 1989 8 p Submitted for publication
(DE90-601096; IC-89/123) Avail: NTIS (US Sales Only) HC A02/MF A01

The cold nuclear fusion process is investigated in terms of barrier penetration calculations by considering both the deuteron-molecule and colliding deuteron-deuteron atoms. Atomic collisions with strongly screened interatomic potential and the resonant state formation can bring agreement with present experimental results. Analysis of the data in terms of the reaction rates is also discussed. DOE

N90-16514# International Centre for Theoretical Physics, Trieste (Italy).
SOME THEORETICAL ASPECTS OF COLD FUSION: A REPORT
S. B. Khadkikar (Physical Research Lab., Ahmedabad, India) Jun. 1989 3 p Sponsored in part by Swedish Agency for Research Cooperation with Developing Countries
(DE90-601098; IC-89/136) Avail: NTIS (US Sales Only) HC A01/MF A01

Some theoretical aspects of cold fusion as discussed at the Erice meeting, namely the theories based on an effective mass of the electron larger than its physical mass are presented. DOE

N90-16515# Kyoto Univ., Uji (Japan). Plasma Physics Lab.
SECOND HARMONIC ELECTRON CYCLOTRON HEATING IN LOW AND OVER DENSITY PLASMAS IN HELIOTRON DR
S. Morimoto, N. Yanagi, Motoyasu Sato, S. Kobayashi, M. Iima, S. Besshou, H. Nakamura, K. Hanatani, Tokuhiro Obiki, and Atsuo Iiyoshi Dec. 1988 37 p
(DE90-719519; PPLK-R-33) Avail: NTIS (US Sales Only) HC A03/MF A01

The experiment of the second harmonic electron cyclotron heating was perfromed on Heliotron DR (R = 90 cm, a-bar(sub p) is approximately or equal to 7 cm) using a 28 GHz, 200 kW gyrotron. The plasmas are observed to be heated effectively in a wide range of electron density even above the Ordinary mode cut-off value (overdense plasma). When electron density is lower than the Extraordinary mode cut-off value, electrons are strongly heated and T(sub eo) of approximately or equal to 1.7keV was achieved at n-bar(sub e) of approximately or equal to 0.25 x 10(exp 13)/cu cm. The heating is found to be less sensitive to the magnetic field intensity than in larger devices such as Heliotron E and Wendelstein VII-A, and most efficient at B(sub o) (central magnetic field) lower than B(sub res) (resonant magnetic field). These phenomena are discussed from a viewpoint of orbit of electrons accelerated in the RF field with dominant reflections at the vessel wall (cavity mode). The overdense plasmas (n-bar(sub e) is greater than 1 x 10(exp 13)/cu cm), are strongly heated at B(sub o) higher than B(sub res). Their typical parameters are n-bar(sub e) of approximately or equal to 2 x 10(exp 13)cu cm, T(sub eo) is approximately or equal to 330 eV and the averaged beta value, is approximately or equal to 0.4 percent. The maximum beta value is limited by onset of MHD instability to greater than or equal to 0.5 percent which agrees well with a theoretical prediction for the pressure driven ideal interchange instability. A possibility of heating the overdense plasmas through mode conversion processes of injected RF waves into electron Bernstein waves is examined, and it is shown to be plausible in the present experimental condition with multiple wall reflections. DOE

N90-16516# Kyoto Univ., Uji (Japan). Plasma Physics Lab.
IN SITU MEASUREMENT OF NEUTRAL BEAM COMPONENTS USING THE DOPPLER-SHIFTED H(SUB ALPHA) EMISSIONS IN HELIOTRON E
Katsumi Kondo, Hideki Zushi, Fumimichi Sano, Tadashi Kawabata, Tohru Mizuuchi, Hiroshi Kaneko, Shigeru Sudo, Motoyasu Sato, Tokuhiro Obiki, and Atsuo Iiyoshi Sep. 1988 11 p
(DE90-719521; PPLK-R-29) Avail: NTIS (US Sales Only) HC A03/MF A01

The density fraction of energy components (E, E/2, E/3, E/18) of the neutral beam was measured at the plasma center, using the Doppler-shifted H(sub alpha) emissions, which were excited by electron and proton collisions in the plasma. This measurement will be useful in understanding the heating process by neutral beam injection. DOE

N90-16517# Japan Atomic Energy Research Inst., Tokyo. Dept. of Thermonuclear Fusion Research.
LOW ENERGY NEUTRAL PARTICLE ENERGY ANALYSER BY TIME OF FLIGHT METHOD
Yukitoshi Miura, Fuminori Okano, and Yoshimi Matsuzaki Mar. 1989 19 p In JAPANESE; ENGLISH summary
(DE90-719529; JAERI-M-89-018) Avail: NTIS (US Sales Only) HC A03/MF A01

The design study of a low energy neutral particle analyzer by using the time of flight method is performed. The chopper system can be made by a modified turbo molecular pump. A modified photo-electron-multiplier with a gate assembly may be suitable for the detector of this system. If a turbo molecular pump can rotate with a speed of about 40000 rpm, then the energy resolution (delta E/E) of 1 keV hydrogen particles is less than 20 percent with the flight length of 2 m (it is assumed that the chopper radius is 50 mm and the width of a slit is 0.15 mm). DOE

N90-16518# Japan Atomic Energy Research Inst., Ibaraki. Dept. of Thermonuclear Fusion Research.
FRACTO-FUSION. MECHANISM OF COLD FUSION
Tatsuoki Takeda and Tomonori Takizuka Jul. 1989 19 p
(DE90-719573; JAERI-M-89-093) Avail: NTIS (US Sales Only) HC A03/MF A01

As a cold fusion mechanism, a fracto-fusion was investigated by which reacting particles are accelerated by the electric field generated between the crack surfaces in a crystal and the beam fusion occurs. By assuming the possible magnitude of the potential difference the fusion rate and energy multiplication factor were calculated. These results are consistent with cold fusion experiments. On the basis of a simple model it is conjectured that necessary electric potential difference to accelerate particles can be generated even in a metal crystal with rather low resistivity, and it was concluded that the fracto-fusion mechanism can explain the cold fusion phenomena successfully. DOE

N90-16519# Kyoto Univ., Kumatori (Japan). Research Reactor Inst.
PROCEEDINGS OF THE SPECIALISTS' MEETING ON PHYSICS AND ENGINEERING OF FISSION AND SPALLATION
Yoshihiro Nakagome, ed. Feb. 1989 115 p Meeting held in Kumatori, Japan, 10 Aug. and 19 Dec. 1988
(DE90-719706; KURRI-TR-315; CONF-8812116) Avail: NTIS (US Sales Only) HC A06/MF A01

The meeting was held on August 10 and December 19, 1988. The proceedings carry a total of 13 reports concerning the physics and engineerings of fission and spallation. The first and second reports, entitled IAEA Consultant's Meeting on the Physics of Neutron Emission in Fission (I) and (II), respectively, give brief comments on major topics discussed in the meeting, recently obtained information, and issues of physical interest in the field of fission and spallation. The other 11 reports are entitled A Study on Mass Division in Low-Energy Nuclear Fission, Recent Topics on The Nuclear Fission Accompanied with High Spin, Nuclear Spallation Engineering and Strong Neutron Source, Nuclear Spallation by Gamma-Rays, Comment: Photopion Reaction and Photospallation, Report on the International Meeting on Physics and Chemistry of Nuclear Fission in Commemoration of the 50th Anniversary of the Discovery of Nuclear Fission, Charge Distribution and Neutron Systematics in Heavy-Ion Fission, High-Energy Gamma-Rays from Fission of (sup 252)Cf, Behavior of FP in Chromatographic Separation, Formation of Neutron by Light Ion, and Annihilation Treatment and Annihilation Furnace Equipped with Proton Accelerator. DOE

N90-16520# Los Alamos National Lab., NM.
RECENT PROGRESS ON THE HESS (HIGH EXPLOSIVE SPHEROMAK SOURCE) EXPERIMENT
Robert M. Mayo, D. C. Barnes, B. Freeman, Ivars Henins, Thomas

R. Jarboe, and D. Platts 1989 4 p Presented at the 11th US/Japan Workshop on Field-Reversed Configurations and Compact Toroids, Los Alamos, NM, 7-9 Nov. 1989
(Contract W-7405-eng-36)
(DE90-003218; LA-UR-89-3827; CONF-8911130-4) Avail: NTIS HC A01/MF A01

The new objective of the Los Alamos spheromak program is to assess the use of magnetized plasmas as an energy transfer medium to accelerate material objects to hyper-velocities ((approx gt) 20 km/s). In meeting this objective, we are committed to the subordinate goals of creating high field, long lived spheromak discharges, examining the technical feasibility of employing High Explosives (HE) to compress seed spheromaks, and investigate the technical requirements involved in forming spheromaks by Mechanical Helicity Injection (MHI) using HE. The recent efforts are described of the CTR-5, M-4, and M-6 groups at Los Alamos in assessing the feasibility of generating magnetic helicity by mechanical means in the High Explosive Spheromak Source (HESS) experiment. DOE

N90-16521# Los Alamos National Lab., NM.
ATOMIC PROCESSES IN PLASMAS UNDER ULTRA-INTENSE LASER IRRADIATION
G. T. Schappert, D. E. Casperson, J. A. Cobble, J. C. Comly, L. A. Jones, G. A. Kyrala, K. J. LaGattuta, P. H. Y. Lee, G. L. Olson, and A. J. Taylor Nov. 1989 16 p Presented at the 7th American Physical Society Topical Conference on Atomic Processes in Plasmas, Gaithersburg, MD, Nov. 1989
(Contract W-7405-eng-36)
(DE90-003221; LA-UR-89-4047; CONF-8911138-1) Avail: NTIS HC A03/MF A01

Lasers delivering subpicosecond pulses with energies of a fraction of a Joule have made it possible to generate irradiance levels approaching 10(exp 20) W/sq cm. Two such systems are presently operated: a KrF based excimer laser capable of producing a few 10(exp 17) W/sq cm at 248 nm with a repetition rate of 3 to 5 Hz and a XeCl based excimer laser capable of producing mid 10(sup 19) W/sq cm at 308 nm and 1 Hz. Some experimental results are discussed along with the theory and modeling of the interaction of such intense laser pulses with aluminum. Because of a small Amplified Spontaneous Emission (ASE) prepulse the high intensity interaction is not at the solid surface but rather at the n(sub e) = 2 x 10(exp 22) cu cm critical density of the blowoff plasma generated by the ASE. The transient behavior of the plasma following the energy deposition by the intense subpicosecond pulse can be viewed as the energy-impulse response of the plasma. Experimental results and modeling of the x ray emission from this plasma is presented. DOE

N90-16522# Johns Hopkins Univ., Baltimore, MD.
SPECTROSCOPIC DIAGNOSTICS OF HIGH TEMPERATURE PLASMAS
W. Moos 1989 12 p
(Contract DE-FG02-86ER-53214)
(DE90-003912; DOE/ER-53214/1) Avail: NTIS HC A03/MF A01

A research program in soft x ray/ultraviolet/visible diagnostics for magnetic fusion is described. Recent results include the electron temperature, electron density and impurity densities during EML activity on the TEXT tokamak. The Zeeman effect induced circular polarization in Li neutral beam emissions was analyzed to determine the safety factor in sawtoothing and ECRH heated discharge. The reflective properties of multilayer mirrors (10 to 200 A) were measured. Future work includes an order of magnitude improvement in the time resolution of the circular-polarimeter, development of a soft x ray normal incidence spectrometer and a feasibility study for a narrow band x ray photometer. DOE

N90-16523# California Univ., Berkeley. Lawrence Berkeley Lab. Nuclear Science Div.
LOWER LIMIT FOR THE AVERAGE ANGULAR MOMENTUM LEADING TO FUSION
D. E. DiGregorio (Comision Nacional de Energia Atomica, Buenos Aires, Argentina), K. T. Lesko, B. A. Harmon, E. B. Norman, J. Pouliot, B. Sur, Y. D. Chan, and R. G. Stokstad Oct. 1989 5 p Presented at the 12th Workshop on Nuclear Physics, Iguazu Falls, Argentina, 28 Aug. - 1 Sep. 1989 Submitted for publication
(Contract DE-AC03-76SF-00098)
(DE90-004027; LBL-27654; CONF-8908129-4) Avail: NTIS HC A01/MF A01

The existence of a finite and essentially energy-independent lower limit for the average angular momentum leading to fusion at energies well below the Coulomb barrier was experimentally confirmed. The observation is reported of this angular momentum limit for the systems C-12 + Te-128, Li-7 + Cs-133, and He-3 + Ba-136. It was found that the predicted values of (bar l) are consistent with experiment. The expected variation of (bar l) with entrance channel is also observed. DOE

N90-16524# General Atomic Co., San Diego, CA.
MODELING ENERGY OUTPUT OF INERTIAL STORAGE DEVICES FOR THE DIII-D TOKAMAK
W. V. Torre, P. Petersen, and A. Kellman Dec. 1989 4 p Presented at the 13th IEEE Symposium on Fusion Engineering, Knoxville, TN, 2-6 Oct. 1989 Submitted for publication
(Contract DE-AC03-89ER-51114; GA Proj. 3466)
(DE90-004096; GA-A-19745; CONF-891007-108) Avail: NTIS HC A01/MF A01

The DIII-D fusion experiment utilizes two large motor-generator sets for supplying energy to the toroidal and poloidal field coils of the tokamak. One generator has an energy capability of 2250 MJ and the other has 794 MJ. The development of a computer program is documented which models the energy requirements of a fusion tokamak and compares them to the limitations of a large motor-generator set. The program models the energy requirements of the magnetic confinement coils and also determines the current (Amperes) requirements (as a function of time) reflected to the generator depending on the physics parameters under study for the plasma. This program is used on a daily basis and by optimizing for minimum energy usage, a significant annual cost savings is realized. DOE

N90-16525# TRW Space Technology Labs., Redondo Beach, CA. Applied Technology Div.
MHD INTEGRATED TOPPING CYCLE PROJECT Quarterly Technical Progress Report No. 7, 1 Feb. - 30 Apr. 1989
Oct. 1989 179 p
(Contract DE-AC22-87PC-90274)
(DE90-004141; DOE/PC-90274/T7; MHD-ITC-89-285) Avail: NTIS HC A09/MF A01

The ITC Project will advance the state-of-the-art in MHD power systems with the design, construction, and integrated testing of 50 MWt power train components which are prototypical of the equipment that will be used in an early commercial scale MHD utility retrofit. Long duration testing of the integrated power train at the Component Development and Integration Facility (CDIF) in Butte, Montana, will be performed, so that by the early 1990's, an engineering data base on the reliability, availability, maintainability and performance of the system will be available to allow scale up of the prototypical designs to the next development level. This Progress Report covers the period February 1, 1989 to April 30, 1989. A number of test and evaluation activities provided data to support the prototypical design efforts. Phase 1 of the 20 MWt power train testing at Avco was completed, providing a baseline for upcoming coal-fired power train testing in the Mark VI facility. Gas-side corrosion tests of candidate combustor materials and brazing and explosion bonding tests on Glidcop were used to obtain information on prototypical combustor design and fabrication details. Evaluation of CDIF test data on the performance of the 50 MWt power train with iron oxide addition indicated that while specific benefits (such as increased channel life) can be derived from iron oxide addition, it has yet to be demonstrated that iron oxide addition improves power output. DOE

N90-16526# Argonne National Lab., IL. Energy and Environmental Systems Div.
USER'S MANUAL FOR MGMHD: A MULTIGRID THREE-DIMENSIONAL COMPUTER CODE FOR THE ANALYSIS OF MAGNETOHYDRODYNAMIC GENERATORS AND DIFFUSERS
J. X. Bouillard, J. L. Krazinski, S. P. Vanka, and G. F. Berry Nov. 1989 124 p
(Contract W-31-109-eng-38)
(DE90-004453; ANL/MHD-89/1) Avail: NTIS HC A07/MF A01

The Multigrid Magnetohydrodynamic (MGMHD) computer code is an updated and improved version of the single-grid Three-Dimensional Magnetohydrodynamic (TDMHD) code developed at Argonne National Laboratory in 1982 for the analysis of magnetohydrodynamic generators and diffusers. The new code retains the TDMHD formulation of three-dimensional partial differential equations for flow and electrical fields but incorporates an advanced multigrid solution algorithm. The magnetohydrodynamic equation set comprises the mass continuity equation, three momentum equations, the energy equation, two turbulence equations, and Maxwell's electrical equations. Turbulence is represented by a two-equation model in which partial differential equations are solved for the turbulence energy and its dissipation rate. Two unique features are provided in the MGMHD code: (1) a full approximation storage (FAS), block implicit multigrid, finite-difference solution procedure for the cross-stream hydrodynamic equations, and (2) an FAS multigrid finite-difference solution procedure for the cross-stream electrical potential equations. Detailed descriptions of the equations, solution procedures, options available to the user, and input instructions are presented. Numerical solutions of three sample problems (two Faraday generators and a diagonally connected generator) are discussed. For two of the problems, the multigrid and single-grid codes are compared in terms of computational speed and solution accuracy. DOE

N90-16527# Los Alamos National Lab., NM.
PROGRESS WITH SMALL, HIGH-MAGNETIC-FIELD SPHEROMAKS IN CTX
Fred J. Wysocki, Juan C. Fernandez, Ivars Henins, Thomas R. Jarboe, G. J. Marklin, and Robert M. Mayo 1989 5 p Presented at the 11th US/Japan Workshop on Field-Reversed Configurations and Compact Toroids, Los Alamos, NM, 7-9 Nov. 1989
(Contract W-7405-eng-36)
(DE90-003395; LA-UR-89-3767; CONF-8911130-7) Avail: NTIS HC A01/MF A01

The current CTX program is directed towards using spheromaks as an energy transfer medium to accelerate metal plates to hypervelocity. In the proposed scheme, the spheromak is first compressed by accelerating a large plate to moderate velocity (3 to 5 km/s) with high explosives (HE). Another smaller plate is designed such that it experiences little force until the spheromak is compressed to a size comparable to the small plate. Then the force on the small plate rises quickly, accelerating this plate to high velocity. Present theoretical calculations indicate velocity gain of the small plate over the large plate as high as four, which could produce 20 km/s small plate velocity. In principle, the final velocity is limited only by the sound speed of the spheromak, and in practice, is probably limited by ohmic heating in the plate, the amount of energy that can be delivered to the large compression plate, and the energy dissipated by the spheromak during compression. Taking these effects into account, final velocities in the range 40 to 100 km/s might be achievable. DOE

N90-16528# Sandia National Labs., Albuquerque, NM.
LIGHT ION BEAM DRIVERS FOR INERTIAL CONFINEMENT FUSION
Juan J. Ramirez 1989 17 p Presented at the 9th International Workshop on Laser Interaction and Related Plasma Phenomena, Monterey, CA, 6-10 Nov. 1989
(Contract DE-AC04-76DP-00789)
(DE90-004196; SAND-89-2997C; CONF-891136-1) Avail: NTIS HC A03/MF A01

Intense beams of light ions are being developed at Sandia National Laboratories as a promising driver option for Inertial Confinement Fusion (ICF) implosions. The Particle Beam Fusion Accelerator II (PBFA II) will provide the physics basis for light ion beam driven ICF targets. Recent progress made in ion beam generation focusing on PBFA II has led to a record 5.4 TW/sq cm peak focal intensity with (gt)80 kJ proton energy delivered to a 6 mm diameter sphere. The driver-development program on PBFA II is reviewed. A design concept for a light ion beam driver for the Laboratory Microfusion Facility is also presented. DOE

N90-16529# Los Alamos National Lab., NM.
MHD STABLE HIGH BETA SPHEROMAK EQUILIBRIUM
G. J. Marklin 1989 5 p Presented at the 11th US/Japan Workshop on Field-Reversed Configurations and Compact Toroids, Los Alamos, NM, 7-9 Nov. 1989 Submitted for publication
(Contract W-7405-eng-36)
(DE90-004873; LA-UR-89-4271; CONF-8911130-10) Avail: NTIS HC A01/MF A01

Recent observations of a pressure driven mode in CTX indicate that its performance is being limited by the low beta stability requirements typical of conventional spheromak designs. Improved designs with higher beat limits therefore have the potential to dramatically increase the temperature and lifetime of CTX and other spheromak experiments. The results of an optimization study are presented to examine radically different geometries, but all with minimum energy current profiles which can easily be created experimentally and should be automatically stable to all ideal and resistive current drive modes. DOE

76 SOLID-STATE PHYSICS

Includes superconductivity.

For related information, see also *33 Electronics and Electrical Engineering* and *36 Lasers and Masers.*

N90-16530# California Univ., Berkeley. Lawrence Berkeley Lab. Center for Advanced Materials.
THE INFLUENCE OF RESIDUAL CONTAMINATION ON THE STRUCTURE AND PROPERTIES OF METAL/GaAs INTERFACES
Zuzanna Liliental-Weber Oct. 1988 14 p Presented at the Workshop of the International School of Materials Science and Technology, Erice, Italy, 2-7 Nov. 1988
(Contract DE-AC03-76SF-00098)
(DE90-000549; LBL-26140; CONF-8811270-1) Avail: NTIS HC A03/MF A01

This study shows that interface morphology, orientation relationship, and formation of new phases strongly depend on the surface preparation of GaAs before metal deposition and/or on the annealing environment. The metals investigated (Au, Ag, and Al, with lattice parameters close to each other) deposited in situ on a UHV-cleaved GaAs surface show very similar relationships with GaAs upon annealing. This relationship changes when GaAs is exposed to air before metal deposition. All metals investigated, when deposited on UHV-cleaved GaAs substrate, are stable upon annealing. The interface between metal and GaAs remains abrupt upon annealing. In the case of Cr almost perfect matching to GaAs was observed for UHV deposited samples, but random orientation for air-exposed samples. This study shows that impurities at the semiconductor surface can affect the stability of the barrier height of Schottky contacts. These changes in barrier height depend on the metal used, and on the intensity and direction of the potential and current during the electrical aging. The dramatic example of Ag contacts and their change upon current stressing only for air-exposed samples confirms the importance of surface preparation before metalization. DOE

N90-16531# Helsinki Univ. of Technology, Espoo (Finland). Low Temperature Lab.
SUPERFLOW INDUCED PHASE TRANSITION IN THE AXIAL VORTEX-FREE TEXTURE OF ROTATING SUPERFLUID He-3-B

J. S. Korhonen, Z. Janu, Y. Kondo, M. Krusius, Yu. M. Mukharsky, and A. D. Gongadze (Academy of Sciences of the Georgian SSR, Tbilisi.) 1989 25 p Sponsored in part by Academy of Finland; Koerber Stiftung; and Jenny and Antti Wihuri Foundation
(PB90-110388; TKK-F-A65; ISBN-951-754-909-1) Avail: NTIS HC A03/MF A01 CSCL 20L

In an axial magnetic field the order parameter texture of superfluid He-3-B has the well known flare-out structure. Under homogeneous rotation in the vortex free state with superfluid counterflow the flare-out texture is observed to undergo a 1st order phase transition. The critical rotation velocity has a temperature, pressure and magnetic field dependence which, when compared with calculations of the relative energies of axial textures, prove that counterflow causes the simple flare-out structure to become unstable with respect to a new solution to the texture problem. GRA

N90-16532# International Centre for Theoretical Physics, Trieste (Italy).
THE MODIFIED GINZBURG-LANDAU THEORY FOR ANISOTROPIC HIGH TEMPERATURE SUPERCONDUCTORS
L. N. Shehata (Atomic Energy Establishment, Cairo, Egypt) Mar. 1989 23 p Submitted for publication
(DE89-635909; IC-89/45) Avail: NTIS (US Sales Only) HC A03/MF A01

The modified Ginzburg-Landau theory, MGL, for strongly anisotropic high temperature superconductors (HTSC's) is reviewed and the MGL equations are re-derived to be used in solving two important fundamental problems. The first one concerns the evaluation of the domain-wall energy problem by a complete solution of the derived equations. The modified free energy functional is used to calculate the maximum supercurrents in both HTSC's and the conventional superconductors. The calculations show that the surface energy vanishes at the critical value of the GL parameter kappa(sub c)=1/square root of 2((-M)(1+M/3)) (sup 1/2), where 0 is less than or = M less than 1. Therefore, the transformation from type II to type I superconductivity is possible at temperatures very close to the transition critical one, at which kappa(T) becomes zero. The generalized formulas of the superconducting current allows the calculation of the maximum supercurrents for both the HTSC's and the conventional ones. The possible maximum currents are anisotropic and have higher values for HTSC's. The results are in good agreement with the related theoretical works as well as with the experimental data. DOE

N90-16533# Los Alamos National Lab., NM.
ROTATIONAL MAGNETIC PROCESSES IN YB2Cu3O7
Liwen Liu, J. S. Kouvel, and T. O. Brun (Argonne National Lab., IL.) 1989 12 p Presented at the 34th Conference on Magnetism and Magnetic Materials, Boston, MA, 28 Nov. - 1 Dec. 1989 Submitted for publication
(Contract W-7405-eng-36; NSF DMR-84-06898; NSF DMR-87-22880)
(DE90-000541; LA-UR-89-3001; CONF-891117-2) Avail: NTIS HC A03/MF A01

A polycrystalline superconducting thin disk sample was rotated in a fixed field rvec H at 4.2 K, and the vector magnitude and orientation of the total magnetization rvec M were measured as the sample-rotation angle (Theta) was slowly cycled between 0 and 360 deg. The measured rvec M was decomposed into a penetrating vortex flux component rvec M(sub p) that rotates rigidly with the sample at very small Theta and a diamagnetic (shielding) component rvec M(sub d) that stays antiparallel to rvec H. As Theta is raised, rvec M(sub p) deviates from rigid rotation, and the deviations are very different for the zero-field-cooled (ZFC) and field-cooled (FC) states at the same H, indicating different distributions in the strengths of the initial pinning forces. However, M(sub d) is exactly the same for both states and closely equals Chi(sub o)H, where Chi(sub o) is the low-H (ZFC) diamagnetic susceptibility. At still higher Theta, rvec M(sub p) rotates up to some critical angle relative to rvec H, where it remains as the sample continues to turn. This frictional behavior presumably derives from the dissipative motion of the vortices between pinning centers. DOE

N90-16534# Argonne National Lab., IL. Materials Science Div.
La(SUB 2)MO(SUB 4 + DELTA) (M = Cu, Ni, Co): PHASE SEPARATION AND SUPERCONDUCTIVITY RESULTING FROM EXCESS OXYGEN DEFECTS
B. Dabrowski, J. D. Jorgensen, D. G. Hinks, Shiyou Pei, D. R. Richards, K. G. Vandervoort, G. W. Crabtree, H. B. Vanfleet, and D. L. Decker (Brigham Young Univ., Provo, UT.) 1989 10 p Presented at the 3rd Annual Conference on Superconductivity and Applications, Buffalo, NY, 19-21 Sep. 1989
(Contract W-31-109-eng-38)
(DE90-001988; CONF-890971-4) Avail: NTIS HC A02/MF A01

The structural, superconducting and normal-state properties of La(sub 2)MO(sub 4 + delta) (M = Cu, Ni, Co) were studied by neutron powder diffraction, thermogravimetric analysis and resistivity measurements. La(sub 2)CuO(sub 4 + delta) was found to undergo phase separation near room temperature into antiferromagnetic La2CuO4 and superconducting La(sub 2)-CuO(sub 4.08). Single-phase, metallic, superconducting La(sub 2)CuO(sub 4.08) was prepared under 25 kbar of O2 at 500 C. The excess oxygen present as O(sup =) ions provides a doping mechanism analogous to alkaline-earth metal ion substitution. La(sub 2)NiO(sub 4 + delta) and La(sub 2)CoO(sub 4 + delta) undergo a similar phase separation for 0.02 less than delta less than 0.12 and 0 less than delta less than 0.16, respectively. The structure of the interstitial excess oxygen defect was determined for a single-phase La(sub 2)NiO(sub 4.18) sample. A different excess oxygen defect forms for material with 0 less than or = delta less than or = 0.02. All stoichiometric (delta =0) compounds have the same Cmca orthorhombic structure and are semiconducting and antiferromagnetic. DOE

N90-16535# National Inst. for Research in Inorganic Materials, Ibaraki (Japan).
RESEARCHES ON AMORPHOUS PEROVSKITE
21 Nov. 1988 98 p In JAPANESE
(DE89-900733; IRIM-8801) Avail: NTIS (US Sales Only) HC A05/MF A01

Researches on amorphous perovskite were conducted and thereby the quenching production of fragile oxide by a soft roller method was made possible. The film of KNbO3 added with other materials were produced by this method. These films have the possibility to develop to the infrared detection element. In addition, the film sample has large electrical resistivity. The quenching method is now applied to the oxide superconductive materials, and films of small critical current and of 100 percent density are being produced. As for the researches on high temperature superconductors; researches on crystal chemistry of La-Sr system were conducted, tetragonal and rhombic Y-Ba system was researched and its pressure effect was studied, and then their relations with the average values of T(sub c) and Cu were studied using solid solution. The value of pressure effect of Bi system determined here was quite contrary to the predicted value by the RVB theory. In the study of high pressure composition of sulfide which was conducted with the purpose of producing superconductive perovskite compound, sulfide proved to be hard to become perovskite. DOE

N90-16536# California Univ., Berkeley. Lawrence Berkeley Lab. Center for Advanced Materials.
CONFORMATION, ORIENTATION AND INTERACTION IN MOLECULAR MONOLAYERS: A SURFACE SECOND HARMONIC AND SUM FREQUENCY GENERATION STUDY
R. Superfine, J. Y. Huang, and Y. R. Shen Dec. 1988 5 p Presented at NICOLS '89: 9th International Conference on Laser Spectroscopy, Bretton Woods, NH, 18-23 Jun. 1989
(Contract DE-AC03-76SF-00098)
(DE90-003108; LBL-26490; CONF-890618-5) Avail: NTIS HC A01/MF A01

Sum frequency generation (SFG) was used to study the order

in a silane monolayer before and after the deposition of a coadsorbed liquid crystal monolayer. An increase was observed in the order of the chain of the silane molecule induced by the interpenetration of the liquid crystal molecules. By using second harmonic generation (SHG) and SFG, the orientation and conformation of the liquid crystal molecule on clean and silane coated glass surfaces was studied. On both surfaces, the biphenyl group is tilted by 70 deg with the alkyl chain end pointing away from the surface. The shift in the C-H stretch frequencies in the coadsorbed system indicates a significant interaction between molecules. DOE

N90-16537# Los Alamos National Lab., NM.
MICROSTRUCTURES OF Y123 FILMS ON SrTiO3, LaGaO3, AND LaAlO3
Tapan Roy, I. D. Raistrick, and T. E. Mitchell 1989 5 p Presented at the Materials Research Society Fall Meeting, Boston, MA, 27 Nov. - 2 Dec. 1989 Submitted for publication
(Contract W-7405-eng-36)
(DE90-003367; LA-UR-89-4011; CONF-891119-10) Avail: NTIS HC A01/MF A01

Transmission electron microscopy (TEM) and scanning electron microscopy (SEM) were used to study the microstructural features of YBa2Cu3O7 (hereafter referred to as Y123) films grown on various single crystal substrates by electron beam deposition. The films are all of high quality with the best observed J(sub c) value being 3 x 10(exp7) A/sq cm at 7 K. Cross-sectional views in TEM have shown that the morphology of the film depends on its thickness. Thinner films (2500 A) have a single layer of Y123 oriented with its c-axis perpendicular to the substrate while thicker films (8000 A) have this same c-axis perpendicular layer closest to the interface with a c-axis parallel layer above it. The interface between the film and the substrate is well defined in all cases with no amorphous region at the interface. Chemical analysis shows some inter-diffusion between the film and the substrate. DOE

N90-16538# North Carolina Univ., Chapel Hill. Chemistry Lab.
SOLID STATE VOLTAMMETRY AND SENSORS IN SOLIDS AND GASES Progress Report, 1 Apr. 1989 - 31 Mar. 1990
Royce W. Murray 1989 9 p
(Contract DE-FG05-87ER-13675)
(DE90-003234; DOE/ER-13675/3) Avail: NTIS HC A02/MF A01

A brief synopsis is given of the work under the present award. Seventeen solid state voltammetry projects in various stages: two completed prior to initiation of DOE support, six published, one in press, two submitted, four in advanced draft form, and two advanced but still in experimental phase. DOE

N90-16539# Argonne National Lab., IL. Materials Science Div.
PHONON ANOMALY AT T(SUB c) IN (Y/ER)Ba2Cu3O(7-DELTA)
Rajeshwar P. Sharma, L. E. Rehn, P. M. Baldo, and J. Z. Liu Nov. 1989 5 p Presented at the Materials Research Society Fall Meeting, Boston, MA, 27 Nov. - 2 Dec. 1989
(Contract W-31-109-eng-38)
(DE90-003562; CONF-891119-25) Avail: NTIS HC A01/MF A01

Ion channeling in single crystals of (Y/Er)Ba2Cu3O(7-delta) reveal an abrupt change (approx. 0.01A) at the superconducting transition temperature T(sub c) in displacements of the Cu and O atoms perpendicular to the (001) direction. This anomalous change in atomic displacements shifts directly with stoichiometry-induced changes in T(sub c). Blocking patterns indicate no large structural changes across T(sub c). DOE

N90-16540# Aerospace Corp., El Segundo, CA. Lab. Operations.
RESONANCE ENHANCED RAMAN STUDIES OF AS-GROWN AND LASER-PROCESSED HgCdTe
A. Compaan, B. Aggarwal, R. C. Bowman, Jr., and D. E. Cooper (Rockwell International Science Center, Thousand Oaks, CA.) 22 Sep. 1989 28 p
(Contract F04701-88-C-0089)
(AD-A213855; TR-0089(4945-07)-1; SD-TR-89-76) Avail: NTIS HC A03/MF A01 CSCL 20/12

Raman spectroscopy in Hg(1-x)Cd(x)Te (MCT) is a powerful, nondestructive surface probe of alloy composition and crystallinity. The frequencies and the relative amplitudes of the HGTe-like and CdTe-like phonon modes change with Cd fraction; the E1 and E1 + Delta 1 critical points shift with x value and strongly influence the Raman spectra obtained with the green and blue lines of the argon laser. The resonance enhancement of the two LO and two TO modes and a cluster mode in as-grown samples of MCT are studied for x values between 0.20 and 0.31. Also studied are the changes that occur in the Raman spectra after exposure of the MCT surfaces to single pulses from a dye laser with pulse energies above the melt threshold. The Raman spectra show clear evidence of compositional changes near the surface when processing occurs in air. However, when the irradiation occurs in an ambient of about atm of argon, the major effect is a reduction of the peak associated with a cluster mode. The results are consistent with a strong suppression of clustering after pulsed laser annealing. GRA

N90-16541# Department of the Air Force, Washington, DC.
REFLECTION TECHNIQUE FOR THERMAL MAPPING OF SEMICONDUCTORS Patent
Martin J. Walter, inventor (to Air Force) 20 Jun. 1989 6 p Filed 28 Dec. 1987 Supersedes US-Patent-Appl-SN-138238 (AD-D014263; US-Patent-4,841,150; US-Patent-Appl-SN-138238) Avail: U.S. Patent and Trademark Office CSCL 14/2

Semiconductors may be optically tested for their temperatures by illuminating them with tunable monochromatic electromagnetic radiation and observing the light reflected off of them. A transition point will occur when the wavelength of the light corresponds with the actual band gap energy of the semiconductor. At the transition point, the image of the semiconductor will appreciably darken as the light is transmitted through it, rather than being reflected off of it. The wavelength of the light at the transition point corresponds to the actual band gap energy and the actual temperature of the semiconductor. GRA

N90-16542# Princeton Univ., NJ. Dept. of Electrical Engineering and Computer Science.
GROUP 2 CUBIC FLUORIDES AS DIELECTRICS FOR III-V COMPOUND SEMICONDUCTORS Final Report, Jun. 1986 - May 1989
Antoine Kahn Sep. 1989 8 p
(Contract DAAL03-86-K-0059)
(AD-A214096; ARO-23323.2-EL) Avail: NTIS HC A02/MF A01 CSCL 20/12

The epitaxial growth of lattice matched Ca(x)Sr(1-x)F2/Gallium Arsenide and GaAs/Ca(x)Sr(1-x)F2 heterojunctions by molecular beam epitaxy is investigated. These heterojunctions are potential candidates for realizing opto-electronic devices involving III-V Compound Semiconductors. The composition x=0.5 is chosen to minimize the lattice mismatch at room and growth temperatures. The fabrication of the layers involves the sequential growth of GaAs wafers of a GaAs buffer layer, a 2000 to 3000A Ca5SrF3 layer, and a top 500 to 3000A GaAs layer. The growth along the (100), (111), (511) and (711) orientations is investigated. Optimum growth temperatures range from 500 to 550 C for the fluorides, and 550 to 600 C for the GaAs. The orientation of the substrate is conserved throughout the three epitaxial layers. The bulk crystallinity, studied with ion scattering, is found to be excellent in the GaAs buffer layer, fair to good in the fluoride layer, and poor to fair in the top GaAs layer. The high Miller-index GaAs surfaces (511, 711) exhibit a regular stepped structure (100 terraces) which contributes to the reduction of anti-phase disorder in the fluoride layer. It is also found that the (511) orientation is favorable for the growth of the top GaAs layer. Rough morphology and facetting at fluoride surfaces are identified as the main problems for the growth of high quality top GaAs layers. GRA

N90-16543# Washington Univ., Seattle. Dept. of Chemistry.
SCANNING TUNNELING MICROSCOPE STUDIES OF SURFACE DEFECTS Final Report, 1 Oct. 1987 - 30 Sep. 1989
Thomas Engel and Kevin E. Johnson 16 Oct. 1989 11 p
(Contract N00014-84-K-0544)
(AD-A214121) Avail: NTIS HC A03/MF A01 CSCL 14/2

Experiments proposed for our UHV Scanning Tunneling Microscope systems focus on the study of surface roughness and defect formation. The objective is to study the formation of surface defects of the nature where surface crystalline structure is maintained but periodicity is not. Two complementary systems are studied, one where defects are thermodynamically produced on stepped vicinal surfaces of silver, and a second system where epitaxial growth - surfaces grown using a commercial molecular beam epitaxy (MBE) apparatus - on GaAs substrates produces kinetically induced surface roughness. STM as a real space measure can probe defect type and distributions, information not available to surface diffraction techniques which measure a complementary value of averaged surface disorder. Interest is in the study of the energetics of these processes, both of which have important technological implications. The current state of development is described of the experimental instrumentation and its planned completion. Following that is a discussion of the results obtained so far in the development of the STM. GRA

N90-16544# Boston Coll., Chestnut Hill, MA. Dept. of Physics.
THEORY OF THE ELECTRONIC AND OPTICAL PROPERTIES OF SEMICONDUCTOR HETEROSTRUCTURES Final Report
David A. Broido 1989 9 p
(Contract N00014-88-K-0268)
(AD-A214132) Avail: NTIS HC A02/MF A01 CSCL 20/5

The optical spectrum of quantum wells is characterized by a series of excitonic peaks corresponding roughly to transitions between valence and conduction subband pairs subject to appropriate selection rules. In a simple model where these subbands are taken to be parabolic, the exciton spectrum for each subband pair follows a hydrogen-like series, with each exciton characterized by a two dimensional (2D) angular momentum symmetry e.g., 1s, 2s, 2p, 3d, etc. Accounting for the two types of valence subbands (heavy hole and light hole) and for the fact that only excitons with s symmetry are optically active (i.e., contribute to the oscillator strength), the excitonic transitions can then be labeled 11H(1s), 11L(1s), etc. Here, the first two indices designate the conduction and heavy (H) or light (L) hole valence subbands, respectively. For zincblende structures such as GaAs the conduction subbands can in fact be approximated accurately by parabolas. The valance subbands are, however, much more complicated because of the four-fold degeneracy of the bulk heavy and light hole valence bands at the valence band edge. This degeneracy causes the heavy and light hole subbands to be coupled resulting in the so-called valence band mixing (VBM) effects, such as: (1) Strong nonparabolicities and anisotropy in the valence subband structure; (2) Magnetic field dependent cyclotron masses; and (3) Mixing of Excitons and resulting field effects on the optical absorption. GRA

N90-16545# International Centre for Theoretical Physics, Trieste (Italy).
THERMODYNAMIC STUDIES ON THE FERROELECTRIC PHASE TRANSITION IN NEUTRON IRRADIATED (Li(SUB x)K(1-x))2SO4 CRYSTALS AT HIGH TEMPERATURE
M. E. Kassem, A. M. El-Khatib, E. A. Ammar, and M. M. Denton (Alexandria Univ., Egypt) May 1989 14 p Submitted for publication
(DE89-635786; IC-89/75) Avail: NTIS (US Sales Only) HC A03/MF A01

Thermodynamic studies of (Li(x)K(1-x))2SO4, LKS, mixed crystals have been made in the concentration range (x=0.1,0.2,..., x=0.5). The thermal behavior has been investigated by differential thermal analysis, DTA, and differential scanning calorimeter, DSC, in the vicinity of high temperature phases. Also, the effect of the mixed neutron field of fast and thermal neutrons (10 percent of the reactor neutron pile is fast neutrons) on the thermal properties of mixed crystals was studied. The results show a change in the transition temperature Tc, as well as the value of specific heat Cp at transition temperature, due to the change of the stoichiometric ratio and the radiation doses. The changes of enthalpy and entropy of mixed crystals have been estimated numerically. The obtained small values of Delta S/R is characteristic of incommensurate phase transition as previously confirmed by the results of neutron diffraction technique. DOE

N90-16546# International Centre for Theoretical Physics, Trieste (Italy).
THERMAL EXPANSION OF LATGS CRYSTALS
M. E. Kassem, S. H. Kandil, A. E. Hamed, and J. Stankowska (Adam Mickiewicz Univ., Poznan, Poland) Apr. 1989 17 p Submitted for publication
(DE89-636239; IC-89/62) Avail: NTIS (US Sales Only) HC A03/MF A01

The thermal expansion of triglycine sulphate crystals doped with L-alpha alanine (LATGS) was studied around the phase transition temperature (30 to 60 C) using thermomechanical analysis TMA. With increasing the content of admixture, the transition temperature (T sub c) was shifted towards higher values, while the relative changes in the dimension of the crystals (Delta L/L sub 0) of the studied directions varied both in the para- and ferroelectric phases. The transition width in the case of doped crystals was found to be broad, and this broadening increases with increasing the content of L-alpha alanine. DOE

N90-16547# Argonne National Lab., IL. Materials Science Div.
EFFECTS OF ION DOSE ON THE MORPHOLOGY AND CRYSTALLIZATION OF AMORPHOUS GERMANIUM
L. M. Wang, R. C. Birtcher, and L. E. Rehn Nov. 1989 7 p Presented at the Materials Research Society Fall Meeting, Boston, MA, 27 Nov. - 2 Dec. 1989
(Contract W-31-109-eng-38)
(DE90-003564; CONF-891119-18) Avail: NTIS HC A02/MF A01

The 1.5 MeV Kr(+) irradiation of polycrystalline Ge at room temperature, and subsequent annealing were carried out with in situ TEM observations. After a Kr(+) dose of 1.2 x 10(exp 14) ions/sq cm, Ge in the electron transparent region was completely amorphized. Continuous irradiation of the amorphized Ge resulted in a high density of small cavities. These cavities, first observed after 7 x 10(exp 14) ions/sq cm with an average diameter of approx. 3 nm, grew into large (approx. 50 nm) irregular-shaped holes, transforming the irradiated Ge into a sponge-like material after 8.5 x 10(exp 15) ions/sq cm. The crystallization temperature and the morphology of the crystallized Ge after annealing were found to be dependent on the Kr(+) dose. The sponge-like structure was retained after crystallization at approx. 600 C. DOE

N90-16548# Lawrence Livermore National Lab., CA. Chemistry and Materials Science Div.
USE OF COMPUTER SIMULATIONS TO ANALYZE LIMITATIONS OF KINETIC MODELS FOR RECRYSTALLIZATION
C. W. Price 20 Oct. 1989 7 p Presented at the International Conference on Recrystallization in Metallic Materials, Wollongong, Australia, 22-26 Jan. 1990
(Contract W-7405-eng-48)
(DE90-003618; UCRL-100615; CONF-900128-1) Avail: NTIS HC A02/MF A01

Only two kinetic models appear to be appropriate for recrystallization of metals and crystallization of metallic glasses: Kolmogorov-Johnson-Mehl-Avrami (KJMA) and Speich-Fisher (SF). However, much confusion prevails on the proper use of these models because their limitations are not well understood. Fortunately, computer simulations are proving to be effective for simulating kinetic behavior. In particular, a simplified computer model, which simulates a regular geometric grain growing in an impingement cell, provides kinetic simulations that agree with experimental data. The computer model isolates specific concepts

that the kinetic models were formulated on, and it also simulates different time-dependent growth relations. The KJMA model is based on linear interfacial growth and uses an extended-volume concept to compensate for impingement. The computer model isolated the effect of the extended-volume concept, and it also was used to determine why some experimental data conform to KJMA kinetics while others do not. The analysis indicated that essentially linear KJMA behavior can occur in recrystallization of metals that have reached an effectively constant state of recovery or in crystallization of amorphous metals that have reached a constant state of disorder. DOE

N90-16549# Lawrence Livermore National Lab., CA. Chemistry and Materials Science Dept.

THE CONCEPT OF AXIAL-SYMMETRY CONSTRAINT AND ITS SIGNIFICANCE IN RECRYSTALLIZATION

C. W. Price 20 Oct. 1989 7 p Presented at the International Conference on Recrystallization in Metallic Materials, Wollongong, Australia, 22-26 Jan. 1990

(Contract W-7405-eng-48)

(DE90-003620; UCRL-100614; CONF-900128-2) Avail: NTIS HC A02/MF A01

Grain growth and grain impingement that occur during recrystallization are simulated reasonably well with a simplified computer model that is based on a regular geometric grain growing in an impingement cell. The model also generates effective kinetic simulations, but only when the axial symmetry of the grain is constrained to the axial symmetry of the impingement cell. This condition is defined as the axial-symmetry constraint. When the simulated grain geometry deviates from the axial-symmetry constraint, the simulated kinetic behavior shows corresponding deviation from predicted kinetic behavior. These results imply that the geometry by which recrystallized grains fill space is more important than the actual shape if recrystallized grains. The physical significance of this concept is that the geometric shape of the interface between recrystallized and unrecrystallized material is dictated by the local deformation geometry. Once grain impingement commences and clusters of contiguous recrystallized grains form, the model interface corresponds to the interface formed by the grain clusters. The simulations reveal that interfacial areas dictated by deformation geometry are significantly greater for rolling than for extrusion, and this result correlates with experimental observations that recrystallization is more rapid in rolled materials than in extruded materials for the same initial grain size and similar reductions. DOE

N90-16550# Argonne National Lab., IL. Chemistry and Materials Science Div.

STRUCTURE-PROPERTY CORRELATIONS IN THE DESIGN OF ORGANIC METALS AND SUPERCONDUCTORS: AN OVERVIEW

Aravinda M. Kini, Mark A. Beno, K. Douglas Carlson, John R. Ferraro, Urs Geiser, Arthur J. Schultz, Hau H. Wang, and Jack M. Williams 1989 8 p Presented at the 1st ISSP International Symposium on the Physics and Chemistry of Organic Superconductors, Tokyo, Japan, 27-30 Aug. 1989

(Contract W-31-109-eng-38)

(DE90-003794; CONF-8908191-2) Avail: NTIS HC A02/MF A01

Molecular structure and, more importantly, molecular packing in organic superconducting salts (TMTSF)(2)X, beta-(BEDT-TTF)(2)X and kappa-(BEDT-TTF)(2)X will be examined in the context of deducing structure property correlations in these systems. Such an approach was instrumental in the discovery of superconductivity at 10.4 K in kappa-(BEDT-TTF)(2)Cu(NCS)(2), and it will continue to serve as an important tool in the rational design of new organic superconductors with even higher superconducting transition temperatures. DOE

N90-16551# California Univ., Berkeley. Lawrence Berkeley Lab. Center for Advanced Materials.

HETEROEPITAXY OF GaAs ON Si: METHODS TO DECREASE THE DEFECT DENSITY IN THE EPILAYER

Zuzanna Liliental-Weber, E. R. Weber, and J. Washburn Sep. 1989 10 p Presented at the 3rd Meeting on Defect Recognition and Image Processing in Semiconductors (DRIP-3), Yokohama, Japan, 17-22 Sep. 1989

(Contract DE-AC03-76SF-00098)

(DE90-004028; LBL-27886; CONF-890946-3) Avail: NTIS HC A03/MF A01

The fundamental mechanisms of defects formation and procedures used to improve the structural quality of GaAs grown on Si are discussed. Patterned growth, strained-layer superlattices, and proper thermal cycling are promising approaches to help achieve high quality GaAs layers grown on Si substrates. DOE

N90-16552# Stanford Linear Accelerator Center, CA.

B-FACTORY FINAL FOCUS SYSTEM USING SUPERCONDUCTING QUADRUPOLES

W. W. Ash Oct. 1989 6 p Presented at the Workshop on Towards Establishing B Factory, Syracuse, NY, 6-9 Sep. 1989

(Contract DE-AC03-76SF-00515)

(DE90-004432; SU-SLAC-PUB-5127; CONF-8909233-2) Avail: NTIS HC A02/MF A01

Experience with the superconducting final focus quadrupoles for the SLAC Linear Collider can be applied to a B-Factory built into the existing CESR tunnel. Such a system appears to accommodate detector and machine requirements. DOE

N90-16553# Tokyo Univ., Tanashi (Japan). Inst. for Nuclear Study.

DESIGN OF A LARGE SUPERCONDUCTING SPECTROMETER MAGNET

T. Shintomi, Y. Makida, T. Mito, Y. Yamanoi (National Lab. for High Energy Physics, Ibaraki, Japan), O. Hashimito, and T. Nagae Apr. 1989 4 p Presented at the 1988 Applied Superconductivity Conference, San Francisco, CA

(DE90-719505; INS-744) Avail: NTIS (US Sales Only) HC A01/MF A01

The superconducting spectrometer magnet for nuclear physics experiments was under construction by Institute for Nuclear Study, University of Tokyo with collaboration from KEK. The magnet has a sector type coil. The magnetic field is 3 T with the magnet gap of 50 cm and the stored energy is 11.8 MJ. The easy operation and maintenance are taken into consideration in addition to usual design concept. Three dimensional magnetic field calculation and the stress analysis were performed. The code QUENCH was applied to decide the operation current and to check the safety of the coil. As a result, the current of 500 A was selected. The heat leaks were checked and estimated less than 2 W at 4 K. A small refrigerator is to be used for thermal insulations at 80 and 20 K. DOE

N90-16554# Japan Atomic Energy Research Inst., Takasaki. Dept. of Development.

THE 1MeV-ELECTRON IRRADIATION INDUCED DEFECTS IN EPITAXIALLY GROWN 3C-SiC

Hisayoshi Itoh, Naohiro Hayakawa, Isamu Nashiyama, and Eiichiro Sakuma Jul. 1989 16 p

(DE90-719574; JAERI-M-89-094) Avail: NTIS (US Sales Only) HC A03/MF A01

Electron spin resonance (ESR) measurements were performed for 1MeV-electron irradiated 3C-SiC crystals epitaxially grown by chemical vapor deposition method. The results indicate the presence of at least four paramagnetic defects (T1-T4 centers). The T1 center was found to consist of isotropic five lines equally spaced at about 1.5 G and to have a g-value of 2.0029 + or - 0.0001. The anisotropic T2 center could be detected below about 100 K. The T3 and T4 centers were both anisotropic at room temperature. Isochronal annealing of electron irradiated 3C-SiC showed that the T1 center was annealed at three stages (150, 350, and 750 C) and that the T3 and T4 centers were annealed at 100 and at 350 C respectively. DOE

N90-16555# Sandia National Labs., Albuquerque, NM.
FUNDAMENTAL ISSUES IN HETEROEPITAXY (CONDENSED FROM THE DOE PANEL REPORT)
Paul S. Peercy 1989 12 p Presented at the Materials Research Society Fall Meeting, Boston, MA, 27 Nov. - 2 Dec. 1989 Submitted for publication
(Contract DE-AC04-76DP-00789)
(DE90-003980; SAND-89-1534C; CONF-891119-34) Avail: NTIS HC A03/MF A01

The Department of Energy's Council on Materials Science convened a Panel charged with assessing the present scientific understanding of epitaxial growth and identifying fruitful research opportunities in this area. The Panel, chaired by Paul S. Peercy, a member of the Department of Energy's Council on Materials Science and of the Solid State Sciences Committee, was composed of scientists in materials science, physics, and chemistry from academia, government labs and industry. Panel members were: Ernst G. Bauer, Brian W. Dodson, Daniel J. Ehrlich, Leonard C. Feldman, C. Peter Flynn, Michael W. Geis, James P. Harbison, Richard J. Matyi, Pierre M. Petroff, Paul S. Peercy, Julia M. Phillips, Gerald B. Stringfellow and Andrew Zangwill. The Panel met in January, 1989; its activities were supported by the Materials Sciences Division of Basic Energy Sciences. Deliberations emphasized artificially structured materials and resulted in a Panel Report which has been submitted to the Journal of Materials Research. With permission from the Department of Energy, this article excerpts from the report. DOE

N90-16556# Oak Ridge National Lab., TN. Solid State Div.
ION BEAM ANNEALING OF Si CO-IMPLANTED WITH Ga AND As
S. P. Withrow, O. W. Holland, S. J. Pennycook, J. Pankove, and A. Mascarenhas (Midwest Research Inst., Golden, CO.) Nov. 1989 8 p Presented at the Materials Research Society Fall Meeting, Boston, MA, 27 Nov. - 1 Dec. 1989 Submitted for publication
(Contract DE-AC05-84OR-21400)
(DE90-004297; CONF-891119-41) Avail: NTIS HC A02/MF A01

Ion beam annealing of amorphous Si(100) layers formed by co-implantation of overlapping Ga and As distributions is studied. Annealing was done using 750 keV Si(+) ions with the Si substrate held at 300 C. The samples were characterized using 2.0 and 5.0 MeV He(+) backscattering/channeling as well as by transmission electron microscopy (TEM). Crystallization of the amorphous Si layer occurs during irradiation via solid-phase-epitaxial growth without impurity precipitation or segregation. Both the Ga and As are nearly substitutional in the Si lattice, even at concentrations in excess of 7 at. percent for each species. These results are attributed to compensation effects, most likely through ion pairing of the electrically-attractive dopants. DOE

N90-16557# European Space Agency, Paris (France).
CONTRIBUTION TO THE STUDY OF ORDER EFFECTS IN THE ISING MODEL FRAMEWORK: GROUND STATES AND PHASE DIAGRAMS
Alphonse Finel Oct. 1989 437 p Transl. into ENGLISH of Contribution a l'Etude des Effets dOrdre dans le Cadre du Modele dIsing: Etats de Base et Diagrammes de Phase Original language document was announced as N88-27095
(ESA-TT-1118; ONERA-NT-1987-3; ETN-90-96188) Avail: NTIS HC A19/MF A01

Some aspects of order phenomena on a fixed underlying lattice are studied. The Ising model framework is considered. The ground states at zero temperature are determined. An algorithm is developed to determine exactly the ground states of the linear chain with pair and multiplet interactions up to 5th neighbors and, partially, those of the body centered cubic lattice with interactions between 1st, 2nd, 3rd and 5th neighbors. Approximate methods for calculating a phase diagram at finite temperatures are used. The cluster variation method and a hierarchy of approximations for three-dimensional lattices are studied. The frustation and degeneracy effects on the face-centered cubic lattice with 1st and 2nd neighbor interactions are analyzed. The investigations include two versions on two-dimensional lattices, the square lattice and the brick-work lattice, and a three-dimensional version where the interactions between 2nd neighbors are replaced by interactions between arbitrarily distant neighbors. ESA

N90-16558# Zeiss (Carl), Oberkochen (Germany, F.R.).
EUROLASER. HIGH POWER EXCIMER LASER: OPTICAL CRYSTALS Final Report
Bernhard Gaenswein Sep. 1987 19 p In GERMAN; ENGLISH summary
(Contract BMFT-13-EU-0022)
(ETN-90-95901) Avail: NTIS HC A03/MF A01

The crystals used in excimer lasers because of their excellent optical properties in the ultra violet spectrum are described. The crystals are fluorides of the alkaline earth metals magnesium, calcium and barium and the alkaline fluorides of lithium and sodium. It is possible to grow optical monocrystals of these compounds up to weights of 15 kg with a diameter of 180 mm. Some problems develop in growing crystals larger than this. To do so greater plants and improved automatic temperature monitoring and regulation are required. Special tools are needed for handling such large and heavy monocrystals. Understanding of the interaction between laser radiation and crystal must be improved upon in order to meet all the requirements to be placed on optical components in the future. ESA

N90-16559# Oak Ridge National Lab., TN. Solid State Div.
NEUTRON EXPERIMENTS ON HIGH-TEMPERATURE SUPERCONDUCTORS Foreign Travel Report, 8-21 Nov. 1989
H. A. Mook, Jr. Dec. 1989 7 p
(Contract DE-AC05-84OR-21400)
(DE90-003978; ORNL/FTR-3500) Avail: NTIS HC A02/MF A01

This report details the trip to the ILL to perform neutron scattering research on high-temperature superconductivity. The trip was very successful because of the excellent users' facilities available at the ILL. The data we accumulated were of high quality and will make an impact on our understanding of high-temperature superconductivity. However, we cannot continue to run a research program in this field with the limited beam time available at the ILL. To make substantial progress in this field, we must restart the High Flux Isotope Reactor. DOE

N90-16560# Los Alamos National Lab., NM.
MAGNETIC INTERACTIONS IN Sn-119 SUBSTITUTED FOR Cu IN ANTIFERROMAGNETIC AND SUPERCONDUCTING LAMELLAR CUPRATES
Moshe Paz Pasternak (Tel-Aviv Univ., Israel) and Raymond Dean Taylor Nov. 1989 16 p Presented at the International Conference on the Applications of the Mossbauer Effect, Budapest, Hungary, 4-8 Sep. 1989 Submitted for publication
(Contract W-7405-eng-36)
(DE90-003661; LA-UR-89-3883; CONF-890933-5) Avail: NTIS HC A03/MF A01

Moessbauer Spectroscopy (MS) studies of Sn-119 were carried out in antiferromagnetic La2Cu(0.99)Sn(0.01)O2(214) and in superconducting GdBa2Cu(0.99)Sn(0.01)3O7 (123). Non-magnetic Sn4(+) substitutes for Cu if the right procedure for diffusing (119)SnO2 in CuO is carried out. Studies performed in 214 show a large quadrupole splitting (QS) down to 120 K followed by an onset of a magnetic interaction reaching a saturation internal field of H(eff) = 8.7(5) KOe at T = 30 K. From the combined magnetic-quadrupole interaction the angle theta formed by q(zz) and H(eff), the eta-parameter, and the sign of QS were deduced and information on the local spin structure is derived. Studies conducted with the 123 material T(c) = 90 K reveal a broad unsplit line at temperatures down to 60 K followed by an abrupt onset of a magnetic interaction corresponding to H(eff) (Sn) = 8.3 (7) KOe. The hyperfine field decreases with decreasing temperature reaching 6.0(1) KOe at 16 K. The onset of the magnetic interaction at the Sn-119 nucleus is explained as due to a local

depletion of holes following the Sn4(+) doping and a consequent quenching of the magnetic fluctuations in its vicinity. DOE

N90-16561# Oak Ridge National Lab., TN. Solid State Div.
THE EFFECTS OF OXYGEN AND STRONTIUM VACANCIES ON THE SUPERCONDUCTIVITY OF SINGLE CRYSTALS OF Bi2Sr(2-x)CuO(6-y)
B. C. Sales, Edward Sonder, and B. C. Chakoumakos 1989 4 p Presented at the Materials Research Society Fall Meeting, Boston, MA, 27 Nov. - 2 Dec. 1989
(Contract DE-AC05-84OR-21400)
(DE90-004242; CONF-891119-43) Avail: NTIS HC A01/MF A01

Single crystals of Bi2Sr(2-x)CuO(6-y) were grown from CuO-rich melts. The Sr content in the crystals was varied from x=0.1 to x=0.5 by varying the starting composition of the melt and the oxygen content was adjusted using an appropriate heat treatment of the crystals in a thermogravimetric system. With decreasing Sr content the superconducting transition temperature, (Tc), of the crystals decreased rapidly from 10 K to below 4.2 K and the resistivity in the a-b plane changed from metallic (linear in T from 30 to 300 K) to semiconducting. Reducing the oxygen content in the crystals had a similar effect on the resistivity. Only crystals with close to the maximum oxygen content (y=0) were superconducting, and removal of oxygen from previously superconducting crystals resulted in a rapid decrease of (Tc), and the eventual loss of superconductivity ((Tc) less than 4.2 K). Although crystals of Bi2Sr(2-x)CuO(6-y) could be made sequentially superconducting-semiconducting-superconducting by the addition-removal-addition of oxygen, the process was not totally reversible. After only one such cyclic heat treatment x ray diffraction indicated that for some compositions such cycling resulted in the appearance of CuO and another layered structure that was identified previously and is slightly deficient in CuO. The new layers structure is semiconducting and has a layer-stacking repeat distance that is 1A smaller than the superconducting 221 phase. DOE

N90-16562# Oak Ridge National Lab., TN. Solid State Div.
MAGNETIC PENETRATION DEPTH AND INTRAGRAIN CRITICAL CURRENT DENSITY IN GAIN-ALIGNED Tl2Ca2Ba2Cu3O10 SUPERCONDUCTOR
J. R. Thompson, D. K. Christen, H. A. Deeds, Y. C. Kim, J. Brynestad, S. T. Sekula, J. Budai, and J. G. Ossandon (Tennessee Univ., Knoxville.) Nov. 1989 6 p Presented at the Materials Research Society Fall Meeting, Boston, MA, 27 Nov. - 2 Dec. 1989 Submitted for publication
(Contract DE-AC05-84OR-21400)
(DE90-004245; CONF-891119-42) Avail: NTIS HC A02/MF A01

Magnetic studies were performed on the high temperature superconductor Tl2Ca2Ba2Cu3O10 (Tc = 123 K) in the form of a grain aligned composite. Investigations with the magnetic field applied parallel and perpendicular to the sample's common c-axes were analyzed to obtain the magnetic penetration depth as a function of temperature and the critical current density J(sub c)(H,T). DOE

N90-16563# Oak Ridge National Lab., TN. Solid State Div.
PHYSICAL PROPERTIES OF Bi2Sr2CuO6, THE SEMICONDUCTING PHASE, STRUCTURALLY DISTINCT FROM THE n = 1 Bi-CUPRATE SUPERCONDUCTOR
B. C. Chakoumakos, Edward Sonder, and B. C. Sales 1989 4 p Presented at the Fabrication, Characterization, and Applications of High-Temperature Superconducting Materials, Boston, MA, 26-27 Nov. 1989
(Contract DF-AC05-84OR-21400)
(DE90-004299; CONF-891181-1) Avail: NTIS HC A01/MF A01

The stable phase that forms near 2:2:1 in the Bi-Sr-Cu oxide system is now recognized as a semiconducting phase structurally distinct from the n = 1 Bi-cuprate superconductor, whose actual composition (Bi2Sr(2-x)CuO(6-y), x = 0.1 to 0.25, y = 0 to 0.5) is deficient in Sr. The 2:2:1 phase forms by a slow solid-state replacement of the superconducting phase for compositions near 2:2:1. It also can be grown from melt compositions involving several phase assemblages, but single phase products are not obtained, implying incongruent melting. Alumina and zirconia crucibles promote the growth of the superconducting phase by reacting with the melt to remove Sr, whereas Au crucibles promote the growth of the 2:2:1 phase. Owing to its fine grained, fibrous habit, structural characterization was difficult. Of the unit cells proposed, the C-centered monoclinic cell of Roth et al. provides the best fit to the x ray powder and single crystal precession data, a = 24.522(9), b = 5.426(2), c = 21.983(9)A, beta = 105.00(3)(deg). Perfect prismatic cleavages intersecting at (approx. 148 deg) and (approx. 32 deg) are indexed as (100) and (-201) forms. Although, the superconducting n = 1 Bi-cuprate exhibits variable Sr and O contents, the 2:2:1 phase appears to be a single composition with no oxygen exchange observed by TGA, although it may be somewhat deficient in Cu. The 2:2:1 phase is semiconducting as determined by electrical resistivity measurements, with an apparent activation energy of 0.013 eV. For a 2:2:1 stoichiometry, the measured density of approx. 7.2 g/cu cm implies 16 formula units per cell. DOE

N90-16564# Tufts Univ., Medford, MA. Electro-Optics Technology Center.
LITHIUM COBALT OXIDE THIN FILM AND ITS ELECTROCHROMISM
Guang Wei, Terry E. Haas, and Ronald B. Goldner 1989 10 p Presented at the Electrochemical Society Fall Meeting, Hollywood, FL, 15-20 Oct. 1989 Submitted for publication
(Contract DE-FG03-85SF-15927)
(DE90-004570; CONF-8910107-5) Avail: NTIS HC A02

Thin films of lithium cobalt oxide have been prepared by RF-sputtering from powdered LiCoO2. These films permit reversible electrolytic removal of lithium ions upon application of an anodic voltage in a propylene carbonate-lithium perchlorate electrolyte, the films changing in color from a pale amber transparent state to a dark brown. A polycrystalline columnar film structure was revealed with SEM and TEM. X ray examination of the films suggests that the layered rhombohedral LiCoO2 structure is the major crystalline phase present. Oxidation-reduction titration and atomic absorption were used for the determination of the film stoichiometry. The results show that the as deposited-films on glass slides are lithium deficient (relative to the starting material) and show a high average cobalt oxidation state near +3.5. The measurements of dc conductivity suggest a band to band conduction at high temperature (300 to 430 K) and hopping conduction in localized states at low temperature (4 to 270 K). The thermoelectric power data show that the films behave as p-type semiconductors. Transmission and reflectance measurements from 400 nm to 2500 nm show significant near-IR reflectivity. DOE

N90-16565# Los Alamos National Lab., NM.
ELECTRON BEAM INDUCED OXYGEN IN YBa2Cu3O(7-x) SUPERCONDUCTORS
Soumendra Nath Basu, Tapan Roy, Terence E. Mitchell, and Michael Nastasi 1989 7 p Presented at the Materials Research Society Fall Meeting, Boston, MA, 27 Nov. - 2 Dec. 1989 Submitted for publication
(Contract W-7405-eng-36)
(DE90-004839; LA-UR-89-4102; CONF-891119-53) Avail: NTIS HC A02/MF A01

Thin foils of bulk YBa2Cu3O(sub 7-x) YBCO superconductors were subjected to electron irradiation in a Transmission Electron Microscope (TEM). The resulting disordering of the oxygen atoms and vacancies in the Cu-O planes was monitored by measuring the splitting of the (110) diffraction spots in the (001) diffraction pattern. Samples were irradiated at 83K with 100, 150, 200 and 300kV electrons. The 100kV electrons did not cause any disordering, even after prolonged irradiation. The results of the higher energy irradiations showed an excellent fit to a disordering model, indicating a lack of radiation assisted ordering at 83K. This was further confirmed by the insensitivity of the disordering

to the dose rate of 300kV electrons at 83K. However, at 300K, an increase in the dose rate of 300kV electrons increased the disordering rate, indicating that radiation assisted reordering was occurring at that temperature. DOE

N90-16566# Northwestern Univ., Evanston, IL.
SOLID STATE, SURFACE, AND CATALYTIC STUDIES OF OXIDES Progress Report, 1 May 1987 - 1 Dec. 1989
Harold H. Kung Dec. 1989 22 p
(Contract DE-FG02-87ER-13725)
(DE90-004850; DOE/ER-13725/3) Avail: NTIS HC A03/MF A01

This research program consists of two projects: selective oxidation of alkanes, and catalytic decomposition of methanol on single crystal ZnO surfaces. In the first project, the selective oxidation of light alkanes were studied over mixed magnesium-vanadium oxides. The active phase in these catalysts was identified as magnesium orthovanadate after studying the catalysts with various spectroscopies, which included x ray diffraction, infrared, laser Raman, Auger electron spectroscopy, and scanning electron microscopy. DOE

N90-16567# Arizona Univ., Tucson. Dept. of Physics.
ARTIFICIALLY STRUCTURED SUPERCONDUCTORS Final Progress Report, 1 Apr. 1987 - 31 Mar. 1990
Charles M. Falco 17 Nov. 1989 18 p
(Contract DE-FG02-87ER-45297)
(DE90-004851; DOE/ER-45297/12) Avail: NTIS HC A03/MF A01

This report describes progress during the previous 2 1/2 years of DOE funding; description of the research to be conducted during the remaining months of the present grant; a description of the status of the graduate students working on this research; lists of the invited talks, seminars and colloquia, of other recognition of the research, and of the publications crediting DOE sponsorship; and a summary of current and pending Federal support. Work proposed to be conducted during the next three years is described in detail in a separate proposal submitted to the DOE. Because of the specific capabilities given by significant enhancements to the thin film preparation and analysis facilities (e.g., two heavily instrumented molecular beam epitaxy machines), research efforts were increasingly directed toward studies of magnetism at surfaces and interfaces. Thus, the proposal submitted to DOE for the next three years involves studies of such magnetic thin films and superlattices. This DOE grant is for research on Artificially Structured Superconductors. When the original proposal was written in mid-1986 this meant low (Tc) metallic superlattices. However, after announcement of the new high (Tc) compounds in late-1986, and after consultation with my former DOE contract monitor in January 1987 work was begun on the new high (Tc) superconductors. DOE

N90-16568# Argonne National Lab., IL. Materials Science Div.
HIGH TEMPERATURE NEUTRON DIFFRACTION STUDY OF THE FORMATION REACTION OF BISMUTH SUPERCONDUCTORS
Mary F. Garbauskas, Ronald H. Arendt (General Electric Co., Schenectady, NY.), James D. Jorgensen, and Richard L. Hitterman 1989 5 p Presented at the Materials Research Society Fall Meeting, Boston, MA, 27 Nov. - 2 Dec. 1989 Submitted for publication
(Contract W-31-109-eng-38)
(DE90-004883; CONF-891119-55) Avail: NTIS HC A01/MF A01

High temperature neutron powder diffraction was used to study the formation of the 110K transition temperature material, Bi2Ca2Sr2Cu3O(x) (2223), both from synthetic reaction mixtures and after partial melting. The results indicate that the 80K transition temperature material, Bi2CaSr2Cu2O(x) (2122), is the precursor to the (2223) material. The reaction to form the (2122) occurs rapidly at 860 C, while the conversion of this material to the (2223) is much slower. DOE

N90-16569# Battelle Columbus Labs., OH.
PROPERTIES AND DESIGN OF MULTIFILAMENTARY NbTi COMPOSITE SUPERCONDUCTORS Technical Progress Report
31 Oct. 1989 15 p
(Contract DE-AC02-86ER-40296)
(DE90-004904; DOE/ER-40296/T1) Avail: NTIS HC A03/MF A01

For the past three years we have been conducting research in support of multifilamentary conductor development for Superconducting Supercollider (SSC) applications. We have been concerned not only with alloy design -- NbTi-base alloys for the superconductor and Cu-base alloys for the stabilizer -- but also with the design of the multifilamentary strand itself. DOE

N90-16570# Battelle Memorial Inst., Columbus, OH.
MAGNETIC STUDIES OF PROXIMITY-EFFECT COUPLING IN A VERY CLOSELY SPACED FINE-FILAMENT NbTi/CuMn COMPOSITE SUPERCONDUCTOR
E. W. Collings, K. R. Marken, Jr., M. D. Sumption, E. Gregory, and T. S. Kreilick (Supercon, Inc., Shrewsbury, MA.) 1989 8 p Presented at the International Cryogenic Materials Conference, Los Angeles, CA, 24-28 Jul. 1989
(Contract DE-AC02-86ER-40296)
(DE90-005387; CONF-890701-22) Avail: NTIS HC A02/MF A01

Magnetization studies have been conducted on a 23,000-filament composite (with a filament-spacing/filament-diameter ratio, sd, of about 0.19) drawn down to d = 11.5 to 0.5 (mu)m. Various techniques have been used to explore the occurrence and properties of proximity-effect coupling between the filaments across the Cu-0.5 wt. percent Mn matrix. This coupling, which sets in at d less than 1.5 (mu)m -- much smaller than 2.5 (mu)m intended for superconducting supercollider (SSC) magnet applications -- is studied both at low fields (well below the H sub c1 of the NbTi) and at high fields (of up to 1.5 tesla (15 kG)). DOE

77 THERMODYNAMICS AND STATISTICAL PHYSICS

Includes quantum mechanics; theoretical physics; and Bose and Fermi statistics.

For related information see also *25 Inorganic and Physical Chemistry* and *34 Fluid Mechanics and Heat Transfer.*

N90-16571# International Centre for Theoretical Physics, Trieste (Italy).
THE OFF-SHELL CLOSED STRINGS AS THE TOPOLOGICAL OPEN MEMBRANES: DYNAMICAL TRANSMUTATION OF WORLD SHEET DIMENSION
Yan I. Kogan (Gosudarstvennyi Komitet po Ispolzovaniyu Atomnoi Energii, Moscow, USSR) May 1989 9 p Submitted for publication
(DE89-635721; IC-89/65) Avail: NTIS (US Sales Only) HC A02/MF A01

Using the connection between (2+1) Chern-Simons gauge theory and 2d Conformal Field Theory, the on-shell string condition is obtained as a condition of the full independence of the interior of a (2+1) world. The new method for off-shell continuation is considered based on the introduction of the Maxwell term in (2+1) theory. This leads to a dynamical transmutation of the world-sheet dimensions - the off-shell string becomes a topological membrane (topological means that the (2+1) theory has a topological mass term). The dependence of the parameters of the (2+1) theory under external fields is discussed. DOE

N90-16572# Instituto de Fisica Teorica, Sao Paulo (Brazil).
STUDY OF PRIMITIVE UNIVERSE IN THE BIANCHI 9 MODEL M.S. Thesis
George Emanuel Avraa Matsas Mar. 1988 114 p In

PORTUGUESE; ENGLISH summary
(DE89-635903; INIS-BR-1572) Avail: NTIS (US Sales Only) HC A06/MF A01

The theory of general relativity is used to study the homogeneous cosmological model Bianchi 9 with isometry group SO(3) near the cosmological singularity. The Bogoyavlenskii-Novikov formalism is introduced to explain the unusual behavior of the Liapunov exponent associated with this chaotic system.
DOE

N90-16573# International Centre for Theoretical Physics, Trieste (Italy).
CONTINUOUS SPONTANEOUS REDUCTION MODEL INVOLVING GRAVITY
GianCarlo Ghirardi, Renata Grassi, and Alberto Rimini Jun. 1989 29 p
(DE90-600730; IC-89/105) Avail: NTIS (US Sales Only) HC A03/MF A01

A continuous reduction model implying the dynamical suppression of linear superpositions of macroscopically distinguishable states, presented recently by L. Diosi, is investigated. The model exhibits appealing features, in particular it relates reduction to gravity and contains no constants besides Newton's gravitational constant G. It turns out, however, that the model is not fully consistent. A modification of it is proposed, which overcomes the difficulties and retains partially its nice features. The resulting model deals with systems containing distinguishable or identical constituents, allows the derivation from microdynamics of wave packet reduction and accounts for the emergency of definite macroscopic properties for macro-objects. Reduction is related to gravity in the same way as in Diosi's model, but a fundamental length must be introduced to avoid inconsistencies.
DOE

N90-16574# International Centre for Theoretical Physics, Trieste (Italy).
ON GAUGE FIXING AND QUANTIZATION OF CONSTRAINED HAMILTONIAN SYSTEMS
Omer F. Dayi Jun. 1989 11 p
(DE90-600732; IC-89/118) Avail: NTIS (US Sales Only) HC A03/MF A01

In constrained Hamiltonian systems which possess first class constraints some subsidiary conditions should be imposed for detecting physical observables. This issue and quantization of the system are clarified. It is argued that the reduced phase space and Dirac method of quantization, generally, differ only in the definition of the Hilbert space one should use. For the dynamical systems possessing second class constraints the definition of physical Hilbert space in the BFV-BRST operator quantization method is different from the usual definition.
DOE

N90-16575# International Centre for Theoretical Physics, Trieste (Italy).
ON THE DOMAIN OF STRING PERTURBATION THEORY
Simon Davis Jun. 1989 19 p Submitted for publication
(Grant NSF PHY-82-15249)
(DE90-600759; IC-89/112) Avail: NTIS (US Sales Only) HC A03/MF A01

For a large class of effectively closed surfaces, it is shown that the only divergences in string scattering amplitudes at each order in perturbation theory are those associated with the coincidence of vertex operators and the boundary of moduli space. This class includes all closed surfaces of finite genus, and infinite-genus surfaces which can be uniformized by a group of Schottky type. While the computation is done explicitly for bosonic strings in their ground states, it can also be extended to excited states and to superstrings. The properties of these amplitudes lead to a definition of the domain of perturbation theory as the set of effectively closed surfaces. The implications of the restriction to effectively closed surfaces on the behavior of the perturbation series are discussed.
DOE

N90-16576# International Centre for Theoretical Physics, Trieste (Italy).
PRODUCTION OF PHOTONS IN ANISOTROPIC SPACETIMES
K.-H. Lotze (Friedrich-Schiller Univ., Jena, German D.R.) Jun. 1989 17 p Submitted for publication
(DE90-600760; IC-89/114) Avail: NTIS (US Sales Only) HC A03/MF A01

Under the main aspect of the creation of photon pairs from vacuum, the Maxwell equations in anisotropic universes with a diagonal Bianchi type I metric is investigated. Thereby, a method was employed developed earlier by Sagnotti and Zwiebach (1981). For two axisymmetric expansion laws, exact photon solutions was obtained of the Maxwell equations making use of a WKB particle concept. The number densities was computed of created photons and the importance of singularity avoidance for getting finite results is emphasized. In the case of weak anisotropies the results by Zel'dovich, and Starobinsky (1977) are regained and commented on.
DOE

N90-16577# Stellenbosch Univ. (South Africa). Organization of Theoretical Physicists.
PROCEEDINGS OF THE 23RD ANNUAL SEMINAR ON THEORETICAL PHYSICS
1988 324 p Seminar held in Grahamstown, South Africa, 5-8 Jul. 1988 Prepared in cooperation with South African Inst. of Physics, South Africa
(DE90-601827; INIS-mf-11540; CONF-8807191;
ISBN-0-86960-861-4) Avail: NTIS (US Sales Only) HC A14/MF A01

This seminar contains 18 papers. Twelve papers are indexed separately. Topics covered include: the Dirac equation in arbitrary space-time dimensions; next-to-leading corrections to jet multiplicity distributions in QCD; propagators and one loop diagrams in cavity field theory; cavity quantum chromodynamics in the presence of a classical background field; quark gluon plasma and hadronic matter in the early universe; deconfinement and chiral transitions in lattice QCD; J/PSI suppression as a signal for quark deconfinement; geometrical interpretation of boson models of nuclear structure; the interacting boson model, BCS-RPA theory and the theory of pairing interactions applied to the Ge-nuclei; fluctuations and chaotic behavior; test of the Bonn nucleon-nucleon potential in nucleon-antinucleon scattering; and new relativistic center-of-mass corrections for the nucleon.
DOE

N90-16578# Tokyo Univ., Tanashi (Japan). Inst. for Nuclear Study.
UNIVERSE AS A TOPOLOGICAL DEFECT IN A HIGHER-DIMENSIONAL EINSTEIN-YANG-MILLS THEORY
A. Nakamura (Tokyo Metropolitan Univ., Japan) and K. Shiraishi Apr. 1989 12 p Sponsored in part by Ministry of Education, Science, and Culture and Japan Society for the Promotion of Science
(DE90-719507; INS-746; TMUP-HEL-8904) Avail: NTIS (US Sales Only) HC A03/MF A01

An interpretation is suggested that a spontaneous compactification of space-time can be regarded as a topological defect in a higher-dimensional Einstein-Yang-Mills (EYM) theory. It starts with D-dimensional EYM theory in the present analysis. A compactification leads to a D-2 dimensional effective action of Abelian gauge-Higgs theory. A vortex solution was found in the effective theory. The universe appears to be confined in a center of a vortex, which has D-4 large dimensions. An example is shown with SU (2) symmetry in the original EYM theory, and the resulting solution is found to be equivalent to the instanton-induced compactification. The cosmological implication is also mentioned.
DOE

N90-16579# Japan Atomic Energy Research Inst., Tokyo. Dept. of Fuels and Materials Research.
ESTIMATION OF THERMODYNAMIC PROPERTIES OF ALLOYS FROM PHASE DIAGRAM AND OTHER LOOSE BOUNDARY CONDITIONS
Toru Ogawa and Takashi Iwai May 1989 50 p In JAPANESE;

ENGLISH summary
(DE90-719511; JAERI-M-89-063) Avail: NTIS (US Sales Only) HC A03/MF A01

A set of computer programs has been made, which is used to predict thermodynamic properties of an alloy system from phase diagram and other loose boundary conditions. Loose boundary conditions include fragmentary thermodynamic data and predictions based on several empirical or theoretical hypotheses. In program TOHSG, m equations with n (m greater than n) unknowns which are parameters concerning atomic interactions are assembled from the equilibria collected on experimental phase diagram, and also from the loose boundary conditions. Then, the unknowns are obtained as Chebyshev solutions. Thermodynamic properties of the alloys are also calculated. In order to test their validity, the parameters are then fed into the other two programs TOGAP and TOCOMP, which calculate the phase diagram. The set of programs can: (1) generate a working data set of a system whose thermodynamic properties are unknown, and (2) test various hypotheses against experimental data such as phase diagrams. As an example of application, U-Zr system has been analyzed. Source list of TOHSG and input/output guides are attached. DOE

N90-16580# Hiroshima Univ., Takehara (Japan). Research Inst. for Theoretical Physics.
THE (2+1)-DIMENSIONAL QUANTUM GRAVITY
Akio Hosoya and Ken-ichi Nakao (National Lab. for High Energy Physics, Ibaraki, Japan) May 1989 21 p
(DE90-719556; RRK-89-16) Avail: NTIS (US Sales Only) HC A03/MF A01

The (2+1)-dimensional pure Einstein gravity is studied in the canonical ADM formalism, assuming that the spatial surface is closed and compact. Owing to the constraints, the dynamical variables are reduced to the moduli parameters of the 2-surface. Upon quantization, the system becomes a quantum mechanics of moduli parameters in a curved space endowed with the Weil-Petersson metric. In the case of torus in particular, the superspace, on which the wave function of universe is defined, turns out to be the fundamental region is the moduli space. The solution of the Wheeler-DeWitt equation is explicitly given as the Maass form which is perfectly regular in the superspace. DOE

N90-16581# Tokyo Univ., Tanashi (Japan). Inst. for Nuclear Study.
DOUBLE-PERIODIC WORMHOLES IN THEORIES WITH GLOBAL SYMMETRIES
Shoichi Midorikawa Jun. 1989 12 p Sponsored in part by Iwanami Fujukai Foundation
(DE90-719575; INS-754) Avail: NTIS (US Sales Only) HC A03/MF A01

We examine the quantum theory of a complex scalar field with global U(1) symmetry minimally coupled to gravity. We find numerically that there exists a double-periodic wormhole solution in addition to a single-periodic one if a potential has a local maximum at a finite value of the scalar field. Spontaneous breakdown of the U(1) symmetry is irrelevant to the existence of the wormholes of finite action. DOE

N90-16582# Tokyo Univ., Tanashi (Japan). Inst. for Nuclear Study.
AN ESTIMATION OF THE ONE-LOOP MASS SHIFTS IN OPEN SUPERSTRING THEORY
Tsuyoshi Nishioka, Akihiko Tsuchiya (Tokyo Inst. of Tech., Japan), and Hisashi Yamamoto Jul. 1989 15 p Sponsored in part by Ministry of Education, Science, and Culture, Japan
(DE90-719578; INS-756; UT-Komaba-89-14; TIT/HEP-137)
Avail: NTIS (US Sales Only) HC A03/MF A01

The quantitative studies of the one-loop mass shifts for the first excited states in ten dimensional open superstring are given. Removing the apparent singularities in the on-shell integral expressions by an off-shell analytic continuation, the finite mass shifts with imaginary parts were obtained. The real part was numerically evaluated to find the smallness of the magnitude of one-loop effect. DOE

80 SOCIAL SCIENCES (GENERAL)

Includes educational matters.

No abstracts in this category.

81 ADMINISTRATION AND MANAGEMENT

Includes management planning and research.

N90-16583# Advisory Group for Aerospace Research and Development, Neuilly-Sur-Seine (France).
INTERNATIONAL CONFERENCE MANAGEMENT
George Zinnemann Oct. 1989 21 p Revised
Avail: NTIS HC A03/MF A01

Guidelines and helpful hints to individuals involved in managing and participating in international conferences are provided. The guidelines are intended for individuals involved in international conference management, namely, the conference project officer, the host organization and its coordinator, the meeting chairman, and the individual speaker. The aim is to help conference planners to elude the traps, embarrassments, and obstacles which appear to be built into any meeting ever held. B.G.

N90-16584# Oak Ridge National Lab., TN.
INVENTION AND INNOVATION: ALTERNATIVE MECHANISMS FOR ENHANCING ORGANIZATIONAL COMPETITIVENESS
Terry Lynn Payne and Donald Tippett 1989 7 p Presented at the 2nd International Conference on Technology Management, Miami, CA, 28 Feb. - 2 Mar. 1990
(Contract DE-AC05-84OR-21400)
(DE89-015858; CONF-900215-1) Avail: NTIS HC A02/MF A01

This paper explores the concepts of invention and innovation as mechanisms which play a vital role in achieving a firm's strategic objectives. Too often the terms invention and innovation are used interchangeably. However, a definition for each is provided that clearly shows their distinguishing characteristics. Included is a comparison of the environments that support invention and innovation. Similarities, such as the fact that neither is highly compatible with sustaining operations, are described and discussed. Key differences inherent in the fact that invention is an event and innovation is a process are also discussed. This paper includes a statement of the impacts of innovation and invention on organizational competitiveness. Also included are guidelines for considering innovation and invention as distinct strategic alternatives in the strategic planning process. DOE

82 DOCUMENTATION AND INFORMATION SCIENCE

Includes information management; information storage and retrieval technology; technical writing; graphic arts; and micrography.

For computer documentation see *61 Computer Programming and Software.*

N90-16585# Advisory Group for Aerospace Research and Development, Neuilly-Sur-Seine (France). Technical Information Panel.
AGARD INDEX OF PUBLICATIONS, 1986-1988
Aug. 1989 401 p
(AGARD-INDEX-86-88; ISBN-92-835-1563-3) Copyright Avail:

NTIS HC A18/MF A03; Non-NATO Nationals requests available only from AGARD/Scientific Publications Executive

This bibliography presents abstracts and indexes for approximately 1,500 AGARD unclassified publications published during the period 1986 through 1988. Six indexes are included: subject, personal author, corporate source, AGARD Panel, report/accession number, and accession number. Author

N90-16586 California Univ., Berkeley.

NEW OPTIMIZATION TECHNIQUES IN DATABASE ACCESS AND MAINTENANCE Ph.D. Thesis

Jaideep Srivastava 1988 168 p

Avail: Univ. Microfilms Order No. DA8916900

The past two decades have seen the use of computers as information processing devices in applications other than transaction processing. This dissertation focuses on applications which include statistical and scientific analysis, demographic and actuarial studies, planning and forecasting, and market survey and analysis. One way of looking at information is as a hierarchy of views, i.e., windows on the database. Proposed extensions allow new kinds of views, called aggregate views, to be defined in addition to the regular relation model views, or logical views. For aggregate views defined over numeric information, a degree of precision can be attached, which specifies the consistency it has to maintain with the basic data. The problem of dynamic view maintenance, for logical and aggregate view, is modeled analytically, and optimal algorithms are derived. For the case of logical view maintenance, an integrated approach based on both the users' viewpoint, i.e., response time, and system's viewpoint, i.e., throughput, is developed. This approach provides a taxonomy for past research, and solutions that generalize existing ones. From a practical viewpoint, the usefulness of any system depends on its efficiency. This translates to the response time of a user's query. Two ways of reducing response time are discussed. Firstly, a careful look at target applications revealed a class of queries, called aggregate queries, which are a performance bottleneck for existing systems. This leads to the design of a new access method, based on the pre-computation of carefully chosen information, which helps process these queries very rapidly. Secondly, application domain specific knowledge, expressed in terms of integrity constraints, was used during query optimization to produce better execution plans than would be possible otherwise. Dissert. Abstr.

N90-16587# California Univ., Berkeley. Lawrence Berkeley Lab. Computing Science Research and Development Information and Computing Sciences Div.

ABBREVIATED QUERY INTERPRETATION IN EXTENDED ENTITY-RELATIONSHIP ORIENTED DATABASES

Victor M. Markowitz and Arie Shoshani Aug. 1989 29 p Presented at the 8th International Conference on Entity-Relationship Approach, Toronto, Ontario, 18-20 Oct. 1989

(Contract DE-AC03-76SF-00098)

(DE90-003114; LBL-25337; CONF-8910295-1) Avail: NTIS HC A03/MF A01

In order to express database queries, users are often required to understand large, complex database structures. It is important to relax this requirement by allowing users to express concise (abbreviated) queries, so that they can manage with partial, or even no knowledge of the database structure. Abbreviated queries involve only the specification of the objects that are relevant to the users. The main problem with abbreviated queries is to derive the corresponding full queries. A methodology is presented to support the expression of abbreviated queries in Extended Entity-Relationship (EER) oriented relational databases, that is, relational databases whose schemas are translations of EER schemas. In EER-oriented databases, abbreviated queries can be represented by disconnected subgraphs of the corresponding EER diagrams. A criterion is proposed for determining the connected subgraphs corresponding to such abbreviated queries. The criterion is based on the robustness of the relational view corresponding to a connected subgraph of an EER diagram. View robustness expresses the capability of performing side effect free updates via the view. Techniques are also investigated that take advantage of specific properties of EER diagrams in order to reduce the complexity of finding the subgraphs that correspond to a given abbreviated query. DOE

N90-16588# California Univ., Berkeley. Lawrence Berkeley Lab. Computing Science Research and Development Information and Computing Sciences Div.

EVENT-JOIN OPTIMIZATION IN TEMPORAL RELATIONAL DATABASES

Arie Segev and Himawan Gunadhi Jan. 1989 32 p Presented at the 15th International Conference on Very Large Data Bases, Amsterdam, Netherlands, 22-25 Aug. 1989

(Contract DE-AC03-76SF-00098)

(DE90-003117; LBL-26600; CONF-8908116-2) Avail: NTIS HC A03/MF A01

An Event-Join is mostly used to group several temporal attributes of an entity into a single relation. It combines temporal equi-join components into one operation. The temporal outerjoin component is different than a non-temporal outer-join operations. The need to support the efficient processing of event-joins is examined, and several optimization algorithms are introduced, both for a general data organization and for specialized organizations (sorted and append-only databases). For the append-only database, a new data structure, that can improve the performance of event-joins as well as other queries, is introduced. Finally, the performance of the proposed algorithms is evaluated. DOE

N90-16589*# National Aeronautics and Space Administration. Lyndon B. Johnson Space Center, Houston, TX.

JSC DOCUMENT INDEX

Aug. 1988 450 p

(NASA-TM-102923; JSCM-2314-Rev-A; NAS 1.15:102923) Avail: NTIS HC A19/MF A03 CSCL 05B

The Johnson Space Center (JSC) document index is intended to provide a single source listing of all published JSC-numbered documents their authors, and the designated offices of prime responsibility (OPR's) by mail code at the time of publication. The index contains documents which have been received and processed by the JSC Technical Library as of January 13, 1988. Other JSC-numbered documents which are controlled but not available through the JSC Library are also listed. Author

N90-16590# European Space Agency. European Space Research and Technology Center, ESTEC, Noordwijk (Netherlands).

CATALOGUE OF ESA PUBLICATIONS IN 1987

Bruce Battrick, comp. and F. deZwaan, comp. Sep. 1988 53 p

(ESA-SP-1087) Avail: NTIS HC A04/MF A01

This catalogue lists over 270 publications prepared by the ESA Publications Division in the course of 1987. Items are listed by subject area and document type (i.e., special publications, brochures, technical reports and memoranda, standards and specifications, and contractor reports). Author

N90-16591# Los Alamos National Lab., NM. Military Systems Analysis and Simulation Group.

EXPERIENCES WITH KNOWLEDGE-BASE AND LARGE DATABASE INTEGRATION

Christie Michelsen, Donna Smith, and Glenda McGrath 1989 23 p Presented at the Hawaii International Conference on Systems Sciences: Massive Databases and Ill-Defined Objects, Kailua-Kona, HI, 2-5 Jan. 1990

(Contract W-7405-eng-36)

(DE90-000686; LA-UR-89-3244; CONF-900137-1) Avail: NTIS HC A03/MF A01

This paper will discuss the integration of several knowledge-bases (network data structures providing inheritance and rule-base definition/execution) and a large database in the context of a manufacturing simulation. The simulation represents the production activities at numerous facilities and is used to determine if a production schedule can be satisfied. The simulation is supplied with data from a large relational database which includes production facility characteristics as well as piece part information.

The simulation is currently in use with new functionality being incorporated at this time. This paper will also illustrate the problems inherent in loosely-coupled knowledge-base and database data exchanges. DOE

N90-16592# Sandia National Labs., Albuquerque, NM.
DATABASE DESIGN USING NIAM (NIJSSEN INFORMATION ANALYSIS METHOD) MODELING
Norman H. Stevens 1989 15 p Presented at the 6th International Conference on Data Engineering, Los Angeles, CA, 5-9 Feb. 1990
(Contract DE-AC04-76DP-00789)
(DE89-014631; SAND-89-1561C; CONF-900214-1) Avail: NTIS HC A03/MF A01

The Nijssen Information Analysis Method (NIAM) is an information modeling technique based on semantics and founded in set theory. A NIAM information model is a graphical representation of the information requirements for some universe of discourse. Information models facilitate data integration and communication within an organization about data semantics. An information model is sometimes referred to as the semantic model or the conceptual schema. It helps in the logical and physical design and implementation of databases. NIAM information modeling is used at Sandia National Laboratories to design and implement relational databases containing engineering information which meet the users' information requirements. The paper focuses on the design of one database which satisfied the data needs of four disjoint but closely related applications. The applications as they existed before did not talk to each other even though they stored much of the same data redundantly. NIAM was used to determine the information requirements and design the integrated database. DOE

N90-16593# Department of Energy, Washington, DC. Office of Organization and Management Systems.
FY 1989 UPDATE TO THE INFORMATION RESOURCES MANAGEMENT REVIEW PLAN Report, FY 1989 - FY 1991
Nov. 1989 125 p
(DE90-004185; DOE/MA-0364) Avail: NTIS HC A06/MF A01

The Federal Information Resources Management (IRM) Review Program was initiated in fiscal year (FY) 1986 to ensure that federal agencies' IRM activities are selectively reviewed at least once during a triennial review cycle. This requirement is satisfied predominantly by agency-conducted reviews, the primary purpose being to improve the management of information resources so that the agency can accomplish its missions more efficiently and effectively. The Department's first triennial cycle covered the period FY 1986 to FY 1988. The current cycle covers the period FY 1989 to 1991. IRM reviews may encompass any or all activities of planning, budgeting, organizing, directing, training, and control associated with the creation, collection, processing, transmission, dissemination, use, storage, and disposition of information by agencies. Agencies have been encouraged to take advantage of all ongoing review activity in the IRM area, such as reviews preparing for or resulting from the Office of Management and Budget spring planning and management reviews and/or fall budget reviews; vulnerability assessments and internal control reviews; financial management systems reviews; performance of commercial activity reviews; privacy and security reviews; information collection reviews; records management assessments; and internal audits, among others. DOE

83 ECONOMICS AND COST ANALYSIS

Includes cost effectiveness studies.

No abstracts in this category.

84 LAW, POLITICAL SCIENCE AND SPACE POLICY

Includes NASA appropriation hearings; aviation law; space law and policy; international law; international cooperation; and patent policy.

No abstracts in this category.

85 URBAN TECHNOLOGY AND TRANSPORTATION

Includes applications of space technology to urban problems; technology transfer; technology assessment; and surface and mass transportation.

For related information see also *03 Air Transportation and Safety, 16 Space Transportation,* and *44 Energy Production and Conversion.*

N90-16594# West Virginia Univ., Morgantown. Dept. of Mechanical and Aerospace Engineering.
ESTABLISHMENT OF THE INNOVATIVE TECHNOLOGY UTILIZATION CENTER AT WEST VIRGINIA UNIVERSITY Final Report, 1 Jan. - 31 Dec. 1988
Emil Steinhardt 20 Mar. 1989 70 p Sponsored by Appalachian Regional Commission, Washington, DC
(Contract ARC-87-86/CO-9684)
(PB90-114711) Avail: NTIS HC A04/MF A01 CSCL 05A

An Innovative Technology Utilization Center was established at the College of Engineering at West Virginia University. The center is to serve as a demonstration that a bond can be established between industries and a college of engineering. The center's establishment and first year of operation is described. Author

88 SPACE SCIENCES (GENERAL)

N90-16595# Defence Science and Technology Organization, Salisbury (Australia).
SCIENTIFIC INVESTIGATIONS OF THE SPACE RESEARCH GROUP
J. S. Gubbay and K. J. W. Lynn 1989 45 p
(ISBN-0-642-13252-6) Avail: NTIS HC A03/MF A01

The origin and charter of the Space Research Group of the American Projects Division is presented. Some of the achievements of the Very Long Base Interferometer (VLBI) team is traced through the deployment of outstanding personnel and facilities to which it had access. The pioneering work in charting the higher regions of the ionosphere to define features and trace progress over time are examined. The potential of the resources within the American Projects Division to determine VLF propagation characteristics are discussed. B.G.

89 ASTRONOMY

Includes radio, gamma-ray, and infrared astronomy, and astrometry.

N90-16596*# National Aeronautics and Space Administration, Washington, DC.
REPORTS OF PLANETARY ASTRONOMY, 1986
Aug. 1987 129 p
(NASA-TM-100776; NAS 1.15:100776) Avail: NTIS HC A07/MF A01 CSCL 03A

A compilation of abstracts of reports from Principal Investigators

funded through NASA's Planetary Astronomy Program, Office of Space Science and Applications, is presented. The purpose is to provide a document which succinctly summarizes work conducted in this program for 1986. Each report contains a brief statement on the strategy of investigation and lists significant accomplishments within the area of the author's funded grant or contract, plans for future work, and publications. Author

N90-16597 Leicester Univ. (England).
GALACTIC X RAY ASTRONOMY WITH EXOSAT Ph.D. Thesis
Andrew John Norton 1988 219 p
Avail: Univ. Microfilms Order No. BRD-86046

The results of two separate studies of Galactic x ray sources made with EXOSAT are presented. Both studies are in the form of surveys, the first being a survey of the class of cataclysmic variable stars known as Intermediate Polars and the second being a survey of the ray emission from the Galactic Plane, in the form of scanning and pointed observations. The EXOSAT observatory and the methods of data analysis which were used are described. The results of the Intermediate Polar study and the relevant background information and theoretical models are described. The set of observations used and the analytical results obtained from the x ray light curves and spectra are presented. The results are discussed and interpreted in terms of a model for the accretion process. Comparisons are made between the properties of Polars and Intermediate Polars based on the results derived here and the differences are explained in terms of the model presented. The results of the scanning observations are given. Also given are the results of 7 pointed observations made at some of the unknown sources detected in the Galactic Plane map. Future prospects for x ray astronomy are considered by discussing some of the missions which are planned for launch before the end of the century. Consideration is given to how the understanding of the galactic sources discussed here may be improved, as a result of these missions. Dissert. Abstr.

N90-16598# Los Alamos National Lab., NM. Theoretical Div.
PULSATIONS OF DELTA SCUTI STARS
Arthur N. Cox 1989 30 p Presented at the 5th Workshop in Nonlinear Astronomy: Nonlinear Astrophysical Fluid Dynamics, Gainesville, FL, 5-7 Oct. 1989
(Contract W-7405-eng-36)
(DE90-003213; LA-UR-89-3772; CONF-8910308-1) Avail: NTIS HC A03/MF A01

A general review of the pulsating delta Scuti variables is given including the observed light curves and positions of the stars in the Hertzsprung-Russell diagram. Theoretical interpretations from evolution and pulsation calculations give their masses, radii, luminosities, and even their approximate internal compositions. Three models of these stars are discussed and used to study the nonlinear hydrodynamic behavior of these stars. The hydrodynamic equations and the Stellingwerf method for obtaining strictly periodic solutions are outlined. Problems of allowing for time-dependent convection and its great sensitivity to temperature and density are presented. Tentative results to date do not show any tendency for amplitudes to grow to large unobserved amplitudes, in disagreement with an earlier suggestion by Stellingwerf. It is found that the very small growth rates of the pulsations may even be too small to be useful in seeking a periodic solution. DOE

N90-16599# Lockheed Aircraft Corp., Palo Alto, CA. Research Lab.
X RAY SPECTROPHOTOMETRIC REMOTE SENSING OF DIFFUSE AURORAL IONIZATION
R. R. Vondrak, R. M. Robinson, P. F. Mizera, and D. J. Gorney (Aerospace Corp., El Segundo, CA.) 20 Mar. 1989 24 p
(Contract F04701-85-C-0086)
(SD-TR-89-09; TR-0088(3940-06)-3) Avail: NTIS HC A03/MF A01

Auroral electron precipitation produces both E region ionization and bremsstrahlung x rays. In a set of coordinated observations, these atmospheric effects of electron precipitation were measured simultaneously by the x ray sensor on the DMSP/F2 spacecraft and by the incoherent scatter radar at Chatanika, Alaska. In all data sets there was good agreement between the locations of the x ray source regions and the regions of enhanced E region ionization. Detailed comparisons were made between the measured and derived altitude profiles of ionization for two auroral conditions, a premidnight auroral band and a sunlit diffuse aurora. These comparisons validate the ability to derive auroral ionization from satellite-based x ray measurements. Author

N90-16600# Los Alamos National Lab., NM.
A LOW-THRESHOLD EAS (EXTENSIVE-AIR-SHOWER) ARRAY FOR GAMMA-RAY ASTRONOMY AT LOS ALAMOS
R. L. Burman, C. M. Hoffman, D. E. Nagle, M. E. Potter, V. Sandberg, D. Berley, B. L. Dingus, J. A. Goodman, T. J. Haines, and M. Stark (Maryland Univ., College Park.) et al 1990 6 p Presented at the 21st International Cosmis Ray Conference, Adelaide, Australia, 6-19 Jan. 1990 Prepared in cooperation with George Mason Univ., Fairfax, VA; California Univ., Irvine; California Univ., Riverside; Argonne National Lab., IL and Iowa State Univ. of Science and Tech., Ames
(Contract W-7405-eng-36)
(DE89-016780; LA-UR-89-2971; CONF-900122-1) Avail: NTIS HC A02/MF A01

A new type of extensive-air-shower (EAS) array is described that achieves a low energy threshold, large area, high duty factor and large muon coverage. By placing a regularly-spaced grid of phototubes just below the surface of a shallow pond, the Cherenkov light of particles in an air shower striking the water can be detected, resulting in a primary energy threshold of less than 1 TeV. This highly sensitive array can thus be used to span the gap of information between the existing air Cherenkov techniques at 1 TeV and the existing EAS arrays at 100 TeV. DOE

N90-16601# Los Alamos National Lab., NM.
STATUS OF THE EXPANSION OF THE CYGNUS ARRAY AT LOS ALAMOS
D. Berley, C. Y. Chang, B. L. Dingus, J. A. Goodman, T. J. Haines, M. Stark (Maryland Univ., College Park.), R. L. Burman, D. R. Cady, C. M. Hoffman, and J. Lloyd-Evans et al 1989 5 p Presented at the 21st International Cosmic Ray Conference, Adelaide, Australia, 6-19 Jan. 1990 Prepared in cooperation with California Univ., Irvine and George Mason Univ., Fairfax, VA
(Contract W-7405-eng-36)
(DE89-016781; LA-UR-89-2970; CONF-900122-2) Avail: NTIS HC A01/MF A01

The CYGNUS air shower array, located in Los Alamos, New Mexico, has been operating since April, 1986. The expansion of the array from 108 to 200 counters is described along with the increase in muon detection area. The new array, to be fully operational by the end of 1989, will have three times the sensitivity to UHE sources. DOE

N90-16602# Geneva Observatory (Switzerland).
THE UPPER MAIN SEQUENCE OF OB ASSOCIATIONS. PART 2: THE SINGLE-LINED O STARS: SPECTRAL CLASSIFICATION OF NORTHERN STARS AND LINES OF C AND N
G. Mathys 1989 21 p Submitted for publication
(Ser-C-Prepubl-Fasc-39; ETN-90-96150) Avail: NTIS HC A03/MF A01

The properties of the steps close to the upper main sequence of OB associations are studied. The aim of the work is to provide constraints on the theory of evolution of massive stars. In the present work, the spectral classification of northern single-lined O stars, most of them belonging to the associations Cyg OB1, Per OB1 and Cas OB6, is presented. The classification is performed according to Conti's classification scheme for O stars. The new classificatin criteria are discussed and refined. The behavior of the C and N lines of the stars classified is studied, in order to determine whether CNO-processed material is visible at their surface. Three new ON stars are discovered. Nine ON stars and 25 other stars showing some morphological N enhancement are discussed. ESA

N90-16603# Consiglio Nazionale delle Ricerche, Frascati (Italy). Inst. di Fisica dello Spazio Interplanetario.
SHORT TIME SCALE VARIABILITY OF THE BL LAC OBJECT OJ 287 IN THE NEAR-INFRARED
D. Lorenzetti, E. Massaro, G. C. Perola (Rome Univ., Italy), and L. Spinoglio Jan. 1989 27 p Previously announced in IAA as A90-12681 Submitted for publication Sponsored by the Italian Ministry of Public Education
(IFSI-89-3; ETN-90-96165) Avail: NTIS HC A03/MF A01

The results of a near infrared photometric monitoring of the BL Lacertae object OJ 287 are presented. The standard photometry of the J, H and K bands shows variability of maximum amplitude about 0.7 mag over the entire observing period of 23 months and about 0.3 mag on time intervals as short as 3 hours. No spectral variability is found. A fast monitoring performed in the H band, with a sampling period of approximately 4 minutes, provides evidence that variations can occur in this object. These variations show slow increasing and fast decreasing trends, but no clear indication of periodicity is available. ESA

N90-16604# Max-Planck-Inst. fuer Physik und Astrophysik, Garching (Germany, F.R.). Inst. fuer Extraterrestrische Physik.
ON THE INTERACTION OF A PULSAR WITH THE AMBIENT MEDIUM UTILIZING X RAY IMAGES OF THE CRAB NEBULA Thesis
Thomas Bork Aug. 1989 189 p Original contains color illustrations
(MPE-Rept-215; ISSN-0178-0719; ETN-90-96179) Copyright Avail: NTIS HC A09/MF A02

The measured soft x ray brightness of Crab nebula and simulated data are compared. The aim is a better understanding of the conversion of the Crab pulsar's rotational energy into synchrotron radiation. The soft x ray data obtained in 1979 by the high resolution imager on the Einstein observatory is compared with the brightness distribution of a three dimensional model, based on theoretical concepts developed by Rees and Gunn in 1974 and by Aschenbach and Brinkmann in 1975. ESA

N90-16605 Max-Planck-Inst. fuer Physik und Astrophysik, Garching (Germany, F.R.). Inst. fuer Extraterrestrische Physik.
AN ATLAS OF APERIODIC VARIABILITY IN HMXB
T. Belloni and G. Hasinger Aug. 1989 52 p Submitted for publication Sponsored by the Della Riccia Foundations
(MPE-Preprint-158; ETN-90-96047) Copyright Avail: Fachinformationszentrum Karlsruhe, 7514 Eggenstein-Leopoldshafen 2, Fed. Republic of Germany

Broadband power spectra and color-color diagrams made from EXOSAT archive data of 14 x ray binaries are discussed. The aperiodic (noise) variability of the sources is studied. All the x ray pulsars present in the sample show strong noise components in their emission, with a fractional variability between 20 and 30 percent. The power spectrum of each of the pulsars is investigated individually. Twelve are High Mass X ray Binaries (HMXB) and two are Low Mass X ray Binaries (LMXB). Correlations between the variations and other characteristics of the sources are analyzed. ESA

N90-16606 Max-Planck-Inst. fuer Physik und Astrophysik, Garching (Germany, F.R.). Inst. fuer Extraterrestrische Physik.
RECENT AND FUTURE X RAY OBSERVATIONS OF CLASSICAL NOVAE DURING THE OUTBURST STAGE
Hakki Oegelman Sep. 1989 10 p Submitted for publication
(MPE-Preprint-159; ETN-90-96048) Copyright Avail: Fachinformationszentrum Karlsruhe, 7514 Eggenstein-Leopoldshafen 2, Fed. Republic of Germany

Difficulties inherent in soft x ray detection of classical novae during outburst is described. The advent of spaceborne focusing telescopes has eliminated some of these difficulties although x ray absorbtion by cold interstellar gas remains a problem. Observations of three of the brightest novae whose outburst stage coincided with the lifetime of the EXOSAT satellite are described. A graph presenting the thin Lexan counting rates for the three novae as a function of elapsed time since optical maximum is provided. How these x ray observations will contribute to better understanding novae phenomena is discussed. ESA

90 ASTROPHYSICS

Includes cosmology; celestial mechanics; space plasmas; and interstellar and interplanetary gases and dust.
For related information see also *75 Plasma Physics*.

N90-16607*# Lunar and Planetary Inst., Houston, TX.
WORKSHOP ON ANALYSIS OF RETURNED COMET NUCLEUS SAMPLES
1989 98 p Workshop held in Milpitas, CA, 16-18 Jan. 1989; sponsored by Lunar and Planetary Inst., Houston, TX and NASA, Ames Research Center, Moffett Field, CA
(Contract NASw-4066)
(NASA-CR-184821; NAS 1.26:184821; LPI-Contrib-691) Avail: NTIS HC A05/MF A01 CSCL 03B

This volume contains abstracts that were accepted by the Program Committee for presentation at the workshop on the analysis of returned comet nucleus samples held in Milpitas, California, January 16 to 18, 1989. The abstracts deal with the nature of cometary ices, cryogenic handling and sampling equipment, origin and composition of samples, and spectroscopic, thermal and chemical processing methods of cometary nuclei. Laboratory simulation experimental results on dust samples are reported. Some results obtained from Halley's comet are also included. Microanalytic techniques for examining trace elements of cometary particles, synchrotron x ray fluorescence and instrument neutron activation analysis (INAA), are presented. For individual titles, see N90-16608 through N90-16656.

N90-16608*# California Inst. of Tech., Pasadena.
ANALYTICAL STUDY OF COMET NUCLEUS SAMPLES
A. L. Albee *In* Lunar and Planetary Inst., Workshop on Analysis of Returned Comet Nucleus Samples 1989 p 1-2 (For primary document see N90-16607 08-90)
Avail: NTIS HC A05/MF A01 CSCL 03B

Analytical procedures for studying and handling frozen (130 K) core samples of comet nuclei are discussed. These methods include neutron activation analysis, x ray fluorescent analysis and high resolution mass spectroscopy. K.C.D.

N90-16609*# National Aeronautics and Space Administration. Ames Research Center, Moffett Field, CA.
THE ORIGIN, COMPOSITION AND HISTORY OF COMETARY ICES FROM SPECTROSCOPIC STUDIES
L. J. Allamandola *In* Lunar and Planetary Inst., Workshop on Analysis of Returned Comet Nucleus Samples 1989 p 3-4 (For primary document see N90-16607 08-90)
Avail: NTIS HC A05/MF A01 CSCL 03B

The spectroscopic analysis of pristine cometary material provides a very important probe of the chemical identity of the material as well as of the physical and chemical conditions which prevailed during the comet's history. Concerning classical spectroscopy, the spectral regions which will most likely prove most useful are the infrared, the visible and ultraviolet. Newer spectroscopic techniques which have the potential to provide equally important information include nuclear magnetic resonance (NMR) and electron spin resonance (ESR). Each technique is summarized with emphasis placed on the kind of information which can be obtained. Author

N90-16610*# Tel-Aviv Univ. (Israel). Dept. of Geophysics and Planetary Sciences.
EXPERIMENTAL STUDIES OF GAS TRAPPING IN AMORPHOUS ICE AND THERMAL MODELLING OF COMETS: IMPLICATIONS FOR ROSETTA
Akiva Bar-Nun *In* Lunar and Planetary Inst., Workshop on Analysis of Returned Comet Nucleus Samples 1989 p 5-7 (For

primary document see N90-16607 08-90)
Avail: NTIS HC A05/MF A01 CSCL 03B

The trapping of mixtures of CO, CH4, N2 and Ar in amorphous water ice was studied experimentally. It is shown that the ice particles could not have been formed at a higher temperature and, subsequently, cool down. Experiments where ice was deposited at elevated temperatures, then cooled down and gas was flowed into the ice, showed that the amount of trapped gas depends only on the highest temperature at which the ice was formed, or resided, prior to cooling and gas flow into it. Consequently, the cometary ice had to be formed at approx. 48 K and the ice is therefore amorphous. The thermal profile of a comet in Halley's orbit was calculated, including the build-up of an insulating dust layer. It was found that an insulating dust layer a few cm thick is enough to choke most of the water emission from the surface. A similar thermal model was calculated for comet P/Temple-1, a candidate for both CRAF and Rosetta (CNSR) missions. The temperature at a depth of 10 m is approx. 160 K for all models considered and, hence, the ice at this depth is crystalline. A crystalline ice layer 40 to 240 m thick was found to overly the gas-laden amorphous ice. Consequently, it should be difficult for the probes of the two comet missions to sample pristine amorphous ice, unless they are aimed at the bottom of an active crater. Author

N90-16611*# Max-Planck-Inst. fuer Chemie, Mainz (Germany, F.R.).
ON THE ISOTOPE ANALYSIS OF COMETARY DUST Abstract Only
Friedrich Begemann *In* Lunar and Planetary Inst., Workshop on Analysis of Returned Comet Nucleus Samples 1989 p 8 (For primary document see N90-16607 08-90)
Avail: NTIS HC A05/MF A01 CSCL 03B

It is thought that comets are an intimate mixture of ices and sub-micron to pebble sized silicates. Based on experience with carbonaceous chrondrites, part of the smallest grains are expected to be primary condensates carrying the unadulterated isotopic signature of their place of origin. In order to extract this information a grain-by-grain analysis will be necessary. Author

N90-16612*# National Aeronautics and Space Administration. Ames Research Center, Moffett Field, CA.
DIRECT DETERMINATION OF THE MORPHOLOGY, STRUCTURE AND COMPOSITION OF COMETARY AND INTERSTELLAR ICE ANALOGS IN THE LABORATORY Abstract Only
D. F. Blake and L. J. Allamandola *In* Lunar and Planetary Inst., Workshop on Analysis of Returned Comet Nucleus Samples 1989 p 9-10 (For primary document see N90-16607 08-90)
Avail: NTIS HC A05/MF A01 CSCL 03B

Ices of various kinds (H2O, CO, CO2, CH4, NH3, CH3OH, etc.) comprise a volumetrically significant proportion of objects in the solar system (comets, outer planets, planetary rings, satellites) as well as in interstellar space (astrophysical ices). The refinement of analytical electron microscopy (AEM) procedures for storing, preparing and analyzing ices and other materials at cryogenic temperatures is discussed. These procedures will be essential to the successful analysis of returned comet nucleus samples. Author

N90-16613*# McCrone Associates, Inc., Westmont, IL.
ELECTRON BEAM ANALYSIS OF PARTICULATE COMETARY MATERIAL Abstract Only
John Bradley *In* Lunar and Planetary Inst., Workshop on Analysis of Returned Comet Nucleus Samples 1989 p 11 (For primary document see N90-16607 08-90)
Avail: NTIS HC A05/MF A01 CSCL 03B

Electron microscopy will be useful for characterization of inorganic dust grains in returned comet nucleus samples. The choice of instrument(s) will depend primarily on the nature of the samples, but ultimately a variety of electron-beam methods could be employed. Scanning and analytical (transmission) electron microscopy are the logical choise for morphological, mineralogical, and bulk chemical analyses of dust grains removed from ices. It may also be possible to examine unmelted ice/dust mixtures using an environmental scanning electron microscope equipped with a cryo-transfer unit and a cold stage. Electron microscopic observations of comet nuclei might include: (1) porosities of dust grains; (2) morphologies and microstructures of individual mineral grains; (3) relative abundances of olivine, pyroxene, and glass; and (4) the presence of phases that might have resulted from aqueous alteration (layer silicates, carbonates, sulfates). Author

N90-16614*# Science Applications International Corp., La Jolla, CA. Planetary Science Inst.
THERMAL AND CHEMICAL PROCESSING OF THE OUTERMOST LAYER OF COMETARY NUCLEI Abstract Only
Humberto Campins and E. Philip Krider (Arizona Univ., Tucson.) *In* Lunar and Planetary Inst., Workshop on Analysis of Returned Comet Nucleus Samples 1989 p 12 (For primary document see N90-16607 08-90)
Avail: NTIS HC A05/MF A01 CSCL 03B

A non-equilibrium mechanism that may produce substantial thermal and chemical processing of the outermost layer of cometary nuclei is proposed. If this phenomenon does occur, its effects will impact the interpretation of results from the CNSR and CRAF missions. Author

N90-16615*# National Aeronautics and Space Administration. Ames Research Center, Moffett Field, CA.
THE CARBON CHEMISTRY OF METEORITES: RELATIONSHIPS TO COMETS
S. Chang *In* Lunar and Planetary Inst., Workshop on Analysis of Returned Comet Nucleus Samples 1989 p 13-14 (For primary document see N90-16607 08-90)
Avail: NTIS HC A05/MF A01 CSCL 03B

The carbonaceous meteorites exhibiting alteration by liquid water bear a strong relationship to comets. Not only is their elemental composition closer to solar in relative abundances than other meteorites, they are water rich; and they contain isotopic compositions among refractory and volatile elements indicative of presolar components. Some of these isotopic anomalies occur in organic compounds and carbonaceous grains signifying the presence of discrete and identifiable carbon components derived from interstellar and circumstellar matter. Insofar as comets and meteorites are ultimately formed from interstellar gas and dust, and comets have been subjected to considerably less aqueous and thermal evolution than carbonaceous meteorites, the interstellar imprint should be much stronger and better preserved in comets. Author

N90-16616*# European Space Agency. European Space Research and Technology Center, ESTEC, Noordwijk (Netherlands). Space Science Dept.
LABORATORY ANALYSES OF MICRON-SIZED SOLID GRAINS: EXPERIMENTAL TECHNIQUES AND RECENT RESULTS Abstract Only
L. Colangeli, E. Bussoletti, A. Blanco, A. Borghesi, S. Fonti, V. Orofino (Lecce Univ., Italy), and G. Schwehm *In* Lunar and Planetary Inst., Workshop on Analysis of Returned Comet Nucleus Samples 1989 p 15 (For primary document see N90-16607 08-90)
Avail: NTIS HC A05/MF A01 CSCL 03B

Morphological and spectrophotometric investigations have been extensively applied in the past years to various kinds of micron and/or submicron-sized grains formed by materials which are candidate to be present in space. The samples are produced in the laboratory and then characterized in their physio-chemical properties. Some of the most recent results obtained on various kinds of carbonaceous materials are reported. Main attention is devoted to spectroscopic results in the VUV and IR wavelength ranges, where many of the analyzed samples show typical fingerprints which can be identified also in astrophysical and cometary materials. The laboratory methodologies used so far are also critically discussed in order to point out capabilities and present limitations, in the view of possible application to returned comet

samples. Suggestions are given to develop new techniques which should overcome some of the problems faced in the manipulation and analysis of micron solid samples. Author

N90-16617*# Arizona State Univ., Tempe. Dept. of Chemistry.
ANALYSIS OF ORGANIC COMPOUNDS IN RETURNED COMET NUCLEUS SAMPLES
J. R. Cronin *In* Lunar and Planetary Inst., Workshop on Analysis of Returned Comet Nucleus Samples 1989 p 16-17 (For primary document see N90-16607 08-90)
Avail: NTIS HC A05/MF A01 CSCL 03B

Techniques for analysis of organic compounds in returned comet nucleus samples are described. Interstellar, chondritic and transitional organic components are discussed. Appropriate sampling procedures will be essential to the success of these analyses. It will be necessary to return samples that represent all the various regimes found in the nucleus, e.g., a complete core, volatile components (deep interior), and crustal components (surface minerals, rocks, processed organics such as macromolecular carbon and polymers). Furthermore, sampling, storage, return, and distribution of samples must be done under conditions that preclude contamination of the samples by terrestrial matter. Author

N90-16618*# Massachusetts Inst. of Tech., Cambridge. Dept. of Earth, Atmospheric and Planetary Sciences.
NON-EQUILIBRIUM CHEMISTRY IN THE SOLAR NEBULA AND EARLY SOLAR SYSTEM: IMPLICATIONS FOR THE CHEMISTRY OF COMETS
Bruce Fegley, Jr. *In* Lunar and Planetary Inst., Workshop on Analysis of Returned Comet Nucleus Samples 1989 p 18-19 (For primary document see N90-16607 08-90)
Avail: NTIS HC A05/MF A01 CSCL 03B

Theoretical models of solar nebula and early solar system chemistry which take into account the interplay between chemical, physical, and dynamical processes have great utility for deciphering the origin and evolution of the abundant chemically reactive volatiles (H, O, C, N, S) observed in comets. In particular, such models are essential for attempting to distinguish between presolar and solar nebula products and for quantifying the nature and duration of nebular and early solar system processing to which the volatile constituents of comets have been subjected. The diverse processes and energy sources responsible for chemical processing in the solar nebula and early solar system are discussed. The processes considered include homogeneous and heterogeneous thermochemical and photochemical reactions, and disequilibration resulting from fluid transport, condensation, and cooling whenever they occur on timescales shorter than those for chemical reactions. Author

N90-16619*# State Univ. of New York, Plattsburgh. Dept. of Physics.
TRACE ELEMENT ABUNDANCE DETERMINATIONS BY SYNCHROTRON X RAY FLUORESCENCE (SXRF) ON RETURNED COMET NUCLEUS MINERAL GRAINS
G. J. Flynn and S. R. Sutton (Brookhaven National Lab., Upton, NY.) *In* Lunar and Planetary Inst., Workshop on Analysis of Returned Comet Nucleus Samples 1989 p 20-21 (For primary document see N90-16607 08-90)
Avail: NTIS HC A05/MF A01 CSCL 03B

Trace element analyses were performed on bulk cosmic dust particles by Proton Induced X Ray Emission (PIXE) and Synchrotron X Ray Fluorescence (SXRF). When present at or near chondritic abundances the trace elements K, Ti, Cr, Mn, Cu, Zn, Ga, Ge, Se, and Br are presently detectable by SXRF in particles of 20 micron diameter. Improvements to the SXRF analysis facility at the National Synchrotron Light Source presently underway should increase the range of detectable elements and permit the analysis of smaller samples. In addition the Advanced Photon Source will be commissioned at Argonne National Laboratory in 1995. This 7 to 8 GeV positron storage ring, specifically designed for high-energy undulator and wiggler insertion devices, will be an ideal source for an x ray microprobe with one micron spatial resolution and better than 100 ppb elemental sensitivity for most elements. Thus trace element analysis of individual micron-sized grains should be possible by the time of the comet nucleus sample return mission. Author

N90-16620*# Leiden Univ. (Netherlands).
FROM INTERSTELLAR DUST TO COMETS
J. M. Greenberg *In* Lunar and Planetary Inst., Workshop on Analysis of Returned Comet Nucleus Samples 1989 p 22-23 (For primary document see N90-16607 08-90)
Avail: NTIS HC A05/MF A01 CSCL 03B

The bulk and microstructure of comet nuclei are derived from the morphological structure and chemical composition of submicron sized interstellar dust grains which have undergone cold aggregation in the pre-solar nebula. The evolutionary picture of dust which is emerging is a cyclic one in which the particles, before being destroyed or going into solar system bodies, find themselves during their 5 billion year lifetime alternately in diffuse clouds and in molecular clouds. A small silicate core captured within a molecular cloud accretes various ices and gradually builds up an inner mantle of organic refractory material which has been produced by photoprocessing of the volatile ices. Clumps of grains form, and then clumps of clumps, and so on, until finally we reach the size of the comet nucleus. Author

N90-16621*# Max-Planck-Inst. fuer Kernphysik, Heidelberg (Germany, F.R.).
MODIFICATIONS OF COMET MATERIALS BY THE SUBLIMATION PROCESS: RESULTS FROM SIMULATION EXPERIMENTS
E. Gruen, Akiva Bar-Nun, P. Lammerzahl, J. Klinger, H. Kochan, H. U. Keller, G. Neukum, K. Roessler, D. Stoeffler, and T. Spohn (Muenster Univ., Germany, F.R.) et al *In* Lunar and Planetary Inst., Workshop on Analysis of Returned Comet Nucleus Samples 1989 p 24-25 Prepared in cooperation with Cologne Univ., Fed. Republic of Germany (For primary document see N90-16607 08-90)
Avail: NTIS HC A05/MF A01 CSCL 03B

An active comet like comet Halley loses by sublimation a surface layer of the order of 1 m thickness per perihelion passage. In situ measurements show that water ice is the main constituent which contributes to the gas emission although even more volatile species (CO, NH3, CH4, CO2 etc.) have been identified. Dust particles which were embedded in the ices are carried by the sublimating gases. Measurements of the chemical composition of cometary grains indicate that they are composed of silicates of approximate chondritic composition and refractory carbonaceous material. Comet simulation experiments show that significant modifications of cometary materials occur due to sublimation process in near surface layers which have to be taken into account in order to derive the original state of the material. Author

N90-16622*# Planetary Science Inst., Tucson, AZ.
COMMENTS ON COMET SHAPES AND AGGREGATION PROCESSES
William K. Hartmann *In* Lunar and Planetary Inst., Workshop on Analysis of Returned Comet Nucleus Samples 1989 p 26-27 (For primary document see N90-16607 08-90)
Avail: NTIS HC A05/MF A01 CSCL 03B

An important question for a comet mission is whether comet nuclei preserve information clarifying aggregation processes of planetary matter. New observational evidence shows that Trojan asteroids, as a group, display a higher fraction of highly-elongated objects than the belt. More recently evidence has accumulated that comet nuclei, as a group, also display highly-elongated shapes at macro-scale. This evidence comes from the several comets whose nuclear lightcurves or shapes have been well studied. Trojans and comet nuclei share other properties. Both groups have extremely low albedos and reddish-to neutral-black colors typical of asteroids of spectral class D, P, and C. Both groups may have had relatively low collision frequencies. An important problem to resolve with spacecraft imaging is whether these elongated shapes are primordial, or due to evolution of the objects.

Two hypotheses that might be tested by a combination of global-scale and close-up imaging from various directions are: (1) The irregular shapes are primordial and related to the fact that these bodies have had lower collision frequencies than belt asteroids; or (2) The irregular shapes may be due to volatile loss. Author

N90-16623*# Rutgers Univ., New Brunswick, NJ. Dept. of Chemistry.
COSMOGENIC NUCLIDES IN COMETARY MATERIALS: IMPLICATIONS FOR RATE OF MASS LOSS AND EXPOSURE HISTORY
G. F. Herzog, P. A. J. Englert, and R. C. Reedy (Los Alamos National Lab., NM.) *In* Lunar and Planetary Inst., Workshop on Analysis of Returned Comet Nucleus Samples 1989 p 28-29 (For primary document see N90-16607 08-90)
Avail: NTIS HC A05/MF A01 CSCL 03B

As planned, the Rosetta mission will return to earth with a 10-kg core and a 1-kg surface sample from a comet. The selection of a comet with low current activity will maximize the chance of obtaining material altered as little as possible. Current temperature and level of activity, however, may not reliably indicate previous values. Fortunately, from measurements of the cosmogenic nuclide contents of cometary material, one may estimate a rate of mass loss in the past and perhaps learn something about the exposure history of the comet. Perhaps the simplest way to estimate the rate of mass loss is to compare the total inventories of several long-lived cosmogenic radionuclides with the values expected on the basis of model calculations. Although model calculations have become steadily more reliable, application to bodies with the composition of comets will require some extension beyond the normal range of use. In particular, the influence of light elements on the secondary particle cascade will need study, in part through laboratory irradiations of volatile-rich materials. In the analysis of cometary data, it would be valuable to test calculations against measurements of short-lived isotopes. Author

N90-16624*# Southwest Research Inst., San Antonio, TX.
MORPHOLOGY AND COMPOSITIONAL DIFFERENTIATION OF THE SURFACE OF COMETS Abstract Only
W. F. Huebner and D. C. Boice *In* Lunar and Planetary Inst., Workshop on Analysis of Returned Comet Nucleus Samples 1989 p 30 (For primary document see N90-16607 08-90)
Avail: NTIS HC A05/MF A01 CSCL 03B

The spacecraft missions to Comet Halley gave us the first detailed view of a comet nucleus. What was suspected before, that the nucleus surface was heterogeneous, was confirmed. The Halley Multicolor Camera aboard Giotto recorded jet-like dust features emanating from active regions covering approximately 15 percent of the surface that were responsible for emitting most of the dust and gas. An intensity gradient across the nucleus originating at the active areas and falling off to the darker, inactive region on the night side is caused by small particles that are more easily entrained by surface winds than larger particles that tend to remain in the jets. Data from the PIA (Giotto) and PUMA (Vega 1,2) instruments indicate that the smallest dust particles are enriched with organics (CHON particles). Some of this fine dust gravitationally settles creating a thin surface layer rich in organics. Particularly strong dust jets may cause wind-blown surface structures over inactive areas, such as, leeward dust accumulation behind hills. At close heliocentric distances the fine dust may be sintered on the surface. Author

N90-16625*# Academy of Sciences of the Tajik SSR, Doushanbe. Inst. of Astrophysics.
ROLE OF DUST TO GAS PRODUCTION RATE RATIO IN COMETARY PHYSICS Abstract Only
S. Ibadov *In* Lunar and Planetary Inst., Workshop on Analysis of Returned Comet Nucleus Samples 1989 p 31 (For primary document see N90-16607 08-90)
Avail: NTIS HC A05/MF A01 CSCL 03B

According to results of Earth based observations and in situ measurements cometary nuclei are intensive sources of both the gaseous and the dusty matter. Investigations of the interaction between gas-dust cometary atmospheres and dust grains of the Zodiacal dust cloud reveals the presence of two principally possible mechanisms: meteor-like and explosive-type ones. The meteor-like mechanism is connected with bombardment of zodiacal dust particles by cometary molecules when the temperatures T = 2000 to 3000 K are developed. This mechanism can create over-saturated vapors of refractory elements (Fe, Si, C etc.) in cometary heads. The explosion-type mechanism is connected with high-velocity impacts between cometary and zodiacal dust particles resulting in the generation of high-temperature plasma (T = 10(exp 5) to 10(exp 7) K) and, hence, of x ray radiation and multicharged ions, i.e., with the processes not yet realized in the laboratory conditions. Author

N90-16626*# Virginia Univ., Charlottesville.
RADIATION MODIFICATION OF COMETARY MATERIALS: LABORATORY SIMULATIONS Abstract Only
R. E. Johnson *In* Lunar and Planetary Inst., Workshop on Analysis of Returned Comet Nucleus Samples 1989 p 32 (For primary document see N90-16607 08-90)
Avail: NTIS HC A05/MF A01 CSCL 03B

Cosmic rays and solar photons can modify precometary materials, comet surfaces, and ejected cometary materials. This can be of importance for describing the primordial crust of a comet, the composition of the ejected dust, and the degradation of the dust in the solar environment. The laboratory results of interest to radiation modification of materials, the effects of radiation on cometary materials and the relevance of these materials for comet surface analysis, are described. Author

N90-16627*# Maryland Univ., College Park.
SULFUR COMPOUNDS IN COMETS Abstract Only
S. Kim and M. AHearn *In* Lunar and Planetary Inst., Workshop on Analysis of Returned Comet Nucleus Samples 1989 p 33-34 (For primary document see N90-16607 08-90)
Avail: NTIS HC A05/MF A01 CSCL 03B

Cometary atmospheres exhibit abundant sulfur and sulfur compounds, which are absent in planetary atmospheres. Sulfur compounds were also detected in interstellar media, including SO, SO2, CS, etc., but excluding S2 which was identified only in IRAS-Araki-Alcock 1983d. Fluorescence calculations are used to analyze the B-X system of S2 which appeared in IUE and ground-based spectra of IRAS-Araki-Alcock 1983d. Single- and multiple-cycle fluorescence calculations indicate that fluorescent equilibrium accounts for the observed spectra despite the fact that the S2 lifetime against solar ultraviolet radiation is relatively short. This analysis confirms unambiguously that emission peaks in the 3000 to 4000 A spectral range of the ground-based data are due to the B-X bands of S2. New evidence is presented of at least one S2 outburst before it was detected by A'Hearn, Feldman, and Schleicher. The time variation of S2 outgassing rates and discussion on the correlation between solar wind flux and the S2 outbursts will be presented. Author

N90-16628*# Max-Planck-Inst. fuer Kernphysik, Heidelberg (Germany, F.R.).
ORGANIC CHEMISTRY OF COMETARY DUST AS DERIVED FROM PUMA 1 DATA
J. Kissel and F. R. Krueger (Ingenieurbuero Krueger, Darmstadt, Germany, F.R.) *In* Lunar and Planetary Inst., Workshop on Analysis of Returned Comet Nucleus Samples 1989 p 35 (For primary document see N90-16607 08-90)
Avail: NTIS HC A05/MF A01 CSCL 03B

Onboard the Halley Fly-By spacecrafts Vega 1, Vega 2, and Giotto were the dust impact mass spectrometers PUMA 1, PUMA 2, and PIA respectively. PUMA 1 was the most sensitive instrument among them. From its data the occurrence of masslines greater than 60 Daltons could be shown to be statistically significant. An analysis of these masslines lead to a scenario, which could explain the masslines as fragment ions from larger molecules which characterize the chemical nature of cometary organic matter as: (1) highly unsaturated hydrocarbons; (2) some of them containing

oxygen; (3) less containing nitrogen; and (4) a few containing oxygen and nitrogen as heteroatoms. From the properties of the spectrometer, also some physical parameters of the dust particles could be inferred, such as their density and structure. Author

N90-16629*# National Aeronautics and Space Administration. Lyndon B. Johnson Space Center, Houston, TX.
IDENTIFICATION OF SOLAR NEBULA CONDENSATES IN INTERPLANETARY DUST PARTICLES AND UNEQUILIBRATED ORDINARY CHONDRITES
W. Kloeck, K. L. Thomas (Lockheed Corp., Houston, TX.), and D. S. McKay *In* Lunar and Planetary Inst., Workshop on Analysis of Returned Comet Nucleus Samples 1989 p 36-37 (For primary document see N90-16607 08-90)
Avail: NTIS HC A05/MF A01 CSCL 03B

Orthopyroxene and olivine grains, low in FeO, but containing MnO contents up to 5 wt percent were found in interplanetary dust particles (IDP) collected in the stratosphere. The majority of olivines and pyroxenes in meteorites contain less than 0.5 wt percent MnO. Orthopyroxenes and olivines high in Mn and low in FeO have only been reported from a single coarse grained chondrule rim in the Allende meteorite and from a Tieschitz matrix augite grain. The bulk MnO contents of the extraterrestrial dust particles with high MnO olivines and pyroxenes are close to CI chondrite abundances. High MnO, low FeO olivines and orthopyroxenes were also found in the matrix of Semarkona, an unequilibrated ordinary chondrite. This may indicate a related origin for minerals in extraterrestrial dust particles and in the matrix of unequilibrated ordinary chondrites. Author

N90-16630*# Max-Planck-Inst. fuer Astrophysik, Garching (Germany, F.R.).
SPECTROPHOTOMETRIC OBSERVATIONS OF COMET P/GIACOBINI-ZINNER
I. Konno, S. Wyckoff, and P. A. Wehinger (Arizona State Univ., Tempe.) *In* Lunar and Planetary Inst., Workshop on Analysis of Returned Comet Nucleus Samples 1989 p 38-39 (For primary document see N90-16607 08-90)
Avail: NTIS HC A05/MF A01 CSCL 03B

Spectroscopic observations of the Giacobini-Zinner comet were performed on March 20, June 20 and 21, September 11, and October 19, 1985. The September observations were performed at perihelion, exactly at the time of the International Cometary Explorer (ICE) encounter with the comet. The March and June observations were obtained with an intensified image dissector scanner (IIDS) on the 2.1-meter Kitt Peak telescope and the September and the October observations were obtained with a charge-coupled device (CCD) on the 4-meter Kitt Peak telescope. The nucleus spectra from these observations are presented.
Author

N90-16631*# Centre National de la Recherche Scientifique, Orsay (France).
COMPOSITION OF DUST FROM COMET P/HALLEY: THE MINERAL FRACTION Abstract Only
Y. Langevin *In* Lunar and Planetary Inst., Workshop on Analysis of Returned Comet Nucleus Samples 1989 p 40 (For primary document see N90-16607 08-90)
Avail: NTIS HC A05/MF A01 CSCL 03B

The composition of dust from Comet Halley was investigated in situ during the Vega 1, Vega 2, and Giotto encounters by the PIA/PUMA impact mass spectrometers. More than 5000 meaningful spectra of individual dust particles were obtained, most in a compressed mode. The interpretation of these spectra in terms of elemental and mineralogical composition will be discussed. Accounting for these difficulties, the following conclusions can be derived for the mineral fraction of dust particles: (1) the observed compositions are compatible with the full range of observed meteoritic minerals (in particular mafic silicates, plagioclases, sulfides, oxides); and (2) within each mineralogical class, the spread in composition appears much wider and more uniform than in meteorites. The low overall density and very large excess of light elements will be discussed. These first direct results on cometary dust considerably strengthen the case for a comet sample return mission. Author

N90-16632*# National Aeronautics and Space Administration. Ames Research Center, Moffett Field, CA.
COMPUTER SIMULATION OF DUST GRAIN EVOLUTION
K. Liffman *In* Lunar and Planetary Inst., Workshop on Analysis of Returned Comet Nucleus Samples 1989 p 41-42 (For primary document see N90-16607 08-90)
Avail: NTIS HC A05/MF A01 CSCL 03B

The latest results are reported from a Monte Carlo code that is being developed at NASA Ames. The goal of this program, is to derive from the observed and presumed properties of the interstellar medium (ISM) the following information: (1) the size spectrum of interstellar dust; (2) the chemical structure of interstellar dust; (3) interstellar abundances; and (4) the lifetime of a dust grain in the ISM. Presently this study is restricted to refractory interstellar material, i.e., the formation and destruction of ices are not included in the program. The program is embedded in an analytic solution for the bulk chemical evolution of a two-phase interstellar medium in which stars are born in molecular clouds, but new nucleosynthesis products and stellar return are entered into a complementary intercloud medium. The well-mixed matter of each interstellar phase is repeatedly cycled stochastically through the complementary phase and back. Refractory dust is created by thermal condensation as stellar matter flows away from sites of nucleosynthesis such as novae and supernovae and/or from the matter returned from evolved intermediate stars. The history of each particle is traced by standard Monte Carlo techniques as it is sputtered and fragmented by supernova shock waves in the intercloud medium. It also accretes an amorphous mantle of gaseous refractory atoms when its local medium joins with the molecular cloud medium. Finally it encounters the possibility of astration (destruction by star formation) within the molecular clouds. Author

N90-16633*# Lockheed Engineering and Sciences Co., Houston, TX.
PROMPT GAMMA ACTIVATION ANALYSIS (PGAA): TECHNIQUE OF CHOICE FOR NONDESTRUCTIVE BULK ANALYSIS OF RETURNED COMET SAMPLES
David J. Lindstrom and Richard M. Lindstrom (National Inst. of Standards and Technology, Gaithersburg, MD.) *In* Lunar and Planetary Inst., Workshop on Analysis of Returned Comet Nucleus Samples 1989 p 43-44 (For primary document see N90-16607 08-90)
Avail: NTIS HC A05/MF A01 CSCL 03B

Prompt gamma activation analysis (PGAA) is a well-developed analytical technique. The technique involves irradiation of samples in an external neutron beam from a nuclear reactor, with simultaneous counting of gamma rays produced in the sample by neutron capture. Capture of neutrons leads to excited nuclei which decay immediately with the emission of energetic gamma rays to the ground state. PGAA has several advantages over other techniques for the analysis of cometary materials: (1) It is nondestructive; (2) It can be used to determine abundances of a wide variety of elements, including most major and minor elements (Na, Mg, Al, Si, P, K, Ca, Ti, Cr, Mn, Fe, Co, Ni), volatiles (H, C, N, F, Cl, S), and some trace elements (those with high neutron capture cross sections, including B, Cd, Nd, Sm, and Gd); and (3) It is a true bulk analysis technique. Recent developments should improve the technique's sensitivity and accuracy considerably.
Author

N90-16634*# Arizona Univ., Tucson. Lunar and Planetary Lab.
SOLAR NEBULA CONDENSATES AND THE COMPOSITION OF COMETS
J. I. Lunine *In* Lunar and Planetary Inst., Workshop on Analysis of Returned Comet Nucleus Samples 1989 p 45-46 (For primary document see N90-16607 08-90)
Avail: NTIS HC A05/MF A01 CSCL 03B

Interpretation of the volatile abundances in Halley's comet in

terms of models for chemical and physical processes in the solar nebula are discussed. Key ratios of the oxidized and reduced species of nitrogen and carbon are identified which tell something of the chemical history of the environment in which cometary grains accreted to form the nucleus. Isotopic abundances are also applied to this problem. It will be shown that the abundances of methane and carbon monoxide are consistent both with models of solar nebula chemistry and chemical processing on grains in star-forming regions. Ultimately, limitations of the current data set on molecular abundances in comets and star-forming regions prevent a definitive choice between the two. Processes important to the composition of outer solar system bodies are: (1) gas phase chemistry in the solar nebula; (2) imperfect mixing in the solar nebula; (3) condensation; (4) clathration; (5) adsorption; and (6) processing of interstellar material. Author

N90-16635*# Tecnospazio S.p.A., Milan (Italy).
CANDIDATE SAMPLE ACQUISITION SYSTEMS FOR THE ROSETTA Abstract Only
P. G. Magnani, C. Gerli, G. Colombina, and P. Vielmo (Tecnomare S.p.A., Italy) *In* Lunar and Planetary Inst., Workshop on Analysis of Returned Comet Nucleus Samples 1989 p 47 (For primary document see N90-16607 08-90)
Avail: NTIS HC A05/MF A01 CSCL 03B

The Comet Nucleus Sample Return (CNSR) mission, one of the four cornerstones of the ESA scientific program, is one of the most complex space ventures within the next century, both from technological and deep space exploration point of view. In the Rosetta scenario the sample acquisition phase represents the most critical point for the global mission's success. The proposed paper illustrates the main results obtained in the context of the CNSR-SAS ongoing activity. The main areas covered are related to: (1) sample properties characterization (comet soil model, physical/chemical properties, reference material for testing); (2) concepts identification for coring, shovelling, harpooning and anchoring; (3) preferred concept (trade off among concepts, identification of the preferred configuration); and (4) proposed development activity for gaining the necessary confidence before finalizing the CNSR mission. Particular emphasis will be given to the robotic and flexibility aspects of the identified sample acquisition systems (SAS) configuration, intended as a means for the overall system performance enhancement. Author

N90-16636*# Wisconsin Univ., Madison.
INTERSTELLAR AND COMETARY DUST
John S. Mathis *In* Lunar and Planetary Inst., Workshop on Analysis of Returned Comet Nucleus Samples 1989 p 48-49 (For primary document see N90-16607 08-90)
Avail: NTIS HC A05/MF A01 CSCL 03B

Aspects of interstellar dust which are known from direct observation will be discussed. Some specific difficulties that various theories have in explaining the observations will be presented. Several theoretical interpretations which have been advanced will be discussed, highlighting first their similarities and then their differences. Also discussed will be the author's ideas about the conditions of interstellar dust throughout its life cycle, from origin to incorporation in pre-cometary ices. Dust is primarily observed by its effects on the spectra of background stars, so observations at optical and ultraviolet (UV) wavelengths are confined to the diffuse interstellar medium (ISM) or to the outer regions of dense clouds. Within this somewhat limited range of environments there are very few lines of sight which show any evidence for icy mantles, but there are major variations in the wavelength dependence of the extinction. In the infrared region of the spectrum, it is possible to observe a few stellar sources deeply embedded within molecular clouds. Author

N90-16637*# Kent Univ., Canterbury (England). Unit for Space Sciences.
THE IN-SITU COMETARY PARTICULATE SIZE DISTRIBUTION MEASURED FOR ONE COMET: P/HALLEY
J. A. M. McDonnell and G. S. Pankiewicz *In* Lunar and Planetary Inst., Workshop on Analysis of Returned Comet Nucleus Samples 1989 p 50-51 (For primary document see N90-16607 08-90)
Avail: NTIS HC A05/MF A01 CSCL 03B

The close approach of Giotto to comet Halley during its 1986 apparition offered an opportunity to study the particulate mass distribution to masses of up to one gram. Data acquired by the front end channels of the highly sensitive mass spectrometer PIA and the dust shield detector system, DIDSY, provide definition to the detected distribution as close as 1000 km to the nucleus. Dynamic motion of the particulates after emission leads to a spatial differentiation affecting the size distribution in several forms: (1) ejecta velocity dispersion; (2) radiation pressure; (3) varying heliocentric distance; and (4) anisotropic nucleus emission. Transformation of the in-situ distribution from PIA and DIDSY weighted heavily by the near-nucleus fluxes leads to a presumed nucleus distribution. The data lead to a puzzling distribution at large masses, not readily explained in an otherwise monotonous power law distribution. Although temporal changes in nucleus activity could and do modify the in-situ size distribution, such an explanation is not wholly possible, because the same form is observed at differing locations in the coma where the time of flight from the nucleus greatly varies. Thus neither a general change in comet activity nor spatial variations lead to a satisfactory explanation. Author

N90-16638*# Tennessee Univ., Knoxville. Dept. of Geological Sciences.
EVOLUTION OF CARBONACEOUS CHONDRITE PARENT BODIES: INSIGHTS INTO COMETARY NUCLEI
Harry Y. McSween, Jr. *In* Lunar and Planetary Inst., Workshop on Analysis of Returned Comet Nucleus Samples 1989 p 52-53 (For primary document see N90-16607 08-90)
Avail: NTIS HC A05/MF A01 CSCL 03B

It is thought that cometary samples will comprise the most primitive materials that are able to be sampled. Although parent body alteration of such samples would not necessarily detract from scientists' interest in them, the possibility exists that modification processes may have affected cometary nuclei. Inferences about the kinds of modifications that might be encountered can be drawn from data on the evolution of carbonaceous chondrite parent bodies. Observations suggest that, of all the classes of chondrites, these meteorites are most applicable to the study of comets. If the proportion of possible internal heat sources such as Al-26 in cometary materials are similar to those in chondrites, and if the time scale of comet accretion was fast enough to permit incorporation of live radionuclides, comets might have had early thermal histories somewhat like those of carbonaceous chondrite parent bodies. Author

N90-16639*# National Aeronautics and Space Administration. Ames Research Center, Moffett Field, CA.
THE COMET RENDEZVOUS ASTEROID FLYBY MISSION
David Morrison, Marcia Neugebauer, and Paul R. Weissman (Jet Propulsion Lab., California Inst. of Tech., Pasadena.) *In* Lunar and Planetary Inst., Workshop on Analysis of Returned Comet Nucleus Samples 1989 p 54-55 (For primary document see N90-16607 08-90)
Avail: NTIS HC A05/MF A01 CSCL 03B

The Comet Rendezvous Asteroid Flyby (CRAF) mission is designed to answer the many questions raised by the Halley missions by exploring a cometary nucleus in detail, following it around its orbit and studying its changing activity as it moves closer to and then away from the Sun. In addition, on its way to rendezvous with the comet, CRAF will fly by a large, primitive class main belt asteroid and will return valuable data for comparison with the comet results. The selected asteroid is 449 Hamburga with a diameter of 88 km and a surface composition of carbonaceous chondrite meteorites. The expected flyby date is January, 1998. The CRAF spacecraft will continue to make measurements in orbit around the cometary nucleus as they both move closer to the Sun, until the dust and gas hazard becomes unsafe. At that point the spacecraft will move in and out between

50 and 2,500 kilometers to study the inner coma and the cometary ionosphere, and to collect dust and gas samples for onboard analysis. Following perihelion, the spacecraft will make a 50,000 km excursion down the comet's tail, further investigating the solar wind interaction with the cometary atmosphere. The spacecraft will return to the vicinity of the nucleus about four months after perihelion to observe the changes that have taken place. If the spacecraft remains healthy and adequate fuel is still onboard, an extended mission to follow the comet nucleus out to aphelion is anticipated. Author

N90-16640*# California Univ., La Jolla. Dept. of Chemistry.
MEASUREMENTS OF LONG-LIVED COSMOGENIC NUCLIDES IN RETURNED COMET NUCLEUS SAMPLES
K. Nishiizumi, C. P. Kohl, and J. R. Arnold *In* Lunar and Planetary Inst., Workshop on Analysis of Returned Comet Nucleus Samples 1989 p 56-57 (For primary document see N90-16607 08-90)
Avail: NTIS HC A05/MF A01 CSCL 03B

Measurements of long lived cosmic ray produced radionuclides have given much information on the histories and rates of surface evolution for meteorites, the Moon and the Earth. These nuclides can be equally useful in studying cometary histories and post nebular processing of cometary surfaces. The concentration of these nuclides depends on the orbit of the comet (cosmic ray intensity changes with distance from the sun), the depth of the sampling site in the comet surface, and the rate of continuous evolution of the surface (erosion rate of surface materials). If the orbital parameters and the sampling depth are known, production rates of cosmogenic nuclides can be fairly accurately calculated by theoretical models normalized to measurement on lunar surface materials and meteoritic samples. Due to the continuous evaporation of surface materials, it is expected that the long lived radioactivities will be undersaturated. Accurate measurements of the degree of undersaturation in nuclides of different half-lives allows for the determination of the rate of surface material loss over the last few million years. Author

N90-16641*# National Aeronautics and Space Administration. Goddard Space Flight Center, Greenbelt, MD.
METAMORPHISM OF COSMIC DUST: PROCESSING FROM CIRCUMSTELLAR OUTFLOWS TO THE COMETARY REGOLITH
Joseph A. Nuth, III *In* Lunar and Planetary Inst., Workshop on Analysis of Returned Comet Nucleus Samples 1989 p 58 (For primary document see N90-16607 08-90)
Avail: NTIS HC A05/MF A01 CSCL 03B

Metamorphism of refractory particles continues in the interstellar medium (ISM) where the driving forces are sputtering by cosmic ray particles, annealing by high energy photons, and grain destruction in supernova generated shocks. Studies of the depletion of the elements from the gas phase of the interstellar medium tell us that if grain destruction occurs with high efficiency in the ISM, then there must be some mechanism by which grains can be formed in the ISM. Most grains in a cloud which collapses to form a star will be destroyed; many of the surviving grains will be severely processed. Grains in the outermost regions of the nebula may survive relatively unchanged by thermal processing or hydration. It is these grains which one hopes to find in comets. However, only those grains encased in ice at low temperature can be considered pristine since a considerable degree of hydrous alteration might occur in a cometary regolith if the comet enters the inner solar system. The physical, chemical and isotopic properties of a refractory grain at each stage of its life cycle will be discussed. Author

N90-16642*# New Mexico Univ., Albuquerque. Dept. of Geology.
WHAT IF CHONDRITIC POROUS INTERPLANETARY DUST PARTICLES ARE NOT THE REAL MCCOY
Frans J. M. Rietmeijer *In* Lunar and Planetary Inst., Workshop on Analysis of Returned Comet Nucleus Samples 1989 p 60-61 (For primary document see N90-16607 08-90)
Avail: NTIS HC A05/MF A01 CSCL 03B

To select a target comet for a Comet Nucleus Sample Return Mission (CNSRM) it is necessary to have an experimental data base to evaluate the extent of diversity and similarity of comets. For example, the physical properties (e.g., low density) of chondritic porous (CP) interplanetary dust particles (IDPs) are believed to resemble these properties of cometary dust although it is yet to be demonstrated that the porous structure of CP IDPs is inherent to presolar dust particles stored in comet nuclei. Porous structures of IDPs could conceivably form during sublimation at the surface of active comet nuclei. Porous structures are also obtained during annealing of amorphous Mg-SiO smokes which initially forms porous aggregates of olivine + platey tridymite and which, upon continued annealing, react to fluffy enstatite aggregates. It is therefore uncertain that CP IDPs are entirely composed of unmetamorphosed presolar dust. Conceivably, new minerals and textures may form in situ in nuclei of active comets as a function of their individual thermal history. Unmetamorphosed comet dust is probably structurally amorphous. Thermal annealing of this dust can produce ultra fine-grained minerals and this ultrafine grain size of CP IDPs should be considered in assessments of aqueous alterations that could affect presolar dust in comet nuclei between 200 and 400 K. Devitrification and hydration may occur in situ in ice-dust mixtures and the mantle of active comet nuclei. Devitrification, or uncontrolled crystallization, of amorphous precursor dust can produce a range of chemical compositions of ultrafine-grained minerals and (non-equilibrium) mineral assemblages and textures in dust contained in comet nuclei as a function of period and trajectory of orbit and number of perihelion passages (not considering internal heating). Thus, experimental data on relevant processes and reaction rates between 200 and 400 K are needed in order to evaluate comet selection, penetration depth for sampling device and curation of samples for CNSRM. Author

N90-16643*# Kernforschungsanlage, Juelich (Germany, F.R.). Inst. fuer Nuklearchemie.
HANDLING AND ANALYSIS OF ICES IN CRYOSTATS AND GLOVE BOXES IN VIEW OF COMETARY SAMPLES
K. Roessler, G. Eich, M. Heyl, H. Kochan, A. Oehler, A. Patnaik, W. Schlosser (Ruhr Univ., Bochum, Germany, F.R.), and R. Schulz *In* Lunar and Planetary Inst., Workshop on Analysis of Returned Comet Nucleus Samples 1989 p 62-63 (For primary document see N90-16607 08-90)
Avail: NTIS HC A05/MF A01 CSCL 03B

Comet nucleus sample return mission and other return missions from planets and satellites need equipment for handling and analysis of icy samples at low temperatures under vacuum or protective gas. Two methods are reported which were developed for analysis of small icy samples and which are modified for larger samples in cometary matter simulation experiments (KOSI). A conventional optical cryostat system was modified to allow for transport of samples at 5 K, ion beam irradiation, and measurement in an off-line optical spectrophotometer. The new system consists of a removable window plug containing nozzles for condensation of water and volatiles onto a cold finger. This plug can be removed in a vacuum system, changed against another plug (e.g., with other windows (IR, VIS, VUV) or other nozzles). While open, the samples can be treated under vacuum with cooling by manipulators (cut, removal, sample taking, irradiation with light, photons, or ions). After bringing the plug back, the samples can be moved to another site of analysis. For handling the 30 cm diameter mineral-ice samples from the KOSI experiments an 80x80x80 cm glove box made out of plexiglass was used. The samples were kept in a liquid nitrogen bath, which was filled from the outside. A stream a dry N2 and evaporating gas from the bath purified the glove box from impurity gases and, in particular, H2O, which otherwise would condense onto the samples. Author

N90-16644*# Chicago Univ., IL. Lab. for Astrophysics and Space Research.
TRAJECTORY-CAPTURE CELL INSTRUMENTATION FOR MEASUREMENT OF DUST PARTICLE MASS, VELOCITY AND TRAJECTORY, AND PARTICLE CAPTURE

J. A. Simpson and A. J. Tuzzolino *In* Lunar and Planetary Inst., Workshop on Analysis of Returned Comet Nucleus Samples 1989 p 64-65 (For primary document see N90-16607 08-90)
(Contract NASw-4196)
Avail: NTIS HC A05/MF A01 CSCL 03B

The development of the polyvinylidene fluoride (PVDF) dust detector for space missions--such as the Halley Comet Missions where the impact velocity was very high as well as for missions where the impact velocity is low was extended to include: (1) the capability for impact position determination - i.e., x,y coordinate of impact; and (2) the capability for particle velocity determination using two thin PVDF sensors spaced a given distance apart - i.e., by time-of-flight. These developments have led to space flight instrumentation for recovery-type missions, which will measure the masses (sizes), fluxes and trajectories of incoming dust particles and will capture the dust material in a form suitable for later Earth-based laboratory measurements. These laboratory measurements would determine the elemental, isotopic and mineralogical properties of the captured dust and relate these to possible sources of the dust material (i.e., comets, asteroids), using the trajectory information. The instrumentation described here has the unique advantages of providing both orbital characteristics and physical and chemical properties--as well as possible origin--of incoming dust. Author

N90-16645*# Westfaelische Wilhelms Univ., Muenster (Germany, F.R.). Inst. fuer Planetologie.
THERMAL HISTORIES OF THE SAMPLES OF TWO KOSI COMET NUCLEUS SIMULATION EXPERIMENTS
T. Spohn, J. Benkhoff, J. Klinger, E. Gruen, and H. Kochan (Deutsche Forschungs- und Versuchsanstalt fuer Luft- und Raumfahrt, Cologne, Germany, F.R.) *In* Lunar and Planetary Inst., Workshop on Analysis of Returned Comet Nucleus Samples 1989 p 66-67 Prepared in cooperation with Centre National de la Recherche Scientifique, Saint Martin d'Heres, France (For primary document see N90-16607 08-90)
Avail: NTIS HC A05/MF A01 CSCL 03B

Temperatures recorded during two KOSI comet nucleus simulation experiments strongly suggest that heat transport by vapor flow into the interior of the sample is very important. Two comet nucleus simulation experiments have been done by the KOSI team in a big space simulator. The thermal evolution of the sample during insolation and the results of simplified thermal evolution calculations are discussed. The observed thermal histories cannot be explained by a simple model with heat transferred by heat conduction at a constant conductivity, so a coupled heat and mass transfer problem was considered. The porous ice matrix was assumed to have a constant thermal conductivity and to be in thermal equilibrium with vapor in the pores, the internal pressure being the vapor pressure. The vapor was modelled as an ideal gas because, at the temperatures relevant to the problem, the mean free path length of the vapor molecules is large in comparison with the pore dimensions. The heat capacity at constant volume per unit mass of the two phase mixture was also assumed constant. The vapor was allowed to flow and transfer heat in response to an internal pressure gradient. Author

N90-16646*# Chicago Univ., IL. Dept. of Geophysical Sciences.
ANALYSIS OF PARTICULATES OF COMET NUCLEUS SAMPLES: POSSIBLE USE OF OLIVINE AS INDICATOR PHASE
I. M. Steele *In* Lunar and Planetary Inst., Workshop on Analysis of Returned Comet Nucleus Samples 1989 p 68-69 (For primary document see N90-16607 08-90)
(Grants NAG9-47; NSF EAR-84-15791; NSF EAR-86-08299)
Avail: NTIS HC A05/MF A01 CSCL 03B

The electron microprobe is a proven instrument for particulate analysis and modifications are possible for in situ analysis of particulates in ice at temperatures near that of liquid nitrogen. Present sample requirements allow for polished samples with 0.25 x 0.25 dimensions to be maintained in the sample chamber of a modern electron probe (CAMECA SX-50) at a temperature of -150 C; larger samples are possible but at higher temperatures as determined by thermal conductivity. The major problem is transport and insertion of samples into the instrument through vacuum interlocks. The manufacturer of the above microprobe has designed an exchange mechanism to allow storage and transport of samples previously prepared for their sample holder which attaches to their instrument allowing extraction and insertion of samples while maintaining -150 C temperature. An important test will be the capability of preparing polished surfaces of an ice-particulate sample without loss of particles and at low temperatures. While thin sections of water ice are routine, these are not examined for particulate material and are prepared at temperatures easily obtained in room-size volumes. Anticipated problems include rounding of small grains in the relatively soft ice matrix and the technical problem of dry polishing. Author

N90-16647*# Jet Propulsion Lab., California Inst. of Tech., Pasadena.
THE NATURE OF COMETARY MATERIALS
James Stephens *In* Lunar and Planetary Inst., Workshop on Analysis of Returned Comet Nucleus Samples 1989 p 70 (For primary document see N90-16607 08-90)
Avail: NTIS HC A05/MF A01 CSCL 03B

Because cometary surfaces are likely to be far colder and of a different composition than planetary surfaces, there are some new considerations that must be examined in regards to placing instrumented packages or sample return devices on their surfaces. The qualitative analysis of the problem of attaching hardware to a comet and not being ejected back into space can be divided into two parts. The first problem is to pierce the mantle and obtain access to the icy core. Drilling through the mantle requires that the drilling forces be reacted. Reacting such forces probably requires attachment to the icy core below. Therefore, some kinetic impact piercing device is likely to be required as the first act of attachment. The second problem for a piercing device to overcome is the force produced by the impact kinetic energy that tries to eject the piercing device back into space. The mantle and icy core can absorb some of the impact kinetic energy in the form of fracture formation and friction energy. The energy that is not absorbed in these two ways is stored by the core as elastic deformation of the mantle and icy core. It is concluded that because the cometary materials are almost certainly brittle and the icy core is likely to be self lubricating, the elastic rebound and gas pressure expulsion forces must be counteracted by forces greater than those that may be provided by a piercing device or its capture devices (barbs). Author

N90-16648*# Muenster Univ. (Germany, F.R.). Inst. fuer Planetologie.
METHODS FOR THE MINERALOGICAL AND TEXTURAL ANALYSIS OF COMET NUCLEUS SAMPLES
D. Stoeffler, H. Dueren, and J. Knoelker *In* Lunar and Planetary Inst., Workshop on Analysis of Returned Comet Nucleus Samples 1989 p 71-72 (For primary document see N90-16607 08-90)
Avail: NTIS HC A05/MF A01 CSCL 03B

The objectives and instrumental requirements of a petrographic analysis of porous comet nucleus material are reviewed. Assumptions about its composition and texture, and the available techniques for the microscopic analysis of comet analogue material are investigated. New techniques required for the petrographic investigation of natural and artificial comet nucleus samples are also considered. Author

N90-16649*# Chicago Univ., IL. Dept. of the Geophysical Sciences.
NON-DESTRUCTIVE TRACE ELEMENT MICROANALYSIS OF AS-RECEIVED COMETARY NUCLEUS SAMPLES USING SYNCHROTRON X RAY FLUORESCENCE
S. R. Sutton *In* Lunar and Planetary Inst., Workshop on Analysis of Returned Comet Nucleus Samples 1989 p 73-74 Prepared in cooperation with Brookhaven National Lab., Upton, NY (For primary document see N90-16607 08-90)

(Contract NAG9-106; DE-AC02-76CH-00016; NSF EAR-86-18346)
Avail: NTIS HC A05/MF A01 CSCL 03B

The Synchrotron X ray Fluorescence (SXRF) microprobe at the National Synchrotron Light Source (NSLS), Brookhaven National Laboratory, will be an excellent instrument for non-destructive trace element analyses of cometary nucleus samples. Trace element analyses of as-received cometary nucleus material will also be possible with this technique. Bulk analysis of relatively volatile elements will be important in establishing comet formation conditions. However, as demonstrated for meteorites, microanalyses of individual phases in their petrographic context are crucial in defining the histories of particular components in unequilibrated specimens. Perhaps most informative in comparing cometary material with meteorites will be the halogens and trace metals. In-situ, high spatial resolution microanalyses will be essential in establishing host phases for these elements and identifying terrestrial (collection/processing) overprints. The present SXRF microprobe is a simple, yet powerful, instrument in which specimens are excited with filtered, continuum synchrotron radiation from a bending magnet on a 2.5 GeV electron storage ring. A refrigerated cell will be constructed to permit analyses at low temperatures. The cell will consist essentially of an air tight housing with a cold stage. Kapton windows will be used to allow the incident synchrotron beam to enter the cell and fluorescent x rays to exit it. The cell will be either under vacuum or continuous purge by ultrapure helium during analyses. Several other improvements of the NSLS microprobe will be made prior to the cometary nucleus sample return mission that will greatly enhance the sensitivity of the technique. Author

N90-16650*# Cologne Univ. (Germany, F.R.). Nuklearchemie.
MECHANICAL AND SEM ANALYSIS OF ARTIFICIAL COMET NUCLEUS SAMPLES
K. Thiel, H. Kochan, K. Roessler, E. Gruen, G. Schwehm, H. Hellmann, P. Hsiung (Kernforschungsanlage, Juelich, Germany, F.R.), and G. Koelzer *In* Lunar and Planetary Inst., Workshop on Analysis of Returned Comet Nucleus Samples 1989 p 75-76 (For primary document see N90-16607 08-90)
Avail: NTIS HC A05/MF A01 CSCL 03B

Since 1987 experiments dealing with comet nucleus phenomena have been carried out in the DFVLR space simulation chambers. The main objective of these experiments is a better understanding of thermal behavior, surface phenomena and especially the gas dust interaction. As a function of different sample compositions and exposure to solar irradiation (xenon-bulbs) crusts of different hardness and thickness were measured. The measuring device consists of a motor driven pressure foot (5 mm diameter), which is pressed into the sample. The applied compressive force is electronically monitored. The microstructure of the crust and dust residuals is investigated by scanning electron microscopy (SEM) techniques. Stress-depth profiles of an unirradiated and an irradiated model comet are given. Author

N90-16651*# Jet Propulsion Lab., California Inst. of Tech., Pasadena.
ELECTRON SPIN RESONANCE (ESR) STUDIES OF RETURNED COMET NUCLEUS SAMPLES
Fun-Dow Tsay, Soon Sam Kim, and Ranty H. Liang *In* Lunar and Planetary Inst., Workshop on Analysis of Returned Comet Nucleus Samples 1989 p 77-78 (For primary document see N90-16607 08-90)
Avail: NTIS HC A05/MF A01 CSCL 03B

The most important objective of the Comet Nucleus Sample Returm Mission is to return samples which could reflect formation conditions and evolutionary processes in the early solar nebula. It is expected that the returned samples will consist of fine-grained silicate materials mixed with ices composed of simple molecules such as H2O, NH3, CH4 as well as organics and/or more complex compounds. Because of the exposure to ionizing radiation from cosmic-ray, gamma-ray, and solar wind protons at low temperature, free radicals are expected to be formed and trapped in the solid ice matrices. The kind of trapped radical species together with their concentration and thermal stability can be used as a dosimeter as well as a geothermometer to determine thermal and radiation histories as well as outgassing and other possible alternation effects since the nucleus material was formed. Since free radicals that are known to contain unpaired electrons are all paramagnetic in nature, they can be readily detected and characterized in their native form by the Electron Spin Resonance (ESR) method. In fact, ESR has been shown to be a non-destructive, highly sensitive tool for the detection and characterization of paramagnetic, ferromagnetic, and radiation damage centers in terrestrial and extraterrestrial geological samples. The potential use of ESR as an effective method in the study of returned comet nucleus samples, in particular, in the analysis of fine-grained solid state icy samples is discussed. Author

N90-16652*# Alabama Univ., Birmingham. Dept. of Physics.
ION BOMBARDMENT EXPERIMENTS SUGGESTING AN ORIGIN FOR ORGANIC PARTICLES IN PRE-COMETARY AND COMETARY ICES
Thomas J. Wdowiak, Edward L. Robinson, Gregory C. Flickinger, and David A. Boyd *In* Lunar and Planetary Inst., Workshop on Analysis of Returned Comet Nucleus Samples 1989 p 79-80 (For primary document see N90-16607 08-90)
(Grant NAGw-749)
Avail: NTIS HC A05/MF A01 CSCL 03B

During the Giotto and Vega encounters with Comet Halley both organic particles called CHON and energetic ions were detected. The acceleration of ions to hundreds of keV in the vicinity of the bow shock and near the nucleus may be a demonstration of a situation occurring in the early solar system (perhaps during the T Tauri stage) that led to the formation of organic particles only now released. Utilizing a Van de Graaff accelerator and a target chamber having cryogenic and mass spectrometer capabilities, frozen gases were bombarded at 10 K with 175 keV protons with the result that fluffy solid material remains after sublimation of the ice. Initial experiments were carried out with a gas mixture in parts of 170 carbon monoxide, 170 argon, 25 water, 20 nitrogen, and 15 methane formulated to reflect an interstellar composition in experiments involving the freezing out of the products of a plasma. The plasma experiments resulted in a varnish-like film residue that exhibited luminescence when excited with ultraviolet radiation, while the ion bombardment created particulate material that was not luminescent. Author

N90-16653*# Jet Propulsion Lab., California Inst. of Tech., Pasadena.
PHYSICAL PROCESSING OF COMETARY NUCLEI
Paul R. Weissman and S. Alan Stern (Colorado Univ., Boulder.) *In* Lunar and Planetary Inst., Workshop on Analysis of Returned Comet Nucleus Samples 1989 p 81-82 (For primary document see N90-16607 08-90)
Avail: NTIS HC A05/MF A01 CSCL 03B

Cometary nuclei were formed far from the Sun in the colder regions of the solar nebula, and have been stored in distant orbits in the Oort cloud over most of the history of the solar system. It had been thought that this benign environment would preserve comets in close to their original pristine state. However, recent studies have identified a number of physical processes that have likely acted to modify cometary nuclei in a variety of significant ways. It is important to consider all of these possible processes, both in deciding on a site on the nucleus for collection of cometary samples, and in interpreting the results of analyses of returned cometary samples. Although it can no longer be said that comets are pristine samples of original solar nebula material, they are still the best obtainable samples of that unique period in the formation of the planetary system. Author

N90-16654*# Smithsonian Astrophysical Observatory, Cambridge, MA. Center for Astrophysics.
REFRACTORY SOLIDS IN CHONDRITES AND COMETS: HOW SIMILAR
John A. Wood *In* Lunar and Planetary Inst., Workshop on Analysis of Returned Comet Nucleus Samples 1989 p 84-85

(For primary document see N90-16607 08-90)
Avail: NTIS HC A05/MF A01 CSCL 03B

The grains of ice, dust, and organic material that came together to form the solar system have been preserved to differing degrees in the most primitive solar system bodies, asteroids and comets. The study of samples of asteroids (in the form of chondritic meteorites) reveals that the dust component was extensively altered by high-temperature events and processes in the early solar system, before it was aggregated into chondritic planetesimals. The nature of these high-temperature events and processes is not known, but the evidence of their operation is pervasive and unequivocal. Are the refractory particles in comets likely to be similar to these chondrite components. Probably not (except for the presolar carbonaceous grains in chondrites), because the chondritic components are products of severe thermal processing, and all imaginable energy sources that could have provided the heat tend to diminish with distance from the sun. Every indication is that comets formed at much greater radial distances than asteroids, so the particles they incorporated would have experienced less heating. The possibilities cannot be completely ruled out that comets, too, formed inside the present orbit of Jupiter, or that thermally-processed grains were able to diffuse great radial distances before being incorporated in accreting objects, but it is far more likely that most of the refractory grains in comets have been spared the extreme thermal processing that shaped the character of chondritic components. Author

N90-16655*# Washington Univ., Saint Louis, MO. Center for the Space Sciences.
ISOTOPIC MICROANALYSIS OF RETURNED COMET NUCLEUS SAMPLES
Ernst Zinner *In* Lunar and Planetary Inst., Workshop on Analysis of Returned Comet Nucleus Samples 1989 p 86-87 (For primary document see N90-16607 08-90)
Avail: NTIS HC A05/MF A01 CSCL 03B

If isotopic measurements of interplanetary dust particles (IDPs) and primitive meteorites can serve as a guide to the isotopic analysis of returned comet nucleus material, an essential requirement will be the capability for microanalysis. The reason is that in both types of extraterrestrial samples large isotopic heterogeneities on a small spatial scale have become apparent once it was possible to measure isotopes in small samples. In the discovery of large isotopic anomalies the ion microprobe has played a significant role because of its high spatial resolution for isotopic ratio measurements. The largest isotopic anomalies in C, N, O, Mg, Si, Ca and Ti found to date were measured by ion microprobe mass spectrometry. The most striking examples are D/H measurements in IDPs and isotopic measurements of C, N and Si in SiC from the CM chondrites Murray and Murchison.
Author

N90-16656*# National Aeronautics and Space Administration. Lyndon B. Johnson Space Center, Houston, TX.
THE MEASUREMENT OF TRACE ELEMENTS IN INTERPLANETARY DUST AND COMETARY PARTICLES BY ULTRA-HIGH SENSITIVITY INAA
M. E. Zolensky, David J. Lindstrom, Richard M. Lindstrom (National Inst. of Standards and Technology, Gaithersburg, MD.), and M. M. Lindstrom *In* Lunar and Planetary Inst., Workshop on Analysis of Returned Comet Nucleus Samples 1989 p 88-89 (For primary document see N90-16607 08-90)
Avail: NTIS HC A05/MF A01 CSCL 03B

Today the major elemental composition of interplanetary dust particles (IDPs) is routinely determined in many laboratories. These and mineralogical studies have revealed the presence of at least two major types of IDPs, chondritic and refractory. Preliminary results of a successful attempt to determine abundances of a large suite of trace elements from both chondritic and refractory IDPs are reported. The analytical procedure can be used in the grain-by-grain analysis of returned cometary samples. Chondritic and refractory IDPs are characterized by standard scanning electron microscopy and energy dispersive x ray spectroscopy (SEM-EDX) techniques. With this system, detection limits for many elements are well below picogram levels, and some approach femtogram levels. This technique is non-destructive, although some sample handling is required, so particles can be analyzed by other techniques after instrument neutron activation analysis (INAA) is completed. Data is presently being reduced from the analyses of 7 IDPs. These are U2015E10, U2015F1, W7029-A2, W7029-A3, W7013A8, LACI (all chondritic) and 705 (refractory). So far, 17 different major and trace elements were detected and measured in these particles, including rare earths and some very volatile elements (Br and Zn). Author

N90-16657 California Inst. of Tech., Pasadena.
OUTFLOWS IN HIGH MASS STAR-FORMING REGIONS Ph.D. Thesis
Mary Anne Barsony 1989 178 p
Avail: Univ. Microfilms Order No. DA8908412

In the last decade, observations of star-forming regions in the millimeter wavelength range have led to the discovery of supersonic molecular outflows from embedded sources, a heretofore unsuspected, but now generally accepted, phase in the star formation process. In order to better understand the outflow phenomenon in high mass (i.e., high luminosity) pre-main sequence stars, the three sources S87, LkH(alpha)101, and S106 were chosen for closer study. Observations from the recently completed Owens Valley Radio Observatory's millimeter wave interferometer afford the highest spatial-resolution, molecular line maps of these sources to date. The maps were combined with data from the 14 m FCRAO millimeter wave radio telescope, the VLA, IRAS, and the Palomar 5 m and 1.5 m optical telescopes. A synthesis of the data reveals that although all three pre-main sequence objects are the sources of powerful, ionized stellar winds, only one, S87/IRS1, currently drives a bipolar molecular outflow. In all cases the wind velocities are lower, and the mass loss rates higher, than for main sequence stars of the same spectral types. Radiation pressure is inadequate to drive these winds, which can be anisotropic in their velocity fields. The existence of massive, large-scale disks, necessary for numerous proposed molecular outflow models, can now be ruled out. Only one of the many proposed molecular outflow models is consistent with the new observations (Konigl 1982). Although the observed winds can disperse a good portion of the cloud cores they inhabit, they cannot completely destroy these cores. Consequently, outflows from pre-main sequence stars alone cannot account for the dispersal of molecular clouds, as some investigators have suggested. Dissert. Abstr.

N90-16658 Cornell Univ., Ithaca, NY.
THE DYNAMICS OF DUST IN PLANETARY MAGNETOSPHERES Ph.D. Thesis
Leslie E. Schaffer 1989 334 p
Avail: Univ. Microfilms Order No. DA8915075

Dust grains orbiting through corotating magnetospheres of the outer planets acquire an electric charge determined by the ambient plasma and a grain's velocity. The equilibrium charge and stochastic variations arising from the quantized charging process are computed. Momentum transfer between grains and plasma is estimated. For time scales over which plasma drag and collisions are negligible, dust dynamics can be treated with Hamiltonian methods. For axisymmetric magnetic fields, equatorial orbits, and constant charge, trajectories can be followed regardless of charge-to-mass ratio, epsilon. It is shown that small epsilon grains are the likely inhabitants of dusty ring systems. For small epsilon, the equations of motion about circular, equatorial orbits are expanded, allowing for an asymmetric magnetic field. It is shown that the radial and vertical excursions from the reference orbit satisfy forced harmonic oscillator equations. Trajectories deep in resonance zones are studied via numerical integration, and a closer examination of the perturbation theory explains the long-time dynamical behavior. Any likely stochastic variations in q cannot break the grain's resonant response. Plasma drag causes grains to spiral away from synchronous orbit, and through resonances. The consequences of resonance passage are explored numerically and it is found that inclinations increase by an order of magnitude.

Since orbital ascending nodes are uniformly distributed downstream of resonance, Lorentz resonances can explain much of the vertical structure of the ethereal Jovian ring. Dissert. Abstr.

N90-16659 Purdue Univ., West Lafayette, IN.
THE ROLE OF AN UPSTREAM CYCLONE AND CORRESPONDING SYNOPTIC/PLANETARY-SCALE INTERACTIONS DURING THE DEVELOPMENT OF A BLOCKING ANTICYCLONE Ph.D. Thesis
Chih-Hua Tsou 1988 106 p
Avail: Univ. Microfilms Order No. DA8912007

Using fields derived from Goddard Laboratory for Atmospheres (GLA) analyses of the FGGE SOP-I data set, the general behavior of an Atlantic blocking anticyclone is diagnosed using the extended height tendency equation and several energy quantities. In addition, comparison between quasigeostrophic (QG) and extended height tendencies are made. To further analyze the relative importance of planetary-scale, synoptic-scale, and scale-interaction forcing of this block, height tendencies and energy quantities are also calculated from a scale-partitioned form. The scale partitioning is accomplished using the Barnes objective analysis scheme. Results indicate that vorticity advection is the primary forcing mechanism during the block development. Much of the vorticity advection is attributed to the northward advection of negative relative vorticity east of a jet streak that formed between the cyclone and anticyclone. Further, height rises associated with this advection occurred as the ridge downstream from the exploding cyclone became stationary. In fact, the strong northward advection of relative vorticity is primarily due to the advection of synoptic-scale vorticity by the planetary-scale and synoptic-scale winds. This indicates the importance of the proper phasing of the synoptic-scale vorticity with the winds of both scales. Lack of proper phasing between vorticity and wind fields, weaker winds, and weaker flow across the vorticity contours caused the QG model to seriously underestimate the northward amplification of the ridge as the ridge became stationary. Dissert. Abstr.

N90-16660 California Univ., Santa Cruz.
MASS FUNCTIONS FOR EIGHT GALACTIC CLUSTERS IN THE SOLAR NEIGHBORHOOD Ph.D. Thesis
Stephen Paul Francic 1989 341 p
Avail: Univ. Microfilms Order No. DA8916184

Mass functions for eight galactic clusters in the solar neighborhood were obtained. The mass functions were determined from proper motion membership probabilities and unlike similar investigations, corrected for outlying cluster stars. The membership probabilities were determined from the joint proper motion and surface density distributions for the field and cluster stars. They also were corrected for any magnitude dependences. Comparison of the mass functions with the Salpeter initial mass function (IMF) shows that the older clusters tend to be deficient in the number of low mass stars, while the younger clusters tend to have more. Analysis of the relaxation times shows that the deficiency of faint stars in the older clusters is likely due to their evaporation from the cluster. The combined mass function for six of the clusters results in a power law with a power law index of -1.97 + or - 0.17 for 1.1 less than M/M solar mass less than 2.5. This agrees with a recent determination of the field star IMF where the power law index is -2.00 + or - 0.18 for 0.8 less than M/M solar mass less than 18. If the older clusters are not considered, then comparison of the combined mass function with the individual cluster mass functions shows that the universality hypothesis cannot be denied. Dissert. Abstr.

N90-16661 Northwestern Univ., Evanston, IL.
GAMMA-RAY OBSERVATIONS AND THE DISTRIBUTION OF INTERSTELLAR ALUMINUM-26 Ph.D. Thesis
William Richard Purcell 1989 136 p
Avail: Univ. Microfilms Order No. DA8914014

The discovery of radioactive Al-26 in the Interstellar Medium has provided direct evidence for the recent nucleosynthesis of intermediate mass nuclei in the Galaxy. While modern nucleosynthesis theories suggest that Al-26 production may occur in a variety of astrophysical objects, they have not been able to identify the dominant production site of the observed Al-26. Observationally, the greatest hope for identifying the source of the observed Al-26 is through a comparison of the angular distribution of the observed 1.809 MeV radiation, emitted during the decay of Al-26, with the angular distributions of the suggested production sites. In order to provide limits on the angular distribution of the 1.809 MeV radiation, a technique was developed which significantly improves the angular resolution of the Solar Maximum Mission Gamma-Ray Spectrometer (GRS). This technique, which uses the Earth as an occulting disk in the large GRS field-of-view, was applied to observations of the Galactic 1.809 MeV radiation. The results of this analysis are given and discussed.
Dissert. Abstr.

N90-16662# Centro Brasileiro de Pesquisas Fisicas, Rio de Janeiro.
QUANTUM FIELDS IN COSMOLOGICAL SPACE-TIMES: A SOLUBLE EXAMPLE
Isaias Costa, M. Novello, Nami F. Svaiter, and Nathalie Deruelle (Paris VI Univ., France) 1988 49 p Submitted for publication Sponsored by MRE; Centre National de la Recherche Scientifique; Conselho Nacional de Pesquisas; and COPECUB
(DE89-618837; CBPF-NF-059/88; ISSN-0029-3965) Avail: NTIS (US Sales Only) HC A03/MF A01

The Klein-Gordon equation is solved for a massive real scalar field in the Novello-Salim Eternal Universe, i.e., non singular spatial homogeneous and isotropic cosmological background. This background is tangent to Milne universes in the distant past and future (and hence asymptotically flat) and evolves between these two geometries via a phase of contraction to a point of maximum curvature followed by expansion. This allows a computation of the Bogolyubov coefficients of the scalar field, usually interpreted as the rate of creation of matter by the time varying gravitational field, either when the vacuum is defined at the moment of maximum curvature (the false Big-Bang) or at the far beginning of the cosmic evolution. This new exact solution is compared to the results obtained when the geometry is that of the Milne universe. DOE

N90-16663# Centro Brasileiro de Pesquisas Fisicas, Rio de Janeiro.
DISSIPATIVE EFFECTS IN FRIEDMANN UNIVERSES
J. A. S. Lima and I. Waga (Universidade Federal de Paraiba, Brazil) 1988 27 p Sponsored in part by Brazilian Research Agency
(DE89-618838; CBPF-NF-064/88; ISSN-0029-3865) Avail: NTIS (US Sales Only) HC A03/MF A01

The relationship between the the different temperatures present in a radiative plasma is examined. In particular, the physical and the operational meanings of Eckart's temperature are discussed. An entropy density formula for the radiative component and its fractional rate are derived. We have also suggested a reformulation of Weinberg's conditions for maximum entropy production. The effect of radiative bulk viscosity in diluting monopoles in the very early universe is estimated. DOE

N90-16664*# Space Telescope Science Inst., Baltimore, MD.
ACCRETION SHOCK GEOMETRIES IN THE MAGNETIC VARIABLES
H. S. Stockman Jul. 1988 23 p Presented at the Workshop on Circumstellar Polarization, Vatican City, 1987 Submitted for publication
(NASA-CR-186290; Preprint-Series-293; NAS 1.26:186290)
Avail: NTIS HC A03/MF A01 CSCL 03B

The first self consistent shock models for the AM Herculis-type systems successfully identified the dominant physical processes and their signatures. These homogenous shock models predict unpolarized, Rayleigh-Jeans optical spectra with sharp cutoffs and rising polarizations as the shocks become optically thin in the ultraviolet. However, the observed energy distributions are generally flat with intermediate polarizations over a broad optical band. These and other observational evidence support a non-homogenous accretion profile which may extend over a considerable fraction

of the stellar surface. Both the fundamental assumptions underlying the canonical 1-D shock model and the extension of this model to inhomogenous accretion shocks were identified, for both radial and linear structures. The observational evidence was also examined for tall shocks and little evidence was found for relative shock heights in excess of h/R(1) greater than or equal to 0.1. For several systems, upper limits to the shock height can be obtained from either x ray or optical data. These lie in the region h/R(1) is approximately 0.01 and are in general agreement with the current physical picture for these systems. The quasi-periodic optical variations observed in several magnetic variables may eventually prove to be a major aid in further understanding their accretion shock geometries. Author

N90-16665# Los Alamos National Lab., NM.
RELATIVE MUON CONTENT OF UHE SHOWERS ASSOCIATED WITH HERCULES X-1
D. E. Alexandreas, R. C. Allen, S. Biller, G. Dion, X-Q. Lu, P. R. Vishwanath, G. B. Yodh, R. W. Ellsworth (George Mason Univ., Fairfax, VA.), R. L. Burman, and D. R. Cady et al 1989 5 p Presented at the 21st International Cosmis Ray Conference, Adelaide, Australia, 6-19 Jan. 1990 Prepared in cooperation with Maryland Univ., College Park
(Contract W-7405-eng-36)
(DE90-000609; LA-UR-89-2989; CONF-900122-3) Avail: NTIS HC A01/MF A01

An analysis is presented of the muon content associated with the July, 1986 UHE (ultrahigh energy) observation of the Hercules X-1 system, previously reported by the CYGNUS collaboration. The probability for observing comparable muon content in a set of background showers similar to those of the Hercules burst is given. DOE

N90-16666# Lawrence Livermore National Lab., CA. Inst. of Geophysics and Planetary Physics.
NUCLEAR REACTION UNCERTAINTIES IN STANDARD AND NON-STANDARD COSMOLOGIES
Robert A. Malaney Oct. 1989 14 p Presented at the Workshop on Primordial Nucleosynthesis, Chapel Hill, NC, 6-8 Oct. 1989
(Contract W-7405-eng-48)
(DE90-003594; UCRL-102181; CONF-8910320-1) Avail: NTIS HC A03/MF A01

The uncertainties in the nuclear input data relevant for calculations of standard and non-standard primordial nucleosynthesis are discussed. It is shown how these uncertainties can affect the predictive power of such calculations, and those key nuclear reactions for which improved experimental data on the associated reaction rates is most needed are identified. Such experimental data can lead to more accurate discriminatory tests between the differing primordial nucleosynthesis scenarios. DOE

N90-16667# Lawrence Livermore National Lab., CA. Physics Dept.
ION-HEATED THERMAL COMPTONIZATION MODELS AND X RAY SPECTRAL CORRELATIONS IN ACTIVE GALACTIC NUCLEI
Charles D. Dermer Nov. 1989 7 p Presented at the 23rd ESLAB Symposium on X Ray Astronomy, Bologna, Italy, 13-20 Sep. 1989
(Contract W-7405-eng-48)
(DE90-003597; UCRL-102238; CONF-8909275-1) Avail: NTIS HC A02/MF A01

Recent Ginga observations of the Seyfert 1 galaxies NGC 4051 and MCG 6-30-15 show a positive correlation between the 2 to 10 keV luminosity and photon spectral index (alpha). Similar behavior has also been reported in Exosat and Einstein observations of other active galactic nuclei, and is suggested in hard x ray low-state data of the galactic black-hole candidate Cygnus X-1. A two-temperature thermal Comptonization model with internal soft-photon production provides a simple explanation for this correlation. The electron temperature, determined by a balance between ion heating and radiative cooling, decreases in response to an enhancement of the soft photon flux, resulting in a softening of the spectrum and an increase in the soft x ray luminosity. The bulk of the soft photons are produced through pion production in collisions between the hot ions. Pivoting of the spectrum at photon energies epsilon greater than 50 keV is a consequence of variations in the ion temperature. An important test of the model would be time correlations between soft and hard x ray bands. DOE

N90-16668# International Centre for Theoretical Physics, Trieste (Italy).
ON QUANTUM EFFECTS NEAR A BLACK HOLE SINGULARITY
Asghar Qadir and Azad A. Siddiqui (Quaid-i-Azam Univ., Islamabad, Pakistan) Jun. 1989 5 p
(DE90-600754; IC-89/153) Avail: NTIS (US Sales Only) HC A01/MF A01

It is pointed out that the claim made by Joshi and Joshi, was not rigorously demonstrated by them. A simpler and more correct proof is provided. DOE

N90-16669# Geneva Observatory (Switzerland).
NEW DEVELOPMENTS IN STELLAR AGES AND MODELLING OF POP. I STARS
A. Maeder and E. Vaugioni-Flam, ed. 1989 10 p Presented at the 5th IAP Astrophysics Meeting on Astrophysical Ages and Dating Methods, Jun. 1989 Submitted for publication
(Ser-C-Prepubl-Fasc-41; ETN-90-96152) Avail: NTIS HC A02/MF A01

Basic sets of isochrones and stellar lifetimes with up to date ingredients are given. The large changes in the age determinations, due to the overshooting from convective cores, are discussed. Comparisons with observations confirm the need of overshooting for stars with M equal or superior to 45 of the solar mass. Below this mass limit, there is a short transition interval such that, at about 1.2 of the solar mass in population 1 stars, there is no longer evidence of overshooting and convective cores. In the case of massive stars it is shown that dependence of the mass loss rates on metallicity Z of the form M approximately equal to Z to the 0.5th power allows the distribution of O and WR stars in different galaxies to be explained. The important consequences of this M versus Z relation on the stellar nucleosynthesis are mentioned, in particular on the (delta Y)/(delta Z) ratios. ESA

N90-16670# Consiglio Nazionale delle Ricerche, Frascati (Italy). Ist. di Fisica dello Spazio Interplanetario.
CORRELATIVE ANALYSES FOR GEOMAGNETIC INDICES, COSMIC-RAY INTENSITIES AND SUNSPOT NUMBERS RECORDED SINCE 1937
Marisa Storini, Ottavia BorelloFilisetti, Vittorio Mussino, and Mario Parisi (Rome Univ., Italy) Feb. 1989 25 p Presented at the 1st Latin-American Conference on Space Geophysics, Aguas de Lindoia, Brazil, 21-25 Nov. 1988 Sponsored in part by the Italian Ministry of Public Education
(IFSI-89-4; ETN-90-96166) Avail: NTIS HC A03/MF A01

A statistical study between the cosmic ray intensities, the sigma Kp geomagnetic indices and the sunspot numbers, from 1937 to 1986 on a monthly basis, is presented. The results suggest that the latitudinal dependence for the charged particle propagation in the interplanetary space, is badly checked by correlative analyses inside solar cycle phases. The strong correlation between cosmic ray intensities and the sigma Kp values obtained between the 19th solar cycle maximum and the 20th one and the poor correlation between the 20th solar cycle maximum and the 21st one can be explained. The negligible areas towards the helioequator covered by polar coronal holes, during the descending phase of the 19th cycle and vast areas during the 20th one, are taken into account. ESA

N90-16671# Consiglio Nazionale delle Ricerche, Frascati (Italy). Ist. di Fisica dello Spazio Interplanetario.
A COMPUTER PROGRAM TO CALCULATE THE POPULATION NUMBERS OF MULTI-LEVEL SPECIES
J. Michael (Jacksonville Univ., FL.) Sep. 1989 39 p
(IFSI-89-15; ETN-90-96177) Avail: NTIS HC A03/MF A01

A program designed to calculate the ratio of the intensities of the transition of one ion to the transistion of another (or the same) ion is presented. It is useful in astrophysical applications. The determination of how the ions and molecules, in the regions where stars may form, are distributed. This is achieved for non-degenerate matter by solving the equations of statistical equilibrium. The computer program solves the equations assuming steady state conditions. The calculations of the program are coded in a general way so that it may be expanded for ions of N levels, which improves the accuracy in all cases. The level populations are calculated for various values of the temperature and density of the gas where the ion is located, and the intensities of transistions found. The ions are considered as having two or three fine structure levels. ESA

N90-16672# European Space Agency, Paris (France).
IUE-ULDA ACCESS GUIDE NO. 1: INTERNATIONAL ULTRAVIOLET EXPLORER-UNIFORM LOW DISPERSION ARCHIVE. DWARF NOVAE AND NOVA-LIKE STARS
Constanze laDous, comp. Sep. 1989 179 p
(ESA-SP-1114; ISBN-92-9092-024-6; ISSN-0379-6566; ETN-90-96198) Copyright Avail: NTIS HC A09/MF A01; ESA Publications Div., ESTEC, Noordwijk, Netherlands, 40 Dutch guilders

Background information on all the low resolution International Ultraviolet Explorer (IUE) spectra of dwarf novae and nova-like stars taken until the end of 1987 is presented. The work is performed in order to enable optimum usage of the low resolution IUE - ULDA (uniform low dispersion archive). Details on the individual exposures and their position in the outburst light curves are given. Physical information about each system, and a comprehensive list of references for published observations in all wavelength ranges, are provided. In particular, the following topics are also considered: description of the data, system parameters, the American Association of Variable Star Observers light curves and published IUE observations. ESA

N90-16673 Max-Planck-Inst. fuer Physik und Astrophysik, Garching (Germany, F.R.). Inst. fuer Extraterrestrische Physik.
EXOSAT MEASUREMENTS OF THE PULSE PERIOD OF VELA X-1
B. C. Raubenheimer and Hakki Oegelman Jul. 1989 13 p Submitted for publication
(Contract DFG-Mo-416/3-3)
(MPE-Preprint-157; ISSN-0178-0719; ETN-90-96046) Copyright Avail: Fachinformationszentrum Karlsruhe, 7514 Eggenstein-Leopoldshafen 2, Fed. Republic of Germany

Seven pulse period determinations of Vela X-1 are performed, using the existing EXOSAT data. The measurements span one year and partly fill in the 3.2 year gap between Tenma and Ginga measurements. The results show that the pulse period of Vela X-1 continued with an epoch of near constant period (from 1981 up to at least May 1985). Using all the period determinations from 1975 to 1988, the model in which white torque noise is responsible for the pulse period changes of the neutron is confirmed. It is also shown that the reported TeV gamma ray period measuremnts do not fall in the allowed range of this model. ESA

N90-16674# Lawrence Livermore National Lab., CA. Inst. of Geophysics and Planetary Physics.
TURBULENT STRIPPING OF INTERSTELLAR CLOUDS BY INTERACTION WITH SUPERNOVA REMNANTS
Richard I. Klein, Christopher F. McKee, Philip Colella, and Leo Blitz, ed. Sep. 1989 21 p Presented at the Centennial Meeting of the American Astronomical Society of the Pacific, Berkeley, CA, 21-23 Jun. 1989 Submitted for publication
Prepared in cooperation with California Univ., Berkeley
(Contract W-7405-eng-48)
(DE90-003622; UCRL-101851; CONF-8906257-1) Avail: NTIS HC A03/MF A01

Results are presented for the interaction of a supernovae remnant blast wave with a small interstellar cloud, using for the first time high resolution local adaptive mesh refinement techniques with an underlying second order accurate 2-D Godunov hydrodynamic scheme. The cloud shock is assumed to be strong enough that it is non-radiative. The morphological evolution of the cloud is followed in great detail as it undergoes a series of complex shock-shock interactions and Kelvin-Helmholtz and Rayleigh-Taylor instabilities. It is demonstrated over a large range of cloud densities and shock strengths, that clouds are efficiently destroyed in a few cloud crushing times (essentially, the Rayleigh Taylor time) by a combination of instabilities and large scale shear flow. The scaling properties of clouds of different densities and shocks of different strengths are investigated. The results have uncovered the development of copious supersonic vortex rings produced in the shear flow layer of the interaction. These vortex rings may wrap up ambient magnetic fields, enhancing the synchrotron emission and possibly explaining the compact radio hot spots seen in Cas A. Calculations have carried, for the first time, the cloud-shock interaction well into the fragmentation regime. It is demonstrated that similar calculations with standard fixed grid hydrodynamic schemes would require one to two orders of magnitude more computational time than is needed with the adaptive mesh approach to achieve comparable results. DOE

91 LUNAR AND PLANETARY EXPLORATION

Includes planetology; and manned and unmanned flights.
For spacecraft design or space stations see *18 Spacecraft Design, Testing and Performance.*

N90-16675*# Jet Propulsion Lab., California Inst. of Tech., Pasadena.
NEPTUNE'S TRITON: A MOON RICH IN DRY ICE AND CARBON
A. J. R. Prentice 15 Aug. 1989 18 p Submitted for publication
(Contract NAS7-918)
(NASA-CR-186298; NAS 1.26:186298; JPL-89-37) Avail: NTIS HC A03/MF A01 CSCL 03B

The encounter of the spacecraft Voyager 2 with Neptune and its large satellite Triton in August 1989 will provide a crucial test of ideas regarding the origin and chemical composition of the outer solar system. In this pre-encounter publication, the possibility is quantified that Titron is a captured moon which, like Pluto and Charon, originally condensed as a major planetesimal within the gas ring that was shed by the contracting protosolar cloud at Neptune's orbit. Ideas of supersonic convective turbulence are used to compute the gas pressure, temperature and rat of catalytic synthesis of CH4, CO2, and C(s) within the protosolar cloud, assuming that all C is initially present as CO. The calculations lead to a unique composition for Triton, Pluto, Charon: each body consists of, by mass, 18 1/2 percent solid CO2 ice, 4 percent graphite, 1/2 percent CH4 ice, 29 percent methanated water ice and 48 percent of anhydrous rock. This mix has a density consistent with that of the Pluto-Charon system and yields a predicted mean density for Triton of 2.20 + or - 0.5 g/cu cm, for satellite radius equal to 1,750 km. Author

92 SOLAR PHYSICS

Includes solar activity, solar flares, solar radiation and sunspots.

For related information see *93 Space Radiation.*

N90-16676*# California Univ., San Diego, La Jolla. Center for Astrophysics and Space Sciences.

DETERMINATION OF SOLAR FLARE ACCELERATED ION ANGULAR DISTRIBUTIONS FROM SMM GAMMA RAY AND NEUTRON MEASUREMENTS AND DETERMINATION OF THE He-3/H RATIO IN THE SOLAR PHOTOSPHERE FROM SMM GAMMA RAY MEASUREMENTS Final Technical Report, 1 Jul. 1987 - 31 Aug. 1989

Richard E. Lingenfelter Aug. 1989 7 p

(Grant NAG5-945)

(NASA-CR-186038; NAS 1.26:186038) Avail: NTIS HC A02/MF A01 CSCL 03B

Comparisons of Solar Maximum Mission (SMM) observations of gamma-ray line and neutron emission with theoretical calculation of their expected production by flare accelerated ion interactions in the solar atmosphere have led to significant advances in the understanding of solar flare particle acceleration and interaction, as well as the flare process itself. These comparisons have enabled the determination of, not only the total number and energy spectrum of accelerated ions trapped at the sun, but also the ion angular distribution as they interact in the solar atmosphere. The Monte Carlo program was modified to include in the calculations of ion trajectories the effects of both mirroring in converging magnetic fields and of pitch angle scattering. Comparing the results of these calculations with the SMM observations, not only the angular distribution of the interacting ions can be determined, but also the initial angular distribution of the ions at acceleration. The reliable determination of the solar photospheric He-3 abundance is of great importance for understanding nucleosynthesis in the early universe and its implications for cosmology, as well as for the study of the evolution of the sun. It is also essential for the determinations of the spectrum and total number of flare accelerated ions from the SMM/GRS gamma-ray line measurements. Systematic Monte Carlo calculations of the time dependence were made as a function of the He-3 abundance and other variables. A new series of calculations were compared for the time-dependent flux of 2.223 MeV neutron capture line emission and the ratio of the time-integrated flux in the 2.223 MeV line to that in the 4.1 to 6.4 MeV nuclear deexcitation band. Author

N90-16677# Geneva Observatory (Switzerland).

A LOOK ON NON-STANDARD SOLAR MODELS

A. Maeder, G. Berthomiev, ed., and M. Cribier, ed. 1989 7 p Presented at the IAU Colloquium 121 on Inside the Sun, Versailles, France, May 1989 Submitted for publication

(Ser-C-Prepubl-Fasc-40; ETN-90-96151) Avail: NTIS HC A02/MF A01

Some of the nonstandard solar models, proposed in the last two decades, are reviewed. Their main physical assumptions are shown. The way they meet or do not meet the observational constraints are discussed. The models with additional effects in classical physics and the exotic models are studied. The question whether a model must be changed or not, is considered. The large number of observational tests, more accurate than 30 years ago, are listed. None of the non standard models are submitted to these tests. The observational data plays an important role with respect to progress in stellar evolution. ESA

N90-16678# Consiglio Nazionale delle Ricerche, Frascati (Italy). Ist. di Fisica dello Spazio Interplanetario.

SOME PROPERTIES OF SO-CALLED MAGNETIC CLOUD STRUCTURES IN THE SOLAR WIND

B. Bavassano, Marisa Storini, N. Iucci, and Mario Parisi (Rome Univ., Italy) Oct. 1988 9 p Presented at 27th COSPAR Plenary Meeting, Espoo, Finland, 18-29 Jul. 1988 Previously announced in IAA as A89-46163

(IFSI-88-16; ETN-90-96155) Avail: NTIS HC A02/MF A01

Three short term increases observed in the nucleonic component of galactic cosmic rays from 2 to 6 Apr. 1979 are investigated. Their relation to mesoscale structures of the solar wind to bidirectional fluxes of low energy (lower than 1 MeV) cosmic rays is analyzed. For each event an isolated rotational structure is identified in the Interplanetary Magnetic Field (IMF). Good agreement between the magnetic behavior and short term cosmic ray increases is found. Cosmic ray features suggest, for the associated solar-wind structure, a spatial dimension bigger than that derived from the IMF rotational period ESA

N90-16679# Consiglio Nazionale delle Ricerche, Frascati (Italy). Ist. di Fisica dello Spazio Interplanetario.

GALACTIC COSMIC-RAY MODULATION AND SOLAR-TERRESTRIAL RELATIONSHIPS

Marisa Storini Oct. 1988 29 p Presented at the 4th Cosmic-Physics National Conference, Anacapri, Italy, 11-14 Sep. 1988

(IFSI-88-17; ETN-90-96156) Avail: NTIS HC A03/MF A01

Examples of the recent Italian scientific undertaking on galactic cosmic ray modulation, are given. Current ideas from the international community on long-term effects are discussed. The nucleonic component of primary cosmic rays is the appropriate one to study solar modulation from ground based measurements. Continuous registrations of this component started in the fifties in different sites of the Earth and since then a world wide network of neutron monitors, was established. Nucleonic intensities were recorded since July 1957 at Rome. Only a brief selection among many valuable works related to cosmic rays modulation. Space limitations do not permit a deeper discussion on the subject. Indirect methods to study cosmic ray modulation phenomena emerge from the analysis of cosmogenic nuclei contained in terrestrial and extraterrestrial samples. ESA

93 SPACE RADIATION

Includes cosmic radiation; and inner and outer earth's radiation belts.

For biological effects of radiation see *52 Aerospace Medicine.* For theory see *73 Nuclear and High-Energy Physics.*

N90-16680# California Univ., Berkeley. Lawrence Berkeley Lab. Nuclear Science Div.

COSMIC RAY HALF LIFE OF Ni-56

E. B. Norman, B. Sur, K. T. Lesko, R.-M. Larimer, and E. Browne Aug. 1989 3 p Presented at the 21st International Cosmic Ray Conference, Adelaide, Australia, 6-19 Jan. 1990

(Contract DE-AC03-76SF-00098)

(DE90-000132; LBL-27673; CONF-900129-2) Avail: NTIS HC A01/MF A01

A search for the beta(+) decay of Ni-56 established an upper limit on the branching ratio of 7.2 x 10(exp -7) for the most likely such transition. This provides a lower limit of 2.3 x 10(exp 4) years for the cosmic ray half life of Ni-56. DOE

N90-16681*# National Aeronautics and Space Administration. Goddard Space Flight Center, Greenbelt, MD.

A DATABASE OF FRAGMENTATION CROSS SECTION MEASUREMENTS APPLICABLE TO COSMIC RAY PROPAGATION CALCULATIONS

H. J. Crawford, J. Engelage, F. C. Jones, T. G. Guzik, J. W. Mitchell, J. P. Wefel, C. J. Waddington, W. R. Webber, A. Soutoul, and P. Ferrando (Commissariat a l'Energie Atomique, Saclay, France) et al Aug. 1989 6 p Presented at the 21st International Cosmic Ray Conference, Adelaide, Australia, 6-19 Jan. 1990 Prepared in cooperation with California Univ., Berkeley. Lawrence Berkeley Lab.

(Contract DE-AC03-76SF-00098)

(NASA-CR-186328; NAS 1.26:186328; DE90-002683; LBL-27725; CONF-900122-5) Avail: NTIS HC A02/MF A01 CSCL 03B

A database of single particle inclusive fragment production cross section measurements was established and is accessible

over common computer networks. These measurements were obtained from both published literature and direct communication with experimenters and include cross sections for nuclear beams on H, He, and heavier targets, and for H and He beams on nuclear targets, for energies greater than 30 MeV/nucleon. These cross sections are directly applicable to calculations involving cosmic ray nuclear interactions with matter. The data base includes projectile, target, and fragment specifications, beam energy, cross section with uncertainty, literature reference, and comment code. It is continuously updated to assure accuracy and completeness. Also available are widely used semi-empirical formulations for calculating production cross sections and excitation functions. The data base is discussed in detail and how it can be accessed, is described. The measurements are compared with semi-empirical calculations and areas are pointed out where improved calculations and further cross section measurements are required. DOE

N90-16682# Lawrence Livermore National Lab., CA.
USE OF THE EGRET INSTRUMENT IN STUDIES OF THE ORIGIN OF THE COSMIC RADIATION. 2: SPECTRAL SIGNATURES OF DISCRETE COSMIC-RAY SOURCES
Charles D. Dermer 27 Oct. 1989 6 p Presented at the 21st International Cosmic Ray Conference, Adelaide, Australia, 6-19 Jan. 1990 Submitted for publication
(Contract W-7405-eng-48)
(DE90-003595; UCRL-102243-2; CONF-900129-4-2) Avail: NTIS HC A02/MF A01

This is a continuation of previous studies aimed at predicting spectral signatures of discrete cosmic ray sources. A formalism is developed and presented for calculating gamma ray spectra observed at Earth from the decay of neutral pions formed in collisions of cosmic ray protons and ions with galactic gas and dust. The cosmic rays are assumed to be emitted by discrete sources, and their intensities and spectra are described by solutions to a diffusion equation. Calculations of spectral signatures expected from these hypothetical point sources of cosmic rays are presented. In particular, a steady source of cosmic rays could show a harder gamma ray spectrum than the spectrum of the diffuse galactic background, whereas an impulsive source of cosmic rays could show a much softer spectrum. Observations of the angular variations of gamma ray intensities and spectra near point sources will provide information on cosmic ray propagation in other parts of our galaxy, as well as on the nature of the discrete sources themselves. Capabilities of the Egret telescope in mapping spectra from cosmic ray point sources are briefly discussed. DOE

N90-16683*# National Aeronautics and Space Administration. Goddard Space Flight Center, Greenbelt, MD.
THE EXCESS FLUX IN THE COSMIC SUBMILLIMETER BACKGROUND RADIATION AND THE PRIMORDIAL DEUTERIUM ABUNDANCE
Charles D. Dermer (Lawrence Livermore National Lab., CA.) and N. Guessoum 27 Oct. 1989 6 p Presented at the 21st International Cosmic Ray Conference, Adelaide, Australia, 6-19 Jan. 1990 Submitted for publication
(Contract W-7405-eng-48)
(NASA-CR-186312; NAS 1.26:186312; DE90-003602; UCRL-102240; CONF-900129-3) Avail: NTIS HC A02/MF A01 CSCL 03B

Recent measurements of the cosmic background radiation (CBR) show an enhanced flux in the submillimeter regime, compared to the spectrum of a 2.7 K blackbody. Thermal Comptonization of the relic radiation by a hot nonrelativistic plasma has long been known to produce distortions in the CBR spectrum, similar to what has now been observed. Heating of the primeval plasma to temperatures T approx. 10(exp 6) to 10(exp 8) K could result from the injection of subcosmic ray protons at epoch z approx. 10 to 100. The intensity of the subcosmic ray flux that provide conditions needed to explain the submillimeter excess by thermal Comptonization also leads to the production of cosmologically significant amounts of deuterium in collisions between subcosmic ray protons and primordial protons and alpha-particles. However, the amount of lithium produced through alpha-alpha reactions is in conflict with the observed Li abundance. If lithium is depleted, for example, by processing through Population II stars, arguments for the baryon content of the universe based on primordial deuterium and He abundances are weakened. DOE

N90-16684# Consiglio Nazionale delle Ricerche, Frascati (Italy). Ist. Fisica Spazio Interplanetario.
COSMIC RAY NM-64 NEUTRON MONITOR DATA 16 Annual Report, Jan. - Dec. 1987
N. Iucci, F. Re, F. Signoretti, C. Signorini, G. Villoresi, and N. L. Zangrilli Dec. 1988 56 p Prepared in cooperation with Rome Univ., Italy
(IFSI-88-21; ETN-90-96160) Avail: NTIS HC A04/MF A01

Pressure corrected data from the Rome neutron monitor and barometric pressure data for the year 1987 are given. Tables and graphs of the corrected intensity are provided. Details on the devices employed, operational mode and data handling are considered. The following topics are examined: monitor, atmospheric pressure measurement, data acquisition system, stability, efficiency changes, barometric correction, references, normalization factors, and section ratios. ESA

N90-16685# Oak Ridge National Lab., TN. Engineering Physics and Mathematics Div.
THE EFFECTS OF NATURAL AND ENHANCED VAN ALLEN BELT RADIATION ON A SPACE BASED WEAPON PLATFORM
R. T. Santoro, J. M. Barnes, and J. O. Johnson 1990 5 p Presented at the HEART Conference, Monterey, CA, 12-16 Feb. 1990 Sponsored in part by AF
(Contract DE-AC05-84OR-21400)
(DE89-016219; CONF-900216-2) Avail: NTIS HC A01/MF A01

Monte Carlo radiation transport calculations have been performed to estimate the effects of natural (protons and electrons) and weapon enhanced (electron) Van Allen Belt (VAB) radiation on a space deployed weapon platform. (The satellite configuration adopted for this study represents the authors' concept of such a system.) The purpose of this study was to evaluate the long term and transient effects of these radiation modes on the components of a satellite deployed in a circular orbit at an altitude of 500 km and inclination angle of 0-deg. These kinds of satellites must survive long-term (up to 10 years) exposure to the natural radiation environment and the effects of enhanced radiation introduced when nuclear weapons are detonated in space. This paper describes the platform/weapon system and its components, the Van Allen Belt spectra, the methods of calculation, and summarizes the radiation damage to platform components from VAB protons and electrons and enhanced electron belt radiation. DOE

99 GENERAL

N90-16686*# University of Central Florida, Orlando.
NASA/ASEE SUMMER FACULTY FELLOWSHIP PROGRAM
E. Ramon Hosler, ed. and Dennis W. Armstrong, ed. (National Aeronautics and Space Administration. John F. Kennedy Space Center, Cocoa Beach, FL.) Oct. 1989 420 p Program held at Merritt Island, FL, 5 Jun. - 11 Aug. 1989; sponsored by the Univ. of Central Florida and NASA, Washington
(NASA-CR-166837; NAS 1.26:166837) Avail: NTIS HC A18/MF A03 CSCL 05I

The contractor's report contains all sixteen final reports prepared by the participants in the 1989 Summer Faculty Fellowship Program. Reports describe research projects on a number of different topics. Interface software, metal corrosion, rocket triggering lightning, automatic drawing, 60-Hertz power, carotid-cardiac baroreflex, acoustic fields, robotics, AI, CAD/CAE, cryogenics, titanium, and flow measurement are discussed. For individual titles, see N90-16687 through N90-16702.

N90-16687*# California State Univ., Fresno. Dept. of Computer Science.
FORMALISMS FOR USER INTERFACE SPECIFICATION AND DESIGN **c60**
Brent J. Auernheimer *In* University of Central Florida, NASA/ASEE Summer Faculty Fellowship Program Oct. 1989 p 1-23 (For primary document see N90-16686 08-99)
Avail: NTIS HC A18/MF A03 CSCL 09B

The application of formal methods to the specification and design of human-computer interfaces is described. A broad outline of human-computer interface problems, a description of the field of cognitive engineering and two relevant research results, the appropriateness of formal specification techniques, and potential NASA application areas are described. Author

N90-16688*# Randolph-Macon Coll., Ashland, VA. Dept. of Chemistry.
STUDY OF METAL CORROSION USING ac IMPEDANCE TECHNIQUES IN THE STS LAUNCH ENVIRONMENT **c26**
Luz M. Calle *In* University of Central Florida, NASA/ASEE Summer Faculty Fellowship Program Oct. 1989 p 24-57 (For primary document see N90-16686 08-99)
Avail: NTIS HC A18/MF A03 CSCL 11F

AC impedance measurements were performed to investigate the corrosion resistance of 19 alloys under conditions similar to the STS launch environment. The alloys were: Zirconium 702, Hastelloy C-22, Inconel 625, Hastelloy C-276, Hastelloy C-4, Inconel 600, 7Mo + N, Ferralium 255, Inco Alloy G-3, 20Cb-3, SS 904L, Inconel 825, SS 304LN, SS 316L, SS 317L, ES 2205, SS 304L, Hastelloy B-2, and Monel 400. AC impedance data were gathered for each alloy after one hour immersion time in each of the following three electrolyte solutions: 3.55 percent NaCl, 3.55 percent NaCl-0.1N HCl, and 3.55 percent NaCl-1.0N HCl. The data were analyzed qualitatively using the Nyquist plot and quantitatively using the Bode plot. Polarization resistance, Rp, values were obtained using the Bode plot. Zirconium 702 was the most corrosion resistant alloy in the three electrolytes. The ordering of the other alloys according the their resistance to corrosion varied as the concentration of hydrochloric acid in the electrolyte increased. The corrosion resistance of Zirconium 702 and Ferralium 255 increased as the concentration of hydrochloric acid in the electrolyte increased. The corrosion resistance of the other 17 alloys decreased as the concentration of the hyrdochloric acid in the electrolyte increased. Author

N90-16689*# Massachusetts Univ., Amherst. Dept. of Plant and Soil Sciences.
DYNAMICS OF CARBON DIOXIDE EXCHANGE OF A WHEAT COMMUNITY GROWN IN A SEMI-CLOSED ENVIRONMENT **c51**
Kenneth A. Corey *In* University of Central Florida, NASA/ASEE Summer Faculty Fellowship Program Oct. 1989 p 58-84 (For primary document see N90-16686 08-99)
Avail: NTIS HC A18/MF A03 CSCL 06B

A wheat (Triticum aestivum Yecora Rojo) community was grown in the semi-closed conditions of the NASA/KSC Biomass Production Chamber (BPC). Experiments were conducted to determine whole community carbon dioxide exchange rates as influenced by growth and development, carbon dioxide concentration, time within the photoperiod, irradiance, and temperature. Plants were grown at a population of about 1500 per sq meter using a 20 hour light/4 hour dark daily regime. Light was supplied by HPS vapor lamps and irradiance was maintained in the range of 590 to 675 mu mol per sq meter. The temperature regime was 20 C light/16 C dark and nutrients were supplied hydroponically as a thin film. Fractional interception of PPF by the community increased rapidly during growth reaching a maximum of 0.96, 24 days after planting. This time corresponded to canopy closure and maximum rates of net photosynthesis (NP). Net daily CO2 utilization rates were calculated to day 48 and a 4th order regression equation integrated to obtain total moles of CO2 fixed by the community. This procedure may be useful for monitoring and prediction of biomass yields in a closed ecology life support system (CELSS). Author

N90-16690*# Auburn Univ., AL. Dept. of Aerospace Engineering.
ROCKET-TRIGGERED LIGHTNING STRIKES AND FOREST FIRE IGNITION **c47**
James H. Fenner *In* University of Central Florida, NASA/ASEE Summer Faculty Fellowship Program Oct. 1989 p 85-101 (For primary document see N90-16686 08-99)
Avail: NTIS HC A18/MF A03 CSCL 04B

Background information on the rocket-triggered lightning project at Kennedy Space Center (KSC), a summary of the forecasting problem there, the facilities and equipment available for undertaking field experiments at KSC, previous research activity performed, a description of the atmospheric science field laboratory near Mosquito Lagoon on the KSC complex, methods of data acquisition, and present results are discussed. New sources of data for the 1989 field experiment include measuring the electric field in the lower few thousand feet of the atmosphere by suspending field measuring devices below a tethered balloon. Problems encountered during the 1989 field experiment are discussed. Future prospects for both triggered lightning and lightning-kindled forest fire research at KSC are listed. Author

N90-16691*# Oklahoma State Univ., Stillwater. Dept. of Psychology.
THE DAB MODEL OF DRAWING PROCESSES **c63**
Larry W. Hochhaus *In* University of Central Florida, NASA/ASEE Summer Faculty Fellowship Program Oct. 1989 p 102-124 (For primary document see N90-16686 08-99)
Avail: NTIS HC A18/MF A03 CSCL 09B

The problem of automatic drawing was investigated in two ways. First, a DAB model of drawing processes was introduced. DAB stands for three types of knowledge hypothesized to support drawing abilities, namely, Drawing Knowledge, Assimilated Knowledge, and Base Knowledge. Speculation concerning the content and character of each of these subsystems of the drawing process is introduced and the overall adequacy of the model is evaluated. Second, eight experts were each asked to understand six engineering drawings and to think aloud while doing so. It is anticipated that a concurrent protocol analysis of these interviews can be carried out in the future. Meanwhile, a general description of the videotape database is provided. In conclusion, the DAB model was praised as a worthwhile first step toward solution of a difficult problem, but was considered by and large inadequate to the challenge of automatic drawing. Suggestions for improvements on the model were made. Author

N90-16692*# Savannah State Coll., GA. Dept. of Engineering Technology.
ANALYSIS OF THE 60-Hz POWER SYSTEM AT KSC: THE ORSINO SUBSTATION **c31**
Alex O. Kalu *In* University of Central Florida, NASA/ASEE Summer Faculty Fellowship Program Oct. 1989 p 125-158 (For primary document see N90-16686 08-99)
Avail: NTIS HC A18/MF A03 CSCL 10B

An analysis of the Orsino Substation, a component (50 percent) of the 60-Hertz electric power system at the Kennedy Space Center, is presented. Presented here are separate single-line diagrams of the sixteen feeder circuits to permit easy access to information on the individual feeders for future planning. The load condition of each feeder and load break switch are presented and a heuristic reliability analysis of the system is performed. Information is given about the system fashion useful for decision making purposes. The beauty of it is in the simplified manner by which information about the system can be obtained. Author

N90-16693*# North Carolina Univ., Greensboro. Dept. of Mathematics.
FACTOR ANALYTIC REDUCTION OF THE CAROTID-CARDIAC BAROREFLEX PARAMETERS **c52**
David A. Ludwig *In* University of Central Florida, NASA/ASEE

Summer Faculty Fellowship Program Oct. 1989 p 159-170
(For primary document see N90-16686 08-99)
Avail: NTIS HC A18/MF A03 CSCL 06P

An accepted method for measuring the responsiveness of the carotid-cardiac baroreflex to arterial pressure changes is to artificially stimulate the baroreceptors in the neck. This is accomplished by using a pressurized neck cuff which constricts and distends the carotid artery and subsequently stimulates the baroreceptors. Nine physiological responses to this type of stimulation are quantified and used as indicators of the baroreflex. Thirty male humans between the ages 27 and 46 underwent the carotid-cardiac baroreflex test. The data for the nine response parameters were analyzed by principle component factor analysis. The results of this analysis indicated that 93 percent of the total variance across all nine parameters could be explained in four dimensions. Examination of the factor loadings following an orthogonal rotation of the principle components indicated four well defined dimensions. The first two dimensions reflected location points for R-R interval and carotid distending pressure respectively. The third dimension was composed of measures reflecting the gain of the reflex. The fourth dimension was the ratio of the resting R-R interval to R-R interval during simulated hypertension. The data suggests that the analysis of all nine baroreflex parameters is redundant. Author

N90-16694*# Indiana Univ.-Purdue Univ., Fort Wayne. Dept. of Engineering.
MODELING THE NEAR ACOUSTIC FIELD OF A ROCKET DURING LAUNCH **c71**
David W. Mauritzen *In* University of Central Florida, NASA/ASEE Summer Faculty Fellowship Program Oct. 1989 p 171-202
(For primary document see N90-16686 08-99)
Avail: NTIS HC A18/MF A03 CSCL 20A

The design of launch pad structures is critically dependent upon the stresses imposed by the acoustical pressure field generated by the rocket engines during launch. The purpose of this effort is to better describe the acoustical field in the immediate launch area. Since the problem is not analytically tractable, empirical modeling will be employed so that useful results may be obtained for structural design purposes. The plume of the rocket is considered to be a volumetric acoustic source, and is broken down into incremental contributing volumes. A computer program has been written to sum all the contributions to find the total sound pressure level at an arbitrary point. A constant density source is initially assumed and the acoustic field evaluated for several cases to verify the correct operation of the program. Author

N90-16695*# Purdue Univ., West Lafayette, IN. Dept. of Agricultural Engineering.
PLANT FEATURES MEASUREMENTS FOR ROBOTICS **c51**
Gaines E. Miles *In* University of Central Florida, NASA/ASEE Summer Faculty Fellowship Program Oct. 1989 p 203-225
(For primary document see N90-16686 08-99)
Avail: NTIS HC A18/MF A03 CSCL 06C

Initial studies of the technical feasibility of using machine vision and color image processing to measure plant health were performed. Wheat plants were grown in nutrient solutions deficient in nitrogen, potassium, and iron. An additional treatment imposed water stress on wheat plants which received a full complement of nutrients. The results for juvenile (less than 2 weeks old) wheat plants show that imaging technology can be used to detect nutrient deficiencies. The relative amount of green color in a leaf declined with increased water stress. The absolute amount of green was higher for nitrogen deficient leaves compared to the control plants. Relative greenness was lower for iron deficient leaves, but the absolute green values were higher. The data showed patterns across the leaf consistent with visual symptons. The development of additional color image processing routines to recognize these patterns would improve the performance of this sensor of plant health. Author

N90-16696*# Florida Inst. of Tech., Melbourne. Dept. of Mechanical and Aerospace Engineering.
ON THE SELECTION OF MATERIALS FOR CRYOGENIC SEALS AND THE TESTING OF THEIR PERFORMANCE **c37**
John M. Russell *In* University of Central Florida, NASA/ASEE Summer Faculty Fellowship Program Oct. 1989 p 226-269
(For primary document see N90-16686 08-99)
Avail: NTIS HC A18/MF A03 CSCL 11A

Three questions are addressed: what mission must a cryogenic seal perform; what are the contrasts between desirable and available seal materials; and how realistic must test conditions be. The question of how to quantify the response of a material subject to large strains and which is susceptible to memory effects leads to a discussion of theoretical issues. Accordingly, the report summarizes some ideas from the rational mechanics of materials. The report ends with a list of recommendations and a conclusion. Author

N90-16697*# Mississippi State Univ., State College. Dept. of Mechanical Engineering.
ARTIFICIAL INTELLIGENCE IN PROCESS CONTROL: KNOWLEDGE BASE FOR THE SHUTTLE ECS MODEL **c63**
A. Kent Stiffler *In* University of Central Florida, NASA/ASEE Summer Faculty Fellowship Program Oct. 1989 p 270-291
(For primary document see N90-16686 08-99)
Avail: NTIS HC A18/MF A03 CSCL 09B

The general operation of KATE, an artificial intelligence controller, is outlined. A shuttle environmental control system (ECS) demonstration system for KATE is explained. The knowledge base model for this system is derived. An experimental test procedure is given to verify parameters in the model. Author

N90-16698*# Murray State Univ., KY. Dept. of Engineering Technology.
THE EFFECTS OF HYDROGEN EMBRITTLEMENT OF TITANIUM **c26**
Delbert J. Taylor *In* University of Central Florida, NASA/ASEE Summer Faculty Fellowship Program Oct. 1989 p 292-302
(For primary document see N90-16686 08-99)
Avail: NTIS HC A18/MF A03 CSCL 11F

Titanium alloys, by virtue of their attractive strength to density ratio, fatigue, fracture toughness and corrosion resistance are now commonly used in various aerospace and marine applications. The cost, once very expensive, has been reduced, making titanium even more of a competitive material today. Titanium and titanium alloys have a great affinity to several elements. Hydrogen, even in small amounts, can cause embrittlement, which in turn causes a reduction in strength and ductility. The reduction of strength and ductility is the subject of this investigation. Author

N90-16699*# Lehigh Univ., Bethlehem, PA. Dept. of Industrial Engineering.
OFF-LINE ROBOT PROGRAMMING AND GRAPHICAL VERIFICATION OF PATH PLANNING **c61**
Gregory L. Tonkay *In* University of Central Florida, NASA/ASEE Summer Faculty Fellowship Program Oct. 1989 p 303-323
(For primary document see N90-16686 08-99)
Avail: NTIS HC A18/MF A03 CSCL 09B

The objective of this project was to develop or specify an integrated environment for off-line programming, graphical path verification, and debugging for robotic systems. Two alternatives were compared. The first was the integration of the ASEA Off-line Programming package with ROBSIM, a robotic simulation program. The second alternative was the purchase of the commercial product IGRIP. The needs of the RADL (Robotics Applications Development Laboratory) were explored and the alternatives were evaluated based on these needs. As a result, IGRIP was proposed as the best solution to the problem. Author

N90-16700*# Pennsylvania State Univ., Erie. Dept. of Mechanical Engineering.
LOW FLOW VORTEX SHEDDING FLOWMETER **c35**
Charles J. Waugaman *In* University of Central Florida,

NASA/ASEE Summer Faculty Fellowship Program Oct. 1989 p 324-357 (For primary document see N90-16686 08-99)
Avail: NTIS HC A18/MF A03 CSCL 14B

The purpose was to continue a development project on a no moving parts vortex shedding flowmeter used for flow measurement of hypergols. The project involved the design and construction of a test loop to evaluate the meter for flow of Freon which simulates the hypergol fluids. Results were obtained on the output frequency characteristics of the flow meter as a function of flow rate. A family of flow meters for larger size lines and ranges of flow was sized based on the results of the tested meter. Author

N90-16701*# California Polytechnic State Univ., San Luis Obispo. Dept. of Engineering Technology.
MATHEMATICAL MODEL FOR ADAPTIVE CONTROL SYSTEM OF ASEA ROBOT AT KENNEDY SPACE CENTER c37
Omar Zia *In* University of Central Florida, NASA/ASEE Summer Faculty Fellowship Program Oct. 1989 p 358-381 (For primary document see N90-16686 08-99)
Avail: NTIS HC A18/MF A03 CSCL 13I

The dynamic properties and the mathematical model for the adaptive control of the robotic system presently under investigation at Robotic Application and Development Laboratory at Kennedy Space Center are discussed. NASA is currently investigating the use of robotic manipulators for mating and demating of fuel lines to the Space Shuttle Vehicle prior to launch. The Robotic system used as a testbed for this purpose is an ASEA IRB-90 industrial robot with adaptive control capabilities. The system was tested and it's performance with respect to stability was improved by using an analogue force controller. The objective of this research project is to determine the mathematical model of the system operating under force feedback control with varying dynamic internal perturbation in order to provide continuous stable operation under variable load conditions. A series of lumped parameter models are developed. The models include some effects of robot structural dynamics, sensor compliance, and workpiece dynamics. Author

N90-16702*# Missouri Univ., Rolla. Dept. of Computer Science.
INVESTIGATION OF IGES FOR CAD/CAE DATA TRANSFER c61
George W. Zobrist *In* University of Central Florida, NASA/ASEE Summer Faculty Fellowship Program Oct. 1989 p 382-413 (For primary document see N90-16686 08-99)
Avail: NTIS HC A18/MF A03 CSCL 09B

In a CAD/CAE facility there is always the possibility that one may want to transfer the design graphics database from the native system to a non-native system. This may occur because of dissimilar systems within an organization or a new CAD/CAE system is to be purchased. The Initial Graphics Exchange Specification (IGES) was developed in an attempt to solve this scenario. IGES is a neutral database format into which the CAD/CAE native database format can be translated to and from. Translating the native design database format to IGES requires a pre-processor and transling from IGES to the native database format requires a post-processor. IGES is an artifice to represent CAD/CAE product data in a neutral environment to allow interfacing applications, archive the database, interchange of product data between dissimilar CAD/CAE systems, and other applications. The intent here is to present test data on translating design product data from a CAD/CAE system to itself and to translate data initially prepared in IGES format to various native design formats. This information can be utilized in planning potential procurement and developing a design discipline within the CAD/CAE community. Author

N90-16703*# National Aeronautics and Space Administration. Langley Research Center, Hampton, VA.
RESEARCH AND TECHNOLOGY, 1989: LANGLEY RESEARCH CENTER
Feb. 1990 201 p Original contains color illustrations
(NASA-TM-4150; L-16657; NAS 1.15:4150) Avail: NTIS HC A10/MF A02 CSCL 05A

The mission of the NASA Langley Research Center is to increase the knowledge and capability of the United States in a full range of aeronautics disciplines and in selected space disciplines. This mission will be accomplished by performing innovative research relevant to national needs and Agency goals, transferring technology to users in a timely manner, and providing development support to other United States Government agencies, industry, and other NASA centers. Highlights of the major accomplishments and applications that were made during the past year are presented. The highlights illustrate both the broad range of the research and technology activities at NASA Langley Research Center and the contributions of this work toward maintaining United States leadership in aeronautics and space research. Author

N90-16704# Society of Exploration Geophysicists, Tokyo (Japan).
PROCEEDINGS OF THE 79TH SEGJ CONFERENCE
Oct. 1988 320 p Conference held in Tokyo, Japan, Oct. 1988 (DE89-760006; SEGJ-8802; CONF-8810363) Avail: NTIS (US Sales Only) HC A14/MF A02

The proceedings contain 73 reports on seismic measurements, data analyses, developments of software, applications of various methods, effects, seismic explorations, seismic prospecting works, phenomena and explorations relating to earthquake, system, etc. Some of them are introduced as follows: Evaluation of liquefaction by geophysical survey, Field experiment for geotomography, Reflection seismic exploration in geothermal area, Examples and availability of full waveform acoustic logging, Development of digital borehole televiewer system, Study on accuracy of resistivity modeling by MT method, Development of a new MT system using the commercial power line as a source, Discrimination of surface alteration using 63 channel airborne imaging scanner, Imaging conditions in the migration of magnetotelluric data, Microgravity survey, etc. DOE

N90-16705# Istituto Elettrotecnico Nazionale (Galileo Ferraris), Turin (Itlay).
[ACTIVITIES REPORT OF THE NATIONAL ELECTROTECHNIC INSTITUTE GALILEO FERRARIS] Annual Report, 1988
Jun. 1989 202 p Original contains color illustrations
(ETN-90-96178) Avail: NTIS HC A10/MF A02

The 1988 technical and research activities of the National Electrotechnic Institut (NEI) (Italy), are reported. The activities are developed in the following fields: metrology, regarding time and frequency, electrical and magnetic quantities, photometric and acoustic quantities, for which quantities NEI realizes, maintains and disseminates the measurement units; engineering materials, with research on magnetic materials and study of magnetic, electrical, radiometric, photometric and acoustic properties of materials; electrical equipment and safety, regarding protection and reliability of low voltage electrical installations and requirements to ensure electrical safety; computer science, with the development of techniques for image understanding, research on reliability of complex systems, and application of numerical techniques to computer aided design of electrical devices; and environment protection and human health, with the development of measurement and analysis techniques. ESA

N90-16706# European Space Agency, Paris (France).
FOCUS 88: THE ACTIVITIES OF THE EUROPEAN SPACE AGENCY Annual Report, 1988
Valerie David, comp. and Norman Longdon, comp. Sep. 1989 60 p Original contains color illustrations
(ESA-BR-43; ISSN-0250-1589; ETN-90-96204) Copyright Avail: NTIS HC A04/MF A01

The 1988 activities of ESA are summarized. The research programs are carried out in the following areas: solar-terrestrial physics, Earth observations, microgravity, telecommunications, space transportation systems and space stations and platforms. The research activities are split into three parts: the generation of

new technology needed for future missions; the program which demonstrates the flight worthiness of the systems; and the program providing in-orbit demonstration opportunities. The support areas, including satellite operations, ground facilities, technical infrastructures, data handling and archiving, are considered. ESA

Typical Subject Index Listing

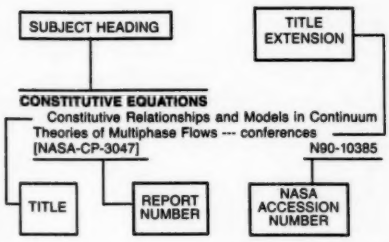

The subject heading is a key to the subject content of the document. Titles, report numbers, and accession numbers of pertinent documents are provided under each subject heading. When the title is insufficiently descriptive of the document content, a title extension has been added, separated from the title by three hyphens. The report number helps to indicate the type of document cited (e.g., NASA report, NASA translation, NASA contractor report). The NASA accession number is the number by which the document abstracts are arranged in this journal and by which the document is sold or requested. The titles, with title extensions if present, are arranged under each subject heading in ascending accession number order. The subject headings have been selected from the latest revision of the *NASA Thesaurus* (NASA SP-7064).

A

ABLATION
Investigation of ablation phenomena using IR thermography in a hypersonic wind tunnel N90-16258

ABSORPTIVITY
Absorption fluids data survey: 1989 update [DE90-003985] N90-16346

ABSTRACTS
Advances in techniques and technologies for air vehicle navigation and guidance [AGARD-AR-276] N90-15899
Reports of planetary astronomy, 1986 [NASA-TM-100776] N90-16596

ABUNDANCE
Trace element abundance determinations by Synchrotron X Ray Fluorescence (SXRF) on returned comet nucleus mineral grains N90-16619
Prompt Gamma Activation Analysis (PGAA): Technique of choice for nondestructive bulk analysis of returned comet samples N90-16633
Solar nebula condensates and the composition of comets N90-16634
The excess flux in the cosmic submillimeter background radiation and the primordial deuterium abundance [NASA-CR-186312] N90-16683

ACCELERATION (PHYSICS)
The use of hypervelocity launchers to explore previously inaccessible states of matter [DE90-004088] N90-15973
An introduction to shaker shock simulations [DE90-003057] N90-16298
Progress with small, high-magnetic-field spheromaks in CTX [DE90-003395] N90-16527

ACCESS CONTROL
Sequential rapid communication visual displays [AD-D014282] N90-16106

ACCESS TIME
New optimization techniques in database access and maintenance N90-16586

ACID RAIN
Assessment of the importance of acidic fogwater and cloudwater in affecting terrestrial vegetation: Some important case-studies [DE90-002216] N90-16361

ACOUSTIC EMISSION
A computational and experimental study of steady and transient acoustic energy flow from a complex mechanical structure N90-16478

ACOUSTIC FREQUENCIES
A computational and experimental study of steady and transient acoustic energy flow from a complex mechanical structure N90-16478

ACOUSTICS
SAW (Surface Acoustic Wave) transducer with improved bus-bar design [AD-D014250] N90-16125
Measurement of reflection and impedance in a beam by the structural intensity technique [DE90-728212] N90-16299
NASA/ASEE Summer Faculty Fellowship Program [NASA-CR-166837] N90-16686
Modeling the near acoustic field of a rocket during launch N90-16694
Proceedings of the 79th SEGJ Conference [DE89-760006] N90-16704

ACTIVATION ANALYSIS
Prompt Gamma Activation Analysis (PGAA): Technique of choice for nondestructive bulk analysis of returned comet samples N90-16633

ACTIVE GALACTIC NUCLEI
Ion-heated thermal Comptonization models and x ray spectral correlations in active galactic nuclei [DE90-003597] N90-16667

ADA (PROGRAMMING LANGUAGE)
Basic mathematical function libraries for scientific computation [NASA-TM-102256] N90-16423

ADAPTIVE CONTROL
Mathematical model for adaptive control system of ASEA robot at Kennedy Space Center N90-16701

ADAPTIVE FILTERS
An analysis of the time variation of the frequency response of the LMS adaptive line enhancer [ISVR-TR-175] N90-16115

ADAPTIVE OPTICS
Enhanced performance IR focal plane arrays using adaptive subtraction [RSRE-MEMO-4286] N90-16502

ADHESION
The effect of primer age on adhesion of polysulphide sealant N90-15909
Improved performance polysulfide based sealant N90-15910
Fuel resistant coatings for metal and composite fuel tanks N90-15911

ADVANCED VERY HIGH RESOLUTION RADIOMETER
Determination of optical porperties of clouds from NOAA-AVHRR data using Apollo N90-16321
Recognition and distinction of clouds, snow, and ice using AVHRR data N90-16322

ADVECTION
Triangle based TVD schemes for hyperbolic conservation laws [NASA-CR-181984] N90-16401

AERIAL PHOTOGRAPHY
Use of remote sensing data for land and building statistics N90-16335

AERIAL RECONNAISSANCE
Evaluation of the pasture potential in the dry areas of Kenya using combined Earth reconnaissance N90-16327

AEROASSIST
Singular perturbation analysis of AOTV-related trajectory optimization problems [NASA-CR-186202] N90-15936

AERODYNAMIC CHARACTERISTICS
The US National Transonic Facility, NTF N90-15942

AERODYNAMIC CONFIGURATIONS
Models for cryogenic wind tunnels N90-15956

AERODYNAMIC INTERFERENCE
Wind tunnel investigations on the configuration of the international vortex flow experiment N90-16181

AERODYNAMIC LOADS
A survey of nonuniform inflow models for rotorcraft flight dynamics and control applications [NASA-TM-102219] N90-15938
Cryogenic balances for the US NTF N90-15959

AERODYNAMICS
Weapon aerodynamics overview [RAE-TM-AERO-2150] N90-15888
Aerodynamic and heat transfer measurements on blading for a high rim-speed transonic turbine [RAE-TM-P-1151] N90-15920
High frequency pulsed diode lasers and phase-coupled diode arrays for aerodynamics N90-16238
Research and technology, 1989: Langley Research Center [NASA-TM-4150] N90-16703

AEROELASTICITY
Structural dynamics division research and technology accomplishments for FY 1989 and plans for FY 1990 [NASA-TM-101683] N90-15894

AERONAUTICAL ENGINEERING
Research and technology, 1989: Langley Research Center [NASA-TM-4150] N90-16703

AERONAUTICS
AGARD index of publications, 1986-1988 [AGARD-INDEX-86-88] N90-16585

AEROSOLS
Lidar technique for adjusting aerosol model number densities to existing conditions [AD-A213846] N90-16374
Short-term bioassays may be useful in evaluating fiber/whisker hazards [DE90-003707] N90-16393

AEROSPACE ENGINEERING
A foundation for the design of an astronautics specification system based on dynamic motivation analysis [ILR-MITT-220] N90-15969
AGARD index of publications, 1986-1988 [AGARD-INDEX-86-88] N90-16585
JSC document index [NASA-TM-102923] N90-16589
Catalogue of ESA publications in 1987 [ESA-SP-1087] N90-16590

AEROSPACE INDUSTRY
Structural characterization of Spacelab [ETN-90-95214] N90-16289

AEROSPACE MEDICINE
Assessment of visual function in aerospace medicine [BMVG-FBWM-89-5] N90-16397

AEROSPACE SCIENCES
JSC document index [NASA-TM-102923] N90-16589
Catalogue of ESA publications in 1987 [ESA-SP-1087] N90-16590

AEROSPACE TECHNOLOGY TRANSFER
Research and technology, 1989: Langley Research Center [NASA-TM-4150] N90-16703

AGRICULTURE
Computer-aided boundary delineation of agricultural lands [NASA-TM-102243] N90-16313
Use of remote sensing in operational inventory and monitoring agricultural and forestry tasks N90-16336

AIR NAVIGATION
Navigation of autonomous air vehicles by passive imaging sensors N90-15927
Navigation and guidance testing of the Lockheed/US Army Aquila remotely piloted vehicle N90-15935

AIR POLLUTION
Environmental, health, and CFC substitution aspects of the ozone depletion issue [DE90-004404] N90-16363

Simulation of pollutant transport using a mesoscale grid circulation model
[GKSS-89/E/24] N90-16365

AIR QUALITY
Environmental, health, and safety concerns associated with nonpetroleum fuel use in US transportation
[DE90-004367] N90-16362

AIR TO SURFACE MISSILES
Navigation up-date using radar mapping: Assessment and optimisation simulation tool N90-15928

AIR TRAFFIC CONTROL
Piloted simulation of a ground-based time-control concept for air traffic control
[NASA-TM-101085] N90-15898

AIR TRANSPORTATION
UK airmisses involving commercial air transport, September to December 1988
[ISSN-0951-6301] N90-15897

AIR WATER INTERACTIONS
The chemistry and dynamics of marine stratocumulus N90-16381

AIRCRAFT ACCIDENT INVESTIGATION
Aircraft accident report: Delta Air Lines, Inc., Boeing 727-232, N473DA, Dallas-Fort Worth International Airport, Texas, August 31, 1988
[PB89-910406] N90-15895

AIRCRAFT ACCIDENTS
Aircraft accident report: Delta Air Lines, Inc., Boeing 727-232, N473DA, Dallas-Fort Worth International Airport, Texas, August 31, 1988
[PB89-910406] N90-15895

AIRCRAFT APPROACH SPACING
Piloted simulation of a ground-based time-control concept for air traffic control
[NASA-TM-101085] N90-15898

AIRCRAFT DESIGN
Application of Lagrangian blending functions for grid generation around airplane geometries
[NASA-CR-186318] N90-15891
Fuel Tank Technology
[AGARD-R-771] N90-15904
The repair of aircraft integral fuel tanks in the RAF: A user's view of fuel tank technology N90-15908
Integral fuel tank certification and test methods N90-15916
Semi-empirical transition criteria for the design of laminar profiles N90-16174

AIRCRAFT ENGINES
An experimental investigation of thrust vectoring two-dimensional convergent-divergent nozzles installed in a twin-engine fighter model at high angles of attack
[NASA-TM-4155] N90-15884

AIRCRAFT FUEL SYSTEMS
Integral fuel tanks - design, production, aging, repair N90-15906

AIRCRAFT FUELS
Aircraft fuel tank construction and testing experience N90-15907
The repair of aircraft integral fuel tanks in the RAF: A user's view of fuel tank technology N90-15908

AIRCRAFT LIGHTS
The automatic detection of anti-collision lights
[RSRE-MEMO-4272] N90-15896

AIRCRAFT MAINTENANCE
Integral fuel tanks - design, production, aging, repair N90-15906
The repair of aircraft integral fuel tanks in the RAF: A user's view of fuel tank technology N90-15908
Fuel resistant coatings for metal and composite fuel tanks N90-15911
Spray sealing: A breakthrough in integral fuel tank sealing technology N90-15912
Design philosophy and construction techniques for integral fuselage fuel tanks N90-15913
Integral fuel tank certification and test methods N90-15916

AIRCRAFT MODELS
The precise calculation of the inviscid leading edge flow on a laminar airfoil using simple methods and verification by measurements on the TLF pilot model N90-16180

AIRCRAFT PERFORMANCE
A UK perspective on the uniform engine test programme
[RAE-TM-P-1172] N90-15922

AIRCRAFT STRUCTURES
Integral fuel tanks - design, production, aging, repair N90-15906
A dynamicist's view of fuel tank skin durability N90-15915

AIRCRAFT TIRES
Evaluation of two transport aircraft and several ground test vehicle friction measurements obtained for various runway surface types and conditions. A summary of test results from joint FAA/NASA Runway Friction Program
[NASA-TP-2917] N90-15902

AIRFOIL PROFILES
Detection of flow instabilities at airfoil profiles using piezoelectric arrays N90-16175
Determination of dynamic surface forces using piezoelectric arrays N90-16249
Use of the film-of-oil technique for profile measurements in the Transonic Wind tunnel Brunswick (TWB) N90-16252
Definition, transformation-formulae and measurements of tipvane angles
[IW-R510] N90-16351

AIRFOILS
Test techniques for cryogenic wind tunnels N90-15952
Models for cryogenic wind tunnels N90-15956
An interactive method for the flow calculation of airfoils with local separation regions N90-16190
Convergence speeding up in the calculation of the viscous flow about an airfoil N90-16194
Periodically unsteady effects on profiles, induced by separation N90-16196

AIRGLOW
Metal vaporisers: Bicentennial series of five historical monographs
[ISBN-0-642-13584-3] N90-16081
Effects of gravity waves on the polar O2 and OH airglow N90-16373

ALCOHOLS
Alcohol and blends as motor fuels
[DE90-003517] N90-16085

ALGEBRA
The algebra of the NODEN analyser
[RSRE-89012] N90-16432

ALGOL
A persistent heap for ALGOL 68
[RSRE-MEMO-4268] N90-16427

ALGORITHMS
Personal computer study of finite-difference methods for the transonic small disturbance equation
[NASA-TM-102582] N90-15892
Advances in techniques and technologies for air vehicle navigation and guidance
[AGARD-AR-276] N90-15899
Navigation of autonomous air vehicles by passive imaging sensors N90-15927
Experience with strain-gage balances for cryogenic wind tunnels N90-15958
A numerical simulation of the flow in the diffuser of the NASA Lewis icing research tunnel
[NASA-TM-102480] N90-15965
Digital system for monitoring and controlling remote processes
[DE90-003935] N90-16094
MT's algorithm: A new algorithm to search for the optimum set of modulation indices for simultaneous range, command, and telemetry
[NASA-CR-186259] N90-16110
Evaluation of a new charge algorithm for a lead-acid battery with gelled electrolyte using a 96V gel cell 4 as a test battery
[DE90-003420] N90-16133
Parallel asynchronous systems and image processing algorithms N90-16218
Element-by-element preconditioning techniques for large-scale, vectorized finite element analysis in nonlinear solid and structural mechanics N90-16291
Ice floe identification in satellite images using mathematical morphology and clustering about principal curves
[AD-A213854] N90-16311
Rainflow counting algorithm for the LIFE2 fatigue analysis code
[DE90-002834] N90-16344
A space-time discretization procedure for wave propagation problems
[NASA-TM-102215] N90-16399
Spanning trees of hypercubes with a maximum of sixteen peaks
[IMAG-RR-755-I] N90-16406
Case tool evaluation system
[DE90-003698] N90-16413
Algorithms for fault tolerant distributed systems
[AD-A214447] N90-16416
An algorithm to compute the square root of 3x3 positive definite matrix
[DE89-635711] N90-16417
The theory of hybrid stochastic algorithms
[DE90-003941] N90-16421
Basic mathematical function libraries for scientific computation
[NASA-TM-102256] N90-16423
The inside-outside algorithm: Further experiments on three and four letter word spelling and implementation on an array processor
[RSRE-MEMO-4256] N90-16426
Beamforming pre-processors for high discrimination algorithms
[RSRE-MEMO-4304] N90-16429
Optimization of monotonic inference algorithms in propositional and first order logic
[LAAS-89204] N90-16436
Design and implementation of a multi-sensor fusion algorithm on a hypercube computer architecture
[DE90-003682] N90-16438
Interpretation of CAD (Computer Aided Design) models through IGES (Initial Graphics Exchange Specification) interface
[PB90-121294] N90-16441
Parallel algorithm for determining motion vectors in ice floe images by matching edge features N90-16451
Optimal step sizes in semi-stochastic approximation procedures
[ETN-90-95888] N90-16469
Solving time harmonic wave problems on vector processors
[DE90-003956] N90-16480
Scaling study for SP-100 reactor technology
[NASA-TM-897140] N90-16496
Abbreviated query interpretation in extended entity-relationship oriented databases
[DE90-003114] N90-16587
Event-join optimization in temporal relational databases
[DE90-003117] N90-16588

ALIGNMENT
Mechanical strain isolator mount
[NASA-CASE-LAR-13580-1] N90-16272
B-Factory Final Focus System using superconducting quadrupoles
[DE90-004432] N90-16552

ALKALI METALS
The onset of boiling of the liquid alkali metals
[DE90-002276] N90-16036

ALLENDE METEORITE
Identification of solar nebula condensates in interplanetary dust particles and unequilibrated ordinary chondrites N90-16629

ALLOYING
Long term creep strength of silver alloyed copper
[DE90-602367] N90-16039

ALTERNATING CURRENT
Study of metal corrosion using ac impedance techniques in the STS launch environment N90-16688

ALUMINIDES
Shock-induced reaction synthesis of aluminides and silicides
[DE90-003948] N90-16066

ALUMINUM ALLOYS
High temperature aluminum-base alloy
[AD-D014270] N90-16028

ALUMINUM OXIDES
Microstructures of Y123 films on SrTiO3, LaGaO3, and LaAlO3
[DE90-003367] N90-16537

ALUMINUM 26
Gamma-ray observations and the distribution of interstellar aluminum-26 N90-16661

AMINES
Advanced biosensors for amino acid detection
[AD-A214029] N90-16225

AMMETERS
Solid state voltammetry and sensors in solids and gases
[DE90-003234] N90-16538

AMORPHOUS MATERIALS
Researches on amorphous perovskite
[DE89-900733] N90-16535
Effects of ion dose on the morphology and crystallization of amorphous germanium
[DE90-003564] N90-16547
Experimental studies of gas trapping in amorphous ice and thermal modelling of comets: Implications for Rosetta N90-16610

AMPLIFICATION
Vorticity amplification in nonorthogonal stagnation flow N90-16152

ANALOGS
Mathematical model for adaptive control system of ASEA robot at Kennedy Space Center N90-16701

ANALYTICAL CHEMISTRY
Analytical study of comet nucleus samples N90-16608

ANALYZERS
Two possible configurations for the top-hat electrostatic analyzer: A numerical study
[IFSI-88-18] N90-16229
CIS-2 analyzer derivation of hardware parameters
[IFSI-89-13] N90-16230

ANEMOMETERS
Miniature laser Doppler anemometer with a diode laser
[ISL-CO-224/88] N90-16232
ANGULAR DISTRIBUTION
Studies of elastic scattering and cross sections of the C-12 + Si-28 system
[DE89-635990] N90-16486
Determination of solar flare accelerated ion angular distributions from SMM gamma ray and neutron measurements and determination of the He-3/H ratio in the solar photosphere from SMM gamma ray measurements
[NASA-CR-186038] N90-16676
ANGULAR MOMENTUM
Lower limit for the average angular momentum leading to fusion
[DE90-004027] N90-16523
ANGULAR RESOLUTION
CIS-2 analyzer derivation of hardware parameters
[IFSI-89-13] N90-16230
ANISOTROPIC MEDIA
Geometrical optics in inhomogeneous chiral media with application to polarization correction in inhomogeneous lens antennas
[PB90-110669] N90-16497
ANISOTROPY
Multigrid methods for two- and three-dimensional Poisson-type equations on the sphere
[GMD-391] N90-16468
Anisotropy and microstructure of high coercivity rare earth iron permanent magnets, list of papers published
[AD-A214160] N90-16476
The modified Ginzburg-Landau theory for anisotropic high temperature superconductors
[DE89-635909] N90-16532
Production of photons in anisotropic spacetimes
[DE90-600760] N90-16576
ANNEALING
Irradiation creep and swelling of annealed type 304L stainless steel at approximately 390 C and high neutron fluence
[DE90-004521] N90-16047
The influence of residual contamination on the structure and properties of metal/GaAs interfaces
[DE90-000549] N90-16530
Ion beam annealing of Si co-implanted with Ga and As
[DE90-004297] N90-16556
ANOMALIES
Multiple flow regimes in the Northern Hemisphere winter N90-16372
Phonon anomaly at T(sub c) in (Y/ER)Ba2Cu3O(7-delta)
[DE90-003562] N90-16539
ANTENNA ARRAYS
Stripline feed for a microstrip array of patch elements with teardrop shaped probes
[NASA-CASE-NPO-17548-1-CU] N90-16104
ANTENNA DESIGN
Satellite broadcasting: Requirements for the receiving antenna
[BBC-RD-1989/5] N90-16098
ANTENNA FEEDS
Stripline feed for a microstrip array of patch elements with teardrop shaped probes
[NASA-CASE-NPO-17548-1-CU] N90-16104
ANTICYCLONES
The role of an upstream cyclone and corresponding synoptic/planetary-scale interactions during the development of a blocking anticyclone N90-16659
ANTIFERROMAGNETISM
Magnetic interactions in Sn-119 substituted for Cu in antiferromagnetic and superconducting lamellar cuprates
[DE90-003661] N90-16560
ANTIPARTICLES
Possible measurement of the gravitational acceleration of molecules, atoms, nuclei, elementary particles, and antiparticles
[DE90-719559] N90-16490
APERTURES
Coded-aperture imaging in nuclear medicine N90-16208
Diffraction limited dichroic combiner diode laser
[AD-D014291] N90-16263
APOLLO SOYUZ TEST PROJECT
Systems interoperability approach Apollo/Soyuz test project N90-15979
APPEARANCE
Appearance analysis from CAD models
[IMAG-RR-756-I-IMAG-88-LIFIA] N90-16434
APPLICATIONS PROGRAMS (COMPUTERS)
ZBTAB: Zenith-248 version of BLUGTAB
[AD-A214279] N90-16415
Creating the next generation control system software
[DE90-003391] N90-16419
APPROXIMATION
Triangle based TVD schemes for hyperbolic conservation laws
[NASA-CR-181984] N90-16401
Optimal step sizes in semi-stochastic approximation procedures
[ETN-90-95888] N90-16469
ARCHITECTURE (COMPUTERS)
Issues and approaches for electronic document approval and transmittal using digital signatures and text authentication: Prototype documentation
[DE90-003382] N90-16119
The Suprenum architecture and its application to computational fluid dynamics
[GMD-389] N90-16161
Parallel asynchronous systems and image processing algorithms N90-16218
Expert system control of a six-legged walking telerobot
[DE90-004661] N90-16285
Dynamic architecture computer
[AD-A214262] N90-16402
The SMITE approach to security
[RSRE-89014] N90-16404
Spanning trees of hypercubes with a maximum of sixteen peaks
[IMAG-RR-755-I] N90-16406
FRAC-IN-THE-BOX utilization
[DE90-003648] N90-16412
Algorithms for fault tolerant distributed systems
[AD-A214447] N90-16416
Creating the next generation control system software
[DE90-003391] N90-16419
A 3-D measurement system using object-oriented FORTH
[DE90-003393] N90-16420
Design and implementation of a multi-sensor fusion algorithm on a hypercube computer architecture
[DE90-003682] N90-16438
Overview and extensions of a system for routing directed graphs on SIMD architectures N90-16444
BLITZEN: A highly integrated massively parallel machine N90-16453
On the efficient exploitation of speculation under data flow paradigms of control
[AD-A214112] N90-16455
Abbreviated query interpretation in extended entity-relationship oriented databases
[DE90-003114] N90-16587
ARRAYS
Detection of flow instabilities at airfoil profiles using piezoelectric arrays N90-16175
Optical flow measuring method using diode lasers, phase coupled arrays, and high frequency pulsed diode lasers N90-16176
A low-threshold EAS (Extensive-Air-Shower) array for gamma-ray astronomy at Los Alamos
[DE89-016780] N90-16600
Status of the expansion of the CYGNUS array at Los Alamos
[DE89-016781] N90-16601
ARTERIES
Apparatus for imaging deep arterial and coronary lesions
[NASA-CASE-NPO-17439-1-CU] N90-16391
Factor analytic reduction of the carotid-cardiac baroreflex parameters N90-16693
ARTIFICIAL INTELLIGENCE
An intelligence-driven RPV mission planner N90-15932
NASA/ASEE Summer Faculty Fellowship Program
[NASA-CR-166837] N90-16686
The DAB model of drawing processes N90-16691
ASPECT RATIO
Definition, transformation-formulae and measurements of tipvane angles
[IW-R510] N90-16351
ASPHALT
Evaluation of two transport aircraft and several ground test vehicle friction measurements obtained for various runway surface types and conditions. A summary of test results from joint FAA/NASA Runway Friction Program
[NASA-TP-2917] N90-15902
ASPHERICITY
Surface topography measurements over the 1 meter to 10 micrometer spatial period bandwidth
[DE90-003642] N90-16501
ASTEROIDS
Comments on comet shapes and aggregation processes N90-16622
The comet rendezvous asteroid flyby mission N90-16639
ASTRONAUT LOCOMOTION
EVA space suit. General concepts of design and arrangement N90-15976
ASTRONAUTICS
A foundation for the design of an astronautics specification system based on dynamic motivation analysis
[ILR-MITT-220] N90-15969
ASTRONOMICAL MODELS
Neutrino oscillations: An essay in honor of Felix Boehm
[DE90-003223] N90-16491
Study of primitive universe in the Bianchi 9 model
[DE89-635903] N90-16572
Pulsations of delta Scuti stars
[DE90-003213] N90-16598
ASTRONOMY
Reports of planetary astronomy, 1986
[NASA-TM-100776] N90-16596
ASYMPTOTIC METHODS
High-frequency asymptotic methods for analyzing the EM scattering by open-ended waveguide cavities
[NASA-CR-186244] N90-16103
Asymptotically fast triangularization of matrices over rings
[DE90-003161] N90-16471
ATMOSPHERIC ATTENUATION
X-band atmospheric attenuation for an Earth terminal measurement system
[PB90-100736] N90-16101
Helsinki University of Technology Radio Laboratory
[PB90-110677] N90-16102
The physical foundations of radiometry and their applications in the mm-waveband
[REPT-12-88] N90-16114
Atmospheric transmittance determination from a two-angle measurement of radiance change
[AD-A213847] N90-16375
ATMOSPHERIC BOUNDARY LAYER
The response of the atmospheric convective boundary layer to surface inhomogeneities N90-16369
ATMOSPHERIC CHEMISTRY
ECC (Electrochemical Concentration Cell) ozonesonde observations at Mirny, Antarctica, during 1988
[PB90-113960] N90-16357
Upper atmosphere research
[ISBN-0-642-13582-7] N90-16368
The chemistry and dynamics of marine stratocumulus N90-16381
ATMOSPHERIC CIRCULATION
Simulation of pollutant transport using a mesoscale grid circulation model
[GKSS-89/E/24] N90-16365
The effect of orographic forcing on the mean flow of the stratosphere N90-16367
The response of the atmospheric convective boundary layer to surface inhomogeneities N90-16369
Multiple flow regimes in the Northern Hemisphere winter N90-16372
ATMOSPHERIC COMPOSITION
ECC (Electrochemical Concentration Cell) ozonesonde observations at South Pole, Antarctica, during 1988
[PB90-110172] N90-16355
Scientific linkages in global change
[PB90-112608] N90-16356
ECC (Electrochemical Concentration Cell) ozonesonde observations at Mirny, Antarctica, during 1988
[PB90-113960] N90-16357
Operational ozone monitoring with the Global Ozone Monitoring Radiometer (GOMR)
[PB90-114034] N90-16359
Potential impact of stratospheric ozone depletion on marine ecosystems
[PB90-112616] N90-16360
Upper atmosphere research
[ISBN-0-642-13582-7] N90-16368
ATMOSPHERIC MODELS
Interconnectedness in nature and in science: The case of climate and climate modeling
[PB90-113986] N90-16358
The effect of orographic forcing on the mean flow of the stratosphere N90-16367
Lidar technique for adjusting aerosol model number densities to existing conditions
[AD-A213846] N90-16374
Verification study of a three-dimensional local scale atmospheric model PHYSIC at seacoast region
[DE90-719560] N90-16384
ATMOSPHERIC PHYSICS
Upper atmosphere research
[ISBN-0-642-13582-7] N90-16368
Rocket-triggered lightning strikes and forest fire ignition N90-16690
ATMOSPHERIC PRESSURE
Cosmic ray NM-64 neutron monitor data 16
[IFSI-88-21] N90-16684

ATMOSPHERIC SOUNDING
A dynamic model for forecasting new cloud development
[AD-A213939] N90-16383
ATMOSPHERIC TEMPERATURE
Vibration damping composition suitable for outer space temperature variations
[AD-D014288] N90-16296
ECC (Electrochemical Concentration Cell) ozonesonde observations at South Pole, Antarctica, during 1988
[PB90-110172] N90-16355
Climatic summaries and documentation for the primary meteorological Station, H. J. Andrews Experimental Forest, 1972 to 1984
[PB90-104373] N90-16382
ATMOSPHERIC TURBULENCE
Statistics of a reflected laser beam in the turbulent atmosphere (path correlation)
[PB90-113994] N90-16261
New atmospheric turbulence model for shuttle applications
[NASA-TM-4168] N90-16389
ATOMIC PHYSICS
General contraction of Gaussian basis sets. Part 2: Atomic natural orbitals and the calculation of atomic and molecular properties
[NASA-CR-186201] N90-16482
Atomic processes in plasmas under ultra-intense laser irradiation
[DE90-003221] N90-16521
ATOMIC STRUCTURE
Surface studies at the NSLS
[DE90-003173] N90-16027
Elastic moduli of copper: Electronic structure contributions from pseudopotentials and full-potential linear muffin-tin orbital band structure calculations
[DE90-004423] N90-16037
Theoretical studies of chemisorption and surface reactions on nickel and silicon
[DE90-004849] N90-16050
Pairs of chalcogen impurities in silicon
[DE89-635767] N90-16063
ATOMS
Theoretical investigations of the structures and binding energies of Be(sub n) and Mg(sub n) (n = 3-5) clusters
[NASA-TM-101931] N90-16483
Possible measurement of the gravitational acceleration of molecules, atoms, nuclei, elementary particles, and antiparticles
[DE90-719559] N90-16490
ATTITUDE CONTROL
Plume shape optimization of small attitude control thrusters with respect to impingement and thrust
[ISL-CO-220/88] N90-16153
AURORAL IONIZATION
X ray spectrophotometric remote sensing of diffuse auroral ionization
[SD-TR-89-09] N90-16599
AUSTENITIC STAINLESS STEELS
An XPS and electrochemical study of the influence of molybdenum and nitrogen on the passivity of austenitic stainless steel
[AD-A214267] N90-16034
Interplanar spacing for various phases in austenitic stainless steels
[DE90-602350] N90-16038
AUSTRALIA
The development of over-the-horizon radar in Australia
[ISBN-0-642-13561-4] N90-16099
AUTOCORRELATION
A simple fiber optic autocorrelation tachometer
[ETN-90-96146] N90-16228
AUTOMATIC CONTROL
Special Course on Advances in Cryogenic Wind Tunnel Technology
[AGARD-R-774] N90-15939
Automatic control of KKK: Requirements, sensors, actuators, and control performance results N90-15944
Automatic control of cryogenic wind tunnels N90-15957
AUTOMOBILES
Flow visualization using the laser light sheet method in vehicle aerodynamics and combustion chamber engineering N90-16246
Results from the third year of operation of the Federal Methanol Fleet at Lawrence Berkeley Laboratory
[DE90-003308] N90-16277
AUTONOMY
Navigation of autonomous air vehicles by passive imaging sensors N90-15927
Technology and evaluation of unmanned air vehicles N90-15934
AUTOREGRESSIVE PROCESSES
Analysis of nonlinear systems using ARMA (Autoregressive Moving Average) models
[DE90-002395] N90-16297
AVAILABILITY
Complex availability problems solved with simulation
[DE89-012610] N90-16459
AVIONICS
Advances in techniques and technologies for air vehicle navigation and guidance
[AGARD-AR-276] N90-15899
Synthesis of control law, on a RPV, in order to minimize the number of sensors N90-15925
Mirach 100 flight control system N90-15926
AXIAL COMPRESSION LOADS
Analysis and testing of axial compression in imperfect slender truss struts
[NASA-TM-4174] N90-16292

B

BACKGROUND RADIATION
Natural and man-made emissions at 1.0 to 5.6 MHz measured between 10 and 18 R sub E
[MPE-PREPRINT-146] N90-16116
The excess flux in the cosmic submillimeter background radiation and the primordial deuterium abundance
[NASA-CR-186312] N90-16683
BACKSCATTERING
Backscattering effects in DIAL due to water vapor
[SER-WISS-ABHANDL-89] N90-16265
Investigation of the backscatter behavior of selected test areas in two geocoded SEASAT-SAR scenes in greater Bonn (Fed. Republic of Germany) N90-16331
Lidar technique for adjusting aerosol model number densities to existing conditions
[AD-A213846] N90-16374
BANACH SPACE
Uniform stability for time-varying infinite-dimensional discrete linear systems
[DE89-635712] N90-16460
BAROCLINIC INSTABILITY
Laboratory studies of isolated eddies in a rotating fluid
[AD-A213903] N90-16146
BARORECEPTORS
Factor analytic reduction of the carotid-cardiac baroreflex parameters N90-16693
BARS
Open-mode delamination stress concentrations in horseshoe and elliptic composite curved bars subjected to end forces
[NASA-TM-4164] N90-16004
BARYON RESONANCE
Q-2 and A dependence of delta (1232) electroexcitation in nuclei
[DE90-003470] N90-16492
BATTERY CHARGERS
Evaluation of a new charge algorithm for a lead-acid battery with gelled electrolyte using a 96V gel cell 4 as a test battery
[DE90-003420] N90-16133
BEAM CURRENTS
Broad-beam multi-ampere metal ion source
[DE90-003106] N90-16123
BEAM INJECTION
Broad-beam multi-ampere metal ion source
[DE90-003106] N90-16123
BEAM INTERACTIONS
Lecture notes on supersonic molecular beam sources
[MPIS-20/1988] N90-16494
BEAMS (RADIATION)
Large angle off-axis beam steering of a phased telescope array
[AD-D014269] N90-16127
BEAMS (SUPPORTS)
Measurement of reflection and impedance in a beam by the structural intensity technique
[DE90-728212] N90-16299
BEND TESTS
Experiences with three-point bending test specimens for determining the crack-arrest fracture toughness K(sub Ia) in low-alloy steel
[DE90-004120] N90-16306
BENDING FATIGUE
Cyclic fatigue of hot-isostatic-pressed silicon nitride
[PB90-122649] N90-16308
BIBLIOGRAPHIES
AGARD index of publications, 1986-1988
[AGARD-INDEX-86-88] N90-16585
JSC document index
[NASA-TM-102923] N90-16589
Catalogue of ESA publications in 1987
[ESA-SP-1087] N90-16590
BIG BANG COSMOLOGY
Nuclear reaction uncertainties in standard and non-standard cosmologies
[DE90-003594] N90-16666
BINARY STARS
EXOSAT measurements of the pulse period of Vela X-1
[MPE-PREPRINT-157] N90-16673
BIOASSAY
Advanced biosensors for amino acid detection
[AD-A214029] N90-16225
Short-term bioassays may be useful in evaluating fiber/whisker hazards
[DE90-003707] N90-16393
BIOINSTRUMENTATION
Advanced biosensors for amino acid detection
[AD-A214029] N90-16225
BIOLOGICAL MODELS (MATHEMATICS)
Computation of the unsteady facilitated transport of oxygen in hemoglobin
[NASA-TM-102251] N90-16400
BIOMASS
Dynamics of carbon dioxide exchange of a wheat community grown in a semi-closed environment N90-16689
BIPOLAR TRANSISTORS
A physical and numerical study of the turn-off behavior of bipolar power transistors
[LAAS-89185] N90-16136
BISMUTH OXIDES
Development of planar geometry solid oxide fuel cells
[PB90-100769] N90-16341
High temperature neutron diffraction study of the formation reaction of bismuth superconductors
[DE90-004883] N90-16568
BL LACERTAE OBJECTS
Short time scale variability of the BL Lac object OJ 287 in the near-infrared
[IFSI-89-3] N90-16603
BLACK HOLES (ASTRONOMY)
An atlas of aperiodic variability in HMXB
[MPE-PREPRINT-158] N90-16605
On quantum effects near a black hole singularity
[DE90-600754] N90-16668
BLADE TIPS
Rotor induced-inflow-ratio measurements and CAMRAD calculations
[NASA-TP-2946] N90-15882
BLADE-VORTEX INTERACTION
Rotor induced-inflow-ratio measurements and CAMRAD calculations
[NASA-TP-2946] N90-15882
BLOCK DIAGRAMS
The algebra of the NODEN analyser
[RSRE-89012] N90-16432
BLOCKING
The role of an upstream cyclone and corresponding synoptic/planetary-scale interactions during the development of a blocking anticyclone N90-16659
BLUNT BODIES
Demonstration of the feasibility of laser induced fluorescence for arc jet flow diagnostics
[NASA-CR-185595] N90-16013
BLURRING
Model-based quantification of image quality N90-16206
BODY CENTERED CUBIC LATTICES
Surface studies at the NSLS
[DE90-003173] N90-16027
BOILING
The onset of boiling of the liquid alkali metals
[DE90-002276] N90-16036
BOLTZMANN DISTRIBUTION
The Eighteenth Conference on Stochastic Processes and their Applications
[AD-A212301] N90-16010
BONDING
An investigation of elastic guided waves for ceramic joint evaluation
[DE90-004400] N90-16071
BORON
Characterization of B and N implanted fused silica
[DE90-004198] N90-16069
BOROSILICATE GLASS
Characterization of B and N implanted fused silica
[DE90-004198] N90-16069
BOSONS
Proceedings of the 23rd Annual Seminar on Theoretical Physics
[DE90-601827] N90-16577
BOUNDARIES
Computer-aided boundary delineation of agricultural lands
[NASA-TM-102243] N90-16313
BOUNDARY ELEMENT METHOD
Electroplating simulation
[DE90-003683] N90-16091

BOUNDARY LAYER EQUATIONS
An efficient solver of the Eigenvalue problem of the linear stability equations for three dimensional, compressible boundary-layer flows N90-16172
Numerical boundary layer calculations on the DFVLR ellipsoid of revolution N90-16193
Grid-independent wall layer turbulence model for complex flow calculations
[DE90-003500] N90-16200
BOUNDARY LAYER FLOW
Flow visualization in the cryogenic wind tunnel N90-15953
Application of the singularity-separating method to computing problems of solid-propellant combustion in a closed vessel
[PREPRINT-489] N90-16086
Method for the primary stability analysis of the three dimensional, compressible boundary layer flows N90-16171
BOUNDARY LAYER PLASMAS
On the structure of the tail magnetic field
[IFSI-88-19] N90-16378
BOUNDARY LAYER SEPARATION
Flow separation in shock wave boundary layer interactions at hypersonic speeds
[NASA-CR-4274] N90-15885
A numerical and experimental investigation of multiple shock wave/turbulent boundary layer interactions in a rectanular duct N90-16141
Flows with Separation
[DGLR-PAPERS-88-05] N90-16169
An interactive method for the flow calculation of airfoils with local separation regions N90-16190
Calculation of the flap profile flows with separation based on coupled potential and boundary layer solutions N90-16191
Inverse solutions for boundary layers with separation or close to separation under locally infinite swept wing conditions N90-16192
Periodically unsteady effects on profiles, induced by separation N90-16196
BOUNDARY LAYER STABILITY
Experiments on the laminar-turbulent transition on swept wings N90-16170
Method for the primary stability analysis of the three dimensional, compressible boundary layer flows N90-16171
An efficient solver of the Eigenvalue problem of the linear stability equations for three dimensional, compressible boundary-layer flows N90-16172
Detection of flow instabilities at airfoil profiles using piezoelectric arrays N90-16175
Direct measurement of laminar instability amplification factors in flight N90-16178
BOUNDARY LAYER TRANSITION
Flows with Separation
[DGLR-PAPERS-88-05] N90-16169
Numerical simulation of the nonlinear evolution of a perturbation in a three dimensional boundary layer N90-16173
Semi-empirical transition criteria for the design of laminar profiles N90-16174
Determination of the N-factor in the Brunswick (Federal Rep. of Germany) transonic wind tunnel using measurements of pressure distributions and transition points, and the Sally method N90-16177
Development of transition criteria on the basis of e to the N power for three dimensional wing boundary layers N90-16179
BOUNDARY LAYERS
Flow separation in shock wave boundary layer interactions at hypersonic speeds
[NASA-CR-4274] N90-15885
BOUNDARY VALUE PROBLEMS
Finite element calculations for transonic flows taking into account several far field boundary conditions N90-16188
On the reciprocity of state vectors in boundary value models
[AD-A214104] N90-16458
Solving time harmonic wave problems on vector processors
[DE90-003956] N90-16480
BREADBOARD MODELS
Knowledge-based imaging-sensor fusion system N90-16220
BREMSSTRAHLUNG
X ray spectrophotometric remote sensing of diffuse auroral ionization
[SD-TR-89-09] N90-16599
BROADCASTING
Use of an HF active monitoring array in the presence of high level interference
[BBC-RD-1989/7] N90-16096
Satellite broadcasting: Requirements for the receiving antenna
[BBC-RD-1989/5] N90-16098
BROMIDES
Carbon-13 nuclear magnetic resonance of heterocyclic salts and its precursors
[DE89-635768] N90-16016
BUBBLES
Numerical simulation of a bubble shaped bursting vortex N90-16187
BUDGETS
International conference management N90-16583
BUFFETING
Assessment of computational prediction of tail buffeting
[NASA-TM-101613] N90-15886
BUILDINGS
Use of remote sensing data for land and building statistics N90-16335
BURNERS
Externally vaporizing system for turbine combustor
[AD-D014284] N90-15918
BURST TESTS
Burst pressure prediction of metallic/fibre reinforced rocket motor cases using an elasto-plastic instability analysis
[RARDE-1/89] N90-15997

C

CALCIUM COMPOUNDS
Cycle-life improvement of Zn/NiOOH cells by the addition of Ca(OH)2 to the zinc electrode
[DE90-004040] N90-16139
CALIBRATING
Cryogenic balances for the US NTF N90-15959
Modeling a self-calibrating thermocouple for use in a smart temperature measurement system
[DE90-003697] N90-16259
Calibration of a pulsed potential crack monitor for use in fatigue crack growth studies
[RAE-TM-M/S-1126] N90-16301
CAMERAS
Knowledge-based imaging-sensor fusion system N90-16220
A knowledge-based machine vision system for space station automation N90-16221
CANARD CONFIGURATIONS
Some recent developments in materials and techniques for model fabrication N90-15955
Wind tunnel investigations on the configuration of the international vortex flow experiment N90-16181
CANCER
Short-term bioassays may be useful in evaluating fiber/whisker hazards
[DE90-003707] N90-16393
CANOPIES (VEGETATION)
Dynamics of carbon dioxide exchange of a wheat community grown in a semi-closed environment N90-16689
CANS
Long term creep strength of silver alloyed copper
[DE90-602367] N90-16039
CANTILEVER BEAMS
Load-shortening behavior of an initially curved eccentrically loaded column
[NASA-TM-101643] N90-16293
CARBON
Effect of carbon on ion beam mixing of Fe-Ti bilayers
[DE90-003650] N90-16056
The carbon chemistry of meteorites: Relationships to comets N90-16615
Neptune's Triton: A moon rich in dry ice and carbon
[NASA-CR-186298] N90-16675
CARBON DIOXIDE
Solid-state electrolyte catalysis for methane and oxygen synthesis
[PB90-100231] N90-16011
Mechanisms of the electrochemistry of small organic molecules
[PB90-100785] N90-16012
Method of making carbon dioxide and chlorine free fluoride-based glass
[AD-D014260] N90-16060
Dynamics of carbon dioxide exchange of a wheat community grown in a semi-closed environment N90-16689
CARBON DIOXIDE CONCENTRATION
A qualitative architecture for understanding policy responses to global change
[DE90-003936] N90-16364
Dynamics of carbon dioxide exchange of a wheat community grown in a semi-closed environment N90-16689
CARBON FIBERS
Instrumented impact and residual tensile strength testing of eight-ply carbon epoxy specimens
[NASA-TP-2981] N90-16007
CARBON MONOXIDE
Mechanisms of the electrochemistry of small organic molecules
[PB90-100785] N90-16012
CARBON 12
Studies of elastic scattering and cross sections of the C-12 + Si-28 system
[DE89-635990] N90-16486
CARBON 13
Carbon-13 nuclear magnetic resonance of heterocyclic salts and its precursors
[DE89-635768] N90-16016
CARBONACEOUS CHONDRITES
Evolution of carbonaceous chondrite parent bodies: Insights into cometary nuclei N90-16638
CARBONACEOUS MATERIALS
Laboratory analyses of micron-sized solid grains: Experimental techniques and recent results N90-16616
CARBONACEOUS METEORITES
The carbon chemistry of meteorites: Relationships to comets N90-16615
CASE HISTORIES
CAE (Computer-Aided Engineering) tools' limitations case study: An SSI (Small Scale Integrated) design to an ASIC (Application Specific Integrated Circuit)
[DE90-002902] N90-16418
CASTING
High temperature aluminum-base alloy
[AD-D014270] N90-16028
CATACLYSMIC VARIABLES
Galactic x ray astronomy with EXOSAT N90-16597
Accretion shock geometries in the magnetic variables
[NASA-CR-186290] N90-16664
CATALOGS (PUBLICATIONS)
Catalogue of ESA publications in 1987
[ESA-SP-1087] N90-16590
CATALYSIS
Solid-state electrolyte catalysis for methane and oxygen synthesis
[PB90-100231] N90-16011
CATHODES
Organic cathode for a secondary battery
[NASA-CASE-NPO-17604-1-CU] N90-16124
CAVITIES
High-frequency asymptotic methods for analyzing the EM scattering by open-ended waveguide cavities
[NASA-CR-186244] N90-16103
CCD STAR TRACKER
The MPI/AIT X ray Imager (MAXI): High speed PN-CCD's for x ray detection
[MPE-PREPRINT-154] N90-16234
CELL ANODES
Improved anode catalysts for coal gas-fueled phosphoric acid fuel cells
[DE90-004016] N90-16347
CENTRAL PROCESSING UNITS
CPU timing routines for a CONVEX C220 computer system
[NASA-CR-181950] N90-16424
The inside-outside algorithm: Further experiments on three and four letter word spelling and implementation on an array processor
[RSRE-MEMO-4256] N90-16426
Beamforming pre-processors for high discrimination algorithms
[RSRE-MEMO-4304] N90-16429
Dynamically allocating sets of fine-grained processors to running computations N90-16447
Scan line graphics generation on the massively parallel processor N90-16450
CERAMICS
Structure-property relationships in ion-beam surface-modified ceramics: Theory and applications
[AD-A212785] N90-16054
Porous ceramic bodies
[AD-D014277] N90-16061
Metals and Ceramics Division Materials Sciences Program
[DE90-004371] N90-16070
An investigation of elastic guided waves for ceramic joint evaluation
[DE90-004400] N90-16071
Thermodynamic analysis of chemical stability of ceramic materials in hydrogen-containing atmospheres at high temperatures
[NASA-CR-4271] N90-16072
Assessment of strength limiting flaws in ceramic heat exchanger components
[DE90-004086] N90-16077
Analytical study on the decreasing method of thermal stress for ceramic gas turbines
[DE90-734934] N90-16078

CERTIFICATION
Integral fuel tank certification and test methods N90-15916

CESIUM VAPOR
Development of a wet vapor homogeneous liquid metal MHD power system
[DE90-001468] N90-16508

CHALCOGENIDES
Pairs of chalcogen impurities in silicon
[DE89-635767] N90-16063

CHANGE DETECTION
Satellite image sequences for motion analysis and change detection N90-16323

CHANNELS (DATA TRANSMISSION)
MT's algorithm: A new algorithm to search for the optimum set of modulation indices for simultaneous range, command, and telemetry
[NASA-CR-186259] N90-16110

CHARACTER RECOGNITION
Alvey MMI007. Object identification from 2D images: The RSRE contribution
[RSRE-MEMO-4277] N90-16428

CHARACTERIZATION
Piezoelectric ceramic modeling and characterization at high levels of mechanical activity
[ISAL-89-0030] N90-16074
Candidate sample acquisition systems for the Rosetta N90-16635

CHARGE DISTRIBUTION
On the observation of a transition from fusion to multifragmentation in high multiplicity O16 induced reactions
[LUIP-8812] N90-16481

CHARGE TRANSFER
Solid state voltammetry and sensors in solids and gases
[DE90-003234] N90-16538

CHARGED PARTICLES
Stochastic simulation of charged particle transport on the massively parallel processor N90-16448
Possible measurement of the gravitational acceleration of molecules, atoms, nuclei, elementary particles, and antiparticles
[DE90-719559] N90-16490

CHARON
Neptune's Triton: A moon rich in dry ice and carbon
[NASA-CR-186298] N90-16675

CHECKOUT
The US National Transonic Facility, NTF N90-15942
The Kryo-Kanal Koeln (KKK): Description of the tunnel conversion. Thermal insulation, instrumentation, operational experience, test results and operating costs N90-15943

CHEMICAL ANALYSIS
Performance of an Inductively Coupled Plasma-Mass Spectrometer Analyzer system
[DE90-004002] N90-16025
Selection of corrosion-resistant materials for use in molten nitrate salts
[DE90-004351] N90-16048
Silicon-based coatings on niobium metal
[DE90-003851] N90-16057
Thermodynamic analysis of chemical stability of ceramic materials in hydrogen-containing atmospheres at high temperatures
[NASA-CR-4271] N90-16072
Microstructures of Y123 films on SrTiO3, LaGaO3, and LaAlO3
[DE90-003367] N90-16537
Workshop on Analysis of Returned Comet Nucleus Samples
[NASA-CR-184821] N90-16607
On the isotope analysis of cometary dust N90-16611
Electron beam analysis of particulate cometary material N90-16613
Thermal and chemical processing of the outermost layer of cometary nuclei N90-16614
Analysis of organic compounds in returned comet nucleus samples N90-16617
Prompt Gamma Activation Analysis (PGAA): Technique of choice for nondestructive bulk analysis of returned comet samples N90-16633
Methods for the mineralogical and textural analysis of comet nucleus samples N90-16648

CHEMICAL COMPOSITION
Improved performance polysulfide based sealant N90-15910
On-line chemical composition analyzer development
[DE90-004079] N90-16026
Researches on amorphous perovskite
[DE89-900733] N90-16535
The origin, composition and history of cometary ices from spectroscopic studies N90-16609
Direct determination of the morphology, structure and composition of cometary and interstellar ice analogs in the laboratory N90-16612
The carbon chemistry of meteorites: Relationships to comets N90-16615
From interstellar dust to comets N90-16620
Modifications of comet materials by the sublimation process: Results from simulation experiments N90-16621
Morphology and compositional differentiation of the surface of comets N90-16624
Identification of solar nebula condensates in interplanetary dust particles and unequilibrated ordinary chondrites N90-16629
Composition of dust from Comet P/Halley: The mineral fraction N90-16631
Computer simulation of dust grain evolution N90-16632
Solar nebula condensates and the composition of comets N90-16634
Candidate sample acquisition systems for the Rosetta N90-16635
The comet rendezvous asteroid flyby mission N90-16639
What if chondritic porous interplanetary dust particles are not the real McCoy N90-16642
Neptune's Triton: A moon rich in dry ice and carbon
[NASA-CR-186298] N90-16675

CHEMICAL EVOLUTION
Workshop on Analysis of Returned Comet Nucleus Samples
[NASA-CR-184821] N90-16607
Computer simulation of dust grain evolution N90-16632
Evolution of carbonaceous chondrite parent bodies: Insights into cometary nuclei N90-16638
The comet rendezvous asteroid flyby mission N90-16639
Physical processing of cometary nuclei N90-16653

CHEMICAL INDICATORS
Flow visualization of water flows using the crystal violet method N90-16253
Unsteady heat transfer measurement using thermochromatic liquid crystals as temperature indicators N90-16254

CHEMICAL PROPERTIES
Spray sealing: A breakthrough in integral fuel tank sealing technology N90-15912
Mechanoelectric conversion by uniaxial constraint in piezoelectric generators: Optimization of electrical, mechanical, and physico-chemical parameters of materials
[ISAL-89-0020] N90-16235

CHEMICAL REACTIONS
The continuous crystallization of sulfur formed by the liquid-phase reaction of hydrogen sulfide and sulfur dioxide
[DE90-003991] N90-16018
Selectivity of the reactions of oxygenates on transition metal surfaces
[DE90-003911] N90-16040
Shock-induced reaction synthesis of aluminides and silicides
[DE90-003948] N90-16066
High temperature neutron diffraction study of the formation reaction of bismuth superconductors
[DE90-004883] N90-16568
Non-equilibrium chemistry in the solar nebula and early solar system: Implications for the chemistry of comets N90-16618

CHEMISORPTION
Theoretical studies of chemisorption and surface reactions on nickel and silicon
[DE90-004849] N90-16050

CHIPS
BLITZEN: A highly integrated massively parallel machine N90-16453

CHLORINE
Method of making carbon dioxide and chlorine free fluoride-based glass
[AD-D014260] N90-16060

CHONDRITES
Identification of solar nebula condensates in interplanetary dust particles and unequilibrated ordinary chondrites N90-16629
What if chondritic porous interplanetary dust particles are not the real McCoy N90-16642
Refractory solids in chondrites and comets: How similar N90-16654

CHROMATOGRAPHY
On-line chemical composition analyzer development
[DE90-004079] N90-16026
Copolymers for drag reduction in marine propulsion: New molecular structures with enhanced effectiveness
[AD-A214444] N90-16062

CHROMITES
Synthesis of air-sinterable lanthanum chromite powders
[DE90-004681] N90-16049

CHROMIUM ALLOYS
Microstructural explanation for irradiation embrittlement of V-15Cr-5Ti
[DE90-004112] N90-16041
Production and processing of Cu-Cr-Nb alloys
[NASA-TM-102495] N90-16053

CHRONOLOGY
New developments in stellar ages and modelling of Pop. I stars
[SER-C-PREPUBL-FASC-41] N90-16669

CIRCUIT PROTECTION
Steep front impulse tests on a solid-state relay
[DE90-004243] N90-16140
Analysis of the 60-Hz power system at KSC: The Orsino substation N90-16692

CIRCUIT RELIABILITY
VLSI integrated circuit tests
[IMAG-RR-763-I] N90-16135

CIRCUITS
Analysis of the 60-Hz power system at KSC: The Orsino substation N90-16692

CIRCULAR POLARIZATION
Stripline feed for a microstrip array of patch elements with teardrop shaped probes
[NASA-CASE-NPO-17548-1-CU] N90-16104

CIRCULATION
Expandable radiator
[AD-D014258] N90-16147

CIVIL AVIATION
Aircraft accident report: Delta Air Lines, Inc., Boeing 727-232, N473DA, Dallas-Fort Worth International Airport, Texas, August 31, 1988
[PB89-910406] N90-15895

CLAMPS
Quick disconnect duct coupler
[AD-D014265] N90-16274

CLASSIFICATIONS
Context dependent anti-aliasing image reconstruction N90-16209
TM land use classification of a region. Utilization for planning and statistics N90-16339
The upper main sequence of OB associations. Part 2: The single-lined O stars: Spectral classification of northern stars and lines of C and N
[SER-C-PREPUBL-FASC-39] N90-16602

CLASSIFYING
Sort computation N90-16446

CLEARANCES
Assessment of worm gearing for helicopter transmissions
[NASA-TM-102441] N90-15923

CLIMATE CHANGE
Scientific linkages in global change
[PB90-112608] N90-16356

CLIMATOLOGY
Interconnectedness in nature and in science: The case of climate and climate modeling
[PB90-113986] N90-16358
The chemistry and dynamics of marine stratocumulus N90-16381
Climatic summaries and documentation for the primary meteorological Station, H. J. Andrews Experimental Forest, 1972 to 1984
[PB90-104373] N90-16382

CLOSED ECOLOGICAL SYSTEMS
Dynamics of carbon dioxide exchange of a wheat community grown in a semi-closed environment N90-16689

CLOSURES
Automatic prestart or post shutoff engine lubricator
[AD-D014259] N90-16273

CLOUDS
Turbulent stripping of interstellar clouds by interaction with supernova remnants
[DE90-003622] N90-16674

CLOUDS (METEOROLOGY)
Determination of optical porperties of clouds from NOAA-AVHRR data using Apollo N90-16321
Recognition and distinction of clouds, snow, and ice using AVHRR data N90-16322
Support of hydrological models calculations by satellite data N90-16337

COAL
Development and evaluation of a process to produce hydrogen from coal
[DE90-003937] N90-16084
Improved anode catalysts for coal gas-fueled phosphoric acid fuel cells
[DE90-004016] N90-16347

COAL GASIFICATION
Development and evaluation of a process to produce hydrogen from coal
[DE90-003937] N90-16084

COASTS
Lightning observations on Japan Sea coast in winter
[DE90-702485] N90-16387

COATINGS
Silicon-based coatings on niobium metal
[DE90-003851] N90-16057
COAXIAL CABLES
Theoretical and experimental investigation of axial power extraction from a magnetically insulated transmission line oscillator
[DE90-003486] N90-16131
COBALT COMPOUNDS
Lithium cobalt oxide thin film and its electrochromism
[DE90-004570] N90-16564
COBALT OXIDES
Lithium cobalt oxide thin film and its electrochromism
[DE90-004570] N90-16564
COCKPITS
Keeping the pilot in the loop
[RAE-TM-FM-18] N90-16396
CODING
Visual Information Processing for Television and Telerobotics
[NASA-CP-3053] N90-16204
Coded-aperture imaging in nuclear medicine N90-16208
Context dependent prediction and category encoding for DPCM image compression N90-16210
Image gathering and coding for digital restoration: Information efficiency and visual quality N90-16211
Data compression for the microgravity experiments N90-16212
High compression image and image sequence coding N90-16214
From primal sketches to the recovery of intensity and reflectance representations N90-16216
Parallel asynchronous systems and image processing algorithms N90-16218
Neural networks for data compression and invariant image recognition N90-16219
A programmable image compression system N90-16222
Hybrid LZW compression N90-16223
Digital image coding and compression
[PB90-110958] N90-16409
COERCIVITY
Anisotropy and microstructure of high coercivity rare earth iron permanent magnets, list of papers published
[AD-A214160] N90-16476
COGNITIVE PSYCHOLOGY
Formalisms for user interface specification and design N90-16687
COLD FLOW TESTS
Aerodynamic and heat transfer measurements on blading for a high rim-speed transonic turbine
[RAE-TM-P-1151] N90-15920
COLLISION AVOIDANCE
The automatic detection of anti-collision lights
[RSRE-MEMO-4272] N90-15896
UK airmisses involving commercial air transport, September to December 1988
[ISSN-0951-6301] N90-15897
COLLISIONS
Anomalous waves in shock wave - fluid interface collisions
[AD-A213584] N90-16144
COLOR
Plant features measurements for robotics N90-16695
COLOR-COLOR DIAGRAM
An atlas of aperiodic variability in HMXB
[MPE-PREPRINT-158] N90-16605
COLUMBUS SPACE STATION
Columbus: A user's introduction
[ESA-BR-62] N90-15989
DNSS: German/Norwegian work team Space Subsea. Environmental control and life support subsystems (technical matters), phase 2
[ETN-90-95905] N90-16398
COMBUSTION
Comprehensive mechanisms for combustion chemistry: An experimental and numerical study with emphasis on applied sensitivity analysis
[DE90-003904] N90-16017
COMBUSTION CHAMBERS
Solid fuel combustion chamber, phase 10
[LR-536] N90-16000
Solid fuel combustion chamber
[LR-555] N90-16001
Conceptual design for the space station Freedom modular combustion facility
[NASA-TM-102037] N90-16087
Flow visualization using the laser light sheet method in vehicle aerodynamics and combustion chamber engineering N90-16246
MHD integrated topping cycle project
[DE90-004141] N90-16525
COMBUSTION CHEMISTRY
Comprehensive mechanisms for combustion chemistry: An experimental and numerical study with emphasis on applied sensitivity analysis
[DE90-003904] N90-16017
COMBUSTION PHYSICS
Solid fuel combustion chamber, phase 10
[LR-536] N90-16000
MHD integrated topping cycle project
[DE90-004141] N90-16525
COMET NUCLEI
Workshop on Analysis of Returned Comet Nucleus Samples
[NASA-CR-184821] N90-16607
Analytical study of comet nucleus samples N90-16608
On the isotope analysis of cometary dust N90-16611
Direct determination of the morphology, structure and composition of cometary and interstellar ice analogs in the laboratory N90-16612
Electron beam analysis of particulate cometary material N90-16613
Thermal and chemical processing of the outermost layer of cometary nuclei N90-16614
Analysis of organic compounds in returned comet nucleus samples N90-16617
Trace element abundance determinations by Synchrotron X Ray Fluorescence (SXRF) on returned comet nucleus mineral grains N90-16619
From interstellar dust to comets N90-16620
Comments on comet shapes and aggregation processes N90-16622
Cosmogenic nuclides in cometary materials: Implications for rate of mass loss and exposure history N90-16623
Morphology and compositional differentiation of the surface of comets N90-16624
Role of dust to gas production rate ratio in cometary physics N90-16625
Spectrophotometric observations of comet P/Giacobini-Zinner N90-16630
Candidate sample acquisition systems for the Rosetta N90-16635
Interstellar and cometary dust N90-16636
The in-situ cometary particulate size distribution measured for one comet: P/Halley N90-16637
Evolution of carbonaceous chondrite parent bodies: Insights into cometary nuclei N90-16638
The comet rendezvous asteroid flyby mission N90-16639
Measurements of long-lived cosmogenic nuclides in returned comet nucleus samples N90-16640
What if chondritic porous interplanetary dust particles are not the real McCoy N90-16642
Handling and analysis of ices in cryostats and glove boxes in view of cometary samples N90-16643
Thermal histories of the samples of two KOSI comet nucleus simulation experiments N90-16645
Analysis of particulates of comet nucleus samples: Possible use of olivine as indicator phase N90-16646
Methods for the mineralogical and textural analysis of comet nucleus samples N90-16648
Non-destructive trace element microanalysis of as-received cometary nucleus samples using synchrotron x ray fluorescence N90-16649
Mechanical and SEM analysis of artificial comet nucleus samples N90-16650
Electron Spin Resonance (ESR) studies of returned comet nucleus samples N90-16651
Physical processing of cometary nuclei N90-16653
Isotopic microanalysis of returned comet nucleus samples N90-16655
COMET RENDEZVOUS ASTEROID FLYBY MISSION
The comet rendezvous asteroid flyby mission N90-16639
COMETARY ATMOSPHERES
Role of dust to gas production rate ratio in cometary physics N90-16625
Sulfur compounds in comets N90-16627
The comet rendezvous asteroid flyby mission N90-16639
What if chondritic porous interplanetary dust particles are not the real McCoy N90-16642
COMETS
Workshop on Analysis of Returned Comet Nucleus Samples
[NASA-CR-184821] N90-16607
The origin, composition and history of cometary ices from spectroscopic studies N90-16609
Experimental studies of gas trapping in amorphous ice and thermal modelling of comets: Implications for Rosetta N90-16610
On the isotope analysis of cometary dust N90-16611
Electron beam analysis of particulate cometary material N90-16613
The carbon chemistry of meteorites: Relationships to comets N90-16615
Laboratory analyses of micron-sized solid grains: Experimental techniques and recent results N90-16616
Non-equilibrium chemistry in the solar nebula and early solar system: Implications for the chemistry of comets N90-16618
Modifications of comet materials by the sublimation process: Results from simulation experiments N90-16621
Comments on comet shapes and aggregation processes N90-16622
Cosmogenic nuclides in cometary materials: Implications for rate of mass loss and exposure history N90-16623
Role of dust to gas production rate ratio in cometary physics N90-16625
Radiation modification of cometary materials: Laboratory simulations N90-16626
Spectrophotometric observations of comet P/Giacobini-Zinner N90-16630
Prompt Gamma Activation Analysis (PGAA): Technique of choice for nondestructive bulk analysis of returned comet samples N90-16633
Candidate sample acquisition systems for the Rosetta N90-16635
Interstellar and cometary dust N90-16636
Evolution of carbonaceous chondrite parent bodies: Insights into cometary nuclei N90-16638
The comet rendezvous asteroid flyby mission N90-16639
Measurements of long-lived cosmogenic nuclides in returned comet nucleus samples N90-16640
Metamorphism of cosmic dust: Processing from circumstellar outflows to the cometary regolith N90-16641
What if chondritic porous interplanetary dust particles are not the real McCoy N90-16642
Trajectory-capture cell instrumentation for measurement of dust particle mass, velocity and trajectory, and particle capture N90-16644
The nature of cometary materials N90-16647
Methods for the mineralogical and textural analysis of comet nucleus samples N90-16648
Mechanical and SEM analysis of artificial comet nucleus samples N90-16650
Ion bombardment experiments suggesting an origin for organic particles in pre-cometary and cometary ices N90-16652
Physical processing of cometary nuclei N90-16653
The measurement of trace elements in interplanetary dust and cometary particles by ultra-high sensitivity INAA N90-16656
COMMERCIAL AIRCRAFT
UK airmisses involving commercial air transport, September to December 1988
[ISSN-0951-6301] N90-15897
COMMUNICATION EQUIPMENT
X-band atmospheric attenuation for an Earth terminal measurement system
[PB90-100736] N90-16101
Helsinki University of Technology Radio Laboratory
[PB90-110677] N90-16102
COMMUNICATION NETWORKS
The first year's work of race project 1036 WTDM broadband customer premises network
[BBC-RD-1989/6] N90-16097
COMPACTING
Method for refining microstructures on prealloyed titanium powder compacts
[AD-D014280] N90-16030
COMPATIBILITY
Improved performance polysulfide based sealant N90-15910
COMPILERS
A generic fine-grained parallel C N90-16454
COMPLEX COMPOUNDS
New electrically conducting solids based on nickel(II) - bis(1,3-dithiole-2-thione-4,5-diselenolate)
[DE90-003788] N90-16020
COMPOSITE MATERIALS
Advanced composite polar boss
[AD-D014287] N90-15994
Assessing the flammability of composite materials
[PB90-112996] N90-16002
Evaluation of potential cold x ray shield materials tested on Proto II
[DE90-004348] N90-16003
The structure of silica-polysiloxane composites and its effects on their elastomeric properties
[DE89-014768] N90-16005
Design of coupled or uncoupled multifilamentary SSC-type strands with almost zero retained magnetization at fields near 0.3 T
[DE90-005391] N90-16052
The physical properties of microcellular composite foams
[DE90-003658] N90-16058

Review of investigations on aeronautical fatigue in the Federal Republic of Germany
[LBF-S-182] N90-16302

COMPOSITION (PROPERTY)
Resonance enhanced Raman studies of as-grown and laser-processed HgCdTe
[AD-A213855] N90-16540

COMPRESSED AIR
Investigation and study on compressed air storage power generation system, part 2
[DE90-702648] N90-16354

COMPRESSIBLE FLOW
Adaptive local grid refinement for the compressible 3-D Euler equations
[FFA-TN-1989-40] N90-16155
Method for the primary stability analysis of the three dimensional, compressible boundary layer flows N90-16171
An efficient solver of the Eigenvalue problem of the linear stability equations for three dimensional, compressible boundary-layer flows N90-16172
Digital image interpretation for optical flow measurement methods: System description and preliminary application examples N90-16244

COMPRESSIBLE FLUIDS
Decay estimates for the compressible Navier-Stokes equations in the half-space
[PREPRINT-46] N90-16163

COMPRESSOR BLADES
Performance of a highly-loaded HP compressor
[RAE-TM-P-1149] N90-15919

COMPRESSORS
Externally vaporizing system for turbine combustor
[AD-D014284] N90-15918

COMPUTATION
An algorithm to compute the square root of 3x3 positive definite matrix
[DE89-635711] N90-16417

COMPUTATIONAL FLUID DYNAMICS
Assessment of computational prediction of tail buffeting
[NASA-TM-101613] N90-15886
Weapon aerodynamics overview
[RAE-TM-AERO-2150] N90-15888
A numerical simulation of the flow in the diffuser of the NASA Lewis icing research tunnel
[NASA-TM-102480] N90-15965
The Suprenum architecture and its application to computational fluid dynamics
[GMD-389] N90-16161
Decay estimates for the compressible Navier-Stokes equations in the half-space
[PREPRINT-46] N90-16163
Calculation of the flow field of a multiblade helicopter rotor using a Euler method including the wake N90-16189
Calculation of the flap profile flows with separation based on coupled potential and boundary layer solutions N90-16191
A finite volume calculation method for three dimensional, complex flows N90-16195
A space-time discretization procedure for wave propagation problems
[NASA-TM-102215] N90-16399
A new finite element formulation for CFD:8. The Galerkin/least-squares method for advective-diffusive equations
[DE89-636437] N90-16462

COMPUTATIONAL GRIDS
Personal computer study of finite-difference methods for the transonic small disturbance equation
[NASA-TM-102582] N90-15892
Euler and Navier-Stokes computations for two-dimensional geometries using unstructured meshes
[NASA-CR-181977] N90-15893
Adaptive local grid refinement for the compressible 3-D Euler equations
[FFA-TN-1989-40] N90-16155
Grid-independent wall layer turbulence model for complex flow calculations
[DE90-003500] N90-16200
FRAC-IN-THE-BOX utilization
[DE90-003648] N90-16412
Parallel algorithms for interactive manipulation of digital terrain models N90-16445
Multigrid methods for two- and three-dimensional Poisson-type equations on the sphere
[GMD-391] N90-16468

COMPUTER AIDED DESIGN
Case tool evaluation system
[DE90-003698] N90-16413
CAE (Computer-Aided Engineering) tools' limitations case study: An SSI (Small Scale Integrated) design to an ASIC (Application Specific Integrated Circuit)
[DE90-002902] N90-16418
Appearance analysis from CAD models
[IMAG-RR-756-I-IMAG-88-LIFIA] N90-16434
Low-cost volumetric modeling
[CRIF-MC-85] N90-16435
Computer aided design based optical system modeling
[DE90-003453] N90-16440
Interpretation of CAD (Computer Aided Design) models through IGES (Initial Graphics Exchange Specification) interface
[PB90-121294] N90-16441
NASA/ASEE Summer Faculty Fellowship Program
[NASA-CR-166837] N90-16686
Investigation of IGES for CAD/CAE data transfer N90-16702

COMPUTER GRAPHICS
Dynamic architecture computer
[AD-A214262] N90-16402
EZVIDEO, FORTRAN graphics routines for the IBM AT
[DE90-004409] N90-16422
Computer aided design based optical system modeling
[DE90-003453] N90-16440
Interpretation of CAD (Computer Aided Design) models through IGES (Initial Graphics Exchange Specification) interface
[PB90-121294] N90-16441
Parallel algorithms for interactive manipulation of digital terrain models N90-16445
Scan line graphics generation on the massively parallel processor N90-16450
NASA/ASEE Summer Faculty Fellowship Program
[NASA-CR-166837] N90-16686
The DAB model of drawing processes N90-16691
Investigation of IGES for CAD/CAE data transfer N90-16702

COMPUTER INFORMATION SECURITY
Issues and approaches for electronic document approval and transmittal using digital signatures and text authentication: Prototype documentation
[DE90-003382] N90-16119
The SMITE approach to security
[RSRE-89014] N90-16404
Tool support for the production of high integrity software
[RSRE-89005] N90-16433

COMPUTER NETWORKS
PVM (Parallel Virtual Machine): A framework for parallel distributed computing
[DE90-004390] N90-16403
Overview and extensions of a system for routing directed graphs on SIMD architectures N90-16444

COMPUTER PROGRAM INTEGRITY
An empirical comparison of software fault tolerance and fault elimination
[NASA-CR-186313] N90-16414
Tool support for the production of high integrity software
[RSRE-89005] N90-16433

COMPUTER PROGRAMMING
Diesel starting system monitor: Prototype development
[DE90-004425] N90-16276
Bus programmable slave module
[NASA-CASE-MSC-21387-1] N90-16411
An empirical comparison of software fault tolerance and fault elimination
[NASA-CR-186313] N90-16414
ZBTAB: Zenith-248 version of BLUGTAB
[AD-A214279] N90-16415
EZVIDEO, FORTRAN graphics routines for the IBM AT
[DE90-004409] N90-16422
The new programming
[RSRE-MEMO-4249] N90-16425
A persistent heap for ALGOL 68
[RSRE-MEMO-4268] N90-16427
Alvey MMI007. Object identification from 2D images: The RSRE contribution
[RSRE-MEMO-4277] N90-16428
Tool support for the production of high integrity software
[RSRE-89005] N90-16433
Computer aided design based optical system modeling
[DE90-003453] N90-16440
Off-line robot programming and graphical verification of path planning N90-16699

COMPUTER PROGRAMS
Rotor induced-inflow-ratio measurements and CAMRAD calculations
[NASA-TP-2946] N90-15882
Improved tangent-cone method for the Aerodynamic Preliminary Analysis System (APAS) version of the hypersonic arbitrary-body program
[NASA-TM-4165] N90-15890
The application of Z to the specification of air traffic control systems. 1: An initial specification of the radar processing activity
[RSRE-MEMO-4280] N90-15900
Automated search techniques applied to optical payloads in unmanned air vehicles N90-15931
Distribution of hardware and software elements in unmanned air vehicle systems N90-15933
A numerical simulation of the flow in the diffuser of the NASA Lewis icing research tunnel
[NASA-TM-102480] N90-15965
Dynamics analyses of space power systems using the salt code
[DE90-002274] N90-15995
MT's algorithm: A new algorithm to search for the optimum set of modulation indices for simultaneous range, command, and telemetry
[NASA-CR-186259] N90-16110
Stand Alone Pressure Measurement Device (SAPMD) for the space shuttle Orbiter, part 2
[NASA-CR-172119-PT-2] N90-16203
Stochastic model of the NASA/MSFC ground facility for large space structures with uncertain parameters: The maximum entropy approach, part 2
[NASA-CR-186009] N90-16407
FRAC-IN-THE-BOX utilization
[DE90-003648] N90-16412
Case tool evaluation system
[DE90-003698] N90-16413
An empirical comparison of software fault tolerance and fault elimination
[NASA-CR-186313] N90-16414
CPU timing routines for a CONVEX C220 computer system
[NASA-CR-181950] N90-16424
Software dependability growth characterization, modeling and evaluation
[LAAS-89320] N90-16437
Design and implementation of a multi-sensor fusion algorithm on a hypercube computer architecture
[DE90-003682] N90-16438
Results of error correction techniques applied on two high accuracy coordinate measuring machines
[DE90-003341] N90-16439
On the efficient exploitation of speculation under data flow paradigms of control
[AD-A214112] N90-16455
An implicit time-integration procedure for a set of internal variable constitutive equations for isotropic elasto-viscoplasticity
[PB90-121302] N90-16470
Modeling energy output of inertial storage devices for the DIII-D tokamak
[DE90-004096] N90-16524
User's manual for MGMHD: A multigrid three-dimensional computer code for the analysis of magnetohydrodynamic generators and diffusers
[DE90-004453] N90-16526
Estimation of thermodynamic properties of alloys from phase diagram and other loose boundary conditions
[DE90-719511] N90-16579
A computer program to calculate the population numbers of multi-level species
[IFSI-89-15] N90-16671
The DAB model of drawing processes N90-16691
Off-line robot programming and graphical verification of path planning N90-16699
Activities report of the National Electrotechnic Institute Galileo Ferraris
[ETN-90-96178] N90-16705

COMPUTER SYSTEMS DESIGN
The Suprenum architecture and its application to computational fluid dynamics
[GMD-389] N90-16161
Dynamic architecture computer
[AD-A214262] N90-16402
UNIX internals. Part 1: Intertask communication in UNIX. Part 2: UNIX file system
[CNES-NT-122-PT-1/2] N90-16405
Creating the next generation control system software
[DE90-003391] N90-16419

COMPUTER SYSTEMS PERFORMANCE
Dynamic architecture computer
[AD-A214262] N90-16402
UNIX internals. Part 1: Intertask communication in UNIX. Part 2: UNIX file system
[CNES-NT-122-PT-1/2] N90-16405
A 3-D measurement system using object-oriented FORTH
[DE90-003393] N90-16420
The NODEN hardware description language
[RSRE-89011] N90-16431
The algebra of the NODEN analyser
[RSRE-89012] N90-16432
Low-cost volumetric modeling
[CRIF-MC-85] N90-16435

Computer aided design based optical system modeling
[DE90-003453] N90-16440
Solving time harmonic wave problems on vector processors
[DE90-003956] N90-16480
New optimization techniques in database access and maintenance N90-16586
Event-join optimization in temporal relational databases
[DE90-003117] N90-16588

COMPUTER SYSTEMS PROGRAMS
The NODEN hardware description language
[RSRE-89011] N90-16431

COMPUTER TECHNIQUES
Computer-aided boundary delineation of agricultural lands
[NASA-TM-102243] N90-16313
The development of two-dimensional object identification techniques
[NASA-CR-186203] N90-16408
An empirical comparison of software fault tolerance and fault elimination
[NASA-CR-186313] N90-16414
CAE (Computer-Aided Engineering) tools' limitations case study: An SSI (Small Scale Integrated) design to an ASIC (Application Specific Integrated Circuit)
[DE90-002902] N90-16418
New optimization techniques in database access and maintenance N90-16586

COMPUTER VISION
Visual Information Processing for Television and Telerobotics
[NASA-CP-3053] N90-16204
Parallel asynchronous systems and image processing algorithms N90-16218
A knowledge-based machine vision system for space station automation N90-16221
Plant features measurements for robotics N90-16695

COMPUTERIZED SIMULATION
Piloted simulation of a ground-based time-control concept for air traffic control
[NASA-TM-101085] N90-15898
Navigation of autonomous air vehicles by passive imaging sensors N90-15927
Navigation up-date using radar mapping: Assessment and optimisation simulation tool N90-15928
Automatic control of KKK: Requirements, sensors, actuators, and control performance results N90-15944
Probabilistic simulation of uncertainties in composite uniaxial strengths
[NASA-TM-102483] N90-16008
Multidimensional numerical simulation of large caliber ignition processes
[ISL-CO-233/88] N90-16021
Fundamental studies of beta phase decomposition modes in titanium alloys
[AD-A214424] N90-16035
Electroplating simulation
[DE90-003683] N90-16091
Sizing and selection of batteries for stand-alone photovoltaic systems
[DE90-002990] N90-16129
Grid-independent wall layer turbulence model for complex flow calculations
[DE90-003500] N90-16200
On-line estimation of mechanical nonlinearities in compliant two-link robot manipulators N90-16280
Design of a spheromak compressor driven by high explosives
[DE90-003652] N90-16283
Element-by-element preconditioning techniques for large-scale, vectorized finite element analysis in nonlinear solid and structural mechanics N90-16291
Rainflow counting algorithm for the LIFE2 fatigue analysis code
[DE90-002834] N90-16344
Simulation of pollutant transport using a mesoscale grid circulation model
[GKSS-89/E/24] N90-16365
A dynamic model for forecasting new cloud development
[AD-A213939] N90-16383
New atmospheric turbulence model for shuttle applications
[NASA-TM-4168] N90-16389
Mechanisms of microwave induced damage in biologic materials
[AD-A213480] N90-16390
Discrete event simulation tool for analysis of qualitative models of continuous processing systems
[NASA-CASE-MSC-21465-1] N90-16410
FRAC-IN-THE-BOX utilization
[DE90-003648] N90-16412
Use of computer simulations to analyze limitations of kinetic models for recrystallization
[DE90-003618] N90-16548
The concept of axial-symmetry constraint and its significance in recrystallization
[DE90-003620] N90-16549
On the interaction of a pulsar with the ambient medium utilizing x ray images of the Crab nebula
[MPE-REPT-215] N90-16604
Computer simulation of dust grain evolution N90-16632
Off-line robot programming and graphical verification of path planning N90-16699

COMPUTERS
Bus programmable slave module
[NASA-CASE-MSC-21387-1] N90-16411

CONCRETES
Evaluation of two transport aircraft and several ground test vehicle friction measurements obtained for various runway surface types and conditions. A summary of test results from joint FAA/NASA Runway Friction Program
[NASA-TP-2917] N90-15902

CONDENSATES
Identification of solar nebula condensates in interplanetary dust particles and unequilibrated ordinary chondrites N90-16629
Solar nebula condensates and the composition of comets N90-16634

CONDENSATION NUCLEI
Study of phase transformations liquid-solid-solid of ultrafine particles
[ISAL-89-0019] N90-16022

CONDENSERS (LIQUEFIERS)
Experimental investigation of condensation of steam in the presence of noncondensable gases for open-cycle surface condensers
[DE90-003552] N90-16353

CONDENSING
Experimental investigation of condensation of steam in the presence of noncondensable gases for open-cycle surface condensers
[DE90-003552] N90-16353
On condensation driven by electrostatic interactions in macroionic solutions
[DE89-636072] N90-16487

CONDUCTING FLUIDS
Command operated liquid metal opening switch
[AD-D014262] N90-16126

CONDUCTION BANDS
Theory of the electronic and optical properties of semiconductor heterostructures
[AD-A214132] N90-16544

CONFERENCES
Advances in techniques and technologies for air vehicle navigation and guidance
[AGARD-AR-276] N90-15899
Fuel Tank Technology
[AGARD-R-771] N90-15904
Guidance and Control of Unmanned Air Vehicles
[AGARD-CP-436] N90-15924
Special Course on Advances in Cryogenic Wind Tunnel Technology
[AGARD-R-774] N90-15939
Crew Safety and Rescue in Space: An International Approach
[ESA-SP-300] N90-15974
The Eighteenth Conference on Stochastic Processes and their Applications
[AD-A212301] N90-16010
Structure-property relationships in ion-beam surface-modified ceramics: Theory and applications
[AD-A212785] N90-16054
Ninth Battery and Electrochemical Contractors' Conference: Extended abstracts
[DE89-016837] N90-16120
Visual Information Processing for Television and Telerobotics
[NASA-CP-3053] N90-16204
Proceedings of the 5th User Seminar of the German Remote Sensing Data Center of the DFVLR
[DFVLR-MITT-89-04] N90-16318
Proceedings of the Conference on Technology-Based Confidence Building: Energy and Environment
[DE90-003363] N90-16366
The 2nd Symposium on the Frontiers of Massively Parallel Computations
[NASA-TM-101918] N90-16442
Proceedings of the specialists' meeting on physics and engineering of fission and spallation
[DE90-719706] N90-16519
International conference management N90-16583
Proceedings of the 79th SEGJ Conference
[DE89-760006] N90-16704

CONFIGURATION INTERACTION
General contraction of Gaussian basis sets. Part 2: Atomic natural orbitals and the calculation of atomic and molecular properties
[NASA-CR-186201] N90-16482

CONFIGURATION MANAGEMENT
Distribution of hardware and software elements in unmanned air vehicle systems N90-15933

CONFORMAL MAPPING
The off-shell closed strings as the topological open membranes: Dynamical transmutation of world sheet dimension
[DE89-635721] N90-16571

CONGRESSIONAL REPORTS
Round trip to orbit. Human spaceflight alternatives: Special report
[OTA-ISC-419] N90-15966

CONNECTORS
Connector selection program implementation notes, version 1.0
[DE90-004983] N90-16279

CONSTITUTIVE EQUATIONS
An implicit time-integration procedure for a set of internal variable constitutive equations for isotropic elasto-viscoplasticity
[PB90-121302] N90-16470

CONSTRAINTS
Use of an HF active monitoring array in the presence of high level interference
[BBC-RD-1989/7] N90-16096

CONSTRUCTION
Aircraft fuel tank construction and testing experience N90-15907
The US National Transonic Facility, NTF N90-15942
The Kryo-Kanal Koeln (KKK): Description of the tunnel conversion. Thermal insulation, instrumentation, operational experience, test results and operating costs N90-15943
The European Transonic Windtunnel (ETW) N90-15945
Materials and techniques for model construction N90-15954
Some recent developments in materials and techniques for model fabrication N90-15955
Models for cryogenic wind tunnels N90-15956

CONSTRUCTION MATERIALS
Special Course on Advances in Cryogenic Wind Tunnel Technology
[AGARD-R-774] N90-15939

CONTAMINATION
Method of making carbon dioxide and chlorine free fluoride-based glass
[AD-D014260] N90-16060
The influence of residual contamination on the structure and properties of metal/GaAs interfaces
[DE90-000549] N90-16530

CONTEXT
Context dependent anti-aliasing image reconstruction N90-16209
Context dependent prediction and category encoding for DPCM image compression N90-16210

CONTINUOUS WAVE LASERS
Eurolaser definition phase: A comparison of high power lasers available
[ETN-90-96061] N90-16268

CONTOUR SENSORS
Order filters, median recursive filter: Analysis and evaluation of performance in image processing
[ISAL-89-0017] N90-16505

CONTOURS
Isolating contour information from arbitrary images N90-16217

CONTRACTION
General contraction of Gaussian basis sets. Part 2: Atomic natural orbitals and the calculation of atomic and molecular properties
[NASA-CR-186201] N90-16482

CONTROL SYSTEMS DESIGN
Crew emergency return vehicle autoland feasibility study
[NASA-CR-181940] N90-15937
The US National Transonic Facility, NTF N90-15942
Automatic control of KKK: Requirements, sensors, actuators, and control performance results N90-15944
On-line chemical composition analyzer development
[DE90-004079] N90-16026
D3-D cryogenic control system upgrade
[DE90-003290] N90-16092
Digital system for monitoring and controlling remote processes
[DE90-003935] N90-16094
Diesel starting system monitor: Prototype development
[DE90-004425] N90-16276
Expert system control of a six-legged walking telerobot
[DE90-004661] N90-16285

Stochastic model of the NASA/MSFC ground facility for large space structures with uncertain parameters: The maximum entropy approach, part 2
[NASA-CR-186009] N90-16407

CONTROL THEORY
Guidance and Control of Unmanned Air Vehicles
[AGARD-CP-436] N90-15924
Synthesis of control law, on a RPV, in order to minimize the number of sensors N90-15925
Automatic control of cryogenic wind tunnels N90-15957
Bilateral force reflection for teleoperators with masters and slaves with dissimilar and possibly redundant kinematics
[DE90-004392] N90-16132

CONTROLLERS
Knowledge-based imaging-sensor fusion system N90-16220
Expert system control of a six-legged walking telerobot
[DE90-004681] N90-16285
Artificial intelligence in process control: Knowledge base for the shuttle ECS model N90-16697
Mathematical model for adaptive control system of ASEA robot at Kennedy Space Center N90-16701

CONVECTION
The response of the atmospheric convective boundary layer to surface inhomogeneities N90-16369

CONVECTION CLOUDS
Mesoscale analysis by numerical modelling coupled with satellite-based sounding N90-16370
A dynamic model for forecasting new cloud development
[AD-A213939] N90-16383

CONVECTIVE FLOW
Feed back Petrov-Galerkin methods for convection dominated problems
[DE89-636436] N90-15148
Simultaneous determination of temperature and velocity fields in a thermal convection flow with non-enclosed liquid crystal tracers N90-16239

CONVERGENCE
Convergence speeding up in the calculation of the viscous flow about an airfoil N90-16194

CONVERGENT-DIVERCENT NOZZLES
An experimental investigation of thrust vectoring two-dimensional convergent-divergent nozzles installed in a twin-engine fighter model at high angles of attack
[NASA-TM-4155] N90-15884

COOLANTS
The onset of boiling of the liquid alkali metals
[DE90-002276] N90-16036

COOLERS
Feasibility of cool storage systems in refrigeration
[DE90-728179] N90-16093

COOLING
Productivity and cryogenic wind tunnels N90-15961
Synthesis of tetrafluorohydrazine
[AD-D014281] N90-16083

COORDINATES
A 3-D measurement system using object-oriented FORTH
[DE90-003393] N90-16420
Results of error correction techniques applied on two high accuracy coordinate measuring machines
[DE90-003341] N90-16439

COPOLYMERS
Copolymers for drag reduction in marine propulsion: New molecular structures with enhanced effectiveness
[AD-A214444] N90-16062
Diblock copolymers at surfaces
[DE90-005406] N90-16079

COPPER
Surface studies at the NSLS
[DE90-003173] N90-16027
Elastic moduli of copper: Electronic structure contributions from pseudopotentials and full-potential linear muffin-tin orbital band structure calculations
[DE90-004423] N90-16037
Long term creep strength of silver alloyed copper
[DE90-602367] N90-16039

COPPER ALLOYS
Production and processing of Cu-Cr-Nb alloys
[NASA-TM-102495] N90-16053

COPPER OXIDES
Rotational magnetic processes in YB2Cu3O7
[DE90-000541] N90-16533
The effects of oxygen and strontium vacancies on the superconductivity of single crystals of Bi2Sr(2-x)CuO(6-y)
[DE90-004242] N90-16561
Physical properties of Bi2Sr2CuO6, the semiconducting phase, structurally distinct from the n = 1 Bi-cuprate superconductor
[DE90-004299] N90-16563

CORE SAMPLING
Analytical study of comet nucleus samples N90-16608
The nature of cometary materials N90-16647

CORRELATION COEFFICIENTS
Correlative analyses for geomagnetic indices, cosmic-ray intensities and sunspot numbers recorded since 1937
[IFSI-89-4] N90-16670

CORROSION
Study of metal corrosion using ac impedance techniques in the STS launch environment N90-16688

CORROSION RESISTANCE
Stainless steel passivity
[AD-A214108] N90-16033
Selection of corrosion-resistant materials for use in molten nitrate salts
[DE90-004351] N90-16048
MHD integrated topping cycle project
[DE90-004141] N90-16525
Study of metal corrosion using ac impedance techniques in the STS launch environment N90-16688
The effects of hydrogen embrittlement of titanium N90-16698

COSMIC DUST
The carbon chemistry of meteorites: Relationships to comets N90-16615
Trace element abundance determinations by Synchrotron X Ray Fluorescence (SXRF) on returned comet nucleus mineral grains N90-16619
From interstellar dust to comets N90-16620
Role of dust to gas production rate ratio in cometary physics N90-16625
Computer simulation of dust grain evolution N90-16632
Interstellar and cometary dust N90-16636
Metamorphism of cosmic dust: Processing from circumstellar outflows to the cometary regolith N90-16641

COSMIC PLASMA
Correlative analyses for geomagnetic indices, cosmic-ray intensities and sunspot numbers recorded since 1937
[IFSI-89-4] N90-16670

COSMIC RAY SHOWERS
A low-threshold EAS (Extensive-Air-Shower) array for gamma-ray astronomy at Los Alamos
[DE89-016780] N90-16600
Status of the expansion of the CYGNUS array at Los Alamos
[DE89-016781] N90-16601
Relative muon content of UHE showers associated with Hercules X-1
[DE90-000609] N90-16665

COSMIC RAYS
Stochastic simulation of charged particle transport on the massively parallel processor N90-16448
Correlative analyses for geomagnetic indices, cosmic-ray intensities and sunspot numbers recorded since 1937
[IFSI-89-4] N90-16670
A database of fragmentation cross section measurements applicable to cosmic ray propagation calculations
[NASA-CR-186328] N90-16681
The excess flux in the cosmic submillimeter background radiation and the primordial deuterium abundance
[NASA-CR-186312] N90-16683
Cosmic ray NM-64 neutron monitor data 16
[IFSI-88-21] N90-16684

COSMOCHEMISTRY
Cosmogenic nuclides in cometary materials: Implications for rate of mass loss and exposure history N90-16623
Metamorphism of cosmic dust: Processing from circumstellar outflows to the cometary regolith N90-16641
Physical processing of cometary nuclei N90-16653

COSMOLOGY
Study of primitive universe in the Bianchi 9 model
[DE89-635903] N90-16572
Universe as a topological defect in a higher-dimensional Einstein-Yang-Mills theory
[DE90-719507] N90-16578
Cosmogenic nuclides in cometary materials: Implications for rate of mass loss and exposure history N90-16623
Measurements of long-lived cosmogenic nuclides in returned comet nucleus samples N90-16640
Quantum fields in cosmological space-times: A soluble example
[DE89-618837] N90-16662
Dissipative effects in Friedmann universes
[DE89-618838] N90-16663
Determination of solar flare accelerated ion angular distributions from SMM gamma ray and neutron measurements and determination of the He-3/H ratio in the solar photosphere from SMM gamma ray measurements
[NASA-CR-186038] N90-16676

COST ANALYSIS
A qualitative architecture for understanding policy responses to global change
[DE90-003936] N90-16364

COST EFFECTIVENESS
The European Transonic Windtunnel (ETW) N90-15945

COULOMB POTENTIAL
Lower limit for the average angular momentum leading to fusion
[DE90-004027] N90-16523

COUNTERFLOW
Superflow induced phase transition in the axial vortex-free texture of rotating superfluid He-3-B
[PB90-110388] N90-16531

COUPLERS
Quick disconnect duct coupler
[AD-D014265] N90-16274

CRAB NEBULA
On the interaction of a pulsar with the ambient medium utilizing x ray images of the Crab nebula
[MPE-REPT-215] N90-16604

CRACK ARREST
Experiences with three-point bending test specimens for determining the crack-arrest fracture toughness K(sub Ia) in low-alloy steel
[DE90-004120] N90-16306

CRACK INITIATION
Numerical simulation of creep crack growth experiments
[IWM-W-4/88] N90-16303

CRACK PROPAGATION
Calibration of a pulsed potential crack monitor for use in fatigue crack growth studies
[RAE-TM-M/S-1126] N90-16301
Numerical simulation of creep crack growth experiments
[IWM-W-4/88] N90-16303
A quantitative analysis of slip phenomena along a dry contact surface between two bodies in comparison to interfacial crack propagation
[ISAL-89-0032] N90-16304
BAM: German Federal Institute for Materials Research and Testing, Berlin
[DE90-004293] N90-16307

CRACKS
Electroplating simulation
[DE90-003683] N90-16091
Fracto-fusion. Mechanism of cold fusion
[DE90-719573] N90-16518

CRASHES
Aircraft accident report: Delta Air Lines, Inc., Boeing 727-232, N473DA, Dallas-Fort Worth International Airport, Texas, August 31, 1988
[PB89-910406] N90-15895

CREEP ANALYSIS
Numerical simulation of creep crack growth experiments
[IWM-W-4/88] N90-16303

CREEP PROPERTIES
Method of marking titanium alloy articles having distinct microstructural regions corresponding to high creep and fatigue resistance
[AD-D014283] N90-16031
Irradiation creep and swelling of annealed type 304L stainless steel at approximately 390 C and high neutron fluence
[DE90-004521] N90-16047
Modeling dislocation evolution in irradiated alloys
[DE90-004921] N90-16051
Theoretical study on creep damage detection by ultra-sonic wave measurement
[DE90-702472] N90-16290

CREEP RUPTURE STRENGTH
The influence of carbide precipitation on the creep rupture behavior of high temperature alloys
[JUEL-2211] N90-16044

CREEP STRENGTH
Long term creep strength of silver alloyed copper
[DE90-602367] N90-16039

CREEP TESTS
The influence of carbide precipitation on the creep rupture behavior of high temperature alloys
[JUEL-2211] N90-16044
Theoretical study on creep damage detection by ultra-sonic wave measurement
[DE90-702472] N90-16290

CREW WORKSTATIONS
The first 1000 days of a future lunar base
[ILR-MITT-224] N90-15970

CRITERIA
Case tool evaluation system
[DE90-003698] N90-16413
CROP INVENTORIES
Quantitative evaluation of object-changes in multitemporal AGRISAR imagery
[FIM-195] N90-16314
Use of remote sensing in operational inventory and monitoring agricultural and forestry tasks N90-16336
CRUSTS
Radiation modification of cometary materials: Laboratory simulations N90-16626
CRYOGENIC FLUIDS
On the selection of materials for cryogenic seals and the testing of their performance N90-16696
CRYOGENIC WIND TUNNELS
Special Course on Advances in Cryogenic Wind Tunnel Technology
[AGARD-R-774] N90-15939
Introduction to cryogenic wind tunnels N90-15940
The NASA Langley 0.3-meter transonic cryogenic tunnel N90-15941
The Kryo-Kanal Koeln (KKK): Description of the tunnel conversion. Thermal insulation, instrumentation, operational experience, test results and operating costs N90-15943
Automatic control of KKK: Requirements, sensors, actuators, and control performance results N90-15944
The cryogenic induction tunnel T2 at Toulouse N90-15946
The cryogenic Ludwieg tube tunnel at Goettingen N90-15947
Other cryogenic wind tunnel projects N90-15948
Instrumentation for cryogenic wind tunnels N90-15950
Fundamental considerations in testing in cryogenic wind tunnels N90-15951
Test techniques for cryogenic wind tunnels N90-15952
Flow visualization in the cryogenic wind tunnel N90-15953
Materials and techniques for model construction N90-15954
Some recent developments in materials and techniques for model fabrication N90-15955
Models for cryogenic wind tunnels N90-15956
Automatic control of cryogenic wind tunnels N90-15957
Experience with strain-gage balances for cryogenic wind tunnels N90-15958
Safety and cryogenic wind tunnels N90-15960
Productivity and cryogenic wind tunnels N90-15961
Energy management and recovery N90-15962
CRYOGENICS
The NASA Langley 0.3-meter transonic cryogenic tunnel N90-15941
The US National Transonic Facility, NTF N90-15942
Cryogenic engineering and materials N90-15949
Cryogenic balances for the US NTF N90-15959
D3-D cryogenic control system upgrade
[DE90-003290] N90-16092
Analysis of particulates of comet nucleus samples: Possible use of olivine as indicator phase N90-16646
On the selection of materials for cryogenic seals and the testing of their performance N90-16696
CRYOSTATS
Handling and analysis of ices in cryostats and glove boxes in view of cometary samples N90-16643
CRYOTRAPPING
Experimental studies of gas trapping in amorphous ice and thermal modelling of comets: Implications for Rosetta N90-16610
CRYSTAL DEFECTS
Pairs of chalcogen impurities in silicon
[DE89-635767] N90-16063
Slow positron defect profiling of silicon epilayers
[DE90-003958] N90-16288
Fracto-fusion. Mechanism of cold fusion
[DE90-719573] N90-16518
La(sub 2)MO(sub 4 + delta) (M = Cu, Ni, Co): Phase separation and superconductivity resulting from excess oxygen defects
[DE90-001988] N90-16534
The 1MeV-electron irradiation induced defects in epitaxially grown 3C-SiC
[DE90-719574] N90-16554
CRYSTAL DISLOCATIONS
Modeling dislocation evolution in irradiated alloys
[DE90-004921] N90-16051
CRYSTAL GROWTH
Use of computer simulations to analyze limitations of kinetic models for recrystallization
[DE90-003618] N90-16548
The concept of axial-symmetry constraint and its significance in recrystallization
[DE90-003620] N90-16549
Eurolaser. High power excimer laser: Optical crystals
[ETN-90-95901] N90-16558
CRYSTAL LATTICES
Elastic moduli of copper: Electronic structure contributions from pseudopotentials and full-potential linear muffin-tin orbital band structure calculations
[DE90-004423] N90-16037
Interplanar spacing for various phases in austenitic stainless steels
[DE90-602350] N90-16038
Contribution to the study of order effects in the Ising model framework: Ground states and phase diagrams
[ESA-TT-1118] N90-16557
CRYSTAL STRUCTURE
ZrO2 sintered compact and method for its production
[DE90-004125] N90-16006
Fundamental studies of beta phase decomposition modes in titanium alloys
[AD-A214424] N90-16035
Conformation, orientation and interaction in molecular monolayers: A surface second harmonic and sum frequency generation study
[DE90-003108] N90-16536
Phonon anomaly at T(sub c) in (Y/ER)Ba2Cu3O(7-delta)
[DE90-003562] N90-16539
Group 2 cubic fluorides as dielectrics for III-V compound semiconductors
[AD-A214096] N90-16542
Scanning tunneling microscope studies of surface defects
[AD-A214121] N90-16543
Fundamental issues in heteroepitaxy (condensed from the DOE panel report)
[DE90-003980] N90-16555
Physical properties of Bi2Sr2CuO6, the semiconducting phase, structurally distinct from the n = 1 Bi-cuprate superconductor
[DE90-004299] N90-16563
Electron beam induced oxygen in YBa2Cu3O(7-x) superconductors
[DE90-004839] N90-16565
CRYSTAL SURFACES
Surface studies at the NSLS
[DE90-003173] N90-16027
CRYSTALLIZATION
The continuous crystallization of sulfur formed by the liquid-phase reaction of hydrogen sulfide and sulfur dioxide
[DE90-003991] N90-16018
Effects of ion dose on the morphology and crystallization of amorphous germanium
[DE90-003564] N90-16547
Ion beam annealing of Si co-implanted with Ga and As
[DE90-004297] N90-16556
CRYSTALS
Thermal expansion of LATGS crystals
[DE89-636239] N90-16546
CULTIVATION
Statistical information system for cultivation of the soil. Use of remote sensing in official statistics N90-16338
CUMULATIVE DAMAGE
Fatigue life estimates for helicopter loading spectra
[NASA-CR-181941] N90-16294
CUMULONIMBUS CLOUDS
Cloud phase discrimination by near-infrared remote sensing N90-16310
CURRENT DENSITY
Magnetic penetration depth and intragrain critical current density in gain-aligned Tl2Ca2Ba2Cu3O10 superconductor
[DE90-004245] N90-16562
CURVATURE
The structure of supersonic turbulent boundary layers subjected to concave surface curvature N90-15883
Load-shortening behavior of an initially curved eccentrically loaded column
[NASA-TM-101643] N90-16293
CURVES
Stochastic action of dynamical systems on curved manifolds. The isokinetic developing map on trajectories
[PREPRINT-666] N90-16466
CURVES (GEOMETRY)
Ice floe identification in satellite images using mathematical morphology and clustering about principal curves
[AD-A213854] N90-16311
CUTTING
Electrode/workpiece combinations
[DE90-003919] N90-16095
CYCLIC LOADS
Cyclic fatigue of hot-isostatic-pressed silicon nitride
[PB90-122649] N90-16308
CYCLONES
The role of an upstream cyclone and corresponding synoptic/planetary-scale interactions during the development of a blocking anticyclone N90-16659
CYGNUS CONSTELLATION
Relative muon content of UHE showers associated with Hercules X-1
[DE90-000609] N90-16665
CYLINDRICAL BODIES
Flow separation in shock wave boundary layer interactions at hypersonic speeds
[NASA-CR-4274] N90-15885
CYLINDRICAL SHELLS
Colinear fluctuating wall shear stress and fluctuating pressure transducer
[AD-D014296] N90-16226
CYLINDRICAL TANKS
Linear liquid oscillations in cylindrical containers under zero-gravity
[LRT-WE-9-FB-5(1989)] N90-16168

D

DAMAGE
Theoretical study on creep damage detection by ultra-sonic wave measurement
[DE90-702472] N90-16290
DATA ACQUISITION
D3-D cryogenic control system upgrade
[DE90-003290] N90-16092
Stand Alone Pressure Measurement Device (SAPMD) for the space shuttle Orbiter, part 1
[NASA-CR-172119-PT-1] N90-16202
Stand Alone Pressure Measurement Device (SAPMD) for the space shuttle Orbiter, part 2
[NASA-CR-172119-PT-2] N90-16203
DATA BASE MANAGEMENT SYSTEMS
RETE experiment activity at the TSS-1 POCC
[IFSI-89-12] N90-15988
Connector selection program implementation notes, version 1.0
[DE90-004983] N90-16279
Introduction to the framework and tasks of the DFD — German Remote Sensing Data Center (DFD) N90-16319
Computer aided design based optical system modeling
[DE90-003453] N90-16440
Abbreviated query interpretation in extended entity-relationship oriented databases
[DE90-003114] N90-16587
Event-join optimization in temporal relational databases
[DE90-003117] N90-16588
Database design using NIAM (Nijssen Information Analysis Method) modeling
[DE89-014631] N90-16592
A database of fragmentation cross section measurements applicable to cosmic ray propagation calculations
[NASA-CR-186328] N90-16681
DATA BASES
Connector selection program implementation notes, version 1.0
[DE90-004983] N90-16279
A persistent heap for ALGOL 68
[RSRE-MEMO-4268] N90-16427
New optimization techniques in database access and maintenance N90-16586
Event-join optimization in temporal relational databases
[DE90-003117] N90-16588
Experiences with knowledge-base and large database integration
[DE90-000686] N90-16591
Database design using NIAM (Nijssen Information Analysis Method) modeling
[DE89-014631] N90-16592
A database of fragmentation cross section measurements applicable to cosmic ray propagation calculations
[NASA-CR-186328] N90-16681
The DAB model of drawing processes N90-16691
Investigation of IGES for CAD/CAE data transfer N90-16702
DATA COMPRESSION
Context dependent prediction and category encoding for DPCM image compression N90-16210
Data compression for the microgravity experiments N90-16212
From primal sketches to the recovery of intensity and reflectance representations N90-16216
Neural networks for data compression and invariant image recognition N90-16219

A programmable image compression system N90-16222
Hybrid LZW compression N90-16223
Digital image coding and compression [PB90-110958] N90-16409
Image segmentation by iterative parallel region growing with application to data compression and image analysis N90-16452

DATA FLOW ANALYSIS
The development of a low cost data logging system for flight trials based on an IBM compatible PC [RAE-TM-FM-16] N90-15917

DATA INTEGRATION
Experiences with knowledge-base and large database integration [DE90-000686] N90-16591

DATA LINKS
Satellite systems integrated with the terrestrial cellular network for mobile communications [ESA-STR-228] N90-16113

DATA MANAGEMENT
Hybrid LZW compression N90-16223
Experiences with knowledge-base and large database integration [DE90-000686] N90-16591

DATA PROCESSING
The development of a low cost data logging system for flight trials based on an IBM compatible PC [RAE-TM-FM-16] N90-15917
The new programming [RSRE-MEMO-4249] N90-16425
Pattern matching in ML: A case study in refinement [RSRE-89004] N90-16430
Sort computation N90-16446
On the efficient exploitation of speculation under data flow paradigms of control [AD-A214112] N90-16455
New optimization techniques in database access and maintenance N90-16586
FY 1989 update to the Information Resources Management review plan [DE90-004185] N90-16593

DATA REDUCTION
RETE experiment activity at the TSS-1 POCC [IFSI-89-12] N90-15988

DATA RETRIEVAL
EXOSAT measurements of the pulse period of Vela X-1 [MPE-PREPRINT-157] N90-16673

DATA STORAGE
IUE-ULDA access guide no. 1: International Ultraviolet Explorer-Uniform Low Dispersion Archive. Dwarf novae and nova-like stars [ESA-SP-1114] N90-16672

DATA SYSTEMS
MT's algorithm: A new algorithm to search for the optimum set of modulation indices for simultaneous range, command, and telemetry [NASA-CR-186259] N90-16110
IUE-ULDA access guide no. 1: International Ultraviolet Explorer-Uniform Low Dispersion Archive. Dwarf novae and nova-like stars [ESA-SP-1114] N90-16672
Cosmic ray NM-64 neutron monitor data 16 [IFSI-88-21] N90-16684
Investigation of IGES for CAD/CAE data transfer N90-16702

DEBRIS
Studies of density distributions in one-dimensional shock-induced debris clouds [DE90-004089] N90-16282

DECARBURIZATION
The influence of carbide precipitation on the creep rupture behavior of high temperature alloys [JUEL-2211] N90-16044

DECISION MAKING
A qualitative architecture for understanding policy responses to global change [DE90-003936] N90-16364

DECOMPOSITION
Fundamental studies of beta phase decomposition modes in titanium alloys [AD-A214424] N90-16035

DEDUCTION
Optimization of monotonic inference algorithms in propositional and first order logic [LAAS-89204] N90-16436

DEFECTS
Fuel resistant coatings for metal and composite fuel tanks N90-15911
Assessment of strength limiting flaws in ceramic heat exchanger components [DE90-004086] N90-16077
Analysis and testing of axial compression in imperfect slender truss struts [NASA-TM-4174] N90-16292
Heteroepitaxy of GaAs on Si: Methods to decrease the defect density in the epilayer [DE90-004028] N90-16551
Universe as a topological defect in a higher-dimensional Einstein-Yang-Mills theory [DE90-719507] N90-16578

DEFENSE COMMUNICATIONS SYSTEM (DCS)
Tactical UK military satellite ground terminals: A research and development review [RSRE-MEMO-4262] N90-15972

DEFORMATION
Effects of high rate shear on the microstructure and deformation and fracture behavior of two high strength steels [AD-A214107] N90-16032
An implicit time-integration procedure for a set of internal variable constitutive equations for isotropic elasto-viscoplasticity [PB90-121302] N90-16470

DEGRADATION
Fracture toughness of ferritic alloys at very high neutron exposures [DE90-004519] N90-16046
Application of ac impedance method for diagnosis of lithium secondary battery degradation. Preliminary study with AA size Li/MoS2 cells [DE90-702474] N90-16137
Model-based quantification of image quality N90-16206

DELAMINATING
Open-mode delamination stress concentrations in horseshoe and elliptic composite curved bars subjected to end forces [NASA-TM-4164] N90-16004

DELINEATION
Computer-aided boundary delineation of agricultural lands [NASA-TM-102243] N90-16313

DELTA WINGS
Flows with Separation [DGLR-PAPERS-88-05] N90-16169
Flow field visualization study on a 65 deg delta wing at M = 0.85 N90-16182
Research on three different Euler's schemes applied to a delta wing with vortical flows N90-16184
Force and moment measurements on delta wings in unsteady flow N90-16185
Numerical simulation of the laminar and turbulent three dimensional flow on a delta wing with sharp leading edge N90-16186

DEMODULATORS
OPFET (Optical Field-Effect Transistor) demodulator-downconverter for detecting microwave modulated optical signals [AD-D014294] N90-16128

DEMULTIPLEXING
The first year's work of race project 1036 WTDM broadband customer premises network [BBC-RD-1989/6] N90-16097

DENSITY DISTRIBUTION
Laboratory studies of isolated eddies in a rotating fluid [AD-A213903] N90-16146
Studies of density distributions in one-dimensional shock-induced debris clouds [DE90-004089] N90-16282

DENSITY MEASUREMENT
Shock thickness measurements with laser beams [MPIS-7/1989] N90-16267
Upper atmosphere research [ISBN-0-642-13582-7] N90-16368

DEOXYRIBONUCLEIC ACID
Mechanisms of microwave induced damage in biologic materials [AD-A213480] N90-16390

DEPOSITION
The influence of residual contamination on the structure and properties of metal/GaAs interfaces [DE90-000549] N90-16530

DESALINIZATION
Conceptual design analysis for hybrid-cycle OTEC plants for co-production of electric power and desalinated water [DE90-003551] N90-16350

DESCENT
Piloted simulation of a ground-based time-control concept for air traffic control [NASA-TM-101085] N90-15898

DESIGN ANALYSIS
Performance of a highly-loaded HP compressor [RAE-TM-P-1149] N90-15919
EVA space suit. General concepts of design and arrangement N90-15976
The visible channel of OMEGA-VIMS [IFSI-89-14] N90-16231
Low risk low power heat pipe/thermoelectric space power supply [DE89-014817] N90-16342
Conceptual design analysis for hybrid-cycle OTEC plants for co-production of electric power and desalinated water [DE90-003551] N90-16350
ATF-2 studies [DE90-004380] N90-16510
Properties and design of multifilamentary NbTi composite superconductors [DE90-004904] N90-16569

DETECTION
Study of silicon nitride pH response to the fabrication of microelectronic sensors [LAAS-89229] N90-16023
An empirical comparison of software fault tolerance and fault elimination [NASA-CR-186313] N90-16414

DEUTERIUM
Initial deuterium confinement studies in DIII-D tokamak: DIII-D milestone report number 58 [DE90-003942] N90-16509
Theoretical study of cold nuclear fusion using barrier penetration approach [DE90-601096] N90-16513
Some theoretical aspects of cold fusion: A report [DE90-601098] N90-16514
The excess flux in the cosmic submillimeter background radiation and the primordial deuterium abundance [NASA-CR-186312] N90-16683

DEUTERIUM COMPOUNDS
Isotope driven critical scattering and phase separation from mixtures of deuterated and protonated polymers [DE90-003976] N90-16076

DEVELOPING NATIONS
Utilization of remote sensing in geoscientific development and projects N90-16334

DIAGNOSIS
Demonstration of the feasibility of laser induced fluorescence for arc jet flow diagnostics [NASA-CR-185595] N90-16013

DIAMONDS
Development of a diamond insulator for thermionic applications [DE90-002849] N90-16055

DICHROISM
Diffraction limited dichroic combiner diode laser [AD-D014291] N90-16263

DIELECTRIC PROPERTIES
Mechanoelectric conversion by uniaxial constraint in piezoelectric generators: Optimization of electrical, mechanical, and physico-chemical parameters of materials [ISAL-89-0020] N90-16235
Group 2 cubic fluorides as dielectrics for III-V compound semiconductors [AD-A214096] N90-16542

DIESEL ENGINES
Diesel starting system monitor: Prototype development [DE90-004425] N90-16276

DIFFERENTIAL EQUATIONS
Integrable classical systems in higher dimensions [DE90-600737] N90-16473

DIFFERENTIAL GEOMETRY
The Eighteenth Conference on Stochastic Processes and their Applications [AD-A212301] N90-16010

DIFFERENTIAL INTERFEROMETRY
Quantative interferometry N90-16237

DIFFERENTIAL PULSE CODE MODULATION
Context dependent prediction and category encoding for DPCM image compression N90-16210

DIFFRACTION
Diffraction limited dichroic combiner diode laser [AD-D014291] N90-16263

DIFFUSERS
User's manual for MGMHD: A multigrid three-dimensional computer code for the analysis of magnetohydrodynamic generators and diffusers [DE90-004453] N90-16526

DIFFUSION
And still, a new beginning: The Galerkin least-squares gradient method [DE89-636435] N90-16461
Solid state voltammetry and sensors in solids and gases [DE90-003234] N90-16538

DIFFUSION COEFFICIENT
Kinetics of the graphite/oxygen reaction in the in-pore diffusion controlled regime. Part 3: Influence of boundary layer diffusion in kinetic experiments at temperatures 970K to 1170K [JUEL-2284-PT-3] N90-16024

DIFFUSION WELDING
Fatigue and impact strength of diffusion bonded titanium alloy joints
[RAE-TM-MAT/STR-1123] N90-16043
DIGITAL COMPUTERS
Synthesis of control law, on a RPV, in order to minimize the number of sensors N90-15925
DIGITAL DATA
Multidimensional numerical simulation of large caliber ignition processes
[ISL-CO-233/88] N90-16021
Direct Monte Carlo calculations on expansion wave structure near a wall
[ISL-CO-249/88] N90-16154
Context dependent anti-aliasing image reconstruction N90-16209
Digital image coding and compression
[PB90-110958] N90-16409
DIGITAL SIMULATION
Flows with Separation
[DGLR-PAPERS-88-05] N90-16169
Numerical simulation of the nonlinear evolution of a perturbation in a three dimensional boundary layer N90-16173
Numerical simulation of the laminar and turbulent three dimensional flow on a delta wing with sharp leading edge N90-16186
Numerical simulation of a bubble shaped bursting vortex N90-16187
Numerical simulation of laminar hypersonic flows about an ellipsoid N90-16198
DIGITAL SYSTEMS
Microwave screening on digital radio communication links due to multicircuit power transmission lines
[DE90-734950] N90-16118
Linear digital imaging system fidelity analysis N90-16205
Digital image interpretation for optical flow measurement methods: System description and preliminary application examples N90-16244
DIGITAL TECHNIQUES
Proceedings of the 5th User Seminar of the German Remote Sensing Data Center of the DFVLR
[DFVLR-MITT-89-04] N90-16318
Attempt to draw conclusions concerning the geological subsoil from the vegetation using digital image processing of TM data N90-16329
Focal research effort points of the Institute of Applied Geodesy in the field of digital image processing N90-16333
Digital image coding and compression
[PB90-110958] N90-16409
DIGITAL TRANSDUCERS
Digital system for monitoring and controlling remote processes
[DE90-003935] N90-16094
DIMENSIONLESS NUMBERS
A space-time discretization procedure for wave propagation problems
[NASA-TM-102215] N90-16399
DIMERS
New electrically conducting solids based on nickel(II) - bis(1,3-dithiole-2-thione-4,5-diselenolate)
[DE90-003788] N90-16020
DIODES
Miniature laser Doppler anemometer with a diode laser
[ISL-CO-224/88] N90-16232
DIPOLE MOMENTS
A search for the electric dipole of the electron
[DE90-001572] N90-16484
DIRAC EQUATION
Theory of singular Lagrangians
[DE90-600735] N90-16456
Proceedings of the 23rd Annual Seminar on Theoretical Physics
[DE90-601827] N90-16577
DISCONNECT DEVICES
Quick disconnect duct coupler
[AD-D014265] N90-16274
DISCRIMINATION
Recognition and distinction of clouds, snow, and ice using AVHRR data N90-16322
DISCRIMINATORS
Beamforming pre-processors for high discrimination algorithms
[RSRE-MEMO-4304] N90-16429
DISPLACEMENT MEASUREMENT
Dynamic analysis of the geodetic networks originating from the Navstar/Global Positioning System (GPS) satellites
[SER-C-346] N90-16316
Preliminary experiences with a novel method for the determination of displacement vector fields and satellite image sequences N90-16324
DISPLAY DEVICES
An electronic pressure profile display system for aeronautic test facilities
[NASA-TM-102478] N90-15964
Sequential rapid communication visual displays
[AD-D014282] N90-16106
Image processing by Intensity-Dependent Spread (IDS) N90-16215
Liquid level measurement system for analog and digital readout
[AD-D014297] N90-16227
Keeping the pilot in the loop
[RAE-TM-FM-18] N90-16396
Assessment of visual function in aerospace medicine
[BMVG-FBWM-89-5] N90-16397
DISSIPATION
Dissipation mechanism of the large-amplitude collective motion. Dynamical evolution of a collective bundle of trajectories in the TDHF phase space for a simple soluble model
[DE90-719557] N90-16477
Dissipative effects in Friedmann universes
[DE89-618838] N90-16663
DISTANCE MEASURING EQUIPMENT
Distance measurement using laser diodes
[ETN-90-96144] N90-16264
DISTILLATION
On-line chemical composition analyzer development
[DE90-004079] N90-16026
DISTRIBUTED PROCESSING
PVM (Parallel Virtual Machine): A framework for parallel distributed computing
[DE90-004390] N90-16403
Algorithms for fault tolerant distributed systems
[AD-A214447] N90-16416
DISTRIBUTION FUNCTIONS
Dissipation mechanism of the large-amplitude collective motion. Dynamical evolution of a collective bundle of trajectories in the TDHF phase space for a simple soluble model
[DE90-719557] N90-16477
DOPPLER EFFECT
Rotating Doppler frequency shifter
[AD-D014279] N90-16475
In situ measurement of neutral beam components using the Doppler-shifted H(sub alpha) emissions in Heliotron E
[DE90-719521] N90-16516
DOWN-CONVERTERS
OPFET (Optical Field-Effect Transistor) demodulator-downconverter for detecting microwave modulated optical signals
[AD-D014294] N90-16128
DRAG
Crew emergency return vehicle autoland feasibility study
[NASA-CR-181940] N90-15937
DRAG REDUCTION
Copolymers for drag reduction in marine propulsion: New molecular structures with enhanced effectiveness
[AD-A214444] N90-16062
DRILLING
The nature of cometary materials N90-16647
DRYING
Porous ceramic bodies
[AD-D014277] N90-16061
DUCTED FLOW
A numerical and experimental investigation of multiple shock wave/turbulent boundary layer interactions in a rectangular duct N90-16141
DUCTILITY
The effects of hydrogen embrittlement of titanium N90-16698
DUCTS
Low-altitude millimeter-wave propagation in the evaporation duct
[AD-A214432] N90-16108
DURABILITY
A dynamicist's view of fuel tank skin durability N90-15915
Structural characterization of Spacelab
[ETN-90-95214] N90-16289
DUST
Ambient flow studies and particulate collection measurements: A laminar flow, reduced entrainment electrostatic precipitator
[DE90-001457] N90-16149
Workshop on Analysis of Returned Comet Nucleus Samples
[NASA-CR-184821] N90-16607
On the isotope analysis of cometary dust N90-16611
Laboratory analyses of micron-sized solid grains: Experimental techniques and recent results N90-16616
Organic chemistry of cometary dust as derived from PUMA 1 data N90-16628
Composition of dust from Comet P/Halley: The mineral fraction N90-16631
The in-situ cometary particulate size distribution measured for one comet: P/Halley N90-16637
Trajectory-capture cell instrumentation for measurement of dust particle mass, velocity and trajectory, and particle capture N90-16644
Mechanical and SEM analysis of artificial comet nucleus samples N90-16650
Refractory solids in chondrites and comets: How similar N90-16654
The dynamics of dust in planetary magnetospheres N90-16658
DUST COLLECTORS
Trajectory-capture cell instrumentation for measurement of dust particle mass, velocity and trajectory, and particle capture N90-16644
DWARF NOVAE
IUE-ULDA access guide no. 1: International Ultraviolet Explorer-Uniform Low Dispersion Archive. Dwarf novae and nova-like stars
[ESA-SP-1114] N90-16672
DYNAMIC CHARACTERISTICS
The use of hypervelocity launchers to explore previously inaccessible states of matter
[DE90-004088] N90-15973
Performance predictions for an intermediate-sized VAWT based on performance of the 34-m VAWT test bed
[DE90-002835] N90-16345
Continuous spontaneous reduction model involving gravity
[DE90-600730] N90-16573
DYNAMIC PRESSURE
Determination of dynamic surface forces using piezoelectric arrays N90-16249
DYNAMIC RESPONSE
Structural dynamics division research and technology accomplishments for FY 1989 and plans for FY 1990
[NASA-TM-101683] N90-15894
Interdisciplinary research in viscoelasticity and rheology
[AD-A213630] N90-16145
Restoring force method and response estimation
[DE90-002394] N90-16463
DYNAMIC STRUCTURAL ANALYSIS
Structural dynamics division research and technology accomplishments for FY 1989 and plans for FY 1990
[NASA-TM-101683] N90-15894
Dynamic analysis of geared rotors by finite elements
[NASA-TM-102349] N90-16286
DYNAMIC TESTS
Conceptual design of a moving belt radiator shuttle-attached experiments: Technical requirement Document
[NASA-CR-185168] N90-15996
Load-shortening behavior of an initially curved eccentrically loaded column
[NASA-TM-101643] N90-16293
DYNAMICAL SYSTEMS
Integrable classical systems in higher dimensions
[DE90-600737] N90-16473
On gauge fixing and quantization of constrained Hamiltonian systems
[DE90-600732] N90-16574

E

EARTH MAGNETOSPHERE
Terrestrial magnetosphere magnetic field models
[REPT-89/CT/DTI/MS/AS/154] N90-16380
EARTH OBSERVATIONS (FROM SPACE)
Necessity and benefit of the X-SAR Space Shuttle experiment
[ESA-TT-1164] N90-16112
Introduction to the framework and tasks of the DFD — German Remote Sensing Data Center (DFD) N90-16319
SPOT after two years in operation: An appraisal of results and a review of selected applications N90-16326
Focal research effort points of the Institute of Applied Geodesy in the field of digital image processing N90-16333
EARTH TERMINAL MEASUREMENT SYSTEM
X-band atmospheric attenuation for an Earth terminal measurement system
[PB90-100736] N90-16101
EARTHNET
ESA/Earthnet N90-16325
EARTHQUAKES
Proceedings of the 79th SEGJ Conference
[DE89-760006] N90-16704

ECHOES
Method for eliminating self-screening noise jamming in radar systems
[AD-D014271] N90-16105
ECONOMIC ANALYSIS
Feasibility of cool storage systems in refrigeration
[DE90-726179] N90-16093
Industrial heat pump assessment study
[DE90-004541] N90-16201
FY 1989 update to the Information Resources Management review plan
[DE90-004185] N90-16593
ECOSYSTEMS
Potential impact of stratospheric ozone depletion on marine ecosystems
[PB90-112616] N90-16360
EDGE DETECTION
Detection of edges using local geometry N90-16213
Isolating contour information from arbitrary images N90-16217
Alvey MMI007. Object identification from 2D images: The RSRE contribution
[RSRE-MEMO-4277] N90-16428
Order filters, median recursive filter: Analysis and evaluation of performance in image processing
[ISAL-89-0017] N90-16505
EDGES
Detection of edges using local geometry N90-16213
From primal sketches to the recovery of intensity and reflectance representations N90-16216
EDITING ROUTINES (COMPUTERS)
Issues and approaches for electronic document approval and transmittal using digital signatures and text authentication: Prototype documentation
[DE90-003382] N90-16119
EDUCATION
Electrical safety in the high voltage laboratory
[DE90-003026] N90-16130
EIGENVALUES
An efficient solver of the Eigenvalue problem of the linear stability equations for three dimensional, compressible boundary-layer flows N90-16172
An algorithm to compute the square root of 3x3 positive definite matrix
[DE89-635711] N90-16417
EJECTA
Stability and fragmentation of ejecta in hypervelocity impact
[DE90-004087] N90-16278
EJECTION SEATS
On the selection of crewmember rescue means for manned space launch systems N90-15978
ELASTIC PROPERTIES
Interdisciplinary research in viscoelasticity and rheology
[AD-A213630] N90-16145
ELASTIC SCATTERING
Studies of elastic scattering and cross sections of the C-12 + Si-28 system
[DE89-635990] N90-16486
Q-2 and A dependence of delta (1232) electroexcitation in nuclei
[DE90-003470] N90-16492
ELASTIC WAVES
An investigation of elastic guided waves for ceramic joint evaluation
[DE90-004400] N90-16071
Direct Monte Carlo calculations on expansion wave structure near a wall
[ISL-CO-249/88] N90-16154
ELASTOHYDRODYNAMICS
Investigation of rough elastohydrodynamic contact
[ISAL-89-0029] N90-16281
ELASTOMERS
Spray sealing: A breakthrough in integral fuel tank sealing technology N90-15912
Development of an elastomeric additive to improve the impact resistance of unsaturated polyester networks
[ISAL-89-0006] N90-16073
ELECTRIC BATTERIES
Ninth Battery and Electrochemical Contractors' Conference: Extended abstracts
[DE89-016837] N90-16120
Assessment of battery technologies for electric vehicles, volume 1
[DE90-002049] N90-16122
Organic cathode for a secondary battery
[NASA-CASE-NPO-17604-1-CU] N90-16124
Sizing and selection of batteries for stand-alone photovoltaic systems
[DE90-002990] N90-16129
An approach for testing fuel-cell/battery hybrid power sources for bus applications
[DE90-002090] N90-16270
Electric and hybrid vehicles: Technical background report for the DOE flexible and alternative fuels study
[DE90-002218] N90-16271
Fault tree analysis: A tool for battery safety and reliability studies
[DE90-002582] N90-16287
ELECTRIC BRIDGES
Very low energy ignition of pyrotechnics using a Semiconductor Bridge (SCB)
[DE90-002645] N90-16062
ELECTRIC CHARGE
The dynamics of dust in planetary magnetospheres N90-16658
ELECTRIC DIPOLES
A search for the electric dipole of the electron
[DE90-001572] N90-16484
ELECTRIC DISCHARGES
Electrode/workpiece combinations
[DE90-003919] N90-16095
ELECTRIC FIELDS
Geometrical optics in inhomogeneous chiral media with application to polarization correction in inhomogeneous lens antennas
[PB90-110669] N90-16497
Rocket-triggered lightning strikes and forest fire ignition N90-16690
ELECTRIC GENERATORS
Mechanoelectric conversion by uniaxial constraint in piezoelectric generators: Optimization of electrical, mechanical, and physico-chemical parameters of materials
[ISAL-89-0020] N90-16235
ELECTRIC HYBRID VEHICLES
National program plan for electric vehicle battery research and development: Technical plan
[DE90-002023] N90-16269
Electric and hybrid vehicles: Technical background report for the DOE flexible and alternative fuels study
[DE90-002218] N90-16271
ELECTRIC MOTOR VEHICLES
Assessment of battery technologies for electric vehicles, volume 1
[DE90-002049] N90-16122
National program plan for electric vehicle battery research and development: Technical plan
[DE90-002023] N90-16269
ELECTRIC MOTORS
A simple fiber optic autocorrelation tachometer
[ETN-90-96146] N90-16228
Electric and hybrid vehicles: Technical background report for the DOE flexible and alternative fuels study
[DE90-002218] N90-16271
ELECTRIC POWER PLANTS
Conceptual design analysis for hybrid-cycle OTEC plants for co-production of electric power and desalinated water
[DE90-003551] N90-16350
Investigation and study on compressed air storage power generation system, part 2
[DE90-702648] N90-16354
ELECTRIC POWER TRANSMISSION
A physical and numerical study of the turn-off behavior of bipolar power transistors
[LAAS-89185] N90-16136
Analysis of the 60-Hz power system at KSC: The Orsino substation N90-16692
ELECTRIC PROPULSION
Design of a thrust stand for high power electric propulsion devices
[NASA-TM-102372] N90-15992
ELECTRIC RELAYS
Steep front impulse tests on a solid-state relay
[DE90-004243] N90-16140
ELECTRICAL INSULATION
Stress analysis of the Princeton Plasma Physics Laboratory 1/2- x 1/2-inch shear/compression test fixture
[DE90-004401] N90-16512
ELECTRICAL RESISTIVITY
Electrical characteristics measurements for the TSS-1 satellite painting
[IFSI-89-7] N90-15987
New electrically conducting solids based on nickel(II) - bis(1,3-dithiole-2-thione-4,5-diselenolate)
[DE90-003788] N90-16020
Command operated liquid metal opening switch
[AD-D014262] N90-16126
ELECTRO-OPTICS
Electro-optic sensors for surveillance and target acquisition N90-15929
Analysis and evaluation of technical data on the photochromic and non-linear optical properties of materials
[AD-A214050] N90-16014
High speed signal extraction using electro-optic techniques
[AD-A214446] N90-16500
ELECTROCATALYSTS
Improved anode catalysts for coal gas-fueled phosphoric acid fuel cells
[DE90-004016] N90-16347
ELECTROCHEMICAL CELLS
Solid-state electrolyte catalysis for methane and oxygen synthesis
[PB90-100231] N90-16011
Application of ac impedance method for diagnosis of lithium secondary battery degradation. Preliminary study with AA size Li/MoS2 cells
[DE90-702474] N90-16137
ECC (Electrochemical Concentration Cell) ozonesonde observations at South Pole, Antarctica, during 1988
[PB90-110172] N90-16355
ECC (Electrochemical Concentration Cell) ozonesonde observations at Mirny, Antarctica, during 1988
[PB90-113960] N90-16357
ELECTROCHEMICAL OXIDATION
New electrically conducting solids based on nickel(II) - bis(1,3-dithiole-2-thione-4,5-diselenolate)
[DE90-003788] N90-16020
ELECTROCHEMISTRY
Mechanisms of the electrochemistry of small organic molecules
[PB90-100785] N90-16012
Electrochemical parameterization of metal complex redox potentials, using the ruthenium(III)/ruthenium(II) couple to generate a ligand electrochemical series
[AD-A214439] N90-16015
An XPS and electrochemical study of the influence of molybdenum and nitrogen on the passivity of austenitic stainless steel
[AD-A214267] N90-16034
Ninth Battery and Electrochemical Contractors' Conference: Extended abstracts
[DE89-016837] N90-16120
Organic cathode for a secondary battery
[NASA-CASE-NPO-17604-1-CU] N90-16124
ELECTROCHROMISM
Lithium cobalt oxide thin film and its electrochromism
[DE90-004570] N90-16564
ELECTRODES
Solid-state electrolyte catalysis for methane and oxygen synthesis
[PB90-100231] N90-16011
Electrode/workpiece combinations
[DE90-003919] N90-16095
Command operated liquid metal opening switch
[AD-D014262] N90-16126
Cycle-life improvement of Zn/NiOOH cells by the addition of Ca(OH)2 to the zinc electrode
[DE90-004040] N90-16139
ELECTROLYSIS
Lithium cobalt oxide thin film and its electrochromism
[DE90-004570] N90-16564
ELECTROLYTES
Evaluation of a new charge algorithm for a lead-acid battery with gelled electrolyte using a 96V gel cell 4 as a test battery
[DE90-003420] N90-16133
Study of metal corrosion using ac impedance techniques in the STS launch environment N90-16688
ELECTROMAGNETIC FIELDS
On averaged force acting on a particle in HF electromagnetic field
[DE90-600984] N90-16109
Characteristics of electromagnetic wave forms with lightning in winter season (2): Characteristics in frequency domain
[DE90-734989] N90-16388
ELECTROMAGNETIC INTERACTIONS
Hollow-cathode experiments to support electrodynamic tether applications
[IFSI-89-5] N90-15986
ELECTROMAGNETIC NOISE
Method for eliminating self-screening noise jamming in radar systems
[AD-D014271] N90-16105
ELECTROMAGNETIC PULSES
On the HEMP (High-Altitude Electromagnetic Pulse) response of protective relays
[DE90-003718] N90-16138
Steep front impulse tests on a solid-state relay
[DE90-004243] N90-16140
Characteristics of electromagnetic wave forms with lightning in winter season (2): Characteristics in frequency domain
[DE90-734989] N90-16388
ELECTROMAGNETIC SCATTERING
High-frequency asymptotic methods for analyzing the EM scattering by open-ended waveguide cavities
[NASA-CR-186244] N90-16103

Plasmon excitation in the scattering of electromagnetic waves from good conductors
[AD-A214026] N90-16107

ELECTRON BEAMS
Recent progress in relativistic klystron research
[DE90-000942] N90-16121
Remote use of an Electron Beam Tester (EBT)
[IMAG-RR-760-I] N90-16233
Proposal for a study of laser acceleration of electrons using micrograting structures at ATF
[DE90-003699] N90-16262
Electron beam induced oxygen in YBa2Cu3O(7-x) superconductors
[DE90-004839] N90-16565

ELECTRON CYCLOTRON HEATING
Second harmonic electron cyclotron heating in low and over density plasmas in Heliotron DR
[DE90-719519] N90-16515
Spectroscopic diagnostics of high temperature plasmas
[DE90-003912] N90-16522

ELECTRON DENSITY (CONCENTRATION)
Atomic processes in plasmas under ultra-intense laser irradiation
[DE90-003221] N90-16521

ELECTRON DISTRIBUTION
X ray spectrophotometric remote sensing of diffuse auroral ionization
[SD-TR-89-09] N90-16599

ELECTRON MICROSCOPY
Direct determination of the morphology, structure and composition of cometary and interstellar ice analogs in the laboratory N90-16612
Electron beam analysis of particulate cometary material N90-16613
Mechanical and SEM analysis of artificial comet nucleus samples N90-16650

ELECTRON ORBITALS
General contraction of Gaussian basis sets. Part 2: Atomic natural orbitals and the calculation of atomic and molecular properties
[NASA-CR-186201] N90-16482

ELECTRON PARAMAGNETIC RESONANCE
Electron Spin Resonance (ESR) studies of returned comet nucleus samples N90-16651

ELECTRON PROBES
Analysis of particulates of comet nucleus samples: Possible use of olivine as indicator phase N90-16646

ELECTRON SCATTERING
Neutrino oscillations: An essay in honor of Felix Boehm
[DE90-003223] N90-16491
Q-2 and A dependence of delta (1232) electroexcitation in nuclei
[DE90-003470] N90-16492

ELECTRON STATES
A search for the electric dipole of the electron
[DE90-001572] N90-16484

ELECTRON TRANSITIONS
Determination of hyperfine structures and Rydberg convergence limits of selected optical transitions in Nb-93 using resonance ionization spectroscopy
[PB90-110719] N90-16498

ELECTRONIC EQUIPMENT
An electronic pressure profile display system for aeronautic test facilities
[NASA-TM-102478] N90-15964

ELECTRONIC EQUIPMENT TESTS
Built in test of folded PLAs
[IMAG-RR-758-I] N90-16134
Remote use of an Electron Beam Tester (EBT)
[IMAG-RR-760-I] N90-16233

ELECTRONS
A search for the electric dipole of the electron
[DE90-001572] N90-16484
Electron beam induced oxygen in YBa2Cu3O(7-x) superconductors
[DE90-004839] N90-16565

ELECTROPLATING
Electroplating simulation
[DE90-003683] N90-16091

ELECTROSTATIC PRECIPITATORS
Ambient flow studies and particulate collection measurements: A laminar flow, reduced entrainment electrostatic precipitator
[DE90-001457] N90-16149

ELECTROSTATIC PROBES
Two possible configurations for the top-hat electrostatic analyzer: A numerical study
[IFSI-88-18] N90-16229
CIS-2 analyzer derivation of hardware parameters
[IFSI-89-13] N90-16230

ELECTROSTATIC WAVES
Langmuir wave interaction with ion-sound one. Part 1: Stochastic effects
[DE90-603368] N90-16474
On condensation driven by electrostatic interactions in macroionic solutions
[DE89-636072] N90-16487

ELEMENTARY PARTICLES
Possible measurement of the gravitational acceleration of molecules, atoms, nuclei, elementary particles, and antiparticles
[DE90-719559] N90-16490

ELLIPSOIDS
Numerical boundary layer calculations on the DFVLR ellipsoid of revolution N90-16193
Numerical simulation of laminar hypersonic flows about an ellipsoid N90-16198

EMBRITTLEMENT
Microstructural explanation for irradiation embrittlement of V-15Cr-5Ti
[DE90-004112] N90-16041

EMERGENCIES
Aircraft accident report: Delta Air Lines, Inc., Boeing 727-232, N473DA, Dallas-Fort Worth International Airport, Texas, August 31, 1988
[PB89-910406] N90-15895

EMISSION SPECTRA
Natural and man-made emissions at 1.0 to 5.6 MHz measured between 10 and 18 R sub E
[MPE-PREPRINT-146] N90-16116
Determination of hyperfine structures and Rydberg convergence limits of selected optical transitions in Nb-93 using resonance ionization spectroscopy
[PB90-110719] N90-16498
Use of the Egret instrument in studies of the origin of the cosmic radiation. 2: Spectral signatures of discrete cosmic-ray sources
[DE90-003595] N90-16682

ENERGY BANDS
Theory of the electronic and optical properties of semiconductor heterostructures
[AD-A214132] N90-16544

ENERGY CONSERVATION
Federal roles to realize national energy-efficiency opportunities in the 1990s
[DE90-004410] N90-16348
Proceedings of the Conference on Technology-Based Confidence Building: Energy and Environment
[DE90-003363] N90-16366

ENERGY CONVERSION
Organic cathode for a secondary battery
[NASA-CASE-NPO-17604-1-CU] N90-16124
Mechanoelectric conversion by uniaxial constraint in piezoelectric generators: Optimization of electrical, mechanical, and physico-chemical parameters of materials
[ISAL-89-0020] N90-16235

ENERGY DISSIPATION
Experimental investigation of a three-dimensional wake. Part 2: Spectral and turbulent energy analysis
[ONERA-RT-32/5025-AYD-PT-2] N90-15887

ENERGY LEVELS
On the observation of a transition from fusion to multifragmentation in high multiplicity O16 induced reactions
[LUIP-8812] N90-16481
A computer program to calculate the population numbers of multi-level species
[IFSI-89-15] N90-16671

ENERGY METHODS
Low energy neutral particle energy analyser by time of flight method
[DE90-719529] N90-16517

ENERGY POLICY
Energy management and recovery N90-15962
A qualitative architecture for understanding policy responses to global change
[DE90-003936] N90-16364

ENERGY REQUIREMENTS
Energy management and recovery N90-15962

ENERGY SPECTRA
Experimental investigation of a three-dimensional wake. Part 2: Spectral and turbulent energy analysis
[ONERA-RT-32/5025-AYD-PT-2] N90-15887

ENERGY STORAGE
Ninth Battery and Electrochemical Contractors' Conference: Extended abstracts
[DE89-016837] N90-16120
Investigation and study on compressed air storage power generation system, part 2
[DE90-702648] N90-16354
Modeling energy output of inertial storage devices for the DIII-D tokamak
[DE90-004096] N90-16524

ENERGY TECHNOLOGY
SERI (Solar Energy Research Institute) solar radiation resource assessment project
[DE89-009456] N90-16352

ENERGY TRANSFER
Rotational energy transfer in metastable states of heteronuclear molecules
[AD-A214425] N90-16485
Recent progress on the HESS (High Explosive Spheromak Source) experiment
[DE90-003218] N90-16520
Progress with small, high-magnetic-field spheromaks in CTX
[DE90-003395] N90-16527

ENGINE CONTROL
Automatic prestart or post shutoff engine lubricator
[AD-D014259] N90-16273

ENGINE PARTS
Advanced composite polar boss
[AD-D014287] N90-15994

ENGINEERING DRAWINGS
The DAB model of drawing processes N90-16691

ENGLISH LANGUAGE
The inside-outside algorithm: Further experiments on three and four letter word spelling and implementation on an array processor
[RSRE-MEMO-4256] N90-16426

ENTRAINMENT
Ambient Test Rig (ATR) flow studies: A laminar flow, reduced entrainment electrostatic precipitator
[DE90-000144] N90-16142
Ambient flow studies and particulate collection measurements: A laminar flow, reduced entrainment electrostatic precipitator
[DE90-001457] N90-16149

ENTROPY
Dissipative effects in Friedmann universes
[DE89-618838] N90-16663

ENVIRONMENT EFFECTS
Interconnectedness in nature and in science: The case of climate and climate modeling
[PB90-113986] N90-16358
Assessment of the importance of acidic fogwater and cloudwater in affecting terrestrial vegetation: Some important case studies
[DE90-002216] N90-16361
A qualitative architecture for understanding policy responses to global change
[DE90-003936] N90-16364

ENVIRONMENT POLLUTION
Environmental, health, and safety concerns associated with nonpetroleum fuel use in US transportation
[DE90-004367] N90-16362

ENVIRONMENT SIMULATION
Artificial intelligence in process control: Knowledge base for the shuttle ECS model N90-16697

ENVIRONMENTAL CONTROL
DNSS: German/Norwegian work team Space Subsea. Environmental control and life support subsystems (technical matters), phase 2
[ETN-90-95905] N90-16398
Artificial intelligence in process control: Knowledge base for the shuttle ECS model N90-16697

ENVIRONMENTAL ENGINEERING
A modular habitation unit adapted for service in low earth and geostationary earth orbits
[ILR-MITT-217] N90-15990
Activities report of the National Electrotechnic Institute Galileo Ferraris
[ETN-90-96178] N90-16705

ENVIRONMENTAL MONITORING
Operational ozone monitoring with the Global Ozone Monitoring Radiometer (GOMR)
[PB90-114034] N90-16359

ENVIRONMENTAL QUALITY
The US National Transonic Facility, NTF N90-15942

ENVIRONMENTAL RESEARCH SATELLITES
World Weather Watch. Global observing system-satellite sub-system. Information on meteorological and other environmental satellites, second edition
[WMO-411-ED-2] N90-16386

EPITAXY
Metals and Ceramics Division Materials Sciences Program
[DE90-004371] N90-16070
Heteroepitaxy of GaAs on Si: Methods to decrease the defect density in the epilayer
[DE90-004028] N90-16551
The 1MeV-electron irradiation induced defects in epitaxially grown 3C-SiC
[DE90-719574] N90-16554
Fundamental issues in heteroepitaxy (condensed from the DOE panel report)
[DE90-003980] N90-16555

EPOXY MATRIX COMPOSITES
Instrumented impact and residual tensile strength testing of eight-ply carbon eopoxy specimens
[NASA-TP-2981] N90-16007

EQUATIONS OF MOTION
Calculation of the flow field of a multiblade helicopter rotor using a Euler method including the wake N90-16189
Restoring force method and response estimation [DE90-002394] N90-16463
Integrable classical systems in higher dimensions [DE90-600737] N90-16473
EQUIPMENT SPECIFICATIONS
Stand Alone Pressure Measurement Device (SAPMD) for the space shuttle Orbiter, part 1 [NASA-CR-172119-PT-1] N90-16202
Stand Alone Pressure Measurement Device (SAPMD) for the space shuttle Orbiter, part 2 [NASA-CR-172119-PT-2] N90-16203
ERROR ANALYSIS
Analytical techniques for tracking filter implementation N90-15903
Results of error correction techniques applied on two high accuracy coordinate measuring machines [DE90-003341] N90-16439
ERROR CORRECTING CODES
Results of error correction techniques applied on two high accuracy coordinate measuring machines [DE90-003341] N90-16439
ESCAPE SYSTEMS
Crew emergency return vehicle autoland feasibility study [NASA-CR-181940] N90-15937
Safety and rescue during STS operations N90-15975
Assured crew return capability architecture N90-15977
ESTIMATES
Theoretical investigations of the structures and binding energies of Be(sub n) and Mg(sub n) (n = 3-5) clusters [NASA-TM-101931] N90-16483
ESTIMATING
On-line estimation of mechanical nonlinearities in compliant two-link robot manipulators N90-16280
Estimating water flow through a hillslope using the massively parallel processor N90-16449
ETA-MESONS
Theoretical aspects of electroweak and other interactions in medium energy nuclear physics [DE90-004015] N90-16493
ETCHING
Silicon membrane formation [DE90-003022] N90-16064
ETHYLENE
Mechanisms of the electrochemistry of small organic molecules [PB90-100785] N90-16012
EULER EQUATIONS OF MOTION
Euler and Navier-Stokes computations for two-dimensional geometries using unstructured meshes [NASA-CR-181977] N90-15893
Adaptive local grid refinement for the compressible 3-D Euler equations [FFA-TN-1989-40] N90-16155
Research on three different Euler's schemes applied to a delta wing with vortical flows N90-16184
Calculation of two and three dimensional super and hypersonic flows by solving the Euler equations N90-16197
Definition, transformation-formulae and measurements of tipvane angles [IW-R510] N90-16351
EULER-LAGRANGE EQUATION
Application of Lagrangian blending functions for grid generation around airplane geometries [NASA-CR-186318] N90-15891
And still, a new beginning: The Galerkin least-squares gradient method [DE89-636435] N90-16461
EURECA (ESA)
Experiment facilities for materials and fluid sciences embarked on Eureca-1 [ESA-SP-1118] N90-16088
Eurolaser definition phase, solid state lasers working group: Active medium, laser active crystals [ETN-90-95899] N90-16266
EUROPEAN SPACE AGENCY
From small beginnings... The story of ESRO's sounding rocket programme in celebration of the twenty-fifth anniversary of the first ESRO sounding rocket launch [ESA-BR-60] N90-15999
Science plan for the Alaska SAR facility program. Phase 1: Data from the first European sensing satellite, ERS-1 [NASA-CR-185028] N90-16312
ESA/Earthnet N90-16325
Catalogue of ESA publications in 1987 [ESA-SP-1087] N90-16590
Focus 88: The activities of the European Space Agency [ESA-BR-43] N90-16706
EUROPEAN SPACE PROGRAMS
Mission to Mars. Report of the Mars exploration study team [ESA-SP-1117] N90-15968
Flight experiment hardware for sounding rocket investigations. Materials science and fluid sciences [ESA-SP-1116] N90-15998
The HERMES development program N90-16199
ESA/Earthnet N90-16325
Focus 88: The activities of the European Space Agency [ESA-BR-43] N90-16706
EVALUATION
Software dependability growth characterization, modeling and evaluation [LAAS-89320] N90-16437
EVAPORATION
Externally vaporizing system for turbine combustor [AD-D014284] N90-15918
Low-altitude millimeter-wave propagation in the evaporation duct [AD-A214432] N90-16108
EXCIMER LASERS
Eurolaser. High power excimer laser: Optical crystals [ETN-90-95901] N90-16558
EXCITATION
Plasmon excitation in the scattering of electromagnetic waves from good conductors [AD-A214026] N90-16107
Q-2 and A dependence of delta (1232) electroexcitation in nuclei [DE90-003470] N90-16492
An estimation of the one-loop mass shifts in open superstring theory [DE90-719578] N90-16582
EXCITONS
Theory of the electronic and optical properties of semiconductor heterostructures [AD-A214132] N90-16544
EXHAUST FLOW SIMULATION
Application of the singularity-separating method to computing problems of solid-propellant combustion in a closed vessel [PREPRINT-489] N90-16086
EXHAUST GASES
A qualitative architecture for understanding policy responses to global change [DE90-003936] N90-16364
EXOSAT SATELLITE
Galactic x ray astronomy with EXOSAT N90-16597
An atlas of aperiodic variability in HMXB [MPE-PREPRINT-158] N90-16605
Recent and future x ray observations of classical novae during the outburst stage [MPE-PREPRINT-159] N90-16606
EXOSAT measurements of the pulse period of Vela X-1 [MPE-PREPRINT-157] N90-16673
EXPANDABLE STRUCTURES
Expandable radiator [AD-D014258] N90-16147
EXPERIMENT DESIGN
Conceptual design of a moving belt radiator shuttle-attached experiments: Technical requirement Document [NASA-CR-185168] N90-15996
EXPERIMENTATION
Fundamental considerations in testing in cryogenic wind tunnels N90-15951
EXPERT SYSTEMS
An intelligence-driven RPV mission planner N90-15932
Knowledge-based imaging-sensor fusion system N90-16220
A knowledge-based machine vision system for space station automation N90-16221
Expert system control of a six-legged walking telerobot [DE90-004661] N90-16285
User interaction with self-learning systems [AD-A214280] N90-16395
Discrete event simulation tool for analysis of qualitative models of continuous processing systems [NASA-CASE-MSC-21465-1] N90-16410
On the efficient exploitation of speculation under data flow paradigms of control [AD-A214112] N90-16455
Experiences with knowledge-base and large database integration [DE90-000686] N90-16591
Artificial intelligence in process control: Knowledge base for the shuttle ECS model N90-16697
EXPLOSION SUPPRESSION
Fuel tank explosion protection N90-15914
EXPLOSIVES
Design of a spheromak compressor driven by high explosives [DE90-003652] N90-16283
EXPOSURE
Fuel resistant coatings for metal and composite fuel tanks N90-15911
Integral fuel tank certification and test methods N90-15916
Fracture toughness of ferritic alloys at very high neutron exposures [DE90-004519] N90-16046
Short-term bioassays may be useful in evaluating fiber/whisker hazards [DE90-003707] N90-16393
EXPULSION
The nature of cometary materials N90-16647
EXTINCTION
Lidar technique for adjusting aerosol model number densities to existing conditions [AD-A213846] N90-16374
Interstellar and cometary dust N90-16636
EXTRACTION
Isolating contour information from arbitrary images N90-16217
EXTRAGALACTIC RADIO SOURCES
Short time scale variability of the BL Lac object OJ 287 in the near-infrared [IFSI-89-3] N90-16603
EXTRAVEHICULAR ACTIVITY
EVA space suit. General concepts of design and arrangement N90-15976
EXTRAVEHICULAR MOBILITY UNITS
EVA space suit. General concepts of design and arrangement N90-15976
EYE PROTECTION
Analysis and evaluation of technical data on the photochromic and non-linear optical properties of materials [AD-A214050] N90-16014

F

F REGION
Scientific investigations of the Space Research Group [ISBN-0-642-13252-6] N90-16595
FABRICATION
Materials and techniques for model construction N90-15954
Some recent developments in materials and techniques for model fabrication N90-15955
Models for cryogenic wind tunnels N90-15956
Experience with strain-gage balances for cryogenic wind tunnels N90-15958
Cryogenic balances for the US NTF N90-15959
Performance of an Inductively Coupled Plasma-Mass Spectrometer Analyzer system [DE90-004002] N90-16025
Synthesis of air-sinterable lanthanum chromite powders [DE90-004681] N90-16049
Porous ceramic bodies [AD-D014277] N90-16061
Artificially structured superconductors [DE90-004851] N90-16567
FACTOR ANALYSIS
Factor analytic reduction of the carotid-cardiac baroreflex parameters N90-16693
FACTORIZATION
Asymptotically fast triangularization of matrices over rings [DE90-003161] N90-16471
FAILURE
Cryogenic engineering and materials N90-15949
FAILURE ANALYSIS
Diesel starting system monitor: Prototype development [DE90-004425] N90-16276
Cyclic fatigue of hot-isostatic-pressed silicon nitride [PB90-122649] N90-16308
Rainflow counting algorithm for the LIFE2 fatigue analysis code [DE90-002834] N90-16344
Complex availability problems solved with simulation [DE89-012610] N90-16459
FAILURE MODES
Discrete event simulation tool for analysis of qualitative models of continuous processing systems [NASA-CASE-MSC-21465-1] N90-16410
FATIGUE (MATERIALS)
Review of investigations on aeronautical fatigue in the Federal Republic of Germany [LBF-S-182] N90-16302
Rainflow counting algorithm for the LIFE2 fatigue analysis code [DE90-002834] N90-16344

FATIGUE LIFE
Fatigue life estimates for helicopter loading spectra
[NASA-CR-181941] N90-16294
FATIGUE TESTS
Fatigue and impact strength of diffusion bonded titanium alloy joints
[RAE-TM-MAT/STR-1123] N90-16043
FRAG requirements for control of fatigue testing
[RAE-TM-MAT/STR-1130] N90-16300
Calibration of a pulsed potential crack monitor for use in fatigue crack growth studies
[RAE-TM-M/S-1126] N90-16301
Review of investigations on aeronautical fatigue in the Federal Republic of Germany
[LBF-S-182] N90-16302
FAULT TOLERANCE
VLSI integrated circuit tests
[IMAG-RR-763-I] N90-16135
An empirical comparison of software fault tolerance and fault elimination
[NASA-CR-186313] N90-16414
Algorithms for fault tolerant distributed systems
[AD-A214447] N90-16416
Software dependability growth characterization, modeling and evaluation
[LAAS-89320] N90-16437
FAULT TREES
Fault tree analysis: A tool for battery safety and reliability studies
[DE90-002582] N90-16287
FEASIBILITY ANALYSIS
Spectral sensitivity of device power output for tandem a-Si alloy solar cells
[DE89-009421] N90-16340
Conceptual design analysis for hybrid-cycle OTEC plants for co-production of electric power and desalinated water
[DE90-003551] N90-16350
Investigation and study on compressed air storage power generation system, part 2
[DE90-702648] N90-16354
ATF-2 studies
[DE90-004380] N90-16510
FEEDBACK
Bilateral force reflection for teleoperators with masters and slaves with dissimilar and possibly redundant kinematics
[DE90-004392] N90-16132
FEEDBACK CONTROL
Feed back Petrov-Galerkin methods for convection dominated problems
[DE89-636436] N90-16148
Mathematical model for adaptive control system of ASEA robot at Kennedy Space Center N90-16701
FEEDERS
Analysis of the 60-Hz power system at KSC: The Orsino substation N90-16692
FERROELECTRICITY
Thermodynamic studies on the ferroelectric phase transition in neutron irradiated (Li(sub x)K(1-x))2SO4 crystals at high temperature
[DE89-635786] N90-16545
FIBER COMPOSITES
Probabilistic simulation of uncertainties in composite uniaxial strengths
[NASA-TM-102483] N90-16008
FIBER OPTICS
A simple fiber optic autocorrelation tachometer
[ETN-90-96146] N90-16228
Chromatic dispersion compensation in a Fresnel lens by means of a diffraction grating
[DE90-004030] N90-16506
FIBERS
Short-term bioassays may be useful in evaluating fiber/whisker hazards
[DE90-003707] N90-16393
FIELD ALIGNED CURRENTS
On the structure of the tail magnetic field
[IFSI-88-19] N90-16378
FIELD EFFECT TRANSISTORS
OPFET (Optical Field-Effect Transistor) demodulator-downconverter for detecting microwave modulated optical signals
[AD-D014294] N90-16128
FIELD OF VIEW
Appearance analysis from CAD models
[IMAG-RR-756-I-IMAG-88-LIFIA] N90-16434
FIELD THEORY (PHYSICS)
On averaged force acting on a particle in HF electromagnetic field
[DE90-600984] N90-16109
The theory of hybrid stochastic algorithms
[DE90-003941] N90-16421
Multiplet classification of highest weight modules over quantum universal enveloping algebras: The U(sub q)(sl(3,C)) example
[DE90-600720] N90-16464
The off-shell closed strings as the topological open membranes: Dynamical transmutation of world sheet dimension
[DE89-635721] N90-16571
Proceedings of the 23rd Annual Seminar on Theoretical Physics
[DE90-601827] N90-16577
Quantum fields in cosmological space-times: A soluble example
[DE89-616837] N90-16662
FIGHTER AIRCRAFT
An experimental investigation of thrust vectoring two-dimensional convergent-divergent nozzles installed in a twin-engine fighter model at high angles of attack
[NASA-TM-4155] N90-15884
FILE MAINTENANCE (COMPUTERS)
UNIX internals. Part 1: Intertask communication in UNIX. Part 2: UNIX file system
[CNES-NT-122-PT-1/2] N90-16405
FINITE DIFFERENCE THEORY
Personal computer study of finite-difference methods for the transonic small disturbance equation
[NASA-TM-102582] N90-15892
Computation of the unsteady facilitated transport of oxygen in hemoglobin
[NASA-TM-102251] N90-16400
Stochastic simulation of charged particle transport on the massively parallel processor N90-16448
FINITE ELEMENT METHOD
Space shuttle Production Verification Motor 1 (PV-1) static fire
[NASA-CR-183784] N90-15991
Open-mode delamination stress concentrations in horseshoe and elliptic composite curved bars subjected to end forces
[NASA-TM-4164] N90-16004
Feed back Petrov-Galerkin methods for convection dominated problems
[DE89-636436] N90-16148
Extrapolation techniques for finite element approximations of Stokes and Navier-Stokes flow over a backward facing step
[PREPRINT-499] N90-16160
Finite element calculations for transonic flows taking into account several far field boundary conditions N90-16188
Dynamic analysis of geared rotors by finite elements
[NASA-TM-102349] N90-16286
Element-by-element preconditioning techniques for large-scale, vectorized finite element analysis in nonlinear solid and structural mechanics N90-16291
BAM: German Federal Institute for Materials Research and Testing, Berlin
[DE90-004293] N90-16307
And still, a new beginning: The Galerkin least-squares gradient method
[DE89-636435] N90-16461
A new finite element formulation for CFD:8. The Galerkin/least-squares method for advective-diffusive equations
[DE89-636437] N90-16462
FINITE VOLUME METHOD
A finite volume calculation method for three dimensional, complex flows N90-16195
FISSION
Proceedings of the specialists' meeting on physics and engineering of fission and spallation
[DE90-719706] N90-16519
FISSION PRODUCTS
Proceedings of the specialists' meeting on physics and engineering of fission and spallation
[DE90-719706] N90-16519
FIXTURES
Stress analysis of the Princeton Plasma Physics Laboratory 1/2- x 1/2-inch shear/compression test fixture
[DE90-004401] N90-16512
FLAME PROPAGATION
Fuel tank explosion protection N90-15914
Assessing the flammability of composite materials
[PB90-112996] N90-16002
FLAME STABILITY
Swirl-stabilized flames: Fluid dynamics, mixing, and flame stability limits N90-16009
FLAMES
Swirl-stabilized flames: Fluid dynamics, mixing, and flame stability limits N90-16009
FLAMMABILITY
Assessing the flammability of composite materials
[PB90-112996] N90-16002
FLAPS (CONTROL SURFACES)
Calculation of the flap profile flows with separation based on coupled potential and boundary layer solutions N90-16191
FLARES
Tracking flares
[ISBN-0-642-13583-5] N90-16080
FLAT PLATES
Flow separation in shock wave boundary layer interactions at hypersonic speeds
[NASA-CR-4274] N90-15885
FLIGHT CONDITIONS
A survey of nonuniform inflow models for rotorcraft flight dynamics and control applications
[NASA-TM-102219] N90-15938
FLIGHT CONTROL
Guidance and Control of Unmanned Air Vehicles
[AGARD-CP-436] N90-15924
Mirach 100 flight control system N90-15926
A survey of nonuniform inflow models for rotorcraft flight dynamics and control applications
[NASA-TM-102219] N90-15938
FLIGHT MANAGEMENT SYSTEMS
The development of a low cost data logging system for flight trials based on an IBM compatible PC
[RAE-TM-FM-16] N90-15917
FLIGHT OPERATIONS
Fuel tank explosion protection N90-15914
FLIGHT SIMULATION
A survey of nonuniform inflow models for rotorcraft flight dynamics and control applications
[NASA-TM-102219] N90-15938
The NASA Langley 0.3-meter transonic cryogenic tunnel N90-15941
FLIGHT SIMULATORS
Simulator sickness in the UH-60 (Black Hawk) flight simulator
[AD-A214434] N90-16392
FLIGHT TESTS
Mirach 100 flight control system N90-15926
Navigation and guidance testing of the Lockheed/US Army Aquila remotely piloted vehicle N90-15935
Pulsed plasma mission endurance test
[AD-A213462] N90-15993
FLIGHT TRAINING
Simulator sickness in the UH-60 (Black Hawk) flight simulator
[AD-A214434] N90-16392
FLOATING POINT ARITHMETIC
Basic mathematical function libraries for scientific computation
[NASA-TM-102256] N90-16423
FLOW CHARACTERISTICS
The cryogenic induction tunnel T2 at Toulouse N90-15946
Automatic control of cryogenic wind tunnels N90-15957
A numerical simulation of the flow in the diffuser of the NASA Lewis icing research tunnel
[NASA-TM-102480] N90-15965
A numerical and experimental investigation of multiple shock wave/turbulent boundary layer interactions in a rectangular duct N90-16141
Study of flow around a sphere in a hydraulic test tunnel
[CERT-1/2313/MES] N90-16156
Extrapolation techniques for finite element approximations of Stokes and Navier-Stokes flow over a backward facing step
[PREPRINT-499] N90-16160
FLOW DISTRIBUTION
The structure of supersonic turbulent boundary layers subjected to concave surface curvature N90-15883
Performance of a highly-loaded HP compressor
[RAE-TM-P-1149] N90-15919
Flow visualization in the cryogenic wind tunnel N90-15953
Application of the singularity-separating method to computing problems of solid-propellant combustion in a closed vessel
[PREPRINT-489] N90-16086
Ambient Test Rig (ATR) flow studies: A laminar flow, reduced entrainment electrostatic precipitator
[DE90-000144] N90-16142
Using the singularity-separating method to study how to decrease the pressure at the end of a tube
[PREPRINT-490] N90-16158
Numerical analysis of nonstationary fluid flow (a survey)
[PREPRINT-492] N90-16159
Two-Dimensional Measuring Techniques
[DGLR-PAPERS-88-04] N90-16236
Coded trajectories for the investigation of strongly unsteady flow fields N90-16240
Visualization of instability forms of a round free jet using a light sheet method N90-16241

Visualization of gas flows using the smoke wire technique N90-16242
Flow field visualization using laser light sheet methods. Quantitative analysis using image processing N90-16243
Digital image interpretation for optical flow measurement methods: System description and preliminary application examples N90-16244
The determination of vortex separation frequencies by means of laser light sheet images [DNW-WTI-88.038] N90-16245
Flow visualization using the laser light sheet method in vehicle aerodynamics and combustion chamber engineering N90-16246
Analysis of the measuring range and the accuracy of an existing particle image velocimetry system N90-16247
Determination of dynamic surface forces using piezoelectric arrays N90-16249
The use of sublimation methods for the recognition of transition at low speed N90-16251
Use of the film-of-oil technique for profile measurements in the Transonic Wind tunnel Brunswick (TWB) N90-16252
Flow visualization of water flows using the crystal violet method N90-16253
Unsteady heat transfer measurement using thermochromatic liquid crystals as temperature indicators N90-16254
Surface flow visualization with shear stress sensitivive liquid crystals [DNW-WTI-88.039] N90-16255
Quantitative heat transfer measurements using heated liquid crystals N90-16256
Determination of the heat transfer coefficients in separated flows using an infrared camera N90-16257
Investigation of ablation phenomena using IR thermography in a hypersonic wind tunnel N90-16258
Multiple flow regimes in the Northern Hemisphere winter N90-16372

FLOW EQUATIONS
The Eighteenth Conference on Stochastic Processes and their Applications [AD-A212301] N90-16010
A new finite element formulation for CFD:8. The Galerkin/least-squares method for advective-diffusive equations [DE89-636437] N90-16462

FLOW MEASUREMENT
Rotor induced-inflow-ratio measurements and CAMRAD calculations [NASA-TP-2946] N90-15882
Ambient flow studies and particulate collection measurements: A laminar flow, reduced entrainment electrostatic precipitator [DE90-001457] N90-16149
Measurement of the p, v, T behavior under microgram conditions [ETN-90-95906] N90-16162
Optical flow measuring method using diode lasers, phase coupled arrays, and high frequency pulsed diode lasers N90-16176
Low flow vortex shedding flowmeter N90-16700

FLOW STABILITY
Detection of flow instabilities at airfoil profiles using piezoelectric arrays N90-16175
Visualization of instability forms of a round free jet using a light sheet method N90-16241

FLOW VELOCITY
Ambient Test Rig (ATR) flow studies: A laminar flow, reduced entrainment electrostatic precipitator [DE90-000144] N90-16142
Analysis of the measuring range and the accuracy of an existing particle image velocimetry system N90-16247
Further development of the PIV method for use in the large wind tunnel N90-16248
A space-time discretization procedure for wave propagation problems [NASA-TM-102215] N90-16399
Low flow vortex shedding flowmeter N90-16700

FLOW VISUALIZATION
Special Course on Advances in Cryogenic Wind Tunnel Technology [AGARD-R-774] N90-15939
Flow visualization in the cryogenic wind tunnel N90-15953
Study of flow around a sphere in a hydraulic test tunnel [CERT-1/2313/MES] N90-16156
Visualization of 2 and 3 dimensional flows [REPT-1] N90-16164
Flow field visualization study on a 65 deg delta wing at M = 0.85 N90-16182
Two-Dimensional Measuring Techniques [DGLR-PAPERS-88-04] N90-16236
Visualization of instability forms of a round free jet using a light sheet method N90-16241
Visualization of gas flows using the smoke wire technique N90-16242
Flow field visualization using laser light sheet methods. Quantitative analysis using image processing N90-16243
Flow visualization using the laser light sheet method in vehicle aerodynamics and combustion chamber engineering N90-16246
Analysis of the measuring range and the accuracy of an existing particle image velocimetry system N90-16247
Further development of the PIV method for use in the large wind tunnel N90-16248
Flow visualization of water flows using the crystal violet method N90-16253
Surface flow visualization with shear stress sensitivive liquid crystals [DNW-WTI-88.039] N90-16255

FLOWMETERS
Low flow vortex shedding flowmeter N90-16700

FLUID BOUNDARIES
Anomalous waves in shock wave - fluid interface collisions [AD-A213584] N90-16144

FLUID DYNAMICS
Swirl-stabilized flames: Fluid dynamics, mixing, and flame stability limits N90-16009
Experiment facilities for materials and fluid sciences embarked on Spacelab [ESA-SP-1120] N90-16089
Measurement of the p, v, T behavior under microgram conditions [ETN-90-95906] N90-16162

FLUID FILMS
Thickness, velocity, and temperature measurements in falling liquid films [DE90-004290] N90-16151
Use of the film-of-oil technique for profile measurements in the Transonic Wind tunnel Brunswick (TWB) N90-16252

FLUID FLOW
Thickness, velocity, and temperature measurements in falling liquid films [DE90-004290] N90-16151
Measurement of the p, v, T behavior under microgram conditions [ETN-90-95906] N90-16162
Colinear fluctuating wall shear stress and fluctuating pressure transducer [AD-D014296] N90-16226
Studies of density distributions in one-dimensional shock-induced debris clouds [DE90-004089] N90-16282

FLUID MANAGEMENT
Flight experiment hardware for sounding rocket investigations. Materials science and fluid sciences [ESA-SP-1116] N90-15998

FLUID MECHANICS
Test techniques for cryogenic wind tunnels N90-15952
Absorption fluids data survey: 1989 update [DE90-003985] N90-16346

FLUORESCENCE
Sulfur compounds in comets N90-16627

FLUORIDES
Method of making carbon dioxide and chlorine free fluoride-based glass [AD-D014260] N90-16060
Group 2 cubic fluorides as dielectrics for III-V compound semiconductors [AD-A214096] N90-16542

FLUX PINNING
Rotational magnetic processes in YB2Cu3O7 [DE90-000541] N90-16533

FLY ASH
Ambient flow studies and particulate collection measurements: A laminar flow, reduced entrainment electrostatic precipitator [DE90-001457] N90-16149

FLYBY MISSIONS
Experimental studies of gas trapping in amorphous ice and thermal modelling of comets: Implications for Rosetta N90-16610
Trajectory-capture cell instrumentation for measurement of dust particle mass, velocity and trajectory, and particle capture N90-16644

FOAMS
The physical properties of microcellular composite foams [DE90-003658] N90-16058

FOCAL PLANE DEVICES
The MPI/AIT X ray Imager (MAXI): High speed PN-CCD's for x ray detection [MPE-PREPRINT-154] N90-16234
Enhanced performance IR focal plane arrays using adaptive subtraction [RSRE-MEMO-4286] N90-16502

FOCUSING
B-Factory Final Focus System using superconducting quadrupoles [DE90-004432] N90-16552

FOG
Assessment of the importance of acidic fogwater and cloudwater in affecting terrestrial vegetation: Some important case studies [DE90-002216] N90-16361

FORCE DISTRIBUTION
Wind tunnel tests of the influence of aerofoil thickness on the normal force and pitching moment of two slender wings at transonic and supersonic Mach numbers [ESA-TT-1129] N90-15889
Force and moment measurements on delta wings in unsteady flow N90-16185

FORCED VIBRATION
Dynamic analysis of geared rotors by finite elements [NASA-TM-102349] N90-16286

FORECASTING
Diesel starting system monitor: Prototype development [DE90-004425] N90-16276

FOREST FIRES
Rocket-triggered lightning strikes and forest fire ignition N90-16690

FOREST MANAGEMENT
Forest mapping Nuerenberg German national forest with special emphasis on the spectral reflection behavior of pine trees N90-16328
Use of remote sensing in operational inventory and monitoring agricultural and forestry tasks N90-16336

FORESTS
Assessment of the importance of acidic fogwater and cloudwater in affecting terrestrial vegetation: Some important case studies [DE90-002216] N90-16361

FORMALISM
Formalisms for user interface specification and design N90-16687

FORMAT
Sequential rapid communication visual displays [AD-D014282] N90-16106

FORTRAN
EZVIDEO, FORTRAN graphics routines for the IBM AT [DE90-004409] N90-16422

FRACTURE MECHANICS
Effects of high rate shear on the microstructure and deformation and fracture behavior of two high strength steels [AD-A214107] N90-16032
Rainflow counting algorithm for the LIFE2 fatigue analysis code [DE90-002834] N90-16344

FRACTURE STRENGTH
Method to produce titanium alloy articles with high fatigue and fracture resistance [AD-D014278] N90-16029
Fracture toughness of ferritic alloys at very high neutron exposures [DE90-004519] N90-16046
Experiences with three-point bending test specimens for determining the crack-arrest fracture toughness K(sub Ia) in low-alloy steel [DE90-004120] N90-16306
The effects of hydrogen embrittlement of titanium N90-16698

FRACTURES (MATERIALS)
BAM: German Federal Institute for Materials Research and Testing, Berlin [DE90-004293] N90-16307
Some considerations on resource evaluation of The Geysers [DE90-002119] N90-16343

FRACTURING
Assessment of strength limiting flaws in ceramic heat exchanger components [DE90-004086] N90-16077

FRAGMENTATION
Stability and fragmentation of ejecta in hypervelocity impact [DE90-004087] N90-16278
On the observation of a transition from fusion to multifragmentation in high multiplicity O16 induced reactions [LUIP-8812] N90-16481
A database of fragmentation cross section measurements applicable to cosmic ray propagation calculations [NASA-CR-186328] N90-16681

FREE CONVECTION
Simultaneous determination of temperature and velocity fields in a thermal convection flow with non-enclosed liquid crystal tracers N90-16239
FREE FLOW
Demonstration of the feasibility of laser induced fluorescence for arc jet flow diagnostics [NASA-CR-185595] N90-16013
FREE JETS
Plume shape optimization of small attitude control thrusters with respect to impingement and thrust [ISL-CO-220/88] N90-16153
Visualization of instability forms of a round free jet using a light sheet method N90-16241
Lecture notes on supersonic molecular beam sources [MPIS-20/1988] N90-16494
FREE RADICALS
Electron Spin Resonance (ESR) studies of returned comet nucleus samples N90-16651
FREEZING
Soft modes, freezing, and nonlinear response of a dipolar glass [DE90-003647] N90-16075
Feasibility of cool storage systems in refrigeration [DE90-728179] N90-16093
FREQUENCY ANALYZERS
An analysis of the time variation of the frequency response of the LMS adaptive line enhancer [ISVR-TR-175] N90-16115
FREQUENCY SHIFT
Rotating Doppler frequency shifter [AD-D014279] N90-16475
FRESNEL DIFFRACTION
Chromatic dispersion compensation in a Fresnel lens by means of a diffraction grating [DE90-004030] N90-16506
FRESNEL LENSES
Chromatic dispersion compensation in a Fresnel lens by means of a diffraction grating [DE90-004030] N90-16506
FRICTION MEASUREMENT
Evaluation of two transport aircraft and several ground test vehicle friction measurements obtained for various runway surface types and conditions. A summary of test results from joint FAA/NASA Runway Friction Program [NASA-TP-2917] N90-15902
Investigation of rough elastohydrodynamic contact [ISAL-89-0029] N90-16281
FUEL CELLS
Synthesis of air-sinterable lanthanum chromite powders [DE90-004681] N90-16049
Ninth Battery and Electrochemical Contractors' Conference: Extended abstracts [DE89-016837] N90-16120
An approach for testing fuel-cell/battery hybrid power sources for bus applications [DE90-002090] N90-16270
Electric and hybrid vehicles: Technical background report for the DOE flexible and alternative fuels study [DE90-002218] N90-16271
Development of planar geometry solid oxide fuel cells [PB90-100769] N90-16341
FUEL COMBUSTION
Solid fuel combustion chamber [LR-555] N90-16001
FUEL CONSUMPTION
Industrial heat pump assessment study [DE90-004541] N90-16201
FUEL INJECTION
Externally vaporizing system for turbine combustor [AD-D014284] N90-15918
FUEL SYSTEMS
Fuel resistant coatings for metal and composite fuel tanks N90-15911
Externally vaporizing system for turbine combustor [AD-D014284] N90-15918
Diesel starting system monitor: Prototype development [DE90-004425] N90-16276
FUEL TANKS
Fuel Tank Technology [AGARD-R-771] N90-15904
Integral fuel tank sealing practice at British Aerospace (Kingston) N90-15905
Integral fuel tanks - design, production, aging, repair N90-15906
Aircraft fuel tank construction and testing experience N90-15907
The repair of aircraft integral fuel tanks in the RAF: A user's view of fuel tank technology N90-15908
The effect of primer age on adhesion of polysulphide sealant N90-15909
Fuel resistant coatings for metal and composite fuel tanks N90-15911
Spray sealing: A breakthrough in integral fuel tank sealing technology N90-15912
Design philosophy and construction techniques for integral fuselage fuel tanks N90-15913
Fuel tank explosion protection N90-15914
A dynamicist's view of fuel tank skin durability N90-15915
Integral fuel tank certification and test methods N90-15916
Linear liquid oscillations in cylindrical containers under zero-gravity [LRT-WE-9-FB-5(1989)] N90-16168
FUELS
Improved performance polysulfide based sealant N90-15910
Alcohol and blends as motor fuels [DE90-003517] N90-16085
Improved anode catalysts for coal gas-fueled phosphoric acid fuel cells [DE90-004016] N90-16347
Environmental, health, and safety concerns associated with nonpetroleum fuel use in US transportation [DE90-004367] N90-16362
FUSELAGES
Design philosophy and construction techniques for integral fuselage fuel tanks N90-15913

G

GALACTIC CLUSTERS
Mass functions for eight galactic clusters in the solar neighborhood N90-16660
GALACTIC COSMIC RAYS
Galactic cosmic-ray modulation and solar-terrestrial relationships [IFSI-88-17] N90-16679
Use of the Egret instrument in studies of the origin of the cosmic radiation. 2: Spectral signatures of discrete cosmic-ray sources [DE90-003595] N90-16682
GALACTIC EVOLUTION
Computer simulation of dust grain evolution N90-16632
Evolution of carbonaceous chondrite parent bodies: Insights into cometary nuclei N90-16638
GALACTIC NUCLEI
Gamma-ray observations and the distribution of interstellar aluminum-26 N90-16661
GALACTIC RADIATION
Gamma-ray observations and the distribution of interstellar aluminum-26 N90-16661
GALAXIES
Galactic x ray astronomy with EXOSAT N90-16597
GALERKIN METHOD
Feed back Petrov-Galerkin methods for convection dominated problems [DE89-636436] N90-16148
And still, a new beginning: The Galerkin least-squares gradient method [DE89-636435] N90-16461
A new finite element formulation for CFD:8. The Galerkin/least-squares method for advective-diffusive equations [DE89-636437] N90-16462
GALLIUM ARSENIDES
Radiation resistance of solar cells for space application. 1: Study on the irradiation procedure of electron beams [DE90-719546] N90-16349
The influence of residual contamination on the structure and properties of metal/GaAs interfaces [DE90-000549] N90-16530
Group 2 cubic fluorides as dielectrics for III-V compound semiconductors [AD-A214096] N90-16542
Scanning tunneling microscope studies of surface defects [AD-A214121] N90-16543
Heteroepitaxy of GaAs on Si: Methods to decrease the defect density in the epilayer [DE90-004028] N90-16551
GALLIUM OXIDES
Microstructures of Y123 films on SrTiO3, LaGaO3, and LaAlO3 [DE90-003367] N90-16537
GAMMA RAY ASTRONOMY
A low-threshold EAS (Extensive-Air-Shower) array for gamma-ray astronomy at Los Alamos [DE89-016780] N90-16600
Status of the expansion of the CYGNUS array at Los Alamos [DE89-016781] N90-16601
GAMMA RAY BURSTS
Relative muon content of UHE showers associated with Hercules X-1 [DE90-000609] N90-16665
GAMMA RAY SPECTRA
Gamma-ray observations and the distribution of interstellar aluminum-26 N90-16661
Use of the Egret instrument in studies of the origin of the cosmic radiation. 2: Spectral signatures of discrete cosmic-ray sources [DE90-003595] N90-16682
GAMMA RAYS
Coded-aperture imaging in nuclear medicine N90-16208
GAS EXCHANGE
Dynamics of carbon dioxide exchange of a wheat community grown in a semi-closed environment N90-16689
GAS FLOW
A brief description of lattice gas models for multiphase flows and magnetohydrodynamics [DE90-003653] N90-16143
Visualization of gas flows using the smoke wire technique N90-16242
Experimental studies of gas trapping in amorphous ice and thermal modelling of comets: Implications for Rosetta N90-16610
GAS JETS
Swirl-stabilized flames: Fluid dynamics, mixing, and flame stability limits N90-16009
GAS MIXTURES
Externally vaporizing system for turbine combustor [AD-D014284] N90-15918
Swirl-stabilized flames: Fluid dynamics, mixing, and flame stability limits N90-16009
GAS PRESSURE
Neptune's Triton: A moon rich in dry ice and carbon [NASA-CR-186298] N90-16675
GAS TURBINE ENGINES
Cycle analysis for helicopter gas turbine engines [RAE-TM-P-1154] N90-15921
GAS TURBINES
Analytical study on the decreasing method of thermal stress for ceramic gas turbines [DE90-734934] N90-16078
The use of piezofoil sensors for the determination of the unsteady pressure distribution at the surface of a gas turbine blade N90-16250
GAS-METAL INTERACTIONS
Mechanisms of the electrochemistry of small organic molecules [PB90-100785] N90-16012
GASEOUS DIFFUSION
Computation of the unsteady facilitated transport of oxygen in hemoglobin [NASA-TM-102251] N90-16400
GASEOUS FUELS
Externally vaporizing system for turbine combustor [AD-D014284] N90-15918
GASES
Using inorganic membranes to separate gases: R and D status review [DE90-004386] N90-16019
Improved anode catalysts for coal gas-fueled phosphoric acid fuel cells [DE90-004016] N90-16347
GAUGE INVARIANCE
Universe as a topological defect in a higher-dimensional Einstein-Yang-Mills theory [DE90-719507] N90-16578
GAUGE THEORY
The off-shell closed strings as the topological open membranes: Dynamical transmutation of world sheet dimension [DE89-635721] N90-16571
GEARS
Assessment of worm gearing for helicopter transmissions [NASA-TM-102441] N90-15923
Continuously variable gear drive transmission [AD-D014268] N90-16275
Dynamic analysis of geared rotors by finite elements [NASA-TM-102349] N90-16286
GELS
Evaluation of a new charge algorithm for a lead-acid battery with gelled electrolyte using a 96V gel cell 4 as a test battery [DE90-003420] N90-16133
Development of low density silica aerogel as a capture medium for hyper-velocity particles [NASA-CR-185930] N90-16489
GEOCHEMISTRY
Summaries of physical research in the geosciences [DE90-004993] N90-16309
GEODESY
Integrated geodetic network analysis with stochastic prior information about the gravity field and reference ellipsoid [SER-C-351] N90-16317

Focal research effort points of the Institute of Applied Geodesy in the field of digital image processing N90-16333

GEODETIC ACCURACY
Regional height determination using gravimetric and topographical data [UH-156] N90-16315

GEODETIC COORDINATES
Dynamic analysis of the geodetic networks originating from the Navstar/Global Positioning System (GPS) satellites [SER-C-346] N90-16316

GEOGRAPHIC APPLICATIONS PROGRAM
Investigation of the backscatter behavior of selected test areas in two geocoded SEASAT-SAR scenes in greater Bonn (Fed. Republic of Germany) N90-16331

GEOLOGICAL SURVEYS
Computer-aided boundary delineation of agricultural lands [NASA-TM-102243] N90-16313

GEOLOGY
Attempt to draw conclusions concerning the geological subsoil from the vegetation using digital image processing of TM data N90-16329

GEOMAGNETIC TAIL
On the structure of the tail magnetic field [IFSI-88-19] N90-16378

GEOMAGNETISM
On the structure of the tail magnetic field [IFSI-88-19] N90-16378
Correlative analyses for geomagnetic indices, cosmic-ray intensities and sunspot numbers recorded since 1937 [IFSI-89-4] N90-16670

GEOMETRICAL OPTICS
High-frequency asymptotic methods for analyzing the EM scattering by open-ended waveguide cavities [NASA-CR-166244] N90-16103
Geometrical optics in inhomogeneous chiral media with application to polarization correction in inhomogeneous lens antennas [PB90-110669] N90-16497

GEOMETRICAL THEORY OF DIFFRACTION
Chromatic dispersion compensation in a Fresnel lens by means of a diffraction grating [DE90-004030] N90-16506

GEOMETRY
Application of Lagrangian blending functions for grid generation around airplane geometries [NASA-CR-166318] N90-15891
Euler and Navier-Stokes computations for two-dimensional geometries using unstructured meshes [NASA-CR-181977] N90-15893
Vorticity amplification in nonorthogonal stagnation flow N90-16152
Detection of edges using local geometry N90-16213

GEOPHYSICS
Summaries of physical research in the geosciences [DE90-004993] N90-16309
Proceedings of the 79th SEGJ Conference [DE89-760006] N90-16704

GEOPOTENTIAL HEIGHT
On mean elements for satellite orbits perturbed by the zonal harmonics of the geopotential [RAE-TM-SPACE-371] N90-15971
Multiple flow regimes in the Northern Hemisphere winter N90-16372

GEYSERS
Some considerations on resource evaluation of The Geysers [DE90-002119] N90-16343

GIACOBINI-ZINNER COMET
Spectrophotometric observations of comet P/Giacobini-Zinner N90-16630

GIOTTO MISSION
Morphology and compositional differentiation of the surface of comets N90-16624
Organic chemistry of cometary dust as derived from PUMA 1 data N90-16628
Composition of dust from Comet P/Halley: The mineral fraction N90-16631
The in-situ cometary particulate size distribution measured for one comet: P/Halley N90-16637

GLASS
Soft modes, freezing, and nonlinear response of a dipolar glass [DE90-003647] N90-16075

GLASS TRANSITION TEMPERATURE
Soft modes, freezing, and nonlinear response of a dipolar glass [DE90-003647] N90-16075

GLOBAL ATMOSPHERIC RESEARCH PROGRAM
Guide on the global observing system [WMO-488-REV] N90-16385
The role of an upstream cyclone and corresponding synoptic/planetary-scale interactions during the development of a blocking anticyclone N90-16659

GLOBAL POSITIONING SYSTEM
Advances in techniques and technologies for air vehicle navigation and guidance [AGARD-AR-276] N90-15899
GPS network analysis: The influence of stochastic prior information of orbital elements on ground station position measures [TR-4-1988] N90-15901
Regional height determination using gravimetric and topographical data [UH-156] N90-16315
Dynamic analysis of the geodetic networks originating from the Navstar/Global Positioning System (GPS) satellites [SER-C-346] N90-16316

GLOBAL WARMING
Scientific linkages in global change [PB90-112608] N90-16356

GLOVES
Handling and analysis of ices in cryostats and glove boxes in view of cometary samples N90-16643

GLYCINE
Thermal expansion of LATGS crystals [DE89-636239] N90-16546

GLYCOLS
Thickness, velocity, and temperature measurements in falling liquid films [DE90-004290] N90-16151

GOVERNMENTS
Federal roles to realize national energy-efficiency opportunities in the 1990s [DE90-004410] N90-16348

GRADIENTS
And still, a new beginning: The Galerkin least-squares gradient method [DE89-636435] N90-16461

GRAMMARS
The inside-outside algorithm: Further experiments on three and four letter word spelling and implementation on an array processor [RSRE-MEMO-4256] N90-16426

GRAND TOURS
The Gevaltig: An inertial fusion powered manned spacecraft design for outer solar system missions [NASA-CR-185163] N90-15985

GRAPH THEORY
Overview and extensions of a system for routing directed graphs on SIMD architectures N90-16444

GRAPHITE
Kinetics of the graphite/oxygen reaction in the in-pore diffusion controlled regime. Part 3: Influence of boundary layer diffusion in kinetic experiments at temperatures 970K to 1170K [JUEL-2284-PT-3] N90-16024

GRAPHITE-EPOXY COMPOSITES
Probabilistic simulation of uncertainties in composite uniaxial strengths [NASA-TM-102483] N90-16008
Review of investigations on aeronautical fatigue in the Federal Republic of Germany [LBF-S-182] N90-16302

GRASSLANDS
Evaluation of the pasture potential in the dry areas of Kenya using combined Earth reconnaissance N90-16327

GRATINGS (SPECTRA)
Chromatic dispersion compensation in a Fresnel lens by means of a diffraction grating [DE90-004030] N90-16506

GRAVITATION
Continuous spontaneous reduction model involving gravity [DE90-600730] N90-16573
The (2+1)-dimensional quantum gravity [DE90-719556] N90-16580

GRAVITATIONAL EFFECTS
Data compression for the microgravity experiments N90-16212
Effects of gravity waves on the polar O2 and OH airglow N90-16373
Possible measurement of the gravitational acceleration of molecules, atoms, nuclei, elementary particles, and antiparticles [DE90-719559] N90-16490

GRAVITATIONAL FIELDS
Integrated geodetic network analysis with stochastic prior information about the gravity field and reference ellipsoid [SER-C-351] N90-16317
The (2+1)-dimensional quantum gravity [DE90-719556] N90-16580
Double-periodic wormholes in theories with global symmetries [DE90-719575] N90-16581
On quantum effects near a black hole singularity [DE90-600754] N90-16668

GRAVITATIONAL WAVES
Are gravitons windows to higher dimensions [DE90-600756] N90-16376

GRAVITONS
Are gravitons windows to higher dimensions [DE90-600756] N90-16376

GRAVITY WAVES
Effects of gravity waves on the polar O2 and OH airglow N90-16373

GREASES
Molybdenum disulfide-molybdenum oxide lubricants [AD-D014253] N90-16059

GREEN'S FUNCTIONS
Simple proof of renormalization group equation in the minimal subtraction scheme [DE90-600758] N90-16457

GREENHOUSE EFFECT
Scientific linkages in global change [PB90-112608] N90-16356
Proceedings of the Conference on Technology-Based Confidence Building: Energy and Environment [DE90-003363] N90-16366

GRID GENERATION (MATHEMATICS)
Application of Lagrangian blending functions for grid generation around airplane geometries [NASA-CR-166318] N90-15891
FRAC-IN-THE-BOX utilization [DE90-003648] N90-16412

GROUND OPERATIONAL SUPPORT SYSTEM
Tactical UK military satellite ground terminals: A research and development review [RSRE-MEMO-4262] N90-15972

GROUND STATE
Contribution to the study of order effects in the Ising model framework: Ground states and phase diagrams [ESA-TT-1118] N90-16557

GROUND STATIONS
GPS network analysis: The influence of stochastic prior information of orbital elements on ground station position measures [TR-4-1988] N90-15901
Satellite systems integrated with the terrestrial cellular network for mobile communications [ESA-STR-228] N90-16113

GROUND SUPPORT EQUIPMENT
Tactical UK military satellite ground terminals: A research and development review [RSRE-MEMO-4262] N90-15972
RETE experiment activity at the TSS-1 POCC [IFSI-89-12] N90-15988
X-band atmospheric attenuation for an Earth terminal measurement system [PB90-100736] N90-16101

GROUND TESTS
Evaluation of two transport aircraft and several ground test vehicle friction measurements obtained for various runway surface types and conditions. A summary of test results from joint FAA/NASA Runway Friction Program [NASA-TP-2917] N90-15902

GROUP THEORY
Simple proof of renormalization group equation in the minimal subtraction scheme [DE90-600758] N90-16457
Multiplet classification of highest weight modules over quantum universal enveloping algebras: The U(sub q)(sl(3,C)) example [DE90-600720] N90-16464

GUIDANCE (MOTION)
Navigation and guidance testing of the Lockheed/US Army Aquila remotely piloted vehicle N90-15935
Singular perturbation analysis of AOTV-related trajectory optimization problems [NASA-CR-186202] N90-15936

H

HADRONS
Proceedings of the 23rd Annual Seminar on Theoretical Physics [DE90-601827] N90-16577

HAFNIUM OXIDES
ZrO2 sintered compact and method for its production [DE90-004125] N90-16006

HALF LIFE
Cosmic ray half life of Ni-56 [DE90-000132] N90-16680

HALLEY'S COMET
Morphology and compositional differentiation of the surface of comets N90-16624

Organic chemistry of cometary dust as derived from PUMA 1 data N90-16628
Composition of dust from Comet P/Halley: The mineral fraction N90-16631
Solar nebula condensates and the composition of comets N90-16634
The in-situ cometary particulate size distribution measured for one comet: P/Halley N90-16637

HALOGEN COMPOUNDS
Rotational energy transfer in metastable states of heteronuclear molecules
[AD-A214425] N90-16485

HAMILTONIAN FUNCTIONS
Theory of singular Lagrangians
[DE90-600735] N90-16456
On gauge fixing and quantization of constrained Hamiltonian systems
[DE90-600732] N90-16574

HANDLING EQUIPMENT
Handling and analysis of ices in cryostats and glove boxes in view of cometary samples N90-16643

HARDWARE
Columbus: A user's introduction
[ESA-BR-62] N90-15989
The NODEN hardware description language
[RSRE-89011] N90-16431
The algebra of the NODEN analyser
[RSRE-89012] N90-16432

HARMONIC GENERATIONS
Conformation, orientation and interaction in molecular monolayers: A surface second harmonic and sum frequency generation study
[DE90-003108] N90-16536

HARTREE APPROXIMATION
Dissipation mechanism of the large-amplitude collective motion. Dynamical evolution of a collective bundle of trajectories in the TDHF phase space for a simple soluble model
[DE90-719557] N90-16477

HAZARDS
Safety and cryogenic wind tunnels N90-15960
MANPRINT (Manpower and Personnel Integration) evaluation: AN/TRC-170 digital troposcatter radio system
[AD-A211799] N90-16100
Short-term bioassays may be useful in evaluating fiber/whisker hazards
[DE90-003707] N90-16393

HEAD MOVEMENT
Helmet-mounted head restraint
[AD-D014233] N90-16394

HEALTH
MANPRINT (Manpower and Personnel Integration) evaluation: AN/TRC-170 digital troposcatter radio system
[AD-A211799] N90-16100
Environmental, health, and safety concerns associated with nonpetroleum fuel use in US transportation
[DE90-004367] N90-16362

HEAT EXCHANGERS
Cycle analysis for helicopter gas turbine engines
[RAE-TM-P-1154] N90-15921
Assessment of strength limiting flaws in ceramic heat exchanger components
[DE90-004086] N90-16077
Thickness, velocity, and temperature measurements in falling liquid films
[DE90-004290] N90-16151

HEAT FLUX
The response of the atmospheric convective boundary layer to surface inhomogeneities N90-16369

HEAT PIPES
Low risk low power heat pipe/thermoelectric space power supply
[DE89-014817] N90-16342

HEAT PUMPS
Industrial heat pump assessment study
[DE90-004541] N90-16201

HEAT RESISTANT ALLOYS
Method to produce titanium alloy articles with high fatigue and fracture resistance
[AD-D014278] N90-16029

HEAT SOURCES
Expandable radiator
[AD-D014258] N90-16147

HEAT TRANSFER
Aerodynamic and heat transfer measurements on blading for a high rim-speed transonic turbine
[RAE-TM-P-1151] N90-15920
Conceptual design of a moving belt radiator shuttle-attached experiments: Technical requirement Document
[NASA-CR-185168] N90-15996
The onset of boiling of the liquid alkali metals
[DE90-002276] N90-16036
Selection of corrosion-resistant materials for use in molten nitrate salts
[DE90-004351] N90-16048
Electroplating simulation
[DE90-003683] N90-16091
Expandable radiator
[AD-D014258] N90-16147
Thickness, velocity, and temperature measurements in falling liquid films
[DE90-004290] N90-16151
Modeling a self-calibrating thermocouple for use in a smart temperature measurement system
[DE90-003697] N90-16259
Thermal histories of the samples of two KOSI comet nucleus simulation experiments N90-16645

HEAT TRANSFER COEFFICIENTS
Unsteady heat transfer measurement using thermochromatic liquid crystals as temperature indicators N90-16254
Quantitative heat transfer measurements using heated liquid crystals N90-16256
Determination of the heat transfer coefficients in separated flows using an infrared camera N90-16257

HEAT TREATMENT
Silicon-based coatings on niobium metal
[DE90-003651] N90-16057

HEAVY IONS
Heavy ion inelastic scattering with a 4(pi) gamma detector
[DE90-002709] N90-16488
Lower limit for the average angular momentum leading to fusion
[DE90-004027] N90-16523

HELICOPTER ENGINES
Cycle analysis for helicopter gas turbine engines
[RAE-TM-P-1154] N90-15921

HELICOPTER PERFORMANCE
Fatigue life estimates for helicopter loading spectra
[NASA-CR-181941] N90-16294

HELICOPTER WAKES
Rotor induced-inflow-ratio measurements and CAMRAD calculations
[NASA-TP-2946] N90-15882
Calculation of the flow field of a multiblade helicopter rotor using a Euler method including the wake N90-16189

HELICOPTERS
Assessment of worm gearing for helicopter transmissions
[NASA-TM-102441] N90-15923

HELIOTRONS
Second harmonic electron cyclotron heating in low and over density plasmas in Heliotron DR
[DE90-719519] N90-16515
In situ measurement of neutral beam components using the Doppler-shifted H(sub alpha) emissions in Heliotron E
[DE90-719521] N90-16516

HELIUM ISOTOPES
Superflow induced phase transition in the axial vortex-free texture of rotating superfluid He-3-B
[PB90-110388] N90-16531

HELMET MOUNTED DISPLAYS
Helmet-mounted head restraint
[AD-D014233] N90-16394

HELMHOLTZ VORTICITY EQUATION
Solving time harmonic wave problems on vector processors
[DE90-003956] N90-16480

HEMOGLOBIN
Computation of the unsteady facilitated transport of oxygen in hemoglobin
[NASA-TM-102251] N90-16400

HERCULES NOVA
Relative muon content of UHE showers associated with Hercules X-1
[DE90-000609] N90-16665

HERMES MANNED SPACEPLANE
RVD scenari and interfaces between Hermes and space station N90-15982
Flows with Separation
[DGLR-PAPERS-88-05] N90-16169
The HERMES development program N90-16199
DNSS: German/Norwegian work team Space Subsea. Environmental control and life support subsystems (technical matters), phase 2
[ETN-90-95905] N90-16398

HERTZSPRUNG-RUSSELL DIAGRAM
Pulsations of delta Scuti stars
[DE90-003213] N90-16598

HETEROJUNCTION DEVICES
Group 2 cubic fluorides as dielectrics for III-V compound semiconductors
[AD-A214096] N90-16542

HETEROJUNCTIONS
Theory of the electronic and optical properties of semiconductor heterostructures
[AD-A214132] N90-16544

HIERARCHIES
Connectionist model-based stereo vision for telerobotics N90-16224

HIGH ALTITUDE
On the HEMP (High-Altitude Electromagnetic Pulse) response of protective relays
[DE90-003718] N90-16138

HIGH FREQUENCIES
Use of an HF active monitoring array in the presence of high level interference
[BBC-RD-1989/7] N90-16096
Optical flow measuring method using diode lasers, phase coupled arrays, and high frequency pulsed diode lasers N90-16176
High frequency pulsed diode lasers and phase-coupled diode arrays for aerodynamics N90-16238

HIGH POWER LASERS
Diffraction limited dichroic combiner diode laser
[AD-D014291] N90-16263

HIGH REYNOLDS NUMBER
The cryogenic induction tunnel T2 at Toulouse N90-15946

HIGH STRENGTH STEELS
Effects of high rate shear on the microstructure and deformation and fracture behavior of two high strength steels
[AD-A214107] N90-16032

HIGH TEMPERATURE
The influence of carbide precipitation on the creep rupture behavior of high temperature alloys
[JUEL-2211] N90-16044

HIGH TEMPERATURE PLASMAS
Spectroscopic diagnostics of high temperature plasmas
[DE90-003912] N90-16522

HIGH TEMPERATURE SUPERCONDUCTORS
The modified Ginzburg-Landau theory for anisotropic high temperature superconductors
[DE89-635909] N90-16532
La(sub 2)MO(sub 4 + delta) (M = Cu, Ni, Co): Phase separation and superconductivity resulting from excess oxygen defects
[DE90-001988] N90-16534
Phonon anomaly at T(sub c) in (Y/ER)Ba2Cu3O(7-delta)
[DE90-003562] N90-16539
Structure-property correlations in the design of organic metals and superconductors: An overview
[DE90-003794] N90-16550
Neutron experiments on high-temperature superconductors
[DE90-003978] N90-16559
Magnetic interactions in Sn-119 substituted for Cu in antiferromagnetic and superconducting lamellar cuprates
[DE90-003661] N90-16560
Magnetic penetration depth and intragrain critical current density in gain-aligned Tl2Ca2Ba2Cu3O10 superconductor
[DE90-004245] N90-16562
Artificially structured superconductors
[DE90-004851] N90-16567
High temperature neutron diffraction study of the formation reaction of bismuth superconductors
[DE90-004883] N90-16568

HIGH VOLTAGES
Electrical safety in the high voltage laboratory
[DE90-003026] N90-16130

HILBERT SPACE
On gauge fixing and quantization of constrained Hamiltonian systems
[DE90-600732] N90-16574

HISTORIES
The NASA Langley 0.3-meter transonic cryogenic tunnel N90-15941
A foundation for the design of an astronautics specification system based on dynamic motivation analysis
[ILR-MITT-220] N90-15969
The development of over-the-horizon radar in Australia
[ISBN-0-642-13561-4] N90-16099

HOLLOW CATHODES
Hollow-cathode experiments to support electrodynamic tether applications
[IFSI-89-5] N90-15986

HOLOGRAPHIC INTERFEROMETRY
Quantative interferometry N90-16237

HOT ISOSTATIC PRESSING
Cyclic fatigue of hot-isostatic-pressed silicon nitride
[PB90-122649] N90-16308

HOT PRESSING
Production and processing of Cu-Cr-Nb alloys
[NASA-TM-102495] N90-16053

HOT WORKING
An implicit time-integration procedure for a set of internal variable constitutive equations for isotropic elasto-viscoplasticity
[PB90-121302] N90-16470
HUMAN FACTORS ENGINEERING
MANPRINT (Manpower and Personnel Integration) evaluation: AN/TRC-170 digital troposcatter radio system
[AD-A211799] N90-16100
Electrical safety in the high voltage laboratory
[DE90-003026] N90-16130
Assessment of visual function in aerospace medicine
[BMVG-FBWM-89-5] N90-16397
HUMAN RESOURCES
Project summaries
[PB90-103987] N90-16472
HYDRAULIC TEST TUNNELS
Study of flow around a sphere in a hydraulic test tunnel
[CERT-1/2313/MES] N90-16156
HYDROCHLORIC ACID
Study of metal corrosion using ac impedance techniques in the STS launch environment N90-16688
HYDRODYNAMICS
Thickness, velocity, and temperature measurements in falling liquid films
[DE90-004290] N90-16151
Material responses to incident x rays
[DE89-015366] N90-16305
HYDROGEN EMBRITTLEMENT
The effects of hydrogen embrittlement of titanium N90-16698
HYDROGEN PRODUCTION
Development and evaluation of a process to produce hydrogen from coal
[DE90-003937] N90-16084
HYDROGEN SULFIDE
The continuous crystallization of sulfur formed by the liquid-phase reaction of hydrogen sulfide and sulfur dioxide
[DE90-003991] N90-16018
HYDROGENATION
Method for refining microstructures on prealloyed titanium powder compacts
[AD-D014280] N90-16030
HYDROLOGY
Utilization of remote sensing in geoscientific development and projects N90-16334
HYDROLOGY MODELS
Support of hydrological models calculations by satellite data N90-16337
HYDROLYSIS
Synthesis of tetrafluorohydrazine
[AD-D014281] N90-16083
HYDROSTATICS
Assessment of worm gearing for helicopter transmissions
[NASA-TM-102441] N90-15923
HYDROXIDES
Cycle-life improvement of Zn/NiOOH cells by the addition of Ca(OH)2 to the zinc electrode
[DE90-004040] N90-16139
HYDROXYL EMISSION
Effects of gravity waves on the polar O2 and OH airglow N90-16373
HYPERCUBE MULTIPROCESSORS
Spanning trees of hypercubes with a maximum of sixteen peaks
[IMAG-RR-755-I] N90-16406
Design and implementation of a multi-sensor fusion algorithm on a hypercube computer architecture
[DE90-003682] N90-16438
HYPERFINE STRUCTURE
Determination of hyperfine structures and Rydberg convergence limits of selected optical transitions in Nb-93 using resonance ionization spectroscopy
[PB90-110719] N90-16498
HYPERSONIC FLOW
Calculation of two and three dimensional super and hypersonic flows by solving the Euler equations N90-16197
Numerical simulation of laminar hypersonic flows about an ellipsoid N90-16198
HYPERSONIC SPEED
Flow separation in shock wave boundary layer interactions at hypersonic speeds
[NASA-CR-4274] N90-15885
HYPERSONIC WIND TUNNELS
Investigation of ablation phenomena using IR thermography in a hypersonic wind tunnel N90-16258
HYPERSONICS
Improved tangent-cone method for the Aerodynamic Preliminary Analysis System (APAS) version of the hypersonic arbitrary-body program
[NASA-TM-4165] N90-15890
HYPERTENSION
Factor analytic reduction of the carotid-cardiac baroreflex parameters N90-16693
HYPERVELOCITY GUNS
Progress with small, high-magnetic-field spheromaks in CTX
[DE90-003395] N90-16527
HYPERVELOCITY IMPACT
Stability and fragmentation of ejecta in hypervelocity impact
[DE90-004087] N90-16278
HYPERVELOCITY LAUNCHERS
The use of hypervelocity launchers to explore previously inaccessible states of matter
[DE90-004088] N90-15973
HYPERVELOCITY PROJECTILES
Studies of density distributions in one-dimensional shock-induced debris clouds
[DE90-004089] N90-16282

I

IBM COMPUTERS
The development of a low cost data logging system for flight trials based on an IBM compatible PC
[RAE-TM-FM-16] N90-15917
ICE
Recognition and distinction of clouds, snow, and ice using AVHRR data N90-16322
Workshop on Analysis of Returned Comet Nucleus Samples
[NASA-CR-184821] N90-16607
The origin, composition and history of cometary ices from spectroscopic studies N90-16609
Experimental studies of gas trapping in amorphous ice and thermal modelling of comets: Implications for Rosetta N90-16610
Direct determination of the morphology, structure and composition of cometary and interstellar ice analogs in the laboratory N90-16612
Modifications of comet materials by the sublimation process: Results from simulation experiments N90-16621
Interstellar and cometary dust N90-16636
Handling and analysis of ices in cryostats and glove boxes in view of cometary samples N90-16643
Analysis of particulates of comet nucleus samples: Possible use of olivine as indicator phase N90-16646
The nature of cometary materials N90-16647
Electron Spin Resonance (ESR) studies of returned comet nucleus samples N90-16651
Ion bombardment experiments suggesting an origin for organic particles in pre-cometary and cometary ices N90-16652
Refractory solids in chondrites and comets: How similar N90-16654
Neptune's Triton: A moon rich in dry ice and carbon
[NASA-CR-186298] N90-16675
ICE FLOES
Ice floe identification in satellite images using mathematical morphology and clustering about principal curves
[AD-A213854] N90-16311
Parallel algorithm for determining motion vectors in ice floe images by matching edge features N90-16451
ICE FORMATION
A numerical simulation of the flow in the diffuser of the NASA Lewis icing research tunnel
[NASA-TM-102480] N90-15965
IDENTIFYING
The development of two-dimensional object identification techniques
[NASA-CR-186203] N90-16408
IGNITION
The Gevaltig: An inertial fusion powered manned spacecraft design for outer solar system missions
[NASA-CR-185163] N90-15985
Assessing the flammability of composite materials
[PB90-112996] N90-16002
Multidimensional numerical simulation of large caliber ignition processes
[ISL-CO-233/88] N90-16021
Very low energy ignition of pyrotechnics using a Semiconductor Bridge (SCB)
[DE90-002645] N90-16082
Automatic prestart or post shutoff engine lubricator
[AD-D014259] N90-16273
Rocket-triggered lightning strikes and forest fire ignition N90-16690
IMAGE ANALYSIS
A knowledge-based machine vision system for space station automation N90-16221
Digital image interpretation for optical flow measurement methods: System description and preliminary application examples N90-16244
Quantitative evaluation of object-changes in multitemporal AGRISAR imagery
[FIM-195] N90-16314
Image segmentation by iterative parallel region growing with application to data compression and image analysis N90-16452
IMAGE ENHANCEMENT
Order filters, median recursive filter: Analysis and evaluation of performance in image processing
[ISAL-89-0017] N90-16505
IMAGE FILTERS
The lidar experiment at Andoya, Norway, during the Summer of 1988
[BONN-IR-89-16] N90-16117
Order filters, median recursive filter: Analysis and evaluation of performance in image processing
[ISAL-89-0017] N90-16505
IMAGE PROCESSING
Optimal focal-plane restoration N90-16207
Detection of edges using local geometry N90-16213
Image processing by Intensity-Dependent Spread (IDS) N90-16215
From primal sketches to the recovery of intensity and reflectance representations N90-16216
Parallel asynchronous systems and image processing algorithms N90-16218
Neural networks for data compression and invariant image recognition N90-16219
Two-Dimensional Measuring Techniques
[DGLR-PAPERS-88-04] N90-16236
Quantative interferometry N90-16237
Flow field visualization using laser light sheet methods. Quantitative analysis using image processing N90-16243
Digital image interpretation for optical flow measurement methods: System description and preliminary application examples N90-16244
End-on soft x ray imaging of Field-Reversed Configurations (FRCs) on the Field-Reversal-C (FRX-C)/Large Scale Modification (LSM) experiment
[DE90-004863] N90-16260
Science plan for the Alaska SAR facility program. Phase 1: Data from the first European sensing satellite, ERS-1
[NASA-CR-185028] N90-16312
Computer-aided boundary delineation of agricultural lands
[NASA-TM-102243] N90-16313
Proceedings of the 5th User Seminar of the German Remote Sensing Data Center of the DFVLR
[DFVLR-MITT-89-04] N90-16318
The Interactive System Meteorology and its use in meteorology and oceanography N90-16320
Satellite image sequences for motion analysis and change detection N90-16323
Attempt to draw conclusions concerning the geological subsoil from the vegetation using digital image processing of TM data N90-16329
The determination of subscale structures in thermal images N90-16330
Focal research effort points of the Institute of Applied Geodesy in the field of digital image processing N90-16333
Utilization of remote sensing in geoscientific development and projects N90-16334
Digital image coding and compression
[PB90-110958] N90-16409
Alvey MMI007. Object identification from 2D images: The RSRE contribution
[RSRE-MEMO-4277] N90-16428
Parallel algorithm for determining motion vectors in ice floe images by matching edge features N90-16451
Order filters, median recursive filter: Analysis and evaluation of performance in image processing
[ISAL-89-0017] N90-16505
Plant features measurements for robotics N90-16695
IMAGE RECONSTRUCTION
Visual Information Processing for Television and Telerobotics
[NASA-CP-3053] N90-16204
Linear digital imaging system fidelity analysis N90-16205
Context dependent anti-aliasing image reconstruction N90-16209
Image gathering and coding for digital restoration: Information efficiency and visual quality N90-16211
IMAGE RESOLUTION
Model-based quantification of image quality N90-16206
Context dependent anti-aliasing image reconstruction N90-16209
Context dependent prediction and category encoding for DPCM image compression N90-16210
Isolating contour information from arbitrary images N90-16217
Distance measurement using laser diodes
[ETN-90-96144] N90-16264

IMAGE VELOCITY SENSORS
The automatic detection of anti-collision lights
[RSRE-MEMO-4272] N90-15896
IMAGERY
Context dependent anti-aliasing image reconstruction
N90-16209
Context dependent prediction and category encoding for DPCM image compression N90-16210
IMAGES
High compression image and image sequence coding
N90-16214
From primal sketches to the recovery of intensity and reflectance representations N90-16216
Reflection technique for thermal mapping of semiconductors
[AD-D014263] N90-16541
IMAGING SPECTROMETERS
The visible channel of OMEGA-VIMS
[IFSI-89-14] N90-16231
IMAGING TECHNIQUES
Navigation of autonomous air vehicles by passive imaging sensors N90-15927
Electro-optic sensors for surveillance and target acquisition N90-15929
Visual Information Processing for Television and Telerobotics
[NASA-CP-3053] N90-16204
Linear digital imaging system fidelity analysis
N90-16205
Model-based quantification of image quality
N90-16206
Optimal focal-plane restoration N90-16207
Coded-aperture imaging in nuclear medicine
N90-16208
Image gathering and coding for digital restoration: Information efficiency and visual quality N90-16211
Data compression for the microgravity experiments
N90-16212
Image processing by Intensity-Dependent Spread (IDS) N90-16215
Knowledge-based imaging-sensor fusion system
N90-16220
A programmable image compression system
N90-16222
The MPI/AIT X ray Imager (MAXI): High speed PN-CCD's for x ray detection
[MPE-PREPRINT-154] N90-16234
Science plan for the Alaska SAR facility program. Phase 1: Data from the first European sensing satellite, ERS-1
[NASA-CR-185028] N90-16312
Quantitative evaluation of object-changes in multitemporal AGRISAR imagery
[FIM-195] N90-16314
Apparatus for imaging deep arterial and coronary lesions
[NASA-CASE-NPO-17439-1-CU] N90-16391
Digital image coding and compression
[PB90-110958] N90-16409
Image segmentation by iterative parallel region growing with application to data compression and image analysis
N90-16452
Proposed concept for the visible/infrared imaging radiometer for second generation Meteosat
[ETN-90-96145] N90-16503
Plant features measurements for robotics N90-16695
IMPACT LOADS
Stability and fragmentation of ejecta in hypervelocity impact
[DE90-004087] N90-16278
IMPACT RESISTANCE
Development of an elastomeric additive to improve the impact resistance of unsaturated polyester networks
[ISAL-89-0006] N90-16073
IMPACT STRENGTH
Instrumented impact and residual tensile strength testing of eight-ply carbon eopoxy specimens
[NASA-TP-2981] N90-16007
Fatigue and impact strength of diffusion bonded titanium alloy joints
[RAE-TM-MAT/STR-1123] N90-16043
IMPACT TESTS
Instrumented impact and residual tensile strength testing of eight-ply carbon eopoxy specimens
[NASA-TP-2981] N90-16007
Studies of density distributions in one-dimensional shock-induced debris clouds
[DE90-004089] N90-16282
IMPEDANCE
Application of ac impedance method for diagnosis of lithium secondary battery degradation. Preliminary study with AA size Li/MoS2 cells
[DE90-702474] N90-16137
Measurement of reflection and impedance in a beam by the structural intensity technique
[DE90-728212] N90-16299
IMPEDANCE MEASUREMENT
Measurement of reflection and impedance in a beam by the structural intensity technique
[DE90-728212] N90-16299
IMPLOSIONS
Design of a spheromak compressor driven by high explosives
[DE90-003652] N90-16283
IMPURITIES
Pairs of chalcogen impurities in silicon
[DE89-635767] N90-16063
Synthesis of tetrafluorohydrazine
[AD-D014281] N90-16083
IN-FLIGHT MONITORING
Direct measurement of laminar instability amplification factors in flight N90-16178
INCIDENT RADIATION
Reflection from layered media with special attention to the microwave region
[ESA-TT-1155] N90-16111
INCOMPRESSIBLE FLOW
A numeric analysis of incompressible, viscous flow around a symmetrical body of revolution
[ISL-CO-215/87] N90-16157
INCONEL (TRADEMARK)
The influence of carbide precipitation on the creep rupture behavior of high temperature alloys
[JUEL-2211] N90-16044
INDEXES (DOCUMENTATION)
AGARD index of publications, 1986-1988
[AGARD-INDEX-86-88] N90-16585
JSC document index
[NASA-TM-102923] N90-16589
INDUSTRIAL PLANTS
Industrial heat pump assessment study
[DE90-004541] N90-16201
INDUSTRIAL SAFETY
Electrical safety in the high voltage laboratory
[DE90-003026] N90-16130
INELASTIC SCATTERING
Heavy ion inelastic scattering with a 4(pi) gamma detector
[DE90-002709] N90-16488
INERTIAL CONFINEMENT FUSION
The Gevaltig: An inertial fusion powered manned spacecraft design for outer solar system missions
[NASA-CR-185163] N90-15985
Light ion beam drivers for inertial confinement fusion
[DE90-004196] N90-16528
INERTIAL NAVIGATION
Advances in techniques and technologies for air vehicle navigation and guidance
[AGARD-AR-276] N90-15899
INFERENCE
Optimization of monotonic inference algorithms in propositional and first order logic
[LAAS-89204] N90-16436
INFORMATION
Isolating contour information from arbitrary images
N90-16217
INFORMATION MANAGEMENT
Introduction to the framework and tasks of the DFD — German Remote Sensing Data Center (DFD)
N90-16319
FY 1989 update to the Information Resources Management review plan
[DE90-004185] N90-16593
INFORMATION SYSTEMS
Statistical information system for cultivation of the soil.
Use of remote sensing in official statistics N90-16338
Database design using NIAM (Nijssen Information Analysis Method) modeling
[DE89-014631] N90-16592
FY 1989 update to the Information Resources Management review plan
[DE90-004185] N90-16593
INFORMATION THEORY
High compression image and image sequence coding
N90-16214
INFORMATION TRANSFER
Investigation of IGES for CAD/CAE data transfer
N90-16702
INFRARED ASTRONOMY SATELLITE
Outflows in high mass star-forming regions
N90-16657
INFRARED DETECTORS
Determination of the heat transfer coefficients in separated flows using an infrared camera N90-16257
Enhanced performance IR focal plane arrays using adaptive subtraction
[RSRE-MEMO-4286] N90-16502
INFRARED IMAGERY
Investigation of ablation phenomena using IR thermography in a hypersonic wind tunnel N90-16258
INFRARED PHOTOMETRY
Short time scale variability of the BL Lac object OJ 287 in the near-infrared
[IFSI-89-3] N90-16603
INFRARED RADIOMETERS
Proposed concept for the visible/infrared imaging radiometer for second generation Meteosat
[ETN-90-96145] N90-16503
INFRARED SOURCES (ASTRONOMY)
Short time scale variability of the BL Lac object OJ 287 in the near-infrared
[IFSI-89-3] N90-16603
Outflows in high mass star-forming regions
N90-16657
INFRARED SPECTRA
Cloud phase discrimination by near-infrared remote sensing N90-16310
INFRARED SPECTROMETERS
The visible channel of OMEGA-VIMS
[IFSI-89-14] N90-16231
INHOMOGENEITY
The response of the atmospheric convective boundary layer to surface inhomogeneities N90-16369
INLET FLOW
Rotor induced-inflow-ratio measurements and CAMRAD calculations
[NASA-TP-2946] N90-15882
INSOLATION
SERI (Solar Energy Research Institute) solar radiation resource assessment project
[DE89-009456] N90-16352
INSULATION
Energy management and recovery N90-15962
Command operated liquid metal opening switch
[AD-D014262] N90-16126
INSULATORS
Development of a diamond insulator for thermionic applications
[DE90-002849] N90-16055
INTEGERS
Basic mathematical function libraries for scientific computation
[NASA-TM-102256] N90-16423
INTEGRAL EQUATIONS
Simple proof of renormalization group equation in the minimal subtraction scheme
[DE90-600758] N90-16457
INTEGRALS
Integrable classical systems in higher dimensions
[DE90-600737] N90-16473
INTEGRATED CIRCUITS
CAE (Computer-Aided Engineering) tools' limitations case study: An SSI (Small Scale Integrated) design to an ASIC (Application Specific Integrated Circuit)
[DE90-002902] N90-16418
INTEGRATED MISSION CONTROL CENTER
RETE experiment activity at the TSS-1 POCC
[IFSI-89-12] N90-15988
INTEGRITY
Fuel Tank Technology
[AGARD-R-771] N90-15904
Mechanical strain isolator mount
[NASA-CASE-LAR-13580-1] N90-16272
INTERACTIONS
On the interaction of a pulsar with the ambient medium utilizing x ray images of the Crab nebula
[MPE-REPT-215] N90-16604
INTERACTIVE CONTROL
An interactive method for the flow calculation of airfoils with local separation regions N90-16190
The Interactive System Meteorology and its use in meteorology and oceanography N90-16320
INTERCONTINENTAL BALLISTIC MISSILES
Complex availability problems solved with simulation
[DE89-012610] N90-16459
INTERFACE STABILITY
Anomalous waves in shock wave - fluid interface collisions
[AD-A213584] N90-16144
INTERFACES
RVD scenari and interfaces between Hermes and space station N90-15982
A generic fine-grained parallel C N90-16454
INTERFACIAL TENSION
Development of an elastomeric additive to improve the impact resistance of unsaturated polyester networks
[ISAL-89-0006] N90-16073
Determination of dynamic surface forces using piezoelectric arrays N90-16249
A quantitative analysis of slip phenomena along a dry contact surface between two bodies in comparison to interfacial crack propagation
[ISAL-89-0032] N90-16304

INTERFERENCE
Use of an HF active monitoring array in the presence of high level interference
[BBC-RD-1989/7] N90-16096
INTERIOR BALLISTICS
Multidimensional numerical simulation of large caliber ignition processes
[ISL-CO-233/88] N90-16021
INTERMETALLICS
Design of coupled or uncoupled multifilamentary SSC-type strands with almost zero retained magnetization at fields near 0.3 T
[DE90-005391] N90-16052
Metals and Ceramics Division Materials Sciences Program
[DE90-004371] N90-16070
INTERNAL COMBUSTION ENGINES
Results from the third year of operation of the Federal Methanol Fleet at Lawrence Berkeley Laboratory
[DE90-003J06] N90-16277
INTERNATIONAL COOPERATION
Crew Safety and Rescue in Space: An International Approach
[ESA-SP-300] N90-15974
Systems interoperability approach Apollo/Soyuz test project N90-15979
Crew safety and rescue aids N90-15980
Guide on the global observing system
[WMO-488-REV] N90-16385
INTERNATIONAL SUN EARTH EXPLORER 3
Spectrophotometric observations of comet P/Giacobini-Zinner N90-16630
INTERPLANETARY DUST
Identification of solar nebula condensates in interplanetary dust particles and unequilibrated ordinary chondrites N90-16629
What if chondritic porous interplanetary dust particles are not the real McCoy N90-16642
Isotopic microanalysis of returned comet nucleus samples N90-16655
The measurement of trace elements in interplanetary dust and cometary particles by ultra-high sensitivity INAA N90-16656
INTERPLANETARY FLIGHT
Reports of planetary astronomy, 1986
[NASA-TM-100776] N90-16596
INTERPLANETARY MAGNETIC FIELDS
Polar cusps latitudinal shift and its relation to the IMF-By component
[IFSI-88-14] N90-16377
Some properties of so-called magnetic cloud structures in the solar wind
[IFSI-88-16] N90-16678
INTERPLANETARY SPACE
Stochastic simulation of charged particle transport on the massively parallel processor N90-16448
INTERPOLATION
Application of Lagrangian blending functions for grid generation around airplane geometries
[NASA-CR-186318] N90-15891
Context dependent anti-aliasing image reconstruction N90-16209
INTERPROCESSOR COMMUNICATION
UNIX internals. Part 1: Intertask communication in UNIX. Part 2: UNIX file system
[CNES-NT-122-PT-1/2] N90-16405
Algorithms for fault tolerant distributed systems
[AD-A214447] N90-16416
INTERSTELLAR CHEMISTRY
Non-equilibrium chemistry in the solar nebula and early solar system: Implications for the chemistry of comets N90-16618
INTERSTELLAR GAS
Role of dust to gas production rate ratio in cometary physics N90-16625
INTERSTELLAR MATTER
Workshop on Analysis of Returned Comet Nucleus Samples
[NASA-CR-184821] N90-16607
Direct determination of the morphology, structure and composition of cometary and interstellar ice analogs in the laboratory N90-16612
The carbon chemistry of meteorites: Relationships to comets N90-16615
Analysis of organic compounds in returned comet nucleus samples N90-16617
From interstellar dust to comets N90-16620
Comments on comet shapes and aggregation processes N90-16622
Computer simulation of dust grain evolution N90-16632
Solar nebula condensates and the composition of comets N90-16634
Interstellar and cometary dust N90-16636
Metamorphism of cosmic dust: Processing from circumstellar outflows to the cometary regolith N90-16641
Gamma-ray observations and the distribution of interstellar aluminum-26 N90-16661
Turbulent stripping of interstellar clouds by interaction with supernova remnants
[DE90-003622] N90-16674
INVENTIONS
Invention and innovation: Alternative mechanisms for enhancing organizational competitiveness
[DE89-015858] N90-16584
INVISCID FLOW
The precise calculation of the inviscid leading edge flow on a laminar airfoil using simple methods and verification by measurements on the TLF pilot model N90-16180
ION ACOUSTIC WAVES
Langmuir wave interaction with ion-sound one. Part 1: Stochastic effects
[DE90-603368] N90-16474
ION BEAMS
Structure-property relationships in ion-beam surface-modified ceramics: Theory and applications
[AD-A212785] N90-16054
Effect of carbon on ion beam mixing of Fe-Ti bilayers
[DE90-003650] N90-16056
Silicon-based coatings on niobium metal
[DE90-003651] N90-16057
Light ion beam drivers for inertial confinement fusion
[DE90-004196] N90-16528
Effects of ion dose on the morphology and crystallization of amorphous germanium
[DE90-003564] N90-16547
Ion beam annealing of Si co-implanted with Ga and As
[DE90-004297] N90-16556
ION CURRENTS
Solid state voltammetry and sensors in solids and gases
[DE90-003234] N90-16538
ION DENSITY (CONCENTRATION)
A double focussing mass-spectrometer for simultaneous ion measurements in the stratosphere
[AERONOMICA-ACTA-A-350-1989] N90-16379
ION DISTRIBUTION
A computer program to calculate the population numbers of multi-level species
[IFSI-89-15] N90-16671
Determination of solar flare accelerated ion angular distributions from SMM gamma ray and neutron measurements and determination of the He-3/H ratio in the solar photosphere from SMM gamma ray measurements
[NASA-CR-186038] N90-16676
ION IMPLANTATION
Effect of carbon on ion beam mixing of Fe-Ti bilayers
[DE90-003650] N90-16056
Characterization of B and N implanted fused silica
[DE90-004198] N90-16069
Metals and Ceramics Division Materials Sciences Program
[DE90-004371] N90-16070
Ion beam annealing of Si co-implanted with Ga and As
[DE90-004297] N90-16556
ION IRRADIATION
Structure-property relationships in ion-beam surface-modified ceramics: Theory and applications
[AD-A212785] N90-16054
Mass loss during x ray microanalysis
[DE90-003954] N90-16067
Ion bombardment experiments suggesting an origin for organic particles in pre-cometary and cometary ices N90-16652
ION PROBES
Isotopic microanalysis of returned comet nucleus samples N90-16655
ION SCATTERING
Heavy ion inelastic scattering with a 4(pi) gamma detector
[DE90-002709] N90-16488
ION SOURCES
Broad-beam multi-ampere metal ion source
[DE90-003106] N90-16123
In situ measurement of neutral beam components using the Doppler-shifted H(sub alpha) emissions in Heliotron E
[DE90-719521] N90-16516
IONIZATION
Upper atmosphere research
[ISBN-0-642-13582-7] N90-16368
IONOSPHERIC ELECTRON DENSITY
Scientific investigations of the Space Research Group
[ISBN-0-642-13252-6] N90-16595
IRAS-ARAKI-ALCOCK COMET
Sulfur compounds in comets N90-16627
IRON ALLOYS
Fracture toughness of ferritic alloys at very high neutron exposures
[DE90-004519] N90-16046
Effect of carbon on ion beam mixing of Fe-Ti bilayers
[DE90-003650] N90-16056
Anisotropy and microstructure of high coercivity rare earth iron permanent magnets, list of papers published
[AD-A214160] N90-16476
IRRADIATION
Defense to laser light irradiation
[AD-D014286] N90-15984
Evaluation of potential cold x ray shield materials tested on Proto II
[DE90-004348] N90-16003
Microstructural explanation for irradiation embrittlement of V-15Cr-5Ti
[DE90-004112] N90-16041
Phase evolution during neutron irradiation of commercial Fe-Cr-Mn alloys
[DE90-004113] N90-16042
Irradiation creep and swelling of annealed type 304L stainless steel at approximately 390 C and high neutron fluence
[DE90-004521] N90-16047
Modeling dislocation evolution in irradiated alloys
[DE90-004921] N90-16051
Structure-property relationships in ion-beam surface-modified ceramics: Theory and applications
[AD-A212785] N90-16054
Metals and Ceramics Division Materials Sciences Program
[DE90-004371] N90-16070
Radiation resistance of solar cells for space application. 1: Study on the irradiation procedure of electron beams
[DE90-719546] N90-16349
Mechanisms of microwave induced damage in biologic materials
[AD-A213480] N90-16390
Atomic processes in plasmas under ultra-intense laser irradiation
[DE90-003221] N90-16521
Effects of ion dose on the morphology and crystallization of amorphous germanium
[DE90-003564] N90-16547
The 1MeV-electron irradiation induced defects in epitaxially grown 3C-SiC
[DE90-719574] N90-16554
ISING MODEL
Contribution to the study of order effects in the Ising model framework: Ground states and phase diagrams
[ESA-TT-1118] N90-16557
ISOLATORS
Mechanical strain isolator mount
[NASA-CASE-LAR-13580-1] N90-16272
ISOTOPE SEPARATION
Isotope driven critical scattering and phase separation from mixtures of deuterated and protonated polymers
[DE90-003976] N90-16076
ISOTOPES
Isotope driven critical scattering and phase separation from mixtures of deuterated and protonated polymers
[DE90-003976] N90-16076
On the isotope analysis of cometary dust N90-16611
Isotopic microanalysis of returned comet nucleus samples N90-16655
ITERATION
Improved solution techniques for the eigenstructure of fractional order systems
[AD-A213844] N90-16295
ITERATIVE SOLUTION
Element-by-element preconditioning techniques for large-scale, vectorized finite element analysis in nonlinear solid and structural mechanics N90-16291
IUE
Sulfur compounds in comets N90-16627

J

JAMMING
Method for eliminating self-screening noise jamming in radar systems
[AD-D014271] N90-16105
JAPAN
Lightning observations on Japan Sea coast in winter
[DE90-702485] N90-16387
JAPANESE SPACE PROGRAM
NASDA's approach to the interoperability of safety and rescue in space N90-15981
JET FLOW
Swirl-stabilized flames: Fluid dynamics, mixing, and flame stability limits N90-16009
Demonstration of the feasibility of laser induced fluorescence for arc jet flow diagnostics
[NASA-CR-185595] N90-16013

JET IMPINGEMENT
Plume shape optimization of small attitude control thrusters with respect to impingement and thrust
[ISL-CO-220/88] N90-16153
JET STREAMS (METEOROLOGY)
Diagnostic and kinematic fields associated with curved and straight jet streaks using a two-layer primitive equation model N90-16371
JETTISON SYSTEMS
On the selection of crewmember rescue means for manned space launch systems N90-15978
JOINTS (JUNCTIONS)
An investigation of elastic guided waves for ceramic joint evaluation
[DE90-004400] N90-16071

K

KENYA
Evaluation of the pasture potential in the dry areas of Kenya using combined Earth reconnaissance N90-16327
KERNEL FUNCTIONS
Optimal focal-plane restoration N90-16207
KINEMATICS
Bilateral force reflection for teleoperators with masters and slaves with dissimilar and possibly redundant kinematics
[DE90-004392] N90-16132
Diagnostic and kinematic fields associated with curved and straight jet streaks using a two-layer primitive equation model N90-16371
KINETIC ENERGY
Stability and fragmentation of ejecta in hypervelocity impact
[DE90-004087] N90-16278
KINETICS
The continuous crystallization of sulfur formed by the liquid-phase reaction of hydrogen sulfide and sulfur dioxide
[DE90-003991] N90-16018
Theoretical studies of chemisorption and surface reactions on nickel and silicon
[DE90-004849] N90-16050
Bilateral force reflection for teleoperators with masters and slaves with dissimilar and possibly redundant kinematics
[DE90-004392] N90-16132
MHD integrated topping cycle project
[DE90-004141] N90-16525
Use of computer simulations to analyze limitations of kinetic models for recrystallization
[DE90-003618] N90-16548
KLEIN-GORDON EQUATION
Quantum fields in cosmological space-times: A soluble example
[DE89-618837] N90-16662
KLYSTRONS
Recent progress in relativistic klystron research
[DE90-000942] N90-16121
KNOWLEDGE BASES (ARTIFICIAL INTELLIGENCE)
Experiences with knowledge-base and large database integration
[DE90-000686] N90-16591
Artificial intelligence in process control: Knowledge base for the shuttle ECS model N90-16697
KNOWLEDGE REPRESENTATION
Optimization of monotonic inference algorithms in propositional and first order logic
[LAAS-89204] N90-16436

L

LABORATORIES
FRAG requirements for control of fatigue testing
[RAE-TM-MAT/STR-1130] N90-16300
Activities report of the National Electrotechnic Institute Galileo Ferraris
[ETN-90-96178] N90-16705
LAGRANGE MULTIPLIERS
Theory of singular Lagrangians
[DE90-600735] N90-16456
LAMINAR BOUNDARY LAYER
Experiments on the laminar-turbulent transition on swept wings N90-16170
Direct measurement of laminar instability amplification factors in flight N90-16178
LAMINAR FLOW
Ambient Test Rig (ATR) flow studies: A laminar flow, reduced entrainment electrostatic precipitator
[DE90-000144] N90-16142
Numerical simulation of the laminar and turbulent three dimensional flow on a delta wing with sharp leading edge N90-16186
Numerical simulation of laminar hypersonic flows about an ellipsoid N90-16198
LAMINAR FLOW AIRFOILS
Semi-empirical transition criteria for the design of laminar profiles N90-16174
The precise calculation of the inviscid leading edge flow on a laminar airfoil using simple methods and verification by measurements on the TLF pilot model N90-16180
LAMINATES
Reflection from layered media with special attention to the microwave region
[ESA-TT-1155] N90-16111
LAND MANAGEMENT
Use of remote sensing data for land and building statistics N90-16335
LAND MOBILE SATELLITE SERVICE
Satellite systems integrated with the terrestrial cellular network for mobile communications
[ESA-STR-228] N90-16113
LAND USE
Computer-aided boundary delineation of agricultural lands
[NASA-TM-102243] N90-16313
Support of hydrological models calculations by satellite data N90-16337
TM land use classification of a region. Utilization for planning and statistics N90-16339
LANDAU-GINZBURG EQUATIONS
The modified Ginzburg-Landau theory for anisotropic high temperature superconductors
[DE89-635909] N90-16532
LANDING
Crew emergency return vehicle autoland feasibility study
[NASA-CR-181940] N90-15937
LANDSAT SATELLITES
Evaluation of the pasture potential in the dry areas of Kenya using combined Earth reconnaissance N90-16327
Image segmentation by iterative parallel region growing with application to data compression and image analysis N90-16452
LANTHANUM COMPOUNDS
Synthesis of air-sinterable lanthanum chromite powders
[DE90-004681] N90-16049
LANTHANUM OXIDES
La(sub 2)MO(sub 4 + delta) (M = Cu, Ni, Co): Phase separation and superconductivity resulting from excess oxygen defects
[DE90-001988] N90-16534
Microstructures of Y123 films on SrTiO3, LaGaO3, and LaAlO3
[DE90-003367] N90-16537
LASER APPLICATIONS
Electro-optic sensors for surveillance and target acquisition N90-15929
The first year's work of race project 1036 WTDM broadband customer premises network
[BBC-RD-1989/6] N90-16097
Backscattering effects in DIAL due to water vapor
[SER-WISS-ABHANDL-89] N90-16265
Shock thickness measurements with laser beams
[MPIS-7/1989] N90-16267
Results of error correction techniques applied on two high accuracy coordinate measuring machines
[DE90-003341] N90-16439
Resonance enhanced Raman studies of as-grown and laser-processed HgCdTe
[AD-A213855] N90-16540
LASER BEAMS
Analysis and evaluation of technical data on the photochromic and non-linear optical properties of materials
[AD-A214050] N90-16014
Flow field visualization using laser light sheet methods. Quantitative analysis using image processing N90-16243
The determination of vortex separation frequencies by means of laser light sheet images
[DNW-WTI-88.038] N90-16245
Flow visualization using the laser light sheet method in vehicle aerodynamics and combustion chamber engineering N90-16246
Statistics of a reflected laser beam in the turbulent atmosphere (path correlation)
[PB90-113994] N90-16261
Diffraction limited dichroic combiner diode laser
[AD-D014291] N90-16263
High speed signal extraction using electro-optic techniques
[AD-A214446] N90-16500
LASER DAMAGE
Analysis and evaluation of technical data on the photochromic and non-linear optical properties of materials
[AD-A214050] N90-16014
LASER DOPPLER VELOCIMETERS
Solid fuel combustion chamber
[LR-555] N90-16001
Miniature laser Doppler anemometer with a diode laser
[ISL-CO-224/88] N90-16232
High frequency pulsed diode lasers and phase-coupled diode arrays for aerodynamics N90-16238
LASER INDUCED FLUORESCENCE
Demonstration of the feasibility of laser induced fluorescence for arc jet flow diagnostics
[NASA-CR-185595] N90-16013
LASER OUTPUTS
Defense to laser light irradiation
[AD-D014286] N90-15984
Atomic processes in plasmas under ultra-intense laser irradiation
[DE90-003221] N90-16521
LASER PLASMAS
Atomic processes in plasmas under ultra-intense laser irradiation
[DE90-003221] N90-16521
LASER TARGETS
Studies of density distributions in one-dimensional shock-induced debris clouds
[DE90-004089] N90-16282
LATERAL CONTROL
Synthesis of control law, on a RPV, in order to minimize the number of sensors N90-15925
LATITUDE
Polar cusps latitudinal shift and its relation to the IMF-By component
[IFSI-88-14] N90-16377
LATTICES (MATHEMATICS)
A nonlinear vortex-lattice method for the calculation of interference effects between free vortex sheets and wings N90-16183
LAUNCHERS
From small beginnings... The story of ESRO's sounding rocket programme in celebration of the twenty-fifth anniversary of the first ESRO sounding rocket launch
[ESA-BR-60] N90-15999
LAUNCHING SITES
From small beginnings... The story of ESRO's sounding rocket programme in celebration of the twenty-fifth anniversary of the first ESRO sounding rocket launch
[ESA-BR-60] N90-15999
LEAD ACID BATTERIES
Evaluation of a new charge algorithm for a lead-acid battery with gelled electrolyte using a 96V gel cell 4 as a test battery
[DE90-003420] N90-16133
LEADING EDGES
The precise calculation of the inviscid leading edge flow on a laminar airfoil using simple methods and verification by measurements on the TLF pilot model N90-16180
LEAKAGE
Fuel Tank Technology
[AGARD-R-771] N90-15904
Integral fuel tank sealing practice at British Aerospace (Kingston) N90-15905
Integral fuel tanks - design, production, aging, repair N90-15906
Aircraft fuel tank construction and testing experience N90-15907
The repair of aircraft integral fuel tanks in the RAF: A user's view of fuel tank technology N90-15908
Spray sealing: A breakthrough in integral fuel tank sealing technology N90-15912
Design philosophy and construction techniques for integral fuselage fuel tanks N90-15913
A dynamicist's view of fuel tank skin durability N90-15915
Integral fuel tank certification and test methods N90-15916
LEAST SQUARES METHOD
And still, a new beginning: The Galerkin least-squares gradient method
[DE89-636435] N90-16461
A new finite element formulation for CFD:8. The Galerkin/least-squares method for advective-diffusive equations
[DE89-636437] N90-16462
LENS ANTENNAS
Geometrical optics in inhomogeneous chiral media with application to polarization correction in inhomogeneous lens antennas
[PB90-110669] N90-16497
LEPTONS
Dissipative effects in Friedmann universes
[DE89-618838] N90-16663

LESIONS
Apparatus for imaging deep arterial and coronary lesions
[NASA-CASE-NPO-17439-1-CU] N90-16391
LIE GROUPS
Multiplet classification of highest weight modules over quantum universal enveloping algebras: The U(sub q)(sl(3,C)) example
[DE90-600720] N90-16464
LIFE (DURABILITY)
Fuel Tank Technology
[AGARD-R-771] N90-15904
The effect of primer age on adhesion of polysulphide sealant N90-15909
Long term creep strength of silver alloyed copper
[DE90-602367] N90-16039
Assessment of strength limiting flaws in ceramic heat exchanger components
[DE90-004086] N90-16077
LIFE SUPPORT SYSTEMS
DNSS: German/Norwegian work team Space Subsea. Environmental control and life support subsystems (technical matters), phase 2
[ETN-90-95905] N90-16396
LIGANDS
Electrochemical parameterization of metal complex redox potentials, using the ruthenium(III)/ruthenium(II) couple to generate a ligand electrochemical series
[AD-A214439] N90-16015
LIGHT (VISIBLE RADIATION)
The visible channel of OMEGA-VIMS
[IFSI-89-14] N90-16231
LIGHT EMITTING DIODES
Liquid level measurement system for analog and digital readout
[AD-D014297] N90-16227
LIGHT IONS
Light ion beam drivers for inertial confinement fusion
[DE90-004196] N90-16528
LIGHT SCATTERING
The determination of vortex separation frequencies by means of laser light sheet images
[DNW-WTI-88.038] N90-16245
LIGHT SOURCES
Liquid level measurement system for analog and digital readout
[AD-D014297] N90-16227
LIGHTNING
Lightning observations on Japan Sea coast in winter
[DE90-702485] N90-16387
Characteristics of electromagnetic wave forms with lightning in winter season (2): Characteristics in frequency domain
[DE90-734989] N90-16388
Rocket-triggered lightning strikes and forest fire ignition N90-16690
LINE SPECTRA
The upper main sequence of OB associations. Part 2: The single-lined O stars: Spectral classification of northern stars and lines of C and N
[SER-C-PREPUBL-FASC-39] N90-16602
LINEAR ACCELERATORS
Proposal for a study of laser acceleration of electrons using micrograting structures at ATF
[DE90-003699] N90-16262
LINEAR FILTERS
An analysis of the time variation of the frequency response of the LMS adaptive line enhancer
[ISVR-TR-175] N90-16115
LINEAR QUADRATIC GAUSSIAN CONTROL
Crew emergency return vehicle autoland feasibility study
[NASA-CR-181940] N90-15937
LINEAR SYSTEMS
Linear digital imaging system fidelity analysis N90-16205
Element-by-element preconditioning techniques for large-scale, vectorized finite element analysis in nonlinear solid and structural mechanics N90-16291
Uniform stability for time-varying infinite-dimensional discrete linear systems
[DE89-635712] N90-16460
LINEAR VIBRATION
Analysis of nonlinear systems using ARMA (Autoregressive Moving Average) models
[DE90-002395] N90-16297
LIQUID CRYSTALS
Simultaneous determination of temperature and velocity fields in a thermal convection flow with non-enclosed liquid crystal tracers N90-16239
Unsteady heat transfer measurement using thermochromatic liquid crystals as temperature indicators N90-16254
Surface flow visualization with shear stress sensitivive liquid crystals
[DNW-WTI-88.039] N90-16255
Quantitative heat transfer measurements using heated liquid crystals N90-16256
Conformation, orientation and interaction in molecular monolayers: A surface second harmonic and sum frequency generation study
[DE90-003108] N90-16536
LIQUID FLOW
Command operated liquid metal opening switch
[AD-D014262] N90-16126
LIQUID LEVELS
Liquid level measurement system for analog and digital readout
[AD-D014297] N90-16227
LIQUID METALS
The onset of boiling of the liquid alkali metals
[DE90-002276] N90-16036
Command operated liquid metal opening switch
[AD-D014262] N90-16126
Development of a wet vapor homogeneous liquid metal MHD power system
[DE90-001468] N90-16508
LIQUID SLOSHING
Small amplitude liquid oscillations in a rectangular container under zero-gravity
[LRT-WE-9-FB-2(1989)] N90-16167
Linear liquid oscillations in cylindrical containers under zero-gravity
[LRT-WE-9-FB-5(1989)] N90-16168
LIQUID SURFACES
Response of a rotating finite annular liquid layer to axial excitation
[LRT-WE-9-FB-15(1988)] N90-16090
LIQUID-VAPOR INTERFACES
On condensation driven by electrostatic interactions in macroionic solutions
[DE89-636072] N90-16487
LIQUIDS
Thickness, velocity, and temperature measurements in falling liquid films
[DE90-004290] N90-16151
LITHIUM ALLOYS
Lithium cobalt oxide thin film and its electrochromism
[DE90-004570] N90-16564
LITHIUM OXIDES
Lithium cobalt oxide thin film and its electrochromism
[DE90-004570] N90-16564
LITHIUM SULFATES
Thermodynamic studies on the ferroelectric phase transition in neutron irradiated (Li(sub x)K(1-x))2SO4 crystals at high temperature
[DE89-635786] N90-16545
LITHIUM SULFUR BATTERIES
Application of ac impedance method for diagnosis of lithium secondary battery degradation. Preliminary study with AA size Li/MoS2 cells
[DE90-702474] N90-16137
LOAD DISTRIBUTION (FORCES)
Fatigue life estimates for helicopter loading spectra
[NASA-CR-181941] N90-16294
LOAD TESTS
Analysis and testing of axial compression in imperfect slender truss struts
[NASA-TM-4174] N90-16292
LOCAL AREA NETWORKS
Issues and approaches for electronic document approval and transmittal using digital signatures and text authentication: Prototype documentation
[DE90-003382] N90-16119
LOCKS (FASTENERS)
Quick disconnect duct coupler
[AD-D014265] N90-16274
LOGIC CIRCUITS
Fault tree analysis: A tool for battery safety and reliability studies
[DE90-002582] N90-16287
Algorithms for fault tolerant distributed systems
[AD-A214447] N90-16416
The NODEN hardware description language
[RSRE-89011] N90-16431
The algebra of the NODEN analyser
[RSRE-89012] N90-16432
LOGIC PROGRAMMING
D3-D cryogenic control system upgrade
[DE90-003290] N90-16092
Built in test of folded PLAs
[IMAG-RR-758-I] N90-16134
LOGISTICS
International conference management N90-16583
LONG DURATION EXPOSURE FACILITY
Experiment facilities for materials and fluid sciences embarked on Eureca-1
[ESA-SP-1118] N90-16086
LONGITUDINAL CONTROL
An experimental investigation of thrust vectoring two-dimensional convergent-divergent nozzles installed in a twin-engine fighter model at high angles of attack
[NASA-TM-4155] N90-15884
LORENTZ FORCE
Command operated liquid metal opening switch
[AD-D014262] N90-16126
LOW ALTITUDE
Low-altitude millimeter-wave propagation in the evaporation duct
[AD-A214432] N90-16108
LOW SPEED WIND TUNNELS
The use of sublimation methods for the recognition of transition at low speed N90-16251
LUBRICATING OILS
Automatic prestart or post shutoff engine lubricator
[AD-D014259] N90-16273
LUBRICATION
Automatic prestart or post shutoff engine lubricator
[AD-D014259] N90-16273
Investigation of rough elastohydrodynamic contact
[ISAL-89-0029] N90-16281
LUNAR BASES
The first 1000 days of a future lunar base
[ILR-MITT-224] N90-15970

M

MACHINE LEARNING
User interaction with self-learning systems
[AD-A214280] N90-16395
MACHINE TOOLS
Electrode/workpiece combinations
[DE90-003919] N90-16095
MAGNET COILS
Modeling energy output of inertial storage devices for the DIII-D tokamak
[DE90-004096] N90-16524
MAGNETIC CLOUDS
Some properties of so-called magnetic cloud structures in the solar wind
[IFSI-88-16] N90-16678
MAGNETIC EFFECTS
Magnetic interactions in Sn-119 substituted for Cu in antiferromagnetic and superconducting lamellar cuprates
[DE90-003661] N90-16560
MAGNETIC FIELD CONFIGURATIONS
End-on soft x ray imaging of Field-Reversed Configurations (FRCs) on the Field-Reversal-C (FRX-C)/Large Scale Modification (LSM) experiment
[DE90-004863] N90-16260
On the structure of the tail magnetic field
[IFSI-88-19] N90-16378
Terrestrial magnetosphere magnetic field models
[REPT-89/CT/DTI/MS/AS/154] N90-16380
Recent progress on the HESS (High Explosive Spheromak Source) experiment
[DE90-003218] N90-16520
MAGNETIC FIELDS
Design of coupled or uncoupled multifilamentary SSC-type strands with almost zero retained magnetization at fields near 0.3 T
[DE90-005391] N90-16052
Terrestrial magnetosphere magnetic field models
[REPT-89/CT/DTI/MS/AS/154] N90-16380
Geometrical optics in inhomogeneous chiral media with application to polarization correction in inhomogeneous lens antennas
[PB90-110669] N90-16497
Toroidal magnetic fields in terms of field-line invariants
[DE89-016610] N90-16507
Magnetic penetration depth and intragrain critical current density in gain-aligned Tl2Ca2Ba2Cu3O10 superconductor
[DE90-004245] N90-16562
The dynamics of dust in planetary magnetospheres N90-16658
MAGNETIC MATERIALS
Electron Spin Resonance (ESR) studies of returned comet nucleus samples N90-16651
Activities report of the National Electrotechnic Institute Galileo Ferraris
[ETN-90-96178] N90-16705
MAGNETIC MIRRORS
Spectroscopic diagnostics of high temperature plasmas
[DE90-003912] N90-16522
MAGNETIC PROPERTIES
Properties and design of multifilamentary NbTi composite superconductors
[DE90-004904] N90-16569

Magnetic studies of proximity-effect coupling in a very closely spaced fine-filament NbTi/CuMn composite superconductor
[DE90-005387] N90-16570

MAGNETIC SHIELDING
On the HEMP (High-Altitude Electromagnetic Pulse) response of protective relays
[DE90-003718] N90-16138

MAGNETIC SPECTROSCOPY
Spectroscopic diagnostics of high temperature plasmas
[DE90-003912] N90-16522

MAGNETIC STARS
Accretion shock geometries in the magnetic variables
[NASA-CR-186290] N90-16664

MAGNETIC SURVEYS
Proceedings of the 79th SEGJ Conference
[DE89-760006] N90-16704

MAGNETIZATION
Design of coupled or uncoupled multifilamentary SSC-type strands with almost zero retained magnetization at fields near 0.3 T
[DE90-005391] N90-16052
Rotational magnetic processes in YB2Cu3O7
[DE90-000541] N90-16533
Magnetic studies of proximity-effect coupling in a very closely spaced fine-filament NbTi/CuMn composite superconductor
[DE90-005387] N90-16570

MAGNETOHYDRODYNAMIC FLOW
User's manual for MGMHD: A multigrid three-dimensional computer code for the analysis of magnetohydrodynamic generators and diffusers
[DE90-004453] N90-16526

MAGNETOHYDRODYNAMIC GENERATORS
Development of a wet vapor homogeneous liquid metal MHD power system
[DE90-001468] N90-16508
MHD Integrated topping cycle project
[DE90-004141] N90-16525
User's manual for MGMHD: A multigrid three-dimensional computer code for the analysis of magnetohydrodynamic generators and diffusers
[DE90-004453] N90-16526

MAGNETOHYDRODYNAMIC STABILITY
MHD stable high beta spheromak equilibrium
[DE90-004873] N90-16529

MAGNETOHYDRODYNAMICS
A brief description of lattice gas models for multiphase flows and magnetohydrodynamics
[DE90-003653] N90-16143
Development of a wet vapor homogeneous liquid metal MHD power system
[DE90-001468] N90-16508
MHD Integrated topping cycle project
[DE90-004141] N90-16525
User's manual for MGMHD: A multigrid three-dimensional computer code for the analysis of magnetohydrodynamic generators and diffusers
[DE90-004453] N90-16526

MAGNETOPLASMADYNAMICS
Design of a thrust stand for high power electric propulsion devices
[NASA-TM-102372] N90-15992

MAIN SEQUENCE STARS
Outflows in high mass star-forming regions
N90-16657

MAINTAINABILITY
The repair of aircraft integral fuel tanks in the RAF: A user's view of fuel tank technology N90-15908
Spray sealing: A breakthrough in integral fuel tank sealing technology N90-15912
Complex availability problems solved with simulation
[DE89-012610] N90-16459

MAINTENANCE
Fuel Tank Technology
[AGARD-R-771] N90-15904
Integral fuel tank sealing practice at British Aerospace (Kingston) N90-15905
The effect of primer age on adhesion of polysulphide sealant N90-15909
Fuel tank explosion protection N90-15914
New optimization techniques in database access and maintenance N90-16586

MAN MACHINE SYSTEMS
Distribution of hardware and software elements in unmanned air vehicle systems N90-15933
Formalisms for user interface specification and design N90-16687

MAN-COMPUTER INTERFACE
User interaction with self-learning systems
[AD-A214280] N90-16395
NASA/ASEE Summer Faculty Fellowship Program
[NASA-CR-166837] N90-16686
Formalisms for user interface specification and design N90-16687

MANAGEMENT
Invention and innovation: Alternative mechanisms for enhancing organizational competitiveness
[DE89-015858] N90-16584

MANAGEMENT METHODS
Discrete event simulation tool for analysis of qualitative models of continuous processing systems
[NASA-CASE-MSC-21465-1] N90-16410
International conference management N90-16583
FY 1989 update to the Information Resources Management review plan
[DE90-004185] N90-16593

MANAGEMENT PLANNING
International conference management N90-16583

MANEUVERABLE REENTRY BODIES
Singular perturbation analysis of AOTV-related trajectory optimization problems
[NASA-CR-186202] N90-15936

MANIFOLDS (MATHEMATICS)
Stochastic action of dynamical systems on curved manifolds. The isokinetic developing map on trajectories
[PREPRINT-666] N90-16466

MANIPULATORS
Bilateral force reflection for teleoperators with masters and slaves with dissimilar and possibly redundant kinematics
[DE90-004392] N90-16132
On-line estimation of mechanical nonlinearities in compliant two-link robot manipulators N90-16280
Examples of robots and teleoperators at the Savannah River Site
[DE90-004659] N90-16284
Mathematical model for adaptive control system of ASEA robot at Kennedy Space Center N90-16701

MANNED ORBITAL LABORATORIES
A modular habitation unit adapted for service in low earth and geostationary earth orbits
[ILR-MITT-217] N90-15990

MANNED SPACE FLIGHT
The Gevaltig: An inertial fusion powered manned spacecraft design for outer solar system missions
[NASA-CR-185163] N90-15985

MANNED SPACECRAFT
Systems interoperability approach Apollo/Soyuz test project N90-15979

MANPOWER
MANPRINT (Manpower and Personnel Integration) evaluation: AN/TRC-170 digital troposcatter radio system
[AD-A211799] N90-16100

MANUALS
Columbus: A user's introduction
[ESA-BR-62] N90-15989

MANUFACTURING
Aircraft fuel tank construction and testing experience N90-15907
Method of making carbon dioxide and chlorine free fluoride-based glass
[AD-D014260] N90-16060

MAP MATCHING GUIDANCE
Navigation up-date using radar mapping: Assessment and optimisation simulation tool N90-15928

MAPPING
Parallel algorithms for interactive manipulation of digital terrain models N90-16445
Scientific investigations of the Space Research Group
[ISBN-0-642-13252-6] N90-16595

MARINE ENVIRONMENTS
Potential impact of stratospheric ozone depletion on marine ecosystems
[PB90-112616] N90-16360

MARINE METEOROLOGY
The chemistry and dynamics of marine stratocumulus N90-16381

MARINE PROPULSION
Copolymers for drag reduction in marine propulsion: New molecular structures with enhanced effectiveness
[AD-A214444] N90-16062

MARKING
Method of marking titanium alloy articles having distinct microstructural regions corresponding to high creep and fatigue resistance
[AD-D014283] N90-16031

MARKOV PROCESSES
The theory of hybrid stochastic algorithms
[DE90-003941] N90-16421

MARS OBSERVER
Mission to Mars. Report of the Mars exploration study team
[ESA-SP-1117] N90-15968

MARS SAMPLE RETURN MISSIONS
Mission to Mars. Report of the Mars exploration study team
[ESA-SP-1117] N90-15968

MARS SURFACE
Mission to Mars. Report of the Mars exploration study team
[ESA-SP-1117] N90-15968

MASS
Mass loss during x ray microanalysis
[DE90-003954] N90-16067
Some theoretical aspects of cold fusion: A report
[DE90-601098] N90-16514

MASS SPECTROMETERS
Performance of an Inductively Coupled Plasma-Mass Spectrometer Analyzer system
[DE90-004002] N90-16025
A double focussing mass-spectrometer for simultaneous ion measurements in the stratosphere
[AERONOMICA-ACTA-A-350-1989] N90-16379
The in-situ cometary particulate size distribution measured for one comet: P/Halley N90-16637

MASS SPECTROSCOPY
Organic chemistry of cometary dust as derived from PUMA 1 data N90-16628
Composition of dust from Comet P/Halley: The mineral fraction N90-16631

MASS TRANSFER
Thermal histories of the samples of two KOSI comet nucleus simulation experiments N90-16645

MASSIVELY PARALLEL PROCESSORS
How to cluster in parallel with neural networks N90-16443
Parallel algorithms for interactive manipulation of digital terrain models N90-16445
Stochastic simulation of charged particle transport on the massively parallel processor N90-16448
Estimating water flow through a hillslope using the massively parallel processor N90-16449
Scan line graphics generation on the massively parallel processor N90-16450
BLITZEN: A highly integrated massively parallel machine N90-16453
A generic fine-grained parallel C N90-16454

MATERIALS HANDLING
Examples of robots and teleoperators at the Savannah River Site
[DE90-004659] N90-16284
Handling and analysis of ices in cryostats and glove boxes in view of cometary samples N90-16643

MATERIALS SCIENCE
Flight experiment hardware for sounding rocket investigations. Materials science and fluid sciences
[ESA-SP-1116] N90-15998

MATHEMATICAL LOGIC
Optimization of monotonic inference algorithms in propositional and first order logic
[LAAS-89204] N90-16436

MATHEMATICAL MODELS
Rotor induced-inflow-ratio measurements and CAMRAD calculations
[NASA-TP-2946] N90-15882
Assessment of computational prediction of tail buffeting
[NASA-TM-101613] N90-15886
Euler and Navier-Stokes computations for two-dimensional geometries using unstructured meshes
[NASA-CR-181977] N90-15893
Automatic control of KKK: Requirements, sensors, actuators, and control performance results N90-15944
The continuous crystallization of sulfur formed by the liquid-phase reaction of hydrogen sulfide and sulfur dioxide
[DE90-003991] N90-16018
Elastic moduli of copper: Electronic structure contributions from pseudopotentials and full-potential linear muffin-tin orbital band structure calculations
[DE90-004423] N90-16037
Modeling dislocation evolution in irradiated alloys
[DE90-004921] N90-16051
Piezoelectric ceramic modeling and characterization at high levels of mechanical activity
[ISAL-89-0030] N90-16074
On averaged force acting on a particle in HF electromagnetic field
[DE90-600984] N90-16109
A brief description of lattice gas models for multiphase flows and magnetohydrodynamics
[DE90-003653] N90-16143
Vorticity amplification in nonorthogonal stagnation flow N90-16152
Calculation of turbulent choppy flow mixing
[ETN-90-95929] N90-16165
Grid-independent wall layer turbulence model for complex flow calculations
[DE90-003500] N90-16200
Improved solution techniques for the eigenstructure of fractional order systems
[AD-A213844] N90-16295

Analysis of nonlinear systems using ARMA (Autoregressive Moving Average) models
[DE90-002395] N90-16297
Integrated geodetic network analysis with stochastic prior information about the gravity field and reference ellipsoid
[SER-C-351] N90-16317
Some considerations on resource evaluation of The Geysers
[DE90-002119] N90-16343
Mesoscale analysis by numerical modelling coupled with satellite-based sounding N90-16370
Diagnostic and kinematic fields associated with curved and straight jet streaks using a two-layer primitive equation model N90-16371
Terrestrial magnetosphere magnetic field models
[REPT-89/CT/DTI/MS/AS/154] N90-16380
Stochastic model of the NASA/MSFC ground facility for large space structures with uncertain parameters: The maximum entropy approach, part 2
[NASA-CR-186009] N90-16407
Discrete event simulation tool for analysis of qualitative models of continuous processing systems
[NASA-CASE-MSC-21465-1] N90-16410
Dissipation mechanism of the large-amplitude collective motion. Dynamical evolution of a collective bundle of trajectories in the TDHF phase space for a simple soluble model
[DE90-719557] N90-16477
On the observation of a transition from fusion to multifragmentation in high multiplicity O16 induced reactions
[LUIP-8812] N90-16481
Development of a wet vapor homogeneous liquid metal MHD power system
[DE90-001468] N90-16508
Fracto-fusion. Mechanism of cold fusion
[DE90-719573] N90-16518
Continuous spontaneous reduction model involving gravity
[DE90-600730] N90-16573
Modeling the near acoustic field of a rocket during launch N90-16694
Mathematical model for adaptive control system of ASEA robot at Kennedy Space Center N90-16701

MATRICES (MATHEMATICS)
An algorithm to compute the square root of 3x3 positive definite matrix
[DE89-635711] N90-16417
Asymptotically fast triangularization of matrices over rings
[DE90-003161] N90-16471

MATTER (PHYSICS)
The use of hypervelocity launchers to explore previously inaccessible states of matter
[DE90-004088] N90-15973

MAXIMUM ENTROPY METHOD
Stochastic model of the NASA/MSFC ground facility for large space structures with uncertain parameters: The maximum entropy approach, part 2
[NASA-CR-186009] N90-16407

MAXWELL EQUATION
Production of photons in anisotropic spacetimes
[DE90-600760] N90-16576

MEASURING INSTRUMENTS
Calibration of a pulsed potential crack monitor for use in fatigue crack growth studies
[RAE-TM-M/S-1126] N90-16301
Surface topography measurements over the 1 meter to 10 micrometer spatial period bandwidth
[DE90-003642] N90-16501
On gauge fixing and quantization of constrained Hamiltonian systems
[DE90-600732] N90-16574

MECHANICAL DRIVES
Assessment of worm gearing for helicopter transmissions
[NASA-TM-102441] N90-15923
Continuously variable gear drive transmission
[AD-D014268] N90-16275

MECHANICAL PROPERTIES
Spray sealing: A breakthrough in integral fuel tank sealing technology N90-15912
Cryogenic engineering and materials N90-15949
Materials and techniques for model construction N90-15954
The use of hypervelocity launchers to explore previously inaccessible states of matter
[DE90-004088] N90-15973
Structure-property relationships in ion-beam surface-modified ceramics: Theory and applications
[AD-A212785] N90-16054
Interdisciplinary research in viscoelasticity and rheology
[AD-A213630] N90-16145
Absorption fluids data survey: 1989 update
[DE90-003985] N90-16346

MELT SPINNING
High temperature aluminum-base alloy
[AD-D014270] N90-16028

MELTING
Production and processing of Cu-Cr-Nb alloys
[NASA-TM-102495] N90-16053

MEMBRANES
Using inorganic membranes to separate gases: R and D status review
[DE90-004386] N90-16019
Study of silicon nitride pH response to the fabrication of microelectronic sensors
[LAAS-89229] N90-16023
Silicon membrane formation
[DE90-003022] N90-16064

MEMORY (COMPUTERS)
Bus programmable slave module
[NASA-CASE-MSC-21387-1] N90-16411

MERCURY CADMIUM TELLURIDES
Resonance enhanced Raman studies of as-grown and laser-processed HgCdTe
[AD-A213855] N90-16540

MESOSCALE PHENOMENA
Mesoscale analysis by numerical modelling coupled with satellite-based sounding N90-16370
A dynamic model for forecasting new cloud development
[AD-A213939] N90-16383
Some properties of so-called magnetic cloud structures in the solar wind
[IFSI-88-16] N90-16678

MESSAGE PROCESSING
A 3-D measurement system using object-oriented FORTH
[DE90-003393] N90-16420

METAL BONDING
Fatigue and impact strength of diffusion bonded titanium alloy joints
[RAE-TM-MAT/STR-1123] N90-16043

METAL FATIGUE
Method to produce titanium alloy articles with high fatigue and fracture resistance
[AD-D014278] N90-16029
Method of marking titanium alloy articles having distinct microstructural regions corresponding to high creep and fatigue resistance
[AD-D014283] N90-16031

METAL IONS
Broad-beam multi-ampere metal ion source
[DE90-003106] N90-16123

METAL SURFACES
The effect of primer age on adhesion of polysulphide sealant N90-15909
Selectivity of the reactions of oxygenates on transition metal surfaces
[DE90-003911] N90-16040
Solid state, surface, and catalytic studies of oxides
[DE90-004850] N90-16566

METAL VAPORS
Metal vaporisers: Bicentennial series of five historical monographs
[ISBN-0-642-13584-3] N90-16081

METALLIC GLASSES
Method of making carbon dioxide and chlorine free fluoride-based glass
[AD-D014260] N90-16060

METALLIC PLASMAS
Plasmon excitation in the scattering of electromagnetic waves from good conductors
[AD-A214026] N90-16107

METALS
Fuel resistant coatings for metal and composite fuel tanks N90-15911
Metals and Ceramics Division Materials Sciences Program
[DE90-004371] N90-16070

METAMORPHISM (GEOLOGY)
Metamorphism of cosmic dust: Processing from circumstellar outflows to the cometary regolith N90-16641

METASTABLE STATE
Rotational energy transfer in metastable states of heteronuclear molecules
[AD-A214425] N90-16485

METEORITES
The carbon chemistry of meteorites: Relationships to comets N90-16615
Evolution of carbonaceous chondrite parent bodies: Insights into cometary nuclei N90-16638
Isotopic microanalysis of returned comet nucleus samples N90-16655

METEORITIC COMPOSITION
Identification of solar nebula condensates in interplanetary dust particles and unequilibrated ordinary chondrites N90-16629
Composition of dust from Comet P/Halley: The mineral fraction N90-16631
The comet rendezvous asteroid flyby mission N90-16639

METEOROLOGICAL PARAMETERS
Climatic summaries and documentation for the primary meteorological Station, H. J. Andrews Experimental Forest, 1972 to 1984
[PB90-104373] N90-16382

METEOROLOGICAL SATELLITES
Polar cusps latitudinal shift and its relation to the IMF-By component
[IFSI-88-14] N90-16377
World Weather Watch. Global observing system-satellite sub-system. Information on meteorological and other environmental satellites, second edition
[WMO-411-ED-2] N90-16386

METEOROLOGY
Backscattering effects in DIAL due to water vapor
[SER-WISS-ABHANDL-89] N90-16265
The Interactive System Meteorology and its use in meteorology and oceanography N90-16320
Guide on the global observing system
[WMO-488-REV] N90-16385
Rocket-triggered lightning strikes and forest fire ignition N90-16690

METEOSAT SATELLITE
Proposed concept for the visible/infrared imaging radiometer for second generation Meteosat
[ETN-90-96145] N90-16503

METHANE
Solid-state electrolyte catalysis for methane and oxygen synthesis
[PB90-100231] N90-16011
Mechanisms of the electrochemistry of small organic molecules
[PB90-100785] N90-16012

METHYL ALCOHOL
Results from the third year of operation of the Federal Methanol Fleet at Lawrence Berkeley Laboratory
[DE90-003306] N90-16277

METRIC SPACE
How to cluster in parallel with neural networks N90-16443

METROLOGY
Activities report of the National Electrotechnic Institute Galileo Ferraris
[ETN-90-96178] N90-16705

MICROANALYSIS
Mass loss during x ray microanalysis
[DE90-003954] N90-16067
Workshop on Analysis of Returned Comet Nucleus Samples
[NASA-CR-184821] N90-16607
Trace element abundance determinations by Synchrotron X Ray Fluorescence (SXRF) on returned comet nucleus mineral grains N90-16619
Analysis of particulates of comet nucleus samples: Possible use of olivine as indicator phase N90-16646
Non-destructive trace element microanalysis of as-received cometary nucleus samples using synchrotron x ray fluorescence N90-16649
Isotopic microanalysis of returned comet nucleus samples N90-16655
The measurement of trace elements in interplanetary dust and cometary particles by ultra-high sensitivity INAA N90-16656

MICROCOMPUTERS
Digital system for monitoring and controlling remote processes
[DE90-003935] N90-16094

MICROELECTRONICS
Study of silicon nitride pH response to the fabrication of microelectronic sensors
[LAAS-89229] N90-16023

MICROMECHANICS
Probabilistic simulation of uncertainties in composite uniaxial strengths
[NASA-TM-102483] N90-16008
Effects of high rate shear on the microstructure and deformation and fracture behavior of two high strength steels
[AD-A214107] N90-16032

MICROPARTICLES
Study of phase transformations liquid-solid-solid of ultrafine particles
[ISAL-89-0019] N90-16022
From interstellar dust to comets N90-16620

MICROSTRIP TRANSMISSION LINES
Stripline feed for a microstrip array of patch elements with teardrop shaped probes
[NASA-CASE-NPO-17548-1-CU] N90-16104

MICROSTRUCTURE
The structure of silica-polysiloxane composites and its effects on their elastomeric properties
[DE89-014768] N90-16005
Method to produce titanium alloy articles with high fatigue and fracture resistance
[AD-D014278] N90-16029
Method for refining microstructures on prealloyed titanium powder compacts
[AD-D014280] N90-16030
Method of marking titanium alloy articles having distinct microstructural regions corresponding to high creep and fatigue resistance
[AD-D014283] N90-16031
Effects of high rate shear on the microstructure and deformation and fracture behavior of two high strength steels
[AD-A214107] N90-16032
Interplanar spacing for various phases in austenitic stainless steels
[DE90-602350] N90-16038
Microstructural explanation for irradiation embrittlement of V-15Cr-5Ti
[DE90-004112] N90-16041
Phase evolution during neutron irradiation of commercial Fe-Cr-Mn alloys
[DE90-004113] N90-16042
Selection of corrosion-resistant materials for use in molten nitrate salts
[DE90-004351] N90-16048
Effect of carbon on ion beam mixing of Fe-Ti bilayers
[DE90-003650] N90-16056
Proposal for a study of laser acceleration of electrons using micrograting structures at ATF
[DE90-003699] N90-16262
Anisotropy and microstructure of high coercivity rare earth iron permanent magnets, list of papers published
[AD-A214160] N90-16476
Development of low density silica aerogel as a capture medium for hyper-velocity particles
[NASA-CR-185930] N90-16489
Microstructures of Y123 films on SrTiO3, LaGaO3, and LaAlO3
[DE90-003367] N90-16537
Direct determination of the morphology, structure and composition of cometary and interstellar ice analogs in the laboratory N90-16612
Mechanical and SEM analysis of artificial comet nucleus samples N90-16650

MICROWAVE FREQUENCIES
Helsinki University of Technology Radio Laboratory
[PB90-110677] N90-16102

MICROWAVE IMAGERY
Laboratory of Space Technology
[PB90-110651] N90-15967

MICROWAVE POWER BEAMING
Theoretical and experimental investigation of axial power extraction from a magnetically insulated transmission line oscillator
[DE90-003486] N90-16131

MICROWAVES
Helsinki University of Technology Radio Laboratory
[PB90-110677] N90-16102
Reflection from layered media with special attention to the microwave region
[ESA-TT-1155] N90-16111
Microwave screening on digital radio communication links due to multicircuit power transmission lines
[DE90-734950] N90-16118
Mechanisms of microwave induced damage in biologic materials
[AD-A213480] N90-16390

MILITARY TECHNOLOGY
Tactical UK military satellite ground terminals: A research and development review
[RSRE-MEMO-4262] N90-15972

MILLIMETER WAVES
Helsinki University of Technology Radio Laboratory
[PB90-110677] N90-16102
Low-altitude millimeter-wave propagation in the evaporation duct
[AD-A214432] N90-16108
The physical foundations of radiometry and their applications in the mm-waveband
[REPT-12-88] N90-16114
Outflows in high mass star-forming regions N90-16657

MIMD (COMPUTERS)
The 2nd Symposium on the Frontiers of Massively Parallel Computations
[NASA-TM-101918] N90-16442
Dynamically allocating sets of fine-grained processors to running computations N90-16447

MINERALOGY
Composition of dust from Comet P/Halley: The mineral fraction N90-16631
Methods for the mineralogical and textural analysis of comet nucleus samples N90-16648

MINIATURIZATION
Miniature laser Doppler anemometer with a diode laser
[ISL-CO-224/88] N90-16232

MIRROR FUSION
Spectroscopic diagnostics of high temperature plasmas
[DE90-003912] N90-16522

MIRRORS
Material responses to incident x rays
[DE89-015366] N90-16305
Surface topography measurements over the 1 meter to 10 micrometer spatial period bandwidth
[DE90-003642] N90-16501

MISSILE CONTROL
Navigation up-date using radar mapping: Assessment and optimisation simulation tool N90-15928

MISSILE SYSTEMS
Complex availability problems solved with simulation
[DE89-012610] N90-16459

MISSILES
Weapon aerodynamics overview
[RAE-TM-AERO-2150] N90-15888
Navigation of autonomous air vehicles by passive imaging sensors N90-15927
Tracking flares
[ISBN-0-642-13583-5] N90-16080

MISSION PLANNING
Mirach 100 flight control system N90-15926
An intelligence-driven RPV mission planner N90-15932
Distribution of hardware and software elements in unmanned air vehicle systems N90-15933
Experiment facilities for materials and fluid sciences embarked on Eureca-1
[ESA-SP-1118] N90-16088

MIXED CRYSTALS
Thermodynamic studies on the ferroelectric phase transition in neutron irradiated (Li(sub x)K(1-x))2SO4 crystals at high temperature
[DE89-635766] N90-16545

MIXING
Swirl-stabilized flames: Fluid dynamics, mixing, and flame stability limits N90-16009
Silicon-based coatings on niobium metal
[DE90-003651] N90-16057

MIXTURES
Alcohol and blends as motor fuels
[DE90-003517] N90-16085

MOBILE COMMUNICATION SYSTEMS
Satellite systems integrated with the terrestrial cellular network for mobile communications
[ESA-STR-228] N90-16113

MODAL RESPONSE
Restoring force method and response estimation
[DE90-002394] N90-16463

MODELS
Ion-heated thermal Comptonization models and x ray spectral correlations in active galactic nuclei
[DE90-003597] N90-16667

MODULATION
MT's algorithm: A new algorithm to search for the optimum set of modulation indices for simultaneous range, command, and telemetry
[NASA-CR-186259] N90-16110

MODULES
Conceptual design for the space station Freedom modular combustion facility
[NASA-TM-102037] N90-16087
Bus programmable slave module
[NASA-CASE-MSC-21387-1] N90-16411

MODULUS OF ELASTICITY
Elastic moduli of copper: Electronic structure contributions from pseudopotentials and full-potential linear muffin-tin orbital band structure calculations
[DE90-004423] N90-16037

MOISTURE CONTENT
Thermodynamic analysis of chemical stability of ceramic materials in hydrogen-containing atmospheres at high temperatures
[NASA-CR-4271] N90-16072

MOLECULAR BEAM EPITAXY
Slow positron defect profiling of silicon epilayers
[DE90-003958] N90-16288
Group 2 cubic fluorides as dielectrics for III-V compound semiconductors
[AD-A214096] N90-16542

MOLECULAR BEAMS
Lecture notes on supersonic molecular beam sources
[MPIS-20/1988] N90-16494

MOLECULAR CLOUDS
From interstellar dust to comets N90-16620
Outflows in high mass star-forming regions N90-16657
A computer program to calculate the population numbers of multi-level species
[IFSI-89-15] N90-16671

MOLECULAR COLLISIONS
Rotational energy transfer in metastable states of heteronuclear molecules
[AD-A214425] N90-16485

MOLECULAR EXCITATION
Rotational energy transfer in metastable states of heteronuclear molecules
[AD-A214425] N90-16485

MOLECULAR STRUCTURE
Carbon-13 nuclear magnetic resonance of heterocyclic salts and its precursors
[DE89-635768] N90-16016
Copolymers for drag reduction in marine propulsion: New molecular structures with enhanced effectiveness
[AD-A214444] N90-16062
Structure-property correlations in the design of organic metals and superconductors: An overview
[DE90-003794] N90-16550
Solid state, surface, and catalytic studies of oxides
[DE90-004850] N90-16566

MOLECULES
Mechanisms of the electrochemistry of small organic molecules
[PB90-100785] N90-16012

MOLTEN SALTS
Selection of corrosion-resistant materials for use in molten nitrate salts
[DE90-004351] N90-16048
Organic cathode for a secondary battery
[NASA-CASE-NPO-17604-1-CU] N90-16124

MOLYBDENUM
Stainless steel passivity
[AD-A214108] N90-16033
An XPS and electrochemical study of the influence of molybdenum and nitrogen on the passivity of austenitic stainless steel
[AD-A214267] N90-16034

MOLYBDENUM OXIDES
Molybdenum disulfide-molybdenum oxide lubricants
[AD-D014253] N90-16059

MOMENT DISTRIBUTION
Force and moment measurements on delta wings in unsteady flow N90-16185

MOMENTUM TRANSFER
The dynamics of dust in planetary magnetospheres N90-16658

MONITORS
Diesel starting system monitor: Prototype development
[DE90-004425] N90-16276
Keeping the pilot in the loop
[RAE-TM-FM-18] N90-16396
Cosmic ray NM-64 neutron monitor data 16
[IFSI-88-21] N90-16684

MONTE CARLO METHOD
Probabilistic simulation of uncertainties in composite uniaxial strengths
[NASA-TM-102483] N90-16008
Direct Monte Carlo calculations on expansion wave structure near a wall
[ISL-CO-249/88] N90-16154
The theory of hybrid stochastic algorithms
[DE90-003941] N90-16421
Computer simulation of dust grain evolution N90-16632
Determination of solar flare accelerated ion angular distributions from SMM gamma ray and neutron measurements and determination of the He-3/H ratio in the solar photosphere from SMM gamma ray measurements
[NASA-CR-186038] N90-16676

MORPHOLOGY
Ice floe identification in satellite images using mathematical morphology and clustering about principal curves
[AD-A213854] N90-16311
Effects of ion dose on the morphology and crystallization of amorphous germanium
[DE90-003564] N90-16547
Direct determination of the morphology, structure and composition of cometary and interstellar ice analogs in the laboratory N90-16612

MOSSBAUER EFFECT
Magnetic interactions in Sn-119 substituted for Cu in antiferromagnetic and superconducting lamellar cuprates
[DE90-003661] N90-16560

MOTION SICKNESS
Simulator sickness in the UH-60 (Black Hawk) flight simulator
[AD-A214434] N90-16392

MOTIVATION
A foundation for the design of an astronautics specification system based on dynamic motivation analysis
[ILR-MITT-220] N90-15969
MOTOR VEHICLES
An approach for testing fuel-cell/battery hybrid power sources for bus applications
[DE90-002090] N90-16270
MULTIPHASE FLOW
A brief description of lattice gas models for multiphase flows and magnetohydrodynamics
[DE90-003653] N90-16143
MULTIPOLES
General contraction of Gaussian basis sets. Part 2: Atomic natural orbitals and the calculation of atomic and molecular properties
[NASA-CR-186201] N90-16482
MULTISENSOR APPLICATIONS
Design and implementation of a multi-sensor fusion algorithm on a hypercube computer architecture
[DE90-003682] N90-16438
MUONS
A low-threshold EAS (Extensive-Air-Shower) array for gamma-ray astronomy at Los Alamos
[DE89-016780] N90-16600
Status of the expansion of the CYGNUS array at Los Alamos
[DE89-016781] N90-16601
Relative muon content of UHE showers associated with Hercules X-1
[DE90-000609] N90-16665

N

NAVIER-STOKES EQUATION
Euler and Navier-Stokes computations for two-dimensional geometries using unstructured meshes
[NASA-CR-181977] N90-15893
Numerical analysis of nonstationary fluid flow (a survey)
[PREPRINT-492] N90-16159
Extrapolation techniques for finite element approximations of Stokes and Navier-Stokes flow over a backward facing step
[PREPRINT-499] N90-16160
Decay estimates for the compressible Navier-Stokes equations in the half-space
[PREPRINT-46] N90-16163
Visualization of 2 and 3 dimensional flows
[REPT-1] N90-16164
Calculation of turbulent choppy flow mixing
[ETN-90-95929] N90-16165
NAVIGATION
Mirach 100 flight control system N90-15926
NAVIGATION AIDS
The automatic detection of anti-collision lights
[RSRE-MEMO-4272] N90-15896
NAVSTAR SATELLITES
Dynamic analysis of the geodetic networks originating from the Navstar/Global Positioning System (GPS) satellites
[SER-C-346] N90-16316
NEAR INFRARED RADIATION
Cloud phase discrimination by near-infrared remote sensing N90-16310
Short time scale variability of the BL Lac object OJ 287 in the near-infrared
[IFSI-89-3] N90-16603
NEBULAE
Non-equilibrium chemistry in the solar nebula and early solar system: Implications for the chemistry of comets N90-16618
From interstellar dust to comets N90-16620
Solar nebula condensates and the composition of comets N90-16634
NECK (ANATOMY)
Factor analytic reduction of the carotid-cardiac baroreflex parameters N90-16693
NEODYMIUM LASERS
Eurolaser definition phase: A comparison of high power lasers available
[ETN-90-96061] N90-16268
NEPTUNE (PLANET)
Neptune's Triton: A moon rich in dry ice and carbon
[NASA-CR-186298] N90-16675
NETWORK ANALYSIS
Integrated geodetic network analysis with stochastic prior information about the gravity field and reference ellipsoid
[SER-C-351] N90-16317
NEURAL NETS
Parallel asynchronous systems and image processing algorithms N90-16218
Neural networks for data compression and invariant image recognition N90-16219
Knowledge-based imaging-sensor fusion system N90-16220
Connectionist model-based stereo vision for telerobotics N90-16224
How to cluster in parallel with neural networks N90-16443
NEUROPHYSIOLOGY
High compression image and image sequence coding N90-16214
NEUTRAL BEAMS
In situ measurement of neutral beam components using the Doppler-shifted H(sub alpha) emissions in Heliotron E
[DE90-719521] N90-16516
NEUTRAL PARTICLES
Low energy neutral particle energy analyser by time of flight method
[DE90-719529] N90-16517
NEUTRINOS
Neutrino interactions
[NOTA-INTERNA-934] N90-16495
NEUTRON ACTIVATION ANALYSIS
The measurement of trace elements in interplanetary dust and cometary particles by ultra-high sensitivity INAA N90-16656
NEUTRON COUNTERS
Cosmic ray NM-64 neutron monitor data 16
[IFSI-88-21] N90-16684
NEUTRON DIFFRACTION
High temperature neutron diffraction study of the formation reaction of bismuth superconductors
[DE90-004883] N90-16568
NEUTRON IRRADIATION
Phase evolution during neutron irradiation of commercial Fe-Cr-Mn alloys
[DE90-004113] N90-16042
Fracture toughness of ferritic alloys at very high neutron exposures
[DE90-004519] N90-16046
Thermodynamic studies on the ferroelectric phase transition in neutron irradiated (Li(sub x)K(1-x))2SO4 crystals at high temperature
[DE89-635786] N90-16545
NEUTRONS
Isotope driven critical scattering and phase separation from mixtures of deuterated and protonated polymers
[DE90-003976] N90-16076
Neutron experiments on high-temperature superconductors
[DE90-003978] N90-16559
NICKEL
Theoretical studies of chemisorption and surface reactions on nickel and silicon
[DE90-004849] N90-16050
NICKEL COMPOUNDS
New electrically conducting solids based on nickel(II) - bis(1,3-dithiole-2-thione-4,5-diselenolate)
[DE90-003788] N90-16020
NICKEL ISOTOPES
Cosmic ray half life of Ni-56
[DE90-000132] N90-16680
NICKEL ZINC BATTERIES
Cycle-life improvement of Zn/NiOOH cells by the addition of Ca(OH)2 to the zinc electrode
[DE90-004040] N90-16139
NIOBIUM
Silicon-based coatings on niobium metal
[DE90-003651] N90-16057
NIOBIUM ALLOYS
Production and processing of Cu-Cr-Nb alloys
[NASA-TM-102495] N90-16053
Properties and design of multifilamentary NbTi composite superconductors
[DE90-004904] N90-16569
NIOBIUM ISOTOPES
Determination of hyperfine structures and Rydberg convergence limits of selected optical transitions in Nb-93 using resonance ionization spectroscopy
[PB90-110719] N90-16498
NITRATES
Selection of corrosion-resistant materials for use in molten nitrate salts
[DE90-004351] N90-16048
NITRIDING
An XPS and electrochemical study of the influence of molybdenum and nitrogen on the passivity of austenitic stainless steel
[AD-A214267] N90-16034
NITROGEN
Stainless steel passivity
[AD-A214108] N90-16033
An XPS and electrochemical study of the influence of molybdenum and nitrogen on the passivity of austenitic stainless steel
[AD-A214267] N90-16034
Characterization of B and N implanted fused silica
[DE90-004198] N90-16069
NITROGEN FLUORIDES
Synthesis of tetrafluorohydrazine
[AD-D014281] N90-16083
NITROGEN POLYMERS
Synthesis and analysis of novel polymers with potential for providing both high permselectivity and permeability in gas separation applications
[DE90-003907] N90-16065
NOAA SATELLITES
Determination of optical porperties of clouds from NOAA-AVHRR data using Apollo N90-16321
NOISE MEASUREMENT
Multisqueezing of mechanical states and back-action evasion measurements
[IFSI-89-6] N90-16504
NONCONDENSABLE GASES
Experimental investigation of condensation of steam in the presence of noncondensable gases for open-cycle surface condensers
[DE90-003552] N90-16353
NONDESTRUCTIVE TESTS
Assessment of strength limiting flaws in ceramic heat exchanger components
[DE90-004086] N90-16077
Slow positron defect profiling of silicon epilayers
[DE90-003958] N90-16288
Theoretical study on creep damage detection by ultra-sonic wave measurement
[DE90-702472] N90-16290
Prompt Gamma Activation Analysis (PGAA): Technique of choice for nondestructive bulk analysis of returned comet samples N90-16633
Non-destructive trace element microanalysis of as-received cometary nucleus samples using synchrotron x ray fluorescence N90-16649
NONEQUILIBRIUM CONDITIONS
Non-equilibrium chemistry in the solar nebula and early solar system: Implications for the chemistry of comets N90-16618
NONLINEAR EQUATIONS
Interdisciplinary research in viscoelasticity and rheology
[AD-A213630] N90-16145
Hidden regularity for a strongly nonlinear wave equation
[DE90-600742] N90-16465
NONLINEAR EVOLUTION EQUATIONS
A space-time discretization procedure for wave propagation problems
[NASA-TM-102215] N90-16399
NONLINEAR SYSTEMS
Element-by-element preconditioning techniques for large-scale, vectorized finite element analysis in nonlinear solid and structural mechanics N90-16291
NONLINEARITY
Soft modes, freezing, and nonlinear response of a dipolar glass
[DE90-003647] N90-16075
Numerical simulation of the nonlinear evolution of a perturbation in a three dimensional boundary layer N90-16173
On-line estimation of mechanical nonlinearities in compliant two-link robot manipulators N90-16280
NORMALIZING
Simple proof of renormalization group equation in the minimal subtraction scheme
[DE90-600758] N90-16457
NORTHERN HEMISPHERE
Multiple flow regimes in the Northern Hemisphere winter N90-16372
NOVAE
Recent and future x ray observations of classical novae during the outburst stage
[MPE-PREPRINT-159] N90-16606
NOZZLE DESIGN
Space shuttle Production Verification Motor 1 (PV-1) static fire
[NASA-CR-183784] N90-15991
NUCLEAR BINDING ENERGY
Theoretical investigations of the structures and binding energies of Be(sub n) and Mg(sub n) (n = 3-5) clusters
[NASA-TM-101931] N90-16483
NUCLEAR ENGINE FOR ROCKET VEHICLES
Dynamics analyses of space power systems using the salt code
[DE90-002274] N90-15995
NUCLEAR FUEL ELEMENTS
Scaling study for SP-100 reactor technology
[NASA-TM-897140] N90-16496

NUCLEAR FUSION
Toroidal magnetic fields in terms of field-line invariants
[DE89-016610] N90-16507
Near-term directions in the world stellarator program
[DE90-004381] N90-16511
Theoretical study of cold nuclear fusion using barrier penetration approach
[DE90-601096] N90-16513
Fracto-fusion. Mechanism of cold fusion
[DE90-719573] N90-16518
Lower limit for the average angular momentum leading to fusion
[DE90-004027] N90-16523
Gamma-ray observations and the distribution of interstellar aluminum-26 N90-16661
Nuclear reaction uncertainties in standard and non-standard cosmologies
[DE90-003594] N90-16666
Determination of solar flare accelerated ion angular distributions from SMM gamma ray and neutron measurements and determination of the He-3/H ratio in the solar photosphere from SMM gamma ray measurements
[NASA-CR-186038] N90-16676
NUCLEAR MAGNETIC RESONANCE
Carbon-13 nuclear magnetic resonance of heterocyclic salts and its precursors
[DE89-635768] N90-16016
NUCLEAR MEDICINE
Coded-aperture imaging in nuclear medicine N90-16208
NUCLEAR REACTIONS
Theoretical study of cold nuclear fusion using barrier penetration approach
[DE90-601096] N90-16513
Some theoretical aspects of cold fusion: A report
[DE90-601098] N90-16514
Fracto-fusion. Mechanism of cold fusion
[DE90-719573] N90-16518
NUCLEAR REACTORS
The Gevaltig: An inertial fusion powered manned spacecraft design for outer solar system missions
[NASA-CR-185163] N90-15985
Nuclear reaction uncertainties in standard and non-standard cosmologies
[DE90-003594] N90-16666
NUCLEAR STRUCTURE
Heavy ion inelastic scattering with a 4(pi) gamma detector
[DE90-002709] N90-16488
Theoretical aspects of electroweak and other interactions in medium energy nuclear physics
[DE90-004015] N90-16493
NUCLEATION
Study of phase transformations liquid-solid-solid of ultrafine particles
[ISAL-89-0019] N90-16022
NUCLEI
Q-2 and A dependence of delta (1232) electroexcitation in nuclei
[DE90-003470] N90-16492
NUCLEONS
Theoretical aspects of electroweak and other interactions in medium energy nuclear physics
[DE90-004015] N90-16493
NUCLIDES
Cosmogenic nuclides in cometary materials: Implications for rate of mass loss and exposure history N90-16623
Measurements of long-lived cosmogenic nuclides in returned comet nucleus samples N90-16640
NUMERICAL ANALYSIS
Improved tangent-cone method for the Aerodynamic Preliminary Analysis System (APAS) version of the hypersonic arbitrary-body program
[NASA-TM-4165] N90-15890
A physical and numerical study of the turn-off behavior of bipolar power transistors
[LAAS-89185] N90-16136
A numeric analysis of incompressible, viscous flow around a symmetrical body of revolution
[ISL-CO-215/87] N90-16157
Two possible configurations for the top-hat electrostatic analyzer: A numerical study
[IFSI-88-18] N90-16229
NUMERICAL CONTROL
D3-D cryogenic control system upgrade
[DE90-003290] N90-16092
Diesel starting system monitor: Prototype development
[DE90-004425] N90-16276
Bus programmable slave module
[NASA-CASE-MSC-21387-1] N90-16411
NUMERICAL INTEGRATION
Numerical boundary layer calculations on the DFVLR ellipsoid of revolution N90-16193

O

O RING SEALS
Space shuttle Production Verification Motor 1 (PV-1) static fire
[NASA-CR-183784] N90-15991
O STARS
The upper main sequence of OB associations. Part 2: The single-lined O stars: Spectral classification of northern stars and lines of C and N
[SER-C-PREPUBL-FASC-39] N90-16602
OBJECT PROGRAMS
A 3-D measurement system using object-oriented FORTH
[DE90-003393] N90-16420
OBLIQUE SHOCK WAVES
Flow separation in shock wave boundary layer interactions at hypersonic speeds
[NASA-CR-4274] N90-15885
OCEAN BOTTOM
ZBTAB: Zenith-248 version of BLUGTAB
[AD-A214279] N90-16415
OCEAN THERMAL ENERGY CONVERSION
Conceptual design analysis for hybrid-cycle OTEC plants for co-production of electric power and desalinated water
[DE90-003551] N90-16350
OCEANOGRAPHIC PARAMETERS
ZBTAB: Zenith-248 version of BLUGTAB
[AD-A214279] N90-16415
OCEANOGRAPHY
The Interactive System Meteorology and its use in meteorology and oceanography N90-16320
OCEANS
Multiple flow regimes in the Northern Hemisphere winter N90-16372
OLIVINE
Analysis of particulates of comet nucleus samples: Possible use of olivine as indicator phase N90-16646
ON-LINE SYSTEMS
On-line chemical composition analyzer development
[DE90-004079] N90-16026
On-line estimation of mechanical nonlinearities in compliant two-link robot manipulators N90-16280
OORT CLOUD
Physical processing of cometary nuclei N90-16653
OPACITY
Development of low density silica aerogel as a capture medium for hyper-velocity particles
[NASA-CR-185930] N90-16489
OPEN CLUSTERS
The upper main sequence of OB associations. Part 2: The single-lined O stars: Spectral classification of northern stars and lines of C and N
[SER-C-PREPUBL-FASC-39] N90-16602
OPERATING COSTS
The Kryo-Kanal Koeln (KKK): Description of the tunnel conversion. Thermal insulation, instrumentation, operational experience, test results and operating costs N90-15943
OPERATOR PERFORMANCE
User interaction with self-learning systems
[AD-A214280] N90-16395
OPTICAL COMMUNICATION
OPFET (Optical Field-Effect Transistor) demodulator-downconverter for detecting microwave modulated optical signals
[AD-D014294] N90-16128
OPTICAL COUNTERMEASURES
Defense to laser light irradiation
[AD-D014286] N90-15984
OPTICAL EQUIPMENT
Instrumentation for cryogenic wind tunnels N90-15950
Flow visualization in the cryogenic wind tunnel N90-15953
Analysis and evaluation of technical data on the photochromic and non-linear optical properties of materials
[AD-A214050] N90-16014
Reflectometers
[AD-D014249] N90-16499
Surface topography measurements over the 1 meter to 10 micrometer spatial period bandwidth
[DE90-003642] N90-16501
OPTICAL HETERODYNING
Distance measurement using laser diodes
[ETN-90-96144] N90-16264
OPTICAL PROPERTIES
Design, characterization, and optical properties of phosphazene-based polymers
[DE90-004111] N90-16068
Determination of optical porperties of clouds from NOAA-AVHRR data using Apollo N90-16321
Eurolaser. High power excimer laser: Optical crystals
[ETN-90-95901] N90-16558
Lithium cobalt oxide thin film and its electrochromism
[DE90-004570] N90-16564
OPTICAL RADAR
The lidar experiment at Andoya, Norway, during the Summer of 1988
[BONN-IR-89-16] N90-16117
Backscattering effects in DIAL due to water vapor
[SER-WISS-ABHANDL-89] N90-16265
Lidar technique for adjusting aerosol model number densities to existing conditions
[AD-A213846] N90-16374
OPTICAL REFLECTION
Forest mapping Nuerenberg German national forest with special emphasis on the spectral reflection behavior of pine trees N90-16328
OPTIMAL CONTROL
The algebraic Riccati equation and singular optimal control
[MEMO-COSOR-89-11] N90-16467
OPTIMIZATION
Synthesis of control law, on a RPV, in order to minimize the number of sensors N90-15925
Built in test of folded PLAs
[IMAG-RR-758-I] N90-16134
Plume shape optimization of small attitude control thrusters with respect to impingement and thrust
[ISL-CO-220/88] N90-16153
Mechanoelectric conversion by uniaxial constraint in piezoelectric generators: Optimization of electrical, mechanical, and physico-chemical parameters of materials
[ISAL-89-0020] N90-16235
Optimization of monotonic inference algorithms in propositional and first order logic
[LAAS-89204] N90-16436
Optimal step sizes in semi-stochastic approximation procedures
[ETN-90-95888] N90-16469
Enhanced performance IR focal plane arrays using adaptive subtraction
[RSRE-MEMO-4286] N90-16502
Near-term directions in the world stellarator program
[DE90-004381] N90-16511
MHD stable high beta spheromak equilibrium
[DE90-004873] N90-16529
New optimization techniques in database access and maintenance N90-16586
Event-join optimization in temporal relational databases
[DE90-003117] N90-16588
OPTOELECTRONIC DEVICES
Characterization of B and N implanted fused silica
[DE90-004198] N90-16069
ORBIT PERTURBATION
On mean elements for satellite orbits perturbed by the zonal harmonics of the geopotential
[RAE-TM-SPACE-371] N90-15971
ORBIT TRANSFER VEHICLES
Singular perturbation analysis of AOTV-related trajectory optimization problems
[NASA-CR-186202] N90-15936
ORDER-DISORDER TRANSFORMATIONS
Contribution to the study of order effects in the Ising model framework: Ground states and phase diagrams
[ESA-TT-1118] N90-16557
ORGANIC CHEMISTRY
Organic chemistry of cometary dust as derived from PUMA 1 data N90-16628
ORGANIC COMPOUNDS
Mechanisms of the electrochemistry of small organic molecules
[PB90-100785] N90-16012
Organic cathode for a secondary battery
[NASA-CASE-NPO-17604-1-CU] N90-16124
Analysis of organic compounds in returned comet nucleus samples N90-16617
ORGANIC MATERIALS
Ion bombardment experiments suggesting an origin for organic particles in pre-cometary and cometary ices N90-16652
Refractory solids in chondrites and comets: How similar N90-16654
ORGANIC SULFUR COMPOUNDS
New electrically conducting solids based on nickel(II) - bis(1,3-dithiole-2-thione-4,5-diselenolate)
[DE90-003788] N90-16020
ORGANOMETALLIC POLYMERS
Porous ceramic bodies
[AD-D014277] N90-16061
OROGRAPHY
The effect of orographic forcing on the mean flow of the stratosphere N90-16367

ORTHOGONAL FUNCTIONS
Vorticity amplification in nonorthogonal stagnation flow N90-16152

OSCILLATIONS
Neutrino oscillations: An essay in honor of Felix Boehm
[DE90-003223] N90-16491

OSCILLATORS
Theoretical and experimental investigation of axial power extraction from a magnetically insulated transmission line oscillator
[DE90-003486] N90-16131

OVER-THE-HORIZON RADAR
The development of over-the-horizon radar in Australia
[ISBN-0-642-13561-4] N90-16099

OXIDATION
Comprehensive mechanisms for combustion chemistry: An experimental and numerical study with emphasis on applied sensitivity analysis
[DE90-003904] N90-16017
Solid state, surface, and catalytic studies of oxides
[DE90-004850] N90-16566

OXIDATION-REDUCTION REACTIONS
Electrochemical parameterization of metal complex redox potentials, using the ruthenium(III)/ruthenium(II) couple to generate a ligand electrochemical series
[AD-A214439] N90-16015
Kinetics of the graphite/oxygen reaction in the in-pore diffusion controlled regime. Part 3: Influence of boundary layer diffusion in kinetic experiments at temperatures 970K to 1170K
[JUEL-2284-PT-3] N90-16024

OXIDE FILMS
Lithium cobalt oxide thin film and its electrochromism
[DE90-004570] N90-16564
Solid state, surface, and catalytic studies of oxides
[DE90-004850] N90-16566

OXYGEN
Solid-state electrolyte catalysis for methane and oxygen synthesis
[PB90-100231] N90-16011
Effects of gravity waves on the polar O2 and OH airglow N90-16373
Computation of the unsteady facilitated transport of oxygen in hemoglobin
[NASA-TM-102251] N90-16400
The effects of oxygen and strontium vacancies on the superconductivity of single crystals of Bi2Sr(2-x)CuO(6-y)
[DE90-004242] N90-16561
Electron beam induced oxygen in YBa2Cu3O(7-x) superconductors
[DE90-004839] N90-16565

OXYGEN ISOTOPES
On the observation of a transition from fusion to multifragmentation in high multiplicity O16 induced reactions
[LUIP-8812] N90-16481

OXYGENATION
Selectivity of the reactions of oxygenates on transition metal surfaces
[DE90-003911] N90-16040

OZONE
ECC (Electrochemical Concentration Cell) ozonesonde observations at Mirny, Antarctica, during 1988
[PB90-113960] N90-16357
Operational ozone monitoring with the Global Ozone Monitoring Radiometer (GOMR)
[PB90-114034] N90-16359
Environmental, health, and CFC substitution aspects of the ozone depletion issue
[DE90-004404] N90-16363
The chemistry and dynamics of marine stratocumulus N90-16381

OZONE DEPLETION
ECC (Electrochemical Concentration Cell) ozonesonde observations at South Pole, Antarctica, during 1988
[PB90-110172] N90-16355
Scientific linkages in global change
[PB90-112608] N90-16356
Potential impact of stratospheric ozone depletion on marine ecosystems
[PB90-112616] N90-16360
Environmental, health, and CFC substitution aspects of the ozone depletion issue
[DE90-004404] N90-16363

OZONOMETRY
Operational ozone monitoring with the Global Ozone Monitoring Radiometer (GOMR)
[PB90-114034] N90-16359

P

PAINTS
Electrical characteristics measurements for the TSS-1 satellite painting
[IFSI-89-7] N90-15987
Ultrasonic assisted paint removal method
[AD-D014264] N90-16479

PAIR PRODUCTION
Production of photons in anisotropic spacetimes
[DE90-600760] N90-16576

PARABOLOID MIRRORS
Reflectometers
[AD-D014249] N90-16499

PARALLEL PROCESSING (COMPUTERS)
PVM (Parallel Virtual Machine): A framework for parallel distributed computing
[DE90-004390] N90-16403
The 2nd Symposium on the Frontiers of Massively Parallel Computations
[NASA-TM-101918] N90-16442
How to cluster in parallel with neural networks N90-16443
Overview and extensions of a system for routing directed graphs on SIMD architectures N90-16444
Parallel algorithms for interactive manipulation of digital terrain models N90-16445
Sort computation N90-16446
Stochastic simulation of charged particle transport on the massively parallel processor N90-16448
Estimating water flow through a hillslope using the massively parallel processor N90-16449
Scan line graphics generation on the massively parallel processor N90-16450
BLITZEN: A highly integrated massively parallel machine N90-16453
A generic fine-grained parallel C N90-16454
On the efficient exploitation of speculation under data flow paradigms of control
[AD-A214112] N90-16455

PARALLEL PROGRAMMING
Design and implementation of a multi-sensor fusion algorithm on a hypercube computer architecture
[DE90-003682] N90-16438

PARALLELEPIPEDS
FRAC-IN-THE-BOX utilization
[DE90-003648] N90-16412

PARTICLE ACCELERATION
Proposal for a study of laser acceleration of electrons using micrograting structures at ATF
[DE90-003699] N90-16262
Possible measurement of the gravitational acceleration of molecules, atoms, nuclei, elementary particles, and antiparticles
[DE90-719559] N90-16490
Fracto-fusion. Mechanism of cold fusion
[DE90-719573] N90-16518
Determination of solar flare accelerated ion angular distributions from SMM gamma ray and neutron measurements and determination of the He-3/H ratio in the solar photosphere from SMM gamma ray measurements
[NASA-CR-186038] N90-16676

PARTICLE ACCELERATOR TARGETS
Lower limit for the average angular momentum leading to fusion
[DE90-004027] N90-16523

PARTICLE COLLISIONS
On the observation of a transition from fusion to multifragmentation in high multiplicity O16 induced reactions
[LUIP-8812] N90-16481

PARTICLE ENERGY
Low energy neutral particle energy analyser by time of flight method
[DE90-719529] N90-16517

PARTICLE INTERACTIONS
Neutrino interactions
[NOTA-INTERNA-934] N90-16495
Proceedings of the 23rd Annual Seminar on Theoretical Physics
[DE90-601827] N90-16577

PARTICLE MASS
An estimation of the one-loop mass shifts in open superstring theory
[DE90-719578] N90-16582
Trajectory-capture cell instrumentation for measurement of dust particle mass, velocity and trajectory, and particle capture N90-16644

PARTICLE SIZE DISTRIBUTION
Study of phase transformations liquid-solid-solid of ultrafine particles
[ISAL-89-0019] N90-16022
Development of an elastomeric additive to improve the impact resistance of unsaturated polyester networks
[ISAL-89-0006] N90-16073

PARTICLE TRAJECTORIES
Coded trajectories for the investigation of strongly unsteady flow fields N90-16240
Analysis of the measuring range and the accuracy of an existing particle image velocimetry system N90-16247
Trajectory-capture cell instrumentation for measurement of dust particle mass, velocity and trajectory, and particle capture N90-16644

PARTICLES
Development of low density silica aerogel as a capture medium for hyper-velocity particles
[NASA-CR-185930] N90-16489

PARTICULATES
High temperature aluminum-base alloy
[AD-D014270] N90-16028
Ambient flow studies and particulate collection measurements: A laminar flow, reduced entrainment electrostatic precipitator
[DE90-001457] N90-16149
Electron beam analysis of particulate cometary material N90-16613
The in-situ cometary particulate size distribution measured for one comet: P/Halley N90-16637
Analysis of particulates of comet nucleus samples: Possible use of olivine as indicator phase N90-16646
Ion bombardment experiments suggesting an origin for organic particles in pre-cometary and cometary ices N90-16652

PASCAL (PROGRAMMING LANGUAGE)
Parallel algorithms for interactive manipulation of digital terrain models N90-16445

PASSIVITY
Stainless steel passivity
[AD-A214108] N90-16033
An XPS and electrochemical study of the influence of molybdenum and nitrogen on the passivity of austenitic stainless steel
[AD-A214267] N90-16034

PATENTS
Continuously variable gear drive transmission
[AD-D014268] N90-16275

PATHOGENS
Short-term bioassays may be useful in evaluating fiber/whisker hazards
[DE90-003707] N90-16393

PATTERN RECOGNITION
Connectionist model-based stereo vision for telerobotics N90-16224
Ice floe identification in satellite images using mathematical morphology and clustering about principal curves
[AD-A213854] N90-16311
The development of two-dimensional object identification techniques
[NASA-CR-186203] N90-16408
Pattern matching in ML: A case study in refinement
[RSRE-89004] N90-16430
Interpretation of CAD (Computer Aided Design) models through IGES (Initial Graphics Exchange Specification) interface
[PB90-121294] N90-16441
High speed signal extraction using electro-optic techniques
[AD-A214446] N90-16500
Order filters, median recursive filter: Analysis and evaluation of performance in image processing
[ISAL-89-0017] N90-16505

PATTERN REGISTRATION
Pattern matching in ML: A case study in refinement
[RSRE-89004] N90-16430

PAYLOADS
Unmanned air vehicles payloads and sensors N90-15930
Automated search techniques applied to optical payloads in unmanned air vehicles N90-15931
Proposed concept for the visible/infrared imaging radiometer for second generation Meteosat
[ETN-90-96145] N90-16503

PENETRATION
Theoretical study of cold nuclear fusion using barrier penetration approach
[DE90-601096] N90-16513
Magnetic penetration depth and intragrain critical current density in gain-aligned Tl2Ca2Ba2Cu3O10 superconductor
[DE90-004245] N90-16562

PERFORMANCE PREDICTION
Improved tangent-cone method for the Aerodynamic Preliminary Analysis System (APAS) version of the hypersonic arbitrary-body program
[NASA-TM-4165] N90-15890

Multidimensional numerical simulation of large caliber ignition processes
[ISL-CO-233/88] N90-16021
CIS-2 analyzer derivation of hardware parameters
[IFSI-89-13] N90-16230
Performance predictions for an intermediate-sized VAWT based on performance of the 34-m VAWT test bed
[DE90-002835] N90-16345

PERFORMANCE TESTS
Fuel Tank Technology
[AGARD-R-771] N90-15904
Aircraft fuel tank construction and testing experience N90-15907
Design philosophy and construction techniques for integral fuselage fuel tanks N90-15913
Performance of a highly-loaded HP compressor
[RAE-TM-P-1149] N90-15919
A UK perspective on the uniform engine test programme
[RAE-TM-P-1172] N90-15922
Space shuttle Production Verification Motor 1 (PV-1) static fire
[NASA-CR-183784] N90-15991
Pulsed plasma mission endurance test
[AD-A213462] N90-15993
Theoretical and experimental investigation of axial power extraction from a magnetically insulated transmission line oscillator
[DE90-003486] N90-16131
Stand Alone Pressure Measurement Device (SAPMD) for the space shuttle Orbiter, part 1
[NASA-CR-172119-PT-1] N90-16202
Stand Alone Pressure Measurement Device (SAPMD) for the space shuttle Orbiter, part 2
[NASA-CR-172119-PT-2] N90-16203
Results from the third year of operation of the Federal Methanol Fleet at Lawrence Berkeley Laboratory
[DE90-003306] N90-16277
Performance predictions for an intermediate-sized VAWT based on performance of the 34-m VAWT test bed
[DE90-002835] N90-16345
On the selection of materials for cryogenic seals and the testing of their performance N90-16696

PERIODIC VARIATIONS
Periodically unsteady effects on profiles, induced by separation N90-16196

PERMANENT MAGNETS
Anisotropy and microstructure of high coercivity rare earth iron permanent magnets, list of papers published
[AD-A214160] N90-16476

PERMEABILITY
Improved performance polysulfide based sealant N90-15910
Synthesis and analysis of novel polymers with potential for providing both high permselectivity and permeability in gas separation applications
[DE90-003907] N90-16065
Some considerations on resource evaluation of The Geysers
[DE90-002119] N90-16343

PERMITTIVITY
Porous ceramic bodies
[AD-D014277] N90-16061
Plasmon excitation in the scattering of electromagnetic waves from good conductors
[AD-A214026] N90-16107

PEROVSKITES
Researches on amorphous perovskite
[DE89-900733] N90-16535

PERSONAL COMPUTERS
Personal computer study of finite-difference methods for the transonic small disturbance equation
[NASA-TM-102582] N90-15892

PERSONNEL
MANPRINT (Manpower and Personnel Integration) evaluation: AN/TRC-170 digital troposcatter radio system
[AD-A211799] N90-16100

PERSONNEL DEVELOPMENT
Project summaries
[PB90-103987] N90-16472

PERTURBATION
Singular perturbation analysis of AOTV-related trajectory optimization problems
[NASA-CR-186202] N90-15936

PERTURBATION THEORY
On the domain of string perturbation theory
[DE90-600759] N90-16575
The dynamics of dust in planetary magnetospheres N90-16658

PETROLOGY
Summaries of physical research in the geosciences
[DE90-004993] N90-16309

PH
Study of silicon nitride pH response to the fabrication of microelectronic sensors
[LAAS-89229] N90-16023

PHARMACOLOGY
Coded-aperture imaging in nuclear medicine N90-16208

PHASE DIAGRAMS
Surface studies at the NSLS
[DE90-003173] N90-16027
Contribution to the study of order effects in the Ising model framework: Ground states and phase diagrams
[ESA-TT-1118] N90-16557
Physical properties of Bi2Sr2CuO6, the semiconducting phase, structurally distinct from the n = 1 Bi-cuprate superconductor
[DE90-004299] N90-16563
Estimation of thermodynamic properties of alloys from phase diagram and other loose boundary conditions
[DE90-719511] N90-16579

PHASE SEPARATION (MATERIALS)
La(sub 2)MO(sub 4 + delta) (M = Cu, Ni, Co): Phase separation and superconductivity resulting from excess oxygen defects
[DE90-001988] N90-16534

PHASE TRANSFORMATIONS
Study of phase transformations liquid-solid-solid of ultrafine particles
[ISAL-89-0019] N90-16022
Fundamental studies of beta phase decomposition modes in titanium alloys
[AD-A214424] N90-16035
Phase evolution during neutron irradiation of commercial Fe-Cr-Mn alloys
[DE90-004113] N90-16042
Soft modes, freezing, and nonlinear response of a dipolar glass
[DE90-003647] N90-16075
On the observation of a transition from fusion to multifragmentation in high multiplicity O16 induced reactions
[LUIP-8812] N90-16481
Superflow induced phase transition in the axial vortex-free texture of rotating superfluid He-3-B
[PB90-110388] N90-16531
Thermodynamic studies on the ferroelectric phase transition in neutron irradiated (Li(sub x)K(1-x))2SO4 crystals at high temperature
[DE89-635786] N90-16545
Physical properties of Bi2Sr2CuO6, the semiconducting phase, structurally distinct from the n = 1 Bi-cuprate superconductor
[DE90-004299] N90-16563

PHASED ARRAYS
Large angle off-axis beam steering of a phased telescope array
[AD-D014269] N90-16127

PHENYLALANINE
Advanced biosensors for amino acid detection
[AD-A214029] N90-16225

PHONONS
Phonon anomaly at T(sub c) in (Y/ER)Ba2Cu3O(7-delta)
[DE90-003562] N90-16539

PHOSPHAZENE
Design, characterization, and optical properties of phosphazene-based polymers
[DE90-004111] N90-16068

PHOSPHORIC ACID FUEL CELLS
Improved anode catalysts for coal gas-fueled phosphoric acid fuel cells
[DE90-004016] N90-16347

PHOTOCHEMICAL REACTIONS
The chemistry and dynamics of marine stratocumulus N90-16381

PHOTOGRAMMETRY
Focal research effort points of the Institute of Applied Geodesy in the field of digital image processing N90-16333

PHOTOINTERPRETATION
Computer-aided boundary delineation of agricultural lands
[NASA-TM-102243] N90-16313

PHOTON DENSITY
Production of photons in anisotropic spacetimes
[DE90-600760] N90-16576

PHOTONUCLEAR REACTIONS
Proceedings of the specialists' meeting on physics and engineering of fission and spallation
[DE90-719706] N90-16519

PHOTOPRODUCTION
Theoretical aspects of electroweak and other interactions in medium energy nuclear physics
[DE90-004015] N90-16493

PHOTOSPHERE
Determination of solar flare accelerated ion angular distributions from SMM gamma ray and neutron measurements and determination of the He-3/H ratio in the solar photosphere from SMM gamma ray measurements
[NASA-CR-186038] N90-16676

PHOTOSYNTHESIS
Dynamics of carbon dioxide exchange of a wheat community grown in a semi-closed environment N90-16689

PHOTOVOLTAIC CELLS
Sizing and selection of batteries for stand-alone photovoltaic systems
[DE90-002990] N90-16129

PHYSICAL CHEMISTRY
Physical processing of cometary nuclei N90-16653

PHYSIOLOGICAL RESPONSES
Cryogenic engineering and materials N90-15949
Factor analytic reduction of the carotid-cardiac baroreflex parameters N90-16693

PIERCING
The nature of cometary materials N90-16647

PIEZOELECTRIC CERAMICS
Piezoelectric ceramic modeling and characterization at high levels of mechanical activity
[ISAL-89-0030] N90-16074

PIEZOELECTRIC GAGES
Mechanoelectric conversion by uniaxial constraint in piezoelectric generators: Optimization of electrical, mechanical, and physico-chemical parameters of materials
[ISAL-89-0020] N90-16235

PIEZOELECTRIC TRANSDUCERS
Detection of flow instabilities at airfoil profiles using piezoelectric arrays N90-16175
Colinear fluctuating wall shear stress and fluctuating pressure transducer
[AD-D014296] N90-16226
Determination of dynamic surface forces using piezoelectric arrays N90-16249
The use of piezofoil sensors for the determination of the unsteady pressure distribution at the surface of a gas turbine blade N90-16250

PIEZOELECTRICITY
SAW (Surface Acoustic Wave) transducer with improved bus-bar design
[AD-D014250] N90-16125
Mechanoelectric conversion by uniaxial constraint in piezoelectric generators: Optimization of electrical, mechanical, and physico-chemical parameters of materials
[ISAL-89-0020] N90-16235

PILOT PERFORMANCE
Piloted simulation of a ground-based time-control concept for air traffic control
[NASA-TM-101085] N90-15898
Keeping the pilot in the loop
[RAE-TM-FM-18] N90-16396

PILOTLESS AIRCRAFT
Guidance and Control of Unmanned Air Vehicles
[AGARD-CP-436] N90-15924
Unmanned air vehicles payloads and sensors N90-15930
Distribution of hardware and software elements in unmanned air vehicle systems N90-15933
Technology and evaluation of unmanned air vehicles N90-15934

PIPES (TUBES)
Using the singularity-separating method to study how to decrease the pressure at the end of a tube
[PREPRINT-490] N90-16158

PIXELS
Detection of edges using local geometry N90-16213

PLANAR STRUCTURES
High temperature aluminum-base alloy
[AD-D014270] N90-16028
Development of planar geometry solid oxide fuel cells
[PB90-100769] N90-16341

PLANE WAVES
A space-time discretization procedure for wave propagation problems
[NASA-TM-102215] N90-16399

PLANETARY EVOLUTION
Mission to Mars. Report of the Mars exploration study team
[ESA-SP-1117] N90-15968

PLANETARY MAGNETOSPHERES
The dynamics of dust in planetary magnetospheres N90-16658

PLANETARY NEBULAE
Identification of solar nebula condensates in interplanetary dust particles and unequilibrated ordinary chondrites N90-16629

PLANETARY SURFACES
The nature of cometary materials N90-16647

PLANETARY WAVES
The effect of orographic forcing on the mean flow of the stratosphere N90-16367
PLANNING
The first 1000 days of a future lunar base [ILR-MITT-224] N90-15970
Federal roles to realize national energy-efficiency opportunities in the 1990s [DE90-004410] N90-16348
Invention and innovation: Alternative mechanisms for enhancing organizational competitiveness [DE89-015858] N90-16584
PLANTING
Dynamics of carbon dioxide exchange of a wheat community grown in a semi-closed environment N90-16689
PLASMA COMPRESSION
Design of a spheromak compressor driven by high explosives [DE90-003652] N90-16283
PLASMA CONTROL
Hollow-cathode experiments to support electrodynamic tether applications [IFSI-89-5] N90-15986
Initial deuterium confinement studies in DIII-D tokamak: DIII-D milestone report number 58 [DE90-003942] N90-16509
Recent progress on the HESS (High Explosive Spheromak Source) experiment [DE90-003218] N90-16520
PLASMA DENSITY
Langmuir wave interaction with ion-sound one. Part 1: Stochastic effects [DE90-603368] N90-16474
PLASMA DIAGNOSTICS
In situ measurement of neutral beam components using the Doppler-shifted H(sub alpha) emissions in Heliotron E [DE90-719521] N90-16516
Low energy neutral particle energy analyser by time of flight method [DE90-719529] N90-16517
Spectroscopic diagnostics of high temperature plasmas [DE90-003912] N90-16522
PLASMA DRIFT
Nonlinear wave coupling and clumps in drift wave turbulence theory [DE90-004103] N90-16150
PLASMA ENGINES
Pulsed plasma mission endurance test [AD-A213462] N90-15993
PLASMA GUNS
Progress with small, high-magnetic-field spheromaks in CTX [DE90-003395] N90-16527
PLASMA PHYSICS
Stress analysis of the Princeton Plasma Physics Laboratory 1/2- x 1/2-inch shear/compression test fixture [DE90-004401] N90-16512
PLASMA RESONANCE
Plasmon excitation in the scattering of electromagnetic waves from good conductors [AD-A214026] N90-16107
PLASMA SPRAYING
Structural analysis of zirconium-aluminum plasma deposits [ETCA-89-R-073] N90-16045
PLASMA TURBULENCE
Nonlinear wave coupling and clumps in drift wave turbulence theory [DE90-004103] N90-16150
PLASMA WAVES
On averaged force acting on a particle in HF electromagnetic field [DE90-600984] N90-16109
Nonlinear wave coupling and clumps in drift wave turbulence theory [DE90-004103] N90-16150
Design of a spheromak compressor driven by high explosives [DE90-003652] N90-16283
PLASMAS (PHYSICS)
Second harmonic electron cyclotron heating in low and over density plasmas in Heliotron DR [DE90-719519] N90-16515
Ion bombardment experiments suggesting an origin for organic particles in pre-cometary and cometary ices N90-16052
Dissipative effects in Friedmann universes [DE89-618838] N90-16663
PLASMONS
Plasmon excitation in the scattering of electromagnetic waves from good conductors [AD-A214026] N90-16107
PLASTIC FLOW
An implicit time-integration procedure for a set of internal variable constitutive equations for isotropic elasto-viscoplasticity [PB90-121302] N90-16470
PLASTIC PROPERTIES
Burst pressure prediction of metallic/fibre reinforced rocket motor cases using an elasto-plastic instability analysis [RARDE-1/89] N90-15997
BAM: German Federal Institute for Materials Research and Testing, Berlin [DE90-004293] N90-16307
An implicit time-integration procedure for a set of internal variable constitutive equations for isotropic elasto-viscoplasticity [PB90-121302] N90-16470
PLOTTERS
EZVIDEO, FORTRAN graphics routines for the IBM AT [DE90-004409] N90-16422
PLUMES
Plume shape optimization of small attitude control thrusters with respect to impingement and thrust [ISL-CO-220/88] N90-16153
Simulation of pollutant transport using a mesoscale grid circulation model [GKSS-89/E/24] N90-16365
POINT SOURCES
Use of the Egret instrument in studies of the origin of the cosmic radiation. 2: Spectral signatures of discrete cosmic-ray sources [DE90-003595] N90-16682
POISSON EQUATION
Multigrid methods for two- and three-dimensional Poisson-type equations on the sphere [GMD-391] N90-16468
POLAR CUSPS
Polar cusps latitudinal shift and its relation to the IMF-By component [IFSI-88-14] N90-16377
POLAR REGIONS
The effect of orographic forcing on the mean flow of the stratosphere N90-16367
Polar cusps latitudinal shift and its relation to the IMF-By component [IFSI-88-14] N90-16377
POLARIZATION (CHARGE SEPARATION)
A search for the electric dipole of the electron [DE90-001572] N90-16484
POLICIES
Safety and cryogenic wind tunnels N90-15960
Round trip to orbit. Human spaceflight alternatives: Special report [OTA-ISC-419] N90-15966
The SMITE approach to security [RSRE-89014] N90-16404
POLLUTION TRANSPORT
Simulation of pollutant transport using a mesoscale grid circulation model [GKSS-89/E/24] N90-16365
POLYCARBONATES
Synthesis and analysis of novel polymers with potential for providing both high permselectivity and permeability in gas separation applications [DE90-003907] N90-16065
POLYESTERS
Synthesis and analysis of novel polymers with potential for providing both high permselectivity and permeability in gas separation applications [DE90-003907] N90-16065
Development of an elastomeric additive to improve the impact resistance of unsaturated polyester networks [ISAL-89-0006] N90-16073
POLYMER CHEMISTRY
Design, characterization, and optical properties of phosphazene-based polymers [DE90-004111] N90-16068
POLYMERIC FILMS
Mass loss during x ray microanalysis [DE90-003954] N90-16067
POLYMERIZATION
The structure of silica-polysiloxane composites and its effects on their elastomeric properties [DE89-014766] N90-16005
The physical properties of microcellular composite foams [DE90-003658] N90-16058
Synthesis and analysis of novel polymers with potential for providing both high permselectivity and permeability in gas separation applications [DE90-003907] N90-16065
Design, characterization, and optical properties of phosphazene-based polymers [DE90-004111] N90-16068
POLYSTYRENE
The physical properties of microcellular composite foams [DE90-003658] N90-16058
Diblock copolymers at surfaces [DE90-005406] N90-16079
POLYSULFIDES
Integral fuel tank sealing practice at British Aerospace (Kingston) N90-15905
The effect of primer age on adhesion of polysulphide sealant N90-15909
Improved performance polysulfide based sealant N90-15910
POROSITY
Porous ceramic bodies [AD-D014277] N90-16061
POROUS BOUNDARY LAYER CONTROL
Kinetics of the graphite/oxygen reaction in the in-pore diffusion controlled regime. Part 3: Influence of boundary layer diffusion in kinetic experiments at temperatures 970K to 1170K [JUEL-2284-PT-3] N90-16024
POSITION (LOCATION)
Analytical techniques for tracking filter implementation N90-15903
Parallel algorithm for determining motion vectors in ice floe images by matching edge features N90-16451
POSITION ERRORS
Analytical techniques for tracking filter implementation N90-15903
POSITION INDICATORS
GPS network analysis: The influence of stochastic prior information of orbital elements on ground station position measures [TR-4-1988] N90-15901
POSITIVE IONS
A double focussing mass-spectrometer for simultaneous ion measurements in the stratosphere [AERONOMICA-ACTA-A-350-1989] N90-16379
POSITRONS
Slow positron defect profiling of silicon epilayers [DE90-003958] N90-16288
POTASSIUM COMPOUNDS
Thermodynamic studies on the ferroelectric phase transition in neutron irradiated (Li(sub x)K(1-x))2SO4 crystals at high temperature [DE89-635786] N90-16545
POWDER (PARTICLES)
Synthesis of air-sinterable lanthanum chromite powders [DE90-004681] N90-16049
POWDER METALLURGY
Method for refining microstructures on prealloyed titanium powder compacts [AD-D014280] N90-16030
Structural analysis of zirconium-aluminum plasma deposits [ETCA-89-R-073] N90-16045
Shock-induced reaction synthesis of aluminides and silicides [DE90-003948] N90-16066
POWDERED ALUMINUM
Structural analysis of zirconium-aluminum plasma deposits [ETCA-89-R-073] N90-16045
POWER EFFICIENCY
Piezoelectric ceramic modeling and characterization at high levels of mechanical activity [ISAL-89-0030] N90-16074
POWER LINES
Microwave screening on digital radio communication links due to multicircuit power transmission lines [DE90-734950] N90-16118
POWER TRANSMISSION
Microwave screening on digital radio communication links due to multicircuit power transmission lines [DE90-734950] N90-16118
PRE-MAIN SEQUENCE STARS
Outflows in high mass star-forming regions N90-16657
PRECIPITATION (CHEMISTRY)
The influence of carbide precipitation on the creep rupture behavior of high temperature alloys [JUEL-2211] N90-16044
PRECONDITIONING
Element-by-element preconditioning techniques for large-scale, vectorized finite element analysis in nonlinear solid and structural mechanics N90-16291
PREDICTION ANALYSIS TECHNIQUES
On the observation of a transition from fusion to multifragmentation in high multiplicity O16 induced reactions [LUIP-8812] N90-16481
PREPARATION
Ultrasonic assisted paint removal method [AD-D014264] N90-16479

PREPOLYMERS
Design, characterization, and optical properties of phosphazene-based polymers
[DE90-004111] N90-16068
PRESSURE DISTRIBUTION
Pressure measurement technique in the wind tunnel division of DFVLR
[ESA-TT-1145] N90-15963
An electronic pressure profile display system for aeronautic test facilities
[NASA-TM-102478] N90-15964
Laboratory studies of isolated eddies in a rotating fluid
[AD-A213903] N90-16146
Determination of the N-factor in the Brunswick (Federal Rep. of Germany) transonic wind tunnel using measurements of pressure distributions and transition points, and the Saily method N90-16177
Two-Dimensional Measuring Techniques
[DGLR-PAPERS-88-04] N90-16236
The use of piezofoil sensors for the determination of the unsteady pressure distribution at the surface of a gas turbine blade N90-16250
Use of the film-of-oil technique for profile measurements in the Transonic Wind tunnel Brunswick (TWB) N90-16252
PRESSURE EFFECTS
The use of hypervelocity launchers to explore previously inaccessible states of matter
[DE90-004088] N90-15973
Space shuttle Production Verification Motor 1 (PV-1) static fire
[NASA-CR-183784] N90-15991
Thermodynamic analysis of chemical stability of ceramic materials in hydrogen-containing atmospheres at high temperatures
[NASA-CR-4271] N90-16072
PRESSURE MEASUREMENT
Pressure measurement technique in the wind tunnel division of DFVLR
[ESA-TT-1145] N90-15963
Stand Alone Pressure Measurement Device (SAPMD) for the space shuttle Orbiter, part 1
[NASA-CR-172119-PT-1] N90-16202
Stand Alone Pressure Measurement Device (SAPMD) for the space shuttle Orbiter, part 2
[NASA-CR-172119-PT-2] N90-16203
PRESSURE OSCILLATIONS
Small amplitude liquid oscillations in a rectangular container under zero-gravity
[LRT-WE-9-FB-2(1989)] N90-16167
PRESSURE REDUCTION
Using the singularity-separating method to study how to decrease the pressure at the end of a tube
[PREPRINT-490] N90-16158
PRESSURE SENSORS
Pressure measurement technique in the wind tunnel division of DFVLR
[ESA-TT-1145] N90-15963
Stand Alone Pressure Measurement Device (SAPMD) for the space shuttle Orbiter, part 1
[NASA-CR-172119-PT-1] N90-16202
Stand Alone Pressure Measurement Device (SAPMD) for the space shuttle Orbiter, part 2
[NASA-CR-172119-PT-2] N90-16203
Colinear fluctuating wall shear stress and fluctuating pressure transducer
[AD-D014296] N90-16226
PRESSURE VESSELS
BAM: German Federal Institute for Materials Research and Testing, Berlin
[DE90-004293] N90-16307
PRIMERS
The effect of primer age on adhesion of polysulphide sealant N90-15909
PRIMITIVE EQUATIONS
Diagnostic and kinematic fields associated with curved and straight jet streaks using a two-layer primitive equation model N90-16371
PROBABILITY DENSITY FUNCTIONS
Multiple flow regimes in the Northern Hemisphere winter N90-16372
PROBLEM SOLVING
Recent progress in relativistic klystron research
[DE90-000942] N90-16121
An algorithm to compute the square root of 3x3 positive definite matrix
[DE89-635711] N90-16417
Complex availability problems solved with simulation
[DE89-012610] N90-16459
Hidden regularity for a strongly nonlinear wave equation
[DE90-600742] N90-16465
PROCESS CONTROL (INDUSTRY)
On-line chemical composition analyzer development
[DE90-004079] N90-16026
Silicon membrane formation
[DE90-003022] N90-16064
Development and evaluation of a process to produce hydrogen from coal
[DE90-003937] N90-16084
Digital system for monitoring and controlling remote processes
[DE90-003935] N90-16094
PRODUCT DEVELOPMENT
Further development of the PIV method for use in the large wind tunnel N90-16248
PRODUCTION ENGINEERING
Sequential rapid communication visual displays
[AD-D014282] N90-16106
PRODUCTIVITY
Productivity and cryogenic wind tunnels N90-15961
PROGRAM VERIFICATION (COMPUTERS)
Stochastic model of the NASA/MSFC ground facility for large space structures with uncertain parameters: The maximum entropy approach, part 2
[NASA-CR-186009] N90-16407
Pattern matching in ML: A case study in refinement
[RSRE-89004] N90-16430
PROGRAMMING LANGUAGES
The application of Z to the specification of air traffic control systems. 1: An initial specification of the radar processing activity
[RSRE-MEMO-4280] N90-15900
Pattern matching in ML: A case study in refinement
[RSRE-89004] N90-16430
The NODEN hardware description language
[RSRE-89011] N90-16431
PROJECT MANAGEMENT
Solid fuel combustion chamber, phase 10
[LR-536] N90-16000
Establishment of the Innovative Technology Utilization Center at West Virginia University
[PB90-114711] N90-16594
PROJECT PLANNING
National program plan for electric vehicle battery research and development: Technical plan
[DE90-002023] N90-16269
PROJECTILES
The use of hypervelocity launchers to explore previously inaccessible states of matter
[DE90-004088] N90-15973
Stability and fragmentation of ejecta in hypervelocity impact
[DE90-004087] N90-16278
PROJECTS
Activities report of the National Electrotechnic Institute Galileo Ferraris
[ETN-90-96178] N90-16705
PROTECTION
Fuel tank explosion protection N90-15914
PROTECTIVE COATINGS
Fuel resistant coatings for metal and composite fuel tanks N90-15911
Ultrasonic assisted paint removal method
[AD-D014264] N90-16479
PROTOCOL (COMPUTERS)
Satellite systems integrated with the terrestrial cellular network for mobile communications
[ESA-STR-228] N90-16113
The DAB model of drawing processes N90-16691
PROTOPLANETS
Neptune's Triton: A moon rich in dry ice and carbon
[NASA-CR-186298] N90-16675
PSYCHOLOGICAL FACTORS
Simulator sickness in the UH-60 (Black Hawk) flight simulator
[AD-A214434] N90-16392
PSYCHOPHYSICS
High compression image and image sequence coding N90-16214
PULSARS
Pulsations of delta Scuti stars
[DE90-003213] N90-16598
On the interaction of a pulsar with the ambient medium utilizing x ray images of the Crab nebula
[MPE-REPT-215] N90-16604
An atlas of aperiodic variability in HMXB
[MPE-PREPRINT-158] N90-16605
Relative muon content of UHE showers associated with Hercules X-1
[DE90-000609] N90-16665
PULSE AMPLITUDE
Calibration of a pulsed potential crack monitor for use in fatigue crack growth studies
[RAE-TM-M/S-1126] N90-16301
PULSE COMMUNICATION
Microwave screening on digital radio communication links due to multicircuit power transmission lines
[DE90-734950] N90-16118
PULSE DURATION
Pulsed plasma mission endurance test
[AD-A213462] N90-15993
EXOSAT measurements of the pulse period of Vela X-1
[MPE-PREPRINT-157] N90-16673
PULSE GENERATORS
Electrical safety in the high voltage laboratory
[DE90-003026] N90-16130
PULSE MODULATION
High speed signal extraction using electro-optic techniques
[AD-A214446] N90-16500
PULSED LASERS
Optical flow measuring method using diode lasers, phase coupled arrays, and high frequency pulsed diode lasers N90-16176
High frequency pulsed diode lasers and phase-coupled diode arrays for aerodynamics N90-16238
Eurolaser definition phase: A comparison of high power lasers available
[ETN-90-96061] N90-16268
Resonance enhanced Raman studies of as-grown and laser-processed HgCdTe
[AD-A213855] N90-16540
PYRIDINES
Carbon-13 nuclear magnetic resonance of heterocyclic salts and its precursors
[DE89-635768] N90-16016
PYROLYSIS
Comprehensive mechanisms for combustion chemistry: An experimental and numerical study with emphasis on applied sensitivity analysis
[DE90-003904] N90-16017
Method of making carbon dioxide and chlorine free fluoride-based glass
[AD-D014260] N90-16060
PYROTECHNICS
Very low energy ignition of pyrotechnics using a Semiconductor Bridge (SCB)
[DE90-002645] N90-16082

Q

QUADRUPOLES
B-Factory Final Focus System using superconducting quadrupoles
[DE90-004432] N90-16552
QUALITATIVE ANALYSIS
Discrete event simulation tool for analysis of qualitative models of continuous processing systems
[NASA-CASE-MSC-21465-1] N90-16410
QUANTUM CHROMODYNAMICS
Neutrino interactions
[NOTA-INTERNA-934] N90-16495
Proceedings of the 23rd Annual Seminar on Theoretical Physics
[DE90-601827] N90-16577
QUANTUM ELECTRONICS
Rotational energy transfer in metastable states of heteronuclear molecules
[AD-A214425] N90-16485
QUANTUM MECHANICS
Continuous spontaneous reduction model involving gravity
[DE90-600730] N90-16573
The (2+1)-dimensional quantum gravity
[DE90-719556] N90-16580
Double-periodic wormholes in theories with global symmetries
[DE90-719575] N90-16581
QUANTUM OPTICS
Multisqueezing of mechanical states and back-action evasion measurements
[IFSI-89-6] N90-16504
QUANTUM THEORY
The theory of hybrid stochastic algorithms
[DE90-003941] N90-16421
Multiplet classification of highest weight modules over quantum universal enveloping algebras: The U(sub q)(sl(3,C)) example
[DE90-600720] N90-16464
The off-shell closed strings as the topological open membranes: Dynamical transmutation of world sheet dimension
[DE89-635721] N90-16571
Double-periodic wormholes in theories with global symmetries
[DE90-719575] N90-16581
Quantum fields in cosmological space-times: A soluble example
[DE89-618837] N90-16662

QUANTUM WELLS
Theory of the electronic and optical properties of semiconductor heterostructures
[AD-A214132] N90-16544
QUARK PARTON MODEL
Neutrino interactions
[NOTA-INTERNA-934] N90-16495
QUASARS
Scientific investigations of the Space Research Group
[ISBN-0-642-13252-6] N90-16595
QUERY LANGUAGES
Abbreviated query interpretation in extended entity-relationship oriented databases
[DE90-003114] N90-16587

R

RADAR APPROACH CONTROL
The application of Z to the specification of air traffic control systems. 1: An initial specification of the radar processing activity
[RSRE-MEMO-4280] N90-15900
RADAR CROSS SECTIONS
Plasmon excitation in the scattering of electromagnetic waves from good conductors
[AD-A214026] N90-16107
RADAR DETECTION
The lidar experiment at Andoya, Norway, during the Summer of 1988
[BONN-IR-89-16] N90-16117
RADAR EQUIPMENT
Method for eliminating self-screening noise jamming in radar systems
[AD-D014271] N90-16105
RADAR IMAGERY
Investigation of the topographic components of the image content of radar pictures N90-16332
RADAR MAPS
Navigation up-date using radar mapping: Assessment and optimisation simulation tool N90-15928
RADAR MEASUREMENT
Analytical techniques for tracking filter implementation N90-15903
RADAR NAVIGATION
Navigation up-date using radar mapping: Assessment and optimisation simulation tool N90-15928
RADIANCE
Atmospheric transmittance determination from a two-angle measurement of radiance change
[AD-A213847] N90-16375
RADIATION ABSORPTION
Cloud phase discrimination by near-infrared remote sensing N90-16310
Atmospheric transmittance determination from a two-angle measurement of radiance change
[AD-A213847] N90-16375
Mechanisms of microwave induced damage in biologic materials
[AD-A213480] N90-16390
RADIATION BELTS
The effects of natural and enhanced Van Allen Belt radiation on a space based weapon platform
[DE89-016219] N90-16685
RADIATION DAMAGE
Material responses to incident x rays
[DE89-015366] N90-16305
Mechanisms of microwave induced damage in biologic materials
[AD-A213480] N90-16390
RADIATION DETECTORS
Reflectometers
[AD-D014249] N90-16499
RADIATION DOSAGE
Analysis and evaluation of technical data on the photochromic and non-linear optical properties of materials
[AD-A214050] N90-16014
RADIATION EFFECTS
Interplanar spacing for various phases in austenitic stainless steels
[DE90-602350] N90-16038
Phase evolution during neutron irradiation of commercial Fe-Cr-Mn alloys
[DE90-004113] N90-16042
Modeling dislocation evolution in irradiated alloys
[DE90-004921] N90-16051
Development of a diamond insulator for thermionic applications
[DE90-002849] N90-16055
On the HEMP (High-Altitude Electromagnetic Pulse) response of protective relays
[DE90-003718] N90-16138
Mechanisms of microwave induced damage in biologic materials
[AD-A213480] N90-16390
The 1MeV-electron irradiation induced defects in epitaxially grown 3C-SiC
[DE90-719574] N90-16554
Electron beam induced oxygen in YBa2Cu3O(7-x) superconductors
[DE90-004839] N90-16565
Radiation modification of cometary materials: Laboratory simulations N90-16626
The effects of natural and enhanced Van Allen Belt radiation on a space based weapon platform
[DE89-016219] N90-16685
RADIATION HARDENING
Analysis and evaluation of technical data on the photochromic and non-linear optical properties of materials
[AD-A214050] N90-16014
RADIATION PROTECTION
On the HEMP (High-Altitude Electromagnetic Pulse) response of protective relays
[DE90-003718] N90-16138
RADIATION SHIELDING
Evaluation of potential cold x ray shield materials tested on Proto II
[DE90-004348] N90-16003
Scaling study for SP-100 reactor technology
[NASA-TM-897140] N90-16496
RADIATION TOLERANCE
Improved performance polysulfide based sealant N90-15910
Radiation resistance of solar cells for space application. 1: Study on the irradiation procedure of electron beams
[DE90-719546] N90-16349
RADIO ASTRONOMY
Scientific investigations of the Space Research Group
[ISBN-0-642-13252-6] N90-16595
RADIO COMMUNICATION
Helsinki University of Technology Radio Laboratory
[PB90-110677] N90-16102
Satellite systems integrated with the terrestrial cellular network for mobile communications
[ESA-STR-228] N90-16113
Microwave screening on digital radio communication links due to multicircuit power transmission lines
[DE90-734950] N90-16118
RADIO EQUIPMENT
MANPRINT (Manpower and Personnel Integration) evaluation: AN/TRC-170 digital troposcatter radio system
[AD-A211799] N90-16100
RADIOACTIVE DECAY
Cosmic ray half life of Ni-56
[DE90-000132] N90-16680
RADIOACTIVE ISOTOPES
Measurements of long-lived cosmogenic nuclides in returned comet nucleus samples N90-16640
RADIOACTIVE MATERIALS
Examples of robots and teleoperators at the Savannah River Site
[DE90-004659] N90-16284
RADIOACTIVITY
Coded-aperture imaging in nuclear medicine N90-16208
RADIOMETERS
The physical foundations of radiometry and their applications in the mm-waveband
[REPT-12-88] N90-16114
Model-based quantification of image quality N90-16206
Operational ozone monitoring with the Global Ozone Monitoring Radiometer (GOMR)
[PB90-114034] N90-16359
RADIOMETRIC RESOLUTION
The physical foundations of radiometry and their applications in the mm-waveband
[REPT-12-88] N90-16114
RAIN
Estimating water flow through a hillslope using the massively parallel processor N90-16449
RANGEFINDING
MT's algorithm: A new algorithm to search for the optimum set of modulation indices for simultaneous range, command, and telemetry
[NASA-CR-186259] N90-16110
Parallel algorithm for determining motion vectors in ice floe images by matching edge features N90-16451
RANKING
Case tool evaluation system
[DE90-003698] N90-16413
RAPID QUENCHING (METALLURGY)
Production and processing of Cu-Cr-Nb alloys
[NASA-TM-102495] N90-16053
RARE EARTH ALLOYS
Anisotropy and microstructure of high coercivity rare earth iron permanent magnets, list of papers published
[AD-A214160] N90-16478
RAYLEIGH SCATTERING
Backscattering effects in DIAL due to water vapor
[SER-WISS-ABHANDL-89] N90-16265
REACTION KINETICS
Dynamics analyses of space power systems using the salt code
[DE90-002274] N90-15995
Kinetics of the graphite/oxygen reaction in the in-pore diffusion controlled regime. Part 3: Influence of boundary layer diffusion in kinetic experiments at temperatures 970K to 1170K
[JUEL-2284-PT-3] N90-16024
Solid state, surface, and catalytic studies of oxides
[DE90-004850] N90-16566
Nuclear reaction uncertainties in standard and non-standard cosmologies
[DE90-003594] N90-16666
REACTOR MATERIALS
Interplanar spacing for various phases in austenitic stainless steels
[DE90-602350] N90-16038
Fracture toughness of ferritic alloys at very high neutron exposures
[DE90-004519] N90-16046
REACTOR SAFETY
Dynamics analyses of space power systems using the salt code
[DE90-002274] N90-15995
REACTOR TECHNOLOGY
Scaling study for SP-100 reactor technology
[NASA-TM-897140] N90-16496
READOUT
Liquid level measurement system for analog and digital readout
[AD-D014297] N90-16227
REAL TIME OPERATION
Electro-optic sensors for surveillance and target acquisition N90-15929
An intelligence-driven RPV mission planner N90-15932
An electronic pressure profile display system for aeronautic test facilities
[NASA-TM-102478] N90-15964
RETE experiment activity at the TSS-1 POCC
[IFSI-89-12] N90-15988
Digital system for monitoring and controlling remote processes
[DE90-003935] N90-16094
Sequential rapid communication visual displays
[AD-D014282] N90-16106
Keeping the pilot in the loop
[RAE-TM-FM-18] N90-16396
Dynamic architecture computer
[AD-A214262] N90-16402
RECEIVERS
Satellite broadcasting: Requirements for the receiving antenna
[BBC-RD-1989/5] N90-16098
Helsinki University of Technology Radio Laboratory
[PB90-110677] N90-16102
RECIPROCAL THEOREMS
On the reciprocity of state vectors in boundary value models
[AD-A214104] N90-16458
RECOGNITION
Recognition and distinction of clouds, snow, and ice using AVHRR data N90-16322
RECONNAISSANCE
Automated search techniques applied to optical payloads in unmanned air vehicles N90-15831
RECOVERY
Energy management and recovery N90-15962
RECRYSTALLIZATION
Use of computer simulations to analyze limitations of kinetic models for recrystallization
[DE90-003618] N90-16548
The concept of axial-symmetry constraint and its significance in recrystallization
[DE90-003620] N90-16549
REDUCED GRAVITY
Experiment facilities for materials and fluid sciences embarked on Eureca-1
[ESA-SP-1118] N90-16088
Experiment facilities for materials and fluid sciences embarked on Spacelab
[ESA-SP-1120] N90-16089
Data compression for the microgravity experiments N90-16212
REFINING
Method for refining microstructures on prealloyed titanium powder compacts
[AD-D014280] N90-16030
REFLECTANCE
From primal sketches to the recovery of intensity and reflectance representations N90-16216

Reflectometers
[AD-D014249] N90-16499
REFLECTED WAVES
Statistics of a reflected laser beam in the turbulent atmosphere (path correlation)
[PB90-113994] N90-16261
REFLECTION
Measurement of reflection and impedance in a beam by the structural intensity technique
[DE90-728212] N90-16299
Reflection technique for thermal mapping of semiconductors
[AD-D014263] N90-16541
REFLECTOMETERS
Reflectometers
[AD-D014249] N90-16499
REFLEXES
Factor analytic reduction of the carotid-cardiac baroreflex parameters N90-16693
REFRACTORIES
Refractory solids in chondrites and comets: How similar N90-16654
REFRACTORY METALS
High temperature aluminum-base alloy
[AD-D014270] N90-16028
REFRIGERANTS
Absorption fluids data survey: 1989 update
[DE90-003985] N90-16346
REFRIGERATING
Feasibility of cool storage systems in refrigeration
[DE90-728179] N90-16093
REFRIGERATORS
Feasibility of cool storage systems in refrigeration
[DE90-728179] N90-16093
REGOLITH
Metamorphism of cosmic dust: Processing from circumstellar outflows to the cometary regolith N90-16641
REGULARITY
Hidden regularity for a strongly nonlinear wave equation
[DE90-600742] N90-16465
REGULATIONS
Diesel starting system monitor: Prototype development
[DE90-004425] N90-16276
REINFORCING MATERIALS
Vibration damping composition suitable for outer space temperature variations
[AD-D014288] N90-16296
RELATIVITY
Study of primitive universe in the Bianchi 9 model
[DE89-635903] N90-16572
Universe as a topological defect in a higher-dimensional Einstein-Yang-Mills theory
[DE90-719507] N90-16578
RELIABILITY
From small beginnings... The story of ESRO's sounding rocket programme in celebration of the twenty-fifth anniversary of the first ESRO sounding rocket launch
[ESA-BR-60] N90-15999
Fault tree analysis: A tool for battery safety and reliability studies
[DE90-002582] N90-16287
Software dependability growth characterization, modeling and evaluation
[LAAS-89320] N90-16437
Complex availability problems solved with simulation
[DE89-012610] N90-16459
REMOTE CONSOLES
Remote use of an Electron Beam Tester (EBT)
[IMAG-RR-760-I] N90-16233
REMOTE CONTROL
Digital system for monitoring and controlling remote processes
[DE90-003935] N90-16094
Connectionist model-based stereo vision for telerobotics N90-16224
Remote use of an Electron Beam Tester (EBT)
[IMAG-RR-760-I] N90-16233
REMOTE SENSING
Laboratory of Space Technology
[PB90-110651] N90-15967
Cloud phase discrimination by near-infrared remote sensing N90-16310
Science plan for the Alaska SAR facility program. Phase 1: Data from the first European sensing satellite, ERS-1
[NASA-CR-185028] N90-16312
Proceedings of the 5th User Seminar of the German Remote Sensing Data Center of the DFVLR
[DFVLR-MITT-89-04] N90-16318
Introduction to the framework and tasks of the DFD --- German Remote Sensing Data Center (DFD) N90-16319
Attempt to draw conclusions concerning the geological subsoil from the vegetation using digital image processing of TM data N90-16329
Utilization of remote sensing in geoscientific development and projects N90-16334
Use of remote sensing data for land and building statistics N90-16335
Use of remote sensing in operational inventory and monitoring agricultural and forestry tasks N90-16336
Statistical information system for cultivation of the soil. Use of remote sensing in official statistics N90-16338
X ray spectrophotometric remote sensing of diffuse auroral ionization
[SD-TR-89-09] N90-16599
REMOTE SENSORS
Liquid level measurement system for analog and digital readout
[AD-D014297] N90-16227
Trajectory-capture cell instrumentation for measurement of dust particle mass, velocity and trajectory, and particle capture N90-16644
REMOTELY PILOTED VEHICLES
Guidance and Control of Unmanned Air Vehicles
[AGARD-CP-436] N90-15924
Synthesis of control law, on a RPV, in order to minimize the number of sensors N90-15925
Mirach 100 flight control system N90-15926
Unmanned air vehicles payloads and sensors N90-15930
Automated search techniques applied to optical payloads in unmanned air vehicles N90-15931
An intelligence-driven RPV mission planner N90-15932
Technology and evaluation of unmanned air vehicles N90-15934
Navigation and guidance testing of the Lockheed/US Army Aquila remotely piloted vehicle N90-15935
REMOVAL
Environmental, health, and CFC substitution aspects of the ozone depletion issue
[DE90-004404] N90-16363
Ultrasonic assisted paint removal method
[AD-D014264] N90-16479
REPORTS
Reports of planetary astronomy, 1986
[NASA-TM-100776] N90-16596
Focus 88: The activities of the European Space Agency
[ESA-BR-43] N90-16706
REQUIREMENTS
Pulsed plasma mission endurance test
[AD-A213462] N90-15993
RESCUE OPERATIONS
Crew Safety and Rescue in Space: An International Approach
[ESA-SP-300] N90-15974
Safety and rescue during STS operations N90-15975
Assured crew return capability architecture N90-15977
On the selection of crewmember rescue means for manned space launch systems N90-15978
Crew safety and rescue aids N90-15980
NASDA's approach to the interoperability of safety and rescue in space N90-15981
RESEARCH AND DEVELOPMENT
Structural dynamics division research and technology accomplishments for FY 1989 and plans for FY 1990
[NASA-TM-101683] N90-15894
Other cryogenic wind tunnel projects N90-15948
Metal vaporisers: Bicentennial series of five historical monographs
[ISBN-0-642-13584-3] N90-16081
The first year's work of race project 1036 WTDM broadband customer premises network
[BBC-RD-1989/6] N90-16097
The development of over-the-horizon radar in Australia
[ISBN-0-642-13561-4] N90-16099
Eurolaser definition phase, solid state lasers working group: Active medium, laser active crystals
[ETN-90-95899] N90-16266
National program plan for electric vehicle battery research and development: Technical plan
[DE90-002023] N90-16269
Project summaries
[PB90-103987] N90-16472
Research and technology, 1989: Langley Research Center
[NASA-TM-4150] N90-16703
RESEARCH FACILITIES
A burst compression and expansion technique for variable-rate users in satellite-switched TDMA networks
[NASA-TM-102414] N90-15983
Conceptual design for the space station Freedom modular combustion facility
[NASA-TM-102037] N90-16087
Experiment facilities for materials and fluid sciences embarked on Eureca-1
[ESA-SP-1118] N90-16088
Experiment facilities for materials and fluid sciences embarked on Spacelab
[ESA-SP-1120] N90-16089
RESEARCH MANAGEMENT
The HERMES development program N90-16199
Focus 88: The activities of the European Space Agency
[ESA-BR-43] N90-16706
RESEARCH VEHICLES
Singular perturbation analysis of AOTV-related trajectory optimization problems
[NASA-CR-186202] N90-15936
RESIN BONDING
Molybdenum disulfide-molybdenum oxide lubricants
[AD-D014253] N90-16059
RESOLUTION
The lidar experiment at Andoya, Norway, during the Summer of 1988
[BONN-IR-89-16] N90-16117
RESONANCE
Resonance enhanced Raman studies of as-grown and laser-processed HgCdTe
[AD-A213855] N90-16540
RESONANT FREQUENCIES
Conformation, orientation and interaction in molecular monolayers: A surface second harmonic and sum frequency generation study
[DE90-003108] N90-16536
RESONANT VIBRATION
Piezoelectric ceramic modeling and characterization at high levels of mechanical activity
[ISAL-89-0030] N90-16074
RESOURCES MANAGEMENT
FY 1989 update to the Information Resources Management review plan
[DE90-004185] N90-16593
RESPIRATION
Short-term bioassays may be useful in evaluating fiber/whisker hazards
[DE90-003707] N90-16393
RESPONSE TIME (COMPUTERS)
New optimization techniques in database access and maintenance N90-16586
RESTORATION
Optimal focal-plane restoration N90-16207
Image gathering and coding for digital restoration: Information efficiency and visual quality N90-16211
RETINA
Image processing by Intensity-Dependent Spread (IDS) N90-16215
RETINAL IMAGES
Neural networks for data compression and invariant image recognition N90-16219
RETROREFLECTORS
Defense to laser light irradiation
[AD-D014286] N90-15984
REVERSE FIELD PINCH
End-on soft x ray imaging of Field-Reversed Configurations (FRCs) on the Field-Reversal-C (FRX-C)/Large Scale Modification (LSM) experiment
[DE90-004863] N90-16260
REYNOLDS NUMBER
Introduction to cryogenic wind tunnels N90-15940
Numerical analysis of nonstationary fluid flow (a survey)
[PREPRINT-492] N90-16159
REYNOLDS STRESS
The structure of supersonic turbulent boundary layers subjected to concave surface curvature N90-15883
RHEOLOGY
Interdisciplinary research in viscoelasticity and rheology
[AD-A213630] N90-16145
RICCATI EQUATION
The algebraic Riccati equation and singular optimal control
[MEMO-COSOR-89-11] N90-16467
ROBOT ARMS
A knowledge-based machine vision system for space station automation N90-16221
On-line estimation of mechanical nonlinearities in compliant two-link robot manipulators N90-16280
ROBOT DYNAMICS
Mathematical model for adaptive control system of ASEA robot at Kennedy Space Center N90-16701
ROBOTICS
Visual Information Processing for Television and Telerobotics
[NASA-CP-3053] N90-16204
Connectionist model-based stereo vision for telerobotics N90-16224
Expert system control of a six-legged walking telerobot
[DE90-004661] N90-16285

Interpretation of CAD (Computer Aided Design) models through IGES (Initial Graphics Exchange Specification) interface
[PB90-121294] N90-16441
Plant features measurements for robotics N90-16695
Off-line robot programming and graphical verification of path planning N90-16699
Mathematical model for adaptive control system of ASEA robot at Kennedy Space Center N90-16701

ROBOTS
Bilateral force reflection for teleoperators with masters and slaves with dissimilar and possibly redundant kinematics
[DE90-004392] N90-16132
Visual Information Processing for Television and Telerobotics
[NASA-CP-3053] N90-16204
Examples of robots and teleoperators at the Savannah River Site
[DE90-004659] N90-16284
Expert system control of a six-legged walking telerobot
[DE90-004661] N90-16285
Off-line robot programming and graphical verification of path planning N90-16699
Mathematical model for adaptive control system of ASEA robot at Kennedy Space Center N90-16701

ROCKET ENGINE CASES
Advanced composite polar boss
[AD-D014287] N90-15994
Burst pressure prediction of metallic/fibre reinforced rocket motor cases using an elasto-plastic instability analysis
[RARDE-1/89] N90-15997

ROCKET LAUNCHING
Tracking flares
[ISBN-0-642-13583-5] N90-16080
Modeling the near acoustic field of a rocket during launch N90-16694

ROCKET NOZZLES
Advanced composite polar boss
[AD-D014287] N90-15994

ROCKET VEHICLES
Rocket-triggered lightning strikes and forest fire ignition N90-16690

ROCKET-BORNE INSTRUMENTS
Metal vaporisers: Bicentennial series of five historical monographs
[ISBN-0-642-13584-3] N90-16081

ROLLING
Production and processing of Cu-Cr-Nb alloys
[NASA-TM-102495] N90-16053

ROTARY WING AIRCRAFT
A survey of nonuniform inflow models for rotorcraft flight dynamics and control applications
[NASA-TM-102219] N90-15938

ROTARY WINGS
Calculation of the flow field of a multiblade helicopter rotor using a Euler method including the wake N90-16189

ROTATING FLUIDS
Response of a rotating finite annular liquid layer to axial excitation
[LRT-WE-9-FB-15(1988)] N90-16090
Laboratory studies of isolated eddies in a rotating fluid
[AD-A213903] N90-16146
Superflow induced phase transition in the axial vortex-free texture of rotating superfluid He-3-B
[PB90-110388] N90-16531

ROTATION
Rotating Doppler frequency shifter
[AD-D014279] N90-16475

ROTORS
Dynamic analysis of geared rotors by finite elements
[NASA-TM-102349] N90-16286

ROUGHNESS
Investigation of rough elastohydrodynamic contact
[ISAL-89-0029] N90-16281

RUN TIME (COMPUTERS)
CPU timing routines for a CONVEX C220 computer system
[NASA-CR-181950] N90-16424

RUNWAY CONDITIONS
Evaluation of two transport aircraft and several ground test vehicle friction measurements obtained for various runway surface types and conditions. A summary of test results from joint FAA/NASA Runway Friction Program
[NASA-TP-2917] N90-15902

RUNWAYS
Crew emergency return vehicle autoland feasibility study
[NASA-CR-181940] N90-15937

RUTHENIUM
Electrochemical parameterization of metal complex redox potentials, using the ruthenium(III)/ruthenium(II) couple to generate a ligand electrochemical series
[AD-A214439] N90-16015

RYDBERG SERIES
Determination of hyperfine structures and Rydberg convergence limits of selected optical transitions in Nb-93 using resonance ionization spectroscopy
[PB90-110719] N90-16498

S

SAFETY
Aircraft accident report: Delta Air Lines, Inc., Boeing 727-232, N473DA, Dallas-Fort Worth International Airport, Texas, August 31, 1988
[PB89-910406] N90-15895
Cryogenic engineering and materials N90-15949
Safety and cryogenic wind tunnels N90-15960
Energy management and recovery N90-15962
Environmental, health, and safety concerns associated with nonpetroleum fuel use in US transportation
[DE90-004367] N90-16362

SAFETY DEVICES
Helmet-mounted head restraint
[AD-D014233] N90-16394

SAFETY FACTORS
Safety and rescue during STS operations N90-15975
Assured crew return capability architecture N90-15977
Crew safety and rescue aids N90-15980
NASDA's approach to the interoperability of safety and rescue in space N90-15981
MANPRINT (Manpower and Personnel Integration) evaluation: AN/TRC-170 digital troposcatter radio system
[AD-A211799] N90-16100
The SMITE approach to security
[RSRE-89014] N90-16404

SAMPLING
Linear digital imaging system fidelity analysis N90-16205
Analysis of organic compounds in returned comet nucleus samples N90-16617
Candidate sample acquisition systems for the Rosetta N90-16635
Methods for the mineralogical and textural analysis of comet nucleus samples N90-16648

SANDWICH STRUCTURES
Open-mode delamination stress concentrations in horseshoe and elliptic composite curved bars subjected to end forces
[NASA-TM-4164] N90-16004

SATELLITE ALTIMETRY
Regional height determination using gravimetric and topographical data
[UH-156] N90-16315

SATELLITE COMMUNICATION
Tactical UK military satellite ground terminals: A research and development review
[RSRE-MEMO-4262] N90-15972
X-band atmospheric attenuation for an Earth terminal measurement system
[PB90-100736] N90-16101
Helsinki University of Technology Radio Laboratory
[PB90-110677] N90-16102

SATELLITE CONFIGURATIONS
Pulsed plasma mission endurance test
[AD-A213462] N90-15993

SATELLITE IMAGERY
Ice floe identification in satellite images using mathematical morphology and clustering about principal curves
[AD-A213854] N90-16311
Quantitative evaluation of object-changes in multitemporal AGRISAR imagery
[FIM-195] N90-16314

SATELLITE NETWORKS
World Weather Watch. Global observing system-satellite sub-system. Information on meteorological and other environmental satellites, second edition
[WMO-411-ED-2] N90-16386

SATELLITE OBSERVATION
Science plan for the Alaska SAR facility program. Phase 1: Data from the first European sensing satellite, ERS-1
[NASA-CR-185028] N90-16312
Use of remote sensing data for land and building statistics N90-16335
Support of hydrological models calculations by satellite data N90-16337
Scientific investigations of the Space Research Group
[ISBN-0-642-13252-6] N90-16595

SATELLITE ORBITS
On mean elements for satellite orbits perturbed by the zonal harmonics of the geopotential
[RAE-TM-SPACE-371] N90-15971

SATELLITE SOUNDING
Mesoscale analysis by numerical modelling coupled with satellite-based sounding N90-16370

SATELLITE-BORNE PHOTOGRAPHY
Satellite image sequences for motion analysis and change detection N90-16323
Preliminary experiences with a novel method for the determination of displacement vector fields and satellite image sequences N90-16324

SCALE EFFECT
Scaling study for SP-100 reactor technology
[NASA-TM-897140] N90-16496

SCALERS
Double-periodic wormholes in theories with global symmetries
[DE90-719575] N90-16581

SCANNING TUNNELING MICROSCOPY
Scanning tunneling microscope studies of surface defects
[AD-A214121] N90-16543

SCATTERING
Isotope driven critical scattering and phase separation from mixtures of deuterated and protonated polymers
[DE90-003976] N90-16076
High-frequency asymptotic methods for analyzing the EM scattering by open-ended waveguide cavities
[NASA-CR-186244] N90-16103

SCATTERING AMPLITUDE
On the domain of string perturbation theory
[DE90-600759] N90-16575

SCATTERING COEFFICIENTS
Lidar technique for adjusting aerosol model number densities to existing conditions
[AD-A213846] N90-16374

SCATTERING CROSS SECTIONS
Studies of elastic scattering and cross sections of the C-12 + Si-28 system
[DE89-635990] N90-16486
Heavy ion inelastic scattering with a 4(pi) gamma detector
[DE90-002709] N90-16488
Neutrino oscillations: An essay in honor of Felix Boehm
[DE90-003223] N90-16491
A database of fragmentation cross section measurements applicable to cosmic ray propagation calculations
[NASA-CR-186328] N90-16681

SCENE ANALYSIS
High compression image and image sequence coding N90-16214
A knowledge-based machine vision system for space station automation N90-16221
Alvey MMI007. Object identification from 2D images: The RSRE contribution
[RSRE-MEMO-4277] N90-16428

SCHEDULING
Piloted simulation of a ground-based time-control concept for air traffic control
[NASA-TM-101085] N90-15898
Dynamically allocating sets of fine-grained processors to running computations N90-16447
International conference management N90-16583
Experiences with knowledge-base and large database integration
[DE90-000686] N90-16591

SCHWARZSCHILD METRIC
On quantum effects near a black hole singularity
[DE90-600754] N90-16668

SCIENTISTS
Reports of planetary astronomy, 1986
[NASA-TM-100776] N90-16596

SCINTILLATION COUNTERS
A low-threshold EAS (Extensive-Air-Shower) array for gamma-ray astronomy at Los Alamos
[DE89-016780] N90-16600
Status of the expansion of the CYGNUS array at Los Alamos
[DE89-016781] N90-16601

SCUTUM CONSTELLATION
Pulsations of delta Scuti stars
[DE90-003213] N90-16598

SEA BREEZE
Verification study of a three-dimensional local scale atmospheric model PHYSIC at seacoast region
[DE90-719560] N90-16384

SEALERS
The effect of primer age on adhesion of polysulphide sealant N90-15909
Improved performance polysulfide based sealant N90-15910

Fuel resistant coatings for metal and composite fuel tanks N90-15911

SEALING

Integral fuel tank sealing practice at British Aerospace (Kingston) N90-15905

The repair of aircraft integral fuel tanks in the RAF: A user's view of fuel tank technology N90-15908

Fuel resistant coatings for metal and composite fuel tanks N90-15911

Spray sealing: A breakthrough in integral fuel tank sealing technology N90-15912

Design philosophy and construction techniques for integral fuselage fuel tanks N90-15913

Integral fuel tank certification and test methods N90-15916

SEALS (STOPPERS)

On the selection of materials for cryogenic seals and the testing of their performance N90-16696

SEASAT PROGRAM

Investigation of the backscatter behavior of selected test areas in two geocoded SEASAT-SAR scenes in greater Bonn (Fed. Republic of Germany) N90-16331

SEASAT SATELLITES

Parallel algorithm for determining motion vectors in ice floe images by matching edge features N90-16451

SEISMOLOGY

Summaries of physical research in the geosciences [DE90-004993] N90-16309

Proceedings of the 79th SEGJ Conference [DE89-760006] N90-16704

SELECTIVE DISSEMINATION OF INFORMATION

The SMITE approach to security [RSRE-89014] N90-16404

SELENIUM COMPOUNDS

New electrically conducting solids based on nickel(II) - bis(1,3-dithiole-2-thione-4,5-diselenolate) [DE90-003788] N90-16020

SELF ORGANIZING SYSTEMS

User interaction with self-learning systems [AD-A214280] N90-16395

SELF SEALING

Spray sealing: A breakthrough in integral fuel tank sealing technology N90-15912

SELF TESTS

Built in test of folded PLAs [IMAG-RR-758-I] N90-16134

SEMICONDUCTOR DEVICES

Very low energy ignition of pyrotechnics using a Semiconductor Bridge (SCB) [DE90-002645] N90-16082

Theory of the electronic and optical properties of semiconductor heterostructures [AD-A214132] N90-16544

SEMICONDUCTOR DIODES

Optical flow measuring method using diode lasers, phase coupled arrays, and high frequency pulsed diode lasers N90-16176

SEMICONDUCTOR LASERS

Optical flow measuring method using diode lasers, phase coupled arrays, and high frequency pulsed diode lasers N90-16176

Distance measurement using laser diodes [ETN-90-96144] N90-16264

SEMICONDUCTORS (MATERIALS)

Slow positron defect profiling of silicon epilayers [DE90-003958] N90-16288

Resonance enhanced Raman studies of as-grown and laser-processed HgCdTe [AD-A213855] N90-16540

Reflection technique for thermal mapping of semiconductors [AD-D014263] N90-16541

Group 2 cubic fluorides as dielectrics for III-V compound semiconductors [AD-A214096] N90-16542

SEPARATED FLOW

Flows with Separation [DGLR-PAPERS-88-05] N90-16169

An interactive method for the flow calculation of airfoils with local separation regions N90-16190

Calculation of the flap profile flows with separation based on coupled potential and boundary layer solutions N90-16191

Inverse solutions for boundary layers with separation or close to separation under locally infinite swept wing conditions N90-16192

Periodically unsteady effects on profiles, induced by separation N90-16196

Determination of the heat transfer coefficients in separated flows using an infrared camera N90-16257

SEQUENCING

Preliminary experiences with a novel method for the determination of displacement vector fields and satellite image sequences N90-16324

SERVICE LIFE

Cycle-life improvement of Zn/NiOOH cells by the addition of Ca(OH)2 to the zinc electrode [DE90-004040] N90-16139

SET THEORY

The algebraic Riccati equation and singular optimal control [MEMO-COSOR-89-11] N90-16467

SEYFERT GALAXIES

Ion-heated thermal Comptonization models and x ray spectral correlations in active galactic nuclei [DE90-003597] N90-16667

SHAFTS (MACHINE ELEMENTS)

Continuously variable gear drive transmission [AD-D014268] N90-16275

SHAPES

Stripline feed for a microstrip array of patch elements with teardrop shaped probes [NASA-CASE-NPO-17548-1-CU] N90-16104

The development of two-dimensional object identification techniques [NASA-CR-186203] N90-16408

Comments on comet shapes and aggregation processes N90-16622

SHARP LEADING EDGES

Numerical simulation of the laminar and turbulent three dimensional flow on a delta wing with sharp leading edge N90-16186

SHEAR PROPERTIES

Stress analysis of the Princeton Plasma Physics Laboratory 1/2- x 1/2-inch shear/compression test fixture [DE90-004401] N90-16512

SHEAR STRENGTH

Effects of high rate shear on the microstructure and deformation and fracture behavior of two high strength steels [AD-A214107] N90-16032

SHEAR STRESS

The structure of supersonic turbulent boundary layers subjected to concave surface curvature N90-15883

Colinear fluctuating wall shear stress and fluctuating pressure transducer [AD-D014296] N90-16226

Surface flow visualization with shear stress sensitivive liquid crystals [DNW-WTI-88.039] N90-16255

SHOCK ABSORBERS

An introduction to shaker shock simulations [DE90-003057] N90-16298

SHOCK FRONTS

Shock thickness measurements with laser beams [MPIS-7/1989] N90-16267

SHOCK LAYERS

Demonstration of the feasibility of laser induced fluorescence for arc jet flow diagnostics [NASA-CR-185595] N90-16013

A numerical and experimental investigation of multiple shock wave/turbulent boundary layer interactions in a rectanular duct N90-16141

SHOCK MEASURING INSTRUMENTS

Shock thickness measurements with laser beams [MPIS-7/1989] N90-16267

SHOCK WAVE INTERACTION

Flow separation in shock wave boundary layer interactions at hypersonic speeds [NASA-CR-4274] N90-15885

Automatic control of cryogenic wind tunnels N90-15957

Anomalous waves in shock wave - fluid interface collisions [AD-A213584] N90-16144

Turbulent stripping of interstellar clouds by interaction with supernova remnants [DE90-003622] N90-16674

SHOCK WAVES

Shock-induced reaction synthesis of aluminides and silicides [DE90-003948] N90-16066

A numerical and experimental investigation of multiple shock wave/turbulent boundary layer interactions in a rectanular duct N90-16141

Anomalous waves in shock wave - fluid interface collisions [AD-A213584] N90-16144

An introduction to shaker shock simulations [DE90-003057] N90-16298

Accretion shock geometries in the magnetic variables [NASA-CR-186290] N90-16664

SHUTTLE DERIVED VEHICLES

Round trip to orbit. Human spaceflight alternatives: Special report [OTA-ISC-419] N90-15966

SHUTTLE IMAGING RADAR

Necessity and benefit of the X-SAR Space Shuttle experiment [ESA-TT-1164] N90-16112

SIGNAL DETECTION

Beamforming pre-processors for high discrimination algorithms [RSRE-MEMO-4304] N90-16429

SIGNAL FADING

Use of an HF active monitoring array in the presence of high level interference [BBC-RD-1989/7] N90-16096

SIGNAL PROCESSING

Use of an HF active monitoring array in the presence of high level interference [BBC-RD-1989/7] N90-16096

Satellite broadcasting: Requirements for the receiving antenna [BBC-RD-1989/5] N90-16098

Method for eliminating self-screening noise jamming in radar systems [AD-D014271] N90-16105

Knowledge-based imaging-sensor fusion system N90-16220

A programmable image compression system N90-16222

Apparatus for imaging deep arterial and coronary lesions [NASA-CASE-NPO-17439-1-CU] N90-16391

Restoring force method and response estimation [DE90-002394] N90-16463

A computational and experimental study of steady and transient acoustic energy flow from a complex mechanical structure N90-16478

High speed signal extraction using electro-optic techniques [AD-A214446] N90-16500

SIGNAL REFLECTION

Rotating Doppler frequency shifter [AD-D014279] N90-16475

SIGNAL TRANSMISSION

Low-altitude millimeter-wave propagation in the evaporation duct [AD-A214432] N90-16108

SIGNATURE ANALYSIS

Issues and approaches for electronic document approval and transmittal using digital signatures and text authentication: Prototype documentation [DE90-003382] N90-16119

SILICIDES

Shock-induced reaction synthesis of aluminides and silicides [DE90-003948] N90-16066

SILICON

Theoretical studies of chemisorption and surface reactions on nickel and silicon [DE90-004849] N90-16050

Silicon-based coatings on niobium metal [DE90-003651] N90-16057

Pairs of chalcogen impurities in silicon [DE89-635767] N90-16063

Silicon membrane formation [DE90-003022] N90-16064

Slow positron defect profiling of silicon epilayers [DE90-003958] N90-16288

Heteroepitaxy of GaAs on Si: Methods to decrease the defect density in the epilayer [DE90-004028] N90-16551

SILICON ALLOYS

Spectral sensitivity of device power output for tandem a-Si alloy solar cells [DE89-009421] N90-16340

SILICON CARBIDES

Analytical study on the decreasing method of thermal stress for ceramic gas turbines [DE90-734934] N90-16078

The 1MeV-electron irradiation induced defects in epitaxially grown 3C-SiC [DE90-719574] N90-16554

SILICON DIOXIDE

Characterization of B and N implanted fused silica [DE90-004198] N90-16069

SILICON ISOTOPES

Studies of elastic scattering and cross sections of the C-12 + Si-28 system [DE89-635990] N90-16486

SILICON NITRIDES

Study of silicon nitride pH response to the fabrication of microelectronic sensors [LAAS-89229] N90-16023

Cyclic fatigue of hot-isostatic-pressed silicon nitride [PB90-122649] N90-16308

SILOXANES

The structure of silica-polysiloxane composites and its effects on their elastomeric properties [DE89-014768] N90-16005

SILVER
Long term creep strength of silver alloyed copper
[DE90-602367] N90-16039
SIMD (COMPUTERS)
The 2nd Symposium on the Frontiers of Massively Parallel Computations
[NASA-TM-101918] N90-16442
How to cluster in parallel with neural networks N90-16443
Overview and extensions of a system for routing directed graphs on SIMD architectures N90-16444
Sort computation N90-16446
Scan line graphics generation on the massively parallel processor N90-16450
SIMULATION
Hybrid LZW compression N90-16223
Load-shortening behavior of an initially curved eccentrically loaded column
[NASA-TM-101643] N90-16293
An introduction to shaker shock simulations
[DE90-003057] N90-16296
Numerical simulation of creep crack growth experiments
[IWM-W-4/88] N90-16303
Stochastic simulation of charged particle transport on the massively parallel processor N90-16448
Complex availability problems solved with simulation
[DE89-012610] N90-16459
Modifications of comet materials by the sublimation process: Results from simulation experiments N90-16621
Radiation modification of cometary materials: Laboratory simulations N90-16626
Thermal histories of the samples of two KOSI comet nucleus simulation experiments N90-16645
SINGLE CRYSTALS
Eurolaser. High power excimer laser: Optical crystals
[ETN-90-95901] N90-16558
The effects of oxygen and strontium vacancies on the superconductivity of single crystals of Bi2Sr(2-x)CuO(6-y)
[DE90-004242] N90-16561
SINGULARITY (MATHEMATICS)
Using the singularity-separating method to study how to decrease the pressure at the end of a tube
[PREPRINT-490] N90-16158
Theory of singular Lagrangians
[DE90-600735] N90-16456
On quantum effects near a black hole singularity
[DE90-600754] N90-16668
SINTERING
ZrO2 sintered compact and method for its production
[DE90-004125] N90-16006
Synthesis of air-sinterable lanthanum chromite powders
[DE90-004681] N90-16049
SIZE DISTRIBUTION
The in-situ cometary particulate size distribution measured for one comet: P/Halley N90-16637
SKIN (STRUCTURAL MEMBER)
A dynamicist's view of fuel tank skin durability N90-15915
SKIN FRICTION
Test techniques for cryogenic wind tunnels N90-15952
SLENDER BODIES
Improved tangent-cone method for the Aerodynamic Preliminary Analysis System (APAS) version of the hypersonic arbitrary-body program
[NASA-TM-4165] N90-15890
SLIDING
Quick disconnect duct coupler
[AD-D014265] N90-16274
SLIDING FRICTION
Investigation of rough elastohydrodynamic contact
[ISAL-89-0029] N90-16281
A quantitative analysis of slip phenomena along a dry contact surface between two bodies in comparison to interfacial crack propagation
[ISAL-89-0032] N90-16304
SMOKE
Ambient flow studies and particulate collection measurements: A laminar flow, reduced entrainment electrostatic precipitator
[DE90-001457] N90-16149
Visualization of gas flows using the smoke wire technique N90-16242
SMOOTHING
Numerical analysis of nonstationary fluid flow (a survey)
[PREPRINT-492] N90-16159
SNOW
Recognition and distinction of clouds, snow, and ice using AVHRR data N90-16322
SOFTWARE ENGINEERING
Using the singularity-separating method to study how to decrease the pressure at the end of a tube
[PREPRINT-490] N90-16158
The Suprenum architecture and its application to computational fluid dynamics
[GMD-389] N90-16161
The new programming
[RSRE-MEMO-4249] N90-16425
Low-cost volumetric modeling
[CRIF-MC-85] N90-16435
Software dependability growth characterization, modeling and evaluation
[LAAS-89320] N90-16437
NASA/ASEE Summer Faculty Fellowship Program
[NASA-CR-166837] N90-16686
Formalisms for user interface specification and design N90-16687
SOFTWARE TOOLS
The application of Z to the specification of air traffic control systems. 1: An initial specification of the radar processing activity
[RSRE-MEMO-4280] N90-15900
The new programming
[RSRE-MEMO-4249] N90-16425
A persistent heap for ALGOL 68
[RSRE-MEMO-4268] N90-16427
Tool support for the production of high integrity software
[RSRE-89005] N90-16433
A computer program to calculate the population numbers of multi-level species
[IFSI-89-15] N90-16671
SOIL SCIENCE
Utilization of remote sensing in geoscientific development and projects N90-16334
Statistical information system for cultivation of the soil. Use of remote sensing in official statistics N90-16338
SOILS
Attempt to draw conclusions concerning the geological subsoil from the vegetation using digital image processing of TM data N90-16329
Estimating water flow through a hillslope using the massively parallel processor N90-16449
SOL-GEL PROCESSES
Development of low density silica aerogel as a capture medium for hyper-velocity particles
[NASA-CR-185930] N90-16489
SOLAR CELLS
Spectral sensitivity of device power output for tandem a-Si alloy solar cells
[DE89-009421] N90-16340
Radiation resistance of solar cells for space application. 1: Study on the irradiation procedure of electron beams
[DE90-719546] N90-16349
SOLAR COLLECTORS
Chromatic dispersion compensation in a Fresnel lens by means of a diffraction grating
[DE90-004030] N90-16506
SOLAR CORONA
Solar nebula condensates and the composition of comets N90-16634
SOLAR ENERGY
SERI (Solar Energy Research Institute) solar radiation resource assessment project
[DE89-009456] N90-16352
SOLAR ENERGY CONVERSION
SERI (Solar Energy Research Institute) solar radiation resource assessment project
[DE89-009456] N90-16352
SOLAR FLARES
Determination of solar flare accelerated ion angular distributions from SMM gamma ray and neutron measurements and determination of the He-3/H ratio in the solar photosphere from SMM gamma ray measurements
[NASA-CR-186038] N90-16676
SOLAR INTERIOR
A look on non-standard solar models
[SER-C-PREPUBL-FASC-40] N90-16677
SOLAR NEIGHBORHOOD
Mass functions for eight galactic clusters in the solar neighborhood N90-16660
SOLAR NEUTRINOS
Neutrino oscillations: An essay in honor of Felix Boehm
[DE90-003223] N90-16491
SOLAR RADIATION
SERI (Solar Energy Research Institute) solar radiation resource assessment project
[DE89-009456] N90-16352
Climatic summaries and documentation for the primary meteorological Station, H. J. Andrews Experimental Forest, 1972 to 1984
[PB90-104373] N90-16382
A look on non-standard solar models
[SER-C-PREPUBL-FASC-40] N90-16677
Galactic cosmic-ray modulation and solar-terrestrial relationships
[IFSI-88-17] N90-16679
SOLAR RADIO BURSTS
Natural and man-made emissions at 1.0 to 5.6 MHz measured between 10 and 18 R sub E
[MPE-PREPRINT-146] N90-16116
SOLAR SYSTEM
Non-equilibrium chemistry in the solar nebula and early solar system: Implications for the chemistry of comets N90-16618
SOLAR TERRESTRIAL INTERACTIONS
Galactic cosmic-ray modulation and solar-terrestrial relationships
[IFSI-88-17] N90-16679
SOLAR WIND
Some properties of so-called magnetic cloud structures in the solar wind
[IFSI-88-16] N90-16678
SOLID ELECTROLYTES
Solid-state electrolyte catalysis for methane and oxygen synthesis
[PB90-100231] N90-16011
Development of planar geometry solid oxide fuel cells
[PB90-100769] N90-16341
SOLID LUBRICANTS
Molybdenum disulfide-molybdenum oxide lubricants
[AD-D014253] N90-16059
SOLID MECHANICS
Element-by-element preconditioning techniques for large-scale, vectorized finite element analysis in nonlinear solid and structural mechanics N90-16291
SOLID PROPELLANT COMBUSTION
Solid fuel combustion chamber, phase 10
[LR-536] N90-16000
Solid fuel combustion chamber
[LR-555] N90-16001
Application of the singularity-separating method to computing problems of solid-propellant combustion in a closed vessel
[PREPRINT-489] N90-16086
SOLID PROPELLANTS
Pulsed plasma mission endurance test
[AD-A213462] N90-15993
SOLID STATE
Solid-state electrolyte catalysis for methane and oxygen synthesis
[PB90-100231] N90-16011
Steep front impulse tests on a solid-state relay
[DE90-004243] N90-16140
Solid state voltammetry and sensors in solids and gases
[DE90-003234] N90-16538
Solid state, surface, and catalytic studies of oxides
[DE90-004850] N90-16566
SOLID STATE LASERS
Eurolaser definition phase, solid state lasers working group: Active medium, laser active crystals
[ETN-90-95899] N90-16266
SOLID SURFACES
Surface topography measurements over the 1 meter to 10 micrometer spatial period bandwidth
[DE90-003642] N90-16501
SOLID-SOLID INTERFACES
The influence of residual contamination on the structure and properties of metal/GaAs interfaces
[DE90-000549] N90-16530
SOLIDIFICATION
High temperature aluminum-base alloy
[AD-D014270] N90-16028
SOLIDS
Refractory solids in chondrites and comets: How similar N90-16654
SOLUBILITY
Solid state voltammetry and sensors in solids and gases
[DE90-003234] N90-16538
SOUND FIELDS
Modeling the near acoustic field of a rocket during launch N90-16694
SOUND GENERATORS
Modeling the near acoustic field of a rocket during launch N90-16694
SOUND PRESSURE
Modeling the near acoustic field of a rocket during launch N90-16694
SOUND WAVES
SAW (Surface Acoustic Wave) transducer with improved bus-bar design
[AD-D014250] N90-16125
Measurement of reflection and impedance in a beam by the structural intensity technique
[DE90-728212] N90-16299

A computational and experimental study of steady and transient acoustic energy flow from a complex mechanical structure N90-16478

SOUNDING

Operational ozone monitoring with the Global Ozone Monitoring Radiometer (GOMR) [PB90-114034] N90-16359

SOUNDING ROCKETS

Flight experiment hardware for sounding rocket investigations. Materials science and fluid sciences [ESA-SP-1116] N90-15998

From small beginnings... The story of ESRO's sounding rocket programme in celebration of the twenty-fifth anniversary of the first ESRO sounding rocket launch [ESA-BR-60] N90-15999

SPACE COLONIES

The first 1000 days of a future lunar base [ILR-MITT-224] N90-15970

SPACE ENVIRONMENT SIMULATION

Hollow-cathode experiments to support electrodynamic tether applications [IFSI-89-5] N90-15986

SPACE EXPLORATION

Reports of planetary astronomy, 1986 [NASA-TM-100776] N90-16596

SPACE FLIGHT

A foundation for the design of an astronautics specification system based on dynamic motivation analysis [ILR-MITT-220] N90-15969

SPACE FLIGHT TRACKING AND DATA NETWORK

GPS network analysis: The influence of stochastic prior information of orbital elements on ground station position measures [TR-4-1988] N90-15901

SPACE MISSIONS

NASDA's approach to the interoperability of safety and rescue in space N90-15981

SPACE PLASMAS

The dynamics of dust in planetary magnetospheres N90-16658

SPACE PLATFORMS

The effects of natural and enhanced Van Allen Belt radiation on a space based weapon platform [DE89-016219] N90-16685

SPACE POWER REACTORS

Dynamics analyses of space power systems using the salt code [DE90-002274] N90-15995

The onset of boiling of the liquid alkali metals [DE90-002276] N90-16036

Low risk low power heat pipe/thermoelectric space power supply [DE89-014817] N90-16342

Scaling study for SP-100 reactor technology [NASA-TM-897140] N90-16496

SPACE PROGRAMS

Crew Safety and Rescue in Space: An International Approach [ESA-SP-300] N90-15974

SPACE RENDEZVOUS

Crew Safety and Rescue in Space: An International Approach [ESA-SP-300] N90-15974

Systems interoperability approach Apollo/Soyuz test project N90-15979

RVD scenari and interfaces between Hermes and space station N90-15982

SPACE SHUTTLE ORBITERS

Conceptual design of a moving belt radiator shuttle-attached experiments: Technical requirement Document [NASA-CR-185168] N90-15996

SPACE SHUTTLES

Safety and rescue during STS operations N90-15975

New atmospheric turbulence model for shuttle applications [NASA-TM-4168] N90-16389

Artificial intelligence in process control: Knowledge base for the shuttle ECS model N90-16697

SPACE SIMULATORS

Thermal histories of the samples of two KOSI comet nucleus simulation experiments N90-16645

Mechanical and SEM analysis of artificial comet nucleus samples N90-16650

SPACE STATION STRUCTURES

A modular habitation unit adapted for service in low earth and geostationary earth orbits [ILR-MITT-217] N90-15990

SPACE STATIONS

RVD scenari and interfaces between Hermes and space station N90-15982

Conceptual design for the space station Freedom modular combustion facility [NASA-TM-102037] N90-16087

A knowledge-based machine vision system for space station automation N90-16221

SPACE SUITS

EVA space suit. General concepts of design and arrangement N90-15976

SPACE TECHNOLOGY EXPERIMENTS

Laboratory of Space Technology [PB90-110651] N90-15967

SPACE TEMPERATURE

Vibration damping composition suitable for outer space temperature variations [AD-D014288] N90-16296

SPACE TRANSPORTATION

Round trip to orbit. Human spaceflight alternatives: Special report [OTA-ISC-419] N90-15966

SPACE TRANSPORTATION SYSTEM

Study of metal corrosion using ac impedance techniques in the STS launch environment N90-16688

SPACE WEAPONS

The effects of natural and enhanced Van Allen Belt radiation on a space based weapon platform [DE89-016219] N90-16685

SPACE-TIME FUNCTIONS

Quantum fields in cosmological space-times: A soluble example [DE89-616837] N90-16662

SPACEBORNE EXPERIMENTS

Flight experiment hardware for sounding rocket investigations. Materials science and fluid sciences [ESA-SP-1116] N90-15998

Experiment facilities for materials and fluid sciences embarked on Spacelab [ESA-SP-1120] N90-16089

SPACECRAFT CONTROL

Pulsed plasma mission endurance test [AD-A213462] N90-15993

Assessment of visual function in aerospace medicine [BMVG-FBWM-89-5] N90-16397

SPACECRAFT DEFENSE

Defense to laser light irradiation [AD-D014286] N90-15984

SPACECRAFT DESIGN

Crew emergency return vehicle autoland feasibility study [NASA-CR-181940] N90-15937

Round trip to orbit. Human spaceflight alternatives: Special report [OTA-ISC-419] N90-15966

NASDA's approach to the interoperability of safety and rescue in space N90-15981

The Gevaltig: An inertial fusion powered manned spacecraft design for outer solar system missions [NASA-CR-185163] N90-15985

SPACECRAFT DOCKING

Crew Safety and Rescue in Space: An International Approach [ESA-SP-300] N90-15974

Systems interoperability approach Apollo/Soyuz test project N90-15979

RVD scenari and interfaces between Hermes and space station N90-15982

SPACECRAFT ENVIRONMENTS

A modular habitation unit adapted for service in low earth and geostationary earth orbits [ILR-MITT-217] N90-15990

Study of metal corrosion using ac impedance techniques in the STS launch environment N90-16688

Artificial intelligence in process control: Knowledge base for the shuttle ECS model N90-16697

SPACECRAFT MODELS

Artificial intelligence in process control: Knowledge base for the shuttle ECS model N90-16697

SPACECRAFT POWER SUPPLIES

Conceptual design of a moving belt radiator shuttle-attached experiments: Technical requirement Document [NASA-CR-185168] N90-15996

SPACECRAFT PROPULSION

Design of a thrust stand for high power electric propulsion devices [NASA-TM-102372] N90-15992

SPACECRAFT RADIATORS

Conceptual design of a moving belt radiator shuttle-attached experiments: Technical requirement Document [NASA-CR-185168] N90-15996

Expandable radiator [AD-D014258] N90-16147

SPACECRAFT SHIELDING

Material responses to incident x rays [DE89-015366] N90-16305

SPACECREWS

The first 1000 days of a future lunar base [ILR-MITT-224] N90-15970

Crew Safety and Rescue in Space: An International Approach [ESA-SP-300] N90-15974

Assured crew return capability architecture N90-15977

On the selection of crewmember rescue means for manned space launch systems N90-15978

Crew safety and rescue aids N90-15980

SPACELAB

Experiment facilities for materials and fluid sciences embarked on Spacelab [ESA-SP-1120] N90-16089

Structural characterization of Spacelab [ETN-90-95214] N90-16289

SPACING

Interplanar spacing for various phases in austenitic stainless steels [DE90-602350] N90-16038

SPALLATION

Proceedings of the specialists' meeting on physics and engineering of fission and spallation [DE90-719706] N90-16519

SPARK MACHINING

Electrode/workpiece combinations [DE90-003919] N90-16095

SPATIAL FILTERING

Neural networks for data compression and invariant image recognition N90-16219

SPATIAL RESOLUTION

Context dependent anti-aliasing image reconstruction N90-16209

Context dependent prediction and category encoding for DPCM image compression N90-16210

The determination of subscale structures in thermal images N90-16330

SPECIFICATIONS

Sizing and selection of batteries for stand-alone photovoltaic systems [DE90-002990] N90-16129

Eurolaser definition phase: A comparison of high power lasers available [ETN-90-96061] N90-16268

SPECTRA

Soft modes, freezing, and nonlinear response of a dipolar glass [DE90-003647] N90-16075

SPECTRAL CORRELATION

Ion-heated thermal Comptonization models and x ray spectral correlations in active galactic nuclei [DE90-003597] N90-16667

SPECTRAL REFLECTANCE

Cloud phase discrimination by near-infrared remote sensing N90-16310

SPECTRAL SENSITIVITY

Spectral sensitivity of device power output for tandem a-Si alloy solar cells [DE89-009421] N90-16340

SPECTRAL SIGNATURES

Use of the Egret instrument in studies of the origin of the cosmic radiation. 2: Spectral signatures of discrete cosmic-ray sources [DE90-003595] N90-16682

SPECTROMETERS

Design of a large superconducting spectrometer magnet [DE90-719505] N90-16553

SPECTROPHOTOMETRY

Laboratory analyses of micron-sized solid grains: Experimental techniques and recent results N90-16616

SPECTROSCOPIC ANALYSIS

Carbon-13 nuclear magnetic resonance of heterocyclic salts and its precursors [DE89-635768] N90-16016

Workshop on Analysis of Returned Comet Nucleus Samples [NASA-CR-184821] N90-16607

Analytical study of comet nucleus samples N90-16608

The origin, composition and history of cometary ices from spectroscopic studies N90-16609

Laboratory analyses of micron-sized solid grains: Experimental techniques and recent results N90-16616

Sulfur compounds in comets N90-16627

Organic chemistry of cometary dust as derived from PUMA 1 data N90-16628

Composition of dust from Comet P/Halley: The mineral fraction N90-16631

Handling and analysis of ices in cryostats and glove boxes in view of cometary samples N90-16643

Methods for the mineralogical and textural analysis of comet nucleus samples N90-16648

Electron Spin Resonance (ESR) studies of returned comet nucleus samples N90-16651

The measurement of trace elements in interplanetary dust and cometary particles by ultra-high sensitivity INAA N90-16656

SPECTROSCOPY
The origin, composition and history of cometary ices from spectroscopic studies N90-16609
Spectrophotometric observations of comet P/Giacobini-Zinner N90-16630
SPECTRUM ANALYSIS
Experimental investigation of a three-dimensional wake. Part 2: Spectral and turbulent energy analysis [ONERA-RT-32/5025-AYD-PT-2] N90-15887
Natural and man-made emissions at 1.0 to 5.6 MHz measured between 10 and 18 R sub E [MPE-PREPRINT-146] N90-16116
Spectroscopic diagnostics of high temperature plasmas [DE90-003912] N90-16522
SPEED REGULATORS
Continuously variable gear drive transmission [AD-D014268] N90-16275
SPHERES
Study of flow around a sphere in a hydraulic test tunnel [CERT-1/2313/MES] N90-16156
Multigrid methods for two- and three-dimensional Poisson-type equations on the sphere [GMD-391] N90-16468
Surface topography measurements over the 1 meter to 10 micrometer spatial period bandwidth [DE90-003642] N90-16501
SPHEROMAKS
Design of a spheromak compressor driven by high explosives [DE90-003652] N90-16283
Recent progress on the HESS (High Explosive Spheromak Source) experiment [DE90-003218] N90-16520
Progress with small, high-magnetic-field spheromaks in CTX [DE90-003395] N90-16527
MHD stable high beta spheromak equilibrium [DE90-004873] N90-16529
SPIN DYNAMICS
Electrochemical parameterization of metal complex redox potentials, using the ruthenium(III)/ruthenium(II) couple to generate a ligand electrochemical series [AD-A214439] N90-16015
SPLINES
Application of Lagrangian blending functions for grid generation around airplane geometries [NASA-CR-186318] N90-15891
SPONTANEOUS EMISSION
Atomic processes in plasmas under ultra-intense laser irradiation [DE90-003221] N90-16521
SPOT (FRENCH SATELLITE)
SPOT after two years in operation: An appraisal of results and a review of selected applications N90-16326
SPRAYERS
Spray sealing: A breakthrough in integral fuel tank sealing technology N90-15912
SPUTTERING
Lithium cobalt oxide thin film and its electrochromism [DE90-004570] N90-16564
Artificially structured superconductors [DE90-004851] N90-16567
SQUEEZED STATES (QUANTUM THEORY)
Multisqueezing of mechanical states and back-action evasion measurements [IFSI-89-6] N90-16504
STABILITY
Stability and fragmentation of ejecta in hypervelocity impact [DE90-004087] N90-16278
STAGNATION FLOW
Vorticity amplification in nonorthogonal stagnation flow N90-16152
STAINLESS STEELS
Stainless steel passivity [AD-A214108] N90-16033
Irradiation creep and swelling of annealed type 304L stainless steel at approximately 390 C and high neutron fluence [DE90-004521] N90-16047
STANDARDS
FRAG requirements for control of fatigue testing [RAE-TM-MAT/STR-1130] N90-16300
STAR CLUSTERS
Mass functions for eight galactic clusters in the solar neighborhood N90-16660
STAR FORMATION
Outflows in high mass star-forming regions N90-16657
STATE VECTORS
On the reciprocity of state vectors in boundary value models [AD-A214104] N90-16458
STATIC TESTS
Space shuttle Production Verification Motor 1 (PV-1) static fire [NASA-CR-183784] N90-15991
STATIONKEEPING
Pulsed plasma mission endurance test [AD-A213462] N90-15993
STATISTICAL ANALYSIS
Use of remote sensing data for land and building statistics N90-16335
Statistical information system for cultivation of the soil. Use of remote sensing in official statistics N90-16338
STATISTICAL CORRELATION
Statistics of a reflected laser beam in the turbulent atmosphere (path correlation) [PB90-113994] N90-16261
STEADY STATE
Euler and Navier-Stokes computations for two-dimensional geometries using unstructured meshes [NASA-CR-181977] N90-15893
A computational and experimental study of steady and transient acoustic energy flow from a complex mechanical structure N90-16478
STEAM
Experimental investigation of condensation of steam in the presence of noncondensable gases for open-cycle surface condensers [DE90-003552] N90-16353
STEAM FLOW
Experimental investigation of condensation of steam in the presence of noncondensable gases for open-cycle surface condensers [DE90-003552] N90-16353
STEELS
Experiences with three-point bending test specimens for determining the crack-arrest fracture toughness K(sub Ia) in low-alloy steel [DE90-004120] N90-16306
STEERING
Large angle off-axis beam steering of a phased telescope array [AD-D014269] N90-16127
STELLAR COLOR
New developments in stellar ages and modelling of Pop. I stars [SER-C-PREPUBL-FASC-41] N90-16669
STELLAR ENVELOPES
Metamorphism of cosmic dust: Processing from circumstellar outflows to the cometary regolith N90-16641
STELLAR EVOLUTION
Pulsations of delta Scuti stars [DE90-003213] N90-16598
New developments in stellar ages and modelling of Pop. I stars [SER-C-PREPUBL-FASC-41] N90-16669
A look on non-standard solar models [SER-C-PREPUBL-FASC-40] N90-16677
STELLAR MASS
Mass functions for eight galactic clusters in the solar neighborhood N90-16660
STELLAR MASS ACCRETION
Accretion shock geometries in the magnetic variables [NASA-CR-186290] N90-16664
STELLAR MODELS
Accretion shock geometries in the magnetic variables [NASA-CR-186290] N90-16664
New developments in stellar ages and modelling of Pop. I stars [SER-C-PREPUBL-FASC-41] N90-16669
A look on non-standard solar models [SER-C-PREPUBL-FASC-40] N90-16677
STELLAR PHYSICS
Some properties of so-called magnetic cloud structures in the solar wind [IFSI-88-16] N90-16678
STELLAR RADIATION
IUE-ULDA access guide no. 1: International Ultraviolet Explorer-Uniform Low Dispersion Archive. Dwarf novae and nova-like stars [ESA-SP-1114] N90-16672
STELLAR WINDS
Outflows in high mass star-forming regions N90-16657
STELLARATORS
ATF-2 studies [DE90-004380] N90-16510
Near-term directions in the world stellarator program [DE90-004381] N90-16511
STEREOSCOPIC VISION
Connectionist model-based stereo vision for telerobotics N90-16224
STOCHASTIC PROCESSES
The Eighteenth Conference on Stochastic Processes and their Applications [AD-A212301] N90-16010
Integrated geodetic network analysis with stochastic prior information about the gravity field and reference ellipsoid [SER-C-351] N90-16317
Stochastic simulation of charged particle transport on the massively parallel processor N90-16448
Stochastic action of dynamical systems on curved manifolds. The isokinetic developing map on trajectories [PREPRINT-666] N90-16466
Optimal step sizes in semi-stochastic approximation procedures [ETN-90-95888] N90-16469
Langmuir wave interaction with ion-sound one. Part 1: Stochastic effects [DE90-603368] N90-16474
STOICHIOMETRY
La(sub 2)MO(sub 4 + delta) (M = Cu, Ni, Co): Phase separation and superconductivity resulting from excess oxygen defects [DE90-001988] N90-16534
Lithium cobalt oxide thin film and its electrochromism [DE90-004570] N90-16564
STOKES FLOW
Extrapolation techniques for finite element approximations of Stokes and Navier-Stokes flow over a backward facing step [PREPRINT-499] N90-16160
STORAGE BATTERIES
Application of ac impedance method for diagnosis of lithium secondary battery degradation. Preliminary study with AA size Li/MoS2 cells [DE90-702474] N90-16137
STORMS (METEOROLOGY)
Diagnostic and kinematic fields associated with curved and straight jet streaks using a two-layer primitive equation model N90-16371
STRAIN DISTRIBUTION
Mechanical strain isolator mount [NASA-CASE-LAR-13580-1] N90-16272
STRAIN GAGE BALANCES
Experience with strain-gage balances for cryogenic wind tunnels N90-15958
Cryogenic balances for the US NTF N90-15959
STRAIN RATE
Irradiation creep and swelling of annealed type 304L stainless steel at approximately 390 C and high neutron fluence [DE90-004521] N90-16047
Fatigue life estimates for helicopter loading spectra [NASA-CR-181941] N90-16294
STRANDS
Design of coupled or uncoupled multifilamentary SSC-type strands with almost zero retained magnetization at fields near 0.3 T [DE90-005391] N90-16052
STRAPS
Helmet-mounted head restraint [AD-D014233] N90-16394
STRATOCUMULUS CLOUDS
The chemistry and dynamics of marine stratocumulus N90-16381
STRATOSPHERE
Environmental, health, and CFC substitution aspects of the ozone depletion issue [DE90-004404] N90-16363
The effect of orographic forcing on the mean flow of the stratosphere N90-16367
A double focussing mass-spectrometer for simultaneous ion measurements in the stratosphere [AERONOMICA-ACTA-A-350-1989] N90-16379
STRATOSPHERIC WARMING
The effect of orographic forcing on the mean flow of the stratosphere N90-16367
STRESS ANALYSIS
Burst pressure prediction of metallic/fibre reinforced rocket motor cases using an elasto-plastic instability analysis [RARDE-1/89] N90-15997
Stress analysis of the Princeton Plasma Physics Laboratory 1/2- x 1/2-inch shear/compression test fixture [DE90-004401] N90-16512
Design of a large superconducting spectrometer magnet [DE90-719505] N90-16553
STRESS CONCENTRATION
Open-mode delamination stress concentrations in horseshoe and elliptic composite curved bars subjected to end forces [NASA-TM-4164] N90-16004
STRESS CORROSION
Interplanar spacing for various phases in austenitic stainless steels [DE90-602350] N90-16038

STRESS-STRAIN RELATIONSHIPS
Improved solution techniques for the eigenstructure of fractional order systems
[AD-A213844] N90-16295
STRESSES
Material responses to incident x rays
[DE89-015366] N90-16305
STRING THEORY
The off-shell closed strings as the topological open membranes: Dynamical transmutation of world sheet dimension
[DE89-635721] N90-16571
On the domain of string perturbation theory
[DE90-600759] N90-16575
An estimation of the one-loop mass shifts in open superstring theory
[DE90-719578] N90-16582
STRONTIUM
The effects of oxygen and strontium vacancies on the superconductivity of single crystals of Bi2Sr(2-x)CuO(6-y)
[DE90-004242] N90-16561
STRONTIUM COMPOUNDS
Microstructures of Y123 films on SrTiO3, LaGaO3, and LaAlO3
[DE90-003367] N90-16537
STRUCTURAL ANALYSIS
Structural analysis of zirconium-aluminum plasma deposits
[ETCA-89-R-073] N90-16045
Interdisciplinary research in viscoelasticity and rheology
[AD-A213630] N90-16145
Element-by-element preconditioning techniques for large-scale, vectorized finite element analysis in nonlinear solid and structural mechanics N90-16291
Load-shortening behavior of an initially curved eccentrically loaded column
[NASA-TM-101643] N90-16293
Measurement of reflection and impedance in a beam by the structural intensity technique
[DE90-728212] N90-16299
STRUCTURAL DESIGN
Design philosophy and construction techniques for integral fuselage fuel tanks N90-15913
Unmanned air vehicles payloads and sensors N90-15930
Special Course on Advances in Cryogenic Wind Tunnel Technology
[AGARD-R-774] N90-15939
The European Transonic Windtunnel (ETW) N90-15945
The cryogenic Ludwieg tube tunnel at Goettingen N90-15947
Design of a thrust stand for high power electric propulsion devices
[NASA-TM-102372] N90-15992
Tracking flares
[ISBN-0-642-13583-5] N90-16080
Metal vaporisers: Bicentennial series of five historical monographs
[ISBN-0-642-13584-3] N90-16081
Conceptual design for the space station Freedom modular combustion facility
[NASA-TM-102037] N90-16087
Organic cathode for a secondary battery
[NASA-CASE-NPO-17604-1-CU] N90-16124
Sizing and selection of batteries for stand-alone photovoltaic systems
[DE90-002990] N90-16129
MHD stable high beta spheromak equilibrium
[DE90-004873] N90-16529
Design of a large superconducting spectrometer magnet
[DE90-719505] N90-16553
STRUCTURAL DESIGN CRITERIA
Analytical study on the decreasing method of thermal stress for ceramic gas turbines
[DE90-734934] N90-16078
Semi-empirical transition criteria for the design of laminar profiles N90-16174
Development of transition criteria on the basis of e to the N power for three dimensional wing boundary layers N90-16179
STRUCTURAL ENGINEERING
Aircraft fuel tank construction and testing experience N90-15907
STRUCTURAL STABILITY
Analysis and testing of axial compression in imperfect slender truss struts
[NASA-TM-4174] N90-16292
STRUCTURAL VIBRATION
Measurement of reflection and impedance in a beam by the structural intensity technique
[DE90-728212] N90-16299
STRUCTURAL WEIGHT
Scaling study for SP-100 reactor technology
[NASA-TM-897140] N90-16496
STRUTS
Analysis and testing of axial compression in imperfect slender truss struts
[NASA-TM-4174] N90-16292
SUBGROUPS
The algebraic Riccati equation and singular optimal control
[MEMO-COSOR-89-11] N90-16467
SUBLIMATION
The use of sublimation methods for the recognition of transition at low speed N90-16251
Modifications of comet materials by the sublimation process: Results from simulation experiments N90-16621
SUBMILLIMETER WAVES
The excess flux in the cosmic submillimeter background radiation and the primordial deuterium abundance
[NASA-CR-186312] N90-16683
SUBROUTINE LIBRARIES (COMPUTERS)
Basic mathematical function libraries for scientific computation
[NASA-TM-102256] N90-16423
SUBSTRATES
Improved performance polysulfide based sealant N90-15910
Heteroepitaxy of GaAs on Si: Methods to decrease the defect density in the epilayer
[DE90-004028] N90-16551
SUBSTRUCTURES
Design philosophy and construction techniques for integral fuselage fuel tanks N90-15913
SULFATES
Thermal expansion of LATGS crystals
[DE89-636239] N90-16546
SULFIDES
Molybdenum disulfide-molybdenum oxide lubricants
[AD-D014253] N90-16059
Researches on amorphous perovskite
[DE89-900733] N90-16535
SULFUR COMPOUNDS
Sulfur compounds in comets N90-16627
SULFUR DIOXIDES
The continuous crystallization of sulfur formed by the liquid-phase reaction of hydrogen sulfide and sulfur dioxide
[DE90-003991] N90-16018
SULFUR FLUORIDES
Measurement of the p, v, T behavior under microgram conditions
[ETN-90-95906] N90-16162
SUNSPOTS
Correlative analyses for geomagnetic indices, cosmic-ray intensities and sunspot numbers recorded since 1937
[IFSI-89-4] N90-16670
SUPERCONDUCTING FILMS
Microstructures of Y123 films on SrTiO3, LaGaO3, and LaAlO3
[DE90-003367] N90-16537
SUPERCONDUCTING MAGNETS
Design of a large superconducting spectrometer magnet
[DE90-719505] N90-16553
SUPERCONDUCTING SUPER COLLIDER
Properties and design of multifilamentary NbTi composite superconductors
[DE90-004904] N90-16569
SUPERCONDUCTIVITY
Rotational magnetic processes in YB2Cu3O7
[DE90-000541] N90-16533
La(sub 2)MO(sub 4 + delta) (M = Cu, Ni, Co): Phase separation and superconductivity resulting from excess oxygen defects
[DE90-001988] N90-16534
Structure-property correlations in the design of organic metals and superconductors: An overview
[DE90-003794] N90-16550
B-Factory Final Focus System using superconducting quadrupoles
[DE90-004432] N90-16552
Neutron experiments on high-temperature superconductors
[DE90-003978] N90-16559
Magnetic interactions in Sn-119 substituted for Cu in antiferromagnetic and superconducting lamellar cuprates
[DE90-003661] N90-16560
The effects of oxygen and strontium vacancies on the superconductivity of single crystals of Bi2Sr(2-x)CuO(6-y)
[DE90-004242] N90-16561
Physical properties of Bi2Sr2CuO6, the semiconducting phase, structurally distinct from the n = 1 Bi-cuprate superconductor
[DE90-004299] N90-16563
High temperature neutron diffraction study of the formation reaction of bismuth superconductors
[DE90-004883] N90-16568
Magnetic studies of proximity-effect coupling in a very closely spaced fine-filament NbTi/CuMn composite superconductor
[DE90-005387] N90-16570
SUPERCONDUCTORS
Design of coupled or uncoupled multifilamentary SSC-type strands with almost zero retained magnetization at fields near 0.3 T
[DE90-005391] N90-16052
Researches on amorphous perovskite
[DE89-900733] N90-16535
Magnetic interactions in Sn-119 substituted for Cu in antiferromagnetic and superconducting lamellar cuprates
[DE90-003661] N90-16560
Physical properties of Bi2Sr2CuO6, the semiconducting phase, structurally distinct from the n = 1 Bi-cuprate superconductor
[DE90-004299] N90-16563
Electron beam induced oxygen in YBa2Cu3O(7-x) superconductors
[DE90-004839] N90-16565
Properties and design of multifilamentary NbTi composite superconductors
[DE90-004904] N90-16569
Magnetic studies of proximity-effect coupling in a very closely spaced fine-filament NbTi/CuMn composite superconductor
[DE90-005387] N90-16570
SUPERCRITICAL FLOW
Calculation of turbulent choppy flow mixing
[ETN-90-95929] N90-16165
SUPERFLUIDITY
Superflow induced phase transition in the axial vortex-free texture of rotating superfluid He-3-B
[PB90-110388] N90-16531
SUPERHEATING
The onset of boiling of the liquid alkali metals
[DE90-002276] N90-16036
SUPERHIGH FREQUENCIES
X-band atmospheric attenuation for an Earth terminal measurement system
[PB90-100736] N90-16101
SUPERLATTICES
Heteroepitaxy of GaAs on Si: Methods to decrease the defect density in the epilayer
[DE90-004028] N90-16551
Fundamental issues in heteroepitaxy (condensed from the DOE panel report)
[DE90-003980] N90-16555
Artificially structured superconductors
[DE90-004851] N90-16567
SUPERNOVA REMNANTS
Turbulent stripping of interstellar clouds by interaction with supernova remnants
[DE90-003622] N90-16674
SUPERSONIC BOUNDARY LAYERS
The structure of supersonic turbulent boundary layers subjected to concave surface curvature N90-15883
SUPERSONIC FLOW
A numerical and experimental investigation of multiple shock wave/turbulent boundary layer interactions in a rectangular duct N90-16141
Calculation of two and three dimensional super and hypersonic flows by solving the Euler equations N90-16197
Lecture notes on supersonic molecular beam sources
[MPIS-20/1988] N90-16494
SUPERSONIC SPEED
A numerical and experimental investigation of multiple shock wave/turbulent boundary layer interactions in a rectangular duct N90-16141
SUPERSONIC TURBINES
Aerodynamic and heat transfer measurements on blading for a high rim-speed transonic turbine
[RAE-TM-P-1151] N90-15920
SUPERSYMMETRY
Are gravitons windows to higher dimensions
[DE90-600756] N90-16376
SUPPORT SYSTEMS
Load-shortening behavior of an initially curved eccentrically loaded column
[NASA-TM-101643] N90-16293
SUPPORTS
Mechanical strain isolator mount
[NASA-CASE-LAR-13580-1] N90-16272
SURFACE ACOUSTIC WAVE DEVICES
SAW (Surface Acoustic Wave) transducer with improved bus-bar design
[AD-D014250] N90-16125
SURFACE CRACKS
BAM: German Federal Institute for Materials Research and Testing, Berlin
[DE90-004293] N90-16307

SURFACE DEFECTS
Scanning tunneling microscope studies of surface defects
[AD-A214121] N90-16543
SURFACE LAYERS
Modifications of comet materials by the sublimation process: Results from simulation experiments N90-16621
Morphology and compositional differentiation of the surface of comets N90-16624
Radiation modification of cometary materials: Laboratory simulations N90-16626
SURFACE PROPERTIES
Selectivity of the reactions of oxygenates on transition metal surfaces
[DE90-003911] N90-16040
Theoretical studies of chemisorption and surface reactions on nickel and silicon
[DE90-004849] N90-16050
Structure-property relationships in ion-beam surface-modified ceramics: Theory and applications
[AD-A212785] N90-16054
Diblock copolymers at surfaces
[DE90-005406] N90-16079
The influence of residual contamination on the structure and properties of metal/GaAs interfaces
[DE90-000549] N90-16530
SURFACE REACTIONS
Theoretical studies of chemisorption and surface reactions on nickel and silicon
[DE90-004849] N90-16050
SURFACE ROUGHNESS
Surface topography measurements over the 1 meter to 10 micrometer spatial period bandwidth
[DE90-003642] N90-16501
Scanning tunneling microscope studies of surface defects
[AD-A214121] N90-16543
SURFACE TEMPERATURE
Mesoscale analysis by numerical modelling coupled with satellite-based sounding N90-16370
SURFACES
Material responses to incident x rays
[DE89-015366] N90-16305
Stochastic action of dynamical systems on curved manifolds. The isokinetic developing map on trajectories
[PREPRINT-566] N90-16466
SURVEILLANCE
Electro-optic sensors for surveillance and target acquisition N90-15929
SURVEYS
A survey of nonuniform inflow models for rotorcraft flight dynamics and control applications
[NASA-TM-102219] N90-15938
Absorption fluids data survey: 1989 update
[DE90-003965] N90-16346
SWELLING
Irradiation creep and swelling of annealed type 304L stainless steel at approximately 390 C and high neutron fluence
[DE90-004521] N90-16047
SWEPT WINGS
Experiments on the laminar-turbulent transition on swept wings N90-16170
The precise calculation of the inviscid leading edge flow on a laminar airfoil using simple methods and verification by measurements on the TLF pilot model N90-16180
SWIRLING
Swirl-stabilized flames: Fluid dynamics, mixing, and flame stability limits N90-16009
SWITCHES
Command operated liquid metal opening switch
[AD-D014262] N90-16126
SWITCHING CIRCUITS
A physical and numerical study of the turn-off behavior of bipolar power transistors
[LAAS-89185] N90-16136
SYMBOLIC PROGRAMMING
On the efficient exploitation of speculation under data flow paradigms of control
[AD-A214112] N90-16455
SYMMETRICAL BODIES
A numeric analysis of incompressible, viscous flow around a symmetrical body of revolution
[ISL-CO-215/87] N90-16157
SYMMETRY
Double-periodic wormholes in theories with global symmetries
[DE90-719575] N90-16581
SYNCHRONISM
A burst compression and expansion technique for variable-rate users in satellite-switched TDMA networks
[NASA-TM-102414] N90-15983
Parallel asynchronous systems and image processing algorithms N90-16218
Multisqueezing of mechanical states and back-action evasion measurements
[IFSI-89-6] N90-16504
SYNCHROTRON RADIATION
Non-destructive trace element microanalysis of as-received cometary nucleus samples using synchrotron x ray fluorescence N90-16649
SYNCHROTRONS
Trace element abundance determinations by Synchrotron X Ray Fluorescence (SXRF) on returned comet nucleus mineral grains N90-16619
SYNOPTIC METEOROLOGY
The role of an upstream cyclone and corresponding synoptic/planetary-scale interactions during the development of a blocking anticyclone N90-16659
SYNTHESIS (CHEMISTRY)
Solid-state electrolyte catalysis for methane and oxygen synthesis
[PB90-100231] N90-16011
Carbon-13 nuclear magnetic resonance of heterocyclic salts and its precursors
[DE89-635768] N90-16016
Synthesis of air-sinterable lanthanum chromite powders
[DE90-004681] N90-16049
Silicon-based coatings on niobium metal
[DE90-003651] N90-16057
Copolymers for drag reduction in marine propulsion: New molecular structures with enhanced effectiveness
[AD-A214444] N90-16062
Shock-induced reaction synthesis of aluminides and silicides
[DE90-003948] N90-16066
Synthesis of tetrafluorohydrazine
[AD-D014281] N90-16083
High temperature neutron diffraction study of the formation reaction of bismuth superconductors
[DE90-004883] N90-16568
SYNTHETIC APERTURE RADAR
Necessity and benefit of the X-SAR Space Shuttle experiment
[ESA-TT-1164] N90-16112
Science plan for the Alaska SAR facility program. Phase 1: Data from the first European sensing satellite, ERS-1
[NASA-CR-185028] N90-16312
Investigation of the backscatter behavior of selected test areas in two geocoded SEASAT-SAR scenes in greater Bonn (Fed. Republic of Germany) N90-16331
Investigation of the topographic components of the image content of radar pictures N90-16332
Parallel algorithm for determining motion vectors in ice floe images by matching edge features N90-16451
SYSTEMS ANALYSIS
A UK perspective on the uniform engine test programme
[RAE-TM-P-1172] N90-15922
Dynamics analyses of space power systems using the salt code
[DE90-002274] N90-15995
Linear digital imaging system fidelity analysis N90-16205
Two possible configurations for the top-hat electrostatic analyzer: A numerical study
[IFSI-88-18] N90-16229
Fault tree analysis: A tool for battery safety and reliability studies
[DE90-002582] N90-16287
Appearance analysis from CAD models
[IMAG-RR-756-I-IMAG-88-LIFIA] N90-16434
SYSTEMS ENGINEERING
Advances in techniques and technologies for air vehicle navigation and guidance
[AGARD-AR-276] N90-15899
Guidance and Control of Unmanned Air Vehicles
[AGARD-CP-436] N90-15924
Mirach 100 flight control system N90-15926
An electronic pressure profile display system for aeronautic test facilities
[NASA-TM-102478] N90-15964
MANPRINT (Manpower and Personnel Integration) evaluation: AN/TRC-170 digital troposcatter radio system
[AD-A211799] N90-16100
SYSTEMS INTEGRATION
A burst compression and expansion technique for variable-rate users in satellite-switched TDMA networks
[NASA-TM-102414] N90-15983
Experiences with knowledge-base and large database integration
[DE90-000686] N90-16591
SYSTEMS STABILITY
Uniform stability for time-varying infinite-dimensional discrete linear systems
[DE89-635712] N90-16460

T

TACHOMETERS
A simple fiber optic autocorrelation tachometer
[ETN-90-96146] N90-16228
TAIL ASSEMBLIES
Assessment of computational prediction of tail buffeting
[NASA-TM-101613] N90-15886
TANK GEOMETRY
Small amplitude liquid oscillations in a rectangular container under zero-gravity
[LRT-WE-9-FB-2(1989)] N90-16167
TARGET ACQUISITION
Guidance and Control of Unmanned Air Vehicles
[AGARD-CP-436] N90-15924
Electro-optic sensors for surveillance and target acquisition N90-15929
Automated search techniques applied to optical payloads in unmanned air vehicles N90-15931
TARGET RECOGNITION
Mirach 100 flight control system N90-15926
TECHNOLOGICAL FORECASTING
Establishment of the Innovative Technology Utilization Center at West Virginia University
[PB90-114711] N90-16594
TECHNOLOGY ASSESSMENT
Technology and evaluation of unmanned air vehicles N90-15934
Assessment of battery technologies for electric vehicles, volume 1
[DE90-002049] N90-16122
National program plan for electric vehicle battery research and development: Technical plan
[DE90-002023] N90-16269
SERI (Solar Energy Research Institute) solar radiation resource assessment project
[DE89-009456] N90-16352
Project summaries
[PB90-103987] N90-16472
TECHNOLOGY TRANSFER
Establishment of the Innovative Technology Utilization Center at West Virginia University
[PB90-114711] N90-16594
TECHNOLOGY UTILIZATION
Establishment of the Innovative Technology Utilization Center at West Virginia University
[PB90-114711] N90-16594
Research and technology, 1989: Langley Research Center
[NASA-TM-4150] N90-16703
TELECOMMUNICATION
A burst compression and expansion technique for variable-rate users in satellite-switched TDMA networks
[NASA-TM-102414] N90-15983
MT's algorithm: A new algorithm to search for the optimum set of modulation indices for simultaneous range, command, and telemetry
[NASA-CR-186259] N90-16110
TELEMETRY
MT's algorithm: A new algorithm to search for the optimum set of modulation indices for simultaneous range, command, and telemetry
[NASA-CR-186259] N90-16110
TELEOPERATORS
Bilateral force reflection for teleoperators with masters and slaves with dissimilar and possibly redundant kinematics
[DE90-004392] N90-16132
Visual Information Processing for Television and Telerobotics
[NASA-CP-3053] N90-16204
Connectionist model-based stereo vision for telerobotics N90-16224
Examples of robots and teleoperators at the Savannah River Site
[DE90-004659] N90-16284
TELESCOPES
Large angle off-axis beam steering of a phased telescope array
[AD-D014269] N90-16127
TELEVISION SYSTEMS
Visual Information Processing for Television and Telerobotics
[NASA-CP-3053] N90-16204
TELEVISION TRANSMISSION
Satellite broadcasting: Requirements for the receiving antenna
[BBC-RD-1989/5] N90-16098
TEMPERATURE DISTRIBUTION
Two-Dimensional Measuring Techniques
[DGLR-PAPERS-88-04] N90-16236
Simultaneous determination of temperature and velocity fields in a thermal convection flow with non-enclosed liquid crystal tracers N90-16239

TEMPERATURE EFFECTS
Cryogenic engineering and materials N90-15949
The use of hypervelocity launchers to explore previously inaccessible states of matter
[DE90-004088] N90-15973
ZrO2 sintered compact and method for its production
[DE90-004125] N90-16006
Development of a diamond insulator for thermionic applications
[DE90-002849] N90-16055
Silicon membrane formation
[DE90-003022] N90-16064
Thermodynamic analysis of chemical stability of ceramic materials in hydrogen-containing atmospheres at high temperatures
[NASA-CR-4271] N90-16072
Magnetic penetration depth and intragrain critical current density in gain-aligned Tl2Ca2Ba2Cu3O10 superconductor
[DE90-004245] N90-16562
Mechanical and SEM analysis of artificial comet nucleus samples N90-16650
TEMPERATURE MEASUREMENT
Thickness, velocity, and temperature measurements in falling liquid films
[DE90-004290] N90-16151
Modeling a self-calibrating thermocouple for use in a smart temperature measurement system
[DE90-003697] N90-16259
Upper atmosphere research
[ISBN-0-642-13582-7] N90-16368
TEMPERATURE PROFILES
Thermal histories of the samples of two KOSI comet nucleus simulation experiments N90-16645
TENSILE TESTS
Fatigue and impact strength of diffusion bonded titanium alloy joints
[RAE-TM-MAT/STR-1123] N90-16043
Fracture toughness of ferritic alloys at very high neutron exposures
[DE90-004519] N90-16046
TERMINAL GUIDANCE
Navigation up-date using radar mapping: Assessment and optimisation simulation tool N90-15928
TERRAIN
Parallel algorithms for interactive manipulation of digital terrain models N90-16445
TERRAIN ANALYSIS
Advances in techniques and technologies for air vehicle navigation and guidance
[AGARD-AR-276] N90-15899
TEST CHAMBERS
The NASA Langley 0.3-meter transonic cryogenic tunnel N90-15941
TEST FIRING
Space shuttle Production Verification Motor 1 (PV-1) static fire
[NASA-CR-183784] N90-15991
TEST STANDS
Design of a thrust stand for high power electric propulsion devices
[NASA-TM-102372] N90-15992
TESTING TIME
VLSI integrated circuit tests
[IMAG-RR-763-I] N90-16135
TETHERED SATELLITES
Hollow-cathode experiments to support electrodynamic tether applications
[IFSI-89-5] N90-15986
Electrical characteristics measurements for the TSS-1 satellite painting
[IFSI-89-7] N90-15987
RETE experiment activity at the TSS-1 POCC
[IFSI-89-12] N90-15988
TETRAFLUOROHYDRAZINE
Synthesis of tetrafluorohydrazine
[AD-D014281] N90-16083
TEXTURES
Methods for the mineralogical and textural analysis of comet nucleus samples N90-16648
THEMATIC MAPPERS (LANDSAT)
Computer-aided boundary delineation of agricultural lands
[NASA-TM-102243] N90-16313
Image segmentation by iterative parallel region growing with application to data compression and image analysis N90-16452
THEMATIC MAPPING
The visible channel of OMEGA-VIMS
[IFSI-89-14] N90-16231
Forest mapping Nuerenberg German national forest with special emphasis on the spectral reflection behavior of pine trees N90-16328
Attempt to draw conclusions concerning the geological subsoil from the vegetation using digital image processing of TM data N90-16329
TM land use classification of a region. Utilization for planning and statistics N90-16339
THEORETICAL PHYSICS
Some theoretical aspects of cold fusion: A report
[DE90-601098] N90-16514
Proceedings of the 23rd Annual Seminar on Theoretical Physics
[DE90-601827] N90-16577
THERMAL ANALYSIS
Thermal and chemical processing of the outermost layer of cometary nuclei N90-16614
THERMAL CONDUCTIVITY
The physical properties of microcellular composite foams
[DE90-003658] N90-16058
Analytical study on the decreasing method of thermal stress for ceramic gas turbines
[DE90-734934] N90-16078
Thermal histories of the samples of two KOSI comet nucleus simulation experiments N90-16645
THERMAL CONTROL COATINGS
Electrical characteristics measurements for the TSS-1 satellite painting
[IFSI-89-7] N90-15987
THERMAL EXPANSION
Thermal expansion of LATGS crystals
[DE89-636239] N90-16546
THERMAL FATIGUE
Cryogenic engineering and materials N90-15949
THERMAL INSULATION
The Kryo-Kanal Koeln (KKK): Description of the tunnel conversion. Thermal insulation, instrumentation, operational experience, test results and operating costs N90-15943
Investigation of ablation phenomena using IR thermography in a hypersonic wind tunnel N90-16258
Federal roles to realize national energy-efficiency opportunities in the 1990s
[DE90-004410] N90-16348
THERMAL MAPPING
The determination of subscale structures in thermal images N90-16330
Reflection technique for thermal mapping of semiconductors
[AD-D014263] N90-16541
THERMAL SHOCK
Analytical study on the decreasing method of thermal stress for ceramic gas turbines
[DE90-734934] N90-16078
THERMAL STRESSES
Analytical study on the decreasing method of thermal stress for ceramic gas turbines
[DE90-734934] N90-16078
THERMIONIC CONVERTERS
Development of a diamond insulator for thermionic applications
[DE90-002849] N90-16055
THERMOCHROMATIC MATERIALS
Unsteady heat transfer measurement using thermochromatic liquid crystals as temperature indicators N90-16254
THERMOCOUPLES
Modeling a self-calibrating thermocouple for use in a smart temperature measurement system
[DE90-003697] N90-16259
THERMODYNAMIC CYCLES
Cycle analysis for helicopter gas turbine engines
[RAE-TM-P-1154] N90-15921
THERMODYNAMIC PROPERTIES
Reflection technique for thermal mapping of semiconductors
[AD-D014263] N90-16541
Thermodynamic studies on the ferroelectric phase transition in neutron irradiated (Li(sub x)K(1-x))2SO4 crystals at high temperature
[DE89-635786] N90-16545
Estimation of thermodynamic properties of alloys from phase diagram and other loose boundary conditions
[DE90-719511] N90-16579
THERMODYNAMICS
The use of hypervelocity launchers to explore previously inaccessible states of matter
[DE90-004088] N90-15973
Thermodynamic analysis of chemical stability of ceramic materials in hydrogen-containing atmospheres at high temperatures
[NASA-CR-4271] N90-16072
Modeling a self-calibrating thermocouple for use in a smart temperature measurement system
[DE90-003697] N90-16259
THERMOELECTRIC POWER GENERATION
Low risk low power heat pipe/thermoelectric space power supply
[DE89-014817] N90-16342
THERMOGRAPHY
Investigation of ablation phenomena using IR thermography in a hypersonic wind tunnel N90-16258
THERMOPLASTIC RESINS
Vibration damping composition suitable for outer space temperature variations
[AD-D014288] N90-16296
THERMOSTATS
Measurement of the p, v, T behavior under microgram conditions
[ETN-90-95906] N90-16162
THICKNESS
Thickness, velocity, and temperature measurements in falling liquid films
[DE90-004290] N90-16151
THIN AIRFOILS
Some recent developments in materials and techniques for model fabrication N90-15955
THIN FILMS
Solid state voltammetry and sensors in solids and gases
[DE90-003234] N90-16538
Lithium cobalt oxide thin film and its electrochromism
[DE90-004570] N90-16564
Artificially structured superconductors
[DE90-004851] N90-16567
THIN WINGS
Wind tunnel tests of the influence of aerofoil thickness on the normal force and pitching moment of two slender wings at transonic and supersonic Mach numbers
[ESA-TT-1129] N90-15889
THREE DIMENSIONAL BODIES
Appearance analysis from CAD models
[IMAG-RR-756-I-IMAG-88-LIFIA] N90-16434
THREE DIMENSIONAL BOUNDARY LAYER
Method for the primary stability analysis of the three dimensional, compressible boundary layer flows N90-16171
An efficient solver of the Eigenvalue problem of the linear stability equations for three dimensional, compressible boundary-layer flows N90-16172
Numerical simulation of the nonlinear evolution of a perturbation in a three dimensional boundary layer N90-16173
Development of transition criteria on the basis of e to the N power for three dimensional wing boundary layers N90-16179
THREE DIMENSIONAL FLOW
Adaptive local grid refinement for the compressible 3-D Euler equations
[FFA-TN-1989-40] N90-16155
Visualization of 2 and 3 dimensional flows
[REPT-1] N90-16164
Numerical simulation of the laminar and turbulent three dimensional flow on a delta wing with sharp leading edge N90-16186
A finite volume calculation method for three dimensional, complex flows N90-16195
Calculation of two and three dimensional super and hypersonic flows by solving the Euler equations N90-16197
Coded trajectories for the investigation of strongly unsteady flow fields N90-16240
THREE DIMENSIONAL MODELS
Experimental investigation of a three-dimensional wake. Part 2: Spectral and turbulent energy analysis
[ONERA-RT-32/5025-AYD-PT-2] N90-15887
The cryogenic induction tunnel T2 at Toulouse N90-15946
Verification study of a three-dimensional local scale atmospheric model PHYSIC at seacoast region
[DE90-719560] N90-16384
Design of a large superconducting spectrometer magnet
[DE90-719505] N90-16553
THRUST
Design of a thrust stand for high power electric propulsion devices
[NASA-TM-102372] N90-15992
Pulsed plasma mission endurance test
[AD-A213462] N90-15993
THRUST CONTROL
Plume shape optimization of small attitude control thrusters with respect to impingement and thrust
[ISL-CO-220/88] N90-16153
THRUST VECTOR CONTROL
An experimental investigation of thrust vectoring two-dimensional convergent-divergent nozzles installed in a twin-engine fighter model at high angles of attack
[NASA-TM-4155] N90-15884
TIME
Uniform stability for time-varying infinite-dimensional discrete linear systems
[DE89-635712] N90-16460

TIME DEPENDENCE
Uniform stability for time-varying infinite-dimensional discrete linear systems
[DE89-635712] N90-16460
TIME DIVISION MULTIPLE ACCESS
A burst compression and expansion technique for variable-rate users in satellite-switched TDMA networks
[NASA-TM-102414] N90-15983
TIME DIVISION MULTIPLEXING
The first year's work of race project 1036 WTDM broadband customer premises network
[BBC-RD-1989/6] N90-16097
TIME MEASUREMENT
An analysis of the time variation of the frequency response of the LMS adaptive line enhancer
[ISVR-TR-175] N90-16115
TIME OF FLIGHT SPECTROMETERS
Low energy neutral particle energy analyser by time of flight method
[DE90-719529] N90-16517
TISSUES (BIOLOGY)
Apparatus for imaging deep arterial and coronary lesions
[NASA-CASE-NPO-17439-1-CU] N90-16391
TITANIUM ALLOYS
Method to produce titanium alloy articles with high fatigue and fracture resistance
[AD-D014278] N90-16029
Method for refining microstructures on prealloyed titanium powder compacts
[AD-D014280] N90-16030
Method of marking titanium alloy articles having distinct microstructural regions corresponding to high creep and fatigue resistance
[AD-D014283] N90-16031
Fundamental studies of beta phase decomposition modes in titanium alloys
[AD-A214424] N90-16035
Microstructural explanation for irradiation embrittlement of V-15Cr-5Ti
[DE90-004112] N90-16041
Fatigue and impact strength of diffusion bonded titanium alloy joints
[RAE-TM-MAT/STR-1123] N90-16043
Effect of carbon on ion beam mixing of Fe-Ti bilayers
[DE90-003650] N90-16056
Magnetic penetration depth and intragrain critical current density in gain-aligned Tl2Ca2Ba2Cu3O10 superconductor
[DE90-004245] N90-16562
Properties and design of multifilamentary NbTi composite superconductors
[DE90-004904] N90-16569
The effects of hydrogen embrittlement of titanium N90-16698
TITANIUM OXIDES
Microstructures of Y123 films on SrTiO3, LaGaO3, and LaAlO3
[DE90-003367] N90-16537
TOKAMAK DEVICES
Initial deuterium confinement studies in DIII-D tokamak: DIII-D milestone report number 58
[DE90-003942] N90-16509
Modeling energy output of inertial storage devices for the DIII-D tokamak
[DE90-004096] N90-16524
TOLERANCES (MECHANICS)
FRAG requirements for control of fatigue testing
[RAE-TM-MAT/STR-1130] N90-16300
TOOLS
Case tool evaluation system
[DE90-003698] N90-16413
TOPOGRAPHY
Regional height determination using gravimetric and topographical data
[UH-156] N90-16315
Investigation of the topographic components of the image content of radar pictures N90-16332
Surface topography measurements over the 1 meter to 10 micrometer spatial period bandwidth
[DE90-003642] N90-16501
TOROIDAL PLASMAS
Toroidal magnetic fields in terms of field-line invariants
[DE89-016610] N90-16507
TORQUE
Continuously variable gear drive transmission
[AD-D014268] N90-16275
TOUGHNESS
Fracture toughness of ferritic alloys at very high neutron exposures
[DE90-004519] N90-16046
TRACE ELEMENTS
Scientific linkages in global change
[PB90-112608] N90-16356
Trace element abundance determinations by Synchrotron X Ray Fluorescence (SXRF) on returned comet nucleus mineral grains N90-16619
Prompt Gamma Activation Analysis (PGAA): Technique of choice for nondestructive bulk analysis of returned comet samples N90-16633
Non-destructive trace element microanalysis of as-received cometary nucleus samples using synchrotron x ray fluorescence N90-16649
The measurement of trace elements in interplanetary dust and cometary particles by ultra-high sensitivity INAA N90-16656
TRACKING (POSITION)
Analytical techniques for tracking filter implementation N90-15903
Tracking flares
[ISBN-0-642-13583-5] N90-16080
TRACKING FILTERS
Analytical techniques for tracking filter implementation N90-15903
TRACKING RADAR
The application of Z to the specification of air traffic control systems. 1: An initial specification of the radar processing activity
[RSRE-MEMO-4280] N90-15900
TRAJECTORIES
Singular perturbation analysis of AOTV-related trajectory optimization problems
[NASA-CR-186202] N90-15936
Dissipation mechanism of the large-amplitude collective motion. Dynamical evolution of a collective bundle of trajectories in the TDHF phase space for a simple soluble model
[DE90-719557] N90-16477
The dynamics of dust in planetary magnetospheres N90-16658
TRAJECTORY ANALYSIS
Stochastic action of dynamical systems on curved manifolds. The isokinetic developing map on trajectories
[PREPRINT-666] N90-16466
TRAJECTORY CONTROL
Off-line robot programming and graphical verification of path planning N90-16699
TRAJECTORY MEASUREMENT
Trajectory-capture cell instrumentation for measurement of dust particle mass, velocity and trajectory, and particle capture N90-16644
TRAJECTORY OPTIMIZATION
Singular perturbation analysis of AOTV-related trajectory optimization problems
[NASA-CR-186202] N90-15936
TRANSDUCERS
SAW (Surface Acoustic Wave) transducer with improved bus-bar design
[AD-D014250] N90-16125
Apparatus for imaging deep arterial and coronary lesions
[NASA-CASE-NPO-17439-1-CU] N90-16391
TRANSFORMERS
Analysis of the 60-Hz power system at KSC: The Orsino substation N90-16692
TRANSITION FLOW
Experiments on the laminar-turbulent transition on swept wings N90-16170
Development of transition criteria on the basis of e to the N power for three dimensional wing boundary layers N90-16179
The use of sublimation methods for the recognition of transition at low speed N90-16251
TRANSITION METALS
Selectivity of the reactions of oxygenates on transition metal surfaces
[DE90-003911] N90-16040
TRANSITION POINTS
Determination of the N-factor in the Brunswick (Federal Rep. of Germany) transonic wind tunnel using measurements of pressure distributions and transition points, and the Sally method N90-16177
TRANSITION TEMPERATURE
Study of phase transformations liquid-solid-solid of ultrafine particles
[ISAL-89-0019] N90-16022
The modified Ginzburg-Landau theory for anisotropic high temperature superconductors
[DE89-635909] N90-16532
Structure-property correlations in the design of organic metals and superconductors: An overview
[DE90-003794] N90-16550
TRANSMISSION LINES
Microwave screening on digital radio communication links due to multicircuit power transmission lines
[DE90-734950] N90-16118
Theoretical and experimental investigation of axial power extraction from a magnetically insulated transmission line oscillator
[DE90-003486] N90-16131
TRANSMISSIONS (MACHINE ELEMENTS)
Assessment of worm gearing for helicopter transmissions
[NASA-TM-102441] N90-15923
Continuously variable gear drive transmission
[AD-D014268] N90-16275
TRANSMITTANCE
Atmospheric transmittance determination from a two-angle measurement of radiance change
[AD-A213847] N90-16375
TRANSMITTERS
Diffraction limited dichroic combiner diode laser
[AD-D014291] N90-16263
TRANSONIC FLOW
Personal computer study of finite-difference methods for the transonic small disturbance equation
[NASA-TM-102582] N90-15892
Finite element calculations for transonic flows taking into account several far field boundary conditions N90-16188
Digital image interpretation for optical flow measurement methods: System description and preliminary application examples N90-16244
TRANSONIC SPEED
Wind tunnel tests of the influence of aerofoil thickness on the normal force and pitching moment of two slender wings at transonic and supersonic Mach numbers
[ESA-TT-1129] N90-15889
TRANSONIC WIND TUNNELS
The NASA Langley 0.3-meter transonic cryogenic tunnel N90-15941
The US National Transonic Facility, NTF N90-15942
The European Transonic Windtunnel (ETW) N90-15945
The cryogenic Ludwieg tube tunnel at Goettingen N90-15947
Other cryogenic wind tunnel projects N90-15948
Test techniques for cryogenic wind tunnels N90-15952
Automatic control of cryogenic wind tunnels N90-15957
Cryogenic balances for the US NTF N90-15959
Safety and cryogenic wind tunnels N90-15960
Determination of the N-factor in the Brunswick (Federal Rep. of Germany) transonic wind tunnel using measurements of pressure distributions and transition points, and the Sally method N90-16177
Use of the film-of-oil technique for profile measurements in the Transonic Wind tunnel Brunswick (TWB) N90-16252
TRANSPORT AIRCRAFT
Evaluation of two transport aircraft and several ground test vehicle friction measurements obtained for various runway surface types and conditions. A summary of test results from joint FAA/NASA Runway Friction Program
[NASA-TP-2917] N90-15902
TRANSPORT PROPERTIES
La(sub 2)MO(sub 4 + delta) (M = Cu, Ni, Co): Phase separation and superconductivity resulting from excess oxygen defects
[DE90-001988] N90-16534
TRANSPORTATION
Environmental, health, and safety concerns associated with nonpetroleum fuel use in US transportation
[DE90-004367] N90-16362
TRANSPORTATION ENERGY
An approach for testing fuel-cell/battery hybrid power sources for bus applications
[DE90-002090] N90-16270
TRANSVERSE OSCILLATION
Dynamic analysis of geared rotors by finite elements
[NASA-TM-102349] N90-16286
TRAVELING WAVE MODULATION
Galactic cosmic-ray modulation and solar-terrestrial relationships
[IFSI-88-17] N90-16679
TREES (MATHEMATICS)
Spanning trees of hypercubes with a maximum of sixteen peaks
[IMAG-RR-755-I] N90-16406
TREES (PLANTS)
Forest mapping Nuerenberg German national forest with special emphasis on the spectral reflection behavior of pine trees N90-16328
TRIANGLES
Triangle based TVD schemes for hyperbolic conservation laws
[NASA-CR-181984] N90-16401
TRIANGULATION
Asymptotically fast triangularization of matrices over rings
[DE90-003161] N90-16471
TRITON
Neptune's Triton: A moon rich in dry ice and carbon
[NASA-CR-186298] N90-16675

TROPOSPHERE
The chemistry and dynamics of marine stratocumulus N90-16381
TROPOSPHERIC SCATTERING
MANPRINT (Manpower and Personnel Integration) evaluation: AN/TRC-170 digital troposcatter radio system
[AD-A211799] N90-16100
TRUSSES
Analysis and testing of axial compression in imperfect slender truss struts
[NASA-TM-4174] N90-16292
TRYPTOPHAN
Advanced biosensors for amino acid detection
[AD-A214029] N90-16225
TURBINE BLADES
Aerodynamic and heat transfer measurements on blading for a high rim-speed transonic turbine
[RAE-TM-P-1151] N90-15920
The use of piezofoil sensors for the determination of the unsteady pressure distribution at the surface of a gas turbine blade N90-16250
Performance predictions for an intermediate-sized VAWT based on performance of the 34-m VAWT test bed
[DE90-002835] N90-16345
TURBOCOMPRESSORS
Performance of a highly-loaded HP compressor
[RAE-TM-P-1149] N90-15919
TURBULENCE
A numerical and experimental investigation of multiple shock wave/turbulent boundary layer interactions in a rectanular duct N90-16141
Vorticity amplification in nonorthogonal stagnation flow N90-16152
The response of the atmospheric convective boundary layer to surface inhomogeneities N90-16369
Turbulent stripping of interstellar clouds by interaction with supernova remnants
[DE90-003622] N90-16674
TURBULENCE MODELS
Euler and Navier-Stokes computations for two-dimensional geometries using unstructured meshes
[NASA-CR-181977] N90-15893
Nonlinear wave coupling and clumps in drift wave turbulence theory
[DE90-004103] N90-16150
Grid-independent wall layer turbulence model for complex flow calculations
[DE90-003500] N90-16200
New atmospheric turbulence model for shuttle applications
[NASA-TM-4168] N90-16389
TURBULENT BOUNDARY LAYER
The structure of supersonic turbulent boundary layers subjected to concave surface curvature N90-15883
Flow separation in shock wave boundary layer interactions at hypersonic speeds
[NASA-CR-4274] N90-15885
A numerical and experimental investigation of multiple shock wave/turbulent boundary layer interactions in a rectanular duct N90-16141
Experiments on the laminar-turbulent transition on swept wings N90-16170
An interactive method for the flow calculation of airfoils with local separation regions N90-16190
Inverse solutions for boundary layers with separation or close to separation under locally infinite swept wing conditions N90-16192
TURBULENT FLOW
Assessment of computational prediction of tail buffeting
[NASA-TM-101613] N90-15886
Calculation of turbulent choppy flow mixing
[ETN-90-95929] N90-16165
Numerical simulation of the laminar and turbulent three dimensional flow on a delta wing with sharp leading edge N90-16186
A finite volume calculation method for three dimensional, complex flows N90-16195
Grid-independent wall layer turbulence model for complex flow calculations
[DE90-003500] N90-16200
Colinear fluctuating wall shear stress and fluctuating pressure transducer
[AD-D014296] N90-16226
Turbulent stripping of interstellar clouds by interaction with supernova remnants
[DE90-003622] N90-16674
TURBULENT MIXING
Calculation of turbulent choppy flow mixing
[ETN-90-95929] N90-16165
TURBULENT WAKES
Experimental investigation of a three-dimensional wake. Part 2: Spectral and turbulent energy analysis
[ONERA-RT-32/5025-AYD-PT-2] N90-15887
TVD SCHEMES
Triangle based TVD schemes for hyperbolic conservation laws
[NASA-CR-181984] N90-16401
TWO DIMENSIONAL FLOW
Visualization of 2 and 3 dimensional flows
[REPT-1] N90-16164
Calculation of two and three dimensional super and hypersonic flows by solving the Euler equations N90-16197
Two-Dimensional Measuring Techniques
[DGLR-PAPERS-88-04] N90-16236
Coded trajectories for the investigation of strongly unsteady flow fields N90-16240
Analysis of the measuring range and the accuracy of an existing particle image velocimetry system N90-16247
TWO DIMENSIONAL MODELS
Element-by-element preconditioning techniques for large-scale, vectorized finite element analysis in nonlinear solid and structural mechanics N90-16291
The development of two-dimensional object identification techniques
[NASA-CR-186203] N90-16408
Alvey MMI007. Object identification from 2D images: The RSRE contribution
[RSRE-MEMO-4277] N90-16428
Universe as a topological defect in a higher-dimensional Einstein-Yang-Mills theory
[DE90-719507] N90-16578

U

ULTRASONIC FLAW DETECTION
Theoretical study on creep damage detection by ultra-sonic wave measurement
[DE90-702472] N90-16290
ULTRASONIC TESTS
Theoretical study on creep damage detection by ultra-sonic wave measurement
[DE90-702472] N90-16290
ULTRASONICS
Apparatus for imaging deep arterial and coronary lesions
[NASA-CASE-NPO-17439-1-CU] N90-16391
Ultrasonic assisted paint removal method
[AD-D014264] N90-16479
ULTRAVIOLET RADIATION
Potential impact of stratospheric ozone depletion on marine ecosystems
[PB90-112616] N90-16360
ULTRAVIOLET SPECTRA
Eurolaser. High power excimer laser: Optical crystals
[ETN-90-95901] N90-16558
UNDERWATER ACOUSTICS
ZBTAB: Zenith-248 version of BLUGTAB
[AD-A214279] N90-16415
UNITED KINGDOM
UK airmisses involving commercial air transport, September to December 1988
[ISSN-0951-6301] N90-15897
A UK perspective on the uniform engine test programme
[RAE-TM-P-1172] N90-15922
Tactical UK military satellite ground terminals: A research and development review
[RSRE-MEMO-4262] N90-15972
UNIVERSE
Study of primitive universe in the Bianchi 9 model
[DE89-635903] N90-16572
Universe as a topological defect in a higher-dimensional Einstein-Yang-Mills theory
[DE90-719507] N90-16578
The (2+1)-dimensional quantum gravity
[DE90-719556] N90-16580
Dissipative effects in Friedmann universes
[DE89-618838] N90-16663
UNIX (OPERATING SYSTEM)
UNIX internals. Part 1: Intertask communication in UNIX. Part 2: UNIX file system
[CNES-NT-122-PT-1/2] N90-16405
CPU timing routines for a CONVEX C220 computer system
[NASA-CR-181950] N90-16424
UNSTEADY AERODYNAMICS
Structural dynamics division research and technology accomplishments for FY 1989 and plans for FY 1990
[NASA-TM-101683] N90-15894
Test techniques for cryogenic wind tunnels N90-15952
UNSTEADY FLOW
Force and moment measurements on delta wings in unsteady flow N90-16185
Periodically unsteady effects on profiles, induced by separation N90-16196
Coded trajectories for the investigation of strongly unsteady flow fields N90-16240
Unsteady heat transfer measurement using thermochromatic liquid crystals as temperature indicators N90-16254
A computational and experimental study of steady and transient acoustic energy flow from a complex mechanical structure N90-16478
UNSTEADY STATE
The use of piezofoil sensors for the determination of the unsteady pressure distribution at the surface of a gas turbine blade N90-16250
UPPER ATMOSPHERE
Metal vaporisers: Bicentennial series of five historical monographs
[ISBN-0-642-13584-3] N90-16081
Upper atmosphere research
[ISBN-0-642-13582-7] N90-16368
UPSTREAM
The role of an upstream cyclone and corresponding synoptic/planetary-scale interactions during the development of a blocking anticyclone N90-16659
URANIUM ALLOYS
Estimation of thermodynamic properties of alloys from phase diagram and other loose boundary conditions
[DE90-719511] N90-16579
URBAN TRANSPORTATION
An approach for testing fuel-cell/battery hybrid power sources for bus applications
[DE90-002090] N90-16270
USER MANUALS (COMPUTER PROGRAMS)
User's manual for MGMHD: A multigrid three-dimensional computer code for the analysis of magnetohydrodynamic generators and diffusers
[DE90-004453] N90-16526
USER REQUIREMENTS
Columbus: A user's introduction
[ESA-BR-62] N90-15989
User interaction with self-learning systems
[AD-A214280] N90-16395
UTILIZATION
SPOT after two years in operation: An appraisal of results and a review of selected applications N90-16326

V

VACANCIES (CRYSTAL DEFECTS)
The effects of oxygen and strontium vacancies on the superconductivity of single crystals of Bi2Sr(2-x)CuO(6-y)
[DE90-004242] N90-16561
VALENCE
Theory of the electronic and optical properties of semiconductor heterostructures
[AD-A214132] N90-16544
VALVES
Automatic prestart or post shutoff engine lubricator
[AD-D014259] N90-16273
VAN DE GRAAFF ACCELERATORS
Ion bombardment experiments suggesting an origin for organic particles in pre-cometary and cometary ices N90-16652
VAPORIZERS
Metal vaporisers: Bicentennial series of five historical monographs
[ISBN-0-642-13584-3] N90-16081
VAPORIZING
Externally vaporizing system for turbine combustor
[AD-D014284] N90-15918
VAPORS
Studies of density distributions in one-dimensional shock-induced debris clouds
[DE90-004089] N90-16282
VARIABLE STARS
Pulsations of delta Scuti stars
[DE90-003213] N90-16598
VARIATIONS
Uniform stability for time-varying infinite-dimensional discrete linear systems
[DE89-635712] N90-16460
VECTOR PROCESSING (COMPUTERS)
Solving time harmonic wave problems on vector processors
[DE90-003956] N90-16480
VEGA PROJECT
Organic chemistry of cometary dust as derived from PUMA 1 data N90-16628
VEGETATION
Assessment of the importance of acidic fogwater and cloudwater in affecting terrestrial vegetation: Some important case studies
[DE90-002216] N90-16361
VEGETATIVE INDEX
Quantitative evaluation of object-changes in multitemporal AGRISAR imagery
[FIM-195] N90-16314

VELOCITY DISTRIBUTION
Two-Dimensional Measuring Techniques
[DGLR-PAPERS-88-04] N90-16236
Simultaneous determination of temperature and velocity fields in a thermal convection flow with non-enclosed liquid crystal tracers N90-16239
VELOCITY MEASUREMENT
Solid fuel combustion chamber
[LR-555] N90-16001
Thickness, velocity, and temperature measurements in falling liquid films
[DE90-004290] N90-16151
Miniature laser Doppler anemometer with a diode laser
[ISL-CO-224/88] N90-16232
Analysis of the measuring range and the accuracy of an existing particle image velocimetry system N90-16247
Further development of the PIV method for use in the large wind tunnel N90-16248
VENTING
The repair of aircraft integral fuel tanks in the RAF: A user's view of fuel tank technology N90-15908
VERY LARGE SCALE INTEGRATION
VLSI integrated circuit tests
[IMAG-RR-763-I] N90-16135
BLITZEN: A highly integrated massively parallel machine N90-16453
VERY LONG BASE INTERFEROMETRY
Scientific investigations of the Space Research Group
[ISBN-0-642-13252-6] N90-16595
VERY LOW FREQUENCIES
Scientific investigations of the Space Research Group
[ISBN-0-642-13252-6] N90-16595
VIBRATION DAMPING
Vibration damping composition suitable for outer space temperature variations
[AD-D014288] N90-16296
VIBRATION TESTS
Vibrational behavior of a viscous column with a free liquid surface
[LRT-WE-9-FB-1(1989)] N90-16166
VIBRATIONAL SPECTRA
Vibrational behavior of a viscous column with a free liquid surface
[LRT-WE-9-FB-1(1989)] N90-16166
Conformation, orientation and interaction in molecular monolayers: A surface second harmonic and sum frequency generation study
[DE90-003108] N90-16536
VIBRATIONAL STRESS
Vibrational behavior of a viscous column with a free liquid surface
[LRT-WE-9-FB-1(1989)] N90-16166
VIDEO EQUIPMENT
A programmable image compression system N90-16222
VIDEO SIGNALS
Satellite broadcasting: Requirements for the receiving antenna
[BBC-RD-1989/5] N90-16098
VIRTUAL MEMORY SYSTEMS
PVM (Parallel Virtual Machine): A framework for parallel distributed computing
[DE90-004390] N90-16403
VISCOELASTIC DAMPING
Improved solution techniques for the eigenstructure of fractional order systems
[AD-A213844] N90-16295
VISCOELASTICITY
Interdisciplinary research in viscoelasticity and rheology
[AD-A213630] N90-16145
VISCOUS FLOW
Using inorganic membranes to separate gases: R and D status review
[DE90-004386] N90-16019
A numeric analysis of incompressible, viscous flow around a symmetrical body of revolution
[ISL-CO-215/87] N90-16157
Numerical boundary layer calculations on the DFVLR ellipsoid of revolution N90-16193
Convergence speeding up in the calculation of the viscous flow about an airfoil N90-16194
VISCOUS FLUIDS
Decay estimates for the compressible Navier-Stokes equations in the half-space
[PREPRINT-46] N90-16163
Vibrational behavior of a viscous column with a free liquid surface
[LRT-WE-9-FB-1(1989)] N90-16166
VISUAL ACUITY
Assessment of visual function in aerospace medicine
[BMVG-FBWM-89-5] N90-16397
VISUAL PERCEPTION
Isolating contour information from arbitrary images N90-16217
Simulator sickness in the UH-60 (Black Hawk) flight simulator
[AD-A214434] N90-16392
VOLTAGE REGULATORS
Steep front impulse tests on a solid-state relay
[DE90-004243] N90-16140
VOLTMETERS
Solid state voltammetry and sensors in solids and gases
[DE90-003234] N90-16536
VOLUMETRIC ANALYSIS
Low-cost volumetric modeling
[CRIF-MC-85] N90-16435
VORTEX BREAKDOWN
Numerical simulation of a bubble shaped bursting vortex N90-16187
VORTEX GENERATORS
Laboratory studies of isolated eddies in a rotating fluid
[AD-A213903] N90-16146
VORTEX SHEDDING
Low flow vortex shedding flowmeter N90-16700
VORTEX SHEETS
A nonlinear vortex-lattice method for the calculation of interference effects between free vortex sheets and wings N90-16183
VORTICES
Laboratory studies of isolated eddies in a rotating fluid
[AD-A213903] N90-16146
Vorticity amplification in nonorthogonal stagnation flow N90-16152
Wind tunnel investigations on the configuration of the international vortex flow experiment N90-16181
Flow field visualization study on a 65 deg delta wing at M = 0.85 N90-16182
A nonlinear vortex-lattice method for the calculation of interference effects between free vortex sheets and wings N90-16183
Research on three different Euler's schemes applied to a delta wing with vortical flows N90-16184
The determination of vortex separation frequencies by means of laser light sheet images
[DNW-WTI-88.038] N90-16245
The response of the atmospheric convective boundary layer to surface inhomogeneities N90-16369
VORTICITY
Assessment of computational prediction of tail buffeting
[NASA-TM-101613] N90-15886
Vorticity amplification in nonorthogonal stagnation flow N90-16152
The role of an upstream cyclone and corresponding synoptic/planetary-scale interactions during the development of a blocking anticyclone N90-16659
VULNERABILITY
Fuel tank explosion protection N90-15914

W

WAKES
Study of flow around a sphere in a hydraulic test tunnel
[CERT-1/2313/MES] N90-16156
WALKING MACHINES
Expert system control of a six-legged walking telerobot
[DE90-004661] N90-16285
WALL FLOW
Direct Monte Carlo calculations on expansion wave structure near a wall
[ISL-CO-249/88] N90-16154
Grid-independent wall layer turbulence model for complex flow calculations
[DE90-003500] N90-16200
WALL PRESSURE
Colinear fluctuating wall shear stress and fluctuating pressure transducer
[AD-D014296] N90-16226
WARNING SYSTEMS
The automatic detection of anti-collision lights
[RSRE-MEMO-4272] N90-15896
WATER
Conceptual design analysis for hybrid-cycle OTEC plants for co-production of electric power and desalinated water
[DE90-003551] N90-16350
WATER FLOW
Flow visualization of water flows using the crystal violet method N90-16253
Estimating water flow through a hillslope using the massively parallel processor N90-16449
WATER VAPOR
Backscattering effects in DIAL due to water vapor
[SER-WISS-ABHANDL-89] N90-16265
Assessment of the importance of acidic fogwater and cloudwater in affecting terrestrial vegetation: Some important case studies
[DE90-002216] N90-16361
Mesoscale analysis by numerical modelling coupled with satellite-based sounding N90-16370
WAVE DIFFRACTION
Anomalous waves in shock wave - fluid interface collisions
[AD-A213584] N90-16144
WAVE DISPERSION
A space-time discretization procedure for wave propagation problems
[NASA-TM-102215] N90-16399
Chromatic dispersion compensation in a Fresnel lens by means of a diffraction grating
[DE90-004030] N90-16506
WAVE EQUATIONS
Hidden regularity for a strongly nonlinear wave equation
[DE90-600742] N90-16465
WAVE FUNCTIONS
General contraction of Gaussian basis sets. Part 2: Atomic natural orbitals and the calculation of atomic and molecular properties
[NASA-CR-186201] N90-16482
Continuous spontaneous reduction model involving gravity
[DE90-600730] N90-16573
The (2+1)-dimensional quantum gravity
[DE90-719556] N90-16580
WAVE INTERACTION
Langmuir wave interaction with ion-sound one. Part 1: Stochastic effects
[DE90-603368] N90-16474
On condensation driven by electrostatic interactions in macroionic solutions
[DE89-636072] N90-16487
WAVE PROPAGATION
Personal computer study of finite-difference methods for the transonic small disturbance equation
[NASA-TM-102582] N90-15892
An investigation of elastic guided waves for ceramic joint evaluation
[DE90-004400] N90-16071
Helsinki University of Technology Radio Laboratory
[PB90-110677] N90-16102
Low-altitude millimeter-wave propagation in the evaporation duct
[AD-A214432] N90-16108
Direct Monte Carlo calculations on expansion wave structure near a wall
[ISL-CO-249/88] N90-16154
A space-time discretization procedure for wave propagation problems
[NASA-TM-102215] N90-16399
Solving time harmonic wave problems on vector processors
[DE90-003956] N90-16480
Geometrical optics in inhomogeneous chiral media with application to polarization correction in inhomogeneous lens antennas
[PB90-110669] N90-16497
Scientific investigations of the Space Research Group
[ISBN-0-642-13252-6] N90-16595
WAVE REFLECTION
Reflection from layered media with special attention to the microwave region
[ESA-TT-1155] N90-16111
WAVEFORMS
Characteristics of electromagnetic wave forms with lightning in winter season (2): Characteristics in frequency domain
[DE90-734989] N90-16388
WAVEGUIDES
Method of making carbon dioxide and chlorine free fluoride-based glass
[AD-D014260] N90-16060
Characterization of B and N implanted fused silica
[DE90-004198] N90-16069
High-frequency asymptotic methods for analyzing the EM scattering by open-ended waveguide cavities
[NASA-CR-186244] N90-16103
WAVELENGTH DIVISION MULTIPLEXING
The first year's work of race project 1036 WTDM broadband customer premises network
[BBC-RD-1989/6] N90-16097
WEAPONS
Weapon aerodynamics overview
[RAE-TM-AERO-2150] N90-15888

WEAR RESISTANCE
Structure-property relationships in ion-beam surface-modified ceramics: Theory and applications
[AD-A212785] N90-16054
Investigation of rough elastohydrodynamic contact
[ISAL-89-0029] N90-16281
WEATHER FORECASTING
A dynamic model for forecasting new cloud development
[AD-A213939] N90-16383
World Weather Watch. Global observing system-satellite sub-system. Information on meteorological and other environmental satellites, second edition
[WMO-411-ED-2] N90-16386
WEATHER STATIONS
Climatic summaries and documentation for the primary meteorological Station, H. J. Andrews Experimental Forest, 1972 to 1984
[PB90-104373] N90-16382
WEIGHT REDUCTION
Advanced composite polar boss
[AD-D014267] N90-15994
Low risk low power heat pipe/thermoelectric space power supply
[DE89-014817] N90-16342
WEIGHTLESSNESS
Response of a rotating finite annular liquid layer to axial excitation
[LRT-WE-9-FB-15(1988)] N90-16090
WEIGHTLESSNESS SIMULATION
Small amplitude liquid oscillations in a rectangular container under zero-gravity
[LRT-WE-9-FB-2(1989)] N90-16167
Linear liquid oscillations in cylindrical containers under zero-gravity
[LRT-WE-9-FB-5(1989)] N90-16168
WELDED JOINTS
Structural characterization of Spacelab
[ETN-90-95214] N90-16289
WHEAT
Dynamics of carbon dioxide exchange of a wheat community grown in a semi-closed environment N90-16689
Plant features measurements for robotics N90-16695
WIND (METEOROLOGY)
Diagnostic and kinematic fields associated with curved and straight jet streaks using a two-layer primitive equation model N90-16371
A dynamic model for forecasting new cloud development
[AD-A213939] N90-16383
WIND DIRECTION
ECC (Electrochemical Concentration Cell) ozonesonde observations at South Pole, Antarctica, during 1988
[PB90-110172] N90-16355
WIND TUNNEL APPARATUS
Instrumentation for cryogenic wind tunnels N90-15950
WIND TUNNEL CALIBRATION
The US National Transonic Facility, NTF N90-15942
The Kryo-Kanal Koeln (KKK): Description of the tunnel conversion. Thermal insulation, instrumentation, operational experience, test results and operating costs N90-15943
The cryogenic Ludwieg tube tunnel at Goettingen N90-15947
Instrumentation for cryogenic wind tunnels N90-15950
WIND TUNNEL MODELS
Fundamental considerations in testing in cryogenic wind tunnels N90-15951
Test techniques for cryogenic wind tunnels N90-15952
Flow visualization in the cryogenic wind tunnel N90-15953
Materials and techniques for model construction N90-15954
Some recent developments in materials and techniques for model fabrication N90-15955
Models for cryogenic wind tunnels N90-15956
Experience with strain-gage balances for cryogenic wind tunnels N90-15958
The determination of vortex separation frequencies by means of laser light sheet images
[DNW-WTI-88.038] N90-16245
Quantitative heat transfer measurements using heated liquid crystals N90-16256
WIND TUNNEL TESTS
Wind tunnel tests of the influence of aerofoil thickness on the normal force and pitching moment of two slender wings at transonic and supersonic Mach numbers
[ESA-TT-1129] N90-15889
Special Course on Advances in Cryogenic Wind Tunnel Technology
[AGARD-R-774] N90-15939
Introduction to cryogenic wind tunnels N90-15940
Fundamental considerations in testing in cryogenic wind tunnels N90-15951
Test techniques for cryogenic wind tunnels N90-15952
Wind tunnel investigations on the configuration of the international vortex flow experiment N90-16181
Further development of the PIV method for use in the large wind tunnel N90-16248
WIND TUNNELS
Pressure measurement technique in the wind tunnel division of DFVLR
[ESA-TT-1145] N90-15963
WIND TURBINES
Performance predictions for an intermediate-sized VAWT based on performance of the 34-m VAWT test bed
[DE90-002835] N90-16345
WIND VELOCITY
ECC (Electrochemical Concentration Cell) ozonesonde observations at South Pole, Antarctica, during 1988
[PB90-110172] N90-16355
Climatic summaries and documentation for the primary meteorological Station, H. J. Andrews Experimental Forest, 1972 to 1984
[PB90-104373] N90-16382
WINDMILLS (WINDPOWERED MACHINES)
Definition, transformation-formulae and measurements of tipvane angles
[IW-R510] N90-16351
WINGS
Test techniques for cryogenic wind tunnels N90-15952
WINTER
Multiple flow regimes in the Northern Hemisphere winter N90-16372
Lightning observations on Japan Sea coast in winter
[DE90-702485] N90-16387
Characteristics of electromagnetic wave forms with lightning in winter season (2): Characteristics in frequency domain
[DE90-734989] N90-16388
WORLD METEOROLOGICAL ORGANIZATION
Guide on the global observing system
[WMO-488-REV] N90-16385

X

X RAY ANALYSIS
Mass loss during x ray microanalysis
[DE90-003954] N90-16067
Atomic processes in plasmas under ultra-intense laser irradiation
[DE90-003221] N90-16521
X RAY ASTRONOMY
Galactic x ray astronomy with EXOSAT N90-16597
A low-threshold EAS (Extensive-Air-Shower) array for gamma-ray astronomy at Los Alamos
[DE89-016780] N90-16600
On the interaction of a pulsar with the ambient medium utilizing x ray images of the Crab nebula
[MPE-REPT-215] N90-16604
Recent and future x ray observations of classical novae during the outburst stage
[MPE-PREPRINT-159] N90-16606
X RAY BINARIES
An atlas of aperiodic variability in HMXB
[MPE-PREPRINT-158] N90-16605
X RAY FLUORESCENCE
Trace element abundance determinations by Synchrotron X Ray Fluorescence (SXRF) on returned comet nucleus mineral grains N90-16619
Non-destructive trace element microanalysis of as-received cometary nucleus samples using synchrotron x ray fluorescence N90-16649
X RAY IMAGERY
Necessity and benefit of the X-SAR Space Shuttle experiment
[ESA-TT-1164] N90-16112
End-on soft x ray imaging of Field-Reversed Configurations (FRCs) on the Field-Reversal-C (FRX-C)/Large Scale Modification (LSM) experiment
[DE90-004863] N90-16260
X RAY INSPECTION
Structural characterization of Spacelab
[ETN-90-95214] N90-16289
X RAY SOURCES
Galactic x ray astronomy with EXOSAT N90-16597
Status of the expansion of the CYGNUS array at Los Alamos
[DE89-016781] N90-16601
X RAY SPECTRA
Mass loss during x ray microanalysis
[DE90-003954] N90-16067
X ray spectrophotometric remote sensing of diffuse auroral ionization
[SD-TR-89-09] N90-16599
Ion-heated thermal Comptonization models and x ray spectral correlations in active galactic nuclei
[DE90-003597] N90-16667
X RAY STARS
An atlas of aperiodic variability in HMXB
[MPE-PREPRINT-158] N90-16605
X RAY TELESCOPES
The MPI/AIT X ray Imager (MAXI): High speed PN-CCD's for x ray detection
[MPE-PREPRINT-154] N90-16234
Recent and future x ray observations of classical novae during the outburst stage
[MPE-PREPRINT-159] N90-16606
X RAYS
Evaluation of potential cold x ray shield materials tested on Proto II
[DE90-004348] N90-16003
Material responses to incident x rays
[DE89-015366] N90-16305

Y

YAG LASERS
Eurolaser definition phase: A comparison of high power lasers available
[ETN-90-96061] N90-16268
YTTRIUM OXIDES
ZrO2 sintered compact and method for its production
[DE90-004125] N90-16006

Z

ZENITH
Atmospheric transmittance determination from a two-angle measurement of radiance change
[AD-A213847] N90-16375
ZINC ALLOYS
Cycle-life improvement of Zn/NiOOH cells by the addition of Ca(OH)2 to the zinc electrode
[DE90-004040] N90-16139
ZIRCONIUM
Structural analysis of zirconium-aluminum plasma deposits
[ETCA-89-R-073] N90-16045
ZIRCONIUM ALLOYS
Estimation of thermodynamic properties of alloys from phase diagram and other loose boundary conditions
[DE90-719511] N90-16579
ZIRCONIUM OXIDES
ZrO2 sintered compact and method for its production
[DE90-004125] N90-16006
Development of planar geometry solid oxide fuel cells
[PB90-100769] N90-16341
ZONAL HARMONICS
On mean elements for satellite orbits perturbed by the zonal harmonics of the geopotential
[RAE-TM-SPACE-371] N90-15971

Typical Personal Author Index Listing

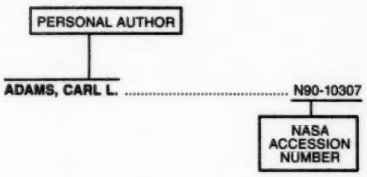

Listings in this index are arranged alphabetically by personal author. The NASA accession number denotes the number by which the citation is identified.

A

AARONSON, HUBERT I. N90-16035
AARSVOLD, JOHN N. N90-16208
ABDULLAH, KAMAL FUAD N90-16484
ABE, T. N90-16078
ABOLHASSANI, JAMSHID S. N90-15891
ABRAMOV, I. P. N90-15976
ADDY, HAROLD E., JR. N90-15965
ADRIANI, A. N90-16231
ADUOL, FRANCIS W. ODHIAMBO N90-16317
AERENS, RICHARD N90-16435
AERS, G. C. N90-16288
AGEMATSU, TAKASHI N90-16349
AGGARWAL, B. N90-16540
AGUILAR, JERRY L. N90-15996
AHEARN, M. N90-16627
AHLBRECHT, HORST N90-16256
ALBEE, A. L. N90-16608
ALDROVANDI, ETTORE N90-16466
ALEXANDREAS, D. E. N90-16665
ALLAMANDOLA, L. J. N90-16609
N90-16612
ALLEN, M. A. N90-16121
ALLEN, R. C. N90-16665
ALLRED, JOHN C. N90-16366
ALMLOEF, JAN N90-16482
ALPERS, MATTHIAS N90-16117
ALT, THORSTEN N90-15970
ALTER-GARTENBERG, RACHEL N90-16216
AMATA, E. N90-16230
AMICK, GROVER S. N90-15930
AMMAR, E. A. N90-16545
ANAND, L. N90-16470
ANASTASIADIS, SPIROS H. N90-16079
ANDERSON, K. D. N90-16108
ANDERSON, KAREN S. N90-16212
ANDERSSON, CLARENCE A. N90-16061
ANDREAE, P. V. N90-16413
ANDRES, JAMES R. N90-16273
ANGELICI, GARY L. N90-16313
ANGRILLI, F. N90-16231
ANSMANN, ALBERT N90-16265
ARBUZOVA, V. N. N90-16357
ARCHAMBAUD, JEAN-PIERRE N90-15946
ARENDT, RONALD H. N90-16568
AREPALLI, SIVARAM N90-16013
ARIJS, E. N90-16379
ARLIA, N. N90-16209
ARMSTRONG, DENNIS W. N90-16686
ARNOLD, F. N90-16190
ARNOLD, G. W. N90-16069
ARNOLD, J. R. N90-16640
ASAY, J. R. N90-15973
N90-16282
ASCOUGH, J. C. N90-15922
ASH, W. W. N90-16552
AUERKARI, PERTTI N90-16039
AUERNHEIMER, BRENT J. N90-16687
AUTERINEN, I. H. N90-16498

B

BABCOCK, S. M. N90-16132
BACIAK, MARK G. N90-16127
BADIRKHAN, Z. N90-16487
BAE, GYOUNG H. N90-15936
BAE, INTAK N90-16280
BAHNER, MARK A. N90-16149
BAILEY, A. D., III N90-16260
BAILLE, G. N90-16233
BAKER, T. S. N90-16043
BALAKRISHNA, S. N90-15957
BALDASARE, PAUL N90-15902
BALDETTI, P. N90-16230
BALDO, P. M. N90-16539
BALLINGALL, R. A. N90-16502
BALOCCO, MARIO N90-16289
BALSIGER, H. N90-16378
BANFIELD, JEFFREY D. N90-16311
BANKSTON, CLYDE P. N90-16124
BANNERT, D. N90-16334
BAR-NUN, AKIVA N90-16610
N90-16621
BARASSIN, A. N90-16379
BARBOUR, J. C. N90-16069
BARNES, D. C. N90-16520
BARNES, J. M. N90-16685
BARNES, PAUL R. N90-16138
N90-16140
BARNEY, MEL N90-15932
BARRETT, HARRISON H. N90-16208
BARRON, ANDY R. N90-16057
BARROS, SAULO R. M. N90-16468
BARRY, JAMES D. N90-15984
BARSIKOW, B. N90-16241
BARSONY, MARY ANNE N90-16657
BARTEAU, MARK A. N90-16040
BARTELS, H.-H. N90-16237
BASHAM, BRYAN D. N90-16410
BASU, SOUMENDRA NATH N90-16585
BATES, J. L. N90-16049
BATHIA, R. N90-16231
BATTRICK, BRUCE N90-15988
N90-16590
BAUER, HELMUT F. N90-16090
N90-16166
N90-16167
N90-16168
BAVASSANO-CATTANEO, M. B. N90-16229
BAVASSANO, B. N90-16678
BAVASSANO, M. B. N90-16230
BAYER, THOMAS N90-16332
BAZIN, MAURICE N90-15950
BEAUDET, PAUL R. N90-16209
N90-16210
BECKER, CHRISTIAN N90-15970
BECKER, K. N90-16180
BEEKE, K. L. N90-16096
BEGEMANN, FRIEDRICH N90-16611
BEHR, R. N90-16183
BEHRENS, K. N90-16314
BELLONI, T. N90-16605
BELLUCCI, G. N90-16230
N90-16231
BENEDICT, J. J. N90-16095
BENKHOFF, J. N90-16645
BENO, MARK A. N90-16020
N90-16550
BERENS, A. P. N90-16294
BERGER, CHRISTIAN N90-16156
BERGER, H. N90-16188
BERLEY, D. N90-16600
N90-16601
BERNARD, MARTINIE N90-16022
BERRY, G. F. N90-16526
BERTHOMIEV, G. N90-16677
BESSHOU, S. N90-16515
BEWLEY, A. D. N90-15921
BEZY, J. L. N90-16503
BHATTACHARYYA, SAMIT K. N90-15995
N90-16055
BIANCO, CORRADO N90-15907
BICKES, R. W., JR. N90-16082
BIELER, H. N90-16179
BIERLMAIER, FREDERICK A. N90-16382
BIGALKE, K. N90-16365
BIGGS, ALBERT W. N90-16131
BILLER, S. N90-16665
BIPPES, H. N90-16170
BIRTCHER, R. C. N90-16547
BISHOP, P. S. N90-16048
BLAKE, D. F. N90-16612
BLAKE, H. W. N90-16512
BLANCO, A. N90-16616
BLAND, SAMUEL R. N90-15892
BLECHINGER, F. N90-16503
BLENKINSOP, I. D. N90-16502
BLEVINS, CREED E. N90-16296
BLEVINS, D. W. N90-16453
BLITZ, LEO N90-16674
BLOCH, A. N90-16247
BLUM, H. N90-16160
BODVARSSON, GUDMUNDUR S. N90-16343
BOEHM, M. H. N90-16116
BOENSCH, EVA N90-16331
BOFF, KENNETH R. N90-16106
BOICE, D. C. N90-16624
BOIFFIER, JEAN-LUC N90-15925
BOLING, M. E. N90-16119
BORCHARDT, B. N90-16439
BORCHERS, INGO N90-16398
BORDERS, M. E. N90-15914
BORDONI, FRANCO N90-16504
BORELLOFILISETTI, OTTAVIA N90-16670
BORGESON, PETER N90-16056
BORGHESI, A. N90-16616
BORK, THOMAS N90-16604
BOSSI, J. A. N90-15937
BOUILLARD, J. X. N90-16526
BOUIS, XAVIER N90-15945
BOWER, J. R. N90-16077
BOWMAN, R. C., JR. N90-16540
BOWSER, SAMUEL E. N90-16100
BOYD, DAVID A. N90-16652
BRADLEY, JOHN N90-16613
BRAEUNINGER, H. N90-16234
BRAMSON, B. D. N90-16425
BRANDON, DEBORAH N90-16145
BRETTHAUER, B. N90-16237
BREUER, M. N90-16187
BROIDO, DAVID A. N90-16544
BROW, R. K. N90-16069
BROWN, IAN G. N90-16123
BROWNE, E. N90-16680
BRUCE, WALTER E., JR. N90-15942
BRUINING, A. N90-16351
BRUN, T. O. N90-16533
BRUNO, R. N90-16229
N90-16230
BRYNESTAD, J. N90-16562
BUCHELNIKOVA, N. S. N90-16474
BUDAI, J. N90-16562
BUDDE, KLAUS N90-15901
BUDINGER, JAMES M. N90-15983
BUDZ, S. N90-16020
BUETEFISCH, KARL-ALOYS N90-16182
N90-16256
BUGGA, RATNAKUMAR V. N90-16124
BULLOCK, J. S. N90-16091
BURKE, W. R. N90-16113
BURKHOLDER, R. J. N90-16103
BURMAN, R. L. N90-16600
N90-16601
N90-16665
BURRELL, K. N90-16509
BUSSOLETTI, E. N90-16616
BUTTERFIELD, KENNETH B. N90-16420
BUXBAUM, O. N90-16302
BYNUM, MARY ANN N90-16424

C

CADY, D. R. N90-16601
N90-16665
CAIRNS, ELTON J. N90-16139
CALISE, ANTHONY J. N90-15936

CALLE, LUZ M. N90-16686
CALLIN, R. S. N90-16121
CALVERT, W. J. N90-15919
CAMILLO, P. J. N90-16449
CAMPBELL, C. W. N90-16389
CAMPBELL, G. L. N90-16092
CAMPINS, HUMBERTO N90-16614
CANDIDI, M. N90-16230
N90-16377
N90-16378
CAPACCIONI, F. N90-16231
CAPART, J.-J. N90-15982
CAPONE, FRANCIS J. N90-15884
CARINENA, JOSE F. N90-16456
CARLSON, K. DOUGLAS N90-16550
CARLSSON, LENNART N90-16308
CARR, M. J. N90-16069
CARRERAS, B. A. N90-16510
CARRERAS, RICHARD A. N90-16127
CARROLL, BRUCE FREDERICK N90-16141
CARSEY, FRANK D. N90-16312
CARUSI, A. N90-16231
CASEY, WILLIAM L. N90-16263
CASPERSON, D. E. N90-16521
CASSIDY, JOSEPH R. N90-15993
CATTANEO, P. N90-16234
CENTERS, PHILLIP W. N90-16059
CERULLI-IRELLI, P. N90-16230
CHAIKO, LEV N90-15923
CHAKOUMAKOS, B. C. N90-16561
N90-16563
CHAMBERLIN, JAY L. N90-16129
CHAMIS, C. C. N90-16008
CHAMP, PASCAL N90-16074
CHAN, Y. D. N90-16523
CHANG, C. Y. N90-16601
CHANG, S. N90-16615
CHAPMAN, RICHARD N. N90-16129
CHAPPELL, R. N. N90-16201
CHEN, GE N90-16434
CHEN, H. N90-16143
CHEN, ROBERT T. N. N90-15936
CHEN, RUEY-HUNG N90-16009
CHEN, S. N90-16143
CHEN, W. N90-16262
CHENG, THOMAS D. N90-16313
CHETYRKIN, K. G. N90-16457
CHICARRO, A. F. N90-15968
CHICK, L. A. N90-16049
CHIONCHIO, G. N90-16230
N90-16231
CHIPMAN, LAURE J. N90-16221
CHOU, H. N90-16075
CHRISTEN, D. K. N90-16562
CHRISTENSEN, THOMAS M. N90-16079
CHRISTIAN, T. F., JR. N90-15914
CHRISTIE, W. H. N90-16025
CHRISTOPHE, J. N90-15961
CHUN, DU HWAN N90-16478
CHURCH, EUGENE L. N90-16501
CHURNSIDE, JAMES H. N90-16261
CIMA, MONIQUE N90-16405
CINNIBULK, M. N90-16012
CIPRI, FRANCO N90-16289
CLARKSON, CHARLES B. N90-16105
CLAUS, J. N90-16262
CLAYTON, C. R. N90-16033
N90-16034
CLIFF, G. N90-16427
CLINARD, L. A. N90-16413
COATES, ELINOR L. N90-16127
COBBLE, J. A. N90-16521
COLANGELI, L. N90-16616
COLELLA, PHILIP N90-16674
COLLINGS, E. W. N90-16052
N90-16570
COLLINS, DAVE G. N90-16412
COLOMBINA, G. N90-15635
COLSON, THOMAS E. N90-16084
COMLY, J. C. N90-16521
COMPAAN, A. N90-16540
CONQUET, F. N90-16233
COOK, R. N90-16300
COOK, R. L. N90-16225
COON, D. D. N90-16218
COOPER, D. E. N90-16540
CORADINI, A. N90-16231
CORADINI, M. N90-15968
COREY, KENNETH A. N90-16689
CORNSWEET, TOM N. N90-16215
COSMOVICI, C. B. N90-15986
COSTA, ISAIAS N90-16662
COSTELLO, M. J. N90-16066
COTTON, WILLIAM R. N90-16383
COUNTS, D. L. N90-16130
COURTOIS, B. N90-16134
COX, ARTHUR N. N90-16598
COZZENS, ROBERT F. N90-16014
CRABTREE, G. W. N90-16534
CRAIG, J. W. N90-15977
CRAWFORD, H. J. N90-16681
CRIBIER, M. N90-16677
CRONIN, J. R. N90-16617
CRUZ, CHRISTOPHER I. N90-15890
CUTTER, M. A. N90-16503
CZICHOWSKY, W. N90-16157
CZYRSKA-FILEMONOWICZ, A. N90-16044

D

DABROWSKI, B. N90-16534
DAHL, ERNEST A. N90-16227
DALLMANN, DANIEEL N90-15970
DAMP, S. N90-16232
DANNENBERG, KLAUS N90-15932
DARGEL, G. N90-16191
DATHE, INGO N90-16398
DAVID, VALERIE N90-15974
N90-16088
N90-16706
DAVIS, E. W. N90-16445
N90-16453
DAVIS, SANFORD N90-16399
N90-16400
DAVIS, SIMON N90-16575
DAVIS, STEVEN J. N90-16485
DAVIS, THOMAS J. N90-15898
DAWSON, G. N90-15908
DAY, J. N90-15909
DAYI, OMER F. N90-16574
DEBEY, T. M. N90-16276
DEBIASSE, ROBERT A. N90-16501
DEBOO, J. C. N90-16509
DECKELNICK, KLAUS N90-16163
DECKER, D. L. N90-16534
DEEDS, H. A. N90-16562
DEFRAINE, JAN N90-16435
DELRE, E. N90-16113
DEMUTH, GARY E. N90-16131
DENHOFF, M. W. N90-16288
DENIEL, MARC N90-16435
DENKER, HEINER N90-16315
DENTON, M. M. N90-16545
DEREP, J. L. N90-16045
DERMER, CHARLES D. N90-16667
N90-16682
N90-16683
DERUELLE, NATHALIE N90-16662
DERUYTER, H. N90-16121
DEVANEY, JUDY E. N90-16443
N90-16449
DEVAUTOUR, B. N90-16233
DEVENUTO, F. N90-15986
DEVERAUX, MICHELE L. N90-16295
DEVRIES, KEVIN R. N90-16285
DEWILDE, J. P. N90-16001
DEZWAAN, F. N90-16590
DIEMOZ, M. N90-16495
DIERKSMEIER, DOUGLAS D. N90-16274
DIGREGORIO, D. E. N90-16523
DIJKSTRA, F. N90-16000
N90-16001
DILELLIS, A. N90-16230
DIMACZEK, G. N90-16253
DINGUS, B. L. N90-16600
N90-16601
DION, G. N90-16665
DISTEFANO, J. R. N90-16048
DISTEFANO, SALVADOR N90-16124
DOBREV, V. K. N90-16464
DOCARMO, EDUARDO G. D. N90-16148
DODD, HENRY M. N90-16345
DODD, LORRAINE N90-16426
DOEBELE, M. N90-16314
DOERFLER, T. N90-16175
DOHRN, DANIELA N90-16466
DOIRON, T. N90-16439
DOMINGUEZ, N. N90-16510
DOMINGUEZ, R. R. N90-16150
DONOVAN, JOHN FRANCIS N90-15883
DONOVAN, MICHELL M. N90-16057
DOOLEN, G. D. N90-16143
DOPHEIDE, D. N90-16176
N90-16238
DORBAND, JOHN E. N90-16448
N90-16450
N90-16454
DOUBLEDAY, M. K. N90-16389
DOUGLAS, DAVID L. N90-16269
DOWLING, N. E. N90-16294
DRESNER, L. N90-16510
DRIVAS, P. J. N90-16342
DRYER, FREDERICK L. N90-16017
DUEREN, H. N90-16648
DULLENKOPF, K. N90-16250
DURLOFSKY, LOUIS J. N90-16401
DUTRADOCARMO, EDUARDO G. N90-16461
DUVENBECK, HARALD N90-16164

E

EAGAR, C. N90-16361
EARL, JAMES A. N90-16448
EASTERLY, CLAY E. N90-16393
EATON, DEREK N90-15999
EBERT, A. N90-16314
ECKHARDT, ROGER C. N90-16366
EDWARDS, JOHN W. N90-15886
EGAN, B. ZANE N90-16019
EH, C. N90-16253
EHRENSTEIN, U. N90-16171
EICH, G. N90-16643
EIDEL, WERNER N90-16167
N90-16168
EKSTEDT, EDWARD E. N90-15918
EL-KHATIB, A. M. N90-16545
ELANDS, P. J. M. N90-16000
N90-16001
ELLIS, DAVID L. N90-16053
ELLSWORTH, R. W. N90-16665
ELMAHGARY, YEHIA N90-16093
ELPHIC, R. C. N90-16378
ELSHOLZ, E. N90-16192
ENCKE, WALTER N90-16397
ENDEBROCK, ELTON G. N90-16463
ENGEL, THOMAS N90-16543
ENGELAGE, J. N90-16681
ENGI, DENNIS N90-16364
ENGLERT, P. A. J. N90-16623
ENGQUIST, BJORN N90-16401
ENNIS, P. J. N90-16044
EPPLEY, K. R. N90-16121
ERIKSSON, ANKE N90-16324
ESCALADA-IMAZ, GONZALO N90-16436
ESCH, HELMUT N90-15889
ESKENAS, K. N90-16340
EVERTS, JEFF N90-16418
EXARHOS, GREGORY J. N90-16068
EYLON, DANIEL N90-16029
N90-16030
N90-16031

F

FABER, M. N90-16176
N90-16238
FAI, G. N90-16481
FAIRCHILD, P. D. N90-16363
FALCO, CHARLES M. N90-16567
FANT, K. S. N90-16121
FARRELLE, PAUL M. N90-16222
FEGLEY, BRUCE, JR. N90-16618
FENNER, JAMES H. N90-16690
FERENCZ, ROBERT MARK N90-16291
FERGUSON, STEVEN L. N90-15935
FERMAN, M. A. N90-15915
FERNANDES, A. O. N90-16134
FERNANDEZ, JUAN C. N90-16283
N90-16527
FERNOW, R. C. N90-16262
FERRANDO, P. N90-16681
FERRARO, JOHN R. N90-16550
FERREIRADEPAULA, HELIO, JR. N90-16063
FERRIS, ALICE T. N90-15959
FERRONI, F. N90-16495
FICHTER, W. B. N90-16293
FINEL, ALPHONSE N90-16557
FISCHER, J. N90-16262
FLAMAND, LOUIS N90-16281
FLEURY, P. A. N90-16075
FLICKINGER, GREGORY C. N90-16652
FLYNN, G. J. N90-16619
FOERSTER, SABINE N90-16243
FONTI, S. N90-16616
FORMISANO, V. N90-16229
N90-16230
N90-16231
FORSYTH, WILLIAM B. N90-16223
FOSTER, D. N. N90-15888
FOUJANET, M. C. N90-16045
FOWKES, W. R. N90-16121
FOWLKES, JENNIFER N90-16392
FRANCA, LEOPOLDO P. N90-16417
N90-16461
N90-16462

FRANCIC, STEPHEN PAUL N90-16660
FRANCIS, MICHAEL H. N90-16101
FREEMAN, B. N90-16520
FREIRE, HAYDEE RODRIGUES N90-16016
FRESE, K. W., JR. N90-16012
FRETWELL, P. N90-16428
FROES, FRANCIS H. N90-16028
N90-16029
N90-16030
N90-16031
FUCHS, H. H. N90-16114
FULKERSON, W. N90-16363
FURENLID, KAREN N90-16501
FURLONG, DALE A. N90-16149
FURUHARA, T. N90-16035
FUSSEN, D. N90-16379

G

GAENSWEIN, BERNHARD N90-16558
GALANT, DAVID C. N90-16423
GALEAO, AUGUSTO CESAR N90-16148
GALLAGHER, J. P. N90-16294
GALLARDO, J. C. N90-16262
GALLOT, DANIEL N90-16156
GALVIN, JAMES E. N90-16123
GARBAUSKAS, MARY F. N90-16568
GARDNER, JAMES E. N90-15894
GARDNER, SHELDON N90-16219
GARNER, F. A. N90-16041
N90-16042
N90-16047
GARRISON, ARLENE A. N90-16026
GAUDIN, PASCAL N90-16156
GAULKE, SCOTT N90-16343
GEERTS, A. H. W. N90-16467
GEISER, URS N90-16550
GELLES, D. S. N90-16041
GENDRE, PASCAL N90-16165
GENENS, L. N90-16350
GEORGIADIS, NICHOLAS N90-16292
GERAGHTY, PAUL N90-16440
GERLI, C. N90-16635
GEROPP, D. N90-16242
GERTEISEN, EDGAR A. N90-16196
GESELL, GERHARD N90-16322
GEWECKE, K. N90-16116
GEYER, HOWARD K. N90-15995
GHIRARDI, GIANCARLO N90-16573
GILES, G. E. N90-16091
GILGALLON, J. J. N90-16092
GINDER, R. B. N90-15919
GLASMACHERS, ROLAND N90-15970
GLEASON, CLIFFORD C. N90-15918
GLEASON, DANIEL N90-15903
GLOSS, BLAIR B. N90-15942
GLOVER, CHARLES W. N90-16438
GOLDBERG, LAURENCE P. N90-16358
GOLDNER, RONALD B. N90-16564
GOLDSTEIN, C. I. N90-16480
GONGADZE, A. D. N90-16531
GOODING, R. H. N90-15971
GOODMAN, J. A. N90-16600
N90-16601
GOODYER, M. J. N90-15940
N90-15953
GORDON, L. B. N90-16130
GORNEY, D. J. N90-16599
GOSMAN, A. D. N90-16195
GOUYON, Y. N90-16233
GOWER, DANIEL W., JR. N90-16392
GRADY, D. E. N90-16278
GRAHAM, R. A. N90-16066
GRASSI, RENATA N90-16573
GRATTAN, K. T. V. N90-16228
GRAY, L. J. N90-16091
GREEN, P. L. N90-16413
GREEN, PETER F. N90-16079
GREEN, STEVEN M. N90-15898
GREENBERG, IRA N90-16416
GREENBERG, J. M. N90-16620
GREGORY, E. N90-16570
GREGSON, P. J. N90-16301
GREINER, GARY P. N90-16149
GRIBBLE, R. J. N90-16260
GRIFFEATH, D. N90-16010
GROENIG, H. N90-16240
GROSS, E. E. N90-16488
GROSSE, C. N90-16390
GROVE, JOHN W. N90-16144
GROVES, A. N90-15997
GRUDEN, JAMES M. N90-16126
GRUEN, E. N90-16621
N90-16645
N90-16650
GUALTIERI, J. A. N90-16213
N90-16443
GUBBAY, J. S. N90-16595
GUCINSKI, HERMANN N90-16360
GUER, TURGUT M. N90-16011
GUERRA, FRANCESCO N90-16466
GUESSOUM, N. N90-16683
GUIDONI, U. N90-15986
N90-15987
N90-15988
GUNADHI, HIMAWAN N90-16588
GUPTA, RAJ K. N90-16513
GUPTA, S. K. N90-16513
GURNEY, R. J. N90-16449
GUYENNE, T. D. N90-15974
GUYVARCH, J. P. N90-15928
GUZIK, T. G. N90-16681

H

HAAG, THOMAS W. N90-15992
HAAS, TERRY E. N90-16564
HACKETT, E. M. N90-16032
HACKSTEIN, JOSEF N90-16398
HADFIELD, MARK GREGORY N90-16369
HAENEL, D. N90-16187
HAFNER, JAMES L. N90-16471
HAGEN, KIRK DEE N90-16152
HAINES, T. J. N90-16600
N90-16601
HALL, WILLIAM A. N90-16411
HALLIKAINEN, MARTTI N90-15967
HAMED, A. N90-15885
HAMED, A. E. N90-16546
HAMET, L. N90-16454
HAMILTON, M. L. N90-16046
HAMILTON, WILLIAM N90-16271
HAMMOND, P. D. N90-16427
HANAN, NELSON A. N90-15995
HANATANI, K. N90-16515
HARA, HISAO N90-16006
HARALSON, DAVID G. N90-16127
HARASGAMA, S. P. N90-15920
HARDY, JOHN T. N90-16360
HARIG, J. N90-16160
HARMON, B. A. N90-16523
HARRIS, RICHARD A. N90-16410
HARTMANN, CLINTON S. N90-16125
HARTMANN, K. N90-16182
HARTMANN, WILLIAM K. N90-16622
HARUYAMA, YASUYUKI N90-16349
HASHIMITO, O. N90-16553
HASINGER, G. N90-16605
HAUFF, D. N90-16234
HAWKE, R. S. N90-15973
HAYAKAWA, NAOHIRO N90-16554
HAZRA, RAJEEB N90-16206
HEALEY, M. D. N90-15915
HEATON, R. A. N90-16453
HECKENDORN, FRANK M. N90-16284
HEDRICK, C. L. N90-16510
HEFER, G. N90-15947
HEISER, R. N90-16021
HELLER, P. N90-16247
HELLMANN, H. N90-16650
HENCKELS, A. N90-16258
HENINS, IVARS N90-16283
N90-16520
N90-16527
HENKE, R. N90-16180
N90-16251
HENRIKSEN, G. L. N90-16122
N90-16269
HENSEL, D. N90-16021
HENTSCHEL, WERNER N90-16246
HERHOLZ, J. N90-16199
HERRMANN, M. N90-16267
HERTEL, J. N90-16189
HERZOG, G. F. N90-16623
HESTER, R. D. N90-16062
HETTLAGE, E. N90-16503
HEYL, M. N90-16643
HEYSER, RICHARD C. N90-16391
HILGENSTOCK, A. N90-16186
HILLER, W. J. N90-16239
HILLIS, S. L. N90-16277
HINKS, D. G. N90-16534
HINSSEN, HANS-KLEMENS N90-16024
HIRSCH, C. N90-16254
HIRSHMAN, S. P. N90-16510
HIRST, ERIC N90-16348
HIRVONEN, JUHA PEKKA N90-16056
HISMATSU, T. N90-16078
HITTERMAN, RICHARD L. N90-16568
HOAD, DANNY R. N90-15882
HOAG, H. A. N90-16121
HOCHHAUS, LARRY W. N90-16691
HODGSON, J. W. N90-16277
HOECKER, RAINER N90-16248
HOFER, W. W. N90-16130
HOFF, WILLIAM N90-16224
HOFFMAN, C. M. N90-16600
N90-16601
HOHRATH, A. N90-16314
HOLDEMAN, J. T. N90-16422
HOLLAND, O. W. N90-16556
HOLLISTER, WALTER M. N90-15899
HOLLSTEIN, THOMAS N90-16303
HOLMES, M. N90-15922
HOLTZ, ROBERT E. N90-16036
HOLTZCLAW, KARL N90-16485
HOMMA, MASANORI N90-15981
HORSTMANN, K.-H. N90-16178
HOSLER, E. RAMON N90-16686
HOSOYA, AKIO N90-16580
HOUPT, RONALD A. N90-16151
HOUSER, DONALD R. N90-16286
HOUSTON, A. N90-15929
HRUBESH, LAWRENCE W. N90-16489
HSIA, WEI SHEN N90-16407
HSIUNG, P. N90-16650
HUANG, F. H. N90-16046
HUANG, J. Y. N90-16536
HUANG, JOHN N90-16104
HUBER, GUENTER N90-16266
HUCK, FRIEDRICH O. N90-16204
N90-16211
HUDMAN, G. D. N90-16047
HUEBNER, W. F. N90-16624
HUFENBACH, BERNHARD N90-15970
HUGGINS, ROBERT A. N90-16011
HUGHES, H. G. N90-16374
N90-16375
HUGHES, THOMAS J. R. N90-16462
HULBERT, GREGORY M. N90-16462
HULSTROM, R. L. N90-16352
HUNT, A. N90-16209
HUNT, CHARLES E. N90-16064
HUNT, J. N90-15998
HUNTER, NORMAN F., JR. N90-16297
HUTH, H. N90-16302
HUTTA, JOSEPH J. N90-16060

I

IBADOV, S. N90-16625
IIMA, M. N90-16515
IIYOSHI, ATSUO N90-16515
N90-16516
INGELS, J. N90-16379
INOUE, RYOJI N90-16006
IREDELL, MARK DOUGLAS N90-16367
IRVING, P. M. N90-16361
ISHIHARA, KARORU N90-16137
ITOH, HISAYOSHI N90-16554
IUCCI, N. N90-16678
N90-16684
IWAI, TAKASHI N90-16579

J

JACK, J. W. N90-15929
JACKMAN, T. E. N90-16288
JACKSON, RAYMOND H. N90-16004
JACKSON, W. L. N90-16422
JAIN, RAJIV N90-16139
JAKOB, H. N90-16180
N90-16191
JAKOBSSON, B. N90-16481
JAMES, GORDON E. N90-16272
JANETOS, ANTHONY C. N90-16356
JANOTH, JUERGEN N90-16328
JANSEN, J. F. N90-16132
JANU, Z. N90-16531
JARBOE, THOMAS R. N90-16283
N90-16520
N90-16527
JAYARAMAN, V. N90-15887
JEFFERSON, A. N90-16301
JENNINGS, MARK J. N90-16200
JENNINGS, T. M. N90-15914
JENZER, U. N90-16379
JERVIS, THOMAS R. N90-16057
JIAN, L. N90-16005
JIANG, C. Y. N90-16005
JIWEI, J. N90-16228
JOBSON, DANIEL J. N90-16217
JOHN, R. Y. N90-16115
JOHN, SARAH N90-16211

JOHNSON, D. L. N90-16389
JOHNSON, J. O. N90-16685
JOHNSON, KENNETH C. N90-16506
JOHNSON, KEVIN E. N90-16543
JOHNSON, MARVIN M. N90-16459
JOHNSON, R. E. N90-16626
JOHNSTON, I. R. N90-16081
JONES, F. C. N90-16681
JONES, KEITH W. N90-16067
JONES, L. A. N90-16521
JONSSON, G. N90-16481
JORDAN, C. W. N90-16130
JORGENSEN, J. D. N90-16534
JORGENSEN, JAMES D. N90-16568
JUSTUS, C. G. N90-16389
JUTRO, PETER R. N90-16356

K

KACKLEY, NANCY N90-16347
KAGERBAUER, G. N90-15913
KAHN, ANTOINE N90-16542
KAHRAMAN, AHMET N90-16286
KAJAVA, T. T. N90-16498
KALU, ALEX O. N90-16692
KAMGAR-PARSI, BEHROOZ N90-16443
KAMGAR-PARSI, BEHZAD N90-16443
KANAZAWA, TAKAO N90-16349
KANDIL, S. H. N90-16546
KANEKO, HIROSHI N90-16516
KANG, TZONG-SHYAN N90-16441
KANOUN, KARAMA N90-16437
KARLSSON, L. N90-16481
KASSEM, M. E. N90-16545
N90-16546
KAWA, STEPHAN RANDOLPH N90-16381
KAWABATA, CURT M. N90-15994
KAWABATA, TADASHI N90-16516
KAYAL, GOEKHAN N90-15969
KAYAL, HAKAN N90-15970
KEITH, THEO G., JR. N90-15965
KEITH, WILLIAM L. N90-16226
KEKKONEN, VEIKKO N90-16093
KELLER, H. U. N90-16621
KELLMAN, A. N90-16524
KENNEDY, A. D. N90-16421
KENNEDY, CHANDLER J. N90-15984
KENNEL, E. N90-16055
KENNEWEG, H. N90-16336
KERRES, W. N90-16240
KETTHAUS, B. N90-16178
KEYDEL, WOLFGANG N90-16112
KHADKIKAR, S. B. N90-16514
KHANDKAR, ASHOK C. N90-16341
KHATTATOV, V. U. N90-16357
KHOSROVANEH, A. K. N90-16294
KIENZLER, REINHOLD N90-16303
KILGORE, ROBERT A. N90-15948
KIM, D. N90-16034
KIM, S. N90-16627
KIM, SOON SAM N90-16651
KIM, Y. C. N90-16562
KIM, YOUNG-WON N90-16028
KIMOTO, MASAHIDE N90-16372
KINGCOMBE, R. C. N90-15920
KINI, ARAVINDA M. N90-16020
N90-16550
KIRK, H. G. N90-16262
KIRKEWOOG, A. E. N90-16130
KIRKLEN, CHUCK N90-15932
KISSEL, J. N90-16628
KISSINGER, H. E. N90-16049
KJEMS, J. N90-16075
KLEESSEN, RENE N90-15970
KLEIN, RICHARD I. N90-16674
KLEISER, L. N90-16173
KLEVENHUSEN, K. D. N90-16180
KLINGER, J. N90-16621
N90-16645
KLOECK, W. N90-16629
KNOELKER, J. N90-16648
KNOWLES, G. E. N90-15914
KNUTH, E. L. N90-16494
KO, WILLIAM L. N90-16004
KOBAYASHI, S. N90-16515
KOCH, ST. N90-16239
KOCHAN, H. N90-16621
N90-16643
N90-16645
N90-16650
KOEHLER, G. N90-16314
KOELLE, H. HERMANN N90-15970
KOELZER, G. N90-16650
KOENIG, THOMAS N90-16320
KOESTER, H. N90-16177
KOGAN, YAN I. N90-16571
KOHL, C. P. N90-16640
KOHSMANN, JAMES J. N90-16415
KOMHYR, W. D. N90-16355
N90-16357
KOMPENHANS, JUERGEN N90-16243
N90-16248
KONDO, KATSUMI N90-16516
KONDO, Y. N90-16531
KONNO, I. N90-16630
KOONTZ, R. F. N90-16121
KOPLJAR, V. N90-16481
KOPP, E. N90-16379
KORHONEN, J. S. N90-16531
KOROS, W. J. N90-16065
KORTING, P. A. O. G. N90-16000
N90-16001
KOSEK, JOHN A. N90-16347
KOSIK, JEAN-CLAUDE N90-16380
KOSKIE, JOHN E. N90-16151
KOUVEL, J. S. N90-16533
KOWALEWSKI, T. A. N90-16239
KRABEL, ECKHARD N90-15970
KRAEMER, E. N90-16189
KRAMER, H. N90-16262
KRAZINSKI, J. L. N90-16526
KREILICK, T. S. N90-16570
KREIS, ANDREAS N90-16398
KRIDER, E. PHILIP N90-16614
KRIEBEL, K. T. N90-16321
KROESCH, VOLKMAR N90-16335
KROHN, GREGORY S. N90-16100
KROLL, N. N90-16197
KRONEN, R. N90-15944
KRUCK, W. N90-16334
KRUECKEBERG, C.-P. N90-16178
KRUEGER, F. R. N90-16628
KRUSIUS, M. N90-16531
KUBRUSLY, C. S. N90-16460
KUECHLER, ANDREAS N90-15970
KUELBS, J. N90-16010
KUMAI, KAZUMA N90-16137
KUNG, HAROLD H. N90-16566
KUNKEL, B. N90-16503
KUNT, MURAT N90-16214
KURTZ, T. N90-16010
KURZEJA, NORBERT N90-16162
KYRALA, G. A. N90-16521

L

LABELLE, J. N90-16116
LABORDE, JEAN-MARIE N90-16406
LADOUS, CONSTANZE N90-16872
LAGATTUTA, K. J. N90-16521
LAHTI, TAPIO N90-16299
LAITINEN, ARI N90-16093
LAKE, MARK S. N90-16292
LAMMERS, UVE H. N90-16475
LAMMERZAHL, P. N90-16621
LAMPORT, LESLIE N90-16416
LANDEAU, JOCELYNE N90-15989
LANGEHOUGH, M. A. N90-15937
LANGEVIN, Y. N90-16631
LAPPALAINEN, REIJO N90-16056
LAPUCHA, DARIUSZ N90-15901
LARIMER, R.-M. N90-16680
LASSMANN, JENS N90-15990
LATAITIS, RICHARD J. N90-16261
LATHROP, J. A. N90-16355
N90-16357
LAUBER, J. N90-16250
LAURANTO, H. M. N90-16498
LAVERGNE, GERARD N90-16156
LAVINE, T. L. N90-16121
LAWING, PIERCE L. N90-15952
N90-15956
N90-15962
LEAVITT, LAURENCE D. N90-15884
LEBBY, GARY N90-16408
LECROISSETTE, DENNIS H. N90-16391
LEDER, A. N90-16242
LEE, K. L. N90-15937
LEE, P. H. Y. N90-16521
LEE, TIMOTHY J. N90-16483
LEFEVRE, CHRISTOPHE N90-16023
LEHMANN, B. N90-16241
LEHNER, PAUL E. N90-16395
LEMKE, RAYMOND W. N90-16131
LEMMER, L. N90-15913
LEMPEREUR, CHRISTINE N90-16156
LESKO, K. T. N90-16523
N90-16680
LEVER, A. B. P. N90-16015
LEVERSUCH, N. P. N90-15920
LEVESON, NANCY G. N90-16414
LEVY, SAMUEL C. N90-16287
LEWIS, H. GARTON, JR. N90-16223
LEWIS, H. RALPH N90-16507
LI, H. N90-16197
LI, Z. N90-16262
LIANG, RANTY H. N90-16651
LICHTENEGGER, JUERG N90-16325
LIFFMAN, K. N90-16632
LILIENTAL-WEBER, ZUZANNA N90-16530
N90-16551
LIMA, J. A. S. N90-16663
LINDELL, ISMO V. N90-16497
LINDLOHR, WOLFGANG N90-16316
LINDSTROM, DAVID J. N90-16633
N90-16656
LINDSTROM, M. M. N90-16656
LINDSTROM, RICHARD M. N90-16633
N90-16656
LINGENFELTER, RICHARD E. N90-16676
LINJAMA, JUKKA N90-16299
LIOSSI, ERNESTO N90-15907
LIPTON, ALAN EDMUND N90-16370
LITOVITZ, T. N90-16390
LIU, J. Z. N90-16539
LIU, LIWEN N90-16533
LIVINGSTON, JULIE M. N90-15995
LLOYD-EVANS, J. N90-16601
LLOYD, K. H. N90-16368
LOBB, D. R. N90-16503
LOEW, G. A. N90-16121
LONGDON, NORMAN N90-15989
N90-15999
N90-16089
N90-16706
LONGO, E. N90-16495
LONGO, J. M. A. N90-16184
LOOMIS, B. A. N90-16041
LORENZETTI, D. N90-16603
LOTTES, PAUL A. N90-16036
LOTZE, K.-H. N90-16576
LU, X-Q. N90-16665
LU, Y. N90-16034
LUBELL, M. S. N90-16510
LUCAS, JAMES P. N90-16003
LUDWIG, DAVID A. N90-16693
LUE, J. W. N90-16510
LUMET, J. P. N90-16045
LUNINE, J. I. N90-16634
LUSH, A. M. N90-16470
LUTZ, G. N90-16234
LYNN, K. G. N90-16288
LYNN, K. J. W. N90-16595
LYNN, SCOTT N90-16018
N90-16084
LYON, J. F. N90-16510
N90-16511
LYONS, K. B. N90-16075
LYU, TAE-HWAN N90-16151

M

MA, MATT N90-16313
MACDONALD, M. P. N90-16077
MACDONALD, R. N90-16430
MACGILL, ROBERT A. N90-16123
MACHIDA, T. N90-16078
MACRISS, R. A. N90-16346
MAECKEL, RUEDIGER N90-16327
MAEDER, A. N90-16669
N90-16677
MAGNANI, P. G. N90-16635
MAHAJAN, YASHWANT R. N90-16028
MAIANI, LUCIANO N90-16495
MAKIDA, Y. N90-16553
MALANEY, ROBERT A. N90-16666
MALIN, JANE T. N90-16410
MALKUS, DAVID S. N90-16145
MANNING, A. P. N90-15917
MANOHAR, M. N90-16213
N90-16451
MARGETSON, J. N90-15997
MARIANI, ELIO A. N90-16125
MARK, J. E. N90-16005
MARKEN, K. R., JR. N90-16052
N90-16570
MARKLIN, G. J. N90-16527
N90-16529
MARKLIN, GEORGE J. N90-16283
MARKOWITZ, VICTOR M. N90-16587
MARKWITZ, WINFRIED N90-16319
MARR, RICHARD A. N90-16475
MARSH, STANLEY P. N90-16283
MARSHALL, A. C. N90-16496
MARTI, KURT N90-16469

MARTINELLI, G. N90-16495
MARTINSDEOLIVEIRU, JOSE, JR. N90-16486
MARUMORI, TOSHIO N90-16477
MASCARENHAS, A. N90-16556
MASON, MARY L. N90-15884
MASSARO, E. N90-16603
MASTRANTONIO, G. N90-16377
MATHER, J. L. N90-16429
MATHIS, DONALD N90-16224
MATHIS, JOHN S. N90-16636
MATHYS, G. N90-16602
MATIN, ETHEL N90-16106
MATOCHKIN, E. P. N90-16474
MATSAS, GEORGE EMANUEL AVRAAM N90-16572
MATSUBARA, MASAAKI N90-16290
MATSUDA, SUMIO N90-16349
MATSUO, MASAYUKI N90-16477
MATSUZAKI, YOSHIMI N90-16517
MATTHAEUS, W. H. N90-16143
MAUER, E. N90-16314
MAUER, F. N90-16258
MAURITZEN, DAVID W. N90-16694
MAVRIPLIS, D. J. N90-15893
MAXWELL, E. N90-16352
MAYO, ROBERT M. N90-16283
N90-16520
N90-16527
MCALLISTER, D. F. N90-16445
MCANELLY, RAY N90-16383
MCCAMPBELL, C. B. N90-16082
MCCARTHY, D. N90-16005
MCCARTHY, J. M. N90-16042
MCCLUNG, R. W. N90-16071
MCCORMICK, C. L. N90-16062
MCCORMICK, JUDITH A. N90-16211
MCCURLEY, KEVIN S. N90-16471
MCDONNELL, J. A. M. N90-16637
MCGILL, R. N. N90-16085
N90-16277
MCGRATH, GLENDA N90-16591
MCKAY, D. S. N90-16629
MCKEE, ARTHUR N90-16382
MCKEE, CHRISTOPHER F. N90-16674
MCKENZIE, I. R. I. N90-15919
MCKENZIE, P. W. N90-16091
MCKISSOCK, B. N90-16496
MCLARNON, FRANK R. N90-16139
MCSWEEN, HARRY Y., JR. N90-16638
MEADOWS, D. E. N90-15914
MEGGITT, B. T. N90-16228
N90-16264
MEIER, G. E. A. N90-16237
MEIER, M. N90-16234
MELLIAR-SMITH, P. MICHAEL N90-16416
MENDEL, HERRMAN G. N90-16337
MENG, C.-I. N90-16377
MENTER, F. N90-16193
METZGER, D. E. N90-16254
MEYER, F. N90-16173
MICHAEL, J. N90-16671
MICHAL, GARY M. N90-16053
MICHELSEN, CHRISTIE N90-16591
MIDDLETON, DAVID N90-16447
MIDORIKAWA, SHOICHI N90-16581
MIGNOSI, ANDRE N90-15951
MILES, GAINES E. N90-16695
MILEY, S. J. N90-16178
MILLER, KEITH W. N90-16206
MILLS, RONNIE N90-16442
MIMAKI, T. N90-16078
MIROW, P. N90-16175
N90-16249
MISHRA, S. C. N90-16473
MISRA, AJAY K. N90-16072
MITCHELL, J. W. N90-16681
MITCHELL, T. E. N90-16537
MITCHELL, TERENCE E. N90-16565
MITO, T. N90-16553
MITSUI, HIROSHI N90-16349
MIURA, YUKITOSHI N90-16517
MIYATA, H. N90-16078
MIZERA, P. F. N90-16599
MIZUUCHI, TOHRU N90-16516
MOHR, R. N90-16390
MOLINARO, RICHARD CHARLES N90-16371
MONNAND, E. N90-16481
MONTROSE, C. N90-16390
MOODY, ROBERT L. N90-15931
MOOK, H. A., JR. N90-16559
MOOR, R. N90-16379
MOORE, CHARLES F. N90-16026
MOORMANN, RAINER N90-16024
MOOS, W. N90-16522
MOREL, THOMAS N90-16200
MORGOWNIK, A. F. J. N90-16503
MORIMOTO, S. N90-16515
MORRIS, R. N. N90-16510
MORRISON, DAVID N90-16639
MOSER, LOUISE N90-16416
MOU, Y. N90-16035
MOUHOUB, MOHAMED N90-16505
MOUROU, GERARD N90-16500
MOUWAKEH, MOUFID N90-16304
MUDAWAR, ISSAM A. N90-16151
MUELLER, B. N90-16170
N90-16198
MUELLER, R. N90-16177
MUELLER, S. N90-16160
MUKHARSKY, YU. M. N90-16531
MUKHOPADHYAY, NIMAI C. N90-16493
MULLEN, T. O. N90-16355
MULLIN, THERESA M. N90-16395
MULLINS, M. N90-16390
MULY, EMIL C. N90-16026
MURRAY, K. A. N90-15985
MURRAY, ROYCE W. N90-16538
MUSSINO, VITTORIO N90-16670

N

NAGAE, T. N90-16553
NAGARAJ, V. N90-16445
NAGLE, D. E. N90-16600
NAKAGOME, YOSHIHIRO N90-16519
NAKAMURA, A. N90-16578
NAKAMURA, H. N90-16515
NAKAO, KEN-ICHI N90-16580
NANDEDKAR, R. V. N90-16038
NARAYANSWAMY, RAMKUMAR N90-16211
N90-16216
NASHIYAMA, ISAMU N90-16554
NASTASI, MICHAEL N90-16056
N90-16057
N90-16565
NAUMANN, K. W. N90-16153
NEES, JOHN N90-16500
NETTLES, A. T. N90-16007
NEUGEBAUER, MARCIA N90-16639
NEUKUM, G. N90-16621
NEVEJANS, D. N90-16379
NEWMAN, J. N90-16301
NGUYEN, TIEN MANH N90-16110
NICHOLS, ARTHUR S. N90-16366
NICKEL, H. N90-16044
NIELSEN, B. N90-16288
NIFENECKER, H. N90-16481
NING, Y. P. N90-16005
NISHIIZUMI, K. N90-16640
NISHIOKA, TSUYOSHI N90-16582
NITSCHE, W. N90-16175
N90-16249
NITTA, AKIHITO N90-16290
NNAJI, BARTHOLOMEW O. N90-16441
NOGUCHI, TAKASHI N90-16349
NOHEL, JOHN A. N90-16145
NOLKER, KAREN S. N90-16216
NOREN, B. N90-16481
NORMAN, E. B. N90-16523
N90-16680
NORTON, ANDREW JOHN N90-16597
NOVELLO, M. N90-16662
NOWAK, DIETER K. N90-16133
NUREYEV, P. G. N90-16357
NUTH, JOSEPH A., III N90-16641
NYHOLM, K. M. N90-16498
NYITRAY, ALICE M. N90-16058

O

OBIKI, TOKUHIRO N90-16515
N90-16516
OCONNOR, BRYAN N90-15975
OEGELMAN, HAKKI N90-16606
N90-16673
OEHLER, A. N90-16643
OELKER, H.-CHR. N90-16181
OETTL, HERWIG N90-16112
OGAWA, TORU N90-16579
OGUNNIYI, J. F. N90-16109
OHANESSIAN, HAGOP N90-16235
OHLEMILLER, THOMAS J. N90-16002
OHNUKI, S. N90-16041
OKANO, FUMINORI N90-16517
OLIPHANT, A. N90-16097
OLSON, G. L. N90-16521
OMONGAIN, E. N90-16503
ONN, DAVID N90-16058
ONOFRIO, R. N90-16504
OROFINO, V. N90-16616
ORSINI, S. N90-16377
N90-16378
ORTH, NORMAN W. N90-16053
OSBORN, A. R. N90-15922
OSHER, STANLEY N90-16401
OSSANDON, J. G. N90-16562
OVERSLUIZEN, M. N90-16034
OZGUVEN, H. NEVZAT N90-16286

P

PACE, C. N90-16439
PACHELSKI, WOJCIECH N90-15901
PAILHAS, G. N90-15887
PAINTER, S. L. N90-16510
PALMER, A. W. N90-16228
N90-16264
PALMER, MILES R. N90-16083
PALMER, R. B. N90-16262
PANCHAL, C. B. N90-16350
N90-16353
PANKIEWICZ, G. S. N90-16637
PANKOVE, J. N90-16556
PAOLONI, FRANK J. N90-16123
PARASHAR, D. N90-16473
PARISI, MARIO N90-16670
N90-16678
PARK, STEPHEN K. N90-16204
N90-16205
N90-16206
N90-16207
PARTLOW, DEBORAH P. N90-16061
PARTRIDGE, P. G. N90-16043
PASSMAN, S. L. N90-16278
PASTERNAK, MOSHE PAZ N90-16560
PATEL, J. N90-16225
PATHAK, P. H. N90-16103
PATNAIK, A. N90-16643
PATTERSON, M. R. N90-16422
PATTERSON, MICHAEL H. N90-16394
PAUL, D. R. N90-16065
PAULSON, M. R. N90-16374
PAYNE, TERRY LYNN N90-16584
PEDERSEN, A. N90-15999
PEDERSON, L. R. N90-16049
PEELING, N. E. N90-16427
PEERCY, PAUL S. N90-16555
PEI, SHIYOU N90-16534
PEI, SU-CHANG N90-16409
PENAFIEL, M. N90-16390
PENGEL, K. N90-16245
N90-16255
PENNEWELL, W. J. N90-16413
PENNYCOOK, S. J. N90-16556
PERERA, A. G. U. N90-16218
PERIC, M. N90-16195
PEROLA, G. C. N90-16603
PERRY, A. M. N90-16363
PETERMAN, KLAUS N90-16266
PETERSEN, P. N90-16524
PFEIFER, H. N90-16238
PFEIFFER, A. N90-16257
PHILLIPS, C. S. E. N90-16425
PICARD, C. A. N90-15906
PIEPERBECK, BRUNO N90-16162
PIHALA, HANNU N90-16093
PILEWSKIE, PETER ANDREW N90-16310
PINSON, MARK W. N90-16293
PIPER, L. G. N90-16485
PITCHER, P. D. N90-16301
PLANET, WALTER G. N90-16359
PLATTS, D. N90-16520
PLATZER, K.-H. N90-16254
PLOECHINGER, ERNST N90-16469
PORTER, D. L. N90-16047
POSTON, R. W. N90-16355
POTTER, M. E. N90-16600
POULIOT, J. N90-16523
POUSSE, M. N90-16326
PREDEHL, P. N90-16234
PREISS, HELMUT N90-16398
PREISSNER, JUERGEN N90-16111
PRENTICE, A. J. R. N90-16675
PRICE, C. W. N90-16548
N90-16549
PRICE, PATRICK E. N90-16402
PRIEBE, S. J. N90-16201
PUFFERT-MEISSNER, W. N90-16252
PURCELL, WILLIAM RICHARD N90-16661
PUROHIT, ANKUR N90-16055
PYGOTT, C. H. N90-16431
N90-16432

Q

QADIR, ASGHAR N90-16668

QUADAKKERS, W. J. N90-16044

R

RAAG, V. N90-16342
RABAS, T. N90-16350
RADERMACHER, WALTER N90-16338
RADESPIEL, R. N90-16194
RAEISAENEN, ANTTI N90-16102
RAFTERY, ADRIAN E. N90-16311
RAISTRICK, I. D. N90-16537
RAJAN, J. B. N90-16362
RAMAPRIYAN, H. K. N90-16451
RAMDANI, MOHAMMED N90-16136
RAMIREZ, JUAN J. N90-16528
RAMSEYER, H. N90-16379
RANDALL, C. C. N90-15914
RANDAZZO, SANTO N90-15911
RANDELL, G. P. N90-16430
RANGANATH, H. S. N90-16221
RANKEN, W. A. N90-16342
RANNACHER, R. N90-16159
RATIER, G. N90-16503
RATNER, E. Z. N90-16122
RAUBENHEIMER, B. C. N90-16673
RAUSCHER, CHRISTEN N90-16128
RAY, EDWARD J. N90-15941
N90-15960
RE, F. N90-16684
REDEKER, G. N90-16179
REEDY, R. C. N90-16623
REES, S. J. N90-16427
REGAN, J. D. N90-16363
REHN, L. E. N90-16539
N90-16547
REICHENBACH, STEPHEN E. N90-16207
REIF, J. H. N90-16453
REIM, G. N90-16176
N90-16238
REINHART, THEODORE J. N90-16479
REINMULLER, DONALD L. N90-16147
RENDELL, ALISTAIR P. N90-16483
RENTSCHLER, INGO N90-16397
REPPIN, C. N90-16234
REYNOLDS, HUGH M. N90-15994
RICHARDS, D. R. N90-16534
RICHARDSON, MARTIN D. N90-15912
N90-15915
N90-15916
RIEDELBAUCH, S. N90-16198
RIETMEIJER, FRANS J. M. N90-16642
RIMINI, ALBERTO N90-16573
RIORDAN, C. N90-16352
RIPPERDA, MARK N90-16343
RIVERA, JAIME E. M. N90-16485
RIVEREAU, J. C. N90-16326
ROACH, DENNIS P. N90-16094
ROBERTS, MICHAEL J. N90-16026
ROBERTSON, M. O. N90-16077
ROBINSON, EDWARD L. N90-16652
ROBINSON, R. M. N90-16599
ROESSLER, K. N90-16621
N90-16643
N90-16650
ROGERS, J. N90-16262
ROGERS, JONATHAN D. N90-16298
ROGERS, ROBERT C. N90-16145
ROONEY, JAMES A. N90-16391
ROSEN, S. P. N90-16491
ROSSOW, C. N90-16194
ROY, TAPAN N90-16537
N90-16565
RUDAKOV, V. V. N90-16357
RUPPEL, F. R. N90-16259
RUSHBY, JOHN N90-16416
RUSSELL, JOHN M. N90-16696
RUSSELL, THOMAS P. N90-16079
RYMES, M. N90-16352
RYTZ, D. N90-16075

S

SADREHAGHIGHI, IDEEN N90-15891
SAKATA, FUMIHIKO N90-16477
SAKUMA, EIICHIRO N90-16554
SALAS, TOM M. N90-16140
SALES, B. C. N90-16561
N90-16563
SALOMAA, R. R. E. N90-16498
SAMMELLS, A. F. N90-16225
SAMUELS, WILLIAM D. N90-16068
SANDBERG, V. N90-16600
SANDIFER, J. P. N90-16077
SANDLIN, STEFAN N90-16039
SANO, FUMIMICHI N90-16516
SANTORO, R. T. N90-16685
SARICKS, C. L. N90-16362
SATO, MOTOYASU N90-16515
N90-16516
SAUVAIN, LARRY D. N90-15933
SAYOOD, KHALID N90-16212
SBUELZ, ANES N90-15926
SCHAEFER, DALE W. N90-16005
SCHAFFER, LESLIE E. N90-16658
SCHALAU, B. N90-16190
SCHAPPERT, G. T. N90-16521
SCHATZMANN, M. N90-16365
SCHERER, D. N90-16330
SCHERER, V. N90-16257
SCHISSEL, D. P. N90-16509
SCHLEICHER, B. R. N90-16130
SCHLOBOHM, S. L. N90-16082
SCHLOSSER, W. N90-16643
SCHLUTER, L. L. N90-16344
SCHMIDT-FALKENBERG, H. N90-16333
SCHMIDT, ALFRED N90-16164
SCHMIDT, B. N90-16154
SCHMIDT, R. N90-15927
SCHMULLIUS, CHRISTIANE N90-16339
SCHNEEWEISS, GUENTHER N90-16306
SCHNERR, G. N90-16244
SCHOENE, J. N90-16197
SCHOENFELD, THILO N90-16155
SCHRAUF, GEZA N90-16172
SCHROEDER, GENE J. N90-16459
SCHULTZ, ARTHUR J. N90-16550
SCHULTZ, DAVID E. N90-16419
SCHULTZ, PETER J. N90-16288
SCHULZ, B.-S. N90-16333
SCHULZ, R. N90-16643
SCHUMACHER, CLIFFORD R. N90-16107
SCHUSSLER, F. N90-16481
SCHUSTER, H. N90-16044
SCHWEHM, G. N90-16616
N90-16650
SCOON, G. E. N. N90-15968
SEALOCK, R. M. N90-16492
SEGEV, ARIE N90-16588
SEILER, F. N90-16154
SEKULA, S. T. N90-16562
SEMYENOV, YURI P. N90-15980
SENNETT, C. T. N90-16430
N90-16433
SERIES, R. N90-16428
SERIZAWA, Y. N90-16118
SEVERIN, G. I. N90-15976
N90-15978
SEVIER, NICOLE E. N90-16279
SEYFANG, GEORGE R. N90-15934
SHALKHAUSER, MARY JO N90-16212
SHAPIRO, S. N90-16075
SHARABY, AHMED N90-15910
SHARMA, RAJESHWAR P. N90-16539
SHEHATA, L. N. N90-16532
SHEN, Y. R. N90-16536
SHERIDAN, G. N. N90-15905
SHERROD, EARNEST E. N90-16408
SHIMEALL, TIMOTHY J. N90-16414
SHINTOMI, T. N90-16553
SHIRAISHI, K. N90-16578
SHOSHANI, ARIE N90-16587
SICKAFUS, KURT N90-16056
SIDDIQUI, AZAD A. N90-16668
SIEBERT, RUEDIGER N90-15963
SIGNORETTI, F. N90-16684
SIGNORINI, C. N90-16684
SIHVOLA, ARI H. N90-16497
SIMCOX, L. N. N90-15900
SIMPSON, J. A. N90-16644
SIMPSON, W. A., JR. N90-16071
SINGH, M. K. N90-16362
SINNOTT, D. H. N90-16099
SKILTON, P. J. N90-15972
SLYE, ROBERT E. N90-16313
SMITH, DONNA N90-16591
SMITH, J. N90-16375
SMITH, JACQUELINE G. N90-15894
SMITH, M. S. N90-16305
SMITH, WARREN E. N90-16208
SNAIL, KEITH A. N90-16499
SODERSTROM, K. N90-16481
SOKOLOWSKI, LESZEK M. N90-16376
SOLCHENBACH, KARL N90-16161
SOLEY, RICHARD M. N90-16455
SONAR, TH. N90-16197
SONDER, EDWARD N90-16561
N90-16563
SONG, I. N90-16066
SOUTOUL, A. N90-16681
SOVA, GREGORY J. N90-15890
SPANNE, PER N90-16067
SPINOGLIO, L. N90-16603
SPOHN, T. N90-16621
N90-16645
SPOONER, STEVE N90-16005
SRIVASTAVA, JAIDEEP N90-16586
STANKOWSKA, J. N90-16546
STARK, M. N90-16600
N90-16601
STECKEMETZ, BERND N90-16185
STEELE, I. M. N90-16646
STEINHARDT, EMIL N90-16594
STEPHAN, FRANCOIS N90-16156
STEPHENS, JAMES N90-16647
STERN, S. ALAN N90-16653
STERZIK, M. N90-16234
STEVENS, CRAIG A. N90-16018
STEVENS, NORMAN H. N90-16592
STEWART, J. H. N90-16025
STIEB-STABEL, MARION N90-16398
STIEGLER, J. O. N90-16070
STIEREN, D. N90-16439
STIFFLER, A. KENT N90-16697
STJOHN, H. N90-16509
STOCK, T. A. N90-16008
STOCKMAN, H. S. N90-16664
STOEFFLER, D. N90-16621
N90-16648
STOEPLER, RAINER N90-16398
STOFFEL, T. N90-16352
STOKHOLM, M. N90-16378
STOKSTAD, R. G. N90-16523
STOLLER, R. E. N90-16051
STORINI, MARISA N90-16670
N90-16678
N90-16679
STOTT, J. H. N90-16098
STRASBURGER, HANS N90-16397
STRAUB, GALEN K. N90-16037
STROH, S. N90-16174
STRONG, J. P. N90-16451
STRUEDER, L. N90-16234
STUPIK, PAUL D. N90-16057
SUDO, SHIGERU N90-16516
SUGIMOTO, S. N90-16260
SUMMERS, ANNE M. N90-16212
SUMPTION, M. D. N90-16052
N90-16570
SUN, C. C. N90-16005
SUNAGA, HIROMI N90-16349
SUNDERAM, V. S. N90-16403
SUPERFINE, R. N90-16536
SUR, B. N90-16523
N90-16680
SUSPENE, LAURENT N90-16073
SUTHERLAND, H. J. N90-16344
SUTTON, S. R. N90-16619
N90-16649
SVAITER, NAMI F. N90-16662
SVERTSHEK, V. I. N90-15976
SYMONS, P. C. N90-16122

T

TAGGART, D. P. N90-16260
TAKACS, PETER Z. N90-16501
TAKAHASHI, H. N90-16041
TAKEDA, TATSUOKI N90-16518
TAKESHITA, K. N90-16118
TAKIZUKA, TOMONORI N90-16518
TAMURA, TAKASHI N90-16349
TANAKA, RYUICHI N90-16349
TANAKA, SUSUMU N90-16349
TANDBERG, ERIK N90-16288
TARRANT, P. M. N90-16413
TAUX, G. N90-16176
TAYLOR, A. J. N90-16521
TAYLOR, B. C. N90-16503
TAYLOR, DELBERT J. N90-16698
TAYLOR, G. E. N90-16363
TAYLOR, PETER R. N90-16482
N90-16483
TAYLOR, RAYMOND DEAN N90-16560
TELOTTE, JOHN C. N90-16353
TERAZAWA, HIDEZUMI N90-16490
TERRY, P. F. N90-16404
THADHANI, N. N. N90-16066
THEMMER, KLAS N90-16067
THIEDE, P. N90-16174
THIEL, K. N90-16650
THIELE, F. N90-16190
THOLE, CLEMENS-AUGUST N90-16161
THOMAS, B., JR. N90-16413
THOMAS, D. E. N90-16138
THOMAS, K. L. N90-16629

THOMPSON, I. L. N90-16080
THOMPSON, J. R. N90-16562
THOMPSON, JAMES L. N90-15931
TICO, BEATRICE N90-16156
TIEDERMAN, WILLIAM G. N90-16151
TILTON, JAMES C. N90-16452
TIPPETT, DONALD N90-16584
TIWARI, SURENDRA N. N90-15891
TOLCOTT, MARTIN A. N90-16395
TOMBOULIAN, SHERRYL N90-16444
TOMLINSON, BILL N90-16202
N90-16203
TONKAY, GREGORY L. N90-16699
TONSO, ARNALDO N90-16289
TORRE, W. V. N90-16524
TORTORELLI, P. F. N90-16048
TOSI, M. P. N90-16487
TREMBACK, CRAIG N90-16383
TRETYAKOV, SERGEI A. N90-16497
TREUMANN, R. A. N90-16116
TREUTWEIN, BERNHARD N90-16397
TROPEA, C. N90-16253
TRUCANO, T. G. N90-15973
N90-16282
TRUEMPER, J. N90-16234
TSAY, FUN-DOW N90-16651
TSKHAKAYA, D. D. N90-16109
TSOU, CHIH-HUA N90-16659
TSUCHIYA, AKIHIKO N90-16582
TUZZOLINO, A. J. N90-16644
TZAVARAS, ATHANASSIOS E. N90-16145

U

UNGER, W. H. N90-15915

V

VANDENBEG, R. P. N90-16000
VANDENBRAND, J. N90-16000
VANDERSANDE, J. N90-16055
VANDERVOORT, K. G. N90-16534
VANDEWLLE, RICHARD C. N90-16284
VANFLEET, H. B. N90-16534
VANHOOK, R. I. N90-16363
VANKA, S. P. N90-16526
VANNARONI, G. N90-15986
N90-15987
VARGA, THOMAS N90-16306
VAUGIONI-FLAM, E. N90-16669
VEALE, R. N90-16439
VERDILLON, A. N90-16135
VIEHWEGER, F. N90-15943
VIELMO, P. N90-16635
VIERECK, RODNEY ALLEN N90-16373
VIITANEN, ARI J. N90-16497
VILLORESI, G. N90-16684
VIRKAR, A. V. N90-16341
VISHWANATH, P. R. N90-16665
VITERBINI, M. N90-16231
VOGLER, WILLIAM A. N90-15902
VOGLSINGER, M. N90-15913
VONDERGRACHT, R. N90-16044
VONDRAK, R. R. N90-16599

W

WADDINGTON, C. J. N90-16681
WADE, DONALD C. N90-15979
WAEBER, K. R. N90-16077
WAGA, I. N90-16663
WAGNER, S. N90-16183
N90-16189
WAGNER, WOLFGANG N90-16162
WALCHLI, U. N90-16379
WALKO, ROBERT N90-16383
WALLENTINE, PATRICIA J. N90-16127
WALSH, W. N90-16122
WALSH, W. J. N90-16362
WALTER, MARTIN J. N90-16541
WANDERT, H. N90-16178
WANG, H. H. N90-16020
WANG, HAU H. N90-16550
WANG, L. M. N90-16547
WARD, CLYDE R. N90-16284
WARD, R. C. N90-16422
WARDE, C. J. N90-16122
N90-16269
WARNECKE, G. N90-16188
WASHBURN, J. N90-16551
WAUGAMAN, CHARLES J. N90-16700
WAY, D. J. N90-15919
WDOWIAK, THOMAS J. N90-16652
WEBBER, W. R. N90-16681
WEBER, E. R. N90-16551
WEBER, G. N90-16470
WEDLAKE, E. T. N90-15920
WEFEL, J. P. N90-16681
WEHINGER, P. A. N90-16630
WEI, GUANG N90-16564
WEINERT, HOWARD L. N90-16458
WEISSMAN, PAUL R. N90-16639
N90-16653
WENDLAND, W. N90-16188
WENSKUS, R. N90-16237
WEST, B. H. N90-16277
WEST, JAMES T. N90-16412
WESTROM, GEORGE N90-16220
WEVER, TOBIAS N90-16329
WHITE, R. G. N90-16396
WHITEHEAD, J. A. N90-16146
WHITTEN, JERRY L. N90-16050
WHYTE, WAYNE A., JR. N90-16212
WIGGINS, CARL M. N90-16138
N90-16140
WIGLEY, D. A. N90-15949
N90-15954
N90-15955
WIGNALL, G. D. N90-16076
WIJCHERS, T. N90-16000
N90-16001
WILFERT, G. L. N90-16201
WILFORD, S. P. N90-15909
WILLENBRUCH, R. D. N90-16034
WILLIAMS, JACK M. N90-16020
N90-16550
WILLIAMS, JOEL M. N90-16058
WILLIAMS, M. SUSAN N90-15958
WILLIAMS, ROGER M. N90-16124
WILLS, JOHN M. N90-16037
WISE, HENRY N90-16011
WITEK, ADAM N90-16058
WITHROW, S. P. N90-16556
WITTENBERG, H. N90-16000
N90-16001
WITTIG, S. N90-16254
N90-16257
WOIKE, MARK R. N90-15964
WOLF, D. N90-15927
WON, VANN Y. N90-16275
WOOD, C. N90-16055
WOOD, JOHN A. N90-16654
WORK, S. N90-16086
WORREST, ROBERT C. N90-16356
N90-16360
WU, XIONGHUA N90-16086
N90-16158
WYCKOFF, S. N90-16630
WYNDHAM, BRIAN A. N90-15896
WYSOCKI, FRED J. N90-16283
N90-16527

Y

YAGER, THOMAS J. N90-15902
YAMAMOTO, HISASHI N90-16582
YAMANOI, Y. N90-16553
YAMAZAWA, HIROMI N90-16384
YANAGI, N. N90-16515
YODH, G. B. N90-16665
YOLDAS, BULENT E. N90-16061

Z

ZADARNOWSKI, J. H. N90-15912
ZAKRAJSEK, JAMES J. N90-16286
ZAMYSHLAYEV, I. V. N90-16357
ZANDBERGEN, B. T. C. N90-16001
ZANGRILLI, N. L. N90-16684
ZAWACKI, T. S. N90-16346
ZHU, YOULAN N90-16086
N90-16158
ZIA, OMAR N90-16701
ZICK, CHRISTIAN N90-16323
ZINNEMANN, GEORGE N90-16583
ZINNER, ERNST N90-16655
ZINNER, H. N90-15927
ZOBRIST, GEORGE W. N90-16702
ZOLENSKY, M. E. N90-16656
ZUSHI, HIDEKI N90-16516

Typical Corporate Source Index Listing

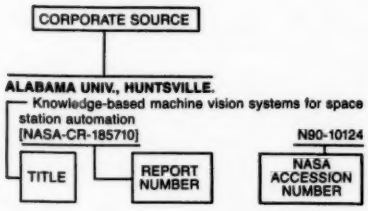

Listings in this index are arranged alphabetically by corporate source. The title of the document provides the user with a brief description of the subject matter. The report number helps to indicate the type of document cited (e.g., NASA report, translation, NASA contractor report). The NASA accession number denotes the number by which the citation is identified. The titles are arranged under each corporate source in ascending accession number order.

A

ACADEMY OF SCIENCES OF THE TAJIK SSR, DOUSHANBE.
Role of dust to gas production rate ratio in cometary physics N90-16625

ACADEMY OF SCIENCES (USSR), NOVOSIBIRSK.
Langmuir wave interaction with ion-sound one. Part 1: Stochastic effects
[DE90-603368] N90-16474

ADVISORY GROUP FOR AEROSPACE RESEARCH AND DEVELOPMENT, NEUILLY-SUR-SEINE (FRANCE).
Advances in techniques and technologies for air vehicle navigation and guidance
[AGARD-AR-276] N90-15899
Fuel Tank Technology
[AGARD-R-771] N90-15904
Guidance and Control of Unmanned Air Vehicles
[AGARD-CP-436] N90-15924
Special Course on Advances in Cryogenic Wind Tunnel Technology
[AGARD-R-774] N90-15939
International conference management N90-16583
AGARD index of publications, 1986-1988
[AGARD-INDEX-86-88] N90-16585

AERITALIA S.P.A., TURIN (ITALY).
Aircraft fuel tank construction and testing experience N90-15907
Structural characterization of Spacelab
[ETN-90-95214] N90-16289

AERONAUTICAL RESEARCH INST. OF SWEDEN, STOCKHOLM.
Adaptive local grid refinement for the compressible 3-D Euler equations
[FFA-TN-1989-40] N90-16155

AEROSPACE CORP., EL SEGUNDO, CA.
Resonance enhanced Raman studies of as-grown and laser-processed HgCdTe
[AD-A213855] N90-16540

AEROSPATIALE, PARIS (FRANCE).
Navigation up-date using radar mapping: Assessment and optimisation simulation tool N90-15928

AIR FORCE INST. OF TECH., WRIGHT-PATTERSON AFB, OH.
Improved solution techniques for the eigenstructure of fractional order systems
[AD-A213844] N90-16295
Dynamic architecture computer
[AD-A214262] N90-16402

AIR FORCE WRIGHT AERONAUTICAL LABS., WRIGHT-PATTERSON AFB, OH.
Spray sealing: A breakthrough in integral fuel tank sealing technology N90-15912

AIR FORCE WRIGHT RESEARCH AND DEVELOPMENT CENTER, WRIGHT-PATTERSON AFB, OH.
Integral fuel tank certification and test methods N90-15916

ALABAMA UNIV., BIRMINGHAM.
Ion bombardment experiments suggesting an origin for organic particles in pre-cometary and cometary ices N90-16652

ALABAMA UNIV., HUNTSVILLE.
Evaluation of a new charge algorithm for a lead-acid battery with gelled electrolyte using a 96V gel cell 4 as a test battery
[DE90-003420] N90-16133
A knowledge-based machine vision system for space station automation N90-16221

ALABAMA UNIV., TUSCALOOSA.
Stochastic model of the NASA/MSFC ground facility for large space structures with uncertain parameters: The maximum entropy approach, part 2
[NASA-CR-186009] N90-16407

ALASKA UNIV., FAIRBANKS.
Effects of gravity waves on the polar O2 and OH airglow N90-16373

ARGONNE NATIONAL LAB., IL.
Dynamics analyses of space power systems using the salt code
[DE90-002274] N90-15995
New electrically conducting solids based on nickel(II) - bis(1,3-dithiole-2-thione-4,5-diselenolate)
[DE90-003788] N90-16020
The onset of boiling of the liquid alkali metals
[DE90-002276] N90-16036
Development of a diamond insulator for thermionic applications
[DE90-002849] N90-16055
Conceptual design analysis for hybrid-cycle OTEC plants for co-production of electric power and desalinated water
[DE90-003551] N90-16350
Experimental investigation of condensation of steam in the presence of noncondensable gases for open-cycle surface condensers
[DE90-003552] N90-16353
Assessment of the importance of acidic fogwater and cloudwater in affecting terrestrial vegetation: Some important case studies
[DE90-002216] N90-16361
Environmental, health, and safety concerns associated with nonpetroleum fuel use in US transportation
[DE90-004367] N90-16362
User's manual for MGMHD: A multigrid three-dimensional computer code for the analysis of magnetohydrodynamic generators and diffusers
[DE90-004453] N90-16526
La(sub 2)MO(sub 4 + delta) (M = Cu, Ni, Co): Phase separation and superconductivity resulting from excess oxygen defects
[DE90-001988] N90-16534
Phonon anomaly at T(sub c) in (Y/ER)Ba2Cu3O(7-delta)
[DE90-003562] N90-16539
Effects of ion dose on the morphology and crystallization of amorphous germanium
[DE90-003564] N90-16547
Structure-property correlations in the design of organic metals and superconductors: An overview
[DE90-003794] N90-16550
High temperature neutron diffraction study of the formation reaction of bismuth superconductors
[DE90-004883] N90-16568
A low-threshold EAS (Extensive-Air-Shower) array for gamma-ray astronomy at Los Alamos
[DE89-016780] N90-16600

ARIZONA STATE UNIV., TEMPE.
Analysis of organic compounds in returned comet nucleus samples N90-16617

ARIZONA UNIV., TUCSON.
Cloud phase discrimination by near-infrared remote sensing N90-16310
Artificially structured superconductors
[DE90-004851] N90-16567
Solar nebula condensates and the composition of comets N90-16634

ARMY AEROMEDICAL RESEARCH LAB., FORT RUCKER, AL.
Simulator sickness in the UH-60 (Black Hawk) flight simulator
[AD-A214434] N90-16392

ARMY AVIATION SYSTEMS COMMAND, CLEVELAND, OH.
Assessment of worm gearing for helicopter transmissions
[NASA-TM-102441] N90-15923
Dynamic analysis of geared rotors by finite elements
[NASA-TM-102349] N90-16286

ASTER, INC., FORT COLLINS, CO.
A dynamic model for forecasting new cloud development
[AD-A213939] N90-16383

AUBURN UNIV., AL.
Rocket-triggered lightning strikes and forest fire ignition N90-16690

AVIONS MARCEL DASSAULT, SAINT-CLOUD (FRANCE).
Integral fuel tanks - design, production, aging, repair N90-15906

B

BABCOCK AND WILCOX CO., LYNCHBURG, VA.
Assessment of strength limiting flaws in ceramic heat exchanger components
[DE90-004086] N90-16077

BATTELLE COLUMBUS LABS., OH.
Design of coupled or uncoupled multifilamentary SSC-type strands with almost zero retained magnetization at fields near 0.3 T
[DE90-005391] N90-16052
Properties and design of multifilamentary NbTi composite superconductors
[DE90-004904] N90-16569

BATTELLE INST., FRANKFURT AM MAIN (GERMANY, F.R.).
Eurolaser definition phase: A comparison of high power lasers available
[ETN-90-96061] N90-16268

BATTELLE MEMORIAL INST., COLUMBUS, OH.
Magnetic studies of proximity-effect coupling in a very closely spaced fine-filament NbTi/CuMn composite superconductor
[DE90-005387] N90-16570

BATTELLE PACIFIC NORTHWEST LABS., RICHLAND, WA.
Ninth Battery and Electrochemical Contractors' Conference: Extended abstracts
[DE89-016837] N90-16120

BOEING AEROSPACE CO., KENT, WA.
Crew emergency return vehicle autoland feasibility study
[NASA-CR-181940] N90-15937

BONN UNIV. (GERMANY, F.R.).
The lidar experiment at Andoya, Norway, during the Summer of 1988
[BONN-IR-89-16] N90-16117
Decay estimates for the compressible Navier-Stokes equations in the half-space
[PREPRINT-46] N90-16163
Visualization of 2 and 3 dimensional flows
[REPT-1] N90-16164

BONNEVILLE POWER ADMINISTRATION, PORTLAND, OR.
Industrial heat pump assessment study
[DE90-004541] N90-16201

BOSTON COLL., CHESTNUT HILL, MA.
Theory of the electronic and optical properties of semiconductor heterostructures
[AD-A214132] N90-16544

BRITISH AEROSPACE PUBLIC LTD. CO., KINGSTON-UPON-THAMES (ENGLAND).
Integral fuel tank sealing practice at British Aerospace (Kingston) N90-15905

BRITISH AEROSPACE PUBLIC LTD. CO., LANCASHIRE (ENGLAND).
Technology and evaluation of unmanned air vehicles N90-15934

BRITISH BROADCASTING CORP., KINGSWOOD (ENGLAND).
Use of an HF active monitoring array in the presence of high level interference [BBC-RD-1989/7] N90-16096
The first year's work of race project 1036 WTDM broadband customer premises network [BBC-RD-1989/6] N90-16097
Satellite broadcasting: Requirements for the receiving antenna [BBC-RD-1989/5] N90-16098

BROOKHAVEN NATIONAL LAB., UPTON, NY.
Mass loss during x ray microanalysis [DE90-003954] N90-16067
Soft modes, freezing, and nonlinear response of a dipolar glass [DE90-003647] N90-16075
The MPI/AIT X ray Imager (MAXI): High speed PN-CCD's for x ray detection [MPE-PREPRINT-154] N90-16234
Proposal for a study of laser acceleration of electrons using micrograting structures at ATF [DE90-003699] N90-16262
Slow positron defect profiling of silicon epilayers [DE90-003958] N90-16288
Solving time harmonic wave problems on vector processors [DE90-003956] N90-16480
Surface topography measurements over the 1 meter to 10 micrometer spatial period bandwidth [DE90-003642] N90-16501
Non-destructive trace element microanalysis of as-received cometary nucleus samples using synchrotron x ray fluorescence N90-16649

BUNDESANSTALT FUER GEOWISSENSCHAFTEN UND ROHSTOFFE, HANNOVER (GERMANY, F.R.).
Utilization of remote sensing in geoscientific development and projects N90-16334

BUNDESANSTALT FUER GEWAESSERKUNDE, KOBLENZ (GERMANY, F.R.).
Support of hydrological models calculations by satellite data N90-16337

BUNDESFORSCHUNGSANSTALT FUER LANDESKUNDE UND RAUMORDNUNG, BONN (GERMANY, F.R.).
Use of remote sensing data for land and building statistics N90-16335

C

CALIFORNIA INST. OF TECH., PASADENA.
Analytical study of comet nucleus samples N90-16608
Outflows in high mass star-forming regions N90-16657

CALIFORNIA POLYTECHNIC STATE UNIV., SAN LUIS OBISPO.
Mathematical model for adaptive control system of ASEA robot at Kennedy Space Center N90-16701

CALIFORNIA STATE UNIV., FRESNO.
Formalisms for user interface specification and design N90-16687

CALIFORNIA UNIV., BERKELEY.
New optimization techniques in database access and maintenance N90-16586
Turbulent stripping of interstellar clouds by interaction with supernova remnants [DE90-003622] N90-16674

CALIFORNIA UNIV., BERKELEY. LAWRENCE BERKELEY LAB.
The continuous crystallization of sulfur formed by the liquid-phase reaction of hydrogen sulfide and sulfur dioxide [DE90-003991] N90-16018
Development and evaluation of a process to produce hydrogen from coal [DE90-003937] N90-16084
Recent progress in relativistic klystron research [DE90-000942] N90-16121
Broad-beam multi-ampere metal ion source [DE90-003106] N90-16123
Cycle-life improvement of Zn/NiOOH cells by the addition of Ca(OH)2 to the zinc electrode [DE90-004040] N90-16139
Some considerations on resource evaluation of The Geysers [DE90-002119] N90-16343
A search for the electric dipole of the electron [DE90-001572] N90-16484
Chromatic dispersion compensation in a Fresnel lens by means of a diffraction grating [DE90-004030] N90-16506
Lower limit for the average angular momentum leading to fusion [DE90-004027] N90-16523
The influence of residual contamination on the structure and properties of metal/GaAs interfaces [DE90-000549] N90-16530
Conformation, orientation and interaction in molecular monolayers: A surface second harmonic and sum frequency generation study [DE90-003108] N90-16536
Heteroepitaxy of GaAs on Si: Methods to decrease the defect density in the epilayer [DE90-004028] N90-16551
Abbreviated query interpretation in extended entity-relationship oriented databases [DE90-003114] N90-16587
Event-join optimization in temporal relational databases [DE90-003117] N90-16588
Cosmic ray half life of Ni-56 [DE90-000132] N90-16680
A database of fragmentation cross section measurements applicable to cosmic ray propagation calculations [NASA-CR-186328] N90-16681

CALIFORNIA UNIV., IRVINE.
Image processing by Intensity-Dependent Spread (IDS) N90-16215
A low-threshold EAS (Extensive-Air-Shower) array for gamma-ray astronomy at Los Alamos [DE89-016780] N90-16600
Status of the expansion of the CYGNUS array at Los Alamos [DE89-016781] N90-16601

CALIFORNIA UNIV., LA JOLLA.
Measurements of long-lived cosmogenic nuclides in returned comet nucleus samples N90-16640

CALIFORNIA UNIV., LOS ANGELES.
Proposal for a study of laser acceleration of electrons using micrograting structures at ATF [DE90-003699] N90-16262
Multiple flow regimes in the Northern Hemisphere winter N90-16372

CALIFORNIA UNIV., RIVERSIDE.
A low-threshold EAS (Extensive-Air-Shower) array for gamma-ray astronomy at Los Alamos [DE89-016780] N90-16600

CALIFORNIA UNIV., SAN DIEGO, LA JOLLA.
Determination of solar flare accelerated ion angular distributions from SMM gamma ray and neutron measurements and determination of the He-3/H ratio in the solar photosphere from SMM gamma ray measurements [NASA-CR-186038] N90-16676

CALIFORNIA UNIV., SANTA CRUZ.
Mass functions for eight galactic clusters in the solar neighborhood N90-16660

CARNEGIE-MELLON UNIV., PITTSBURGH, PA.
Fundamental studies of beta phase decomposition modes in titanium alloys [AD-A214424] N90-16035

CATHOLIC UNIV. OF AMERICA, WASHINGTON, DC.
Mechanisms of microwave induced damage in biologic materials [AD-A213480] N90-16390

CENTRAL AEROLOGICAL OBSERVATORY, DOLGOPRUDNYI (USSR).
ECC (Electrochemical Concentration Cell) ozonesonde observations at Mirny, Antarctica, during 1988 [PB90-113960] N90-16357

CENTRAL RESEARCH INST. OF ELECTRIC POWER INDUSTRY, TOKYO (JAPAN).
Analytical study on the decreasing method of thermal stress for ceramic gas turbines [DE90-734934] N90-16078
Microwave screening on digital radio communication links due to multicircuit power transmission lines [DE90-734950] N90-16118
Application of ac impedance method for diagnosis of lithium secondary battery degradation. Preliminary study with AA size Li/MoS2 cells [DE90-702474] N90-16137
Theoretical study on creep damage detection by ultra-sonic wave measurement [DE90-702472] N90-16290
Lightning observations on Japan Sea coast in winter [DE90-702485] N90-16387
Characteristics of electromagnetic wave forms with lightning in winter season (2): Characteristics in frequency domain [DE90-734989] N90-16388

CENTRE D'ETUDES ET DE RECHERCHES, TOULOUSE (FRANCE).
Experimental investigation of a three-dimensional wake. Part 2: Spectral and turbulent energy analysis [ONERA-RT-32/5025-AYD-PT-2] N90-15887
The cryogenic induction tunnel T2 at Toulouse N90-15946
Fundamental considerations in testing in cryogenic wind tunnels N90-15951
Study of flow around a sphere in a hydraulic test tunnel [CERT-1/2313/MES] N90-16156

CENTRE DE RECHERCHES SCIENTIFIQUES ET TECHNIQUES DE L'INDUSTRIE DES FABRICATIONS METALLIQUES, BRUSSELS (BELGIUM).
Low-cost volumetric modeling [CRIF-MC-85] N90-16435

CENTRE NATIONAL D'ETUDES SPATIALES, TOULOUSE (FRANCE).
Terrestrial magnetosphere magnetic field models [REPT-89/CT/DTI/MS/AS/154] N90-16380
UNIX internals. Part 1: Intertask communication in UNIX. Part 2: UNIX file system [CNES-NT-122-PT-1/2] N90-16405

CENTRE NATIONAL DE LA RECHERCHE SCIENTIFIQUE, ORSAY (FRANCE).
Composition of dust from Comet P/Halley: The mineral fraction N90-16631

CENTRE NATIONAL DE LA RECHERCHE SCIENTIFIQUE, SAINT MARTIN D'HERES (FRANCE).
Thermal histories of the samples of two KOSI comet nucleus simulation experiments N90-16645

CENTRO BRASILEIRO DE PESQUISAS FISICAS, RIO DE JANEIRO.
Quantum fields in cosmological space-times: A soluble example [DE89-618837] N90-16662
Dissipative effects in Friedmann universes [DE89-618838] N90-16663

CERAMATEC, INC., SALT LAKE CITY, UT.
Development of planar geometry solid oxide fuel cells [PB90-100769] N90-16341

CHICAGO UNIV., IL.
Trajectory-capture cell instrumentation for measurement of dust particle mass, velocity and trajectory, and particle capture N90-16644
Analysis of particulates of comet nucleus samples: Possible use of olivine as indicator phase N90-16646
Non-destructive trace element microanalysis of as-received cometary nucleus samples using synchrotron x ray fluorescence N90-16649

CITY UNIV., LONDON (ENGLAND).
A simple fiber optic autocorrelation tachometer [ETN-90-96146] N90-16228

CIVIL AVIATION AUTHORITY, LONDON (ENGLAND).
UK airmisses involving commercial air transport, September to December 1988 [ISSN-0951-6301] N90-15897

COLLEGE OF WILLIAM AND MARY, WILLIAMSBURG, VA.
Linear digital imaging system fidelity analysis N90-16205
Model-based quantification of image quality N90-16206
Optimal focal-plane restoration N90-16207

COLOGNE UNIV. (GERMANY, F.R.).
Modifications of comet materials by the sublimation process: Results from simulation experiments N90-16621
Mechanical and SEM analysis of artificial comet nucleus samples N90-16650

COLORADO STATE UNIV., FORT COLLINS.
The response of the atmospheric convective boundary layer to surface inhomogeneities N90-16369
Mesoscale analysis by numerical modelling coupled with satellite-based sounding N90-16370
The chemistry and dynamics of marine stratocumulus N90-16381

CONGRESS OF THE UNITED STATES, WASHINGTON, DC.
Round trip to orbit. Human spaceflight alternatives: Special report [OTA-ISC-419] N90-15966

CONSIGLIO NAZIONALE DELLE RICERCHE, FRASCATI (ITALY).
Hollow-cathode experiments to support electrodynamic tether applications [IFSI-89-5] N90-15988
Electrical characteristics measurements for the TSS-1 satellite painting [IFSI-89-7] N90-15987
RETE experiment activity at the TSS-1 POCC [IFSI-89-12] N90-15988
Two possible configurations for the top-hat electrostatic analyzer: A numerical study [IFSI-88-18] N90-16229

CIS-2 analyzer derivation of hardware parameters
[IFSI-89-13] N90-16230
The visible channel of OMEGA-VIMS
[IFSI-89-14] N90-16231
Polar cusps latitudinal shift and its relation to the IMF-By component
[IFSI-88-14] N90-16377
On the structure of the tail magnetic field
[IFSI-88-19] N90-16378
Multisqueezing of mechanical states and back-action evasion measurements
[IFSI-89-6] N90-16504
Short time scale variability of the BL Lac object OJ 287 in the near-infrared
[IFSI-89-3] N90-16603
Correlative analyses for geomagnetic indices, cosmic-ray intensities and sunspot numbers recorded since 1937
[IFSI-89-4] N90-16670
A computer program to calculate the population numbers of multi-level species
[IFSI-89-15] N90-16671
Some properties of so-called magnetic cloud structures in the solar wind
[IFSI-88-16] N90-16678
Galactic cosmic-ray modulation and solar-terrestrial relationships
[IFSI-88-17] N90-16679
Cosmic ray NM-64 neutron monitor data 16
[IFSI-88-21] N90-16684

CORNELL UNIV., ITHACA, NY.
The dynamics of dust in planetary magnetospheres N90-16658

CRYOGENIC, MARINE AND MATERIALS CONSULTANTS, SOUTHAMPTON (ENGLAND).
Cryogenic engineering and materials N90-15949
Materials and techniques for model construction N90-15954
Some recent developments in materials and techniques for model fabrication N90-15955

D

DECISION SCIENCE CONSORTIUM, INC., RESTON, VA.
User interaction with self-learning systems
[AD-A214280] N90-16395

DEFENCE SCIENCE AND TECHNOLOGY ORGANIZATION, SALISBURY (AUSTRALIA).
Tracking flares
[ISBN-0-642-13583-5] N90-16080
Metal vaporisers: Bicentennial series of five historical monographs
[ISBN-0-642-13584-3] N90-16081
The development of over-the-horizon radar in Australia
[ISBN-0-642-13561-4] N90-16099
Upper atmosphere research
[ISBN-0-642-13582-7] N90-16368
Scientific investigations of the Space Research Group
[ISBN-0-642-13252-6] N90-16595

DELAWARE UNIV., NEWARK.
Selectivity of the reactions of oxygenates on transition metal surfaces
[DE90-003911] N90-16040

DEPARTMENT OF ENERGY, IDAHO FALLS, ID.
Industrial heat pump assessment study
[DE90-004541] N90-16201

DEPARTMENT OF ENERGY, WASHINGTON, DC.
Summaries of physical research in the geosciences
[DE90-004993] N90-16309
FY 1989 update to the Information Resources Management review plan
[DE90-004185] N90-16593

DEPARTMENT OF THE AIR FORCE, WASHINGTON, DC.
Externally vaporizing system for turbine combustor
[AD-D014284] N90-15918
Defense to laser light irradiation
[AD-D014286] N90-15984
Advanced composite polar boss
[AD-D014287] N90-15994
High temperature aluminum-base alloy
[AD-D014270] N90-16028
Method to produce titanium alloy articles with high fatigue and fracture resistance
[AD-D014278] N90-16029
Method for refining microstructures on prealloyed titanium powder compacts
[AD-D014280] N90-16030
Method of marking titanium alloy articles having distinct microstructural regions corresponding to high creep and fatigue resistance
[AD-D014283] N90-16031
Molybdenum disulfide-molybdenum oxide lubricants
[AD-D014253] N90-16059
Method of making carbon dioxide and chlorine free fluoride-based glass
[AD-D014260] N90-16060
Porous ceramic bodies
[AD-D014277] N90-16061
Synthesis of tetrafluorohydrazine
[AD-D014281] N90-16083
Method for eliminating self-screening noise jamming in radar systems
[AD-D014271] N90-16105
Sequential rapid communication visual displays
[AD-D014282] N90-16106
Command operated liquid metal opening switch
[AD-D014262] N90-16126
Large angle off-axis beam steering of a phased telescope array
[AD-D014269] N90-16127
Expandable radiator
[AD-D014258] N90-16147
Diffraction limited dichroic combiner diode laser
[AD-D014291] N90-16263
Automatic prestart or post shutoff engine lubricator
[AD-D014259] N90-16273
Quick disconnect duct coupler
[AD-D014265] N90-16274
Continuously variable gear drive transmission
[AD-D014268] N90-16275
Vibration damping composition suitable for outer space temperature variations
[AD-D014288] N90-16296
Rotating Doppler frequency shifter
[AD-D014279] N90-16475
Ultrasonic assisted paint removal method
[AD-D014264] N90-16479
Reflection technique for thermal mapping of semiconductors
[AD-D014263] N90-16541

DEPARTMENT OF THE ARMY, WASHINGTON, DC.
SAW (Surface Acoustic Wave) transducer with improved bus-bar design
[AD-D014250] N90-16125

DEPARTMENT OF THE NAVY, WASHINGTON, DC.
OPFET (Optical Field-Effect Transistor) demodulator-downconverter for detecting microwave modulated optical signals
[AD-D014294] N90-16128
Colinear fluctuating wall shear stress and fluctuating pressure transducer
[AD-D014296] N90-16226
Liquid level measurement system for analog and digital readout
[AD-D014297] N90-16227
Helmet-mounted head restraint
[AD-D014233] N90-16394
Reflectometers
[AD-D014249] N90-16499

DEUTSCHE FORSCHUNGS- UND VERSUCHSANSTALT FUER LUFT- UND RAUMFAHRT, BERLIN (GERMANY, F.R.).
Visualization of instability forms of a round free jet using a light sheet method N90-16241

DEUTSCHE FORSCHUNGS- UND VERSUCHSANSTALT FUER LUFT- UND RAUMFAHRT, BRUNSWICK (GERMANY, F.R.).
Determination of the N-factor in the Brunswick (Federal Rep. of Germany) transonic wind tunnel using measurements of pressure distributions and transition points, and the Sally method N90-16177
Direct measurement of laminar instability amplification factors in flight N90-16178
Research on three different Euler's schemes applied to a delta wing with vortical flows N90-16184
Calculation of two and three dimensional super and hypersonic flows by solving the Euler equations N90-16197
Use of the film-of-oil technique for profile measurements in the Transonic Wind tunnel Brunswick (TWB) N90-16252

DEUTSCHE FORSCHUNGS- UND VERSUCHSANSTALT FUER LUFT- UND RAUMFAHRT, GOETTINGEN (GERMANY, F.R.).
Method for the primary stability analysis of the three dimensional, compressible boundary layer flows N90-16171
Numerical simulation of the nonlinear evolution of a perturbation in a three dimensional boundary layer N90-16173
Flow field visualization study on a 65 deg delta wing at M = 0.85 N90-16182
Numerical simulation of the laminar and turbulent three dimensional flow on a delta wing with sharp leading edge N90-16186
Numerical boundary layer calculations on the DFVLR ellipsoid of revolution N90-16193
Numerical simulation of laminar hypersonic flows about an ellipsoid N90-16198
Flow field visualization using laser light sheet methods. Quantitative analysis using image processing N90-16243
Further development of the PIV method for use in the large wind tunnel N90-16248
Quantitative heat transfer measurements using heated liquid crystals N90-16256

DEUTSCHE FORSCHUNGS- UND VERSUCHSANSTALT FUER LUFT- UND RAUMFAHRT, OBERPFAFFENHOFEN (GERMANY, F.R.).
Proceedings of the 5th User Seminar of the German Remote Sensing Data Center of the DFVLR
[DFVLR-MITT-89-04] N90-16318
Introduction to the framework and tasks of the DFD N90-16319
The Interactive System Meteorology and its use in meteorology and oceanography N90-16320
Determination of optical porperties of clouds from NOAA-AVHRR data using Apollo N90-16321
Recognition and distinction of clouds, snow, and ice using AVHRR data N90-16322
Investigation of the backscatter behavior of selected test areas in two geocoded SEASAT-SAR scenes in greater Bonn (Fed. Republic of Germany) N90-16331
Investigation of the topographic components of the image content of radar pictures N90-16332

DEUTSCHE FORSCHUNGS- UND VERSUCHSANSTALT FUER LUFT- UND RAUMFAHRT, PORZ (GERMANY, F.R.).
Investigation of ablation phenomena using IR thermography in a hypersonic wind tunnel N90-16258

DEUTSCHE FORSCHUNGSANSTALT FUER LUFT- UND RAUMFAHRT, COLOGNE (GERMANY, F.R.).
The Kryo-Kanal Koeln (KKK): Description of the tunnel conversion. Thermal insulation, instrumentation, operational experience, test results and operating costs N90-15943
Automatic control of KKK: Requirements, sensors, actuators, and control performance results N90-15944

DEUTSCHE FORSCHUNGSANSTALT FUER LUFT- UND RAUMFAHRT, GOETTINGEN (GERMANY, F.R.).
The cryogenic Ludwieg tube tunnel at Goettingen N90-15947

DEUTSCHE GEODAETISCHE KOMMISSION, MUNICH (GERMANY, F.R.).
Dynamic analysis of the geodetic networks originating from the Navstar/Global Positioning System (GPS) satellites
[SER-C-346] N90-16316
Integrated geodetic network analysis with stochastic prior information about the gravity field and reference ellipsoid
[SER-C-351] N90-16317

DEUTSCHE GESELLSCHAFT FUER LUFT- UND RAUMFAHRT, BONN (GERMANY, F.R.).
Flows with Separation
[DGLR-PAPERS-88-05] N90-16169
Experiments on the laminar-turbulent transition on swept wings N90-16170
Two-Dimensional Measuring Techniques
[DGLR-PAPERS-88-04] N90-16236
Quantative interferometry N90-16237

DORNIER SYSTEM G.M.B.H., FRIEDRICHSHAFEN (GERMANY, F.R.).
Periodically unsteady effects on profiles, induced by separation N90-16196
DNSS: German/Norwegian work team Space Subsea. Environmental control and life support subsystems (technical matters), phase 2
[ETN-90-95905] N90-16398

DU PONT DE NEMOURS (E. I.) AND CO., AIKEN, SC.
Expert system control of a six-legged walking telerobot
[DE90-004661] N90-16285

DUITS-NEDERLANDSE WINDTUNNEL, NORTH EAST POLDER (NETHERLANDS).
The determination of vortex separation frequencies by means of laser light sheet images
[DNW-WTI-88.038] N90-16245
Surface flow visualization with shear stress sensitivive liquid crystals
[DNW-WTI-88.039] N90-16255

E

ECOLE NATIONALE DE L'AERONAUTIQUE ET DE L'ESPACE, TOULOUSE (FRANCE).
Synthesis of control law, on a RPV, in order to minimize the number of sensors N90-15925

ECOLE POLYTECHNIQUE FEDERALE DE LAUSANNE (SWITZERLAND).
High compression image and image sequence coding N90-16214

EDGERTON, GERMESHAUSEN AND GRIER, INC., IDAHO FALLS, ID.
Assessment of battery technologies for electric vehicles, volume 1
[DE90-002049] N90-16122
National program plan for electric vehicle battery research and development: Technical plan
[DE90-002023] N90-16269
An approach for testing fuel-cell/battery hybrid power sources for bus applications
[DE90-002090] N90-16270
Electric and hybrid vehicles: Technical background report for the DOE flexible and alternative fuels study
[DE90-002218] N90-16271
ELECTRIC POWER DEVELOPMENT CO. LTD. (JAPAN).
Investigation and study on compressed air storage power generation system, part 2
[DE90-702648] N90-16354
ELTRON RESEARCH, INC., AURORA, IL.
Advanced biosensors for amino acid detection
[AD-A214029] N90-16225
ENVIRONMENTAL PROTECTION AGENCY, WASHINGTON, DC.
Scientific linkages in global change
[PB90-112608] N90-16356
Potential impact of stratospheric ozone depletion on marine ecosystems
[PB90-112616] N90-16360
ERLANGEN-NUREMBERG UNIV. (GERMANY, F.R.).
Flow visualization of water flows using the crystal violet method N90-16253
ESSEX CORP., WESTLAKE VILLAGE, CA.
MANPRINT (Manpower and Personnel Integration) evaluation: AN/TRC-170 digital troposcatter radio system
[AD-A211799] N90-16100
ETABLISSEMENT TECHNIQUE CENTRAL DE L'ARMEMENT, ARCUEIL (FRANCE).
Structural analysis of zirconium-aluminum plasma deposits
[ETCA-89-R-073] N90-16045
ETS, INC., ROANOKE, VA.
Ambient Test Rig (ATR) flow studies: A laminar flow, reduced entrainment electrostatic precipitator
[DE90-000144] N90-16142
Ambient flow studies and particulate collection measurements: A laminar flow, reduced entrainment electrostatic precipitator
[DE90-001457] N90-16149
ETW G.M.B.H., COLOGNE (GERMANY, F.R.).
The European Transonic Windtunnel (ETW) N90-15945
EUROPEAN SPACE AGENCY, PARIS (FRANCE).
Wind tunnel tests of the influence of aerofoil thickness on the normal force and pitching moment of two slender wings at transonic and supersonic Mach numbers
[ESA-TT-1129] N90-15889
Pressure measurement technique in the wind tunnel division of DFVLR
[ESA-TT-1145] N90-15963
Mission to Mars. Report of the Mars exploration study team
[ESA-SP-1117] N90-15968
Crew Safety and Rescue in Space: An International Approach
[ESA-SP-300] N90-15974
RVD scenari and interfaces between Hermes and space station N90-15982
Columbus: A user's introduction
[ESA-BR-62] N90-15989
Flight experiment hardware for sounding rocket investigations. Materials science and fluid sciences
[ESA-SP-1116] N90-15998
From small beginnings... The story of ESRO's sounding rocket programme in celebration of the twenty-fifth anniversary of the first ESRO sounding rocket launch
[ESA-BR-60] N90-15999
Experiment facilities for materials and fluid sciences embarked on Eureca-1
[ESA-SP-1118] N90-16088
Experiment facilities for materials and fluid sciences embarked on Spacelab
[ESA-SP-1120] N90-16089
Reflection from layered media with special attention to the microwave region
[ESA-TT-1155] N90-16111
Necessity and benefit of the X-SAR Space Shuttle experiment
[ESA-TT-1164] N90-16112
Satellite systems integrated with the terrestrial cellular network for mobile communications
[ESA-STR-228] N90-16113
Contribution to the study of order effects in the Ising model framework: Ground states and phase diagrams
[ESA-TT-1118] N90-16557
IUE-ULDA access guide no. 1: International Ultraviolet Explorer-Uniform Low Dispersion Archive. Dwarf novae and nova-like stars
[ESA-SP-1114] N90-16672
Focus 88: The activities of the European Space Agency
[ESA-BR-43] N90-16706
EUROPEAN SPACE AGENCY. CENTRE SPATIAL DE TOULOUSE (FRANCE).
The HERMES development program N90-16199
EUROPEAN SPACE AGENCY. ESRIN, FRASCATI (ITALY).
ESA/Earthnet N90-16325
EUROPEAN SPACE AGENCY. EUROPEAN SPACE RESEARCH AND TECHNOLOGY CENTER, ESTEC, NOORDWIJK (NETHERLANDS).
Catalogue of ESA publications in 1987
[ESA-SP-1087] N90-16590
Laboratory analyses of micron-sized solid grains: Experimental techniques and recent results N90-16616

F

FAIRCHILD WESTON SYSTEMS, INC., SYOSSET, NY.
Hybrid LZW compression N90-16223
FERMI NATIONAL ACCELERATOR LAB., BATAVIA, IL.
The theory of hybrid stochastic algorithms
[DE90-003941] N90-16421
FERRANTI DEFENCE SYSTEMS LTD., EDINBURGH (SCOTLAND).
Electro-optic sensors for surveillance and target acquisition N90-15929
FLORIDA INST. OF TECH., MELBOURNE.
On the selection of materials for cryogenic seals and the testing of their performance N90-16696
FOREST SERVICE, PORTLAND, OR.
Climatic summaries and documentation for the primary meteorological Station, H. J. Andrews Experimental Forest, 1972 to 1984
[PB90-104373] N90-16382
FORSCHUNGSINSTITUT FUER HOCHFREQUENZPHYSIK, WERTHHOVEN (GERMANY, F.R.).
The physical foundations of radiometry and their applications in the mm-waveband
[REPT-12-88] N90-16114
FORSCHUNGSINSTITUT FUER INFORMATIONSVERARBEITUNG, ETTLINGEN (GERMANY, F.R.).
Quantitative evaluation of object-changes in multitemporal AGRISAR imagery
[FIM-195] N90-16314
FRAUNHOFER-INST. FUER BETRIEBSFESTIGKEIT, DARMSTADT (GERMANY, F.R.).
Review of investigations on aeronautical fatigue in the Federal Republic of Germany
[LBF-S-182] N90-16302
FRAUNHOFER-INST. FUER MICROELECTRONICS, DUISBURG (GERMANY, F.R.).
The MPI/AIT X ray Imager (MAXI): High speed PN-CCD's for x ray detection
[MPE-PREPRINT-154] N90-16234
FRAUNHOFER INST. FUER WERKSTOFFMECHANIK, FREIBURG (GERMANY, F.R.).
Numerical simulation of creep crack growth experiments
[IWM-W-4/88] N90-16303
FREIBURG UNIV. (GERMANY, F.R.).
Evaluation of the pasture potential in the dry areas of Kenya using combined Earth reconnaissance N90-16327
The determination of subscale structures in thermal images N90-16330
FREIE UNIV., BERLIN (GERMANY, F.R.).
Satellite image sequences for motion analysis and change detection N90-16323
Preliminary experiences with a novel method for the determination of displacement vector fields and satellite image sequences N90-16324
TM land use classification of a region. Utilization for planning and statistics N90-16339

G

GANDHI (INDIRA) CENTRE FOR ATOMIC RESEARCH, KALPAKKAM (INDIA).
Interplanar spacing for various phases in austenitic stainless steels
[DE90-602350] N90-16038
GENERAL ATOMIC CO., SAN DIEGO, CA.
D3-D cryogenic control system upgrade
[DE90-003290] N90-16092
Nonlinear wave coupling and clumps in drift wave turbulence theory
[DE90-004103] N90-16150
Initial deuterium confinement studies in DIII-D tokamak: DIII-D milestone report number 58
[DE90-003942] N90-16509
Modeling energy output of inertial storage devices for the DIII-D tokamak
[DE90-004096] N90-16524
GENEVA OBSERVATORY (SWITZERLAND).
The upper main sequence of OB associations. Part 2: The single-lined O stars: Spectral classification of northern stars and lines of C and N
[SER-C-PREPUBL-FASC-39] N90-16602
New developments in stellar ages and modelling of Pop. I stars
[SER-C-PREPUBL-FASC-41] N90-16669
A look on non-standard solar models
[SER-C-PREPUBL-FASC-40] N90-16677
GEORGE MASON UNIV., FAIRFAX, VA.
Analysis and evaluation of technical data on the photochromic and non-linear optical properties of materials
[AD-A214050] N90-16014
A low-threshold EAS (Extensive-Air-Shower) array for gamma-ray astronomy at Los Alamos
[DE89-016780] N90-16600
Status of the expansion of the CYGNUS array at Los Alamos
[DE89-016781] N90-16601
GEORGE WASHINGTON UNIV., WASHINGTON, DC.
Flow separation in shock wave boundary layer interactions at hypersonic speeds
[NASA-CR-4274] N90-15885
GEORGIA INST. OF TECH., ATLANTA.
Singular perturbation analysis of AOTV-related trajectory optimization problems
[NASA-CR-186202] N90-15936
GESELLSCHAFT FUER MATHEMATIK UND DATENVERARBEITUNG, SAINT AUGUSTIN (GERMANY, F.R.).
The Suprenum architecture and its application to computational fluid dynamics
[GMD-389] N90-16161
Multigrid methods for two- and three-dimensional Poisson-type equations on the sphere
[GMD-391] N90-16468
GINER, INC., WALTHAM, MA.
Improved anode catalysts for coal gas-fueled phosphoric acid fuel cells
[DE90-004016] N90-16347
GKSS-FORSCHUNGSZENTRUM GEESTHACHT (GERMANY, F.R.).
Simulation of pollutant transport using a mesoscale grid circulation model
[GKSS-89/E/24] N90-16365
GLAVKOSMOS, MOSCOW (USSR).
EVA space suit. General concepts of design and arrangement N90-15976
On the selection of crewmember rescue means for manned space launch systems N90-15978
Crew safety and rescue aids N90-15980
GRENOBLE-1 UNIV. (FRANCE).
Built in test of folded PLAs
[IMAG-RR-758-I] N90-16134
VLSI integrated circuit tests
[IMAG-RR-763-I] N90-16135
Remote use of an Electron Beam Tester (EBT)
[IMAG-RR-760-I] N90-16233
Spanning trees of hypercubes with a maximum of sixteen peaks
[IMAG-RR-755-I] N90-16406
Appearance analysis from CAD models
[IMAG-RR-756-I-IMAG-88-LIFIA] N90-16434

H

HAIMSON RESEARCH CORP., PALO ALTO, CA.
Recent progress in relativistic klystron research
[DE90-000942] N90-16121
HAMBURG UNIV. (GERMANY, F.R.).
Eurolaser definition phase, solid state lasers working group: Active medium, laser active crystals
[ETN-90-95899] N90-16256
HEIDELBERG UNIV. (GERMANY, F.R.).
Application of the singularity-separating method to computing problems of solid-propellant combustion in a closed vessel
[PREPRINT-489] N90-16086
Using the singularity-separating method to study how to decrease the pressure at the end of a tube
[PREPRINT-490] N90-16158
Numerical analysis of nonstationary fluid flow (a survey)
[PREPRINT-492] N90-16159

Extrapolation techniques for finite element approximations of Stokes and Navier-Stokes flow over a backward facing step
[PREPRINT-499] N90-16160

HELSINKI UNIV. OF TECHNOLOGY, ESPOO (FINLAND).
Laboratory of Space Technology
[PB90-110651] N90-15967
Helsinki University of Technology Radio Laboratory
[PB90-110677] N90-16102
Geometrical optics in inhomogeneous chiral media with application to polarization correction in inhomogeneous lens antennas
[PB90-110669] N90-16497
Determination of hyperfine structures and Rydberg convergence limits of selected optical transitions in Nb-93 using resonance ionization spectroscopy
[PB90-110719] N90-16498
Superflow induced phase transition in the axial vortex-free texture of rotating superfluid He-3-B
[PB90-110388] N90-16531

HIROSHIMA UNIV., TAKEHARA (JAPAN).
The (2+1)-dimensional quantum gravity
[DE90-719556] N90-16580

I

IBM NORWAY, BERGEN.
Electroplating simulation
[DE90-003683] N90-16091

IDAHO NATIONAL ENGINEERING LAB., IDAHO FALLS.
Industrial heat pump assessment study
[DE90-004541] N90-16201

ILLINOIS INST. OF TECH., CHICAGO.
Grid-independent wall layer turbulence model for complex flow calculations
[DE90-003500] N90-16200

ILLINOIS UNIV., URBANA-CHAMPAIGN.
A numerical and experimental investigation of multiple shock wave/turbulent boundary layer interactions in a rectanular duct N90-16141

IMPERIAL COLL. OF SCIENCE AND TECHNOLOGY, LONDON (ENGLAND).
A finite volume calculation method for three dimensional, complex flows N90-16195

INDIANA UNIV.-PURDUE UNIV., FORT WAYNE.
Modeling the near acoustic field of a rocket during launch N90-16694

INSTITUT D'AERONOMIE SPATIALE DE BELGIQUE, BRUSSELS.
A double focussing mass-spectrometer for simultaneous ion measurements in the stratosphere
[AERONOMICA-ACTA-A-350-1989] N90-16379

INSTITUT FRANCO-ALLEMAND DE RECHERCHES, SAINT-LOUIS (FRANCE).
Multidimensional numerical simulation of large caliber ignition processes
[ISL-CO-233/88] N90-16021
Plume shape optimization of small attitude control thrusters with respect to impingement and thrust
[ISL-CO-220/88] N90-16153
Direct Monte Carlo calculations on expansion wave structure near a wall
[ISL-CO-249/88] N90-16154
A numeric analysis of incompressible, viscous flow around a symmetrical body of revolution
[ISL-CO-215/87] N90-16157
Miniature laser Doppler anemometer with a diode laser
[ISL-CO-224/88] N90-16232

INSTITUT FUER ANGEWANDTE GEODAESIE, FRANKFURT AM MAIN (GERMANY, F.R.).
Focal research effort points of the Institute of Applied Geodesy in the field of digital image processing N90-16333

INSTITUT NATIONAL DES SCIENCES APPLIQUEES DE LYON, VILLEURBANNE (FRANCE).
Study of phase transformations liquid-solid-solid of ultrafine particles
[ISAL-89-0019] N90-16022
Development of an elastomeric additive to improve the impact resistance of unsaturated polyester networks
[ISAL-89-0006] N90-16073
Piezoelectric ceramic modeling and characterization at high levels of mechanical activity
[ISAL-89-0030] N90-16074
Mechanoelectric conversion by uniaxial constraint in piezoelectric generators: Optimization of electrical, mechanical, and physico-chemical parameters of materials
[ISAL-89-0020] N90-16235
Investigation of rough elastohydrodynamic contact
[ISAL-89-0029] N90-16281
A quantitative analysis of slip phenomena along a dry contact surface between two bodies in comparison to interfacial crack propagation
[ISAL-89-0032] N90-16304
Order filters, median recursive filter: Analysis and evaluation of performance in image processing
[ISAL-89-0017] N90-16505

INSTITUTE FOR COMPUTER APPLICATIONS IN SCIENCE AND ENGINEERING, HAMPTON, VA.
Euler and Navier-Stokes computations for two-dimensional geometries using unstructured meshes
[NASA-CR-181977] N90-15893
Triangle based TVD schemes for hyperbolic conservation laws
[NASA-CR-181984] N90-16401
Overview and extensions of a system for routing directed graphs on SIMD architectures N90-16444
Dynamically allocating sets of fine-grained processors to running computations N90-16447

INSTITUTE OF GAS TECHNOLOGY, CHICAGO, IL.
Absorption fluids data survey: 1989 update
[DE90-003985] N90-16346

INSTITUTO DE FISICA TEORICA, SAO PAULO (BRAZIL).
Study of primitive universe in the Bianchi 9 model
[DE89-635903] N90-16572

INTERNATIONAL CENTRE FOR THEORETICAL PHYSICS, TRIESTE (ITALY).
On averaged force acting on a particle in HF electromagnetic field
[DE90-600984] N90-16109
Are gravitons windows to higher dimensions
[DE90-600756] N90-16376
Theory of singular Lagrangians
[DE90-600735] N90-16456
Simple proof of renormalization group equation in the minimal subtraction scheme
[DE90-600758] N90-16457
Multiplet classification of highest weight modules over quantum universal enveloping algebras: The U(sub q)(sl(3,C)) example
[DE90-600720] N90-16464
Integrable classical systems in higher dimensions
[DE90-600737] N90-16473
On condensation driven by electrostatic interactions in macroionic solutions
[DE89-636072] N90-16487
Theoretical study of cold nuclear fusion using barrier penetration approach
[DE90-601096] N90-16513
Some theoretical aspects of cold fusion: A report
[DE90-601098] N90-16514
The modified Ginzburg-Landau theory for anisotropic high temperature superconductors
[DE89-635909] N90-16532
Thermodynamic studies on the ferroelectric phase transition in neutron irradiated (Li(sub x)K(1-x))2SO4 crystals at high temperature
[DE89-635786] N90-16545
Thermal expansion of LATGS crystals
[DE89-636239] N90-16546
The off-shell closed strings as the topological open membranes: Dynamical transmutation of world sheet dimension
[DE89-635721] N90-16571
Continuous spontaneous reduction model involving gravity
[DE90-600730] N90-16573
On gauge fixing and quantization of constrained Hamiltonian systems
[DE90-600732] N90-16574
On the domain of string perturbation theory
[DE90-600759] N90-16575
Production of photons in anisotropic spacetimes
[DE90-600760] N90-16576
On quantum effects near a black hole singularity
[DE90-600754] N90-16668

IOWA STATE UNIV. OF SCIENCE AND TECHNOLOGY, AMES.
A low-threshold EAS (Extensive-Air-Shower) array for gamma-ray astronomy at Los Alamos
[DE89-016780] N90-16600

ISTITUTO ELETTROTECNICO NAZIONALE (GALILEO FERRARIS), TURIN (ITLAY).
Activities report of the National Electrotechnic Institute Galileo Ferraris
[ETN-90-96178] N90-16705

J

JAPAN ATOMIC ENERGY RESEARCH INST., IBARAKI.
Verification study of a three-dimensional local scale atmospheric model PHYSIC at seacoast region
[DE90-719560] N90-16384
Fracto-fusion. Mechanism of cold fusion
[DE90-719573] N90-16518

JAPAN ATOMIC ENERGY RESEARCH INST., TAKASAKI.
Radiation resistance of solar cells for space application. 1: Study on the irradiation procedure of electron beams
[DE90-719546] N90-16349
The 1MeV-electron irradiation induced defects in epitaxially grown 3C-SiC
[DE90-719574] N90-16554

JAPAN ATOMIC ENERGY RESEARCH INST., TOKYO.
Low energy neutral particle energy analyser by time of flight method
[DE90-719529] N90-16517
Estimation of thermodynamic properties of alloys from phase diagram and other loose boundary conditions
[DE90-719511] N90-16579

JET PROPULSION LAB., CALIFORNIA INST. OF TECH., PASADENA.
Stripline feed for a microstrip array of patch elements with teardrop shaped probes
[NASA-CASE-NPO-17548-1-CU] N90-16104
MT's algorithm: A new algorithm to search for the optimum set of modulation indices for simultaneous range, command, and telemetry
[NASA-CR-186259] N90-16110
Organic cathode for a secondary battery
[NASA-CASE-NPO-17604-1-CU] N90-16124
Science plan for the Alaska SAR facility program. Phase 1: Data from the first European sensing satellite, ERS-1
[NASA-CR-185028] N90-16312
Apparatus for imaging deep arterial and coronary lesions
[NASA-CASE-NPO-17439-1-CU] N90-16391
The nature of cometary materials N90-16647
Electron Spin Resonance (ESR) studies of returned comet nucleus samples N90-16651
Physical processing of cometary nuclei N90-16653
Neptune's Triton: A moon rich in dry ice and carbon
[NASA-CR-186298] N90-16675

JOHNS HOPKINS UNIV., BALTIMORE, MD.
On the reciprocity of state vectors in boundary value models
[AD-A214104] N90-16458
Spectroscopic diagnostics of high temperature plasmas
[DE90-003912] N90-16522

K

KARLSRUHE UNIV. (GERMANY, F.R.).
Digital image interpretation for optical flow measurement methods: System description and preliminary application examples N90-16244
The use of piezofoil sensors for the determination of the unsteady pressure distribution at the surface of a gas turbine blade N90-16250
Unsteady heat transfer measurement using thermochromatic liquid crystals as temperature indicators N90-16254
Determination of the heat transfer coefficients in separated flows using an infrared camera N90-16257

KENT UNIV., CANTERBURY (ENGLAND).
The in-situ cometary particulate size distribution measured for one comet: P/Halley N90-16637

KERNFORSCHUNGSANLAGE, JUELICH (GERMANY, F.R.).
Kinetics of the graphite/oxygen reaction in the in-pore diffusion controlled regime. Part 3: Influence of boundary layer diffusion in kinetic experiments at temperatures 970K to 1170K
[JUEL-2284-PT-3] N90-16024
The influence of carbide precipitation on the creep rupture behavior of high temperature alloys
[JUEL-2211] N90-16044
Handling and analysis of ices in cryostats and glove boxes in view of cometary samples N90-16643

KYOTO UNIV., KUMATORI (JAPAN).
Proceedings of the specialists' meeting on physics and engineering of fission and spallation
[DE90-719706] N90-16519

KYOTO UNIV., UJI (JAPAN).
Second harmonic electron cyclotron heating in low and over density plasmas in Heliotron DR
[DE90-719519] N90-16515
In situ measurement of neutral beam components using the Doppler-shifted H(sub alpha) emissions in Heliotron E
[DE90-719521] N90-16516

L

LABORATOIRE D'AUTOMATIQUE ET D'ANALYSE DES SYSTEMES, TOULOUSE (FRANCE).
Study of silicon nitride pH response to the fabrication of microelectronic sensors
[LAAS-89229] N90-16023
A physical and numerical study of the turn-off behavior of bipolar power transistors
[LAAS-89185] N90-16136
Optimization of monotonic inference algorithms in propositional and first order logic
[LAAS-89204] N90-16436
Software dependability growth characterization, modeling and evaluation
[LAAS-89320] N90-16437
LABORATORIO DE COMPUTACAO CIENTIFICA, RIO DE JANEIRO (BRAZIL).
Feed back Petrov-Galerkin methods for convection dominated problems
[DE89-636436] N90-16148
An algorithm to compute the square root of 3x3 positive definite matrix
[DE89-635711] N90-16417
Uniform stability for time-varying infinite-dimensional discrete linear systems
[DE89-635712] N90-16460
And still, a new beginning: The Galerkin least-squares gradient method
[DE89-636435] N90-16461
A new finite element formulation for CFD:8. The Galerkin/least-squares method for advective-diffusive equations
[DE89-636437] N90-16462
Hidden regularity for a strongly nonlinear wave equation
[DE90-600742] N90-16465
LAWRENCE LIVERMORE NATIONAL LAB., CA.
Silicon membrane formation
[DE90-003022] N90-16064
Electrode/workpiece combinations
[DE90-003919] N90-16095
Recent progress in relativistic klystron research
[DE90-000942] N90-16121
Electrical safety in the high voltage laboratory
[DE90-003026] N90-16130
Computer aided design based optical system modeling
[DE90-003453] N90-16440
Development of low density silica aerogel as a capture medium for hyper-velocity particles
[NASA-CR-185930] N90-16489
Use of computer simulations to analyze limitations of kinetic models for recrystallization
[DE90-003618] N90-16548
The concept of axial-symmetry constraint and its significance in recrystallization
[DE90-003620] N90-16549
Nuclear reaction uncertainties in standard and non-standard cosmologies
[DE90-003594] N90-16666
Ion-heated thermal Comptonization models and x ray spectral correlations in active galactic nuclei
[DE90-003597] N90-16667
Turbulent stripping of interstellar clouds by interaction with supernova remnants
[DE90-003622] N90-16674
Use of the Egret instrument in studies of the origin of the cosmic radiation. 2: Spectral signatures of discrete cosmic-ray sources
[DE90-003595] N90-16682
LEHIGH UNIV., BETHLEHEM, PA.
Off-line robot programming and graphical verification of path planning N90-16699
LEICESTER UNIV. (ENGLAND).
Galactic x ray astronomy with EXOSAT N90-16597
LEIDEN UNIV. (NETHERLANDS).
From interstellar dust to comets N90-16620
LITTLE (ARTHUR D.), INC., CAMBRIDGE, MA.
Conceptual design of a moving belt radiator shuttle-attached experiments: Technical requirement Document
[NASA-CR-185168] N90-15996
LOCKHEED AERONAUTICAL SYSTEMS CO., MARIETTA, GA.
Fuel tank explosion protection N90-15914
LOCKHEED AIRCRAFT CORP., PALO ALTO, CA.
X ray spectrophotometric remote sensing of diffuse auroral ionization
[SD-TR-89-09] N90-16599
LOCKHEED ENGINEERING AND SCIENCES CO., HOUSTON, TX.
Demonstration of the feasibility of laser induced fluorescence for arc jet flow diagnostics
[NASA-CR-185595] N90-16013
Prompt Gamma Activation Analysis (PGAA): Technique of choice for nondestructive bulk analysis of returned comet samples N90-16633
LOCKHEED MISSILES AND SPACE CO., AUSTIN, TX.
Unmanned air vehicles payloads and sensors N90-15930
Automated search techniques applied to optical payloads in unmanned air vehicles N90-15931
Distribution of hardware and software elements in unmanned air vehicle systems N90-15933
Navigation and guidance testing of the Lockheed/US Army Aquila remotely piloted vehicle N90-15935
LOS ALAMOS NATIONAL LAB., NM.
Elastic moduli of copper: Electronic structure contributions from pseudopotentials and full-potential linear muffin-tin orbital band structure calculations
[DE90-004423] N90-16037
Effect of carbon on ion beam mixing of Fe-Ti bilayers
[DE90-003650] N90-16056
Silicon-based coatings on niobium metal
[DE90-003651] N90-16057
The physical properties of microcellular composite foams
[DE90-003658] N90-16058
A brief description of lattice gas models for multiphase flows and magnetohydrodynamics
[DE90-003653] N90-16143
End-on soft x ray imaging of Field-Reversed Configurations (FRCs) on the Field-Reversal-C (FRX-C)/Large Scale Modification (LSM) experiment
[DE90-004863] N90-16260
Proposal for a study of laser acceleration of electrons using micrograting structures at ATF
[DE90-003699] N90-16262
Design of a spheromak compressor driven by high explosives
[DE90-003652] N90-16283
Analysis of nonlinear systems using ARMA (Autoregressive Moving Average) models
[DE90-002395] N90-16297
Low risk low power heat pipe/thermoelectric space power supply
[DE89-014817] N90-16342
Proceedings of the Conference on Technology-Based Confidence Building: Energy and Environment
[DE90-003363] N90-16366
FRAC-IN-THE-BOX utilization
[DE90-003648] N90-16412
Creating the next generation control system software
[DE90-003391] N90-16419
A 3-D measurement system using object-oriented FORTH
[DE90-003393] N90-16420
Complex availability problems solved with simulation
[DE89-012610] N90-16459
Restoring force method and response estimation
[DE90-002394] N90-16463
Neutrino oscillations: An essay in honor of Felix Boehm
[DE90-003223] N90-16491
Toroidal magnetic fields in terms of field-line invariants
[DE89-016610] N90-16507
Recent progress on the HESS (High Explosive Spheromak Source) experiment
[DE90-003218] N90-16520
Atomic processes in plasmas under ultra-intense laser irradiation
[DE90-003221] N90-16521
Progress with small, high-magnetic-field spheromaks in CTX
[DE90-003395] N90-16527
MHD stable high beta spheromak equilibrium
[DE90-004873] N90-16529
Rotational magnetic processes in YB2Cu3O7
[DE90-000541] N90-16533
Microstructures of Y123 films on SrTiO3, LaGaO3, and LaAlO3
[DE90-003367] N90-16537
Magnetic interactions in Sn-119 substituted for Cu in antiferromagnetic and superconducting lamellar cuprates
[DE90-003661] N90-16560
Electron beam induced oxygen in YBa2Cu3O(7-x) superconductors
[DE90-004839] N90-16565
Experiences with knowledge-base and large database integration
[DE90-000686] N90-16591
Pulsations of delta Scuti stars
[DE90-003213] N90-16598
A low-threshold EAS (Extensive-Air-Shower) array for gamma-ray astronomy at Los Alamos
[DE89-016780] N90-16600
Status of the expansion of the CYGNUS array at Los Alamos
[DE89-016781] N90-16601
Relative muon content of UHE showers associated with Hercules X-1
[DE90-000609] N90-16665
LUDWIG-MAXIMILIANS-UNIVERSITAET, MUNICH (GERMANY, F.R.).
Assessment of visual function in aerospace medicine
[BMVG-FBWM-89-5] N90-16397
LUNAR AND PLANETARY INST., HOUSTON, TX.
Workshop on Analysis of Returned Comet Nucleus Samples
[NASA-CR-184821] N90-16607
LUND UNIV. (SWEDEN).
On the observation of a transition from fusion to multifragmentation in high multiplicity O16 induced reactions
[LUIP-8812] N90-16481

M

MARTIN MARIETTA CORP., DENVER, CO.
Connectionist model-based stereo vision for telerobotics N90-16224
MARYLAND UNIV., COLLEGE PARK.
Stochastic simulation of charged particle transport on the massively parallel processor N90-16448
Sulfur compounds in comets N90-16627
Relative muon content of UHE showers associated with Hercules X-1
[DE90-000609] N90-16665
MASSACHUSETTS INST. OF TECH., CAMBRIDGE.
On the efficient exploitation of speculation under data flow paradigms of control
[AD-A214112] N90-16455
An implicit time-integration procedure for a set of internal variable constitutive equations for isotropic elasto-viscoplasticity
[PB90-121302] N90-16470
Non-equilibrium chemistry in the solar nebula and early solar system: Implications for the chemistry of comets N90-16618
MASSACHUSETTS UNIV., AMHERST.
Interpretation of CAD (Computer Aided Design) models through IGES (Initial Graphics Exchange Specification) interface
[PB90-121294] N90-16441
Dynamics of carbon dioxide exchange of a wheat community grown in a semi-closed environment N90-16689
MAX-PLANCK-INST. FUER ASTROPHYSIK, GARCHING (GERMANY, F.R.).
Spectrophotometric observations of comet P/Giacobini-Zinner N90-16630
MAX-PLANCK-INST. FUER CHEMIE, MAINZ (GERMANY, F.R.).
On the isotope analysis of cometary dust N90-16611
MAX-PLANCK-INST. FUER KERNPHYSIK, HEIDELBERG (GERMANY, F.R.).
Modifications of comet materials by the sublimation process: Results from simulation experiments N90-16621
Organic chemistry of cometary dust as derived from PUMA 1 data N90-16628
MAX-PLANCK-INST. FUER METEOROLOGIE, HAMBURG (GERMANY, F.R.).
Backscattering effects in DIAL due to water vapor
[SER-WISS-ABHANDL-89] N90-16265
MAX-PLANCK-INST. FUER PHYSIK UND ASTROPHYSIK, GARCHING (GERMANY, F.R.).
Natural and man-made emissions at 1.0 to 5.6 MHz measured between 10 and 18 R sub E
[MPE-PREPRINT-146] N90-16116
The MPI/AIT X ray Imager (MAXI): High speed PN-CCD's for x ray detection
[MPE-PREPRINT-154] N90-16234
On the interaction of a pulsar with the ambient medium utilizing x ray images of the Crab nebula
[MPE-REPT-215] N90-16604
An atlas of aperiodic variability in HMXB
[MPE-PREPRINT-158] N90-16605
Recent and future x ray observations of classical novae during the outburst stage
[MPE-PREPRINT-159] N90-16606
EXOSAT measurements of the pulse period of Vela X-1
[MPE-PREPRINT-157] N90-16673
MAX-PLANCK-INST. FUER STROEMUNGSFORSCHUNG, GOETTINGEN (GERMANY, F.R.).
Simultaneous determination of temperature and velocity fields in a thermal convection flow with non-enclosed liquid crystal tracers N90-16239
Shock thickness measurements with laser beams
[MPIS-7/1989] N90-16267
Lecture notes on supersonic molecular beam sources
[MPIS-20/1988] N90-16494

MCCRONE ASSOCIATES, INC., WESTMONT, IL.
Electron beam analysis of particulate cometary material N90-16613
MCDONNELL AIRCRAFT CO., SAINT LOUIS, MO.
A dynamicist's view of fuel tank skin durability N90-15915
MCELROY (RALPH) CO., AUSTIN, TX.
BAM: German Federal Institute for Materials Research and Testing, Berlin
[DE90-004293] N90-16307
MERIT TECHNOLOGY, INC., PLANO, TX.
An intelligence-driven RPV mission planner N90-15932
MESSERSCHMITT-BOELKOW-BLOHM G.M.B.H., BREMEN (GERMANY, F.R.).
An efficient solver of the Eigenvalue problem of the linear stability equations for three dimensional, compressible boundary-layer flows N90-16172
Development of transition criteria on the basis of e to the N power for three dimensional wing boundary layers N90-16179
The precise calculation of the inviscid leading edge flow on a laminar airfoil using simple methods and verification by measurements on the TLF pilot model N90-16180
Research on three different Euler's schemes applied to a delta wing with vortical flows N90-16184
An interactive method for the flow calculation of airfoils with local separation regions N90-16190
Calculation of the flap profile flows with separation based on coupled potential and boundary layer solutions N90-16191
Inverse solutions for boundary layers with separation or close to separation under locally infinite swept wing conditions N90-16192
The use of sublimation methods for the recognition of transition at low speed N90-16251
MESSERSCHMITT-BOELKOW-BLOHM G.M.B.H., MUNICH (GERMANY, F.R.).
Design philosophy and construction techniques for integral fuselage fuel tanks N90-15913
Navigation of autonomous air vehicles by passive imaging sensors N90-15927
MESSERSCHMITT-BOELKOW-BLOHM G.M.B.H., OTTOBRUNN (GERMANY, F.R.).
The MPI/AIT X ray Imager (MAXI): High speed PN-CCD's for x ray detection
[MPE-PREPRINT-154] N90-16234
METEOR COSTRUZIONI AERONAUTICHE ED ELETTRONICHE S.P.A., RONCHI DEI LEGIONARI (ITALY).
Mirach 100 flight control system N90-15926
MICHIGAN UNIV., ANN ARBOR.
Swirl-stabilized flames: Fluid dynamics, mixing, and flame stability limits N90-16009
MICROELECTRONICS CENTER OF NORTH CAROLINA, RESEARCH TRIANGLE PARK.
BLITZEN: A highly integrated massively parallel machine N90-16453
MICROTRONICS ASSOCIATES, PITTSBURGH, PA.
Parallel asynchronous systems and image processing algorithms N90-16218
MIDWEST RESEARCH INST., GOLDEN, CO.
Spectral sensitivity of device power output for tandem a-Si alloy solar cells
[DE89-009421] N90-16340
SERI (Solar Energy Research Institute) solar radiation resource assessment project
[DE89-009456] N90-16352
MINNESOTA UNIV., MINNEAPOLIS.
General contraction of Gaussian basis sets. Part 2: Atomic natural orbitals and the calculation of atomic and molecular properties
[NASA-CR-186201] N90-16482
MISSISSIPPI STATE UNIV., STATE COLLEGE.
Artificial intelligence in process control: Knowledge base for the shuttle ECS model N90-16697
MISSOURI UNIV., ROLLA.
Investigation of IGES for CAD/CAE data transfer N90-16702
MORTON THIOKOL, BRIGHAM CITY, UT.
Space shuttle Production Verification Motor 1 (PV-1) static fire
[NASA-CR-183784] N90-15991
MUENSTER UNIV. (GERMANY, F.R.).
Methods for the mineralogical and textural analysis of comet nucleus samples N90-16648
MURRAY STATE UNIV., KY.
The effects of hydrogen embrittlement of titanium N90-16698

N

NATIONAL AERONAUTICS AND SPACE ADMINISTRATION, WASHINGTON, DC.
Reports of planetary astronomy, 1986
[NASA-TM-100776] N90-16596
NATIONAL AERONAUTICS AND SPACE ADMINISTRATION. AMES RESEARCH CENTER, MOFFETT FIELD, CA.
Piloted simulation of a ground-based time-control concept for air traffic control
[NASA-TM-101085] N90-15898
A survey of nonuniform inflow models for rotorcraft flight dynamics and control applications
[NASA-TM-102219] N90-15938
Computer-aided boundary delineation of agricultural lands
[NASA-TM-102243] N90-16313
A space-time discretization procedure for wave propagation problems
[NASA-TM-102215] N90-16399
Computation of the unsteady facilitated transport of oxygen in hemoglobin
[NASA-TM-102251] N90-16400
Basic mathematical function libraries for scientific computation
[NASA-TM-102256] N90-16423
Theoretical investigations of the structures and binding energies of Be(sub n) and Mg(sub n) (n = 3-5) clusters
[NASA-TM-101931] N90-16483
The origin, composition and history of cometary ices from spectroscopic studies N90-16609
Direct determination of the morphology, structure and composition of cometary and interstellar ice analogs in the laboratory N90-16612
The carbon chemistry of meteorites: Relationships to comets N90-16615
Computer simulation of dust grain evolution N90-16632
The comet rendezvous asteroid flyby mission N90-16639
NATIONAL AERONAUTICS AND SPACE ADMINISTRATION. GODDARD SPACE FLIGHT CENTER, GREENBELT, MD.
Detection of edges using local geometry N90-16213
The 2nd Symposium on the Frontiers of Massively Parallel Computations
[NASA-TM-101918] N90-16442
How to cluster in parallel with neural networks N90-16443
Sort computation N90-16446
Estimating water flow through a hillslope using the massively parallel processor N90-16449
Scan line graphics generation on the massively parallel processor N90-16450
Parallel algorithm for determining motion vectors in ice floe images by matching edge features N90-16451
Image segmentation by iterative parallel region growing with application to data compression and image analysis N90-16452
A generic fine-grained parallel C N90-16454
Metamorphism of cosmic dust: Processing from circumstellar outflows to the cometary regolith N90-16641
A database of fragmentation cross section measurements applicable to cosmic ray propagation calculations
[NASA-CR-186328] N90-16681
The excess flux in the cosmic submillimeter background radiation and the primordial deuterium abundance
[NASA-CR-186312] N90-16683
NATIONAL AERONAUTICS AND SPACE ADMINISTRATION. HUGH L. DRYDEN FLIGHT RESEARCH FACILITY, EDWARDS, CA.
Open-mode delamination stress concentrations in horseshoe and elliptic composite curved bars subjected to end forces
[NASA-TM-4164] N90-16004
NATIONAL AERONAUTICS AND SPACE ADMINISTRATION. LYNDON B. JOHNSON SPACE CENTER, HOUSTON, TX.
Safety and rescue during STS operations N90-15975
Assured crew return capability architecture N90-15977
Systems interoperability approach Apollo/Soyuz test project N90-15979
Discrete event simulation tool for analysis of qualitative models of continuous processing systems
[NASA-CASE-MSC-21465-1] N90-16410
Bus programmable slave module
[NASA-CASE-MSC-21387-1] N90-16411
JSC document index
[NASA-TM-102923] N90-16589
Identification of solar nebula condensates in interplanetary dust particles and unequilibrated ordinary chondrites N90-16629
The measurement of trace elements in interplanetary dust and cometary particles by ultra-high sensitivity INAA N90-16656
NATIONAL AERONAUTICS AND SPACE ADMINISTRATION. LANGLEY RESEARCH CENTER, HAMPTON, VA.
Rotor induced-inflow-ratio measurements and CAMRAD calculations
[NASA-TP-2946] N90-15882
An experimental investigation of thrust vectoring two-dimensional convergent-divergent nozzles installed in a twin-engine fighter model at high angles of attack
[NASA-TM-4155] N90-15884
Assessment of computational prediction of tail buffeting
[NASA-TM-101613] N90-15886
Improved tangent-cone method for the Aerodynamic Preliminary Analysis System (APAS) version of the hypersonic arbitrary-body program
[NASA-TM-4165] N90-15890
Personal computer study of finite-difference methods for the transonic small disturbance equation
[NASA-TM-102582] N90-15892
Structural dynamics division research and technology accomplishments for FY 1989 and plans for FY 1990
[NASA-TM-101683] N90-15894
Evaluation of two transport aircraft and several ground test vehicle friction measurements obtained for various runway surface types and conditions. A summary of test results from joint FAA/NASA Runway Friction Program
[NASA-TP-2917] N90-15902
The NASA Langley 0.3-meter transonic cryogenic tunnel N90-15941
The US National Transonic Facility, NTF N90-15942
Other cryogenic wind tunnel projects N90-15948
Test techniques for cryogenic wind tunnels N90-15952
Models for cryogenic wind tunnels N90-15956
Automatic control of cryogenic wind tunnels N90-15957
Experience with strain-gage balances for cryogenic wind tunnels N90-15958
Cryogenic balances for the US NTF N90-15959
Safety and cryogenic wind tunnels N90-15960
Energy management and recovery N90-15962
Convergence speeding up in the calculation of the viscous flow about an airfoil N90-16194
Visual Information Processing for Television and Telerobotics
[NASA-CP-3053] N90-16204
Image gathering and coding for digital restoration: Information efficiency and visual quality N90-16211
Isolating contour information from arbitrary images N90-16217
Mechanical strain isolator mount
[NASA-CASE-LAR-13580-1] N90-16272
Analysis and testing of axial compression in imperfect slender truss struts
[NASA-TM-4174] N90-16292
Load-shortening behavior of an initially curved eccentrically loaded column
[NASA-TM-101643] N90-16293
Research and technology, 1989: Langley Research Center
[NASA-TM-4150] N90-16703
NATIONAL AERONAUTICS AND SPACE ADMINISTRATION. LEWIS RESEARCH CENTER, CLEVELAND, OH.
Assessment of worm gearing for helicopter transmissions
[NASA-TM-102441] N90-15923
An electronic pressure profile display system for aeronautic test facilities
[NASA-TM-102478] N90-15964
A numerical simulation of the flow in the diffuser of the NASA Lewis icing research tunnel
[NASA-TM-102480] N90-15965
A burst compression and expansion technique for variable-rate users in satellite-switched TDMA networks
[NASA-TM-102414] N90-15983
Design of a thrust stand for high power electric propulsion devices
[NASA-TM-102372] N90-15992
Probabilistic simulation of uncertainties in composite uniaxial strengths
[NASA-TM-102483] N90-16008
Production and processing of Cu-Cr-Nb alloys
[NASA-TM-102495] N90-16053
Conceptual design for the space station Freedom modular combustion facility
[NASA-TM-102037] N90-16087
Data compression for the microgravity experiments N90-16212

Dynamic analysis of geared rotors by finite elements
[NASA-TM-102349] N90-16286
Scaling study for SP-100 reactor technology
[NASA-TM-897140] N90-16496

NATIONAL AERONAUTICS AND SPACE ADMINISTRATION. MARSHALL SPACE FLIGHT CENTER, HUNTSVILLE, AL.

Instrumented impact and residual tensile strength testing of eight-ply carbon epoxy specimens
[NASA-TP-2981] N90-16007
New atmospheric turbulence model for shuttle applications
[NASA-TM-4168] N90-16389

NATIONAL AERONAUTICS AND SPACE ADMINISTRATION. PASADENA OFFICE, CA.

Stripline feed for a microstrip array of patch elements with teardrop shaped probes
[NASA-CASE-NPO-17548-1-CU] N90-16104
Organic cathode for a secondary battery
[NASA-CASE-NPO-17604-1-CU] N90-16124
Apparatus for imaging deep arterial and coronary lesions
[NASA-CASE-NPO-17439-1-CU] N90-16391

NATIONAL CENTER FOR ATMOSPHERIC RESEARCH, BOULDER, CO.

Interconnectedness in nature and in science: The case of climate and climate modeling
[PB90-113986] N90-16358

NATIONAL ENVIRONMENTAL SATELLITE SERVICE, WASHINGTON, DC.

Operational ozone monitoring with the Global Ozone Monitoring Radiometer (GOMR)
[PB90-114034] N90-16359

NATIONAL INST. FOR RESEARCH IN INORGANIC MATERIALS, IBARAKI (JAPAN).

Researches on amorphous perovskite
[DE89-900733] N90-16535

NATIONAL INST. OF STANDARDS AND TECHNOLOGY, BOULDER, CO.

X-band atmospheric attenuation for an Earth terminal measurement system
[PB90-100736] N90-16101

NATIONAL INST. OF STANDARDS AND TECHNOLOGY, GAITHERSBURG, MD.

Assessing the flammability of composite materials
[PB90-112996] N90-16002

NATIONAL OCEANIC AND ATMOSPHERIC ADMINISTRATION, BOULDER, CO.

Statistics of a reflected laser beam in the turbulent atmosphere (path correlation)
[PB90-113994] N90-16261

NATIONAL OCEANIC AND ATMOSPHERIC ADMINISTRATION, SILVER SPRING, MD.

ECC (Electrochemical Concentration Cell) ozonesonde observations at South Pole, Antarctica, during 1988
[PB90-110172] N90-16355
ECC (Electrochemical Concentration Cell) ozonesonde observations at Mirny, Antarctica, during 1988
[PB90-113960] N90-16357

NATIONAL SCIENCE FOUNDATION, WASHINGTON, DC.

Project summaries
[PB90-103987] N90-16472

NATIONAL SPACE DEVELOPMENT AGENCY, TOKYO (JAPAN).

NASDA's approach to the interoperability of safety and rescue in space N90-15981

NATIONAL TAIWAN UNIV., TAIPEI.

Digital image coding and compression
[PB90-110958] N90-16409

NATIONAL TRANSPORTATION SAFETY BOARD, WASHINGTON, DC.

Aircraft accident report: Delta Air Lines, Inc., Boeing 727-232, N473DA, Dallas-Fort Worth International Airport, Texas, August 31, 1988
[PB89-910406] N90-15895

NATO ADVANCED STUDY INST., BRUSSELS (BELGIUM).

Structure-property relationships in ion-beam surface-modified ceramics: Theory and applications
[AD-A212785] N90-16054

NAVAL OCEAN SYSTEMS CENTER, SAN DIEGO, CA.

Low-altitude millimeter-wave propagation in the evaporation duct
[AD-A214432] N90-16108
Lidar technique for adjusting aerosol model number densities to existing conditions
[AD-A213846] N90-16374
Atmospheric transmittance determination from a two-angle measurement of radiance change
[AD-A213847] N90-16375

NAVAL OCEANOGRAPHIC OFFICE, BAY SAINT LOUIS, MS.

ZBTAB: Zenith-248 version of BLUGTAB
[AD-A214279] N90-16415

NAVAL POSTGRADUATE SCHOOL, MONTEREY, CA.

An empirical comparison of software fault tolerance and fault elimination
[NASA-CR-186313] N90-16414

NAVAL RESEARCH LAB., WASHINGTON, DC.

Neural networks for data compression and invariant image recognition N90-16219

NAVAL SHIP RESEARCH AND DEVELOPMENT CENTER, BETHESDA, MD.

Effects of high rate shear on the microstructure and deformation and fracture behavior of two high strength steels
[AD-A214107] N90-16032
Plasmon excitation in the scattering of electromagnetic waves from good conductors
[AD-A214026] N90-16107

NEW ENERGY DEVELOPMENT ORGANIZATION, TOKYO (JAPAN).

Investigation and study on compressed air storage power generation system, part 2
[DE90-702648] N90-16354

NEW MEXICO UNIV., ALBUQUERQUE.

What if chondritic porous interplanetary dust particles are not the real McCoy N90-16642

NIELS BOHR INST., COPENHAGEN (DENMARK).

On the observation of a transition from fusion to multifragmentation in high multiplicity O16 induced reactions
[LUIP-8812] N90-16481

NORTH CAROLINA AGRICULTURAL AND TECHNICAL STATE UNIV., GREENSBORO.

The development of two-dimensional object identification techniques
[NASA-CR-186203] N90-16408

NORTH CAROLINA STATE UNIV., RALEIGH.

Theoretical studies of chemisorption and surface reactions on nickel and silicon
[DE90-004849] N90-16050
Parallel algorithms for interactive manipulation of digital terrain models N90-16445
A computational and experimental study of steady and transient acoustic energy flow from a complex mechanical structure N90-16478

NORTH CAROLINA UNIV., CHAPEL HILL.

Solid state voltammetry and sensors in solids and gases
[DE90-003234] N90-16538

NORTH CAROLINA UNIV., GREENSBORO.

Factor analytic reduction of the carotid-cardiac baroreflex parameters N90-16693

NORTHWESTERN UNIV., EVANSTON, IL.

Solid state, surface, and catalytic studies of oxides
[DE90-004850] N90-16566
Gamma-ray observations and the distribution of interstellar aluminum-26 N90-16661

O

OAK RIDGE GASEOUS DIFFUSION PLANT, TN.

Issues and approaches for electronic document approval and transmittal using digital signatures and text authentication: Prototype documentation
[DE90-003382] N90-16119

OAK RIDGE NATIONAL LAB., TN.

The structure of silica-polysiloxane composites and its effects on their elastomeric properties
[DE89-014768] N90-16005
Using inorganic membranes to separate gases: R and D status review
[DE90-004386] N90-16019
Performance of an Inductively Coupled Plasma-Mass Spectrometer Analyzer system
[DE90-004002] N90-16025
Selection of corrosion-resistant materials for use in molten nitrate salts
[DE90-004351] N90-16048
Modeling dislocation evolution in irradiated alloys
[DE90-004921] N90-16051
Metals and Ceramics Division Materials Sciences Program
[DE90-004371] N90-16070
An investigation of elastic guided waves for ceramic joint evaluation
[DE90-004400] N90-16071
Isotope driven critical scattering and phase separation from mixtures of deuterated and protonated polymers
[DE90-003976] N90-16076
Alcohol and blends as motor fuels
[DE90-003517] N90-16085
Electroplating simulation
[DE90-003683] N90-16091
Bilateral force reflection for teleoperators with masters and slaves with dissimilar and possibly redundant kinematics
[DE90-004392] N90-16132
On the HEMP (High-Altitude Electromagnetic Pulse) response of protective relays
[DE90-003718] N90-16138
Steep front impulse tests on a solid-state relay
[DE90-004243] N90-16140
Modeling a self-calibrating thermocouple for use in a smart temperature measurement system
[DE90-003697] N90-16259
Results from the third year of operation of the Federal Methanol Fleet at Lawrence Berkeley Laboratory
[DE90-003306] N90-16277
Material responses to incident x rays
[DE89-015386] N90-16305
Experiences with three-point bending test specimens for determining the crack-arrest fracture toughness K(sub Ia) in low-alloy steel
[DE90-004120] N90-16306
BAM: German Federal Institute for Materials Research and Testing, Berlin
[DE90-004293] N90-16307
Absorption fluids data survey: 1989 update
[DE90-003985] N90-16346
Federal roles to realize national energy-efficiency opportunities in the 1990s
[DE90-004410] N90-16348
Environmental, health, and CFC substitution aspects of the ozone depletion issue
[DE90-004404] N90-16363
Short-term bioassays may be useful in evaluating fiber/whisker hazards
[DE90-003707] N90-16393
PVM (Parallel Virtual Machine): A framework for parallel distributed computing
[DE90-004390] N90-16403
Case tool evaluation system
[DE90-003698] N90-16413
EZVIDEO, FORTRAN graphics routines for the IBM AT
[DE90-004409] N90-16422
Design and implementation of a multi-sensor fusion algorithm on a hypercube computer architecture
[DE90-003682] N90-16438
Heavy ion inelastic scattering with a 4(pi) gamma detector
[DE90-002709] N90-16488
ATF-2 studies
[DE90-004380] N90-16510
Near-term directions in the world stellarator program
[DE90-004381] N90-16511
Stress analysis of the Princeton Plasma Physics Laboratory 1/2- x 1/2-inch shear/compression test fixture
[DE90-004401] N90-16512
Ion beam annealing of Si co-implanted with Ga and As
[DE90-004297] N90-16556
Neutron experiments on high-temperature superconductors
[DE90-003978] N90-16559
The effects of oxygen and strontium vacancies on the superconductivity of single crystals of Bi2Sr(2-x)CuO(6-y)
[DE90-004242] N90-16561
Magnetic penetration depth and intragrain critical current density in gain-aligned Tl2Ca2Ba2Cu3O10 superconductor
[DE90-004245] N90-16562
Physical properties of Bi2Sr2CuO6, the semiconducting phase, structurally distinct from the n = 1 Bi-cuprate superconductor
[DE90-004299] N90-16563
Invention and innovation: Alternative mechanisms for enhancing organizational competitiveness
[DE89-015858] N90-16584
The effects of natural and enhanced Van Allen Belt radiation on a space based weapon platform
[DE89-016219] N90-16685

OAK RIDGE Y-12 PLANT, TN.

ZrO2 sintered compact and method for its production
[DE90-004125] N90-16006

ODETICS, INC., ANAHEIM, CA.

Knowledge-based imaging-sensor fusion system N90-16220

OFFICE NATIONAL D'ETUDES ET DE RECHERCHES AERONAUTIQUES, PARIS (FRANCE).

Instrumentation for cryogenic wind tunnels N90-15950
Productivity and cryogenic wind tunnels N90-15961

OFFICE NATIONAL D'ETUDES ET DE RECHERCHES AEROSPATIALES, TOULOUSE (FRANCE).

Calculation of turbulent choppy flow mixing
[ETN-90-95929] N90-16165

OHIO STATE UNIV., COLUMBUS.

High-frequency asymptotic methods for analyzing the EM scattering by open-ended waveguide cavities
[NASA-CR-186244] N90-16103

OKLAHOMA STATE UNIV., STILLWATER.
The DAB model of drawing processes N90-16691
OLD DOMINION UNIV., NORFOLK, VA.
Application of Lagrangian blending functions for grid generation around airplane geometries
[NASA-CR-186318] N90-15891
From primal sketches to the recovery of intensity and reflectance representations N90-16216
OPTIVISION, INC., DAVIS, CA.
A programmable image compression system N90-16222

P

PACIFIC NORTHWEST LAB., RICHLAND, WA.
Microstructural explanation for irradiation embrittlement of V-15Cr-5Ti
[DE90-004112] N90-16041
Phase evolution during neutron irradiation of commercial Fe-Cr-Mn alloys
[DE90-004113] N90-16042
Fracture toughness of ferritic alloys at very high neutron exposures
[DE90-004519] N90-16046
Irradiation creep and swelling of annealed type 304L stainless steel at approximately 390 C and high neutron fluence
[DE90-004521] N90-16047
Synthesis of air-sinterable lanthanum chromite powders
[DE90-004681] N90-16049
Design, characterization, and optical properties of phosphazene-based polymers
[DE90-004111] N90-16068
PADUA UNIV. (ITALY).
The visible channel of OMEGA-VIMS
[IFSI-89-14] N90-16231
PAVIA UNIV. (ITALY).
The MPI/AIT X ray Imager (MAXI): High speed PN-CCD's for x ray detection
[MPE-PREPRINT-154] N90-16234
PENNSYLVANIA STATE UNIV., ERIE.
Low flow vortex shedding flowmeter N90-16700
PENNSYLVANIA STATE UNIV., UNIVERSITY PARK.
On-line estimation of mechanical nonlinearities in compliant two-link robot manipulators N90-16280
PHYSICAL SCIENCES, INC., ANDOVER, MA.
Rotational energy transfer in metastable states of heteronuclear molecules
[AD-A214425] N90-16485
PHYSIKALISCH-TECHNISCHE BUNDESANSTALT, BRUNSWICK (GERMANY, F.R.).
Optical flow measuring method using diode lasers, phase coupled arrays, and high frequency pulsed diode lasers N90-16176
High frequency pulsed diode lasers and phase-coupled diode arrays for aerodynamics N90-16238
PLANETARY SCIENCE INST., TUCSON, AZ.
Comments on comet shapes and aggregation processes N90-16622
POLITECNICO DI MILANO (ITALY).
The MPI/AIT X ray Imager (MAXI): High speed PN-CCD's for x ray detection
[MPE-PREPRINT-154] N90-16234
PRC KENTRON, INC., HAMPTON, VA.
CPU timing routines for a CONVEX C220 computer system
[NASA-CR-181950] N90-16424
PRINCETON UNIV., NJ.
The structure of supersonic turbulent boundary layers subjected to concave surface curvature N90-15883
Comprehensive mechanisms for combustion chemistry: An experimental and numerical study with emphasis on applied sensitivity analysis
[DE90-003904] N90-16017
Proposal for a study of laser acceleration of electrons using micrograting structures at ATF
[DE90-003699] N90-16262
Group 2 cubic fluorides as dielectrics for III-V compound semiconductors
[AD-A214096] N90-16542
PRINS MAURITS LAB. TNO, RIJSWIJK (NETHERLANDS).
Solid fuel combustion chamber, phase 10
[LR-536] N90-16000
Solid fuel combustion chamber
[LR-555] N90-16001
PRODUCTS RESEARCH AND CHEMICAL CORP., GLENDALE, CA.
Improved performance polysulfide based sealant N90-15910
Fuel resistant coatings for metal and composite fuel tanks N90-15911
PURDUE UNIV., WEST LAFAYETTE, IN.
Analytical techniques for tracking filter implementation N90-15903
Thickness, velocity, and temperature measurements in falling liquid films
[DE90-004290] N90-16151
The role of an upstream cyclone and corresponding synoptic/planetary-scale interactions during the development of a blocking anticyclone N90-16659
Plant features measurements for robotics N90-16695

R

RANDOLPH-MACON COLL., ASHLAND, VA.
Study of metal corrosion using ac impedance techniques in the STS launch environment N90-16688
RENSSELAER POLYTECHNIC INST., TROY, NY.
Theoretical aspects of electroweak and other interactions in medium energy nuclear physics
[DE90-004015] N90-16493
RISOE NATIONAL LAB., ROSKILDE (DENMARK).
Soft modes, freezing, and nonlinear response of a dipolar glass
[DE90-003647] N90-16075
ROCHESTER UNIV., NY.
Coded-aperture imaging in nuclear medicine N90-16208
High speed signal extraction using electro-optic techniques
[AD-A214446] N90-16500
ROCKET RESEARCH CORP., REDMOND, WA.
Pulsed plasma mission endurance test
[AD-A213462] N90-15993
ROCKWELL INTERNATIONAL CORP., CANOGA PARK, CA.
The Gevaltig: An inertial fusion powered manned spacecraft design for outer solar system missions
[NASA-CR-185163] N90-15985
ROME UNIV. (ITALY).
Stochastic action of dynamical systems on curved manifolds. The isokinetic developing map on trajectories
[PREPRINT-666] N90-16486
Neutrino interactions
[NOTA-INTERNA-934] N90-16495
Cosmic ray NM-64 neutron monitor data 16
[IFSI-88-21] N90-16684
ROYAL AEROSPACE ESTABLISHMENT, FARNBOROUGH (ENGLAND).
Weapon aerodynamics overview
[RAE-TM-AERO-2150] N90-15888
The development of a low cost data logging system for flight trials based on an IBM compatible PC
[RAE-TM-FM-16] N90-15917
Performance of a highly-loaded HP compressor
[RAE-TM-P-1149] N90-15919
Aerodynamic and heat transfer measurements on blading for a high rim-speed transonic turbine
[RAE-TM-P-1151] N90-15920
Cycle analysis for helicopter gas turbine engines
[RAE-TM-P-1154] N90-15921
A UK perspective on the uniform engine test programme
[RAE-TM-P-1172] N90-15922
On mean elements for satellite orbits perturbed by the zonal harmonics of the geopotential
[RAE-TM-SPACE-371] N90-15971
Fatigue and impact strength of diffusion bonded titanium alloy joints
[RAE-TM-MAT/STR-1123] N90-16043
FRAG requirements for control of fatigue testing
[RAE-TM-MAT/STR-1130] N90-16300
Calibration of a pulsed potential crack monitor for use in fatigue crack growth studies
[RAE-TM-M/S-1126] N90-16301
Keeping the pilot in the loop
[RAE-TM-FM-18] N90-16396
ROYAL AIR FORCE, DEREHAM (ENGLAND).
The repair of aircraft integral fuel tanks in the RAF: A user's view of fuel tank technology N90-15908
ROYAL AIRCRAFT ESTABLISHMENT, FARNBOROUGH (ENGLAND).
The effect of primer age on adhesion of polysulphide sealant N90-15909
ROYAL ARMAMENT RESEARCH AND DEVELOPMENT ESTABLISHMENT, FORT HALSTEAD (ENGLAND).
Burst pressure prediction of metallic/fibre reinforced rocket motor cases using an elasto-plastic instability analysis
[RARDE-1/89] N90-15997
ROYAL SIGNALS AND RADAR ESTABLISHMENT, MALVERN (ENGLAND).
The automatic detection of anti-collision lights
[RSRE-MEMO-4272] N90-15896
The application of Z to the specification of air traffic control systems. 1: An initial specification of the radar processing activity
[RSRE-MEMO-4280] N90-15900
Tactical UK military satellite ground terminals: A research and development review
[RSRE-MEMO-4262] N90-15972
The SMITE approach to security
[RSRE-89014] N90-16404
The new programming
[RSRE-MEMO-4249] N90-16425
The inside-outside algorithm: Further experiments on three and four letter word spelling and implementation on an array processor
[RSRE-MEMO-4256] N90-16426
A persistent heap for ALGOL 68
[RSRE-MEMO-4268] N90-16427
Alvey MMI007. Object identification from 2D images: The RSRE contribution
[RSRE-MEMO-4277] N90-16428
Beamforming pre-processors for high discrimination algorithms
[RSRE-MEMO-4304] N90-16429
Pattern matching in ML: A case study in refinement
[RSRE-89004] N90-16430
The NODEN hardware description language
[RSRE-89011] N90-16431
The algebra of the NODEN analyser
[RSRE-89012] N90-16432
Tool support for the production of high integrity software
[RSRE-89005] N90-16433
Enhanced performance IR focal plane arrays using adaptive subtraction
[RSRE-MEMO-4286] N90-16502
RUHR UNIV., BOCHUM (GERMANY, F.R.).
Measurement of the p, v, T behavior under microgram conditions
[ETN-90-95906] N90-16162
RUTGERS UNIV., NEW BRUNSWICK, NJ.
Cosmogenic nuclides in cometary materials: Implications for rate of mass loss and exposure history N90-16823

S

SAINT LOUIS UNIV., MO.
Diagnostic and kinematic fields associated with curved and straight jet streaks using a two-layer primitive equation model N90-16371
SANDIA NATIONAL LABS., ALBUQUERQUE, NM.
The use of hypervelocity launchers to explore previously inaccessible states of matter
[DE90-004088] N90-15973
Evaluation of potential cold x ray shield materials tested on Proto II
[DE90-004348] N90-16003
Shock-induced reaction synthesis of aluminides and silicides
[DE90-003948] N90-16066
Characterization of B and N implanted fused silica
[DE90-004198] N90-16069
Diblock copolymers at surfaces
[DE90-005406] N90-16079
Very low energy ignition of pyrotechnics using a Semiconductor Bridge (SCB)
[DE90-002645] N90-16082
Digital system for monitoring and controlling remote processes
[DE90-003935] N90-16094
Sizing and selection of batteries for stand-alone photovoltaic systems
[DE90-002990] N90-16129
Theoretical and experimental investigation of axial power extraction from a magnetically insulated transmission line oscillator
[DE90-003486] N90-16131
Diesel starting system monitor: Prototype development
[DE90-004425] N90-16276
Stability and fragmentation of ejecta in hypervelocity impact
[DE90-004087] N90-16278
Connector selection program implementation notes, version 1.0
[DE90-004983] N90-16279
Studies of density distributions in one-dimensional shock-induced debris clouds
[DE90-004089] N90-16282
Fault tree analysis: A tool for battery safety and reliability studies
[DE90-002582] N90-16287
An introduction to shaker shock simulations
[DE90-003057] N90-16298
Rainflow counting algorithm for the LIFE2 fatigue analysis code
[DE90-002834] N90-16344

Performance predictions for an intermediate-sized VAWT based on performance of the 34-m VAWT test bed
[DE90-002835] N90-16345
A qualitative architecture for understanding policy responses to global change
[DE90-003936] N90-16364
CAE (Computer-Aided Engineering) tools' limitations case study: An SSI (Small Scale Integrated) design to an ASIC (Application Specific Integrated Circuit)
[DE90-002902] N90-16418
Results of error correction techniques applied on two high accuracy coordinate measuring machines
[DE90-003341] N90-16439
Asymptotically fast triangularization of matrices over rings
[DE90-003161] N90-16471
Light ion beam drivers for inertial confinement fusion
[DE90-004196] N90-16528
Fundamental issues in heteroepitaxy (condensed from the DOE panel report)
[DE90-003980] N90-16555
Database design using NIAM (Nijssen Information Analysis Method) modeling
[DE89-014631] N90-16592

SAO PAULO UNIV. (BRAZIL).
Carbon-13 nuclear magnetic resonance of heterocyclic salts and its precursors
[DE89-635768] N90-16016
Pairs of chalcogen impurities in silicon
[DE89-635767] N90-16063
Studies of elastic scattering and cross sections of the C-12 + Si-28 system
[DE89-635990] N90-16486

SAVANNAH STATE COLL., GA.
Analysis of the 60-Hz power system at KSC: The Orsino substation N90-16692

SCIENCE APPLICATIONS INTERNATIONAL CORP., LA JOLLA, CA.
Thermal and chemical processing of the outermost layer of cometary nuclei N90-16614

SIEGEN UNIV., (GERMANY, F.R.).
Visualization of gas flows using the smoke wire technique N90-16242

SIRA INST. LTD., CHISLEHURST (ENGLAND).
Distance measurement using laser diodes
[ETN-90-96144] N90-16264
Proposed concept for the visible/infrared imaging radiometer for second generation Meteosat
[ETN-90-96145] N90-16503

SMITHSONIAN ASTROPHYSICAL OBSERVATORY, CAMBRIDGE, MA.
Refractory solids in chondrites and comets: How similar N90-16654

SOCIETY OF EXPLORATION GEOPHYSICISTS, TOKYO (JAPAN).
Proceedings of the 79th SEGJ Conference
[DE89-760006] N90-16704

SOLMECS LTD., JERUSALEM (ISRAEL).
Development of a wet vapor homogeneous liquid metal MHD power system
[DE90-001468] N90-16508

SOUTH AFRICAN INST. OF PHYSICS, PRETORIA.
Proceedings of the 23rd Annual Seminar on Theoretical Physics
[DE90-601827] N90-16577

SOUTHAMPTON UNIV. (ENGLAND).
Introduction to cryogenic wind tunnels N90-15940
Flow visualization in the cryogenic wind tunnel N90-15953
An analysis of the time variation of the frequency response of the LMS adaptive line enhancer
[ISVR-TR-175] N90-16115

SOUTHWEST RESEARCH INST., SAN ANTONIO, TX.
Stand Alone Pressure Measurement Device (SAPMD) for the space shuttle Orbiter, part 1
[NASA-CR-172119-PT-1] N90-16202
Stand Alone Pressure Measurement Device (SAPMD) for the space shuttle Orbiter, part 2
[NASA-CR-172119-PT-2] N90-16203
Morphology and compositional differentiation of the surface of comets N90-16624

SPACE TELESCOPE SCIENCE INST., BALTIMORE, MD.
Accretion shock geometries in the magnetic variables
[NASA-CR-186290] N90-16664

SPECTRACOM, CANOGA PARK, CA.
Spectral sensitivity of device power output for tandem a-Si alloy solar cells
[DE89-009421] N90-16340

SPOT IMAGE CORP., TOULOUSE (FRANCE).
SPOT after two years in operation: An appraisal of results and a review of selected applications N90-16326

SRI INTERNATIONAL CORP., MENLO PARK, CA.
Mechanisms of the electrochemistry of small organic molecules
[PB90-100785] N90-16012
Algorithms for fault tolerant distributed systems
[AD-A214447] N90-16416

STANFORD LINEAR ACCELERATOR CENTER, CA.
Recent progress in relativistic klystron research
[DE90-000942] N90-16121
B-Factory Final Focus System using superconducting quadrupoles
[DE90-004432] N90-16552

STANFORD UNIV., CA.
Solid-state electrolyte catalysis for methane and oxygen synthesis
[PB90-100231] N90-16011
Element-by-element preconditioning techniques for large-scale, vectorized finite element analysis in nonlinear solid and structural mechanics N90-16291

STATE UNIV. OF NEW YORK, ALBANY.
Surface studies at the NSLS
[DE90-003173] N90-16027
Stainless steel passivity
[AD-A214108] N90-16033

STATE UNIV. OF NEW YORK, PLATTSBURGH.
Trace element abundance determinations by Synchrotron X Ray Fluorescence (SXRF) on returned comet nucleus mineral grains N90-16619

STATE UNIV. OF NEW YORK, STONY BROOK.
An XPS and electrochemical study of the influence of molybdenum and nitrogen on the passivity of austenitic stainless steel
[AD-A214267] N90-16034
Theoretical studies of chemisorption and surface reactions on nickel and silicon
[DE90-004849] N90-16050
Anomalous waves in shock wave - fluid interface collisions
[AD-A213584] N90-16144

STATISTISCHES BUNDESAMT, WIESBADEN (GERMANY, F.R.).
Statistical information system for cultivation of the soil. Use of remote sensing in official statistics N90-16338

STELLENBOSCH UNIV. (SOUTH AFRICA).
Proceedings of the 23rd Annual Seminar on Theoretical Physics
[DE90-601827] N90-16577

STUTTGART UNIV. (GERMANY, F.R.).
GPS network analysis: The influence of stochastic prior information of orbital elements on ground station position measures
[TR-4-1988] N90-15901
Finite element calculations for transonic flows taking into account several far field boundary conditions N90-16188

SVERDRUP TECHNOLOGY, INC., CLEVELAND, OH.
Thermodynamic analysis of chemical stability of ceramic materials in hydrogen-containing atmospheres at high temperatures
[NASA-CR-4271] N90-16072

SWEDISH INST. FOR MATERIALS TESTING, BORAS.
Cyclic fatigue of hot-isostatic-pressed silicon nitride
[PB90-122649] N90-16308

SYNERGIC COMMUNICATION SERVICES, INC., COLUMBUS, OH.
Ninth Battery and Electrochemical Contractors' Conference: Extended abstracts
[DE89-016837] N90-16120

T

TECHNICAL RESEARCH CENTRE OF FINLAND, ESPOO.
Feasibility of cool storage systems in refrigeration
[DE90-728179] N90-16093
Measurement of reflection and impedance in a beam by the structural intensity technique
[DE90-728212] N90-16299

TECHNICAL RESEARCH CENTRE OF FINLAND, HELSINKI.
Long term creep strength of silver alloyed copper
[DE90-602367] N90-16039

TECHNISCHE HOCHSCHULE, AACHEN (GERMANY, F.R.).
Force and moment measurements on delta wings in unsteady flow N90-16185
Numerical simulation of a bubble shaped bursting vortex N90-16187
Coded trajectories for the investigation of strongly unsteady flow fields N90-16240

TECHNISCHE HOCHSCHULE, DARMSTADT (GERMANY, F.R.).
Semi-empirical transition criteria for the design of laminar profiles N90-16174
Analysis of the measuring range and the accuracy of an existing particle image velocimetry system N90-16247

TECHNISCHE UNIV., BERLIN (GERMANY, F.R.).
A foundation for the design of an astronautics specification system based on dynamic motivation analysis
[ILR-MITT-220] N90-15969
The first 1000 days of a future lunar base
[ILR-MITT-224] N90-15970
A modular habitation unit adapted for service in low earth and geostationary earth orbits
[ILR-MITT-217] N90-15990
Detection of flow instabilities at airfoil profiles using piezoelectric arrays N90-16175
Determination of dynamic surface forces using piezoelectric arrays N90-16249
Use of remote sensing in operational inventory and monitoring agricultural and forestry tasks N90-16336

TECHNISCHE UNIV., BRUNSWICK (GERMANY, F.R.).
Wind tunnel investigations on the configuration of the international vortex flow experiment N90-16181

TECHNISCHE UNIV., DELFT (NETHERLANDS).
Solid fuel combustion chamber, phase 10
[LR-536] N90-16000
Solid fuel combustion chamber
[LR-555] N90-16001
Definition, transformation-formulae and measurements of tipvane angles
[IW-R510] N90-16351

TECHNISCHE UNIV., EINDHOVEN (NETHERLANDS).
The algebraic Riccati equation and singular optimal control
[MEMO-COSOR-89-11] N90-16467

TECHNISCHE UNIV., HANOVER (GERMANY, F.R.).
Regional height determination using gravimetric and topographical data
[UH-156] N90-16315

TECHNISCHE UNIV., MUNICH (GERMANY, F.R.).
Attempt to draw conclusions concerning the geological subsoil from the vegetation using digital image processing of TM data N90-16329

TECHNISCHE UNIV., VIENNA (AUSTRIA).
Anisotropy and microstructure of high coercivity rare earth iron permanent magnets, list of papers published
[AD-A214160] N90-16476

TECNOSPAZIO S.P.A., MILAN (ITALY).
Candidate sample acquisition systems for the Rosetta N90-16635

TEL-AVIV UNIV. (ISRAEL).
Experimental studies of gas trapping in amorphous ice and thermal modelling of comets: Implications for Rosetta N90-16610

TENNESSEE UNIV., KNOXVILLE.
On-line chemical composition analyzer development
[DE90-004079] N90-16026
Evolution of carbonaceous chondrite parent bodies: Insights into cometary nuclei N90-16638

TEXAS UNIV., AUSTIN.
Synthesis and analysis of novel polymers with potential for providing both high permselectivity and permeability in gas separation applications
[DE90-003907] N90-16065

TOKYO UNIV., TANASHI (JAPAN).
Dissipation mechanism of the large-amplitude collective motion. Dynamical evolution of a collective bundle of trajectories in the TDHF phase space for a simple soluble model
[DE90-719557] N90-16477
Possible measurement of the gravitational acceleration of molecules, atoms, nuclei, elementary particles, and antiparticles
[DE90-719559] N90-16490
Design of a large superconducting spectrometer magnet
[DE90-719505] N90-16553
Universe as a topological defect in a higher-dimensional Einstein-Yang-Mills theory
[DE90-719507] N90-16578
Double-periodic wormholes in theories with global symmetries
[DE90-719575] N90-16581
An estimation of the one-loop mass shifts in open superstring theory
[DE90-719578] N90-16582

TRW SPACE TECHNOLOGY LABS., REDONDO BEACH, CA.
MHD integrated topping cycle project
[DE90-004141] N90-16525

TUEBINGEN UNIV. (GERMANY, F.R.).
The MPI/AIT X ray imager (MAXI): High speed PN-CCD's for x ray detection
[MPE-PREPRINT-154] N90-16234

TUFTS UNIV., MEDFORD, MA.
Lithium cobalt oxide thin film and its electrochromism
[DE90-004570] N90-16564

U

UNIVERSITAET DER BUNDESWEHR, NEUBIBERG (GERMANY, F.R.).
Response of a rotating finite annular liquid layer to axial excitation
[LRT-WE-9-FB-15(1988)] N90-16090
Vibrational behavior of a viscous column with a free liquid surface
[LRT-WE-9-FB-1(1989)] N90-16166
Small amplitude liquid oscillations in a rectangular container under zero-gravity
[LRT-WE-9-FB-2(1989)] N90-16167
Linear liquid oscillations in cylindrical containers under zero-gravity
[LRT-WE-9-FB-5(1989)] N90-16168
A nonlinear vortex-lattice method for the calculation of interference effects between free vortex sheets and wings N90-16183
Calculation of the flow field of a multiblade helicopter rotor using a Euler method including the wake N90-16189
Optimal step sizes in semi-stochastic approximation procedures
[ETN-90-95888] N90-16469

UNIVERSITY OF CENTRAL FLORIDA, ORLANDO.
NASA/ASEE Summer Faculty Fellowship Program
[NASA-CR-166837] N90-16686

UNIVERSITY OF SOUTHERN MISSISSIPPI, HATTIESBURG.
Copolymers for drag reduction in marine propulsion: New molecular structures with enhanced effectiveness
[AD-A214444] N90-16062

US FUEL CELLS, INC., IDAHO FALLS, ID.
An approach for testing fuel-cell/battery hybrid power sources for bus applications
[DE90-002090] N90-16270

UTAH UNIV., SALT LAKE CITY.
Vorticity amplification in nonorthogonal stagnation flow N90-16152

V

VIRGINIA POLYTECHNIC INST. AND STATE UNIV., BLACKSBURG.
Fatigue life estimates for helicopter loading spectra
[NASA-CR-181941] N90-16294

VIRGINIA UNIV., CHARLOTTESVILLE.
Q-2 and A dependence of delta (1232) electroexcitation in nuclei
[DE90-003470] N90-16492
Radiation modification of cometary materials: Laboratory simulations N90-16626

VOLKSWAGEN A.G., WOLFSBURG (GERMANY, F.R.).
Flow visualization using the laser light sheet method in vehicle aerodynamics and combustion chamber engineering N90-16246

W

WASHINGTON UNIV., SAINT LOUIS, MO.
Isotopic microanalysis of returned comet nucleus samples N90-16655

WASHINGTON UNIV., SEATTLE.
Ice floe identification in satellite images using mathematical morphology and clustering about principal curves
[AD-A213854] N90-16311
The effect of orographic forcing on the mean flow of the stratosphere N90-16367
Scanning tunneling microscope studies of surface defects
[AD-A214121] N90-16543

WEST VIRGINIA UNIV., MORGANTOWN.
Establishment of the Innovative Technology Utilization Center at West Virginia University
[PB90-114711] N90-16594

WESTFAELISCHE WILHELMS UNIV., MUENSTER (GERMANY, F.R.).
Thermal histories of the samples of two KOSI comet nucleus simulation experiments N90-16645

WESTINGHOUSE ELECTRIC CORP., BALTIMORE, MD.
Context dependent anti-aliasing image reconstruction N90-16209
Context dependent prediction and category encoding for DPCM image compression N90-16210

WESTINGHOUSE SAVANNAH RIVER CO., AIKEN, SC.
Examples of robots and teleoperators at the Savannah River Site
[DE90-004659] N90-16284

WISCONSIN UNIV., MADISON.
The Eighteenth Conference on Stochastic Processes and their Applications
[AD-A212301] N90-16010
Interdisciplinary research in viscoelasticity and rheology
[AD-A213630] N90-16145
Interstellar and cometary dust N90-16636

WOODS HOLE OCEANOGRAPHIC INST., MA.
Laboratory studies of isolated eddies in a rotating fluid
[AD-A213903] N90-16146

WORLD METEOROLOGICAL ORGANIZATION, GENEVA (SWITZERLAND).
Guide on the global observing system
[WMO-488-REV] N90-16385
World Weather Watch. Global observing system-satellite sub-system. Information on meteorological and other environmental satellites, second edition
[WMO-411-ED-2] N90-16386

WUERZBURG UNIV. (GERMANY, F.R.).
Forest mapping Nuerenberg German national forest with special emphasis on the spectral reflection behavior of pine trees N90-16328

Y

YORK UNIV., DOWNSVIEW (ONTARIO).
Electrochemical parameterization of metal complex redox potentials, using the ruthenium(III)/ruthenium(II) couple to generate a ligand electrochemical series
[AD-A214439] N90-16015

Z

ZEISS (CARL), OBERKOCHEN (GERMANY, F.R.).
Eurolaser. High power excimer laser: Optical crystals
[ETN-90-95901] N90-16558

Typical Contract Number Index Listing

AF-AFOSR-0039-88 ..... N90-10330

CONTRACT NUMBER — NASA ACCESSION NUMBER

Listings in this index are arranged alphanumerically by contract number. Under each contract number the NASA accession numbers denoting documents that have been produced as a result of research done under that contract are arranged in ascending order. The NASA accession number denotes the number by which the citation is identified.

AF PROJ. 2303 ..... N90-16485
AF PROJ. 2304 ..... N90-16145
AF PROJ. 2306 ..... N90-16035
AF PROJ. 2338 ..... N90-16500
AF PROJ. 6670 ..... N90-16383
AF-AFOSR-0020-83 ..... N90-16005
AF-AFOSR-0101-88 ..... N90-16377
AF-AFOSR-0191-87 ..... N90-16145
AF-AFOSR-0303-84 ..... N90-16035
AF-AFOSR-0386-87 ..... N90-16453
ARC-87-86/CO-9684 ..... N90-16594
ARPA ORDER 6631 ..... N90-16014
BMFT-FE-01-TQ-8602-AK/PA1 ..... N90-16398
BMFT-FKZ-13-EU-00018/2 ..... N90-16268
BMFT-ITR-8601-9 ..... N90-16161
BMFT-KF-10056 ..... N90-16265
BMFT-KF-10110 ..... N90-16265
BMFT-01-QV-094A N90-16162
BMFT-03-K-0503-3 ..... N90-16303
BMFT-13-EU-0022 ..... N90-16558
BMFT-13-EU-00214 ..... N90-16266
BMFT-514-8891-LFF-8440 ..... N90-16189
BMFT-523-4001-01QS87069 ..... N90-16314
BMVG-INSAN-I-0784-V-6385 ..... N90-16397
BMVG-INSAN-I-0784-V-6386 ..... N90-16397
DA PROJ. 1L1-61102-AH-45 ..... N90-15923
DA PROJ. 1L1-62209-A4-7A N90-16286
DA PROJ. 1L1-62211-A-47-AA N90-15882
DA PROJ. 3E1-6277-A-878 ..... N90-16390
DA PROJ. 793 ..... N90-16100
DAAB07-89-C-F404 ..... N90-16014
DAAG29-85-K-0188 ..... N90-16144
DAAL03-86-K-0032 ..... N90-16005
DAAL03-86-K-0059 ..... N90-16542
DAAL03-88-K-0195 ..... N90-16453
DAAL03-89-G-0029 ..... N90-16010
DAAL03-89-K-0017 ..... N90-16144
DAJA45-86-C-0010 ..... N90-16476
DAMD17-86-C-6260 ..... N90-16390
DE-AC02-76CH-00016 ..... N90-16067
N90-16075
N90-16262
N90-16288
N90-16480
N90-16501
N90-16649
DE-AC02-76CH-03000 ..... N90-16421
DE-AC02-83CH-10093 ..... N90-16340
N90-16352
DE-AC02-86ER-40296 ..... N90-16052
N90-16569
N90-16570
DE-AC03-76SF-00098 ..... N90-16018
N90-16084
N90-16121
N90-16123
N90-16139
N90-16343
N90-16484
N90-16506
N90-16523
N90-16530
N90-16536
N90-16551
N90-16587
N90-16588
N90-16680
N90-16681
DE-AC03-76SF-00515 ..... N90-16121
N90-16552
DE-AC03-89ER-51114 ..... N90-16092
N90-16509
N90-16524
DE-AC03-89ER-53277 ..... N90-16150
DE-AC04-76DP-00789 ..... N90-15973
N90-16005
N90-16066
N90-16069
N90-16079
N90-16082
N90-16094
N90-16129
N90-16131
N90-16276
N90-16278
N90-16279
N90-16282
N90-16287
N90-16298
N90-16344
N90-16345
N90-16364
N90-16418
N90-16439
N90-16471
N90-16496
N90-16528
N90-16555
N90-16592
DE-AC04-76DR-00789 ..... N90-16003
DE-AC04-86AL-33183 ..... N90-16200
DE-AC05-84OR-21400 ..... N90-16005
N90-16019
N90-16025
N90-16048
N90-16051
N90-16070
N90-16071
N90-16076
N90-16085
N90-16091
N90-16132
N90-16138
N90-16140
N90-16259
N90-16277
N90-16305
N90-16306
N90-16307
N90-16346
N90-16348
N90-16363
N90-16393
N90-16403
N90-16413
N90-16422
N90-16438
N90-16488
N90-16510
N90-16511
N90-16512
N90-16556
N90-16559
N90-16561
N90-16562
N90-16563
N90-16584
N90-16685
DE-AC05-84OS-21400 ..... N90-16006
DE-AC05-84OT-21400 ..... N90-16119
DE-AC06-76RL-01830 ..... N90-16041
N90-16042
N90-16046
N90-16047
N90-16049
N90-16068
N90-16120
DE-AC07-76ID-01570 ..... N90-16122
N90-16269
N90-16270
N90-16271
DE-AC07-84ID-12566 ..... N90-16077
DE-AC09-76SR-00001 ..... N90-16285
DE-AC09-89SR-18035 ..... N90-16284
DE-AC21-88MC-25170 ..... N90-16347
DE-AC22-87PC-90274 ..... N90-16525
DE-AC22-88PC-88853 ..... N90-16508
DE-AC22-88PC-88865 ..... N90-16142
N90-16149
DE-AI79-87BP-36246 ..... N90-16201
DE-FC05-85ER-25000 ..... N90-16421
DE-FC07-88ID-12691 ..... N90-16026
DE-FG02-84ER-13290 ..... N90-16040
DE-FG02-84ER-45100 ..... N90-16050
DE-FG02-85ER-13398 ..... N90-16151
DE-FG02-86ER-13503 ..... N90-16017
DE-FG02-86ER-45239 ..... N90-16027
DE-FG02-86ER-53214 ..... N90-16522
DE-FG02-87ER-13725 ..... N90-16566
DE-FG02-87ER-45297 ..... N90-16567
DE-FG02-88ER-40448 ..... N90-16493
DE-FG03-85SF-15927 ..... N90-16564
DE-FG05-86ER-13507 ..... N90-16065
DE-FG05-87ER-13675 ..... N90-16538
DE-FG05-89ER-40501 ..... N90-16492
DE-FG08-87NV-10672 ..... N90-16133
DFG-MO-416/3-3 ..... N90-16673
DFG-WA-424/3 ..... N90-16183
DFG-ZI/18-31-1 ..... N90-16244
DRET-86-34-810-00-470-75-01 ..... N90-16165
DRET-87-002-019 ..... N90-16156
FMV-FLYGFL-82260-88-061-73-001 ..... N90-16155
F04611-84-C-0060 ..... N90-15993
F04701-85-C-0086 ..... N90-16599
F04701-88-C-0089 ..... N90-16540
F19628-87-C-0182 ..... N90-16383
F30602-81-C-0206 ..... N90-16500
F30602-85-C-0024 ..... N90-16416
F33615-88-C-0540 ..... N90-16395
F49620-86-C-0061 ..... N90-16485
GA PROJ. 3466 ..... N90-16092
N90-16524
GA PROJ. 3468 ..... N90-16150
GRI-5083-260-0922 ..... N90-16012
GRI-5086-294-1292 ..... N90-16341
GRI-5087-260-1534 ..... N90-16011
MDA903-86-C-0341 ..... N90-16100
MOD-2040/411/XR-MAT N90-16301
MWMT-323-860-5200 ..... N90-16161
NAGW-749 ..... N90-16652
NAG1-270 ..... N90-16401
NAG1-660 ..... N90-15936
NAG1-668 ..... N90-16414
NAG1-822 ..... N90-16294
NAG1-870 ..... N90-16408
NAG3-476 ..... N90-16103
NAG3-773 ..... N90-16286
NAG3-806 ..... N90-16212
NAG5-916 ..... N90-16212
NAG5-945 ..... N90-16676
NAG5-966 ..... N90-16453
NAG8-081 ..... N90-16407
NAG9-47 ..... N90-16646
NAG9-106 ..... N90-16649
NASA ORDER C-32002-J N90-15985
NASW-4066 ..... N90-16607
NASW-4196 ..... N90-16644
NAS1-18000 ..... N90-16424
NAS1-18107 ..... N90-15893
N90-16444
NAS1-18458 ..... N90-15885
NAS1-18468 ..... N90-16215
NAS1-18584 ..... N90-15891
NAS1-18605 ..... N90-15893
N90-16401
NAS1-18664 ..... N90-16220
NAS1-18762 ..... N90-15937

NAS1-18816 ..... N90-16220
NAS3-25266 ..... N90-16072
NAS3-25356 ..... N90-15996
NAS5-28200 ..... N90-16449
NAS7-918 ..... N90-16104
N90-16110
N90-16124
N90-16312
N90-16391
N90-16675
NAS8-30490 ..... N90-15991
NAS9-17601 ..... N90-16202
N90-16203
NAS9-17900 ..... N90-16013
NCA-2372 ..... N90-16401
NCC2-371 ..... N90-16482
N90-16483
NCC8-16 ..... N90-16221
NGR-21-002-066 ..... N90-16448
NR-83-004 ..... N90-16146
NRA-88-ARC-1(BJY) N90-16072
NSC-76-0404-E002-17 ..... N90-16409
NSF ATM-87-09659 ..... N90-16358
NSF ATM-87-13212 ..... N90-16377
NSF ATM-88-13654 ..... N90-16116
NSF CCR-86-96134 ..... N90-16453
NSF CHE-86-10809 ..... N90-16482
NSF DCR-85-21398 ..... N90-16414
NSF DMC-86-10417 ..... N90-16441
NSF DMR-84-06896 ..... N90-16533
NSF DMR-84-15082 ..... N90-16005
NSF DMR-87-22880 ..... N90-16533
NSF DMS-85-12188 ..... N90-16480
NSF DMS-88-11863 ..... N90-16401
NSF EAR-84-15791 ..... N90-16646
NSF EAR-86-08299 ..... N90-16646
NSF EAR-86-18346 ..... N90-16649
NSF MEA-83-15117 ..... N90-16470
NSF OCE-84-16100 ..... N90-16146
NSF OCE-87-14842 ..... N90-16146
NSF PHY-82-15249 ..... N90-16575
N00014-80-C-0647 ..... N90-16453
N00014-84-G-0201 ..... N90-16015
N00014-84-K-0099 ..... N90-16455
N00014-84-K-0544 ..... N90-16543
N00014-86-K-0691 ..... N90-16401
N00014-87-K-0007 ..... N90-16146
N00014-87-K-0310 ..... N90-16453
N00014-88-K-0265 ..... N90-16311
N00014-88-K-0268 ..... N90-16544
N00014-88-K-0458 ..... N90-16453
N00014-89-C-0250 ..... N90-16225
N00014-89-J-1068 ..... N90-16034
N00014-89-J-1114 ..... N90-16311
N00014-89-J-1642 ..... N90-16458
N00014-89-J-1893 ..... N90-16062
RSRE-A94C/2711 ..... N90-16404
SRI PROJ. PYU-7142 ..... N90-16012
STPA-85-95-004-35 ..... N90-15887
STW-DLR-15-0120 ..... N90-16001
SWRI PROJ. 15-1062 ..... N90-16202
N90-16203
TUDLR-A2L3-81-04 ..... N90-16001
W-31-109-ENG-38 ..... N90-15995
N90-16020
N90-16036
N90-16047
N90-16055
N90-16350
N90-16353
N90-16361
N90-16362
N90-16526
N90-16534
N90-16539
N90-16547
N90-16550
N90-16568
W-7405-ENG-36 ..... N90-16037
N90-16056
N90-16057
N90-16058
N90-16143
N90-16260
N90-16283
N90-16297
N90-16342
N90-16366
N90-16412
N90-16419
N90-16420
N90-16459
N90-16463
N90-16491
N90-16507
N90-16520
N90-16521
N90-16527
N90-16529
N90-16533
N90-16537
N90-16560
N90-16565
N90-16591
N90-16598
N90-16600
N90-16601
N90-16665
W-7405-ENG-48 ..... N90-16064
N90-16095
N90-16121
N90-16130
N90-16440
N90-16489
N90-16548
N90-16549
N90-16666
N90-16667
N90-16674
N90-16682
N90-16683
149-22-03-01 ..... N90-16312
505-61-31 ..... N90-16399
N90-16400
505-61-51 ..... N90-15938
505-61-51-10 ..... N90-15882
505-62-OK N90-15923
505-62-3B N90-15964
505-62-71-01 ..... N90-15884
505-63-01-05 ..... N90-16294
505-63-01-10 ..... N90-16424
505-63-11 ..... N90-16008
505-63-21 ..... N90-15892
505-63-21-01 ..... N90-15886
505-63-21-02 ..... N90-15894
505-63-41-02 ..... N90-15902
505-63-51 ..... N90-16286
505-67-21 ..... N90-15898
505-68-11 ..... N90-15965
505-80-21-06 ..... N90-15885
505-90-21-01 ..... N90-15893
N90-16401
506-42-31 ..... N90-15992
506-43-41-02 ..... N90-16292
506-48-4A N90-15996
506-49-11-01 ..... N90-15890
N90-15937
522-09-01 ..... N90-16004
549-03-61 ..... N90-16423
553-13-00 ..... N90-16053
585-02-31-01 ..... N90-16293
650-60-23 ..... N90-15983
672-90-20-03 ..... N90-16313
694-03-03 ..... N90-16087
763-01-46 ..... N90-16072

Typical Report Number Index Listing

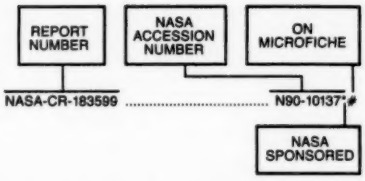

Listings in this index are arranged alphanumerically by report number. The NASA accession number denotes the number by which the citation is identified. An asterisk (*) indicates that the item is a NASA report. A pound sign (#) indicates that the item is available on microfiche.

A-89085 ..... N90-15898* #
A-89212 ..... N90-16399* #
A-89220 ..... N90-15938* #
A-89264 ..... N90-16313* #
A-90011 ..... N90-16400* #
A-90015 ..... N90-16423* #

AAMRL-TR-89-029 ..... N90-16395 #

AD-A211799 ..... N90-16100 #
AD-A212301 ..... N90-16010 #
AD-A212785 ..... N90-16054 #
AD-A213462 ..... N90-15993 #
AD-A213480 ..... N90-16390 #
AD-A213584 ..... N90-16144 #
AD-A213630 ..... N90-16145 #
AD-A213844 ..... N90-16295 #
AD-A213846 ..... N90-16374 #
AD-A213847 ..... N90-16375 #
AD-A213854 ..... N90-16311 #
AD-A213855 ..... N90-16540 #
AD-A213903 ..... N90-16146 #
AD-A213939 ..... N90-16383 #
AD-A214026 ..... N90-16107 #
AD-A214029 ..... N90-16225 #
AD-A214050 ..... N90-16014 #
AD-A214096 ..... N90-16542 #
AD-A214104 ..... N90-16458 #
AD-A214107 ..... N90-16032 #
AD-A214108 ..... N90-16033 #
AD-A214112 ..... N90-16455 #
AD-A214121 ..... N90-16543 #
AD-A214132 ..... N90-16544 #
AD-A214160 ..... N90-16476 #
AD-A214184 ..... N90-16414* #
AD-A214262 ..... N90-16402 #
AD-A214267 ..... N90-16034 #
AD-A214279 ..... N90-16415 #
AD-A214280 ..... N90-16395 #
AD-A214424 ..... N90-16035 #
AD-A214425 ..... N90-16485 #
AD-A214432 ..... N90-16108 #
AD-A214434 ..... N90-16392 #
AD-A214439 ..... N90-16015 #
AD-A214444 ..... N90-16062 #
AD-A214446 ..... N90-16500 #
AD-A214447 ..... N90-16416 #

AD-D014233 ..... N90-16394 #
AD-D014249 ..... N90-16499 #
AD-D014250 ..... N90-16125 #
AD-D014253 ..... N90-16059 #
AD-D014258 ..... N90-16147 #
AD-D014259 ..... N90-16273 #
AD-D014260 ..... N90-16060 #
AD-D014262 ..... N90-16126 #
AD-D014263 ..... N90-16541 #
AD-D014264 ..... N90-16479 #
AD-D014265 ..... N90-16274 #
AD-D014268 ..... N90-16275 #
AD-D014269 ..... N90-16127 #

AD-D014270 ..... N90-16028 #
AD-D014271 ..... N90-16105 #
AD-D014277 ..... N90-16061 #
AD-D014278 ..... N90-16029 #
AD-D014279 ..... N90-16475 #
AD-D014280 ..... N90-16030 #
AD-D014281 ..... N90-16083 #
AD-D014282 ..... N90-16106 #
AD-D014283 ..... N90-16031 #
AD-D014284 ..... N90-15918 #
AD-D014286 ..... N90-15984 #
AD-D014287 ..... N90-15994 #
AD-D014288 ..... N90-16296 #
AD-D014291 ..... N90-16263 #
AD-D014294 ..... N90-16128
AD-D014296 ..... N90-16226
AD-D014297 ..... N90-16227

AERONOMICA-ACTA-A-350-1989 ..... N90-16379

AFAL-TR-88-105 ..... N90-15993 #

AFGL-TR-89-0011 ..... N90-16383 #

AFIT/GAE/AA/88D-08 ..... N90-16295 #

AFIT/GE/ENG/89D-40 ..... N90-16402 #

AFOSR-89-1274TR ..... N90-16145 #
AFOSR-89-1340TR ..... N90-16485 #
AFOSR-89-1356TR ..... N90-16035 #

AGARD-AR-276 ..... N90-15899 #

AGARD-CP-436 ..... N90-15924 #

AGARD-INDEX-86-88 ..... N90-16585 #

AGARD-R-771 ..... N90-15904 #
AGARD-R-774 ..... N90-15939 #

AIAA-89-2829 ..... N90-15992* #
AIAA-90-0488 ..... N90-15965* #
AIAA-90-0850 ..... N90-15983* #

ANL/ES-163 ..... N90-16362 #

ANL/MHD-89/1 ..... N90-16526 #

ARI-RR-1524 ..... N90-16100 #

ARO-23323.2-EL ..... N90-16542 #
ARO-26196.1-MA-CF ..... N90-16010 #
ARO-26616.6-MA ..... N90-16144 #

AVSCOM-TM-89-B-010 ..... N90-15882* #
AVSCOM-TM-89-C-006 ..... N90-16286* #
AVSCOM-TM-89-C-010 ..... N90-15923* #

BBC-RD-1989/5 ..... N90-16098
BBC-RD-1989/6 ..... N90-16097
BBC-RD-1989/7 ..... N90-16096

BMVG-FBWM-89-5 ..... N90-16397

BNL-42519 ..... N90-16501 #
BNL-43410 ..... N90-16075 #
BNL-43452 ..... N90-16067 #
BNL-43465 ..... N90-16262 #
BNL-43477 ..... N90-16480 #
BNL-43482 ..... N90-16288 #

BONN-IR-89-16 ..... N90-16117 #

BR109681 ..... N90-16396 #
BR109992 ..... N90-16427 #
BR110021 ..... N90-16426 #
BR110081 ..... N90-15972 #
BR110168 ..... N90-15896 #
BR110400 ..... N90-15920 #
BR110401 ..... N90-15919 #
BR110402 ..... N90-15921
BR110495 ..... N90-16301 #
BR110498 ..... N90-15888 #
BR110503 ..... N90-16043 #
BR110583 ..... N90-16430 #
BR110718 ..... N90-15997 #
BR110738 ..... N90-16433 #
BR110742 ..... N90-15917 #
BR110773 ..... N90-16300 #
BR110853 ..... N90-16428 #
BR110918 ..... N90-15971 #
BR110949 ..... N90-15922 #
BR111059 ..... N90-16502 #
BR111060 ..... N90-15900 #
BR111061 ..... N90-16425 #
BR111532 ..... N90-16429 #
BR111536 ..... N90-16404 #
BR111545 ..... N90-16432 #
BR111665 ..... N90-16431 #

CBPF-NF-059/88 ..... N90-16662 #
CBPF-NF-064/88 ..... N90-16663 #

CERT-1/2313/MES ..... N90-16156 #

CNES-NT-122-PT-1/2 ..... N90-16405 #

CONF-890304-38 ..... N90-16285 #
CONF-890618-5 ..... N90-16536 #
CONF-890665-52 ..... N90-16130 #
CONF-890692-23 ..... N90-16361 #
CONF-890701-22 ..... N90-16570 #
CONF-890701-26 ..... N90-16052 #
CONF-890703-25 ..... N90-16123 #
CONF-890803-22 ..... N90-16121 #
CONF-890836-20 ..... N90-16501 #
CONF-890836-22 ..... N90-16506 #
CONF-890933-5 ..... N90-16560 #
CONF-890946-3 ..... N90-16551 #
CONF-890971-4 ..... N90-16534 #
CONF-891007-92 ..... N90-16092 #
CONF-891007-108 ..... N90-16524 #
CONF-891024-7 ..... N90-16066 #
CONF-891031-9 ..... N90-16343 #
CONF-891087-12 ..... N90-16284 #
CONF-891094-10 ..... N90-16419 #
CONF-891117-2 ..... N90-16533 #
CONF-891117-12 ..... N90-16068 #
CONF-891119-10 ..... N90-16537 #
CONF-891119-12 ..... N90-16057 #
CONF-891119-12 ..... N90-16058 #
CONF-891119-13 ..... N90-16056 #
CONF-891119-18 ..... N90-16547 #
CONF-891119-25 ..... N90-16539 #
CONF-891119-30 ..... N90-16020 #
CONF-891119-34 ..... N90-16555 #
CONF-891119-40 ..... N90-16069 #
CONF-891119-41 ..... N90-16556 #
CONF-891119-42 ..... N90-16562 #
CONF-891119-43 ..... N90-16561 #
CONF-891119-53 ..... N90-16565 #
CONF-891119-55 ..... N90-16568 #
CONF-891119-59 ..... N90-16079 #
CONF-891132-SUMM ..... N90-16120 #
CONF-891136-1 ..... N90-16528 #
CONF-891181-1 ..... N90-16563 #
CONF-891182-1 ..... N90-16507 #
CONF-891204-8 ..... N90-16041 #
CONF-891204-9 ..... N90-16042 #
CONF-891204-10 ..... N90-16046 #
CONF-891204-11 ..... N90-16047 #
CONF-891208-26 ..... N90-16094 #
CONF-891210-2 ..... N90-16364 #
CONF-891214-12 ..... N90-16282 #
CONF-891214-13 ..... N90-15973 #
CONF-891214-14 ..... N90-16278 #
CONF-900108-1 ..... N90-16459 #
CONF-900109-2 ..... N90-16342 #
CONF-900109-4 ..... N90-16496* #
CONF-900109-12 ..... N90-15995 #
CONF-900109-13 ..... N90-16036 #
CONF-900122-1 ..... N90-16600 #
CONF-900122-2 ..... N90-16601 #
CONF-900122-3 ..... N90-16665 #
CONF-900122-5 ..... N90-16681* #

CONF-900128-1 ..... N90-16548 #
CONF-900128-2 ..... N90-16549 #
CONF-900129-2 ..... N90-16680 #
CONF-900129-3 ..... N90-16683* #
CONF-900129-4-2 ..... N90-16682 #
CONF-900136-3 ..... N90-16344 #
CONF-900136-4 ..... N90-16345 #
CONF-900137-1 ..... N90-16591 #
CONF-900138-2 ..... N90-16287 #
CONF-900138-3 ..... N90-16129 #
CONF-900139-1 ..... N90-16463 #
CONF-900139-2 ..... N90-16297 #
CONF-900140-1 ..... N90-16131 #
CONF-900145-1 ..... N90-16298 #
CONF-900146-1 ..... N90-16418 #
CONF-900147-1 ..... N90-16488 #
CONF-900148-1 ..... N90-16471 #
CONF-900202-3 ..... N90-16138 #
CONF-900202-4 ..... N90-16140 #
CONF-900213-1 ..... N90-16005 #
CONF-900214-1 ..... N90-16592 #
CONF-900215-1 ..... N90-16584 #
CONF-900216-1 ..... N90-16305 #
CONF-900216-2 ..... N90-16685 #
CONF-900228-1 ..... N90-16259 #
CONF-900250-1 ..... N90-16439 #
CONF-8807191 ..... N90-16577 #
CONF-8808122-18 ..... N90-16288 #
CONF-8808196-5 ..... N90-16492 #
CONF-8809322-2 ..... N90-16051 #
CONF-8810363 ..... N90-16704 #
CONF-8811270-1 ..... N90-16530 #
CONF-8812116 ..... N90-16519 #
CONF-8903179-1 ..... N90-16480 #
CONF-8903180-1 ..... N90-16150 #
CONF-8906239-2 ..... N90-16143 #
CONF-8906257-1 ..... N90-16674 #
CONF-8907103-EXC ..... N90-16366 #
CONF-8907111-1 ..... N90-16075 #
CONF-8908116-2 ..... N90-16588 #
CONF-8908129-4 ..... N90-16523 #
CONF-8908163-1 ..... N90-16200 #
CONF-8908165-3 ..... N90-16067 #
CONF-8908186-1 ..... N90-16091 #
CONF-8908189-1 ..... N90-16421 #
CONF-8908191-2 ..... N90-16550 #
CONF-8909233-2 ..... N90-16552 #
CONF-8909273-1 ..... N90-16491 #
CONF-8909275-1 ..... N90-16667 #
CONF-8910107-5 ..... N90-16564 #
CONF-8910107-7 ..... N90-16049 #
CONF-8910220-2 ..... N90-16440 #
CONF-8910224-1 ..... N90-16082 #
CONF-8910295-1 ..... N90-16587 #
CONF-8910301-1 ..... N90-16055 #
CONF-8910308-1 ..... N90-16598 #
CONF-8910318-1 ..... N90-16095 #
CONF-8910320-1 ..... N90-16666 #
CONF-8911125-2 ..... N90-16438 #
CONF-8911130-4 ..... N90-16520 #
CONF-8911130-7 ..... N90-16527 #
CONF-8911130-8 ..... N90-16283 #
CONF-8911130-9 ..... N90-16260 #
CONF-8911130-10 ..... N90-16529 #
CONF-8911138-1 ..... N90-16521 #
CONF-8911140-1 ..... N90-16420 #
CONF-8911148-1-VUGRAPHS ..... N90-16393 #
CONF-8911151-1 ..... N90-16350 #
CONF-8911151-2 ..... N90-16353 #

CRIE-T-10 ..... N90-16387 #
CRIE-T-88010 ..... N90-16137 #
CRIE-T-88014 ..... N90-16290 #
CRIE-T-88079 ..... N90-16118 #
CRIE-T-88092 ..... N90-16388 #

CRIE-W-88014 ..... N90-16078 #

CRIF-MC-85 ..... N90-16435 #

DERAT-32/5025-20-PT-2 ..... N90-15887 #

DE89-009421 ..... N90-16340 #
DE89-009456 ..... N90-16352 #
DE89-012610 ..... N90-16459 #
DE89-014631 ..... N90-16592 #
DE89-014768 ..... N90-16005 #
DE89-014817 ..... N90-16342 #
DE89-014967 ..... N90-16496* #
DE89-015366 ..... N90-16305 #
DE89-015858 ..... N90-16584 #
DE89-016219 ..... N90-16685 #
DE89-016610 ..... N90-16507 #
DE89-016780 ..... N90-16600 #
DE89-016781 ..... N90-16601 #
DE89-016837 ..... N90-16120 #
DE89-618837 ..... N90-16662 #
DE89-618838 ..... N90-16663 #
DE89-635711 ..... N90-16417 #
DE89-635712 ..... N90-16460 #
DE89-635721 ..... N90-16571 #
DE89-635767 ..... N90-16063 #
DE89-635768 ..... N90-16016 #
DE89-635786 ..... N90-16545 #
DE89-635903 ..... N90-16572 #
DE89-635909 ..... N90-16532 #
DE89-635990 ..... N90-16486 #
DE89-636072 ..... N90-16487 #
DE89-636239 ..... N90-16546 #
DE89-636435 ..... N90-16461 #
DE89-636436 ..... N90-16148 #
DE89-636437 ..... N90-16462 #
DE89-760006 ..... N90-16704 #
DE89-900733 ..... N90-16535 #
DE90-000132 ..... N90-16680 #
DE90-000144 ..... N90-16142 #
DE90-000541 ..... N90-16533 #
DE90-000549 ..... N90-16530 #
DE90-000609 ..... N90-16665 #
DE90-000686 ..... N90-16591 #
DE90-000942 ..... N90-16121 #
DE90-001457 ..... N90-16149 #
DE90-001466 ..... N90-16508 #
DE90-001572 ..... N90-16484 #
DE90-001988 ..... N90-16534 #
DE90-002023 ..... N90-16269 #
DE90-002049 ..... N90-16122 #
DE90-002090 ..... N90-16270 #
DE90-002119 ..... N90-16343 #
DE90-002216 ..... N90-16361 #
DE90-002218 ..... N90-16271 #
DE90-002274 ..... N90-15995 #
DE90-002276 ..... N90-16036 #
DE90-002394 ..... N90-16463 #
DE90-002395 ..... N90-16297 #
DE90-002582 ..... N90-16287 #
DE90-002645 ..... N90-16082 #
DE90-002683 ..... N90-16681* #
DE90-002709 ..... N90-16488 #
DE90-002834 ..... N90-16344 #
DE90-002835 ..... N90-16345 #
DE90-002849 ..... N90-16055 #
DE90-002902 ..... N90-16418 #
DE90-002990 ..... N90-16129 #
DE90-003022 ..... N90-16064 #
DE90-003026 ..... N90-16130 #
DE90-003057 ..... N90-16298 #
DE90-003106 ..... N90-16123 #
DE90-003108 ..... N90-16536 #
DE90-003114 ..... N90-16587 #
DE90-003117 ..... N90-16588 #
DE90-003161 ..... N90-16471 #
DE90-003173 ..... N90-16027 #
DE90-003213 ..... N90-16598 #
DE90-003218 ..... N90-16520 #
DE90-003221 ..... N90-16521 #
DE90-003223 ..... N90-16491 #
DE90-003234 ..... N90-16538 #
DE90-003290 ..... N90-16092 #
DE90-003306 ..... N90-16277 #
DE90-003341 ..... N90-16439 #
DE90-003363 ..... N90-16366 #
DE90-003367 ..... N90-16537 #
DE90-003382 ..... N90-16119 #
DE90-003391 ..... N90-16419 #
DE90-003393 ..... N90-16420 #
DE90-003395 ..... N90-16527 #
DE90-003420 ..... N90-16133 #
DE90-003453 ..... N90-16440 #
DE90-003470 ..... N90-16492 #
DE90-003486 ..... N90-16131 #
DE90-003500 ..... N90-16200 #
DE90-003517 ..... N90-16085 #
DE90-003551 ..... N90-16350 #
DE90-003552 ..... N90-16353 #
DE90-003562 ..... N90-16539 #
DE90-003564 ..... N90-16547 #
DE90-003594 ..... N90-16666 #
DE90-003595 ..... N90-16682 #
DE90-003597 ..... N90-16667 #
DE90-003602 ..... N90-16683* #
DE90-003618 ..... N90-16548 #
DE90-003620 ..... N90-16549 #
DE90-003622 ..... N90-16674 #
DE90-003642 ..... N90-16501 #
DE90-003647 ..... N90-16075 #
DE90-003648 ..... N90-16412 #
DE90-003650 ..... N90-16056 #
DE90-003651 ..... N90-16057 #
DE90-003652 ..... N90-16283 #
DE90-003653 ..... N90-16143 #
DE90-003658 ..... N90-16058 #
DE90-003661 ..... N90-16560 #
DE90-003682 ..... N90-16438 #
DE90-003683 ..... N90-16091 #
DE90-003697 ..... N90-16259 #
DE90-003698 ..... N90-16413 #
DE90-003699 ..... N90-16262 #
DE90-003707 ..... N90-16393 #
DE90-003718 ..... N90-16138 #
DE90-003788 ..... N90-16020 #
DE90-003794 ..... N90-16550 #
DE90-003904 ..... N90-16017 #
DE90-003907 ..... N90-16065 #
DE90-003911 ..... N90-16040 #
DE90-003912 ..... N90-16522 #
DE90-003919 ..... N90-16095 #
DE90-003935 ..... N90-16094 #
DE90-003936 ..... N90-16364 #
DE90-003937 ..... N90-16084 #
DE90-003941 ..... N90-16421 #
DE90-003942 ..... N90-16509 #
DE90-003948 ..... N90-16066 #
DE90-003954 ..... N90-16067 #
DE90-003956 ..... N90-16480 #
DE90-003958 ..... N90-16288 #
DE90-003976 ..... N90-16076 #
DE90-003978 ..... N90-16559 #
DE90-003980 ..... N90-16555 #
DE90-003985 ..... N90-16346 #
DE90-003990 ..... N90-16489* #
DE90-003991 ..... N90-16018 #
DE90-004002 ..... N90-16025 #
DE90-004015 ..... N90-16493 #
DE90-004016 ..... N90-16347 #
DE90-004027 ..... N90-16523 #
DE90-004028 ..... N90-16551 #
DE90-004030 ..... N90-16506 #
DE90-004040 ..... N90-16139 #
DE90-004079 ..... N90-16026 #
DE90-004086 ..... N90-16077 #
DE90-004087 ..... N90-16278 #
DE90-004088 ..... N90-15973 #
DE90-004089 ..... N90-16282 #
DE90-004096 ..... N90-16524 #
DE90-004103 ..... N90-16150 #
DE90-004111 ..... N90-16068 #
DE90-004112 ..... N90-16041 #
DE90-004113 ..... N90-16042 #
DE90-004120 ..... N90-16306 #
DE90-004125 ..... N90-16006 #
DE90-004141 ..... N90-16525 #
DE90-004185 ..... N90-16593 #
DE90-004196 ..... N90-16528 #
DE90-004198 ..... N90-16069 #
DE90-004242 ..... N90-16561 #
DE90-004243 ..... N90-16140 #
DE90-004245 ..... N90-16562 #
DE90-004290 ..... N90-16151 #
DE90-004293 ..... N90-16307 #
DE90-004297 ..... N90-16556 #
DE90-004299 ..... N90-16563 #
DE90-004348 ..... N90-16003 #
DE90-004351 ..... N90-16048 #
DE90-004367 ..... N90-16362 #
DE90-004371 ..... N90-16070 #
DE90-004380 ..... N90-16510 #
DE90-004381 ..... N90-16511 #
DE90-004386 ..... N90-16019 #
DE90-004390 ..... N90-16403 #
DE90-004392 ..... N90-16132 #
DE90-004400 ..... N90-16071 #
DE90-004401 ..... N90-16512 #
DE90-004404 ..... N90-16363 #
DE90-004409 ..... N90-16422 #
DE90-004410 ..... N90-16348 #
DE90-004423 ..... N90-16037 #
DE90-004425 ..... N90-16276 #
DE90-004432 ..... N90-16552 #
DE90-004453 ..... N90-16526 #
DE90-004519 ..... N90-16046 #
DE90-004521 ..... N90-16047 #
DE90-004541 ..... N90-16201 #
DE90-004570 ..... N90-16564 #
DE90-004659 ..... N90-16284 #
DE90-004661 ..... N90-16285 #
DE90-004681 ..... N90-16049 #
DE90-004839 ..... N90-16565 #
DE90-004849 ..... N90-16050 #
DE90-004850 ..... N90-16566 #
DE90-004851 ..... N90-16567 #
DE90-004863 ..... N90-16260 #
DE90-004873 ..... N90-16529 #
DE90-004883 ..... N90-16568 #
DE90-004904 ..... N90-16569 #
DE90-004921 ..... N90-16051 #
DE90-004983 ..... N90-16279 #
DE90-004993 ..... N90-16309 #

DE90-005387 N90-16570 #
DE90-005391 N90-16052 #
DE90-005406 N90-16079 #
DE90-600720 N90-16464 #
DE90-600730 N90-16573 #
DE90-600732 N90-16574 #
DE90-600735 N90-16456 #
DE90-600737 N90-16473 #
DE90-600742 N90-16465 #
DE90-600754 N90-16668 #
DE90-600756 N90-16376 #
DE90-600758 N90-16457 #
DE90-600759 N90-16575 #
DE90-600760 N90-16576 #
DE90-600984 N90-16109 #
DE90-601096 N90-16513 #
DE90-601098 N90-16514 #
DE90-601827 N90-16577 #
DE90-602350 N90-16038 #
DE90-602367 N90-16039 #
DE90-603368 N90-16474 #
DE90-702472 N90-16290 #
DE90-702474 N90-16137 #
DE90-702485 N90-16387 #
DE90-702648 N90-16354 #
DE90-719505 N90-16553 #
DE90-719507 N90-16578 #
DE90-719511 N90-16579 #
DE90-719519 N90-16515 #
DE90-719521 N90-16516 #
DE90-719529 N90-16517 #
DE90-719546 N90-16349 #
DE90-719556 N90-16580 #
DE90-719557 N90-16477 #
DE90-719559 N90-16490 #
DE90-719560 N90-16384 #
DE90-719573 N90-16518 #
DE90-719574 N90-16554 #
DE90-719575 N90-16581 #
DE90-719578 N90-16582 #
DE90-719706 N90-16519 #
DE90-728179 N90-16093 #
DE90-728212 N90-16299 #
DE90-734934 N90-16076 #
DE90-734950 N90-16118 #
DE90-734989 N90-16388 #

DFVLR-FB-88-17 N90-15889 #

DFVLR-MITT-88-11 N90-15963 #
DFVLR-MITT-88-29 N90-16112 #
DFVLR-MITT-89-03 N90-16111 #
DFVLR-MITT-89-04 N90-16318 #

DGLR-PAPERS-88-04 N90-16236 #
DGLR-PAPERS-88-05 N90-16169 #

DNW-WTI-88.038 N90-16245 #
DNW-WTI-88.039 N90-16255 #

DOE/BP-36246/1 N90-16201 #

DOE/ER-0430 N90-16309 #
DOE/ER-13290/5 N90-16040 #
DOE/ER-13398/11 N90-16151 #
DOE/ER-13503/3 N90-16017 #
DOE/ER-13507/5 N90-16065 #
DOE/ER-13675/3 N90-16538 #
DOE/ER-13725/3 N90-16566 #
DOE/ER-40296/T1 N90-16569 #
DOE/ER-40448/2 N90-16493 #
DOE/ER-45100/13 N90-16050 #
DOE/ER-45239/T1 N90-16027 #
DOE/ER-45297/12 N90-16567 #
DOE/ER-53214/1 N90-16522 #

DOE/ID-10219 N90-16269 #
DOE/ID-10243 N90-16122 #
DOE/ID-10252 N90-16271 #
DOE/ID-12566/3 N90-16077 #
DOE/ID-12691/1 N90-16026 #

DOE/MA-0364 N90-16593 #

DOE/MC-25170/2779 N90-16347 #

DOE/NV-10672/1 N90-16133 #

DOE/PC-88653/T1 N90-16508 #
DOE/PC-88865/T1 N90-16142 #
DOE/PC-88865/T2 N90-16149 #
DOE/PC-90274/T7 N90-16525 #

DP-MS-88-94 N90-16285 #

DTRC/SME-89/27 N90-16032 #

DTRC/SME-89/025 N90-16107 #

E-4786 N90-16087* #
E-4954 N90-16072* #
E-5058 N90-16286* #
E-5104 N90-15992* #
E-5177 N90-15983* #
E-5212 N90-15923* #
E-5265 N90-15964* #
E-5269 N90-16008* #
E-5270 N90-15965* #
E-5286 N90-16053* #

EGG-EP-8581 N90-16270 #

EPA/600/D-89/125 N90-16360 #
EPA/600/D-89/126 N90-16356 #

ESA-BR-43 N90-16706 #
ESA-BR-60 N90-15999 #
ESA-BR-62 N90-15989 #

ESA-SP-300 N90-15974 #
ESA-SP-1087 N90-16590 #
ESA-SP-1114 N90-16672 #
ESA-SP-1116 N90-15998 #
ESA-SP-1117 N90-15968 #
ESA-SP-1118 N90-16088 #
ESA-SP-1120 N90-16089 #

ESA-STR-228 N90-16113 #

ESA-TT-1118 N90-16557 #
ESA-TT-1129 N90-15889 #
ESA-TT-1145 N90-15963 #
ESA-TT-1155 N90-16111 #
ESA-TT-1164 N90-16112 #

ESL-TR-719630-3 N90-16103* #

ETCA-89-R-073 N90-16045 #

ETEC-89-7 N90-15985* #

ETN-90-95007 N90-16236 #
ETN-90-95008 N90-16169 #
ETN-90-95026 N90-16156 #
ETN-90-95029 N90-16157 #
ETN-90-95032 N90-16232 #
ETN-90-95214 N90-16289 #
ETN-90-95270 N90-16466 #
ETN-90-95272 N90-16467 #
ETN-90-95296 N90-16318 #
ETN-90-95326 N90-16044 #
ETN-90-95332 N90-16494 #
ETN-90-95346 N90-16114
ETN-90-95348 N90-16314
ETN-90-95350 N90-16265 #
ETN-90-95352 N90-16315 #
ETN-90-95355 N90-15990 #
ETN-90-95356 N90-15969 #
ETN-90-95514 N90-16073 #
ETN-90-95530 N90-16115 #
ETN-90-95693 N90-16134 #
ETN-90-95694 N90-16233 #
ETN-90-95697 N90-16135 #
ETN-90-95704 N90-16434 #
ETN-90-95706 N90-16136 #
ETN-90-95707 N90-16074 #
ETN-90-95755 N90-16385 #
ETN-90-95759 N90-16386 #
ETN-90-95816 N90-16495 #
ETN-90-95821 N90-15970 #
ETN-90-95854 N90-16116
ETN-90-95856 N90-16234
ETN-90-95862 N90-15901 #
ETN-90-95872 N90-16397
ETN-90-95873 N90-16302
ETN-90-95876 N90-16086 #
ETN-90-95877 N90-16158 #
ETN-90-95878 N90-16159 #
ETN-90-95879 N90-16160 #
ETN-90-95881 N90-16161
ETN-90-95882 N90-16468
ETN-90-95883 N90-16316
ETN-90-95886 N90-16317
ETN-90-95888 N90-16469 #
ETN-90-95899 N90-16266 #
ETN-90-95901 N90-16558 #
ETN-90-95905 N90-16398 #
ETN-90-95906 N90-16162 #
ETN-90-95908 N90-16303 #
ETN-90-95910 N90-16117 #
ETN-90-95911 N90-16163 #
ETN-90-95912 N90-16164 #
ETN-90-95927 N90-16045 #

ETN-90-95929 N90-16165 #
ETN-90-95998 N90-16000 #
ETN-90-96000 N90-16001 #
ETN-90-96002 N90-16351
ETN-90-96029 N90-16435 #
ETN-90-96034 N90-16379
ETN-90-96035 N90-16281 #
ETN-90-96036 N90-16022 #
ETN-90-96037 N90-16505 #
ETN-90-96038 N90-16235 #
ETN-90-96039 N90-16436 #
ETN-90-96040 N90-16023 #
ETN-90-96041 N90-16437 #
ETN-90-96042 N90-16405 #
ETN-90-96043 N90-16380 #
ETN-90-96044 N90-16304 #
ETN-90-96045 N90-16406 #
ETN-90-96046 N90-16673
ETN-90-96047 N90-16605
ETN-90-96048 N90-16606
ETN-90-96055 N90-16267 #
ETN-90-96061 N90-16268 #
ETN-90-96063 N90-16090 #
ETN-90-96064 N90-16166 #
ETN-90-96065 N90-16167 #
ETN-90-96066 N90-16168 #
ETN-90-96071 N90-16365 #
ETN-90-96073 N90-16024 #
ETN-90-96083 N90-15887 #
ETN-90-96087 N90-16153 #
ETN-90-96092 N90-16021 #
ETN-90-96096 N90-16154 #
ETN-90-96112 N90-16425 #
ETN-90-96113 N90-16426 #
ETN-90-96114 N90-15972 #
ETN-90-96115 N90-16427 #
ETN-90-96116 N90-15896 #
ETN-90-96117 N90-16428 #
ETN-90-96119 N90-15900 #
ETN-90-96120 N90-16502 #
ETN-90-96121 N90-16429 #
ETN-90-96122 N90-16430 #
ETN-90-96123 N90-16431 #
ETN-90-96124 N90-16432 #
ETN-90-96125 N90-16404 #
ETN-90-96126 N90-15919 #
ETN-90-96127 N90-15920 #
ETN-90-96128 N90-15921
ETN-90-96129 N90-15922 #
ETN-90-96130 N90-15917 #
ETN-90-96131 N90-16396 #
ETN-90-96134 N90-15971 #
ETN-90-96135 N90-16043 #
ETN-90-96136 N90-16300 #
ETN-90-96137 N90-15888 #
ETN-90-96138 N90-16301 #
ETN-90-96141 N90-15997 #
ETN-90-96144 N90-16264 #
ETN-90-96145 N90-16503 #
ETN-90-96146 N90-16228 #
ETN-90-96148 N90-15897
ETN-90-96149 N90-16155 #
ETN-90-96150 N90-16602 #
ETN-90-96151 N90-16677 #
ETN-90-96152 N90-16669 #
ETN-90-96153 N90-16377 #
ETN-90-96155 N90-16678 #
ETN-90-96156 N90-16679 #
ETN-90-96157 N90-16229 #
ETN-90-96158 N90-16378 #
ETN-90-96160 N90-16684 #
ETN-90-96165 N90-16603 #
ETN-90-96166 N90-16670 #
ETN-90-96167 N90-15986 #
ETN-90-96168 N90-16504 #
ETN-90-96169 N90-15987 #
ETN-90-96174 N90-15988 #
ETN-90-96175 N90-16230 #
ETN-90-96176 N90-16231 #
ETN-90-96177 N90-16671 #
ETN-90-96178 N90-16705 #
ETN-90-96179 N90-16604 #
ETN-90-96188 N90-16557 #
ETN-90-96189 N90-15889 #
ETN-90-96190 N90-15963 #
ETN-90-96191 N90-16111 #
ETN-90-96192 N90-16112 #
ETN-90-96196 N90-15974 #
ETN-90-96198 N90-16672 #
ETN-90-96199 N90-15998 #
ETN-90-96200 N90-15968 #
ETN-90-96201 N90-16088 #
ETN-90-96202 N90-16089 #
ETN-90-96203 N90-16113 #
ETN-90-96204 N90-16706 #
ETN-90-96205 N90-15999 #

ETN-90-96206 ..... N90-15989 #
ETN-90-96210 ..... N90-16433 #

FFA-TN-1989-40 ..... N90-16155 #

FIM-195 ..... N90-16314

FNAL/C-89/237-T ..... N90-16421 #

FSGTR-PNW-242 ..... N90-16382 #

FSU-SCRI-89-147 ..... N90-16421 #

GA-A-19745 ..... N90-16524 #
GA-A-19747 ..... N90-16092 #
GA-A-19794 ..... N90-16150 #
GA-A-19803 ..... N90-16509 #

GKSS-89/E/24 ..... N90-16365 #

GMD-389 ..... N90-16181
GMD-391 ..... N90-16468

GRI-89/0036 ..... N90-16011 #
GRI-89/0127 ..... N90-16012 #
GRI-89/0154 ..... N90-16341 #

H-1567 ..... N90-16004* #

IC-88/418 ..... N90-16457 #
IC-89/45 ..... N90-16532 #
IC-89/60 ..... N90-16487 #
IC-89/61 ..... N90-16456 #
IC-89/62 ..... N90-16546 #
IC-89/65 ..... N90-16571 #
IC-89/75 ..... N90-16545 #
IC-89/88 ..... N90-16473 #
IC-89/99 ..... N90-16376 #
IC-89/105 ..... N90-16573 #
IC-89/112 ..... N90-16575 #
IC-89/114 ..... N90-16576 #
IC-89/116 ..... N90-16574 #
IC-89/123 ..... N90-16513 #
IC-89/136 ..... N90-16514 #
IC-89/142 ..... N90-16464 #
IC-89/146 ..... N90-16109 #
IC-89/153 ..... N90-16668 #

ICASE-90-3 ..... N90-15893* #
ICASE-90-10 ..... N90-16401* #

IEEE-CATALOG-88CH2649-2 ..... N90-16442* #

IEEE-ORDER-892 ..... N90-16442* #

IFSI-88-14 ..... N90-16377 #
IFSI-88-16 ..... N90-16678 #
IFSI-88-17 ..... N90-16679 #
IFSI-88-18 ..... N90-16229 #
IFSI-88-19 ..... N90-16378 #
IFSI-88-21 ..... N90-16684 #
IFSI-89-3 ..... N90-16603 #
IFSI-89-4 ..... N90-16670 #
IFSI-89-5 ..... N90-15986 #
IFSI-89-6 ..... N90-16504 #
IFSI-89-7 ..... N90-15987 #
IFSI-89-12 ..... N90-15988 #
IFSI-89-13 ..... N90-16230 #
IFSI-89-14 ..... N90-16231 #
IFSI-89-15 ..... N90-16671 #

IGC-104 ..... N90-16038 #

ILR-MITT-217 ..... N90-15990 #
ILR-MITT-220 ..... N90-15969 #
ILR-MITT-224 ..... N90-15970 #

IMAG-RR-755-I ..... N90-16406 #
IMAG-RR-756-I-IMAG-88-LIFIA ..... N90-16434 #
IMAG-RR-758-I ..... N90-16134 #
IMAG-RR-760-I ..... N90-16233 #
IMAG-RR-763-I ..... N90-16135 #

INIS-BR-1567 ..... N90-16063 #
INIS-BR-1569 ..... N90-16486 #
INIS-BR-1572 ..... N90-16572 #
INIS-BR-1583 ..... N90-16016 #

INIS-MF-11540 ..... N90-16577 #

INS-744 ..... N90-16553 #
INS-746 ..... N90-16578 #
INS-751 ..... N90-16477 #
INS-752 ..... N90-16490 #
INS-754 ..... N90-16581 #
INS-756 ..... N90-16582 #

IRIM-8801 ..... N90-16535 #

ISAL-89-0006 ..... N90-16073 #
ISAL-89-0017 ..... N90-16505 #
ISAL-89-0019 ..... N90-16022 #
ISAL-89-0020 ..... N90-16235 #
ISAL-89-0029 ..... N90-16281 #
ISAL-89-0030 ..... N90-16074 #
ISAL-89-0032 ..... N90-16304 #

ISBN-0-642-13252-6 ..... N90-16595 #
ISBN-0-642-13561-4 ..... N90-16099 #
ISBN-0-642-13582-7 ..... N90-16368 #
ISBN-0-642-13583-5 ..... N90-16080 #
ISBN-0-642-13584-3 ..... N90-16081 #
ISBN-0-8186-0892-7 ..... N90-16442* #
ISBN-0-86960-861-4 ..... N90-16577 #
ISBN-3-7696-9394-9 ..... N90-16316
ISBN-3-7696-9399-X N90-16317
ISBN-3-922010-41-5 ..... N90-16236 #
ISBN-3-922010-42-3 ..... N90-16169 #
ISBN-90-6275-424-4 ..... N90-16351
ISBN-91-7848-193-7 ..... N90-16308 #
ISBN-92-63-10486-3 ..... N90-16385 #
ISBN-92-63-12411-6 ..... N90-16386 #
ISBN-92-835-0523-9 ..... N90-15924 #
ISBN-92-835-0526-X ..... N90-15899 #
ISBN-92-835-0532-5 ..... N90-15939 #
ISBN-92-835-0534-4 ..... N90-15904 #
ISBN-92-835-1563-3 ..... N90-16585 #
ISBN-92-9029-042-4 ..... N90-15974 #
ISBN-92-9092-001-7 ..... N90-16113 #
ISBN-92-9092-015-7 ..... N90-15999 #
ISBN-92-9092-024-6 ..... N90-16672 #
ISBN-92-9092-027-0 ..... N90-15989 #
ISBN-92-9092-036-X ..... N90-15998 #
ISBN-92-9092-040-8 ..... N90-15968 #
ISBN-92-9092-044-0 ..... N90-16088 #
ISBN-92-9092-052-1 ..... N90-16089 #
ISBN-951-38-3253-8 ..... N90-16093 #
ISBN-951-38-3498-0 ..... N90-16299 #
ISBN-951-754-888-5 ..... N90-16102 #
ISBN-951-754-909-1 ..... N90-16531 #
ISBN-951-754-914-8 ..... N90-16498 #
ISBN-951-754-928-8 ..... N90-15967 #
ISBN-951-754-929-6 ..... N90-16497 #

ISL-CO-215/87 ..... N90-16157 #
ISL-CO-220/88 ..... N90-16153 #
ISL-CO-224/88 ..... N90-16232 #
ISL-CO-233/88 ..... N90-16021 #
ISL-CO-249/88 ..... N90-16154 #

ISSN-0029-3865 ..... N90-16663 #
ISSN-0029-3965 ..... N90-16662 #
ISSN-0065-3713 ..... N90-16379
ISSN-0065-5325 ..... N90-16316
ISSN-0065-5325 ..... N90-16317
ISSN-0101-6113 ..... N90-16148 #
ISSN-0101-6113 ..... N90-16417 #
ISSN-0101-6113 ..... N90-16460 #
ISSN-0101-6113 ..... N90-16461 #
ISSN-0101-6113 ..... N90-16462 #
ISSN-0101-6113 ..... N90-16465 #
ISSN-0172-8741 ..... N90-16117 #
ISSN-0174-1454 ..... N90-16315 #
ISSN-0178-0719 ..... N90-16116
ISSN-0178-0719 ..... N90-16234
ISSN-0178-0719 ..... N90-16604 #
ISSN-0178-0719 ..... N90-16673
ISSN-0250-1589 ..... N90-15989 #
ISSN-0250-1589 ..... N90-15999 #
ISSN-0250-1589 ..... N90-16706 #
ISSN-0284-5172 ..... N90-16308 #
ISSN-0344-9629 ..... N90-16365 #
ISSN-0348-9329 ..... N90-16481 #
ISSN-0355-5712 ..... N90-16102 #
ISSN-0355-7790 ..... N90-16498 #
ISSN-0358-5077 ..... N90-16093 #
ISSN-0358-5077 ..... N90-16299 #
ISSN-0366-0885 ..... N90-16024 #
ISSN-0366-0885 ..... N90-16044 #
ISSN-0379-4067 ..... N90-16113 #
ISSN-0379-6566 ..... N90-15968 #
ISSN-0379-6566 ..... N90-15974 #
ISSN-0379-6566 ..... N90-15998 #
ISSN-0379-6566 ..... N90-16088 #
ISSN-0379-6566 ..... N90-16089 #
ISSN-0379-6566 ..... N90-16672 #
ISSN-0436-1199 ..... N90-16267 #
ISSN-0436-1199 ..... N90-16494 #
ISSN-0721-5320 ..... N90-16302
ISSN-0723-0508 ..... N90-16161
ISSN-0723-0508 ..... N90-16468
ISSN-0784-848X ..... N90-16497 #
ISSN-0786-8154 ..... N90-15967 #

ISSN-0933-2839 ..... N90-15901 #
ISSN-0951-6301 ..... N90-15897

ISVR-TR-175 ..... N90-16115 #

IW-R510 ..... N90-16351

IWM-W-4/88 ..... N90-16303 #

IYAF-88-139-PT-1 ..... N90-16474 #

JAERI-M-89-018 ..... N90-16517 #
JAERI-M-89-063 ..... N90-16579 #
JAERI-M-89-082 ..... N90-16384 #
JAERI-M-89-085 ..... N90-16349 #
JAERI-M-89-093 ..... N90-16518 #
JAERI-M-89-094 ..... N90-16554 #

JHU/ECE-89-14 ..... N90-16458 #

JPL-PUBL-89-14 ..... N90-16312* #

JPL-89-20 ..... N90-16110* #
JPL-89-37 ..... N90-16675* #

JSCM-2314-REV-A ..... N90-16589* #

JUEL-2211 ..... N90-16044 #
JUEL-2284-PT-3 ..... N90-16024 #

K/DSRD-112-VOL-1 ..... N90-16413 #
K/DSRD-205 ..... N90-16119 #

KURRI-TR-315 ..... N90-16519 #

L-16404 ..... N90-15890* #
L-16536 ..... N90-15902* #
L-16563 ..... N90-15884* #
L-16594 ..... N90-15882* #
L-16657 ..... N90-16703* #
L-16665 ..... N90-16204* #
L-16712 ..... N90-16292* #

LA-UR-89-1383 ..... N90-16459 #
LA-UR-89-1952 ..... N90-16342 #
LA-UR-89-2913 ..... N90-16507 #
LA-UR-89-2970 ..... N90-16601 #
LA-UR-89-2971 ..... N90-16600 #
LA-UR-89-2989 ..... N90-16665 #
LA-UR-89-3001 ..... N90-16533 #
LA-UR-89-3244 ..... N90-16591 #
LA-UR-89-3375 ..... N90-16297 #
LA-UR-89-3376 ..... N90-16463 #
LA-UR-89-3440-EXC ..... N90-16366 #
LA-UR-89-3679 ..... N90-16420 #
LA-UR-89-3685 ..... N90-16419 #
LA-UR-89-3767 ..... N90-16527 #
LA-UR-89-3772 ..... N90-16598 #
LA-UR-89-3827 ..... N90-16520 #
LA-UR-89-3883 ..... N90-16560 #
LA-UR-89-3940 ..... N90-16058 #
LA-UR-89-3984 ..... N90-16143 #
LA-UR-89-4006 ..... N90-16283 #
LA-UR-89-4008 ..... N90-16057 #
LA-UR-89-4009 ..... N90-16056 #
LA-UR-89-4011 ..... N90-16537 #
LA-UR-89-4026 ..... N90-16491 #
LA-UR-89-4047 ..... N90-16521 #
LA-UR-89-4102 ..... N90-16565 #
LA-UR-89-4237 ..... N90-16260 #
LA-UR-89-4271 ..... N90-16529 #

LA-11522-MS ..... N90-16037 #
LA-11606-MS ..... N90-16412 #

LAAS-89185 ..... N90-16136 #
LAAS-89204 ..... N90-16436 #
LAAS-89229 ..... N90-16023 #
LAAS-89320 ..... N90-16437 #

LBF-S-182 ..... N90-16302

LBL-25332 ..... N90-16139 #
LBL-25337 ..... N90-16587 #
LBL-26140 ..... N90-16530 #
LBL-26490 ..... N90-16536 #
LBL-26600 ..... N90-16588 #
LBL-26842 ..... N90-16123 #
LBL-27598 ..... N90-16343 #
LBL-27654 ..... N90-16523 #
LBL-27673 ..... N90-16680 #
LBL-27723 ..... N90-16484 #
LBL-27725 ..... N90-16681* #
LBL-27760 ..... N90-16121 #
LBL-27886 ..... N90-16551 #
LBL-27950 ..... N90-16506 #

LBL-27955 N90-16084 #
LBL-27956 N90-16018 #

LC-88-82088 N90-16442* #
LC-89-600744 N90-15966 #

LESC-27642 N90-16013* #

LFD-281 N90-16114

LNCC-022/88 N90-16417 #
LNCC-028/88 N90-16465 #
LNCC-030/88 N90-16461 #
LNCC-033/88 N90-16460 #
LNCC-034/88 N90-16148 #
LNCC-037/88 N90-16462 #

LPI-CONTRIB-691 N90-16607* #

LR-536 N90-16000 #
LR-555 N90-16001 #

LRT-WE-9-FB-1(1989) N90-16166 #
LRT-WE-9-FB-2(1989) N90-16167 #
LRT-WE-9-FB-5(1989) N90-16168 #
LRT-WE-9-FB-15(1988) N90-16090 #

LUIP-8812 N90-16481 #

LUNFD6/(NFFK-7095)1-24(1988) N90-16481 #

MEMO-COSOR-89-11 N90-16467 #

MHD-ITC-89-285 N90-16525 #

MIT/LCS/TR-443 N90-16455 #

MPE-PREPRINT-146 N90-16116
MPE-PREPRINT-154 N90-16234
MPE-PREPRINT-157 N90-16673
MPE-PREPRINT-158 N90-16605
MPE-PREPRINT-159 N90-16606

MPE-REPT-215 N90-16604 #

MPIS-7/1989 N90-16267 #
MPIS-20/1988 N90-16494 #

NAS 1.15:4150 N90-16703* #
NAS 1.15:4155 N90-15884* #
NAS 1.15:4164 N90-16004* #
NAS 1.15:4165 N90-15890* #
NAS 1.15:4168 N90-16389* #
NAS 1.15:4174 N90-16292* #
NAS 1.15:100776 N90-16596* #
NAS 1.15:101085 N90-15898* #
NAS 1.15:101613 N90-15886* #
NAS 1.15:101643 N90-16293* #
NAS 1.15:101683 N90-15894* #
NAS 1.15:101918 N90-16442* #
NAS 1.15:101931 N90-16483* #
NAS 1.15:102037 N90-16087* #
NAS 1.15:102215 N90-16399* #
NAS 1.15:102219 N90-15938* #
NAS 1.15:102243 N90-16313* #
NAS 1.15:102251 N90-16400* #
NAS 1.15:102256 N90-16423* #
NAS 1.15:102349 N90-16286* #
NAS 1.15:102372 N90-15992* #
NAS 1.15:102414 N90-15983* #
NAS 1.15:102441 N90-15923* #
NAS 1.15:102478 N90-15964* #
NAS 1.15:102480 N90-15965* #
NAS 1.15:102483 N90-16008* #
NAS 1.15:102495 N90-16053* #
NAS 1.15:102582 N90-15892* #
NAS 1.15:102923 N90-16589* #
NAS 1.15:897140 N90-16496* #
NAS 1.26:4271 N90-16072* #
NAS 1.26:4274 N90-15885* #
NAS 1.26:166837 N90-16686* #
NAS 1.26:172119-PT-1 N90-16202* #
NAS 1.26:172119-PT-2 N90-16203* #
NAS 1.26:181940 N90-15937* #
NAS 1.26:181941 N90-16294* #
NAS 1.26:181950 N90-16424* #
NAS 1.26:181977 N90-15893* #
NAS 1.26:181984 N90-16401* #
NAS 1.26:183784 N90-15991* #
NAS 1.26:184821 N90-16607* #
NAS 1.26:185028 N90-16312* #
NAS 1.26:185163 N90-15985* #
NAS 1.26:185168 N90-15996* #
NAS 1.26:185595 N90-16013* #
NAS 1.26:185930 N90-16489* #
NAS 1.26:186009 N90-16407* #
NAS 1.26:186038 N90-16676* #
NAS 1.26:186201 N90-16482* #
NAS 1.26:186202 N90-15936* #
NAS 1.26:186203 N90-16408* #
NAS 1.26:186244 N90-16103* #
NAS 1.26:186259 N90-16110* #
NAS 1.26:186290 N90-16664* #
NAS 1.26:186298 N90-16675* #
NAS 1.26:186312 N90-16683* #
NAS 1.26:186313 N90-16414* #
NAS 1.26:186318 N90-15891* #
NAS 1.26:186328 N90-16681* #
NAS 1.55:3053 N90-16204* #
NAS 1.60:2917 N90-15902* #
NAS 1.60:2946 N90-15882* #
NAS 1.60:2981 N90-16007* #
NAS 1.71:LAR-13580-1 N90-16272* #
NAS 1.71:MSC-21387-1 N90-16411* #
NAS 1.71:MSC-21465-1 N90-16410* #
NAS 1.71:NPO-17439-1-CU N90-16391* #
NAS 1.71:NPO-17548-1-CU N90-16104* #
NAS 1.71:NPO-17604-1-CU N90-16124* #

NASA-CASE-LAR-13580-1 N90-16272* #

NASA-CASE-MSC-21387-1 N90-16411* #
NASA-CASE-MSC-21465-1 N90-16410* #

NASA-CASE-NPO-17439-1-CU N90-16391* #
NASA-CASE-NPO-17548-1-CU N90-16104* #
NASA-CASE-NPO-17604-1-CU N90-16124* #

NASA-CP-3053 N90-16204* #

NASA-CR-4271 N90-16072* #
NASA-CR-4274 N90-15885* #
NASA-CR-166837 N90-16686* #
NASA-CR-172119-PT-1 N90-16202* #
NASA-CR-172119-PT-2 N90-16203* #
NASA-CR-181940 N90-15937* #
NASA-CR-181941 N90-16294* #
NASA-CR-181950 N90-16424* #
NASA-CR-181977 N90-15893* #
NASA-CR-181984 N90-16401* #
NASA-CR-183784 N90-15991* #
NASA-CR-184821 N90-16607* #
NASA-CR-185028 N90-16312* #
NASA-CR-185163 N90-15985* #
NASA-CR-185168 N90-15996* #
NASA-CR-185595 N90-16013* #
NASA-CR-185930 N90-16489* #
NASA-CR-186009 N90-16407* #
NASA-CR-186038 N90-16676* #
NASA-CR-186201 N90-16482* #
NASA-CR-186202 N90-15936* #
NASA-CR-186203 N90-16408* #
NASA-CR-186244 N90-16103* #
NASA-CR-186259 N90-16110* #
NASA-CR-186290 N90-16664* #
NASA-CR-186298 N90-16675* #
NASA-CR-186312 N90-16683* #
NASA-CR-186313 N90-16414* #
NASA-CR-186318 N90-15891* #
NASA-CR-186328 N90-16681* #

NASA-TM-4150 N90-16703* #
NASA-TM-4155 N90-15884* #
NASA-TM-4164 N90-16004* #
NASA-TM-4165 N90-15890* #
NASA-TM-4168 N90-16389* #
NASA-TM-4174 N90-16292* #
NASA-TM-100776 N90-16596* #
NASA-TM-101085 N90-15898* #
NASA-TM-101613 N90-15886* #
NASA-TM-101643 N90-16293* #
NASA-TM-101683 N90-15894* #
NASA-TM-101918 N90-16442* #
NASA-TM-101931 N90-16483* #
NASA-TM-102037 N90-16087* #
NASA-TM-102215 N90-16399* #
NASA-TM-102219 N90-15938* #
NASA-TM-102243 N90-16313* #
NASA-TM-102251 N90-16400* #
NASA-TM-102256 N90-16423* #
NASA-TM-102349 N90-16286* #
NASA-TM-102372 N90-15992* #
NASA-TM-102414 N90-15983* #
NASA-TM-102441 N90-15923* #
NASA-TM-102478 N90-15964* #
NASA-TM-102480 N90-15965* #
NASA-TM-102483 N90-16008* #
NASA-TM-102495 N90-16053* #
NASA-TM-102582 N90-15892* #
NASA-TM-102923 N90-16589* #
NASA-TM-897140 N90-16496* #
NASA-TP-2917 N90-15902* #
NASA-TP-2946 N90-15882* #
NASA-TP-2981 N90-16007* #

NCAR/CT-121 N90-16358 #

NEDOJ-P-8825-PT-2 N90-16354 #

NISTIR-89/3918 N90-16101 #
NISTIR-89/4032 N90-16002 #

NOAA-DR-ERL-ARL-18 N90-16355 #
NOAA-DR-ERL-ARL-19 N90-16357 #

NOAA-TM-ERL-WPL-172 N90-16261 #

NOAA-TM-NESDIS-28 N90-16359 #

NOO-TN-03-89 N90-16415 #

NOSC/TD-1636 N90-16375 #
NOSC/TD-1637 N90-16374 #

NOSC/TR-1300 N90-16108 #

NOTA-INTERNA-934 N90-16495 #

NPS52-89-047 N90-16414* #

NSF-88-336 N90-16472 #

NSF/ENG-89047 N90-16470 #
NSF/ENG-89049 N90-16441 #

NTSB/AAR-89/04 N90-15895 #

ONERA-NT-1987-3 N90-16557 #

ONERA-RT-32/5025-AYD-PT-2 N90-15887 #

ORNL-ESD-3308 N90-16363 #

ORNL-6552 N90-16363 #

ORNL/ATD-23 N90-16512 #

ORNL/CON-290 N90-16348 #

ORNL/CSD/TM-265 N90-16422 #

ORNL/FTR-3488 N90-16025 #
ORNL/FTR-3490 N90-16085 #
ORNL/FTR-3496 N90-16076 #
ORNL/FTR-3500 N90-16559 #

ORNL/SUB-84-47989/4 N90-16346 #

ORNL/TM-10931 N90-16071 #
ORNL/TM-11162 N90-16048 #
ORNL/TM-11254 N90-16510 #
ORNL/TM-11255 N90-16511 #
ORNL/TM-11281 N90-16070 #
ORNL/TM-11326 N90-16132 #
ORNL/TM-11345 N90-16019 #
ORNL/TM-11375 N90-16403 #
ORNL/TM-11401 N90-16277 #

ORNL/TR-89/48 N90-16307 #
ORNL/TR-89/52 N90-16306 #

OTA-ISC-419 N90-15966 #

PB89-910406 N90-15895 #
PB90-100231 N90-16011 #
PB90-100736 N90-16101 #
PB90-100769 N90-16341 #
PB90-100785 N90-16012 #
PB90-103987 N90-16472 #
PB90-104373 N90-16382 #
PB90-110172 N90-16355 #
PB90-110388 N90-16531 #
PB90-110651 N90-15967 #
PB90-110669 N90-16497 #
PB90-110677 N90-16102 #
PB90-110719 N90-16498 #
PB90-110958 N90-16409 #
PB90-112608 N90-16356 #
PB90-112616 N90-16360 #
PB90-112996 N90-16002 #
PB90-113960 N90-16357 #
PB90-113986 N90-16358 #
PB90-113994 N90-16261 #
PB90-114034 N90-16359 #
PB90-114711 N90-16594 #
PB90-121294 N90-16441 #
PB90-121302 N90-16470 #

PB90-122649 ..... N90-16308 #

PML-1987-C141 ..... N90-16000 #
PML-1988-C32 ..... N90-16001 #

PNL-SA-16980 ..... N90-16042 #
PNL-SA-16982 ..... N90-16046 #
PNL-SA-16986 ..... N90-16047 #
PNL-SA-17010 ..... N90-16049 #
PNL-SA-17021 ..... N90-16041 #
PNL-SA-17227 ..... N90-16068 #

PPLK-R-29 ..... N90-16516 #
PPLK-R-33 ..... N90-16515 #

PREPRINT-SERIES-293 ..... N90-16664* #

PREPRINT-46 ..... N90-16163 #
PREPRINT-489 ..... N90-16086 #
PREPRINT-490 ..... N90-16158 #
PREPRINT-492 ..... N90-16159 #
PREPRINT-499 ..... N90-16160 #
PREPRINT-666 ..... N90-16466 #

PROG-88608804 ..... N90-16341 #

PSI-1006/TR-976 ..... N90-16485 #

R/D-5295-MS-01 ..... N90-16476 #
R/D-5956-MS-02 ..... N90-16054 #

RADC-TR-89-162 ..... N90-16416 #
RADC-TR-89-181 ..... N90-16500 #

RAE-TM-AERO-2150 ..... N90-15888 #

RAE-TM-FM-16 ..... N90-15917 #
RAE-TM-FM-18 ..... N90-16396 #

RAE-TM-M/S-1126 ..... N90-16301 #

RAE-TM-MAT/STR-1123 ..... N90-16043 #
RAE-TM-MAT/STR-1130 ..... N90-16300 #

RAE-TM-P-1149 ..... N90-15919 #
RAE-TM-P-1151 ..... N90-15920 #
RAE-TM-P-1154 ..... N90-15921
RAE-TM-P-1172 ..... N90-15922 #

RAE-TM-SPACE-371 ..... N90-15971 #

RARDE-1/89 ..... N90-15997 #

REPT-1 ..... N90-15967 #
REPT-1 ..... N90-16164 #
REPT-1/231/00/DERMES ..... N90-16156 #
REPT-12-88 ..... N90-16114
REPT-48 ..... N90-16497 #
REPT-83-102 ..... N90-16013* #
REPT-89/CT/DTI/MS/AS/154 ..... N90-16380 #

RRK-89-16 ..... N90-16580 #

RSRE-MEMO-4249 ..... N90-16425 #
RSRE-MEMO-4256 ..... N90-16426 #
RSRE-MEMO-4262 ..... N90-15972 #
RSRE-MEMO-4268 ..... N90-16427 #
RSRE-MEMO-4272 ..... N90-15896 #
RSRE-MEMO-4277 ..... N90-16428 #
RSRE-MEMO-4280 ..... N90-15900 #
RSRE-MEMO-4286 ..... N90-16502 #
RSRE-MEMO-4304 ..... N90-16429 #

RSRE-89004 ..... N90-16430 #
RSRE-89005 ..... N90-16433 #
RSRE-89011 ..... N90-16431 #
RSRE-89012 ..... N90-16432 #
RSRE-89014 ..... N90-16404 #

S-179 ..... N90-16102 #

SAN-264-620X ..... N90-16442* #

SAND-88-7056 ..... N90-16276 #
SAND-89-0507C ..... N90-16278 #
SAND-89-0595C ..... N90-16282 #
SAND-89-0596C ..... N90-15973 #
SAND-89-1338C ..... N90-16364 #
SAND-89-1534C ..... N90-16555 #
SAND-89-1536C ..... N90-16345 #
SAND-89-1561C ..... N90-16592 #
SAND-89-1608C ..... N90-16094 #
SAND-89-1619 ..... N90-16279 #
SAND-89-1635C ..... N90-16496* #
SAND-89-1729C ..... N90-16298 #
SAND-89-1795C ..... N90-16344 #

SAND-89-1822C ..... N90-16069 #
SAND-89-2134C ..... N90-16129 #
SAND-89-2259 ..... N90-16082 #
SAND-89-2312C ..... N90-16287 #
SAND-89-2581C ..... N90-16471 #
SAND-89-2703C ..... N90-16066 #
SAND-89-2712 ..... N90-16418 #
SAND-89-2733C ..... N90-16131 #
SAND-89-2788C ..... N90-16079 #
SAND-89-2820C ..... N90-16439 #
SAND-89-2997C ..... N90-16528 #
SAND-89-8224 ..... N90-16003 #

SD-TR-89-09 ..... N90-16599 #
SD-TR-89-76 ..... N90-16540 #

SEGJ-8802 ..... N90-16704 #

SER-C-PREPUBL-FASC-39 ..... N90-16602 #
SER-C-PREPUBL-FASC-40 ..... N90-16677 #
SER-C-PREPUBL-FASC-41 ..... N90-16669 #

SER-C-346 ..... N90-16316
SER-C-351 ..... N90-16317

SER-WISS-ABHANDL-89 ..... N90-16265 #

SERI/PR-215-3500 ..... N90-16352 #

SERI/STR-211-3510 ..... N90-16340 #

SFCC-PUBL-52 ..... N90-16001 #

SP-RAPP-1989-43 ..... N90-16308 #

SU-SLAC-PUB-5070 ..... N90-16121 #
SU-SLAC-PUB-5127 ..... N90-16552 #

TIT/HEP-137 ..... N90-16582 #

TKK-F-A65 ..... N90-16531 #
TKK-F-A654 ..... N90-16498 #

TMUP-HEL-8904 ..... N90-16578 #

TR-4-1988 ..... N90-15901 #
TR-27 ..... N90-16015 #
TR-172 ..... N90-16311 #
TR-0088(3940-06)-3 ..... N90-16599 #
TR-0089(4945-07)-1 ..... N90-16540 #

TWR-17592-REV-B ..... N90-15991* #

UCRL-21193 ..... N90-16064 #
UCRL-21234 ..... N90-16489* #
UCRL-100614 ..... N90-16549 #
UCRL-100615 ..... N90-16548 #
UCRL-100652 ..... N90-16130 #
UCRL-101688 ..... N90-16121 #
UCRL-101851 ..... N90-16574 #
UCRL-101940 ..... N90-16440 #
UCRL-102181 ..... N90-16666 #
UCRL-102200 ..... N90-16095 #
UCRL-102238 ..... N90-16667 #
UCRL-102240 ..... N90-16683* #
UCRL-102243-2 ..... N90-16682 #

UH-156 ..... N90-16315 #

US-PATENT-APPL-SN-011085 ..... N90-16061 #
US-PATENT-APPL-SN-012517 ..... N90-16105 #
US-PATENT-APPL-SN-052641 ..... N90-16275 #
US-PATENT-APPL-SN-054976 ..... N90-16128
US-PATENT-APPL-SN-070499 ..... N90-16479 #
US-PATENT-APPL-SN-090500 ..... N90-16106 #
US-PATENT-APPL-SN-100385 ..... N90-16274 #
US-PATENT-APPL-SN-106469 ..... N90-16499 #
US-PATENT-APPL-SN-107185 ..... N90-16126 #
US-PATENT-APPL-SN-109810 ..... N90-15994 #
US-PATENT-APPL-SN-128842 ..... N90-16030 #
US-PATENT-APPL-SN-138238 ..... N90-16541 #
US-PATENT-APPL-SN-181135 ..... N90-16059 #
US-PATENT-APPL-SN-181480 ..... N90-16127 #
US-PATENT-APPL-SN-183200 ..... N90-16296 #
US-PATENT-APPL-SN-185728 ..... N90-16226
US-PATENT-APPL-SN-187143 ..... N90-16273 #
US-PATENT-APPL-SN-197935 ..... N90-16475 #
US-PATENT-APPL-SN-198804 ..... N90-16029 #
US-PATENT-APPL-SN-213007 ..... N90-16060 #
US-PATENT-APPL-SN-213032 ..... N90-16227
US-PATENT-APPL-SN-219295 ..... N90-16410* #
US-PATENT-APPL-SN-241179 ..... N90-16083 #
US-PATENT-APPL-SN-255803 ..... N90-16147 #
US-PATENT-APPL-SN-266955 ..... N90-16394 #
US-PATENT-APPL-SN-270146 ..... N90-16031 #
US-PATENT-APPL-SN-310448 ..... N90-16028 #

US-PATENT-APPL-SN-323748 ..... N90-16411* #
US-PATENT-APPL-SN-338198 ..... N90-15984 #
US-PATENT-APPL-SN-404288 ..... N90-16124* #
US-PATENT-APPL-SN-404293 ..... N90-16104* #
US-PATENT-APPL-SN-412054 ..... N90-16125 #
US-PATENT-APPL-SN-441673 ..... N90-16272* #
US-PATENT-APPL-SN-444248 ..... N90-16391* #
US-PATENT-APPL-SN-905439 ..... N90-15918 #
US-PATENT-APPL-SN-928356 ..... N90-16263 #

US-PATENT-CLASS-65-32.5 ..... N90-16060 #
US-PATENT-CLASS-73-714 ..... N90-16226
US-PATENT-CLASS-89-1.11 ..... N90-15984 #
US-PATENT-CLASS-134-1 ..... N90-16479 #
US-PATENT-CLASS-252-25 ..... N90-16059 #
US-PATENT-CLASS-264-60 ..... N90-16061 #
US-PATENT-CLASS-340-619 ..... N90-16227
US-PATENT-CLASS-423-406 ..... N90-16083 #
US-PATENT-CLASS-455-619 ..... N90-16128

US-PATENT-4,815,858 ..... N90-16499 #
US-PATENT-4,822,834 ..... N90-16296 #
US-PATENT-4,823,357 ..... N90-16263 #
US-PATENT-4,825,826 ..... N90-16273 #
US-PATENT-4,828,729 ..... N90-16059 #
US-PATENT-4,828,774 ..... N90-16061 #
US-PATENT-4,828,793 ..... N90-16029 #
US-PATENT-4,830,479 ..... N90-16475 #
US-PATENT-4,831,246 ..... N90-16127 #
US-PATENT-4,832,760 ..... N90-16030 #
US-PATENT-4,832,931 ..... N90-16083 #
US-PATENT-4,836,858 ..... N90-16479 #
US-PATENT-4,838,029 ..... N90-15918 #
US-PATENT-4,838,584 ..... N90-16274 #
US-PATENT-4,841,150 ..... N90-16541 #
US-PATENT-4,841,834 ..... N90-16126 #
US-PATENT-4,842,045 ..... N90-16147 #
US-PATENT-4,842,631 ..... N90-16060 #
US-PATENT-4,845,645 ..... N90-16106 #
US-PATENT-4,851,055 ..... N90-16031 #
US-PATENT-4,851,193 ..... N90-16028 #
US-PATENT-4,851,847 ..... N90-16105 #
US-PATENT-4,852,347 ..... N90-15994 #
US-PATENT-4,852,452 ..... N90-15984 #
US-PATENT-4,854,174 ..... N90-16226
US-PATENT-4,854,190 ..... N90-16275 #
US-PATENT-4,856,095 ..... N90-16128
US-PATENT-4,857,894 ..... N90-16227

USAARL-89-25 ..... N90-16392 #

UT-KOMABA-89-14 ..... N90-16582 #

VTT-TUTK-620 ..... N90-16093 #
VTT-TUTK-625 ..... N90-16299 #

WMO-411-ED-2 ..... N90-16386 #
WMO-488-REV ..... N90-16385 #

WSRC-RP-89-799 ..... N90-16284 #

Y/TR-89-8 ..... N90-16006 #

YJT-88-14 ..... N90-16039 #

Appendix—About STAR

Scientific and Technical Aerospace Reports (STAR) is a major component of a comprehensive National Aeronautics and Space Administration information system covering aeronautics, space, and supporting disciplines. *STAR* is issued on the 8th and 23rd of each month and announces current publications of the following types:

- NASA, NASA contractor, and NASA grantee reports
- Reports issued by other U.S. Government agencies, domestic and foreign institutions, universities, and private firms
- Translations in report form
- NASA-owned patents and patent applications
- Other U.S. Government agency and foreign patents and patent applications
- Domestic and foreign dissertations and theses

Journal, book, and conference literature, cover-to-cover journal translations, and certain foreign dissertations are announced in a companion journal, *International Aerospace Abstracts (IAA)*, available on subscription from the American Institute of Aeronautics and Astronautics, Technical Information Service, 555 West 57th Street, 12th Floor, New York, NY 10019.

SUBJECT SCOPE

The subject scope of *STAR* and *IAA* includes all aspects of aeronautics and space research and development, supporting basic and applied research, and applications. Aerospace aspects of earth resources, energy development, conservation, oceanography, environmental protection, urban transportation, and other topics of high national priority are also covered.

OTHER NASA PUBLICATIONS

Other NASA publications and information services are described in the publication, *The NASA Scientific and Technical Information System ... and How to Use It*, available without charge from the NASA Scientific and Technical Information Facility, P.O. Box 8757, BWI Airport, MD 21240.

HOW TO USE *STAR* SUBJECT CATEGORIES

STAR is categorized by 10 major subject divisions broken down further into 76 specific subject categories and one general division/category. The major subject divisions are listed on page ii in the Table of Contents, together with a note for each that defines its scope and provides any cross-references. For example:

AERONAUTICS

Includes aeronautics (general); aerodynamics; air transportation and safety; aircraft communications and navigation; aircraft design, testing and performance; aircraft instrumentation; aircraft propulsion and power; aircraft stability and control; and research and support facilities (air).

For related information see also *Astronautics*.

Each major division is further divided into as many as nine specific categories, which are identified by category numbers.

Abstracts in *STAR* are grouped by subject category, the categories appearing in sequential order. Category breaks in the abstract section are identified by the category number and title, and a scope note. Cross-references to other categories are provided as appropriate. For example:

02 AERODYNAMICS

Includes aerodynamics of bodies, combinations, wings, rotors, and control surfaces; and internal flow in ducts and turbomachinery.

For related information see also *34 Fluid Mechanics and Heat Transfer.*

CROSS-REFERENCES

Individual *STAR* abstracts are not ordinarily cross-referenced, except for certain conference reports or book translations that have had separate abstracts written for their component papers or chapters. Citations and abstracts of the components follow immediately after those of the parent document. When the subject content of a component differs sufficiently from the general content of the parent, a cross-reference citation also is printed at the end of the category to which it normally would have been assigned if it were independent.

DOCUMENTS ON MICROFICHE

Documents on microfiche[1] are designated by a pound sign (#) following the accession number. The pound sign is used without regard to the source or quality of the microfiche.

LIMITED REPRODUCIBILITY

A Note of Limited Reproducibility appears in the citation, if one or a combination of the following factors affect the reproducibility of more than 20% of the document. These factors include: faint or broken type, color photographs, black and white photographs, foldouts, dot matrix print, charts/graphs with script notation, non-Roman alphabet, or some other factor that limits the reproducibility of that document. This notation also appears on the microfiche header, with the specific causing factor checked off on a list visible in the second frame.

AVAILABILITIES

One or more sources from which a document announced in *STAR* is available to the public is given in each citation. The most commonly indicated sources and their acronyms or abbreviations are listed below. If the publication is available from a source other than those listed, the publisher and his address will be displayed on the availability line or in combination with the corporate source line.

Avail: NTIS. Sold by the National Technical Information Service. Prices for hard copy (HC) and microfiche (MF) are indicated by a price code following the letters HC or MF in the *STAR* citation. Current values for the price codes are given in the tables on page A-7.

Initially distributed microfiche under the NTIS SRIM (Selected Research in Microfiche) is available at greatly reduced unit prices. For this service and for information concerning subscription to NASA printed reports, consult the NTIS Subscription Section, Springfield, VA 22161.

NOTE ON ORDERING DOCUMENTS: When ordering NASA publications (those followed by the * symbol), use the N accession number. NASA patent applications (only the specifications are offered) should be ordered by the US-Patent-Appl-SN number. Non-NASA publications (no asterisk) should be ordered by the AD, PB, or other *report number* shown on the last line of the citation, not by the N accession number. It is also advisable to cite the title and other bibliographic identification.

(1) A microfiche is a transparent sheet of film, 105 by 148 mm in size, containing as many as 60 to 98 pages of information reduced to micro images (not to exceed 26:1 reduction).

Avail: SOD (or GPO). Sold by the Superintendent of Documents, U.S. Government Printing Office, in hard copy. The current price and order number are given following the availability line. (NTIS will fill microfiche requests, as indicated above, for those documents identified by a # symbol.)

Avail: BLL (formerly NLL): British Library Lending Division, Boston Spa, Wetherby, Yorkshire, England. Photocopies available from this organization at the price shown. (If none is given, inquiry should be addressed to the BLL.)

Avail: DOE Depository Libraries. Organizations in U.S. cities and abroad that maintain collections of Department of Energy reports, usually in microfiche form, are listed in *Energy Research Abstracts*. Services available from the DOE and its depositories are described in a booklet, *DOE Technical Information Center - Its Functions and Services* (TID-4660), which may be obtained without charge from the DOE Technical Information Center.

Avail: ESDU. Pricing information on specific data, computer programs, and details on Engineering Sciences Data Unit (ESDU) topic categories can be obtained from ESDU International Ltd. Requesters in North America should use the Virginia address while all other requesters should use the London address, both of which are on page A-6.

Avail: Fachinformationszentrum, Karlsruhe. Sold by the Fachinformationszentrum Energie, Physik, Mathematik GMBH, Eggenstein Leopoldshafen, Federal Republic of Germany, at the price shown in deutschmarks (DM).

Avail: HMSO. Publications of Her Majesty's Stationery Office are sold in the U.S. by Pendragon House, Inc. (PHI), Redwood City, CA. The U.S. price (including a service and mailing charge) is given, or a conversion table may be obtained from PHI.

Avail: NASA Public Document Rooms. Documents so indicated may be examined at or purchased from the National Aeronautics and Space Administration, Public Documents Room (Room 126), 600 Independence Ave., S.W., Washington, DC 20546, or public document rooms located at NASA installations, and the NASA Pasadena Office at the Jet Propulsion Laboratory.

Avail: Univ. Microfilms. Documents so indicated are dissertations selected from *Dissertation Abstracts* and are sold by University Microfilms as xerographic copy (HC) and microfilm. All requests should cite the author and the Order Number as they appear in the citation.

Avail: US Patent and Trademark Office. Sold by Commissioner of Patents and Trademarks, U.S. Patent and Trademark Office, at the standard price of $1.50 each, postage free. (See discussion of NASA patents and patent applications below.)

Avail: (US Sales Only). These foreign documents are available to users within the United States from the National Technical Information Service (NTIS). They are available to users outside the United States through the International Nuclear Information Service (INIS) representative in their country, or by applying directly to the issuing organization.

Avail: USGS. Originals of many reports from the U.S. Geological Survey, which may contain color illustrations, or otherwise may not have the quality of illustrations preserved in the microfiche or facsimile reproduction may be examined by the public at the libraries of the USGS field offices whose addresses are listed in this Introduction. The libraries may be queried

concerning the availability of specific documents and the possible utilization of local copying services, such as color reproduction.

Avail: Issuing Activity, or Corporate Author, or no indication of availability. Inquiries as to the availability of these documents should be addressed to the organization shown in the citation as the corporate author of the document.

NASA PATENTS AND PATENT APPLICATIONS

Patents and patent applications owned by NASA are announced in *STAR* under appropriate subject categories and are referenced in the *STAR* indexes. In the Report/Accession Number Index, patents are indexed by the NASA Case Number (which appears in lieu of the report number in other indexes), the U.S. Patent Number, the U.S. Patent Application Serial Number, and the U.S. Patent Class. Patent applications for which patents have not yet been issued are indexed by the NASA Case Number and the U.S. Patent Application Serial Number.

NASA *patent application specifications* are sold in paper copy and microfiche by the National Technical Information Service (NTIS). The US-Patent-Appl-SN- number should be used in ordering either paper copy or microfiche from NTIS. Printed copies of *patents* (which are not microfiched) are available for purchase from:

Commissioner of Patents and Trademarks
U.S. Patent and Trademark Office
Washington, DC 20231

When ordering patents, the U.S. Patent Number should be used, and payment must be remitted in advance, by money order or check payable to the Commissioner of Patents and Trademarks. Prepaid purchase coupons for ordering are also available from the Patent and Trademark Office. The patents and patent applications announced in *STAR* are owned by NASA and are available for royalty-free licensing. Requests for licensing terms and further information should be addressed to:

Associate General Counsel for Intellectual Property/Code GP
National Aeronautics and Space Administration
Washington, DC 20546

ELIGIBILITY AND REGISTRATION FOR NASA INFORMATION PRODUCTS AND SERVICES

A variety of services is available to organizations of the following types that have registered with NASA to receive specific services or products:

1. NASA offices and installations, contractors, subcontractors, grantees, and consultants;
2. Other U.S. Government agencies and their contractors;
3. Libraries in the United States that have arrangements with NASA to maintain collections of NASA documents for public reference;
4. Other organizations in the United States having a need for NASA documents in work related to aeronautics and space research;
5. Organizations abroad that have established reciprocal document exchange arrangements with NASA.

Only the central service points or central points of document acquisition and control within qualified organizations are eligible to register for NASA products and services. Domestic organizations that may be eligible to receive various classes of NASA publications and services should address their requests for registration or for further information to:

NASA Scientific and Technical Information Facility
ATTN: Registration Services
P.O. Box 8757
BWI Airport, MD 21240
301-621-0153

Organizations abroad should direct requests to Manager, International STI Activities, NTT, NASA Headquarters, Washington, DC 20546.

AVAILABILITY OF *STAR* ABSTRACTS ON MICROFICHE

Microfiche of the abstract sections of this issue and other issues of *STAR* are available on annual subscription from NTIS as PB90-911300, Attn: Subscriptions, 5285 Port Royal Road, Springfield, VA 22161. Annual subscription rates are $75.50 North America; $151.00 foreign. Abstract sections for previous years retroactive to 1964 are available at the current rates. Microfiche for individual *STAR* issue abstract sections are not available.

PUBLIC COLLECTIONS OF NASA DOCUMENTS

DOMESTIC: NASA and NASA-sponsored documents and a large number of aerospace publications are available to the public for reference purposes at the library maintained by the American Institute of Aeronautics and Astronautics, Technical Information Service, 555 West 57th Street, 12th Floor, New York, NY 10019

EUROPEAN: An extensive collection of NASA and NASA-sponsored publications is maintained by the British Library Lending Division, Boston Spa, Wetherby, Yorkshire, England, for public access. The British Library Lending Division also has available many of the non-NASA publications cited in *STAR*. European requesters may purchase facsimile copy or microfiche of NASA and NASA-sponsored documents, those identified by both the symbols # and * from ESA - Information Retrieval Service, European Space Agency, 8-10 rue Mario-Nikis, 75738 Paris CEDEX 15, France.

FEDERAL DEPOSITORY LIBRARY PROGRAM

In order to provide the general public with greater access to U.S. Government publications, Congress established the Federal Depository Library Program under the Government Printing Office (GPO), with 51 regional depositories responsible for permanent retention of material, inter-library loan, and reference services. At least one copy of nearly every NASA and NASA-sponsored publication, either in printed or microfiche format, is received and retained by the 51 regional depositories. A list of the regional GPO libraries, arranged alphabetically by state, appears on the inside back cover. These libraries are *not* sales outlets. A local library can contact a Regional Depository to help locate specific reports, or direct contact may be made by an individual.

ADDRESSES OF ORGANIZATIONS

American Institute of Aeronautics and Astronautics
Technical Information Service
555 West 57th Street, 12th Floor
New York, New York 10019

British Library Lending Division,
Boston Spa, Wetherby, Yorkshire,
England

Commissioner of Patents and Trademarks
U.S. Patent and Trademark Office
Washington, DC 20231

Department of Energy
Technical Information Center
P.O. Box 62
Oak Ridge, Tennessee 37830

European Space Agency-Information Retrieval Service
ESRIN
Via Galileo Galilei
00044 Frascati (Rome) Italy

Engineering Sciences Data Unit International
P.O. Box 1633
Manassas, Virginia 22110

Engineering Sciences Data Unit International, Ltd.
251-259 Regent Street
London, W1R 7AD, England

Fachinformationszentrum Energie, Physik, Mathematik
GMBH
7514 Eggenstein Leopoldshafen
Federal Republic of Germany

Her Majesty's Stationery Office
P.O. Box 569, S.E. 1
London, England

NASA Scientific and Technical Information Facility
P.O. Box 8757
BWI Airport, Maryland 21240

National Aeronautics and Space Administration
Scientific and Technical Information Division (NTT)
Washington, DC 20546

National Technical Information Service
5285 Port Royal Road
Springfield, Virginia 22161

Pendragon House, Inc.
899 Broadway Avenue
Redwood City, California 94063

Superintendent of Documents
U.S. Government Printing Office
Washington, DC 20402

University Microfilms
A Xerox Company
300 North Zeeb Road
Ann Arbor, Michigan 48106

University Microfilms, Ltd.
Tylers Green
London, England

U.S. Geological Survey Library National Center
MS 950
12201 Sunrise Valley Drive
Reston, Virginia 22092

U.S. Geological Survey Library
2255 North Gemini Drive
Flagstaff, Arizona 86001

U.S. Geological Survey
345 Middlefield Road
Menlo Park, California 94025

U.S. Geological Survey Library
Box 25046
Denver Federal Center, MS914
Denver, Colorado 80225

NTIS PRICE SCHEDULES

(Effective January 1, 1990)

Schedule A
STANDARD PRICE DOCUMENTS AND MICROFICHE

PRICE CODE	NORTH AMERICAN PRICE	FOREIGN PRICE
A01	$ 8.00	$ 16.00
A02	11.00	22.00
A03	15.00	30.00
A04-A05	17.00	34.00
A06-A09	23.00	46.00
A10-A13	31.00	62.00
A14-A17	39.00	78.00
A18-A21	45.00	90.00
A22-A25	53.00	106.00
A99	*	*
N01	60.00	120.00
N02	59.00	118.00
N03	20.00	40.00

Schedule E
EXCEPTION PRICE DOCUMENTS AND MICROFICHE

PRICE CODE	NORTH AMERICAN PRICE	FOREIGN PRICE
E01	$10.00	$ 20.00
E02	12.00	24.00
E03	14.00	28.00
E04	16.50	33.00
E05	18.50	37.00
E06	21.50	43.00
E07	24.00	48.00
E08	27.00	54.00
E09	29.50	59.00
E10	32.50	65.00
E11	35.00	70.00
E12	38.50	77.00
E13	41.00	82.00
E14	45.00	90.00
E15	48.50	97.00
E16	53.00	106.00
E17	57.50	115.00
E18	62.00	124.00
E19	69.00	138.00
E20	80.00	160.00
E99	*	*

* Contact NTIS for price quote.

IMPORTANT NOTICE

NTIS Shipping and Handling Charges

U.S., Canada, Mexico — ADD $3.00 per TOTAL ORDER

All Other Countries — ADD $4.00 per TOTAL ORDER

Exceptions — Does NOT apply to:

ORDERS REQUESTING NTIS RUSH HANDLING

ORDERS FOR SUBSCRIPTION OR STANDING ORDER PRODUCTS *ONLY*

NOTE: Each additional delivery address on an order requires a separate shipping and handling charge.

FEDERAL REGIONAL DEPOSITORY LIBRARIES

ALABAMA

AUBURN UNIV. AT MONTGOMERY LIBRARY
Documents Department
Montgomery, AL 36193
(205) 279-9110 ext.253

UNIV. OF ALABAMA LIBRARY
Reference Department/Documents
Box S
Tuscaloosa, AL 35486
(205) 348-6046

ARIZONA

DEPT. OF LIBRARY, ARCHIVES, AND PUBLIC RECORDS
Third Floor State Capitol
1700 West Washington
Phoenix, AZ 85007
(602) 255-4121

ARKANSAS

ARKANSAS STATE LIBRARY
Documents Service Section
One Capitol Mall
Little Rock, AR 72201
(501) 371-2090

CALIFORNIA

CALIFORNIA STATE LIBRARY
Govt. Publications Section
914 Capitol Mall
Sacramento, CA 95814
(916) 322-4572

COLORADO

UNIV. OF COLORADO
Norlin Library
Government Publications Division
Campus Box 184
Boulder, CO 80309
(303) 492-8834

DENVER PUBLIC LIBRARY
Govt. Pub. Department
1357 Broadway
Denver, CO 80203
(303) 571-2346

CONNECTICUT

CONNECTICUT STATE LIBRARY
231 Capitol Avenue
Hartford, CT 06106
(203) 566-4971

FLORIDA

UNIV. OF FLORIDA LIBRARIES
Documents Department
Library West
Gainesville, FL 32611
(904) 392-0367

GEORGIA

UNIV. OF GEORGIA LIBRARIES
Government Documents Dept.
Athens, GA 30602
(404) 542-8949

HAWAII

UNIV. OF HAWAII
Hamilton Library
Government Documents Collection
2550 The Mall
Honolulu, HI 96822
(808) 948-8230

IDAHO

UNIV. OF IDAHO LIBRARY
Documents Section
Moscow, ID 83843
(208) 885-6344

ILLINOIS

ILLINOIS STATE LIBRARY
Federal Documents
Centennial Building
Springfield, IL 62756
(217) 782-5012

INDIANA

INDIANA STATE LIBRARY
Serials Section
140 North Senate Avenue
Indianapolis, IN 46204
(317) 232-3686

IOWA

UNIV. OF IOWA LIBRARIES
Government Publications Dept.
Iowa City, IA 52242
(319) 335-5926

KANSAS

UNIVERSITY OF KANSAS
Spencer Research Library
Government Documents
Lawrence, KS 66045
(913) 864-4662

KENTUCKY

UNIV. OF KENTUCKY LIBRARIES
Government Publications/Maps Dept.
Lexington, KY 40506
(606) 257-8400

LOUISIANA

LOUISIANA STATE UNIVERSITY
Middleton Library
Government Documents Dept.
Baton Rouge, LA 70803
(504) 388-2570

LOUISIANA TECHNICAL UNIV.
Prescott Memorial Library
Government Documents Dept.
Ruston, LA 71272
(318) 257-4962

MAINE

UNIVERSITY OF MAINE
Raymond H. Fogler Library
Govt. Documents & Microforms Dept.
Orono, ME 04469
(207) 581-1680

MARYLAND

UNIVERSITY OF MARYLAND
McKeldin Library
Documents/Maps Room
College Park, MD 20742
(301) 454-3034

MASSACHUSETTS

BOSTON PUBLIC LIBRARY
Government Documents Dept.
666 Boylston Street
Boston, MA 02117
(617) 536-5400 ext.226

MICHIGAN

DETROIT PUBLIC LIBRARY
5201 Woodward Avenue
Detroit, MI 48202
(313) 833-1409

LIBRARY OF MICHIGAN
Government Documents
P.O. Box 30007
735 E. Michigan Avenue
Lansing, MI 48909
(517) 373-1593

MINNESOTA

UNIVERSITY OF MINNESOTA
Wilson Library
Government Publications
309 Nineteenth Avenue South
Minneapolis, MN 55455
(612) 373-7813

MISSISSIPPI

UNIV. OF MISSISSIPPI LIB.
Government Documents Dept.
106 Old Gym Bldg.
University, MS 38677
(601) 232-5857

MISSOURI

University of Missouri at Columbia Library
Government Documents
Columbia, MO 65201
(314) 882-6733

MONTANA

UNIV. OF MONTANA
Mansfield Library
Documents Division
Missoula, MT 59812
(406) 243-6700

NEBRASKA

UNIVERSITY OF NEBRASKA - LINCOLN
Love Memorial Library
Documents Department
Lincoln, NE 68588
(402) 472-2562

NEVADA

UNIV. OF NEVADA-RENO LIB.
Govt. Pub. Department
Reno, NV 89557
(702) 784-6579

NEW JERSEY

NEWARK PUBLIC LIBRARY
U.S. Documents Division
5 Washington Street
P.O. Box 630
Newark, NJ 07101
(201) 733-7812

NEW MEXICO

UNIVERSITY OF NEW MEXICO
General Library
Government Publications/Maps Dept.
Albuquerque, NM 87131
(505) 277-5441

NEW MEXICO STATE LIBRARY
325 Don Gaspar Avenue
Santa Fe, NM 87501
(505) 827-3826

NEW YORK

NEW YORK STATE LIBRARY
Documents Sect. Cultural Educ. Ctr.
Empire State Plaza
Albany, NY 12230
(518) 474-5563

NORTH CAROLINA

UNIVERSITY OF NORTH CAROLINA AT CHAPEL HILL
Davis Library 080A
BA/SS Department Documents
Chapel Hill, NC 27514
(919) 962-1151

NORTH DAKOTA

NORTH DAKOTA STATE UNIVERSITY LIBRARY
Government Documents Dept.
Fargo, ND 58105
(701) 237-8352
In cooperation with Univ. of North Dakota, Chester Fritz Library
Grand Forks

OHIO

STATE LIBRARY OF OHIO
Documents Section
65 South Front Street
Columbus, OH 43266
(614) 644-7051

OKLAHOMA

OKLAHOMA DEPT. OF LIBRARIES
Government Documents
200 NE 18th Street
Oklahoma City, OK 73105
(405) 521-2502, ext. 252

OKLAHOMA STATE UNIV. LIB.
Documents Department
Stillwater, OK 74078
(405) 624-0489

OREGON

PORTLAND STATE UNIV.
Millar Library
934 SW Harrison - P.O. Box 1151
Portland, OR 97207
(503) 229-3673

PENNSYLVANIA

STATE LIBRARY OF PENN.
Government Publications Section
Box 1601
Walnut St. & Commonwealth Ave.
Harrisburg, PA 17105
(717) 787-3752

SOUTH CAROLINA

CLEMSON UNIV. COOPER LIB.
Documents Department
Clemson, SC 29634
(803) 656-5174
In cooperation with Univ. of South Carolina, Thomas Cooper Library, Columbia

TEXAS

TEXAS STATE LIBRARY
Public Services Department
P.O. Box 12927 - 1201 Brazos
Austin, TX 78711
(512) 463-5455

TEXAS TECH. UNIV. LIBRARY
Documents Department
Lubbock, TX 79409
(806) 742-2268

UTAH

UTAH STATE UNIVERSITY
Merrill Library & Learning Resources Center, UMC-30
Documents Department
Logan, UT 84322
(801) 750-2682

VIRGINIA

UNIVERSITY OF VIRGINIA
Alderman Library
Government Documents
Charlottesville, VA 22903
(804) 924-3133

WASHINGTON

WASHINGTON STATE LIBRARY
Document Section
Olympia, WA 98504
(206) 753-4027

WEST VIRGINIA

WEST VIRGINIA UNIV. LIB.
Government Documents Section
P.O. Box 6069
Morgantown, WV 26506
(304) 293-3640

WISCONSIN

ST. HIST SOC. OF WISCONSIN LIB.
Government Pub. Section
816 State Street
Madison, WI 53706
(608) 262-2781
In cooperation with Univ. of Wisconsin-Madison, Memorial Library

MILWAUKEE PUBLIC LIBRARY
Documents Division
814 West Wisconsin Avenue
Milwaukee, WI 53233
(414) 278-3065

WYOMING

WYOMING STATE LIBRARY
Supreme Court & Library Bldg.
Cheyenne, WY 82002
(307) 777-5919

National Aeronautics and
Space Administration
Code NTT
Washington, D.C.
20546
Official Business
Penalty for Private Use, $300

SPECIAL FOURTH-CLASS RATE
POSTAGE & FEES PAID
NASA
PERMIT No. G27

POSTMASTER: If Undeliverable (Section 158
Postal Manual) Do Not Return